Biochimica et Biophysica Acta, 1149 (1993) 305–312

BBAMEM 76026

Conjugation of apolipoprotein B with liposomes and targeting to cells in culture

Bo Lundberg [a], Keelung Hong [b] and Demetrios Papahadjopoulos [b,c]

[a] *Department of Biochemistry and Pharmacy, Åbo Akademi University, Åbo (Finland),* [b] *Cancer Research Institute, University of California, San Francisco, CA (USA) and* [c] *Department of Pharmacology, University of California, San Francisco, CA (USA)*

(Received 26 February 1993)

Key words: Drug delivery; Apolipoprotein B; Liposome; Drug targeting

Mixed phospholipid/cholesterol (2:1 molar ratio) liposomes were conjugated with native and acetylated apolipoprotein B (apoB), the protein part of low density lipoprotein (LDL). The objective was to increase the specificity of the cellular uptake of liposomes by utilization of the LDL and scavenger receptor pathways. The method of choice for the conjugation of liposomes with apoB proved to be the detergent solubilization and removal procedure. Two detergents were tested;sodium cholate (NaC) and octyl glucoside (OG). The integrity of the resulting complexes was demonstrated by Sepharose CL-4B gel chromatography and Metrizamide gradient centrifugation. The conjugates showed a good physical stability and the leakiness was only marginally larger than for unconjugated liposomes. The interaction of apoB- and acetyl apoB–liposome conjugates with CV-1 and J774 cells, respectively, was monitored by an encapsulated pH-sensitive fluorophore, pyranine (8-hydroxy-1,3,6-pyrenetrisulfonate (HPTS)). This dye provides means of detecting binding and endocytosis of conjugates in living cells. The internalization was a fast process and about 10-times faster for the OG-conjugates than for the corresponding unconjugated liposomes. The conjugates showed a clear concentration-dependent association of dye with cells, while this was less prominent with liposomes. The uptake was nearly an order of magnitude faster with CV-1 cells than with J774 cells. Acidification of intracellular conjugates proceeded fast during the first 30 min of incubation and reached a minimum value of approx. pH 6 after 3 h. The specificity of binding of apoB–liposome conjugates to CV-1 cells was demonstrated by displacement experiments with native LDL. The results indicate that apoB–liposome conjugates may be used as a delivery vehicle for bioactive subtances to cells.

Introduction

Liposomes have been extensively studied as a delivery system for biomedically active substances to cells in vitro and in vivo (for reviews, see Refs. 1,2). One of the central problems in using liposomes as drug carrier is the lack of target specificity. An attractive strategy to promote efficient and selective delivery of encapsulated molecules to cells is to utilize liposomes that are targeted to specific cell-surface receptors by means of liposome-conjugated proteins or other ligands [3].

In recent years, LDL has been considered as an endogenous drug carrier in cancer chemotherapy [4]. LDL is taken up by cells via a specific receptor that interacts with apoB on LDL [5]. The rationale for using LDL as a carrier for antineoplastic drugs is that many cancer cell lines have higher LDL receptor activity than the corresponding normal cells [6]. LDL can also be directed to non-lipoprotein receptors by chemical modification of apoB [7]. However, targeting by use of drug/LDL complexes can only be applied to lipophilic drugs, while a large majority of the compounds in use today are water-soluble. The present study offers a way to overcome this problem. The targeting properties of apoB are combined with the capacity of the liposomes to carry water-soluble compounds. Two major problems had to be overcome in this work. The method for conjugation should restore both the receptor binding properties of apoB and the integrity of the liposomes. This report describes a simple and reproducible method for the successful conjungation of native and modified apoB with liposomes and the biological activity of these complexes are tested on cells in culture. This system should have potential applications for effective delivery

Correspondence to: B. Lundberg: Department of Biochemistry and Pharmacy, Åbo Akademi University, P.O. Box 66, SF-20521 Åbo, Finland.

Abbreviations: apoB, apolipoprotein B; LDL, low density lipoprotein; NaC, sodium cholate; OG, octyl glucoside; HPTS, 8-hydroxy-1,3,6-pyrenetrisulfonate; POPC, palmitoyloleoylphosphatidylcholine; Na_2EDTA, etylenediaminetetraacetic acid disodium salt; Hepes, *N*-2-hydroxyethylpiperazine-*N'*-2-ethanesulfonic acid; CF, carboxyfluorescein.

of bioactive substances to cells via receptor-mediated endocytosis.

Materials and Methods

Materials. Palmitoyloleoylphosphatidylcholine (POPC) was purchased from Avanti Polar Lipids (Birmingham, AL, USA) and L-3-phosphatidylcholine,1-palmitoyl-2-[1-^{14}C]oleoyl (57 mCi/mmol) from the Radiochemical Centre (Amersham, UK). Cholesterol, n-octyl-β-D-glucopyranoside, sodium cholate and Metrizamide were obtained from Sigma (St. Louis, MO, USA). Pyranine (8-hydroxypyrene-1,3,6-trisulfonic acid, disodium salt) was from Molecular Probes (Eugene, OR, USA), Bio-Beads SM-2 (20–50 mesh) from Bio-Rad Laboratories (Richmond, CA, USA) and carboxyfluorescein (CF) from Eastman Kodak (New York, NY, USA) and was purified on a Sephadex LH-20 column. The scintillation cocktail Liquiscint was obtained from National Diagnostics. All other chemicals were reagent grade.

Lipoprotein isolation. Plasma was obtained from freshly drawn blood from normal human volunteers. LDL (d = 1.019–1.063 g/ml) and high density lipoprotein (HDL) (d = 1.063–1.21 g/ml) was isolated by differential density ultracentrifugation using standard procedures [8]. Isolated LDL was washed by ultracentrifugal flotation through an overlayering solution of d = 1.063 g/ml. The centrifugations were performed in a Beckman SW-28 rotor at 27000 rpm at 4°C for 24 h. The purity of LDL was verified by agarose electrophoresis by staining with Oil Red O and Coomassie brilliant blue. The isolated LDL was dialyzed in the dark at 4°C for 24 h against 0.15 M NaCl and 0.05% Na_2EDTA (pH 7.4), filtered through a 0.22-μm filter and stored at 0°C in sterile ampoules. Acetylation of LDL was performed by reaction with acetic acid anhydride as described in Ref. 9. LDL was labelled with ^{125}I to a specific activity of about 100 cpm/ng using the IODO-GEN™ method [10] (Pierce, Rockford, IL, USA) and subsequently purified by Sephadex G-75 gel chromatography.

Delipidation of apoB. Prior to conjugation with liposomes, apoB, the protein component of LDL, was delipidated by extraction with heptane to remove endogenous neutral lipids, principally as described in Ref. 11. Briefly, 2.5 mg LDL in 400 μl was dialyzed at 4°C for 60 h against three changes of 3 liters of 0.3 mM Na_2EDTA (pH 7.0). Then sucrose was added to a final concentration of 25% (w/v) to stabilize the LDL-protein during lyophilization and heptane extraction. The solution was rapidly frozen and lyophilized over night. The residue was then stored under vacuum at 0°C in a desiccator containing P_2O_5 until it was completely dry (approx. 2 h). The dried LDL was extracted three times with 3 ml heptane at 0°C. The remaining heptane was evaporated in vacuum under argon at 0°C. The resulting delipidated apoB, which is freed of neutral lipids [12], was used for conjugation with liposomes as fast as possible.

Peparation and characterization of apoB–liposome conjugates. Liposomes were produced and conjugated with apoB by the detergent solubilization and removal method. The lipid components of the liposomes POPC and cholesterol (molar ratio 2:1) were mixed from stock solutions with 15 and 2 molar excesses (calculated on POPC basis) of OG and NaC, respectively, and evaporated to dryness under argon. After addition of buffer (2.5 mM Hepes, 75 mM NaCl, 50 μM EDTA (pH 7.4), standard buffer) the mixtures were subjected to a short sonication in a bath sonicator to ensure complete solubilization of the lipids. The mixed micelles were then added to the delipidated apoB in the proportion 2:1 (weight ratio) between POPC and apoB and the mixture was rotated gently until the solution was completely clear. The detergents were then removed from the mixtures by passage through a Bio-Beads SM-2 (20–50 mesh) column (Bio-Rad). This method has been shown to bring about a practically complete removal of detergents from a codispersion with phospholipids and protein [13]. The beads were wetted with the standard buffer before use and the moist beads were then weighed into disposable micro-columns in an amount enough to absorb the whole sample. The mixed micelle/apoB mixture was then added to the column and incubated at 0°C for 30 min. The product was eluted into a collecting tube by centrifugation of the micro-column for 2 min in a table-top centrifuge at approx. 400 × g. These procedures for extracting of detergents by Bio-Beads SM-2 were repeated once. At this stage the solutions were opaque indicating the formation of liposomes. The apoB–liposome conjugates were further purified by passage through a Sephadex G-75 column (1 × 15 cm). Since the size of aggregated apoB might equal that of small liposomes, the conjugates were also isolated by flotation in a Metrizamide gradient to assure their purity. The apoB–liposome complexes were applied in 20% Metrizamide and overlayered with 10% Metrizamide and standard buffer. The conjugates were recovered in the boundary between buffer and 10% Metrizamide. The size of the isolated complexes was measured by quasielastic laser light scattering on a Malvern system 4700 sub-micron particle analyzer (Malvern Instruments, Malvern, UK). The density of the conjugates was determined by density-gradient centrifugation in a linear 0–40% sucrose gradient. The leakage was assessed by dialysis of apoB–liposome conjugates with entrapped CF against a 100-fold excess of standard buffer for 24 h and measuring CF in the dialysate and CF remaining in conjugates after release with Triton X-100.

Cell culture. The macrophage-like cell lines J774 and CV-1, an established line of African green monkey kidney cells, were maintained in monolayer culture in Dulbecco's modified Eagle's medium (DMEM) supplemented with 4.5 g/l glucose and 10% foetal bovine serum and incubated under 7% humidified CO_2 at 37°C. Cells were plated at a concentration of 10^6 cells per 9.6 cm^2 plastic culture dish 24 h prior to use.

Cell incubation with HPTS-containing apoB–liposome conjugates. HPTS-containing conjugates were prepared by using solutions of HPTS (35 mM) in standard buffer for preparation of conjugates. Unencapsulated HPTS was removed by the chromatography on a Sephadex G-75 column (1×15 cm) equilibrated with 150 mM NaCl and 5 mM Hepes (pH 7.4). Before incubation with HPTS-containing conjugates the growth medium was removed and the cells were washed twice with 2 ml 137 mM NaCl, 2.7 mM KCl, 1.5 mM KH_2PO_4, 8.1 mM Na_2HPO_4 (PBS (pH 7.4)) supplemented with 0.4 mM calcium, 0.4 mM magnesium and 5 mM glucose (PBS-CMG). Before the start of incubation the HPTS-containing conjugates were diluted to 80 μM phospholipid in PBS-CMG and 0.5 ml was added to each culture dish (approx. $2 \cdot 10^6$ cells). After incubation in a humidified incubator at 37°C, cells were analyzed for fluorescence.

Fluorometry. Fluorescense was measured with a SPEX Fluorolog 2 fluorometer equipped with a photon-counting detector. The temperature of the stirred cuvette was held at 20°C. After incubation with HPTS-containing apoB–liposome conjugates for different times, cells were washed twice with PBS-CMG and incubated for 5 min at 37°C with 1.5 ml PBS containing 3 mM EDTA. Cells were dislodged and diluted to $5 \cdot 10^5$ cells/ml in PBS. Peak heights were measured at 510 nm emission at the three excitation wavelengths 403, 413 and 450 nm. Fluorescence units are expressed as photon counts per second.

Fluorescence microscopy. After incubation with HPTS-containing apoB–liposome conjugates, cells were washed twice with 2 ml PBS-CMG and viewed with a Leitz fluorescense microscope. The pH-independent fluorescence of HPTS could be viewed with a filter set, which excites in a wide violet band (350–410 nm), or with a filter set having a narrow blue excitation band (450–490 nm), which visualizes the fluorescence of HPTS at neutral or basic pH.

Analytical procedures. Protein was measured by the modified Lowry method [14] or by using the Bio-Rad protein kit (Bio-Rad Laboratories, Richmond, CA, USA), with albumin as standard. Phospholipid concentration was determined by the method of Bartlett [15] or by measurement of [^{3}H]POPC by liquid scintillation. Radioactivity was measured in a Beckman LS-3801 scintillation counter after dissolving the samples in Liquiscint scintillation fluid.

Results

Preparation and characterization of apoB–liposome conjugates

The heptane extraction method for delipdation of LDL used in this study yields a product, which is devoid of neutral lipids but with the phospholipid content essentially intact [12]. In a set of preliminary experiments a panel of different conjugation methods were tested, including spontaneous conjugation, dehydration-rehydration and transient pH jump [16]. However, the method finally adopted, detergent solubilization and removal, proved to be superior to those methods. Two relatively mild 'biological' detergents; NaC and OG were chosen for the experiments. For the appropriate use of the detergent solubilization and removal conjugation method the amount of detergent to be added must be determined for each specific system. The concentration should be enough to totally solubilize the lipids in the presence of the protein, but unnecessary excess should be avoided. The amount of detergent to be added was determined by titration of liposomes containing a self-quencing concentration of carboxyfluorescein (CF, 90 mM) and apo B with the detergent in question. The detergent concentrations showing maximum release of encapsulated CF, corresponded to detergent/POPC ratios of 22 and 3 for OG and NaC, respectively. These values were applied in the conjugation experiments.

The solubilization and detergent removal method proved to to be a fast, convenient and effective method for the conjugation of apoB with POPC-cholesterol liposomes. An almost total (96%) recovery of both protein and phospholipid was noted after removal of detergents by adsorption on Bio-Beads SM-2. Fig. 1 shows the separation on a Sepharose CL-4B column of liposomes composed of POPC/cholesterol (2:1 molar ratio) conjugated with apoB in an initial ratio of 2:1 (weight ratio) between POPC and apoB. The effluent was analyzed for phospholipid and protein and in some experiments the elution profile of encapsulated CF was recorded. The results demonstrate an effective conjugation of apo B with the liposomes. The reproducible elution profiles show two peaks; a sharp peak near V_0 and a small diffuse peak near the V_t of the column. The first large peak represents conjugates, which was demonstrated by the coelution of entrapped CF with phospholipid and protein. Only traces of fluorescence was noted in the second small peak. The POPC/apoB weight ratios in the major peak were found to be very near that of the starting value of 2:1. The integrity of the conjugates was confirmed by Metrizamide gradient centrifugation resulting in a recovery of about 85% of apoB in cojugates. No difference was noted in yield for conjugates formed with native or acetylated apoB.

The analytical gel filtration indicated that the OG

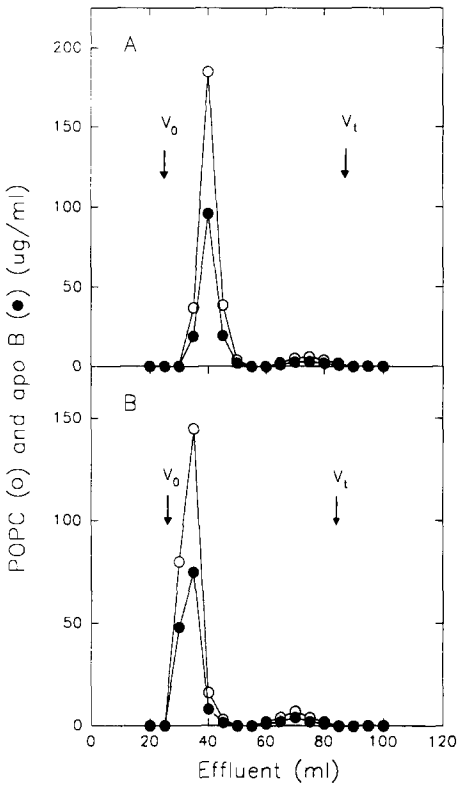

Fig. 1. Gel-filtration chromatography on a Sepharose CL-4B column (2.5×60 cm) of apoB–liposome conjugates prepared by the detergent solubilization and removal method as described in Materials and Methods. (A) Elution profile of conjugates prepared with sodium cholate (NaC) and (B) octyl glucoside (OG) as detergent. Arrows mark the void (V_0) and total (V_t) volumes of the column; (○) μg of POPC and (●) μg of apo B per ml of effluent.

conjugates were somewhat larger than those prepared with NaC. This observation was confirmed by the quasi-elastic light-scattering measurements. The conjugation of liposomes with apoB increased the diameter to some degree giving average values of 222 and 140 nm for OG and NaC conjugates, respectively, and 141 and 92 nm for corresponding liposomes, prepared by the same methods. At sucrose density gradient ultracentrifugation the apoB–liposome conjugates appeared as a distinct band with peak maximum at $d = 1.07$ g/ml. The phospholipid and protein bands overlapped completely. The measurements of the CF leakage showed a somewhat increased leakage for the conjugates compared to corresponding liposomes, giving values of 1.5 and 2.4% per day for OG and NaC conjugates and 1.5 and 0.9% for corresponding liposomes, respectively.

Biological activity

The spectral shifts of HPTS with changes in pH make it a useful marker of the fate of encapsulated dye following endocytosis [17,18]. HPTS exhibits two major fluorescence excitation maxima (403 and 450 nm) with complementary pH-dependence in the range 5–9. The peak at 403 nm is maximal at low pH values while the peak at 450 nm is maximal at high pH values. The cellular fate of the dye encapsulated in apoB–liposome conjugates and unconjugated liposomes was followed by fluorescence microscopy and fluorometry. At microscopy the uptake into acidifying compartments was followed by use of an essentially pH-insensitive violet filter set (350–410 nm) and a blue filter set (450–490 nm) which excites the pH-sensitive 450 nm peak. After a short time of incubation (< 0.5 h) with conjugates and liposomes, punctate fluorescence was seen on the cell surface, as well as in intracellular compartments under both short and long-wavelength excitation. At later times perinuclear vacuoles appear, with strong fluorescence at 350–410 nm illumination, but with much weaker fluorescence when excited with long wavelengths. Cells incubated with conjugates showed a more intense fluorescence than those incubated with liposomes. This fact was especially obvious for cells incubated with the OG conjugates, which after 3 h incubations showed a massive accumulation of dye in large vacuoles visible under violet, but not under under blue illumination (Fig. 2). These large-diameter acidic punctates may result from leakage of encapsulated dye in endosomes and lysosomes. The accumulation of dye was more accenturated for CV-1 than for J774 cells and much so in the large acidic vacuoles.

The cellular uptake of liposomal phospholipid can be calculated starting with the measured fluorescence values and the known values for fluorescence per nmol liposome or conjugate phospholipid. The quantitative measurements of POPC incorporation into cells (Fig. 3) confirmed the observations made by fluorescence microscopy. NaC conjugates showed a clear but only moderate predominance in dye incorporation com-

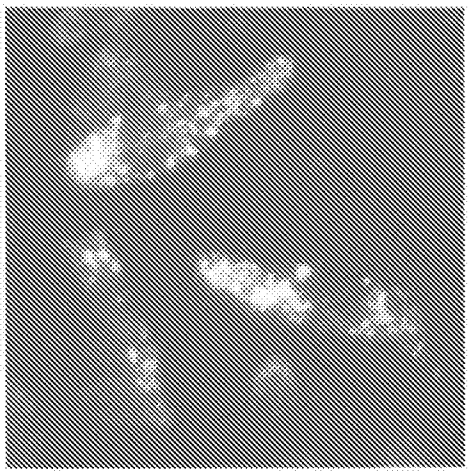

Fig. 2. Fluorescence micrographs of J774 macrophages treated with HPTS-containing aopB-liposome conjugates. The cells were treated with the preparation for 3 h at 37°C, washed, and viewed with a water immersion objective by epifluorescence with λ_{ex} 350–410 filters.

pared to corresponding liposomes. OG conjugates on the other hand gave a 5–6-fold increase in the rate of uptake compared to liposomes. Calculated on the basis of cell number the uptake of conjugates and liposomes was about ten times larger for CV-1 than for J774 cells. The observation by microscopy that much of the fluorescence gradually accumulated in acidic intracellular compartments was also confirmed by calculations of the 450/413 nm ratios. The OG conjugates gave ratios of 0.33 and 0.41 for CV-1 and J774 cells, respectively, after 3 h of incubation. These values correspond to pH values of 6.1 and 6.3, respectively, as estimated from the pH calibration curve of HPTS [18]. Thus, most of the dye endocytosed after 3 h of incubation resides within endosomes and lysosomes at low pH. The corresponding 450/413 nm ratios for OG liposomes were 0.52 and 0.71. NaC conjugates and liposomes gave similar values around 0.70 with both types of cells.

The initial studies clearly showed a preferential cellular uptake of OG conjugates. The further experiments were thus concentrated on this type of preparations. The internalization process was further studied

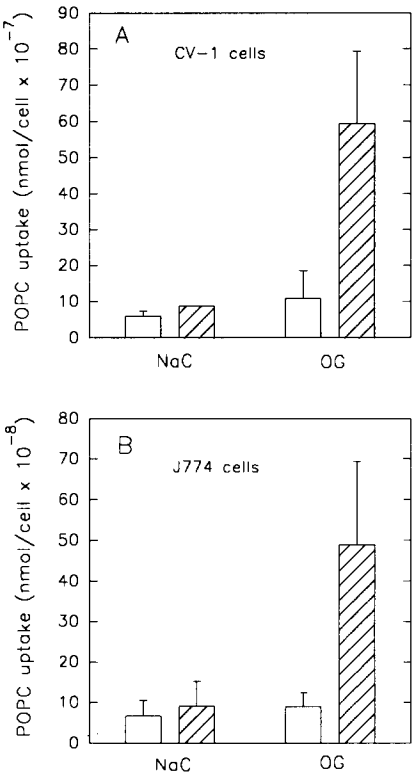

Fig. 3. The cellular uptake of HPTS-containing liposomes (open bars) and apoB–liposome conjugates (hatched bars) expressed as nmol POPC per cell. CV-1 (A) and J774 (B) cells were exposed to preparations prepared with NaC (bars to the left) and OG (bars to the right) as detergents at a concentration of 80 nmol of POPC per ml PBS for 3 h at 37°C. After incubation cells were washed with PBS and the cell-associated fluorescence was measured and the corresponding POPC values calculated.

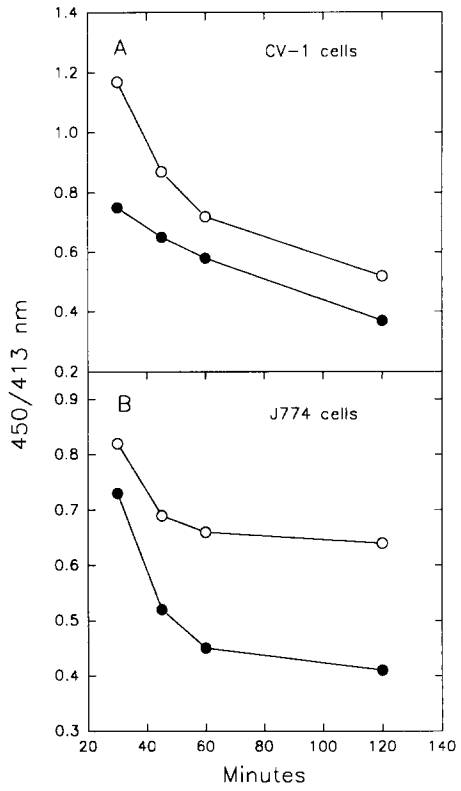

Fig. 4. Internalization into low-pH compartments of HPTS-containing liposomes (○), and apoB–liposome conjugates (●) by (A) CV-1, and (B) J774 cells in culture. The preparations were made with OG as detergent. The cells were incubated with respective preparation for 30 min, then washed with PBS and the incubation proceeded for different lenghts of time. The uptake process was followed by measurements of the 450/413 nm excitation wavelength ratio.

by exposition of cells to the conjugates for 30 min and then they were washed carefully and incubated for different times in PBS. Removal of free liposomes or conjugates resulted in a moderate reduction of total cell-associated HPTS with time at excitation wavelengths of 403 and 413 nm (data not shown). The peaks at 450 nm showed a more dramatic change and decreased progressively and with a faster rate for the conjugates than for the liposomes. The normalized 450 nm values (450/413 nm ratios) from CV-1 and J774 cells incubated with liposomes and conjugates are shown in Fig. 4. The fast decrease in 450/413 ratios noted for both cell types and both preparations is consistent with the expected change due to the acidification of HPTS. This process is somewhat faster for the J774 cells than for the CV-1 cells and becomes largely complete 30 min after removal of the conjugates.

The concentration-dependent uptake of encapsulated dye is shown in Fig. 5. At low concentration, there is an marked increase in uptake with increase in concentration of conjugates, which may in large part be due to binding of the particles to the cell surface. For

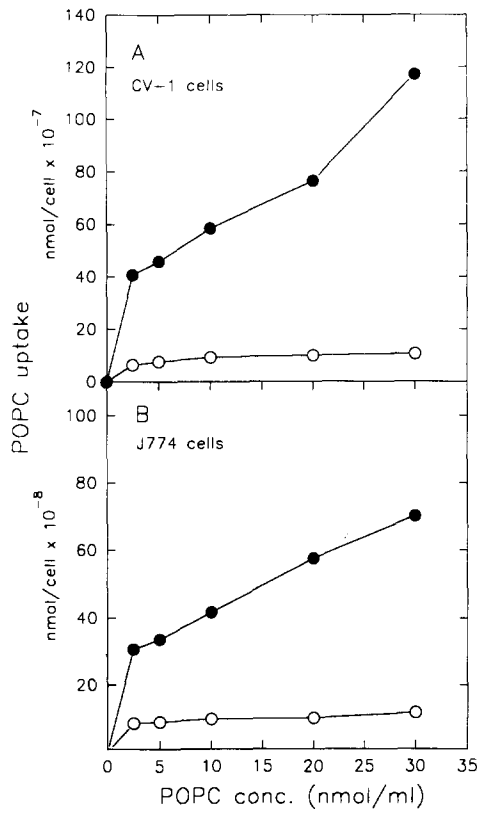

Fig. 5. The concentration-dependent uptake of HPTS-containing liposomes (○) and apoB–liposome conjugates (●) by (A) CV-1 and (B) J774 cells in culture. OG was used as detergent. The amounts of the preparations taken up by cells were calculated from measured values of HPTS fluorescence counts per nmol POPC.

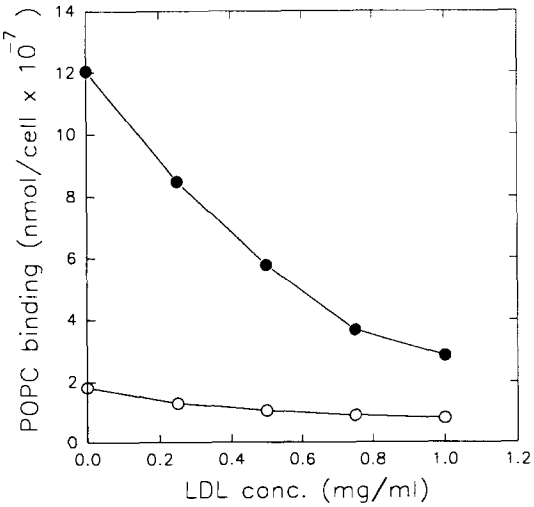

Fig. 6. The ability of native LDL to compete with HPTS-containing liposomes (○) and apo B-liposome conjugates (●) for binding to CV-1 cells in culture. The preparations used were made with OG as detergent. In each sample the final concentration of POPC was 80 nmol/ml and that of LDL as indicated. After incubation for 1 h at 4°C the cells were washed with PBS and the cell-associated fluorescence measured and the corresponding POPC values calculated.

the conjugates the uptake is dependent on the concentration, while the uptake of liposomes was less sensitive to the concentration.

The specificity of the binding of apoB–liposome conjugates to cells was tested by the ability of native LDL to compete with OG conjugates (and liposomes) for the binding to the LDL receptors on CV-1 cells. The addition of LDL to the incubation mixture decreased the binding of conjugates in a concentration-dependent and reproducible way (Fig. 6), demonstrating a competitive binding to the LDL receptor. The specificity of the binding of the conjugates to the cells was further confirmed by displacement experiments with high concentrations of HDL and albumin (1 mg/ml). No significant reduction of conjugate binding was noted. On the other hand, when the incubation was performed in the presence of heparin (3 mg/ml), which is known to displace LDL from the receptor [5], the binding of the apoB liposome conjugates to the cells was abolished. It was also noted that the binding of liposomes to cells was to some degree hindered by LDL (Fig. 6).

Discussion

The LDL receptor pathway has been studied extensively and is known in many details [5]. The use of this pathway to deliver cytotoxic agents to cancer cells has been proposed by several authors [4,19]. In a previous paper, the successful targeting of a lipophilic antineoplastic drug to cancer cells in culture was performed [20]. In the present study the targeting capability of apoB is combined with the capacity of liposomes to encapsulate water-soluble compounds. Drug targeting via the LDL receptor pathway is feasible by means of apoB–liposome conjugates as long as the coupling reaction preserves liposome integrity, as well as the binding properties of apoB to the receptor. Considering the dimensions and complexity of the apoB molecule (apparent molecular mass 550 kDa [21]), the fullfillment of these requirements might seem all but certain. However, the detergent solubilization and removal method proved to work excellent for conjugation of apoB to liposomes. In a fairly short time a stable product was produced with a very good yield. The preparations made by OG solubilization proved to have a good biological activity. The competitive inhibition of the cellular binding of conjugates by native LDL strongly indicates a receptor-mediated uptake. The LDL concentrations needed for displacement of conjugates were higher than those valid for fibroblasts [22], but similar to those obtained with leukemic lymphocytes [23]. The specificity of the binding of apoB–liposome conjugates to CV-1 cells was further confirmed by the lack of competition with HDL and albumin and the displacement by heparin. The experiment with the pH-sensitive

probe HPTS, revealing a cellular uptake to an acid milieu, was also cosistent with a LDL receptor uptake via the endosome-lysosome pathway. It is interesting to note that also the binding of liposomes to some degree was inhibited by LDL. This observation supports the hypothesis that liposomes can enter cells through the coated pit/coated vesicle system [24]. The poor biological activity of the NaC-conjugates is not easily explained and this study offers no answer to this problem.

Special aspects of targeting with apoB are offered by the possibility to chemically modify the protein and thereby change its fate in vivo. The acetylation used in this study leads to modification of the lysine residues of the protein, which results in a more negatively-charged particle [9]. ApoB modified in this way is specifically recognized by the scavenger receptor on macrophages and endothelial cells [7]. The uptake of liposomes by the macrophage cell type J774 was enhanced by conjugation to acetylated apoB. This fact supports the presumption that the conjugates are taken up by the scavenger receptor. Like uptake via the LDL receptor, internalization via the scavenger receptor proceeds through coated vesicles and, finally, degradation in lysosomes [25]. Another possibility to modify apoB is by lactosylation, which induces rapid clearance due to galactose-specific uptake by the liver [7].

The pH-sensitive and membrane-impermeant fluorescence dye HPTS proved to be a very useful tool to study the kinetics of endocytosis. Endocytosis is detected by the large pH-dependent shift in excitation wavelength. As a fluorescence indicator useful for both microscopic and fluorometric analysis, HPTS provides several advantages; good water solubility and photostability, a pK_a value in the physiological range and a high fluorescence quantum yield, and has an isosbestic point at 413 nm, permitting corrections of the measurements to the total amount of dye present in the sample. More detailed descriptions of the properties and use of HPTS have been presented in recent papers [17,18].

The intracellular fate of the conjugates might present a problem. The results of this study shows unequivocally that they end up in acidic compartments like endosomes and lysosomes. As long as a lysosomal route is aimed at this fact is favourable, but often enough this is not the case. However, a special type of liposomes, pH-sensitive liposomes, have been developed to circumvent delivery to the lysosome [26]. The appropriately designed pH-sensitive liposome should transfer its content into the cytoplasm. Such a behaviour is important, e.g., for delivery of DNA to cells, which could be one application of apoB–liposome conjugates.

It can be concluded that apoB- and modified apoB–liposome conjugates obviously have a potential use as effective targeting systems for bioactive agents in vitro. However, their large scale use for drug targeting in vivo might be more problematic. The utility of liposomes for delivery of therapeutic agents was for a long time hampered by the rapid recognition and removal of these carrier particles by cells of the mononuclear phagocytic system (MPS). Recently, however, sterically-stabilized liposomes with long circulation half-lives have been described [27]. Such liposomes contain lipids with special headsgroups such as GM_1, PI, PEG-PE, which contribute to their long blood residence time. Liposomes made up of phosphatidylcholine and cholesterol were considered appropriate for this in-vitro study, but it seems plausible that apoB can be complexed to sterically stabilized liposomes as well. The method for delipidation of apoB applied in this study, involving stabilization of the protein structure by sucrose, was chosen because this procedure preserves the clearance rate of the apoprotein [11]. By the extraction with cold heptane the neutral lipids, but not the phospholipids are removed from LDL [12]. The phospholipids apparently help to stabilize the structure of apoB. The conformation of apoB in LDL is an elongated form that wraps around the LDL particle and interacts with the polar surface with many but short anchoring points [28]. In fact, the surfaces of LDL and liposomes with their surface monolayer of phospholipid and cholesterol offer a similar environment for apoB–lipid interactions. Recent structural studies of apoB have confirmed that it retains its native conformation by recombination with lipid after a mild delipidation [29].

A very important question regarding the feasibility of liposomes as drug carriers is whether they are able to cross the anatomical barriers, such as the capillary wall, which separates the tumor cells from the bloodstream. Targeting of liposomes will be successful only if they are able to exit from the circulation and, thus, gain access to target cells in the extravascular compartments. In this context, the anatomy of the microcirculation can be expected to be of crucial importance. Blood capillaries are classified into three different groups; continous, fenestrated and sinusoidal capillaries. In contrast to the continous and fenestrated capillaries the sinusoidal ones offer relatively large gaps for the liposomes to peneterate the endothelium. A factor, which might favour the access of liposomes to tumors is the increased permeability of tumor vasculature compared to normal tissue [30]. In fact, it seems likely that the ability of some liposome formulations to accumulate in transplantable human tumors, at least in part, is due to increased microvascular permeability [31].

ApoB–liposome conjugates meet many requirements for a good targeted delivery system; all components are biocompatible, biodegradable and nontoxic. LDL/drug complexes, which resemble apoB–liposome

conjugates in many respects, have proven to be effective drug carriers in vitro (for review, see Ref. 19). In recent studies an increased therapeutic effect was obtained through use of LDL as a carrier administered in vivo to both animals [32,33] and humans [34]. These results support the view that also apoB–liposome conjugates may prove to be useful for drug targeting. However, it should be stressed that it is not possible to obtain absolute selectivity, since normal cells also have LDL receptors. This problem can partly be solved by down-regulating the LDL receptors in the liver and the adrenals [35] and, since most antineoplastic drugs in use today are totally untargeted, even partial success would be an appreciable improvement.

References

1 Torchilin, V.P. (1985) CRC Crit. Rev. Ther. Drug Carr. Syst. 2, 65–115.
2 Wright, S. and Huang, L. (1989) Adv. Drug Deliv. Rev. 3, 343–389.
3 Machy, P. and Leserman, L. (1987) Liposomes in Cell Biology and Pharmacology, Editions Inserm, John Libbey Eurotext, London.
4 Shaw, J.M. (ed.) (1991) Lipoproteins as Carriers of Pharmacological Agents, Marcel Dekker, New York.
5 Goldstein, J.L. and Brown, M.S. (1977) Annu. Rev. Biochem. 46, 897–930.
6 Vitols, S., Garthon, G., Öst, Å. and Peterson, C. (1984) Blood 63, 1186–1193.
7 Bijsterbosch, M.K. and Van Berkel, T.J.C. (1990) Adv. Drug Deliv. Rev. 5, 231–251.
8 Lindgren, F.T., Jensen, L.C. and Hatch, F.T. (1972) in Blood Lipids and Lipoproteins: Quantitation, Composition, and Metabolism (Nelson, G.J., ed.), pp. 181–275, Wiley-Interscience, New York.
9 Mahley, R.W., Innerarity, T.L., Weisgraber, K.H. and Oh, S.Y. (1979) J. Clin. Invest. 64, 743–750.
10 Fraker, P.J. and Speck, J.C. (1978) Biochem. Biophys. Res. Commun. 80, 849–857.
11 Masquelier, M., Vitols, S. and Peterson, C. (1986) Cancer Res. 46, 3842–3847.
12 Krieger, M., Brown, M.S., Faust, J.R. and Goldstein, J.L. (1978) J. Biol. Chem. 253, 4093–4101.
13 Bonomo, E.A. and Swaney, J.B. (1988) J. Lipid Res. 29, 380–384.
14 Markwell, M.A.K., Hass, S.M., Bieber, L.L. and Tolbert, N.E. (1978) Anal. Biochem. 87, 206–210.
15 Bartlett, G.R. (1959) J. Biol. Chem. 234, 466–468.
16 Woodle, M.C. and Papahadjopoulos, D. (1989) Methods Enzymol. 171, 193–217.
17 Straubinger, R.M., Papahadjopoulos, D. and Hong, K. (1990) Biochemistry 29, 4929–4939.
18 Daleke, D.L., Hong, K. and Papahajopoulos, D. (1990) Biochim. Biophys. Acta 1024, 352–366.
19 De Smidt, P.C. and Van Berkel T.J.C. (1990) Crit. Rev. Ther. Drug Carr. Syst. 7, 99–120.
20 Lundberg, B. (1987) Cancer Res. 47, 4105–4108.
21 Yang, C.Y., Gu, Z.W., Weng, S.A., Kim, T.W., Chen, S.H., Pownall, H.J., Sharp, P.M., Liu, S.W., Li, W.S., Gotto, A.M. and Chan, L. (1989) Arteriosclerosis 9, 96–108.
22 Weisgraber, K.H., Innerarity, T.L. and Mahley, R.W. (1978) J. Biol. Chem. 253, 9053–9062.
23 Vidal, M., Sainte-Marie, J., Philippot, J.R. and Bienvenue, A. (1985) EMBO J. 4, 2461–2467.
24 Straubinger, R.M., Hong, K., Friend, D.S. and Papahadjopoulos, D. (1983) Cell 32, 1069–1079.
25 Brown, M.S. and Goldstein, J.L. (1983) Annu. Rev. Biochem. 52, 223–261.
26 Woodle, M.C. and Lasic, D.D. (1992) Biochim. Biophys. Acta 1113, 171–199.
27 Chu, C.J., Dijkstra, J., Lai, M.Z., Hong, K. and Szoka, F.C. (1990) Pharm. Res. 7, 824–834.
28 Yang, C.Y., Kim, T.W., Weng, S.A., Lee, B., Yang, M. and Gotto, A.M. (1990) Proc. Natl. Acad. Sci. USA 87, 5523–5527.
29 Singh, S. and Lee, D.M. (1986) Biochim. Biophys. Acta 876, 460–468.
30 Jain, R.K. and Gerlowski, L.E. (1986) Crit. Rev. Oncol. Hematol. 5, 115–170.
31 Gabizon, A. and Papahadjopoulos, D. (1988) Proc. Natl. Acad. Sci. USA 85, 6949–6953.
32 Vitols, S., Söderberg-Reid, K., Masquelier, M., Sjöström, B. and Peterson, C. (1990) Br. J. Cancer 62, 724–729.
33 De Smidt, P.C. and Van Berkel, T.J.C. (1990) Cancer Res. 50, 7476–7482.
34 Filipowska, D., Filipowski, T., Morelowska, B., Kazanowska, W., Laudanski, T., Lapinjoki, S., Åkerlund, M. and Breeze, A. (1992) Cancer Chemother. Pharm. 29, 396–400.
35 Hynds, S.A., Welsh, J., Stewart, J.M., Jack, A., Soukop, M., McArdle, C.S., Calman, K.C., Packard, C.J. and Shepherd, J. (1984) Biochim. Biophys. Acta 795, 589–595.

DEVELOPMENTAL THERAPEUTICS—CLINICAL PHARMACOLOGY AND EXPERIMENTAL THERAPEUTICS

Population pharmacokinetics and exposure-safety relationship of nanoliposomal irinotecan (MM-398, nal-IRI) in patients with solid tumors.

Wen Wee Ma , Ik-Joo Chung , Istvan Lang , Tibor Csőszi ,Miklos Wenczl , Antonio CubilloJen-Shi Chen , Mark Wong ,Joon Oh Park , Jun Suk Kim , Kun-Ming Rau , Bohuslav Melichar , Javier Gallego , Martin Smakal , Jaeyeon Kim , Bruce Belanger , Eliel Bayever , Navreet Dhindsa , Istvan Molnar , Bambang Adiwijaya

Roswell Park Cancer Institute, Buffalo, NY; Department of Hematology-Oncology, Chonnam National University Hwasun Hospital, Hwasun, South Korea; National Institute of Oncology, Budapest, Hungary; JNSZ Megyei Hetényi Géza Kórház-Rendelőintézet, Szolnok, Hungary; Markusovszky Korhaz, Budapest, Hungary; Centro Integral Oncológico Clara Campal, Madrid, Spain; Chang Gung Memorial Hospital, Taipei, Taiwan; Westmead Hospital, Westmead, Australia; Samsung Medical Center, Sungkyunkwan University School of Medicine, Seoul, South Korea; Korea University Guro Hospital, Seoul, South Korea; Chang Gung Memorial Hospital Kaohsiung Branch, Kaohsiung, Taiwan; Onkologicka Klinika, Lekarska Fakulta Univerzity Palackeho a Fakultni Nemocnice, Olomouc, Czech Republic; Hospital General de Elche, Elche, Spain; Institut Onkologie a Rehabilitace na Plesi s.r.o., Nova Ves Pod Plesi, Czech Republic; Merrimack Pharmaceuticals, Inc., Cambridge, MA; Merrimack Pharmaceuticals, Inc., Boston, MA; Merrimack Pharmaceuticals, Inc., Cambridege, MA

Show Less

Abstract Disclosures

Abstract

e13588

Background: MM-398 is a nanoliposomal irinotecan (nal-IRI). This study characterized the population PK and exposure–response with MM-398 in patients with solid tumors. **Methods:**Population PK analysis was performed for total irinotecan (IRI) and its active metabolite SN-38 in 353 patients administered MM-398 60-120 mg/m^{2}in 6 studies. Covariates include body size (BSA), hepatic and renal functions (UGT1A1*28 7/7, bilirubin, liver metastasis, AST, ALT, albumin, CrCl), demographics (sex, race, age), and external factors (co-treatment with 5-FU, manufacturing site). Exposure-safety (neutropenia, diarrhea, and anemia) relationships were evaluated from 6 studies. Predictions of incidence rates of AEs were obtained from exposure-safety and predicted exposure with a dose of 80mg/m^2. **Results:**Population PK of IRI was described as a 2-compartmental model, and SN-38 as a 1-compartmental model. Significant

covariates to IRI were race and BSA; covariates to SN-38 were baseline bilirubin and BSA. No other covariates were significant; association with UGT1A1*28 was not significant. Compared to 120 mg/m^2 q3w, MM398 80 mg/m^2 q2w had similar average (C_{avg}), and 1.5-fold lower C_{max} for both IRI and SN-38. SN-38 C_{max} was associated with incidence of G ≥ 3 neutropenia and anemia, and IRI C_{max} was associated with incidence of G ≥ 3 diarrhea. Compared to Caucasians, Asians had 0.5-fold lower IRI C_{max}, corresponding to 5% lower predicted G ≥ 3 diarrhea. In contrast, Asians had 1.5-fold higher SN-38 C_{max} than Caucasians, corresponding to 7% higher predicted G ≥ 3 neutropenia. Compared to patients with bilirubin < 1 mg/dL, patients with bilirubin 1-2 mg/dL had 1.4-fold higher SN-38. **Conclusions:** MM-398 at a lower dose, given more frequently, was predicted to have similar C_{avg} and lower C_{max}. IRI C_{max} was associated with diarrhea and SN-38 C_{max} was associated with neutropenia and anemia. Asians had lower IRI levels, but higher SN-38. Increasing baseline bilirubin was associated with higher SN-38 levels. Clinical trial information: NCT01494506.

British Journal of Cancer (2006) 94, 1287–1292

www.bjcancer.com

clinical studies

A phase II study of FOLFIRI-3 (double infusion of irinotecan combined with LV5FU) after FOLFOX in advanced colorectal cancer patients

M Mabro*[,1], P Artru[2], T André[3], M Flesch[4], F Maindrault-Goebel[5], B Landi[6], G Liedo[2], A Plantade[1], C Louvet[5] and A de Gramont[5] on behalf of GERCOR

[1]Department of Medical Oncology, Hôpital Foch, 40 rue Worth, 92151 Suresnes Cedex, France; [2]Department of Medical Oncology, Clinique Saint-Jean, Lyon, France; [3]Department of Medical Oncology, Hôpital Tenon, Paris, France; [4]Department of Medicine, Hôpital de Dijon, Dijon, France; [5]Department of Medical Oncology, Hôpital Saint-Antoine, Paris, France; [6]Department of Medical Oncology, Hôpital Européen Georges Pompidou, Paris, France

In advanced colorectal cancer previously treated with oxaliplatin, efficacy of irinotecan-based chemotherapy is poor and the best regimen is not defined. We designed FOLFIRI-3 and conducted a phase II study to establish its efficacy and safety in advanced colorectal cancer patients previously treated with FOLFOX. FOLFIRI-3 consisted of irinotecan 100 mg m^{-2} as a 60-min infusion on day 1, running concurrently with leucovorin 200 mg m^{-2} as a 2-h infusion on day 1, followed by 46-h continuous infusion of 5-fluorouracil (5FU) 2000 mg m^{-2}, and irinotecan 100 mg m^{-2} repeated on day 3, at the end of the 5FU infusion, every 2 weeks. Sixty-five patients entered the study. The intent-to-treat objective response rate was 23% (95% CI 13–33%). Disease was stable in 37% of patients, progressed in 26% and was not assessable in 14%. From the start of FOLFIRI-3, median progression-free survival was 4.7 months and median survival 10.5 months. Main toxicities (% of patients) were grade 3–4 diarrhoea 23% and grade 4 neutropenia 11%. FOLFIRI-3 is a promising regimen achieving high response rate and progression-free survival in patients previously treated with FOLFOX with a moderate toxicity.

British Journal of Cancer (2006) **94**, 1287–1292. doi:10.1038/sj.bjc.6603095 www.bjcancer.com
Published online 11 April 2006

Keywords: colorectal cancer; combination chemotherapy; irinotecan; 5-fluorouracil; leucovorin; phase II study

Colorectal cancer is the one of the commonest cancers worldwide and remains a leading cause of mortality. For many years the main treatment for metastatic colorectal cancer consisted of 5-fluorouracil (5FU) modulated by leucovorin (LV). Since 1990, tremendous progresses have been made through the availability of several new drugs, such as oxaliplatin and irinotecan (Cunningham *et al*, 1998; Rougier *et al*, 1998; De Gramont *et al*, 2000; Douillard *et al*, 2000; Saltz *et al*, 2000; Grothey *et al*, 2002; Goldberg *et al*, 2004).

Irinotecan has definite activity against advanced metastatic colorectal cancer both in chemotherapy-naive patients and after 5FU failure (Cunningham *et al*, 1998; Rougier *et al*, 1998; Douillard *et al*, 2000; Saltz *et al*, 2000). Two randomised studies in patients with 5FU bolus-resistant metastatic colorectal cancer established the superiority of irinotecan over best supportive care (Cunningham *et al*, 1998) or 5FU continuous-infusion regimens (Rougier *et al*, 1998). Later, two large multicentre randomised studies established the superiority of irinotecan combined with 5FU and LV over 5FU–LV as first-line treatment of metastatic colorectal cancer (Douillard *et al*, 2000; Saltz *et al*, 2000). Two additional randomised studies demonstrated the superiority of oxaliplatin combined with LV5FU2 (FOLFOX4) over 5FU and LV as front therapy (De Gramont *et al*, 2000; Grothey *et al*, 2002). More recently, in a large phase III study, FOLFOX4 achieved better response rate, progression-free survival and overall survival than the irinotecan-based IFL regimen as first-line treatment of metastatic colorectal cancer (Goldberg *et al*, 2004). However, few data are available about irinotecan-based chemotherapy in patients previously treated with FOLFOX. Thus, the FOLFIRI regimen achieved a 5% response rate in pretreated patients (André *et al*, 1999; Tournigand *et al*, 2004).

In vitro studies suggested that the synergy between irinotecan and 5FU is sequence dependent, with a higher cytotoxicity when irinotecan is administered before 5FU (Guichard *et al*, 1997; Mullany *et al*, 1998; Mans *et al*, 1999). Clinical data are less documented. In a phase II randomised study evaluating the sequence effect of irinotecan and 5FU, toxicities were affected by the sequence of administration, with a worsened tolerability when 5FU was followed by irinotecan (Falcone *et al*, 2001). These results suggested that cytotoxicity is higher when irinotecan is administered after 5FU (Falcone *et al*, 2001). Thus, we previously designed the FOLFIRI-2 regimen consisting of irinotecan 180 mg m^{-2} combined with a simplified LV5FU regimen, with irinotecan administered at the end of the 5FU infusion (Mabro *et al*, 2003). In this phase II study of patients with heavily pretreated colorectal cancer, efficacy was encouraging, with a 17% confirmed response rate and 4.1 months progression-free survival, but toxicity was high.

*Correspondence: Dr M Mabro; E-mail: m.mabro@hopital-foch.org
Received 9 November 2005; revised 13 March 2006; accepted 13 March 2006; published online 11 April 2006

Thus, irinotecan-based chemotherapy after FOLFOX needs to be improved and the best schedule is not yet established. We designed a new regimen, FOLFIRI-3, in which irinotecan is administered as two infusions: half-dose before 5FU and half-dose at the end of the 5FU infusion, and conducted this multicentre phase II study to evaluate the efficacy of the FOLFIRI-3 regimen in advanced colorectal cancer patients previously treated with FOLFOX regimen.

PATIENTS AND METHODS

This study was an open multicentre phase II study conducted from June 2001 to December 2002. The study fulfilled the Clinical Good Practice Guidelines and was approved by the Ethics Committee of La Pitié – Salpêtrière Hospital, Paris, France. Written informed consent was obtained from all patients prior to study entry.

The main end point of the study was progression-free survival. The other study parameters were: response rate, overall survival and toxicity.

Inclusion criteria

Patients were required to be 18–80 years old, and to have metastatic adenocarcinoma of the colon or the rectum histologically proven and previously treated with a FOLFOX regimen. An interval of at least 2 weeks must have elapsed since prior treatment. Other eligibility criteria were: no central nervous system metastases, WHO performance status 0–2, initial evaluation $\leqslant 2$ weeks before inclusion by computed tomography scan prior to initiation of therapy and feasibility of regular follow-up. Required laboratory parameters included: neutrophil count $\geqslant 1500\,\mu l^{-1}$, platelet count $\geqslant 100\,000\,\mu l^{-1}$, serum alkaline phosphatase < 3 times the upper limit of normal (ULN) and bilirubin < 1.5 times ULN.

Treatment administration

FOLFIRI-3 regimen was given every 14 days as follows: on day 1, irinotecan 100 mg m^{-2} as a 1-h infusion, running concurrently with LV 200 mg m^{-2} as a 2-h infusion via a Y-connector, followed by 5FU 2000 mg m^{-2} as a 46-h infusion using a disposable elastomeric pump. On day 3, irinotecan 100 mg m^{-2} as a 1-h infusion was repeated, at the end of the 5FU infusion (Figure 1). In the absence of grade 2 toxicity after two cycles, the dose of irinotecan was to be increased from 100 to 120 mg m^{-2} at days 1 and 3. Treatment was continued until disease progression or limiting toxicity.

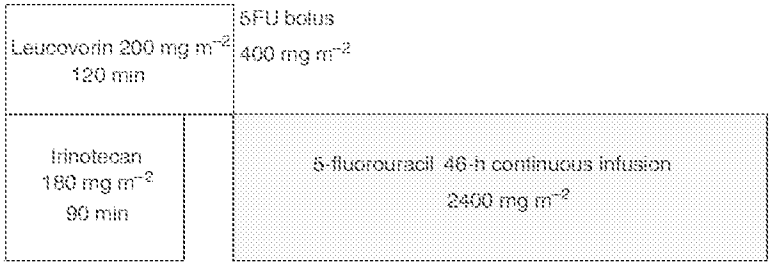

FOLFIRI: Irinotecan day 1 followed by bolus 5FU and 46-h continuous 5FU.

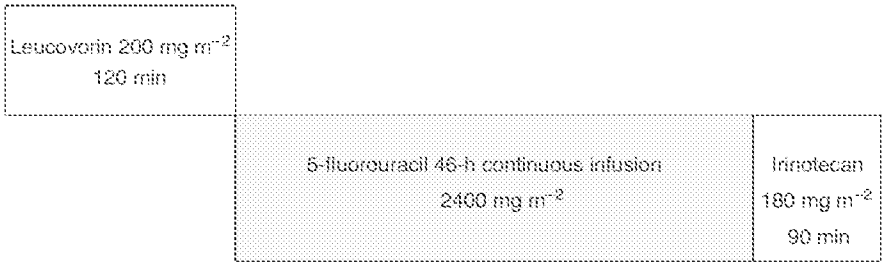

FOLFIRI-2: Irinotecan on day 3 at the end of 5FU infusion, plus hydroxyurea given the day before, day 1 and day 2 of each cycle.

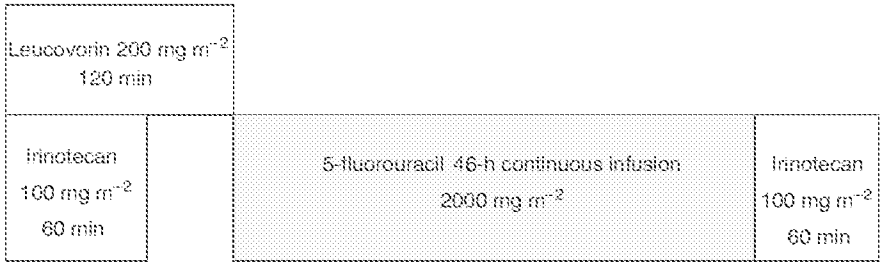

FOLFIRI-3: Double infusion of irinotecan before (day 1) and at the end of 5FU infusion (day 3).

Figure 1 Design of FOLFIRI (André *et al*, 1999), FOLFIRI-2 (Mabro *et al*, 2003) and FOLFIRI-3 regimens; cycles are repeated every 2 weeks.

Blood tests and clinical evaluation were performed every 2 weeks, prior to treatment. Chemotherapy could be administered if neutrophil count was $\geqslant 1500\,\mu l^{-1}$, platelet count $\geqslant 100\,000\,\mu l^{-1}$ and if clinical toxicity was resolved or $<$ grade 2. In case of grade >2 neutropenia, thrombocytopenia or diarrhoea toxicity, the dose of irinotecan was to be reduced from 100 to 80 mg m^{-2}. If neutropenia, thrombocytopenia or diarrhoea $>$ grade 2 persisted at this latter dose, chemotherapy was discontinued.

Supportive care

Specific anti-emetic prophylaxis was left to the investigator's discretion. For patients who experienced an early cholinergic syndrome occurring during or shortly after irinotecan administration, atropine sulphate (0.25 mg) could be given subcutaneously. The use of loperamide was recommended in case of diarrhoea.

Study parameters

Before each cycle, patients underwent a clinical examination, and blood cells were counted. All toxicities were reported according to the National Cancer Institute-Common Toxicity Criteria (NCI-CTC) (MacDonald *et al*, 1995). Carcinoembryogenic antigen, bilirubin, serum alkaline phosphatases, serum creatinine, lactate dehydrogenase, chest X-ray and CT scans were repeated every 8 weeks (i.e. every four cycles) or earlier in the case of worsening of clinical condition. Tumour response was assessed by RECIST criteria (Therasse *et al*, 2000). Tumour growth control was defined by the proportion of patients with response rate or stable disease.

Statistical considerations

Based on previous studies, we expected FOLFIRI-3 to achieve a 40% rate of nonprogressive patients at 6 months. According to a binomial distribution point estimate of proportion, with 5% significance and 80% power, 65 patients were to be enrolled. Survival times were calculated from the start of FOLFIRI-3 until death. Time to progression was calculated from the first day of FOLFIRI-3 to the date of progression for all the patients entering the study. Survival curves were obtained using the Kaplan–Meier method (Kaplan and Meier, 1958).

RESULTS

From 17 June 2001 to 19 December 2002, 65 patients were recruited from nine French institutions. Their characteristics are described in Table 1. All patients had previously been treated with a FOLFOX regimen (combination of oxaliplatin, infusion 5FU and LV), and had experienced disease progression while on FOLFOX (36 patients) or after discontinuation (29 patients). Thirteen patients (20%) had previously been treated with at least two regimens for metastatic purpose before entering the FOLFIRI-3 study.

Treatment

The median number of treatment cycles administered was 7 (range, 1–20). Six patients (9%) refused to continue after the first or the second course (personal convenience without toxicity $>$ grade 2). In six patients (9%) treatment was stopped because of grade 3 or 4 toxicity. Tumour response was not assessable in nine of those 12 patients. In 39 patients (60%) treatment was stopped because of disease progression after a median of eight courses. In 14 additional patients (21%) chemotherapy was interrupted by investigator after 8–20 cycles, without evidence of disease progression nor severe toxicity.

Dose reductions occurred in 25 patients due to grade 3 toxicities, mainly vomiting, diarrhoea or mucositis. Irinotecan dose was increased according to the design of the study only in 12 patients with a median dose level of 120 mg m^{-2} on days 1 and 3. Grade 3 toxicity occurred only in one of these patients.

Table 1 Patient characteristics ($n = 65$)

	N	%
Median age: 60 years (range: 30–79)		
Gender		
Male	32	49
Female	33	51
WHO performance status		
0	32	49
1	22	34
2	11	17
Primary tumour		
Colon	49	75
Rectum	16	25
Site of metastases		
Liver	52	80
Lung	23	35
Peritoneum	9	14
Nodes	11	17
Other	6	9
Involved sites		
1	36	55
2	23	35
>2	6	9
Prior adjuvant chemotherapy	13	20
LVSFU	11	17
FOLFOX	2	3
Number of lines for metastatic purpose received before FOLFIRI-3		
1 line only	52	80
2 lines or more	13	20
FOLFOX regimen received before FOLFIRI-3		
FOLFOX7	27	42
FOLFOX6	13	20
FOLFOX4	25	38

Safety

Side effects were collected for 463 cycles according to the NCI-CTC grade scale. Toxicities are listed in Table 2. Neutropenia reached grade 3/4 in 37% of patients, including three patients (5%) who had one episode of febrile neutropenia. There was one toxic death after the first course of chemotherapy related to a sepsis shock with neutropenia and diarrhoea. Overall, 10 patients (15%) experienced at least one grade 4 toxicity and 20 patients (31%) experienced one grade 3 nonhematological toxicity.

Survival and objective response

Progression free survival for 6 months was 42%. From the start of FOLFIRI-3, median progression-free survival was 20.5 weeks (4.7 months) and median survival was 46 weeks (10.5 months). Survival curves are shown in Figure 2.

Tumour response was assessable in 56 patients and not assessable in nine patients (14%). Response rates were calculated in the intent-to-treat population. Objective response was obtained in 15 patients (1 complete, 14 partial), achieving a 23% (95% CI 13–33%) response rate (15 out of 65). The number of responder

Table 2 Toxicity of FOLFIRI-3 according to NCI-CTC grading (maximal grade per patient, collected from 463 cycles, 65 patients)

	NCI-CTC grade (% of patients)			
	1	2	3	4
Nonhaematological toxicities				
Nausea	28	29	9	0
Vomiting	12	19	8	0
Mucositis	20	19	5	2
Diarrhoea	25	33	22	1
Asthenia	28	20	11	3
Hand–foot syndrome	23	2	0	—
Alopecia	23	54	—	—
Haematological toxicities				
Neutropenia	14	28	26	11
Febrile neutropenia	—	—	2	3
Anaemia	54	26	2	2
Thrombocytopenia	34	5	3	0

NCI-CTC, National Cancer Institute-Common Toxicity Criteria.

Table 3 RECIST number of the responder patients

Patient no.	Response	RECIST at baseline	RECIST at first evaluation	RECIST at second evaluation
103	PR	38	18	20
105	PR	10	6	3
108	PR	275	230	175
112	PR	114	45	50
113	PR	102	81	25
202	PR	90	90	65
212	PR	78	48	55
265	PR	20	10	10
301	PR	74	48	91
306	PR	80	70	44
308	PR	180	160	118
501	PR	100	90	70
505	PR	50	21	19
803	PR	131	90	78
404	CR	85	55	0

RECIST, Response Evaluation Criteria in Solid Tumors.

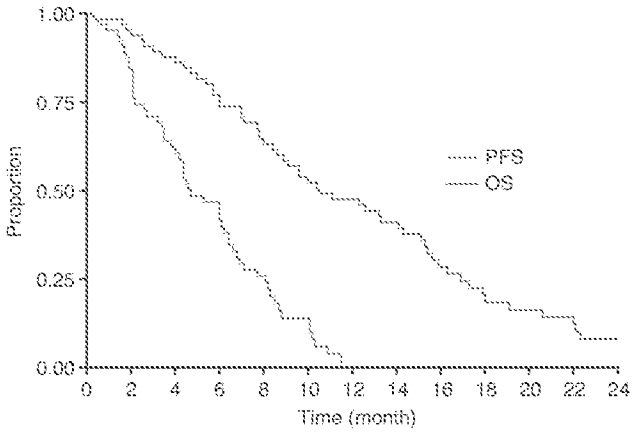

Figure 2 Progression-free survival and overall survival in the FOLFIRI-3 study (65 patients).

patients assessed by RECIST criteria are listed in Table 3. Disease was stable in 24 patients (37%) and progressed in 17 (26%). Tumour growth control was 60% (95% CI 48–72%).

Regarding assessable patients, response rate was 27% (95% CI 15–39%), and 22% in the subset of patients in whom disease progressed while on previous FOLFOX regimen, and 33% in the subset of patients in whom disease progressed after FOLFOX discontinuation.

DISCUSSION

This multicentre phase II study assessed the efficacy and tolerability of the FOLFIRI-3 regimen, a new combination of irinotecan and LV5FU, in patients with metastatic colorectal cancer previously treated with FOLFOX. With 42% of patients free of progression at 6 months, the main objective of the study was reached.

Several phase II studies (Pitot *et al*, 1997; Rougier *et al*, 1997; Rothenberg *et al*, 1999; Van Cutsem *et al*, 1999) and two large phase III studies (Cunningham *et al*, 1998; Rougier *et al*, 1998) established the efficacy of irinotecan after 5FU failure (Table 4). In phase II studies of irinotecan alone, after 5FU failure response rates were 11–16% (Rougier *et al*, 1997; Rothenberg *et al*, 1999; Van Cutsem *et al*, 1999), and progression-free survival was 3–4 months (Pitot *et al*, 1997; Rougier *et al*, 1997; Rothenberg *et al*, 1999; Van Cutsem *et al*, 1999). In phase III studies of irinotecan after 5FU failure, progression-free survival was 3–4 months (Cunningham *et al*, 1998; Rougier *et al*, 1998; Fuchs *et al*, 2003). Response rate was reported in only one of those studies and was 4.5% (Rougier *et al*, 1998).

The combination of irinotecan with 5FU and LV after 5FU failure was evaluated in three phase II studies. Reported response rates were 11.4–21% (Ducreux *et al*, 1999; Gil-Delgado *et al*, 2001; Rougier *et al*, 2002). As shown in Table 4, results observed with regimens combining irinotecan, 5FU and LV after 5FU failure seem slightly better than those with irinotecan alone, in a cross-study comparison. More recently, a large randomised phase III study was conducted enrolling more than 2000 patients. In this study, the addition of irinotecan to 5FU after 5FU failure achieved better survival (14.8 *vs* 13.9 months from the start of front-line 5FU) and higher response rate (21 *vs* 11%) than irinotecan alone after 5FU failure (Seymour *et al*, 2005). These results encourage the administration of 5FU with irinotecan despite previous 5FU failure.

Efficacy of irinotecan in patients previously treated with FOLFOX is less documented. Results of the FOLFIRI, FOLFIRI-2 and FOLFIRI-3 studies are summarised in Table 4. In a randomised trial recently reported, irinotecan alone achieved a 4% response rate and 2.7 progression-free survival in 94 patients previously treated with 5FU as front line and FOLFOX4 as second line (Rowland *et al*, 2005).

In the present study, the progression-free survival was 4.7 months and the intent-to-treat response rate was 23%, higher than those reported with irinotecan alone, FOLFIRI and FOLFIRI-2 after FOLFOX. In a cross-study comparison, efficacy of FOLFIRI-3 seems slightly better than FOLFIRI-2, as FOLFIRI-2 showed a high toxicity profile. The main FOLFIRI-2 grade 3–4 toxicities were diarrhoea (31%), neutropenia (52%), and febrile neutropenia (14%) (Mabro *et al*, 2003). Toxicity of FOLFIRI-3 was moderate, lower than FOLFIRI-2 study and quite higher than FOLFIRI in pretreated patients (André *et al*, 1999). It is difficult to assess if this increased toxicity is related to the divided dose of irinotecan or to the total dose of irinotecan, which is 10% more than in the FOLFIRI (200 instead of 180 mg m^{-2} per cycle). Differences should be also partly due to the subset of patients. In particular, patients

Table 4 Results of main published phase II and III studies of irinotecan in previously treated patients with metastatic colorectal cancer

Reference	Study phase	N	Response rate (%)	Progression-free survival (months)
Irinotecan alone after 5FU				
Van Cutsem *et al*, 1999	II	107	13.7	4
Pitot *et al*, 1997	II	90	12.3	----
Rothenberg *et al*, 1999	II	166	11	----
Rougier *et al*, 1997	II	140	16	----
Cunningham *et al*, 1998	III	189	----	----
Rougier *et al*, 1998	III	133	5	4.2
Fuchs *et al*, 2003	III	291	----	3.5
Irinotecan combined with LV5FU after 5FU				
Ducreux *et al*, 1999	II	55	22	6.3
Gil-Delgado *et al*, 2001	II	39	21	----
Rougier *et al*, 2002	Randomised phase II	101	11.4	----
Irinotecan combined with LV5FU after FOLFOX				
André *et al*, 1999	II	33	5.5	4.1
Tournigand *et al*, 2004	III	66	4	2.5
Mabro *et al*, 2003	II	29	17	4
Maindrault *et al*, 2002	II	20	20	6.7
FOLFIRI-3	II	65	23	4.7

of the FOLFIRI-3 study were less selected and 17% entered the study with a PS 2.

In conclusion, FOLFIRI-3 is a feasible regimen with encouraging response rate and progression-free survival in patients previously treated with FOLFOX. Future studies should evaluate the combination of FOLFIRI-3 with molecular targeted therapies like bevacizumab, cetuximab or new oral anti-REGF molecules.

REFERENCES

André T, Louvet C, Maindrault-Goebel F, Couteau C, Mabro M, Lotz JP, Gilles-Amar V, Krulik M, Carola E, Izrael V, de Gramont A (1999) CPT-11 (irinotecan) addition to bimonthly, high-dose leucovorin and continuous-infusion 5-fluorouracil (FOLFIRI) for pretreated metastatic colorectal cancer. *Eur J Cancer* **35:** 1343–1347

Cunningham D, Pyrhönen S, James RD, Punt CJ, Hickish TF, Heikkila R, Johannesen TB, Starkhammar H, Topham CA, Awad L, Jacques C, Herait P (1998) Randomised trial of irinotecan plus supportive care *vs* supportive care alone after fluorouracil failure for patients with metastatic colorectal cancer. *Lancet* **352:** 1413–1418

de Gramont A, Figer A, Seymour M, Homerin M, Hmissi A, Cassidy J, Boni C, Cortes-Funes H, Cervantes A, Freyer G, Papamichael D, Le Bail N, Louvet C, Hendler D, de Braud F, Wilson C, Morvan F, Bonetti A (2000) Leucovorin and fluorouracil with or without oxaliplatin as first-line treatment in advanced colorectal cancer. *J Clin Oncol* **18:** 2938–2947

Douillard JY, Cunningham D, Roth AD, Navarro M, James RD, Karasek P, Jandik P, Iveson T, Carmichael J, Alakl M, Gruia G, Awad L, Rougier P (2000) Irinotecan combined with fluorouracil compared with fluorouracil alone as first-line treatment for metastatic colorectal cancer: a multicentre randomised trial. *Lancet* **355:** 1041–1047

Ducreux M, Ychou M, Seitz JF, Bonnay M, Bexon A, Armand JP, Mahjoubi M, Mery-Mignard D, Rougier P (1999) Irinotecan combined with bolus fluorouracil, continuous infusion fluorouracil, and high-dose leucovorin every two weeks (LV5FU2 regimen): a clinical dose finding and pharmacokinetic study in patients with pretreated metastatic colorectal cancer. *J Clin Oncol* **17:** 2901–2908

Falcone A, di Paolo A, Masi G, Allegrini G, Danesi R, Lencioni M, Pfanner E, Cornis S, Del Tacca M, Conte P (2001) Sequence effect of irinotecan on pharmacokinetics and toxicity in chemotherapy-naive metastatic colorectal cancer patients. *J Clin Oncol* **19:** 3456–3462

Fuchs CS, Moore MR, Harker G, Villa L, Rinaldi D, Hecht J (2003) Phase III comparison of two irinotecan dosing regimens in second-line therapy of metastatic colorectal cancer. *J Clin Oncol* **21:** 807–814

Gil-Delgado MA, Guinet F, Castaing D, Adam R, Goeffic D, Durrani AK, Bismuth H, Khayat D (2001) Prospective phase II trial of irinotecan, 5-fluorouacil, and leucovorin in combination as salvage therapy for advanced colorectal cancer. *Am J Clin Oncol* **24:** 101–105

Goldberg RM, Sargent DJ, Morton RF, Fuchs CS, Ramanathan RK, Williamson SK, Findlay BP, Pitot HC, Alberts SR (2004) A randomised controlled trial of fluorouracil plus leucovorin, irinotecan, and oxaliplatin combinations in patients with previously untreated metastatic colorectal cancer. *J Clin Oncol* **22:** 4–6

Grothey A, Deschler B, Kroening H, Bidwelski K, Reichardt P, Kretzschmar A, Clemens M, Hirschmann W, Lorenz M, Asperger W, Buechele T, Schmoll HJ (2002) Phase III study of bolus 5-fluorouracil (5FU)/folinic acid (FA) (Mayo) *vs* weekly high-dose 24 h 5-FU infusion/FA+oxaliplatin (OXA) in advanced colorectal cancer (ACRC). *Proc Am Soc Clin Oncol (Orlando, FL, USA)* **21:** 129a (abstract)

Guichard S, Cussac D, Hennebelle I, Bugat R, Canal P (1997) Sequence-dependent activity of the irinotecan-5FU combination in human colon-cancer model HT-29 *in vitro* and *in vivo*. *Int J Cancer* **73:** 729–734

Kaplan EL, Meier P (1958) Nonparametric estimation from incomplete observations. *J Am Stat Assoc* **53:** 457–481

Mabro M, Louvet C, André T, Carola E, Gilles-Amar V, Artru P, Krulik M, de Gramont A, on behalf GERCOR (2003) Bimonthly leucovorin, infusion, 5-fluorouracil, hydroxyurea, and irinotecan (FOLFIRI-2) for pretreated metastatic colorectal cancer. *Am J Clin Oncol* **25:** 254–258

MacDonald J, Haller D, Mayer R (1995) Grading of toxicity. In: *Manual of Oncologic Therapeutics*, MacDonald J, Haller D, Mayer R (eds) pp 519–523. Lippincott: Philadelphia

Maindrault F, Louvet C, Tournigand C, Gervais H, Mabro M, Artru P, Garcia ML, André T, Carola C, de Gramont A (2002) Leucovorin, 5-fluorouracil infusion and irinotecan (FOLFIRI-3) in pretreated patients with metastatic colorectal cancer. *Proc Am Soc Clin Oncol (Orlando, FL, USA)* **21:** 658a (abstract)

Mans DRA, Grivicich I, Peters GJ, Schwartsmann G (1999) Sequence-dependent growth inhibition and DNA damage by the irinotecan–5-fluorouracil combination in human colon carcinoma cell lines. *Eur J Cancer* **35:** 1851–1861

Mullany S, Svingen PA, Kaufmann SH, Erlichman C (1998) Effect of adding the topoisomerase I poison 7-ethyl 10-hydroxycamptothecin (SN 38) to 5-fluorouracil and folinic acid in HCT8 cells: elevated dTTP pools and enhanced cytotoxicity. *Cancer Chemother Pharm* **42:** 391–399

Pitot HC, Wender DB, O'Connell MJ, Schroeder G, Goldberg RM, Rubin J, Mailliard JA, Knost JA, Ghosh C, Kirschling RJ, Levitt R, Windschitl HE (1997) Phase II trial of irinotecan in patients with metastatic colorectal carcinoma. *J Clin Oncol* **15:** 2910–2919

Rothenberg ML, Cox JV, DeVore RF, Hainsworth JD, Pazdur R, Rivkin SE, Macdonald JS, Geyer Jr CE, Sandbach J, Wolf DL, Mohrland JS, Elfring GL, Miller LL, Von Hoff DD (1999) A multicenter, phase II trial of weekly irinotecan (CPT-11) in patients with previously treated colorectal carcinoma. *Cancer* **85:** 786–795

Rougier P, Bugat R, Douillard JY, Culine S, Suc E, Brunet P, Becouarn Y, Ychou M, Marty M, Extra JM, Bonneterre J, Adenis A, Seitz JF, Ganem G, Namer M, Conroy T, Negrier S, Merrouche Y, Burki F, Mousseau M, Herait P, Mahjoubi M (1997) Phase II study of irinotecan in the treatment of advanced colorectal cancer in chemotherapy naive patients and patients pretreated with fluorouracil based chemotherapy. *J Clin Oncol* **15:** 251–260

Rougier P, Lepille D, Bennouna J, Marre A, Ducreux M, Mignot L, Hua A, Mery-Mignard D (2002) Antitumour activity of three second-line treatment combinations in patients with metastatic colorectal cancer after optimal 5-FU regimen failure: a randomised, multicentre phase II study. *Ann Oncol* **13:** 1558–1567

Rougier P, Van Cutsem E, Bajetta E, Niederle N, Possinger K, Labianca R, Navarro M, Morant R, Bleiberg H, Wils J, Awad L, Herait P, Jacques C (1998) Randomised trial of irinotecan *vs* fluorouracil by continuous infusion after fluorouracil failure in patients with metastatic colorectal cancer. *Lancet* **352:** 1407–1412

Rowland KM, Pitot HC, Sargent DJ, Philip PA, Mitchell EP, Mailliard JA, Goldberg RM, Alberts SR (2005) Results of third line therapy on N9841: a randomized phase III trial of oxaliplatin/5-fluorouracil/leucovorin (FOLFOX4) *vs* irinotecan (CPT-11) in patients with advanced colorectal cancer previously treated with prior 5FU chemotherapy. *Proc Am Soc Clin Oncol (Orlando, FL, USA)* **24:** 3519a (abstract)

Saltz LB, Cox JV, Blanke C, Rosen LS, Fehrenbacher L, Moore MJ, Maroun JA, Ackland SP, Locker PK, Pirotta N, Elfring GL, Miller LL (2000) Irinotecan plus fluorouracil and leucovorin for metastatic colorectal cancer. Irinotecan study group. *N Engl J Med* **343:** 905–914

Seymour MT, for the UK NCRI Colorectal Clinical Studies Group and FOCUS Trial Investigators (2005) Fluorouracil, oxaliplatin and CPT-11 (irinotecan), use and sequencing (MRC FOCUS): a 2135-patient randomized trial in advanced colorectal cancer (ACRC). *Proc Am Soc Clin Oncol (Orlando, FL, USA)* **24:** 3518a (abstract)

Therasse P, Arbuck SG, Eisenhauer EA, Wanders J, Kaplan RS, Rubinstein L, Verweij J, Van Glabbeke M, van Oosterom AT, Christian MC, Gwyther SG (2000) New guidelines to establish response to treatment in solid tumors. *J Nat Cancer Inst* **92:** 205–216

Tournigand C, André T, Achille E, Lledo G, Flesh M, Mery-Mignard D, Quinaux E, Couteau C, Buyse M, Ganem G, Landi B, Colin P, Louvet C, de Gramont A (2004) FOLFIRI followed by FOLFOX6 or the reverse sequence in advanced colorectal cancer: a randomized GERCOR study. *J Clin Oncol* **22:** 229–237

Van Cutsem E, Cunningham D, Ten Bokkel Huinink WW, Punt CJ, Alexopoulos CG, Dirix L, Symann M, Blijham GH, Cholet P, Fillet G, Van Groeningen C, Vannetzel JM, Levi F, Panagos G, Unger C, Wils J, Cote C, Blanc C, Herait P, Bleiberg H (1999) Clinical activity and benefit of irinotecan (CPT-11) in patients with colorectal cancer truly resistant to 5-fluorouracil (5-FU). *Eur J Cancer* **35:** 54–59

Am J Clin Oncol (CCT) 26(3): 254–258, 2003

Bimonthly Leucovorin, Infusion 5-Fluorouracil, Hydroxyurea, and Irinotecan (FOLFIRI-2) for Pretreated Metastatic Colorectal Cancer

May Mabro, M.D., Christophe Louvet, M.D., Thierry André, M.D., Elisabeth Carola, M.D., Véronique Gilles-Amar, M.D., Pascal Artru, M.D., Marcel Krulik, M.D., Ph.D., and Aimery de Gramont, M.D., Ph.D., on behalf of GERCOR

Irinotecan has shown activity in advanced colorectal cancer resistant to leucovorin and fluorouracil. Preclinical experiments on cell cultures and human tumor xenografts indicated potential synergy when combining irinotecan and fluorouracil. We designed a new regimen combining leucovorin, fluorouracil, irinotecan, and hydroxyurea (FOLFIRI-2) and conducted a phase II study to establish its efficacy and tolerance in advanced colorectal cancer refractory to fluorouracil and oxaliplatin. Treatment was repeated every 2 weeks and consisted of leucovorin 400 mg/m^2 on day 1, immediately followed by 46 hours of continuous infusion of fluorouracil 2,000 mg/m^2, irinotecan 180 mg/m^2 on day 3, and hydroxyurea 1,500 mg the day before leucovorin, and on days 1 and 2. Treatment was continued until progression or limiting toxicity. Twenty-nine heavily pretreated patients entered the study. Five patients achieved an objective response (17%), and 12 obtained stabilization of disease or minor response (52%). Five patients failed to continue treatment (17%) because of toxicity or worsening condition. From the start of FOLFIRI-2 treatment, median progression-free survival was 4.1 months and median survival was 9.7 months. Grade III/IV National Cancer Institute–Common Toxicity Criteria toxicities were nausea 17%, diarrhea 31%, mucositis 14%, neutropenia 52%, and febrile neutropenia 14%. FOLFIRI-2 achieved a good rate of response and stabilization in heavily pretreated patients despite significant toxicity.

Key Words: Irinotecan (CPT-11)—5-Fluorouracil (5-FU)—Leucovorin—Hydroxyurea—Advanced colorectal cancer—Phase II trials.

Tremendous progress has been made in the treatment of advanced colorectal cancer during the past years due to the availability of several new drugs, especially oxaliplatin and irinotecan.

Irinotecan has definite activity against advanced metastatic colorectal cancer both in chemotherapy-naive and pretreated patients whose disease progressed with 5-fluorouracil (5-FU).[1–4] Two large, randomized, multicenter studies on patients with 5-FU bolus-resistant metastatic colorectal cancer established the superiority of irinotecan over best supportive care[3] or 5-FU continuous-infusion regimens.[4] Irinotecan combined with 5-FU and leucovorin demonstrated an improve in response rate, progression-free survival, and overall survival compared to the same regimen without irinotecan in chemotherapy-naive patients with metastatic colorectal cancer.[5,6] Thus, combining irinotecan and 5-FU is a logical approach to attempt to improve the results obtained with irinotecan or 5-FU-based treatments alone.[7–9] Since the publication of studies showing that leucovorin enhances the efficacy of 5-FU against advanced colorectal carcinoma, progress has been made in developing leucovorin/5-FU (LV5-FU) regimens to improve the therapeutic ratio.[10–12]

Based on these clinical data, irinotecan was combined to the simplified LV5-FU regimen and administered in a previous phase II study in 33 patients with metastatic progressive disease after administration of at least two lines of chemotherapy including bimonthly LV5-FU and oxaliplatin (FOLFOX regimens).[13,14] This FOLFIRI-1 regimen generated an acceptable toxicity and achieved a 6% response rate and a 61% stabilization rate.[15] Preclinical experiments on cell cultures and human tumor xenografts indicated potential synergy when irinotecan was combined with 5-FU and leucovorin.[16–18] Preclinical data are controversial on the best timing to administer irinotecan, i.e., before or after the 5-FU infusion.[16] On the other hand, hydroxyurea could impair the DNA repair mechanisms either directly or by favoring the 5-FU incorporation in RNA.[19,20] We previously obtained restoration of tumor response by administering hydroxyurea before and during 5-FU infusion in pretreated

From the Department of Medical Oncology, Hôpital Saint-Antoine (M.M., C.L., V.G.-A., P.A., M.K., A.G.) Paris; the Department of Medical Oncology, Hôpital Tenon (T.A.) Paris; and the Department of Medicine, Hôpital de Senlis (E.C.) Senlis, France.

Preliminary results of this study were presented at the Annual Meeting of the American Society of Clinical Oncology, New Orleans, May 20 to 23, 2000.

Address correspondence and reprint requests to Dr. M. Mabro, Service d'Oncologie Medicale, Hôpital Saint-Antoine, 184, rue du Faubourg Saint-Antoine, 75571 Paris Cedex 12, France.

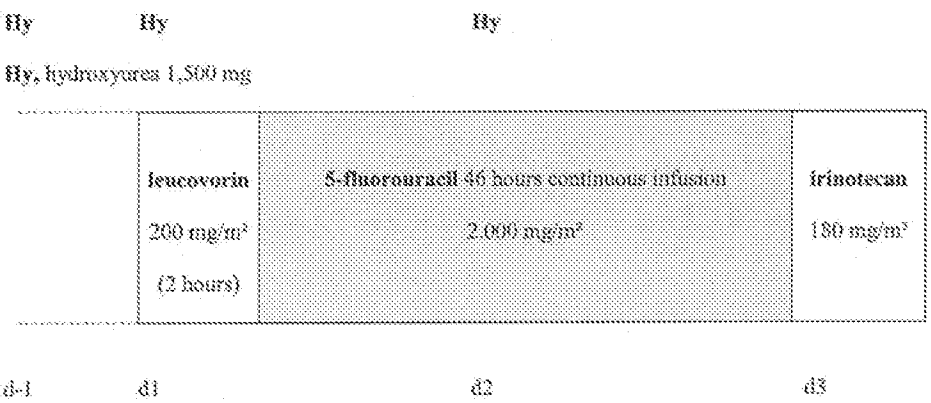

FIG. 1. Leucovorin, fluorouracil, irinotecan, and hydroxyurea (FOLFIRI-2) regimen: irinotecan was administered as a 90-minute infusion at the end of 5-fluorouracil infusion (day 3), and cycles were repeated every 2 weeks.

colorectal cancer resistant or refractory to 5-FU.[21] We hypothesized that the low response rate obtained with FOLFIRI-1 could be improved with a modified regimen. This FOLFIRI-2 regimen consisted of a simplified LV5-FU bimonthly regimen combined with irinotecan 180 mg/m^2 as a 90-minute infusion day 3 at the end of the 5-FU infusion, and with hydroxyurea taken before and during 5-FU infusion.

The objective of this study was to determine the tolerance and the efficacy of this regimen in advanced colorectal cancer refractory to 5-FU and oxaliplatin.

PATIENTS AND METHODS

Inclusion Criteria

This phase II study was conducted from June 1998 to April 1999. Patients were required to be 18 to 80 years old, and to have metastatic, histologically proven adenocarcinoma of the colon or rectum, previously treated with chemotherapy, including leucovorin, 5-FU, and oxaliplatin. An interval of at least 2 weeks must have elapsed since prior treatment. Other eligibility criteria were as follows: no central nervous system metastases, World Health Organization performance status 0 to 2, initial evaluation 2 weeks or less before inclusion by computed tomography (CT) scan prior to initiation of therapy and feasibility of regular follow-up. Required laboratory parameters included neutrophil count greater than 1,500/μl, platelet count greater than 100,000/μl, serum creatinine less than 300 μmol/l, serum alkaline phosphatase less than 3 times the upper normal limit, and bilirubin less than or equal to 1.5 mg/dl. Written informed consent was obtained from all patients.

Treatment Administration

Hydroxyurea (1,500 mg) was given orally the day before each cycle and on days 1 and 2, leucovorin (*dl* racemic mixture 400 mg/m^2) was infused on day 1 over 2 hours, immediately followed by 5-FU 46-hour infusion (2,000 mg/m^2). Irinotecan (180 mg/m^2) was given intravenously in 500 ml 5% dextrose solution over 90 minutes on day 3 at the end of 5-FU infusion, and cycles were repeated every 2 weeks (Fig. 1). This regimen was to be administered until progression as long as the neutrophil count was greater than 1,500/μl, platelet count was greater than 100,000/μl, and if toxicity was tolerable (National Cancer Institute–Common Toxicity Criteria [NCI-CTC] grade 0 to II). In case of neutropenia or thrombocytopenia greater than grade II, hydroxyurea was discontinued. When neutropenia, thrombocytopenia, or diarrhea exceeded grade II, the irinotecan dose was to be lowered from 180 mg/m^2 to 150 mg/m^2. If neutropenia, thrombocytopenia, or diarrhea greater than grade II persisted at this latter dose, therapy was discontinued.

Supportive Care

Specific antiemetic prophylaxis was left to investigator's discretion. For patients who experienced an early cholinergic syndrome (lacrimation, diaphoresis, abdominal cramps and/or diarrhea) occurring during or shortly after irinotecan administration, atropine sulfate (0.25 mg) could be given subcutaneously. To manage delayed diarrhea, it was recommended that loperamide (2 mg every 2 hours) be given immediately after the first liquid stools and discontinued 12 hours after the last loose stool; if the diarrhea was not controlled after 3 days, other supportive measures, including hospitalization, were to be considered.

Study parameters

Before each cycle, patients underwent a clinical examination, and blood cells were counted. Carcinoembryonic antigen (CEA), bilirubin, serum alkaline phosphatases, serum creatinine, lactate dehydrogenase, chest radiograph, and CT scans were repeated every 8 weeks (i.e., every four cycles) or earlier in the case of clinical deterioration. Only patients with bidimensionally measurable lesions on a CT scan were considered assessable for tumor responses. Complete response was defined as the complete disappearance of all assessable disease for at least 4 weeks; partial response was defined as a decrease of at least 50% of the sum of the products of the diameters of measurable lesions for at least 4 weeks. Stable disease was defined as a decrease of less than 50% or an increase of less than 25% of the disease. Progressive disease was defined as an increase of at least 25% or the appearance of new neoplastic lesion(s)[22] or a significant clinical deterioration that could not be attributed to irinotecan or medical conditions other than colorectal cancer. For rectal cancers, assessable metastases had to be outside the irradiated pelvis. All tumor responses were reviewed by an independent radiologist. Therapy was discontinued when disease progressed or intolerable toxicity occurred.

Statistical Considerations

Survival times were calculated from the start of FOLFIRI-2 until death. Time to progression was calculated from the first day of FOLFIRI-2 to the date of progression for all the patients entering the study. Survival curves were obtained using the Kaplan-Meier method.[23] All endpoints were updated on December 31, 1999.

TABLE 1. *Patient characteristics (n = 29)*

Characteristic	n	%
Median age (range) (y)	66 (38–79)	
Gender		
Male	18	62
Female	11	38
Primary tumor		
Colon	19	66
Rectum	10	34
Site of metastases		
Liver	19	66
Lung	13	45
Other	10	34
Involved sites		
1	14	48
2	13	45
>2	2	7
WHO performance status		
0	11	38
1	11	38
2	7	24
Tumor-related symptoms		
None	17	59
Yes	12	41
Elevated carcinoembryonic antigen		
10–50 ng/ml	14	48
>50 ng/ml	12	42
Previous chemotherapy for metastatic disease		
First-line (n = 29)		
Bimonthly LV5FU	24	83
FOLFOX regimen	5	17
Second-line (n = 26)		
FOLFOX regimen	20	
Bimonthly LV5FU	6	
Third-line (n = 5)		
FOLFOX regimen	5	

FOLFOX, bimonthly leucovorin/5-fluorouracil and oxaliplatin; LV5FU, leucovorin/5-fluorouracil; WHO, World Health Organization.

TABLE 2. *Toxicity of FOLFIRI-2 (29 patients, 207 cycles)*

	NCI-CTC grade (% of patients)			
	0 or I	II	III	IV
Nausea/vomiting	62	21	17	0
Mucositis	45	41	14	0
Delayed diarrhea	35	34	28	3
Neutropenia	28	21	21	31
Febrile neutropenia				14
Anemia	83	17	0	0
Thrombocytopenia	93	7	0	0
Hand–foot syndrome	93	7	0	0
Alopecia	55	45	—	—
Maximum nonhematologic toxicity including febrile neutropenia	7	38	38	17

FOLFIRI-2, leucovorin, fluorouracil, irinotecan, hydroxyurea; NCI-CTC, National Cancer Institute/Common Toxicity Criteria.

RESULTS

Patient Characteristics

From June 17, 1998 to April 19, 1999, 29 patients met all eligibility criteria and were included in the study. Their characteristics are given in Table 1. The median age was 66 years (range, 38–79 years). Overall, 41% of the patients had symptoms attributed to advanced disease. All had experienced disease progression while on a FOLFOX regimen (combination of oxaliplatin, bolus and infusion 5-FU, and leucovorin), or 2 months after discontinuation. Twenty-six patients (90%) were heavily treated before the administration of the FOLFIRI-2 regimen.

Treatment

The median number of treatment cycles administered was 7 (range, 1–23). Fourteen patients (48%) received more than 8 cycles. Two patients (7%) refused to continue after the second course (personal convenience with toxicity less than grade II), and 5 patients (17%) stopped treatment after 1, 2, or 3 cycles because of grade III or IV toxicity. In 4 patients (14%), treatment was stopped after 8 courses in stabilization without clinical benefit.

Toxicity

The incidence of the main toxic effects according to the NCI-CTC grade scale[24] are listed in Table 2. Two hundred seven cycles could be evaluated. Neutropenia reached grade III/IV in 15 patients (52%), including 4 patients (14%) who had 1 episode of febrile neutropenia. Grade III/IV delayed diarrhea developed in 9 patients (31%) and required hospitalization and discontinuation of the FOLFIRI-2 in 2 patients (7%). The other grade III/IV toxicities observed were nausea/vomiting in 5 patients (17%) and mucositis in 4 patients (14%). Mild side effects also included conjunctivitis and fatigue. Alopecia was grade I in 9 patients (28%) and grade II in 15 patients (45%). Overall, 16 patients (55%) experienced nonhematology grade III/IV toxicity. Toxicities were lowered after adjustment of doses. Overall grade III/IV toxicities occurred in 26% of cycles. No toxic death occurred.

Objective tumor responses and survival

The objective response rate for all patients was 17% (n = 5; 95% CI : 3–31%). Fifty-two percent had stable disease (n = 15) and 14% had progressive disease (n = 4). CEA level decreased more than 50% in 7 of 19 patients with increased CEA level at baseline (37%).

Median progression-free survival was 18 weeks (4.1 months) and median survival was 42 weeks (9.7 months) from the start of FOLFIRI-2 (Fig. 2).

DISCUSSION

This phase II study assessed the efficacy and toxicity of the FOLFIRI-2 regimen, a new combination of irinotecan and LV5-FU, in heavily pretreated patients with metastatic colorectal cancer. Various combinations of irinotecan and 5-FU with or without leucovorin were

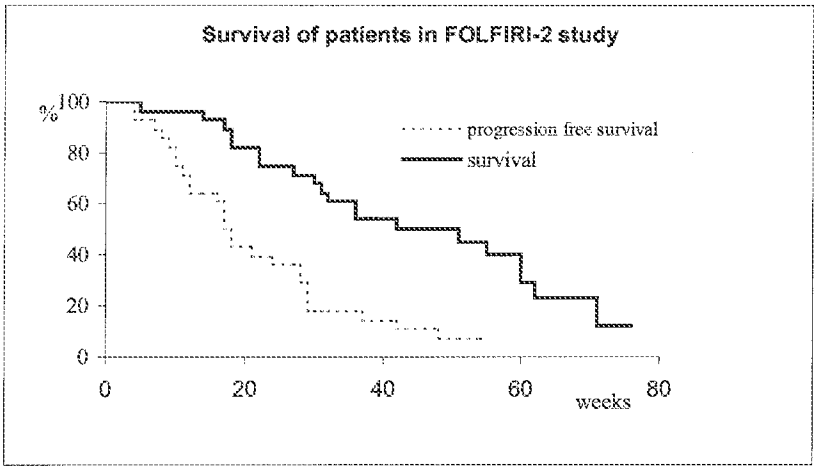

FIG. 2. Survival and progression free-survival in leucovorin, fluorouracil, irinotecan, and hydroxyurea (FOLFIRI-2) study.

tested in phase I-II studies in the United States,[25–27] Europe[8,9,15,28,29] and Japan,[30] and then in phase III studies.[5,6,31] In accordance with the findings of the present study, those studies showed clinical activity against colorectal cancer, including pretreated patients. Neutropenia and diarrhea were the main toxicities and were more frequent and severe when irinotecan was given alone at 350 mg/m^2.[1–4] The predominant toxicities observed with our schedule were 47% grade III to IV neutropenia and 38% grade III to IV diarrhea. The FOLFIRI-1 regimen combining 180 mg/m^2 irinotecan with the simplified LV5-FU achieved a 5% response rate and a 61% stabilization rate in a phase II study of pretreated patients, with mild toxicity.[15] Irinotecan was also combined with the LV5-FU2 regimen. This combination achieved a response rate of 21% and a stabilization rate of 30% in a phase II study of pretreated patients, with poor toxicity.[29] However, the population of this study was less heavily pretreated and with better performance status than in the FOLFIRI-2 study.

The response rate of 17% and the 52% stabilization of FOLFIRI-2 compare favorably with the FOLFIRI-1 regimen in heavily pretreated patients.[15] The administration of irinotecan at the end of the 5-FU infusion and the addition of hydroxyurea as third-line therapy achieved results comparable to irinotecan alone as first-line therapy. The small subset of patients in our study does not allow a conclusion about whether the benefit is related to a hydroxyurea-enhanced RNA pattern or to a schedule-dependent in vivo synergism between 5-FU and irinotecan. The higher rate of toxicity on FOLFIRI-2 in comparison to FOLFIRI-1 and to LV5–FU2–irinotecan can be related to the subset of heavily pretreated patients and could also be explained by a sequence-dependent synergism.

In conclusion, as third-line therapy in patients with metastatic colorectal cancer, FOLFIRI-2 has amazing antitumor activity and, unfortunately, significant toxicity. Based on results of FOLFIRI-1 and FOLFIRI-2 regimen, we are now conducting a new study to evaluate the FOLFIRI-3 regimen combining the simplified LV5-FU with two administrations of irinotecan on day 1 and on day 3, before and after the 5-FU infusion. ₡

REFERENCES

1. Rougier P, Bugat R, Douillard JY, et al. Phase II study of irinotecan in the treatment of advanced colorectal cancer in chemotherapy naive patients and patients pretreated with fluorouracil based chemotherapy. *J Clin Oncol* 1997;15:251–60.
2. Pitot HC, Wender DB, O'Connell MJ, et al. Phase II trial of irinotecan in patients with metastatic colorectal carcinoma. *J Clin Oncol* 1997;15:2910–9.
3. Cunningham D, Pyrhönen S, James RD, et al. Randomised trial of irinotecan plus supportive care versus supportive care alone after fluorouracil failure for patients with metastatic colorectal cancer. *Lancet* 1998;352:1413–8.
4. Rougier P, Van Cutsem E, Bajetta E, et al. Randomised trial of irinotecan versus fluorouracil by continuous infusion after fluorouracil failure in patients with metastatic colorectal cancer. *Lancet* 1998;352:1407–12.
5. Douillard JY, Cunningham D, Roth AD, et al. Irinotecan combined with fluorouracil compared with fluorouracil alone as first-line treatment for metastatic colorectal cancer: a multicentre randomised trial. *Lancet* 2000;355:1041–7.
6. Saltz LB, Cox JV, Blanke C, et al. Irinotecan plus fluorouracil and leucovorin for metastatic colorectal cancer. Irinotecan study group. *N Engl J Med* 2000;343:905–14.
7. Mullany S, Svingen PA, Kaufmann SH, et al. Effect of adding the topoisomerase I poison 7-ethyl 10-hydroxycamptothecin (SN 38) to 5-fluorouracil and folinic acid in HCT8 cells: elevated dTTP pools and enhanced cytotoxicity. *Cancer Chemother Pharm* 1998; 42:391–9.
8. Khayat D, Gil-Delgado M, Antoine EC, et al. European experience with irinotecan plus fluorouracil/folinic acid or mitomycin. *Oncology* 1998;12(suppl 6):64–7.
9. Ducreux M, Ychou M, Seitz JF, et al. Irinotecan combined with bolus fluorouracil, continuous infusion fluorouracil, and high-dose leucovorin every two weeks (LV5FU2 regimen): A clinical dose finding and pharmacokinetic study in patients with pretreated metastatic colorectal cancer. *J Clin Oncol* 1999;17:2901–8.
10. de Gramont A, Bosset JF, Milan C, et al. Randomized trial comparing monthly low dose leucovorin and fluorouracil bolus with bimonthly high dose leucovorin and fluorouracil bolus plus continuous infusion for advanced colorectal cancer. A French intergroup study. *J Clin Oncol* 1997;15:808–15.
11. de Gramont A, Louvet C, André T, et al. A review of GERCOD trials of bimonthly leucovorin plus 5-fluorouracil 48-hour continuous infusion in advanced colorectal cancer. *Eur J Cancer* 1998;34:619–26.

12. Tournigand C, de Gramont A, Louvet C, et al. A simplified bimonthly regimen with leucovorin (LV) and 5-fluorouracil (5FU) for metastatic colorectal cancer (MCRC). *Proc Am Soc Clin Oncol* 1998;17:274a.
13. Maindrault-Goebel F, Louvet C, André T, et al. Oxaliplatin added to the simplified bimonthly leucovorin and 5-fluorouracil regimen as second line therapy for metastatic colorectal cancer (FOLFOX6). *Eur J Cancer* 1999;35:1338–42.
14. de Gramont A, Figer A, Seymour M, et al. Leucovorin and fluorouracil with or without oxaliplatin as first-line treatment in advanced colorectal cancer. *J Clin Oncol* 2000;18:2938–47.
15. André T, Louvet C, Maindrault-Goebel F, et al. CPT-11 (irinotecan) addition to bimonthly, high-dose leucovorin and continuous-infusion 5-fluorouracil (FOLFIRI) for pretreated metastatic colorectal cancer. *Eur J Cancer* 1999;35:1343–7.
16. Guichard S, Hennebelle I, Bugat R, et al. Cellular interactions of 5-fluorouracil and the camptothecin analogue CPT-11 (irinotecan) in a human colorectal carcinoma cell line. *Biochem Pharmacol* 1998;55:667–76.
17. Guichard S, Cussac D, Hennebelle I, et al. Sequence-dependent activity of the irinotecan-5FU combination in human colon-cancer model HT-29 in vitro and in vivo. *Int J Cancer* 1997;73:729–34.
18. Mans DRA, Grivicich I, Peters GJ, et al. Sequence-dependent growth inhibition and DNA damage by the irinotecan-5-fluorouracil combination in human colon carcinoma cell lines. *Eur J Cancer* 1999;35:1851–61.
19. Kobayashi S, Hoshino T. Combined cytotoxic effect of low-dose 5-fluorouracil and hydroxyurea on 9L cells *in vitro*. *Cancer Res* 1983;43:5309–13.
20. Kao AK, Muggia FM, Dubin N, et al. Evaluation of a sequential 5-FU and hydroxyurea combination in advanced bowel cancer. *Cancer Treat Rep* 1984;68:1383–5.
21. de Gramont A, Louvet C, Bennamoun M, et al. Dual modulation of 5-fluorouracil with folinic acid and hydroxyurea in metastatic colorectal cancer. *J Infusion Chemo* 1996;6:97–101.
22. World Health Organization. *WHO handbook for reporting results of cancer treatment*. Geneva: WHO, 1979.
23. Kaplan EL, Meier P. Nonparametric estimation from incomplete observations. *J Am Stat Assoc* 1958;53:457–81.
24. MacDonald J, Haller D, Mayer R. Grading of toxicity. In: MacDonald J, Haller D, Mayer R, eds. *Manual of oncologic therapeutics*. Philadelphia: JB Lippincott, 1995:519–23.
25. Parnes HL, Tait N, Conley B, et al. A phase I study of CPT-11, weekly bolus 5FU and leucovorin in patients with metastatic cancer. *Oncol Rep* 1995;2:1131–4.
26. Saltz LB, Kanowitz J, Kemeny NE, et al. Phase I clinical and pharmacokinetic study of irinotecan, fluorouracil, and leucovorin in patients with advanced solid tumors. *J Clin Oncol* 1996;14:2959–67.
27. Goldberg RM, Erlichman C. Irinotecan plus 5FU and leucovorin in advanced colorectal cancer: North American trials. *Oncology* 1998;12(suppl 6):59–63.
28. Paz-Ares L, Sastre J, Diaz-Rubio B, et al. Phase I dose-finding study of irinotecan (CPT-11) over a short IV infusion combined with fixed dose of 5-fluorouracil (5FU) protracted continuous IV infusion in patients with advanced solid tumor. *Proc Am Soc Clin Oncol* 1997; 16:247a.
29. Gil-Delgado MA, Guinet F, Castaing D, et al. Prospective phase II trial of irinotecan, 5-fluorouracil, and leucovorin in combination as salvage therapy for advanced colorectal cancer. *Am J Clin Oncol* 2001;24:101–5.
30. Matsuoka H, Yano K, Takiguchi S, et al. Advantage of combined treatment of CPT-11 and 5-fluorouracil. *Anticancer Res* 1995;15: 1447–52.
31. Tournigand C, Louvet C, André T, et al. FOLFIRI followed by FOLFOX or FOLFOX followed by FOLFIRI in metastatic colorectal cancer: which is the best sequence? Safety and preliminary efficacy results of a randomized phase III study. *Proc Am Soc Clin Oncol* 2000;19:245a.

Original article

Annals of Oncology 15: 665–670, 2004
DOI: 10.1093/annonc/mdh133

A phase I study of OSI-211 and cisplatin as intravenous infusions given on days 1, 2 and 3 every 3 weeks in patients with solid cancers

M. J. MacKenzie[1], H. W. Hirte[1], L. L. Siu[2], K. Gelmon[3], M. Ptaszynski[4], B. Fisher[5] & E. Eisenhauer[5]*

[1]*Hamilton Regional Cancer Centre, Hamilton, Ontario;* [2]*Princess Margaret Hospital, Toronto, Ontario;* [3]*Vancouver Cancer Centre, Vancouver, British Columbia, Canada;* [4]*OSI Pharmaceuticals, Boulder, CO, USA;* [5]*NCIC Clinical Trials Group, Kingston, Ontario, Canada*

Received 12 September 2003; revised 13 November 2003; accepted 22 December 2003

Background: OSI-211 (also known as NX211) is a liposomal preparation of the topoisomerase I inhibitor, lurtotecan, which has shown antitumor activity in phase I and II clinical trials. Cisplatin is a widely used antineoplastic agent with activity in a broad range of tumor types. This phase I trial was conducted to determine the recommended doses of these agents, and their pharmacokinetic properties and toxicities in patients with advanced solid malignancies.

Patients and methods: Fourteen patients with advanced and/or metastatic solid malignancies were enrolled in this trial. The first planned dose level was OSI-211 0.9 mg/m^2 with cisplatin 25 mg/m^2 administered intravenously daily for the first three consecutive days of a 21-day cycle. Patients were evaluated for hematological and non-hematological toxicities, and pharmacokinetic studies were performed on both agents.

Results: The recommended phase II dose was determined to be 0.7 mg/m^2 OSI-211 given with 25 mg/m^2 cisplatin. Dose-limiting neutropenia was seen in two of three patients at the starting dose level. Three of 11 patients at the second (lower) dose level experienced dose-limiting thrombocytopenia; febrile neutropenia was also seen in one patient. Non-hematological toxicities were generally manageable and included fatigue, nausea and vomiting. Considerable variability was seen in both hematological toxicities and pharmacokinetics. One complete response and three partial responses were seen.

Conclusions: The recommended phase II dose for this combination is 0.7 mg/m^2 OSI-211 with 25 mg/m^2 cisplatin given as an intravenous infusion on days 1, 2 and 3 of a 21-day cycle. The main toxicity was myelosuppression. Preliminary evidence of antitumor activity was seen.

Key words: liposomes, phase I, topoisomerase I

Introduction

Lurtotecan [7(4-methylpiperazinomethylene)-10,11-ethylenedioxy-20-(S)-camptothecin dihydrochloride] is a semisynthetic analog of camptothecin, which is a derivative of the tree *Camptotheca acuminata* [1]. Like other camptothecin analogs, lurtotecan inhibits the ability of topoisomerase I to relax torsionally strained DNA [2].

After the demonstration of its antitumor activity in the preclinical setting, several early-phase trials were conducted with lurtotecan as a single agent. In all phase I trials, the dose-limiting toxicity (DLT) was myelosuppression, mainly neutropenia. Antitumor activity has been documented; Paz-Ares et al. [3] reported that among 44 patients with advanced solid tumors, there were three partial responses and two minor responses. Another phase I trial showed that two patients (out of 38) had partial responses [4]. Responses were observed in ovarian and small-cell lung cancers (SCLC).

A phase II trial of lurtotecan in patients with breast, colorectal and non-small-cell lung cancer (NSCLC) showed that three of 25 patients with breast cancer and two of 23 patients with NSCLC had partial responses [5]. No responses were seen among the 19 patients with colorectal cancer in this trial. In a separate trial involving 67 patients with previously treated SCLC, the overall response rate was 16% [6].

Lurtotecan has since been formulated in a low-clearance, liposomal preparation, OSI-211 (also known as NX211). Liposomal preparations of other antineoplastic agents have shown prolonged plasma exposure, improved tumor delivery and decreased toxicity [7]. In several preclinical studies, compared with lurtotecan, OSI-211 demonstrated a significant increase in plasma residence time. In mouse xenograft models, OSI-211 produced a three-fold or higher increase in therapeutic index compared with lurtotecan [2].

Eisenhauer et al. [8] have presented the results of phase I trials with three different schedules of OSI-211. The first trial (29 patients) administered OSI-211 as a 30 min infusion every 3 weeks. In the second trial OSI-211 was given on days 1, 2 and 3 (37 patients),

**Correspondence to:* Dr E. Eisenhauer, NCIC Clinical Trials Group, Cancer Research Institute, 10 Stuart Street, Queen's University, Kingston, Ontario, Canada K7L 3N6. Tel: +1-613-533-6430; Fax: +1-905-575-6326; E-mail: eeisenhauer@ctg.queensu.ca

and in the third study, OSI-211 was given on days 1 and 8 (26 patients). Eighty-six patients were evaluable for toxicity. DLTs were neutropenia and thrombocytopenia. Other toxicities included anemia, fatigue, nausea and vomiting. Partial responses were observed in patients with breast and ovarian cancers. The divided dose schedules allowed for higher dose intensity delivery, and were selected for further study in phase II trials. The recommended doses were 2.1 and 1.5 mg/m^2 daily ×3 (total 6.3 and 4.5 mg/m^2/cycle) for the day 1, 2 and 3 schedule in minimally and heavily pretreated patients, respectively. For the day 1 and 8 schedule, the recommended dose is 2.4 mg/m^2 (total 4.8 mg/m^2/cycle) [8].

Goetz et al. [9] presented the results of a phase I study of OSI-211 administered weekly for 4 weeks of a 6-week cycle in patients with advanced solid tumors. Again, the major toxicity was neutropenia. The tumor response rate was not reported.

Another topoisomerase inhibitor, topotecan, has been evaluated in combination with cisplatin. Cisplatin has been used widely in the management of malignant disease for decades, and has activity in a broad range of tumor types. Unfortunately, the combination of topotecan and cisplatin caused more neutropenia than expected from either drug given alone at the same doses. Phase I trials combining cisplatin and topotecan found the combination produced additive myelosuppression, and neither drug could be given in its full single-agent dose [10–12].

Preclinical studies of OSI-211 and cisplatin administered in combination in three separate tumor xenograft models (head and neck, lung, and ovarian) have been performed. These studies demonstrated increased antitumor activity in the ovarian and head and neck models compared with the single agent, but bone marrow toxicity of the combination was similar to that caused by OSI-211 alone (OSI Pharmaceuticals; data on file). The primary objective of this present trial was to determine the doses of OSI-211 and cisplatin that could be given in a daily ×3 regimen and to determine whether they could be given in combination without such additive myelotoxicity. The secondary objectives were to evaluate the pharmacokinetic profile of this combination and its preliminary antitumor activity.

Patients and methods

Patient selection

Patients were selected based on the following eligibility criteria: histologically or cytologically documented advanced and/or metastatic solid malignancy that was refractory to standard therapy or for which no curative therapy existed; age >18 years; and an Eastern Cooperative Oncology Group (ECOG) performance status of 0–2. All patients were required to have adequate bone marrow, hepatic and renal function defined as follows: an absolute neutrophil count (ANC) of ≥1.5 × 10^9/l, platelets ≥100 × 10^9/l, creatinine less than upper limit of normal (ULN) (or calculated clearance ≥60 ml/min), bilirubin ≤ULN, aspartate aminotransferase/alanine aminotransferase ≤2.5× ULN (or ≤5× ULN if documented liver metastases). Patients may have had up to one prior chemotherapy regimen (adjuvant and/or metastatic). Prior cisplatin-containing chemotherapy was allowed, providing the total dose of cisplatin was ≤300 mg/m^2. A minimum of 21 days (6 weeks for nitrosoureas or mitomycin C) must have elapsed between the end of treatment and entry into the protocol, and patients must have recovered from any treatment-induced toxicities. Neuropathy and ototoxicity must have been grade ≤1 according to National Cancer Institute common toxicity criteria (NCI CTC) version 2.0. Prior radiotherapy was permitted providing that it had not encompassed >25% of the bone marrow reserve. A minimum of 4 weeks must have elapsed between completion of radiotherapy and protocol entry. Female patients of childbearing potential could not be pregnant, lactating or using inadequate birth control as defined by the protocol, and were required to have a negative pregnancy test at study entry.

Patients were excluded if they had untreated brain or meningeal metastases (patients with previously treated and stable CNS metastases were eligible). Patients with serious medical illnesses were excluded.

All patients gave written informed consent. The study was approved by local hospital and university ethics review boards and met institutional and federal guidelines.

Trial design

This was a phase I, open-label, non-randomized, dose-finding study of the combination of cisplatin and OSI-211 given as intravenous infusions on days 1, 2 and 3 of an 3 week cycle. The schedule of three consecutive days was selected because the phase I trial of OSI-211 given in this schedule was promising in terms of antitumor activity and, at least in some clinical settings such as SCLC, cisplatin may be given in a daily ×3 dosing schedule. The starting dose of OSI-211 was 0.9 mg/m^2 (<50% of the recommended single-agent dose for minimally pretreated patients). The dose of cisplatin was fixed in all dose levels at 25 mg/m^2, which is the standard dose used in daily ×3 regimens.

The study, conducted under the auspices of the National Cancer Institute of Canada Clinical Trials Group (NCIC CTG), accrued patients from three participating centers, the Hamilton Regional Cancer Centre, the Princess Margaret Hospital/University Health Network and the British Columbia Cancer Agency–Vancouver Center Hospital. All patients were registered with the NCIC CTG central office and assigned to a dose level. Data monitoring was performed by NCIC CTG and OSI Pharmaceuticals.

Treatment plan

Pretreatment evaluation included history, physical examination, complete blood count, chemistry, urinalysis, ECG, chest X-ray and radiological assessment, with other scans/X-rays as necessary to document disease. A pregnancy test was performed in women of childbearing potential. A complete toxicity evaluation was performed to document residual toxicity from previous therapy and baseline symptoms.

Patients were reviewed every 3 weeks by one of the investigators to assess symptoms and signs. A complete blood count was performed on day 1 and twice weekly during cycle 1, and on day 1 and weekly during subsequent cycles. Biochemistry was drawn on day 1 and weekly during cycle 1, and then on day 1 of subsequent cycles. Formal tumor measurements were performed after every two cycles of treatment. Toxic effects were monitored continuously according to the NCI CTC version 2. No routine hematopoetic growth factors were given.

OSI-211 was administered by intravenous infusion (over 30 min) on an outpatient basis on days 1, 2 and 3 of a 21-day cycle. Patients received cisplatin 25 mg/m^2/day intravenously over 1 h on days 1, 2 and 3 of the cycle immediately preceding the OSI-211 infusion. All patients were premedicated with dexamethasone 10 mg by mouth or intravenously, and ondansetron 8 mg by mouth before each treatment. Patients routinely received 500 ml normal saline as prehydration. No other routine prophylactic premedications or co-medications were administered.

Treatment was continued until the patient developed disease progression or unacceptable toxicity, or withdrew his or her consent.

Dose escalation and dose modifications

Initially, three patients were to be enrolled at each dose level. If no patients exhibited DLT at a given level, escalation would proceed to the next dose level, according to a modified Fibonacci schedule. If one of three patients had a DLT, then three additional patients were to be enrolled in that cohort. If two or more patients had a DLT, that dose was to be declared the maximum tolerated dose (MTD), and the next lower dose level expanded as the recommended phase II dose. The dose of OSI-211 was not to be escalated in individual patients.

Response criteria

Patients were considered assessable for response if they had received at least one cycle of therapy and had their disease re-evaluated. Measurable lesions were defined as those that could be accurately measured in at least one dimension as ≥20 mm with conventional techniques [physical exam, computed tomography (CT) scan, X-ray, magnetic resonance imaging] or as ≥10 mm with spiral CT scan. All measurable lesions were evaluated at least every two cycles using the RECIST criteria [13]. A complete response was defined as the disappearance of all clinical and radiological evidence of tumor. A partial response was a reduction of at least 30% in the sum of the longest dimension of target lesions. Progressive disease was defined as a 20% or more increase in the sum of the longest dimensions of measured lesions, or the appearance of new lesions.

Pharmacokinetic analysis

The pharmacokinetics of OSI-211 and cisplatin were studied on days 1–5 of the first cycle of treatment only. On days 1 and 3, blood samples were collected before drug administration, and thereafter at 60 min (at the end of the cisplatin infusion and prior to the beginning of the OSI-211 infusion), 90, 120, 150, 180 and 210 min, and at 5 and 8 h after the end of the OSI-211 infusion. One sample was collected on day 2 prior to initiating the day 2 OSI-211 infusion. One sample was taken on day 4 and another on day 5, 23.5 and 46.5 h after the end of the day 3 OSI-211 administration. Plasma samples were analyzed by reverse-phase high-pressure liquid chromatography with fluorescence detection. The total concentration of OSI-211 is reported (lactone and carboxylate forms of OSI-211 were not determined independently).

The maximum plasma concentration (C_{max}), area under the curve from time zero to infinity ($AUC_{0-\infty}$), plasma clearance, volume of distribution (V_d) of the central compartment at steady state and elimination half-life were determined.

Results

Patient characteristics

The patient characteristics are detailed in Table 1. Fourteen patients were enrolled onto the study between March 2000 and November 2001. All were evaluable for hematological and non-hematological toxicity. Eleven were evaluable for response. Of the three patients not evaluable, two did not have repeat radiology to re-assess disease (one of these patients was removed from study due to symptomatic progression after one cycle of treatment; the other was removed due to elevated creatinine). The third non-evaluable patient had non-measurable disease.

Nine patients were female and five were male. All patients had ECOG status <2 at the time of enrollment. Six of the patients had no prior chemotherapy and eight had one previous chemotherapy regimen. Five patients had a diagnosis of ovarian cancer, four had head and neck cancer, and one each had cervical, renal, peritoneal, thyroid and unknown primary carcinoma.

Table 1. Patient characteristics ($n = 14$)

Characteristic	n
Median age (range)	54 (44–73)
Gender	
Female	9
Male	5
ECOG performance status	
0	6
1	8
Malignancy type	
Ovary	5
Head and neck	4
Renal	1
Cervix	1
Peritoneum	1
Thyroid	1
Unknown primary	1
Prior chemotherapy regimens	
0	6
1	8
Prior radiotherapy	7

ECOG, Eastern Cooperative Oncology Group.

Drug delivery

At the first dose level (0.9 mg/m^2/day OSI-211 and 25 mg/m^2 cisplatin), dose-limiting myelosuppression was encountered in two of the three patients entered; thus, further enrolment of patients was undertaken at the −1 dose level of OSI-211, 0.7 mg/m^2 plus cisplatin 25 mg/m^2, the dose level that is recommended for further evaluation. A total of 61 courses of chemotherapy were delivered at the two dose levels. Table 2 outlines the total number of cycles of chemotherapy at each dose level.

The number of cycles given at dose level 1 ranged from two to five (median five cycles). The number of cycles given at dose level −1 ranged from one to six (median six cycles).

Toxicity

Hematological toxicity. Table 3 displays the median nadir of the ANC, hemoglobin and platelets by cohort. As described above, at the starting dose of 0.9 mg/m^2 OSI-211 with 25 mg/m^2 cisplatin, two of three patients experience DLT. One patient was neutropenic (grade 4) for >7 days. A second patient developed febrile neutropenia on day 19 of treatment. This patient was admitted to hospital for treatment with intravenous antibiotics, and subsequently recovered.

Because the first dose level was thus declared the MTD, a reduced dose level of 0.7 mg/m^2 OSI-211 was opened. Initially,

Table 2. Dose levels, number of patients and number of cycles

Dose level (mg/m^2) OSI-211/cisplatin	Total No. of patients	Total No. of cycles	Range (no. of cycles)	No. of patients with DLT
0.9/25 (starting)	3	12	2–5	2
0.7/25 (–1 dose)	11	49	1–6	3

DLT, dose-limiting toxicity.

Table 3. Hematological toxicity (worst ever by starting dose)

Dose OSI-211 (mg/m^2/day)	Median nadir ANC ($\times 10^9$/l) (range)	Median nadir hemoglobin (g/l) (range)	Median nadir platelets ($\times 10^9$/l) (range)
0.9	0.1 (0.1–0.9)	85 (82–89)	37 (36–207)
0.7	0.5 (0.1–3.3)	82 (65–110)	82 (10–299)

ANC, absolute neutrophil count.

Table 4. Non-hematological toxicity: worst grade by patient, any relationship to therapy

Toxicity	No. of patients				Percent of patients
	Grade 1	Grade 2	Grade 3	Grade 4	
Dose level 0.9 mg/m^2/day OSI-211 ($n = 3$)					
Fatigue	2	1		–	100
Nausea	1	2		–	100
Vomiting	1	1		–	66
Taste disturbance	1			–	33
Anorexia	2			–	66
Inner ear/hearing		1		–	33
Neuropathy sensory	1			–	33
Insomnia		2		–	66
Alopecia	2			–	66
Dose level 0.7/m^2/day OSI-211 ($n = 11$)					
Fatigue	2	8	1		100
Nausea	2	4	1		64
Vomiting	3	1	1		45
Anorexia	3	1	1		45
Neuropathy sensory	5				45
Neuropathy motor	3	1			36
Insomnia	3	1			36
Alopecia	2	2			36
Inner ear/hearing	1	2			27

four patients were registered to this dose level, and two of these patients required cycle 2 delays due to neutropenia. As a result, four additional patients were enrolled at this level to obtain a broader picture of the bone marrow effects. When two of these four patients experienced DLTs in the form of thrombocytopenia and febrile neutropenia, three further patients were enrolled. One of these patients experienced grade 3 thrombocytopenia. Therefore, in total, three of 11 patients at this new level had a DLT. However, because wide inter-patient variability was observed (with some patients having little or no toxicity), this dose was declared the recommended level for phase II study.

Non-hematological toxicity. Non-hematological effects occurring on the study are detailed in Table 4. The most common non-hematological effects were fatigue, nausea and vomiting, and none was dose limiting. One 64-year-old patient with peritoneal cancer was admitted to hospital with myocardial infarction on day 9

Table 5. Pharmacokinetics for cisplatin and OSI-211

Drug	OSI-211 dose		$AUC_{0-\infty}$ (g/h/ml)		C_{max} (ng/ml)		V_d (ml/m^2)		Clearance (ml/h/m^2)		Half life (h)	
			Day 1	Day 3	Day 1	Day 3	Day 1	Day 3	Day 1	Day 3	Day 1	Day 3
Cisplatin	0.9	N	3	3	3	3	3	3	3	3	3	3
		M	1138	1258	1088	994	10 559	13 681	14 502	13 119	0.43	1.27
		R	1027–1238	1204–1313	880–1308	804–1156	8646–12 949	12 819–17 198	13 331–15 485	12 569–13 201	0.41–0.45	1.09–1.85
	0.7	N	11	10	11	10	11	10	11	10	11	10
		M	1199	1542	970	1006	16 043	25 634	13 431	10 502	0.81	2.515
		R	833–1728	1057–2283	686–1438	594–1259	10 251–25 504	10 863–115 104	9318–19 690	6921–13 703	0.41–1.09	0.82–13.4
OSI-211	0.9	N	3	3	3	3	3	3	3	3	3	3
		M	258	382	154	283	10 422	8612	3946	2432	3.5	7.7
		R	187–9205	334–9096	145–566	156–671	1150–15 642	1333–19 978	97–4976	98–2744	2.2–9.4	4.9–9.1
	0.7	N	10	11	10	11	10	10	10	11	10	11
		M	3080	4063	317	420	2181	1862	241	175	7.4	7.8
		R	178–8243	310–9814	112–511	159–598	1269–7943	1247–5481	81–4016	70–2303	1.2–14.7	2–13.6

N, number of patients; M, median; R, range.

of her fifth course of therapy. Following appropriate in hospital care she recovered and was discharged. Owing to the temporal sequence of the event with treatment, a relationship to study therapy could not be excluded. She was therefore removed from the study.

In patients with normal baseline biochemistry, some elevations in liver enzymes, primarily grade 1, were seen. However, two patients were removed from study due to elevations in creatinine after one and two cycles of therapy were given. Overall, five patients had creatinine elevations (three patients with grade 1; two patients with grade 2), and, because of the known effects of cisplatin on renal function, these elevations are likely related to the combination protocol therapy.

Pharmacokinetics

Pharmacokinetic results (including AUC, C_{max}, V_d, clearance and half-life) are reported in Table 5. Pharmacokinetic evaluation was performed in 14 patients. OSI-211 pharmacokinetics showed results that were similar to those observed previously in single-agent trials at the dose levels given in this study. There was little intra-patient variability, but marked inter-patient variability. As was the case in the single-agent phase I studies, the variability of toxicity (in particular myelosuppression) could not be explained by the variability in pharmacological behavior of the drug.

A statistically significant rise in the AUC of cisplatin between days 1 and 3 was noted in the group receiving 0.7 mg/m^2 OSI-211 ($P = 0.0090$, paired t-test). Such elevations in AUC and C_{max} have been noted when platinum is administered as monotherapy. Therefore, it is unlikely that the increase is a result of co-administration with OSI-211 [14].

Antitumor response

Eleven patients were evaluable for response. One patient (with anaplastic thyroid cancer) had a complete response. The response was sustained for the duration of treatment (six cycles) and the patient relapsed 6 months after discontinuation. Three had partial responses (ovarian, peritoneal, and head and neck). The median duration for partial response was 4.7 months (range 3.9–14.1). Six patients had stable disease; the median duration of stable disease was 6.9 months (range 2.4–11.2). One patient had progressive disease.

Discussion

OSI-211, a liposomal preparation of the camptothecin analog lurtotecan, has shown antitumor activity in phase II evaluation [15]. Cisplatin is a widely used antineoplastic agent with activity in a broad range of tumor types. Because the combination of camptothecin and platinum is logical given the spectrum of activity of both these classes of agents, we carried out this phase I trial to determine the MTD and toxicity profile of OSI-211 and cisplatin.

Unfortunately, significant myelotoxicity was seen at the starting dose in the first cohort, and therefore subsequent patients were enrolled at a lower dose level. The results of this trial are similar to those documented in previous phase I trials of cisplatin combined with topotecan [10–12], indicating the preclinical toxicology that

suggested there might not be additive myelosuppression when OSI-211 was given in combination with cisplatin were misleading in this regard.

Although myelotoxicity was again seen in this second cohort given reduced doses of OSI-211, there was significant interpatient variability in the toxicities seen. As three of 11 patients had a DLT at the second (lower) level, the recommended dose for phase II studies is 0.7 mg/m^2 OSI-211 and 25 mg/m^2 cisplatin for three consecutive days in a 21-day cycle.

The pharmacokinetic evaluation of these patients also showed interpatient variability in OSI-211 AUC, C_{max}, V_d and clearance. The variability of toxicity (in particular myelosuppression) could not be explained by the variability in pharmacological behaviour of the drug.

Non-hematological adverse effects were manageable, with no DLTs seen. The most common non-hematological toxicities were gastrointestinal.

The study combination did show antitumor activity, with one complete and three partial responses seen. It should be noted, however, that these responses occurred in patients with malignancies that are known to be responsive to platinum analogs; thus it is unclear whether the activity seen was related to the combination being given, or simply administration of the platinum component.

Since this trial was initiated, others have shown that the preferred schedule for OSI-211 administration is the daily ×3 regimen we employed in this study [15]. Thus, should this agent be pursued further in combination with cisplatin, the daily ×3 schedule we have studied may merit further evaluation in solid tumors, where OSI-211 has shown activity.

Acknowledgements

This study was supported by grants from the National Cancer Institute of Canada and OSI Pharmaceuticals.

References

1. Kehrer DFS, Bos AM, Verweij J et al. Phase I and pharmacologic study of liposomal lurtotecan, NX211: urinary excretion predicts hematologic toxicity. J Clin Oncol 2002; 20: 1222–1231.
2. Emerson DL, Bendele R, Brown E et al. Antitumor efficacy, pharmacokinetics, and biodistribution of NX211: a low-clearance liposomal formulation of lurtotecan. Clin Cancer Res 2000; 6: 2903–2912.
3. Paz-Ares L, Kunka R, De Maria D et al. A phase I and pharmacokinetic study of the new topoisomerase inhibitor GI147211 given as a 72-h continuous infusion. Br J Cancer 1998; 78: 1329–1336.
4. Stevenson JP, DeMaria D, Sludden J et al. Phase I/pharmacokinetic study of the topoisomerase I inhibitor GG211 administered as a 21-day infusion. Ann Oncol 1999; 10: 339–344.
5. Gamucci T, Paridaens R, Heinrich B et al. Activity and toxicity of GI147211 in breast, colorectal and non-small-cell lung cancer patients: an EORTC-ECSG phase II clinical study. Ann Oncol 2000; 11: 793–797.
6. Sessa C, Wanders J, Roelvink M et al. Second-line treatment of small-cell lung cancer with the camptothecin-derivative GI147211: a study of the EORTC Early Clinical Studies Group (ECSG). Ann Oncol 2000; 11: 207–210.
7. Mayer LD, Cullis PR, Bally MB. Designing therapeutically optimized liposomal anti-cancer delivery systems: lessons from conventional liposomes. In Lassic D, Papahadjopoulos D (eds): Medical Applications of Liposomes. Amsterdam, The Netherlands: Elsevier Press 1998; 231–256.
8. Eisenhauer EA, Verweij J, Rothenberg ML et al. Phase I evaluation of liposomal topoisomerase I inhibitor, NX211, administered by three schedules to patients with advanced solid tumors. Proc Am Soc Clin Oncol 2001; 20 (Abstr 409).
9. Goetz AD, Hammond LA, Hao D et al. A Phase I and pharmacokinetic study of NX211 (liposomal lurtotecan) administered weekly × 4 every 6 weeks in patients with advanced solid tumors. Proc Am Soc Clin Oncol 2002; 21 (Abstr 388).
10. Miller AA, Hargis JB, Lilenbaum RC et al. Phase I study of topotecan and cisplatin in patients with advanced solid tumors: a Cancer and Leukemia Group B study. J Clin Oncol 1994; 12: 2743–2750.
11. Lilenbaum RC, Miller AA, Batist G et al. Phase I and pharmacologic study of continuous infusion topotecan in combination with cisplatin in patients with advanced cancer. J Clin Oncol 1998; 16: 3302–3309.
12. Raymond E, Burris HA, Rowinsky EK et al. Phase I study of daily times five topotecan and single injection of cisplatin in patients with previously untreated non-small cell lung carcinoma. Ann Oncol 1997; 8: 1003–1008.
13. Therasse P, Arbuck SG, Eisenhauer EA et al. New guidelines to evaluate the response to treatment in solid tumours. European Organization for Research and Treatment of Cancer, National Cancer Institute of United States, National Cancer Institute of Canada. J Natl Cancer Inst 2000; 92: 205–216.
14. Gamelin E, Allain P, Maillart P et al. Long term pharmacokinetic behavior of platinum after cisplatin administration. Cancer Chemother Pharmacol 1995; 37: 97–102.
15. Calvert AH, Grimshaw R, Poole C et al. Randomized phase II trial of two intravenous schedules of the liposomal topoisomerase I inhibitor, NX211, in women with relapsed epithelial ovarian cancer (OVCA): an NCIC CTG study. Proc Am Soc Clin Oncol 2002; 21 (Abstr 830).

The Oncologist®

Clinical Studies of Three Oral Prodrugs of 5-Fluorouracil (Capecitabine, UFT, S-1): A Review

M. Malet-Martino, R. Martino

Groupe de RMN Biomédicale, Laboratoire des IMRCP, Université Paul Sabatier, Toulouse, France

Key Words. *Xeloda® · Orzel™ · TS-1 · Toxicity · Phase I, II, III trials*

Learning Objectives

After completing this course, the reader will be able to:

1. Define the main oral prodrugs of fluorouracil.
2. Know the indications of the new oral prodrugs of fluorouracil.
3. Review the main toxicities and drug interactions of oral prodrugs of fluorouracil.
4. Evaluate the benefit(s) of using an oral prodrug of fluorouracil compared with classical treatments.

Access and take the CME test online and receive one hour of AMA PRA category 1 credit at CME.TheOncologist.com

Abstract

Although 5-fluorouracil (5-FU) was first introduced in 1957, it remains an essential part of the treatment of a wide range of solid tumors. 5-FU has antitumor activity against epithelial malignancies arising in the gastrointestinal tract and breast as well as the head and neck, with single-agent response rates of only 10%-30%. Although 5-FU is still the most widely prescribed agent for the treatment of colorectal cancer, less than one-third of patients achieve objective responses. Recent research has focused on the biomodulation of 5-FU to improve the cytotoxicity and therapeutic effectiveness of this drug in the treatment of advanced disease. As all the anticancer agents, 5-FU leads to several toxicities. The toxicity profile of 5-FU is schedule dependent. Myelotoxicity is the major toxic effect in patients receiving bolus doses. Hand-foot syndrome (palmar-plantar erythrodysesthesia), stomatitis, and neuro- and cardiotoxicities are associated with continuous infusions. Other adverse effects associated with both bolus-dose and continuous-infusion regimens include nausea and vomiting, diarrhea, alopecia, and dermatitis. All these reasons explain the need for more effective and less toxic fluoropyrimidines.

In the first part of this review, we briefly present the metabolic pathways of 5-FU responsible for the efficacy and toxicity of this drug. This knowledge is also necessary to understand the target(s) of biomodulation.

The second part is devoted to a review of the literature on three recent prodrugs of 5-FU, i.e., capecitabine, UFT (ftorafur [FTO] plus uracil), and S-1 (FTO plus 5-chloro-2,4-dihydroxypyridine plus potassium oxonate). The pharmacological principles that have influenced the development of these new drugs and our current knowledge of the clinical pharmacology of these new agents, focusing on antitumor activity and toxicity, are presented.

The literature was analyzed until March 2002. This review is intended to be as exhaustive as possible since it was conceived as a work tool for readers wanting to go further. *The Oncologist* 2002;7:288-323

Correspondence: M. Malet-Martino, Ph.D., Groupe de RMN Biomédicale, Laboratoire des IMRCP (UMR CNRS 5623), Université Paul Sabatier, 118, route de Narbonne, 31062 Toulouse Cédex, France. Telephone: 33-561-556271; Fax: 33-561-557625; e-mail: martino@chimie.ups-tlse.fr *Received January 24, 2002; accepted for publication April 5, 2002.*

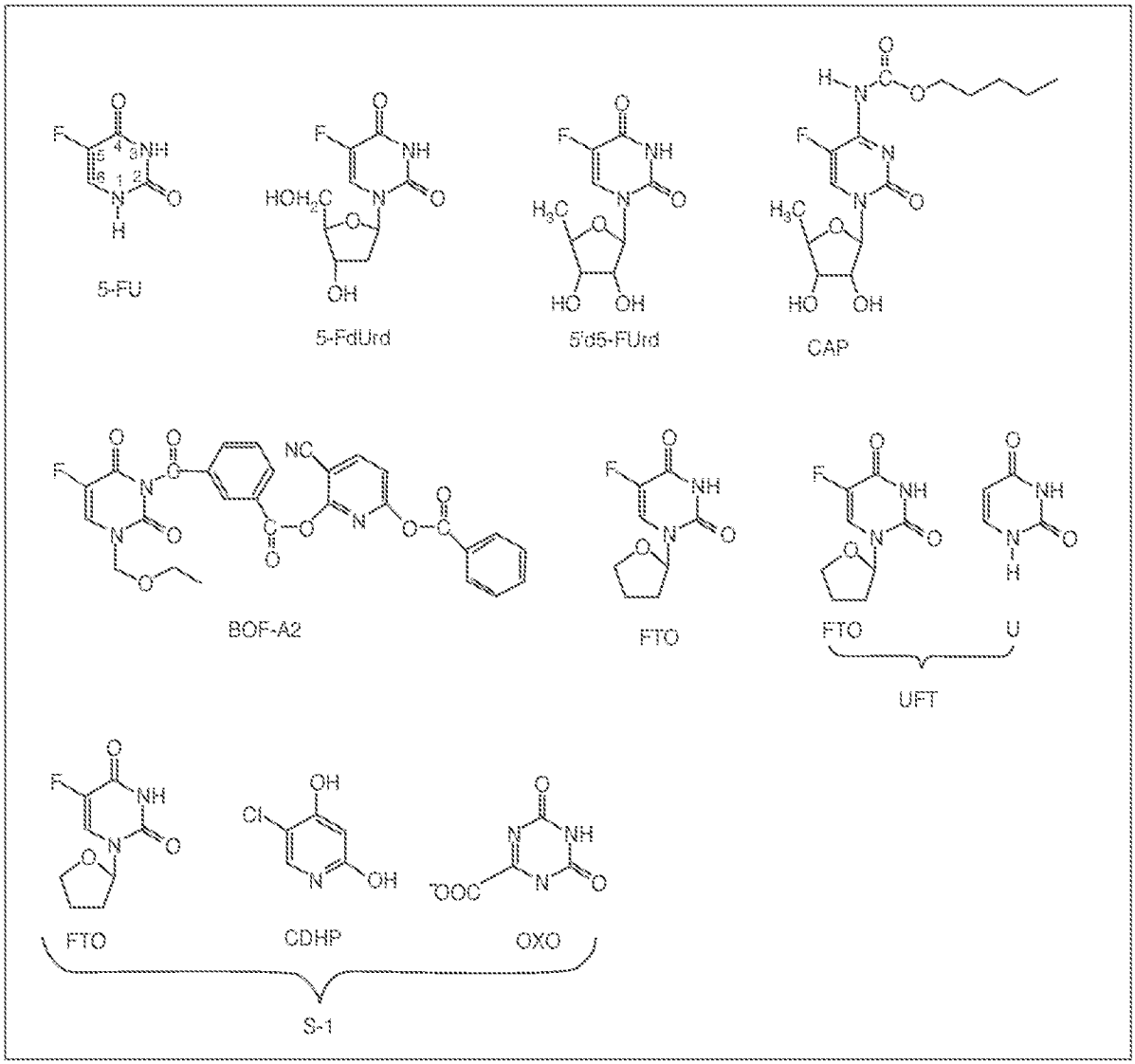

Figure 1. Structures of 5-fluorouracil and its prodrugs. *Abbreviations: 5-FU = 5-fluorouracil; 5-FdUrd = 5-fluoro-2′-deoxyuridine; 5′d5-FUrd = 5′-deoxy-5-fluorouridine; CAP = capecitabine; FTO = ftorafur; U = uracil; CDHP = 5-chloro-2,4-dihydroxypyridine; OXO = potassium oxonate; BOF-A2 = emitefur.*

5-Fluorouracil

5-fluorouracil (5-FU) (Fig. 1) is an example of a rationally designed anticancer agent. The observation that rat hepatomas utilized radiolabeled uracil more avidly than non-malignant tissues implied that the enzymatic pathways for utilization of uracil differ between malignant and normal cells [1]. *Heidelberger et al.* [2], thus, synthesized 5-FU in 1957 as an antimetabolite agent. In this molecule, the hydrogen atom in position 5 of uracil is replaced by the similarly sized atom of fluorine, and the molecule was designed to occupy the active sites of enzyme targets, thereby blocking metabolism in malignant cells. Although this antimetabolite is toxic, its efficacy makes it one of the most widely used agents against solid tumors. As several reviews have been devoted to 5-FU [3-13], we present briefly the main features of its metabolism, mechanism of action, and clinical uses.

Metabolism of 5-FU

After penetration into the cell, 5-FU is metabolized via two routes in competition with each other: the anabolic route, which gives rise to the active metabolites, and the catabolic route, which inactivates 5-FU and leads to elimination of the drug from the organism.

The Anabolic Route

The anabolism of 5-FU is rather complex (Fig. 2) with various parallel reactions. Initially, 5-FU can react in the following three ways. The first, which is quantitatively the least

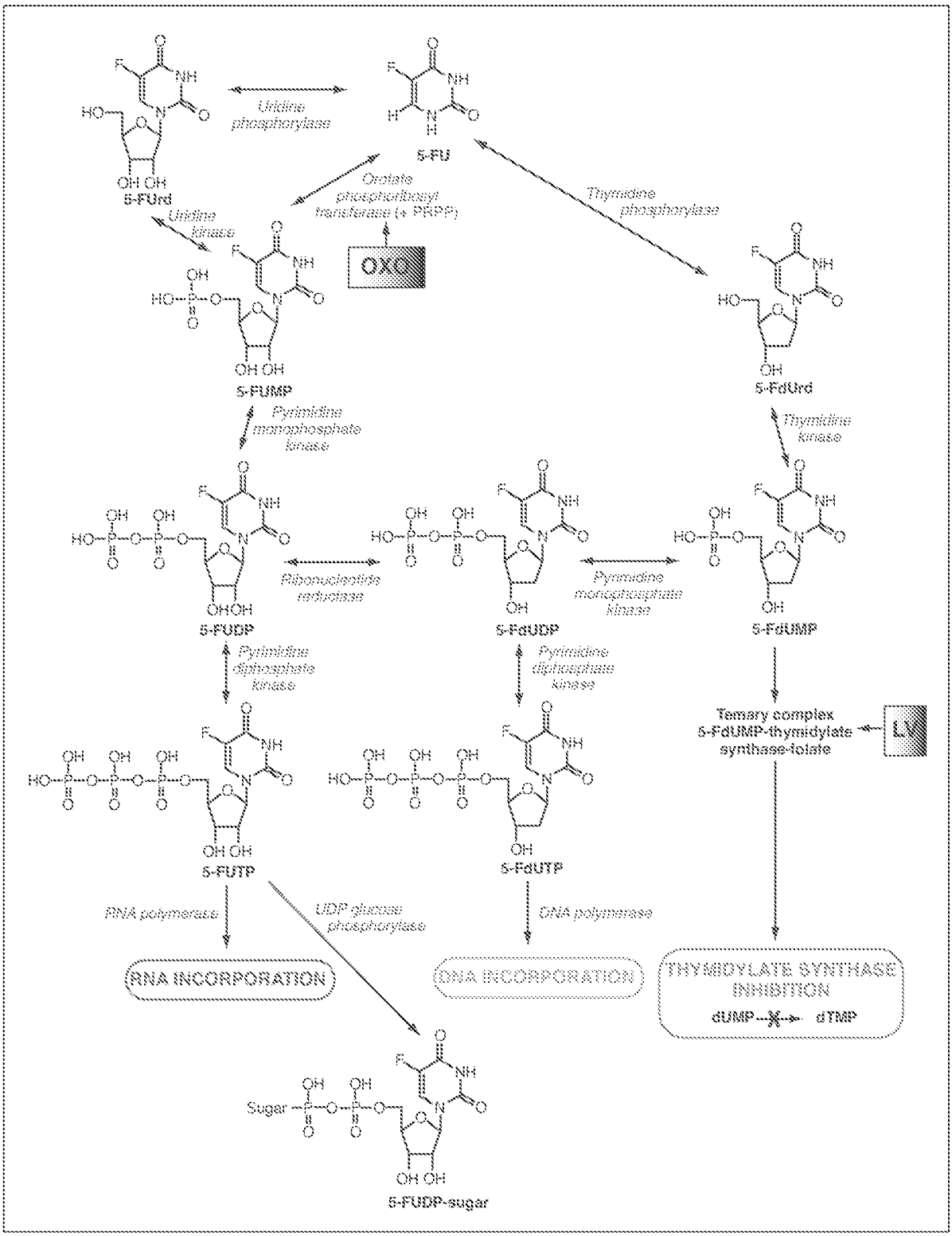

Figure 2. Intracellular anabolism of 5-fluorouracil (5-FU). *All the compounds are represented in neutral form. LV (leucovorin) and OXO (potassium oxonate) are biochemical modulators of 5-FU. Abbreviations: 5-FUrd = 5-fluorouridine; PRPP = 5′-phosphoribosyl-1-pyrophosphate; 5-FUMP = 5-fluorouridine-5′-monophosphate; 5-FUDP = 5-fluorouridine-5′-diphosphate; 5-FUTP = 5-fluorouridine-5′-triphosphate; 5-FUDP-sugars = 5-FU-nucleotide sugars; 5-FdUrd = 5-fluoro-2′-deoxyuridine; 5-FdUMP = 5-fluoro-2′-deoxyuridine-5′-monophosphate; 5-FdUDP = 5-fluoro-2′-deoxyuridine-5′-diphosphate; 5-FdUTP = 5-fluoro-2′-deoxyuridine-5′-triphosphate; dUMP = 2′-deoxyuridine-5′-monophosphate; dTMP = thymidine-5′-monophosphate.*

important, leads in two stages to the formation of 5-fluoro-2′-deoxyuridine-5′-monophosphate (5-FdUMP). The other two routes both form 5-fluorouridine-5′-monophosphate (5-FUMP), which can then undergo two successive phosphorylations to give 5-fluorouridine-5′-diphosphate (5-FUDP) and then 5-fluorouridine-5′-triphosphate (5-FUTP), which can be incorporated into RNA instead of uridine-5′-triphosphate (UTP). 5-FUTP can also be conjugated to sugars giving 5-FU-nucleotide sugars (5-FUDP-sugars).

5-FUDP and 5-FdUMP can be transformed into 5-fluoro-2′-deoxyuridine-5′-diphosphate (5-FdUDP), which is then phosphorylated to 5-fluoro-2′-deoxyuridine-5′-triphosphate (5-FdUTP). 5-FdUTP acts as a substrate for DNA polymerases and can thus be incorporated into DNA.

The Catabolic Route

After administration of 5-FU, more than 80% of the injected dose is degraded according to the scheme shown in Figure 3. The first stage of this degradation occurs very rapidly; under the action of dihydropyrimidine dehydrogenase (DPD), 5-FU is reduced to 5,6-dihydro-5-fluorouracil (5-FUH_2). This first stage effectively governs the rate at which 5-FU is available for anabolism. 5-FUH_2 is then cleaved to give α-fluoro-β-ureidopropionic acid (FUPA). A third stage leads to the formation of α-fluoro-β-alanine (FBAL), the major catabolite of 5-FU.

Most of the catabolic schemes of 5-FU stop at these metabolites, although recent studies using more sophisticated analytic methods have identified other catabolites of 5-FU. They include fluoride ion (F^-), N-carboxy-α-fluoro-β-alanine (CFBAL), three conjugates of FBAL with bile acids, two metabolites of FBAL by transamination (2-fluoro-3-hydroxypropanoic acid [FHPA] and fluoroacetate [FAC]) [14-20].

Mechanism of Action of 5-FU

As seen above, one of the routes of metabolism of 5-FU gives rise to 5-FUTP. The atom of fluorine replacing the hydrogen on position 5 of uracil is of comparable size, and during transcription, this fluoronucleotide thus mimics UTP and is recognized by RNA polymerases. This leads to the incorporation of 5-FU in all classes of RNA. It is thought that the full cytotoxicity stems from a combination of the numerous modifications of RNA due to incorporation of 5-FU rather than alteration of a single function.

The second way that 5-FU is activated, by the formation of 5-FdUMP, could be the most important. Indeed, this fluoronucleotide is an inhibitor of thymidylate synthase (TS), which is involved in the synthesis of DNA. TS is an obvious target for cytotoxic agents since thymidine is the only nucleotide precursor specific to DNA. In the presence of the cofactor 5,10-methylene tetrahydrofolate (MeTHF), serving as the methyl donor, TS and 2′-deoxyuridine-5′-monophosphate (dUMP) form a ternary complex, which enables transfer of a methyl group on carbon 5 of dUMP to form thymidine-5′-monophosphate (dTMP). Following 5-FU exposure and adequate 5-FdUMP formation, the methyl transfer does not take place because the fluorine atom in the C_5 position of 5-FdUMP is much more tightly bound than hydrogen. The enzyme is then trapped in a slowly reversible ternary complex. The formation of dTMP is therefore blocked, thereby decreasing the availability of thymidine-5′-triphosphate (dTTP) for DNA replication and repair. The "genotoxic stress" resulting from TS inhibition may activate programmed cell death pathways.

Throughout the 1970s, it was believed that the anticancer effect of 5-FU was the result of the two previous mechanisms. Later, it was reported that two other mechanisms could be partly responsible for the cytotoxic effect of 5-FU. The first one is the incorporation of 5-FU into DNA. The second mechanism is the alteration of the membrane function of 5-FU-treated cells. This is related to the formation of 5-FUDP sugars and their incorporation into membranes.

The extent to which any of these pathways predominates in human tumors is unknown and is likely to vary across tumor types and with different modes and doses of drug administration. Recent studies suggest that more prolonged exposure to low doses of 5-FU leads to cell death primarily via the TS-directed mechanism, whereas bolus administration of 5-FU results primarily in an RNA-mediated process of cell death [21-23].

Limitations of the Activity of 5-FU

The activity of 5-FU is markedly limited by its rapid degradation into 5-FUH_2 via the action of the cytosolic enzyme DPD, the first enzyme in the catabolic cycle of 5-FU (Fig. 3). It has been demonstrated that this enzyme deactivates more than 85% of the injected dose of 5-FU. Little drug is thus left for anabolism. Moreover, there is considerable variability in the activity of this enzyme between both normal and tumor tissues within one patient and among different patients [24, 25]. The bioavailability of 5-FU, especially after oral administration, is thus unpredictable. In some cases, where DPD possesses strong activity, little 5-FU is available and its efficiency is consequently low. On the other hand, if DPD possesses weak activity, levels of 5-FU are elevated, which may lead to toxicity from overdose.

There are also several other determinants of cellular sensitivity to 5-FU. Among these, the activity of enzymes involved in 5-FU anabolism, the availability of cofactors necessary for 5-FU activation (e.g., 5′-phosphoribosyl-1-pyrophosphate [PRPP]), the level of TS activity or expression,

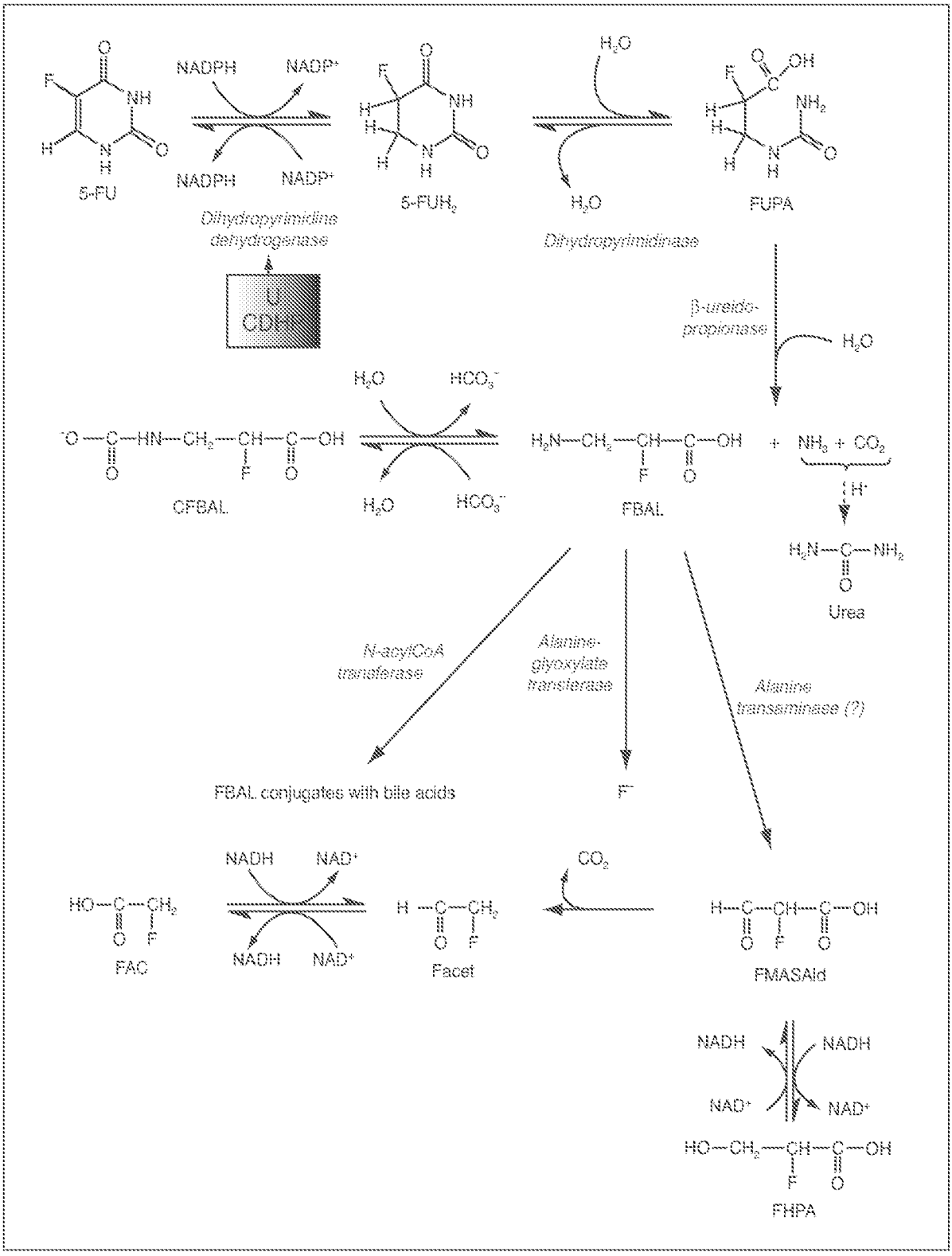

Figure 3. Catabolic pathway of 5-fluorouracil (5-FU). *All the compounds (except N-carboxy-α-fluoro-β-alanine (CFBAL)) are represented in neutral form. U (uracil) and CDHP (5-chloro-2,4-dihydroxypyridine) are inhibitors of the enzyme dihydropyrimidine dehydrogenase. Abbreviations: 5-FUH$_2$ = 5,6-dihydro-5-fluorouracil; FUPA = α-fluoro-β-ureidopropionic acid; FBAL = α-fluoro-β-alanine; F$^-$ = fluoride ion; FMASAld = fluoromalonic acid semi-aldehyde; FHPA = 2-fluoro-3-hydroxypropanoic acid; Facet = fluoroacetaldehyde; FAC = fluoroacetate.*

the size of intracellular reduced folate and endogenous dUMP pools, the extent of 5-FUTP incorporation into RNA and 5-FdUTP into DNA, and the intratumor activity of DPD have been identified as important in determining response to 5-FU chemotherapy in patients with solid tumors [26].

5-FU in Chemotherapy

Since its introduction more than 40 years ago, 5-FU has become a component of the standard therapy for a variety of malignancies, including gastrointestinal cancers, head and neck cancer, and breast cancer.

5-FU is a small molecule with a pK_A (8.0) that should predict excellent absorption and bioavailability. However, the use of oral 5-FU was abandoned decades ago because of its irregular absorption. Plasma levels of 5-FU are quite unpredictable after oral administration with marked intra- and interindividual differences due to the variable activity of DPD, especially in the gastrointestinal mucosa [27, 28]. This effectively rules out oral treatment with 5-FU.

Until recently, the standard regimen for treatment with 5-FU was 400-600 mg/m^2 administered by i.v. bolus once a week for 6 weeks or for five consecutive days every 4 or 5 weeks. However, since the half-life ($t_{1/2}$) of 5-FU is low (5 to 20 min) [29], tumor cells are only exposed to the active principle for a short time. The development of permanent venous access devices and portable infusion pumps has allowed continuous infusion of 5-FU over prolonged periods, designed to prolong exposure of cells to the drug and so confer higher activity [30, 31]. Indeed, the initial clinical results bore out this assumption and showed a twofold increase in response rate for continuous infusion compared with treatment by bolus, with a comparable survival [32]. In 1998, a meta-analysis of six randomized trials on 1,219 patients with colorectal cancers treated by either continuous i.v. infusion of 5-FU over 120 hours or i.v. bolus was published [33]. The response rate was clearly higher for the first than for the second regimen (22% versus 14%). Median survival time (MST) was comparable for the two treatments (12.1 months with bolus treatment versus 11.3 months with infusional therapy).

The toxicity profile of 5-FU is schedule dependent. For the bolus regimen, toxicities include myelosuppression, oral mucositis, and gastrointestinal disturbances (diarrhea, nausea, vomiting) due to phosphorylation of 5-FU into 5-FUMP by orotate phosphoribosyl transferase (OPRT) in the digestive tract [34]. For the continuous regimen, toxic reactions include the hand-foot syndrome (HFS, i.e., dermal pain in hands and feet), which was observed in many cases, but less hematologic and gastrointestinal toxicity. Cardiotoxicity and neurotoxicity may be observed during treatment with 5-FU (2%-5% of cases), but symptoms disappear on stopping the treatment, and resumption of treatment with a lower dose is generally well tolerated.

Treatment by continuous i.v. infusion thus presents advantages compared with treatment by bolus i.v. with respect to both response rate (RR) and toxicity, although mean survival is no better. Despite these benefits, the complex nature of the treatment (requirement for continuous infusion pumps), its high cost, and the added risks mean that it is used relatively infrequently, and i.v. bolus remains the conventional treatment.

To increase the activity of 5-FU, various researchers have proposed utilization of biochemical modulators. A biochemical modulator is a pharmacological agent designed to enhance the biological effect of the chemotherapy, either by selectively increasing the antitumor action or by selectively protecting the host. A 5-FU modulator can act at two levels: A) on the anabolic pathways, which will increase selectively the antitumor activity, or B) on catabolism to enhance bioavailability of the active principle as well as minimize toxic effects.

Several agents modulating the metabolism of 5-FU have been tested. The most efficient during treatment with 5-FU is the calcium salt of folinic acid, also called leucovorin (LV). LV is an intracellular source of reduced folates, which stabilize the ternary complex that they form with TS and 5-FdUMP, and thus increase and prolong the inhibition of TS and so enhance the efficacy of the drug. This modulator thus acts on the anabolism of 5-FU.

The modulation of 5-FU by LV has been extensively developed, and a meta-analysis of 1,381 patients in nine randomized clinical trials has clearly demonstrated its superiority over bolus 5-FU, with a response rate of 23% versus 11%. However, this improvement in RR failed to convey a significant survival advantage; MST in patients treated with 5-FU alone was 11 months compared with 11.5 months in those given 5-FU plus LV [35].

At the present time, the combination 5-FU/LV is considered the standard chemotherapy for colon cancer in both advanced disease and in the adjuvant setting. The two common regimens, which often serve as the control arms for phase III trials evaluating new agents in colorectal cancer, are A) 5-FU (370-425 mg/m^2/day) + LV (low dose: 20 mg/m^2/day or high dose: 200 mg/m^2/day) administered by i.v. bolus during five consecutive days every 4 to 5 weeks [36], and B) 5-FU (600 mg/m^2/week) + LV (500 mg/m^2/week) administered by i.v. bolus during six consecutive weeks and repeated every 8 weeks [37].

Although these two regimens are associated with similar response rates and survival, the toxicities observed with each regimen differ. Dose-limiting toxicities associated with the daily administration are primarily mucositis and neutropenia (affecting 24% and 29% of patients, respectively),

whereas the predominant toxicity seen in patients on the weekly regimen is diarrhea (32% of patients) [38]. Twenty percent to 30% of the patients on these 5-FU/LV regimens require hospitalization for toxicity-related events.

Conclusion

As discussed above, 5-FU is relatively efficient, but has numerous drawbacks. First of all, it is relatively toxic, causing myelosuppression and gastrointestinal disorders, due mainly to phosphorylation of 5-FU in the digestive tract. Toxicity also derives from the lack of selectivity of the drug toward tumors. Its efficiency is limited by the short $t_{1/2}$ of 5-FU in plasma, by its low bioavailability due to the activity of DPD, and by the resistance to 5-FU of some tumors with strong expression of TS or low reserves of reduced folates. Its mode of administration is also a problem. Any i.v. administration, whether by bolus or continuous infusion, requires the presence of the patient in a hospital, whereas oral treatment can be taken at home with a corresponding reduction in stress. Furthermore, i.v. administration is not without risk of complications (venous thrombosis or infection around the catheter).

For these reasons, one of the challenges of cancer research is the development of prodrugs of 5-FU that diminish or circumvent some of these disadvantages: reduction in toxicity by avoiding certain routes of degradation (prodrugs that are not a substrate for the enzymes of degradation) or by targeting the tumor site (prodrugs that liberate the active principle selectively in tumor cells); enhancement of activity by reducing catabolism (use of DPD inhibitors) or by increasing anabolism, and improvement in quality of life of the patient by developing oral prodrugs.

Prodrugs of 5-FU

What is a Prodrug?

A prodrug is defined as a pharmacologically inactive compound that is converted into an active agent by a metabolic biotransformation. The objective is a chemical modification of the antitumor agent to render it temporarily inactive. In vivo, via the action of enzyme(s), this prodrug decomposes, liberating the active principle. In most cases, a judiciously selected chemical group is bound covalently to the active principle. This group must be nontoxic, biologically inactive, and labile in vivo. This group will often govern the solubility of the prodrug, its stability, the rate at which it liberates the active principle, and the particular enzyme(s) required for its transformation.

The prodrugs of 5-FU are characterized by a pyrimidine ring with a fluorine atom in position 5. They differ from 5-FU in a variety of chemical alterations. Their main benefit is that of oral administration. They are designed to be well absorbed intact from the gastrointestinal tract and subsequently enzymatically converted into 5-FU in the liver or within the tumor itself, in order to expose the tumor to 5-FU for a longer time but at lower concentrations than those observed after an i.v. bolus, hence minimizing toxicity. New orally administered fluoropyrimidines thus provide protracted 5-FU delivery, which offers advantages that include schedule flexibility and reductions in professional health care resource requirements, administration costs, and toxicity-related hospitalization. These advantages may reduce the overall cost of treatment [39].

In a study of 103 patients, 89% stated a preference for oral therapy. Reasons for this choice included convenience and fewer problems than with venous access. Nevertheless, 70% of survey respondents were unwilling to accept a lower RR with oral therapy [40]. Thus, although convenience is an important potential advantage, therapeutic equivalence or superiority is required for oral agents.

Each agent has been developed according to a specification with a well-defined mechanism for liberation of the active principle. Some are designed to function alone and others require coadministration of a modulator. The aim is to mimic the pharmacokinetics of 5-FU administered by continuous i.v. infusion, not only by virtue of their chemical structure, but also by careful choice of dosage.

Prodrugs in Clinical Trials or Already Used in Clinic

Over the years, many attempts have been made to synthesize more effective fluoropyrimidine drugs (Fig. 1). 5-fluoro-2′-deoxyuridine (5-FdUrd; Floxuridine®) represents the first generation. It is much more efficiently metabolized by the liver than 5-FU, which explains why its major clinical use is hepatic arterial administration for liver metastases of colorectal cancer [41]. Even if severely compromised by the 5-FdUrd-induced hepatoxicity, it has been demonstrated in a meta-analysis of randomized trials that hepatic arterial administration of 5-FdUrd is superior, in terms of RR and survival, to i.v. treatment [42]. Recently, a high RR (74%) was observed when colorectal cancer patients with unresectable hepatic metastases were treated with concurrent systemic CPT-11 (irinotecan) and hepatic arterial infusion of 5-FdUrd and dexamethasone [43].

Ftorafur (FTO, 1-(2-tetrahydrofuryl)-5-fluorouracil, Tegafur or Futraful) and 5′-deoxy-5-fluorouridine (5′d5-FUrd, doxifluridine or Furtulon®), the second generation, were developed with the hope of permitting oral administration. The third-generation compounds include the enzymatically activated prodrug, capecitabine, and the DPD-inhibitory compounds (UFT [FTO + uracil] eniluracil, S-1 [FTO plus 5-chloro-2,4-dihydroxypyridine plus potassium oxonate], and BOF-A2).

The industrial sponsor of emiluracil discontinued development of the drug in 2000, and further clinical trials of the 5-FU/emiluracil have been abandoned [44, 45]. Several reviews on the new fluoropyrimidine agents have been recently published; only some of the most recent are cited [44-59].

Capecitabine

N^4-pentyloxycarbonyl-5′-deoxy-5-fluorocytidine, more commonly called capecitabine (CAP) (Fig. 1) or Xeloda®, is a cytotoxic agent that is administered orally and should be activated preferentially in tumors. This carbamate of fluoropyrimidine was synthesized in the 1990s by Japanese researchers [60] as an oral formulation designed to circumvent the unacceptable toxicity of 5′d5-FUrd. The main limitation of 5′d5-FUrd derives from its gastrointestinal toxicity, attributed to liberation of 5-FU in the small intestine under the action of thymidine phosphorylase (TP) [61], a tumor-associated angiogenesis factor [62]. CAP was thus designed as a prodrug of 5′d5-FUrd that could not be metabolized by TP in the intestine.

Indeed, after oral administration, CAP crosses the gastrointestinal barrier intact and is rapidly and almost completely absorbed [63, 64]; thus, diarrhea should not occur with its use. It is subsequently converted into 5-FU in a three-stage mechanism involving several enzymes (Fig. 4). In the first step, it is metabolized into 5′-deoxy-5-fluorocytidine (5′-dFCR) by hepatic carboxylesterase. 5′-dFCR is then deaminated into 5′d5-FUrd by cytidine deaminase, mainly localized in liver and tumor tissues. Finally, 5′d5-FUrd is transformed into 5-FU under the action of TP, an enzyme with higher activity in tumor than in normal tissues. Higher levels of 5-FU are thus produced within tumors with minimal exposure of healthy tissue to 5-FU [65]. It must be underlined that a high phosphorylase activity is good for activation of CAP to 5-FU but bad for activation of 5-FU nucleoside derivatives up to the fluoronucleotides level (Fig. 2). This reaction is in fact bidirectional, but the main direction is toward breakdown of the nucleosides to the bases [66].

In theory, this prodrug of 5-FU should have two main advantages, which may translate into an improved therapeutic index. First, it should increase the concentration of the active principle at the tumor site, and so, should have greater activity; second, it should decrease the concentration of drug in healthy tissues with a consequent reduction in systemic toxicity.

A pharmacokinetic study was carried out to verify these expectations [67]. Nineteen patients with colorectal cancers who were undergoing elective resection of either a primary lesion or liver metastases were treated prior to surgery with 1,255 mg/m² of CAP administered twice daily over 5 to 7 days. Analysis of samples removed on operation showed a higher concentration of 5-FU in the tumors than in adjacent healthy tissues. 5-FU concentrations in the colorectal resections were on average 3.2 times greater than in the normal bowel and 21 times greater than in plasma. In liver metastases, the ratio of 5-FU concentrations was 1.4 when metastases

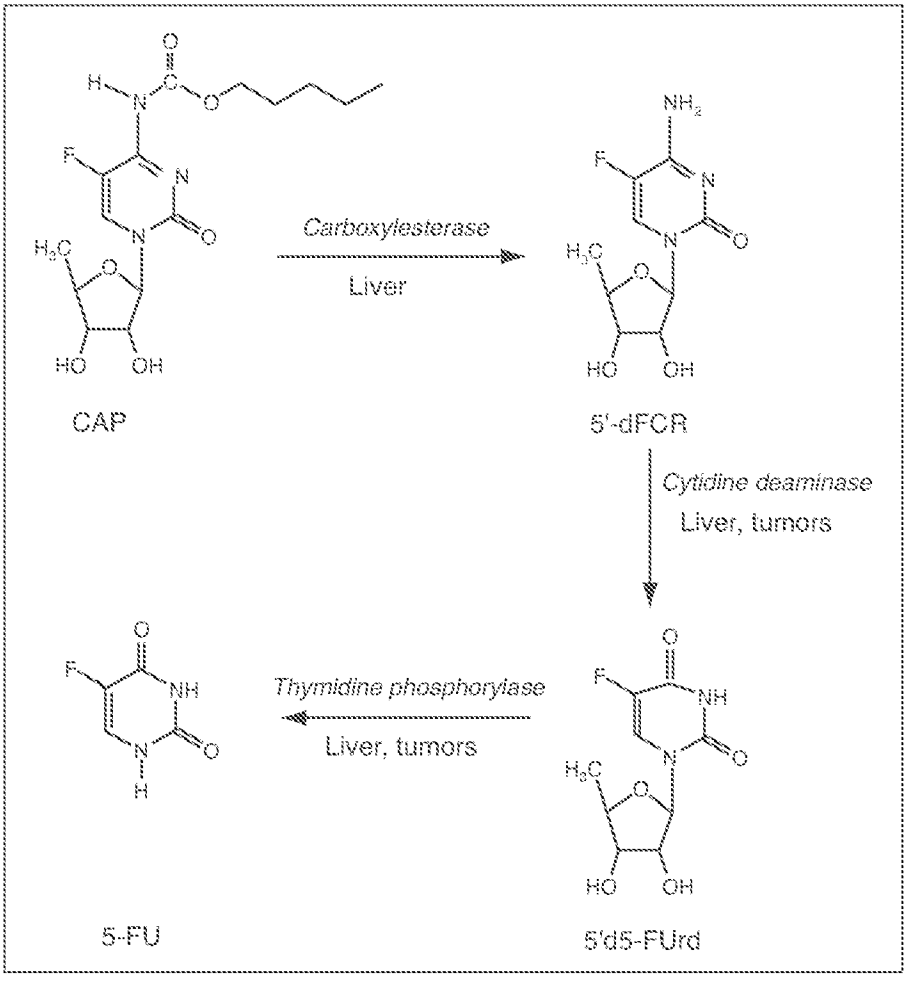

Figure 4. Metabolic pathway of capecitabine (CAP). Abbreviations: 5′-dFCR = 5′-deoxy-5-fluorocytidine; 5′d5-FUrd = 5′-deoxy-5-fluorouridine; 5-FU = 5-fluorouracil.

were compared with normal liver (not statistically significant) and 9.9 when compared with plasma. These data are explained by the fact that the activity of TP is four times higher in colorectal tumor tissue than in healthy colorectal tissue, whereas it is similar in liver metastasis and healthy liver.

These encouraging findings have prompted a number of phase I trials of this drug [68-72]. As LV is frequently used during treatment with 5-FU to enhance inhibition of TS, *Cao et al.* [73] proposed using LV to increase the efficacy of CAP. Their preclinical study confirmed this hypothesis and has led to a phase I clinical trial with LV. Initial clinical studies showed that the maximum-tolerated doses (MTDs) of CAP were schedule dependent, with higher doses possible by employing breaks of 1-2 weeks after 2 weeks of continuous therapy. The dose-limiting toxicities (DLTs) in phase I trials were similar to those observed with continuous infusion of 5-FU, i.e., mainly diarrhea and HFS, but also nausea, vomiting, mucositis, leukopenia, and abdominal pain. The occurrence of bowel toxicity was disappointing as, in theory, it should have been avoided as CAP is not metabolized in the intestinal mucosa. In a recent study on 41 patients with metastatic colorectal cancer treated with the intermittent regimen of CAP at a dose of 2,500 mg/m^2/day, HFS developed in 28 patients (68%; 95% confidence interval [CI] 52%-82%), with five patients (18%) having grade 1, 20 (71%) grade 2, and three (11%) grade 3. HFS starts within the first two cycles of therapy. Dose reduction leads to complete resolution in all cases [74]. The addition of pyridoxine (~200 mg/day) for ameliorating the symptoms of CAP-induced HFS allows for the administration of higher doses of CAP [75]. "Bag balm," which is a topical petroleum-lanolin based ointment with an antiseptic ingredient, hydroxyquinoline sulfate, also improved HFS [76].

Phase II trials have evaluated both continuous and intermittent schedules of CAP, mainly in breast cancer (Table 1) [77-95]. The addition of LV resulted in a greater rate of toxicities, in particular diarrhea and HFS, without any perceptible greater antitumor efficacy. Monotherapy with CAP, given in an intermittent schedule was, thus, chosen for further development.

Two large randomized phase III trials enrolling patients with advanced colorectal carcinoma were recently conducted. Both trials had similar study rationale, objectives, and design. The primary end point evaluated was RR, and it was hoped that at least equivalent RR would be seen in the two treatment arms. Secondary end points included efficacy and safety profile, quality of life, and medical care utilization. *Van Cutsem et al.* [96] compared CAP administered at 2,500 mg/m^2/day in two divided doses for 2 weeks every 3 weeks with 5-FU, 425 mg/m^2, plus LV, 20 mg/m^2, administered daily by i.v. infusion for 5 days every 28 days. The study conducted in Europe, Israel, Australia, New Zealand, and Taiwan enrolled 602 patients divided equally between the two treatment arms. The overall RR was statistically equivalent for patients treated with CAP (18.9%, 95% CI 14.7%-23.8%) and with 5-FU/LV (15.0%, 95% CI 11.1%-19.5%). The median duration of response (MDR) in responding patients was 7.2 months in the CAP group and 9.4 months in the 5-FU/LV group. Median time to disease progression (5.2 months for the CAP group versus 4.7 months for the 5-FU/LV group), median time to treatment failure (4.2 months for the CAP group versus 4.0 months for the 5-FU/LV group), and median overall survival (13.2 months for the CAP group versus 12.1 months for the 5-FU/LV group) were equivalent for both groups. Figure 5 depicts the frequencies of adverse reactions of any grade that occurred in more than 15% of patients. Patients in the CAP group experienced significantly less stomatitis and alopecia of any grade compared with those in the 5-FU/LV group, whereas HFS was more frequent in patients treated with CAP. The frequency of grade 3-4 diarrhea was similar in both arms, but the 5-FU/LV regimen was associated with considerably more grade 3-4 stomatitis and neutropenia, and dose reductions were required in 35.1% of patients. HFS was rare among the 5-FU/LV patients but necessitated dose reduction in 27.3% of the CAP patients. Few patients experienced grade 4 toxicities in either group. A later onset and a lower incidence of grade 3 diarrhea, stomatitis, nausea, vomiting, alopecia, HFS, and neutropenia were observed in the CAP group. CAP patients required substantially fewer hospital visits for drug administration and spent fewer days in hospital for the management of treatment-related adverse events. In addition, CAP reduced the requirement for expensive drugs, in particular antimicrobial fluconazole and 5-HT3 antagonists to manage adverse events. Globally, the CAP treatment of colorectal cancer patients resulted in a substantial resource savings relative to the regimen of 5-FU/LV [97].

Hoff et al. [98] conducted a similar study. CAP was administered orally at 2,500 mg/m^2/day twice daily for 2 weeks every 3 weeks. 5-FU/LV was administered according to the Mayo Clinic regimen, consisting of a rapid i.v. injection of 20 mg/m^2 LV followed by an i.v. bolus injection of 425 mg/m^2 5-FU daily, days 1 to 5 every 4 weeks. The study enrolled 605 patients, with 302 patients randomized to the CAP arm and 303 patients randomized to the 5-FU/LV arm, and was conducted in the U.S., Canada, Mexico, and Brazil. Researchers found a significant difference in the RR (24.8% for CAP versus 15.5% for 5-FU/LV). When an independent review committee reviewed these results, statistical significance was maintained and, in fact, improved with an RR of 25.8% for the CAP arm and 11.6% for the 5-FU/LV arm. However, duration of response (9.1 months versus 9.5 months), median time to disease progression (4.3 months

Table 1. Phase II trials on patients treated with capecitabine (CAP)

Study (year)	*n* of evaluable patients (age), disease	CAP dose	LV dose	Response rate (95% CI)	Median duration of response (MDR); median survival time (MST)	Main side effects
O'Reilly et al. [77] (1998)	22 anthracycline-resistant breast cancer	2,510 mg/m²/d[a]		36% (17%-59%)		
Blum et al. [78] (1999)	162 paclitaxel-resistant breast cancer	2,510 mg/m²/d[a]		20% (14%-28%)	MDR 8.1 mo MST 12.8 mo	Diarrhea, hand-foot syndrome
Cervantes et al. [79] (2000)	32 taxane-resistant breast cancer	2,500 mg/m²/d[a]		16%		
Wong et al. [80] (2000)	22 refractory breast cancer	2,500 mg/m²/d[a]		27%		Hand-foot syndrome
Watanabe et al. [81] (2001)	55 docetaxel-resistant breast cancer	1,657 mg/m²/d[b]		20% (10%-33%)	MDR 221 d	Hand-foot syndrome, hyperbilirubinemia
Blum et al. [82] (2001)	74 taxane-resistant breast cancer	2,510 mg/m²/d[a]		26% (16%-36%) 27% for paclitaxel-resistant patients; 20% for docetaxel-resistant patients	MDR 8.3 mo MST 12.2 mo	Hand-foot syndrome, diarrhea, stomatitis
Thuss-Patience et al. [83] (2001)	100 anthracycline- and taxane-resistant breast cancer	2,500 mg/m²/d[a]		18%		Hand-foot syndrome, nausea, vomiting, diarrhea
Sundaram et al. [84] (2000)	7 breast cancer progressing after HDC-ASCS	2,500 mg/m²/d[a]		71%		Hand-foot syndrome
Jakob et al. [85] (2001)	13 breast cancer progressing after HDC-ASCS	2,500 mg/m²/d[a]		54% (26%-81%)	MST 454 d	Hand-foot syndrome, granulocytopenia, nausea, diarrhea, fever
O'Shaughnessy et al. [86] (2001)	61 (≥55 y) untreated breast cancer	2,510 mg/m²/d[a]		30% (19%-43%) 3 CR	MST 19.6 mo	Hand-foot syndrome, diarrhea
Kusama et al. [87] (2001)	46 breast cancer	1,657 mg/m²/d[b]		28% (16%-44%)	MDR 161 d	Hand-foot syndrome, hyperbilirubinemia
Procopio et al. [88] (2001)	27 (≥65 y) breast cancer	2,500 mg/m²/d[a]		29%		Diarrhea, vomiting hand-foot syndrome, asthenia, stomatitis
Vasey et al. [89] (2000)	15 ovarian cancer	2,500 mg/m²/d[a]		7%		Hand-foot syndrome, diarrhea
Wenzel et al. [90] (2002)	23 renal cell cancer after failing immunotherapy	2,500 mg/m²/d[a]		9%		Hand-foot syndrome, anemia
Lozano et al. [91] (2000)	55 hepatobiliary carcinoma	2,000 mg/m²/d[a]		16% (8%-24%)	MST not reached; 1-year survival rate 70%	Hand-foot syndrome, thrombocytopenia
Cartwright et al. [92] (2002)	42 pancreatic cancer	2,500 mg/m²/d[a]		9.5% (3%-21%)	MDR 208, 260, and 566 d	Hand-foot syndrome, diarrhea, nausea
Heff et al. [93] (2000)	19 5-FU-resistant colorectal cancer	2,500 mg/m²/d[a]		0%		Nausea, vomiting, diarrhea, abdominal pain
Van Cutsem et al. [94] (2000)	109: colorectal cancer — arm A: 39; arm B: 35; arm C: 35	1,331 mg/m²/d[a,c] 2,510 mg/m²/d[a,c] 1,657 mg/m²/d[a,c]	60 mg/d[a]	21% (9%-36%) 24% (11%-41%) 23% (10%-40%)		Diarrhea, hand-foot syndrome
Koizumi and *Taguchi* [95] (2001)	31 gastric cancer	1,657 mg/m²/d[b]		19% (8%-38%)	MST 248 d	Hyperbilirubinemia, skin rash, lymphopenia

[a]Administered orally in two daily doses for 14 days every 21 days (intermittent regimen)

[b]Administered orally for 21 days every 28 days

[c]Administered orally in two daily doses every day for 12 weeks (continuous regimen)

[d]Median duration of treatment: 109 days in arm A, 145 days in arm B, and 130 days in arm C; response assessed after 6 and 12 weeks of treatment

Abbreviations: LV = leucovorin; CI = confidence interval; HDC-ASCS = high-dose chemotherapy with autologous stem cell support; CR = complete response

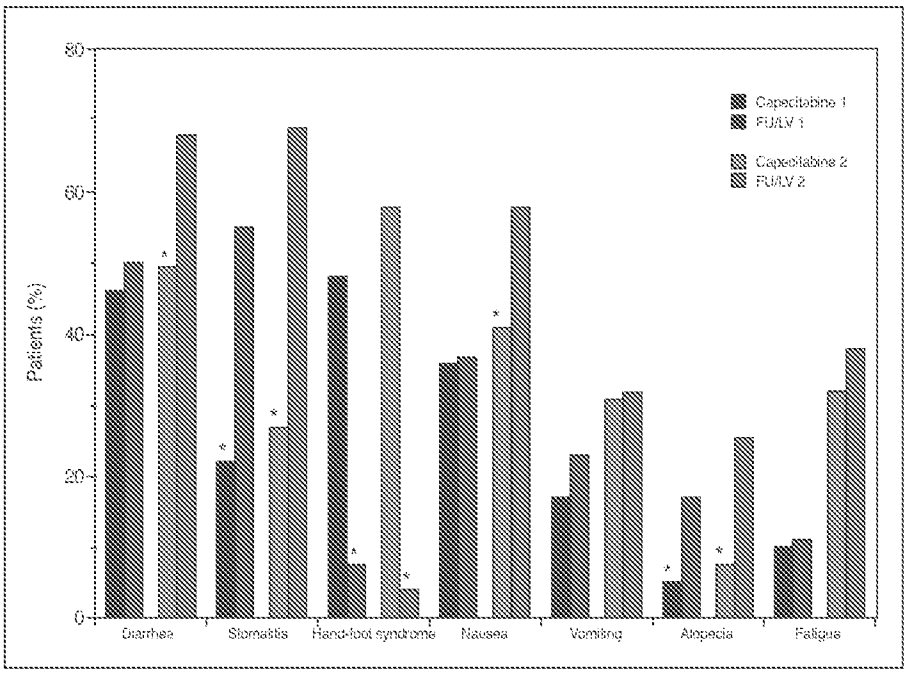

Figure 5. Adverse reactions of any grade that occurred in >15% (bars 1) or ≥20% (bars 2) of patients treated with capecitabine or the combination 5-fluorouracil leucovorin (adapted from [96] and [98]). **Statistically significant difference ($p < 0.00001$ for bars 1 or $p < 0.0002$ for bars 2).*

versus 4.7 months), and median overall survival time (12.5 months versus 13.3 months) were not significantly different. The safety profile significantly favored CAP (Fig. 5). Similar rates of grade 3-4 diarrhea were observed in both arms, but increased neutropenia and stomatitis were reported in the 5-FU/LV arm. However, grade 3 HFS occurred in 18% of the CAP patients versus 1% of the 5-FU/LV group. Fewer patients in the CAP group required hospitalization for adverse reactions than in the 5-FU/LV group (11.4% versus 20.4%). Dose reduction for adverse reactions was required in 40.5% of patients in the CAP group (most commonly for HFS or diarrhea) and 49.3% of patients in the 5-FU/LV group (most commonly for stomatitis or diarrhea).

When data from the two clinical trials were pooled and analyzed, a statistically significant improvement in the overall RR was observed (25.7% for the CAP patients versus 16.7% for the 5-FU/LV group). This result was confirmed by an independent review committee (RR 22.4% for the CAP patients versus 13.2% for the 5-FU/LV group). In patients who had received prior adjuvant treatment, the RR with CAP was 21.1% compared with only 9.0% in patients treated with 5-FU/LV. Median time to disease progression was 4.6 months for CAP and 4.7 months for the 5-FU/LV group. The median survival was 12.9 months in the CAP group and 12.8 months in the 5-FU/LV group. Median time to treatment failure was also similar (4.2 months with CAP versus 3.6 months with 5-FU/LV). Response to treatment occurred as early in patients treated with CAP as in patients treated with 5-FU/LV (median time to response: 1.7 months versus 2.4 months, respectively). Significantly ($p < 0.001$) lower incidences of diarrhea (48% versus 58%), stomatitis (24% versus 62%), nausea (38% versus 47%), and alopecia (6% versus 21%) were observed with CAP compared with 5-FU/LV. The incidences of vomiting and fatigue were similar in both treatment groups. The only adverse event that occurred more frequently with CAP than with 5-FU/LV was HFS (all grades: 53% versus 6%; grade 3: 17% versus 1%). Grade 3/4 stomatitis occurred in only approximately 2% of patients receiving CAP, but was a major side effect of 5-FU/LV treatment (15%, $p < 0.0001$). Grade 3 or 4 neutropenia was significantly more common in the 5-FU/LV group than in the CAP group (21.1% versus 2.2%). The incidence of hyperbilirubinemia was higher in patients receiving CAP. Hospitalization for treatment-related adverse events was significantly less frequent in the CAP group than in the 5-FU/LV group (11.6% versus 18.0%, respectively; $p = 0.002$). Dose reductions for adverse reactions occurred less frequently with CAP than with 5-FU/LV (34% versus 42%, respectively; $p < 0.004$). Furthermore, dose reductions for adverse events occurred later in patients receiving CAP than in patients treated with 5-FU/LV, with a median time to dose reduction of 2.5 months versus 1.2 months [99].

The same regimen of CAP is being evaluated in a large-scale adjuvant trial, which is expected to recruit approximately 1,700 Duke's C colon cancer patients (X-ACT study, Roche; USA). Two large randomized phase III trials have also been designed to evaluate CAP as first-line therapy in patients with previously untreated metastatic breast cancer [100].

Since the conversion of CAP to 5-FU is mediated by TP, the combination of CAP with agents that upregulate TP concentrations in human cancer xenograft models, such as paclitaxel and docetaxel [101], cyclophosphamide (CP) [102], and x-ray irradiation [103], offers the potential to improve efficacy further. Moreover, a study on breast cancer models reported that the most potent and synergistic activity was observed when docetaxel was given on day 8 [104]. Numerous phase I trials with combinations containing CAP and other anticancer agents (taxanes, oxaliplatin, CPT-11, vinorelbine, gemcitabine, R115777 [a farnesyl transferase

Table 2. Phase II trials conducted on patients treated with capecitabine (CAP) combined with other anticancer agents

Study (year)	*n* of evaluable patients, disease	CAP dose	Other compound(s) administered	Response rate (95% CI)	Main side effects
Batista et al. [130] (2000)	64 breast cancer	2,000 mg/m²/d[a]	Paclitaxel 175 mg/m² day 1 every 3 weeks	63% (50%-74%)	Neutropenia, hand-foot syndrome
Meza et al. [131] (2001)	37 metastatic breast cancer	1,650 mg/m²/d[a]	Paclitaxel 175 mg/m² day 1 every 3 weeks	49%	Neutropenia, hand-foot syndrome, fatigue
Tonkin et al. [132] (2001)	11 anthracycline-pretreated metastatic breast cancer	1,800 mg/m²/d[a]	Docetaxel 30 or 36 mg/m² every week	50%	Asthenia, nail loss, diarrhea, neutropenia, mucositis, nausea
Kim et al. [133] (2001)	16 previously untreated advanced gastric cancer	2,500 mg/m²/d[a]	Cisplatin 60 mg/m² i.v. day 1 every 3 weeks	68% (45%-91%)	Neutropenia, anemia, hand-foot syndrome, thrombocytopenia
Borner et al. [134] (2001)	57 advanced or metastatic colorectal cancer	2,500 mg/m²/d[a]	Oxaliplatin 130 mg/m² i.v. day 1 every 3 weeks	44% for previously untreated patients (34); 22% for previously treated patients (23)	Diarrhea, nausea, vomiting
Akhtar et al. [135] (2001)	9 untreated advanced NSCLC	2,000 mg/m²/d[b]	Carboplatin AUC = 5 30-min i.v. infusion day 1 every 4 weeks	44%	Diarrhea
Cassata et al. [136] (2001)	35 (arm A: 18; arm B: 17) untreated advanced colorectal cancer	2,500 mg/m²/d[a]	CPT-11 every 3 weeks 90-min i.v. infusion Arm A: 300 mg/m² day 1 Arm B: 150 mg/m² days 1 and 8	71% (21 evaluable patients)	Arm A: diarrhea, hand-foot syndrome, anemia, neutropenia; Arm B: nausea, neutropenia, diarrhea
Domenech et al. [137] (2001)	12 metastatic breast cancer	2,000 mg/m²/d[a]	Vinorelbine 18 mg/m²/wk	58%	Neutropenia
Campos et al. [138] (2001)	21 advanced pancreatic cancer	1,500 mg/m²/d[a]	Gemcitabine 1,000 mg/m² i.v. days 1 and 8 every 3 weeks	29%	Neutropenia, hand-foot syndrome, anemia
Bangemann et al. [139] (2000)	13 HER2-overexpressing breast cancer	2,250 mg/m²/d[a]	Trastuzumab[c] 2 mg/kg/wk	62%	
Venturini et al. [140] (2001)	22 advanced breast cancer	2,000 mg/m²/d[a]	Docetaxel and epirubicin 75 mg/m² i.v. bolus day 1 every 3 weeks	95%	Neutropenia, asthenia, mucositis

[a]Administered orally in two daily doses for 14 days every 21 days (intermittent regimen)
[b]Administered orally in two daily doses for 14 days every 28 days
[c]Trastuzumab (Herceptin®) is the first humanized antibody against HER2

Abbreviations: CI = confidence interval; NSCLC = Non-small cell lung carcinoma; AUC = area under the concentration curve; CPT-11 = irinotecan

inhibitor], CI-994 [a histone deacetylase inhibitor], or epirubicin [combined with docetaxel, cisplatin, or CP]) or CAP combined with radiotherapy (RT) have been investigated recently [105-129]. DLTs were mainly HFS and neutropenia with taxanes (paclitaxel at 175 mg/m² or docetaxel at 75 or 100 mg/m² administered i.v. every 21 days) [105-109], diarrhea with oxaliplatin (120 or 130 mg/m² administered i.v. every 21 days) [110-113], diarrhea and neutropenia with CPT-11 (70-300 mg/m² with various schedules of administration) [114-116], myelotoxicity and stomatitis with gemcitabine (1 g/m²) [119-120], neutropenia, diarrhea, and HFS with RT (50.4 Gy) [123-126], neutropenia with docetaxel and epirubicin (both injected at 75 mg/m² on day 1 every 21 days) [127], and neutropenia and stomatitis with epirubicin and cisplatin or CP [128-129]. The phase II trials are reported in Table 2 [130-140].

In summary, orally administered CAP mimics continuous-infusion 5-FU, is well tolerated, with HFS and diarrhea the most common toxicities reported, and is more convenient for patients. Mucositis, leopard-like vitiligo, onychomadesis, and onycholysis are recently reported side effects of CAP [141-143]. It has also been shown that CAP reduced treatment costs in patients with metastatic colon cancer (U.S. $381 per cycle versus U.S. $517 for the classic 5-FU/LV regimen, in Uruguay) [144]. The U.S. Food and Drug Administration (FDA) has approved CAP for use in patients with metastatic breast cancer resistant to both paclitaxel and an anthracycline-containing chemotherapy regimen

or resistant to paclitaxel and for whom further anthracycline therapy is not indicated. CAP is now commercialized in Europe as a monotherapy for first-line treatment of metastatic colorectal cancer. In November 2001, the FDA approved CAP combined with docetaxel for treating patients with metastatic breast cancer after failure of prior anthracycline chemotherapy. The combination therapy was approved on the basis of an open-label randomized trial in 75 centers worldwide. Five hundred and eleven patients with metastatic breast cancer resistant to or recurring or relapsing during or after anthracycline-containing therapy were randomized to receive either 100 mg/m^2 of docetaxel every 3 weeks (n = 256) or the intermittent regimen of CAP (2,500 mg/m^2/day) plus 75 mg/m^2 docetaxel (n = 225). The combination therapy resulted in significantly greater median days to disease progression (186 versus 128, $p < 0.001$), overall survival (442 days versus 352 days, $p = 0.01$), and RR (32% versus 22%, $p = 0.009$) compared with docetaxel alone. The most frequent adverse events in both arms were diarrhea (67% versus 48%), stomatitis (67% versus 43%), and HFS (63% versus 8%) [145]. The FDA suggests that dosages of the drugs may have to be modified for patients with impaired kidney function. Moreover, the agency urges people receiving CAP and a coumarin-derivative to have their anticoagulant response monitored frequently, as CAP has a significant drug interaction with oral coumarin derivative anticoagulant therapy, which can cause serious bleeding complications.

The approved dose of CAP (2,500 mg/m^2/day as intermittent regimen) leads to unacceptable toxicities in many patients with metastatic breast cancer. A recent retrospective analysis suggests a standard starting dose of 2,000 mg/m^2/day. If patients still have toxicities, individualization of dosing is necessary [146]. Moreover, the dose of CAP can be reduced to minimize toxicity without compromising efficacy. The impact of dose reduction was evaluated retrospectively from four phase II trials (2,510 mg/m^2/day, intermittent regimen) including 321 patients with advanced or metastatic breast cancer. One hundred thirty-one patients with dose reductions were compared with 190 patients with no dose reductions. There were little differences in duration of response (220 days versus 211 days), time to treatment failure (234 days versus 218 days), and survival time (350 days versus 243 days) [147].

In breast cancer patients with brain metastases, a drug interaction between CAP and the anticonvulsant phenytoin led to cerebellar symptoms indicative of phenytoin intoxication. CAP downregulates the isoenzyme P4502C9, which plays a major role in the hepatic degradation of phenytoin. A frequent monitoring of the phenytoin level is thus imperative [148].

The polymorphism of the human TS gene determines response to CAP in advanced colorectal cancer [149]. The human TS gene promoter is polymorphic, having either double or triple repeats of a 28-base-pair sequence. Colon cancer patients homozygous for the triple tandem repeats (L/L) have significantly higher TS mRNA, which is associated with lower RR to 5-FU and poorer clinical outcome compared with those homozygous for the double repeat variant (S/S). In a study on 22 patients, 80% of individuals with the S/S variant responded to CAP, compared with 10% and 14% of those with the S/L and L/L variants, respectively. Genotyping patients for the TS polymorphism may thus be useful in identifying colon cancer patients who are more likely to respond to CAP treatment.

UFT® and Orzel®

In an effort to improve the therapeutic index of FTO, Japanese researchers [150] prepared a special formulation of FTO, called UFT® (Fig. 1), a mixture of FTO and uracil (U) in molar proportions of 1:4. This ratio was chosen based on preclinical models that suggested maximal tumor selectivity with these relative concentrations. U acts as a modulator on the catabolism of 5-FU. Being a natural substrate for DPD, it competes with 5-FU. Since its molar concentration is much higher than that of 5-FU (in the form of FTO), little 5-FU is degraded by DPD, and thus, is more available to the anabolic route of activation. The coadministration of FTO (slow liberation of 5-FU in the organism) with U (reduced degradation of 5-FU) was designed to produce a constant reserve of 5-FU and its active metabolites and to minimize production of inactive and potentially toxic metabolites [151]. In 10 patients receiving equimolar dosages of 5-FU by continuous infusion (250 mg/m^2/day over 5 days) or oral UFT (370 mg/m^2/day over 28 days), similar systemic 5-FU exposure (measured by the area under the concentration curve [AUC]) was obtained [152]. This study also demonstrated a prolonged elimination $t_{1/2}$ of 5-FU after oral UFT administration.

It has been reported recently that UFT, partly by maintaining a high and long-lasting blood level of 5-FU and partly through its metabolites (γ-hydroxybutyric acid and γ-butyrolactone), had a stronger angiogenesis inhibitory effect in a murine renal carcinoma cell line than 5-FU or 5'd5-FUrd [153]. While the clinical relevance of this observation remains to be determined, it might be another mechanism of action of this compound.

Of the newer oral fluoropyrimidines, UFT has been studied the most extensively. Japanese investigators studied UFT about 20 years ago, but interpretation of the data was difficult because dissimilar methodologies, criteria, and evaluation standards were used [56]. Results of these studies indicated that UFT was well tolerated and had significant activity in patients with colon, stomach, and breast cancers [154]. Since the initial studies using UFT alone have produced encouraging

results, researchers have proposed using an additional modulator, such as LV, to act on the anabolism of 5-FU by increasing available reduced folates and thereby stabilizing the binding of 5-FdUMP to TS. Orzel™ is the trade name for the combination UFT/LV. It is composed of UFT capsules copackaged with LV tablets.

Phase I trials [155-161] have established that the maximal dosage of UFT administered concomitantly with LV over 14 to 28 days in divided doses ranges from 350 to 400 mg/m^2/day, which will thus be employed in the phase II trials. The main toxic reactions at the MTD were gastrointestinal (diarrhea, nausea, vomiting). The occurrence of these toxic effects correlated significantly with the maximum plasma concentration and AUC_{0-6h} of 5-FU [162]. The HFS, characteristic to continuous i.v. infusion of 5-FU, was not observed.

UFT/LV in Colorectal and Rectal Cancers

Phase II Trials in Colorectal Cancer

Phase II trials in advanced colorectal cancer have shown that an oral regimen of UFT/LV is well tolerated and is at least as efficient as treatment with 5-FU administered by continuous i.v. infusion with or without LV [162-174]. The objective RR in these studies ranged from 20%-40%, and median overall survival was around 13 months. The most frequent severe toxicities were diarrhea and nausea/vomiting. The absence of objective responses in patients refractory to previous i.v. bolus 5-FU suggests that UFT is cross-resistant with bolus 5-FU [160, 169]. For elderly patients, the RRs were lower than in the general population [167, 168].

Phase III Trials in Colorectal Cancer

The above results led to two randomized phase III trials comparing oral treatment of UFT/LV (300 mg/m^2/day in three daily doses for 28 days every 5 weeks in combination with 75 or 90 mg/day of oral LV, the doses found to lead to maximum LV bioavailability) with i.v. administration of 5-FU/LV (425 mg/m^2/day of 5-FU + 20 mg/m^2/day of LV administered by i.v. bolus during 5 days every 4 or 5 weeks) in patients with metastatic colorectal cancer [175, 176]. The overall RRs were not significantly different in both studies. In the study of *Pazdur et al.* [175], which enrolled 816 patients, RR was 12% in the UFT/LV arm and 15% in the 5-FU/LV arm. For the 380 patients evaluated in the study of *Carmichael et al.* [176], RR was 11% in the UFT/LV arm and 9% in the 5-FU/LV arm. In the latter study, the median time to progression was 3.4 months and 3.3 months in the UFT/LV arm and the 5-FU/LV arm, respectively. The MSTs were 12.2 months (UFT/LV arm) versus 11.9 months (5-FU/LV arm) in the *Carmichael et al.* study, and 12.4 months (UFT/LV arm) versus 13.2 months (5-FU/LV arm) in the *Pazdur et al.* study. However, UFT/LV was associated with a significantly better safety profile compared with 5-FU/LV. UFT/LV treatment resulted in fewer episodes of febrile neutropenia and documented infection. Significant HFS was not observed with UFT/LV, whereas bilirubin was increased more often in the UFT/LV-treated patients. Both studies concluded that the oral treatment was accompanied by lower toxicity and was thus an acceptable alternative to treatment with i.v. 5-FU/LV.

A recent study examined patient preference for oral UFT/LV or i.v. 5-FU/LV chemotherapy in metastatic colorectal cancer. Thirty-seven previously untreated patients were randomized to start treatment with either oral UFT/LV (300 mg/m^2/day of UFT plus 90 mg/day of LV, both in three daily doses for 28 days every 5 weeks) or bolus i.v. 5-FU/LV (425 mg/m^2/day 5-FU plus LV 20 mg/m^2/day for 5 days every 4 weeks). For the second treatment cycle, patients were crossed over to the alternative treatment regimen. Prior to the first and after the second therapy cycle, patients were required to complete a therapy preference questionnaire. Eighty-four percent of patients ($n = 31$) preferred oral UFT to i.v. 5-FU because they experienced less stomatitis and diarrhea, could take their medication at home, and preferred pill to injection. The authors also showed that oral UFT/LV led to prolonged 5-FU exposure that was comparable with continuous i.v. treatment [177].

Adjuvant Therapy in Colorectal Cancer

Oral UFT or UFT/LV were also explored in the adjuvant setting of colon cancer. Four hundred seventy-six patients were given either i.v. mitomycin C (MMC; 6 g/m^2 on the day of and the day after surgery) or the same dose of MMC plus oral UFT (400 mg/day for 1 year). The disease-free survival rate of the UFT group was significantly higher than that of the control, though no significant difference in the overall survival rate was observed [178].

A clinical trial of oral UFT (600 mg/day for 5 days followed by 2 drug-free days, for a year) as adjuvant chemotherapy for resected colorectal cancer was conducted on 87 patients. This schedule was well tolerated and was favorable in terms of compliance [179]. A recent study on the pharmacokinetics of 5-FU during the 2 days off UFT showed that the 5-FU concentrations in the tumor were maintained at relatively high levels until 48 hours after the final dose of UFT, while serum 5-FU concentrations decreased to very low levels within 24 hours. These data suggest that the two off-drug days reduced the adverse reactions and improved drug tolerance without compromising antitumor efficacy [180].

Espinosa et al. [181] evaluated 269 patients with operated Dukes' stage B2-C colon cancer. The UFT/LV regimen

was oral UFT 390 mg/m²/day for 14 days every 4 weeks and i.v. LV (500 mg/m²) on day 1 followed by oral LV (24 mg/day) on days 2-14. Diarrhea was the primary side effect. After a median follow-up of 36 months, the disease-free survival was 83% for stage B2 and 62% for stage C. The overall survival rates were 94% and 87%, respectively.

The National Surgical Adjuvant Breast and Bowel Project Protocol C-06 is a randomized comparison of the relative efficacies of i.v. 5-FU/LV versus oral UFT/LV. The 5-FU/LV regimen was given for three cycles and consisted of a 2-hour infusion of LV (500 mg/m²) and, 1 hour after beginning LV, an i.v. bolus of 5-FU (500 mg/m²), both given weekly for 6 weeks. The oral UFT/LV regimen consisted of five cycles of UFT (300 mg/m²/day) in three daily doses and LV (90 mg/day) for 28 days every 5 weeks. An interim analysis on 473 patients indicated that both regimens were well tolerated and had similar toxicity profiles [182].

A randomized prospective trial was performed to determine the efficacy of preoperative and postoperative adjuvant oral UFT, administered with MMC after resection for advanced colorectal cancer. The patients received oral UFT (400 mg/day) for 7 days prior to surgery and, after surgery, were randomly assigned to group A, receiving MMC postoperatively, or group B, receiving MMC and oral UFT (400 mg/day) for 1 year. The survival results revealed no significant difference between groups A and B. However, in patients with nuclear DNA aneuploid tumors, the hematogenous recurrence rate after curative surgery was lower in group B than in group A [183].

A recent study on 55 patients compared the effects of sequential methotrexate (MTX; 100 mg/m²) and 5-FU (600 mg/m²) followed by LV rescue (treatment MFL), as an adjuvant chemotherapy, with a combination of MMC (12 mg/m² intraoperatively, then 6 mg/m² every other week after surgery for 2 months) and oral UFT (375 mg/m²/day) for at least 3 years. The overall survival and disease-free survival rates were significantly higher and the recurrence rate significantly lower in the MFL group, demonstrating the superiority of MFL therapy for improving postsurgical survival [184].

It recently has been demonstrated that postoperative adjuvant immunotherapy using protein-bound polysaccharide K (PSK) and UFT was highly effective in preventing recurrence of colorectal cancer. Two hundred seven patients were assigned to two groups. Group A received oral PSK (3 g/day) and UFT (300 mg/day) while group B received only UFT (300 mg/day), for 2 years after surgery. Three years after surgery, disease-free survivals were significantly different (80.5% and 68.7% for groups A and B, respectively, $p = 0.021$), whereas overall survival times were not (87.2% and 80.6% for groups A and B, respectively, $p = 0.247$) [185].

The Future in Colorectal Cancer

Phase I-II trials are being conducted in which UFT alone or UFT/LV is combined with other agents to find more effective regimens for advanced metastatic colorectal cancer that incorporate both i.v. and oral drugs (Table 3).

Another promising approach is the use of pharmacokinetic modulating chemotherapy (PMC), which is based on the concept that the benefit of a continuous i.v. 5-FU infusion can be potentiated by low-dose oral UFT. Fifty-six patients with unresectable colorectal carcinoma received UFT (200-400 mg/day) 5-7 days per week and 5-FU (600 mg/m²/day) once a week. PMC markedly improved the MST (26.6 months versus 9.2 months in the non-PMC group). This significant improvement was observed in unresectable primary colorectal carcinoma, recurrent tumors, local extension, lung metastases, liver metastases, and peritoneal seedings. PMC resulted in a good quality of life as only one patient required toxicity-related hospitalization. The authors recommended the use of PMC for more than 6 months [197, 198]. This efficacy was based on the fact that PMC targets at least two different phases of the cell cycle [198, 199].

PMC was also used as postoperative adjuvant treatment for hepatic colorectal metastases. Sixty-six patients were divided into two groups after hepatectomy. Group A (n = 38) received a hepatic arterial infusion of 5-FU (600 mg/m²/day) for two consecutive days per week and an oral administration of UFT (400 mg/day) for 5-7 days per week, repeated 10 times. Group B (n = 28) received oral UFT (400 mg/day) for 6 months. Cumulative 5-year survival rates after hepatectomy were 62% in group A and 27% in group B ($p = 0.00001$). Median hepatic recurrence-free times were 31.6 months in group A and 18.4 months in group B ($p = 0.0004$). Main cause of death was lung recurrence in 21% of group A and hepatic recurrence in 57% of group B [200].

Rectal Cancer

Preoperative protracted i.v. infusions of 5-FU with concurrent pelvic RT are commonly used to treat rectal carcinoma [201]. Preliminary results suggest that UFT/LV combined with RT has similar efficacy, improved tolerability, and enhanced quality of life in comparison with continuous 5-FU [202-207].

UFT in Gastric Tumors

Several phase II trials were conducted to evaluate UFT alone or in combination with other agents in gastric cancer (Table 4) [163, 208-219].

Gastric cancer, the most frequently occurring malignant tumor in Japan, was studied in a cooperative randomized trial involving 169 patients from 13 institutions that compared the

Table 3. Recent results of phase I/II and II trials conducted on patients treated with UFT combined with other anticancer agents for colorectal carcinoma

Study (year)	MTD or escalating doses	LV dose	Dose-limiting toxicities	*n* of evaluable patients Response rate Median survival time (MST)	Recommended doses for phase II
Hill et al. [186] (2000)	UFT 250 mg/m²/d[a] CPT-11 300 mg/m² [b]	90 mg/d[a]	Neutropenic fever, diarrhea	16 (UFT 250 mg/m²/d[a], CPT-11 250 mg/m² [b]) 25%	UFT 250 mg/m²/d[a] LV 90 mg/d oral[a] CPT-11 250 mg/m² [b]
Gravalos et al. [187] (2000) *Castellano et al.* [188] (2001)	UFT 300 mg/m²/d[c] CPT-11 300 mg/m² [d]	45 mg/d[c]	Diarrhea, neutropenic fever	23 30%	UFT 300 mg/m²/d[c] LV 45 mg/d[c] CPT-11 250 mg/m² [d]
Alonso et al. [189] (2001)	A: UFT 250 mg/m²/d[e] CPT-11 80, 100, 110, or 120 mg/m² [f] B: UFT 300 mg/m²/d[e] CPT-11 100 or 110 mg/m² [f]		A: diarrhea, asthenia B: diarrhea, neutropenia	30 10% (1%-19%) MST 11 mo	A: UFT 250 mg/m²/d[e] CPT-11 110 mg/m² [f] or B: UFT 300 mg/m²/d[e] CPT-11 100 mg/m² [f]
Cruz et al. [190] (2001)	UFT 200 mg/m²/d[g] CPT-11 125 mg/m² [b]	45 mg/d[g]	Diarrhea, alopecia	17 18% (0%-36%)	
Sazaki et al. [191] (2001)	UFT 300 mg/m² [i] CPT-11 30 mg/m² [j]	20 mg/m² i.v. every week	Neutropenia, nausea, vomiting	29 21% MST 16 mo	
Mel et al. [192] (2000) *Vazquez Estevez et al.* [193] (2000)	UFT 200-350 mg/m²/d[k] raltitrexed 2-3 mg/m² [l]		Diarrhea	28 21%	
Dorta et al. [194] (2000)	UFT 390 mg/m²/d[m] oxaliplatin 85 mg/m² [n]	day 1: 250 mg/m² 2-hr i.v. infusion days 2-14: 15 mg/d oral	Diarrhea, nausea, vomiting	34 35%	UFT 300 mg/m²/d[m] LV day 1: 250 mg/m² 2-hr i.v. infusion days 2-14: 15 mg/d oral oxaliplatin 85 mg/m² [n]
Doudiard and *Seitz* [195] (2001)	UFT 200-350 mg/m²/d[g] oxaliplatin 100-130 mg/m² [b]	90 mg/d[g]	Not reached	13 23%	
Jakobsen et al. [196] (2001)	UFT 300 mg/m²/d[o] hydroxyurea 0.5 g/d[p]	levoLV 22.5 mg/d[o]	Gastrointestinal	63 22% MST 11 mo	

[a]Administered orally during 14 days every 3 weeks
[b]Administered i.v. on day 1 every 3 weeks
[c]Administered orally during 14 days in three daily doses every 3 weeks
[d]Administered as a 90-min i.v. infusion on day 1 every 3 weeks
[e]Administered orally for 21 days in two or three daily doses every 4 weeks
[f]Administered as a 60-min i.v. infusion on days 1, 8, and 15 every 4 weeks
[g]Administered orally during 21 days every 4 weeks
[h]Administered as a 90-min i.v. infusion on days 1, 8, and 15 every 4 weeks
[i]Administered orally every day
[j]Administered as a 60-min i.v. infusion every week
[k]Administered orally during 28 days in three daily doses every 6 weeks
[l]Administered as a 15-min i.v. infusion on days 1 and 21 every 6 weeks
[m]Administered orally during 14 days in two daily doses every 4 weeks
[n]Administered on days 1 and 14 every 4 weeks
[o]Administered orally during 28 days every 5 weeks
[p]Administered orally during 28 days every 5 weeks

Abbreviations: MTD = maximum tolerated dose; LV = leucovorin; CPT-11 = irinotecan

efficacy of oral FTO (500 mg/m²/day for 28 days) plus i.v. MMC (5 mg/m²/week) with oral UFT (375 mg/m²/day for 28 days) plus MMC (same schedule) [220]. A superior RR (25.3% versus 7.8%) as well as a survival advantage were observed in the UFT arm. No significant difference in toxicity was noted.

In another small randomized trial, UFT/MMC was compared with 5-FU/MMC. RRs were 23% for the first regimen and 7% for the second [221].

UFT has also been used in adjuvant therapy after resection for gastric cancer. A slight difference in 5-year survival was reported when patients were treated for 2 years with oral FTO

Table 4. Phase II clinical studies conducted on patients with gastric cancer treated with UFT and other anticancer agents

Study (year)	*n* of evaluable patients	UFT dose	Other compound(s) administered	Response rate (95% CI)	Median duration of response (MDR); median survival time (MST)	Main side effects
Hayakawa et al. [208] (1989)	15	400 mg/m²/d[a]	Days 1, 8, 15, and 22: VP16 50 mg/m² i.v. cisplatin 25 mg/m² i.v. adriamycin 10 mg/m² i.v.	40%		Myelosuppression, alopecia, nausea
Malik et al. [163] (1990)	18	600 mg/d[b]		6% (0.3%-30%)	MST 12 wk	Cutaneous eruption
Sawa et al. [209] (1990)	42	400 mg/d[c]	Day 1: cisplatin 75 mg i.v. and mitomycin C 10 mg i.v. days 3, 4, and 5: VP16 50 mg i.v.	54%		Digestive symptoms, epilation, myelopathy
Hashimoto et al. [210] (1993)	13	400 mg/d days 8-28	Cisplatin 50 mg/d continuous infusion days 1-2 5-FU 500-750 mg/d continuous infusion days 2-7	31%		Anorexia, nausea, vomiting, leukocytopenia
Jin et al. [211] (1994)	93	450 mg/d	Mitomycin C 20 mg i.v. once a week	60%		Weakness, leukopenia
Sato et al. [212] (1995)	14	400 mg/m²/d[b]	Cisplatin 30 mg/m² i.v. for 3 days every 4 weeks	43%	MST 11.4 mo	Anorexia, diarrhea, nausea, vomiting, leukocytopenia
Felia et al. [213] (1996)	46	390 mg/m²/d[d]	VP16 day 1: 100 mg/m² i.v. days 2-3: 200 mg/m² oral LV day 1: 500 mg/m² i.v. days 2-14: 30 mg/d oral	35% (22%-51%)	MDR 10 mo MST 9 mo	Diarrhea, anemia, nausea, vomiting
Kim et al. [214] (1996)	14	480 mg/m²/d[e]	LV 25 mg/m²/d oral	29% (5%-52%)	MST 25 wk	Diarrhea, mucositis, nausea, vomiting
Kim et al. [215] (1997)	37	360 mg/m²/d[b]	LV 25 mg/m²/d oral	27% (15%-43%)	MDR 30 wk MST 30 wk	Diarrhea, mucositis, nausea, vomiting
Chaves et al. [216] (2000)	16	300 mg/d	Day 1: epirubicin 50 mg/m² and cisplatin 60 mg/m² i.v.	19%	MST 10 mo	Neutropenia, nausea, vomiting, alopecia
Sato et al. [217] (2000)	41	400 mg/m²/d[f]	Day 8: cisplatin 80 mg/m² i.v.	51% (35%-67%)	MDR 85 d MST 8.3 mo	Neutropenia
Jeen et al. [218] (2001)	47	360 mg/m²/d[g]	Day 1: epirubicin 50 mg/m² i.v. bolus and cisplatin 60 mg/m² 4-hr i.v. infusion days 1-21: LV 45 mg/d oral[g]	58% (43%-72%)	MST 15 mo	Neutropenia, nausea, vomiting, mucositis, diarrhea
Ravaud et al. [219] (2001)	25	300 mg/m²/d[h]	LV 90 mg/d[h]	16% (6%-33%)	MDR 187 d	Diarrhea, nausea, vomiting, asthenia

[a]Administered orally for 28 days
[b]Administered orally in three daily doses; median duration of treatment: 6 weeks
[c]Administered orally for 21 days
[d]Administered orally for 14 days every 4 weeks
[e]Administered orally for 21 days in divided daily doses every 4 weeks
[f]Administered orally for 21 days in two daily doses every 4 weeks
[g]Administered orally for 21 days in three daily doses every 4 weeks
[h]Administered orally for 28 days in three daily doses every 5 weeks

Abbreviations: CI = confidence interval; VP16 = etoposide; LV = leucovorin

or UFT at a dose of 600 mg/day (52.1% versus 68.7%, $p = 0.04$) [222]. One thousand four hundred ten patients from 180 Japanese institutions were allocated into either a low-dose group, receiving MMC (8 mg/m^2 on the day of surgery) and three capsules of UFT (300 mg in FTO) daily for 6 months, or a high-dose group, receiving MMC (8 mg/m^2 on the day of surgery and in weeks 4, 10, 16, and 22 after surgery) and six capsules of UFT (600 mg in FTO) daily for 6 months. Although the number of adverse events was higher, a better prognosis is expected with the high-dose regimen [223].

UFT in Non-Small Cell Lung Cancer

UFT has been used in non-small cell lung cancer in patients with advanced disease and in the adjuvant setting. Several phase II studies (Table 5) [224-236] showed that the combination UFT/cisplatin was comparable with other currently used regimens for this disease.

Several trials have been conducted in the adjuvant setting [237-242]. In a study from the Study Group of Adjuvant Chemotherapy for Lung Cancer [238], the 5-year survival rate and the 5-year disease-free survival rate were slightly improved in a group ($n = 155$) receiving UFT (8 mg/kg/day) for 6 months following immediate postoperative administration of cisplatin (66 mg/m^2 × 1) and doxorubicin (26 mg/m^2 × 1) compared with a surgery alone control group ($n = 154$). In the first study of *Wada et al.* [239], 323 patients were randomized to one of three arms. They were treated with cisplatin (50 mg/m^2), vindesine (2-3 mg/kg body weight) for three courses, and 1 year of oral UFT (400 mg/kg body weight), or 1 year of oral UFT at the same dose, or randomized to receive no postsurgical therapy. The 5-year overall survival rates were 61%, 64%, and 49% for the three arms, respectively. Survival differences among the groups receiving adjuvant therapy and the control group achieved statistical significance ($p = 0.022$). Side effects were significantly lower in the group treated with UFT alone compared with the first group. This study was noteworthy in that it detected a survival advantage from chronic administration of UFT, with only mild toxicity. *Tanaka et al.* [240] performed a retrospective study to examine the efficacy of UFT as postoperative adjuvant therapy. UFT was administered to 98 patients and not to 557 patients. The 5-year survival rate of the UFT group (77%) was significantly better than that of the control group (59%). Stratified with pathological stage, the efficacy of UFT was seen in stages I and IIIa-pN2 diseases, but not in stages II and III-pT3NO1 patients. Multivariate analysis of the prognostic factors also revealed that postoperative oral UFT improved prognosis. In the second study of *Wada et al.* [241], patients with completely resected stages I and II non-small cell lung cancer were randomly assigned to two groups, a surgery alone group ($n = 116$) and an adjuvant chemotherapy group ($n = 109$). The latter group received two 4-week courses of chemotherapy (cisplatin 80 mg/m^2 and MMC 8 mg/m^2 on day 1, vindesine 2-3 mg/m^2 on day 1 and/or day 8) followed by oral UFT (400 mg/day) for 1 year. The 5-year survival rates were not statistically different (71% for the surgery-alone control group and 77% for the adjuvant chemotherapy group). However, a possible role for adjuvant therapy in stage IA disease could be demonstrated. *Ito et al.* [242] evaluated a regimen consisting of low-dose cisplatin (6-10 mg/m^2/day) and oral UFT (600 mg/day) on days 1-5, 15-19, and 29-33 at 4 weeks after operation. Concurrent RT (50 Gy) was given, followed by the administration of UFT (400 mg/day) for 2 years. The regimen was well tolerated and effective, with a disease-free survival rate of 90% at 1 year and 78% at 2 years.

To examine whether the efficacy of postoperative oral administration of UFT may be influenced by incidence of apoptosis or apoptosis-related gene status (*p53* and *bcl-2*), 44 patients were treated with UFT (300-400 mg/day) 1 month after surgery, whereas 118 were not. For patients with a higher apoptotic index (≥10.9), the 5-year survival rate of the UFT group was significantly higher than that of the control group (83% and 68%, respectively), whereas there was no difference for patients with lower apoptotic index (<10.9). Similarly, UFT was effective for patients without *p53* aberrant expression (5-year survival rate of the UFT group was 95% versus 74% for the control group), but not for patients with *p53* aberrant expression. *Bcl-2* status did not influence the efficacy of UFT [243].

UFT in Breast Cancer

Several phase I and I/II trials were conducted with UFT in combination with other anticancer drugs in breast cancer therapy [244-252]. The DLTs were mainly neutropenia and diarrhea when UFT was combined with LV (90 mg/day) and paclitaxel [244-246, 251], oral CP [252], or vinorelbine [249, 250], with LV, paclitaxel, and doxorubicin [247], or with LV, epirubicin, and CP [248]. The phase II studies on patients treated with UFT alone or in combination with other treatments are presented in Table 6 [253-259].

One Japanese study compared the efficacy of oral UFT (400 mg/day) with that of oral FTO (800 mg/day) in 56 patients (28 in each arm) with advanced breast cancer. The RR was 39% in the UFT arm and 21% in the FTO arm, without statistical significance. No significant differences were demonstrated in time to relapse and overall survival. The adverse effects were similar in both arms [260].

More recently, a randomized trial compared the efficacy of oral UFT (350 mg/m^2/day for 14 days; 31 patients) with i.v. 5-FU (500 mg/m^2/day on days 1 and 8; 31 patients), both treatments being combined with doxorubicin (50 mg/m^2 i.v.

Table 5. Phase II clinical studies conducted on patients treated with UFT alone or with other compounds for non-small cell lung cancer

Study (year)	*n* of evaluable patients	UFT dose	Other compound(s) and/or treatment administered	Response rate (95% CI)	Median duration of response (MDR); median survival time (MST)	Main side effects
Shimizu et al. [224] (1986)	12	600 mg/d[a]		8%		Anorexia, nausea, liver dysfunction, skin pigmentation
Keicho et al. [225] (1986)	16	400 mg/m²/d[b]		6%		Myelosuppression, anorexia, nausea, vomiting, epigastralgia
Ichinose et al. [226] (1995)	31	400 mg/m²/d[b]	Day 8: cisplatin 80 mg/m² i.v.	35% (19%-52%)	MDR 6 mo MST 11 mo (stage III), 8 mo (stage IV)	Leukopenia, thrombocytopenia
Gemma et al. [227] (1995)	17	400 mg/m²/d[c]	Days 4, 8: cisplatin 60 mg/m²/d i.v.	47% (23%-71%)		Anorexia nausea, vomiting, leukocytopenia
Felip et al. [228] (1996)	25	390 mg/m²/d[d]	Cisplatin day 1: 90 mg/m² i.v. days 2-3: 200 mg/m² oral LV day 1: 500 mg/m² i.v. days 2-14: 30 mg/d oral	12% (3%-32%)		Nausea, vomiting, leukopenia, diarrhea, epigastralgia
Koinumaru et al. [229] (1997)	21	400 mg/m²/d[e]	Days 8-12: cisplatin 20 mg/m² i.v.	38% overall (17%-59%) step 1: 33% step 2: 33% step 3: 50%	MST 11.6 mo	Neutropenia, nausea, vomiting
Yoshimori et al. [230] (1998)	108	400 mg/m²/d[c]	Day 8: cisplatin 80 mg/m² i.v.	28% (19%-36%)	MST 10 mo	Neutropenia, anemia, vomiting
Ichinose et al. [231] (2000)	103	400 mg/m²/d[f]	Day 8: cisplatin 80 mg/m² i.v.	29% (20%-38%)	MST 40 wk	Vomiting, hyperbilirubinemia
Yoshino et al. [232] (2000)	23	400 mg/m²/d days 1-52	Days 8, 29, 50: cisplatin 80 mg/m² i.v. radiotherapy 60.8 Gy	91%	MST 16 mo	Leukopenia
Nakanishi et al. [233] (2001)	64	400 mg/m²/d[g]	Day 15: cisplatin 80 mg/m²	31% (21%-43%)	MST 9.9 mo for stage IIIb 8.0 mo for stage IV	Anemia, leukopenia
Saito et al. [234] (2001)	47	400 mg/m²/d[h]	Days 8-12: cisplatin 20 mg/m² i.v.	38% (24%-52%)	MDR 113 d MST 12.8 mo	Anorexia, nausea, neutropenia, thrombocytopenia
Vega-Villegas et al. [235] (2001)	29	200 mg/m²/d[i]	Day 1: cisplatin 100 mg/m² i.v. days 1, 8: vinorelbine 25 mg/m² i.v.	48%	MST 12.4 mo for stage IIIb 8.4 mo for stage IV	Neutropenia, vomiting, alopecia, anemia, neurotoxicity
Yoshimori et al. [236] (2001)	26	400 mg/m²/d[j]	Day 8: cisplatin 80 mg/m² and docetaxel 60 mg/m²	58%	MST 387 d	Neutropenia, gastrointestinal

[a]Administered orally for more than 4 weeks
[b]Administered orally for 21 days every 4 weeks
[c]Administered orally for 14 days
[d]Administered orally for 14 days in two daily doses every 4 weeks
[e]Administered orally in two daily doses for 14 days (step 1), or 21 days (step 2), or 28 days (step 3) every 4 weeks
[f]Administered orally for 14 days in two daily doses every 3 or 4 weeks
[g]Administered orally for 14 days every 3 weeks
[h]Administered orally for 21 days in two daily doses every 4 weeks
[i]Administered orally for 21 days every 3 weeks
[j]Administered orally for 14 days every 3-4 weeks

Table 6. Phase II clinical studies conducted on patients treated with UFT and other agents for breast cancer

Study (year)	*n* of evaluable patients	UFT dose	Other compound(s) and/or treatment administered	Response rate (95% CI)	Median duration of response (MDR)	Main side effects
Daniels et al. [253] (1993)	70	10 mg/kg/d for at least 2 months		19%	9 mo	Nausea, vomiting, diarrhea
Kiman et al. [254] (1994)	9: 6 Pr, 3 Po	300 mg/d every day	Pr: oophorectomy then i.v. cyclophosphamide (300 mg/d) and doxorubicin (30 mg/d) every 2 weeks; Po: same drugs + oral tamoxifen (30 mg/d) every day	Pr 50% Po 33%		Leukopenia, anorexia, malaise
Richardet et al. [255] (1999)	24	300 mg/m²/d[a]	LV 45 mg/d[a]	25%		Diarrhea
Fukuda et al. [256] (1999)	19	300 mg/m²/d[b]	Doxorubicin 30 mg/m² i.v. day 1, cyclophosphamide 65 mg/m² oral on days 1-14 tamoxifen 20 mg/d oral days 1-21	58% (29%-87%)		Leukopenia, alopecia
Yardley et al. [257] (2001)	15	BSA ≥ 1.8 m² 600 mg/d[c] 1.6 m² ≤ BSA < 1.8 m² 500 mg/d[c] BSA < 1.6 m² 400 mg/d[c]	LV 60 mg/d[c]	13%		Nausea, vomiting, diarrhea
Rivera et al. [258] (2001)	79	300 mg/m²/d[d]	LV 90 mg/d[d]	6%		Nausea, vomiting, diarrhea, asthenia
Hortobagyi et al. [259] (2001)	54	300 mg/m²/d[a]	LV 60 mg/d[a]	11%		Nausea, vomiting, diarrhea, asthenia

[a]Administered orally for 28 days in two daily doses every 5 weeks
[b]Administered orally for 14 days every 3 weeks
[c]Administered orally for 14 days in two daily doses every 3 weeks
[d]Administered orally for 28 days in three daily doses every 5 weeks

Abbreviations: CI = confidence interval; Pr = premenopausal; Po = postmenopausal; LV = leucovorin; BSA = body surface area

on day 1) and CP (500 mg/m² i.v. on day 1). No statistical difference in overall RR was seen (48% in the UFT arm and 35% in the 5-FU arm). The MDR was 16 weeks for both arms. The median overall survival was 12 months for the UFT arm and 11 months for the 5-FU arm. Toxicity profiles (alopecia, anemia, leukopenia, thrombocytopenia, and diarrhea) were similar in both groups. Anemia and stomatitis were significantly more common in the 5-FU arm [261].

In the adjuvant setting, Spanish investigators have conducted two trials [262]. In the first one, 187 premenopausal women were randomly assigned to either oral UFT (400 mg/day for 6 months) and oral prednimustine (60 mg/m² for 7 consecutive days, every 28 days in six cycles) or six cycles of the standard therapy CMF (CP 600 mg/m², MTX 40 mg/m², 5-FU 600 mg/m², every 4 weeks). Disease-free survival and overall survival were similar in both arms. Toxicities were mild (nausea/vomiting, alopecia) and slightly worse in the CMF arm. In the second trial, 222 postmenopausal patients received 20 mg/day of tamoxifen for 1 year or the same dose of tamoxifen plus UFT at 400 mg/day for 6 months. The disease-free survival and overall survival rates were equal in both arms, but were longer in patients with five or more axillary-involved nodes treated with tamoxifen plus UFT. Toxicities were negligible in both arms.

A large Japanese trial [263] evaluated the combination of UFT, MMC, and tamoxifen as postoperative adjuvant therapy in the treatment of patients with stage II, estrogen receptor (ER)-positive primary breast cancer. All patients received 13 mg/m² of i.v. MMC on the day of surgery. Patients were then randomly allocated to either oral tamoxifen (20 mg/day, 14 days after surgery for 2 years; 213 evaluable patients; group A) or oral UFT plus tamoxifen (400 mg/day and 20 mg/day, respectively; 223 evaluable patients; group B). There was no difference in the 5-year survival rate (93% for group A and 91% for group B). However, there was a significant advantage for the UFT plus tamoxifen group in the 5-year relapse-free survival rate (83% for group A and 91% for group B). In another large Japanese trial, a benefit was also observed in premenopausal ER-positive patients receiving a similar regimen (30 mg/day of tamoxifen, 300 mg/day of UFT) [264].

Table 7. Phase II clinical studies conducted on patients treated with UFT alone or with other anticancer agents for head and neck, pancreatic, or prostate cancer

Study (year)	*n* of evaluable patients	UFT dose	Other(s) compound(s) administered	Response rate (95% CI)	Median duration of response (MDR); median survival time (MST)	Main side effects
Inuyama et al. [265] (1985)	60 head and neck	600 mg/d		30%		Anorexia, nausea, vomiting, stomatitis, diarrhea
Rivera et al. [266] (1997)	47 head and neck	Induction[a] 6 mg/kg/d days 1-21 then 5 mg/kg/d	Induction[a] vinorelbine 25 mg/m^2 i.v. days 1 and 8; cisplatin 100 mg/m^2 i.v. day 1 then carboplatin 100 mg/m^2/wk i.v. and radiotherapy	93%		Neutropenia, nausea, vomiting, stomatitis
Colevas et al. [267] (2001)	42 head and neck	300 mg/m^2/d[b]	LV 90 mg/d[b]	21% (10%-37%)	MST 8.7 mo	Diarrhea, mucositis, anorexia, dehydration
de Castro et al. [268] (2000)	38 pancreas	390 mg/m^2/d[c]	Gemcitabine 1 g/m^2 days 1, 8, and 15 LV day 1: 250 mg/m^2 i.v. days 2-14: 15 mg/d oral	16% (6%-31%)		Diarrhea
de Castro et al. [269] (2001)	23 pancreas	300 mg/m^2/d[d]	Gemcitabine 1.2 g/m^2 days 1, 8, and 15	30% (14%-54%)	MST not yet reached after 6 mo	Neutropenia, thrombocytopenia, anemia
Nishimura et al. [270] (2001)	26 prostate	400 mg/d	Cyclophosphamide 100 mg/d oral estramustine 560 mg/d oral	62% PSA decline ≥50%	MDR 8 mo	Diarrhea
Ukimura et al. [271] (2001)	23 prostate	400 mg/d	Dexamethasone 1 mg/d oral cyclophosphamide 100 mg/d oral	70% PSA decline ≥50%	MDR 6 mo	Hematuria

[a]Combination repeated every 21 days for four courses

[b]Administered orally for 28 days in three daily doses every 5 weeks

[c]Administered orally for 14 days in two daily doses every 4 weeks

[d]Administered orally for 21 days in two daily doses every 4 weeks

Abbreviations: CI = confidence interval; LV = leucovorin; PSA = prostate-specific antigen

UFT in Head and Neck Cancer

The results of the phase II studies of UFT in head and neck cancer are shown in Table 7 [265-271]. In one study, 398 patients had a standard surgical therapy for stage III-IV head and neck cancer with or without adjuvant oral UFT (300 mg/day for 1 year). There was no significant difference in overall survival or relapse-free survival between arms. However, the addition of UFT improved distant metastasis of disease [272].

More recently, a randomized trial compared the classic combination cisplatin/5-FU with cisplatin/UFT in the neoadjuvant treatment of locally advanced stage III or IV head and neck cancer. Sixty-seven patients received cisplatin (100 mg/m^2) on day 1 followed by either a continuous infusion of 5-FU (1 g/m^2) on days 2-6, or oral administration of UFT (300 mg/m^2/day) on days 2-20. Both treatments were repeated every 21 days for four cycles. Responding patients received locoregional standard RT (50 to 70 Gy) after chemotherapy. At a median follow-up of 84 months, RR (73% versus 79%) and disease-free survival rates were comparable in both arms. However, a lower incidence of phlebitis was observed in patients treated with UFT (71% versus 9%) [273].

One study compared the combination UFT/RT with RT alone and showed significantly longer disease-free survival and overall survival for the group of patients treated concomitantly with UFT and RT [274]. More recently, patients with unresectable stage III-IV head and neck carcinoma received two cycles of neoadjuvant chemotherapy (cisplatin [25 mg/m^2 for 5 days], LV [500 mg/m^2 for 5 days], and 5-FU [800 mg/m^2] for 4 days every 3 weeks) followed by radiochemotherapy (carboplatin [300 mg/m^2 every 3 weeks], UFT [600 mg/day], and RT [65-72 Gy]). Higher

complete and partial RRs were obtained after both steps of treatment (complete RR 69%, partial RR 10%) than after neoadjuvant chemotherapy alone (29%, 56%) [275].

A prospective randomized study was conducted to evaluate the benefit of adjuvant levamisole/UFT chemotherapy in head and neck squamous cell carcinoma. A trend of better distant control was observed in the treated group ($n = 29$) with respect to the control group ($n = 34$) ($p = 0.06$). However, there was no statistically significant improvement in overall long-term survival rates (57% and 39% for patients with and without adjuvant chemotherapy, respectively) ($p = 0.207$) [276].

The correlation of the responsiveness of patients with oral squamous cell carcinoma to UFT with the intratumoral levels of DPD and TS mRNA was examined. Biopsy specimens were obtained before treatment, which consisted of oral administration of UFT, cobalt-60 irradiation, and injection of an immunopotentiator (OK-432). Intratumoral levels of DPD mRNA in patients who showed complete or partial responses were significantly lower than those in patients who showed no change. However, they did not correlate with local recurrence of the tumor. On the other hand, intratumoral TS mRNA levels did not correlate with any clinicopathological parameters [277].

UFT in Other Tumors

Pancreatic Cancer

A retrospective analysis of postoperative chemotherapy with UFT in 78 patients showed a significant difference in the MST between the UFT group (204 days) and non-UFT group (123 days) [278]. Recently, a phase I trial examined the use of UFT/LV with conventional RT (45 Gy) in 12 patients. MST was 8 months showing that this treatment is a viable option and compares favorably with continuous-infusion regimens [279]. The combination gemcitabine/UFT/LV (Table 7) is an adequate palliative therapy for this disease as it is moderately active and its toxicity is acceptable [268, 269].

Prostate Cancer

A phase II trial of UFT/LV in 28 patients with hormone-refractory prostate cancer demonstrated a level of activity similar to that obtained with i.v. 5-FU [280]. The combinations of UFT, CP, and estramustine or dexamethasone were reported as active and well-tolerated regimens (Table 7).

Bladder Cancer

A randomized, prospective trial of prophylactic oral UFT (300-400 mg/day for 2 years) for patients with superficial bladder cancer indicated that the recurrence rate was significantly lower in the UFT group (26% versus 43% for control). In particular, UFT was effective in preventing recurrence in patients with single tumors or small lesions. Gastrointestinal toxicities occurred in less than 10% of patients [281].

In conclusion, UFT combined with LV or other cytotoxic agents has shown equivalent efficacy for several advanced carcinomas in comparison with standard therapies. However, its advantages may be in ease of administration and absence of infusion-related side effects, including infection and bleeding.

Of note, UFT should not be given with food, which decreases the systemic exposure to 5-FU [282] and has a lethal interaction with sorivudine, a new antiviral drug for herpes zoster. A major metabolite of sorivudine, (E)-5-(2-bromovinyl)-uracil, formed by gut flora, is absorbed through the intestinal membrane and reduced in the liver by DPD, giving a reactive intermediate that is a suicide inhibitor of the enzyme. The DPD inactivation leads to extremely high concentrations of 5-FU, resulting in severe gastrointestinal and myelotoxicities then death [283].

UFT/LV has been submitted to the FDA for approval as a first-line treatment of advanced colorectal cancer. As of this writing, approval by the FDA was still pending because the overall role of UFT/LV alone remains to be established, since the first-line therapy of advanced colorectal cancer is changing to the combination of 5-FU/LV/CPT-11 [284]. In Europe, UFT/LV has been approved as a first-line treatment of metastatic colorectal cancer.

S-1

Further refinement of the strategy that led to UFT has resulted in a new mixture, called S-1 or TS-1 (Fig. 1). S-1 is a combination of a prodrug of 5-FU, FTO, and two compounds, 5-chloro-2,4-dihydroxypyridine (CDHP; gimestat) and potassium oxonate (OXO; otastat). It was developed in 1996 by Japanese workers in an attempt to circumvent the adverse reactions of FTO, but without compromising efficacy [285].

In this combination, FTO provides stable and prolonged liberation of 5-FU, equivalent to a continuous i.v. infusion of this drug. Neither CDHP nor OXO has any antitumor activity itself, and they act solely as modulators of 5-FU, designed to act at different steps in the metabolism of 5-FU. CDHP is a potent and reversible inhibitor of DPD, thereby prolonging high 5-FU concentration in the circulation. In vitro, CDHP is 180 times more potent than U, another reversible inhibitor of DPD [286]. Animal studies have demonstrated an elevation and a stability over 12 hours in levels of 5-FU in plasma and tumors after coadministration of FTO with CDHP, or S-1 [285, 287, 288]. OXO is employed to limit the gastrointestinal toxicity of FTO. It has already been pointed out that this toxicity stems from the phosphorylation of 5-FU within the digestive tract by OPRT. OXO accumulates in gastrointestinal

tissues more than in other tissues or in the blood of normal or tumor-bearing rats [289, 290]. OXO competitively inhibits this enzyme, which converts 5-FU to 5-FUMP. The levels of 5-FUMP are decreased by 69% in the small intestine, 2% in Yoshida sarcoma, and 0% in bone marrow. The levels of 5-FU incorporated into RNA are thus decreased by 71% in the small intestine, 22% in Yoshida sarcoma, and 0% in bone marrow [289]. OXO also protects the activity of TS by decreasing 5-FdUMP via 5-FUMP in gastrointestinal tissue, which leads to a reduction in gastrointestinal toxicity [291].

The optimal molar ratio of the three constituents (FTO/CDHP/OXO) of this combination is 1:0.4:1. With this formulation, an optimal inhibition of the transformation of 5-FU in the intestine is obtained without affecting its activation in the tumor [285]. Researchers in Japan conducted preclinical evaluation of S-1 and demonstrated its antitumor activity in experimental models of rodent tumors and human xenografts [287, 288, 292-296]. S-1 significantly inhibited tumor growth in rats with subcutaneous Yoshida sarcoma, and in nude rats and mice implanted with human colon, stomach, head and neck, and breast cancer cell lines. S-1 achieved induction of high and sustained apoptosis. S-1 also showed a significant antimetastatic effect on liver metastasis. The animal studies also confirmed that the gastrointestinal toxicity of S-1 was low because of the protection afforded by OXO [293]. Recently, a potentiated antitumor effect in Yoshida sarcoma-bearing rats was demonstrated when S-1 was combined with cisplatin [297].

Phase I studies of S-1 have been conducted in Japan, Europe, and the United States [298-301], and Phase II trials have been conducted in Japan (Table 8) [302-318]. S-1 achieved similar responses to those of conventional treatments, with a lower incidence of grade 3 or 4 toxicities. The DLT of S-1 was myelosuppression in Japan and diarrhea in Western countries. This difference remains unexplained, although it seems that the conversion of FTO to 5-FU occurs more slowly in Asians than in other ethnic groups [299, 300, 319, 320]. Pharmacokinetic studies showed that, in terms of S-1 dosing, three times daily per os is likely to lead to a more stable steady-state 5-FU plasma concentration and make the toxicity mild without compromising efficacy [300, 321].

Based on the good results observed in patients with gastric cancer, S-1 was given a manufacturing approval from the Ministry of Health and Welfare of Japan in January 1999, with indications for advanced and recurrent gastric cancers [322]. Recently, the relationship between immunoreactivity of TS and DPD in biopsy specimens and the effects of chemotherapy were investigated in 41 patients treated with S-1 for advanced gastric cancer. There were no significant differences in RR and MST (Table 8), indicating that S-1 is effective in the treatment of gastric cancer patients, regardless of intratumoral TS and DPD immunoreactivity status [313].

A comparative study of S-1 (80 mg/m^2/day for 28 days followed by 14 days rest) with or without low-dose (7 mg/m^2 three times a week) cisplatin for patients with recurrent or advanced gastric cancer led to an RR of 25% and an MST of 232 days in the S-1 group ($n = 8$) versus 60% and 157 days in the S-1/cisplatin group ($n = 5$) [323].

Every month, in the Japanese journal *Gan To Kagaku Ryoho*, several case reports on patients treated with S-1 (and more recently with S-1 and cisplatin) for various tumors (mainly gastric) are published. They are not detailed here as only the abstract is in English.

Conclusion

5-FU is one of the most widely used cytotoxic drugs. It is usually administered by i.v. bolus or by continuous i.v. infusion. Although the latter route is the most efficient and least toxic, it is costly and inconvenient. Treatment is now increasingly governed by concern for patient quality of life as well as for efficacy. Intravenous infusion requires attendance in a hospital or clinic, which is not without psychological impact on the patient and has a non-negligible risk of complications from catheterization. An oral formulation of 5-FU would be a considerable advance in the treatment of cancer. Unfortunately, due to the activity of DPD, the drug on its own is poorly absorbed and tissue levels are highly variable.

The development of new agents that use a specific property of tumors such as CAP, or which inhibit DPD such as UFT and S-1, or act on 5-FU anabolism such as UFT/LV, has given new impetus to therapeutic strategies using fluoropyrimidines. All these compounds have demonstrated therapeutic efficacy. CAP and UFT/LV are effective, well-tolerated, and convenient treatments for patients with colorectal cancer even if, compared with the classic 5-FU/LV regimen, they do not improve median survival. In the adjuvant setting, PMC, which combined low-dose oral UFT with continuous i.v. 5-FU, seems an attractive approach but needs larger clinical trials. For metastatic breast cancer patients, CAP is active and well tolerated and resulted in an improvement in tumor-related symptoms. It, therefore, provides an effective and tolerable therapy for patients in whom anthracycline and taxane treatment has failed. UFT/LV led to good RR in gastric tumors. In the adjuvant therapy of non-small cell lung cancer, UFT/LV showed a slight advantage with respect to conventional treatments. S-1 is very likely an effective drug against gastric carcinoma, but it is too early in development to know its potential disadvantages. However, a twice-daily administration is necessary for CAP and S-1, and a thrice-daily one is needed for UFT/LV. This raises a potential problem with oral chemotherapy, that is, the reliability of patient compliance with a treatment associated with toxic effects, especially in adjuvant therapy.

Table 8. Phase II trials on patients treated with S-1 alone or combined with cisplatin

Study (year)	*n* of evaluable patients, disease	S-1 dose	Response rate (95% CI)	Median duration of response (MDR); median survival time (MST)	Main side effects
Horikoshi et al. [302] (1996) *Sugimachi et al.* [303] (1999)	58 28 gastric cancer 30 colorectal cancer	150-200 mg/d[a]	Gastric cancer 54% colorectal cancer 17%	Gastric cancer MDR 84 d MST 298 d Colorectal cancer MDR 109 d MST 358 d	Leukopenia, anemia, diarrhea
Taguchi et al. [304, 305] (1996, 1998)	27 breast cancer	100-150 mg/d[a]	41%		Leukopenia, neutropenia, anemia, hemoglobinemia, ↓ anorexia, nausea, vomiting, fatigue
Fujii et al. [306] (1996)	26 head and neck cancer	100-150 mg/d[a]	46%		Hemoglobinemia, ↓ stomatitis, neutropenia, anorexia
Kurihara et al. [307] (1998) *Koizumi et al.* [308] (2000)	50 gastric cancer	BSA < 1.25 m^2 80 mg/d[a] 1.25 < BSA < 1.5 100 mg/d[a] BSA ≥ 1.5 120 mg/d[a]	44% (30%-59%)	MDR 135 d MST 207 d	Hemoglobinemia, ↓ leukopenia, neutropenia, diarrhea
Sakata et al. [309] (1998)	51 gastric cancer	BSA < 1.25 m^2 80 mg/d[a] 1.25 < BSA < 1.5 100 mg/d[a] BSA ≥ 1.5 120 mg/d[a]	49% (36%-62%)	MDR 68 d MST 250 d	Hemoglobinemia, ↓ granulocytopenia, leukopenia, diarrhea, malaise
Baba et al. [310] (1998) *Ohtsu et al.* [311] (2000)	62 colorectal cancer	BSA < 1.25 m^2 80 mg/d[a] 1.25 < BSA < 1.5 100 mg/d[a] BSA ≥ 1.5 120 mg/d[a]	35% (25%-48%)	MDR 171 d MST 12 mo	Neutropenia, thrombocytopenia, anemia, leukopenia, anorexia
Sano et al. [312] (2000)	81 breast cancer	80 mg/m^2/d[a]	42% (31%-54%)	MST 910 d	Neutropenia, anorexia, fatigue, nausea, vomiting, diarrhea, stomatitis
Miyamoto et al. [313] (2000)	41 gastric cancer	80 mg/m^2/d[a]	TS + 54% TS - 53% DPD + 61% DPD - 48%	MST TS + 284 d TS - 189 d DPD + 338 d DPD - 207 d	
Yoshida et al. [314] (2001)	19 gastric cancer	75 mg/m^2/d[a]	47%		Bone marrow suppression, nausea, vomiting,
Kamata et al. [315] (2001)	12 gastric cancer	S-1 80 mg/body oral cisplatin 15 mg/m^2 i.v. biweekly	42%	MST 15.3 mo	Leukopenia
Inuyama et al. [316] (2001) *Shirasaka et al.* [317] (2001)	59 head and neck cancer		29% (18%-42%)	MST 344 d	Anemia, leukopenia, neutropenia, anorexia
Kawahara et al. [318] (2001)	59 chemotherapy-naive non-small cell lung cancer	80 mg/m^2/d[a]	22% (12%-35%)	MDR 3.4 mo MST 10.2 mo	Anorexia, diarrhea, malaise, neutropenia

[a]Administered orally during 28 days in two daily doses every 6 weeks
[b]Administered orally during 28 days every 6 weeks

Abbreviations: CI = confidence interval; BSA = body surface area; TS = thymidylate synthase; DPD = dihydropyrimidine dehydrogenase

The future of these oral drugs will rest on documentation of superior, or at least equivalent to 5-FU, activity, decreased toxicity, patient convenience, or diminished costs. Oral 5-FU prodrugs will undoubtedly join the list of chemotherapeutic agents, but it is too early to predict whether they will eventually replace 5-FU treatment [324]. Combining oral fluoropyrimidines with drugs such as CPT-11 and oxaliplatin is an exciting prospect. However, the economic advantage that can be gained with oral medications can be lost when combinations employing drugs that need a parenteral administration are prescribed. The advantages of 5-FU prodrugs with respect to conventional treatment regimens will thus need to be proven in future clinical trials.

References

1 Rutman RJ, Cantarow A, Paschkis KE. Studies in 2-acetylaminofluorene carcinogenesis. III. The utilization of uracil-2-C^{14} by preneoplastic rat liver and rat hepatoma. Cancer Res 1954;14:119-123.

2 Heidelberger C, Chaudhuri NK, Danneberg PB et al. Fluorinated pyrimidines, a new class of tumor-inhibitory compounds. Nature 1957;179:663-666.

3 Heidelberger C, Danenberg PV, Moran RG. Fluorinated pyrimidines and their nucleosides. In: Meister A, ed. Advances in Enzymology and Related Areas of Molecular Biology. New York: John Wiley & Sons, 1983:57-121.

4 Valeriote F, Santelli G. 5-fluorouracil (FUra). Pharmacol Ther 1984;24:107-132.

5 Pinedo HM, Peters GJ. Fluorouracil: biochemistry and pharmacology. J Clin Oncol 1988;6:1653-1664.

6 Diasio RB, Harris BE. Clinical pharmacology of 5-fluorouracil. Clin Pharmacokinet 1989;16:215-237.

7 Daher GC, Harris BE, Diasio RB. Metabolism of pyrimidine analogs and their nucleosides. Pharmacol Ther 1990;48:189-222.

8 Parker WB, Cheng YC. Metabolism and mechanism of action of 5-fluorouracil. Pharmacol Ther 1990;48:381-395.

9 Weckbecker G. Biochemical pharmacology and analysis of fluoropyrimidines alone and in combination with modulators. Pharmacol Ther 1991;50:367-424.

10 Schilsky RL. Biochemical and clinical pharmacology of 5-fluorouracil. Oncology (Huntingt) 1998;12(suppl 7):13-18.

11 Thomas DM, Zalcberg JR. 5-fluorouracil: a pharmacological paradigm in the use of cytotoxics. Clin Exp Pharmacol Physiol 1998;25:887-895.

12 Lamont EB, Schilsky RL. The oral fluoropyrimidines in cancer chemotherapy. Clin Cancer Res 1999;5:2289-2296.

13 Grem JL. 5-fluorouracil: forty-plus and still ticking. A review of its preclinical and clinical development. Invest New Drugs 2000;18:299-313.

14 Martino R, Lopez A, Malet-Martino MC et al. Release of fluoride ion from 5′-deoxy-5-fluorouridine, an antineoplastic fluoropyrimidine, in humans. Drug Metab Dispos 1985;13:116-118.

15 Porter DJY, Harrington JA, Almond MR et al. Enzymatic elimination of fluoride from alpha-fluoro-beta-alanine. Biochem Pharmacol 1995;50:1475-1484.

16 Martino R, Malet-Martino MC, Vialaneix C et al. ^{19}F nuclear magnetic resonance analysis of the carbamate reaction of α-fluoro-β-alanine (FBAL), the major catabolite of fluoropyrimidines. Application to FBAL carbamate determination in body fluids of patients treated with 5′-deoxy-5-fluorouridine. Drug Metab Dispos 1987;15:897-904.

17 Sweeny DJ, Barnes S, Heggie GD et al. Metabolism of 5-fluorouracil to an N-cholyl-2-fluoro-β-alanine conjugate: previously unrecognized role for bile acids in drug conjugation. Proc Natl Acad Sci USA 1987;84:5439-5443.

18 Malet-Martino MC, Bernadou J, Martino R et al. ^{19}F NMR spectrometry evidence for bile acid conjugates of α-fluoro-β-alanine as the main biliary metabolites of antineoplastic fluoropyrimidines in humans. Drug Metab Dispos 1988;16:78-84.

19 Lemaire L, Malet-Martino MC, de Forni M et al. Cardiotoxicity of commercial 5-fluorouracil vials stems from the alkaline hydrolysis of this drug. Br J Cancer 1992;66:119-127.

20 Lemaire L, Arellano M, Malet-Martino M et al. A novel metabolite of 5-fluorouracil in humans: 2-fluoro-3-hydroxypropionic acid. Proc Am Assoc Cancer Res 1996;37:1225a.

21 Aschele C, Sobrero A, Faderan MA et al. Novel mechanism(s) of resistance to 5-fluorouracil in human colon cancer (HCT-8) sublines following exposure to two different clinically relevant dose schedules. Cancer Res 1992;52:1855-1864.

22 Sobrero AF, Aschele C, Guglielmi AP et al. Synergism and lack of cross-resistance between short-term and continuous exposure to fluorouracil in human colon adenocarcinoma cells. J Natl Cancer Inst 1993;85:1937-1944.

23 Sobrero AF, Aschele C, Bertino JR. Fluorouracil in colorectal cancer — a tale of two drugs: implications for biochemical modulation. J Clin Oncol 1997;15:368-381.

24 Diasio RB, Johnson MR. Dihydropyrimidine dehydrogenase: its role in 5-fluorouracil clinical toxicity and tumor resistance. Clin Cancer Res 1999;5:2672-2673.

25 Guimbaud R, Guichard S, Dusseau C et al. Dihydropyrimidine dehydrogenase activity in normal, inflammatory and tumour tissues of colon and liver in humans. Cancer Chemother Pharmacol 2000;45:477-482.

26 Peters GJ, Jansen G. Resistance to antimetabolites. In: Schilsky RL, Milano GA, Ratain MJ, eds. Principles of Antineoplastic Drug Development and Pharmacology. New York: Marcel Dekker, Inc., 1996:543-585.

27 Fraile RJ, Baker LH, Buroker TR et al. Pharmacokinetics of 5-fluorouracil administered orally, by rapid intravenous and by slow infusion. Cancer Res 1980;40:2223-2228.

28 Diasio RB. The role of dihydropyrimidine dehydrogenase (DPD) modulation in 5-FU pharmacology. Oncology (Huntingt) 1998;12(suppl 7):23-27.

29 Iyer L, Ratain MJ. 5-fluorouracil pharmacokinetics: causes for variability and strategies for modulation in cancer chemotherapy. Cancer Invest 1999;17:494-506.

30 Lokich JJ, Ahlgren JD, Gullo JJ et al. A prospective randomized comparison of continuous infusion fluorouracil with a conventional bolus schedule in metastatic colorectal carcinoma: a Mid-Atlantic Oncology Program Study. J Clin Oncol 1989;7:425-432.

31 Benson 3rd AB. Regional and systemic therapies for advanced colorectal carcinoma: randomized clinical trial results. Oncology (Huntingt) 1998;12(suppl 7):28-34.

32 Seifert P, Baker LH, Reed ML et al. Comparison of continuously infused 5-fluorouracil with bolus injection in treatment of patients with colorectal adenocarcinoma. Cancer 1975;36:123-128.

33 Meta-Analysis Group in Cancer. Efficacy of intravenous continuous infusion of fluorouracil compared with bolus administration in advanced colorectal cancer. J Clin Oncol 1998;16:301-308.

34 Meta-Analysis Group in Cancer. Toxicity of fluorouracil in patients with advanced colorectal cancer: effect of administration schedule and prognostic factors. J Clin Oncol 1998;16:3537-3541.

35 Advanced Colorectal Cancer Meta-Analysis Project. Modulation of fluorouracil by leucovorin in patients with advanced colorectal cancer: evidence in terms of response rate. J Clin Oncol 1992;10:896-903.

36 Poon MA, O'Connell MJ, Wieand HS et al. Biochemical modulation of fluorouracil with leucovorin: confirmatory evidence of improved therapeutic efficacy in advanced colorectal cancer. J Clin Oncol 1991;9:1967-1972.

37 Petrelli N, Douglass Jr HO, Herrera L et al. The modulation of fluorouracil with leucovorin in metastatic colorectal carcinoma: a prospective randomized phase III trial. Gastrointestinal Tumor Study Group. J Clin Oncol 1989;7:1419-1426.

38 Buroker TR, O'Connell MJ, Wieand HS et al. Randomized comparison of two schedules of fluorouracil and leucovorin in the treatment of advanced colorectal cancer. J Clin Oncol 1994;12:14-20.

39 Brito RA, Medgyesy D, Zakowski TH et al. Fluoropyrimidines: a critical evaluation. Oncology 1999;57(suppl 1):2-8.

40 Liu G, Franssen E, Fitch MI et al. Patient preferences for oral versus intravenous palliative chemotherapy. J Clin Oncol 1997;15:110-115.

41 Kemeny N, Daly J, Reichman B et al. Intrahepatic or systemic infusion of fluorodeoxyuridine in patients with liver metastases from colorectal carcinoma. A randomized trial. Ann Intern Med 1987;107:459-465.

42 Meta-Analysis Group in Cancer. Reappraisal of hepatic arterial infusion in the treatment of nonresectable liver metastases from colorectal cancer. J Natl Cancer Inst 1996;88:252-258.

43 Kemeny N, Gonen M, Sullivan D et al. Phase I study of hepatic arterial infusion of floxuridine and dexamethasone with systemic irinotecan for unresectable hepatic metastases from colorectal cancer. J Clin Oncol 2001;19:2687-2695.

44 Royce ME, Medgyesy D, Zakowski TH et al. Colorectal cancer: chemotherapy treatment overview. Oncology (Huntingt) 2000;14(suppl 14):40-46.

45 Cunningham D, James RD. Integrating the oral fluoropyrimidines into the management of advanced colorectal cancer. Eur J Cancer 2001;37:826-834.

46 Peters GJ, Ackland SP. New antimetabolites in preclinical and clinical development. Exp Opin Invest Drugs 1996;5:637-679.

47 Del Vecchio M, Procopio G, Cassata A et al. Fluoropyrimidines in the treatment of advanced neoplastic diseases: role and advantages of UFT. Tumori 1999;85:6-11.

48 Damjanov N, Meropol NJ. Oral therapy for colorectal cancer: how to choose. Oncology (Huntingt) 2000;14:799-807.

49 Bissett D, Ahmed F, McLeod H et al. Oral fluoropyrimidines in the treatment of colorectal cancer. Clin Oncol (R Coll Radiol) 2000;12:240-245.

50 Papamichael D. The use of thymidylate synthase inhibitors in the treatment of advanced colorectal cancer: current status. Stem Cells 2000;18:166-175.

51 Lewis NL, Meropol NJ. Oral fluoropyrimidines in cancer treatment. Cancer Invest 2000;18:747-760.

52 Diasio RB. Oral DPD-inhibitory fluoropyrimidine drugs. Oncology (Huntingt) 2000;14(suppl 9):19-23.

53 Vanhoefer U, Wilke H. Oral fluoropyrimidine-based combination therapy in gastrointestinal cancer. Oncology (Huntingt) 2001;15(suppl 2):79-84.

54 Sharma S. Patient selection for oral chemotherapy. Oncology (Huntingt) 2001;15(suppl 2):33-35.

55 de Bono JS, Twelves CJ. The oral fluorinated pyrimidines. Invest New Drugs 2001;19:41-59.

56 Kuhn JG. Fluorouracil and the new oral fluorinated pyrimidines. Ann Pharmacother 2001;35:217-227.

57 Cunningham D, Coleman R. New options for outpatient chemotherapy. The role of oral fluoropyrimidines. Cancer Treat Rev 2001;27:211-220.

58 Johnston PG, Kaye S. Capecitabine: a novel agent for the treatment of solid tumors. Anticancer Drugs 2001;12:639-646.

59 Jones R, Twelves C. Oral uracil-tegafur: an alternative to intravenous 5-fluorouracil? Expert Opin Pharmacother 2001;2:1495-1505.

60 Arazaki M, Ishitsuka H, Kuruma I et al. N-oxycarbonyl substituted 5'-deoxy-5-fluorocytidines. Eur Patent Appl 1992; no. 92121538.0.

61 Bajetta E, Carnaghi C, Somma L et al. A pilot safety study of capecitabine, a new oral fluoropyrimidine, in patients with advanced neoplastic disease. Tumori 1996;82:450-452.

62 Haraguchi M, Miyadera K, Uemura K et al. Angiogenic activity of enzymes. Nature 1994;368:198.

63 Judson IR, Beale PJ, Trigo JM et al. A human capecitabine excretion balance and pharmacokinetic study after administration of a single oral dose of ^{14}C-labelled drug. Invest New Drugs 1999;17:49-56.

64 Reigner B, Blesch K, Weidekamm E. Clinical pharmacokinetics of capecitabine. Clin Pharmacokinet 2001;40:85-104.

65 Miwa M, Ura M, Nishida M et al. Design of a novel oral fluoropyrimidine carbamate, capecitabine, which generates 5-fluorouracil selectively in tumours by enzymes concentrated in human liver and cancer tissue. Eur J Cancer 1998;34:1274-1281.

66 Sobrero A, Guglielmi A, Grossi F et al. Mechanism of action of fluoropyrimidines: relevance to the new developments in colorectal cancer chemotherapy. Semin Oncol 2000;27(suppl 10):72-77.

67 Schüller J, Cassidy J, Dumont E et al. Preferential activation of capecitabine in tumor following oral administration to colorectal cancer patients. Cancer Chemother Pharmacol 2000;45:291-297.

68 Taguchi T, Ishitani K, Saitoh K et al. A Japanese phase I study of continuous twice daily treatment with capecitabine in patients with advanced and/or metastatic solid tumors. Ann Oncol 1996;7:299a.

69 Hughes M, Planting A, Twelves C et al. A phase I study of intermittent twice daily oral therapy with capecitabine in patients with advanced and/or metastatic solid cancer. Ann Oncol 1996;7:297a.

70 Budman DR, Meropol NJ, Reigner B et al. Preliminary studies of a novel oral fluoropyrimidine carbamate: capecitabine. J Clin Oncol 1998;16:1795-1802.

71 Mackean M, Planting A, Twelves C et al. Phase I and pharmacologic study of intermittent twice-daily oral therapy with capecitabine in patients with advanced and/or metastatic cancer. J Clin Oncol 1998;16:2977-2985.

72 Cassidy J, Dirix L, Bissett D et al. A phase I study of capecitabine in combination with oral leucovorin in patients with intractable solid tumors. Clin Cancer Res 1998;4:2755-2761.

73 Cao S, Lu K, Ishitsuka H et al. Antitumor efficacy of capecitabine against fluorouracil-sensitive and -resistant tumors. Proc Am Soc Clin Oncol 1997;16:795a.

74 Abushullaih S, Saad E, Hoff PM. Characterizing hand-foot syndrome (HFS) caused by capecitabine. Proc Am Soc Clin Oncol 2000;19:2403a.

75 Lauman MK, Morimer J. Effect of pyridoxine on the incidence of palmar plantar erythroderma (PPE) in patients receiving capecitabine. Proc Am Soc Clin Oncol 2001;20:1565a.

76 Chin SF, Tehen N, Oza AM et al. Use of "bag balm" as topical treatment of palmar-plantar erythrodysesthesia syndrome (PPES) in patients receiving selected chemotherapeutic agents. Proc Am Soc Clin Oncol 2001;20:1632a.

77 O'Reilly SM, Moiseyenko V, Talbot DC et al. A randomized phase II study of Xeloda™ (capecitabine) vs paclitaxel in breast cancer patients failing previous anthracycline therapy. Proc Am Soc Clin Oncol 1998;17:627a.

78 Blum JL, Jones SE, Buzdar AU et al. Multicenter phase II study of capecitabine in paclitaxel-refractory metastatic breast cancer. J Clin Oncol 1999;17:485-493.

79 Cervantes G, Torrecillas L, Erazo AA et al. Capecitabine (XELODA) as treatment after failure to taxanes for metastatic breast cancer. Proc Am Soc Clin Oncol 2000;19:469a.

80 Wong ZW, Wong KK, Chew L et al. Capecitabine as an oral chemotherapeutic agent in the treatment of refractory metastatic breast carcinoma (MBC). Proc Am Soc Clin Oncol 2000;19:466a.

81 Watanabe T, Katsumata N, Sasaki Y et al. A multicenter phase II trial of Xeloda™ (capecitabine) in patients with docetaxel-refractory advanced/metastatic breast cancer. Proc Am Soc Clin Oncol 2001;20:1991a.

82 Blum JL, Dieras V, Lo Russo PM et al. Multicenter, phase II study of capecitabine in taxane-pretreated metastatic breast carcinoma patients. Cancer 2001;92:1759-1768.

83 Thuss-Patience PC, Von Minckwitz G, Lück HJ et al. Capecitabine: a new standard in metastatic breast cancer recurring after anthracycline and taxane-containing chemotherapy? Results of a multicenter phase II trial. Proc Am Soc Clin Oncol 2001;20:2012a.

84 Sundaram S, Lancaster D, Silva J et al. Oral capecitabine is an active and well tolerated primary palliative treatment in patients with metastatic breast cancer who progress after high dose chemotherapy and autologous stem cell support. Proc Am Soc Clin Oncol 2000;19:223a.

85 Jakob A, Schupp M, Knop S et al. A phase II study of capecitabine in patients, who relapsed after high dose chemotherapy followed by peripheral blood stem cell transplantation for metastatic breast cancer. Proc Am Soc Clin Oncol 2001;20:1966a.

86 O'Shaughnessy JA, Blum J, Moiseyenko V et al. Randomized, open-label, phase II trial of oral capecitabine (Xeloda) vs. a reference arm of intravenous CMF (cyclophosphamide, methotrexate and 5-fluorouracil) as first-line therapy for advanced/metastatic breast cancer. Ann Oncol 2001;12:1247-1254.

87 Kusama M, Sano M, Ikeda T et al. A phase II study of Xeloda™ (capecitabine) in patients with advanced/metastatic breast carcinoma. Proc Am Soc Clin Oncol 2001;20:1924a.

88 Procopio G, Bajetta E, Catena L et al. A phase II study of capecitabine in elderly patients with advanced breast cancer. Proc Am Soc Clin Oncol 2001;20:3134a.

89 Vasey P, McMahon L, Paul J et al. A phase II trial of capecitabine in relapsed ovarian cancer [abstract]. Ann Oncol 2000;11(suppl 4):373P.

90 Wenzel C, Locker GJ, Schmidinger M et al. Capecitabine in the treatment of metastatic renal cell carcinoma failing immunotherapy. Am J Kidney Dis 2002;39:48-54.

91 Lozano RD, Patt YZ, Hassan MM et al. Oral capecitabine (Xeloda) for the treatment of hepatobiliary cancers (hepatocellular carcinoma, cholangiocarcinoma and gallbladder cancer). Proc Am Soc Clin Oncol 2000;19:1025a.

92 Cartwright TH, Cohn A, Varkey JA et al. Phase II study of oral capecitabine in patients with advanced or metastatic pancreatic cancer. J Clin Oncol 2002;20:160-164.

93 Hoff P, Abbruzzese JL, Medgyesy D et al. A phase II study of Xeloda (capecitabine) in patients with metastatic colorectal cancer demonstrating progression on 5-FU therapy. Proc Am Soc Clin Oncol 2000;19:993a.

94 Van Cutsem E, Findlay M, Osterwalder B et al. Capecitabine, an oral fluoropyrimidine carbamate with substantial activity in advanced colorectal cancer: results of a randomized phase II study. J Clin Oncol 2000;18:1337-1345.

95 Koizumi W, Taguchi T. A phase II study of capecitabine (Xeloda™) in patients with advanced/metastatic gastric carcinoma. Proc Am Soc Clin Oncol 2001;20:2320a.

96 Van Cutsem E, Twelves C, Cassidy J et al. Oral capecitabine compared with intravenous fluorouracil plus leucovorin in patients with metastatic colorectal cancer: results of a large phase III study. J Clin Oncol 2001;19:4097-4106.

97 Twelves C, Boyer M, Findlay M et al. Capecitabine (Xeloda™) improves medical resource use compared with 5-fluorouracil plus leucovorin in a phase III trial conducted in patients with advanced colorectal carcinoma. Eur J Cancer 2001;37:597-604.

98 Hoff PM, Ansari R, Batist G et al. Comparison of oral capecitabine versus intravenous fluorouracil plus leucovorin as first-line treatment in 605 patients with metastatic colorectal cancer: results of a randomized phase III study. J Clin Oncol 2001;19:2282-2292.

99 Twelves C. Capecitabine as first-line treatment in colorectal cancer: pooled data from two large, phase III trials. Eur J Cancer 2002;38(suppl 2):15-20.

100 Blum JL. The role of capecitabine, an oral, enzymatically activated fluoropyrimidine, in the treatment of metastatic breast cancer. ***The Oncologist*** 2001;6:56-64.

101 Sawada N, Ishikawa T, Fukase Y et al. Induction of thymidine phosphorylase activity and enhancement of capecitabine efficacy by taxol/taxotere in human cancer xenografts. Clin Cancer Res 1998;4:1013-1019.

102 Endo M, Shanbodi N, Fukase Y et al. Induction of thymidine phosphorylase expression and enhancement of efficacy of capecitabine or 5'-deoxy-5-fluorouridine by cyclophosphamide in mammary tumor models. Int J Cancer 1999;83:127-134.

103 Sawada N, Ishikawa T, Sekiguchi F et al. X-ray irradiation induces thymidine phosphorylase and enhances the efficacy of capecitabine (Xeloda) in human cancer xenografts. Clin Cancer Res 1999;5:2948-2953.

104 Fujimoto-Ouchi K, Tanaka Y, Tominaga T. Schedule dependency of antitumor activity in combination therapy with capecitabine/5'-deoxy-5-fluorouridine and docetaxel in breast cancer models. Clin Cancer Res 2001;7:1079-1086.

105 Khoury P, Villalona-Calero M, Blum J et al. Phase I study of capecitabine in combination with paclitaxel in patients with previously treated metastatic breast cancer. Proc Am Soc Clin Oncol 1998;17:793a.

106 Villalona-Calero MA, Weiss GR, Burris HA et al. Phase I and pharmacokinetic study of the oral fluoropyrimidine capecitabine in combination with paclitaxel in patients with advanced solid malignancies. J Clin Oncol 1999;17:1915-1925.

107 Elza-Brown K, Dees EC, Wolff AC et al. A phase I study of capecitabine and weekly paclitaxel in advanced solid tumors [abstract]. Proc Am Soc Clin Oncol 2000;19:921J.

108 Villalona-Calero MA, Blum JL, Jones SE et al. A phase I and pharmacologic study of capecitabine and paclitaxel in breast cancer patients. Ann Oncol 2001;12:605-614.

109 Pronk LC, Vasey P, Sparreboom A et al. A phase II and pharmacokinetic study of the combination of capecitabine and docetaxel in patients with advanced solid tumours. Br J Cancer 2000;83:22-29.

110 Diaz-Rubio E, Evans J, Tabernero J et al. Phase I study of capecitabine in combination with oxaliplatin in patients with advanced or metastatic solid tumors. Proc Am Soc Clin Oncol 2000;19:772a.

111 Evans J, Tabernero J, Cassidy J et al. Safety profile and preliminary efficacy of capecitabine (Xeloda®) in combination with oxaliplatin in patients with advanced or metastatic solid tumours: results from a phase I study [abstract]. Ann Oncol 2000;11(suppl 4):222P.

112 DeSantis S, Zeuli M, Di Constanzo F et al. Oxaliplatin and capecitabine in advanced colorectal cancer: a dose-finding trial. Proc Am Soc Clin Oncol 2001;20:559a.

113 Thomas R, Quinn M, Wilson R et al. A phase I trial of capecitabine (CAPE) and oxaliplatin (OHP). Proc Am Soc Clin Oncol 2001;20:530a.

114 Vanhoefer UI, Mayer S, Achterrath W et al. Phase I study of capecitabine in combination with a weekly schedule of irinotecan as first-line chemotherapy in metastatic colorectal cancer [abstract]. Ann Oncol 2000;11(suppl 4):212P.

115 Cassata A, Alù M, Beretta E et al. Capecitabine in combination with two schedules of irinotecan (CPT-11) in advanced colorectal cancer: a pilot experience [abstract]. Ann Oncol 2000;11(suppl 4):192P.

116 Scleucher N, Tewes M, Achterrath W et al. Extended phase I study of capecitabine in combination with a weekly schedule of irinotecan as first-line chemotherapy in metastatic colorectal cancer. Proc Am Soc Clin Oncol 2001;20:561a.

117 Nole F, Catania C, Mandala M et al. Phase I study of vinorelbine (V) and capecitabine (C) in advanced breast cancer (ABC). Proc Am Soc Clin Oncol 2000;19:428a.

118 Welt A, Borquez D, Oberhoff C et al. Phase I study of capecitabine and vinorelbine in pretreated patients with metastatic breast cancer. Proc Am Soc Clin Oncol 2001;20:1979a.

119 Herrmann R, Borner M, Morant R et al. Combining gemcitabine (GEM) and capecitabine (CAP) in advanced pancreatic cancer. Results of a phase I trial. Proc Am Soc Clin Oncol 2000;19:1038a.

120 Schilsky RL, Bertucci D, Vogelzang NJ et al. Dose-escalating study of capecitabine plus gemcitabine combination therapy in patients with advanced cancer. J Clin Oncol 2002;20:582-587.

121 Holden SN, Eckhardt SG, Fisher S et al. A phase I pharmacokinetic (PK) and biological study of the farnesyl transferase inhibitor (FTI) R115777 and capecitabine in patients (PTS) with advanced solid malignancies. Proc Am Soc Clin Oncol 2001;20:316a.

122 Kimmel KH, Kindler HL, Janisch L et al. Phase I dose-finding study of CI-994 in combination with capecitabine in patients with advanced solid tumors. Proc Am Soc Clin Oncol 2001;20:345a.

123 Dunst J, Reese T, Frings S. Phase I study of capecitabine combined with simultaneous radiotherapy rectal cancer. Proc Am Soc Clin Oncol 2001;20:592a.

124 Ngan S, Zalcberg J, Keil A et al. A phase I study of capecitabine combined with radiotherapy for locally advanced potentially operable rectal cancer. Proc Am Soc Clin Oncol 2001;20:591a.

125 Ben-Josef E, Vaishampayan UN, Vaitkevicius VK et al. A single institution experience with concurrent capecitabine and radiation therapy in gastrointestinal malignancies. Proc Am Soc Clin Oncol 2001;20:2324a.

126 Yoon WH, Choi JH, Kim JR et al. Enhanced tumoricidal effect of preoperative chemoradiation using capecitabine for locally advanced rectal cancer. Proc Am Soc Clin Oncol 2001;20:2165a.

127 Venturini M, Del Mastro L, Merlano M et al. Dose finding study of capecitabine in combination with docetaxel and epirubicin in prior untreated advanced breast cancer patients. Proc Am Soc Clin Oncol 2000;19:419a.

128 Evans TRJ, Paul J, McInnes A et al. A phase I and PK study of capecitabine in combination with epirubicin (E) and cisplatin (C) in patients with advanced oesophagogastric (OG) adenocarcinoma. Proc Am Soc Clin Oncol 2001;20:651a.

129 Bonnefoi H, Biganzoli L, Mauriac L et al. An EORTC-IDBBC phase I study of cyclophosphamide (C) and epirubicin (E) in combination with capecitabine (X) (CEX) as primary treatment of locally advanced/inflammatory (LA/I) or large operable (LO) breast cancer (BC). Proc Am Soc Clin Oncol 2001;20:1800a.

130 Batista N, Perez Manga G, Constenla F et al. Phase II study of capecitabine (Xeloda®) in combination with paclitaxel (P) in the treatment of patients with locally advanced or metastatic breast cancer (BC): preliminary results [abstract]. Ann Oncol 2000;11(suppl 4):130P.

131 Meza LA, Amin B, Horsey M et al. A phase II study of capecitabine in combination with paclitaxel as first or second line therapy in patients with metastatic breast cancer (MBC). Proc Am Soc Clin Oncol 2001;20:2029a.

132 Tonkin E, Scarfe AG, Koski S et al. Preliminary results of a phase I/II study of weekly docetaxel (Taxotere) combined with intermittent capecitabine (Xeloda) for patients with anthracycline pre-treated metastatic breast cancer. Proc Am Soc Clin Oncol 2001;20:2016a.

133 Kim TW, Ahn JH, Lee JH et al. A phase II trial of capecitabine (X) and cisplatin (P) in previously untreated advanced gastric cancer (AGC). Proc Am Soc Clin Oncol 2001;20:662a.

134 Borner MM, Mueller S, Roth A et al. Phase II study of capecitabine (CAP) + oxaliplatin (OXA) in first line and second line treatment of advanced or metastatic colorectal cancer (ACC). Proc Am Soc Clin Oncol 2001;20:546a.

135 Akhtar SU, Mathew P, Lin J et al. Phase II trial of capecitabine and carboplatin in patients with newly diagnosed advanced non-small cell carcinoma of the lung (NSCLC). Proc Am Soc Clin Oncol 2001;20:2862a.

136 Cassata A, Chiara Stani S, Alu M et al. Ongoing phase II trial with two schedules of irinotecan (CPT-11) in combination with capecitabine as first line chemotherapy in patients with advanced colorectal cancer (ACRC). Proc Am Soc Clin Oncol 2001;20:573a.

137 Domenech G, Perez A, Vogel C. Vinorelbine/capecitabine (VINOCAP) combination remission induction therapy for metastatic breast cancer (MBC). Proc Am Soc Clin Oncol 2001;20:1939a.

138 Campos LT, Alvarez RH, Sanford B et al. Gemcitabine (GEM) and capecitabine (CPC) in advanced pancreatic cancer (APC) and solid tumors. A single institution experience. Proc Am Soc Clin Oncol 2001;20:2315a.

139 Bangemann N, Kuhle A, Ebert A et al. Capecitabine combined with trastuzumab in the therapy of intensively pretreated HER2-overexpressing metastatic breast cancer (MBC) [abstract]. Ann Oncol 2000;11(suppl 4):653P.

140 Venturini M, Del Mastro L, Durando A et al. TEX (Taxotere, Epirubicin and Xeloda) regimen as first line chemotherapy in advanced breast cancer. A multicenter phase II study. Proc Am Soc Clin Oncol 2001;20:1938a.

141 Bell KA, Perna AG, Hsu S. Mucositis as a treatment-limiting side effect in the use of capecitabine for the treatment of metastatic breast cancer. J Am Acad Dermatol 2001;45:790-791.

142 Schmid-Wendtner MH, Wendtner CM, Volkenandt M et al. Clinical picture: leopard-like vitiligo with capecitabine. Lancet 2001;358:1575.

143 Chen GY, Chen YH, Hsu MM et al. Onychomadesis and onycholysis associated with capecitabine. Br J Dermatol 2001;145:521-522.

144 Arén O, Calveira S, Banchero P et al. Cost comparison of two treatment regimens for metastatic colorectal cancer. 5-fluorouracil plus leucovorin vs. capecitabine. Ann Oncol 2000;11(suppl 4):243a.

145 Schwetz BA. From the Food and Drug Administration. New combination therapy for advanced breast cancer. JAMA 2001;286:2085.

146 Michaud LB, Gauthier MA, Wodjylo JR et al. Improved therapeutic index with lower dose capecitabine in metastatic breast cancer (MBC) patients (Pts). Proc Am Soc Clin Oncol 2000;19:402a.

147 O'Shaughnessy J, Blum J. A retrospective evaluation of the impact of dose reduction in patients treated with Xeloda (capecitabine). Proc Am Soc Clin Oncol 2000;19:400a.

148 Schaller G, Ebert A, Kuhle A et al. Drug interaction of capecitabine and phenytoin in the therapy of cerebral and visceral metastatic breast cancer [abstract]. Ann Oncol 2000;11(suppl 4):637P.

149 Park DJ, Stoehlmacher J, Zhang W et al. Human thymidylate synthase gene polymorphism determines response to

capecitabine chemotherapy in advanced colorectal cancer. Proc Am Soc Clin Oncol 2001;20:514a.

150 Fujii S, Kitano S, Ikenaka K et al. Effect of coadministration of uracil or cytosine on the anti-tumor activity of clinical doses of 1-(2-tetrahydrofuryl)-5-fluorouracil and level of 5-fluorouracil in rodents. Gann 1979;70:209-214.

151 Hoff PM. The tegafur-based dihydropyrimidine dehydrogenase inhibitory fluoropyrimidines, UFT/leucovorin (ORZEL™) and S-1: a review of their clinical development and therapeutic potential. Invest New Drugs 2000;18:331-342.

152 Ho DH, Pazdur R, Covington W et al. Comparison of 5-fluorouracil pharmacokinetics in patients receiving continuous 5-fluorouracil infusion and oral uracil plus N1-(2'-tetrahydrofuryl)-5-fluorouracil. Clin Cancer Res 1998;4:2085-2088.

153 Yonekura K, Basaki Y, Chikahisa L et al. UFT and its metabolites inhibit the angiogenesis induced by murine renal cell carcinoma, as determined by a dorsal air sac assay in mice. Clin Cancer Res 1999;5:2185-2191.

154 Ota K, Taguchi T, Kimura K. Report on nationwide pooled data and cohort investigation in UFT phase II study. Cancer Chemother Pharmacol 1988;22:333-338.

155 Muggia FM, Wu X, Spicer D et al. Phase I and pharmacokinetic study of oral UFT, a combination of the 5-fluorouracil prodrug tegafur and uracil. Clin Cancer Res 1996;2:1461-1467.

156 Pazdur R, Lassere Y, Diaz-Canton E et al. Phase I trials of uracil-tegafur (UFT) using 5 and 28 day administration schedules: demonstration of schedule-dependent toxicities. Anticancer Drugs 1996;7:728-733.

157 Spicer D, Muggia F, Tulpule A et al. Phase I circadian dosing of daily oral uracil (U) plus 1-(tetrahydro-2-furanyl)-5-fluorouracil (FT) with leucovorin (LV). Proc Am Soc Clin Oncol 1991;10:342a.

158 Gonzalez-Baron M, Feliu J, Ordonez A et al. Phase I study of UFT plus leucovorin in advanced colorectal cancer: a double modulation proposal. Anticancer Res 1993;13:759-762.

159 Meropol NJ, Rusum YM, Petrelli NJ et al. A phase I and pharmacokinetic study of oral uracil, ftorafur, and leucovorin in patients with advanced cancer. Cancer Chemother Pharmacol 1996;37:581-586.

160 Pazdur R, Lassere Y, Diaz-Canton E et al. Phase I trial of uracil-tegafur (UFT) plus oral leucovorin: 14-day schedule. Invest New Drugs 1997;15:123-128.

161 Pazdur R, Lassere Y, Diaz-Canton E et al. Phase I trial of uracil-tegafur (UFT) plus oral leucovorin: 28-day schedule. Cancer Invest 1998;16:145-151.

162 Ho DH, Covington W, Brown N et al. Oral uracil and ftorafur plus leucovorin: pharmacokinetics and toxicity in patients with metastatic cancer. Cancer Chemother Pharmacol 2000;46:351-356.

163 Malik STA, Talbot D, Clarke PI et al. Phase II trial of UFT in advanced colorectal and gastric cancer. Br J Cancer 1990;62:1023-1025.

164 Pazdur R, Lassere Y, Rhodes V et al. Phase II trial of uracil and tegafur plus oral leucovorin: an effective oral regimen in the treatment of metastatic colorectal carcinoma. J Clin Oncol 1994;12:2296-2300.

165 Saltz LB, Leichman CG, Young CW et al. A fixed-ratio combination of uracil and tegafur (UFT) with low dose leucovorin. An active oral regimen for advanced colorectal cancer. Cancer 1995;75:782-785.

166 Gonzalez-Baron M, Feliu J, de la Gandara I et al. Efficacy of oral tegafur modulation by uracil and leucovorin in advanced colorectal cancer. A phase II study. Eur J Cancer 1995;31A:2215-2219.

167 Abad A, Navarro M, Sastre J et al. A preliminary report of a phase II trial. UFT plus oral folinic acid as therapy for metastatic colorectal cancer in older patients. Spanish Group for the Treatment of Gastrointestinal Tumors (TTd Group). Oncology (Huntingt) 1997;11(suppl 10):53-57.

168 Feliu J, Gonzalez-Baron M, Espinosa E et al. Uracil and tegafur modulated with leucovorin; an effective regimen with low toxicity for the treatment of colorectal carcinoma in the elderly. Cancer 1997;79:1884-1889.

169 Meropol NJ, Sonnichsen DS, Birkhofer MJ et al. Bioavailability and phase II study of oral UFT plus leucovorin in patients with relapsed or refractory colorectal cancer. Cancer Chemother Pharmacol 1999;43:221-226.

170 Aranda E, Anton-Torres A, Sastre J et al. UFT plus leucovorin (LV) in advanced colorectal cancer (CCR). A phase II trial. Proc Am Soc Clin Oncol 1999;18:940a.

171 Lin JK, Wang WS, Hsieh RK et al. Phase II study of oral tegafur-uracil and folinic acid as first-line therapy for metastatic colorectal cancer: Taiwan experience. Jpn J Clin Oncol 2000;30:510-514.

172 Ichikawa W, Nihei Z, Uetake H et al. UFT plus leucovorin for metastatic colorectal cancer: Japanese experience. Oncology (Huntingt) 2000;14(suppl 9):41-43.

173 Thomas MB, Langleben A, Rinaldi D et al. A phase II study of UFT + leucovorin given as a twice-daily (BID) regimen in the treatment of patients (Pts) with metastatic colorectal cancer (MCC). Proc Am Soc Clin Oncol 2001;20:564a.

174 Hoff PM, Pazdur R. UFT plus oral leucovorin: a new oral treatment for colorectal cancer. ***The Oncologist*** 1998;3:155-164.

175 Pazdur R, Douillard J-Y, Skillings JR et al. Multicenter phase III study of 5-fluorouracil (5-FU) or UFT™ in combination with leucovorin (LV) in patients with metastatic colorectal cancer. Proc Am Soc Clin Oncol 1999;18:1009a.

176 Carmichael J, Popiela T, Radstone D et al. Randomized comparative study of Orzel® (oral Uracil/Tegafur (UFT™) plus leucovorin (LV)) versus parenteral 5-fluorouracil (5-FU) plus LV in patients with metastatic colorectal cancer. Proc Am Soc Clin Oncol 1999;18:1015a.

177 Borner MM, Schöffski P, de Wit R et al. Patient preference and pharmacokinetic of oral modulated UFT versus intravenous fluorouracil and leucovorin: a randomised crossover trial in advanced colorectal cancer. Eur J Cancer 2002;38:349-358.

178 Mitomi T, Tsuchiya S, Hiki Y et al. A randomized controlled study on adjuvant chemotherapy with UFT in curatively resected colorectal cancer. Proc Am Soc Clin Oncol 1993;12:690a.

179 Sadahiro S, Ohki S, Yamaguchi S et al. Feasibility of a novel weekday-on/weekend-off oral UFT schedule as postoperative adjuvant chemotherapy for colorectal cancer. UFT Compliance Study Group, Kanagawa, Japan. Cancer Chemother Pharmacol 2000;46:180-184.

180 Sadahiro S, Suzuki T, Kameya T et al. A pharmacological study of the weekday-on/weekend-off oral UFT schedule in colorectal cancer patients. Cancer Chemother Pharmacol 2001;47:457-460.

181 Espinosa E, Gonzalez-Baron M, Feliu J et al. UFT-leucovorin as adjuvant treatment for Dukes' B2-C colon cancer. Proc Am Soc Clin Oncol 1998;17:1059a.

182 Smith R, Wickerham DL, Wieand HS et al. UFT plus calcium folinate vs 5-FU plus calcium folinate in colon cancer. Oncology (Huntingt) 1999;13(suppl 3):44-47.

183 Nakagoe T, Ishikawa H, Sawai T et al. Multicenter randomized prospective study of adjuvant chemotherapy with UFT and mitomycin C in advanced colorectal cancer. Anticancer Res 2000;20:1069-1075.

184 Tokunaga Y, Kinaoka A, Yagi T et al. Postsurgical sequential methotrexate/5-FU and leucovorin on outpatient basis for advanced colorectal carcinoma. Hepatogastroenterology 2001;48:128-132.

185 Ohwada S, Kawate S, Kawashima Y et al. Postoperative adjuvant immunochemotherapy using protein-bound polysaccharide K (PSK) and tegafur/uracil (UFT) improves disease-free survival: results of a randomized controlled trial (GOSG-C study). Proc Am Soc Clin Oncol 2001;20:582a.

186 Hill M, Mackay H, Cunningham D et al. Phase I/II study of oral uracil/tegafur (UFT®), leucovorin and irinotecan in patients with advanced colorectal cancer [abstract]. Ann Oncol 2000;11(suppl 4):193P.

187 Gravalos C, Garcia-Alfonso P, Castellano D et al. Phase I trial of escalating doses of irinotecan (CPT-11) in combination with UFT/folinic acid (FA) in patients with advanced colorectal cancer (CRC) [abstract]. Ann Oncol 2000;11(suppl 4):199P.

188 Castellano D, Gravalos C, Garcia-Alfonso P et al. Phase I/II study of escalating doses of irinotecan (CPT-11) in combination with UFT/folinic acid (FA) in patients (Pts) with advanced colorectal cancer (CRC). Proc Am Soc Clin Oncol 2001;20:577a.

189 Alonso V, Escudero P, Zorrilla M et al. Phase I trial of weekly irinotecan combined with UFT as second-line treatment for advanced colorectal cancer. Eur J Cancer 2001;37:2385-2391.

190 Cruz JJ, Mendez M, Pujol E et al. Weekly irinotecan (CPT-11) in combination with oral uracil and fiorafur (UFT) plus folinic acid (FA) as first line treatment in advanced colorectal cancer (CRC). Preliminary results. Proc Am Soc Clin Oncol 2001;20:2186a.

191 Sazaki K, Takasaka H, Kawasaki H et al. Weekly low dose irinotecan (CPT-11) combined with oral 5-FU (and isovolin) in patients with metastatic colorectal cancer (CRC) on an out-patient treatment basis. Proc Am Soc Clin Oncol 2001;20:2241a.

192 Mel JR, Vieitez JM, Garcia Alfonso P et al. Raltitrexed (Tomudex) combined with UFT: a phase I/II dose-escalation study in metastatic CRC. Proc Am Soc Clin Oncol 2000;19:1108a.

193 Vazquez Estevez S, Vieitez JM, Garcia AP et al. Raltitrexed combined with UFT: a phase I/II dose escalation study in metastatic colorectal cancer [abstract]. Ann Oncol 2000;11(suppl 4):229P.

194 Dorta FJ, Feliu J, Vicent J et al. Phase II clinical trial with the combination of oxaliplatin-UFT-l,-leucovorin (OXA-UFT-LLV) for the first line treatment of advanced colorectal cancer (ACC). Preliminary results (Oncopaz Cooperative Group—Spain) [abstract]. Ann Oncol 2000;11(suppl 4):220P.

195 Douillard JY, Seitz JF. A phase I study of oral uracil/tegafur (UFT) plus leucovorin (LV) combined with oxaliplatin in patients with metastatic colorectal cancer (CRC). Proc Am Soc Clin Oncol 2001;20:572a.

196 Jakobsen A, Pfeiffer P, Hansen F et al. Dual modulation of UFT with leucovorin and hydroxyurea in metastatic colorectal cancer. Acta Oncol 2001;40:63-66.

197 Kusunoki M, Yanagi H, Noda M et al. The usefulness of pharmacokinetic modulating chemotherapy (UFT + 5-FU) in the treatment of unresectable colorectal carcinomas. Oncol Rep 1999;6:547-552.

198 Yoshikawa R, Kusunoki M, Yanagi H et al. New chemotherapeutic strategy for colorectal cancer by "pharmacokinetic modulating chemotherapy (PMC)". Proc Am Soc Clin Oncol 2001;20:3085a.

199 Yoshikawa R, Kusunoki M, Yanagi H et al. Dual antitumor effects of 5-fluorouracil on the cell cycle in colorectal carcinoma cells: a novel target mechanism concept for pharmacokinetic modulating chemotherapy. Cancer Res 2001;61:1029-1037.

200 Yamagi H, Kusunoki M, Yoshikawa R et al. Clinical results of pharmacokinetic modulating chemotherapy (PMC) in combination with hepatic arterial 5-FU infusion and oral UFT after resection of hepatic colorectal metastases. Proc Am Soc Clin Oncol 2001;20:556a.

201 Minsky BD. UFT® plus oral leucovorin calcium (Orzel™) and radiation in combined modality therapy: a comprehensive review. Int J Cancer 2001;96:1-10.

202 Sanchiz F, Milla A. Tegafur-uracil (UFT) plus folinic acid in advanced rectal cancer. Jpn J Clin Oncol 1994;24:322-326.

203 de la Torre A, Ramos S, Valcarcel FJ et al. Phase II study of radiochemotherapy with UFT and low-dose oral leucovorin in patients with unresectable rectal cancer. Int J Radiat Oncol Biol Phys 1999;45:629-634.

204 Feliu J, Calvillo J, Escribano A et al. Neoadjuvant therapy of rectal carcinoma with UFT-folinic acid (LV) plus radiotherapy (RT). Proc Am Soc Clin Oncol 1999;18:917a.

205 Pfeiffer P. Concurrent UFT/L-leucovorin and curative intended radiotherapy (60 Gy) in patients with locally advanced rectal cancer (LARC): a phase I/II trial. Proc Am Soc Clin Oncol 2000;19:992a.

206 Hoff PM, Janjan N, Saad ED et al. Phase I study of preoperative oral uracil and tegafur plus leucovorin and radiation therapy in rectal cancer. J Clin Oncol 2000;18:3529-3534.

207 Fernandez-Martos C, Aparicio J, Bosch C et al. Pre-operative therapy (PT) with oral uracil and tegafur (UFT) and concomitant irradiation (RT) in operable rectal cancer (RC). Preliminary results of a multicenter phase II study. Proc Am Soc Clin Oncol 2001;20:590a.

208 Hayakawa M, Morise K, Sakai T et al. [Combination chemotherapy with UFT, etoposide, CDDP, adriamycin (FEPA) in advanced gastric cancer.] Gan To Kagaku Ryoho 1989;16:3393-3398. Japanese.

209 Sawa T, Kinoshita K, Takekawa S et al. [Effect of PMUE therapy (CDDP, MMC, UFT, etoposide) in terminal gastric cancer.] Gan To Kagaku Ryoho 1990;17:2381-2386. Japanese.

210 Hashimoto T, Omura K, Ishida F et al. [Clinical efficacy of cis-diamminedichloroplatinum [II] and 5-fluorouracil (UFT) in advanced cancer of the alimentary tract.] Gan To Kagaku Ryoho 1993;20:1333-1338. Japanese.

211 Jin M, Yang B, Zhang W et al. High-dose mitomycin C-containing regimens in the treatment of advanced gastric cancer. Semin Surg Oncol 1994;10:114-116.

212 Sato S, Hasegawa K, Kurihara M et al. [Combination chemotherapy with tegafur-uracil (UFT) and cisplatin (CDDP) for advanced gastric cancer. UFTP Study Group.] Gan To Kagaku Ryoho 1995;22:1355-1362. Japanese.

213 Feliu J, Gonzalez-Baron M, Garcia-Giron C et al. Treatment of patients with advanced gastric carcinoma with the combination of etoposide plus oral tegafur modulated by uracil and leucovorin. A phase II study of the ONCOPAZ Cooperative Group. Cancer 1996;78:211-216.

214 Kim YH, Cheong SK, Lee JD et al. Phase II trial of oral UFT and leucovorin in advanced gastric carcinoma. Am J Clin Oncol 1996;19:212-216.

215 Kim YH, Shin SW, Kim BS et al. A phase II trial. Oral UFT and leucovorin in patients with advanced gastric carcinoma. Oncology (Huntingt) 1997;11(suppl 10):119-123.

216 Chaves M, Bernabe R, Reina JJ et al. A less toxic regime in the treatment of advanced gastric cancer: UFT, epirubicin and cisplatin (ECU) [abstract]. Ann Oncol 2000;11(suppl 4):292P.

217 Sato A, Kurihara M, Koizumi W et al. A phase II study of UFT plus cisplatin (UFTP) therapy in patients with advanced gastric cancer. Proc Am Soc Clin Oncol 2000;19:1087a.

218 Jeen YT, Yoon SY, Shin SW et al. Phase II trial of epirubicin, cisplatin, oral uracil and tegafur, and leucovorin in patients with advanced gastric carcinoma. Cancer 2001;91:2288-2293.

219 Ravaud A, Borner M, Schellens JHM et al. UFT and leucovorin in first-line chemotherapy for patients with metastatic gastric cancer. An Early Clinical Studies Group (ECSG)/European Organization for Research Treatment of Cancer (EORTC) phase II trial. Eur J Cancer 2001;37:1642-1647.

220 Kurihara M, Izumi T, Yoshida S et al. A cooperative randomized study on tegafur plus mitomycin C versus combined tegafur and uracil plus mitomycin C in the treatment of advanced gastric cancer. Jpn J Cancer Res 1991;82:613-620.

221 Sasagawa T, Ho N, Endo T et al. [Randomized controlled trial of MMC + UFT and MMC + 5-FU therapy in advanced gastric cancer.] Gan To Kagaku Ryoho 1994;21:1179-1185. Japanese.

222 Arima S, Ohsato K, Hisatsugu T et al. Multicentre randomised study of adjuvant chemotherapy with mitomycin C and tegafur or tegafur-uracil in gastric cancer. Eur J Surg 1994;160:227-232.

223 Danno M, Shiroto H, Kunii Y et al. [Study on the intensity of MMC and UFT in postoperative adjuvant chemotherapy for gastric cancer. study report of JFMTC study No. 10.] Gan To Kagaku Ryoho 2001;28:195-203. Japanese.

224 Shimizu E, Kimura K, Sone S et al. [A phase II study of UFT in non-small cell lung cancer.] Gan To Kagaku Ryoho 1986;13:2970-2973. Japanese.

225 Keicho N, Saijo N, Shinkai T et al. Phase II study of UFT in patients with advanced non-small cell lung cancer. Jpn J Clin Oncol 1986;16:143-146.

226 Ichinose Y, Takanashi N, Yano T et al. A phase II trial of oral tegafur and uracil plus cisplatin in patients with inoperable nonsmall cell lung cancer. Cancer 1995;75:2677-2680.

227 Genma A, Kudoh S, Yoshimura A et al. Pilot trial of a combination comprising of consecutive oral administration of UFT, and two-divided administration of CDDP in non-small cell lung cancer. Anticancer Res 1995;15:2691-2695.

228 Feliu J, Gonzalez-Baron M, Espinosa E et al. Cisplatin and UFT modulated with leucovorin for the treatment of advanced non-small-cell lung cancer. Am J Clin Oncol 1996;19:121-124.

229 Koinumaru S, Matsuda T, Saitoh J-I et al. Pilot study of UFT combined with 5 consecutive days cisplatin in non-small cell lung cancer. Lung Cancer 1997;18:241-251.

230 Yoshimori K, Yano T, Yoneda S et al. A phase II trial of UFT plus cisplatin in patients with advanced non-small cell lung cancer. Proc Am Soc Clin Oncol 1998;18:1803a.

231 Ichinose Y, Yosimori K, Yoneda S et al. UFT plus cisplatin combination chemotherapy in the treatment of patients with advanced nonsmall cell lung carcinoma: a multiinstitutional phase II trial. For the Japan UFT Lung Cancer Study Group. Cancer 2000;88:318-323.

232 Yoshino I, Yohena T, Kitajima M et al. UFT plus cisplatin with concurrent radiotherapy for locally advanced non-small cell lung cancer (NSCLC). A phase II study. Proc Am Soc Clin Oncol 2000;19:1981a.

233 Nakanishi Y, Fujita M, Ninomiya K et al. A phase II study of UFT plus cisplatin (CDDP) in previously untreated patients with advanced non-small cell lung cancer (NSCLC). Proc Am Soc Clin Oncol 2001;20:2727a.

234 Saito J, Nakai Y, Saijo Y et al. A phase II trial of oral UFT plus cisplatin (CDDP) in patients with non-small cell lung cancer (NSCLC). Lung Cancer 2001;31:285-293.

235 Vega-Villegas ME, Lopez-Brea M, Rivera F et al. A phase II study of UFT, vinorelbine and cisplatin (UFTVP) in advanced

(stage III-B and IV) non small cell lung cancer (NSCLC). Proc Am Soc Clin Oncol 2001;20:2741a.

236 Yoshimori K, Okumura M, Kamio K et al. A phase I/II study of cisplatin (CDDP), docetaxel (TXT) and UFT in patients with advanced non-small cell lung cancer (NSCLC). Proc Am Soc Clin Oncol 2001;20:1367a.

237 Shimizu N. A randomized controlled postoperative adjuvant chemotherapy trial of MMC + Tegafur and MMC + UFT for adenocarcinoma of the lung - first study. West Japan Study Group for Lung Cancer Surgery. Jpn J Lung Cancer 1991;31:1011-1019.

238 The Study Group of Adjuvant Chemotherapy for Lung Cancer (Chubu, Japan). A randomized trial of postoperative adjuvant chemotherapy in non-small cell lung cancer (the second cooperative study). Eur J Surg Oncol 1995;21:69-77.

239 Wada H, Hitomi S, Teramatsu T. Adjuvant chemotherapy after complete resection in non-small-cell lung cancer. West Japan Study Group for Lung Cancer Surgery. J Clin Oncol 1996;14:1048-1054.

240 Tanaka F, Miyahara R, Ohtake Y et al. Advantage of postoperative oral administration of UFT (tegafur and uracil) for completely resected p-stage I-IIIa non-small cell lung cancer (NSCLC). Eur J Cardiothorac Surg 1998;14:256-262.

241 Wada H, Miyahara R, Tanaka F. Postoperative adjuvant chemotherapy with PVM (Cisplatin + Vindesine + Mitomycin C) and UFT (Uracil + Tegafur) in resected stage I-II NSCLC (non-small cell lung cancer): a randomized clinical trial. West Japan Study Group for lung cancer surgery (WJSG). Eur J Cardiothorac Surg 1999;15:438-443.

242 Ito H, Takeda Y, Uno T et al. A phase I/II trial of UFT and low-dose cisplatin plus concurrent thoracic radiotherapy (TRT) for resected P-NII non-small cell lung cancer. Proc Am Soc Clin Oncol 1999;18:1966a.

243 Tanaka F, Otake Y, Yanagihara K et al. Apoptosis and p53 status predict the efficacy of postoperative administration of UFT in non-small cell lung cancer. Br J Cancer 2001;84:263-269.

244 Dickson N, Nicholson BP, Cohen A et al. A phase I trial of UFT, leucovorin (L) and paclitaxel (P) as first or second line therapy in patients (pts) with metastatic breast cancer (MBC). Proc Am Soc Clin Oncol 1999;18:422a.

245 Klaasen U, Lang S, Borquez D et al. Oral UFT/leucovorin (LV) in combination with paclitaxel (P) in the second line treatment of patients (pts) with metastatic breast cancer (MBC): results of a phase I/II trial. Proc Am Soc Clin Oncol 1999;18:404a.

246 Lebedinsky CA, Breier SM, Ayaviri C et al. Dose-finding study of UFT modulated by folic acid in combination with weekly paclitaxel (Taxol) in patients with metastatic breast cancer (MBC). Proc Am Soc Clin Oncol 2000;19:854a.

247 Herrero A, Artal-Cortes A, Martinez-Trufero J et al. Phase I-II trial of increasing dose, continuous UFT plus leucovorin with fixed dose three-weekly doxorubicin (D) and paclitaxel (P) in locally advanced breast cancer (LABC). Proc Am Soc Clin Oncol 2000;19:600a.

248 Gregory RK, Johnston SR, Ellis PA et al. An open label non randomised phase I/II trial of oral UFT/leucovorin therapy in combination with bolus epirubicin and cyclophosphamide (ECU) in patients with locally advanced (LABC) or metastatic (MBC) breast cancer. Proc Am Soc Clin Oncol 2000;19:432a.

249 Fumoleau P, Bonneterre J, Kerbrat P et al. A phase I dose-finding trial of UFT/leucovorin (LV) in combination with vinorelbine (VNB) in patients with metastatic breast cancer (MBC) [abstract]. Ann Oncol 2000;11(suppl 4):134P.

250 Fumoleau P, Bonneterre J, Kerbrat P et al. A phase I dose-finding trial of UFT/leucovorin (LV) in combination with vinorelbine (VNB) in patients with metastatic breast cancer (MBC). Proc Am Soc Clin Oncol 2001;20:1974a.

251 Lueck HJ, Scholz U, Rossner D et al. Phase I study of weekly paclitaxel in combination with oral uracil/ftorafur (UFT) plus leucovorin (LV) in the treatment of patients (Pts) with anthracycline-resistant metastatic breast cancer. Proc Am Soc Clin Oncol 2001;20:2024a.

252 Bunnell CA, Partridge A, Burstein H et al. A phase I study of oral cyclophosphamide and UFT + leucovorin (Orzel) in women with advanced breast cancer. Proc Am Soc Clin Oncol 2001;20:2015a.

253 Daniels M, Diaz-Rubio E, Guillem V et al. Phase II trial of UFT activity in pretreated breast cancer patients. Jpn J Clin Oncol 1993;23:363-365.

254 Kiman K, Suzuki S, Satomi T et al. [Efficacy of combination therapy consisting of cyclophosphamide, adriamycin, UFT and oophorectomy/tamoxifen for advanced or recurrent breast cancer.] Gan To Kagaku Ryoho 1994;21:2445-2552. Japanese.

255 Richardet E, Mickiewicz E, Lerzo G et al. UFT + leucovorin (LV) in advanced breast cancer (ABC): preliminary results in heavily pretreated patients (HPP). Proc Am Soc Clin Oncol 1999;18:869a.

256 Fukuda M, Yamaguchi S, Ohta T et al. Combination therapy for advanced breast cancer: cyclophosphamide, doxorubicin, UFT, and tamoxifen. Oncology (Huntingt) 1999;13(suppl 3):77-81.

257 Yardley DA, Jones SF, Greco FA et al. A phase II trial of Orzel (UFT + leucovorin) in women with previously treated metastatic breast cancer. Proc Am Soc Clin Oncol 2001;20:2031a.

258 Rivera E, Hizinski M, Hutchins L et al. A study of UFT + leucovorin (L) given as a three times daily (TID) regimen in the treatment of patients (Pts) with metastatic breast cancer (MBC). Proc Am Soc Clin Oncol 2001;20:1989a.

259 Hortobagyi GN, Ibrahim N, Young R et al. A study of UFT + leucovorin (L) given as a twice daily (BID) regimen in the treatment of patients (PTS) with metastatic breast cancer (MBC). Proc Am Soc Clin Oncol 2001;20:186a.

260 Tashiro H, Nomura Y, Ohsaki A. A double blind comparative study of tegafur (FT) and UFT (a combination of tegafur and uracil) in advanced breast cancer. Jpn J Clin Oncol 1994;24:212-217.

261 Villalon AH, De Guzman LM, Samson MC et al. A comparative, randomized trial of UFT and 5-fluorouracil in combination with cyclophosphamide and doxorubicin in the treatment

of advanced breast cancer patients at The Philippines General Hospital. Oncology 1997;54(suppl 1):2-6.

262 Iglesias L, Moreno JA, Torrija E et al. UFT in combination as adjuvant therapy for breast cancer. Grupo Oncologico de Sevilla, Seville, Spain. Oncology (Huntingt) 1997;11(suppl 10):74-81.

263 Hata Y, Uchino J, Asaishi K et al. UFT and mitomycin plus tamoxifen for stage II, ER-positive breast cancer. Hokkaido ACETBC Study Group. Oncology (Huntingt) 1999;13(suppl 3):91-95.

264 Sugimachi K, Maehara Y, Akazawa K et al. Postoperative chemo-endocrine treatment with mitomycin C, tamoxifen, and UFT is effective for patients with premenopausal estrogen receptor-positive stage II breast cancer. Nishinihon Cooperative Study Group of Adjuvant Therapy for Breast Cancer. Breast Cancer Res Treat 1999;56:113-124.

265 Inuyama Y, Takeda C, Miyake H et al. [Phase II study of UFT for head and neck cancer.] Gan To Kagaku Ryoho 1985;12:479-484. Japanese.

266 Rivera F, Lopez-Brea M, Lopez-Vega JM et al. High activity of UFT, vinorelbine and cisplatin (UFTVP) as induction chemotherapy for locally advanced squamous cell head and neck carcinoma (SCHNC). Proc Am Soc Clin Oncol 1997;16:1376a.

267 Colevas AD, Amrein PC, Gomolin H et al. A phase II study of combined oral uracil and ftorafur with leucovorin for patients with squamous cell carcinoma of the head and neck. Cancer 2001;92:326-331.

268 de Castro J, Lopez Alvarez M, Rodriguez Jaraiz A et al. Phase II trial of gemcitabine and UFT modulated by leucovorin in patients with advanced pancreatic cancer. Proc Am Soc Clin Oncol 2000;19:1040a.

269 de Castro J, Bolanos M, Cruz MA et al. Phase II trial of prolonged infusion gemcitabine plus UFT for the treatment of advanced pancreatic cancer. Preliminary results. Proc Am Soc Clin Oncol 2001;20:2310a.

270 Nishimura K, Nonomura N, Tokizane T et al. Oral combination chemotherapy for hormone-refractory prostate cancer on an outpatient basis. Proc Am Soc Clin Oncol 2001;20:2385a.

271 Ukimura O, Kamoi K, Hongo F et al. Oral administration of dexamethasone in combination with UFT and cyclophosphamide for the treatment of hormone-refractory prostate cancer. Proc Am Soc Clin Oncol 2001;20:2412a.

272 Horiuchi M, Inuyama Y, Miyake H. Efficacy of surgical adjuvant with tegafur and uracil (UFT) in resectable head and neck cancer: a prospective randomized study. Proc Am Soc Clin Oncol 1994;13:918a.

273 Gonzalez-Larriba JL, Garcia Carbonero I, Sastre Valera J et al. Neoadjuvant therapy with cisplatin/fluorouracil vs cisplatin/UFT in locally advanced squamous cell head and neck cancer. Oncology (Huntingt) 1997;11(suppl 10):90-97.

274 Takahashi H, Yao K, Sawaki S et al. [Investigation of UFT and radiation combination therapy of head and neck cancer, mainly in laryngeal cancer.] Gan To Kagaku Ryoho 1990;17:2037-2042. Japanese.

275 Rueda A, Ribelles N, Mons E et al. Neoadjuvant (Neo) chemotherapy (Ct) followed by radiochemotherapy (Rct) in advanced head and neck carcinoma (Chm) [abstract]. Proc Am Soc Clin Oncol 2000;19:1694E.

276 Lam P, Yuen AP, Ho CM et al. Prospective randomized study of post-operative chemotherapy with levamisole and UFT for head and neck carcinoma. Eur J Surg Oncol 2001;27:750-753.

277 Hoque MO, Kawamata H, Nakashiro KI et al. Dihydropyrimidine dehydrogenase mRNA level correlates with the response to 5-fluorouracil-based chemo-immuno-radiation therapy in human oral squamous cell cancer. Int J Oncol 2001;19:953-958.

278 Ohashi O, Yamamoto M, Ishida H et al. [Retrospective analysis of postoperative chemotherapy with UFT against pancreatic cancer.] Gan To Kagaku Ryoho 1995;22:933-939. Japanese.

279 Childs H, Spencer S, Raben D et al. Phase I study of combined UFT plus leucovorin (L) and radiation therapy (RT) for pancreatic cancer. Proc Am Soc Clin Oncol 1999;18:956a.

280 Pienta KJ, Smith DC, Fardig J et al. Phase II trial of oral uracil/ftorafur (UFT) plus leucovorin in patients with hormone-refractory prostate cancer. Proc Am Soc Clin Oncol 2000;19:1414a.

281 Kubota Y, Hosaka M, Fukushima S et al. Prophylactic oral UFT therapy for superficial bladder cancer. Cancer 1993;71:1842-1845.

282 Damle B, Ravandi F, Kaul S et al. Effect of food on the oral bioavailability of UFT and leucovorin in cancer patients. Clin Cancer Res 2001;7:517-523.

283 Okuda H, Ogura K, Kato A et al. A possible mechanism of eighteen patient deaths caused by interactions of sorivudine, a new antiviral drug, with oral 5-fluorouracil prodrugs. J Pharmacol Exp Ther 1998;287:791-799.

284 Sun W, Haller D. UFT in the treatment of colorectal and breast cancer. Oncology (Huntingt) 2001;15(suppl 2):49-56.

285 Shirasaka T, Shimamato Y, Ohshimo H et al. Development of a novel form of an oral 5-fluorouracil derivative (S-1) directed to the potentiation of the tumor selective cytotoxicity of 5-fluorouracil by two chemical modulators. Anticancer Drugs 1996;7:548-557.

286 Tatsumi K, Fukushima M, Shirasaka T et al. Inhibitory effects of pyrimidine, barbituric acid and pyridine derivatives on 5-fluorouracil degradation in rat liver extracts. Jpn J Cancer Res 1987;78:748-755.

287 Komno H, Tanaka T, Baba M et al. Therapeutic effect of 1 M tegafur-0.4 M 5-chloro-2,4-dihydroxypyridine-1 M potassium oxonate (S-1) on liver metastasis of xenotransplanted human colon carcinoma. Jpn J Cancer Res 1999;90:448-453.

288 Nishimura G, Yanoma S, Mizuno H et al. Therapeutic effect of 1 M tegafur-0.4 M 5-chloro-2,4-dihydroxypyridine-1 M potassium oxonate (S-1) on head and neck squamous carcinoma cells. Cancer Lett 2000;159:1-7.

289 Shirasaka T, Shimamoto Y, Fukushima M. Inhibition by oxonic acid of gastrointestinal toxicity of 5-fluorouracil without loss of its antitumor activity in rats. Cancer Res 1993;53:4004-4009.

290 Yoshisue K, Masuda H, Matsushima E et al. Tissue distribution and biotransformation of potassium oxonate after oral administration of a novel antitumor agent (drug combination of tegafur, 5-chloro-2,4-dihydroxypyridine, and potassium oxonate) to rats. Drug Metab Dispos 2000;28:1162-1167.

291 Yoshisue K, Hironaga K, Yamaguchi S et al. Reduction of 5-fluorouracil (5-FU) gastrointestinal (GI) toxicity resulting from the protection of thymidylate synthase (TS) in GI tissue by repeated simultaneous administration of potassium oxonate (Oxo) in rats. Cancer Chemother Pharmacol 2000;46:51-56.

292 Shirasaka T, Nakano K, Takechi T et al. Antitumor activity of 1 M tegafur-0.4 M 5-chloro-2,4-dihydroxypyridine-1 M potassium oxonate (S-1) against human colon carcinoma orthotopically implanted into nude rats. Cancer Res 1996;56:2602-2606.

293 Takechi T, Nakano K, Uchida J et al. Antitumor activity and low intestinal toxicity of S-1, a new formulation of oral tegafur, in experimental tumor models in rats. Cancer Chemother Pharmacol 1997;39:205-211.

294 Fukushima M, Satake H, Uchida J et al. Preclinical antitumor efficacy of S-1: a new oral formulation of 5-fluorouracil on human tumor xenografts. Int J Oncol 1998;13:693-698.

295 Fukushima M, Shimamoto Y, Kato T et al. Anticancer activity and toxicity of S-1, an oral combination of tegafur and two biochemical modulators, compared with continuous i.v. infusion of 5-fluorouracil. Anticancer Drugs 1998;9:817-823.

296 Cao S, Lu K, Toth K et al. Persistent induction of apoptosis and suppression of mitosis as the basis for curative therapy with S-1, an oral 5-fluorouracil prodrug in a colorectal tumor model. Clin Cancer Res 1999;5:267-274.

297 Araki H, Fukushima M, Kamiyama Y et al. Effect of consecutive lower-dose cisplatin in enhancement of 5-fluorouracil cytotoxicity in experimental tumor cells in vivo. Cancer Lett 2000;160:185-191.

298 Taguchi T, Inuyama Y, Kanamaru R et al. [Phase I study of S-1. S-1 Study Group.] Gan To Kagaku Ryoho 1997;24:2253-2264. Japanese.

299 Hoff PM, Wenske CA, Medgyesy DC et al. Phase I and pharmacokinetic (PK) study of a novel oral fluoropyrimidine S-1. Proc Am Soc Clin Oncol 1999;18:665a.

300 van Groeningen CJ, Peters GJ, Schornagel JH et al. Phase I clinical and pharmacokinetic study of oral S-1 in patients with advanced solid tumors. J Clin Oncol 2000;18:2772-2779.

301 Meropol NJ, Leishman CG, Yeslow G et al. Phase I and pharmacokinetic study of single daily oral administration of S-1. Proc Am Soc Clin Oncol 2001;20:361a.

302 Horikoshi N, Mitachi Y, Sakata Y et al. S-1, new oral fluoropyrimidine is very active in patients with advanced gastric cancer (early phase II study). Proc Am Soc Clin Oncol 1996;15:466a.

303 Sugimachi K, Maehara Y, Horikoshi N et al. An early phase II study of oral S-1, a newly developed 5-fluorouracil derivative for advanced and recurrent gastrointestinal cancers. The S-1 Gastrointestinal Cancer Study Group. Oncology 1999;57:202-210.

304 Taguchi T, Horikoshi N, Kinoshita H et al. Early phase II study of S-1 in patients with advanced breast cancer. Proc Am Soc Clin Oncol 1996;15:151a.

305 Taguchi T, Morimoto K, Horikoshi N et al. [An early phase II clinical study of S-1 in patients with breast cancer. S-1 Cooperative Study Group (Breast Cancer Working Group)]. Gan To Kagaku Ryoho 1998;25:1035-1043. Japanese.

306 Fujii M, Kanzaki J, Satake B et al. Early phase II study of S-1 in patients with advanced head and neck cancer. Proc Am Soc Clin Oncol 1996;15:894a.

307 Kurihara M, Koizumi W, Hasegawa K et al. Late phase II study of S-1, a novel oral fluoropyrimidine derivative in patients with advanced gastric cancer. Proc Am Soc Clin Oncol 1998;17:1007a.

308 Koizumi W, Kurihara M, Nakano S et al. Phase II study of S-1, a novel oral derivative of 5-fluorouracil, in advanced gastric cancer. For the S-1 Cooperative Gastric Cancer Study Group. Oncology 2000;58:191-197.

309 Sakata Y, Ohtsu A, Horikoshi N et al. Late phase II study of novel oral fluoropyrimidine anticancer drug S-1 (1 M tegafur-0.4 M gimestat-1 M otastat potassium) in advanced gastric cancer patients. Eur J Cancer 1998;34:1715-1720.

310 Baba H, Ohtsu A, Sakata Y et al. Late phase II study of S-1 in patients with advanced colorectal cancer in Japan. Proc Am Soc Clin Oncol 1998;17:1065a.

311 Ohtsu A, Baba H, Sakata Y et al. Phase II study of S-1, a novel oral fluoropyrimidine derivative, in patients with metastatic colorectal carcinoma. S-1 Cooperative Colorectal Carcinoma Study Group. Br J Cancer 2000;83:141-145.

312 Sano M, Saeki T, Takashima S et al. Late phase II study of S-1 in patients with advanced and/or recurrent breast cancer. Proc Am Soc Clin Oncol 2000;19:404a.

313 Miyamoto S-I, Boku N, Ohtsu A et al. Clinical implications of immunoreactivity of thymidylate synthase and dihydropyrimidine dehydrogenase in gastric cancer treated with oral fluoropyrimidines (S-1). Study Group of S-1 for Gastric Cancer. Int J Oncol 2000;17:653-658.

314 Yoshida K, Nishimoto N, Kagawa Y et al. [A new therapeutic approach to advanced and recurrent gastric cancer by TS-1.] Gan To Kagaku Ryoho 2001;28:1403-1412. Japanese.

315 Kamata T, Hayashi Y, Minatoya G et al. [A pilot study of low-dose TS-1 and cisplatin combination chemotherapy for advanced gastric cancer.] Gan To Kagaku Ryoho 2001;28:1419-1422. Japanese.

316 Inuyama Y, Kida A, Tsukuda M et al. [Late phase II study of S-1 in patients with advanced head and neck cancer.] Gan To Kagaku Ryoho 2001;28:1381-1390. Japanese.

317 Shirasaka T, Tsukuda M, Inuyama Y et al. [New oral anticancer drug, TS-1 (S-1)—from bench to clinic.] Gan To Kagaku Ryoho 2001;28:855-864. Japanese.

318 Kawahara M, Furuse K, Segawa Y et al. Phase II study of S-1, a novel oral fluorouracil, in advanced non-small-cell lung cancer. Br J Cancer 2001;85:939-943.

319 Hirata K, Horikoshi N, Aiba K et al. Pharmacokinetic study of S-1, a novel oral fluorouracil antitumor drug. Clin Cancer Res 1999;5:2000-2005.

320 Saad ED, Hoff PM. Other fluorinated pyrimidines in the treatment of solid tumors. Oncology (Huntingt) 2001;15(suppl 2):65-68.

321 Yamada Y, Shirao K, Matsumura Y et al. Comparison of 5-fluorouracil and F-β-alanine pharmacokinetics in patients receiving protracted venous infusion of 5-fluorouracil and oral S-1. Proc Am Soc Clin Oncol 2001;20:362a.

322 Shirasaka T, Yamamitsu S, Tsuji A et al. Conceptual changes in cancer chemotherapy: from an oral fluoropyrimidine prodrug, UFT, to a novel oral fluoropyrimidine prodrug, S-1, and low-dose FP therapy in Japan. Invest New Drugs 2000;18:315-329.

323 Tsujitani S, Katano K, Gomyo Y et al. Comparative study of S-1 with and without low-dose cisplatin for patients with recurrent or advanced gastric cancer. Proc Am Soc Clin Oncol 2001;20:2319a.

324 Mayer RJ. Oral versus intravenous fluoropyrimidines for advanced colorectal cancer: by either route, it's all the same. J Clin Oncol 2001;19:4093-4096.

[CANCER RESEARCH 63, 3154–3161, June 15, 2003]

Epidermal Growth Factor Receptor (EGFR)-targeted Immunoliposomes Mediate Specific and Efficient Drug Delivery to EGFR- and EGFRvIII-overexpressing Tumor Cells[1]

Christoph Mamot, Daryl C. Drummond, Udo Greiser, Keelung Hong, Dmitri B. Kirpotin, James D. Marks, and John W. Park[2]

Division of Hematology-Oncology [C. M., J. W. P.] and Department of Anesthesia [J. D. M.], University of California, San Francisco, and California Pacific Medical Center Research Institute, Liposome Research Laboratory [D. C. D., U. G., K. H., D. B. K.], San Francisco, California 94115

ABSTRACT

We hypothesized that immunoliposomes (ILs) that target epidermal growth factor receptor (EGFR) and/or its truncated variant EGFRvIII can be constructed to provide efficient intracellular drug delivery in tumor cells overexpressing these receptors. Monoclonal antibody fragments included Fab′ fragments derived from C225, which binds both EGFR and EGFRvIII, or novel anti-EGFR scFv C10, which binds EGFR only. Monoclonal antibody fragments were covalently linked to liposomes containing various reporters or drugs. ILs were evaluated for specific binding, internalization, and cytotoxicity in EGFR/EGFRvIII-overexpressing cell lines *in vitro*. Flow cytometry and fluorescence microscopy showed that EGFR-targeted ILs, but not nontargeted liposomes or irrelevant ILs, were efficiently bound and internalized by EGFR-overexpressing cells, including glioma cells (U-87), carcinoma cells (A-431 and MDA-MB-468), and EGFRvIII stable transfectants (NR-6M). Furthermore, EGFR-targeted ILs did not bind to non-EGFR-overexpressing cells (MCF-7 and parental NR-6). ILs showed 3 orders of magnitude greater accumulation in NR-6-EGFRvIII stable transfectants *versus* parental NR-6 cells. Quantitative internalization studies indicated binding of EGFR-targeted ILs to target cells within 5 min, followed by intracellular accumulation beginning at 15 min; total uptake reached ~13,000 ILs/cell. ILs were used to deliver cytotoxic drugs doxorubicin, vinorelbine, or methotrexate to EGFR/EGFRvIII-overexpressing target cells *in vitro*. In each case, the IL agent was significantly more cytotoxic than the corresponding nontargeted liposomal drug in target cells, whereas it was equivalent in cells lacking EGFR/EGFRvIII overexpression. We conclude that EGFR-targeted ILs provide efficient and targeted delivery of anticancer drugs in cells overexpressing EGFR or EGFRvIII.

INTRODUCTION

To create agents capable of both drug delivery and molecular targeting, we and others have studied approaches for antibody-targeted liposomes (ILs[3]), in which liposomes are endowed with the specificity of MAbs (1, 2). For example, we have developed ILs directed against HER2 (ErbB2), which bind and internalize in HER2-overexpressing cells but not in normal cells (3, 4).

In principle, this approach can be applied to other antigenic targets, particularly other RTKs capable of mediating endocytosis after ligand binding to enable IL internalization. The EGFR is the prototypic member of the class I (ErbB, HER) family of RTKs, which includes EGFR, HER2 (ErbB2), HER3 (ErbB3), and HER4 (ErbB4). As a target antigen, EGFR is a readily accessible cell surface receptor (5), and when overexpressed, provides a basis for selective antibody-based targeting of tumor cells (6, 7). EGFR overexpression occurs in many human solid tumors, and in some cases has been correlated with poor prognosis (reviewed in Ref. 8).

In addition to overexpression of wild-type EGFR, *EGFR* gene rearrangement also occurs in a number of cancer types. Class III mutants (EGFRvIII) contain a deletion of exons 2–7 within the ECD, resulting in an in-frame deletion of 801 bp of the coding sequence and the generation of a novel glycine residue at the fusion junction (9, 10). This mutant form is the most frequently detected genomic variant in brain tumors and other cancers (11). Expression of EGFRvIII is a potentially tumor-specific event in some cases of breast carcinoma, non-small cell lung carcinoma, and high-grade glioma (12–14), and may represent an ideal antigen for immunotherapies.

MAbs against EGFR such as MAb 225 can inhibit the proliferation of EGFR-overexpressing cells *in vitro* and in tumor xenograft models (15). For example, MAb 225 competitively inhibits binding of growth factors such as EGF and transforming growth factor α to EGFR, thus blocking ligand-dependent EGFR signaling. A chimerized version of this MAb, C225 (cetuximab, Erbitux; Ref. 16), has been generated to retain these properties while reducing the potential for immunogenicity. MAb C225 has been studied in clinical trials for the treatment of various cancer types, such as head/neck and colorectal cancer (17, 18). C225 binds to both EGFR and EGFRvIII.

Here we describe the design, preparation, and characterization of EGFR-targeted ILs, including intracellular delivery of multiple drugs in cancer cells that overexpress EGFR and/or EGFRvIII.

MATERIALS AND METHODS

Materials. Reagents for liposome preparation included: $DiIC_{18}(3)$-DS (Molecular Probes, Eugene, OR); 1–2-oleoyl-3-sn-glycerophosphocholine, DSPC, and mPEG-DSPE (Avanti Polar Lipids, Alabaster, AL); Chol (Calbiochem, San Diego, CA); Mal-PEG-DSPE (Shearwater Polymers, Huntsville, AL); organic solvents, high-performance liquid chromatography grade (Fisher, Pittsburgh, PA); and other chemicals of reagent purity (Sigma Chemicals, St. Louis, MO). Vinorelbine (GlaxoSmithKline, Triangle Park, NC), doxorubicin (Bedford Laboratories, Bedford, OH), and pegylated liposomal doxorubicin (Doxil; Aiza Pharmaceuticals, Palo Alto, CA) were obtained commercially from the pharmacy. Methotrexate was purchased from Sigma Chemicals. MAb C225 was kindly provided by Dr. Daniel Hicklin (ImClone Systems, New York, NY).

Cell Lines. MDA-MB-468 human breast cancer and U-87 human glioblastoma cancer cell lines were obtained from the American Type Culture Collection (Rockville, MD). A-431 epidermoid cancer, and SK-BR-3 and MCF-7 breast cancer cell lines were obtained from the University of California San Francisco Cell Culture Facility (San Francisco, CA). NR-6 and stable EGFR-

Received 8/19/02; accepted 4/14/03.

The costs of publication of this article were defrayed in part by the payment of page charges. This article must therefore be hereby marked *advertisement* in accordance with 18 U.S.C. Section 1734 solely to indicate this fact.

[1] Supported by grants from Accelerated Brain Cancer Cure (ABC2), Expedition Inspiration, and the National Cancer Institute Specialized Programs of Research Excellence (SPORE) in Breast Cancer (P50-CA58207) and Brain Tumors (P50-CA097257). C. M. was supported by a postdoctoral fellowship from the Swiss Academy of Medical Sciences (SAMW)/Swiss National Science Foundation (SNSF) and Cancer League, Basel, Switzerland. D. C. D. is supported in part by a New Investigator Award from California's Breast Cancer Research Program of the University of California (7KB-0066).

[2] To whom requests for reprints should be addressed, at University of California, San Francisco Cancer Center, 1600 Divisadero Street, Second Floor, San Francisco, CA 94115-1710.

[3] The abbreviations used are: IL, immunoliposome; EGFR, epidermal growth factor receptor; Chol, cholesterol; $DiIC_{18}(3)$-DS, 1,1′-dioctadecyl-3,3,3′,3′-tetramethylindocarbocyanine-5,5′-disulfonic acid; DSPC, 1,2-distearoyl-*sn*-glycero-3-phosphocholine; DSPE, 1,2-distearoyl-3-*sn*-glycerophosphoethanolamine; HPTS, 8-hydroxypyrene-1,3,6-trisulfonic acid trisodium salt; Mal-PEG-DSPE, β-(*N*-maleimide)propionyl poly(ethylene glycol)-1,2-distearoyl-3-*sn*-phosphoethanolamine; PEG, poly(ethylene glycol); MAb, monoclonal antibody; RTK, receptor-tyrosine kinase; ECD, extracellular domain; EGF, epidermal growth factor; VRL, vinorelbine.

vIII-transfected NR-6M cells were kindly provided by Dr. Daryl D. Bigner (Duke University, Durham, NC; Ref. 19). MDA-MB-468 cells were maintained in Leibovitz L-15 medium, SK-BR-3 cells in McCoy 5a, and all of the other cell lines in DMEM-F-21 medium supplemented with 10% bovine calf serum, 100 IU/ml penicillin, and 100 μg/ml streptomycin in a humidified atmosphere of 95% air and 5% CO_2 at 37°C (except L-15 medium in 100% air).

Liposome Preparation. Unilamellar liposomes were prepared according to the repeated freeze-thawing method (20) using 1-2-oleoyl-3-sn-glycerophosphocholine and Chol, or DSPC and Chol (molar ratio 3:2) with mPEG-DSPE (0.5–5 mol% of phospholipid). Liposomes were subsequently extruded 10 times through polycarbonate filters with defined pore sizes of 0.1 μm, and yielded liposomes of 100–120 nm diameter as determined by dynamic light scattering. Liposome concentration was measured using a standard phosphate assay (21).

For uptake and internalization studies, liposomes were labeled with 0.1–0.3 mol% $DiIC_{18}(3)$-DS, a fluorescent lipid that can be stably incorporated into liposomal membranes (22, 23). For kinetic analysis, the pH-sensitive probe HPTS (pyranine) was encapsulated in liposomes by hydrating the dry lipid in 35 mM HPTS (pH 7.0); the preparation was adjusted to an osmolarity of 280 mOsm/l with NaCl, followed by extrusion as described above. Unentrapped HPTS was removed by gel filtration using a Sephadex G-75 column.

For encapsulation of chemotherapy drugs doxorubicin and vinorelbine, the remote-loading method using ammonium sulfate was performed (24, 25). First, dry lipids were rehydrated in 250 mM ammonium sulfate at pH 5.5, followed by extrusion as described above. Free ammonium sulfate was removed by size-exclusion chromatography using a Sephadex G-75 column/HEPES buffered saline (pH 7.0). Liposomes were then incubated with either doxorubicin or vinorelbine tartrate (Navelbine) for 30 min at 60°C. Notably, in the case of vinorelbine, the pH of the loading solution as well as reduced levels of PEG-DSPE were found to be important for loading. The relatively low pH of vinorelbine tartrate inhibits loading unless adjusted to pH 6.5 before incubation at 60°C. The presence of high concentrations of PEG-DSPE also reduced loading efficiency, and so we used 0.5% PEG-DSPE in this formulation. All of these liposome compositions have been shown to be long circulating, with or without extensive pegylation (26, 27). Under these conditions, loading efficiencies were typically in the range of 95–100% when 150 μg drug/μmol phospholipid was used. In addition, pegylated liposomal doxorubicin (Doxil) was obtained commercially. Methotrexate-loaded liposomes were prepared by passive encapsulation in an aqueous solution containing methotrexate [200 mM and 5 mM HEPES (pH 7.0)]. All of the unencapsulated drugs were removed by size-exclusion chromatography using a Sephadex G-75 column.

MAb Fragment Preparation, Conjugation, and Liposome Incorporation. For C225-Fab′, intact C225 IgG_1 was incubated with pepsin (weight ratio 1:20) in 0.1 M sodium acetate (pH 3.7) at 37°C for 3 h, followed by dialysis against HEPES-buffered saline (pH 6.0). The resulting C225-$F(ab)_2$ was reduced with 2-mercaptoethylamine (15 mM) under argon for 15 min at 37°C, and then recovered by gel filtration using Sephadex G-25. The efficiency of cysteine reduction was assayed using Ellmann's reagent, and was typically 90%. For scFv C10, cysteine reduction was performed according to this procedure; reduction efficiency was typically 80–90%.

Fab′ or scFv were conjugated to Mal-PEG-DSPE as described (4, 27). Conjugation efficiencies were evaluated by SDS-PAGE, allowing comparison of free MAb fragment *versus* conjugate; the resulting bands were scanned and ratios determined using the software package NIH Image (v.1.62). Conjugation efficiencies were typically 30–50% for Fab′ (C225) and 50–80% for scFv (C10). For incorporation into preformed liposomes, including prepared liposomal drugs and probes or commercial pegylated liposomal doxorubicin, MAb fragment conjugates (Fab′/scFv-PEG-DSPE) which form micellar solutions, were incorporated into liposomes by coincubation at 55°C for 30 min at the indicated protein:liposome ratios. As a result, the conjugates become attached to the outer lipid layer of the liposomes via hydrophobic DSPE domains. Unincorporated conjugates and free drug were separated from ILs by Sepharose CL-4B gel filtration. UV absorbance at 280 nm confirmed that ILs were in the excluded volume, whereas unincorporated micelles were retained as a broad peak easily distinguished from the IL peak. When $DiIC_{18}(3)$-DS-labeled liposomes were used, <5% of the fluorescence was coassociated with the micelle fraction, indicating minimal transfer of this marker. Incorporation efficiency of conjugated MAb fragments was estimated by SDS-PAGE using a series of protein standards, and gel scanning and quantitation as described. Typically, 75–85% of added MAb conjugate was incorporated into ILs.

Binding and Internalization Experiments. For flow cytometric assay, cells underwent 2 h incubation with $DiIC_{18}(3)$-DS labeled liposomes or ILs at 37°C. After extensive washing with PBS, cells were detached and stored on ice until subjected to flow cytometry.

For fluorescence microscopy studies, 250,000 cells were concubated in 12-well plates with liposomes or EGFR-targeted ILs labeled with $DiIC_{18}(3)$-DS for 2 h at 37°C, washed extensively with PBS, incubated for another 2 h without liposomes/ILs, washed with PBS, and subsequently observed using an inverted fluorescence microscope (Nikon Eclipse, TE300) with a 540/25 nm bandpass filter for excitation and a long pass filter at 565 nm for emission.

Cellular Uptake Studies. Quantitative analysis of cell surface bound *versus* endocytosed ILs was performed according to Straubinger *et al.* (28). Various target cells were incubated for 2 h with 0.1 μM (phospholipid concentration) EGFR-targeted ILs, followed by washing three times with ice-cold Hanks solution, and then cell harvesting with PBS/EDTA 0.04%. Fluorescence intensities at excitation wavelengths of 460 nm and 413 nm (isosbestic point) were determined using a Spex Fluorolog 2 spectrofluorometer (Spex Industries, Edison, NJ). On the basis of the pH-sensitivity of the fluorophore HPTS, total uptake, internalized and surface-bound fractions were calculated for various time points (4).

Cellular uptake of doxorubicin was assayed after incubation with EGFR-targeted immunoliposomal doxorubicin or liposomal doxorubicin for 3 h at 37°C. Cells were washed, detached, and subjected to quantitative doxorubicin assay using a FL-600 microplate fluorescence reader (Bio-Tek, Winooski, VT) with a bandpass filter at 485/20 nm for excitation and 590/35 nm for emission.

Cytotoxicity Studies. Specific cytotoxicity of EGFR-targeted ILs containing various anticancer drugs was evaluated in target cells plated at a density of 9000 cells/well in 96-well plates and allowed to grow overnight. ILs or control treatments were applied for 2 h at 37°C, followed by washing with PBS and readding growth medium. Cells were additionally incubated at 37°C for 3 days and analyzed for cell viability using 3-(4,5-dimethylthiazol-2-yl)-2,5-diphenyltetrazolium bromide staining (29).

***In Vitro* Stability of ILs in Human Plasma.** EGFR-targeted ILs were prepared by incorporation of C225-conjugated micelles into preformed Doxil as described. Doxil and ILs were mixed with 50% human plasma and transferred into a 10-well microdialyzer (Spectra/Por; Spectrum Med. Ind., Rancho Dominguez, CA). The stability of these ILs and native Doxil was determined after 4 h and 8 h of continuous dialysis at 37°C. Briefly, Sepharose 4B columns (Sigma) were used for each sample to remove the released doxorubicin and unassociated plasma components before calculating the relative stability by determination of the ratio of measured doxorubicin:phospholipid. The amount of entrapped doxorubicin was measured fluorimetrically using the suitable excitation (λ = 470 nm) and emission (λ = 592 nm) wavelengths. Phospholipid concentration was quantified using a standard phosphate assay (21).

RESULTS

Construction of ILs Targeted to EGFR. EGFR-targeted ILs were constructed using the modular design and methodologies initially developed in conjunction with HER2-targeted ILs (1, 3, 4, 27). This includes liposome compositions optimized previously for systemic delivery, including *in vivo* stability and long circulation times. Briefly, ILs were prepared by conjugation of 100-nm liposomes (DSPC/Chol/PEG-PE) with MAb fragments directed against EGFR and/or EGFR-vIII. Conjugation was performed by direct linkage of MAb fragments to modified termini of PEG chains on liposomes (4), or by initial coupling to Mal-PEG-DSPE linker in solution, followed by incorporation of the resulting micellar conjugates into liposomes (30, 31). The latter method allows conjugation of MAb fragments to existing drug-loaded liposomes, such as pegylated liposomal doxorubicin (Doxil), obviating the need for specially prepared liposomes engineered to contain appropriate functional sites.

EGFR-targeted ILs contained either Fab′ derived from C225 (cetuximab; ImClone Systems, Inc.) or scFv C10, a novel anti-EGFR

scFv generated from screening of a phage antibody library. C225, a chimeric IgG_1, binds the ECD of EGFR and thereby blocks activation by EGFR ligands such as EGF and transforming growth factor α (32). Although EGFRvIII involves deletion of exons 2–7 in the ECD, which abrogates binding of EGF and other cognate growth factors, C225 still binds EGFRvIII. Hence, the ability of this MAb to bind EGFRvIII is irrelevant to its therapeutic mechanism of action of ligand blockade, because EGFRvIII is constitutively active; yet this MAb represents a potentially useful reagent for targeted delivery strategies in EGFRvIII-expressing tumors. Fab′ fragments derived by pepsin cleavage of C225 were attached via their hinge cysteine to Mal-PEG-DSPE, either on liposomes or as an initial coupling reaction in solution.

In addition to Fab′ fragments from MAb C225, novel fully human single-chain antibody fragments (scFv) were isolated for IL targeting. scFv, which consist of variable domains only in a single polypeptide sequence, are attractive targeting ligands, and can be generated from recombinant phage antibody libraries (33). For anti-EGFR scFv, two phage antibody libraries containing human antibody genes (34–36) were screened for binding to recombinant EGFR ECD. Of the multiple novel and independent clones showing specific binding, scFv C10 was selected for IL conjugation based on its expression level and stability. For this purpose, scFv C10 was subcloned into an alternative bacterial expression cassette that affixes a COOH-terminal cysteine residue for covalent conjugation to the Mal-PEG-DSPE linker construct.

Uptake of EGFR-targeted ILs in EGFR- and EGFRvIII-overexpressing Cell Lines. Binding and uptake of EGFR-targeted ILs in EGFR-overexpressing cell lines were evaluated by flow cytometry. In this assay, liposomes were fluorescently labeled with $DiIC_{18}(3)$-DS with/without conjugated MAb fragments, and incubated with MDA-MB-468 breast cancer cells for 2 h at 37°C. ILs containing C225-Fab′ showed >200-fold greater accumulation in MDA-MB-468 cells than did control liposomes, which produced only background levels of fluorescence in these cells (Fig. 1*A*). Similarly, ILs containing scFv C10 showed >100-fold greater uptake in MDA-MB-468 cells than did nontargeted liposomes (Fig. 1*B*).

The uptake of C225-Fab′-containing ILs was also evaluated in EGFRvIII-expressing stable transfectants NR-6M *versus* nontransfected parental NR-6 cells. ILs showed extensive uptake in EGFRvIII-expressing NR6-M cells (Fig. 1*C*) but minimal uptake in parental NR-6 cells, which was indistinguishable from that of nontargeted liposomes (Fig. 1*D*). This result indicated a selectivity of up to 3 orders of magnitude for IL uptake between the two isogenic cell lines differing in EGFRvIII expression.

The observation of minimal fluorescence uptake in target cells after incubation with control liposomes is consistent with the nonreactive properties of pegylated liposomes (3, 4) and also confirms that $DiIC_{18}(3)$-DS can be used as a stable liposome-based marker without significant exchange into cell membranes. Indeed, target cells did not accumulate additional fluorescence even after 24-h incubation with $DiIC_{18}(3)$-DS-labeled control liposomes (data not shown).

Internalization of EGFR-targeted ILs. ILs were designed to exploit both binding and internalization of anti-EGFR MAb fragments, thus enabling endocytosis of ILs in target cells for intracellular drug delivery (1). The internalization of EGFR-targeted ILs was evaluated by confocal fluorescence microscopy in a variety of cell lines. First, fluorescence-labeled ILs and matched control (nontargeted) liposomes were incubated with MDA-MB-468 cells for 2 h at 37°C. ILs were observed to have accumulated profusely throughout the cytoplasm in a pattern consistent with endosomal uptake (Fig. 2, *A* and *B*). In contrast, control liposomes failed to show any detectable binding or internalization (Fig. 2, *C* and *D*), consistent with the flow cytometric assay results.

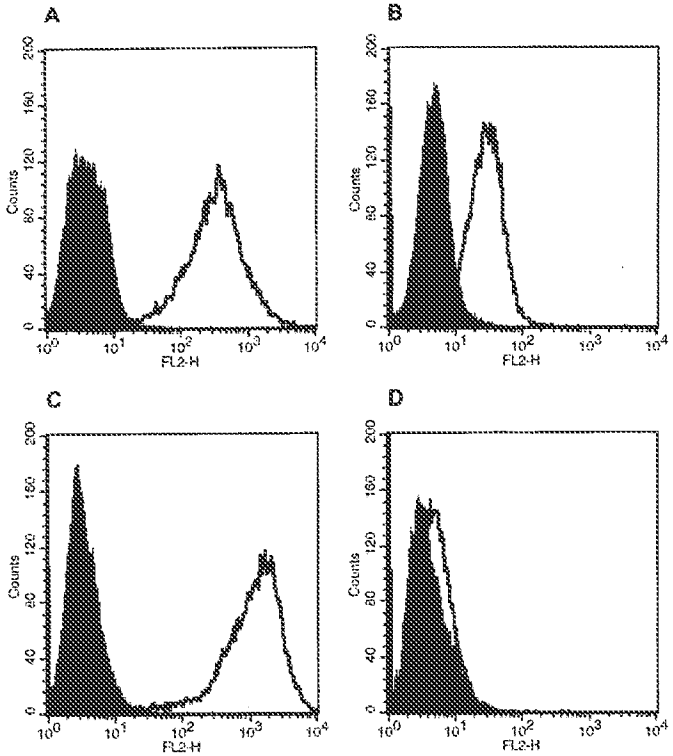

Fig. 1. Uptake of EGFR-targeted ILs in various cell lines. The uptake of EGFR/EGFRvIII-targeted ILs was evaluated in target or control cell lines by flow cytometric assay. The indicated cells were incubated with $DiIC_{18}(3)$-DS-labeled ILs containing either C225-Fab′ or scFv C10 for 2 h at 37°C, extensively washed, detached, and stored on ice until subjected to flow cytometry. *Open histograms*, EGFR/EGFRvIII-targeted ILs. *Filled histograms*, control liposomes prepared identically as ILs except for omission of MAb fragments. *A*, uptake of C225-Fab′-containing ILs in EGFR-overexpressing MDA-MB-468 breast cancer cells. *B*, uptake of scFv C10-containing ILs in MDA-MB-468 cells. *C*, uptake of C225-Fab′-containing ILs in NR-6M, stable transfectants of EGFRvIII. *D*, uptake of C225-Fab′-containing ILs in control cell line NR-6 lacking EGFR or EGFRvIII expression.

IL internalization was further evaluated in additional EGFR-overexpressing or nonoverexpressing cells lines. In EGFR-overexpressing U-87 malignant glioma cells (Fig. 3*A*) and A-431 epidermoid cancer cells (Fig. 3*B*), incubation with EGFR-targeted ILs resulted in extensive internalization and cytoplasmic accumulation. In contrast, irrelevant (HER2-targeted) ILs showed no detectable binding or internalization in either cell type (Fig. 3, *C* and *D*), which was also the case with nontargeted control liposomes (data not shown). Finally, EGFR-targeted ILs were not observed to bind or accumulate in non-EGFR-overexpressing MCF-7 breast cancer cells (Fig. 3*E*). Because MCF-7 cells have low levels of EGFR expression ($\sim 10^4$ receptors/cell), this result indicates a threshold effect in which higher levels of EGFR density than this basal level are required for detectable IL uptake; this appears analogous to the threshold observed for HER2-targeted ILs in HER2-overexpressing target cells (3, 4).

Internalization of C225-Fab′-containing ILs was also studied in cells with EGFRvIII expression. EGFR-targeted ILs demonstrated a high degree of intracellular accumulation in NR-6M cells stably transfected with EGFRvIII (Fig. 3*F*). However, in parental NR-6 cells lacking EGFR or EGFRvIII, no detectable binding or internalization were observed (Fig. 3*G*).

Kinetic Analysis of IL Internalization. Quantitative studies of IL uptake and internalization were performed using EGFR-targeted ILs loaded with the pH-sensitive fluorophore pyranine (HPTS). This method allows quantitative analysis of IL uptake in both neutral pH (surface-bound) and acidic pH (endocytosis-associated) compartments (4). Binding to MDA-MB-468 cells was observed within 5 min,

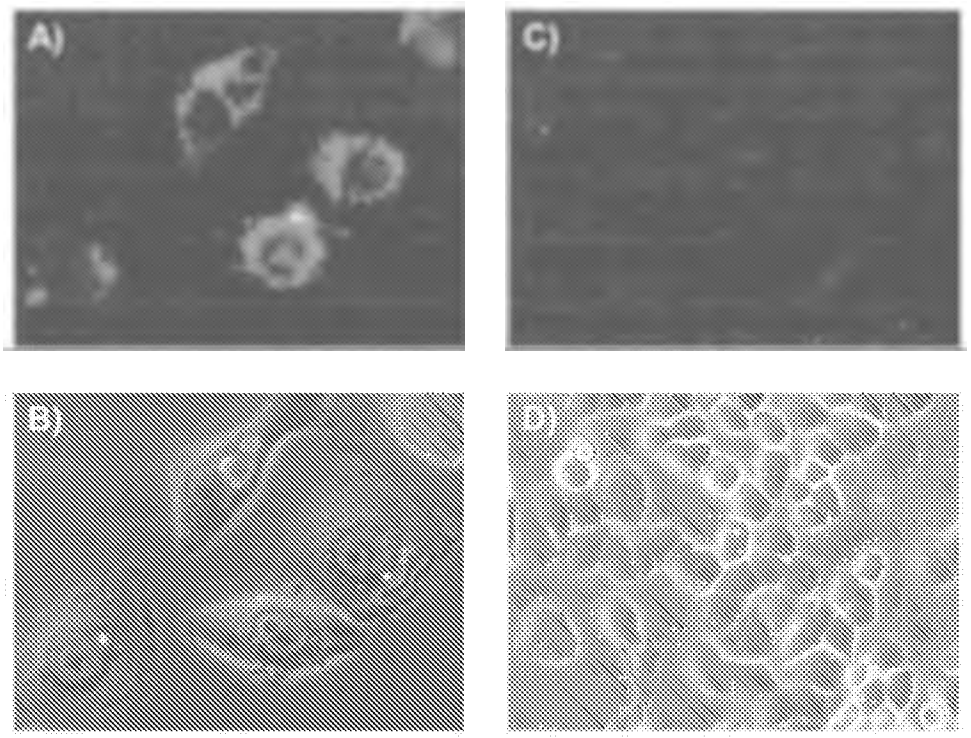

Fig. 2. Internalization of EGFR/EGFRvIII-targeted ILs *versus* nontargeted liposomes in EGFR-overexpressing cells. MDA-MB-468 breast cancer cells were treated with $DiIC_{18}(3)$-DS-labeled liposomes containing or lacking C225-Fab′ for 2 h at 37°C. *A*, internalization of EGFR-targeted ILs in MDA-MB-468 cells as visualized by confocal microscopy. *B*, same field as in *A*, visualized by phase contrast microscopy. *C*, lack of uptake of control (no MAb fragments) liposomes in MDA-MB-468 cells as visualized by confocal microscopy. *D*, same field as in *C*, visualized by phase contrast microscopy.

followed by detectable intracellular accumulation within 15 min, which subsequently increased to a plateau at 240 min (Fig. 4*A*). Total uptake of C225-Fab′ containing ILs at 240 min was 1.70 fmol phospholipid/cell (~13,000 ILs/cell), with virtually the entire uptake in the endocytosed fraction. The uptake of ILs was at least 43-fold greater than that of nontargeted liposomes (<300 liposomes/cell). Similarly, in non-EGFR-overexpressing MCF-7 cells, the uptake of ILs was only 450 ILs/cell. EGFR-targeted ILs containing scFv C10 showed comparable internalization kinetics in MDA-MB-468 cells (Fig. 4*B*). Total uptake for scFv C10-containing ILs reached 1.32 fmol phospholipid/cell (~10,000 ILs/cell) in MDA-MB-468 cells.

The kinetics of internalization of C225-Fab′-containing ILs was similar in cells with EGFRvIII expression. Again, binding to NR-6M (EGFRvIII) stable transfectants started within 5 min, followed by detectable intracellular accumulation after only 15 min and increasing to a plateau after 240 min, reaching 1.45 fmol phospholipid/cell (~11,000 ILs/cell; Fig. 4*C*).

Targeted Drug Delivery Studies. In addition to quantitative analysis of IL internalization, studies of IL-mediated drug delivery were performed using doxorubicin-loaded EGFR-targeted ILs in MDA-MB-468 cells. ILs were prepared by insertion of C225-Fab′ into commercial pegylated liposomal doxorubicin (Doxil) at increasing ratios of Fab′ per liposome and under two reaction conditions. Doxorubicin delivery reached a maximum of 600–700 ng/10^6 cells. Estimating a volume of approximately 0.8–1.2 fl for MDA-MB-468 cells, this number corresponds to an intracellular doxorubicin concentration of 1–2 μM (approximately 0.58–1.16 μg/ml). This is substantially greater than the IC_{50} for doxorubicin in this cell line (~0.3 μg/ml; Table 1*A*). In addition, this uptake corresponds to ~31,500 liposomes/cell, which is somewhat greater than the uptake calculated by the HPTS method. Potential explanations for this 2–3-fold difference in calculated uptake include greater stability and/or less leakiness of commercial liposomal doxorubicin, in which drug is encapsulated in gelated form, than laboratory grade liposomal HPTS, and the possibility of efflux of HPTS via organic anion transporters (37). Doxorubicin delivery was proportional to the amount of Fab′ incorporated in the IL, up to a plateau ratio of 30 μg of Fab′/μmol phospholipid (approximately 30–40 MAb fragments/liposome, Fig. 5). These results are consistent with those observed with HER2-targeted ILs in HER2-overexpressing cells, which similarly show increased uptake with higher MAb fragment density on ILs, up to a plateau of 20–30 MAb fragments/IL (4). Doxil alone without MAb fragments showed negligible delivery of doxorubicin under these *in vitro* conditions.

Targeted Cytotoxicity Studies. For cytotoxicity studies, anti-EGFR ILs containing C225-Fab′ were stably loaded with various chemotherapeutic drugs for targeted delivery to EGFR- or EGFRvIII-overexpressing cells. Drug-loaded ILs were either prepared by active ("remote")-loading or passive loading as described in "Materials and Methods." ILs were incubated with various cell lines, and compared with the respective free and nontargeted liposomal drugs to evaluate efficiency and specificity of delivery.

In EGFR-overexpressing MDA-MB-468 breast cancer cells, EGFR-targeted immunoliposomal doxorubicin showed substantial *in vitro* cytotoxicity after treatment for 2 h (IC_{50} = 1.1 μg/ml), which approached that of free doxorubicin (IC_{50} = 0.8 μg/ml; Fig. 6*A*). Thus, EGFR-targeted IL delivery of doxorubicin was almost as efficient as the rapid diffusion of free doxorubicin, a small, amphipathic molecule that readily transverses cell membranes *in vitro*. On the other hand, EGFR-targeted immunoliposomal doxorubicin, derived by conjugation of C225-Fab′ to Doxil, showed 29-fold greater cytotoxicity than Doxil itself (IC_{50} = 32 μg/ml) in MDA-MB-468 cells, indicating that delivery was antibody-dependent (Fig. 6*A*). Notably, similar treatment with C225 for 2 h showed no cytotoxicity in this assay, confirming that IL activity was due to targeted drug delivery and not related to potential antiproliferative effects of C225 during this brief incubation time. Furthermore, ILs containing C225-Fab′ but lacking encapsulated drug ("empty ILs") similarly showed no cytotoxicity under these assay conditions.

The specificity of EGFR-targeted IL delivery was additionally evaluated in MCF-7 breast cancer cells lacking EGFR-overexpression. Free doxorubicin again showed extremely efficient cytotoxicity (IC_{50} = 0.4 μg/ml) because of its high *in vitro* potency. However, treatment with

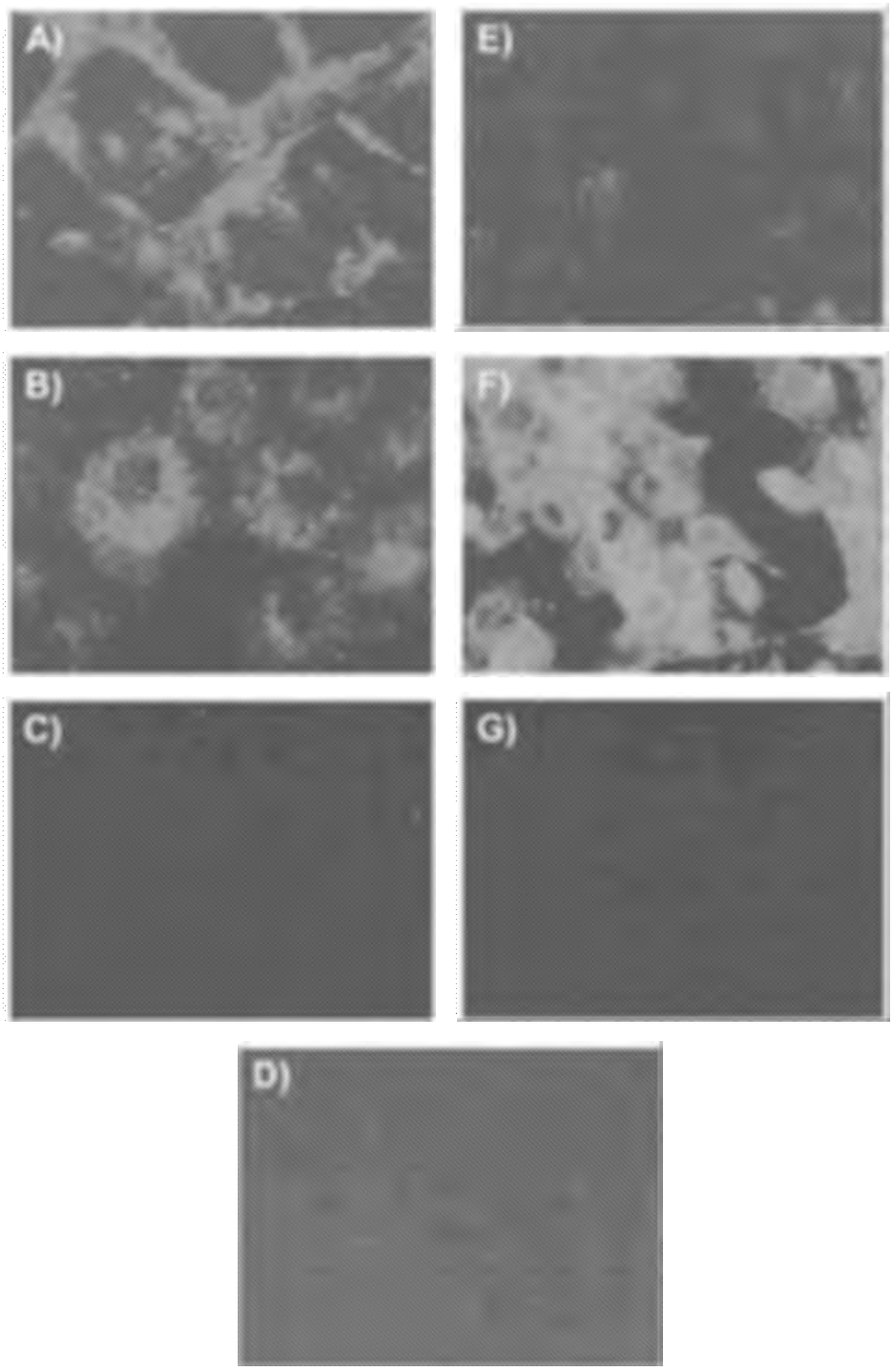

Fig. 3. Internalization of EGFR/EGFRvIII-targeted *versus* irrelevant ILs in various cell lines. Various cell lines were treated with $DiIC_{18}(3)$-DS labeled liposomes containing either anti-EGFR C225-Fab′ or anti-HER2 scFv F5 for 2 h at 37°C. *A*, EGFR-targeted ILs in EGFR-overexpressing U-87 glioma cells. *B*, EGFR-targeted ILs in EGFR-overexpressing A-431 epidermoid cancer cells. *C*, irrelevant (HER2-targeted) ILs in EGFR-overexpressing U-87 glioma cells. *D*, irrelevant (HER2-targeted) ILs in EGFR-overexpressing A-431 epidermoid cancer cells. *E*, EGFR-targeted ILs in non-EGFR-overexpressing MCF-7 breast cancer cells. *F*, EGFR-targeted ILs in NR-6M cells stably transfected with EGFRvIII. *G*, EGFR-targeted ILs in parental NR-6 cells lacking EGFR or EGFRvIII expression.

EGFR-targeted immunoliposomal doxorubicin was >100-fold less efficient than free doxorubicin in these cells and equivalent to Doxil (Fig. 6*B*). Taking together the cytotoxicity results in target (MDA-MB-468) *versus* nontarget (MCF-7) cells, the specificity index (defined as IC_{50} in nontarget cells/IC_{50} in target cells) was 45.5 for EGFR-targeted immunoliposomal doxorubicin, 0.5 for free doxorubicin, and 1.1 for Doxil.

EGFR-targeted ILs were also loaded with vinorelbine (anti-EGFR ILs-VRL) for treatment of MDA-MB-468 and MCF-7 cells. In MDA-MB-468 cells, these constructs were as efficient in delivering vinorelbine as free vinorelbine itself, which has high *in vitro* potency (IC_{50} = 0.3 μg/ml; Fig. 6*C*). EGFR-targeted immunoliposomal vinorelbine was 40-fold more cytotoxic (IC_{50} = 0.3 μg/ml) than nontargeted liposomal vinorelbine (IC_{50} = 12 μg/ml), prepared identically except for omission of MAb fragments. In contrast, in non-EGFR-overexpressing MCF-7 cells, EGFR-targeted ILs showed much reduced cytotoxicity *versus* free vinorelbine, and were comparable with nontargeted liposomal vinorelbine (Fig. 6*D*). For vinorelbine, the specificity index was >90 for EGFR-targeted immunoliposomal vinorelbine, 0.7 for free vinorelbine, and 2.3 for nontargeted liposomal vinorelbine.

EGFR-targeted ILs were also used to deliver methotrexate (anti-EGFR ILs-MTX). Unlike doxorubicin and vinorelbine, methotrexate does not diffuse across the cell membrane, and requires active trans-

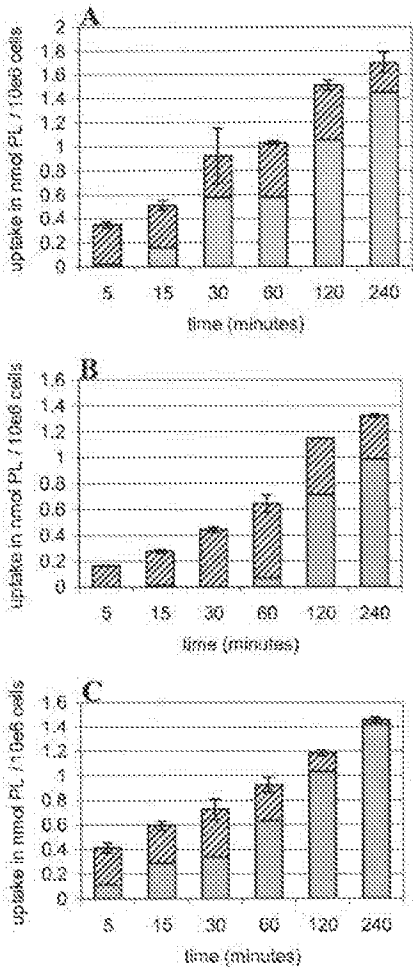

Fig. 4. Kinetics of uptake of EGFR-targeted ILs in cell lines overexpressing EGFR or EGFRvIII. ILs containing the indicated MAb fragments were loaded with the pH-sensitive fluorophore HPTS and incubated with either EGFR-overexpressing MDA-MB-468 cells or EGFRvIII-expressing NR-6M cells for various time points at 37°C. Fluorimetry was then performed to quantify surface-bound ILs at neutral pH (not internalized; ▨) *versus* endocytosed ILs at acidic pH (internalized; ▩). *A*, ILs containing C225-Fab′; MDA-MB-468 cell line. *B*, ILs containing scFv-C10; MDA-MB-468 cell line. *C*, ILs containing C225-Fab′; NR6-M cell line. Data indicate mean; *bars*, ±SD.

port via the folate carrier system for internalization (38). Consistent with this, EGFR-targeted immunoliposomal methotrexate yielded 3-fold more efficient cytotoxicity than free methotrexate in EGFR-overexpressing MDA-MB-468 cells, indicating that IL delivery was superior to cellular active transport mechanisms under these conditions. Anti-EGFR ILs-MTX was also >20-fold more cytotoxic than nontargeted liposomal methotrexate in these cells (Fig. 6*E*). In contrast, in MCF-7 cells, anti-EGFR ILs-MTX and nontargeted liposomal methotrexate showed equivalent minimal cytotoxicity (Fig. 6*F*). For methotrexate, the specificity index was 16.3 for EGFR-targeted immunoliposomal methotrexate, 5 for free methotrexate, and 0.8 for nontargeted liposomal methotrexate.

IL-mediated cytotoxicity with various drugs was also evaluated in EGFRvIII-expressing NR-6M transfectants and compared with results with NR-6 parental cells. These studies permitted an assessment of IL targeting of EGFRvIII alone, because these cells lack wild-type EGFR, and also provided isogenically matched target (NR-6M) *versus* control (NR-6) cells designed to differ only in EGFRvIII expression. ILs containing C225-Fab′ were used to deliver encapsulated doxorubicin, vinorelbine, and methotrexate as described. In each case, the IL drug was markedly more cytotoxic than the corresponding nontargeted liposomal drug in target cells (NR-6M), while equivalent against non-EGFRvIII-expressing cells (NR-6). The specificity indices for doxorubicin were 29.3/1.6/1.1 (EGFR-targeted ILs-drug/free drug/nontargeted liposomes-drug), for vinorelbine 11/2.4/0.9 and for methotrexate 18.7/0.9/1, respectively. A summary of the cytotoxicity studies is shown in Table 1.

Plasma Stability of Anti-EGFR ILs. The EGFR-targeted ILs in this report were derived from an overall design first implemented with HER2-targeted ILs, which were determined previously to be highly stable and with long circulation times *in vivo* (27). To confirm stability and resistance to drug leakage, EGFR-targeted immunoliposomal doxorubicin was prepared by conjugation of C225-Fab′ fragments (approximately 30–40/liposome) to pegylated liposomal doxorubicin (Doxil), and then subjected to prolonged incubation with 50% human plasma. In this model, ILs were stable at temperatures of 37°C for a minimum of 8 h when continuously dialyzed against 50% human plasma. The release of 6% encapsulated doxorubicin after 8 h was comparable with the results observed with commercial pegylated liposomal doxorubicin alone.

DISCUSSION

We have described previously the development of ILs targeting HER2 (3), the relationship of design features to binding and internal-

Table 1 *Immunoliposome delivery of various drugs in NR-6M and NR-6 cells*

Cytotoxic effects (IC_{50}, μg/ml) of various compounds in EGFRvIII-expressing NR-6M cell line compared with NR-6 cell line lacking the mutant EGFRvIII receptor (control): free drug, liposomal encapsulated drug (nt, nontargeted), and EGFR-targeted immunoliposomes (ILs drugs).

	NR-6M cells (IC_{50})	Anti-EGFR ILs *vs.* liposome	NR-6 cells (IC_{50})	Anti-EGFR ILs *vs.* liposome
Doxorubicin (Dox)				
-Free Dox	0.22		0.35	
-nt Doxil	40	27-fold	42	None
-ILs Doxil	1.5		44	
Vinorelbine (VRL)				
-Free VRL	0.23		0.55	
-nt VRL	4.2	13-fold	3.9	None
-ILs VRL	0.31		3.4	
Methotrexate (MTX)				
-Free MTX	32		30	
-nt MTX	>54	>23-fold	54	None
-ILs MTX	2.3		43	

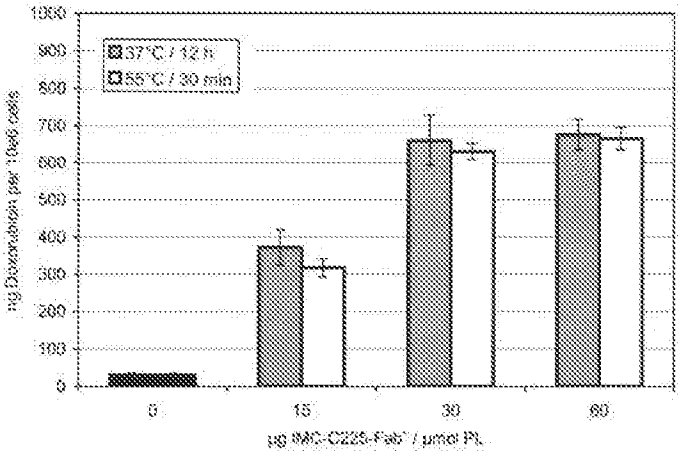

Fig. 5. IL-mediated delivery of doxorubicin *in vitro*. Various amounts of C225-Fab′ (15, 30, and 60 μg/μmol phospholipid) were inserted into pegylated liposomal doxorubicin (Doxil) for conversion of liposomes into ILs. Doxil alone was included as a negative control (liposomal dox). MAb fragment insertion was performed under two different conditions: 37°C for 12 h (▨) or 55°C for 30 min (□). Liposomes or ILs were incubated with MDA-MB-468 breast cancer cells for 3 h at 37°C, washed, detached, and fluorimetry analyzed for quantitation of cellular doxorubicin uptake. Data indicate mean; *bars*, ±SD.

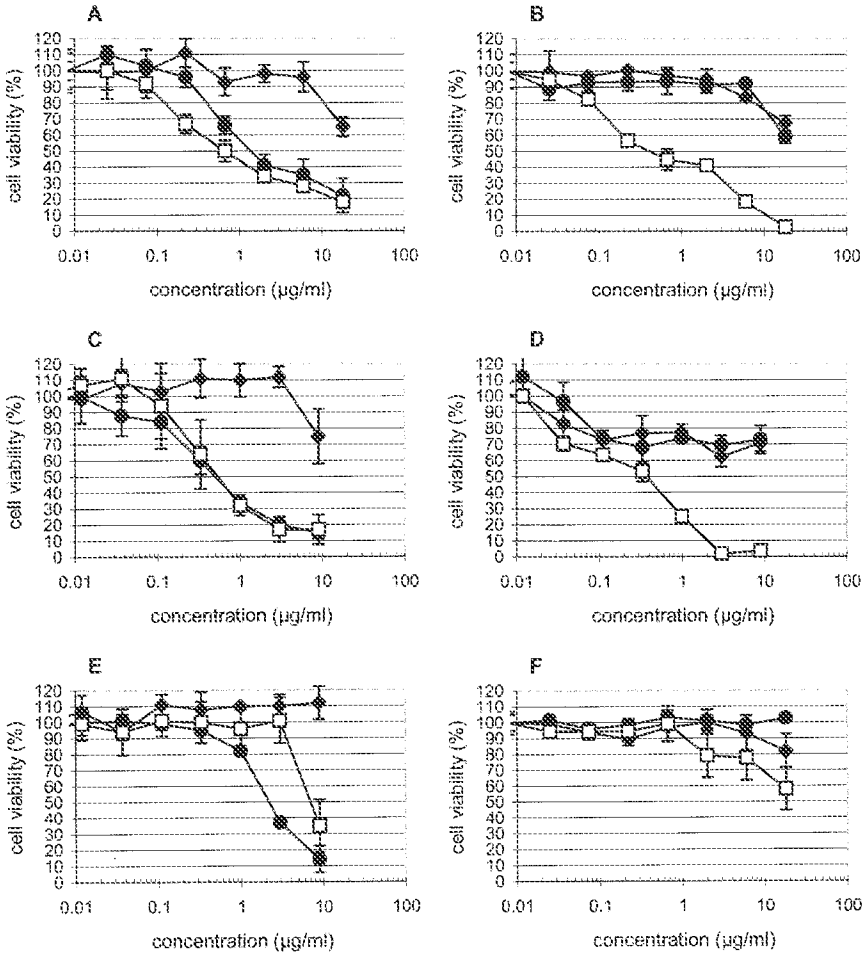

Fig. 6. *In vitro* cytotoxicity of EGFR-targeted ILs containing various drugs. C225-Fab′ were covalently conjugated to stabilized liposomes by incorporation of MAb-linker micelles into preformed liposomes containing various cytotoxic drugs. Cells in culture were treated for 2 h with EGFR-targeted ILs (◉), nontargeted liposomes (◆), or free drug alone (□). Cells were incubated for another 3 days and counted using an 3-(4,5-dimethylthiazol-2-yl)-2,5-diphenyltetrazolium bromide assay. Doxorubicin: *A*, MDA-MB-468; *B*, MCF-7. Vinorelbine: *C*, MDA-MB-468; *D*, MCF-7. Methotrexate: *E*, MDA-MB-468; *F*, MCF-7. Data indicate mean; *bars*, ±SD.

ization properties (4), and their *in vivo* optimization and therapeutic efficacy in HER2-overexpressing tumor models (27). Because of the modular design of these IL constructs, which allows conjugation of various MAb fragments to stabilized and long circulating liposomal carriers, this approach can in principle be extended to other target antigens. In particular, ILs targeting RTKs can potentially trigger endocytosis after binding, resulting in IL internalization and intracellular drug release.

In this report, ILs were constructed with anti-EGFR MAb fragments to deliver drugs selectively to tumor cells with overexpression of EGFR or the truncated mutant EGFRvIII. MAb fragments included C225-Fab′, which provides targeting of both EGFR and EGFRvIII, as well as scFv C10, a novel anti-EGFR scFv derived from a phage antibody library. EGFR-targeted ILs showed specific binding and internalization in EGFR-overexpressing cell lines MDA-MB-468 (breast cancer), U-87 (glioblastoma), and A-431 (epidermoid cancer). Total cellular uptake of EGFR-targeted ILs in these cells was up to 3 orders of magnitude higher than that detected in non-EGFR-overexpressing cells, indicating substantial specificity for target *versus* nontarget cells. ILs containing C225-Fab′ could also target EGFRvIII-expressing cells, as shown by binding and internalization in EGFRvIII-transfected NR-6M cells but not in the nontransfected isogenic control cell line NR-6. Binding and internalization resulted in highly efficient intracellular drug delivery, because of the combined effects of an accumulation of 10^4 ILs/cell with a carrying capacity of 10^4 drugs/IL. The delivery system was used in conjunction with three chemotherapy drugs representing different classes and mechanisms of action. In each case, the IL drug (doxorubicin, vinorelbine, or methotrexate) was markedly more cytotoxic than the corresponding nontargeted liposomal drug in target cells, while equivalent against non-EGFR-overexpressing cell lines.

An important feature of the IL approach is a threshold effect for target receptor expression. EGFR-targeted ILs internalized in EGFR-overexpressing cells, including those with 10^5-10^7 EGFR/cell, but did not detectably accumulate in low EGFR-expressing cells such as MCF-7 (~10^4 EGFR/cell). This suggests that significant drug delivery is unlikely to occur in normal tissues, including epithelial cells expressing up to 10^3-10^4 receptors/cell. These properties of EGFR-targeted ILs are consistent with previous results obtained with HER2-targeted ILs, which indicated a similar threshold for HER2-overexpression (3, 4, 27).

In addition to targeting tumors that overexpress wild-type EGFR, IL agents may be useful against tumors that express truncated mutant receptor EGFRvIII. As a mutant allele, EGFRvIII appears to be a true tumor-specific antigen that is not expressed in normal tissues. Although C225 does not have therapeutic value as a ligand blocker against the ligand-independent EGFRvIII, ILs containing C225-Fab′ can target tumors with overexpression of either EGFR or EGFRvIII. MAbs that specifically recognize the new epitope created by the truncation event in EGFRvIII have also been derived (39). In principle, ILs can be constructed from such MAbs for tumor-specific drug delivery. In addition to existing anti-EGFRvIII MAbs, human scFv can be rapidly selected from phage antibody libraries, which are ideally suited for generation of targeting ligands for IL agents (40). The use of scFv C10 in these studies exemplifies this strategy; this relatively low affinity scFv lacking intrinsic biological activity,

whereas not a therapeutic candidate as a naked MAb, can be very powerful when targeting ILs. Furthermore, the development of methods to select for scFv that internalize in target cells can be rapidly exploited in conjunction with IL technology (36).

In conclusion, these studies describe a molecularly targeted drug delivery system for highly efficient and selective delivery of anticancer drugs in tumor cells overexpressing EGFR or EGFRvIII. This approach may be useful for the delivery of various drugs for enhanced therapeutic index against cancer.

REFERENCES

1. Park, J. W., Hong, K., Kirpotin, D. B., Papahadjopoulos, D., and Benz, C. C. Immunoliposomes for cancer treatment. Adv. Pharmacol., *40:* 399–435, 1997.
2. Drummond, D. C., Meyer, O., Hong, K., Kirpotin, D. B., and Papahadjopoulos, D. Optimizing liposomes for delivery of chemotherapeutic agents to solid tumors. Pharmacol. Rev., *51:* 691–743, 1999.
3. Park, J. W., Hong, K., Carter, P., Asgari, H., Guo, L. Y., Keller, G. A., Wirth, C., Shalaby, R., Kotts, C., Wood, W. I., and *et al.* Development of anti-p185HER2 immunoliposomes for cancer therapy. Proc. Natl. Acad. Sci. USA, *92:* 1327–1331, 1995.
4. Kirpotin, D., Park, J. W., Hong, K., Zalipsky, S., Li, W. L., Carter, P., Benz, C. C., and Papahadjopoulos, D. Sterically stabilized anti-HER2 immunoliposomes: design and targeting to human breast cancer cells *in vitro*. Biochemistry, *36:* 66–75, 1997.
5. Cohen, S., Carpenter, G., and King, L., *Jr.* Epidermal growth factor-receptor-protein kinase interactions. Prog. Clin. Biol. Res., *66:* 557–567, 1981.
6. LeMaistre, C. F., Meneghetti, C., Howes, L., and Osborne, C. K. Targeting the EGF receptor in breast cancer treatment. Breast Cancer Res. Treat., *32:* 97–103, 1994.
7. Mendelsohn, J. The epidermal growth factor receptor as a target for cancer therapy. Endocr. Relat. Cancer, *8:* 3–9, 2001.
8. Nicholson, R. I., Gee, J. M., and Harper, M. E. EGFR and cancer prognosis. Eur. J. Cancer, *37:* S9–15, 2001.
9. Ekstrand, A. J., Sugawa, N., James, C. D., and Collins, V. P. Amplified and rearranged epidermal growth factor receptor genes in human glioblastomas reveal deletions of sequences encoding portions of the N- and/or C-terminal tails. Proc. Natl. Acad. Sci. USA, *89:* 4309–4313, 1992.
10. Yamazaki, H., Fukui, Y., Ueyama, Y., Tamaoki, N., Kawamoto, T., Taniguchi, S., and Shibuya, M. Amplification of the structurally and functionally altered epidermal growth factor receptor gene (c-erbB) in human brain tumors. Mol. Cell. Biol., *8:* 1816–1820, 1988.
11. Wikstrand, C. J., McLendon, R. E., Friedman, A. H., and Bigner, D. D. Cell surface localization and density of the tumor-associated variant of the epidermal growth factor receptor, EGFRvIII. Cancer Res., *57:* 4130–4140, 1997.
12. Humphrey, P. A., Wong, A. J., Vogelstein, B., Friedman, H. S., Werner, M. H., Bigner, D. D., and Bigner, S. H. Amplification and expression of the epidermal growth factor receptor gene in human glioma xenografts. Cancer Res., *48:* 2231–2238, 1988.
13. Wikstrand, C. J., Hale, L. P., Batra, S. K., Hill, M. L., Humphrey, P. A., Kurpad, S. N., McLendon, R. E., Moscatello, D., Pegram, C. N., Reist, C. J., and *et al.* Monoclonal antibodies against EGFRvIII are tumor specific and react with breast and lung carcinomas and malignant gliomas. Cancer Res., *55:* 3140–3148, 1995.
14. Yamazaki, H., Ohba, Y., Tamaoki, N., and Shibuya, M. A deletion mutation within the ligand binding domain is responsible for activation of epidermal growth factor receptor gene in human brain tumors. Jpn. J. Cancer Res., *81:* 773–779, 1990.
15. Sato, J. D., Kawamoto, T., Le, A. D., Mendelsohn, J., Polikoff, J., and Sato, G. H. Biological effects *in vitro* of monoclonal antibodies to human epidermal growth factor receptors. Mol. Biol. Med., *1:* 511–529, 1983.
16. Goldstein, N. I., Prewett, M., Zuklys, K., Rockwell, P., and Mendelsohn, J. Biological efficacy of a chimeric antibody to the epidermal growth factor receptor in a human tumor xenograft model. Clin. Cancer Res., *1:* 1311–1318, 1995.
17. Baselga, J., Pfister, D., Cooper, M. R., Cohen, R., Burtness, B., Bos, M., D'Andrea, G., Seidman, A., Norton, L., Gunnett, K., Falcey, J., Anderson, V., Waksal, H., and Mendelsohn, J. Phase I studies of anti-epidermal growth factor receptor chimeric antibody C225 alone and in combination with cisplatin. J. Clin. Oncol., *18:* 904–914, 2000.
18. Bonner, J. A., Raisch, K. P., Trummell, H. Q., Robert, F., Meredith, R. F., Spencer, S. A., Buchsbaum, D. J., Saleh, M. N., Stackhouse, M. A., LoBuglio, A. F., Peters, G. E., Carroll, W. R., and Waksal, H. W. Enhanced apoptosis with combination C225/radiation treatment serves as the impetus for clinical investigation in head and neck cancers. J. Clin. Oncol., *18:* 47S–53S, 2000.
19. Batra, S. K., Castelino-Prabhu, S., Wikstrand, C. J., Zhu, X., Humphrey, P. A., Friedman, H. S., and Bigner, D. D. Epidermal growth factor ligand-independent, unregulated, cell- transforming potential of a naturally occurring human mutant EGFRvIII gene. Cell Growth Differ., *6:* 1251–1259, 1995.
20. Szoka, F., Jr., and Papahadjopoulos, D. Comparative properties and methods of preparation of lipid vesicles (liposomes). Annu. Rev. Biophys. Bioeng., *9:* 467–508, 1980.
21. Bartlett, G. R. Phosphorus assay in column chromatography. J. Biol. Chem., *234:* 466–468, 1959.
22. Litzinger, D. C., Buiting, A. M., van Rooijen, N., and Huang, L. Effect of liposome size on the circulation time and intraorgan distribution of amphipathic poly(ethylene glycol)-containing liposomes. Biochim. Biophys. Acta, *1190:* 99–107, 1994.
23. Claassen, E. Post-formation fluorescent labelling of liposomal membranes. *In vivo* detection, localisation and kinetics. J. Immunol. Methods, *147:* 231–240, 1992.
24. Lasic, D. D., Frederik, P. M., Stuart, M. C., Barenholz, Y., and McIntosh, T. J. Gelation of liposome interior. A novel method for drug encapsulation. FEBS Lett., *312:* 255–258, 1992.
25. Haran, G., Cohen, R., Bar, L. K., and Barenholz, Y. Transmembrane ammonium sulfate gradients in liposomes produce efficient and stable entrapment of amphipathic weak bases. Biochim. Biophys. Acta, *1151:* 201–215, 1993.
26. Hong, R. L., Huang, C. J., Tseng, Y. L., Pang, V. F., Chen, S. T., Liu, J. J., and Chang, F. H. Direct comparison of liposomal doxorubicin with or without polyethylene glycol coating in C-26 tumor-bearing mice: is surface coating with polyethylene glycol beneficial? Clin. Cancer Res., *5:* 3645–3652, 1999.
27. Park, J. W., Hong, K., Kirpotin, D. B., Colbern, G., Shalaby, R., Baselga, J., Shao, Y., Nielsen, U. B., Marks, J. D., Moore, D., Papahadjopoulos, D., and Benz, C. C. Anti-HER2 immunoliposomes: enhanced efficacy attributable to targeted delivery. Clin. Cancer Res., *8:* 1172–1181, 2002.
28. Straubinger, R. M., Papahadjopoulos, D., and Hong, K. L. Endocytosis and intracellular fate of liposomes using pyranine as a probe. Biochemistry, *29:* 4929–4939, 1990.
29. Scudiero, D. A., Shoemaker, R. H., Paull, K. D., Monks, A., Tierney, S., Nofziger, T. H., Currens, M. J., Seniff, D., and Boyd, M. R. Evaluation of a soluble tetrazolium/formazan assay for cell growth and drug sensitivity in culture using human and other tumor cell lines. Cancer Res., *48:* 4827–4833, 1988.
30. Kirpotin, D. B., Hong, K., Park, J. W., Shalaby, R., Shao, Y., Zhen, W., Nielsen, U., Marks, J. D., Benz, C. C., and Papahadjopoulos, D. Anti-HER2 immunoliposomes produced by spontaneous capture of an amphipathic poly(ethylene glycol)-anti-HER2 antibody conjugate into the liposome membrane. Proc. Am. Assoc. Cancer Res., *41:* 325, 2000.
31. Iden, D. L., and Allen, T. M. *In vitro* and *in vivo* comparison of immunoliposomes made by conventional coupling techniques with those made by a new post-insertion approach. Biochim. Biophys. Acta, *1513:* 207–216, 2001.
32. Fan, Z., Masui, H., Atlas, I., and Mendelsohn, J. Blockade of epidermal growth factor receptor function by bivalent and monovalent fragments of 225 anti-epidermal growth factor receptor monoclonal antibodies. Cancer Res., 4322–4338, 1993.
33. Marks, C., and Marks, J. D. Phage libraries – a new route to clinically useful antibodies. N. Engl. J. Med., *335:* 730–733, 1996.
34. Sheets, M. D., Amersdorfer, P., Finnern, R., Sargent, P., Lindquist, E., Schier, R., Hemingsen, G., Wong, C., Gerhart, J. C., Marks, J. D., and Lindqvist, E. Efficient construction of a large nonimmune phage antibody library: the production of high-affinity human single-chain antibodies to protein antigens. Proc. Natl. Acad. Sci. USA, *95:* 6157–6162, 1998.
35. Huie, M. A., Cheung, M. C., Muench, M. O., Becerril, B., Kan, Y. W., and Marks, J. D. Antibodies to human fetal erythroid cells from a nonimmune phage antibody library. Proc. Natl. Acad. Sci. USA, *98:* 2682–2687, 2001.
36. Nielsen, U. B., Kirpotin, D. B., Pickering, E. M., Hong, K., Park, J. W., Refaat Shalaby, M., Shao, Y., Benz, C. C., and Marks, J. D. Therapeutic efficacy of anti-ErbB2 immunoliposomes targeted by a phage antibody selected for cellular endocytosis. Biochim. Biophys. Acta, *1591:* 109–118, 2002.
37. Steinberg, T. H., Newman, A. S., Swanson, J. A., and Silverstein, S. C. Macrophages possess probenecid-inhibitable organic anion transporters that remove fluorescent dyes from the cytoplasmic matrix. J. Cell Biol., *105:* 2695–2702, 1987.
38. Antony, A. C. The biological chemistry of folate receptors. Blood, *79:* 2807–2820, 1992.
39. Wikstrand, C. J., Cole, V. R., Crotty, L. E., Sampson, J. H., and Bigner, D. D. Generation of anti-idiotypic reagents to the EGFRvIII tumor-associated antigen system. Cancer Immunol. Immunother., *50:* 639–652, 2002.
40. Park, J. W., Kirpotin, D. B., Hong, K., Shalaby, R., Shao, Y., Nielsen, U. B., Marks, J. D., Papahadjopoulos, D., and Benz, C. C. Tumor targeting using anti-her2 immunoliposomes. J. Control Release, *74:* 95–113, 2001.

AACR American Association for Cancer Research

Cancer Research

The Journal of Cancer Research (1916–1930) | The American Journal of Cancer (1931–1940)

Epidermal Growth Factor Receptor (EGFR)-targeted Immunoliposomes Mediate Specific and Efficient Drug Delivery to EGFR- and EGFRvIII-overexpressing Tumor Cells

Christoph Mamot, Daryl C. Drummond, Udo Greiser, et al.

Cancer Res 2003;63:3154-3161.

Available online at www.sciencedirect.com
SCIENCE DIRECT®
Drug Resistance Updates 6 (2003) 271–279
DRUG RESISTANCE Updates
www.elsevier.com/locate/drup

Liposome-based approaches to overcome anticancer drug resistance

Christoph Mamot[a], Daryl C. Drummond[b,c], Keelung Hong[c], Dmitri B. Kirpotin[b,c], John W. Park[a,c,*]

[a] Division of Hematology/Oncology, University of California, San Francisco (UCSF), 2340 Sutter Street, San Francisco, CA 94115, USA
[b] California Pacific Medical Center Research Institute, Liposome Research Laboratory, 2200 Webster Street, San Francisco, CA 94115, USA
[c] Hermes Biosciences, Inc., 61 Airport Blvd., Suite B, San Francisco, CA 94080, USA

Received 24 July 2003; received in revised form 4 August 2003; accepted 5 August 2003

Abstract

Drug resistance remains an important obstacle towards better outcomes in the treatment of cancer. One general approach to overcome this problem has been to inhibit specific resistance mechanisms, such as P-glycoprotein (PGP)-mediated drug efflux, using small molecule agents or other therapeutic strategies. Alternatively, drug delivery approaches using liposomes or other carriers can in principle target drugs to tumor tissue, tumor cells, or even compartments within tumor cells. By increasing bioavailability of drugs at sites of action, these approaches may provide therapeutic advantages, including enhanced efficacy against resistant tumors. Current liposomal anthracyclines have achieved clinical use in cancer treatment by providing efficient encapsulation of drug in stable and non-reactive carriers, and there is evidence indicating potential benefit in some clinical settings involving resistant tumors. Other liposome-based strategies include constructs designed to be taken up by tumor cells, as well as further modifications to allow triggered drug release. These approaches seek to overcome drug resistance by more efficient delivery to tumor cells, and in some cases by concomitant avoidance or inhibition of drug efflux mechanisms. Newer agents employ molecular targeting, such as immunoliposomes using antibody-directed binding and internalization. These agents selectively deliver drug to tumor cells, can efficiently internalize for intracellular drug release, and can potentially enhance both efficacy and safety.

Keywords: Liposomes; Immunoliposomes; Drug delivery; Multidrug resistance; MDR

1. Introduction

Drug resistance continues to be a major challenge in cancer treatment. Intrinsic or acquired drug resistance occurs frequently in most cancers, and often involves resistance to multiple agents simultaneously (multidrug resistance, MDR). A number of mechanisms for drug resistance have been described. These include: overexpressed drug export pumps, such as P-glycoprotein (PGP) and multidrug-resistance protein (MRP); decreased drug uptake, such as altered folate carriers; inactivation of drugs, such as via glutathione-mediated reduction; overexpression of target enzymes, such as upregulated thymidylate synthase; altered drug targets, such as topoisomerase II; increased DNA repair capacity; reduced ability to undergo apoptosis; and others (reviewed in Kellen, 1994; Broxterman et al., 2003). Among these mechanisms, the role of PGP in multidrug resistance has been one of the most intensively studied. PGP, encoded by the *MDR1* gene, is a member of the ABC (ATP-Binding Cassette) transport protein family and is frequently overexpressed in the MDR phenotype. Other membrane-bound transporters capable of mediating drug efflux include multidrug-resistance protein MRP and other related proteins (Renes et al., 2000). These proteins actively transport a variety of heterocyclic substrates, including cytotoxic drugs such as anthracyclines, vinca alkaloids, mitoxantrone, paclitaxel, and others out of the cell or into other cellular compartments (Juranka et al., 1989; Cole and Deeley, 1998; Renes et al., 2000).

Specific inhibitors of these resistance mechanisms have been widely pursued as a means to restore drug sensitivity (for review, see Leonard et al., 2002). Although still actively under investigation, specific resistance inhibitors have yet to gain registration for clinical use. Progress towards therapeutic success has been hampered by such issues as inadequate specificity, both predictable and unforeseen toxicities, uncertainly about the true prevalence and contribution of the known resistance mechanisms, paucity of predictive assays to identify tumors dependent upon particular mechanisms, and multiplicity and redundancy of resistance mechanisms (West et al., 2002).

* Corresponding author. Tel.: +1-415-502-3844; fax: +1-415-353-9571.
E-mail address: jpark@cc.ucsf.edu (J.W. Park).

1368-7646/$ – see front matter © 2003 Elsevier Ltd. All rights reserved.
doi:10.1016/S1368-7646(03)00082-7

An alternative strategy for overcoming drug resistance is based on new drug delivery systems to achieve selective drug accumulation in tumor tissues, tumor cells, or even compartments of tumor cells. Liposomal carriers have become clinically accepted in cancer treatment, and as such are exemplars of delivery systems that can enhance the utility of anticancer drugs. For example, long circulating liposomes and other macromolecular carriers can increase drug deposition in solid tumors, which may help to overcome drug resistance. Other liposome strategies include modifications for controlled release, which may increase drug bioavailability; and ligand-targeted liposomes, such as immunoliposomes, which can internalize in tumor cells for intracellular drug delivery and maximal drug efficacy.

This minireview will update an earlier review in this Journal (Massing and Fuxius, 2000) and discuss the potential of liposome-based strategies, including current liposomal drugs, modified liposomal agents, and ligand-targeted liposomes, for the treatment of drug-resistant cancers.

2. Current liposomal drug delivery

2.1. Long circulating liposomes

Liposomes are membrane-bound vesicles capable of packaging drugs for various delivery applications. For cancer treatment, a number of distinct liposome classes have emerged, based on structural features and associated pharmacologic strategies for delivery (Drummond et al., 1999). Thus, far, the most clinically successful liposomal drugs for cancer treatment have been small unilamellar vesicles (SUV), which consist of a single phospholipid bilayer enclosing an inner aqueous compartment for drug encapsulation. Multilamellar vesicles (MLV) and other structures have been developed as well, and offer an alternative approach to packaging certain drugs. This includes methods for embedding hydrophobic drugs within liposomal membranes. The pharmacokinetics and biodistribution of liposomes depend on properties such as size, surface charge, and membrane composition.

Liposomal drugs currently used in clinical oncology were successfully stabilized to allow for durable drug encapsulation in conjunction with long circulation. Such liposomes tend to accumulate preferentially in tumors as a result of an enhanced permeability and retention (EPR) effect (Matsumura and Maeda, 1986). The EPR effect is attributed to the abnormal microvasculature that arises during tumor angiogenesis, which permits extravasation of macromolecular agents; as well, reduced tumor lymphatics further promote accumulation of such agents. As a result, liposomes or other nanoparticles that have been stabilized for prolonged circulation and limited volume of distribution will slowly accumulate in tumor tissue. Stabilized liposomes, engineered to prevent non-specific interactions with biomembranes, accumulate within the extracellular space of tumor stroma (Huang et al., 1992), and eventually leak their drug into the tumor environment.

Based on these properties, current liposomal delivery systems can potentially provide pharmacologic advantages over free drug, including a means to overcome drug resistance (Table 1). Liposome delivery can yield increases in the area-under-the-concentration-versus-time-curve (AUC) in plasma and tumor by 60–600-fold or greater (Working and Dayan, 1996). At this level, liposomal delivery may overcome the activity of multidrug transporter systems, perhaps even in highly resistant tumors. It should be noted, however, that actual plasma and tumor drug concentrations reflect total drug (free and liposome-encapsulated) in these two compartments. Since only free drug released from its carrier is active, a superior predictor of activity is the AUC of released rather than total drug. This analysis has been technically difficult to perform in experimental models and, especially, in clinical settings.

Liposomal anthracyclines have demonstrated clinical utility, as described below. Other liposomal drugs that have entered clinical development include liposome formulations of paclitaxel (Treat et al., 2001), various camptothecins (Burke and Bom, 2000), and vincristine (Sarris et al., 2000).

2.2. Clinical efficacy of liposomal anthracyclines

At present, two liposomal anthracyclines have been approved by the US FDA for cancer treatment: pegylated

Table 1
Mechanisms for overcoming drug resistance using current liposomal carriers

Mechanism	Rationale	Agents
Increased tumor exposure	• Long-circulating liposomes preferentially extravasate from tumor vessels into tumor tissue • Depot-effect in tissue mimics continuous infusion	• Pegylated liposomal doxorubicin (Doxil®/Caelyx®) • Liposomal daunorubicin (DaunoXome®) • Liposomal doxorubicin (Myocet™)
Reduced or altered toxicity profile	• Liposome encapsulation leads to altered biodistribution and toxicity profiles • Liposome versions can be administered via alternative dose/schedule • Due to reduced or non-overlapping toxicities, liposome versions facilitate new combinations with other chemotherapeutics, which may overcome resistance	• Pegylated liposomal doxorubicin (Doxil®/Caelyx®) • Liposomal daunorubicin (DaunoXome®)

liposomal doxorubicin (PLD, Doxil®, ALZA Pharmaceuticals, Palo Alto, CA; also known as Caelyx®) and liposomal daunorubicin (DaunoXome®, Gilead Sciences, Foster City, CA). Liposomal anthracyclines have achieved extremely robust drug encapsulation, in which drug can be loaded very efficiently, and packed or even crystallized in the aqueous interior. PLD is a small unilamellar vesicle (~100 nm) comprised of neutral lipids, onto which polyethylene glycol (PEG) chains are grafted as an additional surface barrier ("steric stabilization") against non-specific interactions. Liposomal daunorubicin is a small unilamellar vesicle composed exclusively of the neutral lipids distearoylphosphatidylcholine and cholesterol, and thus also features neutral charge and rigid membranes along with very small liposome size (<40 nm) for in vivo stability (Forssen et al., 1992). Liposomal daunorubicin is long-circulating, and PLD even more so; hence, both agents can accumulate in tumor tissues via the EPR effect.

Both liposomal anthracyclines were first approved for the treatment of AIDS-related Kaposi's sarcoma. Notably, there is direct clinical evidence that liposomal doxorubicin is able to overcome drug resistance in this disease. In a study performed by Northfelt and colleagues, 53 patients with advanced AIDS-related Kaposi's sarcoma were treated with PLD in the second-line setting after failing prior combination chemotherapy (Northfelt et al., 1997). In 28 patients who had disease progression following treatment that included standard doxorubicin, the objective response rate to PLD was 32%. This result indicates that PLD can produce clinical responses in patients considered refractory to prior therapy, including standard doxorubicin.

In contrast, PLD did not demonstrate benefit in a small study in advanced breast cancer patients considered to be anthracycline-resistant (Rivera et al., 2002). This phase II study involved 11 patients with metastatic breast cancer who either had disease progression while receiving a standard anthracycline-containing regimen, or who developed evidence of metastatic disease within 6 months of completion of an anthracycline-containing adjuvant regimen. No objective responses were observed in this anthracycline-resistant group. That PLD did not show non-cross-resistance with doxorubicin in this study as in Kaposi's sarcoma may have been due to lesser tumor accumulation of PLD in breast cancer versus the highly vascular lesions of Kaposi's sarcoma, differences in resistance mechanisms between the two cancer types, or other reasons. However, PLD has shown substantial efficacy in breast cancer both as monotherapy and in combination with other chemotherapeutics, and there is continued interest in combinations that include liposomal anthracyclines and their frequently reduced toxicity profile (for review, see Park, 2002). It can be argued that the role of liposomal anthracyclines in anthracycline-resistant breast cancer remains unclear, particularly since there is rationale for combination regimens containing liposomal anthracyclines; such combinations may be useful even in patients resistant to standard anthracyclines.

Current liposomal agents can be combined with other treatment modalities as well as other chemotherapy drugs. In particular, hyperthermia has been used to modulate the biodistribution of liposomal drugs. In animal models, application of hyperthermia to subcutaneous tumors concomitant with or prior to i.v. administration of long circulating liposomes resulted in significantly increases in liposome uptake in tumor tissue (Matteucci et al., 2000). This finding appears due to hyperthermia-induced changes in microcirculatory dynamics and vascular permeability, which further facilitate liposome extravasation from tumor vessels. In a phase I/II clinical trial, patients with metastatic breast cancer of the chest wall received hyperthermia and PLD in close sequence (Park et al., 2001). Treatment was generally well-tolerated, and, in patients with such extensive disease that hyperthermia was limited to portions of tumor, hyperthermia appeared to enhance the efficacy of PLD. Objective responses were observed in over half of the patients, including a number of patients who had previously received standard anthracyclines.

Liposomal anthracyclines have been studied in multiple other cancers. For example, in a randomized phase III clinical trial in ovarian cancer, PLD was found effective in second-line following platinum-based first-line therapy (Gordon et al., 2001). Encouraging results have been reported in multiple myeloma (Mohrbacher et al., 2002) and non-Hodgkin's lymphoma (Aviles et al., 2002) using liposomal anthracyclines in place of standard doxorubicin in commonly used combination regimens.

In addition to these liposomal anthracyclines, a liposomal doxorubicin that features efficient loading of drug has been developed and has received regulatory approval in Europe (Myocet™, Elan Pharma, Munich, Germany). Although not specifically designed for long circulation as liposomal daunorubicin or pegylated liposomal doxorubicin, this agent significantly alters biodistribution, allowing for reduction in the dose-limiting toxicities of doxorubicin (Batist et al., 2002).

2.3. Tumor resistance within the central nervous system

A special problem of drug resistance is posed by primary and metastatic brain tumors, which feature anatomic and physiologic obstacles such as the blood–brain and blood–tumor barriers. In addition, the previously discussed molecular and cellular mechanisms of drug resistance occur as well, and appear to play prominent roles in gliomas (Abe et al., 1994) as well as in metastatic tumors.

Perhaps surprisingly, liposomal drugs may provide a strategy for overcoming these obstacles. Although the blood–brain barrier restricts even small solutes from entering brain parenchyma, the deranged blood–tumor interface may allow sufficient extravasation of long circulating liposomes. Furthermore, the blood–brain barrier is comprised of some of

Table 2
Strategies for overcoming drug resistance using modified liposomes

Strategy	Proposed mechanism
Anionic liposomes	• Anionic lipids may inhibit PGP • Possible internalization
Other inhibitory lipids	• Certain phospholipids may inhibit PGP
Thermosensitive liposomes	• Modified liposomes can release drug upon hyperthermia treatment
Triggered release	• Modified liposomes can increase and optimize drug release in target tissue dependent on pH or other triggers
Combining liposomes and resistance inhibitors	• Liposomal chemotherapeutic may be better than free drug in combination with resistance inhibitors • Liposome delivery of resistance inhibitors may increase therapeutic index
Delivery of hydrophobic drug analogs	• Liposomes can deliver poorly soluble drugs that are not substrates for PGP
Gene therapy approaches	• Non-viral delivery of nucleic acid-based constructs to tumor cells to reverse, circumvent, or exploit drug resistance • Non-viral delivery of resistance genes to normal tissues to protect them from chemotherapy ("chemoprotection")

the same mechanisms that occur in cancer-associated MDR. For example, endothelial PGP activity leads to efflux of drugs out of the CNS; this has been implicated as the mechanism for exclusion of anthracyclines from the blood–brain barrier (Hughes et al., 1998). Liposomes or other particles able to enter tumor tissue may allow circumvention of this resistance mechanism.

Evidence to support this hypothesis includes preclinical studies of stabilized liposomal doxorubicin in a rat intracranial sarcoma model, in which brain tumor drug levels were 14-fold higher with liposome delivery than with free drug (Siegal et al., 1995). Improved drug delivery was accompanied by extended survival in this model. Also, in the rat intracranial 9L gliosarcoma model, stabilized liposomal doxorubicin increased survival, whereas free doxorubicin was no more beneficial than saline control (Zhou et al., 2002). In clinical studies, accumulation of PLD was 7–19 times higher in glioblastomas and metastatic brain tumors compared to the normal brain, and complete responses were observed in 4 out of 10 patients with brain metastasis (Siegal et al., 1995; Koukourakis et al., 2000).

In addition to the possibility of using systemic drug carriers to increase access to brain tumors, local-regional drug delivery approaches are being pursued to completely bypass the blood–brain barrier. For example, polymeric wafers containing BCNU (polifeprosan 20 with carmustine implant, Gliadel®) have been used in patients with primary malignant glioma for continuous release of drug after surgical implantation (Westphal et al., 2003). Advances in convection enhanced delivery (CED), which utilizes bulk flow to infuse high molecular weight agents through solid tissues, enables regional administration of therapeutic agents (Cunningham et al., 2000; Lonser et al., 2002). In rodent and primate models, CED can be used to distribute liposomes extensively in the brain and in regions of brain tumors (Mamot et al., 2003a).

3. Modified liposomes to overcome drug resistance

The versatility of liposomal systems is being actively exploited to develop a variety of new liposome-based constructs for the treatment of drug-resistant cancers (Table 2).

3.1. Liposomes capable of modulating PGP

Many of the earliest studies using liposomal approaches for drug-resistant tumors involved liposomes composed of anionic phospholipids, such as cardiolipin (Oudard et al., 1991; Thierry et al., 1993b) and phosphatidylserine (Poste and Papahadjopoulos, 1976; Fan et al., 1990). The effect of this delivery was increased cellular accumulation and cytotoxicity of the liposomal agent relative to the free drug in drug-resistant cancer cells. Proposed mechanisms of action for these liposomes included direct interaction between anionic lipids and PGP. However, it has also been shown that anionic liposomes are internalized by certain cells (Lee et al., 1992), in contrast to the minimal interaction that occurs with stabilized neutral liposomes. If internalized, anionic liposomes could provide drug release in intracellular compartments to bypass PGP or other membrane-bound transporters. This is similar to the mechanism proposed for ligand-directed liposomes such as immunoliposomes (see Section 4). However, whatever the mechanism for circumventing MDR in experimental models, anionic liposomes have generally not achieved sufficient in vivo stability and circulation time for clinical use (Drummond et al., 1999). Indeed, optimization of liposome design with respect to stability and reduction of membrane reactivity was one of the driving forces in the development of long circulating neutral liposomes.

Neutral phospholipids such as phosphatidylcholine (PC) and phosphatidylethanolamine (PE), the primary constituents of many liposomal membranes, have been suggested

to be PGP substrates (van Helvoort et al., 1996; Bosch et al., 1997) that can compete with drugs for PGP binding (Romsicki and Sharom, 1999). For example, PC- or PE-containing liposomes produced increased drug uptake and enhanced cytotoxicity in MDR cell lines; this occurred not only with liposome-encapsulated drug, but also when empty liposomes were given as pretreatment prior to free drug, indicating a direct interaction between the liposome and the cell (Lo, 2000). Similarly, in MDR cell lines that overexpress PGP, Michieli and coworkers reported that liposomal daunorubicin composed of PC/cholesterol produced significantly higher cellular levels of daunorubicin than free drug, resulting in four- to five-fold greater cytoxic effect (Michieli et al., 1999). However, the mechanism for this effect remains unclear. Neutral liposomes do not appear readily capable of membrane fusion with cells, nor to internalize in most tumor cell types. How then do neutral phospholipids interact with the plasma membrane of target cells, and how do such interactions lead to modulation of drug accumulation/efflux? Further elucidation of these processes will be necessary to fully establish this as a feasible mechanism for overcoming drug resistance.

3.2. Liposomes capable of triggered release: thermosensitive and pH-sensitive liposomes

Once stabilized liposomes extravasate from vessels into tumor tissue, they eventually release drug for eventual uptake in tumor cells. Processes acting to promote drug release may include phagocytosis of liposomes by the reticuloendothelial system as well as destabilization by tissue lipases, oxidizing agents, or other tissue components (Drummond et al., 2000). New liposome strategies include constructs capable of triggered release: such liposomes are designed to undergo structural change in response to physicochemical stimuli, thus allowing more controlled release of encapsulated drug. These approaches include the use of thermosensitive liposomes triggered by exogenous application of heat (hyperthermia), and pH-sensitive liposomes triggered by an acidic milieu.

While hyperthermia can enhance the tumor accumulation of stable and long circulating liposomes (as discussed earlier), another strategy has been to use hyperthermia to destabilize thermosensitive liposomes, thereby inducing drug release in heated regions. Thermosensitive liposomes feature lipid constituents with a relatively sharp phase transition at temperatures only a few degrees above 37 °C. Thus, when hyperthermia is administered, heating induces structural change leading to rapid release of encapsulated drug. For example, thermosensitive liposomes-containing doxorubicin were tested in vitro in a multidrug-resistant subline of MCF-7 breast cancer cells; when liposomal drug and hyperthermia were applied, cell growth was inhibited to the same extent as with non-MDR cells (Merlin et al., 1993). Another thermosensitive formulation has achieved very rapid release of doxorubicin at 39–40 °C, and was highly efficacous with hyperthermia in a squamous cell carcinoma model (Needham et al., 2000). This thermosensitive liposome is entering Phase I clinical trials in conjunction with hyperthermia.

Other strategies for triggering release of liposomal contents within target tissues include modification of the external surface, such as the PEG chains in pegylated liposomes. For example, a disulfide-linked PEG-phospholipid conjugate (mPEG-DTP-DSPE) was used to provide selective detachment from the liposome surface following thiolytic cleavage (Kirpotin et al., 1996). These liposomes are designed to remain pegylated in blood, but in a tumor environment to shed PEG chains for enhanced drug release. Furthermore, fusogenic liposomes can be employed with this approach, so that detachment of PEG can unmask reactive components for liposome fusion with tumor cells.

3.3. Combining liposomes and drug efflux inhibitors

As mentioned, many agents capable of inhibiting drug efflux mechanisms such as PGP have been identified, although thus far none have demonstrated sufficient clinical benefit for regulatory approval. Some of the difficulties in developing PGP inhibitors pertain to pharmacologic limitations of the inhibitor itself and/or the combination with chemotherapy. Liposome-based strategies can potentially be invoked to address such issues.

For example, PSC 833 (Valspodar) is a cyclosporine analogue and potent PGP inhibitor. Although this agent alone appeared to have relatively few toxicities, co-administration with chemotherapeutics such as daunorubicin, doxorubicin and paclitaxel was observed to substantially alter the clearance and pharmacokinetics of the chemotherapeutic drug, resulting in exacerbation of toxicity (Advani et al., 2001; Kang et al., 2001). In preclinical studies, the combination of PSC 833 with liposomal rather than free doxorubicin prevented these undesirable drug–drug interactions; pegylated liposomal doxorubicin in particular was unaffected in its pharmacokinetics by PSC 833 treatment (Krishna and Mayer, 1997; Krishna et al., 1999).

While liposome delivery of chemotherapeutics may mitigate certain pharmacologic problems associated with concomitant anti-resistance therapy, another strategy is to deliver the anti-resistance agent in liposomes. An early example was liposome packaging of the PGP inhibitor valinomycin, which by itself possesses significant toxicities. Liposomal valinomycin was associated with reduction of toxicity without compromising its PGP-inhibitory activity in experimental models (Daoud and Juliano, 1986, 1989).

3.4. Delivery of hydrophobic drug analogs

Liposomes can also be used to deliver hydrophobic drug analogs designed to avoid efflux-mediated resistance, such as the anthracycline annamycin (Zou et al., 1994) and lipophilic platinum derivatives (Perez-Soler et al., 1988).

These compounds are intended to retain the potent anticancer activity of the parent compound, but with structural alterations that render their net cellular uptake relatively independent of PGP and/or other efflux pumps. Because many of these derivatives have resulted in increased hydrophobicity and correspondingly decreased solubility, liposome entrapment or encapsulation have been pursued for the formulation and delivery of these novel analogs. Although liposomal annamycin has shown good preclinical activity in drug-resistant models, a phase II clinical study of liposomal annamycin observed no clear evidence of efficacy in doxorubicin-resistant breast cancer patients (Booser et al., 2002).

4. Immunoliposomes and other ligand-directed liposomal agents

In order to create agents capable of targeting drug carriers to tumor cells, we and others have studied approaches for antibody-targeted liposomes (immunoliposomes, ILs), which combine monoclonal antibody (MAb) and liposome technologies (Park et al., 1997). Immunoliposomes can be designed for specific recognition of a target antigen followed by receptor-mediated endocytosis. In principle, therapeutic index can be increased by targeting liposomes and their contents directly into tumor cells, and this may be useful for resistant cancers (Table 3).

HER2 (ErbB2, Neu) is an oncogenic receptor-tyrosine kinase (RTK) that can be targeted by MAb-based therapy such as trastuzumab (Herceptin). HER2-targeted immunoliposomes were constructed to bind and internalize in HER2-overexpressing cancer cells, resulting in selective intracellular drug delivery (Park et al., 1995; Kirpotin et al., 1997). Immunoliposomes containing either Fab′ or scFv fragments against HER2 were used to deliver doxorubicin, resulting in potent and selective anti-tumor activity in a number of tumor models; this included superior efficacy as compared with free drug, non-targeted liposomal doxorubicin, or non-targeted liposomal doxorubicin plus free anti-HER2 MAb (Park et al., 2002).

Immunoliposomes directed against epidermal growth factor receptor (EGFR/HER1/ErbB1) represent another example of tumor-targeted drug delivery (Mamot et al., 2003b). In cell culture studies, EGFR-targeted immunoliposomes showed extensive internalization in the cytoplasm of EGFR-overexpressing cells (up to 30,000 ILs/cell) but not in non-overexpressing cells. EGFR-targeted ILs demonstrated marked cytotoxicity when encapsulating any of several chemotherapy drugs (doxorubicin, vinorelbine and methotrexate).

Immunoliposomes and other ligand-directed liposomes capable of internalization provide true intracellular drug delivery. By penetrating the plasma membrane and providing drug release within the cytoplasm, drug delivery is not only targeted but also very efficient, and can potentially bypass membrane-bound efflux mechanisms.

Evidence for this includes studies with targeted liposomes containing either growth factor ligands or antibodies against growth factor receptors. For example, folate targeting has been pursued using liposomes conjugated to folic acid, which were rapidly internalized in tumor cells via the folate receptor (for review, see Lu and Low, 2002). In vivo studies in a resistant murine lung carcinoma (M109R-HiFR) tumor model showed superior efficacy of folate-targeted liposomal doxorubicin as compared with free drug or non-targeted liposomal doxorubicin (Goren et al., 2000). The transferrin receptor has also been targeted by immunoliposomes. Anti-transferrin immunoliposomes were used to deliver doxorubicin in a doxorubicin-resistant subline of human leukemia cells (K562/ADR) (Suzuki et al., 1997). Immunoliposome delivery was associated with minimal drug efflux and nearly equivalent dox levels in resistant K562/ADR cells as compared with sensitive parental K562 cells. In contrast, free dox was efficiently effluxed and present at 45-fold lower drug levels in the resistant subline. In separate studies, anti-transferrin immunoliposomes-containing MAb OX26 were used to deliver radiolabeled digoxin in immortalized RBE4 rat brain capillary endothelial cells (Huwyler et al., 2002). Cellular uptake of digoxin was 25-fold higher using immunoliposomes, and was unaffected by the PGP inhibitor ritonavir.

Other immunoliposome-based approaches for drug-resistant cancers include immunoliposomes containing an MAb directed against PGP, which provided increased cytotoxicity of encapulated vinorelbine in resistant K562 cells (Matsuo et al., 2001). Also, immunoliposomes have been constructed to target tumor-associated endothelial cells

Table 3
Strategies for overcoming drug resistance using immunoliposomes and ligand-directed liposomes

Strategy	Proposed mechanism
Immunoliposomes/targeted liposomes against growth factor receptors	• MAb or fragments inserted into liposomes enable targeted drug delivery
	• Targeting of receptor tyrosine kinases or growth factor receptors can induce endocytosis • Intracellular delivery can bypass drug efflux pumps
Immunoliposomes against PGP	• MAbs against PGP can reverse MDR
Immunoliposomes against endothelial receptors	• Endothelial cells are not expected to develop resistance mechanisms as in cancer cells

(Greiser et al., 2002), which are not expected to develop resistance mechanisms similar to tumor cells.

5. Gene therapy using lipidic vectors

A variety of gene therapy approaches have been pursued to inhibit, circumvent, or exploit drug resistance mechanisms. Progress in these areas, and in gene therapy of cancer in general, is currently limited by inadequate gene vector technology for delivery of nucleic acids. Viral vectors feature a host of potential problems, including (among others) carcinogenesis, other toxicities, immunogenicity, non-specificity, downregulation of viral receptors on tumor cells, and difficult manufacturing. Of the non-viral approaches, lipidic or liposome-based delivery systems have been the most commonly pursued. However, these systems have generally relied upon cationic lipids/liposomes for nucleic acid packaging, rather than the highly stabilized neutral liposomes that have become established as efficient and long circulating drug carriers. Gene-containing constructs with comparable stability will be required for systemic gene therapy. Moreover, adding antibody fragments or other targeting ligands to such constructs may enable more specific and efficient gene delivery.

Liposome-based gene therapy approaches, including those directed against drug resistance mechanisms, have been extensively reviewed elsewhere (Kobayashi et al., 2001; Pedroso de Lima et al., 2003). Briefly, examples include cationic liposomes or lipoplexes used to deliver antisense oligonucleotides (Thierry et al., 1993a; Alahari et al., 1996) or ribozymes (Masuda et al., 1998) against sequences of the *MDR1* gene. A related strategy is to use gene therapy technology to overexpress drug resistance genes in healthy tissues, thereby protecting such tissues from chemotherapy-associated toxicity; for example, the *MDR1* gene has been transfected via liposome-based vectors into hematopoietic progenitors in bone marrow (Aksentijevich et al., 1996; Baudard et al., 1996; Lee et al., 2001).

6. Conclusions and outlook

Given the enormous capacity of tumors to deploy various mechanisms to resist anticancer drugs, it is not surprising that strategies to inhibit particular resistance mechanisms have proven difficult to translate into clinical success. Drug delivery approaches are likely to play an increasingly important role to increase the bioavailability of active drug at target sites, including cellular or subcellular sites.

Liposomes represent a validated and established drug delivery system, with several versions now in standard clinical use, as well as a promising technology with further innovations and next-generation systems under active development. Current liposomal anthracyclines can in some cases mitigate drug resistance mechanisms, based on substantially altered pharmacokinetics, biodistribution, and toxicology as compared with free drug. A number of other liposomal drugs are in active development. Alternative liposome-based strategies include attempts to directly modulate drug efflux and/or to achieve triggered drug release, thereby overcoming some resistance mechanisms. Perhaps the most powerful approach involves immunoliposomes or other ligand-linked liposomes that feature integration of molecular targeting and drug delivery. These agents can provide ligand-mediated internalization and intracellular drug delivery, thus achieving greater selectivity and efficiency of delivery to cancer cells, including resistant tumors.

Acknowledgements

This work was supported by grants from Accelerated Brain Cancer Cure (ABC2), Expedition Inspiration, and the National Cancer Institute Specialized Programs of Research Excellence (SPORE) in Breast Cancer (P50-CA 58207-01) and Brain Tumor (P50-CA 097257-01). C.M. was supported by a postdoctoral fellowship from the Swiss Academy of Medical Sciences (SAMW)/Swiss National Science Foundation (SNSF) and Cancer League Basel, Switzerland. D.C.D. is supported in part by a New Investigator Award from California's Breast Cancer Research Program of the University of California (7KB-0066).

References

Abe, T., Hasegawa, S., Taniguchi, K., Yokomizo, A., Kuwano, T., Ono, M., Mori, T., Hori, S., Kohno, K., Kuwano, M., 1994. Possible involvement of multidrug-resistance-associated protein (MRP) gene expression in spontaneous drug resistance to vincristine, etoposide and adriamycin in human glioma cells. Int. J. Cancer 58, 860–864.

Advani, R., Fisher, G.A., Lum, B.L., Hausdorff, J., Halsey, J., Litchman, M., Sikic, B.I., 2001. A phase I trial of doxorubicin, paclitaxel, and valspodar (PSC 833), a modulator of multidrug resistance. Clin. Cancer Res. 7, 1221–1229.

Aksentijevich, I., Pastan, I., Lunardi-Iskandar, Y., Gallo, R.C., Gottesman, M.M., Thierry, A.R., 1996. In vitro and in vivo liposome-mediated gene transfer leads to human MDR1 expression in mouse bone marrow progenitor cells. Hum. Gene Ther. 7, 1111–1122.

Alahari, S.K., Dean, N.M., Fisher, M.H., Delong, R., Manoharan, M., Tivel, K.L., Juliano, R.L., 1996. Inhibition of expression of the multidrug resistance-associated P-glycoprotein of by phosphorothioate and 5′ cholesterol-conjugated phosphorothioate antisense oligonucleotides. Mol. Pharmacol. 50, 808–819.

Aviles, A., Neri, N., Castaneda, C., Talavera, A., Huerta-Guzman, J., Gonzalez, M., 2002. Pegylated liposomal doxorubicin in combination chemotherapy in the treatment of previously untreated aggressive diffuse large B-cell lymphoma. Med. Oncol. 19, 55–58.

Batist, G., Barton, J., Chaikin, P., Swenson, C., Welles, L., 2002. Myocet (liposome-encapsulated doxorubicin citrate): a new approach in breast cancer therapy. Expert Opin. Pharmacother. 12, 1739–1751.

Baudard, M., Flotte, T.R., Aran, J.M., Thierry, A.R., Pastan, I., Pang, M.G., Kearns, W.G., Gottesman, M.M., 1996. Expression of the human multidrug resistance and glucocerebrosidase cDNAs from adeno-associated vectors: efficient promoter activity of AAV sequences and in vivo delivery via liposomes. Hum. Gene Ther. 7, 1309–1322.

Booser, D.J., Esteva, F.J., Rivera, E., Valero, V., Esparza-Guerra, L., Priebe, W., Hortobagyi, G.N., 2002. Phase II study of liposomal annamycin in the treatment of doxorubicin-resistant breast cancer. Cancer Chemother. Pharmacol. 50, 6–8.

Bosch, I., Dumussi-Joannopoulos, K., Wu, R.L., Furlong, S.T., Croop, J., 1997. Phosphatidylcholine and phosphatidylethanolamine behave as substrates of the human MDR1 P-glycoprotein. Biochemistry 36, 5685–5694.

Broxterman, H.J., Lankelma, J., Hoekman, K., 2003. Resistance to cytotoxic and anti-angiogenic agents: similarities and differences. Drug Resist. Update 6, 111–127.

Burke, T.G., Bom, D., 2000. Camptothecin design and delivery approaches for elevating anti-topoisomerase I activities in vivo. Ann. N.Y. Acad. Sci. 922, 36–45.

Cole, S.P., Deeley, R.G., 1998. Multidrug resistance mediated by the ATP-binding cassette transporter protein MRP. Bioessays 20, 931–940.

Cunningham, J., Oiwa, Y., Nagy, D., Podsakoff, G., Colosi, P., Bankiewicz, K.S., 2000. Distribution of AAV-TK following intracranial convection-enhanced delivery into rats. Cell Transplant 9, 585–594.

Daoud, S.S., Juliano, R.L., 1986. Reduced toxicity and enhanced antitumor effects in mice of the ionophoric drug valinomycin when incorporated in liposomes. Cancer Res. 46, 5518–5523.

Daoud, S.S., Juliano, R.L., 1989. Modulation of doxorubicin resistance by valinomycin (NSC 122023) and liposomal valinomycin in Chinese hamster ovary cells. Cancer Res. 49, 2661–2667.

Drummond, D.C., Meyer, O., Hong, K., Kirpotin, D.B., Papahadjopoulos, D., 1999. Optimizing liposomes for delivery of chemotherapeutic agents to solid tumors. Pharmacol. Rev. 51, 691–743.

Drummond, D.C., Zignani, M., Leroux, J., 2000. Current status of pH-sensitive liposomes in drug delivery. Prog. Lipid Res. 39, 409–460.

Fan, D., Bucana, C.D., O'Brian, C.A., Zwelling, L.A., Seid, C., Fidler, I.J., 1990. Enhancement of murine tumor cell sensitivity to adriamycin by presentation of the drug in phosphatidylcholine–phosphatidylserine liposomes. Cancer Res. 50, 3619–3626.

Forssen, E.A., Coulter, D.M., Proffitt, R.T., 1992. Selective in vivo localization of daunorubicin small unilamellar vesicles in solid tumors. Cancer Res. 52, 3255–3261.

Gordon, A.N., Fleagle, J.T., Guthrie, D., Parkin, D.E., Gore, M.E., Lacave, A.J., 2001. Recurrent epithelial ovarian carcinoma: a randomized phase III study of pegylated liposomal doxorubicin versus topotecan. J. Clin. Oncol. 19, 3312–3322.

Goren, D., Horowitz, A.T., Tzemach, D., Tarshish, M., Zalipsky, S., Gabizon, A., 2000. Nuclear delivery of doxorubicin via folate-targeted liposomes with bypass of multidrug-resistance efflux pump. Clin. Cancer Res. 6, 1949–1957.

Greiser, U., Drummond, D.C., Mamot, C., et al., 2002. Targeting immunoliposomes to endothelial receptors. Proc. Am. Assoc. Cancer Res. 43, 410 (Abstract).

Huang, S.K., Lee, K.D., Hong, K., Friend, D.S., Papahadjopoulos, D., 1992. Microscopic localization of sterically stabilized liposomes in colon carcinoma-bearing mice. Cancer Res. 52, 5135–5143.

Hughes, C.S., Vaden, S.L., Manaugh, C.A., Price, G.S., Hudson, L.C., 1998. Modulation of doxorubicin concentration by cyclosporin A in brain and testicular barrier tissues expressing P-glycoprotein in rats. J. Neurooncol. 37, 45–54.

Huwyler, J., Cerletti, A., Fricker, G., Eberle, A.N., Drewe, J., 2002. By-passing of P-glycoprotein using immunoliposomes. J. Drug Target. 10, 73–79.

Juranka, P.F., Zastawny, R.L., Ling, V., 1989. P-glycoprotein: multidrug-resistance and a superfamily of membrane-associated transport proteins. FASEB J. 3, 2583–2592.

Kang, M.H., Figg, W.D., Ando, Y., Blagosklonny, M.V., Liewehr, D., Fojo, T., Bates, S.E., 2001. The P-glycoprotein antagonist PSC 833 increases the plasma concentrations of 6alpha-hydroxypaclitaxel, a major metabolite of paclitaxel. Clin. Cancer Res. 7, 1610–1617.

Kellen, J.A., 1994. The phenomenon of multidrug resistance. In: Kellen, J.A. (Ed.), Reversal of Multidrug Resistance in Cancer. CRC Press, Boca Raton, FL, pp. 1–21.

Kirpotin, D.B., Hong, K., Mullah, N., Papahadjopoulos, D., Zalipsky, S., 1996. Liposomes with detachable polymer coating: destabilization and fusion of dioleoylphosphatidyl-ethanolamine vesicles triggered by cleavage of surface-grafted poly(ethylene glycol). FEBS Lett. 388, 115–118.

Kirpotin, D.B., Park, J.W., Hong, K., Zalipsky, S., Li, W.L., Carter, P., Benz, C.C., Papahadjopoulos, D., 1997. Sterically stabilized anti-HER2 immunoliposomes: design and targeting to human breast cancer cells in vitro. Biochemistry 36, 66–75.

Kobayashi, H., Takemura, Y., Miyachi, H., 2001. Novel approaches to reversing anti-cancer drug resistance using gene-specific therapeutics. Hum. Cell 14, 172–184.

Koukourakis, M.I., Koukouraki, S., Fezoulidis, I., et al., 2000. High intratumoural accumulation of stealth liposomal doxorubicin (Caelyx) in glioblastomas and in metastatic brain tumours. Br. J. Cancer 83, 1281–1286.

Krishna, R., Mayer, L.D., 1997. Liposomal doxorubicin circumvents PSC 833-free drug interactions, resulting in effective therapy of multidrug-resistant solid tumors. Cancer Res. 57, 5246–5253.

Krishna, R., McIntosh, N., Riggs, K.W., Mayer, L.D., 1999. Doxorubicin encapsulated in sterically stabilized liposomes exhibits renal and biliary clearance properties that are independent of valspodar (PSC 833) under conditions that significantly inhibit non-encapsulated drug excretion. Clin. Cancer Res. 5, 2939–2947.

Lee, K.D., Hong, K., Papahadjopoulos, D., 1992. Recognition of liposomes by cells: in vitro binding and endocytosis mediated by specific lipid headgroups and surface charge density. Biochim. Biophys. Acta 1103, 185–197.

Lee, C.G., Vieira, W.D., Pastan, I., Gottesman, M.M., 2001. An episomally maintained MDR1 gene for gene therapy. Hum. Gene Ther. 12, 945–953.

Leonard, G.D., Polgar, O., Bates, S.E., 2002. ABC transporters and inhibitors: new targets, new agents. Curr. Opin. Investig. Drugs 3, 1652–1659.

Lo, Y.L., 2000. Phospholipids as multidrug resistance modulators of the transport of epirubicin in human intestinal epithelial Caco-2 cell layers and everted gut sacs of rats. Biochem. Pharmacol. 60, 1381–1390.

Lonser, R.R., Walbridge, S., Garmestani, K., et al., 2002. Successful and safe perfusion of the primate brainstem: in vivo magnetic resonance imaging of macromolecular distribution during infusion. J. Neurosurg. 97, 905–913.

Lu, Y., Low, P.S., 2002. Folate-mediated delivery of macromolecular anticancer therapeutic agents. Adv. Drug Deliv. Rev. 54, 675–693.

Mamot, C., Bankiewicz, K.S., Hadaczek, P., Drummond, D.C., Guo, Z., Hong, K., Kirpotin, D.B., Marks, J.D., Berger, M., Park, J.W., 2003a. Immunoliposomes target EGFR-overexpressing brain and other tumors for efficient drug delivery and enhanced efficacy. Proc. Am. Soc. Clin. Oncol. 22, 206 (Abstract).

Mamot, C., Drummond, D.C., Greiser, U., Hong, K., Kirpotin, D.B., Marks, J.D., Park, J.W., 2003b. Epidermal growth factor receptor (EGFR)-targeted immunoliposomes mediate specific and efficient drug delivery to EGFR- and EGFRvIII-overexpressing tumor cells. Cancer Res. 63, 3154–3161.

Massing, U., Fuxius, S., 2000. Liposomal formulations of anticancer drugs: selectivity and effectiveness. Drug Resist. Update 3, 171–177.

Masuda, Y., Kobayashi, H., Holland, J.F., Ohnuma, T., 1998. Reversal of multidrug resistance by a liposome-MDR1 ribozyme complex. Cancer Chemother. Pharmacol. 42, 9–16.

Matsumura, Y., Maeda, H., 1986. A new concept for macromolecular therapeutics in cancer chemotherapy: mechanism of tumoritropic accumulation of proteins and the antitumor agent smancs. Cancer Res. 46, 6387–6392.

Matsuo, H., Wakasugi, M., Takanaga, H., Ohtani, H., Naito, M., Tsuruo, T., Sawada, Y., 2001. Possibility of the reversal of multidrug resistance and the avoidance of side effects by liposomes modified with MRK-16, a monoclonal antibody to P-glycoprotein. J. Control. Release 77, 77–86.

Matteucci, M.L., Anyarambhatla, G., Rosner, G., Azuma, C., Fisher, P.E., Dewhirst, M.W., Needham, D., Tirrell, D.E., 2000. Hyperthermia increases accumulation of technetium-99m-labeled liposomes in feline sarcomas. Clin. Cancer Res. 6, 3748–3755.

Merlin, J.L., Marchal, S., Ramacci, C., Notter, D., Vigneron, C., 1993. Antiproliferative activity of thermosensitive liposome-encapsulated doxorubicin combined with 43 degrees C hyperthermia in sensitive and multidrug-resistant MCF-7 cells. Eur. J. Cancer 29A, 2264–2268.

Michieli, M., Damiani, D., Ermacora, A., et al., 1999. Liposome-encapsulated daunorubicin for PGP-related multidrug resistance. Br. J. Haematol. 106, 92–99.

Mohrbacher, A.F., Gregory, S.A., Gabriel, D.A., Rusk, J.M., Giles, F.J., 2002. Liposomal daunorubicin (DaunoXome) plus dexamethasone for patients with multiple myeloma. A phase II International Oncology Study Group study. Cancer 94, 2645–2652.

Needham, D., Anyarambhatla, G., Kong, G., Dewhirst, M.W., 2000. A new temperature-sensitive liposome for use with mild hyperthermia: characterization and testing in a human tumor xenograft model. Cancer Res. 60, 1197–1201.

Northfelt, D.W., Dezube, B.J., Thommes, J.A., et al., 1997. Efficacy of pegylated-liposomal doxorubicin in the treatment of AIDS-related Kaposi's sarcoma after failure of standard chemotherapy. J. Clin. Oncol. 15, 653–659.

Oudard, S., Thierry, A., Jorgensen, T.J., Rahman, A., 1991. Sensitization of multidrug-resistant colon cancer cells to doxorubicin encapsulated in liposomes. Cancer Chemother. Pharmacol. 28, 259–265.

Park, J.W., 2002. Liposome-based drug delivery in breast cancer treatment. Breast Cancer Res. 4, 95–99.

Park, J.W., Hong, K., Carter, P., et al., 1995. Development of anti-p185HER2 immunoliposomes for cancer therapy. Proc. Natl. Acad. Sci. U.S.A. 92, 1327–1331.

Park, J.W., Hong, K., Kirpotin, D.B., Papahadjopoulos, D., Benz, C.C., 1997. Immunoliposomes for cancer treatment. Adv. Pharmacol. 40, 399–435.

Park, J.W., Stauffer, P., Diederich, C., Colbern, G., Lozner, A., Kirpotin, D.B., Rugo, H., Valente, N., Saeed, P., 2001. Hyperthermia (HT) + Doxil significantly enhances drug delivery and efficacy in metastatic breat cancer of the chest wall (CW): a phase I/II study. Proc. Am. Soc. Clin. Oncol. 20, 47a (Abstract).

Park, J.W., Hong, K., Kirpotin, D.B., et al., 2002. Anti-HER2 immunoliposomes: enhanced efficacy attributable to targeted delivery. Clin. Cancer Res. 8, 1172–1181.

Pedroso de Lima, M.C., Neves, S., Filipe, A., Duzgunes, N., Simoes, S., 2003. Cationic liposomes for gene delivery: from biophysics to biological applications. Curr. Med. Chem. 10, 1221–1231.

Perez-Soler, R., Yang, L.Y., Drewinko, B., Lauterzstain, J., Khokhar, A.R., 1988. Increased cytotoxicity and reversal of resistance to cis-diammine-dichloro-platinum(II) with entrapment of *cis*-bis-neodecamoto-*trans*-*R*,*R*-1,2-diaminocyclohexaneplatinum(II) in multilamellar lipid vesicles. Cancer Res. 48, 4509–4512.

Poste, G., Papahadjopoulos, D., 1976. Drug-containing lipid vesicles render drug-resistant cell sensitive to actinomycin D. Nature 261, 699–701.

Renes, J., de Vries, E.G., Jansen, P.L., Muller, M., 2000. The (patho)physiological functions of the MRP family. Drug Resist. Update 3, 289–302.

Rivera, E., Valero, V., Esteva, F.J., et al., 2002. Lack of activity of stealth liposomal doxorubicin in the treatment of patients with antiracycline-resistant breast cancer. Cancer Chemother. Pharmacol. 49, 299–302.

Romsicki, Y., Sharom, F.J., 1999. The membrane lipid environment modulates drug interactions with the P-glycoprotein multidrug transporter. Biochemistry 38, 6887–6896.

Sarris, A.H., Hagemeister, F., Romaguera, J., et al., 2000. Liposomal vincristine in relapsed non-Hodgkin's lymphomas: early results of an ongoing phase II trial. Ann. Oncol. 11, 69–72.

Siegal, T., Horowitz, A., Gabizon, A., 1995. Doxorubicin encapsulated in sterically stabilized liposomes for the treatment of a brain tumor model: biodistribution and therapeutic efficacy. J. Neurosurg. 83, 1029–1037.

Suzuki, S., Inoue, K., Hongoh, A., Hashimoto, Y., Yamazoe, Y., 1997. Modulation of doxorubicin resistance in a doxorubicin-resistant human leukaemia cell by an immunoliposome targeting transferring receptor. Br. J. Cancer 76, 83–89.

Thierry, A.R., Rahman, A., Dritschilo, A., 1993a. Overcoming multidrug resistance in human tumor cells using free and liposomally encapsulated antisense oligodeoxymucleotides. Biochem. Biophys. Res. Commun. 190, 952–960.

Thierry, A.R., Vige, D., Coughlin, S.S., Belli, J.A., Dritschilo, A., Rahman, A., 1993b. Modulation of doxorubicin resistance in multidrug-resistant cells by liposomes. FASEB J. 7, 572–579.

Treat, J., Damjanov, N., Huang, C., Zrada, S., Rahman, A., 2001. Liposomal-encapsulated chemotherapy: preliminary results of a phase I study of a novel liposomal paclitaxel. Oncology (Huntington) 15, 44–48.

van Helvoort, A., Smith, A.J., Sprong, H., Fritzsche, I., Schinkel, A.H., Borst, P., van Meer, G., 1996. MDR1 P-glycoprotein is a lipid translocase of broad specificity, while MDR3 P-glycoprotein specifically translocates phosphatidylcholine. Cell 87, 507–517.

West, K.A., Castillo, S., Dennis, P.A., 2002. Activation of the PI3K/Akt pathway and chemotherapeutic agents. Drug Resist. Update 5, 234–248.

Westphal, M., Hilt, D.C., Bortey, E., Delavault, P., Olivares, R., Warnke, P.C., Whittle, I.R., Jaaskelainen, J., Ram, Z., 2003. A phase 3 trial of local chemotherapy with biodegradable carmustine (BCNU) wafers (Gliadel wafers) in patients with primary malignant glioma. Neurooncology 5, 79–88.

Working, P.K., Dayan, A.D., 1996. Pharmacological-toxicological expert report. Caelyx (stealth liposomal doxorubicin HCl). Hum. Exp. Toxicol. 15, 751–785.

Zhou, R., Mazurchuk, R., Straubinger, R.M., 2002. Antivasculature effects of doxorubicin-containing liposomes in an intracranial rat brain tumor model. Cancer Res. 62, 2561–2566.

Zou, Y., Ling, Y.H., Van, N.T., Priebe, W., Perez-Soler, R., 1994. Antitumor activity of free and liposome-entrapped annamycin, a lipophilic anthracycline antibiotic with non-cross-resistance properties. Cancer Res. 54, 1479–1484.

Chemotherapy Administration Sequence: A Review of the Literature and Creation of a Sequencing Chart

Robert Mancini, PharmD; Jessie Modlin, PharmD

Background: Oncology pharmacists receive numerous questions regarding the sequence of chemotherapy administration. Several chemotherapy agents (eg, doxorubicin, docetaxel, paclitaxel, etc) are extensively metabolized through the cytochrome P450 pathway, and many chemotherapy agents (eg, taxanes, platinum agents) have high degrees of protein binding. In addition, many chemotherapy agents have cell cycle–specific mechanisms of action that may increase the cytotoxicity or antagonize the mechanism of the second agent. We conducted a literature search for data supporting same-day chemotherapy administration sequences. This was achieved by searching PubMed using keyword searches, including any combination of the drug name with "administration," "sequencing," or "interactions."

Results: The literature search yielded 110 articles for evaluation. The original 110 articles provided evidence for 62 potential chemotherapy combination sequences. Based on the types of studies examined, 27 potential sequences remained clinically undefined because of a lack of clinical relevance of the studies that supported them, 21 combinations were justified with a particular sequence, and 14 combinations had evidence that sequence was irrelevant to outcomes. From these data, a chemotherapy administration sequence chart was created as a reference for nurses and pharmacists.

Conclusion: From this literature search, we produced a chemotherapy sequencing chart that helps define recommended sequences of administration based on available published data. The sequence, if not clearly defined in the literature, should follow the sequence of administration published in that regimen's original study.

J Hematol Oncol Pharm. 2011;1(1):17-25.

In an effort to improve response rates to chemotherapy, agents often are combined to give a so-called two-prong attack against tumor cells. This is the basis for combining chemotherapy agents with different mechanisms of action. However, chemotherapy agents are subject to the rules of pharmacokinetics and thus have the potential for drug interactions. A common misconception is that because the agents have been tested as part of a chemotherapy regimen, they are safe and effective. The problem is that many phase 1 and 2 studies of a particular regimen do not give specifics about the order in which these agents were administered.

Several chemotherapy agents (eg, doxorubicin, docetaxel, paclitaxel, and others) are extensively metabolized through the cytochrome P450 pathway, and many chemotherapy agents (eg, taxanes and platinum agents) have high degrees of protein binding. In addition, many chemotherapy agents have cell cycle–specific mechanisms of action that may increase the cytotoxicity or antagonize the mechanism of the second agent.[1] In some situations, the order of administration may dictate whether a particular effect or side effect is encountered based on the principles of pharmacokinetics and pharmacodynamics. Perhaps the most well known is the interaction between cisplatin and paclitaxel.[2] When cisplatin precedes paclitaxel, profound and prolonged neutropenia may occur. This can delay the patient from receiving chemotherapy as prescribed. When the sequence is reversed (ie, paclitaxel before cisplatin), this detrimental side effect is diminished without negating efficacy.[2]

These concerns present real situations and lead to drug information questions that are often asked in a chemotherapy infusion center. Although there are extensive published data for some agents, like the taxanes, about drug interactions and sequencing, the data often can be hard to find, especially for less common or newer agents.[1-5] In addition, drug information resources extrapolate published data from single agents to all agents in the same class, recommending a sequence that

Dr Mancini and Dr Modlin are oncology pharmacists, St. Luke's Mountain States Tumor Institute, Boise, Idaho.

may not be proved clinically. An example is extrapolating the data on cisplatin and paclitaxel to imply the same interaction holds true between oxaliplatin and paclitaxel or carboplatin and docetaxel.

We conducted a thorough review of the literature to examine the data that have been published supporting same-day chemotherapy administration sequences. From these data, we created a chemotherapy administration sequence chart to aid nurses and pharmacists in identifying whether there is a preferred sequence to be used only for agents given on the same day. We then superimposed this chart on a chemotherapy compatibility chart to make a new tool for use in our infusion centers.

Methods

First, a list of all intravenous chemotherapy and monoclonal antibodies commonly used in combination regimens was created. Then, Micromedex Solutions' IV Index with Trissle's compatibility tool was used to assess whether medications were physically compatible via Y-site coinfusion. In addition, base solution compatibilities (lactated Ringers, normal saline, and dextrose 5% in water) for individual chemotherapy agents was evaluated. These steps were performed because they were easy to incorporate into the finalized chart, and it helped to combine existing compatibility charts with the sequencing chart into a single tool.

The combinations with defined sequences or where literature supported no difference in outcomes or toxicity were superimposed onto a compatibility chart for use by our infusion centers.

For the sequencing chart, the administration sequence of the original studies on published regimens was evaluated. Any chemotherapy agent that is not traditionally given on the same day as another agent was excluded from the chart. Lexi-Comp and Micromedex were evaluated, as standards for drug information resources, for recommended sequence specifics in the administration and drug interaction sections. Finally, a thorough PubMed search was conducted using keyword searches including any combination of the drug name with "administration," "sequencing," or "interactions."

After the literature base had been established, studies were evaluated to determine whether they were clinically applicable. Studies were included if they were conducted in humans and evaluated both the forward and reverse sequence of administration. Review articles were also considered if they provided human clinical trial data. All other studies were excluded. These exclusion criteria were selected because those types of studies could not be extrapolated to in vivo results in humans. Studies were also excluded for final evaluation if the agents were not administered on the same day. This exclusion criterion was defined to apply these sequences to how chemotherapy is administered for same-day treatments at an infusion center. If there were conflicting data on a sequence after all studies were evaluated as clinically relevant, recommendations were made to err on the side of safety. In other words, if one study suggested a particular sequence was more toxic and a second study suggested there was no difference, we recommended the sequence that was less toxic rather than stating there was no difference.

Results

The literature search, conducted in October 2009, yielded 110 articles for evaluation. Of those studies, 29 were excluded for testing in vitro sequence only; 11 were excluded as they included only mice; nine were excluded because they did not compare results with the reverse sequence; and four were excluded for other reasons. (Three had trends toward pharmacokinetic changes but did not assess the clinical relevance of these changes, and one used oral agents.) Fifty-seven evaluable articles remained, 44 of which were clinical trials and 13 were literature reviews, typically for a single class of agents.

The original 110 articles provided evidence for 62 potential chemotherapy combination sequences. Based on the types of studies examined, 27 potential sequences remained clinically undefined because of a lack of clinical relevance of the supporting studies (**Table 1**). This left 21 combinations with studies that justified a particular sequence (**Table 2, page 22**), and 14 combinations that provided evidence that sequence was irrelevant to outcomes (**Table 3, page 23**). The combinations with defined sequences or where literature supported no difference in outcomes or toxicity were superimposed onto a compatibility chart for use by our infusion centers (**Figure, pages 20-21**).

Discussion

The goal of this literature search was to create a user-friendly reference chart for pharmacists and nurses who work in outpatient infusion centers and on inpatient oncology floors. We have found that the chart we made has helped quickly define published literature for same-day administration. It must be stated, however, that this chart cannot be used for determining sequences of chemotherapy agents given over several days because that was not the original intent of the literature search.

The literature search revealed that recommendations provided in commonly used drug information resources

Table 1 Suggested Chemotherapy Sequences that Lack Clinical Support

Suggested sequence			
First agent	Second agent	Suggested reason	Reason for exclusion
5-Fluorouracil	Cisplatin	Maximum synergistic activity; less toxicity	In vitro only[6-8]; murine only[9-12]
5-Fluorouracil	Carboplatin	Less overall toxicity	In vitro and murine only[13]
Bleomycin	Paclitaxel	Synergistic effect	In vitro[14]
Dacarbazine	Gemcitabine	Less accumulation of dacarbazine toxic metabolites	Trend toward pharmacoknetic changes; no clinical relevance evaluated[15]
Docetaxel	5-Fluorouracil	Antagonistic in reverse sequence	Murine only[1]
Docetaxel	Oxaliplatin	Lessens neutropenia	No literature found, reference in Lexi-Comp extrapolated from other taxane/platinum combinations
Etoposide	Mitomycin	Antagonistic in reverse sequence	In vitro only[16]
Etoposide	Vincristine	Synergistic interaction, but not related to sequence	Murine[17]
Fludarabine	Cytarabine	Increases accumulation and augments metabolism of Ara-C in chronic lymphocytic leukemia cells leading to better efficacy	Primary analysis was in vitro; secondary analysis separated administration by >24 hours[18]
Gemcitabine	Doxorubicin	Synergistic effect (antagonistic in opposite)	In vitro only[19]
Gemcitabine	Epirubicin	Synergistic effect (antagonistic in opposite)	In vitro only[19]
Gemcitabine	Fluorouracil	Gemcitabine increases fluorouracil area under the curve twofold when fluorouracil given first	Only studied one sequence, not reverse[20]
Gemcitabine	Docetaxel	Synergistic effect (antagonistic in opposite)	Only studied one sequence, not reverse[21,22]; no effect seen, small trial[23]
Gemcitabine	Irinotecan	No sequence-related synergy, toxicity, or pharmacokinetic interactions in this sequence	Single sequence[6]
Gemcitabine	Oxaliplatin	No pharmacokinetic interaction when given 24 hours apart	Not same day (24-hour separation)[24]
Ifosfamide	Paclitaxel	Prevents profound cytopenias	Only studied one sequence, not reverse[25]
Irinotecan	Bevacizumab	Bevacizumab does not affect irinotecan pharmacokinetics in this sequence	Single sequence[26]
Irinotecan	Docetaxel	Significant myelosuppression with this combination, but not related to sequence	Single sequence[27]
Oxaliplatin	5-Fluorouracil	Synergistic effect (antagonistic in opposite)	In vitro[28]
Paclitaxel	Oxaliplatin	Lessens neutropenia; prevents decrease in oxaliplatin clearance	Murine only[29]; only studied one sequence, not reverse[30]
Paclitaxel	5-Fluorouracil	Antagonistic in reverse sequence	In vitro only[1,31]
Paclitaxel	Irinotecan	Less kinetic interactions; less hepatotoxicity	Trend toward pharmacokinetic changes, no clinical relevance evaluated[32]; sequence had no effect[33]
Pemetrexed	Docetaxel	Synergistic effect	In vitro only[34]
Pemetrexed	Paclitaxel	Synergistic effect	In vitro only[35]
Pralatrexate	Gemcitabine	Better therapeutic activity	In vitro and murine[36]
Topotecan	Etoposide	Synergistic effect	In vitro only[37]; oral etoposide used[38]
Vinorelbine	Gemcitabine	Antagonistic in reverse sequence	Single sequence[39]; pharmacokinetic only, no clinical relevance[40]

Figure Chemotherapy Sequencing Chart

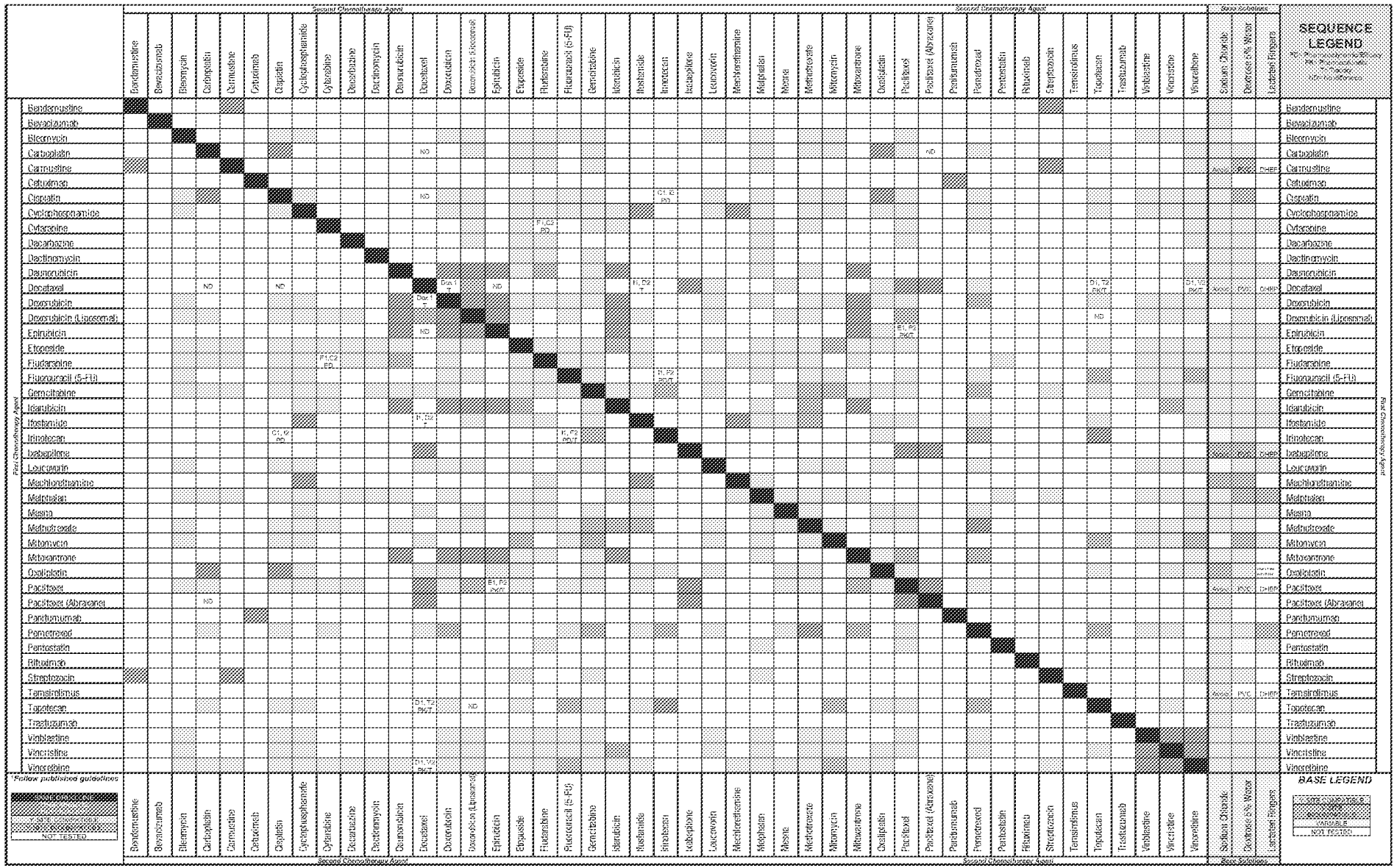

Table 2 Chemotherapy Combinations with Data to Support a Specific Sequence

Preferred sequence		
First agent	Second agent	Sequence benefit
5-Fluorouracil	Methotrexate	Better response and survival rates[41,42]
Cisplatin	Irinotecan	Better response rate; same toxicity[43-45]
Cyclophosphamide	Paclitaxel	Less cytopenias[2,46,47]
Docetaxel	Vinorelbine	Decreased neutropenia (proposed that polysorbate-80 in docetaxel blocks P-glycoprotein–mediated clearance of vinorelbine)[48,49]
Docetaxel	Topotecan	Decreased neutropenia. Reverse sequence causes a 50% reduction in docetaxel clearance[50,51]
Doxorubicin	Paclitaxel[a]	Prevents increased maximum concentration and decreased clearance of doxorubicin; decreases severity of bone marrow suppression and mucositis[2,4,5,52-54]
Doxorubicin	Docetaxel	Less grade 4 neutropenia[2,55]
Epirubicin	Paclitaxel[a]	Reverse sequence leads to increased maximum concentration and decreased clearance of epirubicin; decreases severity of bone marrow suppression and mucositis[2,5,56]
Fludarabine	Cytarabine	Enhances efficacy[57]
Gemcitabine	Cisplatin	Increases platinum-DNA adducts and lessens neutropenia; less toxic[6,58,59]
Ifosfamide	Docetaxel	Less myelosuppression[60,61]
Irinotecan	5-Fluorouracil	Additive efficacy; less diarrhea and neutropenia[6,62,63]
Leucovorin	5-Fluorouracil[a]	Stabilizes thymidylate synthase to increase 5-fluorouracil cytotoxicity and efficacy[64,65]
Liposomal doxorubicin	Docetaxel	Less dose reductions and better tolerance of full dose in this sequence[66]
Liposomal doxorubicin	Vinorelbine	Decreased neutropenia and avoidance of increased vinorelbine area under the curve[67,68]
Methotrexate	Leucovorin[a]	Leucovorin rescues cells after methotrexate administered to reduce toxicity; if leucovorin is given first, there is decreased efficacy of methotrexate[69-73]
Paclitaxel	Cisplatin[a]	Less neutropenia[74,75]
Paclitaxel	Gemcitabine	Synergy; less risk of hepatotoxicity[19,76,77]
Pemetrexed	Gemcitabine	Most efficacious; least toxic[78,79]
Topotecan	Carboplatin	Less risk of neutropenia and thrombocytopenia[80,81]
Topotecan	Cisplatin	Less risk of neutropenia and thrombocytopenia[82,83]

[a]Specific sequence recommended in Lexi-Comp Online.

were based on extrapolated data from drug classes but not studies directly comparing the two agents. An example of this is the taxanes and the platinum agents. We were unable to find any data that directly examine the recommended sequence of docetaxel before oxaliplatin. In addition, the sequence of paclitaxel before carboplatin has been extensively proved to be clinically irrelevant and yet this sequence remains recommended in drug information resources.[2,85-92] These unreferenced recommendations, as one example, could potentially delay treatment, because an oxaliplatin dose could be administered first while docetaxel, which takes longer to reconstitute, is prepared.

The literature search revealed that recommendations provided in commonly used drug information resources were based on extrapolated data from drug classes but not studies directly comparing the two agents.

We found examples throughout the literature indicating that certain studies may not allow extrapolation to a given sequence. A review by Vaishampayan and colleagues, for instance, demonstrates that in vitro studies cannot be applied in clinical practice. The authors evaluated preclinical and clinical data to show that synergy is not always beneficial.[2] When paclitaxel preceded doxorubicin in vitro, they found a threefold increase in cytotoxicity (a synergistic effect); in con-

trast, when this sequence was studied in humans, they found an increased frequency of mucositis, cardiotoxicity, and neutropenia. Synergistic antitumor activity does not necessarily, however, imply worse clinical toxicity. In a study by Zupi and colleagues, paclitaxel followed by gemcitabine was synergistic in vitro,[19] and a study by Poole and colleagues showed that this sequence had less hepatotoxicity and neutropenia than the reverse.[76]

In studies where a given sequence may have toxicity or efficacy issues, we were unable to conclude that the reverse sequence would resolve the issue. This was demonstrated in a review by Smorenburg and colleagues.[1] The authors examined data that suggested the sequence of methotrexate followed by docetaxel was antagonistic and thus had no efficacy, but the reverse sequence caused profound neutropenia, suggesting that this combination of agents should not be used in any sequence. Purely pharmacokinetic studies may not always be applied to their pharmacodynamic properties either. Combination studies of vinorelbine and gemcitabine are an example. In a pharmacokinetic study by Cattel and colleagues, there was an increase in gemcitabine area-under-the-curve and maximum concentration when vinorelbine was administered before gemcitabine.[40] The reverse sequence, gemcitabine followed by vinorelbine, was found to be inactive in vivo.[39]

The comprehensive literature review also revealed several important clinical practice issues that must be evaluated on a consistent basis. One of the common questions encountered by pharmacists in our chemotherapy infusion centers is, "What drug should be administered first?" Pharmacists must use their resources in a timely manner to find the answer—a challenging task given the abundance of literature and resources available. This review has shown that we need solid head-to-head evidence comparing two sequences before we can draw any conclusion. It may not always be the best option to try to extrapolate data from other studies. This includes generalizing data from one agent to the entire therapeutic class, extrapolating data from preclinical studies, or automatically reversing a sequence when the reverse sequence was not directly compared.

Conclusion

As this review has shown, there are several sequences that are well defined in the literature in terms of safety and efficacy. We can use these data, now in a more available format, to help answer some of the common questions regarding chemotherapy administration. At this point, the recommendation for sequence of administration of combination chemotherapy, if not clearly defined in the literature, should follow the sequence of administration published in that regimen's original study. Further clinical studies will be conducted in the future that continue to elucidate the optimal sequence for all combination agents. We hope to evaluate the efficacy of the chart we devised to see whether it has helped increase efficiency and improve workflow for the pharmacists and nurses at our institution. ■

Table 3 Chemotherapy Combinations with Sequence Having No Effect on Efficacy or Toxicity

Nanoparticle albumin-bound paclitaxel plus carboplatin[84]
Carboplatin plus paclitaxel[2,85-92]
Cisplatin plus 5-fluorouracil[93,94]
Docetaxel plus carboplatin[95,a]
Docetaxel plus cisplatin[2,96,97]
Docetaxel plus epirubicin[2-4,98,a]
Doxorubicin plus methotrexate/5-fluorouracil[99]
Etoposide plus topotecan[100]
Etoposide plus paclitaxel[101-103]
Gemcitabine plus carboplatin[104,105]
Gemcitabine plus docetaxel[106,107]
Gemcitabine plus irinotecan[6,108]
Irinotecan plus oxaliplatin[109]
Liposomal doxorubicin plus topotecan[110]

[a]Specific sequence recommended in Lexi-Comp Online.

Disclosure

Drs Mancini and Modlin did not report any potential financial conflicts of interest.

References

1. Smorenburg CH, Sparreboom A, Bontebal M, et al. Combination chemotherapy of the taxanes and antimetabolites: its use and limitations. *Eur J Cancer*. 2001;37:2310-2323.
2. Vaishampayan U, Parchment RE, Jasti BR, et al. Taxanes: an overview of the pharmacokinetics and pharmacodynamics. *Urology*. 1999;54(6A suppl):22-29.
3. Airoldi M, Cattel L, Pedani F, et al. Clinical and pharmacokinetic data of a docetaxel-epirubicin combination in metastatic breast cancer. *Breast Cancer Res Treat*. 2001;70:185-195.
4. Holmes FA, Madden T, Newman RA, et al. Sequence-dependent alteration of doxorubicin pharmacokinetics by paclitaxel in a phase I study of paclitaxel and doxorubicin in patients with metastatic breast cancer. *J Clin Oncol*. 1996;14:2713-2721.
5. Danesi R, Conte PF, Del Tacca M. Pharmacokinetic optimisation of treatment schedules for anthracyclines and paclitaxel in patients with cancer. *Clin Pharmacokinet*. 1999;37:195-211.
6. Goel A, Grossbard ML, Malamud S, et al. Pooled efficacy analysis from a phase I-II study of biweekly irinotecan in combination with gemcitabine, 5-fluorouracil, leucovorin and cisplatin in patients with metastatic pancreatic cancer. *Anticancer Drugs*. 2007;18:263-271.
7. Esaki T, Nakano S, Tatsumoto T, et al. Inhibition by 5-fluorouracil of cis-diammine-dichloroplatinum(II)-induced DNA interstrand cross-link removal in a HST-1 human squamous carcinoma cell line. *Cancer Res*. 1992;52:6501-6506.
8. Cho H, Imada T, Oshima T, et al. In-vitro effect of a combination of 5-fluorouracil (5-FU) and cisplatin (CDDP) on human gastric cancer cell lines: timing of cisplatin treatment. *Gastric Cancer*. 2002;5:43-46.
9. Yu NY, Patawaran MB, Chen JY, et al. Influence of treatment sequence on efficacy of fluorouracil and cisplatin intratumoral drug delivery in vivo. *Cancer J Sci Am*. 1995;1:215-221.

Continued

10. Kuroki M, Nakano S, Mitsugi K, et al. In vivo comparative therapeutic study of optimal administration of 5-fluorouracil and cisplatin using a newly established HST-1 human squamous-carcinoma cell line. *Cancer Chemother Pharmacol.* 1992;29:273-276.
11. Palmeri S, Tiave F, Russello O, et al. The role of drug sequence in therapeutic selectivity of the combination of 5-fluorouracil and cisplatin. *Sel Cancer Ther.* 1989;5:169-177.
12. Pratesi G, Gianni L, Manzotti C, et al. Sequence dependence of the antitumor and toxic effects of 5-fluorouracil and cis-diamminedichloroplatinum combination on primary colon tumors in mice. *Cancer Chemother Pharmacol.* 1988;21:237-240.
13. Saikawa Y, Kubota T, Kuo TH, et al. Combined effect of 5-fluorouracil and carboplatin against human gastric cancer cell lines in vitro and in vivo. *Anticancer Res.* 1994;14:461-464.
14. Waltmire CN, Alberts DS, Dorr RT. Sequence-dependent cytotoxicity of combination chemotherapy using paclitaxel, carboplatin and bleomycin in human lung and ovarian cancer. *Anticancer Drugs.* 2001;12:595-602.
15. Losa R, Fra J, Lopez-Pousa A, et al. Phase II study with the combination of gemcitabine and DTIC in patients with advanced soft tissue sarcomas. *Cancer Chemother Pharmacol.* 2007;59:251-259.
16. Seminara P, Pastore C, Iascone C, et al. Mitomycin C and etoposide in advanced colorectal carcinoma. A clinical and in vitro experience that focuses the problem of schedule dependence in combination therapy. *Chemotherapy.* 2007;53:218-225.
17. Jackson DV Jr, Long TR, Rice DG, et al. Combination vincristine and VP-16-213: evaluation of drug sequence. *Cancer Biochem Biophys.* 1986;8:265-275.
18. Gandhi V, Kemena A, Keating MJ, et al. Fludarabine infusion potentiates arabinosylcytosine metabolism in lymphocytes of patients with chronic lymphocytic leukemia. *Cancer Res.* 1992;52:897-903.
19. Zupi G, Scarsella M, D'Angelo C, et al. Potentiation of the antitumoral activity of gemcitabine and paclitaxel in combination on human breast cancer cells. *Cancer Biol Ther.* 2005;4:866-871.
20. Correale P, Cerretani D, Marsili S, et al. Gemcitabine increases systemic 5-fluorouracil exposure in advanced cancer patients. *Eur J Cancer.* 2003;39:1547-1551.
21. Dumez H, Louwerens M, Pawinsky A, et al. The impact of drug administration sequence and pharmacokinetic interaction in a phase I study of the combination of docetaxel and gemcitabine in patients with advanced solid tumors. *Anticancer Drugs.* 2002;13:583-593.
22. Leu KM, Ostruszka LJ, Shewach D, et al. Laboratory and clinical evidence of synergistic cytotoxicity of sequential treatment with gemcitabine followed by docetaxel in the treatment of sarcoma. *J Clin Oncol.* 2004;22:1706-1712.
23. Bhargava P, Marshall JL, Fried K, et al. Phase I and pharmacokinetic study of two sequences of gemcitabine and docetaxel administered weekly to patients with advanced cancer. *Cancer Chemother Pharmacol.* 2001;48:95-103.
24. Airoldi M, Cattel L, Passera R, et al. Gemcitabine and oxaliplatin in patients with pancreatic adenocarcinoma: clinical and pharmacokinetic data. *Pancreas.* 2006;32:44-50.
25. Forastiere AA, Urba SG. Single-agent paclitaxel and paclitaxel plus ifosfamide in the treatment of head and neck cancer. *Semin Oncol.* 1995;22(suppl 6):24-27.
26. Denlinger CS, Blanchard R, Xu L, et al. Pharmacokinetic analysis of irinotecan plus bevacizumab in patients with advanced solid tumors. *Cancer Chemother Pharmacol.* May 5, 2009. Epub ahead of print.
27. Adjei AA, Klein CE, Kastrissios H, et al. Phase I and pharmacokinetic study of irinotecan and docetaxel in patients with advanced solid tumors: preliminary evidence of clinical activity. *J Clin Oncol.* 2000;18:1116-1123.
28. Qin B, Tanaka R, Shibata Y, et al. In-vitro schedule-dependent interaction between oxaliplatin and 5-fluorouracil in human gastric cancer cell lines. *Anticancer Drugs.* 2006;17:445-453.
29. Liu J, Kraut EH, Balcerzak S, et al. Dosing sequence-dependent pharmacokinetic interaction of oxaliplatin with paclitaxel in the rat. *Cancer Chemother Pharmacol.* 2002;50:445-453.
30. Liu J, Kraut E, Bender J, et al. Pharmacokinetics of oxaliplatin (NSC 266046) alone and in combination with paclitaxel in cancer patients. *Cancer Chemother Pharmacol.* 2002;49:367-374.
31. Toiyama T, Tanaka K, Konishi N, et al. Administration sequence-dependent antitumor effects of paclitaxel and 5-fluorouracil in the human gastric cancer cell line MKN45. *Cancer Chemother Pharmacol.* 2006;57:368-375.
32. Horta K, Ueoka H, Kiura K, et al. A phase I study and pharmacokinetics of irinotecan (CPT-11) and paclitaxel in patients with advanced non-small cell lung cancer. *Lung Cancer.* 2004;45:77-84.
33. Murren JR, Peccerillo K, DiStasio SA, et al. Dose escalation and pharmacokinetic study of irinotecan in combination with paclitaxel in patients with advanced cancer. *Cancer Chemother Pharmacol.* 2000;46:43-50.
34. Kano Y, Tanaka M, Akutsu M, et al. Schedule-dependent synergism and antagonism between pemetrexed and docetaxel in human lung cancer cell lines in vitro. *Cancer Chemother Pharmacol.* 2009;64:1129-1137.
35. Kano Y, Akutsu M, Tsunoda S, et al. Schedule-dependent synergism and antagonism between pemetrexed and paclitaxel in human carcinoma cell lines in vitro. *Cancer Chemother Pharmacol.* 2004;54:505-513.
36. Toner LE, Vrhovac R, Smith EA, et al. The schedule-dependent effects of the novel antifolate pralatrexate and gemcitabine are superior to methotrexate and cytarabine in models of human non-Hodgkin's lymphoma. *Clin Cancer Res.* 2006;12:924-932.
37. Bonnet JA, Kozelsky TF. The significance of the sequence of administration of topotecan and etoposide. *Cancer Chemother Pharmacol.* 1996;39:109-112.
38. Miller AA, Niell HB. Phase I and pharmacologic study of sequential topotecan, carboplatin, and etoposide. *Lung Cancer.* 2001;33:241-248.
39. Juergens R, Brahmer J, Ettinger D. Gemcitabine and vinorelbine in recurrent advanced non-small cell lung cancer: sequence does matter. *Cancer Chemother Pharmacol.* 2007;59:621-629.
40. Cattel L, Airoldi M, Passera R, et al. Gemcitabine plus vinorelbine chemotherapy regimens: a pharmacokinetic study of alternate administration sequences. *Pharm World Sci.* 2004;26:238-241.
41. Mackintosh JR, Coates AS, Tattersall MH, et al. Chemotherapy of advanced head and neck cancer: updated results of a randomized trial of the order of administration of sequential methotrexate and 5-fluorouracil. *Med Pediatr Oncol.* 1988;16:304-307.
42. Coates AS, Tattersall MH, Swanson C, et al. Combination therapy with methotrexate and 5-fluorouracil: a prospective randomized clinical trial of order of administration. *J Clin Oncol.* 1984;2:756-761.
43. Han JY, Lim HS, Lee DH, et al. Randomized phase II study of two opposite administration sequences of irinotecan and cisplatin in patients with advanced non-small cell lung carcinoma. *Cancer.* 2006;106:873-880.
44. de Jonge MJ, Verweij J, de Bruijn P, et al. Pharmacokinetic, metabolic, and pharmacodynamic profiles in a dose-escalating study of irinotecan and cisplatin. *J Clin Oncol.* 2000;18:195-203.
45. de Jonge MJ, Verweij J, Planting AS, et al. Drug-administration sequence does not change pharmacodynamics and kinetics of irinotecan and cisplatin. *Clin Cancer Res.* 1999;5:2012-2017.
46. Kennedy MJ, Zahurak ML, Donehower RC, et al. Sequence-dependent hematologic toxicity associated with the 3-hour paclitaxel/cyclophosphamide doublet. *Clin Cancer Res.* 1998;4:349-356.
47. Kennedy MJ, Zahurak ML, Donehower RC, et al. Phase I and pharmacologic study of sequences of paclitaxel and cyclophosphamide supported by granulocyte colony-stimulating factor in women with previously treated metastatic breast cancer. *J Clin Oncol.* 1996;14:783-791.
48. Airoldi M, Cattell L, Marchionatti S, et al. Docetaxel and vinorelbine in recurrent head and neck cancer: pharmacokinetic and clinical results. *Am J Clin Oncol.* 2003;26:378-381.
49. Airoldi M, Cattel L, Pedani F, et al. Clinical data and pharmacokinetics of a docetaxel-vinorelbine combination in anthracycline resistant/relapsed metastatic breast cancer. *Acta Oncologica.* 2003;42:186-194.
50. Zamboni WC, Egorin MJ, Van Echo DA, et al. Pharmacokinetic and pharmacodynamic study of the combination of docetaxel and topotecan in patients with solid tumors. *J Clin Oncol.* 2000;18:3288-3294.
51. Posey JA, Wang H, Hamilton J, et al. Phase-I dose escalation and sequencing study of docetaxel and continuous infusion topotecan in patients with advanced malignancies. *Cancer Chemother Pharmacol.* 2005;56:182-188.
52. Frassineti GL, Zoli W, Tienghi A, et al. The sequential administration of combined doxorubicin and paclitaxel in the treatment of advanced breast cancer. *Semin Oncol.* 1996;23(suppl 12):22-28.
53. Gianni L, Munzone E, Capri G, et al. Paclitaxel by 3-hour infusion in combination with bolus doxorubicin in women with untreated metastatic breast cancer: high antitumor efficacy and cardiac effects in a dose-finding and sequence-finding study. *J Clin Oncol.* 1995;13:2688-2699.
54. Sledge GW Jr, Robert N, Sparano JA, et al. Eastern Cooperative Oncology Group studies of paclitaxel and doxorubicin in advanced breast cancer. *Semin Oncol.* 1995;22(suppl 6):105-108.
55. Itoh K, Sasak Y, Fujii H, et al. Study of dose escalation and sequence switching of administration of the combination of docetaxel and doxorubicin in advanced breast cancer. *Clin Cancer Res.* 2000;6:4082-4090.
56. Focan C, Graas MP, Beauduin M, et al. Sequential administration of epirubicin and paclitaxel for advanced breast cancer. A phase I randomized trial. *Anticancer Res.* 2005;25:1211-1217.
57. Pastore D, Specchia G, Carluccio P, et al. FLAG-IDA in the treatment of refractory/relapsed acute myeloid leukemia: single-center experience. *Ann Hematol.* 2003;82:231-235.
58. Kroep JR, Peters GJ, van Moorsel CJ, et al. Gemcitabine-cisplatin: a schedule finding study. *Ann Oncol.* 1999;10:1503-1510.
59. Van Moorsel CJA, Kroep JR, Pinedo HM, et al. Pharmacokinetic schedule finding study of the combination of gemcitabine and cisplatin in patients with solid tumors. *Ann Oncol.* 1999;10:444-448.
60. Hervonen P, Jekunen A, Lefebvre P, et al. Docetaxel-ifosfamide combination chemotherapy in patients with metastatic hormone-refractory prostate cancer: a phase I pharmacokinetic study. *Int J Clin Pharmacol Res.* 2003;23:1-7.

61. Schrijvers D, Pronk L, Highley M, et al. Pharmacokinetics of ifosfamide are changed by combination with docetaxel: results of a phase I pharmacologic study. *Am J Clin Oncol.* 2000;23:358-363.
62. Mans DR, Grivicich I, Peters GJ, et al. Sequence-dependent growth inhibition and DNA damage formation by the irinotecan-5-fluorouracil combination in human colon carcinoma cell lines. *Eur J Cancer.* 1999;35:1851-1861.
63. Falcone A, Di Paolo A, Masi G, et al. Sequence effect of irinotecan and fluorouracil treatment on pharmacokinetics and toxicity in chemotherapy-naïve metastatic colorectal cancer patients. *J Clin Oncol.* 2001;19:3456-3462.
64. Rustum YM, Cao S, Zhang Z. Rationale for treatment design: biochemical modulation of 5-fluorouracil by leucovorin. *Cancer J Sci Am.* 1998;4:12-18.
65. Jolivet J. Role of leucovorin dosing and administration schedule. *Eur J Cancer.* 1995;31A:1311-1315.
66. Fracasso PM, Rodriguez LC, Herzog TJ, et al. Phase I dose and sequencing study of pegylated liposomal doxorubicin and docetaxel in patients with advanced malignancies. *Cancer.* 2003;98:610-617.
67. Cattell L, Passera R, Katsaros D, et al. Pegylated liposomal doxorubicin and vinorelbine in recurrent ovarian carcinoma: a pharmacokinetic study on alternate administration sequences. *Anticancer Res.* 2006;26:745-750.
68. Katsaros D, Oletti MV, Rigault de la Longrais IA, et al. Clinical and pharmacokinetic phase II study of pegylated liposomal doxorubicin and vinorelbine in heavily pretreated recurrent ovarian carcinoma. *Ann Oncol.* 2005;16:300-306.
69. Ravelli A, Migliavacca D, Viola S, et al. Efficacy of folinic acid in reducing methotrexate toxicity in juvenile idiopathic arthritis. *Clin Exp Rheumatol.* 1999;17:625-627.
70. Ortiz Z, Shea B, Suarez-Almazor ME, et al. The efficacy of folic acid and folinic acid in reducing methotrexate gastrointestinal toxicity in rheumatoid arthritis. A metaanalysis of randomized controlled trials. *J Rheumatol.* 1998;25:36-43.
71. Alarcon GS, Morgan SL. Folinic acid to prevent side effects of methotrexate in juvenile rheumatoid arthritis. *J Rheumatol.* 1996;23:2184-2185.
72. Joyce DA, Will RK, Hoffman DM, et al. Exacerbation of rheumatoid arthritis in patients treated with methotrexate after administration of folinic acid. *Ann Rheum Dis.* 1991;50:913-914.
73. Morgan SL, Oster RA, Lee JY, et al. The effect of folic acid and folinic acid supplements on purine metabolism in methotrexate-treated rheumatoid arthritis. *Arthritis Rheum.* 2004;50:3104-3011.
74. Milross CG, Peters LJ, Hunter NR. Sequence-dependent antitumor activity of paclitaxel (Taxol) and cisplatin in vivo. *Int J Cancer.* 1995;62:599-604.
75. Rowinsky EK, Gilbert MR, McGuire WP, et al. Sequences of Taxol and cisplatin: a phase I and pharmacologic study. *J Clin Oncol.* 1991;9:1692-1703.
76. Poole CJ, Perren T, Gawande S, et al. Optimized sequence of drug administration and schedule leads to improved dose delivery for gemcitabine and paclitaxel in combination: a phase 1 trial in patients with recurrent ovarian cancer. *Int J Gynecol Cancer.* 2006;16:507-514.
77. Oliveras-Ferraros C, Vazquez-Martin A, Colomer R, et al. Sequence-dependent synergism and antagonism between paclitaxel and gemcitabine in breast cancer cells: the importance of scheduling. *Int J Oncol.* 2008;32:113-120.
78. Adjei AA. Clinical studies of pemetrexed and gemcitabine combinations. *Ann Oncol.* 2006;15(supp 5):v29-v32.
79. Ma CX, Nair S, Thomas S, et al. Randomized phase II trial of three schedules of pemetrexed and gemcitabine as front-line therapy for advanced non-small-cell lung cancer. *J Clin Oncol.* 2005;23:5929-5937.
80. Simpson AB, Calvert PM, Sludden JA, et al. Topotecan in combination with carboplatin: phase I trial evaluation of two treatment schedules. *Ann Oncol.* 2002; 13:399-402.
81. Boss DS, Siegel-Lakhai WS, van Egmond-Schoemaker NE, et al. Phase I pharmacokinetic and pharmacodynamic study of carboplatin and topotecan administered intravenously every 28 days to patients with malignant solid tumors. *Clin Cancer Res.* 2009;15:4475-4483.
82. Rowinsky EK, Kaufmann SH, Baker SD, et al. Sequences of topotecan and cisplatin: phase I, pharmacologic, and in vitro studies to examine sequence dependence. *J Clin Oncol.* 1996;14:3074-3084.
83. Raymond E, Burris HA, Rowinsky EK, et al. Phase I study of daily times five topotecan and single injection of cisplatin in patients with previously untreated non-small-cell lung carcinoma. *Ann Oncol.* 1997;8:1003-1008.
84. Stinchcombe TE, Socinski MA, Walko CM, et al. Phase I and pharmacokinetic trial of carboplatin and albumin-bound paclitaxel, ABI-007 (Abraxane) on three treatment schedules in patients with solid tumors. *Cancer Chemother Pharmacol.* 2007;60:759-766.
85. DiPaola RS, Rubin E, Toppmeyer D, et al. Gemcitabine combined with sequential paclitaxel and carboplatin in patients with urothelial cancers and other advanced malignancies. *Med Sci Monit.* 2003;9:PI5-PI11.
86. Van Warmerdam LJ, Huizing MT, Giaccone G, et al. Clinical pharmacology of carboplatin administered in combination with paclitaxel. *Semin Oncol.* 1997;24 (suppl 2):97-104.
87. Huizing MT, Giaccone G, van Warmerdam LJ, et al. Pharmacokinetics of paclitaxel and carboplatin in a dose-escalating and dose-sequencing study in patients with non-small-cell lung cancer. The European Cancer Centre. *J Clin Oncol.* 1997;15:317-329.
88. Giaccone G, Huizing M, Postmus PE, et al. Dose-finding and sequencing study of paclitaxel and carboplatin in non-small cell lung cancer. *Semin Oncol.* 1995;22(suppl 9):78-82.
89. Perez EA, Hartmann LC. Paclitaxel and carboplatin for advanced breast cancer. *Semin Oncol.* 1996;23(suppl 11):41-45.
90. Obasaju CK, Johnson SW, Rogatko A, et al. Evaluation of carboplatin pharmacokinetics in the absence and presence of paclitaxel. *Clin Cancer Res.* 1996;2:549-552.
91. Belani CP, Kearns CM, Zuhowski EG, et al. Phase I trial, including pharmacokinetic and pharmacodynamic correlations, of combination paclitaxel and carboplatin in patients with metastatic non-small-cell lung cancer. *J Clin Oncol.* 1999;17:676-684.
92. Markman M, Elson P, Kulp B, et al. Carboplatin plus paclitaxel combination chemotherapy: impact of sequence of drug administration on treatment-induced neutropenia. *Gynecol Oncol.* 2003;91:118-122.
93. Koizumi W, Kurihara M, Hasegawa K, et al. Sequence-dependence of cisplatin and 5-fluorouracil in advanced and recurrent gastric cancer. *Oncol Rep.* 2004; 12:557-561.
94. Falcone A, Allegrini G, Masi G, et al. 5-Fluorouracil administered as a 48-hour chronomodulated infusion in combination with leucovorin and cisplatin: a randomized phase II study in metastatic colorectal cancer. *Oncology.* 2001;61:28-35.
95. Ando M, Saka H, Ando Y, et al. Sequence effect of docetaxel and carboplatin on toxicity, tumor response and pharmacokinetics in non-small-cell lung cancer patients: a phase I study of two sequences. *Cancer Chemother Pharmacol.* 2005; 55:552-558.
96. Pronk LC, Schellens JH, Planting AS, et al. Phase I and pharmacologic study of docetaxel and cisplatin in patients with advanced solid tumors. *J Clin Oncol.* 1997;15:1071-1079.
97. Royer I, Monsarrat B, Sonnier M, et al. Metabolism of docetaxel by human cytochromes P450: interactions with paclitaxel and other antineoplastic drugs. *Cancer Res.* 1996;56:58-65.
98. Lunardi G, Venturini M, Vannozzi MO, et al. Influence of alternate sequences of epirubicin and docetaxel on the pharmacokinetic behaviour of both drugs in advanced breast cancer. *Ann Oncol.* 2002;13:280-285.
99. Westermann AM, Taal BG, Swart M, et al. Sequence-dependent toxicity profile in modified FAMTX (fluorouracil-adriamycin-methotrexate) chemotherapy with lenograstim support for advanced gastric cancer: a feasibility study. *Pharmacol Res.* 2000;42:151-156.
100. Huisman C, Postmus PE, Giaccone G, et al. A phase I study of sequential intravenous topotecan and etoposide in lung cancer patients. *Ann Oncol.* 2001;12:1567-1573.
101. Rosell R, Felip E, Massuti B, et al. A sequence-dependent paclitaxel/etoposide phase II trial in patients with non-small cell lung cancer. *Semin Oncol.* 1997;24(suppl 12):56-60.
102. Fleming GF, Roth BJ, Baker SD, et al. Phase I trial of paclitaxel and etoposide for recurrent ovarian carcinoma: a Gynecologic Oncology Group Study. *Am J Clin Oncol.* 2000;23:609-613.
103. Felip E, Massuti B, Camps C, et al. Superiority of sequential versus concurrent administration of paclitaxel with etoposide in advanced non-small cell lung cancer: comparison of two phase II trials. *Clin Cancer Res.* 1998;4:2723-2728.
104. Edelman MJ, Quam H, Mullins B. Interactions of gemcitabine, carboplatin and paclitaxel in molecularly defined non-small-cell lung cancer cell lines. *Cancer Chemother Pharmacol.* 2001;48:141-144.
105. Langer CJ, Calvert P, Ozols RF. Gemcitabine and carboplatin in combination: phase I and phase II studies. *Semin Oncol.* 1998;25(suppl 9):51-54.
106. Harita S, Watanabe Y, Kiura K, et al. Influence of altering administration sequence of docetaxel, gemcitabine and cisplatin in patients with advanced non-small cell lung cancer. *Anticancer Res.* 2006;26:1637-1641.
107. Rizvi NA, Spiridonidis CH, Davis TH, et al. Docetaxel and gemcitabine combinations in non-small cell lung cancer. *Semin Oncol.* 1999;26(suppl 16):27-31, 41-42.
108. Ramnath N, Yu J, Khushalani NI, et al. Scheduled administration of low dose irinotecan before gemcitabine in the second line therapy of non-small cell lung cancer: a phase II study. *Anticancer Drugs.* 2008;19:749-752.
109. Gil-Delgado MA, Bastian G, Guinet F, et al. Oxaliplatin plus irinotecan and FU-FOL combination and pharmacokinetic analysis in advanced colorectal cancer patients. *Am J Clin Oncol.* 2004;27:294-298.
110. Dupont J, Aghajanian C, Andrea G, et al. Topotecan and liposomal doxorubicin in recurrent ovarian cancer: is sequence important? *Int J Gynecol Cancer.* 2006;16(suppl 1):68-73.

Annals of Oncology 23: 2812–2820, 2012
doi:10.1093/annonc/mds134
Published online 5 July 2012

VEGF remains an interesting target in advanced pancreas cancer (APCA): results of a multi-institutional phase II study of bevacizumab, gemcitabine, and infusional 5-fluorouracil in patients with APCA

L. K. Martin[1], X. Li[2], B. Kielber[3], E. C. Ellison[4], M. Bloomston[5], M. Zalupski[6] & T. S. Bekali-Saab[1*]

[1]*Department of Internal Medicine, Division of Medical Oncology, The Ohio State University Comprehensive Cancer Center, Columbus;* [2]*Center for Biostatistics, The Ohio State University, Columbus;* [3]*Comprehensive Cancer Center, The Ohio State University, Columbus;* [4]*Department of Surgery, Division of General Surgery, The Ohio State University Medical Center, Columbus;* [5]*Department of Surgery, Division of Surgical Oncology, The Ohio State University Comprehensive Cancer Center, Columbus;* [6]*Department of Internal Medicine, Division of Hematology-Oncology, University of Michigan Comprehensive Cancer Center, Ann Arbor, USA*

Received 13 January 2012; revised 6 April 2012; accepted 10 April 2012

Background: We investigated the safety and efficacy of bevacizumab combined with gemcitabine followed by infusional 5-fluorouracil (5-FU) in patients with advanced pancreas cancer (APCA).

Design: Patients with untreated APCA received bevacizumab 10 mg/kg, gemcitabine 1000 mg/m^2 over 100 min, and 5-FU 2400 mg/m^2 over 48 h on days 1 and 15 of each 28-day cycle. The primary end point was the proportion of patients with progression-free survival (PFS) at 6 months from initiation of therapy. If PFS at 6 months was ≥41%, the regimen would be considered promising.

Results: Forty-two patients were enrolled in the study; of which, 39 were evaluable for primary end point. PFS at 6 months was 49% (95% CI 34% to 64%). Median PFS was 5.9 months (95% CI 3.5 to 8.1) and median overall survival (OS) was 7.4 months (95% CI 4.7 to 11.2). Partial response and stable disease occurred in 30% and 45% of patients, respectively. Treatment-related hypertension and normal baseline albumin correlated with an improved response rate, PFS and OS. Grade 3 to 4 toxicities included fatigue (14%), hypertension (5%), and venous thrombosis (5%).

Conclusions: The study met its primary end point. Further investigation of anti-VEGF therapy in combination with fluoropyrimidine-based therapy is warranted in APCA. Treatment-related hypertension and normal baseline albumin may predict for the efficacy of bevacizumab and should be investigated in prospective studies.

Key words: bevacizumab, 5-fluorouracil, gemcitabine, pancreas cancer, VEGF

introduction

Pancreas cancer (PCA) is the fourth leading cause of cancer death in the United States [1]. Prognosis remains dismal, with a 5-year survival of <5% for all stages [2]. Surgical resection followed by adjuvant therapy offers the only chance for cure; however, <15% of patients present with resectable disease [3]. Cytotoxic chemotherapy with gemcitabine has been the standard of care and the backbone of experimental regimens in advanced pancreas cancer (APCA) for over a decade based on a modest clinical benefit over bolus 5-fluorouracil (5-FU) [4]. Since the late 1990s, minimal progress has been made to improve survival for these patients with gemcitabine-based combination regimens [5–12]. Recently published phase III data show a significant survival benefit for the combination of 5-FU, oxaliplatin, and irinotecan (FOLFIRINOX) over gemcitabine in patients with untreated metastatic pancreas cancer [13]; however, because of the significant toxicity associated with FOLFIRINOX, the regimen is only appropriate for a select subset of patients. The chemoresistance of pancreas cancer has led to a continuing search for new therapeutic targets.

Vascular endothelial growth factor (VEGF) is a pro-angiogenic growth factor implicated in the pathogenesis of many cancers [14, 15]. In PCA, VEGF promotes tumor growth, invasion, and metastases via activation of the MAPK pathway [16], and also functions as an autocrine growth factor for PCA cells [17, 18]. Overexpression of VEGF and its receptors occurs in >90% of PCA and correlates with poor prognosis [19–23]. Preclinical data suggest that inhibition of VEGF attenuates PCA growth and metastasis [24–26]. Thus, VEGF represents an attractive therapeutic target in human PCA.

Bevacizumab (Avastin®, Roche/Genentech, Inc., South San Francisco, USA) is a recombinant humanized monoclonal

Correspondence to: Dr. T. Bekali-Saab, Department of Internal Medicine, Division of Medical Oncology, The Ohio State University Comprehensive Cancer Center, A454 Starling Loving Hall, 320 West 10th Avenue, Columbus, USA. Tel: +1-11-1-614-293-9863; Fax: +1-11-1-614-293-7529; E-mail: tanios.bekali-saab@osumc.edu

antibody that binds VEGF-A, blocking its interaction with its receptors. Bevacizumab improves outcomes in combination with chemotherapy in a number of advanced malignancies [27–32], however, its role in APCA remains controversial, and current recommendations for its use do not extend outside the investigational setting [33]. Preclinical data and promising results from early clinical studies [24, 25, 34–36] suggested investigation of antiangiogenic therapies in APCA. While phase III studies adding bevacizumab to gemcitabine [37] or gemcitabine and erlotinib [38] failed to confirm an overall survival (OS) benefit in APCA, bevacizumab improved PFS when added to gemcitabine and erlotinib [38]. Correlative work from this trial [39] suggested that pretreatment plasma levels of VEGFA and VEGFR2 may emerge as important predictive biomarkers to identify patients who are most likely to benefit from antiangiogenic therapy. These data suggest that VEGF may remain a valid target in appropriately selected patients with APCA.

Preliminary clinical evidence suggested that gemcitabine given at a fixed dose rate (FDR) of 10 mg/m^2/min had an advantage over standard gemcitabine in patients with APCA [40]. The results of a follow-up three-arm phase III trial reported only a trend toward a survival benefit for FDR gemcitabine over standard gemcitabine, however that study was possibly underpowered [11]. 5-FU has single-agent activity in PCA [41] and phase III data suggest that 5-FU and gemcitabine are equivalent in the adjuvant setting [42]. Of greater interest, gemcitabine has been shown to act as a potential biomodulator of 5-FU activity [43]. Preclinical studies confirm that the sequential administration of prolonged infusion of gemcitabine followed by 5-FU exposure for 24 h results in significant synergistic antitumor activity in cancer cell lines [44]. In early clinical trials of patients with advanced gastrointestinal and genitourinary cancers [45, 46], the combination of prolonged-infusion gemcitabine followed by a fluoropyrimidine showed promising clinical activity. Finally, 5-FU has known clinical synergy with bevacizumab in colon cancer [29–31, 48] and administration of 5-FU as a continuous infusion improves survival and response rate over bolus administration [48].

Based on these observations, we designed a phase II study to investigate the efficacy and safety of the combination of bevacizumab combined with FDR gemcitabine followed by infusional 5-FU over 48 h in patients with untreated APCA.

patients and methods

patient eligibility

Eligible patients were required to have biopsy-proven stage III or IV pancreatic adenocarcinoma with measurable disease by RECIST 1.0 [50], Eastern Cooperative Oncology Group (ECOG) performance status 0–1, no prior treatment for metastatic disease, and adequate bone marrow (neutrophils >1500/μl, hemoglobin >9 g/dl, platelets >100 000/μl), kidney [creatinine < 1.5 × upper limit of normal (ULN)], and liver (bilirubin ≤ ULN, AST/ALT ≤ 1.5 × ULN or ≤ 3 × ULN with liver metastases) function. Prior adjuvant chemotherapy (including gemcitabine) was allowed, provided that >4 weeks had elapsed since the end of therapy. Exclusion criteria included prior treatment with VEGF inhibitors, brain metastases, congestive heart failure requiring active therapy, myocardial infarction or stroke within the past 6 months, bleeding diathesis, uncontrolled hypertension or diabetes mellitus, and proteinuria. All patients provided written informed consent before study enrollment.

treatment plan

This was a multicenter phase II study including the Ohio State University and University of Michigan. Patients received bevacizumab followed by gemcitabine then 5-FU on days 1 and 15 of each 28-day cycle. Bevacizumab was administered intravenously at a dose of 10 mg/kg over 30 min. Gemcitabine was administered intravenously at a dose of 1000 mg/m^2 over 100 min (FDR, 10 mg/m^2/min). 5-FU was given as a continuous 48-h intravenous infusion at a dose of 2400 mg/m^2. Treatment was continued until disease progression, intolerable toxicity, intercurrent illness or death preventing further treatment, or patient withdrawal of consent.

dose delays and modifications

Patients were required to have neutrophils ≥1500/μl, platelets ≥100 000/μl, and all other treatment-related toxicity resolved to grade ≤1 in order to begin a treatment cycle. Dose reductions of gemcitabine were corrected to preserve the FDR. Gemcitabine was reduced to 75% of the original dose for grade 3 or 4 thrombocytopenia, febrile neutropenia (grade 4 neutropenia and ≥grade 2 fever), and grade 3 or 4 nonhematologic toxicity, excluding nausea and vomiting controlled with supportive measures. 5-FU was reduced to 75% of the original dose for febrile neutropenia, grade 3 palmar-plantar erythrodysesthesia (hand and foot syndrome), and any grade 3 or 4 nonhematologic toxicity, excluding nausea and vomiting controlled with supportive measures. There were no recommended dose reductions for bevacizumab. If adverse events occurred that required bevacizumab to be held, the dose remained the same once treatment resumed. Bevacizumab was discontinued and patients were removed from study for grade IV hypertension, venous thrombosis, or hemorrhage, arterial thrombosis of any grade, gastrointestinal perforation, wound dehiscence requiring medical or surgical intervention, recurrent toxicities despite dose modifications, or any toxicity felt by the investigator to prohibit safe continuation of therapy.

assessment of toxicity and response

Adverse events were graded according to the NCI-CTCAE v 3.0. Pretreatment assessment included baseline history and physical, complete blood count, serum chemistry including liver functions, urine protein/creatinine ratio, serum βhCG, EKG, and CA 19-9 level. These assessments (excluding EKG) were repeated on day 1 of each subsequent cycle along with toxicity assessment. On day 15 of every cycle, patients had physical examination, toxicity assessment, complete blood count, and serum chemistries. Radiographic assessment of response was carried out at baseline and every 8 weeks using the same imaging modality [computed tomography (CT) or magnetic resonance imaging (MRI)] used to establish baseline tumor measurements. Responses were measured according to RECIST 1.0 [49]. Hypertension was assessed by blood pressure measurement on days 1 and 15 of each cycle. Baseline albumin was measured before initiation of treatment, and subsequent measurements were obtained on days 1 and 15 of each treatment cycle.

statistical methods

The primary end point was the percentage of patients free from disease progression or death at 6 months (24 weeks) from initiation of therapy. Secondary endpoints include overall response rate (ORR) as defined by RECIST 1.0 [49], 6-month and 1-year survival rates, OS, and the frequency and severity of treatment-associated adverse events. Using a Fleming

single-stage phase II study design, we planned to enroll 39 evaluable patients to determine whether the true 24-week PFS rate was 0.30 or less versus 0.50 or more [$\alpha = 0.10$; $\beta = 0.10$]. Patients were considered nonevaluable for the primary end point if they died from nontreatment related or nondisease related cause before the 6-month assessment period, or if they were removed from the study for treatment-related toxicity with <6 months of follow-up. If at least 16 evaluable patients (41%) were progression-free at 6 months, the regimen will be recommended for further study. *Post hoc* subgroup analyses included patients with and without treatment-related hypertension of any CTCAE grade, and patients with normal (≥3.4 g/dl) and low (<3.4 g/dl) baseline albumin. OS, PFS, and ORR were compared between the subgroups. Survival curves were estimated using the Kaplan–Meier method, and 95% confidence intervals for the medians were provided. The group difference in survival was assessed with the log-rank test. Response rates were compared using Fisher's exact test. For all but the primary endpoints, data were analyzed based on the intention-to-treat principle.

results

patient characteristics (Table 1)

Patient characteristics are detailed in Table 1. Forty-two patients (23 F, 19 M) with a median age 60 (range 36 to 79) and ECOG performance status of zero or one were enrolled between January 2007 and October 2008. Two patients (5%) had stage III disease and 40 patients (95%) had stage IV disease. The most common site of metastatic disease was the liver (75%). Two patients had recurrent metastatic disease after prior surgical resection and adjuvant therapy. Most patients (86%) had elevated baseline CA19-9 levels (>37 U/ml). Sixty-seven percent of patients had normal baseline albumin (≥3.4 g/dl) and 33% of patients had low albumin (<3.4 g/dl) before initiation of treatment.

Of the 42 patients enrolled, 39 were evaluable for the primary end point. Two patients were removed as pre-specified from study, before reaching the 6-month assessment point, due to treatment-related toxicity. Of note, both these patients had stable disease and CA19-9 declines of >25% at the time of removal from study. The third patient was removed from study due to noncompliance unrelated to toxicity. Forty patients were assessable for response. All 42 patients were evaluable for survival and toxicity analyses.

Table 1. Patient characteristics ($N = 42$)

Characteristic	N (%)
Sex	
Male	19 (45)
Female	23 (55)
Age (years)	
Median	60
Range	36 to 79
Race/ethnicity	
Caucasian	37 (88)
African American	3 (7)
Other	2 (5)
ECOG performance status	
0	15 (36)
1	27 (64)
Prior adjuvant therapy	2 (5)
Gemcitabine-based[a]	1 (50)
Chemoradiation[b]	1 (50)
Disease stage	
III	2 (5)
IV	40 (95)
Site of metastasis ($N = 40$)	
Liver only	29 (73)
Liver + other	2 (5)
Other only	9 (23)
CA19-9	
Normal (≤37 U/ml)	6 (14)
Elevated (>37 U/ml)	36 (86)
Albumin	
Normal (≥3.4 g/dl)	28 (67)
Low (<3.4 g/dl)	14 (33)

[a]Patients developed recurrence/metastases while on a clinical trial of gemcitabine ± *Saccharomyces cerevisiae* vaccine.

[b]Patients were treated on a clinical trial of 5-FU, cisplatin, interferon-α, and radiation.

toxicity (Table 2)

Toxic effects are outlined in Table 2. The most frequent treatment-related toxicities were vomiting (69%), anemia (66%), fatigue (61%), and nausea (59%). Chemotherapy-related grade 3–4 toxicities were uncommon and included fatigue (14%), vomiting (5%), lymphopenia (5%), nausea (2%), anemia (2%), thrombocytopenia (2%), and ALT elevation (2%). Grade 3 toxicities attributed to bevacizumab were rare and included

Table 2. Toxic effects observed according to the National Cancer Institute Common Toxicity Criteria Version 3.0[a] ($N = 42$)

	Grade 1 N (%)	Grade 2 N (%)	Grade 3 N (%)	Grade 4 N (%)
Hematologic				
Anemia	19 (45)	8 (19)	0 (0)	1 (2)
Thrombocytopenia	11 (26)	1 (2)	1 (2)	0 (0)
Leukopenia	8 (19)	3 (7)	0 (0)	0 (0)
Neutropenia	4 (10)	2 (5)	0 (0)	0 (0)
Lymphopenia	4 (10)	2 (5)	2 (5)	0 (0)
Non-hematologic				
Fatigue	6 (14)	14 (33)	6 (14)	0 (0)
Vomiting	23 (55)	8 (19)	2 (5)	0 (0)
Nausea	19 (45)	5 (12)	1 (2)	0 (0)
Diarrhea	13 (33)	3 (7)	0 (0)	0 (0)
Elevated ALT	5 (12)	1 (2)	1 (2)	0 (0)
Elevated AST	6 (14)	0 (0)	0 (0)	0 (0)
Mucositis	6 (14)	3 (7)	0 (0)	0 (0)
Altered sense of taste	11 (26)	1 (2)	0 (0)	0 (0)
Hypertension	5 (12)	1 (2)	2 (5)	0 (0)
Fistula formation	0 (0)	0 (0)	1 (2)	0 (0)
Proteinuria	3 (7)	1 (2)	0 (0)	0 (0)
Bleeding	4 (10)	2 (5)	1 (2)	0 (0)
Thrombosis	0 (0)	0 (0)	2 (5)	0 (0)
Headache	5 (12)	0 (0)	0 (0)	0 (0)
Rash	2 (5)	3 (7)	0 (0)	0 (0)
Peripheral sensory neuropathy	5 (12)	1 (2)	0 (0)	0 (0)

[a]Maximum grade per patient.

venous thrombotic events (5%), hypertension (5%), epistaxis (2%), and fistula formation (2%). Only one patient experienced grade 4 toxicity (anemia) and there were no treatment-related deaths. Hypertension was observed in eight patients (19%). Fifteen patients (38%) required treatment delay or dose reduction. Bevacizumab was discontinued in one patient due to progressive renal insufficiency and treatment-related grade 2 proteinuria (urine protein:creatinine ratio 3.4) in the setting of underlying chronic renal insufficiency. Three patients were removed from the study as pre-specified due to treatment-related toxicity including grade 3 venous thrombosis ($n = 2$) and persistent grade 2 thrombocytopenia ($n = 1$).

efficacy (Table 3 and Figure 1A)

Treatment efficacy data are summarized in Table 3. Final data analysis is conducted 4 years from enrollment of the first patient. At the time of the final analysis, 3 patients are still alive and 39 patients have died. Freedom from progression is demonstrated in 19 of 39 patients (49%) at 24 weeks (95% CI 34–64%); therefore, the primary end point of the study is met. Partial response (PR) and stable disease (SD) are seen in 30% and 45% of patients, respectively, with a disease control rate (PR + SD) of 75%. Kaplan–Meier survival curves are provided in Figure 1. Median PFS is 5.9 months (95% CI 3.5 to 8.1) and median OS is 7.4 months (95% CI 4.7 to 11.2). Six-month and 1-year survival were 60 and 36%, respectively. Thirty-six patients (86%) had elevated CA 19-9 levels before therapy. Fifty-nine percent of those patients experienced >25% maximum reduction of CA 19-9 levels, and 54% experienced >50% reduction.

potential predictors of clinical outcome (Table 3 and Figure 1B and C)

Data regarding the relationship between hypertension ($N = 8$), baseline albumin levels and clinical outcomes (ORR, PFS, and OS) are presented in Table 3. Patients with treatment-related hypertension had significantly improved ORR (63 versus 22%; $P = 0.0386$), and mOS (12 versus 6.1 months, $P = 0.0166$) and improved PFS (7.6 versus 4.9 months, $P = 0.38$) that did not reach statistical significance, compared with patients who did not experience treatment-related hypertension. Patients with normal baseline albumin (≥3.4 g/dl, $N = 28$) at study entry had trend toward improvement in ORR (36 versus 17%, $P = 0.2848$), and significantly prolonged mPFS (7.7 versus 2.7 months, $P = 0.0124$) and mOS (11.7 versus 3.2 months, $P = 0.0017$) compared with patients with low baseline albumin (<3.4 g/dl, $N = 14$) (Figure 1B and C).

discussion

The prognosis of PCA remains poor with little progress made in the last few decades. In the last decade, phase III studies of gemcitabine in combination with other cytotoxics have yielded no improvement in survival [5–9, 11, 50–53]. This has led to investigation of biologic targets including anti-VEGF therapy.

We evaluated a rational combination of bevacizumab combined with FDR gemcitabine followed by infusional 5-FU in PCA. The choice of the combination and its schedule focuses on the biomodulation of infusional 5-FU by a prolonged infusion of gemcitabine and the known synergism between 5-FU and bevacizumab [29–31, 47]. In our study, we observed interesting clinical efficacy and reached the primary study end point with 49% of patients being free of disease progression at 24 weeks. The combination was well tolerated with expected and manageable toxicity. Our observed objective response rate, 1-year survival, OS and progression-free survival (PFS) are interesting compared with historical controls in advanced PCA [5–12, 36–38, 50–55]. Confirming the observed

Table 3. Treatment efficacy

Variable	N (%)
PFS at 6 months[a]	19 (49) (95% CI 34 to 64)
Response[b]	
CR	0 (0)
PR	12 (30)
SD	18 (45)
PD	10 (25)
Albumin[c] ≥3.4 g/dl	10 (36)[d]
Albumin <3.4 g/dl	2 (17)[e]
P value	0.2848
Hypertension[f]	5 (63)[g]
No hypertension	7 (22)[h]
P value	0.0386
CA 19-9 maximum reduction[i]	
>25%	23 (59)
>50%	21 (54)
Median PFS (months)[j]	5.9 (95% CI 3.5–8.1)
Albumin[c] ≥3.4 g/dl	7.7
Albumin <3.4 g/dl	2.7
P value	0.0124
Hypertension[f]	7.6
No hypertension	4.9
P value	0.38
Median OS (months)[j]	7.4 (95% CI 4.7–11.2)
Albumin[c] ≥3.4 g/dl	11.7
Albumin <3.4 g/dl	3.2
P value	0.0017
Hypertension[f]	12
No hypertension	6
P value	0.0166
6 month survival[k]	60%
1-year survival[k]	36%

[a]39 patients were considered evaluable.
[b]40 patients were considered evaluable.
[c]Baseline albumin before treatment.
[d]Objective response rate based on 28 evaluable patients with albumin ≥3.4 g/dl.
[e]Objective response rate based on 12 patients with albumin <3.4 g/dl.
[f]Grade ≥1 treatment-related hypertension as defined and graded according to CTCAE v 3.0.
[g]Objective response rate based on eight evaluable patients with hypertension.
[h]Objective response rate based on 32 evaluable patients without hypertension.
[i]36 patients (86%) had baseline elevated CA 19-9.
[j]42 patients were considered evaluable.

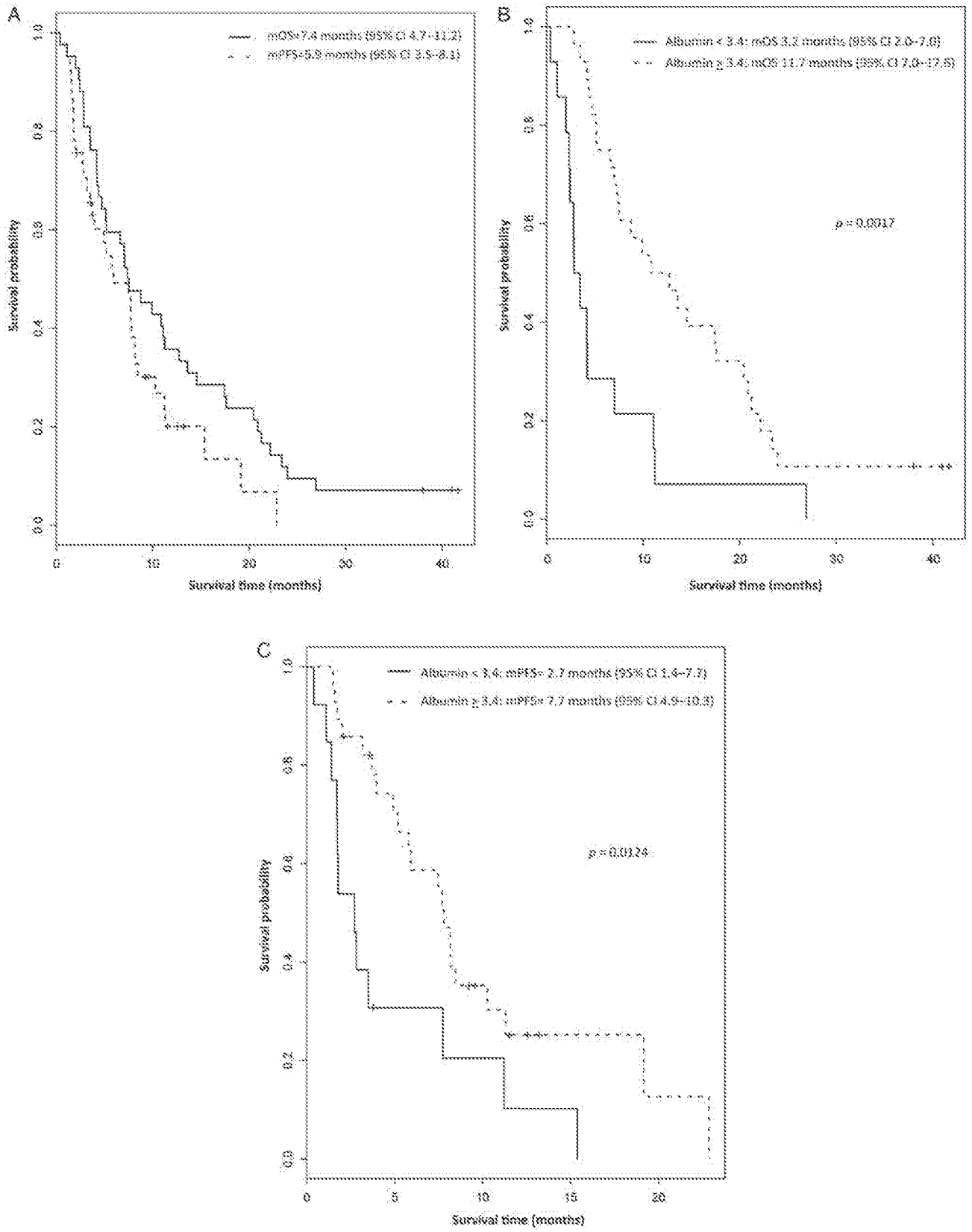

Figure 1. (A) Kaplan–Meier estimation of overall survival (OS) and progression-free survival (PFS). (B) Kaplan–Meier estimation of OS by pretreatment albumin of ≥3.4 versus <3.4 g/dl. (C). Kaplan–Meier estimation of PFS by pretreatment albumin of ≥3.4 versus <3.4 g/dl. mOS, median OS ; mPFS, median PFS.

Table 4. Summary of published phase II and III trials of gemcitabine + antiangiogenic therapy in advanced pancreas cancer

First author	Year	Phase	N	Setting	Investigational therapy[a]	Primary endpoint	P value	mOS (months)	mPFS (months)	ORR
Kindler [36]	2005	II	52	1st line	Gemcitabine + bevacizumab	ORR	—	8.8	5.4	21%
Spano [62]	2008	II	103	1st line	A: Gemcitabine + axitinib	OS	—	A: 6.9	A: 4.2	A: 7%
					B: Gemcitabine			B: 5.6	B: 3.7	B: 3%
Javle [55]	2009	II	50	1st line	Gemcitabine + capecitabine + bevacizumab	PFS	—	9.8	5.8	22%
Van Cutsem [38]	2009	III	607	1st line	A: Gemcitabine + bevacizumab + erlotinib	OS	0.21	A: 7.1	A: 4.6	A:13.5%
					B: Gemcitabine + erlotinib + placebo			B: 6.0	B: 3.6	B: 8.6%
Kindler [37]	2010	III	602	1st line	A: Gemcitabine + bevacizumab	OS	0.95	A: 5.8	A: 3.8	A: 13%
					B: Gemcitabine + placebo			B: 5.9	B: 2.9	B: 10%
Kindler [58]	2011	III	632	1st line	A: Gemcitabine + axitinib	OS	0.54	A: 8.5	A: 4.4	A: 5%
					B: Gemcitabine + placebo			B: 8.3	B: 4.4	B: 2%
Martin[b]	2011	II	42	1st line	FDR gemcitabine + infusional 5-FU + bevacizumab	6-month PFS	—	7.4	5.9	30%

mOS, median overall survival; mPFS, median progression free survival; ORR, objective response rate (complete + partial response); ORR, objective response rate (complete + partial response); FDR, fixed dose rate.

[a]Gemcitabine, standard 30 min infusion unless otherwise specified.

[b]Current study.

interesting activity is the finding that 59% of patients experienced >25% improvement in CA19-9 levels which has been shown to correlate with a favorable outcome [56–59]. These interesting findings argue for continued investigation of antiangiogenic therapies in PCA.

The choice of a chemotherapeutic backbone may impact the efficacy of antiangiogenic therapy in PCA. In a preclinical study, the antitumor activity of paclitaxel and fluoropyrimidines but not that of gemcitabine caused the release of bone marrow derived circulating endothelial progenitor cells (CEPs) and Tie-2 expressing monocytes (TEMs) as well as the induction of pro-angiogenic growth factors. Anti-angiogenic agents inhibit the CEP and TEM mobilization and proangiogenic signaling and thus enhance significantly the antitumor activity of paclitaxel and fluoropyrimidines but not that of gemcitabine [60]. Additionally, gemcitabine-induced myelosuppression in patients with PCA was found to interfere with the mobilization of proangiogenic cell types targeted by bevacizumab and may further counteract antiangiogenic therapy by substantially reducing the angiogenesis inhibitor TSP-1 [61]. These findings may explain why gemcitabine does not elicit TEM and CEP recruitment and may therefore lack synergy with bevacizumab. This phenomenon is not known to occur with fluoropyrimidines. Clinically, this is reinforced by the fact that in addition to our study, the only other study with a combination of gemcitabine plus bevacizumab in PCA to reach its primary end point included a fluoropyrimidine (Table 4) [54].

Several published phase II and III studies investigated antiangiogenic therapy in combination with gemcitabine in PCA [(36–38, 54, 55, 62), Table 4]. All three phase III studies failed to reach their primary end point of OS. However, in the AVITA trial, there was evidence of significant improvements in PFS with the addition of bevacizumab to gemcitabine and erlotinib [38]. More recently, correlative analyses from this trial revealed improved outcomes in bevacizumab-treated patients with baseline elevated plasma levels of VEGFA (OS and PFS) and VEGFR2 (OS) [39] supporting a continued interest in VEGF as a valid therapeutic target in a subset of patients in PCA.

It has also been proposed that hypertension can be used as a pharmacodynamic biomarker for the efficacy of VEGF signaling inhibition [63, 64]. An association between bevacizumab-related hypertension and improved efficacy has been observed in multiple studies with bevacizumab [65] or axitinib [62] in PCA and bevacizumab in other malignancies [66–72]. We confirmed that treatment-related hypertension may be a useful biomarker that predicts for favorable outcomes of antiangiogenic therapy in PCA. Further investigation is warranted to understand the utility of this finding in the clinical setting. For example, studies suggest a relationship between dose intensity of bevacizumab and hypertension [73, 74].

Previous pharmacokinetic studies of bevacizumab showed that a low baseline albumin results in a 15%–20% increased clearance of bevacizumab [75, 76] and patients with low albumin levels may be exposed to lower levels of bevacizumab, which potentially may lead to inferior clinical outcomes. We evaluated the role of pretreatment albumin levels as a potential predictive biomarker for the efficacy of bevacizumab in PCA and found a significant association between normal or above-normal levels and improved clinical outcomes. In the absence of a control arm, albumin levels may be prognostic and future controlled studies are needed to confirm a potential predictive role. Future controlled studies are needed to confirm a potential predictive role. If indeed predictive, pharmacokinetic dose adjustments of bevacizumab based on albumin levels may need to be studied further.

The interpretation of our study results is limited by the small number of patients and the lack of control arm. Our *post hoc* subgroup analyses are exploratory in nature and should be interpreted in this limited context.

In conclusion, the combination of bevacizumab with FDR gemcitabine followed by infusional 5-FU is safe and tolerable

with promising activity in PCA. Our results suggest that angiogenesis remains a viable target in PCA, provided that antiangiogenic agents are paired with a rational chemotherapy backbone, such as a fluoropyrimidine-based regimen (including FOLFIRINOX), to maximize the potential for synergism. Future studies should also focus on identifying subsets of patients more likely to benefit from bevacizumab in PCA. Baseline plasma VEGFA/VEGFR2 and albumin levels may be important for appropriate patient selection for bevacizumab therapy. Treatment-related hypertension may predict for improved outcomes of bevacizumab therapy. These strategies deserve to be further investigated in randomized controlled clinical trials.

funding

This work was supported by funding from Genentech, Inc. and the Roche Group, grant number AVF3571.

disclosures

T.B.-S. has received consultant fees from Genentech. All other authors have declared no conflict of interest.

references

1. Jemal A, Siegel R, Xu J, Ward E. Cancer statistics, 2010. CA Cancer J Clin 2010; 60: 277–300.
2. Weir HK, Thun MJ, Hankey BF et al. Annual report to the nation on the status of cancer, 1975–2000, featuring the uses of surveillance data for cancer prevention and control. J Natl Cancer Inst 2003; 95: 1276–1299.
3. Muller MW, Friess H, Koninger J et al. Factors influencing survival after bypass procedures in patients with advanced pancreatic adenocarcinomas. Am J Surg 2008; 195: 221–228.
4. Burris HA, 3rd, Moore MJ, Andersen J et al. Improvements in survival and clinical benefit with gemcitabine as first-line therapy for patients with advanced pancreas cancer: a randomized trial. J Clin Oncol 1997; 15: 2403–2413.
5. Berlin JD, Catalano P, Thomas JP et al. Phase III study of gemcitabine in combination with fluorouracil versus gemcitabine alone in patients with advanced pancreatic carcinoma: Eastern Cooperative Oncology Group Trial E2297. J Clin Oncol 2002; 20: 3270–3275.
6. Colucci G, Giuliani F, Gebbia V et al. Gemcitabine alone or with cisplatin for the treatment of patients with locally advanced and/or metastatic pancreatic carcinoma: a prospective, randomized phase III study of the Gruppo Oncologia dell'Italia Meridionale. Cancer 2002; 94: 902–910.
7. Colucci G, Labianca R, Di Costanzo F et al. Randomized phase III trial of gemcitabine plus cisplatin compared with single-agent gemcitabine as first-line treatment of patients with advanced pancreatic cancer: the GIP-1 study. J Clin Oncol 2010; 28: 1645–1651.
8. Cunningham D, Chau I, Stocken DD et al. Phase III randomized comparison of gemcitabine versus gemcitabine plus capecitabine in patients with advanced pancreatic cancer. J Clin Oncol 2009; 27: 5513–5518.
9. Heinemann V, Quietzsch D, Gieseler F et al. Randomized phase III trial of gemcitabine plus cisplatin compared with gemcitabine alone in advanced pancreatic cancer. J Clin Oncol 2006; 24: 3946–3952.
10. Philip PA, Benedetti J, Corless CL et al. Phase III study comparing gemcitabine plus cetuximab versus gemcitabine in patients with advanced pancreatic adenocarcinoma: Southwest Oncology Group-directed intergroup trial S0205. J Clin Oncol 2010; 28: 3605–3610.
11. Poplin E, Feng Y, Berlin J et al. Phase III, randomized study of gemcitabine and oxaliplatin versus gemcitabine (fixed-dose rate infusion) compared with gemcitabine (30-minute infusion) in patients with pancreatic carcinoma E6201: a trial of the Eastern Cooperative Oncology Group. J Clin Oncol 2009; 27: 3778–3785.
12. Moore MJ, Goldstein D, Hamm J et al. Erlotinib plus gemcitabine compared with gemcitabine alone in patients with advanced pancreatic cancer: a phase III trial of the National Cancer Institute of Canada Clinical Trials Group. J Clin Oncol 2007; 25: 1960–1966.
13. Conroy T, Desseigne F, Ychou M et al. FOLFIRINOX versus gemcitabine for metastatic pancreatic cancer. N Engl J Med 2011; 364: 1817–1825.
14. Ferrara N. Vascular endothelial growth factor and the regulation of angiogenesis. Recent Prog Horm Res 2000; 55: 15–35; discussion 35–6.
15. Ferrara N, Davis-Smyth T. The biology of vascular endothelial growth factor. Endocr Rev 1997; 18: 4–25.
16. Itakura J, Ishiwata T, Shen B et al. Concomitant over-expression of vascular endothelial growth factor and its receptors in pancreatic cancer. Int J Cancer 2000; 85: 27–34.
17. Masood R, Cai J, Zheng T et al. Vascular endothelial growth factor (VEGF) is an autocrine growth factor for VEGF receptor-positive human tumors. Blood 2001; 98: 1904–1913.
18. von Marschall Z, Cramer T, Hocker M et al. De novo expression of vascular endothelial growth factor in human pancreatic cancer: evidence for an autocrine mitogenic loop. Gastroenterology 2000; 119: 1359–1372.
19. Itakura J, Ishiwata T, Friess H et al. Enhanced expression of vascular endothelial growth factor in human pancreatic cancer correlates with local disease progression. Clin Cancer Res 1997; 3: 1309–1316.
20. Luo J, Guo P, Matsuda K et al. Pancreatic cancer cell-derived vascular endothelial growth factor is biologically active in vitro and enhances tumorigenicity in vivo. Int J Cancer 2001; 92: 361–369.
21. Kuwahara K, Sasaki T, Kuwada Y et al. Expressions of angiogenic factors in pancreatic ductal carcinoma: a correlative study with clinicopathologic parameters and patient survival. Pancreas 2003; 26: 344–349.
22. Karayiannakis AJ, Bolanaki H, Syrigos KN et al. Serum vascular endothelial growth factor levels in pancreatic cancer patients correlate with advanced and metastatic disease and poor prognosis. Cancer Lett 2003; 194: 119–124.
23. Seo Y, Baba H, Fukuda T et al. High expression of vascular endothelial growth factor is associated with liver metastasis and a poor prognosis for patients with ductal pancreatic adenocarcinoma. Cancer 2000; 88: 2239–2245.
24. Solorzano CC, Baker CH, Bruns CJ et al. Inhibition of growth and metastasis of human pancreatic cancer growing in nude mice by PTK 787/ZK222584, an inhibitor of the vascular endothelial growth factor receptor tyrosine kinases. Cancer Biother Radiopharm 2001; 16: 359–370.
25. Bruns CJ, Shrader M, Harbison MT et al. Effect of the vascular endothelial growth factor receptor-2 antibody DC101 plus gemcitabine on growth, metastasis and angiogenesis of human pancreatic cancer growing orthotopically in nude mice. Int J Cancer 2002; 102: 101–108.
26. Buchler P, Reber HA, Ullrich A et al. Pancreatic cancer growth is inhibited by blockade of VEGF-RII. Surgery 2003; 134: 772–782.
27. Reck M, von Pawel J, Zatloukal P et al. Phase III trial of cisplatin plus gemcitabine with either placebo or bevacizumab as first-line therapy for nonsquamous non-small-cell lung cancer: AVAil. J Clin Oncol 2009; 27: 1227–1234.
28. Sobrero A, Ackland S, Clarke S et al. Phase IV study of bevacizumab in combination with infusional fluorouracil, leucovorin and irinotecan (FOLFIRI) in first-line metastatic colorectal cancer. Oncology 2009; 77: 113–119.
29. Fuchs CS, Marshall J, Barrueco J. Randomized, controlled trial of irinotecan plus infusional, bolus, or oral fluoropyrimidines in first-line treatment of metastatic colorectal cancer: updated results from the BICC-C study. J Clin Oncol 2008; 26: 689–690.
30. Giantonio BJ, Catalano PJ, Meropol NJ et al. Bevacizumab in combination with oxaliplatin, fluorouracil, and leucovorin (FOLFOX4) for previously treated metastatic colorectal cancer: results from the Eastern Cooperative Oncology Group Study E3200. J Clin Oncol 2007; 25: 1539–1544.
31. Hurwitz H, Fehrenbacher L, Novotny W et al. Bevacizumab plus irinotecan, fluorouracil, and leucovorin for metastatic colorectal cancer. N Engl J Med 2004; 350: 2335–2342.

32. Sandler A, Gray R, Perry MC et al. Paclitaxel-carboplatin alone or with bevacizumab for non-small-cell lung cancer. N Engl J Med 2006; 355: 2542–2550
33. Javle M, Hauch CT. Updates in Gastrointestinal Oncology - Insights from the 2008 44th annual meeting of the American Society of Clinical Oncology. J Hematol Oncol 2009; 2: 9.
34. Shi Q, Le X, Abbruzzese JL et al. Constitutive Sp1 activity is essential for differential constitutive expression of vascular endothelial growth factor in human pancreatic adenocarcinoma. Cancer Res 2001; 61: 4143–4154.
35. Liu CD, Tilch L, Kwan D et al. Vascular endothelial growth factor is increased in ascites from metastatic pancreatic cancer. J Surg Res 2002; 102: 31–34.
36. Kindler HL, Friberg G, Singh DA et al. Phase II trial of bevacizumab plus gemcitabine in patients with advanced pancreatic cancer. J Clin Oncol 2005; 23: 8033–8040.
37. Kindler HL, Niedzwiecki D, Hollis D et al. Gemcitabine plus bevacizumab compared with gemcitabine plus placebo in patients with advanced pancreatic cancer: phase III trial of the Cancer and Leukemia Group B (CALGB 80303). J Clin Oncol 2010; 28: 3617–3622.
38. Van Cutsem E, Vervenne WL, Bennouna J et al. Phase III trial of bevacizumab in combination with gemcitabine and erlotinib in patients with metastatic pancreatic cancer. J Clin Oncol 2009; 27: 2231–2237.
39. Van Cutsem E, Jayson G, Dive C et al. Analysis of Blood Plasma Factors in the AViTA Phase III Randomized Study of Bevacizumab (bev) with Gemcitabine-Erlotinib (GE) in Patients (pts) with Metastatic Pancreatic Cancer (mPC). Eur J Cancer 2011; 45: 95.
40. Tempero M, Plunkett W, Ruiz Van Haperen V et al. Randomized phase II comparison of dose-intense gemcitabine: thirty-minute infusion and fixed dose rate infusion in patients with pancreatic adenocarcinoma. J Clin Oncol 2003; 21: 3402–3408.
41. Fung MC, Takayama S, Ishiguro H et al. Chemotherapy for advanced or metastatic pancreatic cancer: analysis of 43 randomized trials in 3 decades (1974–2002). Gan To Kagaku Ryoho 2003; 30: 1101–1111.
42. Neoptolemos JP, Stocken DD, Bassi C et al. Adjuvant chemotherapy with fluorouracil plus folinic acid vs gemcitabine following pancreatic cancer resection: a randomized controlled trial. JAMA 2010; 304: 1073–1081.
43. Berlin JD, Alberti DB, Arzoomanian RZ et al. A phase I study of gemcitabine, 5-fluorouracil and leucovorin in patients with advanced, recurrent, and/or metastatic solid tumors. Invest New Drugs 1998; 16: 325–330.
44. Ren Q, Kao V, Grem JL. Cytotoxicity and DNA fragmentation associated with sequential gemcitabine and 5-fluoro-2′-deoxyuridine in HT-29 colon cancer cells. Clin Cancer Res 1998; 4: 2811–2818.
45. Mackiewicz S, Hentschel P, Burns P et al. Phase I chemotherapy study of biochemical modulation of folinic acid and fluorouracil by gemcitabine in patients with solid tumor malignancies. J Clin Oncol 2000; 18: 3553–3557.
46. Attia S, Morgan-Meadows S, Holen KD et al. Dose-escalation study of fixed-dose rate gemcitabine combined with capecitabine in advanced solid malignancies. Cancer Chemother Pharmacol 2009; 64: 45–51.
47. Hurwitz H, Fehrenbacher L, Hainsworth JD et al. Bevacizumab in combination with fluorouracil and leucovorin: an active regimen for first-line metastatic colorectal cancer. J Clin Oncol 2005; 23: 3502–3508.
48. Efficacy of intravenous continuous infusion of fluorouracil compared with bolus administration in advanced colorectal cancer. Meta-analysis Group In Cancer. J Clin Oncol 1998; 16: 301–308.
49. Therasse P, Arbuck SG, Eisenhauer EA et al. New guidelines to evaluate the response to treatment in solid tumors. European Organization for Research and Treatment of Cancer, National Cancer Institute of the United States, National Cancer Institute of Canada. J Natl Cancer Inst 2000; 92: 205–216.
50. Herrmann R, Bodoky G, Ruhstaller T et al. Gemcitabine plus capecitabine compared with gemcitabine alone in advanced pancreatic cancer: a randomized, multicenter, phase III trial of the Swiss Group for Clinical Cancer Research and the Central European Cooperative Oncology Group. J Clin Oncol 2007; 25: 2212–2217.
51. Oettle H, Richards D, Ramanathan RK et al. A phase III trial of pemetrexed plus gemcitabine versus gemcitabine in patients with unresectable or metastatic pancreatic cancer. Ann Oncol 2005; 16: 1639–1645.
52. Stathopoulos GP, Syrigos K, Aravantinos G et al. A multicenter phase III trial comparing irinotecan-gemcitabine (IG) with gemcitabine (G) monotherapy as first-line treatment in patients with locally advanced or metastatic pancreatic cancer. Br J Cancer 2006; 95: 587–592.
53. Louvet C, Labianca R, Hammel P et al. Gemcitabine in combination with oxaliplatin compared with gemcitabine alone in locally advanced or metastatic pancreatic cancer: results of a GERCOR and GISCAD phase III trial. J Clin Oncol 2005; 23: 3509–3516.
54. Javle M, Yu J, Garrett C et al. Bevacizumab combined with gemcitabine and capecitabine for advanced pancreatic cancer: a phase II study. Br J Cancer 2009; 100: 1842–1845.
55. Kindler HL, Ioka T, Richel DJ et al. Axitinib plus gemcitabine versus placebo plus gemcitabine in patients with advanced pancreatic adenocarcinoma: a double-blind randomised phase 3 study. Lancet Oncol 2011; 12: 256–262.
56. Ko AH, Hwang J, Venook AP et al. Serum CA19-9 response as a surrogate for clinical outcome in patients receiving fixed-dose rate gemcitabine for advanced pancreatic cancer. Br J Cancer 2005; 93: 195–199.
57. Ziske C, Schlie C, Gerschlüter M et al. Prognostic value of CA 19-9 levels in patients with inoperable adenocarcinoma of the pancreas treated with gemcitabine. Br J Cancer 2003; 89: 1413–1417.
58. Wong D, Ko AH, Hwang J et al. Serum CA19-9 decline compared to radiographic response as a surrogate for clinical outcomes in patients with metastatic pancreatic cancer receiving chemotherapy. Pancreas 2008; 37: 269–274.
59. Halm U, Schumann T, Schiefke I et al. Decrease of CA 19-9 during chemotherapy with gemcitabine predicts survival time in patients with advanced pancreatic cancer. Br J Cancer 2000; 82: 1013–1016.
60. Shaked Y, Henke E, Roodhart JM et al. Rapid chemotherapy-induced acute endothelial progenitor cell mobilization: implications for antiangiogenic drugs as chemosensitizing agents. Cancer Cell 2008; 14: 263–273.
61. Starlinger P, Brugger P, Schauer D et al. Myelosuppression of thrombocytes and monocytes is associated with a lack of synergy between chemotherapy and anti-VEGF treatment. Neoplasia 2011; 13: 419–427.
62. Spano JP, Chodkiewicz C, Maurel J et al. Efficacy of gemcitabine plus axitinib compared with gemcitabine alone in patients with advanced pancreatic cancer: an open-label randomised phase II study. Lancet 2008; 371: 2101–2108.
63. Maitland ML, Ratain MJ. Terminal ballistics of kinase inhibitors: there are no magic bullets. Ann Intern Med 2006; 145: 702–703.
64. Snider KL, Maitland ML. Cardiovascular toxicities: clues to optimal administration of vascular endothelial growth factor signaling pathway inhibitors. Target Oncol 2009; 4: 67–76.
65. Friberg G, Kasza K, Vokes EE, Kindler HL. Early hypertension (HTN) as a potential pharmacodynamic (PD) marker for survival in pancreatic cancer (PC) patients (pts) treated with bevacizumab (B) and gemcitabine (G). J Clin Oncol 2005; 23: 3020.
66. Baka S, Clamp AR, Jayson GC. A review of the latest clinical compounds to inhibit VEGF in pathological angiogenesis. Expert Opin Ther Targets 2006; 10: 867–876.
67. Schneider BP, Wang M, Radovich M et al. Association of vascular endothelial growth factor and vascular endothelial growth factor receptor-2 genetic polymorphisms with outcome in a trial of paclitaxel compared with paclitaxel plus bevacizumab in advanced breast cancer: ECOG 2100. J Clin Oncol 2008; 26: 4672–4678.
68. Dahlberg SE, Sandler AB, Brahmer JR et al. Clinical course of advanced non-small-cell lung cancer patients experiencing hypertension during treatment with bevacizumab in combination with carboplatin and paclitaxel on ECOG 4599. J Clin Oncol 2010; 28: 949–954.
69. Ryanne Wu R, Lindenberg PA, Slack R et al. Evaluation of hypertension as a marker of bevacizumab efficacy. J Gastrointest Cancer 2009; 40: 101–103.
70. Scartozzi M, Galizia E, Chiorrini S et al. Arterial hypertension correlates with clinical outcome in colorectal cancer patients treated with first-line bevacizumab. Ann Oncol 2009; 20: 227–230.
71. Goodwin R, Ding K, Seymour L et al. Treatment-emergent hypertension and outcomes in patients with advanced non-small-cell lung cancer receiving chemotherapy with or without the vascular endothelial growth factor receptor

inhibitor cediranib: NCIC Clinical Trials Group Study BR24. Ann Oncol 2010; 21: 2220–2226.

72. Rini BI, Cohen DP, Lu DR et al. Hypertension as a biomarker of efficacy in patients with metastatic renal cell carcinoma treated with sunitinib. J Natl Cancer Inst 2011; 103: 763–773.

73. Zhu X, Wu S, Dahut WL, Parikh CR. Risks of proteinuria and hypertension with bevacizumab, an antibody against vascular endothelial growth factor: systematic review and meta-analysis. Am J Kidney Dis 2007; 49: 186–193.

74. Ranpura V, Hapani S, Wu S. Treatment-related mortality with bevacizumab in cancer patients: a meta-analysis. JAMA 2011; 305: 487–494.

75. Lu JF, Bruno R, Eppler S et al. Clinical pharmacokinetics of bevacizumab in patients with solid tumors. Cancer Chemother Pharmacol 2008; 62: 779–786.

76. Gaudreault J, Lieberman G, Kabbinavar F et al. Pharmacokinetics of Bevacizumab (BV) in colorectal cancer (CRC). Clin Pharmacol Ther 2001; 69: 25.

Annals of Oncology 23: 2820–2827, 2012
doi:10.1093/annonc/mds109
Published online 9 May 2012

Neoadjuvant cetuximab, twice-weekly gemcitabine, and intensity-modulated radiotherapy (IMRT) in patients with pancreatic adenocarcinoma

J. M. Pipas[1*], B. I. Zaki[2], M. M. McGowan[1], M. J. Tsapakos[3], G. H. Ripple[1], A. A. Suriawinata[4], G. J. Tsongalis[4], T. A. Colacchio[5], S. R. Gordon[6], J. E. Sutton[7], A. Srivastava[8], K. D. Smith[5], T. B. Gardner[6], M. Korc[9], T. H. Davis[1], M. Preis[1], S. M. Tarczewski[10], T. A. MacKenzie[11] & R. J. Barth, Jr[5]

[1]Section Hematology/Oncology, Department of Medicine; [2]Section Radiation Oncology, Department of Medicine; [3]Department of Radiology; [4]Department of Pathology; [5]Section Surgical Oncology, Department of Surgery; [6]Section Gastroenterology, Department of Medicine, Dartmouth-Hitchcock Medical Center, Lebanon; [7]Department of Surgery, Veterans Administration Medical Center, White River Junction; [8]Department of Pathology, Brigham & Women's Hospital, Boston; [9]Department of Medicine, Indiana University School of Medicine, Indianapolis; [10]Office of Clinical Research, Norris Cotton Cancer Center, Lebanon; [11]Department of Epidemiology & Biostatistics, Dartmouth-Hitchcock Medical Center, Lebanon, USA

Received 14 November 2011; revised 22 February 2012; accepted 23 February 2012

Background: Neoadjuvant therapy has been investigated for localized and locally advanced pancreatic ductal adenocarcinoma (PDAC) but no standard of care exists. Combination cetuximab/gemcitabine/radiotherapy demonstrates encouraging preclinical activity in PDAC. We investigated cetuximab with twice-weekly gemcitabine and intensity-modulated radiotherapy (IMRT) as neoadjuvant therapy in patients with localized or locally advanced PDAC.

Experimental design: Treatment consisted of cetuximab load at 400 mg/m^2 followed by cetuximab 250 mg/m^2 weekly and gemcitabine 50 mg/m^2 twice-weekly given concurrently with IMRT to 54 Gy. Following therapy, patients were considered for resection.

Results: Thirty-seven patients were enrolled with 33 assessable for response. Ten patients (30%) manifested partial response and 20 (61%) manifested stable disease by RECIST. Twenty-five patients (76%) underwent resection, including 18/23 previously borderline and 3/6 previously unresectable tumors. Twenty-three (92%) of these had negative surgical margins. Pathology revealed that 24% of resected tumors had grade III/IV tumor kill, including two pathological complete responses (8%). Median survival was 24.3 months in resected patients. Outcome did not vary by epidermal growth factor receptor status.

Conclusions: Neoadjuvant therapy with cetuximab/gemcitabine/IMRT is tolerable and active in PDAC. Margin-negative resection rates are high and some locally advanced tumors can be downstaged to allow for complete resection with encouraging survival. Pathological complete responses can occur. This combination warrants further investigation.

Key words: cetuximab, gemcitabine, intensity-modulated radiotherapy, neoadjuvant therapy, pancreatic cancer

introduction

Pancreatic ductal adenocarcinoma (PDAC) is highly lethal with 5-year mortality of 95% [1]. Complete resection of localized

*Correspondence to: Dr J. M. Pipas, Section Hematology/Oncology, Dartmouth-Hitchcock Medical Center/Norris Cotton Cancer Center, 1 Medical Center Drive, Lebanon, NH 03756, USA. Tel: +1-603-650-6316; Fax: +1-603-653-0601; E-mail: J.Marc.Pipas@Hitchcock.org

Minireview

Clinical Pharmacokinetics and Metabolism of Irinotecan (CPT-11)

Ron H. J. Mathijssen,[1] Robbert J. van Alphen,[1] Jaap Verweij, Walter J. Loos, Kees Nooter, Gerrit Stoter, and Alex Sparreboom[2]

Department of Medical Oncology, Rotterdam Cancer Institute (Daniel den Hoed Kliniek) and University Hospital Rotterdam, 3008 AE Rotterdam, the Netherlands

Abstract

CPT-11 belongs to the class of topoisomerase I inhibitors, and it acts as a prodrug of SN-38, which is approximately 100–1000-fold more cytotoxic than the parent drug. CPT-11 has shown a broad spectrum of antitumor activity in preclinical models as well as clinically, with responses observed in various disease types including colorectal, lung, cervical, and ovarian cancer. The pharmacokinetics and metabolism of CPT-11 are extremely complex and have been the subject of intensive investigation in recent years. Both CPT-11 and SN-38 are known in an active lactone form and an inactive carboxylate form, between which an equilibrium exists that depends on the pH and the presence of binding proteins. CPT-11 is subject to extensive metabolic conversion by various enzyme systems, including esterases to form SN-38, UGT1A1 mediating glucuronidation of SN-38, as well as CYP3A4, which forms several pharmacologically inactive oxidation products. Elimination routes of CPT-11 also depend on the presence of drug-transporting proteins, notably P-glycoprotein and canalicular multispecific organic anion transporter, present on the bile canalicular membrane. The various processes mediating drug elimination, either through metabolic breakdown or excretion, likely impact substantially on interindividual variability in drug handling. Strategies to individualize CPT-11 administration schedules based on patient differences in enzyme or protein expression or by coadministration of specific agents modulating side effects are under way and may ultimately lead to more selective chemotherapeutic use of this agent.

Introduction

Camptothecin, a plant alkaloid isolated from *Camptotheca acuminata* (family Nyssaceae), was first discovered in the early 1960s (1). Because of severe and unpredictable side effects of camptothecin in early clinical studies, clinical development was halted in the 1970s (2–5). It was later revealed that the water insolubility of camptothecin was an important factor mediating the unpredictable toxic effects (6). The elucidation of the mechanism of action of camptothecin, *i.e.*, inhibition of topoisomerase I, a nuclear enzyme which relaxes torsionally strained (supercoiled) DNA (7–9), resulted in renewed interest in this agent, and subsequently, numerous derivatives have been synthesized and tested clinically (10–12). Some of these agents, including CPT-11[3] (13), topotecan (14), 9-aminocamptothecin and 9-nitrocamptothecin (15–17), lurtotecan (GI147211, GG211; Ref. 18), and DX-8951f (19), have a broad spectrum of antitumor activity both *in vitro* and *in vivo* and show more predictable and clinically manageable toxicities than the originally isolated structure. Two of these agents, topotecan and CPT-11, have recently been introduced into clinical practice for the treatment of ovarian and colorectal cancer, respectively. Of the currently available camptothecin analogues, CPT-11 has an extremely complex pharmacological profile, which is dependent on a host of enzymes involved in metabolic transformation and active transport proteins, regulating intestinal absorption and hepatobiliary secretion mechanisms (Fig. 1). Furthermore, CPT-11 is chemically unique because of the presence of a bulky side chain on the core structure, the enzymatic cleavage of which is a requirement for pharmacological activity. In addition, CPT-11 is known in two distinguishable forms, an active α-hydroxy-δ-lactone ring form and an inactive carboxylate form, between which a pH-dependent equilibrium exists (12) that significantly impacts on the kinetic profile of the compound. In recent years, a wealth of information has become available that has substantially aided in our understanding of the clinical actions of this agent. Here, we will review the clinical pharmacokinetic properties of CPT-11 and its metabolites that appear to be crucial for optimal anticancer chemotherapeutic use.

Pharmacokinetic Properties

Plasma Disposition. The plasma pharmacokinetics of CPT-11 in humans has now been addressed in several studies, and taking into account that these data are from different laboratories, the results are fairly comparable. Most of the initial studies have been performed with the drug administered as a short i.v. infusion (0.5–1.5 h). After such administration, peak plasma concentrations were reached at the end of infusion

Received 3/6/01; revised 5/7/01; accepted 5/10/01.
The costs of publication of this article were defrayed in part by the payment of page charges. This article must therefore be hereby marked *advertisement* in accordance with 18 U.S.C. Section 1734 solely to indicate this fact.

[1] These authors contributed equally to this work.

[2] To whom requests for reprints should be addressed, at Department of Medical Oncology, Rotterdam Cancer Institute (Daniel den Hoed Kliniek) and University Hospital Rotterdam, Groene Hilledijk 301, 3075 EA Rotterdam, the Netherlands. Phone: 31-10-4391112; Fax: 31-10-4391053; E-mail: sparreboom@onch.azr.nl.

[3] The abbreviations used are: CPT-11, irinotecan (7-ethyl-10-[4-(1-piperidino)-1-piperidino]-carbonyloxycamptothecin); SN-38, 7-ethyl-10-hydroxycamptothecin, SN-38G, 7-ethyl-10-[3,4,5-trihydroxy-pyran-2-carboxylic acid]-camptothecin (the β-glucuronide conjugate of SN-38); APC, 7-ethyl-10-[4-*N*-(5-aminopentanoic acid)-1-piperidino]-carbonyloxycamptothecin; NPC, 7-ethyl-10-[4-(1-piperidino)-1-amino]-carbonyloxycamptothecin; CE, carboxylesterase; UGT, UDP glucuronosyltransferase; CYP3A, cytochrome P-450 isoform 3A; AUC, area under the plasma concentration *versus* time curve; cMOAT, canalicular multispecific organic anion transporter; BCRP, breast cancer resistance protein; P-gp, P-glycoprotein.

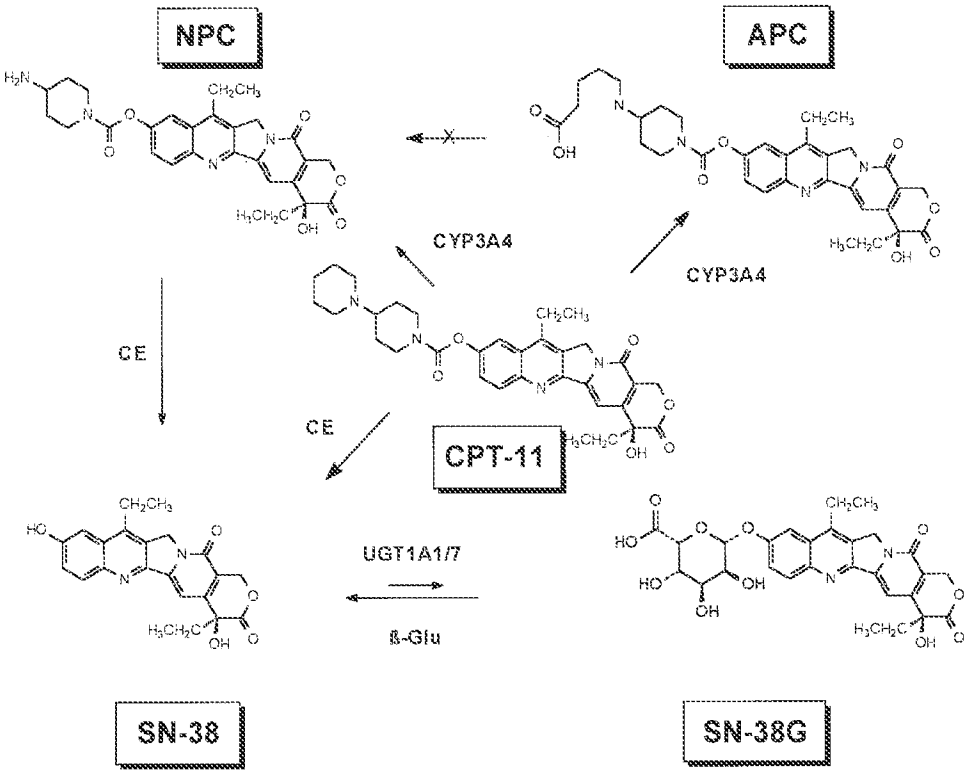

Fig. 1 Metabolic pathways of CPT-11 showing CE-mediated formation of the active metabolite SN-38 and its subsequent conversion to a glucuronide derivative (SN-38G) by UGT1A1 and 1A7 isoforms (UGT1A7), with deglucuronidation by intestinal β-glucuronidase (β-*Glu*). CPT-11 can also undergo CYP3A4-mediated oxidative metabolism to form APC and NPC, of which the latter can be hydrolyzed by CE to release SN-38.

(20–36), with a rapid decrease thereafter as a result of multiple distribution and elimination pathways (32, 36). A rebound peak in the concentration-curve has been noticed in some studies (22, 26, 31, 36) and was initially ascribed to enterohepatic recirculation (22, 26). More recently, it has been suggested that this phenomenon is related to substantial uptake of CPT-11 lactone by erythrocytes and its subsequent release, followed by accumulation of the carboxylate form in the plasma compartment (37). Equilibrium between the two drug forms is rapidly established, and contrary to CPT-11, the principal metabolite SN-38 predominates in its active lactone form (33, 34). The lactone form of SN-38 accounts for approximately 60–70% of total plasma SN-38 after the end of a CPT-11 infusion, declining to of 33–66% at equilibrium (23, 33). The mean lactone:total AUC ratio of SN-38 is high, ~64%, albeit with large interpatient variability (23, 24, 33, 34, 38). This ratio remains constant for the whole dose range measured. Examples of concentration-time profiles for the lactone and carboxylate forms of CPT-11 and SN-38 are shown in Fig. 2.

The peak concentration of CPT-11 appears to be dose-proportional in a large dose range (100–750 mg/m^2), although substantial interpatient variability has been noted (21–23, 25, 26, 39, 40). This variability increases at later time points (41). CPT-11 systemic exposure or AUC also increases in a dose-independent way at doses ranging from 33 to 180 mg/m^2 (24–26, 39, 40, 42), indicating linear pharmacokinetics.

The ratio of the lactone:total AUC remains relatively constant over the entire dose range of CPT-11, with mean values ranging from 34 ± 5% up to 44 ± 4% (33, 34). The conversion of the lactone into the carboxylate form of CPT-11 is rapid, with

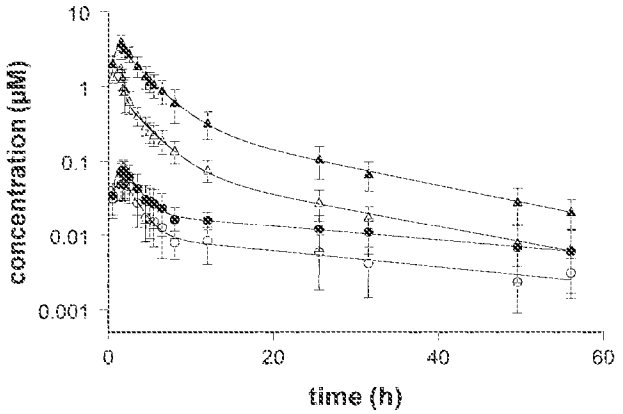

Fig. 2 Plasma concentration-time profiles of the lactone (△, ○) and total drug (*i.e.*, lactone plus carboxylate) forms of CPT-11 (△, ▲) and SN-38 (○, ●) in a group of 17 patients receiving CPT-11 at 200 mg/m^2 as a 90-min i.v. infusion. All pharmacokinetic curves were fit to a three-exponential equation, using Siphar version 4.0 (InnaPhase, Philadelphia, PA), assuming a three-compartmental model for distribution and elimination of the compounds. Data are presented as means; bars, SD. Data were obtained from Mathijssen *et al.* (38).

a mean half-life of 9.5 min (34). The plasma profiles of the two forms of CPT-11 are comparable and can best be fitted in a bi- or tri-exponential equation (22, 25, 43), with mean terminal half-life values of about 9.3–14.2 h (22, 25, 35). More recently, it has been suggested that the terminal disposition half-life of

CPT-11 is much longer, which may be related to the fact that prolonged sampling schedules were applied in combination with a highly sensitive detection method (20, 43).

The volume of distribution at steady state of CPT-11 is large, suggesting extensive tissue distribution, and remained unchanged with an increase in dose (20, 22, 24, 31). Similarly, the total plasma clearance of CPT-11 was found to be dose independent, with a value of 13.5 ± 3.5 L/h/m^2 for the total drug (*i.e.*, lactone plus carboxylate forms) and 45.6 ± 10.8 L/h/m^2 for the lactone form (35). The clearance is unaltered during repeated cycles, despite a mean interpatient variability of ~30% (21, 35), and an intra-patient variability of ~13.5%.

Plasma Protein Binding. An important factor in the pharmacology of drugs is its binding to plasma proteins. In accordance with the hydrophilic nature of CPT-11, in blood, 80% of the drug is mainly bound to and/or localized in erythrocytes, whereas SN-38 is bound for at least 99%, mainly to albumin and lymphocytes, but also to erythrocytes and neutrophils (44). Although binding to plasma proteins appears to be of subordinate importance for CPT-11, binding of the principal metabolite SN-38 to plasma proteins in adults and pediatric patients is thus substantial and independent of (pretherapy) serum albumin levels (~94–96%; Refs. 44–46). In the presence of albumin, the lactone forms of CPT-11 and SN-38 are more stable (47), with higher percentages of the lactone forms available, compared with the situation without this protein. The protein binding is not significantly different for the lactone and carboxylate form of CPT-11. In contrast, SN-38 lactone binds significantly stronger to albumin than its corresponding carboxylate form, which could explain the better stability of SN-38 *in vivo* compared with CPT-11 (47). This, in turn, may play a role in the differential terminal disposition half-lives and volumes of distribution between these molecules. In *in vitro* incubations in the presence of human serum albumin, the apparent half-life of the interconversion of CPT-11 is more than three times higher than that in patients (34). This suggests that there is an early preferential uptake and/or metabolism of the lactone form of CPT-11, thereby altering the ratio of CPT-11 lactone *versus* carboxylate (34).

Metabolism

Several studies have shown that hepatic metabolism and biliary secretion are major pathways of CPT-11 elimination in both animals and humans, with major contributions from various classes of enzymes, including CEs, UGTs, CYP3As, and β-glucuronidases.

Esterase-mediated Biotransformation. The conversion of CPT-11 to SN-38 through cleavage of the ester-bond at C10 by CEs has been studied extensively in recent years. It has been suggested that two human isozymes of liver CE, *i.e.*, hCE-1 and hCE-2, have been characterized that might catalyze this conversion (48, 49). No tumor reduction in SQ20b cells was seen after incubation of CPT-11 with hCE-1, compared with a 60% reduction for hCE-2 (49). Therefore, hCE-2 probably plays the most important role in CPT-11 conversion by CEs in cancer patients. The plasma of several species, including mouse and horse, contains high levels of esterases other than CE and it converts CPT-11 much better into SN-38 than human plasma does. It has been suggested that butyrylcholinesterase, which has CPT-11 converting activity, might be responsible for this phenomenon (50, 51).

SN-38 concentrations have been shown to increase with the CPT-11 dose over the dose range studied (100–750 mg/m^2; Ref. 35). The terminal disposition half lives of SN-38 lactone and total drug are significantly longer than those of CPT-11 (38, 43). In an *in vitro* study of human liver microsomes, twice as much SN-38 was formed when CPT-11 was present in its lactone form in comparison with CPT-11 in its carboxylate form (52). Because CPT-11 lactone is converted easier, this phenomenon might contribute to the predominance of SN-38 in its lactone form in plasma (52).

A clear relationship between CE levels and the chemosensitivity of proliferating tissues and cell lines in general has been suggested (53–55). CPT-11 was significantly more active in five human small-cell lung cancer cell lines than in four non-small cell lung cancer cell lines, and this was attributed to a higher CE activity in the former case (55). CPT-11-converting CE activity in human tumors has also been studied *in vivo* (56). A wide range of variability in enzyme activity in primary colorectal tumors was seen, with no significant difference between primary and secondary tumors. Relatively high CE activity in these tumors, as compared with normal liver tissue has been noticed, which might suggest a local activation of CPT-11 in tumor tissues (56). There were no significant differences between enzyme activity in human liver and colon tissues.

Selective upgrading of CE levels in tumors, thereby producing tumor-specific activity may clearly have substantial clinical implications; it will maximize the exposure of tumors to SN-38 and limit systemic drug concentrations and therefore also limit adverse effects of CPT-11. This upgrading has been studied for several enzyme/prodrug combinations, using antibodies or viruses to attack tumor cells. For the CE/CPT-11 combination, a recombinant replication-deficient adenovirus vector coding for human CE cDNA has been developed (57). This vector effectively suppressed A549 cell growth *in vitro* in the presence of CPT-11 by 7–17-fold. Because SN-38 diffuses from the tumor cell in which it has been produced to its neighbor cells in growth-suppressive concentrations, only 10% of the A549 cells need to be infected for a cytotoxic effect in 48% of the cells (57). In CPT-11-resistant A549 cells, which had a 6-fold resistance and 42% CE activity compared with normal A549 cells, functional CE expression could be accomplished by infection with this vector (57, 58), and these resistant cells could be suppressed efficiently *in vitro* and *in vivo* (58). This sensitivity has also been described for two other human tumor cell lines, although in another eight human cell lines, only a minimal effect was seen (59).

In various studies, the activity of CE isozymes from animal species has been compared with the human enzyme(s), and the latter show consistently lower activity than those of the other species investigated (60, 61). Although the active site amino acids of rabbit and human CEs are almost identical, human CE converts CPT-11 100–1000-fold less efficiently (59). In Rh30 human rhabdomyosarcoma cells, expression of the rabbit enzyme was associated with more rapid tumor regression and a better prevention of tumor recurrence *in vitro* (59, 62). In addition, immune-deprived mice, carrying rabbit CE-expressing

Rh30 cells, were more sensitive to CPT-11 than human CE-expressing cells or control cells. No recurrent tumors occurred in the rabbit-enzyme group, in contrast to 29 and 100% recurrence in the two other groups, respectively (59). The clinical utility of this approach is currently under further investigation.

UGT-mediated Biotransformation. SN-38 itself is further metabolized in human liver by UGT1A1 to an inactive compound, SN-38G (63–65). The lactone functionality of SN-38G could also be hydrolyzed after a pH-dependent equilibrium (65). Mostly, the plasma concentrations of SN-38G are related to SN-38 plasma concentrations, with peak values at ~1.2 h (range, 15 min to 4.5 h) after the end of infusion (31, 43, 66). SN-38G concentrations increase linearly with the administered CPT-11 dose, suggesting that hepatic glucuronidation is not saturated in the dose ranges studied (up to 600 mg/m^2; Refs. 36, 42). The AUC of SN-38G is ~7-fold higher than that of SN-38, suggesting extensive glucuronidation of SN-38 into SN-38G (32, 66), with high interpatient variability (41).

Considerable variation in the conversion of SN-38 into SN-38G in human liver cells has also been noticed *in vitro* (63). This may be attributable to different enzyme activities of the various UGT isoforms. Two distinct gene families of UGT enzymes exist, *UGT1* and *UGT2*, which are both being subclassified into several isoforms. Results obtained from transfection studied have shown that isoform UGT1A1 is primarily responsible for the SN-38 conversion (63), although it was shown more recently that isoform 1A7 is ~21-fold more efficient at physiological pH than UGT1A1 (67).

A genetic polymorphism has been reported in the TATA box sequences of UGT1A1 (68). Normally, the box contains $(TA)_6TAA$ in its promoter region, and sometimes a box contains an extra TA repeat (68, 69). An extra TA repeat in the TATA box has been associated with Gilbert's syndrome (70). The metabolic ratio (SN-38/SN-38G) for these patients is significantly higher compared with the common genotype, suggesting less SN-38 glucuronidation capacity (69). In addition, it has been reported that in patients with the Crigler-Najjar type I syndrome, UGT1 activity is totally lacking (63, 71, 72). As a result, SN-38 cannot be inactivated adequately into SN-38G, and therefore patients with these disorders are at increased risk for severe CPT-11-induced toxicity (63). On the basis of the relative importance of the systemic glucuronidation and the existence of genetic polymorphism, it has been proposed that UGT1A1 genotyping might be an approach to individualize CPT-11 treatment schedules (68, 73).

A significant correlation was observed recently between SN-38 glucuronidation rates and bilirubin glucuronidation by human liver microsomes (63). Interestingly, UGT1A1 is the isozyme that also conjugates bilirubin (72). Also for bilirubin glucuronidation, an inverse correlation between glucuronidation rate and number of TA repeats has been reported (68–70). It has been shown subsequently that baseline values of unconjugated bilirubin correlate significantly with both neutropenia and the AUCs of CPT-11 and SN-38, and this relationship might thus be useful in individual dose prescription or adaptation (72). No relationship has been observed between the glucuronidation of SN-38 and that of para-nitrophenol, which is glucuronidated by several UGTs, including UGT1A1 (63). An intriguing observation has been that valproic acid, an inhibitor of glucuronidation, given 5 min before CPT-11 in rats, caused 99% inhibition in SN-38G formation (74), resulting in a mean increase in SN-38 AUC of 270%. Pretreatment with phenobarbital, an inducer of UGT, resulted in a 72% enhancement in the AUC of SN-38G, with a concomitant reduction in the AUCs of CPT-11 and SN-38 of 31 and 59%, respectively (74). These findings are consistent with data indicating that a patient with Gilbert's syndrome could be treated successfully with simultaneous administration of CPT-11 and phenobarbital (31). CPT-11 and SN-38 were formed in concentrations comparable with those achieved in normal patients, although the AUC of SN-38G appeared to be substantially altered (31).

In human lung cancer cell lines, the role of SN-38 glucuronidation in cytotoxicity profiles has been studied extensively (75). PC-7/CPT cell lines showed an increased glucuronidation in comparison with normal PC-7 cells, and when UGT activity was inhibited, the cells became more sensitive to SN-38. Thus, an up-regulation of the UGT activity may lead to SN-38 resistance in the tumor (75). BCRP or mitoxantrone-resistance half-transporter (MXR) expression was also found to result in 400-1000-fold resistance to SN-38 as compared with parental cell lines (76). Because MXR cells were highly capable to resist drugs that are susceptible to glucuronidation, UGT activity in resistant and normal cell lines were compared. In resistant cells, higher SN-38G levels were seen than in normal cells. Thus, in cancer cells glucuronidation might contribute to drug resistance, but the lack of high UGT levels in resistant MXR cells suggests that BCRP alone is sufficient to induce drug resistance patterns (76).

CYP3A-mediated Biotransformation. Recently, other quantitatively important metabolites of CPT-11 have been identified, the formation of which is dependent of CYP3A. Of these, APC is a major metabolite detectable in plasma and is formed by a CYP3A-mediated oxidation of the distal piperidine group at C10 of CPT-11 (77–79). NPC is also formed through this pathway, by cleavage of the distal piperidino group of CPT-11 (77, 79–82). APC peaks at ~2 h after the end of infusion, and AUC values increase linearly with increasing CPT-11 dose, despite important interpatient variation (36). At equimolar concentrations (as compared with CPT-11), APC did not inhibit the conversion of CPT-11 into SN-38 (83).

Similar to CPT-11, APC shows little cytotoxic activity, although it has some inhibitory effect on acetylcholinesterase, an enzyme involved with the acute cholinergic syndrome observed directly following CPT-11 administration (83). It is likely that APC does not contribute directly to the total activity and toxicity after CPT-11 administration *in vivo*, because it shows minor antitumor activity *in vitro* compared with SN-38 and less toxicity compared with CPT-11. NPC is also a poor inhibitor of cell growth and a poor inducer of topoisomerase I-DNA cleavable complexes, with less antitumor activity in cell lines than CPT-11 (80, 84). In addition, formation of APC and NPC is unlikely to take place in human (colorectal) tumors, where CYP3A levels are generally very low (85). It is of particular interest, though, that human liver microsomes and human liver CE are able to hydrolyze NPC into SN-38 though still to a lesser extent than CPT-11 (80, 84), whereas for APC this conversion has not been demonstrated conclusively (80, 86). Nevertheless, patients with high AUCs of SN-38, also had

high AUCs of CPT-11 and APC, suggesting that some degree of correlation might be present (36). In addition, NPC cannot be formed from APC, in contrast to a formerly suggested conversion (81, 84).

The recognition that CPT-11 is a CYP3A substrate is an important finding, because it makes this agent subject to a host of enzyme-mediated drug interactions, even with commonly prescribed comedication (81, 87). For example, the prototypical CYP3A inhibitors, ketoconazole and troleandomycine, inhibit the conversion of CPT-11 into APC and NPC almost completely (77–79, 81). In addition, both lopemmide and racecadotril inhibit APC and NPC formation by >50%, whereas ondansetron inhibits these formations by 25 and 75%, respectively (78, 81). APC and NPC formation correlated significantly with testosterone 6β hydroxylation, which is also mediated by CYP3A (78, 81). It has been shown recently that the subtype CYP3A4 is the main isozyme involved in formation of both APC and NPC (79, 82), although it was suggested previously that cytosolic aldehyde dehydrogenase might also be involved in APC formation (81). CYP3A5 also showed catalytic activity, but neither APC nor NPC was formed in its presence (79, 82). Instead, a new (unidentified) metabolite was found (79, 82). Because this enzyme is expressed in only 25–30% of adult livers, this might explain some of the interpatient variability in CPT-11 metabolism (82). Preliminary evidence has also been generated indicating that SN-38 might be metabolized by CYP3A4, although the clinical implications of this finding have not yet been evaluated.

β-Glucuronidase-mediated Biotransformation. When SN-38G is excreted in bile and intestines, several bacteria including *Escherichia coli*, *Bacteroides* species, and *Clostridium perfringens* can convert this compound back to the active metabolite SN-38 by producing the enzyme β-glucuronidase (88–90). Various studies have described (microflora-derived) β-glucuronidase activity in nonhuman (91–94) and human intestines (95–97). In rats and athymic mice, within 1 h after the end of infusion, acute diarrheal symptoms with impaired water absorption and increased prostaglandin E_2 levels have been found (92, 93). Histopathological changes in the descending colon, cecum, and ileum were observed after the daily administration of CPT-11 (91–93). Recently, these mucosal abnormalities were confirmed in human colon (97). A good correlation between this histological damage and β-glucuronidase activity in the intestinal lumen has been noticed, whereas a poor correlation was observed with CE activity (91). The lesser damage found in small intestines compared with damage in the colon could be explained by a lower exposure of this tissue to SN-38. This may be attributable to a smaller amount of β-glucuronidase in the lumen of small intestines (94).

Because many drugs could affect the functioning of the intestinal bacteria, comedication may influence the chemotherapeutic treatment of patients with CPT-11 (98). Because bacteria producing β-glucuronidase activity will be killed by antibiotics, it is anticipated that this will lead to a reduction in acute and delayed diarrhea and cecal damage (91). It has been demonstrated that antibiotics had no effects on the plasma concentrations of CPT-11, SN-38, or SN-38G in mice (penicillin/streptomycin; Ref. 94) and in humans (neomycin; Ref. 99). This combined treatment also resulted in reduced SN-38 concentrations in the intestinal contents with concomitantly increased SN-38G levels (94, 99). A potential approach for modulating CPT-11-induced intestinal toxicity may therefore be to reduce bacterial β-glucuronidase-mediated deconjugation of SN-38 and subsequent mucosal destruction. A clinical trial to evaluate the toxicological consequences of pretreatment with neomycin before the administration of CPT-11 is in progress at our institute.

Table 1 Cumulative urinary and fecal excretion of CPT-11 and metabolites

Compound	Urine	Feces	Total
CPT-11	22.4 ± 5.50	32.3 ± 4.47	54.7
SN-38G	3.02 ± 0.77	0.27 ± 0.17	3.29
SN-38	0.43 ± 0.12	8.24 ± 2.51	8.67
APC	2.23 ± 1.53	8.29 ± 2.95	10.5
NPC	0.14 ± 0.08	1.36 ± 0.94	1.50
Total compounds	30.2 ± 6.60	62.0 ± 7.60	92.2
Not extracted	1.25 ± 1.55	9.86 ± 3.77	11.1

Parent drug and metabolite abundance are expressed as percentages of administered dose and were determined by quantitative radiometric high-performance liquid chromatography. Data were obtained from Slatter *et al.* (20).

Excretion

Several studies have examined the excretion of CPT-11 in bile, feces, and urine in animals and humans. In humans, only 52% of the given dose has been recovered using nonradiometric HPLC methods (32, 100), whereas in a recent radiometric study quantitative recovery (95.8 ± 2.7% of radioactivity) was obtained (20). CPT-11 and its three most common metabolites (SN-38, SN-38G, and APC) were responsible for almost all (~93%) detected material (20).

Urinary Elimination. In urine, CPT-11, APC, and SN-38G are the main compounds detected within 24 h after CPT-11 administration (20, 32), with CPT-11 accounting for about 10–22% of the administered dose and SN-38 contributing only 0.18–0.43% (20, 22, 25, 31, 66, 100). Consistent with the highly polar nature of the glucuronic acid group and increased aqueous solubility, SN-38G may be excreted rapidly by the kidneys (32). The cumulative excretion of APC and NPC was very low, amounting to <1% of the dose (32). This suggests that the bulk of CPT-11 and its metabolites is excreted during the first 24 h after infusion, whereas assessing urinary recovery of radiolabeled CPT-11 over 196 h also showed that the excretion was almost complete within 48 h (Table 1; Ref. 20). Similar findings were obtained with daily administration schedules of CPT-11, indicating unchanged urinary excretion profiles (26, 29).

Biliary Secretion. In a few patients, CPT-11 and SN-38 concentrations in bile have been measured (20, 24, 25, 100). CPT-11, SN-38, and SN-38G biliary secretion varies between approximately 3–22, 0.1–0.9, and 0.6–1.1%, respectively (100). NPC was also detected in bile at very low concentrations (80). In a female patient, carrying a biliary T-tube and receiving radiolabeled CPT-11, 30.1% of the administered dose was recovered in bile as radioactive compounds (20).

In rats, a cMOAT located on the bile canalicular membrane was shown to be responsible for the transport of CPT-11 car-

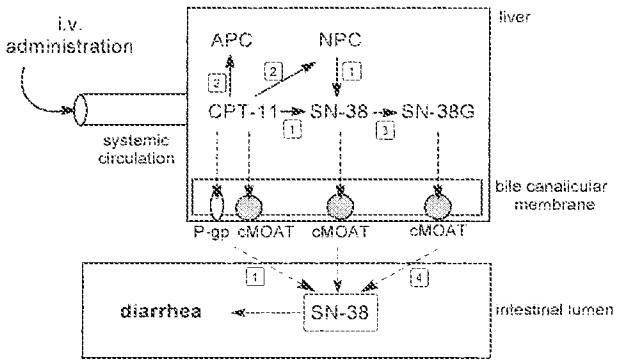

Fig. 3 Primary active transport systems for CPT-11 and its metabolites in the bile canalicular membrane of humans indicating the hypothesis for the mechanism of toxicity caused by i.v. administration of CPT-11 [modified from Sugiyama *et al.* (105)]. *1*, carboxylesterase-mediated conversion; *2*, CYP3A-mediated conversion; *3*, UGT1A-mediated conversion; *4*, β-glucuronidase-mediated conversion.

boxylate, SN-38 carboxylate, and both SN-38G carboxylate and lactone (101). For CPT-11 carboxylate, cMOAT appeared to be a low-affinity transporter, whereas a high-affinity transporter is still unknown (102). For SN-38G lactone and carboxylate, cMOAT is the high-affinity transporter, whereas a low-affinity transporter most likely also exists, presumably P-gp. It has also been found that cMOAT transports SN-38G carboxylate more efficiently than its lactone form (102). In humans, the same transport mechanisms by cMOAT of CPT-11 carboxylate, SN-38 carboxylate, and SN-38G were found as in rats (Fig. 3; Ref. 103).

Cyclosporin A, an inhibitor of the biliary secretion (104), and a known substrate and inhibitor of P-gp (105), significantly increased plasma concentrations of CPT-11, SN-38, and SN-38G in rats (104). At a cyclosporin A dose of 60 mg/kg, the AUCs of CPT-11, SN-38, and SN-38G increased 2–4-fold. This is most likely the result of reduced renal and nonrenal clearance, which simultaneously was reduced by 55 and 81%, respectively. Simultaneously, the terminal disposition half-lives of CPT-11 and its metabolites were substantially prolonged. The conversion of CPT-11 into SN-38 was not altered, but the glucuronidation of SN-38 decreased in comparison to CPT-11 infusion without cyclosporin A (104). In view of these results, it has been suggested that P-gp is one of the high-affinity transporters of CPT-11 carboxylate (106). However, similar to P-gp, cMOAT function may also be inhibited by cyclosporin A or other substrates and modulators (106). Therefore, inhibition has been studied at various concentrations of CPT-11. Because the high-affinity component is most active at substrate concentrations of 5 μM and cMOAT is most active at 250 μM, inhibitors of P-gp and cMOAT were compared at these concentrations. It appeared that P-gp substrates or modulators such as verapamil, PSC-833 (valspodar), or cyclosporin A inhibited the uptake of CPT-11 carboxylate most at concentrations of 5 μM. This suggests that P-gp might be the high-affinity component in CPT-11 carboxylate transport (106).

As an adverse effect, cyclosporin A also inhibits bilirubin excretion, and this may lead to hyperbilirubinemia (104). In the human Dubin-Johnson syndrome, chronic hyperbilirubinemia is seen as a result of a mutation in the *cMOAT* gene (107), and variability in the expression of this protein might play a role in the variability in experienced toxicity during CPT-11 treatment (103).

Fecal Excretion. In a mass balance study using radiolabeled CPT-11, fecal excretion was the major route of drug elimination, with 63.7% of the administered drug recovered (20). The unexpectedly high SN-38 concentrations and relatively low SN-38G concentrations in fecal specimens are suggestive for substantial β-glucuronidase activity in human intestinal contents, and consequently, the SN-38:SN-38G ratio was relatively high in all patients (20, 32). SN-38, APC, and NPC are mainly excreted in feces, 2.5 and 1.7% for SN-38 and NPC, respectively (32).

Considerations of Schedule and Route of Administration

Despite all kinds of dosing schedules, the total CPT-11 dose that can be tolerated in any time period is the same (23–25). Prolonged infusion times might theoretically improve the efficacy of CPT-11, because cytotoxicity of topoisomerase I inhibitors is S-phase specific (10), although the relevance of this principle for CPT-11, given the prolonged terminal disposition half-life of SN-38, is unclear. From xenograft models, it was known that low-dose protracted schedules of CPT-11 administration were more effective and less toxic than the usual higher dose, short infusion periods (108, 109). Chronic low-dose exposure of CPT-11 in patients has been studied recently (29, 39, 45, 110, 111) and revealed that the AUC ratios of lactone to total drug for CPT-11 and SN-38 were in the same range as for the shorter infusion periods (29). The maximal and recommended tolerated doses in these studies, 10–30 mg/m^2/day, are much lower for the prolonged infusions than for the shorter durations. Surprisingly, the SN-38 AUC levels reached similar values as compared with those of the shorter infusion periods, presumably reflecting saturation of enzymatic biotransformation with the latter schedules (29, 39, 45, 110).

Oral Administration. Clearly, the availability of a suitable oral formulation of CPT-11 would allow more convenient use of prolonged dosing schedules. When human liver and intestine S9 fractions were incubated with CPT-11, the agent was mostly hydrolyzed into SN-38 by liver, duodenal, jejunal, and ileal fractions and less by colon and rectal fractions (91, 112). Because it has been discovered that CEs are widely expressed in the human liver and gastrointestinal tract, it may be possible to effectively administer CPT-11 p.o. (112, 113), with the knowledge that substantial presystemic metabolism could take place. The low pH value of the stomach may be favorable for the retention of CPT-11 in its lactone form (113).

Oral administration of CPT-11 in mice resulted in peak concentrations of CPT-11 and SN-38 in plasma within 1 h after administration (114, 115), and the bioavailability of CPT-11 increased with increasing dose and amounted to 10–20% (115). In contrast, and of concern, the SN-38 AUC after oral administration did not correlate linearly with the dose, and in fact even decreased with increasing CPT-11 dose. It has been suggested that saturation of CE might cause this nonlinear correlation

(115), but the high levels of CE expressed in human intestinal tissues do not render this suggestion very likely (113). The higher SN-38 total:CPT-11 total ratios, compared with i.v. administration, suggest a presystemic CPT-11 conversion (116). Lactone *versus* carboxylate CPT-11 ratio was comparable with i.v. infusions, but the SN-38 ratio was much higher (113), suggesting a longer persistence of SN-38 lactone when it is given p.o. When CPT-11 was given orally to nude mice bearing human tumor xenografts, the agent retained its cytotoxic properties (53). Furthermore, in early clinical trials initial antitumor activity has been observed (113), suggesting that oral CPT-11 might be an attractive therapeutic option for the treatment of several human malignancies.

The uptake rates of [^{14}C]CPT-11 and [^{14}C]SN-38 from hamster intestinal epithelial cells and human colon carcinoma HT29 cells were recently published, providing important insight on the absorption characteristics of these agents (117). The lactone forms of CPT-11 and SN-38 were transported mainly by a passive diffusion, whereas the carboxylate forms were absorbed as a result of an active transport mechanism. Both compounds were transported significantly more in their lactone form, and the uptake rates showed a clear pH dependency, because the uptake decreased to 68% when the pH values were higher than 6.8. Lower SN-38 uptake rates also correlated with lower cytotoxicity (117). It was suggested that raising pH values in human intestines might decrease the reabsorption of the drug and as a result it will lower the intestinal side effects (117). The clinical utility of this concept is currently under further investigation. Clearly, demonstration of unaltered pharmacokinetics of SN-38 in the presence of intestinal alkalization is of crucial importance. Thus, although these investigators have shown that this concept can reduce CPT-11-induced intestinal toxicity, this may be a pyrrhic victory if a simultaneously altered metabolic clearance (by way of a decreased enterohepatic recirculation of SN-38) results in reduced antitumor activity.

i.p. Administration. i.p. administration of CPT-11 has also been studied recently and may have some potential advantages over the i.v. route. It appeared that the therapy was more effective and less toxic in mice bearing C26 colon cancers (118). In mice bearing P388 leukemia ascites, substantially elevated peritoneal AUCs of CPT-11 and SN-38 were found, whereas the achieved plasma levels were comparable with those after i.v. dosing (118). If the i.p. administration of CPT-11 does not prove to have major local toxicities, this administration pathway might be an asset for the adjuvant therapy of colorectal cancer.

Pharmacokinetic-Pharmacodynamic Relationships

Relationships between pharmacokinetic parameters and CPT-11-induced side effects have been studied extensively. For abdominal cramps, nausea, vomiting, and anorexia, no correlation with any parameter has been found (23). For myelosuppression and diarrhea in relation to the AUCs of CPT-11 and SN-38, respectively, the findings are highly variable, and final conclusions cannot yet be drawn (Table 2; Refs. 21, 29, 45).

The product of the plasma AUC ratio of SN-38:SN-38G and the plasma CPT-11 AUC (*i.e.*, the biliary index) may be an important kinetic variable because it is thought to be correlated with SN-38 bile concentrations (66). Patients with high biliary indices, suggestive of high SN-38 biliary concentrations, in some studies experienced more severe diarrhea (grades 3 and 4 on the National Cancer Institute-Common Toxicity Criteria scale) than those with low biliary indices (31, 66), but this could not be confirmed in other studies (21, 119, 120). It has been hypothesized that consideration of interindividual differences in fecal β-glucuronidase activity would likely assist in a more accurate prediction of CPT-11-induced intestinal side effects and may provide a basis to modulate the experienced toxicity (32).

Table 2 Correlation between toxicities and the AUCs of CPT-11 and SN-38

Observed toxicity	CPT-11 AUC	SN-38 AUC	Refs.
Neutropenia	No	No	26, 29, 40, 45
	No	Yes	23, 39
	Yes	Yes	21, 22, 25, 27
Diarrhea	No	No	21, 23, 29, 45
	No	Yes	40
	Yes	No	26, 39
	Yes	Yes	22, 25, 27

Evaluation of Drug Interactions

Drug interactions may arise as a result of altered pharmacodynamics or pharmacokinetics of the drugs involved. In the case of pharmacokinetic interactions, this is usually attributable to modification of tissue disposition and metabolism of the drugs. These phenomena are of particular importance in cancer chemotherapy when cytotoxic agents are used, because of the increased risks of severe toxicity. Most of the data available currently to evaluate potential drug interactions with CPT-11 come from clinical trials of CPT-11 given in combination with one or more other anticancer agents (Table 3). Although in several cases only limited information is available, some (preliminary) conclusions can be drawn.

Pharmacokinetic interaction studies have been performed with cisplatin either given alone or in combination with vindesine (121, 122) or ifosfamide (123), and indicated unaltered disposition profiles of both CPT-11 and its metabolites at any dose level or sequence tested (124–126). Likewise, the pharmacokinetics of carboplatin were not influenced by CPT-11, although in one study, the AUC of both CPT-11 and SN-38 was lower than expected, suggesting increased clearance of CPT-11 when given together with carboplatin (127, 128). The basis for this apparent change in pharmacokinetic behavior is unknown, although an effect on CYP3A expression attributable to prior exposure to carboplatin cannot be excluded (129).

In a Japanese study, altered pharmacokinetics were also found when 5-fluorouracil was administered immediately after CPT-11 infusion (130). Compared with an earlier CPT-11 monotherapy study conducted by the same group, the AUC of CPT-11 substantially increased whereas the AUC of SN-38 decreased. An inhibition of CE by 5-FU was suggested to explain these unexpected results (130). Other studies did not find altered pharmacokinetics for this combination therapy or eventually with the further addition of leucovorin (folinic acid;

Table 3 Evaluation of pharmacokinetic interactions between CPT-11 and anticancer agents

Combination drug(s)	Dose (CPT-11) (mg/m^2)	Kinetic alterations	Refs
Carboplatin	5° (60)	AUC_{CPT-11} ↓; AUC_{SN-38} ↓	127, 128
Cisplatin	80 (260)	None	32, 119, 124, 125
Cisplatin/Vindesine	100/3.0 (37.5)	None	120, 121
Cisplatin/Ifosfamide	70/1.5 (60)	None	123
Docetaxel	75 (200)	None	135
	70 (250)	None	149
	50 (60)	None	150
Etoposide	80 (80)	None	30
5-Fluorouracil	500 (125)	AUC_{CPT-11} ↑; AUC_{SN-38} ↓	130
	2600 (80)	None	131, 132, 134
Oxaliplatin	85 (200)	None	148
Paclitaxel	175 (150)	AUC_{CPT-11} ↑; AUC_{SN-38} ↑	136, 137
	75 (50)	None	139
Raltitrexed	3.0 (350)	None	151

° Target AUC in mg·min/ml.

Table 4 Factors contributing to variability in response to CPT-11

Parameter	Source of variability	Example(s)
Dose selection	Patient's condition	Performance status
	Host sensitivity	Previous treatments
Systemic exposure	Concomitant drugs	Cyclosporin A (P-glycoprotein inhibitor)
		Valproic acid (UGT1A1 inhibitor)
		Phenobarbital (UGT1A1 inducer)
		Phenytoin (CYP3A4 inducer)
		Ketoconazole (CYP3A4 inhibitor)
	Pharmacogenetics	Gilbert's syndrome (UGT1A1 mutation)
		Crigler-Najjar type I syndrome (UGT1A1 deficiency)
		Dubin-Johnsson syndrome (cMOAT mutation)
	Altered organ functions	Hepatic dysfunction
Active site levels	Resistance mechanisms	P-glycoprotein
		BCRP
		Topoisomerase I mutations
		CYP3A4 and/or UGT1A1 overexpression

Refs. 131–134). The conclusion from the Japanese study has been criticized in view of the large interpatient variation and noncomparable patient populations (134).

Although no comparative pharmacokinetic data are available, it has also been suggested that an interaction or sequence-dependent effect is present for the combination of CPT-11 and docetaxel. Because both drugs are metabolized by CYP3A, competition might occur when these drugs are given sequentially, and as a result, the clearance of docetaxel might be decreased (135). A significant pharmacokinetic interaction has been observed between CPT-11 and paclitaxel, which is characterized by increased plasma levels of both CPT-11 and SN-38 (136). Similar reactions have also been reported in rats (137) and Cremophor EL, the vehicle used for paclitaxel formulation seems to play a major role (104). This type of interaction appears to be related to micellar encapsulation of certain agents in this vehicle and has also been demonstrated to occur with paclitaxel itself and anthracyclines (138). In any event, because this interaction occurs during the terminal disposition phase of CPT-11, in currently applied dosing schedules the interaction is likely of only minor importance. The combination of weekly administration of CPT-11 with a fixed dose of paclitaxel (75 mg/m^2) indicated that the sequence of drug administration did not affect elimination of CPT-11 (139). There was also no sequence-dependent, chemotherapy-related toxicity. To date, no other cytotoxic drug has been shown to affect the pharmacokinetics of CPT-11 or was affected itself by CPT-11.

Anticonvulsants, phenytoin and phenobarbital in particular, are known to induce several metabolic pathways relevant to xenobiotics. CYP3A4, in particular, has increased expression when patients are treated with these compounds. Indeed, a recent study in patients with recurrent or progressive malignant glioma receiving CPT-11 and phenytoin indicated that AUCs of CPT-11, SN-38, and SN-38G were approximately 40, 25, and 25%, respectively, of those determined previously in patients with metastatic colorectal cancer not receiving antiepileptics (140). Similarly, enzyme-inducing anticonvulsants significantly lowered systemic exposure to CPT-11 and SN-38 in children with newly diagnosed high-grade glioma (141). This interaction is of major importance because it suggests that anticonvulsants thereby largely reduce the potential antitumor effects of CPT-11. In addition to modulation of CYP3A4, another possible explanation for the interaction is the induction of membrane transporters that enhance drug excretion (142).

Conclusions and Perspectives

CPT-11, because of its broad spectrum of antitumor activity, is clearly one of the most important new anticancer drugs developed in the last few decades. The clinical pharmacokinetic behavior of CPT-11 has been explored extensively in recent years, and the generated information has been of fundamental importance in our understanding of the clinical effects of this agent (Table 4). In addition, a wealth of information has become available that has yielded valuable insight into the mechanism of action, the mechanisms of tumor resistance, toxicities, and considerations of dosage and schedule and route of drug administration. Many of these studies have been made possible by the development of selective analytical methodologies to specifically monitor the parent drug and individual metabolites, with sufficient sensitivity to detect the compounds at levels achieved after therapeutic dosing. However, only through further investigations that may allow better definition of the biochemistry and pharmacokinetics of CPT-11 can the rational optimization of therapy involving this agent be achieved. This need has become even more important in light of the current clinical use of CPT-11 in combination with other antineoplastic drugs or agents specifically administered to modify CPT-11-induced toxicity profiles (143). In this respect, the use of mathematical models to predict systemic exposure measures for CPT-11 and its metabolites by application of limited-sampling strategies (38, 41, 144–147), coupled with continued investigations into the role of individual enzyme expression levels and detection of enzyme polymorphism, will allow more rational and selective chemotherapy with this agent.

References

1. Wall, M. E., Wani, M. C., Cook, C. E., Palmer, K. H., McPhail, A. T., and Sim, G. A. Plant antitumor agents. I. The isolation and structure of camptothecine, a novel alkaloidal leukemia and tumor inhibitor from *Camptotheca acuminata*. J. Am. Chem. Soc., *88:* 3888–3890, 1966.

2. Muggia, F. M., Creaven, P. J., Hansen, H. H., Cohen, M. H., and Selawry, O. S. Phase I clinical trial of weekly and daily treatment with camptothecin (NSC-100880): correlation with preclinical studies. Cancer Chemother. Rep., *56:* 515–521, 1972.

3. Moertel, C. G., Schutt, A. J., Reitemeier, R. J., and Hahn, R. G. Phase II study of camptothecin (NSC-100880) in the treatment of advanced gastrointestinal cancer. Cancer Chemother. Rep., *56:* 95–101, 1972.

4. Schaeppi, U., Fleischman, R. W., and Cooney, D. A. Toxicity of camptothecin (NSC-100880). Cancer Chemother. Rep., *5:* 25–36, 1974.

5. Creemers, G. J., Lund, B., and Verweij, J. Topoisomerase I inhibitors. Topotecan and irinotecan. Cancer Treat. Rev., *20:* 73–96, 1994.

6. Rajkumar, S. V., and Adjei, A. A. A review of the pharmacology and clinical activity of new chemotherapeutic agents in lung cancer. Cancer Treat. Rev., *24:* 35–53, 1998.

7. Hsiang, Y-H., Hertzberg, R., Hecht, S., and Liu, L. F. Camptothecin induces protein-linked DNA breaks via mammalian DNA topoisomerase I. J. Biol. Chem., *260:* 14873–14878, 1985.

8. Hsiang, Y-H., and Liu, L. F. Identification of mammalian DNA topoisomerase I as an intracellular target of the anticancer drug camptothecin. Cancer Res., *48:* 1722–1726, 1988.

9. Hsiang, Y-H., Lihou, M. G., and Liu, L. F. Arrest of replication forks by drug-stabilized topoisomerase I-DNA cleavable complexes as a mechanism of cell killing by camptothecin. Cancer Res., *49:* 5077–5082, 1989.

10. Gerrits, C. J. H., de Jonge, M. J. A., Schellens, J. H. M., Stoter, G., and Verweij, J. Topoisomerase I inhibitors: the relevance of prolonged exposure for clinical development. Br. J. Cancer, *76:* 952–962, 1997.

11. O'Leary, J., and Muggia, F. M. Camptothecins: a review of their development and schedules of administration. Eur. J. Cancer, *34:* 1500–1508, 1998.

12. Gelderblom, H. A., de Jonge, M. J. A., Sparreboom, A., and Verweij, J. Oral topoisomerase I inhibitors in adult patients: present and future. Investig. New Drugs, *17:* 401–415, 1999.

13. Kunimoto, T., Nitta, K., Tanaka, T., Uehara, N., Baba, H., Takeuchi, M., Yokokura, T., Sawada, S., Miyasaka, T., and Mutai, M. Antitumor activity of 7-ethyl-10-[4-(1-piperidino)-1-piperidino]carbonyloxy-camptothecin, a novel water-soluble derivative of camptothecin, against murine tumors. Cancer Res., *47:* 5944–5947, 1987.

14. Kingsbury, W. D., Boehm, J. C., Jakas, D. R., Holden, K. G., Hecht, S. M., Gallagher, G., Caranfa, M. J., McCabe, F. L., Faucette, L. F., and Johnson, R. K. Synthesis of water-soluble (aminoalkyl)camptothecin analogues: inhibition of topoisomerase I and antitumor activity. J. Med. Chem., *34:* 98–107, 1991.

15. Pantazis, P., Harris, N., Mendoza, J., and Giovanella, B. The role of pH and serum albumin in the metabolic conversion of 9-nitrocamptothecin to 9-aminocamptothecin by human hematopoietic and other cells. Eur. J. Haematol., *55:* 211–213, 1995.

16. Loos, W. J., Sparreboom, A., Verweij, J., Nooter, K., Stoter, G., and Schellens, J. H. M. Determination of the lactone and lactone plus carboxylate forms of 9-aminocamptothecin in human plasma by sensitive high-performance liquid chromatography with fluorescence detection. J. Chromatogr. B, *694:* 435–441, 1997.

17. Blaney, S., M., Takimoto, C., Murry, D. J., Kuttesch, N., McCully, C., Cole, D. E., Godwin, K., and Balis, F. M. Plasma and cerebrospinal fluid pharmacokinetics of 9-aminocamptothecin (9-AC), irinotecan (CPT-11), and SN-38 in nonhuman primates. Cancer Chemother. Pharmacol., *41:* 464–468, 1998.

18. Emerson, D. L., Besterman, J. M., Brown, H. R., Evans, M. G., Leitner, P. P., Luzzio, M. J., Shaffer, J. E., Sternbach, D. D., Uehling, D., and Vuong, A. *In vivo* antitumor activity of two new seven-substituted water-soluble camptothecin analogues. Cancer Res., *55:* 603–609, 1995.

19. Vey, N., Giles, F. J., Kantarjian, H., Smith, T. L., Beran, M., and Jeha, S. The topoisomerase I inhibitor DX-8951f is active in a severe combined immunodeficient mouse model of human acute myelogenous leukemia. Clin. Cancer Res., *6:* 731–736, 2000.

20. Slatter, J. G., Schaaf, L. J., Sams, J. P., Feenstra, K. L., Johnson, M. G., Bombardt, P. A., Cathcart, K. S., Verburg, M. T., Pearson, L. K., Compton, L. D., Miller, L. L., Baker, D. S., Pesheck, C. V., and Lord, R. S. Pharmacokinetics, metabolism, and excretion of irinotecan (CPT-11) following i.v. infusion of [^{14}C]CPT-11 in cancer patients. Drug Metab. Dispos., *28:* 423–433, 2000.

21. Canal, P., Gay, C., Dezeuze, A., Douillard, J. Y., Bugat, R., Brunet, R., Adems, A., Herait, P., Lokiec, F., and Mathieu-Boue, A. Pharmacokinetics and pharmacodynamics of irinotecan during a Phase II clinical trial in colorectal cancer. J. Clin. Oncol., *14:* 2688–2695, 1996.

22. Abigerges, D., Chabot, G. G., Armand, J-P., Herait, P., Gouyette, A., and Gandia, D. Phase I and pharmacologic studies of the camptothecin analog irinotecan administered every 3 weeks in cancer patients. J. Clin. Oncol., *13:* 210–221, 1995.

23. Rowinsky, E. K., Grochow, L. B., Ettinger, D. S., Sartorius, S. E., Lubejko, B. G., Chen, T. L., Rock, M. K., and Donehower, R. C. Phase I and pharmacological study of the novel topoisomerase I inhibitor 7-ethyl-10-[4-(1-(piperidino)-1-piperidino] carbonyloxycamptothecin (CPT-11) administered as a ninety-minute infusion every 3 weeks. Cancer Res., *54:* 427–436, 1994.

24. Rothenberg, M. L., Kuhn, J. G., Burris, H. A., Nelson, J., Eckardt, J. R., Tristan-Morales, M., Hilsenbeck, S. G., Weiss, G. R., Smith, L. S., and Rodriguez, G. I. Phase I and pharmacokinetic trial of weekly CPT-11. J. Clin. Oncol., *11:* 2194–2204, 1993.

25. de Forni, M., Bugat, R., Chabot, G. G., Culine, S., Extra, J. M., Gouyette, A., Madelaine, I., Marty, M. E., and Mathieu-Boue, A. Phase

I and pharmacokinetic study of the camptothecin derivative irinotecan, administered on a weekly schedule in cancer patients. Cancer Res., *54:* 4347–4354, 1994.

26. Catimel, G., Chabot, G. G., Guastalla, J. P., Dumortier, A., Cote, C., Engel, C., Gouyette, A., Mathieu-Boue, A., Mahjoubi, M., and Clavel, M. Phase I and pharmacokinetic study of irinotecan (CPT-11) administered daily for three consecutive days every three weeks in patients with advanced solid tumors. Ann. Oncol., *6:* 133–140, 1995.

27. Sasaki, Y., Hakusui, H., Mizuno, S., Morita, M., Miya, T., Eguchi, K., Shinkai, T., Tamura, T., Ohe, Y., and Saijo, N. A pharmacokinetic and pharmacodynamic analysis of CPT-11 and its active metabolite SN-38. Jpn. J. Cancer Res., *86:* 101–110, 1995.

28. Pitot, H. C., Goldberg, R. M., Reid, J. M., Sloan, J. A., Skaff, P. A., Erlichman, C., Rubin, J., Burch, P. A., Adjei, A. A., Alberts, S. A., Schaaf, L. J., Elfring, G., and Miller, L. L. Phase I dose-finding and pharmacokinetic trial of irinotecan hydrochloride (CPT-11) using a once-every-three-week dosing schedule for patients with advanced solid tumor malignancy. Clin. Cancer Res., *6:* 2236–2244, 2000.

29. Herben, V. M. M., Schellens, J. H. M., Swart, M., Gruia, G., Vermillet, L., Beijnen, J. H., and ten Bokkel Huinink, W. W. Phase I and pharmacokinetic study of irinotecan administered as a low-dose, continuous intravenous infusion over 14 days in patients with malignant solid tumors. J. Clin. Oncol., *17:* 1897–1905, 1999.

30. Masuda, N., Fukuoka, M., Kudoh, S., Matsui, K., Kusunoki, Y., Takada, M., Nakagawa, K., Hirashima, T., Tsukada, H., and Yana, T. Phase I and pharmacologic study of irinotecan and etoposide with recombinant human granulocyte colony-stimulating factor support for advanced lung cancer. J. Clin. Oncol., *12:* 1833–1841, 1994.

31. Gupta, E., Mick, R., Ramirez, J., Wang, X., Lestingi, T. M., Vokes, E. E., and Ratain, M. J. Pharmacokinetic and pharmacodynamic evaluation of the topoisomerase I inhibitor irinotecan in cancer patients. J. Clin. Oncol., *15:* 1502–1510, 1997.

32. Sparreboom, A., de Jonge, M. J. A., de Bruijn, P., Brouwer, E., Nooter, K., Loos, W. J., van Alphen, R. J., Mathijssen, R. H. J., Stoter, G., and Verweij, J. Irinotecan (CPT-11) metabolism and disposition in cancer patients. Clin. Cancer Res., *4:* 2747–2754, 1998.

33. Sasaki, Y., Yoshida, Y., Sudoh, K., Hakusui, H., Fujii, H., Ohtsu, T., Wakita, H., Igarashi, T., and Itoh, K. Pharmacological correlation between total drug concentration and lactones of CPT-11 and SN-38 in patients treated with CPT-11. Jpn. J. Cancer Res., *86:* 111–116, 1995.

34. Rivory, L. P., Chatelut, E., Canal, P., Mathieu-Boue, A., and Robert, J. Kinetics of the *in vivo* interconversion of the carboxylate and lactone forms of irinotecan and of its metabolite SN-38 in patients. Cancer Res., *54:* 6330–6333, 1994.

35. Chabot, G. G., Abigerges, D., Catimel, G., Culine, S., de Forni, M., Extra, J. M., Mahjoubi, M., Herait, P., Armand, J. P., and Bugat, R. Population pharmacokinetics and pharmacodynamics of irinotecan (CPT-11) and active metabolite SN-38 during Phase I trials. Ann. Oncol., *6:* 141–151, 1995.

36. Rivory, L. P., Haaz, M-C., Canal, P., Lokiec, F., Armand, J. P., and Robert, J. Pharmacokinetic interrelationships of irinotecan (CPT-11) and its three major plasma metabolites in patients enrolled in Phase I/II trials. Clin. Cancer Res., *3:* 1261–1266, 1997.

37. Loos, W. J., Verweij, J., Geiderblom, H. A., de Jonge, M. J. A., Brouwer, E., Dallaire, B. K., and Sparreboom, A. Role of erythrocytes and serum proteins in the kinetic profile of total 9-amino-20(*S*)-camptothecin in humans. Anti-Cancer Drugs, *10:* 705–710, 1999.

38. Mathijssen, R. H. J., van Alphen, R. J., de Jonge, M. J. A., Verweij, J., de Bruijn, P., Loos, W. J., Nooter, K., Vermillet, L., Stoter, G., and Sparreboom, A. Sparse-data set analysis for irinotecan and SN-38 pharmacokinetics in cancer patients co-treated with cisplatin. Anti-Cancer Drugs, *10:* 9–16, 1999.

39. Ohe, Y., Sasaki, Y., Shinkai, T., Eguchi, K., Tamura, T., Kojima, A., Kunikane, H., Okamoto, H., Karato, A., and Ohmatsu, H. Phase I study and pharmacokinetics of CPT-11 with 5-day continuous infusion. J. Natl. Cancer Inst. (Bethesda), *84:* 972–973, 1992.

40. Rothenberg, M. L., Eckardt, J. R., Kuhn, J. G., Burris, H. A., Nelson, J., Hilsenbeck, S. G., Rodriguez, G. I., Thurman, A. M., Smith, L. S., Eckhardt, S. G., Weiss, G. R., Elfring, G. L., Rinaldi, D. A., Schaaf, L. J., and Von Hoff, D. D. Phase II trial of irinotecan in patients with progressive or rapidly recurrent colorectal cancer. J. Clin. Oncol., *14:* 1128–1135, 1996.

41. Mick, R., Gupta, E., Vokes, E. E., and Ratain, M. J. Limited-sampling models for irinotecan pharmacokinetics-pharmacodynamics: prediction of biliary index and intestinal toxicity. J. Clin. Oncol., *14:* 2012–2019, 1996.

42. Rothenberg, M. L., Kuhn, J. G., Schaaf, L. J., Eckhardt, S. G., Villalona-Calero, M. A., Petit, R. G., Miller, L. L., Elfring, G. L., Murphy, T. C., and Von Hoff, D. D. Phase I and pharmacokinetic study of intravenous irinotecan (CPT-11) administered once every 2 weeks +/− G-CSF. Ann. Oncol., *10:* 63, 1998.

43. Kehrer, D. F. S., Yamamoto, W., Verweij, J., de Jonge, M. J. A., de Bruijn, P., and Sparreboom, A. Factors involved in prolongation of the terminal disposition phase of SN-38: clinical and experimental studies. Clin. Cancer Res., *6:* 3451–3458, 2000.

44. Combes, O., Barré, J., Duché, J-C., Vermillet, L., Archimbaud, Y., Marietta, M. P., Tillement, J. P., and Urien, S. *In vitro* binding and partitioning of irinotecan (CPT-11) and its metabolite, SN-38, in human blood. Investig. New Drugs, *18:* 1–5, 2000.

45. Ma, M. K., Zamboni, W. C., Radomski, K. M., Furman, W. L., Santana, V. M., Houghton, P. J., Hanna, S. K., Smith, A. K., and Stewart, C. F. Pharmacokinetics of irinotecan and its metabolites SN-38 and APC in children with recurrent solid tumors after protracted low-dose irinotecan. Clin. Cancer Res., *6:* 813–819, 2000.

46. Burke, T. G., and Mi, Z. H. The structural basis of camptothecin interactions with human serum albumin: impact on drug stability. J. Med. Chem., *37:* 40–46, 1994.

47. Burke, T. G., Munshi, C. B., Mi, Z. H., and Jiang, Y. The important role of albumin in determining the relative human blood stabilities of the camptothecin anticancer drugs. J. Pharm. Sci., *84:* 518–519, 1995.

48. Slatter, J. G., Su, P., Sams, J. P., Schaaf, L. J., and Wienkers, L. C. Bioactivation of the anticancer agent CPT-11 to SN-38 by human hepatic microsomal carboxylesterases and the *in vitro* assessment of potential drug interactions. Drug Metab. Dispos., *25:* 1157–1164, 1997.

49. Humerickhouse, R., Lohrbach, K., Li, L., Bosron, W. F., and Dolan, M. E. Characterization of CPT-11 hydrolysis by human liver carboxylesterase isoforms hCE-1 and hCE-2. Cancer Res., *60:* 1189–1192, 2000.

50. Wierdl, M., Morton, C. L., Danks, M. K., and Potter, P. M. Isolation and characterization of a cDNA encoding a horse liver butyrylcholinesterase: evidence for CPT-11 drug activation. Biochem. Pharmacol., *59:* 773–781, 2000.

51. Morton, C. L., Wadkins, R. M., Danks, M. K., and Potter, P. M. The anticancer prodrug CPT-11 is a potent inhibitor of acetylcholinesterase but is rapidly catalyzed to SN-38 by butyrylcholinesterase. Cancer Res., *59:* 1458–1463, 1999.

52. Haaz, M-C., Rivory, L. P., Riché, C., and Robert, J. The transformation of irinotecan (CPT-11) to its active metabolite SN-38 by human liver microsomes. Naunyn Schmiedebergs Arch. Pharmacol., *356:* 257–262, 1997.

53. Kawato, Y., Furuta, T., Aonuma, M., Yasuoka, M., Yokokura, T., and Matsumoto, K. Antitumor activity of a camptothecin derivative, CPT-11, against human tumor xenografts in nude mice. Cancer Chemother. Pharmacol., *28:* 192–198, 1991.

54. Takaoka, K., Ohtsuka, K., and Jin, M. Conversion of CPT-11 to its active form SN-38, by carboxylesterase of non-small cell lung cancer. Proc. Am. Soc. Clin. Oncol., *16:* 252, 1997.

55. van Ark-Otte, J., Kedde, M. A., van der Vijgh, W. J. F., Dingemans, A. M., Jansen, W. J., Pinedo, H. M., Boven, E., and Giaccone, G. Determinants of CPT-11 and SN-38 activities in human lung cancer cells. Br. J. Cancer, *77:* 2171–2176, 1998.

56. Guichard, S., Terret, C., Hennebelle, I., Lochon, I., Chevreau, P., Fretigny, E., Selves, J., Chatelut, E., Bugat, R., and Canal, P. CPT-11 converting carboxylesterase and topoisomerase I activities in tumour and normal colon and liver tissues. Br. J. Cancer, *80:* 364–370, 1999.

57. Kojima, A., Hackett, N. R., Ohwada, A., and Crystal, R. G. *In vivo* human carboxylesterase cDNA gene transfer to activate the prodrug CPT-11 for local treatment of solid tumors. J. Clin. Investig., *101:* 1789–1796, 1998.

58. Kojima, A., Hackett, N. R., and Crystal, R. G. Reversal of CPT-11 resistance of lung cancer cells by adenovirus-mediated gene transfer of the human carboxylesterase cDNA. Cancer Res., *58:* 4368–4374, 1998.

59. Danks, M. K., Morton, C. L., Krull, E. J., Cheshire, P. J., Richmond, L. B., Naeve, C. W., Pawlik, C. A., Houghton, P. J., and Potter, P. M. Comparison of activation of CPT-11 by rabbit and human carboxylesterases for use in enzyme/prodrug therapy. Clin. Cancer Res., *5:* 917–924, 1999.

60. Satoh, T., Hosokawa, M., Atsumi, R., Suzuki, W., Hakusui, H., and Nagai, E. Metabolic activation of CPT-11, 7-ethyl-10-[4-(1-piperidino)-1-piperidino]carbonyloxycamptothecin, a novel antitumor agent, by carboxylesterase. Biol. Pharm. Bull., *17:* 662–664, 1994.

61. Inaba, M., Ohmichi, Y., Ishii, H., Tanioka, Y., Yoshida, Y., Sudoh, K., Hakusui, H., Mizuno, N., Ito, K., and Sugiyama, Y. Pharmacokinetics of CPT-11 in rhesus monkeys. Cancer Chemother. Pharmacol., *41:* 103–108, 1998.

62. Danks, M. K., Morton, C. L., Pawlik, C. A., and Potter, P. M. Overexpression of a rabbit liver carboxylesterase sensitizes human tumor cells to CPT-11. Cancer Res., *58:* 20–22, 1998.

63. Iyer, L., King, C. D., Whitington, P. F., Green, M. D., Roy, S. K., Tephly, T. R., Coffman, B. L., and Ratain, M. J. Genetic predisposition to the metabolism of irinotecan (CPT-11). J. Clin. Investig., *101:* 847–854, 1998.

64. Rivory, L. P., and Robert, J. Identification and kinetics of a β-glucuronide metabolite of SN-38 in human plasma after administration of the camptothecin derivative irinotecan. Cancer Chemother. Pharmacol., *36:* 176–179, 1995.

65. Atsumi, R., Suzuki, W., and Hakusui, H. Identification of the metabolites of irinotecan, a new derivative of camptothecin, in rat bile and its biliary excretion. Xenobiotica, *21:* 1159–1169, 1991.

66. Gupta, E., Lestingi, T. M., Mick, R., Ramirez, J., Vokes, E. E., and Ratain, M. J. Metabolic fate of irinotecan in humans: correlation of glucuronidation with diarrhea. Cancer Res., *54:* 3723–3725, 1994.

67. Ciotti, M., Basu, N., Brangi, M., and Owens, I. S. Glucuronidation of 7-ethyl-10-hydroxycamptothecin (SN-38) by the human UDP-glucuronosyltransferases encoded at the *UGT1* locus. Biochem. Biophys. Res. Commun., *260:* 199–202, 1999.

68. Ando, Y., Saka, H., Asai, G., Sugiura, S., Shimokata, K., and Kamataki, T. *UGT1A1* genotypes and glucuronidation of SN-38, the active metabolite of irinotecan. Ann. Oncol., *9:* 845–847, 1998.

69. Iyer, L., Hall, D., Das, S., Mortell, M. A., Ramirez, J., Kim, S., di Rienzo, A., and Ratain, M. Phenotype-genotype correlation of *in vitro* SN-38 (active metabolite of irinotecan) and bilirubin glucuronidation in human liver tissue with UGT1A1 promoter polymorphism. Clin. Pharmacol. Ther., *65:* 576–582, 1999.

70. Monaghan, G., Ryan, M., Seddon, R., Hume, R., and Burchell, B. Genetic variation in bilirubin UDP-glucuronosyltransferase gene promoter and Gilbert's syndrome. Lancet, *347:* 578–581, 1996.

71. Wasserman, E., Myara, A., Lokiec, F., Goldwasser, F., Trivin, F., Maljoubi, M., Misset, J. L., and Cvitkovic, E. Severe CPT-11 toxicity in patients with Gilbert's syndrome: two case reports. Ann. Oncol., *8:* 1049–1051, 1997.

72. Wasserman, E., Myara, A., Lokiec, F., Riofio, M., Imadalou, P., Bleuzen, P., Santoni, J., Trivin, F., Herait, P., Mahjoubi, M., Armand, J. P., Misset, J. L., and Cvitkovic, E. Bilirubin (BIL) and SN-38: pharmacokinetic/pharmacodynamics correlation. Ann. Oncol., *10:* 58, 1998.

73. Ando, Y., Saka, H., Ando, M., Sawa, T., Muro, K., Ueoka, H., Yokoyama, A., Saitoh, S., Shimokata, K., and Hasegawa, Y. Polymorphisms of UDP-glucuronosyltransferase gene and irinotecan toxicity: a pharmacogenetic analysis. Cancer Res., *60:* 6921–6926, 2000.

74. Gupta, E., Wang, X., Ramirez, J., and Ratain, M. J. Modulation of glucuronidation of SN-38, the active metabolite of irinotecan, by valproic acid and phenobarbital. Cancer Chemother. Pharmacol., *39:* 440–444, 1997.

75. Takahashi, T., Fujiwara, Y., Yamakido, M., Katoh, O., Watanabe, H., and Mackenzie, P. I. The role of glucuronidation in 7-ethyl-10-hydroxycamptothecin resistance *in vitro*. Jpn. J. Cancer Res., *88:* 1211–1217, 1997.

76. Brangi, M., Litman, T., Ciotti, M., Nishiyama, K., Kohlhagen, G., Takimoto, C., Robey, R., Pommier, Y., Fojo, T., and Bates, S. E. Camptothecin resistance: role of the ATP-binding cassette (ABC), mitoxantrone-resistance half-transporter (MXR), and potential for glucuronidation in MXR-expressing cells. Cancer Res., *59:* 5938–5946, 1999.

77. Lokiec, F., Monegier du Sorbier, B., and Sanderink, G-J. Irinotecan (CPT-11) metabolites in human bile and urine. Clin. Cancer Res., *2:* 1943–1949, 1996.

78. Haaz, M-C., Rivory, L. P., Riché, C., Vernillet, L., and Robert, J. Metabolism of irinotecan (CPT-11) by hepatic microsomes: participation of cytochrome P-450 3A and drug interactions. Cancer Res., *58:* 468–472, 1998.

79. Santos, A., Zannetta, S., Cresteil, T., Deroussent, A., Pein, F., Raymond, E., Vernillet, L., Risse, M. L., Boige, V., Gouyette, A., and Vassal, G. Metabolism of irinotecan (CPT-11) by CYP3A4 and CYP3A5 in humans. Clin. Cancer Res., *6:* 2012–2020, 2000.

80. Dodds, H. M., Haaz, M-C., Riou, J-F., Robert, J., and Rivory, L. P. Identification of a new metabolite of CPT-11 (irinotecan): pharmacological properties and activation to SN-38. J. Pharmacol. Exp. Ther., *286:* 578–583, 1998.

81. Haaz, M-C., Riché, C., Rivory, L. P., and Robert, J. Biosynthesis of an aminopiperidino metabolite of irinotecan [7-ethyl-10-[4-(1-piperidino]carbonyloxycamptothecine] by human hepatic microsomes. Drug Metab. Dispos., *26:* 769–774, 1998.

82. Dodds, H. M., Wunsch, R. M., Gillam, E. M. J., and Rivory, L. P. Further elucidation of the pathways involved in the catabolism of the camptothecin analogue irinotecan. Proc. Am. Assoc. Cancer Res., *40:* 110, 1999.

83. Rivory, L. P., Riou, J-F., Haaz, M-C., Sable, S., Vuilhorgne, M., Commercon, A., Pond, S. M., and Robert, J. Identification and properties of a major plasma metabolite of irinotecan (CPT-11) isolated from the plasma of patients. Cancer Res., *56:* 3689–3694, 1996.

84. Dodds, H. M., Haaz, M-C., Riou, J. F., Robert, J., and Rivory, L. P. Identification of a new metabolite of CPT-11 (irinotecan): pharmacological properties and activation to SN-38. J. Pharmacol. Exp. Ther., *286:* 578–583, 1998.

85. Massaad, L., de Waziers, I., Ribrag, V., Janot, F., Beaune, P. H., Morizet, J., Gouyette, A., and Chabot, G. G. Comparison of mouse and human colon tumors with regard to Phase I and Phase II drug-metabolizing enzyme systems. Cancer Res., *52:* 6567–6575, 1992.

86. Rivory, L. P., Bowles, M. R., Robert, J., and Pond, S. M. Conversion of irinotecan (CPT-11) to its active metabolite, 7-ethyl-10-hydroxycamptothecin (SN-38), by human liver carboxylesterase. Biochem. Pharmacol., *52:* 1103–1111, 1996.

87. Dresser, G. K., Spence, J. D., and Bailey, D. G. Pharmacokinetic-pharmacodynamic consequences and clinical relevance of cytochrome P450 3A4 inhibition. Clin. Pharmacokinet., *38:* 41–57, 2000.

88. Skar, V., Skar, A. G., and Stromme, J. H. β-Glucuronidase activity related to bacterial growth in common bile duct bile in gallstone patients. Scand. J. Gastroenterol., *23:* 83–90, 1988.

89. Yokoi, T., Narita, M., Nagai, E., Hagiwara, H., Aburada, M., and Kamataki, T. Inhibition of UDP-glucuronosyltransferase by aglycons of natural glucuronides in kampo medicines using SN-38 as a substrate. Jpn. J. Cancer Res., *86:* 985–989, 1995.

90. Sperker, B., Backman, J. T., and Kroemer, H. K. The role of β-glucuronidase in drug disposition and drug targeting in humans. Clin. Pharmacokinet., *33:* 18–31, 1997.

91. Takasuna, K., Hagiwara, T., Hirohashi, M., Kato, M., Nomura, M., Nagai, E., Yokoi, T., and Kamataki, T. Involvement of β-glucuronidase in intestinal microflora in the intestinal toxicity of the antitumor camptothecin derivative irinotecan hydrochloride (CPT-11) in rats. Cancer Res., *56:* 3752–3757, 1996.

92. Kase, Y., Hayakawa, T., Togashi, Y., and Kamataki, T. Relevance of irinotecan hydrochloride-induced diarrhea to the level of prostaglandin E2 and water absorption of large intestine in rats. Jpn. J. Pharmacol., *75:* 399–405, 1997.

93. Araki, E., Ishikawa, M., Iigo, M., Koide, T., Itabashi, M., and Hoshi, A. Relationship between development of diarrhea and the concentration of SN-38, an active metabolite of CPT-11, in the intestine and the blood plasma of athymic mice following intraperitoneal administration of CPT-11. Jpn. J. Cancer Res., *84:* 697–702, 1993.

94. Takasuna, K., Hagiwara, T., Hirohashi, M., Kato, M., Nomura, M., Nagai, E., Yokoi, T., and Kamataki, T. Inhibition of intestinal microflora β-glucuronidase modifies the distribution of the active metabolite of the antitumor agent irinotecan hydrochloride (CPT-11) in rats. Cancer Chemother. Pharmacol., *42:* 280–286, 1998.

95. Fujisawa, T., and Mori, M. Influence of various bile salts on β-glucuronide activity of intestinal bacteria. Appl. Microbiol., *25:* 95–97, 1997.

96. Cole, C. B., Fuller, R., Mallet, A. K., and Rowland, I. R. The influence of the host on expression of intestinal microbial enzyme activities involved in metabolism of foreign compounds. J. Appl. Bacteriol., *59:* 549–553, 1985.

97. Van Huyen, J. P., Bloch, F., Attar, A., Levoir, D., Kreft, C., Molina, T., and Bruneval, P. Diffuse mucosal damage in the large intestine associated with irinotecan (CPT-11). Dig. Dis. Sci., *43:* 2649–2651, 1998.

98. Mallett, A. K., Bearne, C. A., and Rowland, I. R. The influence of incubation pH on the activity of rat and human gut flora enzymes. J. Appl. Bacteriol., *66:* 433–437, 1989.

99. Planting, A. S. T. Modulation of irinotecan pharmacokinetics/pharmacodynamics by combined treatment with neomycin. Proc. Am. Soc. Clin. Oncol., *19:* 1007, 2000.

100. Lokiec, F., Canal, P., Gay, C., Chatelut, E., Armand, J. P., Reche, H., Bugat, R., Goncalves, E., and Matieu-Boue, A. Pharmacokinetics of irinotecan and its metabolites in human blood, bile and urine. Cancer Chemother. Pharmacol., *36:* 79–82, 1995.

101. Chu, X-Y., Kato, Y., Niinuma, K., Sudo, K. I., Hakusui, H., and Sugiyama, Y. Multispecific organic anion transporter is responsible for the biliary excretion of the camptothecin derivative irinotecan and its metabolites in rats. J. Pharmacol. Exp. Ther., *281:* 304–314, 1997.

102. Chu, X-Y., Kato, Y., and Sugiyama, Y. Multiplicity of biliary excretion mechanisms for irinotecan, CPT-11, and its metabolites in rats. Cancer Res., *57:* 1934–1938, 1997.

103. Chu, X-Y., Kato, Y., Ueda, K., Suzuki, H., Niinuma, K., Tyson, C. A., Weizer, V., Dabbs, J. E., Froehlich, R., Green, C. E., and Sugiyama, Y. Biliary excretion mechanism of CPT-11 and its metabolites in humans: involvement of primary active transporters. Cancer Res., *58:* 5137–5143, 1998.

104. Gupta, E., Safa, A. R., Wang, X., and Ratain, M. J. Pharmacokinetic modulation of irinotecan and metabolites by cyclosporin A. Cancer Res., *56:* 1309–1314, 1996.

105. Sugiyama, Y., Kato, Y., and Chu, X-Y. Multiplicity of biliary excretion mechanisms for the camptothecin derivative irinotecan (CPT-11), its metabolite SN-38, and its glucuronide: role of canalicular multispecific organic anion transporter and P-glycoprotein. Cancer Chemother. Pharmacol., *42:* S44–S49, 1998.

106. Chu, X-Y., Kato, Y., and Sugiyama, Y. Possible involvement of P-glycoprotein in biliary excretion of CPT-11 in rats. Drug Metab. Dispos., *27:* 440–441, 1999.

107. Paulusma, C. C., Kool, M., Bosma, P. J., Scheffer, G. L., ter Borg, F., Scheper, R. J., Tytgat, G. N., Borst, P., Baas, F., and Oude Elferink, R. P. A mutation in the human canalicular multispecific organic anion transporter gene causes the Dubin-Johnson syndrome. Hepatology, *25:* 1539–1542, 1997.

108. Houghton, P. J., Cheshire, P. J., Hallman, J. D., Lutz, L., Friedman, H. S., Danks, M. K., and Houghton, J. A. Efficacy of topoisomerase I inhibitors, topotecan and irinotecan, administered at low dose levels in protracted schedules to mice bearing xenografts of human tumors. Cancer Chemother. Pharmacol., *36:* 393–403, 1995.

109. Thompson, J., Zamboni, W. C., Cheshire, P. J., Lutz, L., Luo, X., Li, Y., Houghton, J. A., Stewart, C. F., and Houghton, P. J. Efficacy of systemic administration of irinotecan against neuroblastoma xenografts. Clin. Cancer Res., *3:* 423–431, 1997.

110. Takimoto, C. H., Morrison, G., Harold, N., Quinn, M., Monahan, B. P., Band, R. A., Cottrell, J., Guemei, A., Llorens, V., Behman, H., Ismail, A. S., Flemming, D., Gosky, D. M., Hirota, H., Berger, S. J., Berger, N. A., Chen, A. P., Shapiro, J. D., Arbuck, S. G., Wright, J., Hamilton, J. M., Allegra, C. J., and Grem, J. L. Phase I and pharmacologic study of irinotecan administered as a 96-hour infusion weekly to adult cancer patients. J. Clin. Oncol., *18:* 659–667, 2000.

111. Furman, W. L., Stewart, C. F., Poquette, C. A., Pratt, C. B., Santana, V. M., Zamboni, W. C., Bowman, L. C., Ma, M. K., Heffer, F. A., Meyer, W. H., Pappo, A. S., Walter, A. W., and Houghton, P. J. Direct translation of a protracted irinotecan schedule from a xenograft model to a Phase I trial in children. J. Clin. Oncol., *17:* 1815–1824, 1999.

112. Ahmed, F., Vyas, V., Cornfield, A., Goodin, S., Ravikumar, T. S., Rubin, E. H., and Gupta, E. *In vitro* activation of irinotecan to SN-38 by human liver and intestine. Anticancer Res., *19:* 2067–2072, 1999.

113. Drengler, R. L., Kuhn, J. G., Schaaf, L. J., Rodriguez, G. I., Villalona-Calero, M. A., Hammond, L. A., Stephenson, J. A., Hodges, S., Kraynak, M. A., Staton, B. A., Eiring, G. L., Locker, P. K., Miller, L. L., Von Hoff, D. D., and Rothenberg, M. L. Phase I and pharmacokinetic trial of oral irinotecan administered daily for 5 days every 3 weeks in patients with solid tumors. J. Clin. Oncol., *17:* 685–696, 1999.

114. Zamboni, W. C., Houghton, P. J., Thompson, J., Cheshire, P. J., Hanna, S. K., Richmond, L. B., Lou, X., and Stewart, C. F. Altered irinotecan and SN-38 disposition after intravenous and oral administration of irinotecan in mice bearing human neuroblastoma xenografts. Clin. Cancer Res., *4:* 455–462, 1998.

115. Stewart, C. F., Zamboni, W. C., Crom, W. R., and Houghton, P. J. Disposition of irinotecan and SN-38 following oral and intravenous irinotecan dosing in mice. Cancer Chemother. Pharmacol., *41:* 259–265, 1997.

116. Radomski, K. M., Stewart, C. F., Panetta, J. C., Houghton, P. J., and Furman, W. L. Phase I and pharmacokinetic study of oral irinotecan in pediatric patients with solid tumors. Proc. Am. Soc. Clin. Oncol., *41:* 592a, 2000.

117. Kobayashi, K., Bouscarel, B., Matsuzaki, Y., Ceryak, S., Kudoh, S., and Fromm, H. pH-dependent uptake of irinotecan and its active metabolite, SN-38, by intestinal cells. Int. J. Cancer, *83:* 491–496, 1999.

118. Guichard, S., Chatelut, E., Lochon, I., Bugat, R., Mahjoubi, M., and Canal, P. Comparison of the pharmacokinetics and efficacy of irinotecan after administration by the intravenous *versus* intraperitoneal route in mice. Cancer Chemother. Pharmacol., *42:* 165–170, 1998.

119. de Jonge, M. J. A., Sparreboom, A., Planting, A. S. T., van der Burg, M. E. L., de Boer-Dennert, M. M., ter Steeg, J., Jaques, C., and Verweij, J. Phase I study of 3-week schedule of irinotecan combined with cisplatin in patients with advanced solid tumors. J. Clin. Oncol., *18:* 187–194, 2000.

120. de Jonge, M. J. A., Verweij, J., de Bruijn, P., Brouwer, E., Mathijssen, R. H. J., van Alphen, R. J., de Boer-Dennert, M. M., Vermillet, L., Jacques, C., and Sparreboom, A. Pharmacokinetic, metabolic, and pharmacodynamic profiles in a dose-escalating study of irinotecan and cisplatin. J. Clin. Oncol., *18:* 195–203, 2000.

121. Shinkai, T., Arioka, H., Kunikane, H., Eguchi, K., Sasaki, Y., Tamura, T., Ohe, Y., Oshita, F., Nishio, M., and Karato, A. Phase I clinical trial of irinotecan (CPT-11), 7-ethyl-10[4-(1-piperidino)-1-piperidino]carbonyloxy-camptothecin, and cisplatin in combination with fixed dose of vindesine in advanced non-small cell lung cancer. Cancer Res., *54:* 2636–2642, 1994.

122. Mogi, H., Hasegawa, Y., Watanabe, A., Nomura, F., Saka, H., and Shimokata, K. Combination effects of cisplatin, vinorelbine and irinotecan in non-small-cell lung cancer cell lines *in vitro*. Cancer Chemother. Pharmacol., *39:* 199–204, 1997.

123. Fujita, A., Takabatake, H., Tagaki, S., and Sekine, K. Phase I/II study of cisplatin, ifosfamide and irinotecan with rhG-CSF support in

patients with stage IIIB and IV non-small-cell lung cancer. Cancer Chemother. Pharmacol., *45:* 279–283, 2000.

124. DeVore, R. F., Johnson, D. H., Crawford, J., Garst, J., Dimery, I. W., Eckardt, J., Eckhardt, S. G., Elfring, G. L., Schaaf, L. J., Hanover, C. K., and Miller, L. L. Phase II study of irinotecan plus cisplatin in patients with advanced non-small-cell lung cancer. J. Clin. Oncol., *17:* 2710–2720, 1999.

125. Kudoh, S., Fukuoka, M., Masuda, N., Yoshikawa, A., Kusunoki, Y., Matsui, K., Negoro, S., Takifuji, N., Nakagawa, K., and Hirashima, T. Relationship between the pharmacokinetics of irinotecan and diarrhea during combination chemotherapy with cisplatin. Jpn. J. Cancer Res., *86:* 406–413, 1995.

126. de Jonge, M. J. A., Verweij, J., Planting, A. S. T., van der Burg, M. E. L., Stoter, G., de Boer-Dennert, M. M., de Bruijn, P., Brouwer, E., Vermilet, L., and Sparreboom, A. Drug-administration sequence does not change pharmacodynamics and kinetics of irinotecan and cisplatin. Clin. Cancer Res., *5:* 2012–2017, 1999.

127. Okamoto, H., Nagatomo, A., Kunitoh, H., Kunikane, H., and Watanabe, K. A Phase I clinical and pharmacologic study of a carboplatin and irinotecan regimen combined with recombinant human granulocyte-colony stimulating factor in the treatment of patients with advanced non-small cell lung carcinoma. Cancer (Phila.), *82:* 2166–2172, 1998.

128. Fukuda, M., Oka, M., Soda, H., Terashi, K., Kawabata, S., Nakatomi, K., Takatani, H., Tsunetani, J., Tsukamoto, K., Noguchi, Y., Fukuda, M., Kinoshita, A., and Kohno, S. Phase I study of irinotecan combined with carboplatin in previously untreated solid cancers. Clin. Cancer Res., *5:* 3963–3969, 1999.

129. LeBlanc, G. A., Sundseth, S. S., Weber, G. F., and Waxman, D. J. Platinum anticancer drugs modulate P-450 mRNA levels and differentially alter hepatic drug and steroid hormone metabolism in male and female rats. Cancer Res., *52:* 540–547, 1992.

130. Sasaki, Y., Ohtsu, A., Shimada, Y., Ono, K., and Saijo, N. Simultaneous administration of CPT-11 and fluorouracil: alteration of the pharmacokinetics of CPT-11 and SN-38 in patients with advanced colorectal cancer. J. Natl. Cancer Inst. (Bethesda), *86:* 1096–1097, 1994.

131. Saltz, L. B., Kanowitz, J., Kemeny, N. E., Schaaf, L., Spriggs, D., Staton, B. A., Berkery, R., Steger, C., Eng, M., Dietz, A., Locker, P., and Kelsen, D. P. Phase I clinical and pharmacokinetic study of irinotecan, fluorouracil, and leucovorin in patients with advanced solid tumors. J. Clin. Oncol., *14:* 2959–2967, 1996.

132. Vanhoefer, U., Harstrick, A., Köhne, C-H., Achterrath, W., Rustum, Y. M., Seeber, S., and Wilke, H. Phase I study of a weekly schedule of irinotecan, high-dose leucovorin, and infusional fluorouracil as a first-line chemotherapy in patients with advanced colorectal cancer. J. Clin. Oncol., *17:* 907–913, 1999.

133. Benhammouda, A., Bastian, G., and Rixe, O. A Phase I and pharmacokinetic study of CPT-11 and 5-FU (F) combination. Proc. Am. Soc. Clin. Oncol., *16:* 202, 1997.

134. Saltz, L., Shimada, Y., and Khayat, D. CPT-11 (irinotecan) and 5-fluorouracil: a promising combination for therapy of colorectal cancer. Eur. J. Cancer, *32A:* S24–S31, 1996.

135. Adjei, A. A., Klein, C. E., Kastrissios, H., Goldberg, R. M., Alberts, S. R., Patot, H. C., Sloan, J. A., Reid, J. M., Hanson, L. J., Atherton, P., Rubin, J., and Erlichman, C. Phase I and pharmacokinetic study of irinotecan and docetaxel in patients with advanced solid tumors: preliminary evidence of clinical activity. J. Clin. Oncol., *18:* 1116–1123, 2000.

136. Asai, G., Yamamoto, N., and Sakai, S. Paclitaxel (Taxol) affects pharmacokinetics of irinotecan and its metabolites. Proc. Am. Soc. Clin. Oncol., *18:* 201a, 1999.

137. Yamamoto, N., Negoro, S., Chikazawa, H., Shimizu, T., and Fukuoka, M. Pharmacokinetic interaction of the combination of paclitaxel and irinotecan *in vivo* and clinical study. Proc. Am. Soc. Clin. Oncol., *18:* 186a, 1999.

138. van Zuylen, L., Verweij, J., and Sparreboom, A. Role of formulation vehicles in taxane pharmacology. Investig. New Drugs, *19:* 125–141, 2001.

139. Murren, J. R., Peccerillo, K., DiStasio, S. A., Li, X., Leffert, J. J., Pizzorno, G., Burtness, B. A., McKeon, A., and Cheng, Y. Dose escalation and pharmacokinetic study of irinotecan in combination with paclitaxel in patients with advanced cancer. Cancer Chemother. Pharmacol., *46:* 43–50, 2000.

140. Friedman, H. S., Petros, W. P., Friedman, A. H., Schaaf, L. J., Kerby, T., Lawyer, J., Parry, M., Houghton, P. J., Lovell, S., Rasheed, K., Cloughsey, T., Stewart, E. S., Colvin, O. M., Provenzale, J. M., McLendon, R. E., Bigner, D. D., Cokgor, I., Haglund, M., Rich, J., Ashley, D., Malczyn, J., Elfring, G. L., and Miller, L. L. Irinotecan therapy in adults with recurrent or progressive malignant glioma. J. Clin. Oncol., *17:* 1516–1525, 1999.

141. Gajjar, A. J., Radomski, K. M., Bowers, D. C., Chintagumpala, M. M., Thompson, S. J., Houghton, P. J., and Stewart, C. F. Pharmacokinetics of irinotecan (IRN) and metabolites in pediatric high-grade glioma patients with and without co-administration of enzyme-inducing anticonvulsants. Proc. Am. Soc. Clin. Oncol., *19:* 162a, 2000.

142. Grossman, S. A., Hochberg, F., Fisher, J., Chen, T-L., Kim, L., Gregory, R., Grochow, L. B., and Piantadosi, S. Increased 9-aminocamptothecin dose requirements in patients on anticonvulsants. Cancer Chemother. Pharmacol., *42:* 118–126, 1998.

143. Kehrer, D. F. S., Sparreboom, A., Verweij, J., de Bruijn, P., Nierop, C. A., van der Schraaf, J., Ruijgrok, E. J., and de Jonge, M. J. A. Modulation of irinotecan-induced diarrhea by cotreatment with neomycin in cancer patients. Clin. Cancer Res., *7:* 1136–1141, 2001.

144. Chabot, G. G. Limited sampling models for simultaneous estimation of the pharmacokinetics of irinotecan and its active metabolite SN-38. Cancer Chemother. Pharmacol., *36:* 463–472, 1995.

145. Sasaki, Y., Mizuno, S., Fujii, H., Ohtsu, T., Wakita, H., Igarashi, T., Itoh, K., Sekine, I., Miyata, Y., and Saijo, N. A limited sampling model for estimating pharmacokinetics of CPT-11 and its metabolite SN-38. Jpn. J. Cancer Res., *86:* 117–123, 1995.

146. Nakashima, H., Lieberman, R., Kanato, A., Aroka, H., Ohmatsu, H., Nomura, N., Shiraishi, J., Tamura, T., Eguchi, K., and Shinkai, T. Efficient sampling strategies for forecasting pharmacokinetic parameters of irinotecan (CPT-11): implication for area under the concentration-time curve monitoring. Ther. Drug Monit., *17:* 221–229, 1995.

147. Yamamoto, N., Tamura, T., Kanato, A., Uenaka, K., Eguchi, K., Shinkai, T., Ohe, Y., Oshita, F., Arioka, H., and Nakashima, H. CPT-11: population pharmacokinetic model and estimation of pharmacokinetics using the bayesian method in patients with lung cancer. Jpn. J. Cancer Res., *85:* 972–977, 1994.

148. Wasserman, E., Cuvier, C., Lokiec, F., Goldwasser, F., Kaila, S., Mery-Mignard, D., Ouldkaci, M., Besmaine, A., Dupont-Andre, G., Mahjoubi, M., Marty, M., Misset, J. L., and Cvitkovic, E. Combination of oxaliplatin plus irinotecan in patients with gastrointestinal tumors: results of two independent Phase I studies with pharmacokinetics. J. Clin. Oncol., *17:* 902–906, 1999.

149. Couteau, C., Risse, M. L., Ducreux, M., Lefresne-Soulas, F., Riva, A., Lebecq, A., Ruffie, P., Rougier, P., Lokiec, F., Bruno, R., and Armand, J. P. Phase I and pharmacokinetic study of docetaxel and irinotecan in patients with advanced solid tumors. J. Clin. Oncol., *18:* 3545–3552, 2000.

150. Masuda, N., Negoro, S., Kudoh, S., Sugiura, T., Nakagawa, K., Saka, H., Takada, M., Nutani, H., and Fukuoka, M. Phase I and pharmacologic study of docetaxel and irinotecan in advanced non-small-cell lung cancer. J. Clin. Oncol., *18:* 2996–3003, 2000.

151. Ford, H. E., Cunningham, D., Ross, P. J., Rao, S., Aherne, G. W., Benepal, T. S., Price, T., Massey, A., Vermilet, L., and Gnua, G. Phase I study of irinotecan and raltitrexed in patients with advanced gastrointestinal tract adenocarcinoma. Br. J. Cancer, *83:* 146–152, 2000.

Clinical Cancer Research

Clinical Pharmacokinetics and Metabolism of Irinotecan (CPT-11)

Ron H. J. Mathijssen, Robbert J. van Alphen, Jaap Verweij, et al.

Clin Cancer Res 2001;7:2182-2194.

Differential effects of two fluorouracil administration regimens for colorectal cancer

SATOSHI MATSUSAKA[1,2], HAJIME YAMASAKI[2], YOSHIHIRO KITAYAMA[2], TOSHIHIRO OKADA[2] and SHIGETO MAEDA[2]

[1]Department of Surgery, Sano Hospital, Shimizugaoka 2-5-1, Tarumi-ku, Kobe, Hyogo 655-0031; [2]Department of Surgery, Takarazuka Municipal Hospital, Kohama 4-5-1, Takarazuka, Hyogo 665-0827, Japan

Received April 29, 2002; Accepted July 11, 2002

Abstract. Mechanisms of anti-tumor action of 5-fluorouracil (5-FU) are presumed to inhibit DNA synthesis and RNA function, and the balance of these mechanisms is presumed to depend on the modalities of administration. On the other hand, variability of 5-FU sensitivity of the tumors is also presumed to depend on the enzymes of 5-FU metabolism (e.g. dihydropyrimidine dehydrogenase, DPD, rate limiting enzyme of catabolism) and action target (e.g. thymidylate synthase; TS). We studied the effects of modalities of administration and enzyme activities related to metabolism and target of 5-FU on the mechanism of anti-tumor action in patients with colorectal cancer. Thirty-eight patients who were diagnosed at stage II to IV preoperatively were enrolled. Patients were randomly assigned to receive 24-h protracted IV infusion of 5-FU at 320 mg/m²/day for 5 days (CIV group: 18 patients) or 10-min bolus IV infusion of 5-FU at the same dosage for 5 days (BIV group: 20 patients) administered from the 5th preoperative day. Specimens from the tumor and non-tumor regions were obtained by operation. F-RNA (fraudulent-RNA, or 5-FU in RNA) concentration, an indicator for action of 5-FU to RNA, and the enzyme activities of DPD and TS, an indicator for action of 5-FU to DNA, in the collected specimens were measured by GC-MS or RI-HPLC. F-RNA concentration (ng/mg-RNA) in the tumor and non-tumor region in the CIV group was 100.58±16.88 and 50.11±6.03, respectively, with a significant difference between them ($P<0.05$), and in the tumor and non-tumor region in the BIV group was 195.32±16.26 and 121.05±10.62, respectively, with a significant difference between them ($P<0.01$). F-RNA concentration in the tumor and non-tumor regions in the BIV group was significantly higher than those in the CIV group ($P<0.05$). DPD activity and TS activity were not significantly different between the CIV and the BIV groups in the tumor and non-tumor region, respectively. F-RNA concentration was negatively correlated to DPD activity ($r=-0.540$, $P<0.05$) in the tumor region in the CIV group. F-RNA was not correlated to DPD activity in the non-tumor region in the CIV group or in the tumor and non-tumor region in the BIV group. F-RNA was not correlated to TS activity in the tumor or non-tumor region of the two groups. DPD activity was not correlated to TS activity in the tumor or non-tumor region of the two groups. BIV inhibited RNA function more potently than CIV and this was not dependent on TS or DPD activity. As for the inhibition of DNA synthesis, other indicators should be considered further.

Introduction

5-FU is a compound developed by Heidelberger *et al* (1) and Duschinsky *et al* (2) and is important in chemotherapy of gastrointestinal cancer. One of the mechanisms of anti-tumor action of 5-FU is inhibition of DNA synthesis. Fluorodeoxyuridine monophosphate (FdUMP), an active metabolite of 5-FU, inhibits TS activity in the conversion of deoxyuridine monophosphate (dUMP) to thymidine monophosphate (dTMP), essential in DNA synthesis and repair, forming a ternary complex with 5,10-methylene tetrahydrofolate (5,10-CH_2-FH_4), a reduced form of folic acid, and TS (3-8). Another mechanism of anti-tumor action is inhibition of RNA function. Fluorouridine triphosphate (FUTP), another active metabolite of 5-FU, was incorporated into RNA, and, as a result, RNA function was inhibited (9-13) (Nayak *et al*, Proc Am Assoc Cancer Res 19: abs. 63, 1978). High concentration (10 to 100 μM, i.e. 1.3 to 13 μg/ml) of 5-FU is needed to inhibit RNA function (13), while low concentration (0.5 to 1.0 μM) is needed to inhibit DNA synthesis *in vitro* (8). Many studies show that action targets of 5-FU differ by the modality of administration (CIV is thought to be dominant for inhibition of DNA synthesis, BIV for inhibition of RNA function). On the other hand, relative balance of these mechanisms also depends on biochemical features of tumor cells (e.g. DPD and TS activity). It seems to be closely related to the most effective modality of administration of 5-FU and biochemical features of tumor cells, but it has not been clarified clinically (14).

Correspondence to: Dr Satoshi Matsusaka, Department of Surgery, Sano Hospital, Shimizugaoka 2-5-1, Tarumi-ku, Kobe, Hyogo 655-0031, Japan
E-mail: s8matsu@m09.alpha-net.ne.jp

Key words: colorectal cancer, 5-fluorouracil, thymidylate synthase, dihydropyrimidine dehydrogenase, fraudulent-RNA

The purpose of this study was to investigate the effects of modalities of administration and enzyme activities related to target and metabolism of 5-FU on the mechanism of anti-tumor action in patients with colorectal cancer.

Materials and methods

From November 2000 to July 2001 at Takarazuka Municipal Hospital, 38 colorectal cancer patients who were diagnosed at stage II to IV preoperatively were enrolled in this study. Written informed consent was obtained from all patients. Patients were randomly assigned to receive 24-h protracted IV infusion of 5-FU at 320 mg/m^2/day for 5 days (CIV group: 18 patients) or 30-min bolus IV infusion of 5-FU at the same dosage for 5 days (BIV group: 20 patients) administered from the 5th preoperative day. Specimens from the tumor and non-tumor regions were obtained by operation and stored at -80˚C until analyses. F-RNA concentration, an indicator for action of 5-FU to RNA, and the enzyme activities of DPD and TS, an indicator for action of 5-FU to DNA, in the collected specimens were measured by GC-MS or RI-HPLC.

F-RNA concentration. F-RNA concentration was measured according to the method described by Masuike *et al* (15) but followed with the alteration to the below benzylation from trimethylsilylation of 5-FU.

Purification of RNA and preparation of mononucleotide. Frozen tissues were homogenized in cold water and to the homogenate was added cold 10% trichloroacetic acid, and centrifuged (2,330 x g, 5 min, 24˚C). The precipitate was purified by the procedure of mixing, centrifuging and removing the supernatant once with cold 10% trichloroacetic acid, once with 70% ethanol, once with 95% ethanol, and twice with a mixture of ethanol:ether (3:1). The purified precipitate was reacted at 37˚C for 16 to 20 h with 0.3N-KOH, then neutralized with 83.6 µl of 60% $HClO_4$. Then the mixture was centrifuged (2,330 x g, 10 min, 24˚C) and 140 µl of 3N-KOH was added. The mononucleotide was obtained after removing $KClO_4$ precipitate from the mixture.

5-FU concentration in RNA. Mononucleotide was hydrolyzed at 100˚C for 20 h with an equi-volume of hydrochloric acid and the internal standard (IS: 1,3-[$^{15}N_2$]-5-FU) solution. After washing the reaction with chloroform, the solution was evaporated to dryness under stream of nitrogen. The residue was reconstituted with 1 M phosphate buffer (pH 4.0) and extracted with ethyl acetate. The extract was passed through the silica gel column, and then 5-FU fraction was collected. 5-FU was derivatized with 3,5-di-(trifluoromethyl) benzyl bromide described by Bates *et al* (16), and this derivative was assayed by GC-MS to determine 5-FU concentration. RNA content was measured according to the method described by Brown (17) with slight modifications. F-RNA concentration was expressed as ng 5-FU per mg RNA (ng/mg-RNA).

DPD activity in tissues. DPD activity was measured according to the method described by Diasio *et al* (18) with slight modifications. Tissues were homogenized in an enzyme extraction buffer [containing 20 mM phosphate buffer (pH 8.0), 1 mM EDTA-2K and 1 mM 2-mercaptoethanol] and centrifuged (105,000 x g, 1 h, 4˚C). The supernatant (250 µl) was incubated with 12.5 µl of 6.25 mM NADPH and 30 µl of [6-^{3}H]-5-FU (125 µM, 25 µCi/ml) at 37˚C. After 10, 20 and 30-min incubation at 37˚C, the reaction was stopped by addition of 70 µl of 5% $HClO_4$ solution to 70 µl of each sample. The sample was mixed with 140 µl of 20 mM phosphate buffer (pH 3.5) as a mobile phase, and centrifuged, then the supernatant was analyzed by RI-HPLC. Reaction rate was calculated from the amount of 5-FU and its catabolites 5-fluorodihydrouracil (5-FDHU), 2-fluoro-3-ureidopropionate (FUPA) and 2-fluoro-ß-alaninae (FBAL). DPD activity was expressed as pmol of [^{3}H]-5-FU catabolized per min per mg protein (pmol/min/mg protein), based on the linear regression obtained from the incubation time.

TS activity in tissues. TS activity was measured according to the method described by Etienne *et al* (19) with slight modifications. Tissues were homogenized in an enzyme extraction buffer (containing 2 mM dithiothreitol and 50 mM Tris-HCl pH 7.3) and centrifuged (105,000 x g, 1 h, 4˚C). The supernatant (25 µl) was incubated with 20 µl of 0.32 mM methyltetrahydrofolate and 10 µl of 250 µM [^{3}H]-dUMP, as a substrate, at 37˚C. After 10, 20 and 30-min incubation at 37˚C, the reaction was stopped by addition of 300 µl of 4% trichloroacetic acid containing 10% activated charcoal, removing excess of [^{3}H]-dUMP. Reaction rate was calculated from $[^3H]_2O$ formed during the incubation in the supernatant measured using a liquid scintillation counter.

TS activity was expressed as pmol of $[^3H]_2O$ formed per min per mg protein (pmol/min/mg protein), based on the linear regression obtained from the incubation time.

Statistical analysis. Measured values were expressed as mean ± standard error. Software (Statcel company) was used for all calculations. Wilcoxon signed-ranks tests were performed for inter-group and -region analysis of F-RNA concentration, DPD and TS activity. The correlation between F-RNA concentration and DPD activity, as well as the correlation between TS activity and DPD activity, and between F-RNA concentration and TS activity either in the tumor or in the non-tumor regions or the CIV and BIV groups was analyzed by Spearman rank correlation. All P-values cited are two-sided and the limit of statistical significance was P=0.05.

Results

Patient characteristics. Thirty-eight patients were enrolled in this study.The characteristics of the CIV group (7 male, 11 female) were as follows: the mean age was 62.8 years (range: 51 to 80 years), histological stage distribution was I in 4, II in 5, III in 6 and IV in 3, histological tissue type distribution was well differentiated adenocarcinoma in 11, moderately differentiated adenocarcinoma in 6, mucinous adeno-carcinoma in 1, lymphatic invasion (ly) was ly (+) in 14, ly (-) in 4, vessel invasion (v) was v (+) in 12, v (-) in 6. The characteristics of the BIV group (15 male, 5 female) were as follows: the mean age was 61.2 years (range: 49 to 76 years), histological stage distribution was I in 5, II in 7, III in 6 and

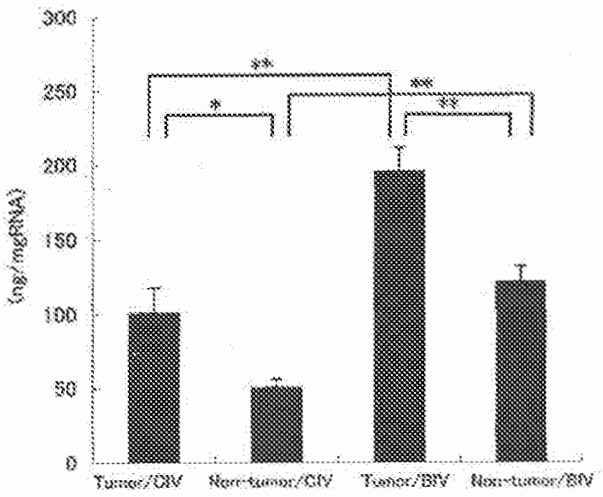

Figure 1. F-RNA concentrations (mean ± standard error) in the tumor and non-tumor regions in the CIV and BIV groups. *P<0.05; **P<0.01.

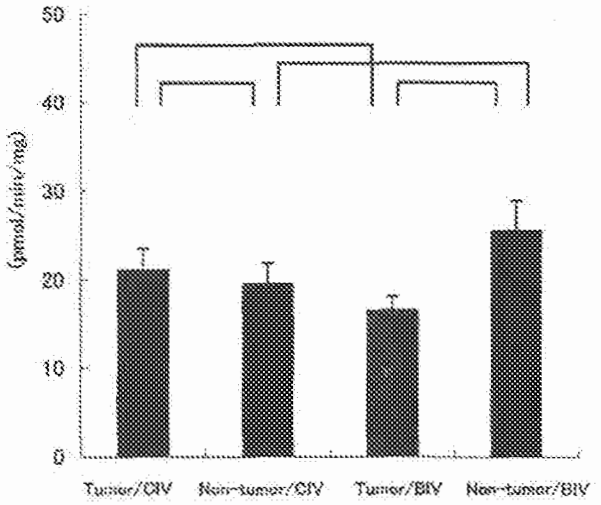

Figure 2. DPD activities (mean ± standard error) in the tumor and non-tumor regions in the CIV and BIV groups.

IV in 2, histological tissue type distribution was well differentiated adenocarcinoma in 13, moderately differentiated adenocarcinoma in 7, lymphatic invasion was ly (+) in 19, ly (-) in 1, vessel invasion was v (+) in 15, v (-) in 5. No significant difference was observed in the above characteristics between the groups.

F-RNA concentration. In the CIV group, F-RNA concentration (ng/mg-RNA) in the tumor and non-tumor region was 100.58±16.88 and 50.11±6.03, respectively, with a significant difference between them (P<0.05). In the BIV group, F-RNA concentration in the tumor and non-tumor region was 195.32±16.26 and 121.05±10.62, respectively, with a significant difference between them (P<0.01). In the tumor region, F-RNA concentration was higher in the BIV group than in the CIV group with a significant difference (P<0.01). The BIV group also showed higher F-RNA concentration in the non-tumor region with a significant difference (P<0.01) (Fig. 1).

DPD activity. In the CIV group, DPD activity (pmol/min/mg protein) in the tumor and non-tumor region was 21.06±2.47 and 19.50±2.36, respectively, with no significant difference between them. In the BIV group, DPD activity in the tumor and non-tumor region was 16.50±1.60 and 25.47±3.38, respectively, with no significant difference between them. There was no significant difference either in the tumor or non-tumor region between the the groups (Fig. 2).

TS activity. In the CIV group, TS activity (pmol/min/mg protein) in the tumor and non-tumor region was 5.45±0.77 and 4.33±1.67, respectively, with no significant difference between them. In the BIV group, TS activity in the tumor and non-tumor region was 4.01±2.51 and 2.68±1.49, respectively, with no significant difference between them. There was no significant difference in the tumor or non-tumor region between the the groups (Fig. 3).

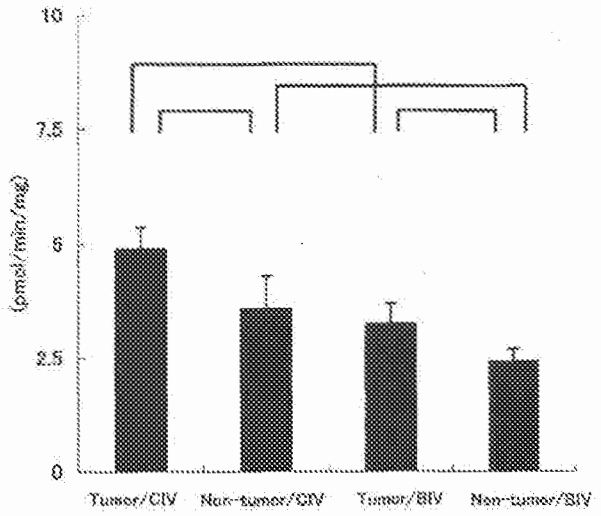

Figure 3. TS activities (mean ± standard error) in the tumor and non-tumor regions in the CIV and BIV groups.

Correlation between F-RNA concentration and DPD activity. The correlation between F-RNA concentration and DPD activity was studied. In the tumor region of the CIV group, these factors were significantly correlated (correlation coefficient; r=-0.540, P<0.05). No correlation was found in the non-tumor region in the CIV group. In the BIV group, there was no correlation in the tumor or non-tumor region.

Correlation between TS activity and DPD activity. The correlation between TS activity and DPD activity was studied. No correlation was found in either of the regions in the CIV or in the BIV group.

Correlation between F-RNA concentration and TS activity. The correlation between F-RNA concentration and TS activity was studied. No correlation was found in either of the regions in the CIV or in the BIV group.

Discussion

In the present study, we approached the questions on the difference of anti-tumor mechanisms of action depending on the modality of administration of 5-FU (CIV and BIV) by measuring F-RNA concentration and the enzyme activities of DPD and TS. F-RNA concentration was measured as indication for action of 5-FU to RNA. Higher F-RNA concentration was achieved by BIV than by CIV. This clinical result is supported by many experimental results *in vitro* and *in vivo* that high concentration of 5-FU had anti-tumor effect rather through inhibition of RNA function compared with inhibition of DNA synthesis (8,13,14).

TS activity was measured as an indicator of action of 5-FU to DNA (3-8,20,21). TS activity after preoperative administration of 5-FU was not significantly different between the CIV group and BIV group in the tumor and non-tumor region. These clinical results were not consistent with previous studies that CIV had anti-tumor effect mainly through inhibition of DNA synthesis (22-28). In the present study, we noted TS activity as an indicator for action of 5-FU to DNA. Further study is required to investigate whether consistent results will be obtained when assessing this action using the amount of TS enzyme or TS inhibition ratio (TSIR; defined as [(total TS amount - FdUMP unbound TS amount)/total TS amount]) as an indicator of action of 5-FU to DNA. We are going to investigate this action using TSIR. Inhibition of DNA synthesis is achieved by inhibiting the conversion of dUMP to FdUMP to form a stable ternary complex with TS, FdUMP and a reduced form of folic acid. Thus, the amount of the reduced form of folic acid in tissues seems to affect the anti-tumor effect of 5-FU (29). It may be necessary to consider measuring its amount in tissues, as an indication of action of 5-FU to DNA.

Negative correlation between F-RNA concentration and DPD activity in the CIV group suggests that, from the aspect of inhibition of RNA function as the anti-tumor effects, patients with elevated DPD activity in the tumor region may not respond well to 5-FU given by CIV. F-RNA concentration dose is not dependent on the DPD activity in the BIV group, on the contrary, it may suggest that more anti-tumor effect is expected by BIV than by CIV in those patients. Tumors with elevated DPD activity have been considered to be 5-FU resistant (20,30-32), but they may respond well to 5-FU changing the modality of administration.

The present study did not show a correlation between TS activity and DPD activity. However, it seems to be difficult to conclude from this result that anti-tumor effect through inhibition of DNA synthesis is independent of DPD. However, mechanism of action of 5-FU to DNA was assessed using only TS activity as an indicator in the present study and the other indication, e.g. the amount of TS protein, TSIR, and the amount of the reduced form of folic acid in tissues, should be also considered in future studies.

We showed that when 5-FU was administered by BIV, higher concentration of F-RNA in the tumor region is achieved than by CIV and this is not dependent on DPD activity. Whereas F-RNA concentration is dependent on DPD activity when administered by CIV. Patients with elevated DPD activity in the tumor region should not be recommended for administration by CIV due to 5-FU (CIV)-resistance from the aspect of inhibition of RNA function in the mechanism of anti-tumor action of 5-FU. We can expect anti-tumor effect of 5-FU by BIV for those patients.

We conclude the administration modality of 5-FU should be considered by DPD activity in the tumor. The effects of TS activity on considering the modality of 5-FU administration is not definitely concluded based on our results. Anti-tumor effect of 5-FU through DNA synthesis inhibition needs further studies.

References

1. Heidelberger C, Chaudhuri NK, Danneberg P, *et al*: Fluorinated pyrimidine, A new class of tumor inhibitory compounds. Nature 179: 663-666, 1957.
2. Duschinsky R, Pleven E and Heidelberger C: The synthesis of 5-fluoropyrimidines. J Am Chem Soc 79: 4559, 1957.
3. Hartman KY and Heidelberger C: Studies on fluorinated pyrimidines, XIII. Inhibition of thymidylate synthase. J Biol Chem 236: 3006-3013, 1961.
4. Langenbach RJ, Danenberg PV and Heidelberger C: Thymidilate synthase: mechanism of inhibition by 5-fluoro-2'-deoxyuridylate. Biochem Biophys Res Commun 48: 1565-1571, 1972.
5. Santi DV and McHenry CS: 5-fluoro-2'-deoxyuridylate; covalent complex with thymidylate synthase. Proc Natl Acad Sci USA 69: 1855-1857, 1972.
6. Spears CP, Shahinian AH, Moran RG, *et al*: *In vivo* kinetics of thymidylate synthase inhibition in 5-fluorouracil-sensitive and-resistant murine colon adenocarcinomas. Cancer Res 42: 450-456, 1982.
7. Spears CP, Gustavsson BG, Mitchell MS, *et al*: Thymidylate synthase inhibition in malignant tumors and normal liver of patients given intravenous 5-fluorouracil. Cancer Res 44: 4144-4150, 1984.
8. Parker WB and Cheng YC: Metabolism and mechanism of action of 5-fluorouracil. Pharmacol Ther 48: 381-395, 1990.
9. Takiuchi H and Ajani JA: Uracil-tegafur in gastric carcinoma; a comprehensive review. J Clin Oncol 16: 2877-2885, 1998.
10. Wilkinson DS and Pilot HC: Inhibition of ribosomal ribonucleic acid maturation in Novikoff hepatoma cells by 5-fluorouracil and 5-fluorouridine. J Biol Chem 248: 63-68, 1973.
11. Wilkinson DS, Tisty TD and Hanas RJ: The inhibition of ribosomal RNA synthesis and maturation in Novikoff hepatoma cells by 5-fluorouridine. Cancer Res 35: 3014-3020, 1975.
12. Carrico CK and Glazer RI: Effect of 5-fluorouracil on the synthesis and translation of polyadenylic acid-containing RNA from regenerating rat liver. Cancer Res 39: 3694-3701, 1979.
13. Spiegelman S, Sawyer R, Nayak R, *et al*: Improving the anti-tumor activity of 5-fluorouracil by increasing its incorporation into RNA via metabolic modulation. Proc Natl Acad Sci USA 77: 4966-4970, 1980.
14. Aschele C, Sobrero A, Faderan MA, *et al*: Novel mechanism(s) of resistance to 5-fluorouracil in human colon cancer (HCT-8) sublines following exposure to two different clinically relevant dose schedules. Cancer Res 52: 1855-1864, 1992.
15. Masuike T, Kikuchi K, Saito A, Hashimoto T and Takemoto Y: Determination of 5-fluorouracil incorporated into RNA in tissue using gas chromatography-mass spectrometry. Antibiot Chemother 11: 162-167, 1995.
16. Bates CD, Watson DG, Willmott N, Logan R and Golberg J: The analysis of 5-fluorouracil in human plasma by gas chromatography-negative ion chemical ionization mass spectrometry (GC-NICIMS) with stable isotope dilution. J Pharm Biomed Anal 9: 19-21, 1991.
17. Brown AH: Determination of pentose in the presence of large quantities of glucose. Arch Biochem 11: 269-278, 1946.

18. Diasio RB, Beavers TL and Carpenter JT: Familial deficiency of dihydropyrimidine dehydrogenase. J Clin Invest 81: 47-51, 1988.
19. Etienne MC, Cheradame S, Fischel JL, *et al*: Response to fluorouracil therapy in cancer patients. The role of tumoral dihydropyrimidine dehydrogenase activity. J Clin Oncol 13: 1663-1670, 1995.
20. Peters GJ, van der Wilt CL, van Triest B, *et al*: Thymidylate synthase and drug resistance. Eur J Cancer 31A: 1299-1305, 1995.
21. Rustum YM, Harstrick A, Cao S, *et al*: Thymidylate synthase inhibitors in cancer therapy: direct and indirect inhibitors. J Clin Oncol 15: 389-400, 1997.
22. Calabro-Jones PM, Byfield JE, Ward JF, *et al*: Time-dose relationships for 5-fluorouracil cytotoxicity against human epithelial cancer cells *in vitro*. Cancer Res 42: 4413-4420, 1982.
23. Drewinko B and Li-Ying Y: Cellular basis for the inefficiency of 5-FU in human colon carcinoma. Cancer Treat Rep 69: 1391-1398, 1985.
24. Link KH, Aigner KR, Peschau K, *et al*: Concentration and time dependence of the toxicity of fluorinated pyrimidines to HT 29 colorectal carcinoma cells. Cancer Chemother Pharmacol 22: 58-62, 1988.
25. Pinedo HM and Peter FI: Fluorouracil: biochemistry and pharmacology. J Clin Oncol 6: 1653-1664, 1988.
26. Seifert PS, Baker LH, Reed ML, *et al*: Comparison of continuously infused 5-fluorouracil with bolus injection in treatment of patients with colorectal adenocarcinoma. Cancer 36: 123-128, 1975.
27. Lokich JJ, Ahlgren JD, Gullo JJ, *et al*: A prospective randomized comparison of continuous infusion fluorouracil with a convention bolus schedule in metastatic colorectal carcinoma; a Mid-Atlantic Oncology Program Study. J Clin Oncol 7: 425-432, 1989.
28. Hansen RM, Ryan L, Anderson T, *et al*: Phase III study of bolus versus infusion fluorouracil with or without cisplatin in advanced colorectal cancer. J Natl Cancer Inst 88: 668-674, 1998.
29. Spears CP, Gustavsson BG, Berne M, *et al*: Mechanism of innate resistance to thymidylate synthase inhibition after 5-fluorouracil. Cancer Res 48: 5894-5900, 1988.
30. Allegra CJ: Dihydropyrimidine dehydrogenase activity: prognostic partner of 5-fluorouracil? Clin Cancer Res 5: 1947-1949, 1999.
31. Beck A, Etienne MC, Cheradame S, *et al*: A role of dihydropyrimidine dehydrogenase and thymidylate synthase in tumour sensitivity to fluorouracil. Eur J Cancer 30A: 1517-1522, 1994.
32. Ishikawa Y, Kubota T, Otani Y, *et al*: Dihydropyrimidine dehydrogenase activity and messenger RNA level may be related to the antitumor effect of 5-fluorouracil on human tumor xenograft in nude mice. Clin Cancer Res 5: 883-889, 1999.

Ratiometric dosing of anticancer drug combinations: Controlling drug ratios after systemic administration regulates therapeutic activity in tumor-bearing mice

Lawrence D. Mayer,[1] Troy O. Harasym,[1] Paul G. Tardi,[1] Natashia L. Harasym,[1] Clifford R. Shew,[1] Sharon A. Johnstone,[1] Euan C. Ramsay,[2] Marcel B. Bally,[2] and Andrew S. Janoff[1,3]

[1]Celator Pharmaceuticals Corp.; [2]Department of Advanced Therapeutics, BC Cancer Agency, Vancouver British Columbia, Canada; and [3]Celator Pharmaceuticals, Inc., Princeton, New Jersey

Abstract

Anticancer drug combinations can act synergistically or antagonistically against tumor cells *in vitro* depending on the ratios of the individual agents comprising the combination. The importance of drug ratios *in vivo*, however, has heretofore not been investigated, and combination chemotherapy treatment regimens continue to be developed based on the maximum tolerated dose of the individual agents. We systematically examined three different drug combinations representing a range of anticancer drug classes with distinct molecular mechanisms (irinotecan/floxuridine, cytarabine/daunorubicin, and cisplatin/daunorubicin) for drug ratio–dependent synergy. In each case, synergistic interactions were observed *in vitro* at certain drug/drug molar ratio ranges (1:1, 5:1, and 10:1, respectively), whereas other ratios were additive or antagonistic. We were able to maintain fixed drug ratios in plasma of mice for 24 hours after i.v. injection for all three combinations by controlling and overcoming the inherent dissimilar pharmacokinetics of individual drugs through encapsulation in liposomal carrier systems. The liposomes not only maintained drug ratios in the plasma after injection, but also delivered the formulated drug ratio directly to tumor tissue. *In vivo* maintenance of drug ratios shown to be synergistic *in vitro* provided increased efficacy in preclinical tumor models, whereas attenuated antitumor activity was observed when antagonistic drug ratios were maintained. Fixing synergistic drug ratios in pharmaceutical carriers provides an avenue by which anticancer drug combinations can be optimized prospectively for maximum therapeutic activity during preclinical development and differs from current practice in which dosing regimens are developed empirically in late-stage clinical trials based on tolerability. (Mol Cancer Ther 2006;5(7):1854–63)

Introduction

Combination chemotherapy regimens for cancer are typically developed by establishing the recommended dose of one agent and then adding subsequent drugs to the combination at increasing concentrations until the aggregate effects of toxicity are considered to be limiting (1–3). This approach assumes, perhaps incorrectly, that maximum therapeutic activity will be achieved with maximum dose intensity for all drugs in the combination and ignores the possibility that more subtle concentration-dependent drug interactions could result in frankly synergistic outcomes (4–6). Although a variety of approaches have been used to investigate whether drug combinations interact synergistically in cell culture systems (7–10), the use of such information to predict clinical activity has been questionable (11, 12).

One factor that clearly impedes the use of screening data to *a priori* predict synergy *in vivo* is the distinct pharmacology of different drugs used in combinations. In contrast to *in vitro* systems where drug concentrations exposed to tumor cells can be tightly controlled, individual agents in a conventional anticancer drug combination will distribute and be eliminated independently of each other after administration *in vivo*. This becomes important if the degree of synergy (or antagonism) depends, as it often does, on the concentration and ratio of the combined drugs (13–18). For example, when camptothecin and doxorubicin were exposed simultaneously to glioma cells at a molar ratio of 5:1, strong antagonism was observed, whereas a 1.5:1 ratio resulted in synergistic activity (18). Initial plasma drug/drug ratios will undoubtedly change within minutes after injection of conventional, aqueous-based drug combinations and such uncoordinated drug pharmacokinetics could lead to exposure of tumor cells to drug ratios with inferior therapeutic activity.

We describe herein the application of drug delivery technology to address this problem by controlling the release of drug combinations from the delivery vehicle such that fixed drug ratios are maintained after injection. Applying this "ratiometric" approach to combinations of common anticancer agents representing a range of drug

Received 3/1/06; revised 5/4/06; accepted 5/16/06.

The costs of publication of this article were defrayed in part by the payment of page charges. This article must therefore be hereby marked advertisement in accordance with 18 U.S.C. Section 1734 solely to indicate this fact.

Requests for reprints: Lawrence D. Mayer, Celator Pharmaceuticals Corp., 1779 West 75th Avenue, Vancouver, BC, Canada V6P 6P2. Phone: 604-675-2103; Fax: 604-708-5883. E-mail: lmayer@celatorpharma.com or Andrew S. Janoff, Celator Pharmaceuticals, Inc., 303B College Road East, Princeton, NJ 08540. Phone: 609-243-0123; Fax: 609-243-0202. E-mail: ajanoff@celatorpharma.com

doi:10.1158/1535-7163.MCT-06-0118

classes and target indications has enabled us to translate *in vitro* synergy information *in vivo*, resulting in fixed-ratio drug combination formulations with potent therapeutic activity.

Materials and Methods

Cell Culture

The human colorectal cell lines HCT-116, LS180, and HT-29; H460 non–small cell lung cancer line; and the Capan-1 pancreatic line were purchased from American Type Culture Collection (Manassas, VA). The murine Colon 26 carcinoma and P388 leukemia lines were obtained from the tumor repository at National Cancer Institute-Frederick. Cells were exposed to fixed ratios of drugs for 72 hours at eight concentrations along the profile of the most cytotoxic drug and viable cells were quantified using standard 3-(4,5-dimethylthiazol-2-yl)-2,5-diphenyltetrazolium bromide detection at 570 nm after DMSO addition (19).

Proliferation Data Analysis

Test data were converted to a percentage mean cell survival value relative to untreated control wells. The fraction of affected cells (f_a) was subsequently determined for each well. Three replicates were averaged and repeats of these data sets (minimum of three) were entered into CalcuSyn (Biosoft, Ferguson, MO) for analysis. This program uses the median effect analysis algorithm that produces the combination index (CI) value as a quantitative indicator of the degree of synergy or antagonism (20, 21). Using this analysis method, CI = 1.0 reflects additive activity, CI > 1 signifies antagonism, and a CI < 1.0 indicates synergy.

Drug Encapsulation

Irinotecan/Floxuridine. Distearoylphosphatidylcholine, distearoylphosphatidylglycerol, and cholesterol were dissolved at a molar ratio of 7:2:1 into dichloromethane/methanol/water (94:5:1), and the mixture was dried using nitrogen gas and then vacuumed overnight. The lipid film was hydrated to form multilamellar liposomes with 100 mmol/L copper gluconate/180 mmol/L TEA (pH 7.0) containing 25 mg/mL floxuridine and tracer quantities of [^{14}C]floxuridine for in-process analysis of encapsulated floxuridine. The hydrated films were extruded through 100 nm polycarbonate filters at 70°C and the mean diameter of the formulations used were 100 ± 20 nm as determined by quasi-elastic light scattering analysis (Submicron Particle Sizer Model 370, Nicomp Particle Systems, Santa Barbara, CA). Following extrusion, preparations were exchanged into 300 mmol/L sucrose/20 mmol/L HEPES/30 mmol/L EDTA (pH 7.0) by cross-flow filtration. Irinotecan was loaded by incubating the drug with the liposomes (0.12:1 molar ratio of irinotecan to lipid) at 50°C for 10 minutes to achieve a 1:1 molar encapsulated irinotecan/floxuridine ratio. Following drug loading, the liposome preparation was exchanged into saline with cross-flow filtration.

Daunorubicin/Cytarabine. Cytarabine containing liposomes were made in the same manner described above for floxuridine using a buffer pH of 7.4 and a cytarabine concentration of 50 mg/mL with a trace of [^{3}H]cytarabine for in-process analysis of cytarabine encapsulation. Following extrusion (22), the liposome preparation was exchanged into 20 mmol/L HEPES/150 mmol/L sodium chloride/1 mmol/L EDTA (pH 7.4) with cross-flow filtration. Daunorubicin loading was achieved by incubating the liposomes in the presence of the drug at 50°C for 30 minutes to achieve a 5:1 molar cytarabine/daunorubicin ratio.

Cisplatin/Daunorubicin. For liposomal cisplatin, dimyristoylphosphatidylcholine/cholesterol (55:45; mol/mol) lipid films were hydrated by vortexing in the presence of hot (80°C) 150 mmol/L NaCl solution containing cisplatin (28.3 mmol/L). The resulting suspension was extruded at 80°C. The preparations were cooled to room temperature, followed by centrifugation (1,250 × *g* for 5 minutes), to pellet any unencapsulated cisplatin. The external buffer was exchanged with 20 mmol/L HEPES, 150 mmol/L NaCl (HBS; pH 7.5) by dialysis. Encapsulated cisplatin concentrations were determined by diluting aliquots 1/10,000 in 0.1% nitric acid and analyzing via atomic absorption spectroscopy (Varian Model AA240Z). For liposomal daunorubicin, lipid films composed of distearoylphosphatidylcholine/2,000 MW polyethylene glycol–conjugated distearoylphosphatidylethanolamine at a 95:5 (mol/mol) ratio were hydrated with 300 mmol/L $CuSO_4$ solution at 70°C followed by extrusion at 70°C. The external buffer was exchanged using Sephadex G-50 columns equilibrated with HBS (pH 7.5). The resulting liposomes were loaded with daunorubicin by incubating for 10 minutes at 60°C at a drug-to-lipid ratio of 0.15:1 (mol/mol).

Pharmacokinetics

Samples were injected i.v. into female Rag2-M mice (Taconic, Germantown, NY) at the indicated doses. Following injection, mice (three per time point) were euthanized at various times and plasma isolated from EDTA-treated blood. For irinotecan analysis, 100 μL saline-diluted plasma samples were mixed with 600 μL acidified methanol and the supernatant was injected onto the high-performance liquid chromatography (HPLC). For floxuridine analysis, saline-diluted plasma samples were extracted in ethyl acetate (to which 5-chlorouracil was added as an internal standard), dried, and reconstituted in water (pH 2). For daunorubicin analysis, 10 μL plasma samples were mixed with 490 μL acidified methanol, centrifuged at 1,500 rpm for 10 minutes, and the supernatant was injected onto the HPLC. For cytarabine analysis, 10 μL plasma samples were mixed with 50 μL methanol by vortexing and were added to 440 μL water. Plasma aliquots of mice receiving liposomal cisplatin were processed as described above for platinum detection using atomic absorption spectrometry (Varian Model AA240Z).

HPLC Drug Analysis

Irinotecan was quantified using a Waters Symmetry C18 column with a multi–λ fluorescence detector (Waters Model 2475) set at excitation/emission wavelengths of 362/425 nm. The mobile phase was 1.5 mL/min acetonitrile–75 mmol/L ammonium acetate containing 7.5 mmol/L tetrabutylammonium bromide (24:76, v/v; pH 6.4). Floxuridine was quantified using a Waters Xterra MS C18

column and a photodiode array detector set at a wavelength of 266 nm. The mobile phase was 100% HPLC grade water adjusted to pH 2.0 using perchloric acid. Cytarabine was evaluated using a Phenomenex Luna C18(2) reverse phase analytic column with photodiode array detector (λ = 273.7 nm). The mobile phase was 1 mL/min 25 mmol/L ammonium acetate (pH 4.8). Daunorubicin was evaluated using a Phenomenex Luna C18(2) reverse phase analytic column with a multi–λ fluorescence detector set at excitation/emission wavelengths of 480/560 nm. The mobile phase was 1 mL/min 25 mmol/L ammonium acetate (pH 4.8)/acetonitrile (67.5:32.5, v/v).

Efficacy Evaluations

For the HT-29, Capan-1, and H460 tumor cells, 2×10^6 cells were inoculated s.c and 1×10^6 cells for the Colon 26 model. Tumor weights were determined according to the equation (length × width^2) / 2 using direct caliper measurements (23, 24). Maximum tolerated dose (MTD) values were defined as survival in the absence of significant tumor burden with ≤15% body weight loss nadir lasting ≤2 days. For P388 studies, mice were inoculated i.p. on day 0 with 1×10^6 cells. Ascitic tumor progression, survival, and body weight were monitored daily. Moribund mice were euthanized and the time of death was logged as the following day. Efficacy experiments were generally repeated to confirm the observed comparative trends. Tumor log cell kill values were determined for individual mice and the statistical significance between different treatment groups was determined using the *post hoc* Student-Newman-Keuls analysis method subsequent to one-way ANOVA (25–27).

Results

We evaluated the *in vitro* cytotoxicity of various anticancer drug combinations using the median-effect analysis method of Chou et al. (20, 28, 29), where the measure of synergy is defined by the CI value. The selection of this drug interaction analysis method was based on its suitability for assessing whether drugs interact synergistically (CI < 1.0), additively (CI ~ 1.0), or antagonistically (CI > 1.0) as a function of drug concentration for different fixed drug/drug ratios. Figure 1A and B summarizes the results of a synergy analysis done by exposing human colorectal and pancreatic cancer cells to various ratios and concentrations of irinotecan and floxuridine. Irinotecan and fluorinated pyrimidine are currently the standard of care in metastatic colorectal cancer, and the combination of irinotecan and the floxuridine-related 5-fluorouracil has been shown previously to interact synergistically *in vitro* under appropriate conditions (30–32). It should be noted that we chose to focus our *in vitro* evaluations on irinotecan rather than its more potent metabolite SN-38, because this reflects the situation experienced for liposomal delivery of irinotecan *in vivo* where preferential extravasation and accumulation of liposomes in tumors provide a local infusion reservoir of irinotecan (see below). Also, in contrast to irinotecan, SN-38 is extremely membrane permeable and was not amenable to stable retention in liposomal delivery systems after injection.

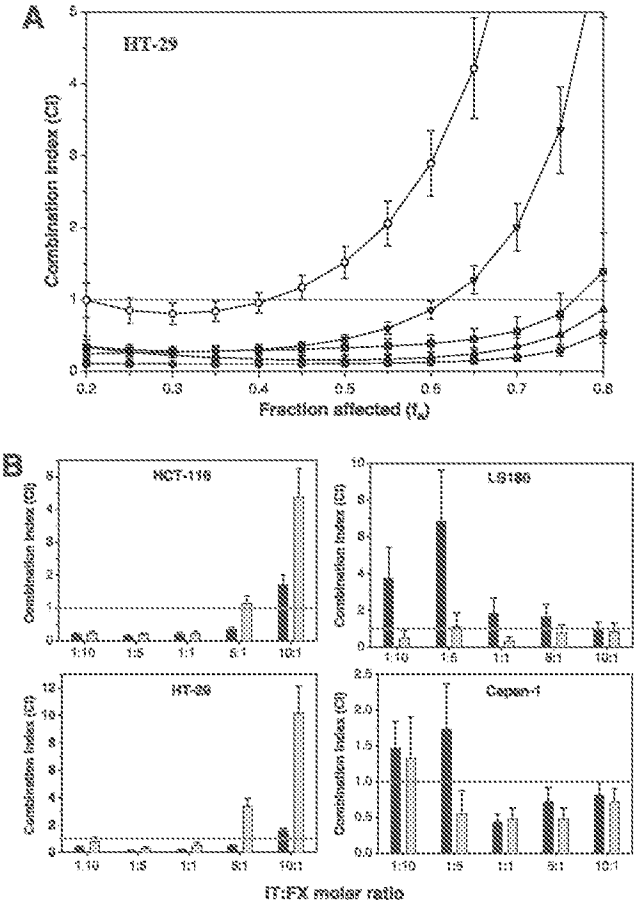

Figure 1. A, *in vitro* screening of irinotecan and floxuridine for synergy in HT-29 colorectal cells as a function of irinotecan/floxuridine ratio and drug concentration. Concentrations of fixed irinotecan/floxuridine molar ratios were titrated to provide a broad range of cell growth inhibition (reflected by f_a). *Points*, average values from triplicate assays repeated a minimum of thrice, where CI values of <1, ~1, and >1 indicate synergy, additivity, and antagonism, respectively. Irinotecan/floxuridine molar ratios were 1:10 (■), 1:5 (●), 1:1 (▲), 5:1 (▼), and 10:1 (○). *Bars*, SE determined for the indicated f_a values. B, *in vitro* screening CI results from various cell types plotted at ED_{50} (*black columns*, f_a = 0.5) and ED_{75} (*gray columns*, f_a = 0.75) as a function of irinotecan/floxuridine (*IT:FX*) ratio.

For HT-29 cells, evidence of significant variation of CI as a function of drug ratio was observed (Fig. 1A and B), particularly at high drug concentrations (high f_a). Strong antagonism reflected by CI values >4 was seen at irinotecan/floxuridine molar ratios of 5:1 and 10:1, whereas synergy was evident at ratios of 1:1, 1:5, and 1:10 (CI values <0.5). At drug concentrations giving rise to 50% and 75% tumor growth inhibition (ED_{50} and ED_{75}, corresponding to f_a = 0.50 and 0.75, respectively), a similar trend of ratio-dependent synergy was observed for HCT-116 human colorectal cancer cells (Fig. 1B), where CI values <0.5 were obtained at irinotecan/floxuridine ratios of 1:1, 1:5, and 1:10, and strong antagonism (ED_{75} CI = 4.4) was seen at an irinotecan/floxuridine ratio of 10:1. Ratio-dependent CI profiles observed for LS180 human colorectal cancer and

Capan-1 human pancreatic tumor lines were different in that antagonism was observed at low irinotecan/floxuridine ratios (1:10 and 1:5); however, the irinotecan/floxuridine molar ratio of 1:1 consistently provided synergy across all four gastrointestinal cell lines and avoided antagonism (Fig. 1B). The degree of drug ratio dependency was greatest in gastrointestinal tumor lines; however, expanded analysis of ratio-dependent synergy in additional tumor cell lines confirmed that the 1:1 irinotecan/floxuridine ratio was optimal (data not shown). We surmised that if similar relationships between drug/drug ratio and antitumor activity were to hold *in vivo*, we would be able to achieve significant increases in efficacy by controlling individual drug pharmacokinetics and maintaining the optimal 1:1 ratio after systemic administration. It should also be noted that ratio-dependent synergy was observed for combinations of floxuridine with SN-38; however, optimal activity occurred at much lower SN-38/floxuridine molar ratios. Specifically, at ED_{75}, in HT-29 cells, CI values >1.0 were observed for SN-38/floxuridine molar ratios of 1:1, 1:10, and 1:100, whereas CI values <1.0 were obtained at a SN-38/floxuridine ratio of 1:1,000 (data not shown).

We coencapsulated irinotecan and floxuridine at a 1:1 molar ratio inside 100-nm-diameter liposomes composed of distearoylphosphatidylcholine/distearoylphosphatidylglycerol/cholesterol (7:2:1 molar ratio) at a 0.1:1 drug-to-lipid ratio (mol/mol). Floxuridine was passively encapsulated during liposome formation and unentrapped floxuridine was subsequently removed via dialysis. Irinotecan was entrapped using a copper-based active loading procedure whereby the drug accumulates inside preformed liposomes containing copper gluconate/TEA (pH 7.0, ref. 33). This formulation (hereafter called CPX-1) maintained the irinotecan/floxuridine molar ratio near 1:1 over extended times (up to 24 hours) after i.v. injection into mice (Fig. 2). In addition, the plasma area under the curve ($AUC_{0\text{-last}}$) values for irinotecan and floxuridine administered as CPX-1 were ~1,500 and 750 times greater, respectively, than observed for the same dose of drugs coadministered in saline (data not shown). HPLC analysis showed that the circulating liposomal drug formulations contained intact drug; no evidence of degradation was observed for either agent. Circulating plasma drug-to-lipid ratios decreased over time with a half-life of ~7.5 hours for both drugs, indicating that irinotecan and floxuridine were released systemically from the liposomes at a 1:1 molar ratio. However, SN-38 was not detected using the HPLC quantification method here for plasma samples obtained from mice.

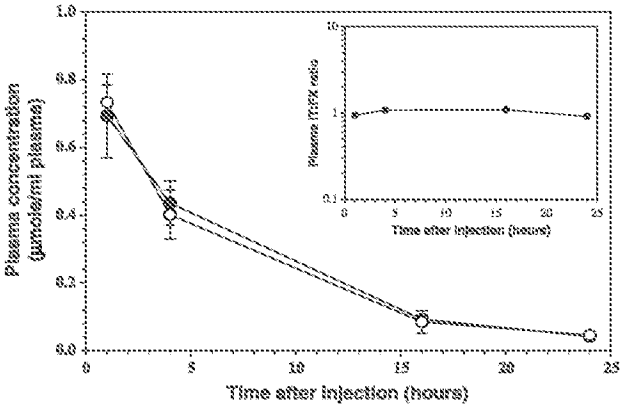

Figure 2. Plasma drug concentrations for irinotecan (●) and floxuridine (○) upon i.v. administration of CPX-1 (37:37 μmol/kg) to Rag2-M female mice ($n = 3$ per time point). *Bars*, SD. Plasma was extracted and analyzed by HPLC as described in Materials and Methods. *Inset*, circulating plasma irinotecan/floxuridine (IT:FX) molar ratio calculated from the absolute plasma concentrations.

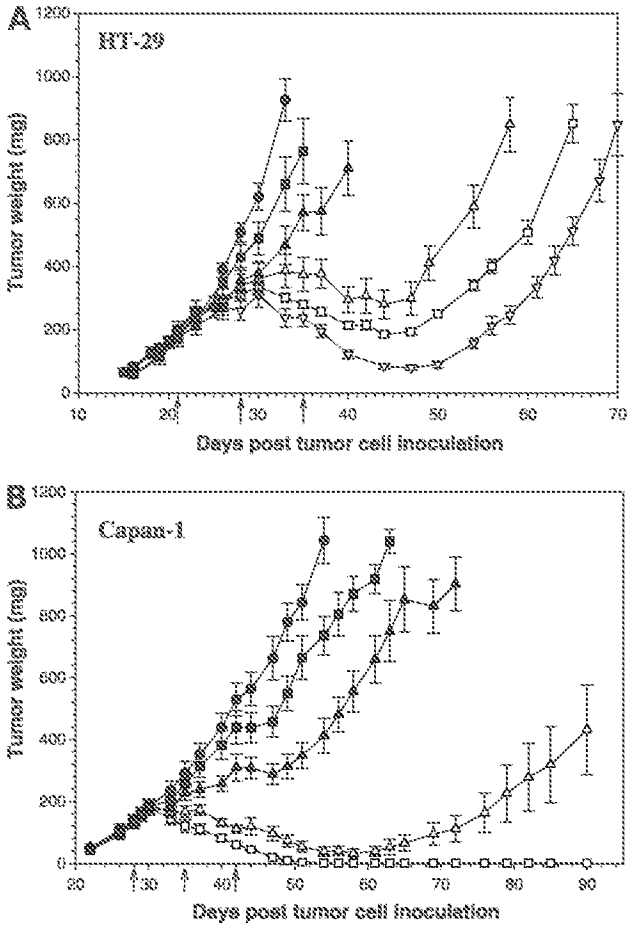

Figure 3. Efficacy of irinotecan and floxuridine codelivered in CPX-1 against gastrointestinal solid tumor models. HT-29 and Capan-1 tumor-bearing Rag2-M mice (six per group) were treated i.v. on the days indicated by the arrows. *Bars*, SE. Doses are expressed in μmol/kg. **A**, irinotecan/floxuridine efficacy in the HT-29 CRC model. ●, saline; ■, irinotecan/floxuridine in saline (37:37); ▲, irinotecan/floxuridine in saline (148:148); △, CPX-1 (irinotecan/floxuridine, 18.5:18.5); □, CPX-1 (irinotecan/floxuridine, 37:37); ▽, CPX-1 (irinotecan/floxuridine, 74:74). **B**, irinotecan/floxuridine efficacy in the Capan-1 pancreatic model. ●, saline; ■, irinotecan/floxuridine in saline (37:37); ▲, irinotecan/floxuridine in saline (148:148); △, CPX-1 (irinotecan/floxuridine, 18.5:18.5); □, CPX-1 (irinotecan/floxuridine, 37:37).

Table 1. Quantitative analysis of CPX-1 *in vivo* antitumor activity in human HT-29 colorectal cancer and Capan-1 pancreatic xenograft tumor models

	Treatment groups								
	Column A	Column B	Column C	Column D	Column E	Column F		Column G		Column H
	CPX-1 (liposomal IT/FX at a 1:1 ratio)	IT in saline	FX in saline	IT/FX in saline at a 1:1 ratio	IT/FX in saline at a IT_{MTD}/FX_{MTD} ratio	Lipo-IT		Lipo-FX		Liposomal IT/FX at the antagonistic ratio
						Low dose	High dose	Low dose	High dose	
HT-29 colorectal										
Log cell kill value	1.71*	0.09	0.09	0.23	0.57	ND	1.51	ND	0.14	1.48
Dose (μmol/kg)	74:74†	148†	1,000†	148:148†	148:1,000†	ND	74†	ND	74†	74:7.4†
Capan-1 pancreatic										
Log cell kill value	1.81*	0.65	0.43	0.69	ND	1.15	1.46	0.36	0.43	0.56
Dose (μmol/kg)	37:37	148†	1,000†	148:148†	ND	7.4	37	37	74†	7.4:74†

NOTE: Log cell kill = $[T - C] / [(3.32) (T_d)]$, where $T - C$ is the treatment-induced delay for tumors to reach 400 to 500 mg, and T_d is the tumor doubling time (7 days for both tumor models).

Abbreviations: IT, irinotecan; FX, floxuridine; ND, not determined.

*Statistically different ($P < 0.05$) from all other groups using Student-Newman-Keuls analysis

†Indicates MTD.

Treatment of established HT-29 tumors with the fixed ratio formulation of irinotecan/floxuridine, CPX-1, yielded dose-dependent therapeutic activity with tumor regression at irinotecan/floxuridine doses of ≥18.5:18.5 μmol/kg (Fig. 3A). This activity was significantly greater than observed with irinotecan and floxuridine coadministered in saline at a 1:1 molar ratio escalated to its MTD of 148:148 μmol/kg (equivalent to a mg/kg-based irinotecan/floxuridine dose of 100:37). Similar results were seen in the Capan-1 tumor model, where CPX-1 at a dose of 37:37 μmol/kg resulted in complete tumor regressions that extended beyond day 90, whereas treatment with a 4-fold greater dose of the combination in saline at its MTD (148:148 μmol/kg) provided only modest tumor growth inhibition (Fig. 3B). Reducing the dose of CPX-1 to 18.5:18.5 μmol/kg lead to prolonged tumor regression and although no long-term complete responses were observed, the antitumor activity in this group was significantly greater than the 8-fold higher dose of the saline-based drug combination. The weekly dosing schedule used here for the human xenograft models was selected based on previous studies demonstrating the superior activity of this schedule for floxuridine as well as the current clinical dosing regimen used for irinotecan/5-fluorouracil combination chemotherapy (34).

We calculated tumor cell kill values from treatment-related delays in tumor growth using well-established analysis methods to compare treatment groups in a more quantitative fashion (Table 1; see ref. 35). Against HT-29 tumors, CPX-1 exhibited a maximum log cell kill value of 1.71 (Table 1, column A), reflecting antitumor activity that was 42 times greater than the MTD of either drug dosed individually in saline [log cell kill value of 0.09 for both 1,000 μmol/kg irinotecan (column B) and 148 μmol/kg floxuridine (column C); Table 1] and 30 times greater than the MTD of the two drugs coadministered in saline at a 1:1 molar ratio (log cell kill value of 0.23 for 148:148 μmol/kg irinotecan/floxuridine; Table 1, column D). In addition, CPX-1 was 14 times more active than a saline-based combination in which each drug was escalated to its MTD (log cell kill value of 0.57 for 148:1,000 μmol/kg irinotecan/floxuridine; Table 1, column E). When compared with liposomal formulations of the individual drugs, CPX-1 was ~1.6 times more active than irinotecan encapsulated in liposomes [log cell kill value of 1.51 for 74 μmol/kg liposome-encapsulated (lipo-) irinotecan; Table 1, column F] despite the fact that lipo-floxuridine was minimally active against this tumor model. In addition, CPX-1 was 1.7 times more active than 74:7.4 μmol/kg irinotecan/floxuridine coencapsulated inside liposomes at the *in vitro* antagonistic ratio of 10:1.

In the more floxuridine-sensitive Capan-1 tumor model, we were able to coencapsulate and dose therapeutically active amounts of both drugs at synergistic and antagonist irinotecan/floxuridine ratios identified *in vitro* (1:1 and 1:10, respectively; see Capan-1 panel of Fig. 1B). Here, it was clear that floxuridine inhibited irinotecan activity at the antagonistic ratio (see Table 1). Specifically, a log cell kill value of 0.56 was obtained for the liposome-formulated antagonistic ratio dosed at 7.4 μmol/kg irinotecan plus 74 μmol/kg floxuridine (Table 1, column H). Surprisingly, the matched dose of liposome encapsulated irinotecan alone (7.4 μmol/kg; Table 1, column F) provided an elevated log cell kill value of 1.15, which was significantly greater than observed for the same dose of irinotecan to which floxuridine was combined in the liposomes at an antagonistic ratio. In contrast, irinotecan and floxuridine coformulated as CPX-1, at the *in vitro* identified synergistic 1:1 molar ratio (37:37 μmol/kg), led to increased antitumor activity, where the log cell kill

Table 2. Quantitative comparison of CPX-1 *in vivo* antitumor activity in the murine Colon 26 colon carcinoma model (treatment days 9, 13, and 17)

Treatment	Dose (μmol/kg)	$T - C$ (d)	Log cell kill
Lipo-FX	30	2.9 ± 0.9	0.7
Lipo-IT	30	2.7 ± 0.3	0.6
CPX-1	30:30	10.4 ± 0.9	2.5*

NOTE: Log cell kill = $[T - C / (3.32)(T_d)]$, where $T - C$ is the treatment-induced delay for tumors to reach 500 mg (±SD, $n = 6$) and T_d is the tumor doubling time.
*Statistically different ($P < 0.001$) from all other groups using Student-Newman-Keuls analysis.

value of 1.81 for CPX-1 (column A) was greater than the value of 1.46 for the matched dose of 37 μmol/kg liposome-entrapped irinotecan (column F). Thus, we were able to conclude that whether irinotecan and floxuridine delivered in liposomes acted synergistically or antagonistically *in vivo* depended on the ratio of the two agents and was not due solely to the altered pharmacokinetics produced by the delivery vehicle. This was corroborated by efficacy results in the yet more floxuridine-sensitive Colon 26 murine colorectal cancer model (Table 2), where CPX-1 treatment yielded a log cell kill value of 2.5, which reflected ~60 times more antitumor activity than the individual liposomal drugs and 10 times greater antitumor activity than predicted for additivity. Specifically, the log cell kill values of lipo-floxuridine (0.7) and lipo-irinotecan (0.6) at the same doses used in CPX-1 predict a log cell kill value of 1.3 for additivity, which is significantly less than the observed value of 2.5 for CPX-1 (Table 2). It is important to note that the ability of distearoylphosphatidylcholine/distearoylphosphatidylglycerol/cholesterol liposomes to maintain fixed drug ratios for extended times after i.v. injection was not dependent on the initially formulated drug ratio between irinotecan/floxuridine molar ratios of 10:1 to 1:10 (data not shown).

To establish whether circulating irinotecan/floxuridine ratios reflected those exposed to tumor tissue, CPX-1 liposomes containing coencapsulated [^{3}H]irinotecan and [^{14}C]floxuridine were administered to mice bearing established Capan-1 solid tumors and tumor-associated drug levels were determined by scintillation counting of tissue homogenates (correcting for tumor blood volume drug contributions). As shown in Fig. 4A, both drugs accumulated in Capan-1 tumors at similar rates with peak tumor concentrations of ~15 nmol/g tumor at 4 hours, which remained associated with the tumor for extended times. As shown in Fig. 4B, these concentrations reflected tumor-associated irinotecan/floxuridine molar ratios near 1:1 through 8 hours after injection, which subsequently increased to 3:1 by 24 hours, all of which were within the synergistic irinotecan/floxuridine ratio range determined *in vitro* (compare Figs. 4B and 1B). It should be noted that tumor-associated irinotecan and floxuridine levels determined here reflect a compilation of drugs both inside and outside of the liposomes as well as radionuclide-bearing metabolites. A more detailed comparison of these data with results from *in vitro* experiments will require separation of intracellular and extracellular drug pools and quantification of active drug metabolites.

We also found a fixed ratio of cytarabine and daunorubicin to be strongly synergistic *in vivo*. These drugs are currently used to treat acute myeloid leukemia and when screened against P388 leukemia cells *in vitro*, we found the combination capable of producing increasing synergy with increasing concentration (Fig. 5A). At drug concentrations providing 90% cell kill (ED_{90}, equivalent to a $f_a = 0.9$), cytarabine/daunorubicin molar ratios of 1:1, 5:1, and 10:1 exhibited synergistic CI values of 0.65, 0.72, and 0.75, respectively, whereas ratios of 1:5 and 1:10 displayed antagonistic CI values of ~1.5 and 1.2, respectively (Fig. 5B).

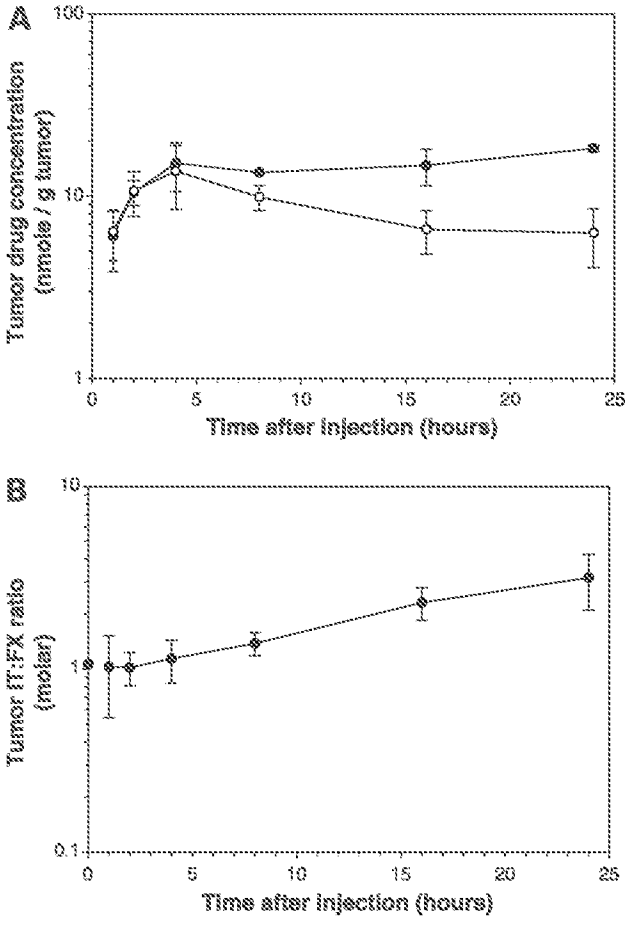

Figure 4. **A**, tumor accumulation of irinotecan (■) and floxuridine (○) after i.v. injection of [^{3}H]irinotecan and [^{14}C]floxuridine containing CPX-1 at an irinotecan/floxuridine dose of 37:37 μmol/kg to Rag2-M mice bearing s.c. Capan-1 tumors. Tumor homogenates were digested, quantified for ^{3}H and ^{14}C by scintillation counting, and tumor drug concentrations were determined after correcting for drug levels contributed by tumor-associated plasma volumes. *Points*, mean of three repeats; *bars*, SD. **B**, corresponding Capan-1 tumor-associated irinotecan/floxuridine (IT:FX) ratios over 24 h after injection of CPX-1.

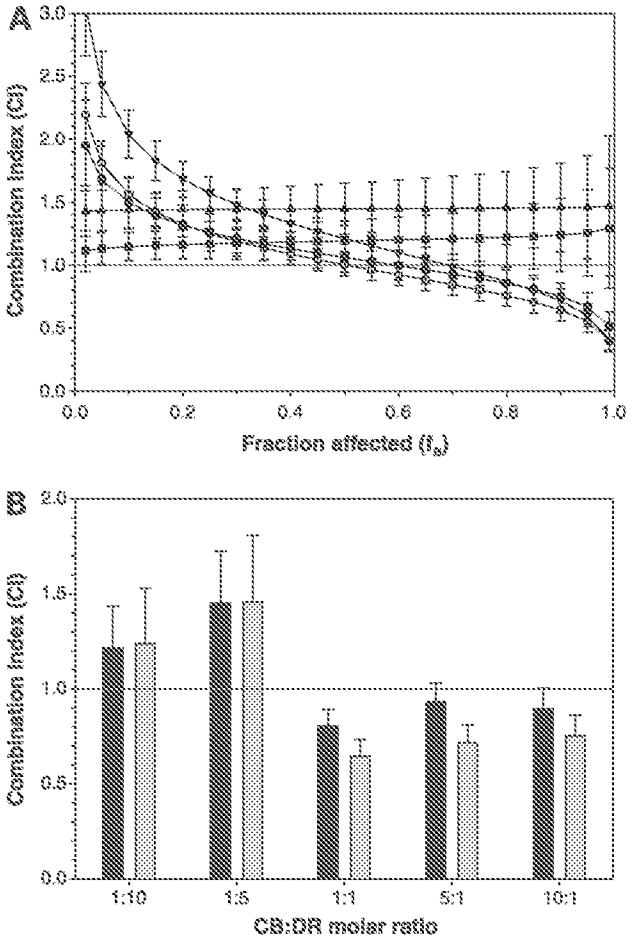

Figure 5. *In vitro* screening of cytarabine and daunorubicin for synergy in murine P388 leukemia cells. **A**, CI values presented as a function of cytarabine/daunorubicin ratio and f_a values. Conditions for assessing *in vitro* synergy were the same as described in Fig. 1. Cytarabine/daunorubicin molar ratios were as follows: 1:10 (▩), 1:5 (▲), 1:1 (○), 5:1 (▼), and 10:1 (◆). *Bars*, SE determined for the indicated f_a values. **B**, *in vitro* CI values at ED_{75} (*black columns*, f_a = 0.75) and ED_{90} (*gray columns*, f_a = 0.90) as a function of cytarabine/daunorubicin (*CB:DR*) ratio.

We developed a liposome formulation fixing cytarabine/daunorubicin at a ratio of 5:1 (hereafter called CPX-351) using the same lipid composition and encapsulation techniques established for CPX-1. CPX-351 maintained circulating cytarabine/daunorubicin molar ratios near 5:1 over 24 hours after i.v. administration (Fig. 6A, *inset*). Plasma drug elimination half-lives for both cytarabine and daunorubicin were ~12 hours, which reflected removal of intact, drug-containing liposomes from the circulation as well as release of the drugs from liposomes in the central blood compartment (release half-life of ~16 hours, data not shown). The latter variable was determined by monitoring the decrease in plasma drug to liposomal lipid ratio over time (determination of drug content by HPLC and liposomal lipid content using [^{14}C]dipalmitoylphosphatidylcholine as a lipid tracer). This formulation administered at a dose of 50:10 μmol/kg cytarabine/daunorubicin (equivalent to a mg/kg-based cytarabine/daunorubicin dose of 12:5.3) achieved a 90% cure rate against P388 tumors *in vivo*, which was superior to the activity of cytarabine and daunorubicin administered as a combination in saline at their respective MTDs (2,500:20 μmol/kg cytarabine/daunorubicin), as well as the matched doses of the individual liposomal drugs (10 μmol/kg lipo-daunorubicin, 50 μmol/kg lipo-cytarabine; see Fig. 6B). Furthermore, the therapeutic activity of CPX-351 administered on a day 1, 4, 7 schedule (90% long-term survival) was superior to a free drug schedule where cytarabine was administered i.v. daily on days 1 to 5 at its MTD of 200 mg/kg per injection (17-day median survival time reflecting an increase in life span of 112%; data not shown).

To address the question of *in vivo* synergy directly, we turned to quantitative analysis and worked at

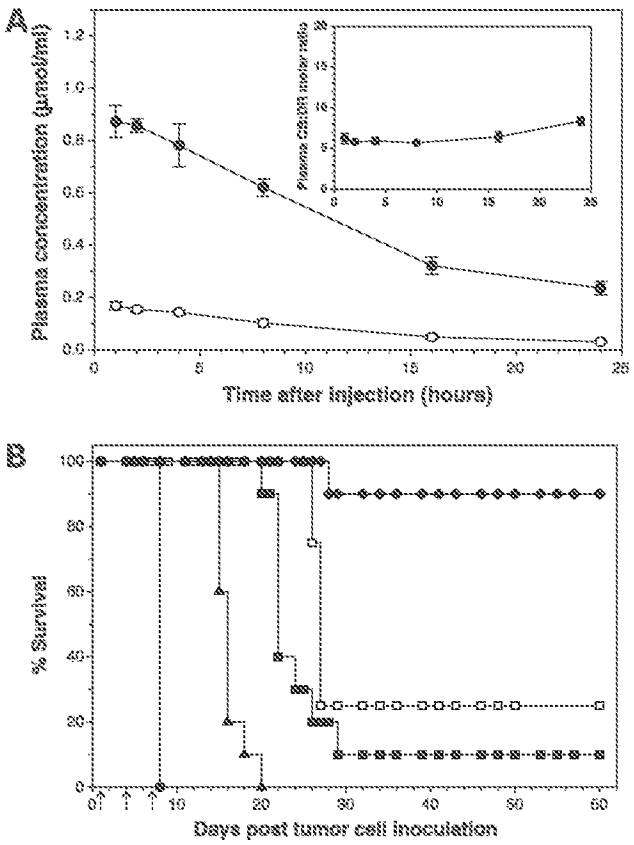

Figure 6. *In vivo* activity of cytarabine/daunorubicin encapsulated inside liposomes at a 5:1 molar ratio. **A**, plasma drug concentrations for cytarabine (▩) and daunorubicin (○) determined by HPLC after i.v. administration of CPX-351 at 50:10 μmol/kg cytarabine/daunorubicin to BDF_1 female mice (n = 3 per time point). *Points*, mean; *bars*, SD. *Inset*, cytarabine/daunorubicin (CB:DR) ratio in plasma over 24 h. **B**, antitumor activity in the murine P388 ascites lymphocytic leukemia model. The following treatments were administered i.v. after i.p. inoculation of tumor cells (6–10 mice per group): ▩, saline; ▲, lipo-daunorubicin (10 μmol/kg); □, cytarabine/daunorubicin in saline (2,500:20 μmol/kg); ▩, lipo-cytarabine (50 μmol/kg); ◆, CPX-351 (cytarabine/daunorubicin, 50:10 μmol/kg). *Arrows*, treatment days.

Table 3. Quantitative comparison of CPX-351 *in vivo* antitumor activity in the murine P388 leukemia model

Treatment	Dose (μmol/kg)	MST (d)	Net MST (d)	Log cell kill
Saline	—	8.0	—	—
Lipo-CB	20	16.0	8.0	3.6
Lipo-DR	4	12.0	4.0	1.8
CPX-351	20:4	27.5	19.5	8.8

NOTE: Log cell kill = $[T - C / (3.32) (T_d)]$, where $T - C$ is the net median survival time of the treatment group compared to control and T_d is the tumor doubling time (0.67 days).

Abbreviations: CB, cytarabine; DR, daunorubicin; MST, median survival time.

intermediate doses to allow comparisons with individual liposomal drugs. CPX-351 dosed at ~50% of its MTD (20:4 μmol/kg cytarabine/daunorubicin) resulted in a net median survival time (median survival time$_{\text{treatment}}$ − median survival time$_{\text{control}}$) of 19.5 days, reflecting a log cell kill of 8.8 (Table 3). This activity was >2,000 times greater than what would be expected if each encapsulated drug had contributed in only an additive fashion to its activity. Specifically, log cell kill values of 3.6 for 20 μmol/kg lipo-cytarabine and 1.8 for 4 μmol/kg lipo-daunorubicin predict a log cell kill value of 5.4 for CPX-351 (see Table 3), which was significantly lower than the observed log cell kill value of 8.8. In addition, decreasing the cytarabine/daunorubicin ratio <5:1 lead to decreased antitumor activity in the P388 tumor model (data not shown).

To further test the concept that we could capture synergistic anticancer drug interactions determined through *in vitro* screening by maintaining fixed drug ratios *in vivo*, we identified a combination in which the antagonistic ratio could be administered at a higher dose than the synergistic ratio. When exposed to H460 cells in culture, cisplatin and daunorubicin interacted synergistically at a 10:1 molar ratio (CI = 0.75 at ED_{80}) and antagonistically at a 1:1 molar ratio (CI = 1.6 at ED_{80}). Encapsulating cisplatin and daunorubicin in separate liposomes enabled us to avoid interactions between daunorubicin and the chemically reactive cisplatin. We encapsulated cisplatin inside 100 nm dimyristoylphosphatidylcholine/cholesterol (55:45 molar ratio) liposomes and daunorubicin in distearoylphosphatidylcholine/2,000 MW polyethylene glycol–conjugated distearoylphosphatidylethanolamine liposomes, and mixed the two liposomal drug preparations at a 10:1 ratio to provide a putatively synergistic formulation and at a 1:1 ratio to provide a putatively antagonistic formulation. Figure 7A shows that each ratio was sustained in plasma over time after i.v. injection in mice. When both formulations were administered to H460 tumor-bearing mice at equivalent doses of cisplatin, the 1:1 antagonistic formulation was less active although it contained 10 times more daunorubicin than the drugs formulated at the 10:1 molar ratio (7.0 versus 0.7 μmol/kg, respectively; see Fig. 7B).

Discussion

Anticancer drug combinations continue to be developed in the clinic by escalating the individual agents to MTD (36). Although intuitive, this approach does not take into account the fact that many agents exert multiple pharmacologic effects with distinct concentration/activity relationships and that many of the molecular pathways associated with these effects have the potential to interact. This opens the possibility that the way in which drug combinations exert their antitumor effects may depend on the ratio of the drugs being combined. We focused our efforts on elucidating whether the ratio of drugs in a combination could dictate antitumor activity *in vitro* and *in vivo*. Although

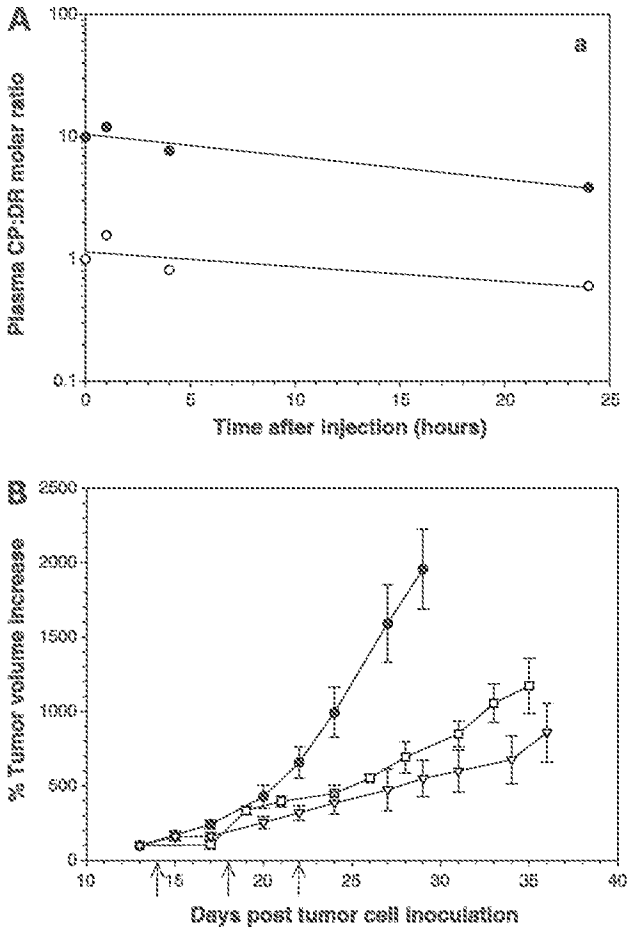

Figure 7. A, plasma drug molar ratios over 24 h for cisplatin (*CP*; determined by atomic absorption) and daunorubicin (*DR*; determined by HPLC) upon i.v. administration of 10:1 (●) and 1:1 (○) molar ratios of lipo-cisplatin and lipo-daunorubicin to female Rag2-M mice. B, *in vivo* evaluation of antitumor activity for 10:1 and 1:1 molar ratios of lipo-cisplatin/lipo-daunorubicin in the H460 human lung cancer xenograft model. Increases in percent tumor volume from day 13 after tumor inoculation were monitored for each group. *Points*, mean; *bars*, SE. Intravenous treatments were administered to mice (8–10 mice per group) on days 14, 18, and 22 after s.c. inoculation of tumor cells (*arrows*, treatment days). Treatment groups were as follows: ●, saline; □, lipo-cisplatin + lipo-daunorubicin (7:7; μmol/kg); ▽, lipo-cisplatin + lipo-daunorubicin (7:0.7; μmol/kg).

such an analysis has not been previously undertaken, the concept that maximum therapeutic activity of drug combinations may occur at doses below the MTD of one or more of the agents is not unprecedented. For example, low-dose suramin combined with paclitaxel has exhibited signs of promising antitumor activity both preclinically and clinically, while avoiding the significant toxicities experienced with suramin administered at MTD (4, 13). Also, optimal activity of certain biological response modifiers and signal transduction inhibitors has been observed at sub-MTD doses (37, 38). In a related treatment approach, "metronomic" dosing, where drugs are administered frequently at doses significantly below their MTD, has led to improved efficacy compared with less frequent dosing at MTD (5, 16). Although this approach uses low-dose administration of cytotoxic agents to induce antitumor effects indirectly through their action on endothelial cells rather than directly on the tumor cells themselves, it highlights the fact that pharmacologic targets can change as the drug dose is altered.

Despite the evidence cited above, drug combinations have not been systematically evaluated for ratio-dependent synergy, nor have there been avenues to exploit this information *in vivo* for combinations where ratio dependency was observed in cell culture. Historically, such correlations have been complicated by the fact that different agents in a conventional drug combination will be disitributed and metabolized differentially and independently after administration, thereby precluding control of the ratio of drugs in a combination that reaches the tumor. However, drug delivery systems, such as the liposome-based carriers used here, provide a means to maintain fixed drug ratios after injection, thus providing an avenue to determine whether drug ratio dependency seen *in vitro* can be translated *in vivo*. Liposomes minimize first-pass metabolism/distribution for encapsulated drugs and preferentially accumulate at sites of tumor growth (see Fig. 4; refs. 39–41). Together, these features provide pharmacokinetic control of drug combinations previously unachievable with conventional, aqueous-based drug formulations, thereby enabling the concept of drug ratio–dependent antitumor activity to be tested directly *in vivo*.

Here, we have taken a mechanistically unbiased approach to assess the importance of drug ratios in determining the therapeutic activity of anticancer drug combinations *in vivo*. Evidence of drug ratio–dependent antitumor activity was observed for three combinations of drugs with very different mechanisms of action and clinical use. This suggests that the role of drug ratios in determining the activity of anticancer drug combinations may be of broad importance. In all cases, drug ratio–dependent synergy/antagonism relationships observed *in vitro* were consistent with *in vivo* trends in efficacy when drug ratios were maintained after injection using liposomal delivery systems. Specifically, liposomal fixed drug ratios shown to interact synergistically provided increased therapeutic activity, whereas drug ratios that yielded antagonism *in vitro* exhibited reduced efficacy when delivered *in vivo* in liposomes. How these relationships are manifested in human cancers, where increased tumor cell heterogeneity is expected, will be revealed through extensive clinical evaluation, which is currently under way with the irinotecan/floxuridine fixed drug ratio formulation, CPX-1 (42).

Although drug combinations were not selected or evaluated on the basis of specific mechanisms, previous literature reports provide evidence that supports the ratio dependency observed here for irinotecan/floxuridine (43, 44). Specifically, examination of cell cycle checkpoint responses to floxuridine exposure in colorectal cancer cell lines has revealed that floxuridine cytotoxicity in HT-29 cells is associated with progression through S phase and drug-induced premature mitotic entry (43). At high irinotecan/floxuridine ratios (e.g., 10:1), irinotecan may antagonize floxuridine activity by arresting cells in S phase (44), which would inhibit mitotic entry. Given that irinotecan will induce DNA single-strand breaks predominantly during G_1 and S phase, it is conceivable that higher relative amounts of floxuridine (e.g., 1:1 irinotecan/floxuridine molar ratio) may drive the progression to mitosis and increase the degree of cytotoxicity in HT-29 cells by propagating deleterious DNA damage before the lesions can be repaired. This type of interaction would reflect a class 2 mechanism as defined by Rideout and Chou (28) where drug A affects cell cycle kinetics, thereby altering the biological effects of drug B after target binding. Furthermore, it is possible that this ratio dependency for simultaneous drug exposure may reflect changes in the tumor cells previously associated with sequential drug exposure where irinotecan preceding 5-fluorouracil was synergistic, whereas the reverse sequence was antagonistic (18). Whether drug ratio effects, such as those observed here for simultaneous treatment, also occur for sequential administration of drug combinations is unknown.

Based on the data presented here as well as historical evidence, we conclude that ratiometric dosing (controlling drug ratios following systemic administration) of anticancer drug combinations can profoundly influence therapeutic outcomes. We raise the possibility that currently used combination regimens, which have been developed principally by considering drug tolerabilities, may be providing less than maximum therapeutic activity. Further, by demonstrating that drug combinations can be optimized preclinically through pharmacokinetic control, we provide a new paradigm by which preclinical information can be used more directly and efficiently in clinical drug combination development. Ultimately, this should yield more effective oncology products.

References

1. Frei E III. Clinical studies of combination chemotherapy for cancer. In: Chou TC, Rideout DC, editors. Synergism and antagonism in chemotherapy. San Diego (California): Academic Press; 1991. p. 103–8.

2. DeVita VT, Jr. Principles of cancer management: chemotherapy. In: DeVita Jr, Hellman S, Rosenberg SA, editors. CANCER: principles and practice of oncology, vol. 1. Philadelphia: Lippincott-Raven; 1997. p. 333–47.

3. Tannock I. In: Tannock IF, Hill RP, editors. Basic science of oncology. New York: McGraw-Hill; 1992. p. 139–96.

4. Villalona-Calero MA, Wientjes MG, Otterson GA, et al. Phase I study of low-dose suramin as a chemosensitizer in patients with advanced non-small cell lung cancer. Clin Cancer Res 2003;9:3303–11.

5. Kerbel R, Folkman J. Clinical translation of angiogenesis inhibitors. Nat Rev Cancer 2002;2:727–39.

6. Hanahan D, Bergers G, Bergsland E. Less is more, regularly: metronomic dosing of cytotoxic drugs can target tumor angiogenesis in mice. J Clin Invest 2000;105:1045–7.

7. Teicher BA. Assays for *in vitro* and *in vivo* synergy. In: Buolamwini JK, Adjei AA, editors. Methods in molecular medicine. Novel anticancer drug protocols, vol. 85. Totowa (New Jersey): Humana Press; 2003. p. 297–321.

8. Greco WR, Bravo G, Parsons JC. The search for synergy: a critical review from a response surface perspective. Pharmacol Rev 1995;47:331–85.

9. Tallarida RJ. Drug synergism, its detection and applications. J Pharmacol Exp Ther 2001;298:865–72.

10. Berenbaum MC. Isobolographic, algebraic, and search methods in the analysis of multiagent synergy. J Am Coll Toxicol 1998;7:927–38.

11. Tsai CM, Gazdar AF, Venzon DJ, et al. Lack of *in vitro* synergy between etoposide and *cis*-diamminedichloroplatinum(II). Cancer Res 1989;49:2390–7.

12. Gitler MS, Monks A, Sausville EA. Preclinical models for defining efficacy of drug combinations: mapping the road to the clinic. Mol Cancer Ther 2003;2:929–32.

13. Song S, Wientjes MG, Walsh C, Au JL. Non-toxic doses of suramin enhance activity of paclitaxel against lung metastases. Cancer Res 2001;61:6145–50.

14. Kanzawa F, Koizumi F, Koh Y, et al. *In vitro* synergistic interactions between the cisplatin analogue nedaplatin and the DNA topoisomerase I inhibitor irinotecan and the mechanism of this interaction. Clin Cancer Res 2001;7:202–9.

15. Raitanen M, Rantanen V, Kulmala J, Helenius H, Grenman R, Grenman S. Supra-additive effect with concurrent paclitaxel and cisplatin in vulvar squamous cell carcinoma *in vitro*. Int J Cancer 2002;100:238–43.

16. Johnston JS, Johnson A, Gan Y, Guillaume Wientjes M, Au L-S. Synergy between 3'-azido-3'-deoxythymidine and paclitaxel in human pharynx FaDu cells. Pharm Res 2003;20:957–61.

17. Aung TT, Davis MA, Ensminger WD, Lawrence TS. Interaction between gemcitabine and mitomycin-C *in vitro*. Cancer Chemother Pharmacol 2000;45:38–42.

18. Pavillard V, Kherfellah D, Richard S, Robert J, Montaudon D. Effects of the combination of camptothecin and doxorubicin or etoposide on rat glioma cells and camptothecin-resistant variants. Br J Cancer 2001;85:1077–83.

19. Mosmann T. Rapid colorimetric assay for cellular growth and survival: application to proliferation and cytotoxicity assays. J Immunol Methods 1983;65:55–63.

20. Chou TC, Talalay P. Quantitative analysis of dose-effect relationships: the combined effects of multiple drugs or enzyme inhibitors. Adv Enzyme Regul 1984;22:27–55.

21. Chou TC, Hayball MP. CalcuSyn: Windows software for dose effects analysis [manual]. Montana: Biosoft; 1996. p. 1–56.

22. Hope MJ, Bally MB, Webb G, Cullis PR. Production of large unilamellar vesicles by a rapid extrusion procedure: characterization of size, trapped volume and ability to maintain a membrane potential. Biochim Biophys Acta 1985;812:55–65.

23. Euhus DM, Hudd C, LaRegina MC, Johnsom FE. Tumor measurement in the nude mouse. J Surg Oncol 1986;31:229–34.

24. Tomayka MM, Reynolds CP. Determination of subcutaneous tumor size in athymic (nude) mice. Cancer Chemother Pharmacol 1989;24:148–54.

25. Skipper HE, Schabel FM, Jr., Wilcox WS. Experimental evaluation of potential anticancer agents XIII. on the criteria and kinetics associated with curability of experimental leukemia. Cancer Chemother Rep 1964;35:1–111.

26. Skipper HE. Laboratory models: the historical perspective. Cancer Treat Rep 1986;70:3–7.

27. Waud WR. Murine L1210 and P388 leukemias. In: Teicher BA, editor. Anticancer drug development guide. Totowa (New Jersey): Humana Press; 1997. p. 59–74.

28. Rideout DC, Chou TC. Synergy, antagonism and potentiation in chemotherapy: An overview. In: Rideout DC, Chou TC, editors. Synergism and antagonism in chemotherapy. San Diego (California): Academic Press; 1991. p. 3–60.

29. Chou JH. Quantitation of synergism and antagonism of two or more drugs by computerized analysis. In: Chou TC, Rideout DC, editors. Synergism and antagonism in chemotherapy. San Diego (California): Academic Press; 1991. p. 223–41.

30. Guichard S, Cussac D, Hennebelle I, Bugat R, Canal P. Sequence-dependent activity of the irinotecan-5FU combination in human colon-cancer model HT-29 *in vitro* and *in vivo*. Int J Cancer 1997;73:729–34.

31. Pavillard V, Formento P, Rostagno P, et al. Combination of irinotecan (CPT-11) and 5-fluorouracil with an analysis of cellular determinants of drug activity. Biochem Pharmaco 1998;56:1315–22.

32. Mans DRA, Grivicich I, Peters GJ, Schwartsmann G. Sequence-dependent growth inhibition and DNA damage formation by the irinotecan-5-fluorouracil combination in human colon carcinoma cell lines. Eur J Cancer 1999;35:1851–62.

33. Ramsay E, Ainajim J, Anantha M, et al. A novel approach to prepare a liposomal irinotecan formulation that exhibits significant therapeutic activity *in vivo*. Proc Am Assoc Cancer Res 2004;45:639.

34. Cao S, Zhang Z, Creaven PJ, Rustum YM. 5-fluoro-2″-deoxyuridine: role of schedule in its therapeutic efficacy. In: Rustum YM, editor. Novel approaches to selective treatments of human solid tumors: laboratory and clinical correlation. New York: Plenum Press; 1993. p. 1–8.

35. Corbett T, Valeriote F, LoRusso P, et al. *In vivo* methods for screening and preclinical testing. In: Teicher BA, editor. Anticancer drug development guide: preclinical screening, clinical trials, and approval. Totowa (New Jersey): Humana Press; 1997. p. 75–99.

36. Frei E III, Cannellos GP. Dose a critical factor in cancer chemotherapy. Am J Med 1980;69:585–94.

37. Rowinsky EK. The pursuit of optimal outcomes in cancer therapy in a new age of rationally designed target-based anticancer agents. Drugs 2000;60:1–14.

38. Talmadge JE. Pharmacodynamic aspects of peptide administration biological response modifiers. Adv Drug Deliv Rev 1998;33:241–52.

39. Allen TM, Cullis PR. Drug delivery systems: entering the mainstream. Science 2004;303:1818–22.

40. Krishna R, McIntosh N, Riggs KW, Mayer LD. Doxorubicin encapsulated in sterically stabilized liposomes exhibits renal and biliary clearance properties that are independent of Valspodar (PSC 833) under conditions that significantly inhibit nonencapsulated drug excretion. Clin Cancer Res 1999;5:2939–47.

41. Harrington KJ, Mohammadtaghi S, Uster PS, et al. Effective targeting of solid tumors in patients with locally advanced cancers by radiolabeled pegylated liposomes. Clin Cancer Res 2001;7:243–54.

42. Batist G, Chi K, Miller W, et al. Phase 1 Study of CPX-1, a fixed ratio formulation of irinotecan (IRI) and floxuridine (FLOX), in patients with advanced solid tumors. Proc Am Soc Clin Oncol 2006;24:82.

43. Parsels LA, Parsels JD, Tai DCH, Coughlin DJ, Maybaum J. 5-Fluoro-2-deoxyuridine-induced cdc25A accumulation correlates with premature mitotic entry and clonogenic death in human colon cancer cells. Cancer Res 2004;64:6538–94.

44. Goldwasser F, Shimizu T, Jackman J, et al. Correlations between S and G_2 arrest and the cytotoxicity of camptothecin in human colon carcinoma cells. Cancer Res 1996;56:4430–7.

Molecular Cancer Therapeutics

Ratiometric dosing of anticancer drug combinations: Controlling drug ratios after systemic administration regulates therapeutic activity in tumor-bearing mice

Lawrence D. Mayer, Troy O. Harasym, Paul G. Tardi, et al.

Mol Cancer Ther 2006;5:1854-1863.

NET-02: A multi-centre, randomised, phase II trial of liposomal irinotecan (nal-IRI) and 5-fluorouracil (5-FU)/folinic acid or docetaxel as second-line therapy in patients (pts) with progressive poorly differentiated extra-pulmonary neuroendocrine carcinoma (PD-EP-NEC)

Mairéad G McNamara[1,2], Jayne Swain[3], Zoe Craig[3], Jonathan Wadsley[4], Lucy Wall5, Nicholas Reed[6], Olusola Faluyi[7], Angela Lamarca[1,2], Richard A Hubner[1,2], Debashis Sarker[8], Tim Meyer[9], Juan W Valle[1,2]

[1]Department of Medical Oncology, The Christie NHS Foundation Trust, Manchester; [2]Division of Cancer Sciences, University of Manchester, Manchester; [3]Leeds Institute of Clinical Trials Research, University of Leeds; [4]Weston Park Hospital, Sheffield; [5]Edinburgh Cancer Centre, Western General Hospital; [6]Beatson Oncology Centre, Glasgow; [7]Clatterbridge Cancer Centre, Wirral; [8]King's College Hospital, London; [9]University College London Cancer Institute, London, United Kingdom.

Background

- Extra-pulmonary (EP) neuroendocrine carcinoma (NEC) is an aggressive rare entity [poorly differentiated (PD) morphology; Ki-67 >20%]1, presenting at an advanced stage in up to 85% of cases[2].
- First-line treatment for patients with advanced PD-EP-NEC, analogous to that of high grade NEC of the lung, has remained unchanged since a study in the early 1990s reported that the etoposide/platinum combination produced anti-tumour activity and high tumour response rates[3].
- The median overall survival (OS) for patients treated with first-line platinum-based chemotherapy in the advanced setting is 11-16.4 months[4,5,6].
- Disease progression inevitably occurs, and there is no established second-line treatment for patients with advanced PD-EP-NEC.
- In a systematic review and meta-analysis of second-line treatment in 595 patients with advanced PD-EP-NEC, the median response rate (RR) was 18%, the median progression-free survival (PFS) was 2.5 months (range 1.2-6.0) and median OS was 7.6 months (range 3.2-22)[7]. Prospective collaborative trials, with translational end-points are warranted, and may inform future biomarker-driven studies.

- **NET-02‡** is a multi-centre, randomised, parallel group, open-label, phase II, single-stage selection trial of liposomal irinotecan (nal-IRI)/5-FU/folinic acid or docetaxel, as **second-line therapy** in patients with progressive PD-EP-NEC, with the overall aim of selecting a treatment for continuation to a phase III trial (The standard arm of NET-02 is that used in high-grade lung NEC, of which docetaxel is a second-line therapy option (National Comprehensive Cancer Network guidelines), and combination regimens such as irinotecan/5-fluorouracil (5-FU) are a second-line therapy option currently used, without trial evidence, for this subset of patients[8]).

Methods

Primary endpoint

- 6-month PFS rate.

Secondary endpoints

- Progression-free survival.
- Overall survival.
- Objective RR using Response Evaluation Criteria in Solid Tumours (RECIST) version 1.1.
- Toxicity.
- Quality of life (QoL) using European Organisation for Research and Treatment of Cancer (EORTC) quality of life validated questionnaires C30 and NET21.
- Serum concentration of neuron-specific enolase.

Exploratory endpoints

- Quantification of circulating tumour cells (CTCs) and circulating tumour deoxyribonucleic acid (ctDNA) at baseline, 6 weeks and on progression, to identify any correlation with disease-related outcomes.
- Molecular profiling of CTCs, ctDNA and tumour tissue (further immunohistochemistry on tumour tissue may also be required) to identify any correlation with disease-related outcomes.
- Potential generation of mouse models of NEC.

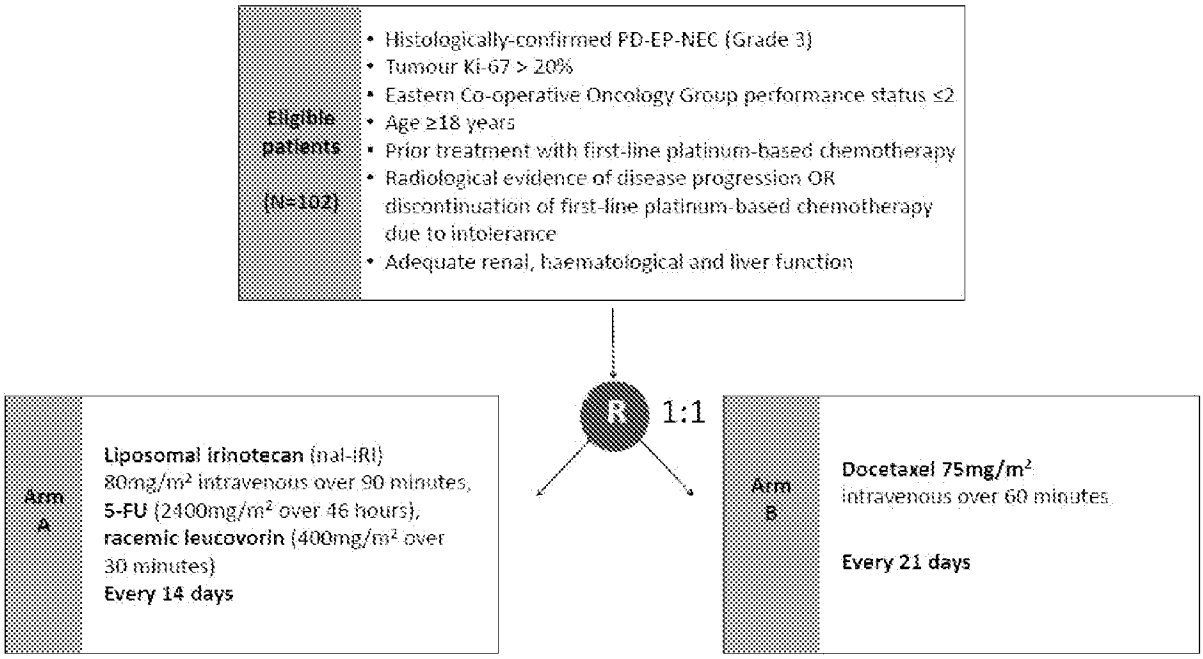

Figure 1: NET-02 Trial schema.

- This study plans to recruit patients from 16 United Kingdom centres over a 37 month duration (under the auspices of the National Institute for Health Research Clinical Research Network).
- Intention is to show that regimens are sufficiently active, but not to show that one regimen is superior.
- Designed to have an 80% chance of demonstrating that the one-sided 95% confidence interval of the 6-month PFS rate excludes 15%, if the true rate is at least 30%, where 30% is the required level of efficacy, and a rate of <15% would give grounds for rejection.
- If both treatment arms exceed the required level of efficacy to warrant further evaluation in a phase III trial, the treatment with the higher PFS rate at 6 months will be selected. However, if the difference in 6 month PFS rates between the treatment arms is less than 5%, alternative selection criteria such as toxicity rates or QoL may be considered, in addition to PFS rate.

- The **NET-02** trial is open (first patient treated November 26th 2018).
- **Clinical Trial information:** *EudraCT Number*: 2017-002453-11, *ISRCTN Number*: 10996604, *Clinical Trials.gov*: NCT03837977

References

(1) Rindi G, Klimstra DS, Abedi-Ardekani B, et al. A common classification framework for neuroendocrine neoplasms: an International Agency for Research on Cancer (IARC) and World Health Organization (WHO) expert consensus proposal. Modern Pathology; 31: 1770-1786, 2018.

(2) Garcia-Carbonero R, Sorbye H, Baudin E, et al. ENETS Consensus Guidelines for High-Grade Gastroenteropancreatic Neuroendocrine Tumours and Neuroendocrine Carcinomas. Neuroendocrinology; 103:186-94, 2016.

(3) Moertel CG, Kvols LK, O'Connell MJ, et al. Treatment of neuroendocrine carcinomas with combined etoposide and cisplatin: evidence of major therapeutic activity in the anaplastic variants of these neoplasms. Cancer; 68:227-232, 1991.

(4) Heetfeld M, Chougnet CN, Olsen IH, et al. Characteristics and treatment of patients with G3 gastroenteropancreatic neuroendocrine neoplasms. Endocr Relat Cancer; 22:657-64, 2015.

(5) Sorbye H, Welin S, Langer SW, et al: Predictive and prognostic factors for treatment and survival in 305 patients with advanced gastrointestinal neuroendocrine carcinoma (WHO G3): The NORDIC NEC study. Annals of Oncol; 24:152-160, 2013.

(6) Yamaguchi T, Machida N, Morizane C et al: Multicenter retrospective analysis of systemic chemotherapy for advanced neuroendocrine carcinoma of the digestive system. Cancer Sci; 105:1176-81, 2014.

(7) McNamara MG, Frizziero M, Jacobs T et al. Second-line treatment in patients (pts) with advanced extra-pulmonary poorly differentiated neuroendocrine carcinoma (EP-PD-NEC): a systematic review and meta-analysis. Neuroendocrinology;108 (Suppl 1):1-273, 2019.

(8) Hentic O, Hammel P, Couvelard A et al. FOLFIRI regimen: an effective second-line chemotherapy after failure of etoposide-platinum combination in patients with neuroendocrine carcinomas grade 3. Endocr Relat Cancer; 19:751-757, 2012.

*NET-02 is investigator-initiated and funded by an unrestricted educational grant (industry-funded) and National Health Service sponsored.

MANCHESTER 1824 The University of Manchester | The Christie NHS Foundation Trust | NIHR National Institute for Health Research | ctru Leeds Institute of Clinical Trials Research

NET-02: A multi-centre, randomised, phase II trial of liposomal irinotecan (nal-IRI) and 5-fluorouracil (5-FU)/folinic acid or docetaxel as second-line therapy in patients (pts) with progressive poorly differentiated extra-pulmonary neuroendocrine carcinoma (PD-EP-NEC)

Mairead G McNamara[1,2], Jayne Swain[3], Zoe Craig[3], Jonathan Wadsley[4], Lucy Wall[5], Nicholas Reed[6], Olusola Faluyi[7], Angela Lamarca[1,2], Richard A Hubner[1,2], Debashis Sarker[8], Tim Meyer[9], Juan W Valle[1,2]

[1]Department of Medical Oncology, The Christie NHS Foundation Trust, Manchester; [2]Division of Cancer Sciences, University of Manchester, Manchester; [3]Leeds Institute of Clinical Trials Research, University of Leeds; [4]Weston Park Hospital, Sheffield; [5]Edinburgh Cancer Centre, Western General Hospital; [6]Beatson Oncology Centre, Glasgow; [7]Clatterbridge Cancer Centre, Wirral; [8]King's College Hospital, London; [9]University College London Cancer Institute, London, United Kingdom.

Background

- Extra-pulmonary (EP) neuroendocrine carcinoma (NEC) is an aggressive rare entity (poorly differentiated (PD) morphology; Ki-67 > 20%), presenting at an advanced stage in up to 85% of cases[1].
- First-line treatment for patients with advanced PD-EP-NEC, analogous to that of high grade NEC of the lung, has remained unchanged since a study in the early 1990s reported that the etoposide/platinum combination produced anti-tumour activity and high tumour response rates[3].
- The median overall survival (OS) for patients treated with first-line platinum-based chemotherapy in the advanced setting is 11-12.4 months[4,5,6].
- Disease progression inevitably occurs, and there is no established second-line treatment for patients with advanced PD-EP-NEC.
- In a systematic review and meta-analysis of second-line treatment in 582 patients with advanced PD-EP-NEC, the median response rate (RR) was 18%, the median progression-free survival (PFS) was 2.5 months (range 1.2-6.0) and median OS was 7.6 months (range 3.2-12)[7]. Prospective collaborative trials, with translational end-points are warranted, and may inform future biomarker-driven studies.

- **NET-02** is a multi-centre, randomised, parallel group, open-label, phase II, single-stage selection trial of liposomal irinotecan (nal-IRI)/5-FU/folinic acid or docetaxel, as **second-line therapy** in patients with progressive PD-EP-NEC, with the overall aim of selecting a treatment for continuation to a phase III trial (The standard arm of NET-02 is that used in high-grade lung NEC, of which docetaxel is a second-line therapy option (National Comprehensive Cancer Network guidelines), and combination regimens such as irinotecan/5-fluorouracil (5-FU) are a second-line therapy option currently used, without trial evidence, for this subset of patients[8]).

Methods

Primary endpoint

- 6-month PFS rate.

Secondary endpoints

- Progression-free survival.
- Overall survival.
- Objective RR using Response Evaluation Criteria in Solid Tumours (RECIST) version 1.1.
- Toxicity.
- Quality of life (QoL) using European Organisation for Research and Treatment of Cancer (EORTC) quality of life validated questionnaires C30 and NET21.
- Serum concentration of neuron-specific enolase.

Eligible patients (N=102)

- Histologically confirmed PD-EP-NEC (Grade 3)
- Tumour Ki-67 > 20%
- Eastern Co-operative Oncology Group performance status ≤1
- Age ≥16 years
- Prior treatment with first-line platinum-based chemotherapy
- Radiological evidence of disease progression OR discontinuation of first-line platinum-based chemotherapy due to intolerance
- Adequate renal, haematological and liver function

Exploratory endpoints

- Quantification of circulating tumour cells (CTCs) and circulating tumour deoxyribonucleic acid (ctDNA) at baseline, 6 weeks and on progression, to identify any correlation with disease-related outcomes.
- Molecular profiling of CTCs, ctDNA and tumour tissue (further immunohistochemistry on tumour tissue may also be required) to identify any correlation with disease-related outcomes.
- Potential generation of mouse models of NEC.

R 1:1

Arm A: **Liposomal irinotecan** (nal-IRI) 70mg/m² intravenous over 90 minutes, **5-FU** (2400mg/m² over 46 hours), **racemic leucovorin** (400mg/m² over 30 minutes) **Every 14 days**

Arm B: **Docetaxel 75mg/m²** intravenous over 60 minutes **Every 21 days**

Figure 1: NET-02 Trial schema.

Computed Tomography every 8 weeks (± 7 days) (QoL every 6 weeks)
Treatment will continue until intolerable toxicity or progressive disease

- This study plans to recruit patients from 16 United Kingdom centres over a 27 month duration (under the auspices of the National Institute for Health Research Clinical Research Network).
- Intention is to show that regimens are sufficiently active, but not to show that one regimen is superior.
- Designed to have an 80% chance of demonstrating that the one-sided 95% confidence interval of the 6-month PFS rate excludes 15%, if the true rate is at least 30%, where 30% is the required level of efficacy, and a rate of <15% would give grounds for rejection.
- If both treatment arms exceed the required level of efficacy to warrant further evaluation in a phase III trial, the treatment with the higher PFS rate at 6 months will be selected. However, if the difference in 6 month PFS rates between the treatment arms is less than 5%, alternative selection criteria such as toxicity rates or QoL may be considered, in addition to PFS rate.

- The **NET-02** trial is open (first patient treated November 26th 2018).
- **Clinical Trial information:** *EudraCT Number: 2017-002453-41; ISRCTN Number: 10996604; Clinical Trials.gov: NCT03837977*

References

(1) Rindi G, Klimstra DS, Abedi-Ardekani B, et al. A common classification framework for neuroendocrine neoplasms: an International Agency for Research on Cancer (IARC) and World Health Organization (WHO) expert consensus proposal. Modern Pathology; 31: 1770-1786, 2018.

(2) Garcia-Carbonero R, Sorbye H, Baudin E, et al. ENETS Consensus Guidelines for High-Grade Gastroenteropancreatic Neuroendocrine Tumours and Neuroendocrine Carcinomas. Neuroendocrinology; 103(2):186-94, 2016.

(3) Moertel CG, Kvols LK, O'Connell MJ, et al. Treatment of neuroendocrine carcinomas with combined etoposide and cisplatin: evidence of major therapeutic activity in the anaplastic variants of these neoplasms. Cancer; 68:227-232, 1991.

(4) Heetfeld M, Chougnet CN, Olsen IH, et al. Characteristics and treatment of patients with G3 gastroenteropancreatic neuroendocrine neoplasms. Endocr Relat Cancer; 22:657-64, 2015.

(5) Sorbye H, Welin S, Langer SW, et al. Predictive and prognostic factors for treatment and survival in 305 patients with advanced gastrointestinal neuroendocrine carcinoma (WHO G3): The NORDIC NEC study. Annals of Oncol; 24:152-160, 2013.

(6) Yamaguchi T, Machida N, Morizane C et al. Multicenter retrospective analysis of systemic chemotherapy for advanced neuroendocrine carcinoma of the digestive system. Cancer Sci; 105:1176-81, 2014.

(7) McNamara MG, Frizziero M, Jacobs T et al. Second-line treatment in patients (pts) with advanced extra-pulmonary poorly differentiated neuroendocrine carcinoma (EP-PD-NEC): a systematic review and meta-analysis. Neuroendocrinology;108 (Suppl 1):1-273, 2019.

(8) Hentic O, Hammel P, Couvelard A, et al. FOLFIRI regimen: an effective second-line chemotherapy after failure of etoposide-platinum combination in patients with neuroendocrine carcinomas grade 3. Endocr Relat Cancer; 19:751-757, 2012.

NET-02 is investigator initiated and funded by an unrestricted educational grant (industry-funded) and National Health Service sponsored.

ENETS

Correspondence to:
Mairead.McNamara@christie.nhs.uk

(P04) - SELECTED FOR Case report

NET-02: A Phase II Trial of Liposomal Irinotecan (nal-IRI) and 5-Fluorouracil (5-FU)/Folinic Acid or Docetaxel as Second-Line Therapy in Patients (pts) with Progressive Poorly Differentiated Extra-Pulmonary Neuroendocrine Carcinoma (PD-EP-NEC)

McNamara M[A], Swain J[B], Craig Z[B], Wadsley J[C], Wall L[D], Reed N[E], Faluyi O[F], Lamarca A[G], Hubner R[G], Sarker D[H], Meyer T[I], Valle JW[A];
[A]University of Manchester, Manchester, United Kingdom
[B]University of Leeds, Leeds, United Kingdom
[C]Weston Park Hospital, Sheffield, United Kingdom
[D]Western General Hospital, Edinburgh, United Kingdom
[E]Beatson West of Scotland Cancer Centre, Glasgow, United Kingdom
[F]Clatterbridge Cancer Centre, Liverpool, United Kingdom
[G]The Christie NHS Foundation Trust, Manchester, United Kingdom
[H]Guys Hospital, London, United Kingdom
[I]UCL, London, United Kingdom

Introduction: The prognosis for pts with PD-EP-NEC is poor. **Aim(s):** First-line treatment for advanced disease is etoposide/platinum-based chemotherapy, with no standard 2nd line treatment, and is an area of unmet need. **Materials and methods:** This is a multi-centre, randomised, phase II trial of nal-IRI; 80mg/m2 intravenously (IV) over 90 mins, prior to 5-FU; 2400 mg/m2 infusion over 46 hrs and folinic acid, Q14 days, or docetaxel; 75mg/m2 IV over 60 mins, Q21 days, as 2nd line therapy in pts with progressive PD-EP-NEC (Ki-67>20%), with the overall aim of selecting a treatment for continuation to a phase III trial. The standard arm is that used in high-grade lung NEC, of which docetaxel is a 2nd line therapy option (NCCN guidelines) and combination regimens such as Irinotecan/5-FU are a 2nd line therapy option currently used without trial evidence for this subset of pts. Pts must have had prior treatment with 1st line platinum-based chemotherapy, have documented disease progression and have an ECOG performance status of ≤2. **Results:** This study plans to recruit 102 pts from 16 UK centres (over 37 mths). Primary endpoint is 6-mth progression-free survival (PFS) rate. If both treatment arms exceed the required level of efficacy to warrant further evaluation in a phase III trial, treatment with the higher PFS rate at 6 mths will be selected. Secondary endpoints include overall survival, objective response rate, toxicity, quality of life, serum neuron-specific enolase. Exploratory endpoints include quantification of circulating tumour cells (CTCs), circulating tumour deoxyribonucleic acid (ctDNA) and molecular profiling of CTCs, ctDNA and tumour tissue, and generation of CTC-derived xenografts. **Conclusion:** This trial is open; 23 pts enrolled to date.
Keywords: poorly differentiated, neuroendocrine carcinoma, second line treatment, docetaxel, liposomal irinotecan, 5-fluorouracil

European

ENETS

Neuroendocrine Tumor Society

17th Annual ENETS Conference for the Diagnosis and Treatment of Neuroendocrine Tumor Disease

Virtual Conference | 11 - 13 March 2020

Abstract Book

Cancer Chemother Pharmacol (2002) 49: 201–210
DOI 10.1007/s002800100371

ORIGINAL ARTICLE

Jetske M. Meerum Terwogt · Gerard Groenewegen
Dick Pluim · Marc Maliepaard · Matthijs M. Tibben
Albert Huisman · Wim W. ten Bokkel Huinink
Margaret Schot · Helen Welbank · Emile E. Voest
Jos H. Beijnen · Jan H. M. Schellens

Phase I and pharmacokinetic study of SPI-77, a liposomal encapsulated dosage form of cisplatin

Received: 9 December 2001 / Accepted: 30 July 2001 / Published online: 22 January 2002

Abstract *Purpose:* To investigate the safety and pharmacokinetics of a new liposomal formulation of cisplatin, SPI-77, in patients with advanced malignancies. *Patients and methods:* Patients with histologically proven malignancies not amenable to other treatment were eligible for this study. The starting dose of SPI-77 (cisplatin in Stealth liposomes) was 40 mg/m^2 administered every 4 weeks in a 2-h infusion, and doses were escalated up to 420 mg/m^2. Pharmacokinetic monitoring was performed in all patients and samples were analysed for platinum content by atomic absorption spectroscopy. Platinum-DNA (Pt-DNA) adduct levels in leucocytes (white blood cells, WBC) and tumour tissue were quantified using a sensitive ^{32}P-postlabelling assay. *Results:* A total of 27 patients were accrued. The main toxicities observed were infusion-related reactions, which could be prevented by lowering the initial infusion rate, and anaemia. The pharmacokinetics of SPI-77-derived platinum were strikingly different from standard cisplatin. Free platinum levels in plasma ultrafiltrate samples were undetectable at the lowest dose levels (40 and 80 mg/m^2), and low but highly variable at higher doses of SPI-77. Plasma pharmacokinetics of total platinum were linear with small interpatient variability. The total body clearance of SPI-77 varied from 14 to 30 ml/h and was significantly lower than reported clearance values for cisplatin of 20 l/m^2 per h, due to the slow release of cisplatin from the liposomes. Pt-DNA adduct levels in WBC ranged from 0.02 to 4.13 fmol/μg DNA for intrastrand Pt-GG (guanine-guanine) adducts and from 0.02 to 1.27 fmol/μg DNA for intrastrand Pt-AG (adenosine-guanine) adducts, which is more than tenfold lower than after administration of a comparable dose of non-liposomal cisplatin. In tumour samples obtained from two patients treated at the highest dose-levels, relatively low levels of Pt-DNA adducts were observed. *Conclusions:* The results of this phase I trial show that the pharmacokinetic behaviour of cisplatin is significantly altered by its encapsulation in Stealth liposomes. The pharmacokinetics of SPI-77 are mainly dominated by the liposomal properties, resulting in high cholesterol concentrations and relatively low concentrations of (free) platinum in plasma, WBC and tumour tissue, which may explain the observed differences between the toxicity profiles of SPI-77 and cisplatin.

Keywords SPI-77 · Liposomal cisplatin · Stealth liposomes · Pharmacokinetics · Phase I study

J.M. Meerum Terwogt (✉) · D. Pluim · M. Maliepaard
M.M. Tibben · W.W. ten Bokkel Huinink · M. Schot
J.H. Beijnen · J.H.M. Schellens
The Netherlands Cancer Institute/Antoni van Leeuwenhoek Hospital, Department of Medical Oncology,
Plesmanlaan 121, 1066 CX, Amsterdam, The Netherlands
E-mail: apjmt@slz.nl
Tel.: +31-20-5124657
Fax: +31-20-5124753

J.M. Meerum Terwogt · M.M. Tibben · W.W. ten Bokkel Huinink · J.H. Beijnen · J.H.M. Schellens
The Netherlands Cancer Institute/Slotervaart Hospital, Department of Pharmacy and Pharmacology,
Louwesweg 6, 1066 EC, Amsterdam, The Netherlands

G. Groenewegen · A. Huisman · E.E. Voest
University Medical Center Utrecht, Department of Internal Medicine – Division of Medical Oncology,
Heidelberglaan 100, 3584 CX, Utrecht, The Netherlands

H. Welbank
SEQUUS Pharmaceuticals, Inc., 950 Great West Road, Brentford, Middlesex TW8 9ES, UK

J.H. Beijnen · J.H.M. Schellens
Faculty of Pharmacy, Utrecht University,
Sorbonnelaan 16, 3584 CA,
Utrecht, The Netherlands

Introduction

Cisplatin is a well-known and very potent anticancer agent frequently used against a variety of tumours, including ovarian, testicular, lung and head and neck cancer [3, 4, 7, 9, 10, 14]. The mechanism of action is based on a direct binding of cisplatin to DNA. The acute

dose-limiting toxicity associated with cisplatin therapy is nephrotoxicity, although this can be largely reduced with adequate hydration. Other commonly observed toxicities that hamper further dose increments are nausea and vomiting, peripheral neuropathies, ototoxicity, hypersensitivity reactions and myelosuppression. Research in the past decade has focused on the development of other platinum compounds with an improved therapeutic index, such as carboplatin [21, 25].

Liposomal encapsulation of cisplatin is an alternative approach to reducing systemic drug exposure and to delivering cisplatin to tumours with increased selectivity. SPI-77, a Stealth liposomal dosage form of cisplatin, was developed in order to increase the total dose of cisplatin that can be administered with no increase, and perhaps even a decrease, in systemic toxicity. Stealth liposomes are coated with methoxy-polyethylene glycol (MPEG) which makes them resistant to recognition by blood opsonins and removal from the blood stream. Due to their small size (approximately 110 nm), long circulation time and reduced interaction with blood components, Stealth liposomes tend to accumulate in tumours [28]. At these tumour sites, the liposomes can become extravasated through the abnormally permeable vessels characteristic of many tumours, thereby entering the interstitial space, where they gradually break down and release cisplatin to the surrounding tumour cells [5, 29]. If successful, the systemic exposure to free cisplatin is low, whereas high concentrations are achieved at the desired site.

SPI-77 has displayed less-acute toxicity in preclinical studies, as compared to cisplatin, and its antitumour effects are at least equivalent to those of cisplatin or carboplatin [12, 20]. In addition, antitumour effects are in general longer-lasting than after administration of cisplatin or carboplatin [20]. In vitro results have suggested that prolonged infusions of cisplatin may be favourable for therapeutic use [14]. The slow release of the drug from the liposomal carrier can mimic a continuous infusion with lower peak plasma levels and a prolonged drug exposure. A phase I dose-escalating study was performed in our institutes to evaluate the safety and the pharmacokinetics of SPI-77 in patients with cancer.

Patients and methods

Patient eligibility criteria

Patients were eligible if they had a histologically or cytologically proven malignancy not amenable to other treatment, and if they had an acceptable performance status (Karnofsky PS ≥70%). Other eligibility criteria included age ≥18 years, life expectancy ≥3 months, and adequate function of bone marrow function (absolute neutrophil count ≥2000/mm^3, platelet count ≥100,000/mm^3 and haemoglobin ≥9.0 g/dl), liver function (total bilirubin ≤ 2.0 mg/dl, ALT and AST not more than 1.5 times the upper limit of normal) and kidney function (creatinine clearance ≥50 ml/min). Previous anticancer chemotherapy, radiotherapy or immunotherapy had to be discontinued for at least 4 weeks before entry to the study (6 weeks in cases of treatment with nitrosourea, suramin or mitomycin C) and prior treatment with SPI-77 was not allowed. Patients were excluded if they had a history of abnormal cardiac function, hearing loss and/or an allergic reaction to cisplatin or other platinum-containing products. Further exclusion criteria were pregnancy, signs or symptoms of an acute infection requiring systemic therapy, neurological symptoms and psychiatric illness. Patients had to give written informed consent.

Treatment plan

Three patients were enrolled per dose level (cohort). Each cohort received SPI-77 every 4 weeks to a total of six doses, or until disease progression, whichever occurred earlier. Initially, the infusion duration was set at 2 h. The three patients in the first cohort received SPI-77 at a dose of 40 mg/m^2 during each cycle and thereafter, dose escalation was scheduled as follows: 80, 120, 200, 320, 520 and 840 mg/m^2, provided that no dose-limiting toxicities were observed (for definition see Patient evaluation section). If a dose-limiting toxicity occurred in one of the three patients within one cohort, then three additional patients were treated at that level. The last patient at a dose level was observed for at least 4 weeks before the first patient at the subsequent dose level was treated. The maximum tolerated dose was defined as the dose below the dose at which two out of six patients experienced dose-limiting toxicity. No prophylactic antiemetic or hydration therapy was given.

Chemicals

SPI-77 was provided by SEQUUS Pharmaceuticals (Brentford, UK) as an isotonic preservative-free suspension for parenteral administration containing 1.18 mg cisplatin/ml. The lipids in SPI-77 consist of fully hydrogenated soy phosphatidylcholine (HSPC) (40.0 mg/ml), cholesterol (17.1 mg/ml), and the polymer MPEG-DSPE (14.3 mg/ml), with a total lipid content of approximately 71 mg/ml. The mean liposome particle diameter is approximately 110 nm and the cisplatin encapsulation exceeds 90%. Prior to infusion, SPI-77 was further diluted with physiological saline (NaCl 0.9%) to a final concentration of 0.2 mg/ml. Nitric acid 65% for dilution of the samples was obtained from Merck, Darmstadt, Germany, and Triton X-100 was obtained from BDH, Poole, UK.

Patient evaluation

Pretreatment evaluation included a complete medical history and a complete physical examination. In addition, an electrocardiogram, an audiogram and a neurological examination were performed. Prior to each administration, haematology and serum chemistry including lipid profile (cholesterol and triglyceride levels including the high density lipoprotein and low density lipoprotein subfractions) were checked. Urine analysis was performed and 24-h creatinine clearance determined. Haematology and serum chemistry were checked weekly. Urine analysis, audiogram and neurological examination were repeated at the end of every cycle. An electrocardiogram was repeated at the end of the treatment. Tumour evaluations were performed every other cycle. Toxicity was graded according to the National Cancer Institute Common Toxicity Criteria [15] and dose-limiting toxicities were defined as nephrotoxicity or non-reversible neurological toxicity grade 2 or higher in severity, or any other toxicity grade 3 or higher, with the exception of untreated nausea, vomiting, alopecia, weight change, fatigue, and allergic reactions, which were not considered dose-limiting. A decrease in creatinine clearance was used as an indicator for evaluation of nephrotoxicity. Creatinine clearances during treatment (between administrations) as well as at the end of the treatment (after the last administration) were determined, to detect acute and cumulative toxicities.

Pharmacokinetic studies

Pharmacokinetic studies were performed in all except two patients. Blood samples were obtained from patients at 12 time-points up to 4 weeks after the first administration: preinfusion, at the end of the infusion, at 1, 3, 5, 24, 48, 72, 96 and 168 h after administration and

weekly thereafter for a total of three additional weeks. The samples (7 ml each) were collected in heparinized tubes, which were placed in an ice-bath (0–4°C) immediately after withdrawal. Whole blood was centrifuged at 4°C for 5 min (3000 *g*). Four 100-µl aliquots of the obtained plasma fraction were diluted tenfold (1:9) with 0.1% Triton X-100 plus 0.2% nitric acid solution. Of the remaining plasma, 1 ml was centrifuged for 10 min using Amicon Centrifree ultrafiltration devices to obtain approximately 0.2 ml plasma ultrafiltrate. All samples were stored at –20°C until analysis.

Urine samples were collected prior to infusion, and at 24, 48, 72 and 96 h after administration. Tumour samples were obtained from three patients: one patient with a melanoma, one patient with ascites from ovarian cancer and one patient with cervix cancer. The melanoma and the cervix cancer were biopsied on day 2 (the day after infusion of SPI-77) and ascites samples were taken on days 1, 5, 9, 15, 18, 26, 30, 36 and 41.

All platinum analyses were performed using a validated flameless atomic absorption spectroscopy method, with a lower limit of quantification of 0.125 µ*M*. [13]. Total platinum, i.e. free plus protein-bound plus liposomal encapsulated platinum, was measured in plasma. Total platinum concentrations were determined in diluted plasma samples and free platinum was determined in ultrafiltrate samples.

Platinum-DNA adduct measurements

Prior to the infusion, at the end of the infusion and at 3, 24 and 48 h after the end of the infusion during course 1, whole blood samples of 14 ml were collected in heparinized tubes for platinum-DNA (Pt-DNA) adduct determination in leucocytes (white blood cells, WBC). Immediately after withdrawal, the samples were centrifuged at 4°C for 5 min (3000 *g*). Subsequently, the WBC fraction was isolated. WBC were purified by lysing contaminating red blood cells in the WBC fraction by incubation in 0.1% (w/v) ammonium chloride, 1 m*M* edetate disodium, and 1% (w/v) potassium bicarbonate for 20 min at 4°C. The WBC were washed twice with phosphate-buffered saline, and lysed in 0.01 *M* Tris-HCl, 2.32% (w/v) NaCl, and 2 m*M* edetate disodium, pH 7.30. The lysed WBC were directly used for DNA isolation or they were stored at –80°C until analysis. Pt-DNA adducts were quantified using a sensitive ^{32}P-postlabelling assay, enabling the selective determination of intrastrand platinum and guanine-guanine (Pt-GG) and platinum and adenosine-guanine (Pt-AG) adducts down to a detection limit of 15 amol platinum/µg DNA [16].

Pharmacokinetic parameters

Non-compartmental methods were applied to calculate the pharmacokinetic parameters of total platinum. The area under the plasma concentration-time curve (AUC) was determined using the linear trapezoidal method with extrapolation to infinity (C_{last}/k, in which C_{last} is the last measured concentration). The AUC of Pt-DNA adducts was calculated up to C_{last} without extrapolation to infinity. The elimination rate constant for total platinum (k) was calculated by linear regression analysis of the logarithmic plasma concentration-time curves. The total body clearance (Cl), the elimination half-life ($t_{1/2}$) and the volume of distribution at steady state (V_{ss}) were calculated using standard equations [6]. Pt-DNA adduct AUC was calculated using the trapezoidal method up to the last measured time-point at 48 h. Statistical analysis of the results was performed using SPSS/PC+ (SPSS/PC+ Advanced Statistics, version 6.1, 1994; Chicago, Ill.).

Results

Patients and treatment

A total of 27 patients were included in the trial. Patient characteristics are presented in Table 1. Six patients were treated at the starting dose of 40 mg/m^2, because of a grade 4 infusion-related reaction observed in one patient (for description see Toxicity section). Three patients were treated at a dose of 80 mg/m^2, three others at a dose of 120 mg/m^2 and three at a dose of 200 mg/m^2. Nine patients were treated at a dose of 320 mg/m^2, because two patients developed muscle weakness proximally in both legs, which was grade 2 to 3 in severity. Three patients were treated at a dose of 420 mg/m^2, after which the study was discontinued. A total of 69 courses of SPI-77 were administered with a median number of two courses per patient (range one to ten). One patient died after the second course due to disease progression. One patient went off-study after the second course due to the grade 4 infusion-related reaction. All other patients went off-study because of disease progression.

Because of the observed infusion-related reactions, the infusion duration was increased from 2 h to approximately 3 h at a dose of 120 mg/m^2 by lowering the infusion rate to 100 ml/h during the first 15 min, followed by an infusion rate of 700 ml/h for the remaining volume. Simultaneously, the final dilution of SPI-77 in 0.9% NaCl was decreased from 0.3 mg/ml to 0.2 mg/ml. As a result, the infusion duration at a dose of 320 mg/m^2 was approximately 5 h. In order to reduce the total infusion volume, the final dilution was reset at 0.3 mg/ml at a dose of 320 mg/m^2, which reduced the infusion duration to approximately 3 h. All patients were considered evaluable for toxicity and response.

Table 1 Patient characteristics and responses. Values are number of patients, except age in years

Number of patients	
Total	27
Male/female	13/14
Age (years)	
Median	57
Range	34–75
Karnofsky performance status (%)	
70	2
80	2
90	11
100	12
Prior therapy	
None	1
Surgery	3
Surgery + radiotherapy	5
Surgery + chemotherapy	10
Surgery + chemotherapy + hormonal therapy	3
Surgery + radiotherapy + hormonal therapy	1
Surgery + radiotherapy + chemotherapy	4
Tumour site	
Colon carcinoma	5
Renal cell carcinoma	4
Ovarian carcinoma	5
Cervix carcinoma	1
Mesothelioma	3
Sigmoid carcinoma	1
Pancreas carcinoma	1
Oesophagus carcinoma	1
Thyroid carcinoma	2
Melanoma	2
Prostate carcinoma	1
Adenocarcinoma with unknown primary	1

Toxicity

Haematological toxicity was mild. Anaemia grade 3 was the most severe haematological toxicity documented, which occurred in two patients (7%) during two courses (3%). Anaemia grade 2 occurred in nine patients (33%) during a total of 11 courses (16%). It should be noted, however, that anaemia grade 2 was pre-existent in three patients (11%) and anaemia grade 1 in ten patients (37%). One patient developed a leucocytopenia grade 1 during one course. Gastrointestinal toxicities were the most frequently observed non-haematological toxicities. One patient suffered from vomiting grade 3 during one course. Vomiting grade 1 or 2 occurred in ten patients (37%) during a total of 14 courses (20%). Nausea grade 1 or 2 was present in 13 patients (48%) during 22 courses (32%).

One patient experienced a grade 4 infusion-related reaction during the first few minutes of the second administration, which was the reason for study discontinuation in this patient. This patient developed hypotension, dizziness, sweating, back pain and paraesthesia within 10 min of the start of the second SPI-77 infusion. All symptoms resolved within 20 min of cessation of the infusion and administration of 10 mg dexamethasone plus 2 mg clemastine intravenously. Three other patients (11%) experienced minor reactions during the first administration. These reactions consisted mainly of flushing and a slight decrease in blood pressure. Typically, the reactions occurred during the first few minutes of administration. It was therefore decided to reduce the rate of infusion during the first 15 min to 100 ml/h (as described under patients and treatment), which prevented further infusion-related reactions. Ototoxicity manifested as transient tinnitus occurred in four patients (15%), during a total of five courses (7%).

Muscle weakness was observed in two patients (7%) during three courses (4%) at a dose of 320 mg/m^2, being severe (grade 2 or 3) in two courses (3%). The onset was after two courses. In both patients the toxicity manifested as a loss of strength of the proximal leg muscles. One patient died shortly thereafter due to disease progression and therefore the relationship between the observed toxicity and the study drug could not be properly assessed in this patient. The other patient underwent extensive neurological examination, but no objective abnormalities were observed on the electromyelogram. During the follow-up, the symptoms improved in this patient, indicating reversibility. It should be noted that the toxicity in both cases manifested as a loss of strength of the leg muscles, and both patients were already considerably weakened due to their disease. These toxicities were also the reason for the recruitment of six additional patients at a dose of 320 mg/m^2. These patients and the patients at a dose of 420 mg/m^2 underwent extensive neurological evaluation, consisting of an electromyelogram and vibration perception measurement, prior to study entry and every other course, or if symptoms developed. No weakness of muscle strength or abnormal test results for neurological side effects were observed in any of these six patients.

No significant decreases in creatinine clearance were observed at any dose administered, either during treatment or at the end of the treatment. Other toxicities consisted of skin toxicities, such as pruritus in five patients (19%) and stomatitis in three patients (11%), and 'flu-like symptoms, such as fever, in seven patients (26%) and fatigue in ten patients (37%). These toxicities were generally mild and never exceeded grade 1 or 2 in severity. Significant toxicities are shown in Table 2.

Responses

Although response measurement was not a primary goal in the study, six patients (22%) had stable disease for at least two consecutive measurements. One of these patients with a renal cell carcinoma, who received four courses of SPI-77, showed a significant regression of tumour metastases, which lasted for 2 months. This patient was a 43-year-old chemonaive male. However, he did not reach a partial response, because no significant reduction was observed in the primary tumour. One patient with advanced pancreatic cancer with liver metastases showed stable disease during ten courses. Responses are further shown according to tumour site in Table 1.

Pharmacokinetic studies

All except two patients underwent pharmacokinetic monitoring during the first course. Total platinum concentrations were measured in diluted plasma samples and free platinum concentrations were measured in plasma ultrafiltrate samples. Complete plasma concentration-time curves for total platinum were obtained in 25 patients during the first course. The mean plasma concentration-time curves per dose level are depicted in Fig. 1. Mean pharmacokinetic parameters for total platinum were derived from these curves and are presented in Table 3. A plot of the total platinum plasma AUC versus the administered dose of SPI-77 is shown in

Table 2 Drug-related toxicity scored according to the CTC criteria

Toxicity	Grade	No. of patients (%)	No. of courses (%)
Haematological			
Anaemia	3	2 (7)	2 (3)
Gastrointestinal			
Nausea	3	1 (4)	1 (1)
Vomiting	3	1 (4)	1 (1)
Infusion-related reactions	4	1 (4)	1 (1)
Neurological			
Sensory	1	1 (4)	1 (1)
Motor	1	1 (4)	1 (1)
Muscle weakness	2	1 (4)	1 (1)
	3	1 (4)	1 (1)

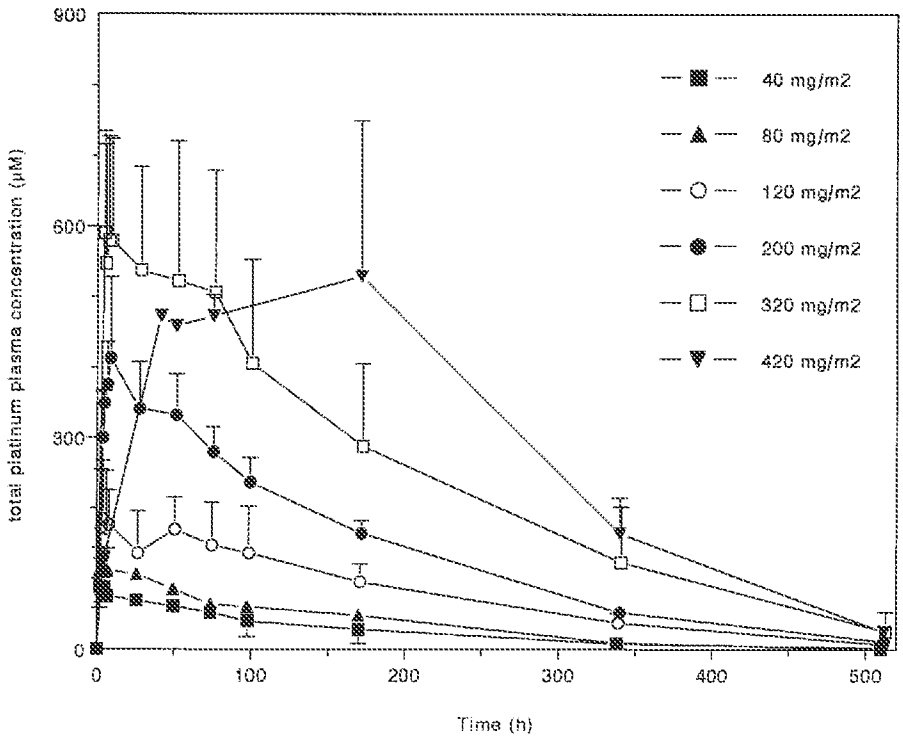

Fig. 1 Plasma concentration-time curves for total platinum. Values are means ± SD. Each curve was derived from the data from at least three patients. SPI-77 was administered over 2–5 h

Table 3 Pharmacokinetic parameters. Values are means ± SD. For abbreviations see Methods section

Dose (mg/m^2)	No. of patients	$AUC_{0-\infty}$ (h·mM)	C_{max} (μM)	Cl (ml/h)	$t_{1/2}$ (h)	V_{ss} (l)
40	6	13.6 ± 1.5	100.8 ± 22.7	19.8 ± 2.5	95 ± 15	2.68 ± 0.37
80	2	18.2 ± 0.2	117.2 ± 24.8	30.0 ± 2.8	79 ± 4	3.45 ± 0.17
120	3	44.5 ± 6.5	193.5 ± 68.9	17.0 ± 2.7	132 ± 35	3.19 ± 0.41
200	3	71.1 ± 2.5	423.1 ± 97.7	17.7 ± 1.0	103 ± 3	2.63 ± 0.10
320	9	145.4 ± 73.8	642.8 ± 141.7	18.1 ± 10.8	116 ± 55	2.86 ± 2.03
420	2	163.3 ± 6.7	589.1 ± 135.1	14.0 ± 0.1	145 ± 107	2.98 ± 2.24

Fig. 2. Pharmacokinetics of total platinum were linear up to a dose of 420 mg/m^2 (Fig. 2). Low interpatient variability was observed at all dose levels, except for the dose of 320 mg/m^2. The calculated AUC values of total platinum after administration of SPI-77 in our study were approximately 100-fold higher than reported AUC values for total platinum after administration of cisplatin at the comparable dose of 100 mg/m^2 [7].

The volume of distribution of total platinum after SPI-77 administration ranged from 2.6 to 3.5 l. Mean elimination half-lives after 2- to 5-h infusions of SPI-77 ranged from 80 to 145 h, and were dose-independent. Total body clearances of SPI-77 were 14–30 ml/h, which is extremely low compared to the reported clearance values for cisplatin, which average 34 l/h [1, 17].

Free (ultrafilterable) platinum levels were below the lower limit of quantification in patients receiving SPI-77 doses of 40 and 80 mg/m^2. At the higher dose levels, free platinum levels were measurable, but highly variable. Maximum measured concentrations ranged from 0.4 to 140 μM and were independent of dose and time.

In addition, several ascites samples were collected from one patient and analysed for platinum content. Total platinum levels in the ascites ranged from 8 to 74 μM and free platinum levels ranged from 0.6 to 1.8 μM.

Lipid profile analysis

The large amount of lipids present in the membrane bilayer of the liposomes may influence the lipid profile of patients receiving SPI-77, especially at high doses. Therefore, serum total cholesterol and triglyceride levels were monitored in all patients. Serum cholesterol levels in patients were highly variable, but increased with increasing doses of SPI-77. In addition, particularly at the higher doses of SPI-77, a fluctuating pattern became apparent. Cholesterol levels tended to increase shortly after administration of SPI-77 and gradually decreased over the 4 weeks following the administration. Maximum cholesterol levels ranged from 5.0 to 20.9 mM, which represented increases from baseline values of 23 to

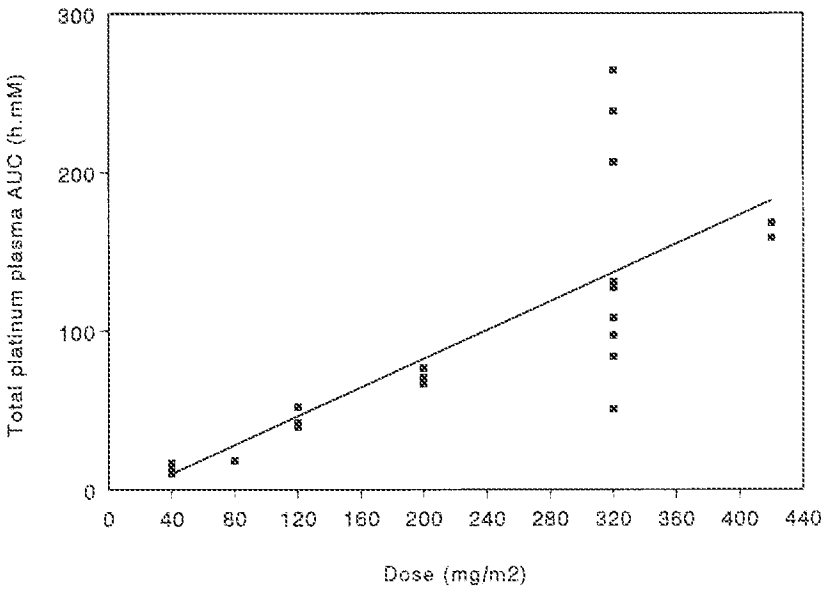

Fig. 2 AUC values of total platinum (derived from the curves in Fig. 1) plotted against the dose of SPI-77. The solid line is the regression line ($R = 0.81$)

214%, the median increase being 64%. Fluctuations in cholesterol levels are shown in Fig. 3. Maximum increases in serum triglyceride levels as a percentage of the baseline values ranged from 38 to 350%, the median increase being 75%. Maximum triglyceride levels varied widely from 1.4 to 12.3 m*M*.

Pt-DNA adduct formation

Pt-DNA adduct formation was quantified in 19 patients. Pt-GG and Pt-AG adducts, the two major Pt-DNA adducts, were measured. Adducts were determined in three patients receiving SPI-77 at a dose of 40 mg/m^2, three a dose of 80 mg/m^2, three a dose of 120 mg/m^2, three a dose of 200 mg/m^2, five a dose of 320 mg/m^2 and two a dose of 420 mg/m^2 during the first course. Pt-GG adduct levels ranged from 0.02 to 4.13 fmol/μg DNA and Pt-AG adduct levels ranged from 0.02 to 1.27 fmol/μg DNA. After administration of SPI-77 at a dose of 80 mg/m^2, maximum Pt-GG levels ranged from 0.4 to 0.9 fmol/μg DNA and maximum Pt-AG levels ranged from 0.1 to 0.3 fmol/μg DNA. Levels of DNA adducts (Pt-AG + PT-GG) at a dose of 420 mg/m^2 ranged from 2.1 to 4.9 fmol/μg DNA. The mean concentration-time curves for all doses are shown in Figs. 4 and 5.

AUC values are presented in Table 4. In Fig. 6, plots of the Pt-DNA adduct AUC versus the administered dose of SPI-77 are shown. A correlation was observed between the AUC values of total plasma platinum and GG-bound platinum ($R = 0.52$, $P = 0.025$), but not between the AUC values of total plasma platinum and AG-bound platinum. No correlation was found between the C_{max} of free platinum and the AUC of Pt-DNA adducts. However, a plot of the AUC of Pt-DNA adducts versus the dose of SPI-77, either in milligrams or in milligrams per square millimetre, revealed a correlation between the Pt-GG adduct AUC and the administered dose of SPI-77 (Fig. 6; $R = 0.74$, $P = 0.0004$; as total dose in milligrams: $R = 0.68$, $P = 0.002$). Total Pt-DNA adduct AUC levels were also significantly correlated with the administered dose of SPI-77 (as milligrams per square millimetre: $R = 0.74$, $P = 0.0004$; as milligrams: $R = 0.67$, $P = 0.002$). No significant correlation was found between the very low Pt-AG adduct AUC and the administered dose of SPI-77.

In addition, it was possible to determine Pt-DNA adduct levels in tumour cells of two patients, one with ovarian carcinoma and one with melanoma. An insufficient amount of DNA was obtained from the third patient (with cervix carcinoma) to allow the measurement of DNA adducts. The Pt-DNA adduct levels (Pt-GG + Pt-AG) in the tumour cells from ascites (in the patient with ovarian carcinoma) ranged from 2.1 to 5.2 fmol/μg DNA, and were approximately tenfold higher than the adduct levels in the WBC from this patient at corresponding time-points (end of infusion, 96 h infusion, and 1, 2, 3, 4, and 5 weeks after infusion) ranging from 0.1 to 0.6 fmol/μg DNA. In the tumour cells from the melanoma biopsy, the Pt-DNA adduct level (Pt-GG + Pt-AG) was 4.4 fmol/μg DNA, compared to 2.9 fmol/μg DNA in the WBC.

Urinary excretion

The cumulative excretion of cisplatin in urine up to 96 h after administration of SPI-77 was measured in 12 patients and ranged from 2.0 to 6.1% of the total dose administered, with a median of 3.3%, which was dose-independent.

Discussion

The liposomal formulation of cisplatin, SPI-77, was developed in order to target cisplatin delivery to tumour

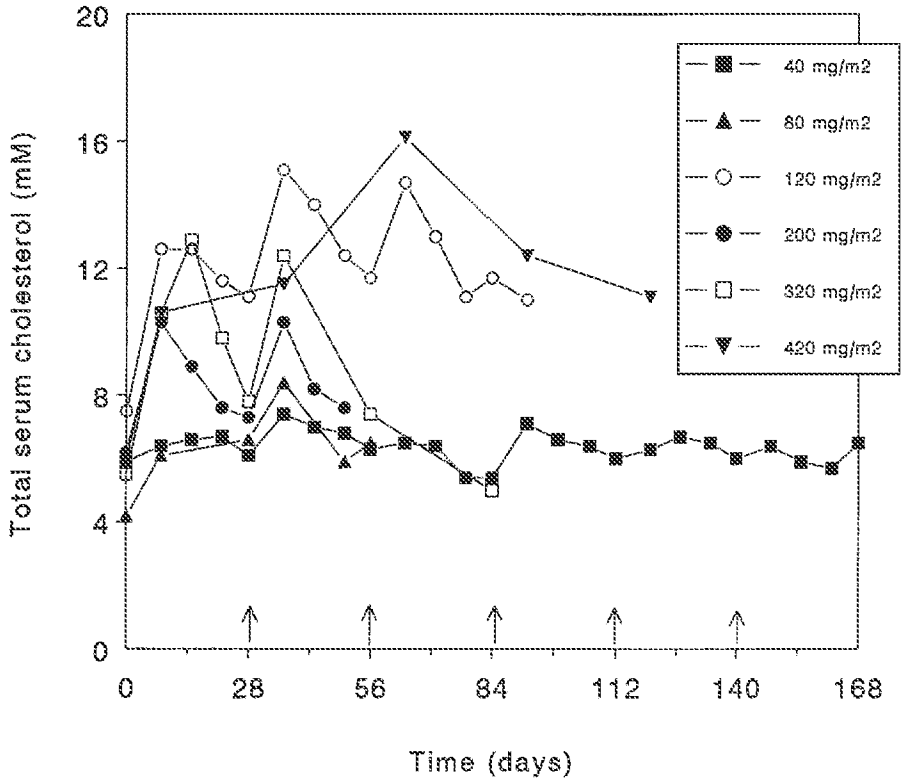

Fig. 3 Mean serum concentration-time curves for total cholesterol. SPI-77 was administered at t = 0, and at 28, 56 and 84 days. The *arrows* indicate the times of administration of SPI-77

cells while reducing the systemic toxicity associated with free cisplatin. The favourable pharmacokinetic properties of Stealth liposomes should facilitate selective release of cisplatin at the tumour site. Encouraged by the preclinical results in various animal species, we performed a phase I study in cancer patients not amenable to other treatment to investigate the pharmacokinetics and toxicity of SPI-77. Tumour biopsies are preferred to investigate whether platinum accumulates in tumours after administration of liposomal cisplatin. However, a validated method for this does not exist currently, and due to ethical and practical considerations tumour biopsies are not routinely obtained from patients.

In blood, three different forms of cisplatin are present following drug administration: free (i.e. active), protein-bound and erythrocyte-bound [10, 14, 18]. After administration of SPI-77 at doses of 40–80 mg/m^2, free, ultrafilterable platinum levels were below the lowest limit of quantification. Administration of SPI-77 at higher doses resulted in free platinum levels varying widely from 0.4 to 140 μM. Apparently, release of cisplatin from the liposomes occurs at a slow rate, resulting in low systemic exposure to free cisplatin. Our analytical method did not distinguish between liposomal and protein-bound platinum. However, as the plasma protein binding is irreversible, the free fraction is mainly the result of liposomal release. Erythrocyte-bound platinum was not measured because in vitro blood partitioning studies have indicated that SPI-77 resides in the plasma and that affinity for erythrocytes is negligible [13]. The volume of distribution of SPI-77-derived platinum was significantly lower than the volume of distribution of total platinum after cisplatin administration (11–24 l) [2, 7], and approximately equal to the plasma volume.

Elimination of cisplatin is usually described by two-compartment models. After administration of cisplatin, elimination half-lives of 42 h to 7.3 days have been reported for total platinum [2, 7, 10, 14, 22, 23, 24]. Plasma concentration versus time data of total platinum after SPI-77 administration were better characterized by a one-compartment model than by a two-compartment model, which is consistent with the assumption that the plasma pharmacokinetics are largely determined by the liposomes, not by the encapsulated material. However, since we observed considerable variation in the shape of the concentration-time curves, non-compartmental methods were applied to calculate pharmacokinetic parameters.

Slow release of cisplatin from the liposomes, rendering the drug unavailable for renal clearance mechanisms, may be responsible for the low total body clearance found in our study. Clearance of standard cisplatin is largely the result of renal processes such as glomerular filtration and tubular secretion. Ultimately, nearly 90% of cisplatin is excreted into the urine following intravenous administration of cisplatin, with most of the drug excreted within the first few days [10]. The nephrotoxicity associated with cisplatin administration may be due to tubular damage caused by high local pharmacologically active platinum concentrations [8]. In our study, the median urinary excretion of cisplatin was comparable to the results from other investigators, and represents a significant reduction in comparison to standard cisplatin administration [1].

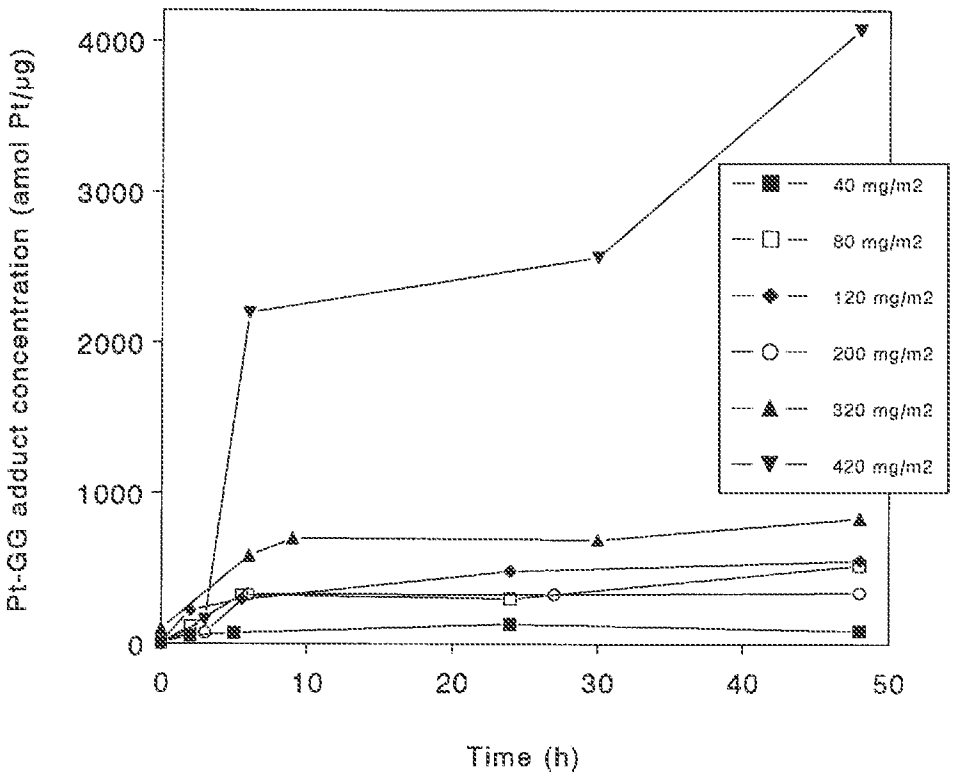

Fig. 4 Mean concentration-time curves for Pt-GG adducts in WBC. Each curve was derived from the data from three patients, except for the 420 mg/m^2 dose which was derived from two patients

The two major Pt-DNA adducts, i.e. Pt-GG and Pt-AG, were found in WBC DNA even at the lowest dose levels, indicating that pharmacologically active cisplatin was released from the liposomes in the blood compartment, at least to some extent. As anticipated, Pt-GG adduct levels were higher than Pt-AG levels, but no correlation was found between the AUC of GG- and AG-bound platinum. It has previously been found that cisplatin doses of 70–80 mg/m^2 result in maximum Pt-DNA adduct levels of 6.6 ± 2.05 fmol/µg DNA [11, 19]. After administration of SPI-77 at a dose of 80 mg/m^2, we found that maximum levels of Pt-DNA adducts were on average tenfold lower than after an equivalent dose of standard cisplatin. It is noteworthy that levels of DNA adducts (Pt-AG + PT-GG) at a dose of 420 mg/m^2 were high compared to the levels at lower dose levels. A correlation was observed between the AUC values of total plasma platinum and GG-bound platinum and between the Pt-GG adduct AUC and the administered dose of SPI-77. No significant correlation was found between the very low Pt-AG adduct AUC and the administered dose of SPI-77.

Pt-DNA adduct levels in tumour cells were determined in two patients. In one patient tumour cells were derived from ascites and in this patient the Pt-DNA adduct levels in the tumour cells were approximately tenfold higher than the Pt-DNA adduct levels in WBC. In the second patient the Pt-DNA adduct levels, determined in tumour cells from a melanoma biopsy, were in the same range of the Pt-DNA adduct levels in the WBC of this patient.

The increase in triglyceride and cholesterol levels after administration of SPI-77 and the subsequent decrease during the following 4 weeks was likely to have been a result of the administration of the liposomes, which contain high levels of cholesterol. The maximum levels of cholesterol detected of 5.0 to 20.9 m*M* represented considerable increases from baseline values. These levels returned to baseline values after discontinuation of the study.

In contrast to cisplatin administration, gastrointestinal toxicity after administration of SPI-77 was limited, eliminating the need for prophylactic antiemetic therapy. No renal toxicity was observed and pre- and/or post-hydration was unnecessary. Infusion-related reactions were observed in four patients, but it was possible to control these by lowering the infusion rate. Two patients experienced severe muscle weakness, which in one patient was possibly related to the administration of SPI-77, although no objective abnormalities were observed on the electromyelogram and the symptoms were reversible. Extensive neurological measurements were performed in all subsequent patients, but no other neurological side effects were observed. Toxicities were not related to the administered dose of SPI-77.

The study was discontinued after the dose of 420 mg/m^2 because platinum accumulation in tumour cells (measured as DNA-bound platinum) and in peripheral tissues was lower than expected, as demonstrated by the low levels of free platinum in ascites, the Pt-DNA adduct levels in tumour cells derived from ascites, and the Pt-DNA adduct levels in tumour cells obtained from tumour biopsies. Although platinum-DNA adduct levels

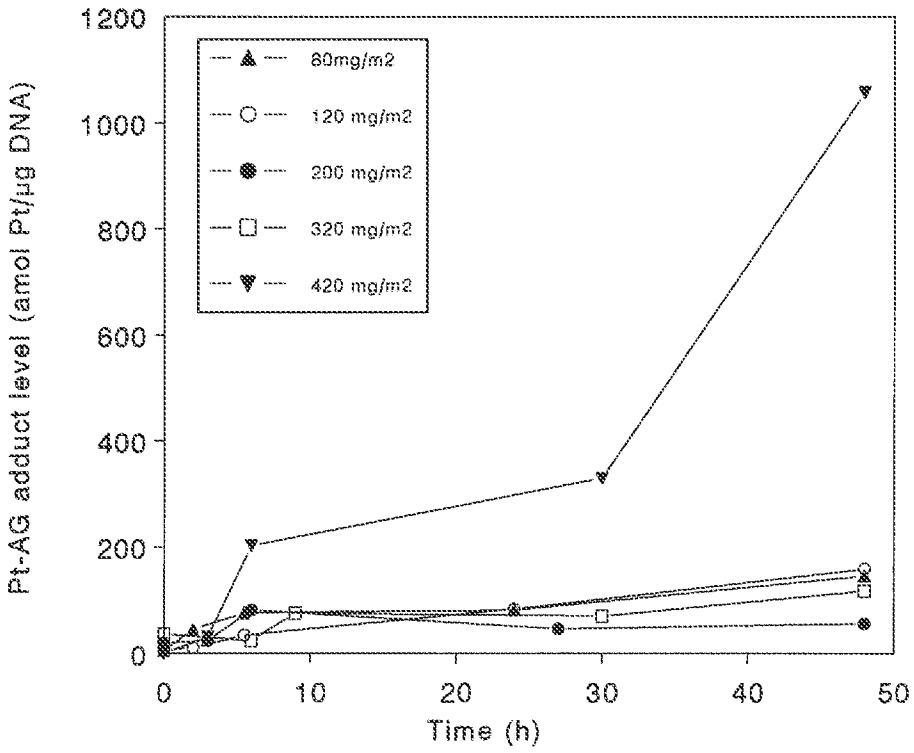

Fig. 5 Mean concentration-time curves for Pt-AG adducts in WBC. Each curve was derived from the data from three patients, except for the 420 mg/m^2 dose which was derived from two patients

Table 4 AUC values of Pt-GG and Pt-AG adducts

Dose (mg/m^2)	No. of patients	AUC (fmol·h/µg)	
		Pt-GG	Pt-AG
40	3	4.3 ± 0.39	–[a]
80	3	16.3 ± 4.81	4.5 ± 1.00
120	3	20.6 ± 11.51	4.3 ± 4.03
200	3	14.6 ± 6.19	4.0[b]
320	5	30.7 ± 10.04	4.6 ± 1.70
420	2	120.9 ± 7.81	19.5 ± 5.60

[a]Actual level too low for calculation
[b]$n = 2$

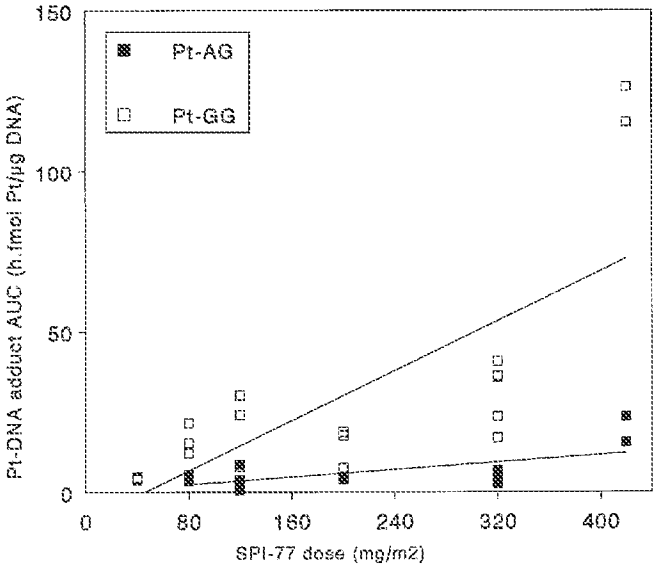

Fig. 6 AUC values (derived from Figs. 3 and 4) of Pt-GG and Pt-AG adducts in WBC plotted against the dose of SPI-77. The lines represent the correlation between the AUC values with $R = 0.75$ ($P = 0.0004$) for the Pt-GG AUC values and $R = 0.61$ (not significant) for the Pt-AG AUC values

in ascites were relatively high compared to adduct levels in WBC of the same patient, Pt-DNA adduct levels were still low compared to Pt-DNA adduct levels in WBC after administration of standard cisplatin [11, 19]. Recent in vivo studies have shown a positive correlations between Pt-adduct levels in tumour tissue and response to cisplatin treatment [26, 27]. Thus, combining these results, we concluded that there was insufficient release of cisplatin from the liposomes due to their prolonged circulation time, resulting in low concentrations of free platinum in plasma and low levels of Pt-DNA adducts in WBC. The second reason for discontinuation of the study was the need for disproportionately high doses of SPI-77 to achieve satisfactory platinum concentrations, resulting in unpredictable large increases in plasma cholesterol values.

In conclusion, we report the results of a phase I study with liposomal encapsulated cisplatin. SPI-77-derived platinum displayed a markedly different pharmacokinetic behaviour, mainly dominated by the liposomes, as compared to cisplatin. Consequently, its toxicity profile differs largely from that of free cisplatin. However, despite the favourable pharmacokinetic properties, enhanced accumulation of platinum in tumour cells following administration of SPI-77 could not be demonstrated. Increased tumour selectivity may be achieved, for example, by using the altered physiological conditions

at the tumour site, such as lower pH, in combination with an acid-sensitive linker at the liposome. Future studies will be performed with Stealth liposomes which have a more favourable release pattern of cisplatin, and with other drugs encapsulated in the liposomes.

References

1. Amantea MA, DeMario MD, Schwartz G, Vogelzang NJ, Tonda M, Pendyala L, Ratain MJ (1998) Single and multiple dose pharmacokinetics of SPI-77 (Stealth® liposomal cisplatin) given every 3 weeks in patients with advanced cancer. Ann Oncol 9:369
2. Andersson A, Fagerberg J, Lewensohn R, Ehrsson H (1996) Pharmacokinetics of cisplatin and its monohydrated complex in humans. J Pharm Sci 85:824–827
3. Bando T, Fujimura M, Kasahara K, Matsuda T (1998) Role of thromboxane receptor on the intracellular accumulation of cis-diamminedichloroplatinum(II) in non-small-cell but not in small-cell lung cancer cell lines. Anticancer Res 18:1079–1084
4. Bando T, Fujimura M, Kasahara K, Matsuda T (1998) Significance of Na^+, K^+-ATPase on the intracellular accumulation of cis-diamminedichloroplatinum(II) in non-small-cell but not in small-cell lung cancer cell lines. Anticancer Res 18:1085–1090
5. Dvorak HF, Nagy JA, Dvorak JT, Dvorak AM (1998) Identification and characterization of the blood vessels of solid tumours that are leaky to circulating macromolecules. Am J Pathol 133:95–109
6. Gibaldi M, Perrier D (1982) Noncompartmental analysis based on the statistical moment theory. In: Gibaldi M, Perrier D (eds) Pharmacokinetics, 2nd edn. Marcel Dekker, New York, pp 409–417
7. Johnsson A, Höglund P, Grubb A, Cavallin-Ståhl E (1996) Cisplatin pharmacokinetics and pharmacodynamics in patients with squamous-cell carcinoma of the head/neck or esophagus. Cancer Chemother Pharmacol 39:25–33
8. Kurose T, Sasaki T, Mochizuki M, Yasuda M, Yamazaji T, Sasagawa M, Tanaka K, Hando T (1989) Pharmacokinetic evidence for the renal absorption of CDDP. Nippon Gan Chiryo Gakkai Shi 24:1229–1237
9. Levin L, Hryniuk WM (1987) Dose intensity analysis of chemotherapy regimens in ovarian carcinoma. J Clin Oncol 5:756–767
10. Loehrer PJ, Einhorn LH (1984) Cisplatin. Ann Intern Med 100:700–714
11. Ma J, Verweij J, Planting AST, de Boer-Dennert M, van Ingen HE, van der Burg MEL, Stoter G, Schellens JHM (1995) Current sample handling methods for measurement of platinum-DNA adducts in leucocytes in man lead to discrepant results in DNA adduct levels and DNA repair. Br J Cancer 71:512–517
12. Meerum Terwogt JM, Beijnen JH, ten Bokkel Huinink WW, Malhepaard M, Tibben MM, Welbank H, Groenewegen G, Schellens JHM (1998) Phase I and pharmacologic study of SPI-77, a novel Stealth® liposomal encapsulated formulation of cisplatin (CDDP). Ann Oncol 9:464
13. Meerum Terwogt JM, Tibben MM, Welbank H, Schellens JHM, Beijnen JH (2000) Validated method for the determination of platinum from a liposomal source (SPI-77) in human plasma using graphite furnace Zeeman atomic absorption spectrometry. Fresenius J Anal Chem 366:298–302
14. Muggia FM, Rozencweig M, Penta J (1980) Clinical implications of cisplatin pharmacology. Recent Results Cancer Res 74:132–138
15. National Cancer Institute (1988) Guidelines for reporting of adverse drug reactions. Division of Cancer Treatment, NCI, Bethesda
16. Pluim D, Maliepaard M, van Waardenburg RCAM, Beijnen JH, Schellens JHM (1999) ^{32}P-postlabelling assay for the quantification of the major platinum-DNA adducts. Anal Biochem 275:30–38
17. Reece PA, Stafford I, Abbot RL, Anderson C, Denham J, Freeman S, Morris RG, Gill PG, Olweny CL (1989) Two- versus 24-hour infusion of cisplatin: pharmacokinetic considerations. J Clin Oncol 7:270–275
18. Roberts JJ (1982) Cisplatin. In: Pinedo HM (ed) Cancer chemotherapy. Excerpta Medica, Amsterdam, pp 95–117
19. Schellens JHM, Ma J, Planting AST, van der Burg ME, van Meerten E, de Boer-Dennert M, Schmitz PI, Stoter G, Verweij J (1996) Relationship between the exposure to cisplatin, DNA-adduct formation in leucocytes and tumour response in patients with solid tumours. Br J Cancer 73:1569–1575
20. SEQUUS Pharmaceuticals (1998) SPI-77: investigator's brochure, edition no. IB17-SPI-77-RP-98-02 (release date 22 January). SEQUUS Pharmaceuticals, Brentford, UK
21. van der Vijgh WJF (1991) Clinical pharmacokinetics of carboplatin. Clin Pharmacokinet 21:242–261
22. Vermorken JB, van der Vijgh WJ, Pinedo HM (1980) Pharmacokinetic evidence for an enterohepatic circulation in a patient treated with cis-dichlorodiammineplatinum(II). Res Commun Chem Pathol Pharmacol 28:319–328
23. Vermorken JB, van der Vijgh WJ, Klein I, Hart AA, Gall HE, Pinedo HM (1984) Pharmacokinetics of free and total platinum species after short-term infusion of cisplatin. Cancer Treat Rep 68:505–513
24. Vermorken JB, van der Vijgh WJ, Klein I, Gall HE, van Groeningen CJ, Hart GA, Pinedo HM (1986) Pharmacokinetics of free and total platinum species after rapid and prolonged infusions of cisplatin. Clin Pharmacol Ther 39:136–144
25. Wagstaff AJ, Ward A, Benfield P, Heel RC (1989) Carboplatin. A preliminary review of its pharmacokinetic properties and therapeutic efficacy in the treatment of cancer. Drugs 37:162–190
26. Welters MJ, Braakhuis BJ, Jacobs-Bergmans AJ, Kegel A, Baan RA, van der Vijgh WJ, Fichtinger-Schepman AM (1999) The potential of platinum-DNA adduct determination in ex vivo treated tumour fragments for the prediction of sensitivity to cisplatin. Ann Oncol 10:97–103
27. Welters MJ, Fichtinger-Schepman AM, Baan RA, Jacobs-Bergmans AJ, Kegel A, van der Vijgh WJ, Braakhuis BJ (1999) Pharmacodynamics of cisplatin in human head and neck cancer: correlation between platinum content, DNA adduct levels and drug sensitivity in vitro and in vivo. Br J Cancer 79:82–88
28. Woodle MC, Newman MS, Working PK (1995) Biological properties of sterically stabilized liposomes. In: Lasic D, Martin F (eds) Stealth liposomes. CRC Press, Boca Raton, pp 103–117
29. Wu NZ, Klitzman B, Rosner G, Needham D, Dewhirst MW (1993) Measure of tissue uptake of intravenously injected macromolecules using fluorescence video-microscopy. Microvasc Res 46:231–253

LIPOSOMAL ENCAPSULATION OF IRINOTECAN AND POTENTIAL FOR THE USE OF LIPOSOMAL DRUG IN THE TREATMENT OF LIVER METASTASES ASSOCIATED WITH ADVANCED COLORECTAL CANCER

by

CORRIE LYNN MESSERER

B.Sc., University of British Columbia, 2000

A THESIS SUBMITTED IN PARTIAL FULFILLMENT OF

THE REQUIREMENT FOR THE DEGREE

OF MASTER OF SCIENCE

in

THE FACULTY OF GRADUATE STUDIES

DEPARTMENT OF PATHOLOGY AND LABORATORY MEDICINE

We accept this thesis as conforming

to the required standard

THE UNIVERSITY OF BRITISH COLUMBIA

August, 2002

In presenting this thesis in partial fulfilment of the requirements for an advanced degree at the University of British Columbia, I agree that the Library shall make it freely available for reference and study. I further agree that permission for extensive copying of this thesis for scholarly purposes may be granted by the head of my department or by his or her representatives. It is understood that copying or publication of this thesis for financial gain shall not be allowed without my written permission.

Department of Pathology

The University of British Columbia
Vancouver, Canada

Date 16.08.02

DE-6 (2/88)

ABSTRACT

Colorectal cancer is the second leading cause of cancer mortality in North America, primarily because of a high incidence of hepatic metastases, which are relatively unresponsive to the systemic chemotherapy. Irinotecan, a camptothecin analogue recently approved for used in conjunction with 5-fluorouricil/leucovorin, is a marginal improvement but toxic and by no means curative. Liposomal drug formulations are argued to be more effective at treating liver-localised carcinomas when compared with their free drug counterparts, because of their intrinsic affinity for the liver and extended lifespan. This work examined the suitability of a liposomal irinotecan formulation in the treatment of colorectal liver metastases. Irinotecan was encapsulated in DSPC/cholesterol liposomes using an ionophore-generated transmembrane proton gradient. After i.v. injection, liposomal drug was eliminated from the plasma much more slowly than free drug, and after 1 h circulating levels of liposome-associated drug were 10 fold greater. In addition, high-performance liquid chromography analysis of plasma samples revealed that liposome-associated irinotecan is protected from inactivating hydrolysis with > 80 % remaining in the active lactone form up to 24 h after administration. These improved pharmacokinetics observed for the liposomal drug were associated with increased efficacy in both solid tumour and orthotopic human models of colorectal metastases. Using a model (LS180) of colorectal metastases in SCID/RAG2M mice it was demonstrated that liposome-encapsulated drug was more effective at arresting tumour growth than was free drug. Further, in the human model of colorectal liver metastases (LS174T), liposomal irinotecan substantially increase life span relative to free drug with all members surviving long-term (75 days) as compared to a survival time of 30 and 50 days for the control and free drug treated groups. These results illustrate that liposomal encapsulation can substantially enhance the therapeutic activity of irinotecan, and emphasize the potential for liposomal irinotecan in the treatment of liver metastases.

TABLE OF CONTENTS

LIST OF FIGURES

LIST OF TABLES

ABBREVIATIONS

^{3}H-CHE	tritiated [^{3}H] cholesteryl hexadeecyl ether
5-FU	5-fluorouracil
APC	7-ethyl-10-[4-N-(5-aminopentanoic acid)-1-piperidino] carbonyloxycamptothecin
CRC	colorectal cancer
CYP3A	cytochrome P450 3A family
DiI	1,1'-dioctadecyl-3,3,3',3'-tetramethylindocarbocyanine perchlorate
DMSO	dimethyl sulfoxide
DSPC	1,2-disteroyl-sn-glycero-3-phosphocholine
EDTA	ethylenediaminetetra-acetic acid
HDL	high-density lipoproteins
HEPES	*N*-2-hydroxyethylpiperazine-*N*-2-ethane-sulphonic acid
HPLC	high-performance liquid chromatography
IC_{50}	concentration necessary for 50% inhibition of growth
i.v.	intravenous
LUV	large unilamellar vesicles
MLV	multilamellar vesicles
MPS	mononuclear phagocytic system
MTD	maximum tolerated dose
MTT	3-(4, 5-dimethylthiazol-2yl)-2, 5-diphenyl tetrazolium bromide
NPC	7-ethyl-10-(4-amino-1-piperidino) carbonyloxycamptothecine
PEG	poly(ethylene glycol)
s.c.	subcutaneous
s.d.	standard deviation
s.e.	standard error
SHE	buffer composed of 300 mM sucrose, 20 mM HEPES and 15 mM EDTA
SUV	small unilamellar vesicles
UGT	uridine diphosphate glucuronsyltransferases

ACKNOWLEDGEMENTS

I would like to thank everyone at Advanced Therapeutics and Celator Technologies, Inc. who were of great assistance through answering my many questions or offering their advice. I must mention, in particular, the animal technicians Dana Masin, Rebecca Ng, Hong Yan and Sophia Tan as well as Natashia Harasym for their expertise and tremendous help with the animal studies. I would especially like to thank Marcel Bally for inviting me to join his lab and for his support, advice and ideas during my time there.

Corrie Messerer
June 2002

To my mum ,

for her unfailing love and support

and

in loving memory of my dad.

CHAPTER 1

INTRODUCTION

1.1 Foreword

Cancer is a general term that encompasses a myriad of discrete diseases, which although sharing the characteristic of inappropriate cell growth and differentiation, otherwise exhibit distinctive behaviours. These behaviours along with a classification, derived from the site of origin and histological appearance, dictate the individual treatment regime prescribed for "each" cancer.

Anticancer treatment strategies fall under one of two modalities, being either localised or systemic treatments. Surgical resection, alone or in combination with radiation therapy, is the leader in achieving cures in localised disease, but is not suitable for treatment of metastatic or disseminated cancers. Chemotherapy, as a single modality, is successful in curing a number of disseminated haematologic and solid tumour malignancies including certain leukaemias, lymphomas, and testicular cancers.

While significant advances have been made in chemotherapeutic strategies over the past thirty years to the extent that some cancers, as previously mentioned, are potentially curable, for many of the most common and fatal cancers such as those originating in the breast, lung and colon, little progress has been made (National Cancer Institute of Canada: Canadian Cancer Statistics 2002, Toronto, Canada, 2002). Short of early detection and intervention by surgical removal of diseased tissues before metastasis, treatment for these cancers relies heavily on chemotherapy

and long term prognosis for the patient is not encouraging. Acknowledgment that current chemotherapeutic standards are unacceptable is reflected in the vast amounts of time, energy and money currently being invested in the arduous process of development and testing of new chemotherapeutic agents. Unfortunately, many chemotherapeutic drugs appear to be inherently problematic, often exhibiting properties far from ideal including poor solubility, rapid metabolism, instability and unfavourable biodistribution most often resulting in dose-limiting toxicities and suboptimal therapy. Ideally drugs would localise directly and specifically with a high therapeutic index (ratio of effective dose to toxic dose) to the disease tissue.

A novel approach for improving cancer chemotherapy, instigated more than three decades ago and recently gaining ground, is based on the principle that chemotherapy's unreliable success is not a consequence of poor drug design, but at least partly caused by ineffective drug delivery to the cancerous cells. Marginally effective or severely toxic drugs can be converted into useful agents simply through improvements in drug delivery. Although several methods have been explored with the aim of improving delivery, including polymer particles, and microspheres, that which is most rapidly gaining popularity and is most advanced in development are lipid-based carriers, and in particular, liposomes. Liposomes are establishing a reputation for converting traditional chemotherapeutic drugs such as vinicristine, doxorubicin and daunorubicin into much more active and efficient anti-cancer agents (see Mayer et al., 2001 for review). The present work investigates the potential for encapsulation of the novel drug irinotecan as an alternative treatment for advanced colorectal cancer.

1.2 Liposomes

Liposomes are among the most commonly employed lipid-based drug delivery systems. A wide

range of potential non-toxic lipid constituents, whose manipulation controls such physical properties as trapping efficacies and release rates (Gregoriadis, 1991), impart tremendous versatility over other carriers. Bangham *et al.* in 1965 were the first to investigate liposomes in the form of multilamellar vesicles (MLVs), which generate spontaneously upon lipid hydration and are characterised by concentric lipid bilayers separated by aqueous channels (Figure 1.1). The distinctive bilayer formation by lipids is due to their amphipathic nature, which drives their hydrophilic head to face outside and their hydrophobic tails to be sheltered on the inside. Liposome technology has not been limited to drug carrier systems, and liposomes were originally described as a tool for studying membrane structure and biophysics (Sessa and Weissmann, 1968), but have since come to play a significant role in drug delivery.

At their most basic level, liposomes serve as solubilising agents and can act as carriers for either water-soluble or water-insoluble drugs. Agents associated with liposomes, particularly those in the aqueous core, exhibit enhanced stability and receive substantial protection from enzyme-mediated degradation and deterioration, other unfavourable physiological processes or pHs. For instance, camptothecin and related analogues require a closed α-hydroxy (lactone) ring moiety for activity, but at physiological pHs rapid hydrolysis to the inactive ring-open compound is observed (Figure 1.2) (reviewed in Burke and Bom, 1996). Liposome entrapment of these drugs in an acidic environment favours the closed-ring version thereby significantly increasing their half-lives *in vivo* (Burke and Gao, 1994). Perhaps of greatest advantage for use in chemotherapy, however, liposome encapsulation often alters the pharmacokinetics and biodistribution properties of the associated drugs (Hwang, 1987; Allen et al., 1995; Scherphof et al., 1997), diminishing toxicities associated with non-specific drug accumulation in healthy tissues while enhancing drug delivery to the disease site, resulting in improved efficacy by increasing selective delivery.

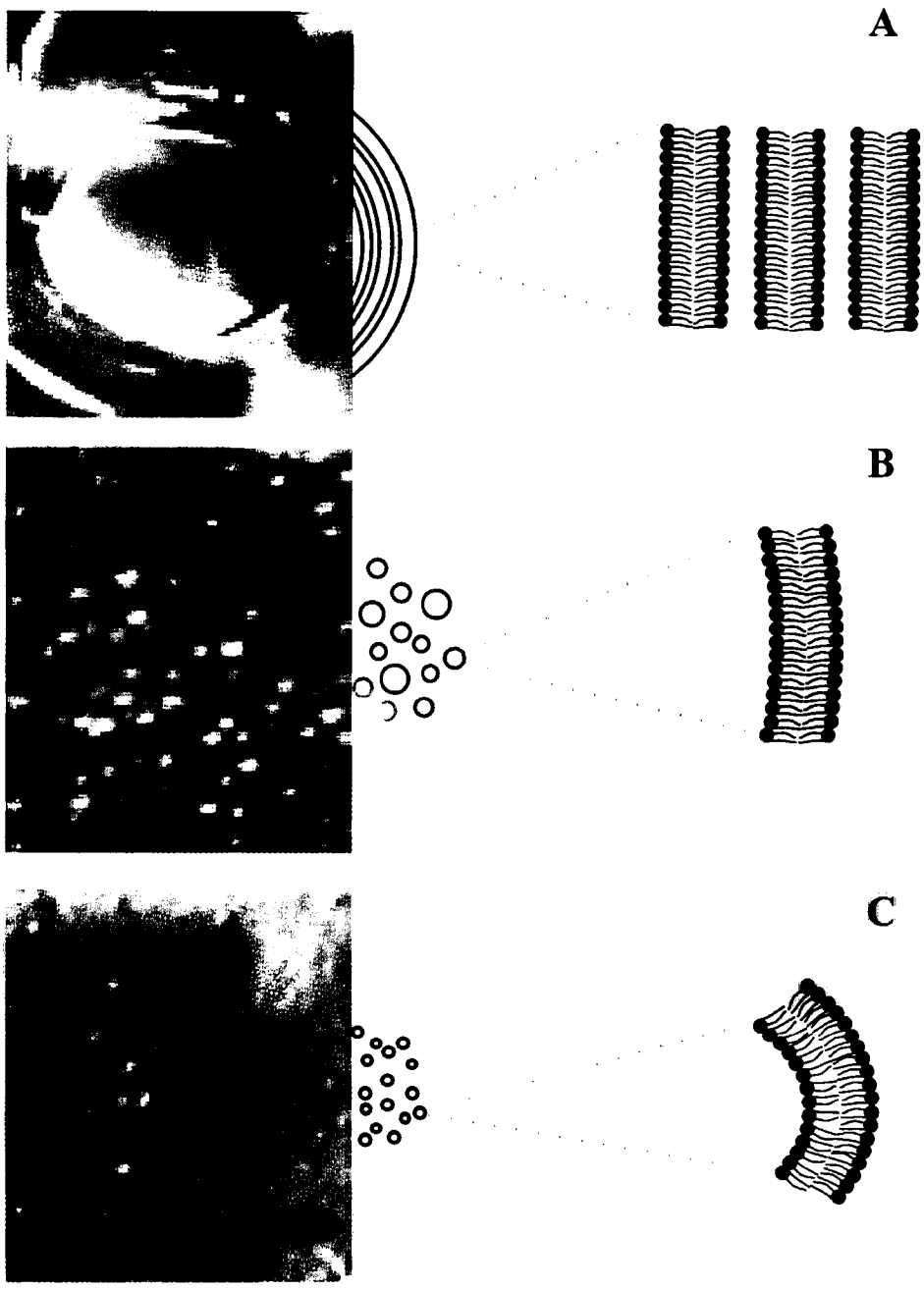

Figure 1.1 Liposome structure. Freeze-fracture electron microscopy of (A) multilamellar vesicles, (B) large unilamellar vesicles, and (C) small unilamellar vesicles composed of phosphatidylcholine.

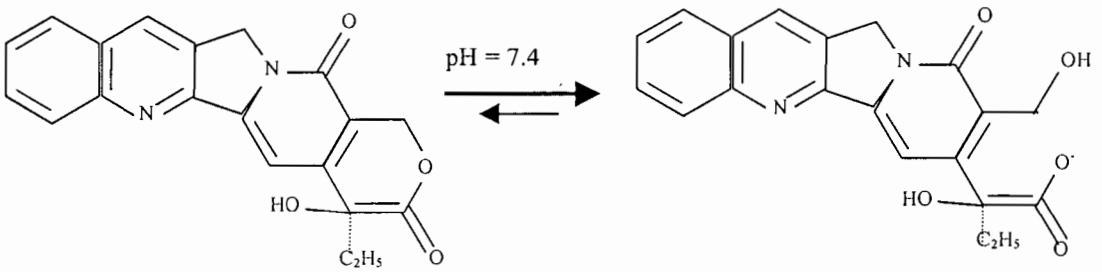

Figure 1.2 Camptothecin ring hydrolysis. An intact lactone ring is necessary for camptothecin-mediated cytotoxicity. pH mediated hydrolysis of camptothecin drives the equation to the right, and the ring-open inactive carboxylate species at physiological pH. Preferential binding of the carboxylate species to serum proteins further drives the reaction in this direction.

1.2.1 Phospholipids

Phospholipids, consisting of a polar headgroup coupled by glycerol-phosphate backbone to an apolar tail (Figure 1.3), comprise one of the major classes of membrane-forming lipids. The versatility of phospholipids as liposome components is attributable to various possible combinations of headgroup and acyl chain tail which together dictate bilayer properties including surface charge and rate of elimination. For example, anionic lipids, such as phosphatidylserine, generally promote serum binding and rapid liposome elimination from the blood stream (Moghimi and Patel, 1989), but this is dependent on chemical properties of the particular anionic lipid used. It has been reported (Gabizon and Papahadjopoulos, 1988) that incorporation of phosphotidylglycerol or phosphotidylionositol can actually enhance circulation lifetime of an infected liposome. In the design of an effective lipid based drug formulation, liposomes must be maintained in the blood stream for a sufficient period of time and concentration to move from the blood compartment to diseased tissue in an extravascular site; consequently, certain charged lipids are not typically used and the focus has been on the zwitterionic phosphatidylcholine (PC).

A key phospholipid characteristic that can dramatically affect its properties as a liposomal carrier is the temperature of its gel to liquid-crystalline phase transition (T_c), which is primarily influenced by its acyl chain structure (McElhaney, 1982; Huang et al., 1993; Wang et al., 1997). At temperatures below the transition temperature, the bilayer is in the highly ordered gel phase in which the tight packing is largely due to the restricted motion of the acyl chains. At temperatures above the phase transition temperature, membrane order is decreased, acyl chains have much greater freedom of movement and membranes exhibit much enhanced permeability to both solvents and solutes. Membrane permeability increases with increased chain unsaturation and decreased acyl chain length (Papahadjopoulos et al., 1973b). The liposomes used in this

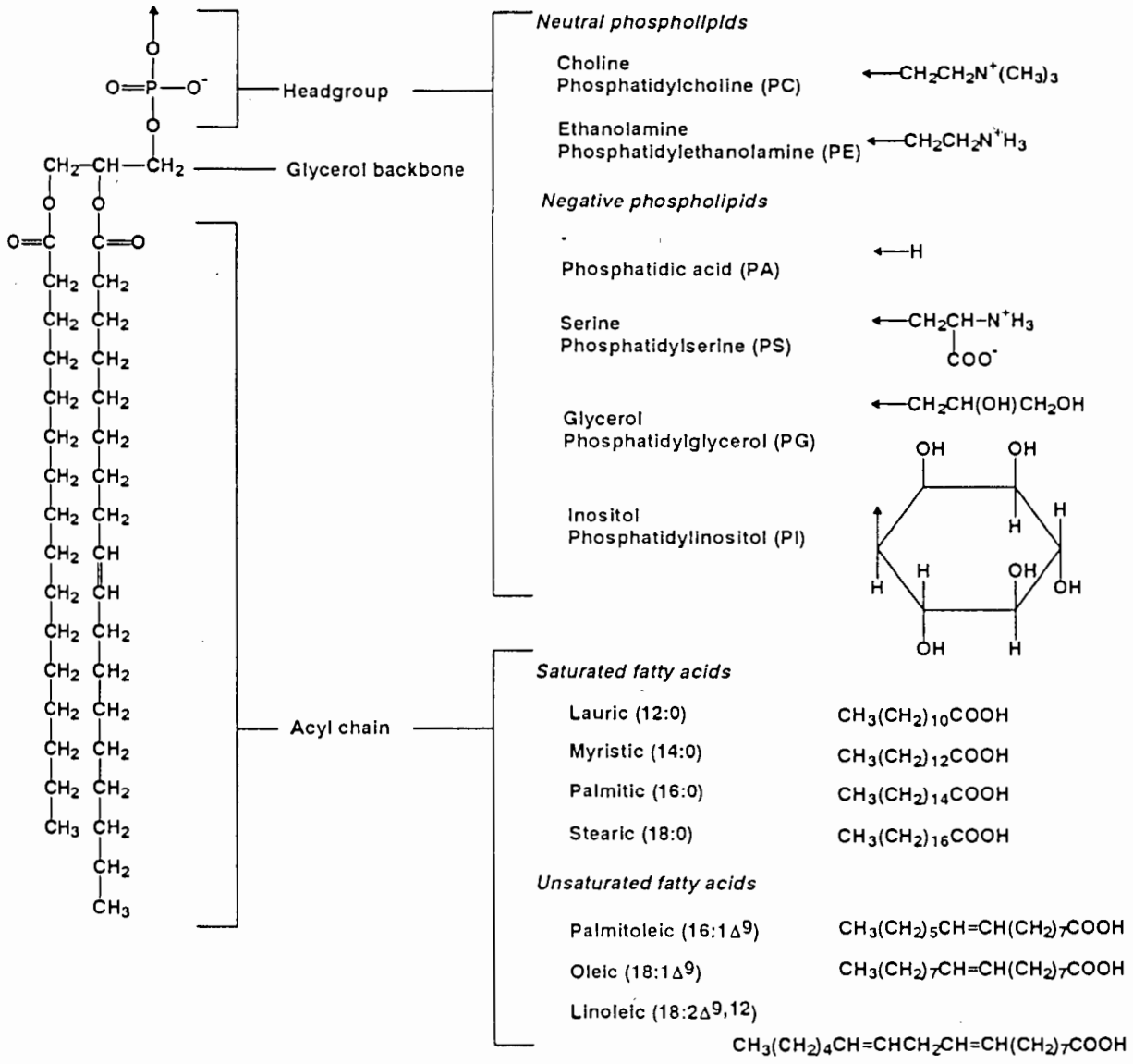

Figure 1.3 Phospholipid structure. (reproduced from Parr, 1995)

thesis were prepared with disteroylphosphatidylcholine (DSPC), a lipid known to exhibit improved drug retention properties.

Phospholipids are not limited to forming lipid bilayers, but display lipid polymorphism, whereby following hydration they form one of a variety of structures (Cullis et al., 1986). The specific structure a group of phospholipids has an affinity to form is greatly influenced by the size of its headgroup in relation to its tail. For instance, lipids with particularly large headgroups, such as those used in emulsifying detergents, are prone to form micelles; whereas, unsaturated PE molecules aggregate into hexagonal structures (Cullis and de Kruijff, 1979). Although the use of non-bilayer forming lipids has been explored for the preparation of liposomal drug carriers that can fuse with cell membranes, the formulations used here have been prepared with the bilayer-forming PC lipids and cholesterol

1.2.2 Cholesterol

Cholesterol, an amphipathic molecule composed of a rigid steroid ring and aliphatic tail (Figure 1.4), is a major neutral lipid component in eukaryotic cell membranes. In the lipid bilayer, its steroid ring associates with the phospholipid acyl chains, while the hydroxyl group is oriented toward the lipid/water interface and positioned next to the carbonyl ester of the neighbouring lipid headgroup, but there is no interaction. Incorporation of cholesterol into the membrane decreases membrane order of phospholipids in the gel phase while increasing order in the liquid-crystalline phase (de Kruyff et al., 1973; Demel and De Kruyff, 1976). At amounts greater than 7 mol %, cholesterol decreases the enthalpy of the gel to liquid-crystalline phase transition, until at 33 mol % it is no longer detected (Hubbell and McConnell, 1971). Cholesterol also moderates lipid bilayer permeability, decreasing permeability of membranes of saturated or

A

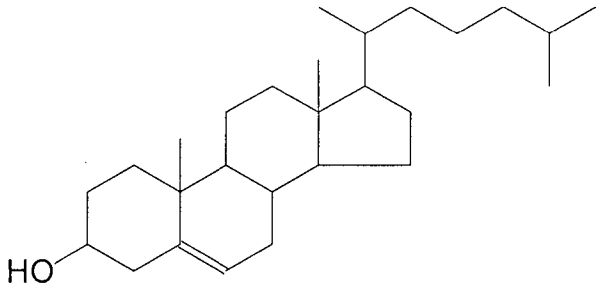

B

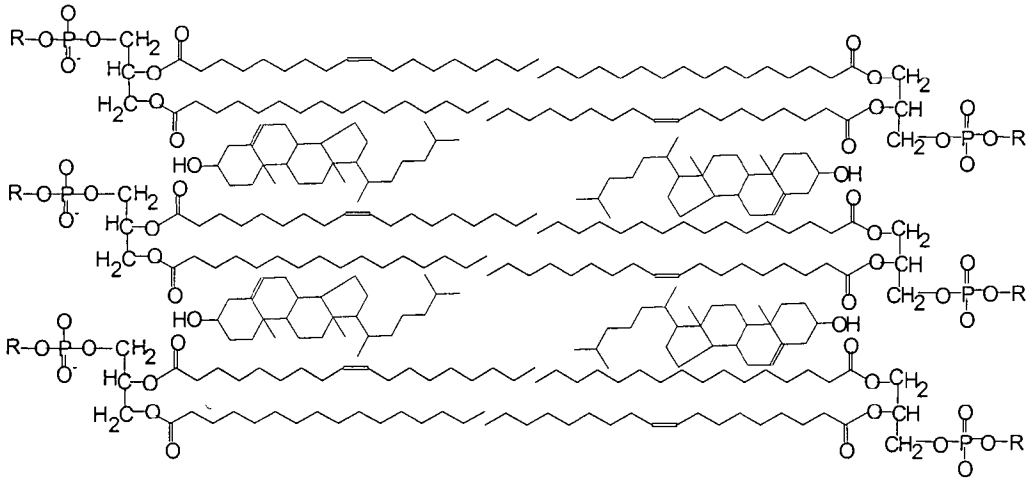

Figure 1.4 Structure of cholesterol (A) and insertion into the lipid bilayer (B).

unsaturated lipids below the transition temperature and increasing permeability of saturated lipids above the transition temperature (Bittman and Blau, 1972).

In the design of lipid-based carriers for drug delivery, incorporation of cholesterol into the liposome membrane has shown the additional benefit of increasing liposome stability (Papahadjopoulos et al., 1973a), primarily by decreasing lipid exchange with lipoproteins (Kirby et al., 1980; Hunt, 1982). Moreover, cholesterol levels in excess of 30 mol % decrease serum protein binding (Patel et al., 1983; Semple et al., 1996), which increases the circulation lifespan of the liposome (Kirby et al., 1980; Patel et al., 1983) and slows release of entrapped contents (Fielding and Abra, 1992). It has recently been suggested (Dos Santos et al., 2002), however, that under certain conditions where PC liposomes are stabilised through the use of polyethylene glycol (PEG), cholesterol may be unnecessary.

1.3 Preparation SUVs and LUVs

Lipid hydration results in the spontaneous formation of MLVs (Figure 1.1A) ranging from 1 to 10 μm in diameter. These vesicles are of little clinical value as carriers, however because their large size causes them to be rapidly eliminated from the circulation. Moreover, the tight packing of their concentric lipid bilayers results in a low trapped volume, which limits the drug loading capacity for these carriers. MLVs are however, useful in making more practical lipid formulations, notably small and large unilamellar vesicles (SUVs and LUVs, respectively) characterised not only by their size, but also by their single lipid bilayer.

Sonication or French press shearing (Barenholtz et al., 1979) of MLVs results in uniformly sized SUVs (Figure 1.1C) with a small diameter (25-50 nm) and low trapped volume (0.5-1.0 μL/μmol

lipid). Their small size bestows a high degree of surface curvature, causing them to be prone to fusion and particularly unstable when administered intravenously.

LUVs (50-500nm diameter) (Figure 1.1B) are made by many procedures including detergent dialysis, infusion and reverse phase evaporation, but the most versatile and frequently used is high pressure extrusion (Szoka et al., 1980; Hope et al., 1985) with inert gas through polycarbonate filters of known pore sizes. This has proven to be both a convenient and reproducible method resulting in the formation of vesicles resistant to fusion, having a large trapped volume 1.5-10 μL/μmol lipid and being of an ideal size for circulation and extravasation (see section 1.5).

1.4 Encapsulation

Drug loading into lipid vesicles can be accomplished through passive or active measures (Figure 1.5). Passively encapsulated drugs are added during the lipid hydration process whereby the liposomes are prepared in a solution containing the agent of interest. This typically results in poor drug entrapment but varies with the individual compound. For example, encapsulation efficiency of aqueous drugs vary with trapped volume and those of lipophilic agents dependent on the capacity of the bilayer to incorporate the agent while maintaining structure. Passive encapsulation is generally used to load hydrophobic drugs that have a propensity to partition into the lipid bilayer, or highly water-soluble drugs that can be retained in the aqueous core of the structure. Other agents, which may possess hydrophobic attributes, as well as charged hydrophilic moieties, may be actively loaded into preformed liposomes through the use of transmembrane ion gradients (Cullis et al., 1983).

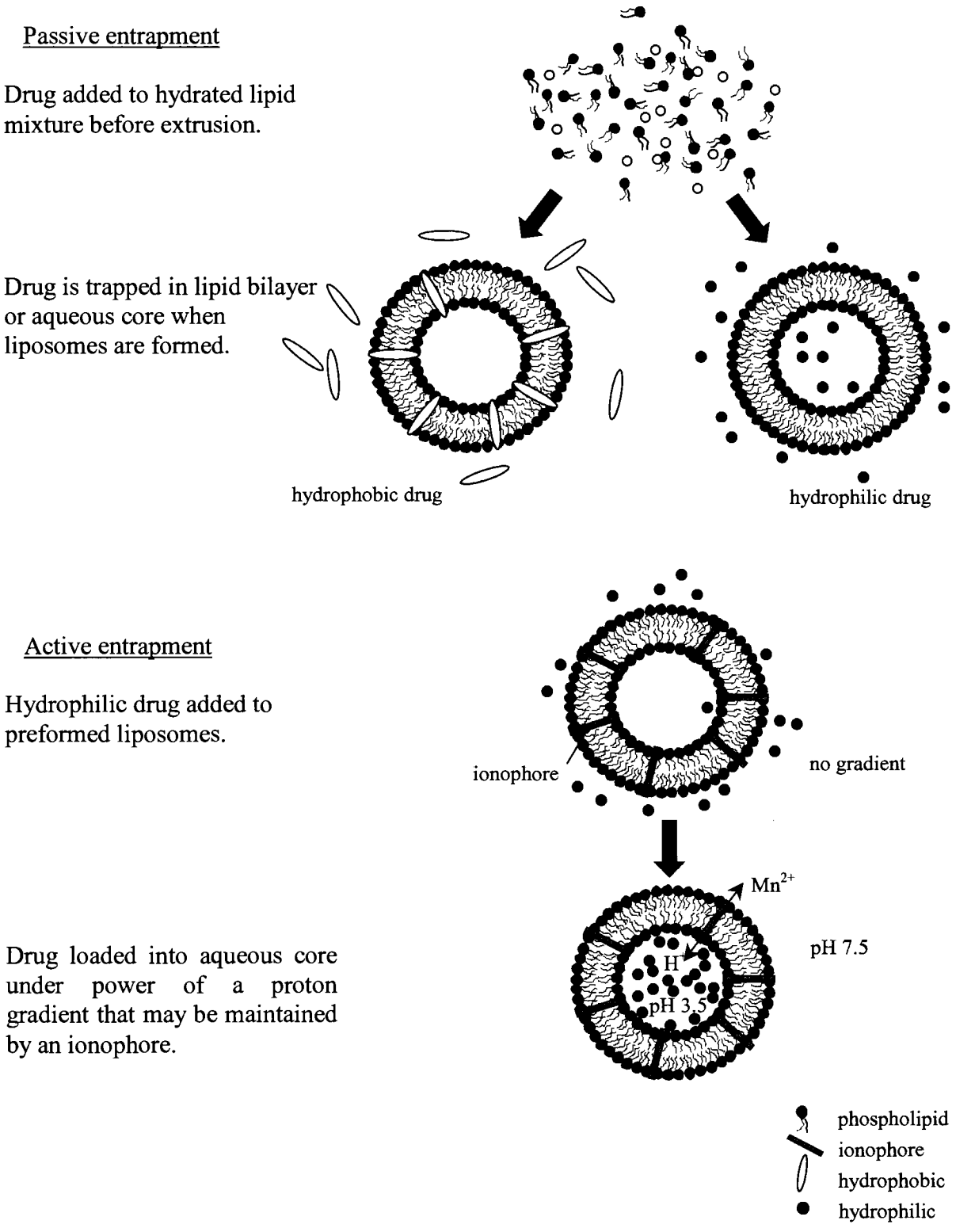

Figure 1.5 Active and passive drug encapsulation.

1.4.1 Passive encapsulation

Passive encapsulation is a method normally used with hydrophobic drugs such as amphotericin B (Madden et al., 1990b) and cyclosporin A (Ouyang et al., 1995) that partition into the lipid bilayer, and is generally characterised by inefficient loading. For such agents trapping efficiency varies with packing constraints of the membrane and the lipid characteristics and while high entrapment efficiency can be achieved it is with a low drug to lipid ratio. Furthermore, hydrophobic drug partitioned into the liposome bilayer can rapidly exchange into other membranes and *in vivo* the drug quickly leaves the carrier (Choice et al., 1995).

It is important to highlight that passive trapping plays a role in preparing liposomes for active drug loading via transmembrane ion gradient-based trapping methods. In this case liposomes are extruded in the presence of a specific buffer that is trapped in the aqueous core, the external buffer is then exchanged in order to generate an ion gradient across the bilayer. This ion gradient can then be used to actively load selected drugs, such as irinotecan, as described in this thesis.

1.4.2 Active encapsulation

Active encapsulation refers to drug loading based on methods whereby the agent is added to preformed liposomes. It is most commonly employed with agents containing protonizable amine or carboxyl functions, and weak bases such as vincristine, and doxorubicin, can accumulate inside in response to a pH gradient (Mayer et al., 1985; Madden et al., 1990a; Mayer et al., 1993). A proton gradient generated across the lipid bilayer (acidic interior) aids entrapment, as the neutral weak base is able to cross the bilayer whereupon it is protonated and

unable to permeate back across it (Addanki et al., 1968; Rottenberg, 1979). Assuming that the pKa of the protonizable function is the same on both sides of the bilayer, at equilibrium intravesicular and external drug concentrations can be derived from the Henderson-Hasselbach equation (Figure 1.6):

$$[HA^+]_{in}/[HA^+]_{out} = [H^+]_{in}/[H^+]_{out}$$

Thus a pH difference of 3 can result in drug accumulation up to a maximum gradient of 10^3 higher inside the liposome compared with outside.

Active loading is generally the preferred mode of drug entrapment as it offers several advantages over passive methods. It is applicable to any lipid formulation capable of maintaining an ion gradient, and typically results in encapsulation efficiencies range of 90-100 %. So long as the internal buffering capacity is maintained, drug trapping is independent of the initial drug to lipid ratio, thereby maximizing the amount of drug loaded into each vesicle. Furthermore, the solubility of drugs of intermediate solubility can be enhanced by manipulation of the internal pH or the addition of counter-ions for the drug to form molecular complexes with and be trapped internally. Finally, because drug is trapped in the liposome core rather than the bilayer, the rate of drug loss can be reduced up to 30 fold (Mayer et al., 1986a). Conventional pH gradient-based loading methods use an internal 300 mM citrate buffer of pH 4.0; however, a more recent variation, which has shown success with agents previously unloadable by this method, uses a proton gradient, $MnSO_4$ and a divalent cation ionophore that maintains the transmembrane gradient (Fenske et al., 1998).

Generation of the transmembrane pH gradient is straightforward and involves the exchange of the external buffer. This can be achieved by one of several methods including size exclusion chromatography, titration to a different pH, or dialysis. The transmembrane pH gradient for

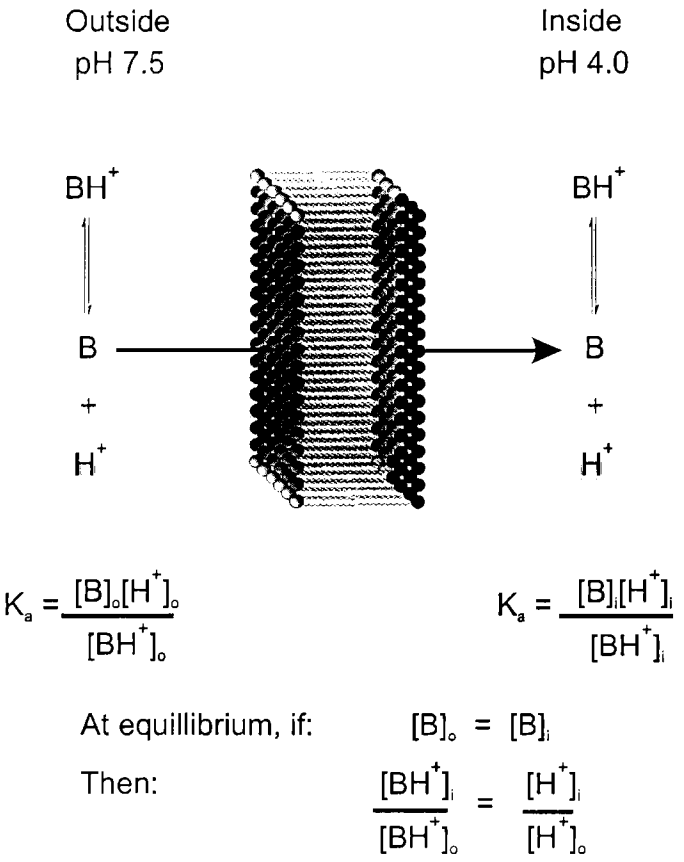

Figure 1.6 Active drug entrapment in liposomes. Equilibrium distribution of a lipophilic amine (weak base) in response to a liposome transmembrane pH gradient. Only the neutral species is able to cross the lipid bilayer in significant amounts. (Reproduced from (Parr, 1995)

several PC-based liposome species are stable for hours or days even at elevated temperatures (Harrigan et al., 1992) and cholesterol further reinforces stability (Madden et al., 1990a).

1.5 Requirements for effective drug delivery

Following intravenous administration, liposomes are exposed to a variety of cells, circulating proteins and other soluble factors resident in the circulating blood volume. Through interactions with the vesicle's lipid bilayer, these factors can instigate bilayer destabilization and/or trigger biological processes that increase membrane permeability or liposome clearance via the mononuclear phagocytic system (MPS). On the most basic level, an effective carrier must withstand these potential deleterious interactions in the blood compartment and be capable of gaining access to an extravascular disease site; consequently, effective delivery of a liposome-associated drug is dictated by the rate of carrier elimination from the plasma compartment; effective drug retention by the carrier en route to the target; and finally, adequate access to, and preferential uptake at the target site enabling direct delivery of drug to diseased cells (Figure 1.7).

1.5.1 Liposome serum protein interactions and clearance

Although pharmacodynamic and pharmacokinetic behaviours of liposomes are dictated primarily by lipid composition and size, they are significantly influenced by liposomal interactions in the blood compartment. Intravenous administration immediately exposes liposomes to cells, lipoproteins and other circulating soluble factors including proteins, carbohydrates and small ions that can compromise drug delivery. To maintain their therapeutic potential in this menacing environment, liposomes must first avoid the bilayer- destabilizing effects of circulating

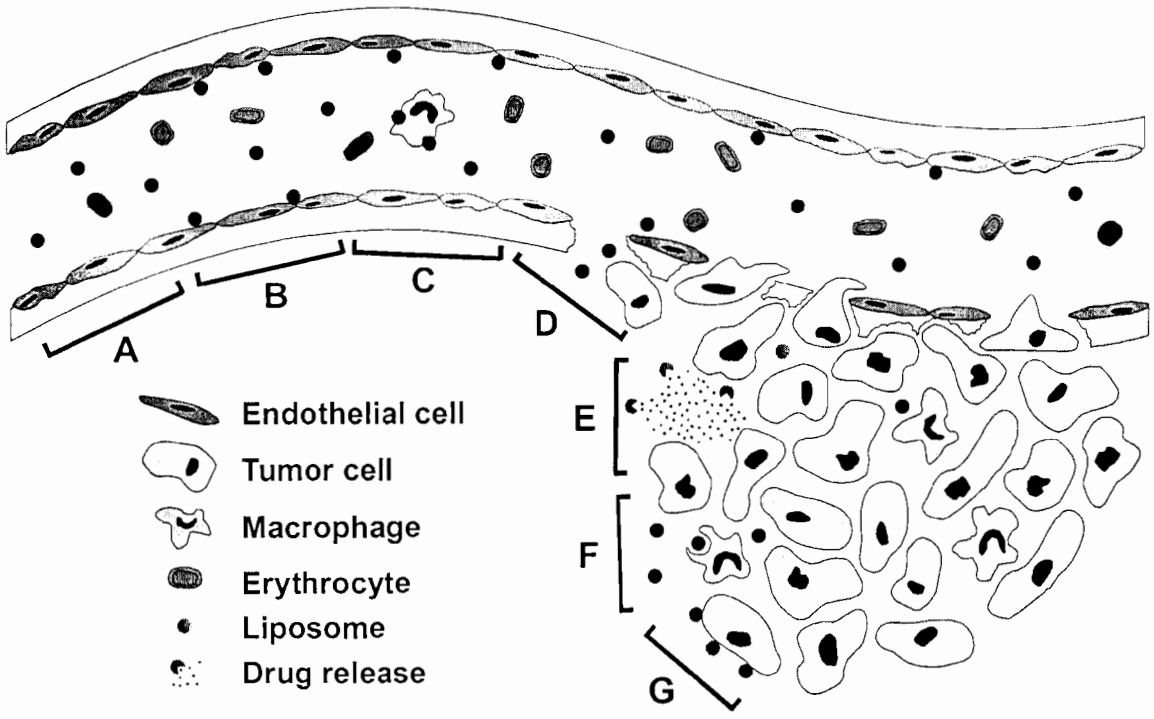

Figure 1.7 Liposome target site accumulation. *A*, in order to effectively reach the target site, i.v. administered liposomes must be retained in the bloodstream for an extended period during which they encounter many different cell types and other soluble factors with which they may interact (*B* and *C*); *D*, passive carrier targeting exploits the characteristic altered leaky vasculature at the disease site which enables liposomes to extravasate into the interstitial space; liposome-associated drug may be released into the intercellular space (*E*) or liposomes may be phagocytosed by tumour-associated macrophages; *G*, surface-bound ligands can increase specificity of liposome targeting.

lipoproteins (Williams et al., 1998). Overcoming this hurdle, their fate is dictated primarily by liposomal surface interactions with serum protein components, which can increase membrane permeability, or immune activation, both of which flag liposomes for recognition and clearance by phagocytic cells of the MPS.

High-density lipoproteins (HDLs), such as Apo A-1, which inserts into the lipid bilayer (Klausner et al., 1985), are able to attack liposomes and "steal" phospholipids, disrupting membrane integrity and initiating liposome disintegration and premature release of their contents into the circulation (Kirby et al., 1980). Opsonizing plasma proteins may also interact with the lipid bilayer, adsorbing to the liposome surface and tagging carriers for recognition phagocytosis by members of the MPS (Aragnol and Leserman, 1986; Alving et al., 1992; Chonn et al., 1992).

The MPS is a part of the host defence system designed to help protect against foreign invaders and is a primary site of liposome and associated drug clearance from the blood (Senior et al., 1985; Hwang, 1987; Woodle and D.D., 1992; Allen et al., 1995). In the absence of a compromised MPS, foreign particulates including bacteria and defined particles such as latex beads (Pretten and Lloyd, 1986) and conventional liposomes (Roerdink et al., 1981), are efficiently removed from the circulation by Kupffer cells in the liver and fixed macrophages in the spleen, lung and bone marrow, leaving little chance of their accumulation in cells other than the phagocytic ones comprising the MPS. Importantly, the rate of liposome elimination from the circulation can decrease through use of formulations designed to minimise their interactions with the cells of the MPS. For example, large liposomes are removed more quickly than small ones, surface charge can promote elimination of liposomes, and this, in turn, affects the degree of opsonin adsorption also play significant roles (Gregoriadis, 1988).

Complement proteins act as primary opsonizing proteins (Coleman, 1986; Moghimi and Patel, 1989), actively flagging objects for recognition and uptake by the MPS (Chonn et al., 1991; Chonn et al., 1992). Proteins coupled to the surface of liposome-based carriers are particularly prone to attacks and can stimulate immune responses by attracting and interacting with complement proteins, resulting in activation of the complement cascade (Devine et al., 1994) and the consequent formation of the membrane attack complex which has pore forming abilities (Silverman et al., 1984).

Although lipoprotein and opsonizing protein interactions with liposomes posed significant obstacles for development of liposomal drug delivery systems, current understanding of the chemical and physical attributes has provided numerous solutions to minimise liposome removal by the MPS and liposome destabilisation by serum protein incorporation. Cholesterol incorporation into the lipid bilayer, for example, enables liposomes to avoid the bilayer destabilizing effects of lipoproteins (Kirby et al., 1980), and inert hydrophobic polymers, such as polyethyleneglycol (PEG), at the liposome surface attracts a water shell to the surface, reducing interactions with circulating proteins (Lasic et al., 1991; Senior et al., 1991; Torchilin et al., 1995), reducing both the rate and extent of liposome uptake into the MPS.

1.5.2 Extravasation through blood vessels

The next hurdle for delivery of lipid vesicles is escape from the confines of the circulatory system and access to the disease site in an extravascular compartment. This entails liposomes crossing the vascular endothelium lining the blood vessels, composed of endothelial cells, a basement membrane and associated smooth muscle cells, into the interstitial space (Figure 1.8).

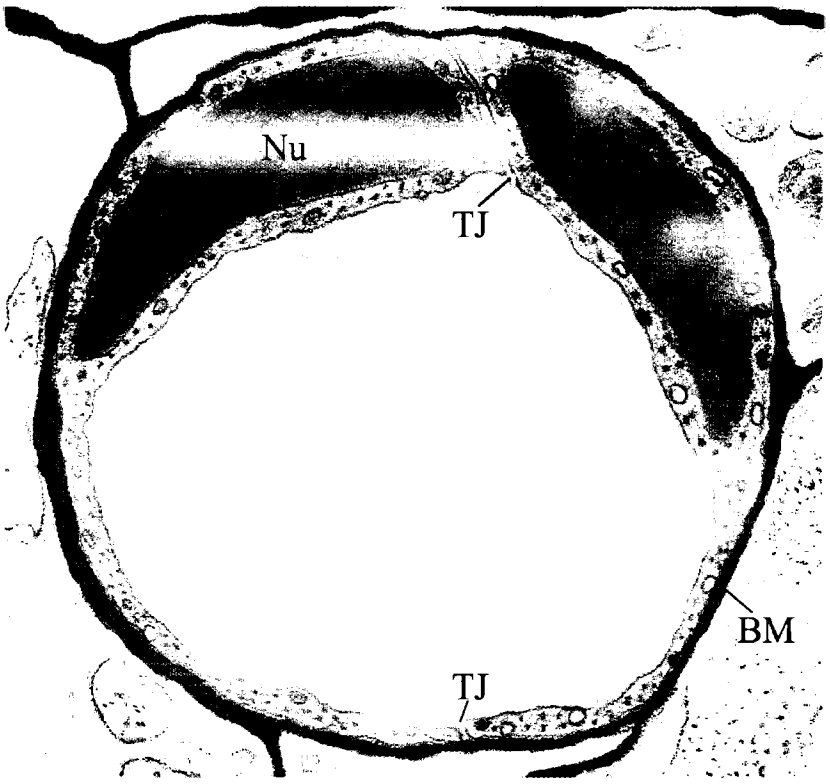

Figure 1.8 Structure of a normal capillary. The capillary is formed from a continuous sheet of endothelial cells, shown with a nucleus (Nu), that encircle the capillary lumen and are connected by tight junctions (TJ). The capillary is supported by a basement membrane (BM).

Liposomes extravasate into the interstitial space through gaps or fenestrae in the vascular endothelial lining (Figure 1.7). In normal tissues, vascular endothelial cells are coupled by tight junctions, which impede rapid and widespread distribution of liposome carriers. While liposomes do not readily accumulate in healthy tissues, an altered vasculature observed in certain disease states enables increased liposome-associated drug levels over extended period of time. Rapidly growing neovasculature and permeabilizing signals from disease cells during tumour growth (Richardson et al., 1979; Proffitt et al., 1983; Papahadjopoulos, 1988), infection (Bakker-Woudenberg et al., 1992) and inflammation (O'Sullivan et al., 1988) enables the filtration of large molecules through fenestrae of 200-500 nm and preferential liposome extravasation at the disease site into the interstitial compartment where the carriers can then act as local drug infusion reservoirs (passive targeting). This selective accumulation is further promoted by impaired or absent lymphatic drainage causing slow diffusion through the interstitial space. Some investigators have argued that additional liposome delivery specificity can be engineered by incorporation of ligands, such as specific antibodies, that can target diseased cells directly (active targeting). This has only been demonstrated successfully when the target cell population is located in the blood compartment (Lopes de Menezes et al., 1998) or lung (Ahmad et al., 1993).

1.5.3 Liposome Accumulation in the Liver

Even in the absence of deliberate targeting, liposomes display an affinity for accumulation within the liver, often to such an extent that it can become a significant obstacle when attempting to target cells beyond this organ. While uptake in the liver can be reduced to some extent by manipulating liposome size and composition (Wu and Zern, 1996), underpinning this phenomenon are: (1) Kupffer cell activity; and (2) the distinctive nature of hepatic circulation.

The liver is uniquely endowed with a dual blood supply from both the hepatic artery and the portal vein. As a result, the liver has an impressive blood flow (25 % of cardiac output) and any intravenously injected substance is assured to pass through this organ (reviewed in Gumucio et al., 1996). This high throughput of blood flow is reflective of its functions in blood detoxification and filtering which is mediated by Kupffer cells and fenestrae in the vascular endothelium. The structure of the liver is such that blood flows through sinusoids lined by endothelial and Kupffer cells (Figure 1.9) (Gumucio et al., 1996). This vascular endothelial lining is discontinuous, enabling molecules and other substances < 100-150 nm to extravasate through fenestrae into the space of Disse where they may have access to hepatocytes, or in theory, other non-native cell populations that may have established. Thus, together with the high volume of blood, the leaky vasculature can act like a sieve, favouring extravasation and accumulation of liposomes not taken up by Kupffer cells in the space of Disse.

Given the natural tendency for liposomes to accumulate in the liver, it has been postulated that liposomal drugs targeting liver localised disease would be highly effective. To date, however, this has not proven to be true. Although reports have demonstrated, using liver-localised cancer cells, that liposomal anticancer drugs can be effective, these studies were completed using highly phagocytic cancer cell lines. Lim and colleagues (Lim et al., 2000) attempted to address the issue associated with treatment of liver-localised cancer and concluded that critical attributes governing the activity of such liposomal drug formulations were the rate of drug release as well as the regional distribution of the carriers following localisation. This thesis explores those topics further, with a focus on a drug better suited for treatment of liver cancer.

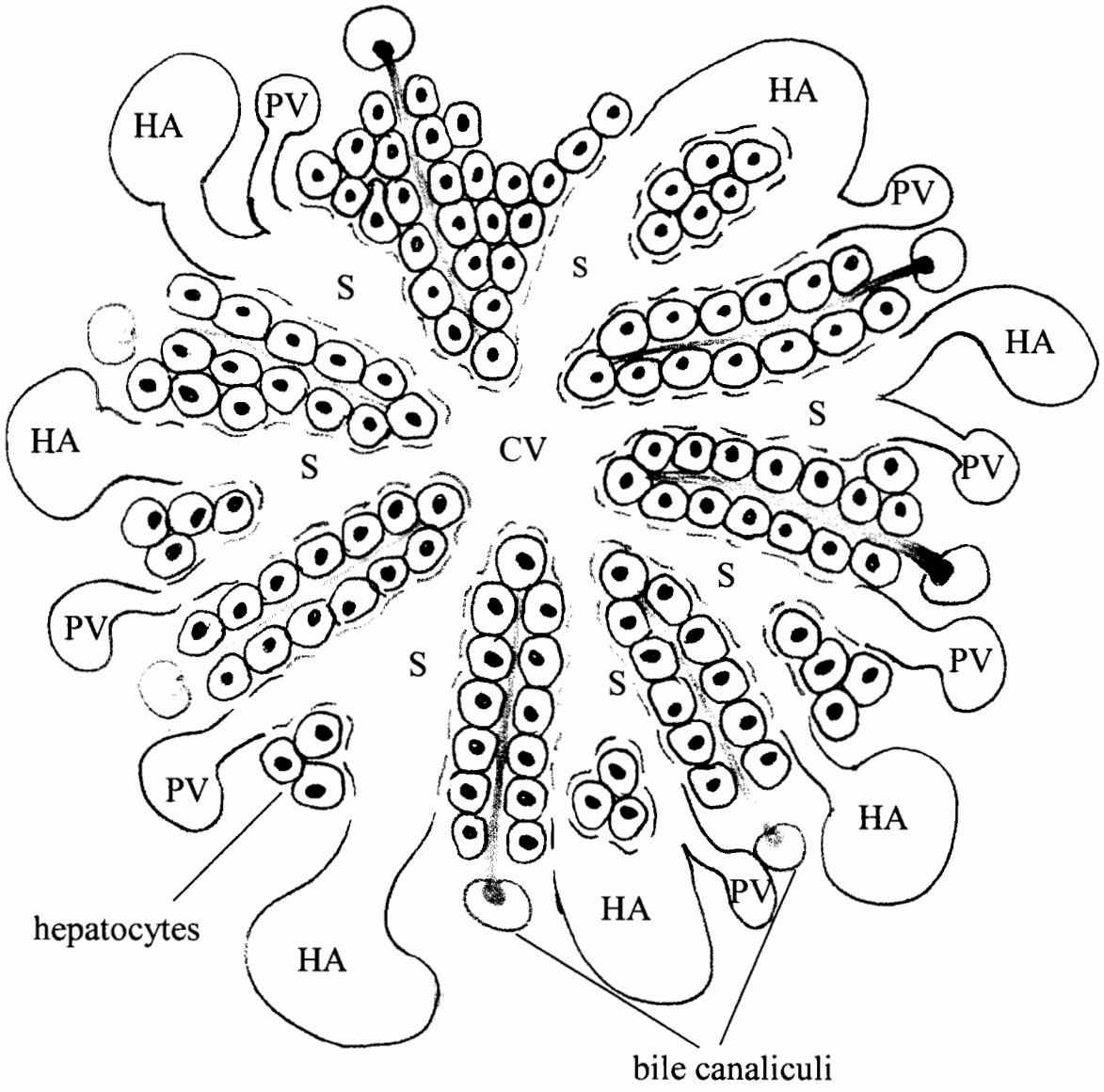

Figure 1.9 Anatomy of the liver sinusoid. Branches of the hepatic artery (HA) from the heart, and the portal vein (PV), from the gastrointestinal tract, supply the blood that percolates through hepatic sinusoids (S) to the central vein (CV). Endothelial cells lining the sinusoids are discontinuous enabling small molecules to escape into the space of Disse where they are in contact with hepatocytes. Hepatocytes are arranged in plates radiating out from the central vein and border bile canaliculi, which receive bile from surrounding hepatocytes and convey it to bile ducts. (Adapted from Paulsen, 1996)

1.5.4 Drug Release

Regardless of liposomal drug dosage, only drug released from the liposome is considered bioavailable and able to mediate a therapeutic effect. Drug release from circulating liposomes is influenced simultaneously by: passive diffusion of the drug across the lipid bilayer; disruption of the liposomal membrane through interactions with circulating factors; and enzymatic degradation of the lipid bilayer, causing premature release of its contents. Although the extent to which enzymatic activity is involved in drug release is specific to the particular enzymes involved, the degree to which passive diffusion or membrane disruption affect drug release can be manipulated by altering the chemical composition of the liposome, the site of liposome administration, for example intraperitoneal administration leads to slower degradation than intravenous administration (Hwang, 1987), and influenced by the tissues involved.

In optimised liposome-drug formulations, lipid-based carriers release their contents gradually, influenced primarily by passive diffusion, and the diseased cells take up the free drug. There does not appear to be significant uptake of discrete lipid-drug packages, however, liposomal drug can become associated with cells through direct liposome interactions with certain cell populations (Szoka and Papahadjopoulos, 1980; Straubinger et al., 1983).

1.6 Liposomes as Drug Carriers

The significance of liposomes as drug delivery vehicles is now well established. Not only does this apply to their ability to buffer the toxicity of encapsulated drugs, but also to protect against degrading factors in the physiological environment as well as acting as a slow release drug reservoir at the disease site, often increasing efficacy of the entrapped drug. Liposomes have

shown promise as carriers in many areas including those for antifungal drugs (Madden et al., 1990b), antibacterials (Nacucchio et al., 1988; Bakker-Woudenberg et al., 1989; Cordeiro et al., 2000), antiparasitics (Madden et al., 1990b), and anticancer agents (Mayer et al., 1998). Among those lipid-based drug carrier-associated anticancer drugs approved for clinical therapy or in late-stage clinical development are: liposomal vincristine (Inex Pharmaceuticals Inc.); liposomal doxil and doxorubicin (Johnson & Johnson); liposomal myocet (Elan); and daunorubicin (NeXstar Pharmaceuticals Inc.). While liposome encapsulation can enhance delivery of a drug, in selecting a drug for encapsulation, it is critical to consider the target cell population and choose a drug that will be therapeutically active in those cells. For example, liver-localised disease has only been poorly managed by drugs such as doxorubicin and vincristine, irrespective of whether they are administered as free or liposomal formulations (Lim et al., 2000).

1.6.1 Selecting a drug for encapsulation

Camptothecin is a natural anti-neoplastic agent derived from the Asian *Camptotheca acuminata* plant (Figure 1.2), which exhibited a significant range of anti-tumour activity against both ascitic and solid animal tumour models. Despite the development of a water-soluble sodium salt and progression through phase I and phase II clinical trials, its further development as a therapeutic agent was hampered by low effectiveness and severe systemic toxicities.

Interest in camptothecin was renewed in the late 1980s motivated by the identification of topoisomerase I as its cellular target (Hsiang and Liu, 1988), the identification of its structure-activity relationship (Jaxel et al., 1989) which spurred the development of water-soluble derivatives (Wall et al., 1993) with lower toxicities than the parent compound, and the finding

that in some tumour tissues, topoisomerase I levels are higher than in their normal tissue counterparts (Giovanella et al., 1989; van der Zee et al., 1991).

Camptothecins are cell cycle specific agents, targeting cells that are actively replicating DNA. Cytotoxicity of all members is dependent on a closed lactone ring, which at physiological pH undergoes rapid hydrolysis to an inactive carboxylate or ring-opened form (Figure 1.2) (reviewed in Burke and Bom, 2000). The poor water solubility of camptothecins and their inactivation at physiological pH have led to their classification as suitable candidates for encapsulation in a carrier that would facilitate intravenous administration, while providing protection from inactivating factors in the biological milieu.

Liposome structure bestows both a hydrophilic and hydrophobic compartment upon the carrier. The ability for both of these compartments to facilitate stabilization of the lactone form of camptothecins was demonstrated in the early 1990s (Burke et al., 1993; Burke and Gao, 1994; Burke, 1996). These studies suggested that camptothecins are capable of associating with membranes, and that bilayer-localized camptothecins preferentially partition as the active lactone form, thereby promoting and stabilizing the active lactone structure. Some of the newer members of the camptothecin family are water soluble, and when encapsulated will associate to a large degree in the aqueous core which can be manipulated to a low pH, thereby also contributing to the stability of the lactone ring (Burke and Gao, 1994; Tardi et al., 2000).

1.7 Irinotecan

Irinotecan (Figure 1.10), a semisynthetic derivative of the natural alkaloid camptothecan and the first of the water-soluble analogues, was introduced into the clinic in the late 1980s and now has

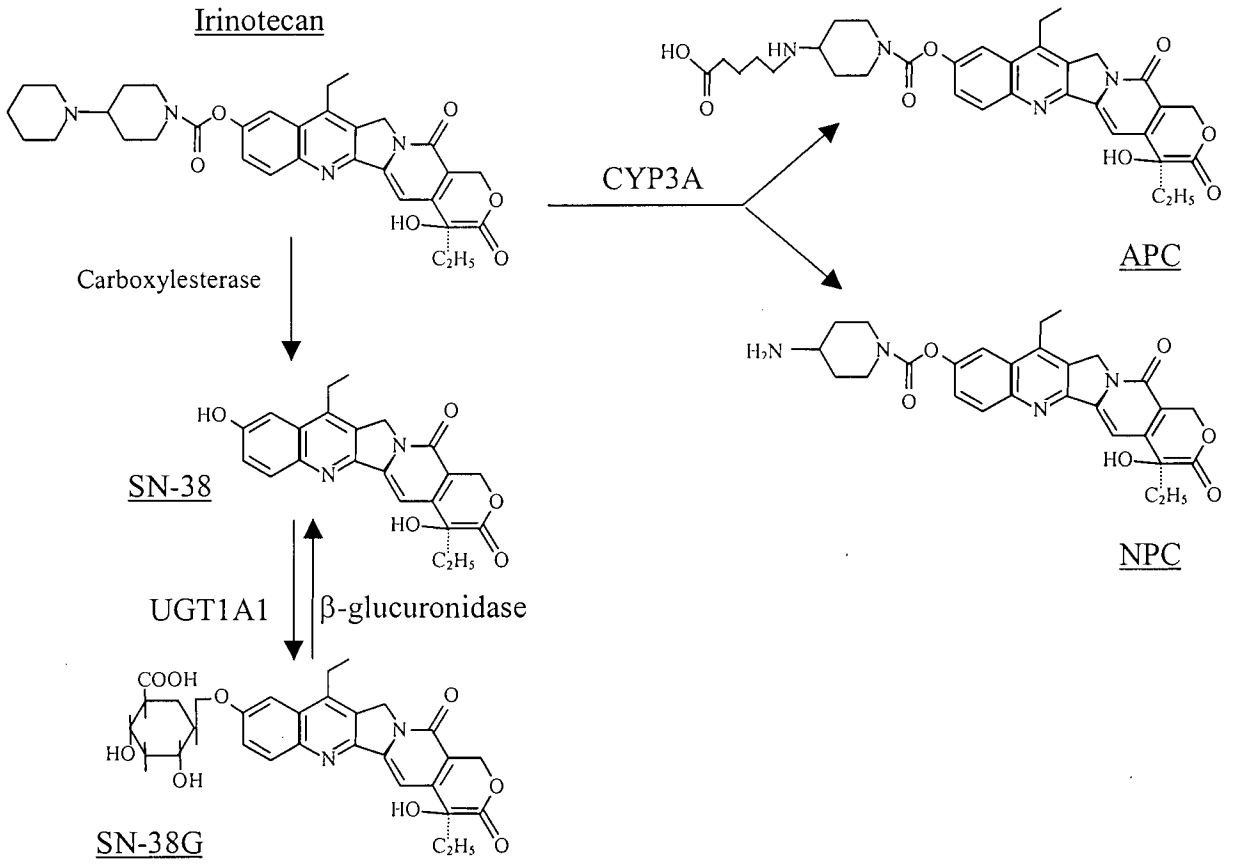

Figure 1.10 Irinotecan metabolism. Irinotecan can undergo activating or deactivating metabolism in the liver. Carboxylesterases mediate activating hydrolysis to form the active drug, SN-38. SN-38 can be further metabolised to SN-38G by uridine diphosphate glucuronosyltransferases (UGTs). Both SN-38 and SN38G are significantly excreted in the bile and may undergo enterohepatic recirculation stimulated by intestinal β-glucuronidase activity. Irinotecan may also undergo detoxifying oxidation by members of the cytochrome p450 3A family of hepatic enzymes resulting primarily in an aminopentanocarboxylic metabolite (APC) and an amino-piperidine derivative (NPC).

become a mainstay of 2nd line treatment of colorectal cancer, non-small cell lung cancer, brain cancer and esophageal cancer.

1.7.1 Mechanism of Action

Camptothecins inhibit topoisomerase I activity, and are active primarily during the S phase of the cell cycle (Li et al., 1972; Liehr et al., 1996). Topoisomerase I is critical for cell growth and proliferation as it makes a transient single-stranded break in the DNA duplex, which allows unwinding of the supercoiled DNA, enabling the replication fork to proceed in duplicating the DNA. After topoisomerase-mediated DNA cleavage, camptothecins bind to and stabilize the topoisomerase I-DNA cleavable complex, thereby preventing religation of the DNA. Subsequent accumulation of cleavable complexes (Hsiang et al., 1988; Hsiang et al., 1989) inside the cell, arrests DNA replication and causes double-stranded DNA breaks, which lead to eventual cell apoptosis (Zhang et al., 1990). The magnitude of camptothecin cytotoxicity is consequently a function of topoisomerase I expression and DNA replication in a cell. Topoisomerase I is overexpressed in several tumour types including breast, lung and colorectal tumours (Potmesil, 1994). Although it is expressed throughout the cell cycle, cells in the S-phase are 1000 times more sensitive to camptothecins than they are during the G phases (Del Bino et al., 1991).

1.7.2 Activation/Metabolism

Irinotecan is a prodrug of limited activity, but which after conversion to its active form, SN-38 (Figure 1.10) by carboxylesterase-mediated de-esterfication in the plasma and the liver, is 1000 times more potent than the parent compound (Kawato et al., 1991). SN-38 can undergo further

conjugation by hepatic uridine diphosphate glucuronosyltransferases (UGTs) to SN-38G, which although inactive, has been found to be the predominant plasma form of SN-38 *in vivo* (Rivory and Robert, 1995a; Lokiec et al., 1996; Rivory et al., 1997;). SN-38 and SN-38G are significantly excreted in the bile, and can undergo enterohepatic recirculation with SN-38 being reconstituted by intestinal β-glucuronidase (Figure 1.10) (Takasuna et al., 1995). Irinotecan can also undergo degrading oxidation reactions mediated by the cytochrome p450 3A (Haaz et al., 1998a; Haaz et al., 1998b) family of hepatic enzymes to form the inactive metabolites, 7-ethyl-10-[4-N-(5-aminopentanoic acid)-1-piperidino] carbonyloxycamptothecin (APC) (Rivory et al., 1996; Rivory et al., 1997; Sparreboom et al., 1998) and 7-ethyl-10-(4-amino-1-piperidino) carbonyloxycamptothecine (NPC), the primary amino-piperidine metabolite (Dodds et al., 1998). Irinotecan and its metabolites are primarily excreted in feces, with irinotecan as the major excretion product (Slatter et al., 2000).

1.7.3 Cellular mechanisms of resistance

Cellular resistance to chemotherapeutic agents can pose a major complication in patient treatment, even so far as resulting in treatment failure. A common mechanism responsible for such resistance is the reduction of the intracellular concentration of the drug via efflux mediated by pumps of the multi-drug resistance family such as P-glycoprotein. Camptothecins do not appear to be good substrates for P-glycoprotein which is commonly overexpressed in colorectal adenocarcinoma (reviewed in Rivory and Robert, 1995b; Jung and Zamboni, 2001), although both irinotecan and SN-38 are transported by the multidrug resistance protein (Chen et al., 1999) and there is further evidence for their efflux by a yet unidentified anionic pump (reviewed in (Jung and Zamboni, 2001).

Modulation of topoisomerase I activity and expression may also mediate drug resistance. Irinotecan cytotoxicity has been linked to cellular levels of topoisomerase I activity (Jansen et al., 1997), thus reductions in topoisomerase I protein levels can directly affect activity. Also, alterations in topoisomerase I mRNA levels or mutations in the gene, causing reduced expression or activity or engendering camptothecin resistance (reviewed in Rivory and Robert, 1995b).

1.8 Advanced Colorectal Cancer And Liver Metastases

Colorectal cancer (CRC) is the second leading cause of cancer mortality in North America, and the most frequent cause of cancer deaths not provoked by a chemical carcinogen (ie. nicotine and lung cancer). Approximately 17,600 Canadians will be diagnosed with colorectal cancer in 2002 and 6,600 will succumb to the disease (National Cancer Institute of Canada: Canadian Cancer Statistics 2002, Toronto, Canada, 2002). If left untreated, only 30% of the patients will survive 3 years and few will survive 5 years beyond the detection of their liver metastasis (Bengmark and Hafstrom, 1969; Adson et al., 1984).

The liver is the primary site of blood borne metastases from cancers of several different origins, including carcinomas of the lung and breast, but colorectal adenocarcinomas, which drain into the portal circulation, are particularly prone to spread to the liver. In contrast to gastric and pancreatic neoplastic spread to the liver, which also reveals spread to other organs, the liver is often the sole site of metastases for CRC. Hepatic metastases are normally asymptomatic until quite advanced and are detected either at the time of primary cancer diagnosis or during a routine follow-up (Choti and Bulkley, 1999). As many as 70% of patients with colorectal cancer will present with (synchronous) liver metastases at the time of their primary diagnosis or develop liver metastases (metachronous) as their disease progresses (Kemeny et al., 1980).

Complications that arise due to neoplasia in the liver include erythrocytosis, hypoglycemia and eventual liver failure.

1.8.1 Current treatment strategies

Neoplasia in the liver are challenging cancers to manage, and despite the development of novel treatment strategies such as intrahepatic arterial chemotherapy and thermal ablation, surgical resection remains the treatment of choice for appropriately selected patients. Systemic chemotherapy is the most common treatment for patients with colorectal hepatic metastases.

1.8.2.1 Systemic chemotherapy

Although systemic chemotherapy is the predominant modality of care for hepatic metastases, it is currently palliative in intent, and at best may induce a transient reduction in tumour size, temporarily increasing the patient's quality of life. Since the 1960s chemotherapeutic intervention of liver metastases has rested almost exclusively on 5-fluorouracil-based treatment regimes, which yield responses in the range of 20-30%. Moreover, most of these responsive patients develop resistance to these cytotoxic agents. Irinotecan was recently introduced as a novel agent for the treatment of advanced colorectal cancer and initially approved for use as a second line treatment for refractory disease. Its remarkable therapeutic ability, eliciting responses in patients resistant to the conventional treatments, lead to its rapid promotion to a first line treatment for advanced CRC administered in conjunction with the conventional therapy of 5-fluorouricil and leucovorin.

1.8.2.2 Liver resection

Surgical resection is the only known potentially curative treatment for liver metastases. However strict qualification criteria including a maximum of three neoplasia in a single lobule restrict this treatment to only 10% of the patient population, and still overall 5-year survival rates of only 25%-40% are obtained (Scheele et al., 1991; Kemeny et al., 1993).

1.9 Specific Aims

The aims of this thesis were to:

1) characterise the DSPC/cholesterol liposomal irinotecan formulation
2) evaluate the potential of liposomal irinotecan to treat liver metastases in a xenograft model of advanced human colorectal cancer.

1.10 Hypothesis

It is argued that liposomal drug formulations should be more effective at treating liver-localised carcinomas, including liver metastases when compared with their free drug counterparts, because of their intrinsic affinity for the liver and extended lifespan.

Although colorectal cancer is the second leading cause of cancer mortality in North America, primarily because of a high incidence of hepatic metastases, the development of new treatment options for these patients is relatively unsuccessful compared to that for several other cancers. Liposomal drugs are currently establishing themselves as powerful chemotherapeutic agents, as liposomes are able to alter the pharmacokinetics of traditional agents, converting marginally

effective or severely toxic drugs into potentially useful agents simply through improvements in drug delivery. Furthermore, liposomes' natural tendency to accumulate in the liver and evidence for increased therapeutic efficacy for liposomal drug formulations in treating liver disease, suggests that encapsulation of the appropriate agent(s) will provide an effective alternative treatment for patients with advanced colorectal cancer. The camptothecin family of anti-neoplastic agents is one group that have been proposed as suitable candidates for encapsulation, primarily due to the importance of their lactone ring, which undergoes inactivating hydrolysis at physiological pH, but which could be stabilized if effectively encapsulated. Recent advancement of the camptothecin analogue irinotecan through clinical trials into the clinic where it continues to perform admirably and has quickly been promoted to first line treatment for advanced colorectal cancer in conjunction with 5-fluorouricil/leucovorin, suggests that it may have further potential which may be exploited by encapsulation.

The results presented in this thesis lend support to the thesis statement. First this work documents that irinotecan is particularly well suited for liposome encapsulation. The results illustrate that under an ionophore-mediated proton gradient, irinotecan can be efficiently trapped even at relatively high drug to lipid ratios. Using improvements in pharmacokinetic properties as a measure of an effective liposome-drug combination, it is demonstrated that DSPC/cholesterol encapsulation of irinotecan significantly improves circulation longevity of the drug as compared to the free agent, which to a large degree is maintained as the active lactone species. Next, the question of a possible role for liposomal drug in the treatment of liver cancer was investigated. Tumour size and growth rate and/or increase in lifespan were used as indicators in efficacy studies of liposomal and free irinotecan conducted in the LS180 solid tumour model of colorectal metastasis, and the LS174T orthotopic model of human colorectal liver metastasis. It is

concluded that DSPC/cholesterol encapsulation of irinotecan offers a significant advantage in the treatment of liver-localised metastases.

CHAPTER 2

MATERIALS AND METHODS

2.1 Materials

Irinotecan hydrochloride (Camptosar®, Pharmacia) was purchased from the British Columbia Cancer Agency Pharmacy. 1,2 Disteroyl-*sn*-glycero-3-phosphocholine (DSPC) was purchased from Avanti Polar Lipids (Alabaster, AL). Cholesterol, the divalent cation ionophore A23187, N-2-hydroxyethylpiperazine-N-2ethane-sulphonic acid (HEPES), and sephadex G-50 (medium) and were obtained from the Sigma Chemical Company (St. Louis, MO). Tritiated [^{3}H]cholesteryl hexadecyl ether (^{3}H-CHE) (NEN, Boston, MA) was used as a liposome marker, and [^{14}C] methylamine hydrochloride, used in determining the pH gradient, was obtained from Amersham Biosciences Corp. (Baie d'Urfe, PQ). DiI, (1,1'-dioctadecyl-3,3,3',3'-tetramethylindocarbocyanine perchlorate) used as a fluorescent lipid probe, was purchased from Molecular Probes (distributed by Cederlane Laboratories Limited, Hornby, ON). All other chemicals used in this study were analytical or HPLC grade. The LS180 and LS174T tumour cell lines were originally purchased from the ATCC (Manassas, VA) and were maintained in tissue culture. Cells were used for experiments when they were between passages three and twenty. After the twentieth passage the cells were discarded and the new cell lines were reverted back to frozen stock. Male SCID/RAG-2M mice (8-10 weeks old) were bred at the British Columbia Cancer Agency Animal Breeding Facility.

2.2 Preparation of liposomes

Large unilamellar vesicles consisting of 1,2-disteroyl-3-*sn*-phosphatidylcholine (DSPC) and cholesterol (55:45 mole percent) were prepared using well-established extrusion technology as previously described by Hope *et al.* (1985). When DiI was used as a fluorescent lipid marker, the DSPC, cholesterol, DiI ratio was 54.5:45:0.5 mole percent. Briefly, the indicated lipids were dissolved in chloroform in the presence of ^{3}H-CHE and dried to a homogenous lipid film under nitrogen gas, which was further dried under vacuum overnight to remove any residual chloroform. The dried lipid films were subsequently hydrated in 300 mM manganese sulfate, pH 3.4, to a final lipid concentration of 50 or 100 mg/ml. The resulting multilamelar vesicle mixture was freeze-thawed five times in liquid nitrogen (Mayer et al., 1986b), and size-reduced using high-pressure extrusion through two-stacked polycarbonate filters, one each of 100 nm and 80 nm pore size (Whatman Inc., Newton, MA) using an extruder (Lipex Biomembranes Inc., Vancouver, BC). The vesicle size of the resulting large unilamellar vesicles (LUVs) was typically in the range of 115 ± 15 nm based on quasi-elastic light scattering (Nicomp Particle Sizer Model 270, Santa Barbara, CA). The external buffer was exchanged by running the sample down a Sephadex G-50 column equilibrated in 300 mM sucrose, 20 mM HEPES and 15 mM EDTA (SHE buffer) at pH 7.4.

2.3 $MnSO_4$ pH gradient loading of irinotecan

Irinotecan was loaded into the liposomes by way of an ionophore-mediated proton gradient (Fenske et al., 1998). Drug uptake was performed at 0.3 mg irinotecan per 1 mg lipid in SHE buffer (pH 7.4). The divalent cation ionophore A23187 (0.5 μg per 1 mg lipid) was first added to the liposomes and the mixture was incubated at 37°C or 60°C for 10 minutes to enable

ionophore incorporation into the lipid bilayer. Subsequently, irinotecan was added and the mixture was incubated at 37°C or 60°C for 1 h. During this process the mixture was protected from the light, as irinotecan has been shown to undergo photodegradation upon extended exposure to light (Dodds et al., 1997). Encapsulation efficiency was determined at several timepoints over a 2-hour period at both 37°C and 60°C. The extent of irinotecan encapsulation was assessed by running an aliquot of the mixture down a Sephadex G-50 mini spin column (Madden et al., 1990a) to remove unencapsulated drug and subsequent measurement of irinotecan and lipid concentrations in the eluent. Irinotecan concentration was quantified at its peak absorbance of 370 nm using a Beckman DU®-64 Spectrophotometer (Beckman Coulter Canada Inc., Mississauga, ON). Radioactivity was assessed by counting a mixture of the sample and 5 ml of Pico-Fluor-15 (Packard, Meriden, CT) scintillation cocktail on a Packard 1900 scintillation counter (Packard, Meriden, CT). The efficiency of irinotecan loading was typically between 90 and 100%. In preparation for intravenous administration, the A23187 ionophore was removed from the liposomal drug preparation and the external buffer exchanged to 0.9 % saline through manual tangential flow as per instructions provided by the column (400 kD cut-off) supplier (Spectrum Laboratories Inc., Rancho Dominguez, CA), which was also employed to reduce volume to achieve an appropriate concentration, based on the desired drug dose, for i.v. administration.

2.4 *In vitro* characteristics of liposomal irinotecan

For drug release studies, drug loaded liposomes were prepared as described in sections 2.2 and 2.3. These were then transferred to Fisherbrand dialysis tubing (10 mm wide, 12,000-14,000 molecular weight cut off, Fischer Scientific, Nepean, ON) and the samples were dialysed against 4 litres of SHE buffer for 72 hours at 37°C. At the indicated time points, 50 μl aliquots, in

triplicate, were removed from the dialysis bag and analysed for relative encapsulated drug and lipid concentrations as previously described (section 2.3). To assess the effect of the transmembrane gradient on drug uptake and vice versa, the magnitude of the proton gradient was measured following a methylamine-based procedure described by (Harrigan et al., 1992), with modifications. Briefly, drug loaded liposomes were prepared as described in sections 2.2 and 2.3 to a total volume of 500 µl. After the loading incubation, 50 µl aliquots from each sample were assayed for loading efficiency, and samples were cooled to room temperature. An appropriate amount of ^{14}C-methylamine (not to exceed a ^{3}H/^{14}C ratio of 1/10) was then added to each sample and allowed to incubate for 1 h at room temperature at which time radioactivity was measured, using a dual label analysis by the Packard instrumentation, in 100 µl aliquots from the samples and the total eluents of 100 µl aliquots, in triplicate, run down mini spin columns. A series of calculations based on these measurements and the assumption that the liposomes used have a trapped volume of 1.2 µl/µmole lipid led to the determination of the transmembrane proton gradients.

2.5 Pharmacokinetic studies in SCID/RAG2M mice

Free irinotecan (50 mg/kg) and liposomal irinotecan (167 mg/kg lipid, 50 mg/kg irinotecan) were injected via the lateral tail vein into male SCID/RAG-2M and the plasma elimination of both the lipid carrier and the drug were determined over a 24-h time course. Animals were terminated by CO_2 asphyxiation at the indicated time points, and blood was retrieved via cardiac puncture and collected into EDTA coated tubes (Microtainers, Becton Dickinson). Blood plasma was isolated from hematocrit following centrifugation of the whole blood at 2500 x *g* for 10 minutes. 25 µl aliquots of plasma were combined with 5 ml Pico-Fluor 15, and scintillation counting of the

marker ^{3}H-CHE (Stein *et al.*, 1980) was used to quantify the liposomal carrier in the plasma. Total irinotecan and relative circulating lactone and carboxylate species concentrations were determined using HPLC analysis as described by (Chollet et al., 1998), with modifications (please refer to the Appendix for details). Briefly, irinotecan was extracted from 100 µl of plasma by diluting the sample in ice-cold methanol to precipitate the proteins and solubilise the liposomes. The samples were analysed immediately. Standard curves for the two species of drug were generated by dissolving the drug in either DMSO for the lactone species or 50% acetonitrile: 50% 20 mM borate buffer (pH 9) for the carboxylate species, (although it was observed that this technique resulted in an incomplete conversion to the carboxylate form, resulting in an over- estimation of the carboxylate species). Separation was achieved using a Symmetry® C_{18} cartridge column (100 Å, particle size 5 µm; 250 x 4.6 mm I.D., Waters) with a Symmetry® Sentry™ C_{18} guard column (particle size 5 µm; 20 x 3.9 I.D., Waters) with a runtime of 20 minutes at a flow rate of 1.5 ml/min, and maintained at 35°C. A two-solvent mobile phase consisted of mobile phase A (75 mM ammonioum acetate, 7.5 mM tetra-butylammoniumbromide, pH 6.4 adjusted with glacial acetic acid) and mobile phase B (100 % acetonitrile), with the elution gradient containing a mixture of 76 % A: 24 % B. For sample analysis, 80 µl of each sample and standard were loaded into 1 ml HPLC sample vials (Waters, Milford, MA) with 200 µl inserts (Chromatographic Specialties Inc., Brockville, ON) and 10 µl was injected into the column. Irinotecan was quantified using an HPLC system equipped with a Waters Model 717 plus autosampler (set to 4°C), a Model 600E pump and controller and a Model 470 Scanning Fluorescence Detector (Waters, Milford, MA) set at an excitation wavelength of 362 nm and an emission wavelength of 425 nm. Data were acquired and processed with the Millenium32® chromatography manager (Version 3.20, Waters, Milford, MA).

2.6 Establishing a maximum tolerated drug dose

Limited dose ranging studies were used in an effort to determine the maximum tolerated dose (MTD). Male SCID/RAG-2M mice in groups of two were given free or encapsulated drug by single or multiple (3 doses, each 4 days apart) i.v. injections into the lateral tail vein. Animals were monitored for weight loss and other signs of stress/toxicity for a period of 30 days. Individual animals that lost more than 20 % of their original weight or those appearing severely stressed, as judged by appearance and/or behaviour and assessed by qualified animal care technicians, were terminated. After 30 days, all remaining animals were terminated by CO_2 asphyxiation and necroscopies were conducted to identify any additional drug toxicities. Toxicity studies aimed at determining the exact LD_{10} dose of a drug formulation are not sanctioned by the Canadian Council on Animal Care nor the institutional Animal Care Committee.

2.7 Liposomal irinotecan anti-tumour efficacy using the human LS180 solid tumour model

Male SCID/RAG-2M mice (20-30 g, 6 per group) were inoculated with 1 x 10^6 cells subcutaneously on the right posterior dorsal side. Once the tumour had established and reached a size accurately measurable with callipers (tumour volume > 0.04 cm^3) (day 11 post inoculation), free or encapsulated irinotecan dosing schedules of single or multiple (day 11, 15, 19) injections of 50 or 100 mg/kg irinotecan via the lateral tail vein were initiated. Animals were monitored daily for any signs of stress or toxicity and were terminated when weight loss exceeded 25% or when animals displayed increasing health deterioration including lethargy, scruffy coats, or dehydration. Survival time for terminated animals was recorded as the

following day. Animals were monitored for sixty days or until all animals had been terminated. Drug mediated off-set of tumour growth was estimated by extrapolation of a line tangential to rapid tumour growth down to the x axis, which indicated a time in days post inoculation.

2.8 Liposomal irinotecan anti-tumour efficacy using the human LS174T orthotopic tumour model

Male SCID/RAG-2M mice (20-30 g, 6 per group) were inoculated intrasplenically with 5 x 10^6 LS174T cells. Following inoculation, these cells travel via the portal vein to the liver were they seed and establish widespread tumour growth. On day 7 post cell inoculation, animals began dosing schedules of single or multiple injections (day 7, 11, 15) of 50 mg/kg free or liposomal irinotecan administered via the lateral tail vein. Animals were monitored daily and terminated upon signs of severe weight loss (> 25%) and/or health deterioration as demonstrated by lethargy, scruffy coats or dehydration. Survival time for terminated animals was recorded as the following day.

2.9 Liposome mediated drug delivery to LS174T liver metastases

To illustrate liposome mediated drug delivery to tumours in the liver, male SCID/RAG-2M mice (20-30 g, 2 per group) were inoculated intrasplenically as described in the previous section. Once the tumours were well established in the liver (day 19 post inoculation), animals were given a single lipid dose of 167 mg/kg, of irinotecan (50 mg/kg) or mock-loaded DSPC/Cholesterol/DiI (54.5:45:0.5, mole percent) liposomes injected via the lateral tail vein. 24 hours later animals were terminated by CO_2 asphyxiation, whole blood was collected via cardiac puncture as outlined in pharmacokinetic studies, and a portion of a lobe of the liver was

harvested for sectioning and histochemistry. DiI inclusion in the liposomes enabled their visualisation using fluorescent microscopy. Liver sections taken from untreated animals (n=2) were H & E stained to reveal tumour-associated cells.

2.10 Statistical analysis

One-way ANOVA (analysis of variance) was performed on the tumour volume results obtained after the administration of free or liposomal irinotecan. Common time points were compared using the post hoc comparison of means, Scheffé test. Survival data was analysed using a multiple-sample test in the Survival Analysis module of Statistica™ (Statsoft Inc, Tulsa, OK). This test is an extension of Gehan's generalized Wilcoxon test, Peto and Peto's generalized Wilcoxon test, and the log-rank test. Differences were considered significant at $p < 0.05$.

CHAPTER 3

LIPOSOMAL IRINOTECAN AND ITS THERAPEUTIC ACTIVITY AGAINST COLORECTAL METASTASES

3.1 *In vitro* irinotecan uptake and release characteristics

Studies illustrating the *in vitro* irinotecan loading in liposomes composed of DSPC and cholesterol at 37°C or 60°C and the importance of the A23187 ionophore are presented in Figure 3.1. At 37°C, less than 30% of the drug was encapsulated over 2 hours, in contrast to 100% encapsulation at 60°C, where the time required to achieve maximum uptake was 20 minutes. In the absence of the A23187 ionophore, drug accumulation in the liposomes was less than 20%, irrespective of the incubation temperature. Moreover, in the absence of the ionophore the transmembrane pH gradient was reduced to approximately 1, emphasizing the ionophore's significant role in maintaining the proton gradient, as well as the dependence of efficient drug encapsulation on this transmembrane gradient. The extent of irinotecan loading was influenced by the starting drug to lipid ratio (Figure 3.2A). Irinotecan encapsulation increased with increasing drug to lipid ratios, but above 0.3:1 (wt:wt) the gain in loading attributable to an increased initial drug to lipid ratio was reduced, and the efficiency of drug encapsulation was also decreased. As illustrated in Figure 3.3, greater than 95% loading could routinely be achieved when the starting drug to lipid ratio was 0.3:1 (wt:wt). If the same experiment was completed at a 0.5:1 (wt:wt) starting drug to lipid ratio, greater drug loading was achieved (final drug to lipid ratio of 0.35:1 (wt:wt), but the efficiency was less than 80%. The reduction in loading efficiency at higher drug to lipid ratios is correlated with degradation of pH gradient (Figure 3.2B). This liposomal irinotecan formulation (prepared at 0.3:1 (wt:wt) drug to lipid

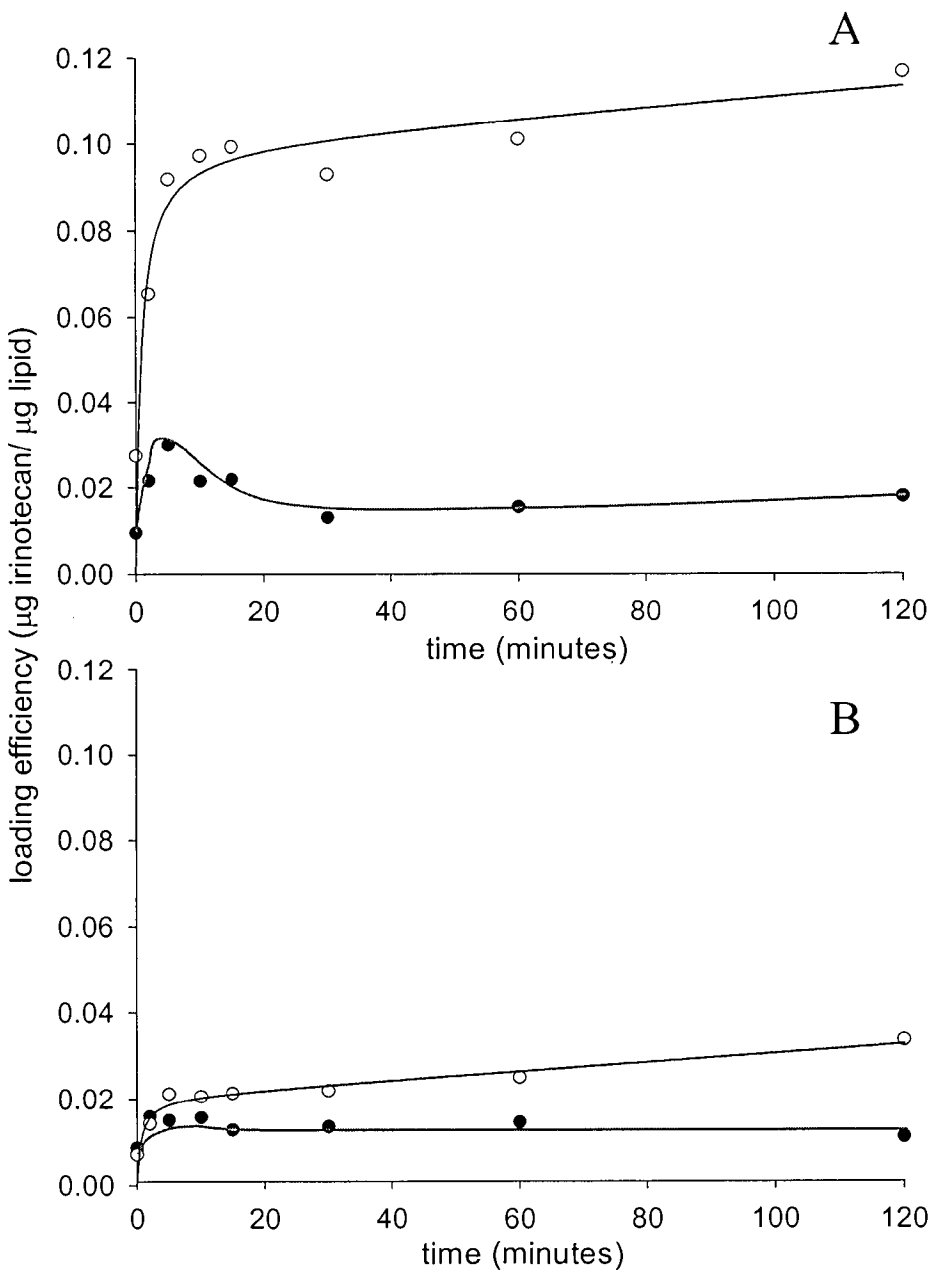

Figure 3.1 Effect of the A23187 ionophore in pH gradient-mediated loading of irinotecan into DSPC/cholesterol liposomes at 60°C (A) or 37°C (B). Loading was evaluated at two temperatures in the presence (○) or absence (●) of the ionophore at a drug to lipid ratio of 0.1:1 (wt:wt). Drug encapsulation was determined by the mini spin column-based procedure described in section 2.3.

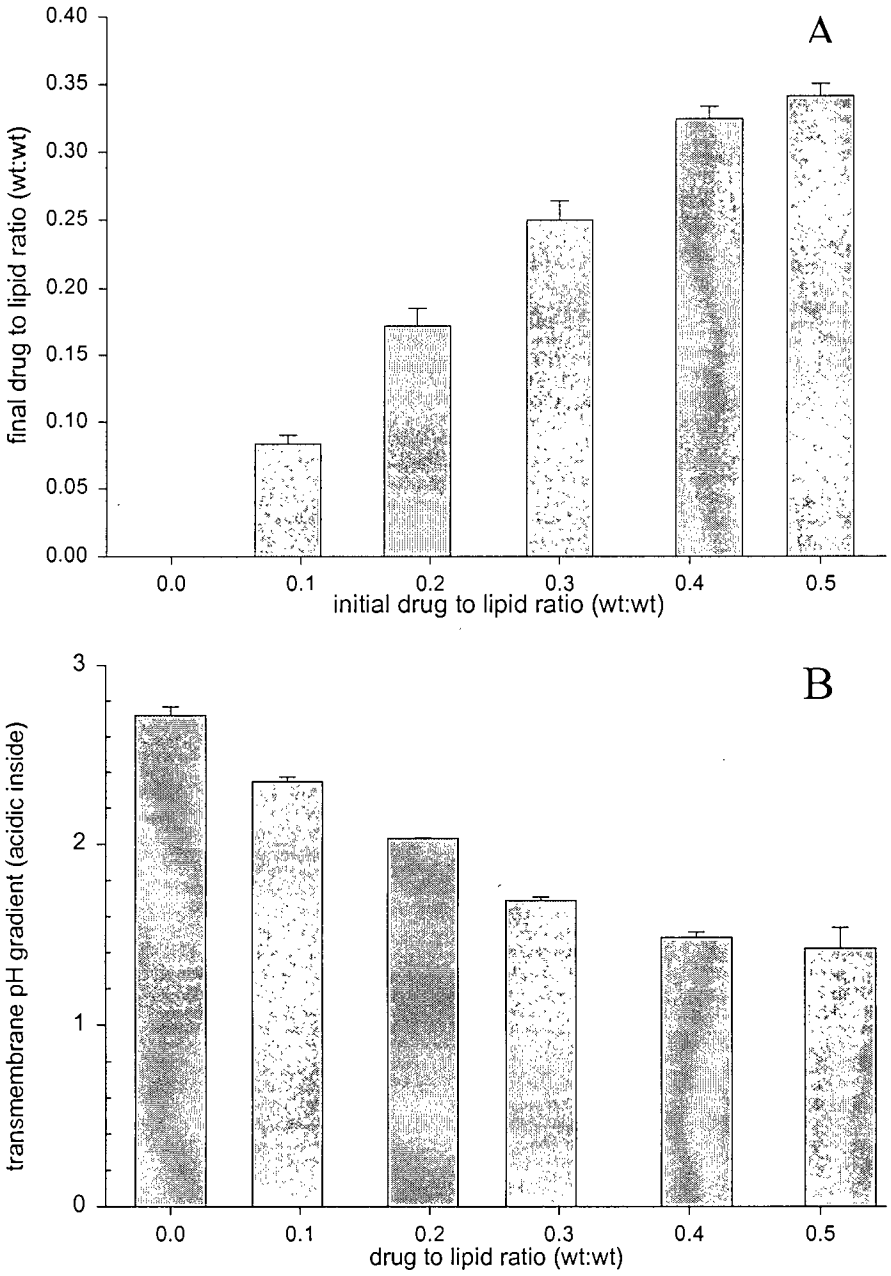

Figure 3.2 The effect of drug to lipid ratio on irinotecan loading (*A*) and the transmembrane pH gradient (*B*). *A*, DSPC/cholesterol liposomes were incubated at 60°C for 1 hour at different drug to lipid ratios, and the extent of irinotecan encapsulation was determined (see section 2.3) and is expressed as the average final drug to lipid ratio ± s.d.. *B*, the transmembrane pH gradient in samples with different drug to lipid ratios was determined, by a ^{14}C-methylamine procedure described in section 2.4, following 1 hour irinotecan incubation with the liposomes.

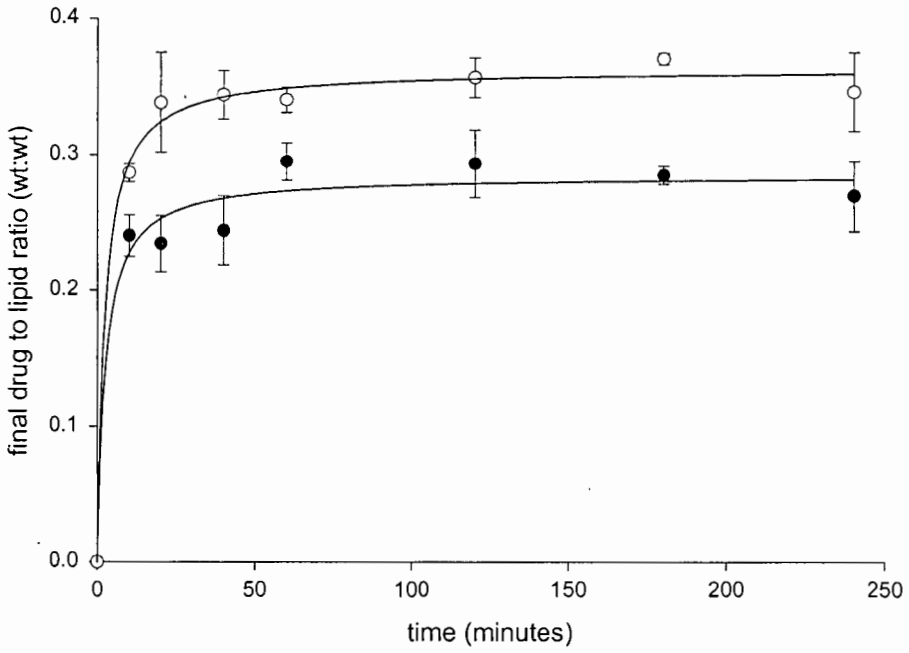

Figure 3.3 Efficiency of irinotecan encapsulation at different drug to lipid ratios. Efficiency of irinotecan loading into DSPC/cholesterol liposomes at 60°C was evaluated for initial drug to lipid ratios of 0.3:1(●) and 0.5:1 (○) (wt:wt). Drug encapsulation was determined as per the procedure described in section 2.3. Aliquots were taken in triplicate over a 2 hour time course, and results are expressed as the average ± s.d..

for up to 72 hours (Figure 3.4) with less than 2% of the trapped irinotecan released, as measured by dialysis of the loaded liposomes against a large volume (4 litres) of SHE buffer.

3.2 *In vivo* plasma elimination of free and liposomal irinotecan

Pharmacokinetic studies investigated plasma elimination rates of irinotecan and the liposomal carrier. Mice were given an i.v. injection of liposomal irinotecan (167 mg/kg lipid; 50 mg/kg drug); free irinotecan (50 mg/kg) or "empty" liposomes (167 mg/kg). DSPC/cholesterol liposomes exhibited an extended circulation lifespan (Figure 3.5A), with similar elimination rates for irinotecan- (filled symbols) and mock-loaded (open symbols) liposomes and approximately 40% of the injected lipid dose could still be found in the plasma compartment 24 h after i.v. injection. Free irinotecan was eliminated rapidly (half-life of less than 15 minutes) from the plasma compartment (Figure 3.5B), while liposome-associated drug was maintained at high levels for up to 24 h, at which time circulating liposomal irinotecan was still 10 fold higher than the concentration of free drug determined at 5 min following injection. The relative amount of irinotecan retained in the circulating liposomes, and conversely the rate of drug release, can be estimated using the data shown in Figure 3.5 A and B to define the irinotecan to lipid ratio (drug to lipid, wt:wt) at each of the measured points (Figure 3.5C). A caveat of this estimation is that it assumes the level of free drug, in the plasma of animals given liposomal irinotecan, is negligible. These data illustrate that DSPC/cholesterol liposomes provide gradual and sustained irinotecan release during the study's 24-hour timecourse, with 75% of the irinotecan originally associated with the liposomes released within 24 hours.

As indicated in sections 1.2 and 1.6.1, irinotecan undergoes reversible hydrolysis between a closed-ring lactone species and an open-ring carboxylate (Figure 1.2). The extent and rate of

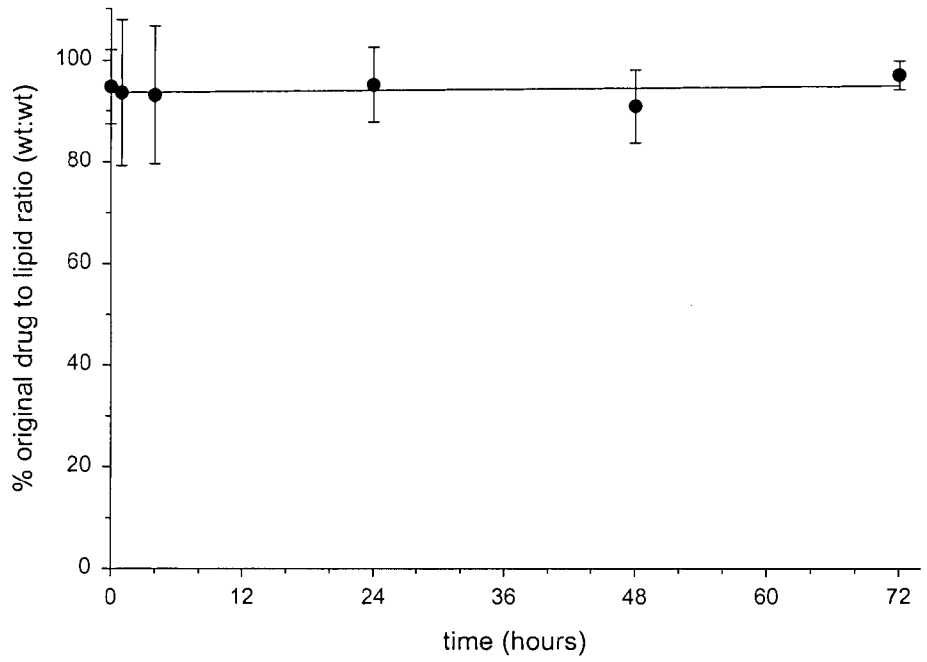

Figure 3.4 Release of irinotecan from DSPC/cholesterol liposomes incubated at 37°C for 72 hours. Irinotecan-loaded liposomes (0.3:1 drug to lipid ratio) were dialized against 4 L of SHE buffer (pH 7.4) over a 72 h period. At the indicated timepoints, 50 μl aliquots, in triplicate, were removed from the dialysis bag and run down mini spin columns, as described in sections 2.3 and 2.4, to determine the amount of drug still associated with lipsomes. Results are expressed as the average ± s.d..

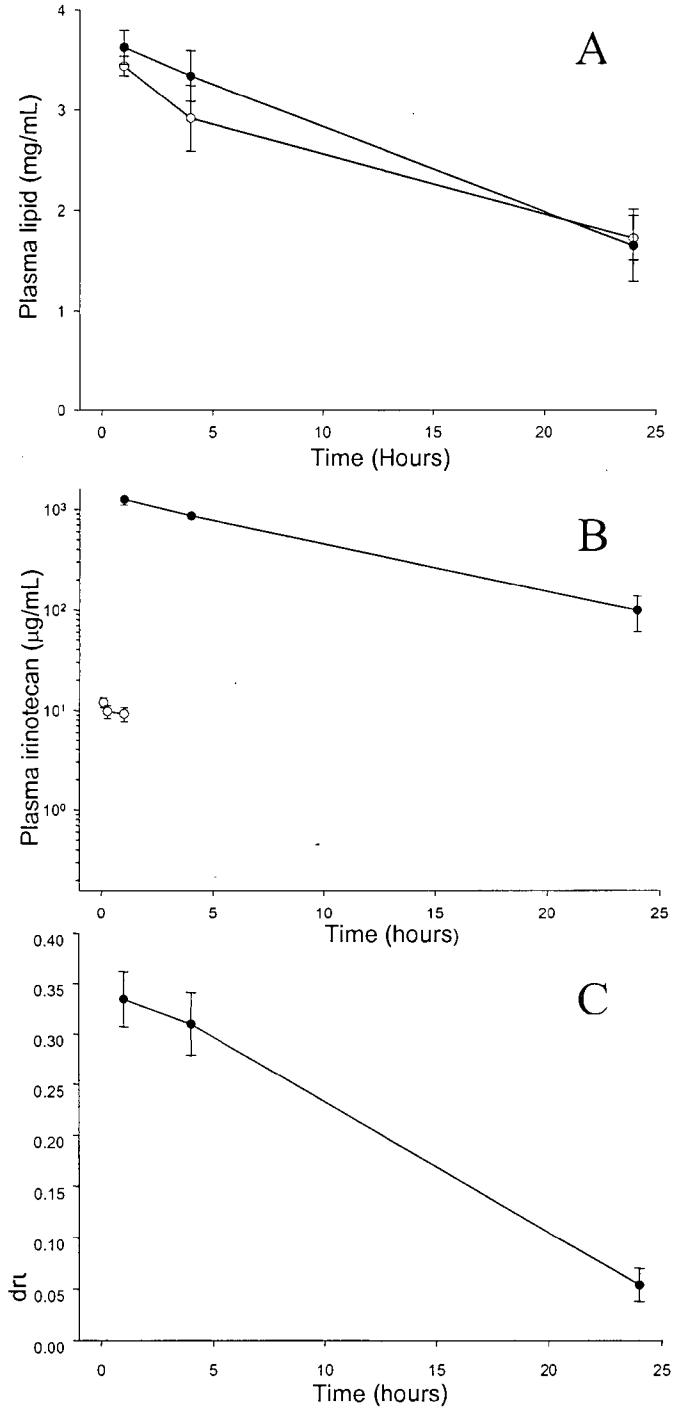

Figure 3.5 Plasma elimination of free and liposomal irinotecan. *A*,mice (n=6) were injected with lipsomal irinotecan (●) or mock-loaded liposomes (○) at a lipid dose of 167 mg/kg and a drug dose of 50 mg/kg. At the indicated times plasma was collected and the circulating lipid concentration was determined as described in section 2.6. *B*, plasma levels of circulating liposomal irinotecan (●) or free drug. (○) were determined at various time points after i.v. injection (50 mg/kg free drug). *C*, irinotecan release rate from circulating liposomes was calculated from data presented in *A* and *B*. All data points represent the mean values obtained from 6 mice per time point and the error bars represent the standard deviation.

hydrolysis is pH dependent, with the carboxylate favoured at physiological pH (Mi and Burke, 1994). Because only the lactone species is active, the relative concentrations of both species are significant from a therapeutic standpoint; hence, the relative proportions of circulating lactone and carboxylate irinotecan species were quantified. Five minutes after injection of the free drug, ~30 % of the measured irinotecan was identified as the carboxylate form (Table 3.1), and this value increased to almost 60% at the 1 hr time point. In contrast, liposome encapsulation protected the lactone species, which up to 4 h after injection represented > 95% of circulating irinotecan, and despite a decrease in relative plasma concentrations by 24 h postinjection to ~80% lactone, the total drug concentration in the plasma remained 10 fold greater than the free drug concentration after only 5 min.

Table 3.1 Analysis of plasma irinotecan following i.v. administration of free or liposomal drug.

	Plasma concentration (μg/ml)			Irinotecan (% of total)	
Time	Lactone	Carboxylate*	Total	Lactone	Carboxylate*
Free irinotecan					
5 min	8.7	3.3	12.0	73	27
15 min	5.4	4.4	9.8	55	45
1 h	3.8	5.5	9.3	41	59
Liposomal irinotecan					
1 h	1236.7	27.0	1263.7	98	2
4 h	838.9	25.5	864.4	97	3
24 h	79.8	18.8	98.6	81	19

* This is an approximation derived from standards at pH 9 to drive irinotecan towards the carboxylate species.

After establishing that liposome encapsulation of irinotecan increases not only circulating total drug levels, but also offers significant protection in maintaining irinotecan as the active lactone species, the therapeutic benefits of the formulations were assessed in two advanced colorectal tumour models.

3.3 Acute toxicity of free and liposomal irinotecan

As the Canadian Council of Animal Care does not authorize formal LD_{10} and LD_{50} studies, toxic dose range finding studies in tumour free male SCID/RAG-2M were conducted using only 2 mice per dose. Unfortunately due to the nature of commercially available irinotecan, (which is supplied, prepared for injection, at 20 mg/ml dissolved with 45 mg/ml sorbitol, 0.9 mg/ml of lactic acid and pH adjusted to 3.5) these limited dose escalation studies were inconclusive. They did, however, reveal an acute dose-limiting toxicity at the 100 mg/kg dose. Because of its rapid onset (within minutes of injection) it can be suggested that this toxicity may be related to drug formulation issues. This toxicity appeared to be slightly reduced by dilution of the drug in 5% dextrose rather than 0.9% saline solution. An evaluation of drug-induced weight loss during the dose escalation studies, suggested DSPC/cholesterol irinotecan was as toxic as the free drug, and necroscopies revealed no gross abnormalities in any of the tissues examined. A more extensive determination of drug induced weight loss was completed as part of the efficacy studies described in section 3.4. Animal weight was monitored over the course of the study and suggested that liposomal irinotecan was more toxic than the free drug when the drug was administered 3X at 100 mg/kg (Figure 3.6D). The nadir in weight loss following this treatment schedule in these tumour-bearing animals occurred between day 21 and day 25 post inoculation (10-15 days after the first drug dose), and at this time animals treated with liposomal drug had lost ~30% (Figure 3.6) of their original body weight and had to be terminated. In contrast, animals treated with other dosing schedules of 50 or 100 mg/kg free or liposomal irinotecan exhibited a weight loss in the range of 7-13 %.

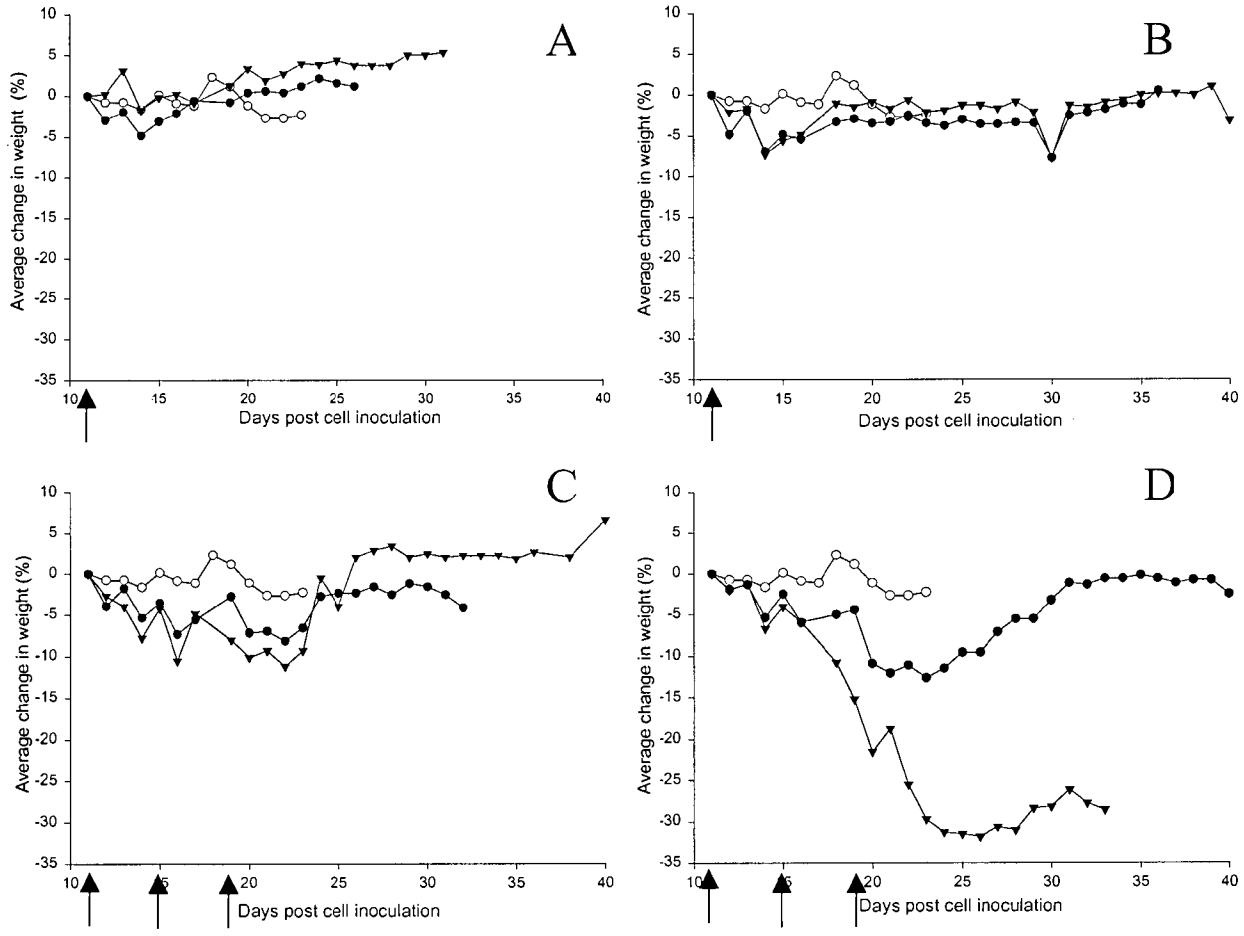

Figure 3.6 Toxicity of free (*A* and *C*) and liposomal (*B* and *D*) irinotecan as assessed by weight loss in LS180 tumour models. Single injections of free (*A*) or liposomal (*B*) irinotecan were administered i.v. on day 11 post cell inoculation, or three injections of free (*C*) or liposomal (*D*) were administered on day 11, 15 and 19 post cell inoculation. Groups shown are control, saline treated animals (○); 50 mg/kg irinotecan/ dose (●); and 100 mg/kg irinotecan/ dose (▼). Arrows indicate drug administration.

3.4 Efficacy of single and multiple dose administration of liposomal and free irinotecan in established LS180 human solid tumours

The human LS180 solid tumour model was used to evaluate the anti-cancer activity of liposomal irinotecan. Eleven days following s.c. inoculation of 10^5 LS180 cells, an easily identifiable and measurable tumour mass arises at the site of injection. The LS180 anti-tumour studies are shown in Figure 3.7, which clearly illustrates that the DSPC/cholesterol irinotecan formulation was therapeutically more active than free drug. These results show that while a single dose of free irinotecan (Figure 3.7A) slows the rate of tumour growth such that the time to reach a 0.4 gm tumour is 19 days if the animals are left untreated, 22 and 26 days if treated with a single i.v. dose of irinotecan at 50 and 100 mg/kg, respectively. In contrast, a single i.v. dose of 50 mg/kg and 100 mg/kg of liposomal irinotecan (Figure 3.7B) delayed the time to progression to a 0.4 gm tumour to 34 and 39 days, respectively. Multiple doses of the free drug provided for increased efficacy (Figure 3.7C), and the tumours reached a mass of 0.4 gm by day 30 and 40 when treated at the 50 and 100 mg/kg dose, respectively. The tumour growth profile for animals treated 3X with 100 mg/kg free drug, closely matched that observed following a single injection of 100 mg/kg liposomal drug. Multiple doses of the liposomal drug showed substantial delays in onset of tumour growth, where no increases in tumour size were noted over the 40 day evaluation period (Figure 3.7D).

3.5 Efficacy of single and multiple dose administration of liposomal and free irinotecan in established LS174T human orthotopic tumours

The results shown in Figure 3.7 suggest that the liposomal formulation is therapeutically more active than free drug, but these results are achieved using a s.c. tumour model. The following studies were initiated to determine whether similar gains in therapeutic activity can be achieved

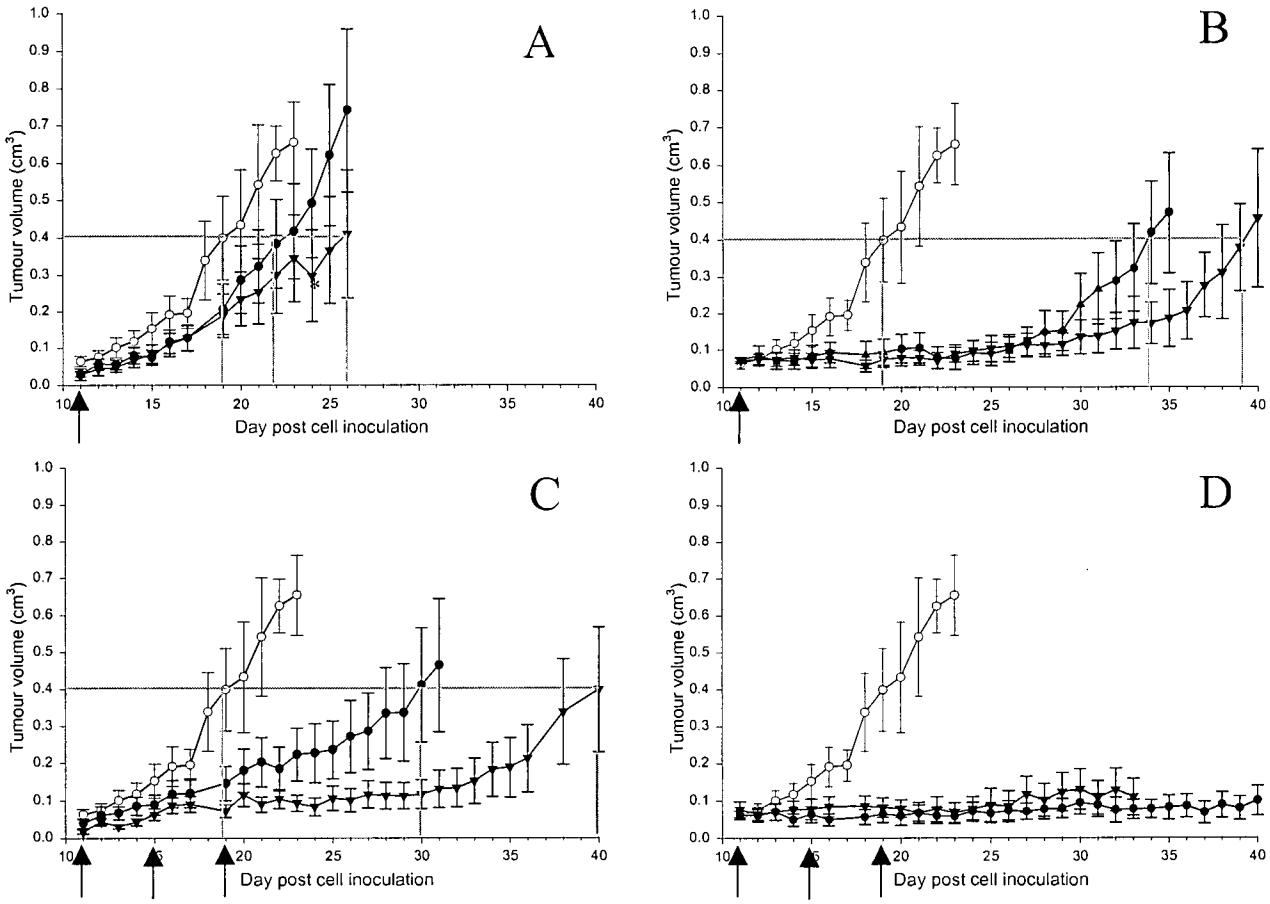

Figure 3.7 Antitumour efficacy of free (*A* and *C*) and liposomal (*B* and *D*) irinotecan as in LS180 tumour models. Drug efficacy was assessed as a function of tumour volume following subcutaneous injuection of LS180 tumour cells on day 0. Single injections of free (*A*) or liposomal (*B*) irinotecan were administered i.v. on day 11 post cell inoculation, or three injections of free (*C*) or liposomal (*D*) were administered on day 11, 15 and 19 post cell inoculation. Groups shown are control, saline treated animals (○); 50 mg/kg irinotecan/ dose (●); and 100 mg/kg irinotecan/ dose (▼). (Average ± s.e.). Arrows indicate drug administration.

* Indicates termination of an animal.

using an animal model which restricts colorectal cancer metastasis to the liver. The orthotopic murine tumour model used to evaluate the anti-cancer activity of liposomal irinotecan against liver metastases was based on intrasplenic injection of LS174T cells. When administered intrasplenically, the primary site of cell seeding is in the liver, although limited growth in the spleen is also common. The LS174T is a relatively slow-growing model, and the effects of a large tumour burden do not become apparent until around day 30 post-inoculation, after which the host condition deteriorates quickly and the animals must be terminated. The effects of multiple dosing of free and liposomal drug in this model are illustrated in Figure 3.8. In the absence of treatment (saline control) the median survival time of inoculated animals is 32 days, while animals treated with free drug exhibited a median survival of 54 days and those treated with liposomal drug showed a median survival time of 79 days This represents a 69% increase in median survival time.

3.6 Liposome mediated delivery to liver metastases

To determine whether the improved outcome observed in animals treated with liposomal drug is due in part to improved drug delivery through passive targeting liposome delivery to animals with LS174T liver tumours was assessed. For these studies animals were dosed with a liposomal irinotecan containing 0.5 mole percent of DiI, a nonexchangable fluorescent marker. Representative photographs are shown in Figure 3.9. Both empty (Figure 3.9B) and irinotecan-loaded (Figure 3.9C) liposomes are seen predominantly in normal liver tissue, as opposed to the tumour mass. These images suggest that peritumour delivery of the liposomal drug is most prominent and, in contrast to results obtained with s.c. tumours, direct delivery into the tumour is not evident 24 hours after i.v. injection of the liposomal drug. These images also illustrate large vacuole-like structures seen only in the tumour tissue. As LS17T cells are derived from a

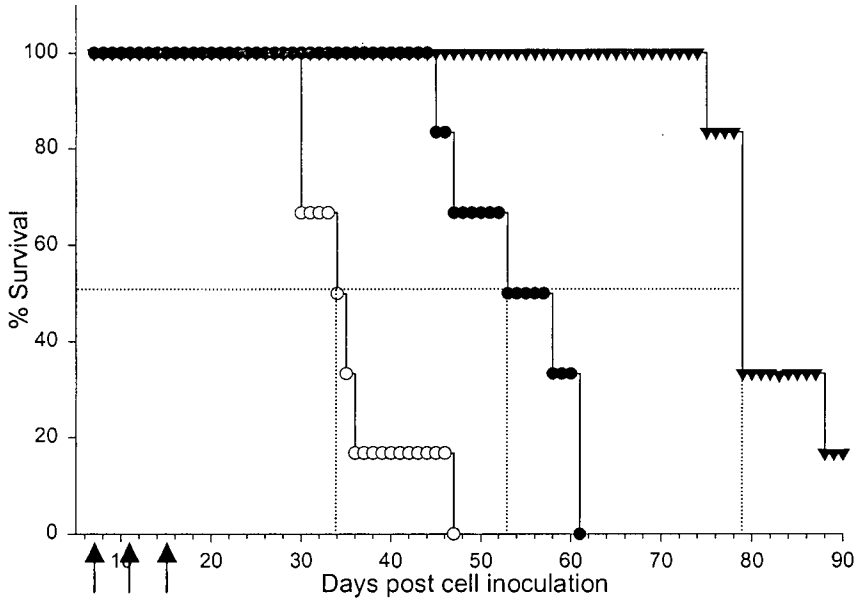

Figure 3.8 Antitumour efficacy of free and liposomal irinotecan in LS174T tumour models. Mouse survival after intrasplenic injection of LS174T tumour cells on day 0. Three injections of 50 mg/kg free or liposomal drug were administered i.v. on days 7, 11, and 15 (indicated by arrows) post cell inoculation. Groups shown are control, untreated (○); free irinotecan (●); or liposomal irinotecan (▼).

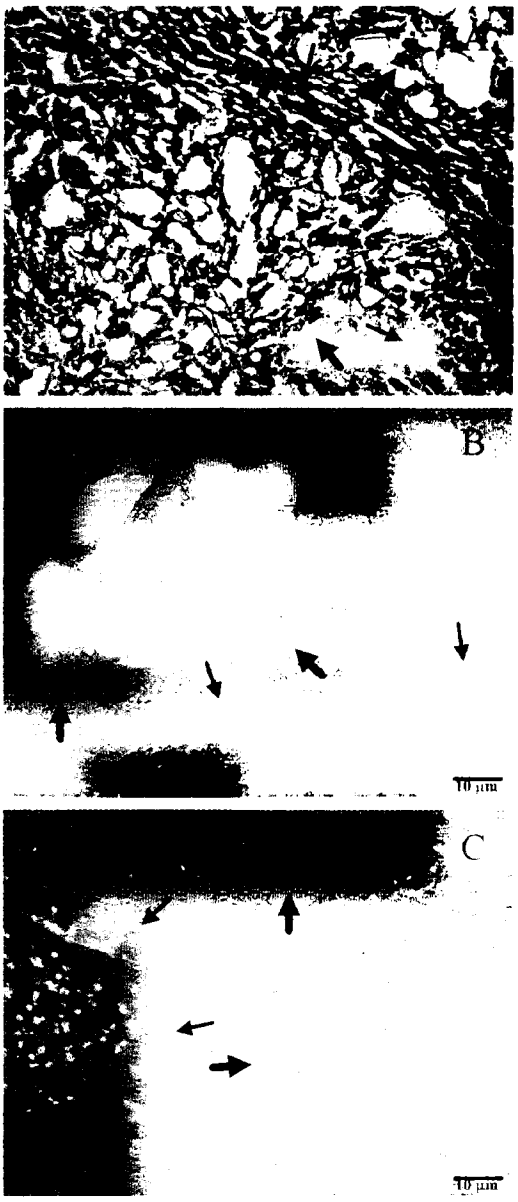

Figure 3.9 Liposome-mediated drug delivery to the tumour. DiI labeled DSPC/cholesterol liposomes, empty or irinotecan loaded, were injected intravenously. At 24 h the livers were harvested for histology. *A*, H & E staining showing healthy and tumour cells; *B*, empty and irinotecan-containing (*C*) liposomes (fluorescent) are the tumour border. The thick arrows indicate tumour tissue, while the narrow arrows indicate normal liver tissue.

mucin-producing adenocarcinoma cell line (Niv et al., 1992), it was postulated that these may be mucous-containing vacuoles.

CHAPTER 4

DISCUSSION

4.1 Summary of results

The objective of the studies presented in this thesis was to outline the potential for a liposomal drug formulation in the treatment of human colorectal liver metastases. A liposomal irinotecan formulation was characterised *in vitro*, prior to evaluating its therapeutic activity in xenograft models of advanced human colorectal cancer.

DSPC/cholesterol is an effective lipid formulation for liposomal irinotecan. Liposome prepared with this lipid combination could be efficiently loaded (>90%) with irinotecan to achieve drug to lipid ratios of 0.3:1 (wt:wt). The loading method relied on use of a transmembrane pH gradient to drive the accumulation of the drug into preformed liposomes. The pH gradient across these liposomes was generated by preparing the liposomes in 300 mM $MnSO_4$ and adding an ionophore (A23187) capable of transferring two protons into the liposome for every one Mn^{2+} transported out. The resulting formulation is stable, with virtually no drug release *in vitro* for up to 72 hours at 37°C. When administered intravenously, irinotecan is gradually released from the carrier, suggesting that the drug will be bioavailable. Liposome encapsulation significantly increased and prolonged circulating irinotecan concentrations, where drug levels were more than 2 orders of magnitude higher following i.v. injection of the liposomal drug. In terms of maintaining irinotecan in its active form, more than 80% of the circulating drug remained in the active lactone form, following injection of the liposomal drug, as compared to only 40% observed just 1 hour after injection of free drug. While free irinotecan was effective in slowing

growth of LS180 solid tumours in SCID/RAG-2M animals, the liposomal drug displayed a much more pronounced effect, arresting tumour growth for an extended time period. Liposomal irinotecan also increased survival in mice bearing the LS174T orthotopic tumours.

4.2 Discussion

The results presented in this thesis highlight the tremendous ability of liposomal encapsulation to potentiate the therapeutic activity of a drug and confirm previous speculation for a possible role of liposomal anti-cancer drugs in treating liver-localised neoplasia. The latter was based on observations of an inherent tendency for significant liposome accumulation in the liver and previous studies establishing a benefit for liposome-based treatments in liver-localized disease. Liposomes are a proven drug delivery system, but the mechanism of action has consistently been defined as due to carrier-mediated increases in tumour delivery. However, the question must be raised regarding localisation within a tissue. This could be best assessed using a tissue that has a natural tendency to accumulate liposomes, such as a liver, and attempts to differentiate between tumour delivery in the liver as opposed to tissue delivery.

Carrier-mediated alterations in drug pharmacokinetics and biodistribution grant liposomes an ability to reduce anticancer drug toxicity while maintaining or increasing efficacy (Boman et al., 1995; Mayer et al., 1998). The former are optimised by manipulation of lipid composition which alters such critical parameters as: (1) drug retention and release; (2) circulation lifespan, and hence propensity to accumulate at the target site; and (3) carrier targeting. Based on these parameters, the application of the highly stable disteroylphosphatidylcholine/cholesterol liposomes in irinotecan transport and delivery to metastatic colorectal cells was explored. DSPC/cholesterol (55:45, mole percent) is an optimised conventional liposome formulation that

exhibits increased blood residency lifetimes due to minimized interactions with opsonizing plasma proteins, reducing the rate of MPS-based carrier elimination (Chonn et al., 1991).

Beyond those advantages of improved pharmacokinetics and biodistribution, an additional benefit begot for camptothecin encapsulation is protection of the active lactone species. Previous camptothecin loading into lipid-based carriers, including attempts at irinotecan encapsulation(Burke et al., 1993; Sadzuka et al., 1999), have exploited their ability to partition into the lipid bilayer. While this has been shown to confer protection of the lactone species (Burke et al., 1993; Sadzuka et al., 1999), therapeutically, this approach is limited by low drug loading efficiencies into the membrane and the rapid exchange of membrane–localised hydrophobic drugs from liposomes to other membranes after i.v. administration (Choice et al., 1995; Ouyang et al., 1995). Tardi and colleagues (Tardi et al., 2000) overcame this limitation by successfully encapsulating topotecan in the aqueous interior of large unilamellar vesicles using an ionophore-generated pH gradient. Results of the present work support their findings that ionophore-mediated encapsulation of a camptothecin analogue in a carrier's acidic interior is not only efficient (>90 % loading), but, as with topotecan, protected irinotecan in its lactone form for an extended length of time, following i.v. administration. In turn, it is logical to assume that this protection will substantially increase the propensity for the active species to be present at the site of tumour growth.

In addition to improving the circulation lifespan of irinotecan, DSPC/cholesterol liposomes provide sustained drug release over 24 h. Together these pharmacokinetic changes are anticipated to prolong tumour cell exposure of this S-phase-specific drug. This, in turn, should increase tumour growth arrest and delays in tumour progression and increases in median survival. It is worth noting that irinotecan cytotoxicity has the additional constraint of requiring

carboxylesterase-mediated conversion to the vastly more potent SN-38. These enzymes are found in high concentrations in hepatic cells, as well as in serum and other tissues, including some tumour populations (Kawato et al., 1991; Guichard et al., 1999;). The environment responsible for liposomal irinotecan activation and the subsequent therapeutic activity observed against colorectal metastases is currently unclear, and depends to some extent on the specificity of drug delivery, although it was likely activated within the vicinity of the tumour, as there was no measurable circulating SN-38.

Initial animal studies evaluated the toxicity and efficacy of liposomal irinotecan in the murine LS180 and LS174T models of metastatic colorectal cancer. While the activity of camptothecins has been evaluated, to a limited extent, in these cell lines *in vitro* (Jansen et al., 1997; te Poele and Joel, 1999; Kouniavsky et al., 2002), no studies involving irinotecan activity in these cells or their corresponding animal models had previously been conducted. In both the LS180 and LS174T models, liposomal irinotecan was considerably more efficacious than free drug. Improvements in tumour growth control and survival time were seen in all liposomal irinotecan-treated groups, in contrast to groups treated with free drug. As shown in Figure 3.7, treatment with liposomal irinotecan did not result in a decrease in tumour size, rather tumour growth was prevented for extended time periods. It can be suggested that liposomal irinotecan provides adequate control of tumour expansion, but alone it is not sufficient to eradicate the disease. This is not surprising as it is generally accepted that tumours represent a heterogenous population of cells and microenvironments. A corollary of this conjecture is that those cells sensitive to irinotecan, are effectively killed, hence the arrest of tumour growth, and those that overcome its cytotoxicity are responsible for reinitiation of tumour growth.

There are numerous possible reasons as to why cells may evade the effects of targeted irinotecan. Irinotecan must be activated, which in the LS180 solid tumour model is presumably mediated by tumour cell associated carboxylesterase, which may not be present at sufficient levels in all cells. Alternatively, it is understood that not all tumour cells are actively dividing within a tumour. Finally, the drug may not have access to all of the tumour cells and at lower doses, not percolate as deeply into the tumour interstitial space. It is presumed that those cells that, for whatever reason, survived irinotecan treatment are responsible for reinstatement of tumour growth. In turn this leads to speculation that, due to an altered cell population, the molecular characteristics of the delayed tumours are distinct from those with little or not disruption of growth, and raises the possibility that they had developed new characteristics that could further challenge treatment. These are questions that have yet to be investigated, but their answers may lead to greater understanding of tumour biology and maturation and perhaps even the development of drug resistance.

Whether free or encapsulated, tumour cell responses to chemotherapeutic agents can vary with tumour physiology and tumour cell heterogeneity. The ideal therapy would be effective in all microenvironments of a heterogeneous tumour population including cells of varying growth rates, in different phases of the cell cycle, originating from different tissues and those capable of rapid adaptation to cytotoxic factors. In practice effective chemotherapy is based on multiple drugs whose cytotoxicity is derived from different mechanisms. Platinum compounds such as cisplatin and the next generation, oxaliplatin, are among those agents proposed to work well in combination with irinotecan and other camptothecins. Evaluation of cisplatin and irinotecan activity *in vitro* confirmed that in the LS180 and LS174T cell lines they do function synergistically (Chew et al., unpublished observations). Current protocols for advanced CRC have incorporated irinotecan in conjunction with 5-FU and leucovorin. It was also confirmed *in*

vitro that irinotecan and 5-FU function synergistically in these cell lines (Chew et al., unpublished observations). These preliminary results, which further support the prevailing understanding that optimal therapy is achieved with multiple drugs in combination, indicates that further studies towards a liposomal-based treatment for colorectal liver metastases should investigate the practicality and *in vivo* effect on efficacy of dual loading of either 5-FU or cisplatin with irinotecan.

In conclusion, liposome encapsulation of irinotecan results in a potent drug formulation for the treatment of liver metastases as a result of increased drug longevity, protection of the active lactone species, and rapid accumulation at the site of tumour development in the liver. Although DSPC/cholesterol has shown itself to be an effective liposome formulation for irinotecan transport to the liver, minor modifications in lipid composition and dosing schedule may further potentiate therapeutic activity. In closing, the use of liposomal irinotecan for the treatment of liver metastases has tremendous potential and continuing studies focussing on optimising the lipid formulation and understanding the role of hepatic cells in processing these carriers, as well as studies with dual loading, could improve liposomal therapy for this cancer.

REFERENCES

Addanki, S., F.D. Cahill, and J.F. Sotos. 1968. Reliability of the quantitation of intramitochondrial pH and pH gradient of heart mitochondria. *Anal Biochem.* 25:17-29.

Adson, M.A., J.A. van Heerden, M.H. Adson, J.S. Wagner, and D.M. Ilstrup. 1984. Resection of hepatic metastases from colorectal cancer. *Arch Surg.* 119:647-51.

Ahmad, I., M. Longenecker, J. Samuel, and T.M. Allen. 1993. Antibody-targeted delivery of doxorubicin entrapped in sterically stabilized liposomes can eradicate lung cancer in mice. *Cancer Res.* 53:1484-8.

Allen, T.M., M.S. Newman, M.C. Woodle, E. Mayhew, and P.S. Uster. 1995. Pharmacokinetics and anti-tumor activity of vincristine encapsulated in sterically stabilized liposomes. *Int.J.Cancer.* 62:199-204.

Alving, C.R., J.N. Verma, M. Rao, U. Krzych, S. Amselem, S.M. Green, and N.M. Wassef. 1992. Liposomes containing lipid A as a potent non-toxic adjuvant. *Res Immunol.* 143:197-8.

Aragnol, D., and L.D. Leserman. 1986. Immune clearance of liposomes inhibited by an anti-Fc receptor antibody in vivo. *Proc Natl Acad Sci U S A.* 83:2699-703.

Bakker-Woudenberg, I.A., A.F. Lokerse, and F.H. Roerdink. 1989. Antibacterial activity of liposome-entrapped ampicillin in vitro and in vivo in relation to the lipid composition. *J Pharmacol Exp Ther.* 251:321-7.

Bakker-Woudenberg, I.A., A.F. Lokerse, M.T. ten Kate, and G. Storm. 1992. Enhanced localization of liposomes with prolonged blood circulation time in infected lung tissue. *Biochim Biophys Acta.* 1138:318-26.

Bangham, A.D., M.M. Standish, and J.C. Watkins. 1965. Diffusion of univalent ions across the lamellae of swollen phospholipids. *J Mol Biol.* 13:238-52.

Barenholtz, Y., S. Amselem, and D. Lichtenberg. 1979. A new method for preparation for phospholipid vesicles (liposomes) - French press. *FEBS Lett.* 99:210-214.

Bengmark, S., and L. Hafstrom. 1969. The natural history of primary and secondary malignant tumors of the liver. I. The prognosis for patients with hepatic metastases from colonic and rectal carcinoma by laparotomy. *Cancer.* 23:198-202.

Bittman, R., and L. Blau. 1972. The phospholipid-cholesterol interaction. Kinetics of water permeability in liposomes. *Biochemistry.* 11:4831-9.

Boman, N.L., M.B. Bally, P.R. Cullis, L.D. Mayer, and M.S. Webb. 1995. Encapsulation of vincristine in liposomes reduces toxicity and improves antitumour efficacy. *Journal of Liposome Research.* 5:523-541.

Burke, T.G. 1996. Chemistry of the camptothecins in the bloodstream. Drug stabilization and optimization of activity. *Ann N Y Acad Sci.* 803:29-31.

Burke, T.G., and X. Gao. 1994. Stabilization of topotecan in low pH liposomes composed of distearoylphosphatidylcholine. *Journal of Pharmaceutical Sciences.* 83:967-969.

Burke, T.G., A.K. Mishra, M.C. Wani, and M.E. Wall. 1993. Lipid bilayer partitioning and stability of camptothecin drugs. *Biochemistry.* 32:5352-64.

Chen, Z.S., T. Furukawa, T. Sumizawa, K. Ono, K. Ueda, K. Seto, and S.I. Akiyama. 1999. ATP-Dependent efflux of CPT-11 and SN-38 by the multidrug resistance protein (MRP) and its inhibition by PAK-104P. *Mol Pharmacol.* 55:921-8.

Choice, E., D. Masin, M.B. Bally, M. Meloche, and T.D. Madden. 1995. Liposomal cyclosporine. Comparison of drug and lipid carrier pharmacokinetics and biodistribution. *Transplantation.* 60:1006-11.

Chollet, D.F., L. Goumaz, A. Renard, G. Montay, L. Vernillet, V. Arnera, and D.J. Mazzo. 1998. Simultaneous determination of the lactone and carboxylate forms of the camptothecin derivative CPT-11 and its metabolite SN-38 in plasma by high-performance liquid chromatography. *J Chromatogr B Biomed Sci Appl.* 718:163-75.

Chonn, A., P.R. Cullis, and D.V. Devine. 1991. The role of surface charge in the activation of the classical and alternative pathways of complement by liposomes. *The Journal of Immunology.* 146.

Chonn, A., S.C. Semple, and P.R. Cullis. 1992. Association of blood proteins with large unilamellar liposomes in vivo. Relation to circulation lifetimes. *Journal of Biological Chemistry.* 267:18759-65.

Choti, M.A., and G.B. Bulkley. 1999. Management of hepatic metastases. *Liver Transpl Surg.* 5:65-80.

Coleman, D.L. 1986. Regulation of macrophage phagocytosis. *Eur J Clin Microbiol.* 5:1-5.

Cordeiro, C., D.J. Wiseman, P. Lutwyche, M. Uh, J.C. Evans, B.B. Finlay, and M.S. Webb. 2000. Antibacterial efficacy of gentamicin encapsulated in pH-sensitive liposomes against an in vivo Salmonella enterica serovar typhimurium intracellular infection model. *Antimicrob Agents Chemother.* 44:533-9.

Cullis, P.R., and B. de Kruijff. 1979. Lipid polymorphism and the functional roles of lipids in biological membranes. *Biochimica et Biophysica Acta.* 559:399-420.

Cullis, P.R., M.J. Hope, M.B. Bally, T.D. Madden, and L.D. Mayer. 1983. Liposomes as pharmaceuticals. *In* Liposomes. M.J. Ostro, editor. Marcel Dekker, Inc., New York. 39-72.

Cullis, P.R., M.J. Hope, and C.P.S. Tilcock. 1986. lipid polymorphism and the roles of lipids in membranes. *Chem.Phys.Lipids.* 40:127-144.

de Kruyff, B., P.W. van Dijck, R.W. Godlbach, R.A. Demel, and L.L. van Deenen. 1973. Influence of fatty acid and sterol composition on the lipid phase transition and activity of membrane-bound enzymes in Acholeplasma laidlawii. *Biochim Biophys Acta*. 330:269-82.

Del Bino, G., P. Lassota, and Z. Darzynkiewicz. 1991. The S-phase cytotoxicity of camptothecin. *Exp Cell Res*. 193:27-35.

Demel, R.A., and B. De Kruyff. 1976. The function of sterols in membranes. *Biochim Biophys Acta*. 457:109-32.

Devine, D.V., K. Wong, K. Serrano, A. Chonn, and P.R. Cullis. 1994. Liposome-complement interactions in rat serum: implications for liposome survival studies. *Biochim Biophys Acta*. 1191:43-51.

Dodds, H.M., D.J. Craik, and L.P. Rivory. 1997. Photodegradation of irinotecan (CPT-11) in aqueous solutions: identification of fluorescent products and influence of solution composition. *J Pharm Sci*. 86:1410-6.

Dodds, H.M., M.C. Haaz, J.F. Riou, J. Robert, and L.P. Rivory. 1998. Identification of a new metabolite of CPT-11 (irinotecan): pharmacological properties and activation to SN-38. *J Pharmacol Exp Ther*. 286:578-83.

Dos Santos, N., L.D. Mayer, S.A. Abraham, R.C. Gallagher, K.A. Cox, P.G. Tardi, and M.B. Bally. 2002. Improved retention of idarubicin after intravenous injection obtained for cholesterol-free liposomes. *Biochim Biophys Acta*. 1561:188-201.

Fenske, D.B., K.F. Wong, E. Maurer, N. Maurer, J.M. Leenhouts, N. Boman, L. Amankwa, and P.R. Cullis. 1998. Ionophore-mediated uptake of ciprofloxacin and vincristine into large unilamellar vesicles exhibiting transmembrane ion gradients. *Biochim Biophys Acta*. 1414:188-204.

Fielding, R.M., and R.M. Abra. 1992. Factors affecting the release rate of terbutaline from liposome formulations after intratracheal instillation in the guinea pig. *Pharm Res*. 9:220-3.

Gabizon, A., and D. Papahadjopoulos. 1988. Liposome formulations with prolonged circulation time in blood and enhanced uptake by tumors. *Proc Natl Acad Sci U S A*. 85:6949-53.

Giovanella, B.C., J.S. Stehlin, M.E. Wall, M.C. Wani, A.W. Nicholas, L.F. Liu, R. Silber, and M. Potmesil. 1989. DNA topoisomerase I--targeted chemotherapy of human colon cancer in xenografts. *Science*. 246:1046-8.

Gregoriadis, G. 1988. Liposomes as a drug delivery system: optimization studies. *Adv Exp Med Biol*. 238:151-9.

Gregoriadis, G. 1991. Overview of liposomes. *J Antimicrob Chemother*. 28:39-48.

Guichard, S., C. Terret, I. Hennebelle, I. Lochon, P. Chevreau, E. Fretigny, J. Selves, E. Chatelut, R. Bugat, and P. Canal. 1999. CPT-11 converting carboxylesterase and topoisomerase activities in tumour and normal colon and liver tissues. *Br J Cancer.* 80:364-70.

Gumucio, J., C. Berkowitz, S. Webster, and A. Thornton. 1996. Structural and functional organization of the liver. *In* Liver and Bilary Diseases. N. Kaptowitz, editor. Williams & Wilkins, Baltimore.

Haaz, M.C., C. Riche, L.P. Rivory, and J. Robert. 1998a. Biosynthesis of an aminopiperidino metabolite of irinotecan [7-ethyl-10- [4-(1-piperidino)-1-piperidino]carbonyloxycamptothecine] by human hepatic microsomes. *Drug Metab Dispos.* 26:769-74.

Haaz, M.C., L. Rivory, C. Riche, L. Vernillet, and J. Robert. 1998b. Metabolism of irinotecan (CPT-11) by human hepatic microsomes: participation of cytochrome P-450 3A and drug interactions. *Cancer Res.* 58:468-72.

Harrigan, P.R., M.J. Hope, T.E. Redelmeier, and P.R. Cullis. 1992. Determination of transmembrane pH gradients and membrane potentials in liposomes. *Biophys J.* 63:1336-45.

Hope, M.J., M.B. Bally, G. Webb, and P.R. Cullis. 1985. Production of large unilamellar vesicles by a rapid extrusion procedure. Characterization of size distribution, trapped volume and ability to maintain a membrane potential. *Biochimica et Biophysica Acta.* 812:55-65.

Hsiang, Y.H., M.G. Lihou, and L.F. Liu. 1989. Arrest of replication forks by drug-stabilized topoisomerase I-DNA cleavable complexes as a mechanism of cell killing by camptothecin. *Cancer Res.* 49:5077-82.

Hsiang, Y.H., and L.F. Liu. 1988. Identification of mammalian DNA topoisomerase I as an intracellular target of the anticancer drug camptothecin. *Cancer Res.* 48:1722-6.

Hsiang, Y.H., H.Y. Wu, and L.F. Liu. 1988. Topoisomerases: novel therapeutic targets in cancer chemotherapy. *Biochem Pharmacol.* 37:1801-2.

Huang, C., S. Li, Z.Q. Wang, and H.N. Lin. 1993. Dependence of the bilayer phase transition temperatures on the structural parameters of phosphatidylcholines. *Lipids.* 28:365-70.

Hubbell, W.L., and H.M. McConnell. 1971. Molecular motion in spin-labeled phospholipids and membranes. *J Am Chem Soc.* 93:314-26.

Hunt, C.A. 1982. Liposomes disposition in vivo. V. Liposome stability in plasma and implications for drug carrier function. *Biochim Biophys Acta.* 719:450-63.

Hwang, K.J. 1987. Liposome pharmacokinetics. *In* Liposomes From Biophysics to Therapeutics. M.J. Ostro, editor. Marcel Dekker, Inc., New York and Basel. 109-156.

Jansen, W.J., B. Zwart, S.T. Hulscher, G. Giaccone, H.M. Pinedo, and E. Boven. 1997. CPT-11 in human colon-cancer cell lines and xenografts: characterization of cellular sensitivity determinants. *Int J Cancer*. 70:335-40.

Jaxel, C., K.W. Kohn, M.C. Wani, M.E. Wall, and Y. Pommier. 1989. Structure-activity study of the actions of camptothecin derivatives on mammalian topoisomerase I: evidence for a specific receptor site and a relation to antitumor activity. *Cancer Res*. 49:1465-9.

Jung, L.L., and W.C. Zamboni. 2001. Cellular, pharmacokinetic, and pharmacodynamic aspects of response to camptothecins: can we improve it? *Drug Resist Updat*. 4:273-88.

Kawato, Y., M. Aonuma, Y. Hirota, H. Kuga, and K. Sato. 1991. Intracellular roles of SN-38, a metabolite of the camptothecin derivative CPT-11, in the antitumor effect of CPT-11. *Cancer Res*. 51:4187-91.

Kemeny, N., J.J. Lokich, N. Anderson, and J.D. Ahlgren. 1993. Recent advances in the treatment of advanced colorectal cancer. *Cancer*. 71:9-18.

Kemeny, N., A. Yagoda, D. Braun, Jr., and R. Golbey. 1980. Therapy for metastatic colorectal carcinoma with a combination of methyl-CCNU, 5-fluorouracil vincristine and streptozotocin (MOF-Strep). *Cancer*. 45:876-81.

Kirby, C., J. Clarke, and G. Gregoriadis. 1980. Effect of the cholesterol content of small unilamellar liposomes on their stability in vivo and in vitro. *Biochem.J.* 186:591-598.

Klausner, R.D., R. Blumenthal, T. Innerarity, and J.N. Weinstein. 1985. The interaction of apolipoprotein A-I with small unilamellar vesicles of L-alpha-dipalmitoylphosphatidylcholine. *J Biol Chem*. 260:13719-27.

Kouniavsky, G., M. Khaikin, I. Zvibel, D. Zippel, S. Brill, Z. Halpern, and M. Papa. 2002. Stromal extracellular matrix reduces chemotherapy-induced apoptosis in colon cancer cell lines. *Clin Exp Metastasis*. 19:55-60.

Lasic, D.D., F.J. Martin, A. Gabizon, S.K. Huang, and D. Papahadjopoulos. 1991. Sterically stabilized liposomes: a hypothesis on the molecular origin of the extended circulation times. *Biochimica et Biophysica Acta*. 1070:187-192.

Li, L.H., T.J. Fraser, E.J. Olin, and B.K. Bhuyan. 1972. Action of camptothecin on mammalian cells in culture. *Cancer Res*. 32:2643-50.

Liehr, J.G., A.E. Ahmed, and B.C. Giovanella. 1996. Pharmacokinetics of camptothecins administered orally. *Ann N Y Acad Sci*. 803:157-63.

Lim, H.J., M.J. Parr, D. Masin, N.L. McIntosh, T.D. Madden, G. Zhang, S. Johnstone, and M.B. Bally. 2000. Kupffer cells do not play a role in governing the efficacy of liposomal mitoxantrone used to treat a tumor model designed to assess drug delivery to liver. *Clin Cancer Res*. 6:4449-60.

Lokiec, F., B.M. du Sorbier, and G.J. Sanderink. 1996. Irinotecan (CPT-11) metabolites in human bile and urine. *Clin Cancer Res.* 2:1943-9.

Lopes de Menezes, D.E., L.M. Pilarski, and T.M. Allen. 1998. In vitro and in vivo targeting of immunoliposomal doxorubicin to human B-cell lymphoma. *Cancer Res.* 58:3320-30.

Madden, T.D., P.R. Harrigan, L.C.L. Tai, M.B. Bally, L.D. Mayer, T.E. Redelmeier, H.C. Loughrey, C.P.S. Tilcock, L.W. Reinish, and P.R. Cullis. 1990a. The accumulation of drugs within large unilamellar vesicles exhibiting a proton gradient: a survey. *Chemistry and Physics of Lipids.* 53:37-46.

Madden, T.D., A.S. Janoff, and P.R. Cullis. 1990b. Incorporation of amphotericin B into large unilamellar vesicles composed of phosphatidylcholine and phosphatidylglycerol. *Chem Phys Lipids.* 52:189-98.

Mayer, L., R. Krishna, and M. Bally. 2001. Liposomes for cancer therapy applications. *In* Polymeric Biomaterials. D. S, editor. Marcel Dekker, Inc., New York.

Mayer, L.D., M.B. Bally, and P.R. Cullis. 1986a. Uptake of adriamycin into large unilamellar vesicles in response to a pH gradient. *Biochimica et Biophysica Acta.* 857:123-126.

Mayer, L.D., M.B. Bally, M.J. Hope, and P.R. Cullis. 1985. Uptake of antineoplastic agents into large unilamellar vesicles in response to a membrane potential. *Biochimica et Biophysica Acta.* 816:294-302.

Mayer, L.D., P.R. Cullis, and M.B. Bally. 1998. Designing therapeutically optimized liposomal anticaner delivery systems: lessons from conventional liposomes. *In* Medical Applications of Liposomes. D. Lasic and D. Papahadjopoulos, editors. 231-257.

Mayer, L.D., M.J. Hope, and P.R. Cullis. 1986b. Vesicles of variable sizes produced by a rapid extrusion procedure. *Biochimica et Biophysica Acta.* 858:161-168.

Mayer, L.D., T.D. Madden, M.B. Bally, and P.R. Cullis. 1993. pH gradient-mediated drug entrapment in liposomes. *In* Liposome Technology. Vol. II. G. Gregoriadis, editor. CRC Press. 27-44.

McElhaney, R.N. 1982. The use of differential scanning calorimetry and differential thermal analysis in studies of model and biological membranes. *Chem Phys Lipids.* 30:229-59.

Moghimi, S., and H. Patel. 1989. Serum opsonins and phagocytosis of saturated and unsaturated phospholipid liposomes. *Biochimica et Biophysica Acta.* 984:384-387.

Nacucchio, M.C., M.J. Gatto Bellora, D.O. Sordelli, and M. D'Aquino. 1988. Enhanced liposome-mediated antibacterial activity of piperacillin and gentamicin against gram-negative bacilli in vitro. *J Microencapsul.* 5:303-9.

Niv, Y., J.C. Byrd, S.B. Ho, R. Dahiya, and Y.S. Kim. 1992. Mucin synthesis and secretion in relation to spontaneous differentiation of colon cancer cells in vitro. *Int J Cancer.* 50:147-52.

O'Sullivan, M.M., N. Powell, A.P. French, K.E. Williams, J.R. Morgan, and B.D. Williams. 1988. Inflammatory joint disease: a comparison of liposome scanning, bone scanning, and radiography. *Ann Rheum Dis*. 47:485-91.

Ouyang, C., E. Choice, J. Holland, M. Meloche, and T.D. Madden. 1995. Liposomal cyclosporine Characterization of drug incorporation and interbilayer exchange. *Transplantation*. 60:999-1006.

Papahadjopoulos, D. 1988. Liposome formation and properties: an evolutionary profile. *Biochem Soc Trans*. 16:910-2.

Papahadjopoulos, D., M. Cowden, and H. Kimelberg. 1973a. Role of cholesterol in membranes. Effects on phospholipid-protein interactions, membrane permeability and enzymatic activity. *Biochim Biophys Acta*. 330:8-26.

Papahadjopoulos, D., K. Jacobson, S. Nir, and T. Isac. 1973b. Phase transitions in phospholipid vesicles. Fluorescence polarization and permeability measurements concerning the effect of temperature and cholesterol. *Biochim Biophys Acta*. 311:330-48.

Parr, M.J. 1995. Circulation lifetimes and tumour accumulation of liposomal drug delivery systems. University of British Columbia.

Patel, H., T. NS., and R. BE. 1983. Inhibitory effect of cholesterol on the uptake of liposomes by liver and spleen. *Biochimica et Biophysica Acta*. 761:142-51.

Paulsen, D.F. 1996. Basic Histology. Appleton and Lange, Stamford.

Potmesil, M. 1994. Camptothecins: from bench research to hospital wards. *Cancer Res*. 54:1431-9.

Pretten, M.K., and J.B. Lloyd. 1986. Pinocytosis and phargocytosis: the effect of size of a particulate substrate on its mode of capture by rat peritoneal macrophages cultured in vitro. *Biochimica et Biophysica Acta*. 881:307-313.

Proffitt, R.T., L.E. Williams, C.A. Presant, G.W. Tin, J.A. Uliana, R.C. Gamble, and J.D. Baldeschwieler. 1983. Tumor-imaging potential of liposomes loaded with In-111-NTA: biodistribution in mice. *J Nucl Med*. 24:45-51.

Richardson, V.J., B.E. Ryman, R.F. Jewkes, K. Jeyasingh, M.N. Tattersall, E.S. Newlands, and S.B. Kaye. 1979. Tissue distribution and tumour localization of 99m-technetium-labelled liposomes in cancer patients. *Br J Cancer*. 40:35-43.

Rivory, L.P., M.C. Haaz, P. Canal, F. Lokiec, J.P. Armand, and J. Robert. 1997. Pharmacokinetic interrelationships of irinotecan (CPT-11) and its three major plasma metabolites in patients enrolled in phase I/II trials. *Clin Cancer Res*. 3:1261-6.

Rivory, L.P., J.F. Riou, M.C. Haaz, S. Sable, M. Vuilhorgne, A. Commercon, S.M. Pond, and J. Robert. 1996. Identification and properties of a major plasma metabolite of irinotecan (CPT-11) isolated from the plasma of patients. *Cancer Res*. 56:3689-94.

Rivory, L.P., and J. Robert. 1995a. Identification and kinetics of a beta-glucuronide metabolite of SN-38 in human plasma after administration of the camptothecin derivative irinotecan. *Cancer Chemother Pharmacol.* 36:176-9.

Rivory, L.P., and J. Robert. 1995b. [Pharmacology of camptothecin and its derivatives]. *Bull Cancer.* 82:265-85.

Roerdink, F., J. Dijkstra, G. Hartman, B. Bolscher, and G. Scherphof. 1981. The involvement of parenchymal, Kupffer and endothelial liver cells in the hepatic uptake of intravenously injected liposomes. Effects of lanthanum and gadolinium salts. *Biochim Biophys Acta.* 677:79-89.

Rottenberg, H. 1979. The measurement of membrane potential and deltapH in cells, organelles, and vesicles. *Methods Enzymol.* 55:547-69.

Sadzuka, Y., S. Hirotsu, and S. Hirota. 1999. Effective irinotecan (CPT-11)-containing liposomes: intraliposomal conversion to the active metabolite SN-38. *Jpn J Cancer Res.* 90:226-32.

Scheele, J., R. Stangl, A. Altendorf-Hofmann, and F.P. Gall. 1991. Indicators of prognosis after hepatic resection for colorectal secondaries. *Surgery.* 110:13-29.

Scherphof, G.L., J.A.M.M. Kamps, and G.A. Koning. 1997. In vivo targeting of surface-modified liposome to metastatically growing colon carcinoma cells and sinusoidal endothelial cells in the rat liver. *Journal of Liposome Research.* 7:419-432.

Semple, S.C., A. Chonn, and P.R. Cullis. 1996. Influence of cholesterol on the association of plasma proteins with liposomes. *Biochemistry.* 35:2521-5.

Senior, J., J.C.W. Crawley, and G. Gregoriadis. 1985. Tissue distribution of liposomes exhibiting long half-lives in the circulation after intravenous injection. *Biochimica et Biophysica Acta.* 839:1-8.

Senior, J., C. Delgado, D. Fisher, C. Tilcock, and G. Gregoriadis. 1991. Influence of surface hydrophilicity of liposomes on their interaction with plasma protein and clearance from the circulation: studies with poly(ethylene glycol)-coated vesicles. *Biochimica et Biophysica Acta.* 1062:77-82.

Sessa, G., and G. Weissmann. 1968. Phospholipid spherules (liposomes) as a model for biological membranes. *J Lipid Res.* 9:310-8.

Silverman, B.A., D.F. Carney, C.A. Johnston, P. Vanguri, and M.L. Shin. 1984. Isolation of membrane attack complex of complement from myelin membranes treated with serum complement. *J Neurochem.* 42:1024-9.

Slatter, J.G., L.J. Schaaf, J.P. Sams, K.L. Feenstra, M.G. Johnson, P.A. Bombardt, K.S. Cathcart, M.T. Verburg, L.K. Pearson, L.D. Compton, L.L. Miller, D.S. Baker, C.V. Pesheck, and R.S. Lord, 3rd. 2000. Pharmacokinetics, metabolism, and excretion of irinotecan (CPT-

11) following I.V. infusion of [(14)C]CPT-11 in cancer patients. *Drug Metab Dispos.* 28:423-33.

Sparreboom, A., M.J. de Jonge, P. de Bruijn, E. Brouwer, K. Nooter, W.J. Loos, R.J. van Alphen, R.H. Mathijssen, G. Stoter, and J. Verweij. 1998. Irinotecan (CPT-11) metabolism and disposition in cancer patients. *Clin Cancer Res.* 4:2747-54.

Straubinger, R.M., K. Hong, D.S. Friend, and D. Papahadjopoulos. 1983. Endocytosis of liposomes and intracellular fate of encapsulated molecules: encounter with a low pH compartment after internalization in coated vesicles. *Cell.* 32:1069-79.

Szoka, F., Jr., and D. Papahadjopoulos. 1980. Comparative properties and methods of preparation of lipid vesicles (liposomes). *Ann.Rev.Biophys.Bioeng.* 9:467-508.

Szoka, F., F. Olson, T. Heath, W. Vail, E. Mayhew, and D. Papahadjopoulos. 1980. Preparation of unilamellar liposomes of intermediate size (0.1-0.2 mumol) by a combination of reverse phase evaporation and extrusion through polycarbonate membranes. *Biochim Biophys Acta.* 601:559-71.

Takasuna, K., Y. Kasai, Y. Kitano, K. Mori, R. Kobayashi, T. Hagiwara, K. Kakihata, M. Hirohashi, M. Nomura, E. Nagai, and et al. 1995. Protective effects of kampo medicines and baicalin against intestinal toxicity of a new anticancer camptothecin derivative, irinotecan hydrochloride (CPT-11), in rats. *Jpn J Cancer Res.* 86:978-84.

Tardi, P., E. Choice, D. Masin, T. Redelmeier, M. Bally, and T.D. Madden. 2000. Liposomal encapsulation of topotecan enhances anticancer efficacy in murine and human xenograft models. *Cancer Res.* 60:3389-93.

te Poele, R.H., and S.P. Joel. 1999. Schedule-dependent cytotoxicity of SN-38 in p53 wild-type and mutant colon adenocarcinoma cell lines. *Br J Cancer.* 81:1285-93.

Torchilin, V.P., V.S. Trubetskoy, K.R. Whiteman, P. Caliceti, P. Ferruti, and F.M. Veronese. 1995. New synthetic amphiphilic polymers for steric protection of liposomes in vivo. *Journal of Pharmaceutical Sciences.* 84:1049-1053.

van der Zee, A.G., H. Hollema, S. de Jong, H. Boonstra, A. Gouw, P.H. Willemse, J.G. Zijlstra, and E.G. de Vries. 1991. P-glycoprotein expression and DNA topoisomerase I and II activity in benign tumors of the ovary and in malignant tumors of the ovary, before and after platinum/cyclophosphamide chemotherapy. *Cancer Res.* 51:5915-20.

Wall, M.E., M.C. Wani, A.W. Nicholas, G. Manikumar, C. Tele, L. Moore, A. Truesdale, P. Leitner, and J.M. Besterman. 1993. Plant antitumor agents. 30. Synthesis and structure activity of novel camptothecin analogs. *J Med Chem.* 36:2689-700.

Wang, G., S. Li, H.N. Lin, and C. Huang. 1997. Influence of cis double bonds in the sn-2 acyl chain of phosphatidylethanolamine on the gel-to-liquid crystalline phase transition. *Biophys J.* 73:283-92.

Williams, K.J., M.C. Phillips, and W.V. Rodrigueza. 1998. Structural and metabolic consequences of liposome-lipoprotein interactions. *Adv Drug Deliv Rev.* 32:31-43.

Woodle, M.C., and L. D.D. 1992. Sterically stabilized liposomes. *Biochimica et Biophysica Acta.* 1113:117-199.

Wu, J., and M.A. Zern. 1996. Modification of liposomes for liver targeting. *J Hepatol.* 24:757-63.

Zhang, H., P. D'Arpa, and L.F. Liu. 1990. A model for tumor cell killing by topoisomerase poisons. *Cancer Cells.* 2:23-7.

APPENDIX

HPLC Assay

Standard solutions

Irinotecan stock solution (20 mg/ml) was diluted in either DMSO or acetonitrile-0.02M borate buffer, pH 9.0 (50:50, v/v), to prepare working solutions of the lactone or carboxylate species, respectively. Aqueous standards were prepared by the dilution of carboxylate and lactone working solutions, which were thought to contain equal amount of the drug, in ice-cold methanol (4°C) to a total volume of 200 μl and frozen immediately until use. Plasma-extracted standards were prepared in the same manner except by dilution of working solutions in plasma. 100 μl of each standard was then transferred to eppendorf tubes containing 5 μl of the internal standard, camptothecin, and 595 μl ice-cold methanol. Standards were immediately frozen at -70°C. All standards contained both the lactone and carboxylate species.

For sample analysis, 80 μl of each standard was loaded into 1-ml HPLC sample vials (Waters, Milford, MA) with 200 μl amber inserts (Chromatographic Specialties Inc., Brockville, ON), and 10 μl were injected into the column.

Calibration curves

Calibration curves were constructed using standard samples containing both the lactone and carboxylate forms of irinotecan. The calibration ranges were from 0.1 to 10 μg/ml for both the

lactone and carboxylate species. The calibration curves were obtained by plotting the peak area of the analytes versus their respective concentrations (Figures A-1 and A-2). For plasma extracted standards (A-2), the peak area of the analytes was divided by that of the internal standard to correct for deficiencies in extraction.

Sample preparation and measurements

Heparinized plasma samples chilled on ice were immediately centrifuged at 1500 g for 10 minutes at 4°C. 100 µl of each sample was then transferred to eppendorf tubes containing 5 µl of the internal standard, camptothecin, and 595 µl ice-cold methanol. Sample analysis was performed as described for analysis of the standards. An example chromatogram is shown in Figure A-3.

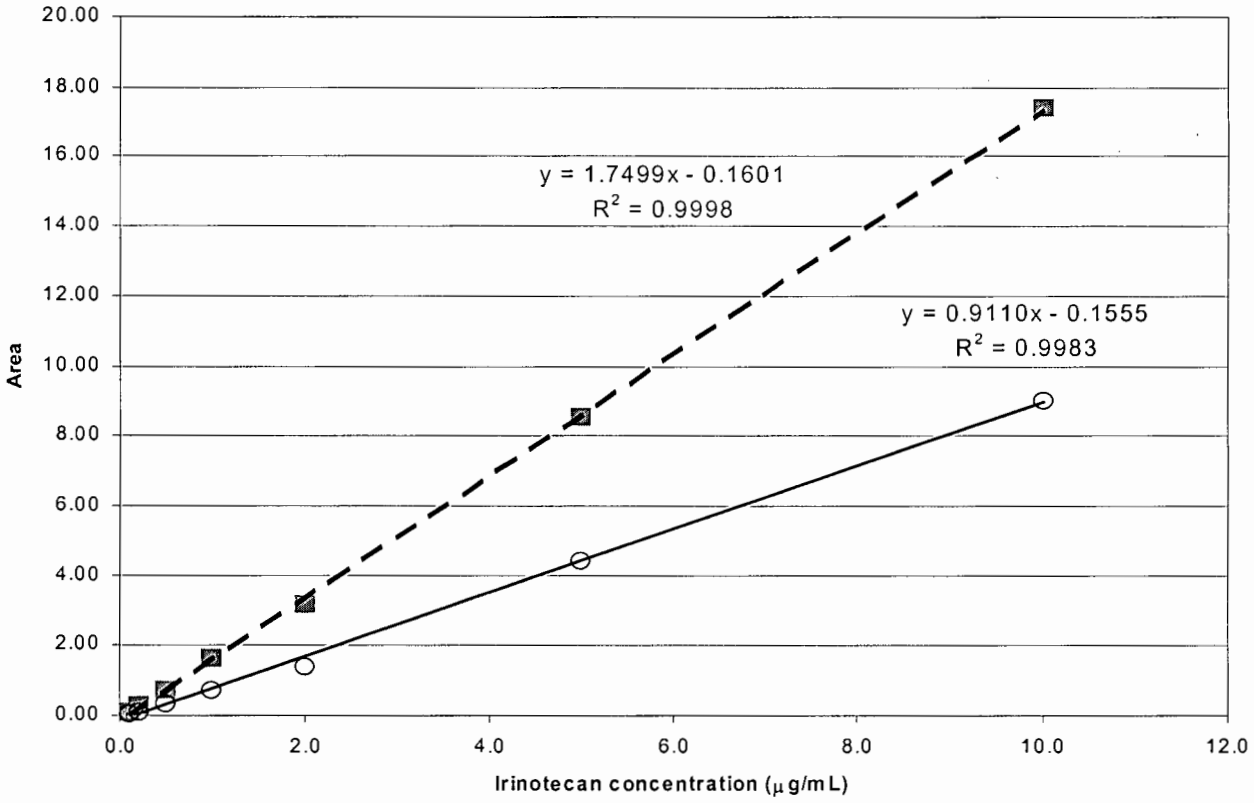

Figure A-1 HPLC calibration curve, aqueous standards. The calibration curves were obtained by plotting the peak area of the analytes versus their respective concentrations. Standards contained both the lactone (■)and carboxylate (o) forms of the irinotecan.

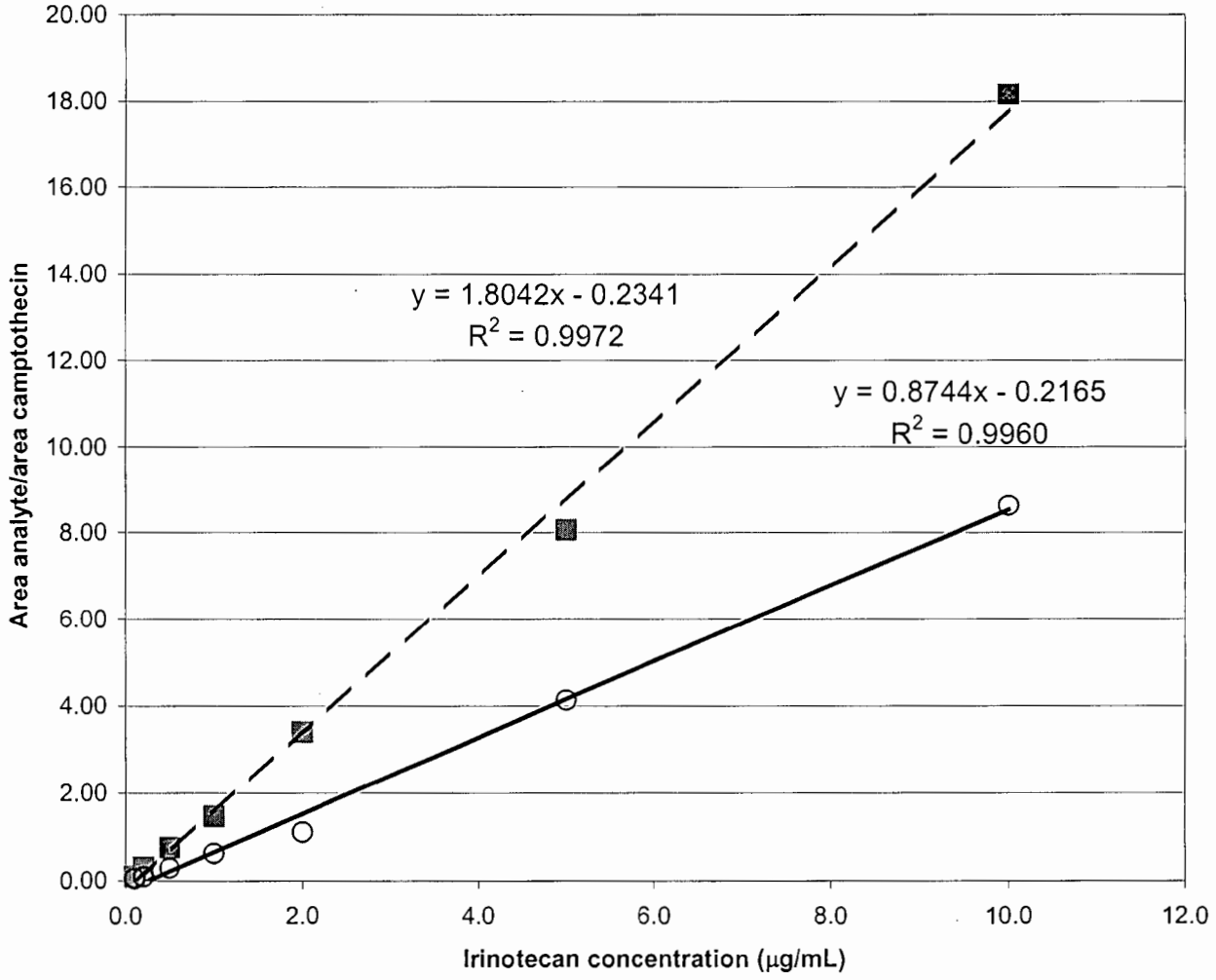

Figure A-2 HPLC calibration curve, plasma standards. The calibration curves were obtained by plotting the peak area of the analytes divided by that of the internal standard, camptothecin, versus their respective concentrations. Standards contained both the (■)and carboxylate (o) forms of the irinotecan.

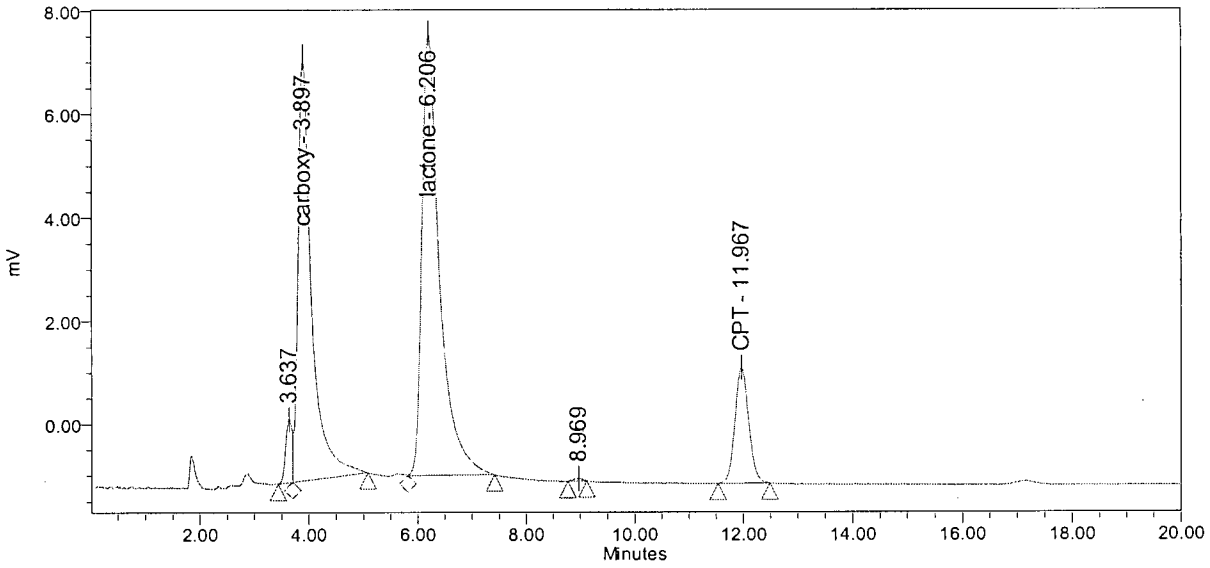

Identified Peaks Summary

	Name	RT	Area	Height	Concentration	Units
1	carboxy	3.897	141930	8221	4.917e+000	ug/ml
2	lactone	6.206	194254	8585	3.055e+000	ug/ml
3	CPT	11.967	39480	2258	1.000e+000	

Figure A-3 Representative chromatogram illustrating irinotecan levels in plasma-extracted samples. Both the carboxylate and the lactone form, as well as the internal standard, camptothecin, are shown as distinct and separate peaks. The associated software (Millennium32® chromatograpy manager, Version 3.20, Waters, Milford, MA) calculates the concentrations based on the area of each peak in relation to standards.

Published in final edited form as:
Am J Med Sci. 2014 February ; 347(2): 167–169. doi:10.1097/MAJ.0000000000000243.

Irinotecan-induced Immune Thrombocytopenia

Barry C. Mirtsching, MD,
Medical City Dallas Hospital, Dallas, Texas

James N. George, MD,
Department of Medicine, College of Medicine, University of Oklahoma Health Sciences Center, Oklahoma City, Oklahoma

Richard H. Aster, MD, and
Platelet and Neutrophil Immunology Laboratory and Blood Research Institute, Blood Center of Wisconsin and Medical College of Wisconsin, Milwaukee, Wisconsin

Brian R. Curtis, PhD
Platelet and Neutrophil Immunology Laboratory and Blood Research Institute, Blood Center of Wisconsin and Medical College of Wisconsin, Milwaukee, Wisconsin

Acute immune-mediated thrombocytopenia caused by drugs is well described but commonly misdiagnosed,[1] because clinicians fail to consider drug exposure as a causative factor. As a consequence, it is not uncommon for patients to experience recurrent episodes of severe thrombocytopenia upon repeated exposure to drug and to receive inappropriate therapy. It is especially likely for a chemotherapeutic agent to be overlooked as a cause of acute immune-mediated thrombocytopenia because of the known tendency of this class of drugs to cause thrombocytopenia related as a consequence of marrow suppression. To date, at least 4 chemotherapeutic agents have been documented as triggers for drug-induced immune thrombocytopenia: fludarabine,[2] dactinomycin,[3] oxaliplatin[4,5] and irinotecan.[6] We describe here the 2nd reported patient with acute, severe immune-mediated thrombocytopenia caused by irinotecan-dependent platelet-reactive antibodies.

A 53-year-old white woman presented with symptoms of partial colonic obstruction. Colon cancer with multiple liver metastases was diagnosed; no other metastases were detected. Carcinoembryonic antigen (CEA) was 6889 μg/L. Treatment with FOLFOX (oxaliplatin, 5-fluorouracil and leucovorin) was begun and continued for 11 two-week cycles. Her platelet count before starting FOLFOX was 347,000/μL. Bevacizumab was added to the FOLFOX regimen when her obstructive symptoms resolved and the potential risk for emergent surgery had passed. FOLFOX treatment required dose reduction and then discontinuation for modest thrombocytopenia (platelet counts, 84,000–100,000/μL). On recovery of the platelet count to 143,000/μL, transverse colectomy was performed with residual tumor of 2 cm and 3/14 regional nodes positive for carcinoma. After surgery, treatment continued with bevacizumab-FOLFIRI (irinotecan, 5-fluorouracil and leucovorin) for 6 two-week cycles

The other authors have no financial or conflict of interest to disclose.

(bevacizumab was omitted in the final 2 cycles) when the liver metastases were potentially amenable to resection or local ablation. Platelet counts were maintained between 113,000–150,000/μL during FOLFIRI therapy. CEA at the end of therapy was 9.1 μg/L. One year after presentation, the remaining liver lesions were treated with left hepatic segmental hepatectomy and radiofrequency ablation, and a hepatic arterial infusion pump was placed. Hepatic arterial floxuridine therapy was initiated (14 days on, 14 days off) approximately 1 month after surgery and continued for 2 months, when multiple lung metastases were discovered. CEA rose to 14 μg/L.

One month later, bevacizumab-FOLFIRI was resumed. The pretreatment platelet count was 150,000/μL. Bevacizumab was administered over 90 minutes without incident, followed by irinotecan (180 mg/m^2 [340 mg]) over 90 minutes, and then leucovorin over 120 minutes. At the completion of the leucovorin administration, the patient developed a sinus tachycardia of 180–200/min, with stable blood pressure. 5-Fluorouracil administration was withheld. The tachycardia spontaneously terminated within 15 minutes. At that time, her platelet count was 2000/μL, verified by repeat analysis (Figure 1A). The patient's examination was normal; she had no signs or symptoms of bleeding. Port and infusion pump contents were immediately emptied and filled with saline. Other laboratory data included: white blood cells 12,900/μL (96% granulocytes, 2% lymphocytes and 2% monocytes), hemoglobin 13.8 g/dL (no schistocytes present in blood smear), D-dimer 1.07 ng/mL (normal, 0.17–0.59 ng/mL), INR 0.9, PTT 25.2 seconds, fibrinogen 321 mg/dL, creatinine 0.7 mg/dL, AST 22 IU/L, ALT 29 IU/L and LDH 193 IU/L.

Laboratory tests for heparin-dependent antibodies by both PF4 enzyme-linked immunosorbent assay and serotonin release assay were negative. Testing for drug-dependent platelet antibodies using a previously described flow cytometry assay[7] was negative for bevacizumab, 5-flurouracil, leucovorin and oxaliplatin (results not shown). However, strong IgG platelet–reactive antibodies were detected in the patient's acute serum only in the presence of irinotecan (Figure 1B), and not with normal control serum and drug (Figure 1C). The patient was observed without specific therapy and her platelet count increased over the ensuing 2 weeks to normal levels (Figure 1A). There was no recurrence of tachycardia. Treatment with bevacizumab, 5-fluorouracil and leucovorin, including the premedications with palonosetron, dexamethasone and atropine, was resumed without incident.

Irinotecan, a synthetic analog of camptothecin, is a topoisomerase I inhibitor often given in combination with 5-fluorouracil, leucovorin and irinotecan (FOLFIRI) for the treatment of metastatic colorectal cancer. Irinotecan is metabolized to its active metabolite, SN-38, which is 1000× more active than the unmodified drug. Common side effects include diarrhea and nausea/vomiting. Neutropenia resulting from myelosuppression is the dominant hematologic side effect and thrombocytopenia, when it occurs, is usually mild.

In the present case, irinotecan was implicated as the cause of acute immune-mediated thrombocytopenia by both clinical criteria and by identification of drug-dependent platelet antibodies. The patient had apparently become sensitized to irinotecan during the initial 6 cycles of FOLFIRI. She had no platelet counts less than 100,000/μL and no systemic symptoms during her previous exposures to the drug. Her only symptom during the acute

irinotecan-induced thrombocytopenia was transient sinus tachycardia. A search of MEDLINE and PubMed on June 3, 2013, identified only 1 previous report of irinotecan-induced thrombocytopenia.[6] In this patient, the irinotecan etiology was confirmed by recurrence of acute severe thrombocytopenia after a repeat irinotecan infusion and by detection of irinotecan-dependent platelet antibodies using a platelet indirect immunofluorescence test.[6] We have previously identified irinotecan-dependent antibodies in 2 patients in whom irinotecan-induced thrombocytopenia was suspected (BR Curtis and RH Aster; unpublished observations). Each patient experienced severe thrombocytopenia (5000 and 20,000 platelets per microliter, respectively) within a few hours of being treated for metastatic carcinoma with combination chemotherapy that included irinotecan, and both patients regained a normal platelet count within 1 week without specific intervention. However, drug-dependent reactions of these 2 antibodies with normal platelets were much weaker than those obtained with antibody from the patient described here. The active form of irinotecan is conjugated to glucuronide, and it is excreted mainly in that form. Glucuronide conjugates of many drugs are capable of inducing drug-induced immune thrombocytopenia, and the responsible antibodies react best when tested with the sensitizing metabolite. It is therefore possible that the weak drug-dependent antibody (DDAb) reactions observed with the 2 patients identified previously were due to metabolite-specific antibodies, but testing for metabolite-specific antibodies was not performed. Metabolite-dependent platelet antibodies were not detected in serum from the single case of irinotecan-induced thrombocytopenia reported previously when serum was tested against platelets in the presence of the SN-38 metabolite.[6]

Because 4 cases of acute, severe thrombocytopenia caused by irinotecan have now been identified, clinicians should consider this possible diagnosis in any patient who experiences an acute and isolated drop in the platelet levels after irinotecan administration. As standard treatment in cases of thrombocytopenia caused by drugs, transfusion would not be recommended in the absence of any bleeding; observation alone is recommended because spontaneous recovery of the platelet counts is expected after discontinuation of the drug. Steroid therapy should only be considered in circumstances of bleeding, or persistence of severe thrombocytopenia (e.g. platelelets $\leq$ 10,000/μL) after some period of observation.

Acknowledgments

RHA currently receives NIH Grant HL-13629 from NHLBI. BRC was a past consultant for Immucor, Inc, and served in past on PNH Advisory Board of Alexion Pharmaceutical.

References

1. Aster RH, Bougie DW. Drug-induced immune thrombocytopenia. N Engl J Med. 2007; 357:580–7. [PubMed: 17687133]
2. Fernandez MJ, Llopis I, Pastor E, et al. Immune thrombocytopenia induced by fludarabine successfully treated with rituximab. Haematologica. 2003; 88:ELT02. [PubMed: 12604433]
3. Khatua S, Nair CN, Ghosh K. Immune-mediated thrombocytopenia following dactinomycin therapy in a child with alveolar rhabdomyosarcoma: the unresolved issues. J Pediatr Hematol Oncol. 2004; 26:777–9. [PubMed: 15543019]
4. Curtis BR, Kaliszewski J, Marques MB, et al. Immune-mediated thrombocytopenia resulting from sensitivity to oxaliplatin. Am J Hematol. 2006; 81:193–8. [PubMed: 16493620]

5. Jardim DL, Rodrigues CA, Novis YA, et al. Oxaliplatin-related thrombocytopenia. Ann Oncol. 2012; 23:1937–42. [PubMed: 22534771]
6. Bozec L, Bierling P, Fromont P, et al. Irinotecan-induced immune thrombocytopenia. Ann Oncol. 1998; 9:453–5. [PubMed: 9636839]
7. Curtis BR, McFarland JG, Wu GG, et al. Antibodies in sulfonamide-induced immune thrombocytopenia recognize calcium-dependent epitopes on the glycoprotein IIb/IIIa complex. Blood. 1994; 84:176–83. [PubMed: 7517207]

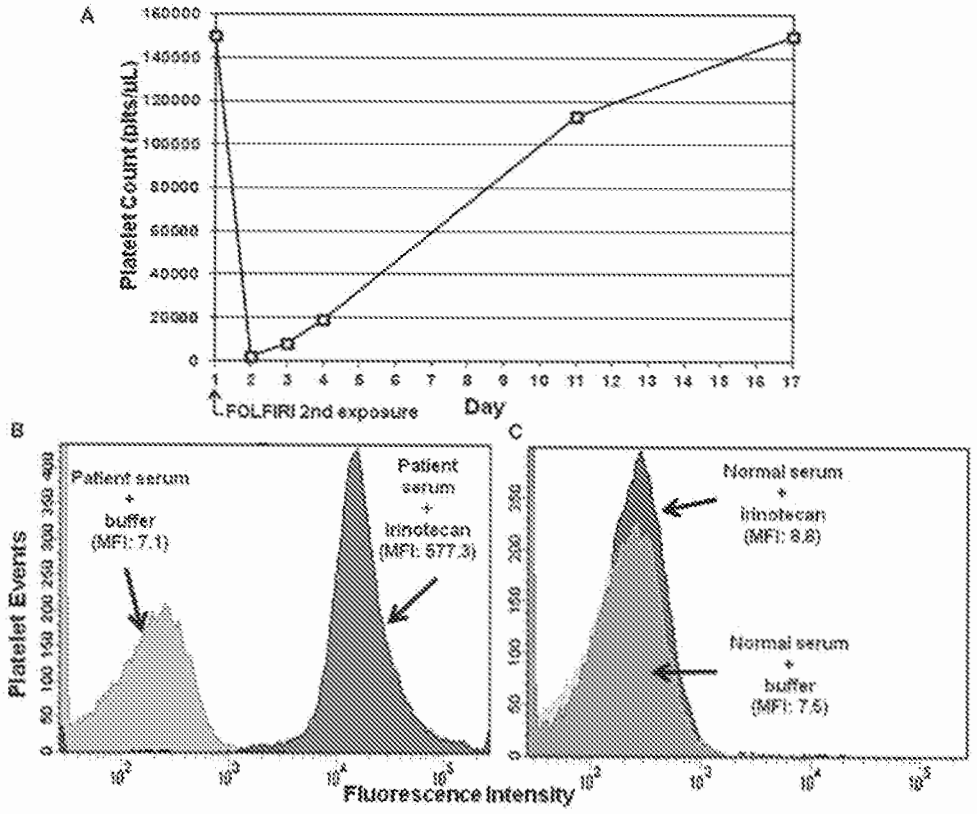

FIGURE 1.

(A) Graph of the patient's platelet levels just before and after bevacizumab-FOLFIRI administration was resumed. Testing of patient's serum for drug-dependent platelet antibodies by flow cytometry assay showed strong IgG antibody reactivity (MFI = 577.3) in the patient's acute serum only in the presence of irinotecan (B) (dark histogram), but not with normal control serum and drug (C) (dark histogram). MFI = median fluorescence intensity.

Adverse side effects associated to metronomic chemotherapy

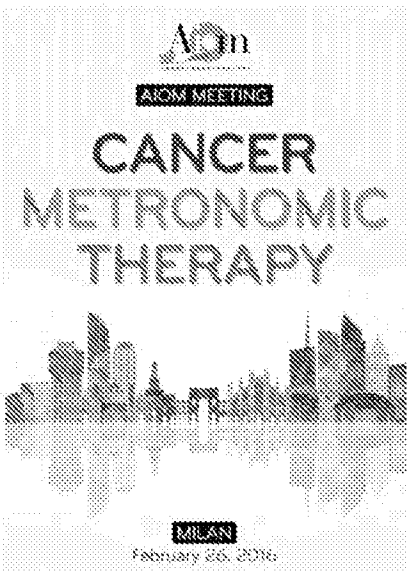

Elisabetta Munzone, MD

Division of Medical Senology
Istituto Europeo di Oncologia
Milano, Italy

LDM: the optimal biological dose

- Although there is no definite clinical data, preclinical studies suggest that the optimal biological LDM dose in terms of anticancer activity appears to coincide with very limited toxicity.
- This would indicate that the lack of severe acute toxicity could be used to optimize LDM chemotherapy dosing in individual patients

Therapeutic index

- The benefit of cancer therapies can be characterized by the therapeutic index: a balance between antitumor activities and treatment-associated toxicities.
- TD50 is the dose of drug that causes a toxic response in 50% of the population and ED50 is the dose of drug that is therapeutically effective in 50% of the population.
- The therapeutic index of metronomic chemotherapy seems particularly beneficial given the combination of excellent antitumor activity with a toxicity profile that is considered to be superior to MTD chemotherapy.

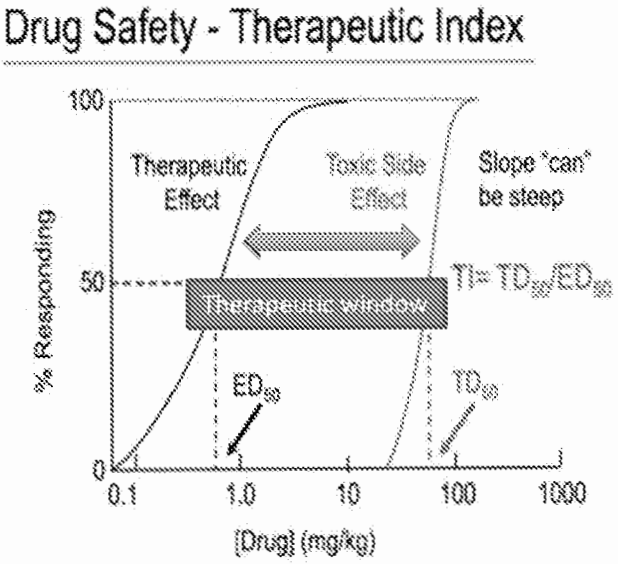

Hypothetical dose-response curves for different effects of cyclophosphamide

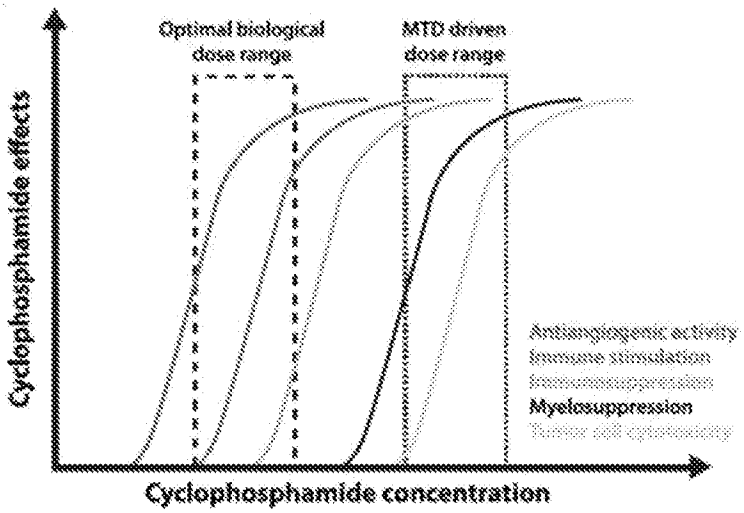

- When given at the **optimal biological dose**, metronomic CTX results in antiangiogenic and immunostimulatory effects.
- Higher CTX doses increase the risk of immuno/myelosuppression, likely without added benefit (MTD dose range)
- **Metronomic schedule may optimize the beneficial therapeutic side effect and minimize host toxicity**

Multi-mechanism of action of metronomic chemotherapy in breast cancer

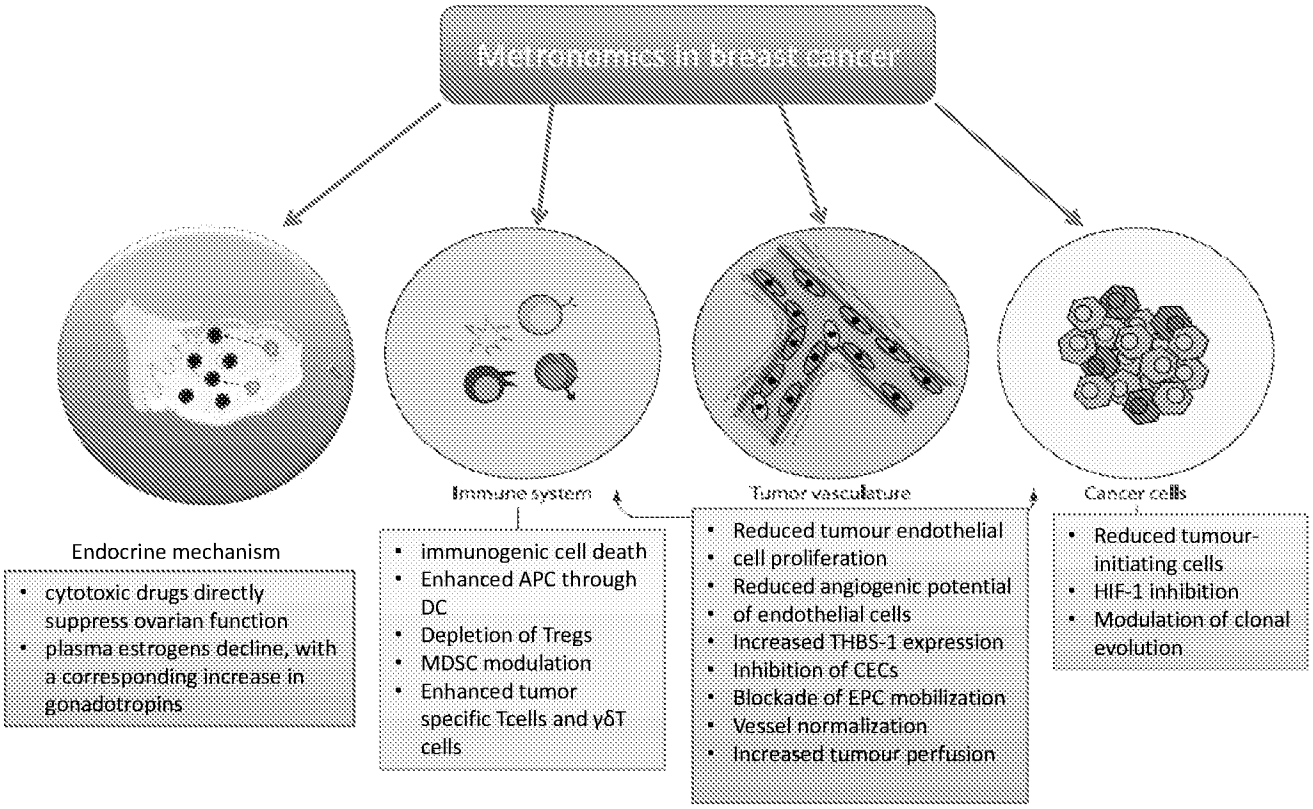

Nat Rev Clin Oncol. 2015 Nov;12(11):631-44.

Immuno side-effects on Tregs

- metronomic CTX strongly decreases immunosuppressive regulatory T cells (preserving other lymphocyte subsets in number and function), favoring a better control of tumor progression.

- these data support CTX regimen as a valuable treatment for reducing tumor-induced immune tolerance before setting to work anticancer immunotherapy aimed at improving T cell or NK cell functions.

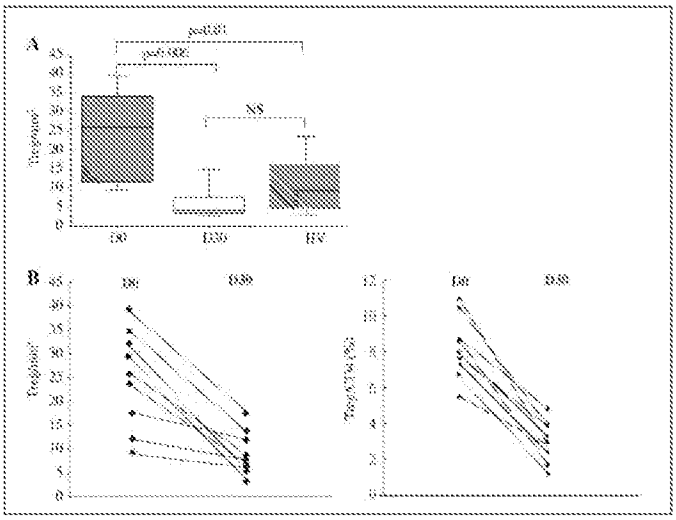

Metronomic CTX selectively depletes regulatory T cells (Treg) in cancer patients

Ghiringhelli F et al (2007) Cancer Immunol Immunother 56(5):641–648

Critical issues to be considered...

- LDM chemotherapy is primarily being studied in advanced disease stages, LDM drug administration is sometimes limited to a few months.
- The overall prognoses of such patients are poor, which could explain why side effects associated with cumulative doses of chemotherapeutics are rarely reported
- Many of the side effects (i.e., grade 1 or 2) reported in LDM trials may be related to the underlying neoplastic condition rather than to LDM therapy itself.
- Low-grade symptoms could negatively impact adherence to treatment itself, particularly to oral regimens administered over prolonged periods of time.

Reports on side effects in a frail population

- Patients initially treated within clinical trials of metronomic chemotherapy were often **heavily pretreated or elderly**
  - High-grade toxic effects were either rare or absent
  - the most common toxic effects were: grade 1 nausea and/or vomiting, grade 1 and 2 anemia, neutropenia, leucopenia, as well as low-grade fatigue.
  - Alopecia grade 1 was rarely reported.

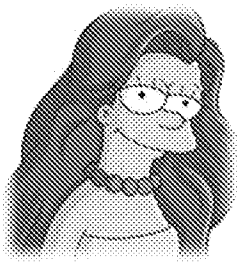

Toxicity of mCT: a systematic analysis

- A recent systematic review of 80 published phase I/II LDM chemotherapy trials included 3,688 patients (only studies with at least 20 patients)
- Varying cancer types and different LDM regimens reported overall low toxicity rates

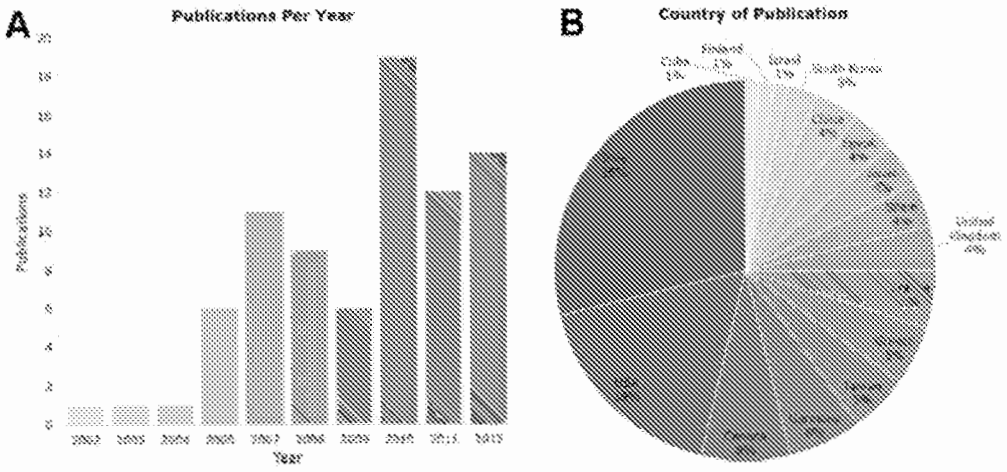

K. Lien et al. / European Journal of Cancer 49 (2013) 3387–3395

Metronomic drugs used

Metronomic drugs.

Metronomic drug	Number of regimens used (%) $N = 107$
Cyclophosphamide	46 (43.0)
Capecitabine	15 (14.0)
Etoposide	15 (14.0)
Vinorelbine	15 (14.0)
Methotrexate	12 (11.2)
Temozolomide	9 (8.4)
Tegafur and uracil (UFT)	6 (5.6)
Trofosfamide	5 (4.7)
Procarbazine	3 (2.8)
5-Fluorouracil (5-FU)	2 (1.9)
Carboplatin	2 (1.9)
Irinotecan (CPT-11)	2 (1.9)
Docetaxel	2 (1.9)
Paclitaxel	2 (1.9)
Vinblastine	2 (1.9)
Carboplatin	1 (0.9)
Doxifluridine	1 (0.9)
Mitomycin C	1 (0.9)

Most frequently used in breast cancer

K. Lien et al. / European Journal of Cancer 49 (2013) 3387–3395

Reported cumulative toxicities

- Severe (grade 3 or 4) side effects were rare and limited to less than 10 % of patients.
- Severe lymphopenia and neutropenia were the most frequent side effects reported, occurring in 6.44 % and 5.71% of patients.
- Elevated transaminases, a known side effect of methotrexate administration, were the most prevalent non-hematological side effect.

Adverse events.

Grade 3 or 4	Number of patients affected (%) $N = 3688$
Haematological	
Neutropenia	199 (5.39)
Lymphopenia	144 (3.91)
Leucopenia	111 (3.01)
Anaemia	64 (1.73)
Thrombocytopenia	53 (1.44)
Febrile neutropenia	20 (0.53)
Non-haematological	
Fatigue	72 (1.95)
Transaminases	68 (1.84)
Hand-foot syndrome	31 (0.84)
Thrombosis	22 (0.59)
Colitis/mucositis/stomatitis	21 (0.57)
Nausea/vomiting	21 (0.57)
Infection	18 (0.50)
Neurological	17 (0.47)
Diarrhoea	14 (0.38)
Hypertension	13 (0.35)

Comparative studies: LDM versus an MTD treatment arm in parallel

	Stopeck et al. 2011 (%)		Clarke 2009 (%)		Cascinu 2011 (%)	
	MTD (n = 36)	LDM (n = 28)	MTD (n = 31)	LDM (n = 26)	MTD (n = 37)	LDM (n = 35)
	TAX 75 mg/m² iv q3 weeks	CPA 50 mg po od continuously	TMZ 150 mg/m² 5/28 weeks	TMZ 50 mg/m² od continuously	PLD 20 mg/m² iv q3 weeks	CPA 50 mg po od + MTX 2.5 mg po D8 [28 days]
Hematological						
Anemia [G3/4]	28	8	–	–	–	–
Neutropenia [G3/4]	19	8	16	7	–	–
Leukopenia [G3/4]	8	4	19	14	–	–
Thrombocytopenia [G3/4]	3	0	3	7	–	–
Lymphopenia [G3/4]	8	8	68	61	–	–
Non-hematological						
Elevated transaminases [G3/4]	–	–	3	18	–	–
Fatigue [G3/4]	–	–	10	4	2.7	0
Constipation [G3]	–	–	–	–	2.7	0
Mucositis/stomatitis [G3]	–	–	–	–	5.4	0
Infection [G3]	–	–	–	–	8.1	0
Rash, hand–foot skin reaction [G3]	–	–	–	–	21.6	0
Other rash [G3]	–	–	–	–	5.4	0
Hypertension [G3]	–	–	–	–	10.8	20
Neurological [G3]	–	–	–	–	0	2.8
Fever/fractures [G3]	–	–	–	–	5.2	0
Pain [G3]	–	–	–	–	5.4	2.8
Allergic reaction/ hypersensitivity [G3]	–	–	–	–	5.4	0
Undefined [G3]	–	–	–	–	0	11.42

Abbreviations: '–' data not available/reported, *bid* twice daily, *CPA* cyclophosphamide, *G* grade, *iv* intravenously, *LDM* low-dose metronomic, *MTD* maximum-tolerated dose, *MTX* methotrexate, *od* daily, *PLD* pegylated liposomal doxorubicin, *po* oral, *TAX* docetaxel, *TMZ* temozolomide

Three comparative studies reporting the rates of adverse events associated with LDM versus MTD regimens indicate superior tolerance and safety of LDM chemotherapy while still displaying comparable antitumor effects.

Risk of secondary cancers

- Prolonged metronomic chemotherapy may lead to high total cumulated doses of anticancer agents, which **can be associated with secondary diseases**
- High cumulated dose of etoposide, cyclophosphamide or temozolomide can lead to the development of secondary **leukemia**.
- Because of its alkylating properties, cyclophosphamide has been shown to increase the risk of secondary malignancies such as leukemia and **urothelial cell carcinomas**

The issue of cumulative doses

- A cumulative CTX dose of >10 g/m2 (approximately 200 days of treatment with 50 mg of CTX po daily in a patient with 1.8 m2) is considered to increase the leukemia risk

- Some increased risk was associated with total CTX doses up to 30,000 mg, the relative risk was 4.7 (*N Engl J Med. 1992*).

- 972 patients evaluated from IBCSG Trials I-III, only one case of leukemia was observed. The patients, who received 12 cycles of CMF (cumulative total CTX dose 25,000-33,600 mg), had a median follow-up of 18 years.

- The long-term effect of prolonged exposure to metronomic chemotherapy on normal endothelial and vascular tissues is unknown.

Cumulative doses in autoimmune disorders

- Oral CTX regimens are used for the treatment of autoimmune disorders, albeit at higher daily doses than 50 mg (168 pts; time frame:25 yrs)

Table 3: Grading of adverse events.

Adverse events	Number (%)	Female	Male
Grade 1 or 2			
Infections	38		
Nausea	63 (37.5)	33	30
Vomiting	23 (13.6)	16	7
Hair loss	38 (22.6)	26	12
Cytopenia	38 (22.6)	19	19
Amenorrhoea	7 (7.6)		
Grade 3			
Secondary sterility	6	5	1
Infections	15		
Haemorrhagic cystitis	1 (0.5)		1
Grade 4			
Infections	4		
Grade 5			
Infection	1		

Swiss Med Wkly. 2014;144:w14030

Commonly used metronomic drugs toxicities

MetroCapecitabine toxicity

- The daily doses of capecitabine varied from 500 mg flat-dosed twice daily to 2,250 mg once daily (1,250 mg/m2), assuming an average body surface of 1.8 m2
- The most frequently observed severe hematological side effects were neutropenia, and anemia.
- Non- hematological side effects were reported with a higher frequency, including fatigue, hand–foot syndrome, stomatitis, elevated transaminases, and diarrhea

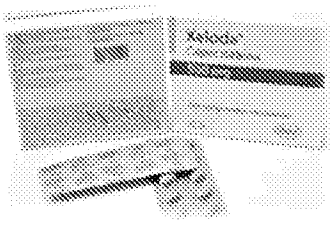

MetroVinorelbine Toxicity

- Oral vinorelbine at 70 mg/m2, fractionated on days 1, 3, and 5, for 3 weeks on and 1 week off, every 4 weeks;
- 50 mg given three times a week
- Main toxicities: neutropenia and anemia, nausea

MetroEtoposide Toxicity

- Daily oral etoposide, ranging from 50 to 100 mg daily
- LDM etoposide had myelosuppressive profile comparable to cyclophosphamide. No incidence of severe lymphopenia was observed
- LDM etoposide was associated with some severe non-hematological toxicities: renal failure, hemoptysis, thromboembolic complications, mucositis, fatigue/asthenia.

MetroCyclophosphamide toxicity

- Most studies used an oral cyclophosphamide flat dose of 50 mg
- Neutropenia and anemia were the most frequently reported side effects reflecting the known myelosuppressive potential of cyclophosphamide
- Most commonly reported non-hematological adverse events included skin rash, fatigue, nausea, and hypertension

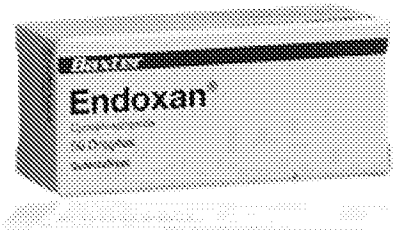

CM toxicity

- Roughly 10 studies were published with CM mainly in breast cancer
- Overall, the rate of severe hematological side effects was well below 10 % in the majority of studies
- Elevated transaminases, a known side effect of methotrexate, were the most prevalent non-hematological side effect.

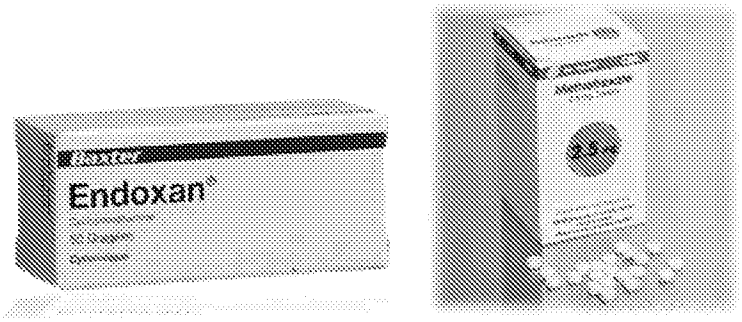

vinorelbine, cyclophosphamide plus capecitabine (VEX) combination

More frequent toxicities (naive)

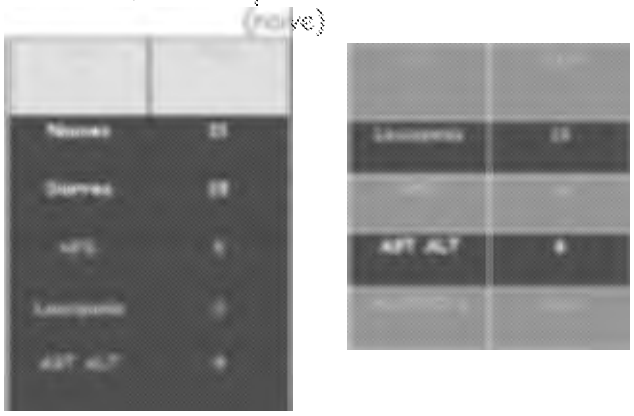

G3:1 anemia, 1 diarrea, 2 HFS, 2 increase AST ALT, 2 neutropenia

More frequent toxicities (pretreated)

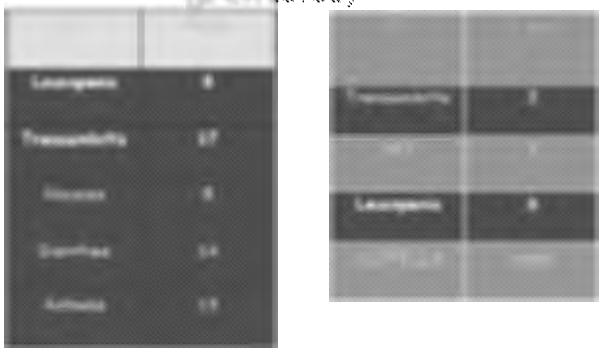

G3:1 leucopenia, 1 vomiting, 1 mucosite,1 neutropenia , 2 HFS

Montagna E et al. Eur J Cancer 2015;51:S291-S292

Strenghts and weakeness of oral CT

- Surveys have shown that most patients prefer oral to i.v.[1]
- A minority prefer i.v. due to possible less effectiveness of oral therapies (last resort)[2]
- Robust data are required to convince the full benefit of oral chemotherapy[3]
- Adherence[4]

[1]J Clin Oncol 1997; 15: 110–115
[2]Ann Oncol 2006; 17: 205–210
[3]Breast Cancer Res Treat 2005; 92: 265–272
[4]CA Cancer J Clin 2009;59(1):56-66

Patients' perception on efficacy of oral chemotherapy

Attributes	n	Rank in order of importance %				
		Highest				Least
		1	2	3	4	5
What do you expect from an oral chemotherapy?						
Reduction of side effects	57	33	25	14	25	3
Ease of dispensation	55	36	33	24	5	2
A reduction in hospital visits	55	13	22	33	27	4
Avoidance of needle	55	20	16	22	38	4
Other	9	55		11		33
Which is the most negative thing about an oral chemotherapy?						
Reduced efficacy	53	21	19	28	26	6
Mistaken administration	54	24	35	28	9	4
Variability in absorption of medicine	53	43	28	15	11	2
Reduction in hospital visits	53	11	15	23	47	4
Other	9	33		22		44
At the idea of beginning an oral chemo, how do you feel?						
Fearful	53	11	11	40	36	2
Neglected	53	6	13	32	45	4
Free	36	58	28	11	5	
Avoiding an uncomfortable procedure	53	26	47	15	11	
Other	5	20		20		60

oral chemotherapy is well accepted by patients and makes them feel less sick than if they were given intravenous therapy

Breast Cancer Research and Treatment (2005)

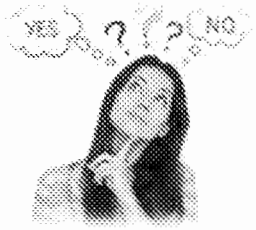

Patients' belief

In the overall population the majority of patients tended not to believe in fewer side effects due to oral administration

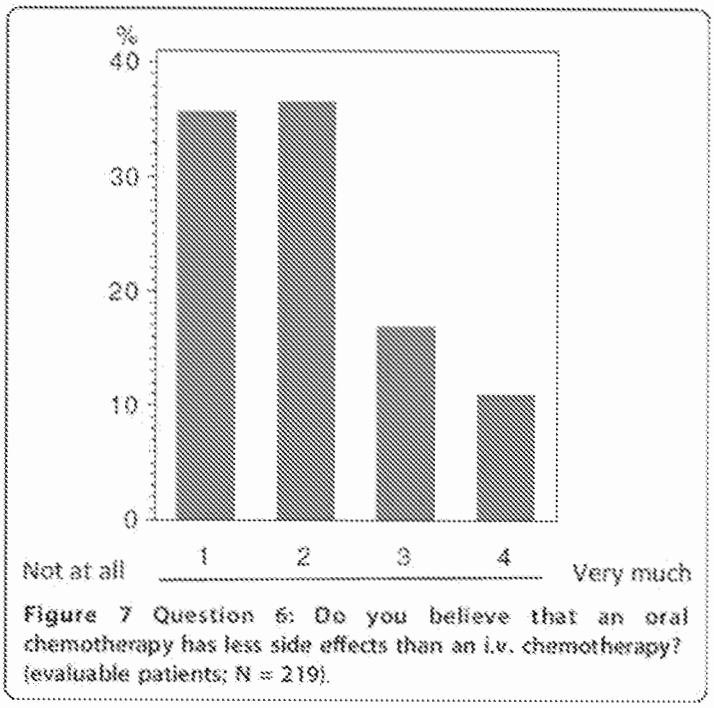

Figure 7 Question 6: Do you believe that an oral chemotherapy has less side effects than an i.v. chemotherapy? (evaluable patients; N = 219).

Schott et al. BMC Cancer 2011

Acceptance of oral chemotherapy in breast cancer patients: oral vs. iv

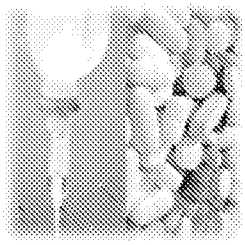

- 224 patients completed the questionnaire: 164 (73.2%) and 60 (26.8%) patients received i.v. and p.o. chemotherapy, respectively
- Significant differences were especially found in terms of:
  - personal benefit (55% i.v., 92% p.o.)
  - reduced feeling of being ill due to p.o. treatment (26% i.v., 65% p.o.)
  - better coping with disease due to p.o. therapy (36% i.v., 68% p.o.).
- Side effects were significantly less often reported under p.o. treatment (19% p.o. vs. 53% i.v.).

Schott et al. BMC Cancer 2011

Patient adherence and persistence with oral anticancer treatment

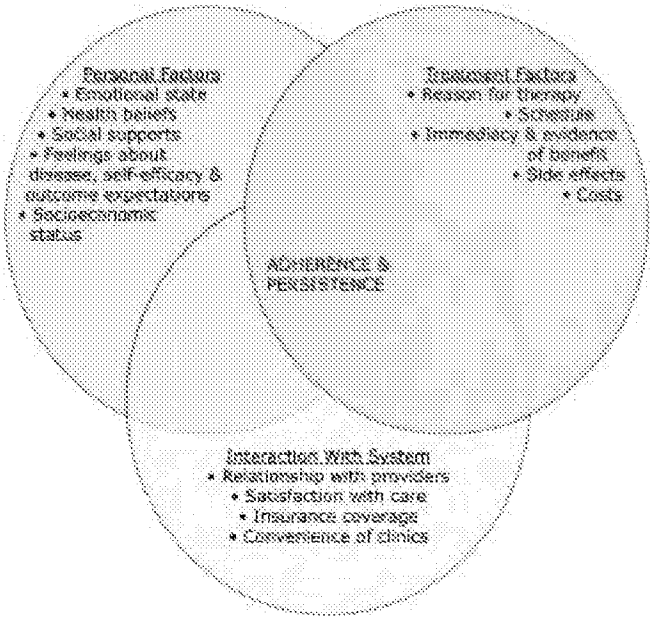

Reasons for non-adherence are complex in most situations.
A large meta-analysis of 76 studies demonstrated that adherence is adversely proportional to medication dosing frequency (prescribed number of doses per day.)

CA: A Cancer Journal for Clinicians
Volume 59, Issue 1, pages 56-66, 16 JAN 2009

FIGURE 1. ADHERENCE, OVERADHERENCE, AND UNDERADHERENCE AMONG PATIENTS BY DRUG CYCLE COMPLEXITY

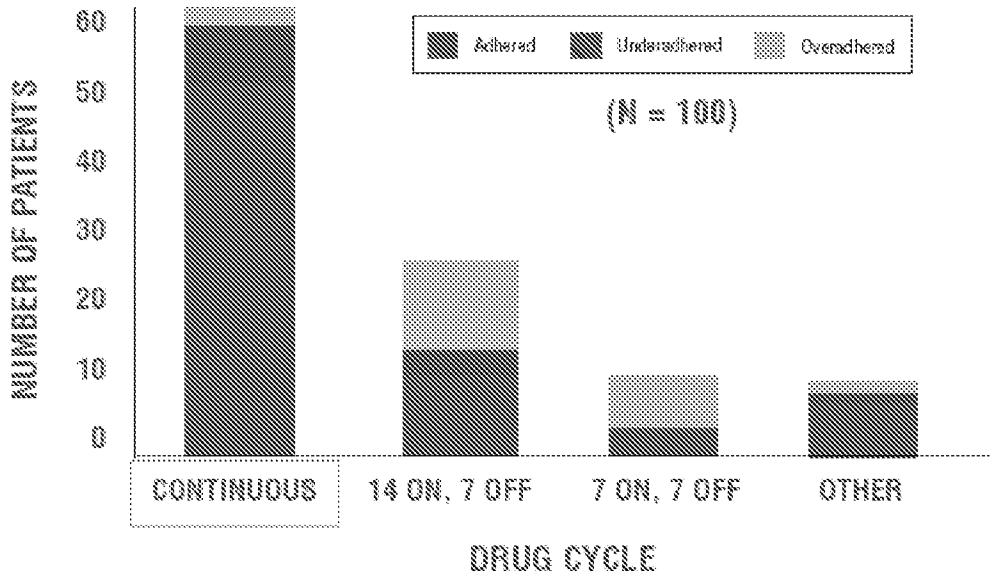

complexity of the treatment regimen and symptom severity were the primary factors affecting adherence.

Spoelstra S et al. CJON 2013,

Factors associated with non adherence to prescribed oral chemotherapy

Complex treatment regimen
Substantial behavioral change required
Inconvenient or inefficient clinics
Inadequate supervision
Poor communication with health care providers
Patient dissatisfaction with care
Patient health beliefs in favor of nonadherence
Inadequate social support
History of nonadherence
History of mental illness

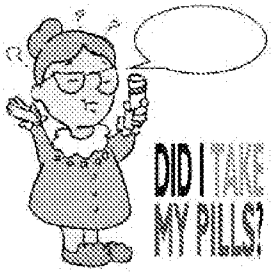

JNCI, 2002; 94: 652-661

Conclusions

- Metronomic chemotherapy is an alternative treatment, especially for palliative indications and for the elderly and/or frail patients that otherwise would not be candidates for MTD chemotherapy
- The low burden of personal costs to the patient and the possibility to continue the treatment for several months support the use of metronomic CT as an additional therapeutic tool
- Increased attention to patients' quality of life favors the use of active oral treatments

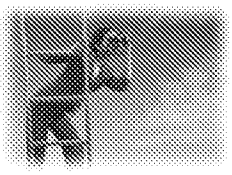

Future tools: how to select?

- Patients may have tumors, preferences and characteristics with little evidence supporting the use of i.v. single agent chemotherapy or polychemotherapy
- Patients and their physicians must weight the risks and benefits of all therapeutic options
- In the absence of validated predictive or pharmacodynamic markers of LDM chemotherapy, additional clinical studies are warranted to further improve the therapeutic index of LDM chemotherapy.

Less is more?

- A number of chemotherapy dose intensification strategies have either failed or resulted in only incremental benefits, they were often associated with increased toxicity
- By making treatments more tolerable and accessible to a broader range of cancer patients, LDM chemotherapy is an example that less can sometimes be more.

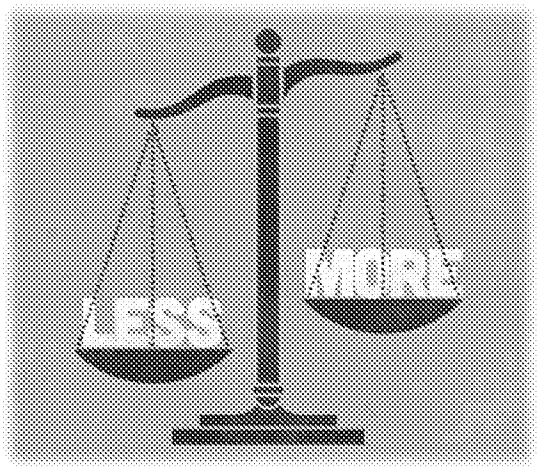

a balance between beneficial therapeutic side effect and minimize host toxicity

ANNEX I

SUMMARY OF PRODUCT CHARACTERISTICS

1. NAME OF THE MEDICINAL PRODUCT

Myocet liposomal 50 mg powder, dispersion and solvent for concentrate for dispersion for infusion.

2. QUALITATIVE AND QUANTITATIVE COMPOSITION

Liposome–encapsulated doxorubicin–citrate complex corresponding to 50 mg doxorubicin hydrochloride (HCl).

Excipient(s) with known effect: The reconstituted medicinal product contains approximately 108 mg sodium for a 50 mg doxorubicin HCl dose.

For the full list of excipients, see section 6.1.

3. PHARMACEUTICAL FORM

Powder, dispersion and solvent for concentrate for dispersion for infusion

Myocet liposomal is supplied as a three-vial system as follows:
Vial 1 - doxorubicin HCl is a red lyophilised powder.
Vial 2 - liposomes is a white to off-white, opaque and homogeneous dispersion.
Vial 3 - buffer is a clear colourless solution.

4. CLINICAL PARTICULARS

4.1 Therapeutic indications

Myocet liposomal, in combination with cyclophosphamide, is indicated for the first line treatment of metastatic breast cancer in adult women.

4.2 Posology and method of administration

The use of Myocet liposomal should be confined to units specialised in the administration of cytotoxic chemotherapy and should only be administered under the supervision of a physician experienced in the use of chemotherapy.

Posology
When Myocet liposomal is administered in combination with cyclophosphamide (600 mg/m^2) the initial recommended dose of Myocet liposomal is 60-75 mg/m^2 every three weeks.

Older people
Safety and efficacy of Myocet liposomal have been assessed in 61 patients with metastatic breast cancer, age 65 and over. Data from randomised controlled clinical trials show that the efficacy and cardiac safety of Myocet liposomal in this population was comparable to that observed in patients less than 65 years old.

Patients with hepatic impairment
As metabolism and excretion of doxorubicin occurs primarily by the hepatobiliary route, evaluation of hepatobiliary function should be performed before and during therapy with Myocet liposomal.
Based on limited data in patients with liver metastases, it is recommended that the initial dose of Myocet liposomal is reduced in accordance with the following table

Liver function tests	Dose
Bilirubin < ULN and normal AST	Standard dose of 60 - 75mg/m^2

Liver function tests	Dose
Bilirubin < ULN and raised AST	Consider a 25% dose reduction
Bilirubin > ULN but < 50 µmol/l	50% dose reduction
Bilirubin > 50 µmol/l	75% dose reduction

If possible, Myocet liposomal should be avoided in patients with bilirubin > 50 µmol/l as the recommendation is based mainly on extrapolations.

For dose reductions due to other toxicity, see section 4.4.

Patients with renal impairment
Doxorubicin is metabolised largely by the liver and excreted in the bile. Therefore dose modification is not required for patients with renal function impairment.

Paediatric population
The safety and efficacy of Myocet liposomal in children aged up to 17 years has not been established. No data are available.

Method of administration
Myocet liposomal must be reconstituted and further diluted prior to administration. A final concentration of between 0.4 mg/ml to 1.2 mg/ml doxorubicin HCl, is required. Myocet liposomal is administered by intravenous infusion over a period of 1 hour.

Myocet liposomal must not be administered by the intramuscular or subcutaneous route or as a bolus injection.

For instructions on reconstitution of the medicinal product before administration, see section 6.6.

4.3 Contraindications

Hypersensitivity to the active substance or to any of the excipients listed in section 6.1.

4.4 Special warnings and precautions for use

Myelosuppression
Therapy with Myocet liposomal causes myelosuppression. Myocet liposomal should not be administered to individuals with absolute neutrophil counts (ANC) lower than 1,500 cells/µl or platelets less than 100,000/µl prior to the next cycle. Careful haematological monitoring (including white blood cell and platelet count, and haemoglobin) should be performed during therapy with Myocet liposomal.
A meta-analysis showed a statistically significant lower rate of grade 4 neutropenia (RR = 0.82, p=0.005) in patients treated with Myocet liposomal versus conventional doxorubicin. However, no significant differences were identified in the occurrence of anaemia, thrombocytopenia and episodes of neutropenic fever.

Haematological as well as other toxicity may require dose reductions or delays. The following dosage modifications are recommended during therapy and should be performed in parallel for both Myocet liposomal and cyclophosphamide. Dosing subsequent to a dose reduction is left to the discretion of the physician in charge of the patient.

Haematological Toxicity			
Grade	**Nadir ANC (cells/µl)**	**Nadir Platelet Count (cells/µl)**	**Modification**
1	1500 – 1900	75,000 – 150,000	None
2	1000 – Less than 1500	50,000 – Less than 75,000	None
3	500 – 999	25,000 – Less than 50,000	Wait until ANC 1500 or

Haematological Toxicity			
Grade	**Nadir ANC (cells/μl)**	**Nadir Platelet Count (cells/μl)**	**Modification**
			more and/or platelets 100,000 or more then redose at 25% dose reduction
4	Less than 500	Less than 25,000	Wait until ANC 1500 and/or platelets 100,000 or more then redose at 50% dose reduction

If myelotoxicity delays treatment to greater than 35 days after the first dose of the previous cycle, then consideration should be given to stopping treatment.

Mucositis		
Grade	**Symptoms**	**Modification**
1	Painless ulcers, erythema, or mild soreness.	None
2	Painful erythema, oedema or ulcers but can eat.	Wait one week and if the symptoms improve redose at 100% dose
3	Painful erythema, oedema or ulcers and cannot eat	Wait one week and if symptoms improve redose at 25% dose reduction
4	Requires parenteral or enteral support	Wait one week and if symptoms improve redose at 50% dose reduction

For dose reduction of Myocet liposomal due to liver function impairment, see section 4.2.

Cardiac toxicity

Doxorubicin and other anthracyclines can cause cardiotoxicity. The risk of toxicity rises with increasing cumulative doses of those medicinal products and is higher in individuals with a history of cardiomyopathy, or mediastinal irradiation or pre-existing cardiac disease.

Analyses of cardiotoxicity in clinical trials have shown a statistically significant reduction in cardiac events in patients treated with Myocet liposomal compared to patients treated with conventional doxorubicin at the same dose in mg. A meta-analysis showed a statistically significant lower rate of both clinical heart failure (RR = 0.20, p=0.02) and clinical and subclinical heart failure combined (RR = 0.38, p<0.0001) in patients treated with Myocet liposomal versus conventional doxorubicin. The reduced risk of cardiotoxicity has also been shown in a retrospective analysis in patients who had received prior adjuvant doxorubicin (log-rank P=0.001, Hazard Ratio=5.42).

In a phase III study in combination with cyclophosphamide (CPA) comparing Myocet liposomal (60 mg/m^2) + CPA (600 mg/m^2) versus doxorubicin (60 mg/m^2) + CPA (600 mg/m^2), 6% versus 21% of patients, respectively, developed a significant decrease in left ventricular ejection fraction (LVEF). In a phase III study comparing single-agent Myocet liposomal (75 mg/m^2) versus single-agent doxorubicin (75 mg/m^2), 12% versus 27% of patients, respectively developed a significant decrease in LVEF. The corresponding figures for congestive heart failure, which was less accurately assessed, were 0% for Myocet liposomal + CPA versus 3% for doxorubicin + CPA, and 2% for Myocet liposomal versus 8% for doxorubicin. The median lifetime cumulative dose of Myocet liposomal in combination with CPA to a cardiac event was > 1260 mg/m^2, compared to 480 mg/m^2 for doxorubicin combination with CPA.

There is no experience with Myocet liposomal in patients with a history of cardiovascular disease, e.g. myocardial infarction within 6 months prior to treatment. Thus, caution should be exercised in patients with impaired cardiac function. The cardiac function of the patients treated concomitantly with Myocet liposomal and trastuzumab must be appropriately monitored as described below.

The total dose of Myocet liposomal should also take into account any previous, or concomitant, therapy with other cardiotoxic compounds, including anthracyclines and anthraquinones.

Before initiation of Myocet liposomal therapy a measurement of left ventricular ejection fraction (LVEF) is routinely recommended, either by Multiple Gated Arteriography (MUGA) or by echocardiography. These methods should also be applied routinely during Myocet liposomal treatment. The evaluation of left ventricular function is considered mandatory before each additional administration of Myocet liposomal once a patient exceeds a lifetime cumulative anthracycline dose of 550 mg/m^2 or whenever cardiomyopathy is suspected. If LVEF has decreased substantially from baseline e.g. by > 20 points to a final value > 50% or by > 10 points to a final value of < 50%, the benefit of continued therapy must be carefully evaluated against the risk of producing irreversible cardiac damage. However, the most definitive test for anthracycline myocardial injury, i.e., endomyocardial biopsy, should be considered.

All patients receiving Myocet liposomal should also routinely undergo ECG monitoring. Transient ECG changes such as T-wave flattening, S-T segment depression and benign arrhythmias are not considered mandatory indications for the cessation of Myocet liposomal therapy. However, reduction of the QRS complex is considered more indicative of cardiac toxicity.

Congestive heart failure due to cardiomyopathy may occur suddenly, and may also be encountered after discontinuation of therapy.

Gastroinstestinal disorders
A meta-analysis showed a statistically significant lower rate of nausea/vomiting grade ≥ 3 (RR = 0.65, p=0.04) and diarrhoea grade ≥ 3(RR = 0.33, p=0.03) in patients treated with Myocet liposomal versus conventional doxorubicin.

Injection site reactions
Myocet liposomal should be considered an irritant and precautions should be taken to avoid extravasation. If extravasation occurs, the infusion should be immediately terminated. Ice may be applied to the affected area for approximately 30 minutes. Subsequently, the Myocet liposomal infusion should be restarted in a different vein than that in which the extravasation has occurred. Note that Myocet liposomal may be administered through a central or peripheral vein. In the clinical program, there were nine cases of accidental extravasation of Myocet liposomal, none of which were associated with severe skin damage, ulceration or necrosis.

Infusion associated reactions
When infused rapidly acute reactions associated with liposomal infusions have been reported. Reported symptoms have included flushing, dyspnoea, fever, facial swelling, headache, back pain, chills, tightness in the chest and throat, and/or hypotension. These acute phenomena may be avoided by using a 1-hour infusion time.

Other
For precautions regarding the use of Myocet liposomal with other medicinal products, see section 4.5.
As for other anthracyclines and doxorubicin products, radiation recall may occur in previously irradiated fields.
Efficacy and safety of Myocet liposomal in the adjuvant treatment of breast cancer have not been determined. The importance of apparent differences in tissue distribution between Myocet liposomal and conventional doxorubicin has not been elucidated with respect to long-term antitumour efficacy.

Excipients
Sodium
This medicinal product contains approximately 108 mg sodium per 50 mg doxorubicin HCL dose, equivalent to 5.4 % of the WHO recommended maximum daily intake of 2 g sodium for an adult.

4.5 Interactions with other medicinal products and other forms of interactions

Specific medicinal product compatibility studies have not been performed with Myocet liposomal. Myocet liposomal is likely to interact with substances that are known to interact with conventional doxorubicin. Plasma levels of doxorubicin and its metabolite, doxorubicinol, may be increased when doxorubicin is administered with cyclosporin, verapamil, paclitaxel or other agents that inhibit P-glycoprotein (P-Gp). Interactions with doxorubicin have also been reported for streptozocin, phenobarbital, phenytoin and warfarin. Studies of the effect of Myocet liposomal on other substances are also lacking. However, doxorubicin may potentiate the toxicity of other antineoplastic agents. Concomitant treatment with other substances reported to be cardiotoxic or with cardiologically active substances (e.g. calcium antagonists) may increase the risk for cardiotoxicity. Concomitant therapy with other liposomal or lipid-complexed substances or intravenous fat emulsions could change the pharmacokinetic profile of Myocet liposomal.

4.6 Fertility, pregnancy and lactation

Women of childbearing potential
Women of childbearing potential should use an effective contraceptive during treatment with Myocet liposomal and up to 6 months following discontinuation of therapy.

Pregnancy
Due to the known cytotoxic, mutagenic and embryotoxic properties of doxorubicin, Myocet liposomal should not be used during pregnancy unless clearly necessary.

Breast-feeding
Women receiving Myocet liposomal should not breastfeed.

4.7 Effects on ability to drive and use machines

Myocet liposomal has been reported to cause dizziness. Patients who suffer from this should avoid driving and operating machinery.

4.8 Undesirable effects

During clinical trials, the most frequently reported adverse reactions were nausea/vomiting (73%), leucopoenia (70%), alopecia (66%), neutropenia (46%), asthenia/fatigue (46%), stomatitis/mucositis (42%), thrombocytopenia (31%) and anaemia (30%).

The following adverse reactions have been reported with Myocet liposomal during clinical studies and post marketing experience. Adverse reactions are listed below as MedDRA preferred term by system organ class and frequency (frequencies are defined as: very common ≥1/10, common ≥1/100 to <1/10, uncommon ≥ 1/1,000 to <1/100, not known (cannot be estimated from the available data)).

	All grades	**Grades ≥ 3**
Infections and infestations		
Neutropenic fever	Very common	Very common
Infections	Very common	Common
Herpes zoster	Uncommon	Uncommon
Sepsis	Uncommon	Uncommon
Injection site infection	Uncommon	Not known
Blood and lymphatic system disorders		
Neutropenia	Very common	Very common
Thrombocytopenia	Very common	Very common
Anaemia	Very common	Very common
Leucopenia	Very common	Very common
Lymphopenia	Common	Common

	All grades	Grades ≥ 3
Pancytopenia	Common	Uncommon
Neutropenic sepsis	Uncommon	Uncommon
Purpura	Uncommon	Uncommon
Metabolism and nutrition disorders		
Anorexia	Very common	Very common
Dehydration	Common	Very common
Hypokalaemia	Common	Uncommon
Hyperglycaemia	Uncommon	Uncommon
Psychiatric disorders		
Agitation	Uncommon	Not known
Nervous system disorders		
Insomnia	Common	Uncommon
Abnormal gait	Uncommon	Uncommon
Dysphonia	Uncommon	Not known
Somnolence	Uncommon	Not known
Cardiac disorders		
Arrhythmia	Common	Uncommon
Cardiomyopathy	Common	Common
Congestive cardiac failure	Common	Common
Pericardial effusion	Uncommon	Uncommon
Vascular disorders		
Hot flushes	Common	Uncommon
Hypotension	Uncommon	Uncommon
Respiratory, thoracic and mediastinal disorders		
Chest pain	Common	Uncommon
Dyspnoea	Common	Uncommon
Epistaxis	Common	Uncommon
Haemoptysis	Uncommon	Not known
Pharyngitis	Uncommon	Not known
Pleural effusion	Uncommon	Uncommon
Pneumonitis	Uncommon	Uncommon
Gastrointestinal disorders		
Nausea/vomiting	Very common	Very common
Stomatitis/mucositis	Very common	Common
Diarrhoea	Very common	Common
Constipation	Common	Uncommon
Oesophagitis	Common	Uncommon
Gastric ulcer	Uncommon	Uncommon
Hepatobiliary disorders		
Increased hepatic transaminases	Common	Uncommon
Increased alkaline phosphatase	Uncommon	Uncommon
Jaundice	Uncommon	Uncommon
Increased serum bilirubin	Uncommon	Not known
Skin and subcutaneous tissue disorders		
Alopecia	Very Common	Common

	All grades	Grades ≥ 3
Rash	Common	Not known
Palmar-plantar erythrodysaesthesia syndrome	Not known	Not known
Nail disorder	Common	Uncommon
Pruritus	Uncommon	Uncommon
Folliculitis	Uncommon	Uncommon
Dry skin	Uncommon	Not known
Musculoskeletal and connective tissue disorders		
Back pain	Common	Uncommon
Myalgia	Common	Uncommon
Muscle weakness	Uncommon	Uncommon
Renal and urinary disorders		
Haemorrhagic cystitis	Uncommon	Uncommon
Oliguria	Uncommon	Uncommon
General disorders and administration site conditions		
Asthenia/Fatigue	Very Common	Common
Fever	Very common	Common
Pain	Very Common	Common
Rigors	Very Common	Uncommon
Dizziness	Common	Uncommon
Headache	Common	Uncommon
Weight loss	Common	Uncommon
Injection site reaction	Uncommon	Uncommon
Malaise	Uncommon	Not known

Reporting of suspected adverse reactions
Reporting suspected adverse reactions after authorisation of the medicinal product is important. It allows continued monitoring of the benefit/risk balance of the medicinal product. Healthcare professionals are asked to report any suspected adverse reactions via the national reporting system listed in Appendix V.

4.9 Overdose

Acute overdose with Myocet liposomal will worsen toxic side effects. Treatment of acute overdose should focus on supportive care for expected toxicity and may include hospitalisation, antibiotics, platelet and granulocyte transfusions and symptomatic treatment of mucositis.

5. PHARMACOLOGICAL PROPERTIES

5.1 Pharmacodynamic properties

Pharmacotherapeutic group: Antineoplastic agents, anthracyclines and related substances, ATC code: L01DB01

The active substance in Myocet liposomal is doxorubicin HCl. Doxorubicin may exert its antitumour and toxic effects by a number of mechanisms including inhibition of topoisomerase II, intercalation with DNA and RNA polymerases, free radical formation and membrane binding. Liposomal-encapsulated doxorubicin compared with conventional doxorubicin was not found more active in doxorubicin resistant cell lines *in vitro.* In animals, liposome-encapsulated doxorubicin reduced the

distribution to heart and gastrointestinal mucosa compared with conventional doxorubicin, while antitumoural efficacy in experimental tumours was maintained.

Myocet liposomal (60 mg/m^2) + CPA (600 mg/m^2) was compared with conventional doxorubicin + CPA (at the same doses) and Myocet liposomal (75 mg/m^2) + CPA (600 mg/m^2) was compared to epirubicin + CPA (at the same doses). In a third trial, Myocet liposomal (75 mg/m^2) monotherapy was compared with conventional doxorubicin monotherapy (at the same dose). Findings regarding response rate and progression-free survival are provided in Table 3.

Table 3
Antitumour efficacy summary for combination and single-agent studies

	Myocet liposomal/CPA (60/600 mg/m^2) (n=142)	Dox 60/CPA (60/600 mg/m^2) (n=155)	Myocet liposomal/CPA (75/600 mg/m^2) (n=80)	Epi/CPA (75/600 mg/m^2) (n=80)	Myocet liposomal (75 mg/m^2) (n=108)	Dox (75 mg/m^2) (n=116)
Tumour response rate	43%	43%	46%	39%	26%	26%
Relative Risk (95% C.I.)	1.01 (0.78-1.31)		1.19 (0.83-1.72)		1.00 (0.64-1.56)	
Median PFS (months)[a]	5.1	5.5	7.7	5.6	2.9	3.2
Risk Ratio (95% C.I.)	1.03 (0.80-1.34)		1.52 (1.06-2.20)		0.87 (0.66-1.16)	

Abbreviations: PFS, progression-free survival; Dox, doxorubicin; Epi, epirubicin; Relative Risk, comparator taken as reference; Risk Ratio, Myocet liposomal taken as reference
[a] Secondary endpoint

5.2 Pharmacokinetic properties

The plasma pharmacokinetics for total doxorubicin in patients receiving Myocet liposomal shows a high degree of inter-patient variability. In general however, the plasma levels of total doxorubicin are substantially higher with Myocet liposomal than with conventional doxorubicin, while the data indicate that peak plasma levels of free (not liposome-encapsulated) doxorubicin are lower with Myocet liposomal than with conventional doxorubicin. Available pharmacokinetic data preclude conclusions regarding the relationship between plasma levels of total/free doxorubicin and its influence on the efficacy/safety of Myocet liposomal. The clearance of total doxorubicin was 5.1 ± 4.8 l/h and the volume of distribution at steady state (V_d) was 56.6 ± 61.5 l whereas after conventional doxorubicin, clearance and V_d were 46.7 ± 9.6 l/h and 1,451 ± 258 l, respectively. The major circulating metabolite of doxorubicin, doxorubicinol, is formed via aldo-keto-reductase. The peak levels of doxorubicinol occur in the plasma later with Myocet liposomal than with conventional doxorubicin.

The pharmacokinetics of Myocet liposomal have not been specifically studied in patients with renal insufficiency. Doxorubicin is known to be eliminated in large part by the liver. A dose reduction of Myocet liposomal has been shown to be appropriate in patients with impaired hepatic function (see section 4.2 for dosage recommendations).

Substances that inhibit P-glycoprotein (P-Gp) have been shown to alter the disposition of doxorubicin and doxorubicinol (see also section 4.5).

5.3 Preclinical safety data

Studies of genotoxicity, carcinogenicity and reproductive toxicity of Myocet liposomal have not been performed but doxorubicin is known to be both mutagenic and carcinogenic and may cause toxicity to reproduction.

6. PHARMACEUTICAL PARTICULARS

6.1 List of excipients

Vial 1 - doxorubicin HCl
- lactose

Vial 2 - liposomes
- phosphatidylcholine
- cholesterol
- citric acid
- sodium hydroxide
- water for injections

Vial 3 - buffer
- sodium carbonate
- water for injections

6.2 Incompatibilities

This medicinal product must not be mixed with other medicinal products except those mentioned in section 6.6.

6.3 Shelf life

18 months

Chemical and physical in-use stability after reconstitution has been demonstrated for up to 8 hours at 25°C, and for up to 5 days at 2°C – 8°C.

From a microbiological point of view, the medicinal product should be used immediately. If not used immediately, in-use storage times and conditions prior to use are the responsibility of the user and would normally not be longer than 24 hours at 2°C – 8°C, unless reconstitution and dilution has taken place in controlled and validated aseptic conditions.

6.4 Special precautions for storage

Store in a refrigerator (2°C – 8°C).

For storage conditions after reconstitution of the medicinal product, see section 6.3.

6.5 Nature and contents of container

Myocet liposomal is available in cartons containing 1 set or 2 sets of the three constituent vials. Not all pack-sizes may be marketed.

Vial 1 - doxorubicin HCl
Type I glass vials sealed with grey butyl rubber stoppers and orange flip-off aluminium seals, containing 50 mg of doxorubicin HCl lyophilised powder.

Vial 2 - liposomes
Type I flint glass tubing vials sealed with siliconised grey stopper and green flip-off aluminium seals, containing not less than 1.9 ml of liposomes.

Vial 3 - buffer
Glass vials sealed with siliconised grey stopper and blue aluminium flip-off seals, containing not less than 3 ml of buffer.

6.6 Special precautions for disposal and other handling

Preparation of Myocet liposomal
Aseptic technique must be strictly observed throughout handling of Myocet liposomal, since no preservative is present.

Caution should be exercised in the handling and preparation of Myocet liposomal. The use of gloves is required

Step 1. Set up
Two alternative heating methods can be used : a Techne DB-3 Dri Block heater or a water bath:

- Turn on the Techne DB-3 Dri Block heater and set the controller to 75°C-76°C. Verify the temperature set point by checking the thermometer(s) on each heat block insert.
- If using a water bath, turn on the water bath and allow it to equilibrate at 58°C (55°C-60°C). Verify the temperature set point by checking the thermometer.

(Please note that whilst the control settings on the water bath and heat block are set to different levels the temperature of the vial contents are in the same range (55°C-60°C)).

Remove the carton of constituents from the refrigerator.

Step 2. Reconstitute doxorubicin HCl

- Withdraw 20 ml sodium chloride solution for injection (0.9%), (not provided in the package), and inject into each vial of doxorubicin HCl, intended for preparation.
- Shake well in the inverted position to ensure doxorubicin is fully dissolved.

Step 3. Heat in water bath or dry heat block

- Heat the reconstituted doxorubicin HCl vial in the Techne DB-3 Dri Block heater with the thermometer in the block reading (75°C-76°C) for 10 minutes (not to exceed 15 minutes). If using a water bath, heat the doxorubicin HCl vial with the thermometer temperature reading 55°C-60°C for 10 minutes (not to exceed 15 minutes).
- While heating proceed to step 4

Step 4. Adjust pH of liposomes

- Withdraw 1.9 ml of liposomes. Inject into the buffer vial to adjust the pH of liposomes. Pressure build-up may require venting.
- Shake well.

Step 5. Add pH-adjusted liposomes to doxorubicin

- Using a syringe, withdraw the entire vial contents of pH-adjusted liposomes from the buffer vial.
- Remove the reconstituted doxorubicin HCl vial from the water bath or dry heat block. SHAKE VIGOROUSLY. Carefully insert a pressure-venting device equipped with a hydrophobic filter. Then IMMEDIATELY (within 2 minutes) inject pH-adjusted liposomes into vial of heated reconstituted doxorubicin HCl. Remove venting device.
- SHAKE VIGOROUSLY.
- WAIT for a minimum of 10 MINUTES before using, keeping the medicine at room temperature.

- The Techne DB-3 Dri Block Heater is fully validated for use in the constitution of Myocet liposomal. Three inserts, each with two 43.7mm openings per insert must be used. To ensure correct temperature control the use of a 35mm immersion thermometer is recommended.

The resulting reconstituted preparation of Myocet liposomal contains 50 mg of doxorubicin HCl/25 ml of liposomal dispersion (2 mg/ml).

After reconstitution the finished product must be further diluted in 0.9% (w/v) sodium chloride for injection, or 5% (w/v) glucose solution for injection to a final volume of 40 ml to 120 ml so that a final concentration of 0.4 mg/ml to 1.2 mg/ml doxorubicin is obtained.
Once constituted, the liposomal dispersion for infusion containing liposome-encapsulated doxorubicin should be a red orange opaque homogeneous dispersion. All parenteral solutions should be inspected visually for particulate matter and discoloration prior to administration. Do not use the preparation if foreign particulate matter is present.

Procedure for proper disposal
Any unused medicinal product or waste material should be disposed of in accordance with local requirements.

7. MARKETING AUTHORISATION HOLDER

Teva B.V.
Swensweg 5
2031 GA Haarlem
Netherlands

8. MARKETING AUTHORISATION NUMBER(S)

EU/1/00/141/001-002

9. DATE OF FIRST AUTHORISATION/RENEWAL OF THE AUTHORISATION

Date of first authorisation: 13 July 2000
Date of latest renewal: 02 July 2010

10. DATE OF REVISION OF THE TEXT

Detailed information on this medicinal product is available on the website of the European Medicines Agency http://www.ema.europa.eu.

ANNEX II

A. MANUFACTURER(S) RESPONSIBLE FOR BATCH RELEASE

B. CONDITIONS OR RESTRICTIONS REGARDING SUPPLY AND USE

C. OTHER CONDITIONS AND REQUIREMENTS OF THE MARKETING AUTHORISATION

D. CONDITIONS OR RESTRICTIONS WITH REGARD TO THE SAFE AND EFFECTIVE USE OF THE MEDICINAL PRODUCT

A. MANUFACTURER(S) RESPONSIBLE FOR BATCH RELEASE

Name and address of the manufacturer(s) responsible for batch release

GP-Pharm
Polígon Industrial Els Vinyets - Els Fogars,
Sector 2, Carretera Comarcal C244, km 22
08777 Sant Quintí de Mediona (Barcelona)
Spain

B. CONDITIONS OR RESTRICTIONS REGARDING SUPPLY AND USE

Medicinal product subject to restricted medical prescription (see Annex I: Summary of Product Characteristics, section 4.2)

C. OTHER CONDITIONS AND REQUIREMENTS OF THE MARKETING AUTHORISATION

- **Periodic safety update reports (PSURs)**

The requirements for submission of PSURs for this medicinal product are set out in the list of Union reference dates (EURD list) provided for under Article 107c(7) of Directive 2001/83/EC and any subsequent updates published on the European medicines web-portal.

D. CONDITIONS OR RESTRICTIONS WITH REGARD TO THE SAFE AND EFFECTIVE USE OF THE MEDICINAL PRODUCT

- **Risk management plan (RMP)**

Not applicable.

ANNEX III

LABELLING AND PACKAGE LEAFLET

A. LABELLING

PARTICULARS TO APPEAR ON THE OUTER PACKAGING

Outer carton (2 sets of 3 constituents)

1. NAME OF THE MEDICINAL PRODUCT

Myocet liposomal 50 mg powder, dispersion and solvent for concentrate for dispersion for infusion
Liposomal doxorubicin hydrochloride

2. STATEMENT OF ACTIVE SUBSTANCE(S)

Liposome–encapsulated doxorubicin corresponding to 50 mg doxorubicin hydrochloride

3. LIST OF EXCIPIENTS

Excipients:
Vial 1- doxorubicin HCl
lactose

Vial 2 - liposomes
phosphatidylcholine, cholesterol, citric acid, sodium hydroxide, water for injections

Vial 3 - buffer
sodium carbonate, water for injections

Contains sodium. See leaflet for further information.

4. PHARMACEUTICAL FORM AND CONTENTS

Powder, dispersion and solvent for concentrate for dispersion for infusion

Carton contents:
2 sets each containing:
1 vial doxorubicin HCl
1 vial liposomes
1 vial buffer

5. METHOD AND ROUTE(S) OF ADMINISTRATION

For intravenous use after reconstitution and dilution.
Read the package leaflet before use.

6. SPECIAL WARNING THAT THE MEDICINAL PRODUCT MUST BE STORED OUT OF THE SIGHT AND REACH OF CHILDREN

Keep out of the sight and reach of children.

7. OTHER SPECIAL WARNING(S), IF NECESSARY

For single use only.

8. EXPIRY DATE

EXP

9. SPECIAL STORAGE CONDITIONS

Store in a refrigerator.

10. SPECIAL PRECAUTIONS FOR DISPOSAL OF UNUSED MEDICINAL PRODUCTS OR WASTE MATERIALS DERIVED FROM SUCH MEDICINAL PRODUCTS, IF APPROPRIATE

Cytotoxic. Any unused product or waste material should be disposed of in accordance with local requirements.

11. NAME AND ADDRESS OF THE MARKETING AUTHORISATION HOLDER

Teva B.V.
Swensweg 5
2031 GA Haarlem
Netherlands

12. MARKETING AUTHORISATION NUMBER(S)

EU/1/00/141/001

13. BATCH NUMBER

Lot

14. GENERAL CLASSIFICATION FOR SUPPLY

Medicinal product subject to medical prescription

15. INSTRUCTIONS ON USE

16. INFORMATION IN BRAILLE

Justification for not including Braille accepted

17. UNIQUE IDENTIFIER – 2D BARCODE

2D barcode carrying the unique identifier included.

18. UNIQUE IDENTIFIER - HUMAN READABLE DATA

PC
SN
NN

PARTICULARS TO APPEAR ON THE INTERMEDIATE PACKAGING

(used with outer carton of 2 sets of 3 constituents)

1. NAME OF THE MEDICINAL PRODUCT

Myocet liposomal 50 mg powder, dispersion and solvent for concentrate for dispersion for infusion
Liposomal doxorubicin hydrochloride

2. STATEMENT OF ACTIVE SUBSTANCE(S)

Liposome–encapsulated doxorubicin corresponding to 50 mg doxorubicin hydrochloride

3. LIST OF EXCIPIENTS

Excipients:
Vial 1 - doxorubicin HCl
lactose

Vial 2 - liposomes
phosphatidylcholine, cholesterol, citric acid, sodium hydroxide, water for injections

Vial 3 - buffer
sodium carbonate, water for injections

Contains sodium. See leaflet for further information.

4. PHARMACEUTICAL FORM AND CONTENTS

Powder, dispersion and solvent for concentrate for dispersion for infusion

Carton contents:
1 vial doxorubicin HCl
1 vial liposomes
1 vial buffer

5. METHOD AND ROUTE(S) OF ADMINISTRATION

For intravenous use after reconstitution and dilution.
Read the package leaflet before use.

6. SPECIAL WARNING THAT THE MEDICINAL PRODUCT MUST BE STORED OUT OF THE SIGHT AND REACH OF CHILDREN

Keep out of the sight and reach of children.

7. OTHER SPECIAL WARNING(S), IF NECESSARY

For single use only.

8. EXPIRY DATE

EXP

9. SPECIAL STORAGE CONDITIONS

Store in a refrigerator.

10. SPECIAL PRECAUTIONS FOR DISPOSAL OF UNUSED MEDICINAL PRODUCTS OR WASTE MATERIALS DERIVED FROM SUCH MEDICINAL PRODUCTS, IF APPROPRIATE

Cytotoxic. Any unused product or waste materials should be disposed of in accordance with local requirements.

11. NAME AND ADDRESS OF THE MARKETING AUTHORISATION HOLDER

Teva B.V.
Swensweg 5
2031 GA Haarlem
Netherlands

12. MARKETING AUTHORISATION NUMBER(S)

EU/1/00/141/001

13. BATCH NUMBER

Lot

14. GENERAL CLASSIFICATION FOR SUPPLY

Medicinal product subject to medical prescription

15. INSTRUCTIONS ON USE

16. INFORMATION IN BRAILLE

Justification for not including Braille accepted

17. UNIQUE IDENTIFIER – 2D BARCODE

18. UNIQUE IDENTIFIER - HUMAN READABLE DATA

PARTICULARS TO APPEAR ON THE OUTER PACKAGING

Outer carton (1 set of 3 constituents)

1. NAME OF THE MEDICINAL PRODUCT

Myocet liposomal 50 mg powder, dispersion and solvent for concentrate for dispersion for infusion
Liposomal doxorubicin hydrochloride

2. STATEMENT OF ACTIVE SUBSTANCE(S)

Liposome–encapsulated doxorubicin corresponding to 50 mg doxorubicin hydrochloride

3. LIST OF EXCIPIENTS

Excipients:
Vial 1 - doxorubicin HCl
lactose

Vial 2 - liposomes
phosphatidylcholine, cholesterol, citric acid, sodium hydroxide, water for injections

Vial 3 - buffer
sodium carbonate, water for injections

Contains sodium. See leaflet for further information.

4. PHARMACEUTICAL FORM AND CONTENTS

Powder, dispersion and solvent for concentrate for dispersion for infusion

Carton contents:
1 vial doxorubicin HCl
1 vial liposomes
1 vial buffer

5. METHOD AND ROUTE(S) OF ADMINISTRATION

For intravenous use after reconstitution and dilution.
Read the package leaflet before use.

6. SPECIAL WARNING THAT THE MEDICINAL PRODUCT MUST BE STORED OUT OF THE SIGHT AND REACH OF CHILDREN

Keep out of the sight and reach of children.

7. OTHER SPECIAL WARNING(S), IF NECESSARY

For single use only.

8. EXPIRY DATE

EXP

9. SPECIAL STORAGE CONDITIONS

Store in a refrigerator.

10. SPECIAL PRECAUTIONS FOR DISPOSAL OF UNUSED MEDICINAL PRODUCTS OR WASTE MATERIALS DERIVED FROM SUCH MEDICINAL PRODUCTS, IF APPROPRIATE

Cytotoxic. Any unused product or waste material should be disposed of in accordance with local requirements.

11. NAME AND ADDRESS OF THE MARKETING AUTHORISATION HOLDER

Teva B.V.
Swensweg 5
2031 GA Haarlem
Netherlands

12. MARKETING AUTHORISATION NUMBER(S)

EU/1/00/141/002

13. BATCH NUMBER

Lot

14. GENERAL CLASSIFICATION FOR SUPPLY

Medicinal product subject to medical prescription

15. INSTRUCTIONS ON USE

16. INFORMATION IN BRAILLE

Justification for not including Braille accepted

17. UNIQUE IDENTIFIER – 2D BARCODE

2D barcode carrying the unique identifier included.

18. UNIQUE IDENTIFIER - HUMAN READABLE DATA

PC
SN
NN

MINIMUM PARTICULARS TO APPEAR ON SMALL IMMEDIATE PACKAGING UNITS

DOXORUBICIN HCL VIAL

1. NAME OF THE MEDICINAL PRODUCT AND ROUTE(S) OF ADMINISTRATION

Myocet liposomal
doxorubicin HCl
IV use

2. METHOD OF ADMINISTRATION

Read the package leaflet before use

3. EXPIRY DATE

EXP

4. BATCH NUMBER

Lot

5. CONTENTS BY WEIGHT, BY VOLUME OR BY UNIT

50 mg

6. OTHER

STICKER/TEAR OFF SECTION OF LABEL FOR RELABELLING THE DOXORUBICIN HCL VIAL CONTAINING RECONSTITUTED FINISHED CONCENTRATE FOR DISPERSION FOR INFUSION

1. NAME OF THE MEDICINAL PRODUCT AND ROUTE(S) OF ADMINISTRATION

Myocet liposomal 50 mg concentrate for dispersion for infusion
Liposomal doxorubicin HCl
IV

2. METHOD OF ADMINISTRATION

Read the package leaflet before use

3. EXPIRY DATE

4. BATCH NUMBER

5. CONTENTS BY WEIGHT, BY VOLUME OR BY UNIT

6. OTHER

Preparation Date: _____
Preparation Time: _____
Prepared By: _____

MINIMUM PARTICULARS TO APPEAR ON SMALL IMMEDIATE PACKAGING UNITS

LIPOSOMES

1. NAME OF THE MEDICINAL PRODUCT AND ROUTE(S) OF ADMINISTRATION

Myocet liposomal
liposomes

2. METHOD OF ADMINISTRATION

Read the package leaflet before use

3. EXPIRY DATE

EXP

4. BATCH NUMBER

Lot

5. CONTENTS BY WEIGHT, BY VOLUME OR BY UNIT

1.9 ml

6. OTHER

MINIMUM PARTICULARS TO APPEAR ON SMALL IMMEDIATE PACKAGING UNITS

BUFFER

1. NAME OF THE MEDICINAL PRODUCT AND ROUTE(S) OF ADMINISTRATION

Myocet liposomal
buffer

2. METHOD OF ADMINISTRATION

Read the package leaflet before use

3. EXPIRY DATE

EXP

4. BATCH NUMBER

Lot

5. CONTENTS BY WEIGHT, BY VOLUME OR BY UNIT

3 ml

6. OTHER

B. PACKAGE LEAFLET

Package leaflet: Information for the user

Myocet liposomal 50 mg powder, dispersion and solvent for concentrate for dispersion for infusion
Liposomal doxorubicin hydrochloride

Read all of this leaflet carefully before you start using this medicine because it contains important information for you.
- Keep this leaflet. You may need to read it again.
- If you have any further questions, ask your doctor, pharmacist or nurse.
- This medicine has been prescribed for you only. Do not pass it on to others. It may harm them, even if their signs of illness are the same as yours.
- If you get any side effects, talk to your doctor or nurse. This includes any possible side effects not listed in this leaflet. See section 4.

What is in this leaflet

1. What Myocet liposomal is and what it is used for

Myocet liposomal contains a medicine called "doxorubicin", which damages tumour cells. This type of medicine is called "chemotherapy". The medicine is contained inside very small droplets of fat called "liposomes".

Myocet liposomal is used in adult women for the first-line treatment of breast cancer that has spread ("metastatic breast cancer"). It is used with another medicine called "cyclophosphamide". Please also read the patient information leaflet carefully that comes with that medicine.

2. What you need to know before you are given Myocet liposomal

Do not have Myocet liposomal:
- if you are allergic to doxorubicin or any of the other ingredients of this medicine (listed in section 6).

Do not have Myocet liposomal if this applies to you. If you are not sure, talk to your doctor or nurse before having Myocet liposomal.

Warning and precautions
Talk to your doctor or nurse before having Myocet liposomal.

Check with your doctor or nurse before having your medicine if:
- you have ever had heart problems such as a heart attack, heart failure or you have had high blood pressure for a long time
- you have liver problems.

If any of the above apply to you (or you are not sure), talk to your doctor or nurse before having Myocet liposomal.

Tests
Your doctor will do tests during your treatment to check that the medicine is working properly. They will also look out for any side effects such as blood problems or heart problems.

Radiation therapy
If you have already had radiation therapy, this may react with Myocet liposomal. You may get painful, red or dry skin. This can happen straight away or later on in your treatment.

Other medicines and Myocet liposomal
Tell your doctor or pharmacist if you are taking, have recently taken or might take any other medicines. This includes medicines obtained without a prescription and herbal medicines. This is because Myocet liposomal can affect the way some other medicines work. Also some other medicines can affect the way Myocet liposomal works.

In particular tell your doctor or nurse if you are taking any of the following medicines:
- phenobarbital or phenytoin – for epilepsy
- warfarin – for thinning the blood
- streptozotocin – for cancer of the pancreas
- cyclosporine – for changing your immune system.

If any of the above apply to you (or you are not sure), please talk to your doctor or nurse before having Myocet liposomal.

Pregnancy and breast-feeding
If you are pregnant or breast-feeding, think you may be pregnant or are planning to have a baby, ask your doctor or nurse for advice before having Myocet liposomal.
- Myocet liposomal should not be used during pregnancy unless clearly necessary.
- Women having Myocet liposomal should not breast-feed.
- Women who could get pregnant should use effective contraception during treatment with Myocet liposomal and for 6 months after treatment.

Driving and using machines
You may feel dizzy after having Myocet liposomal. If you feel dizzy or are not sure how you feel, do not drive or use any tools or machines.

Myocet liposomal contains sodium
Myocet liposomal is available in cartons containing 1 set or 2 sets of 3 vials (not all pack-sizes may be marketed). When the 3 vials have been mixed together, your medicine contains about 108 mg sodium (main component of cooking/table salt). This is equivalent to 5.4 % of the recommended maximum daily dietary intake of sodium for an adult.

3. How Myocet liposomal is given

This medicine is normally given by a doctor or nurse. It is given as a drip (infusion) into a vein.

How much you will be given
Your doctor will work out exactly how much you need. This is based on the size of your body (measured in "square metres" or "m^2").

The recommended dose is between 60 and 75 mg of the medicine for each square meter of your body:
- this is given once every 3 weeks
- the medicine "cyclophosphamide" is given on the same day.

The doctor may give you a lower dose if they think you need it.

The number of times you have the drip depends on:
- the stage of your breast cancer
- how well your body responds to the medicine.

Treatment usually lasts for about 3 to 6 months.

If you get Myocet liposomal on your skin

Tell your doctor or nurse straight away if any medicine leaks from the drip (infusion) onto your skin. This is because Myocet liposomal can damage your skin. The drip will be stopped straight away. Ice will be put on the affected area for 30 minutes. Then the drip will be started in another vein.

If you have any further questions on the use of this medicine, ask your doctor or nurse.

4. Possible side effects

Like all medicines, this medicine can cause side effects, although not everybody gets them. The following side effects may happen with this medicine.

Tell your doctor or nurse straight away if you notice any of the following side effects. These are signs of an allergic reaction and your drip (infusion) may have to be stopped:
- feeling breathless or a tight chest or throat
- headache or back pain
- fever or chills
- swollen or flushed face
- feeling tired, dizzy or light-headed.

If you notice any of the side effects listed above, tell your doctor or nurse straight away.

Other side effects

Very common (may affect more than 1 in 10 people)
- hair loss
- fever, chills, pain
- loss of appetite, diarrhoea, feeling or being sick (nausea or vomiting)
- reduced levels of certain blood cells – your doctor will regularly check your blood for this and decide if any treatment is required. Signs may include:
  - increased bruising
  - sore mouth, throat or mouth ulcers
  - reduced resistance to infection or fever
  - feeling tired or dizzy, having a lack of energy.

Common (may affect up to 1 in 10 people):
- muscle aches, back pain, headache
- difficulty breathing, chest pains
- feeling thirsty, pain or swelling of your food pipe
- shortness of breath, swollen ankles, muscle cramps. These may be signs of heart failure, uneven heart beat or a low potassium level in your blood
- liver function tests abnormal
- difficulty sleeping
- nose bleeds, hot flushes
- constipation, weight loss
- skin rash and nail problems.

Uncommon (may affect up to 1 in 100 people):
- coughing up blood
- feeling agitated, feeling sleepy
- low blood pressure, feeling unwell
- a change in how you walk, speech problems
- stomach pains which may be a sign of a stomach ulcer forming
- muscle weakness
- itchy, dry skin or swollen areas around hair roots
- swollen, red and blistering skin around where the drip was given

- high blood glucose level (your doctor will see this in a blood test)
- yellow skin or eyes. These may be signs of a liver problem called jaundice.
- change in how often you pass water (urine), pain on passing water or blood in your urine

Not Known: frequency cannot be estimated from the available data:
Redness and pain on the hands and feet

Myocet liposomal may cause some side effects that are related to how fast the drip is given. These include flushing, fever, chills, headaches and back pain. These side effects may stop if the drip is given more slowly over a longer period of time.

Reporting of side effects
If you get any side effects, talk to your doctor, pharmacist or nurse. This includes any possible side effects not listed in this leaflet. You can also report side effects directly via the national reporting system listed in Appendix V. By reporting side effects you can help provide more information on the safety of this medicine.

5. How to store Myocet liposomal

- Keep this medicine out of the sight and reach of children.
- Do not use this medicine after the expiry date which is stated on the label and carton.
- Store in a refrigerator (2°C to 8°C).
- From a microbiological point of view, the product should be used immediately. If not used immediately, in-use storage times and conditions prior to use are the responsibility of the user and would normally not be longer than 24 hours at 2°C – 8°C, unless reconstitution and dilution has taken place in controlled and validated aseptic conditions.
- Do not use this medicine if you notice that it shows evidence of discoloration, precipitation or any other particulate matter.
- Do not throw away any medicines via wastewater or household waste. Ask your pharmacist how to throw away medicines you no longer use. These measures will help protect the environment.

6. Content of the pack and other information

What Myocet liposomal contains
- The active substance is liposome–encapsulated doxorubicin. This corresponds to 50 mg doxorubicin hydrochloride.
- The other ingredients are lactose (in the doxorubicin HCl vial), phosphatidylcholine, cholesterol, citric acid, sodium hydroxide and water for injections (in the liposomes vial), and sodium carbonate and water for injections (in the buffer vial).

What Myocet liposomal looks like and contents of the pack
Myocet liposomal consists of a powder, dispersion and solvent for concentrate for dispersion for infusion. It is supplied as a three-vial system: doxorubicin HCl, liposomes and buffer.

Once the content of the vials has been mixed together the resulting liposomal dispersion is orange-red and opaque.

Myocet liposomal is available in cartons containing 1 set or 2 sets of the three constituents. Not all pack-sizes may be marketed.

Marketing Authorisation Holder
Teva B.V.
Swensweg 5
2031 GA Haarlem
Netherlands

Manufacturer
GP-Pharm
Polígon Industrial Els Vinyets - Els Fogars,
Sector 2, Carretera Comarcal C244, km 22
08777 Sant Quintí de Mediona (Barcelona)
Spain

This leaflet was last revised in {MM/YYYY}.

Detailed information on this medicine is available on the European Medicines Agency website: http://www.ema.europa.eu.

The following information is intended for healthcare professionals only:

PREPARATION GUIDE

Myocet liposomal 50 mg powder, dispersion and solvent for concentrate for dispersion for infusion
Liposomal doxorubicin hydrochloride

It is important you read the entire contents of this guide prior to the preparation of this medicinal product.

1. PRESENTATION

Myocet liposomal is supplied as a three-vial system: (1) doxorubicin HCl, (2) liposomes, and (3) buffer. In addition to these three components, 0.9% (w/v) sodium chloride solution for injection will also be required for the reconstitution of the doxorubicin HCl. Myocet liposomal must be reconstituted prior to administration.

2. RECOMMENDATIONS FOR SAFE HANDLING

The normal procedures for proper handling and disposal of anti-tumour medicinal products should be adopted, namely:

- Personnel should be trained to reconstitute the medicinal product.
- Pregnant staff should be excluded from handling the medicinal product.
- Personnel handling this medicinal product during reconstitution should wear protective clothing including masks, goggles and gloves.
- All items for administration or cleaning, including gloves, should be placed in a high-risk, waste disposal bag for high-temperature incineration. Liquid waste may be flushed with large amounts of water.
- Accidental contact with the skin or eyes should be treated immediately with copious amounts of water.

3. PREPARATION FOR THE INTRAVENOUS ADMINISTRATION

Aseptic technique must be strictly observed throughout handling of Myocet liposomal since no preservative is present.

3.1 Preparation of Myocet liposomal

Step 1. Set up

Two alternative heating methods can be used : a Techne DB-3 Dri Block heater or a water bath:

- Turn on the Techne DB-3 Dri Block heater and set the controller to 75°C-76°C. Verify the temperature set point by checking the thermometer(s) on each heat block insert.
- If using a water bath, turn on the water bath and allow it to equilibrate at 58°C (55°C-60°C). Verify the temperature set point by checking the thermometer.

(Please note that whilst the control settings on the water bath and heat block are set to different levels the temperature of the vial contents are in the same range (55°C-60°C)).

- Remove the carton of constituents from the refrigerator.

Step 2. Reconstitute doxorubicin HCl

- Withdraw 20 ml sodium chloride solution for injection (0.9%), (not provided in the package), and inject into each vial of doxorubicin HCl, intended for preparation.
- Shake well in the inverted position to ensure doxorubicin is fully dissolved.

Step 3. Heat in water bath or dry heat block

- Heat the reconstituted doxorubicin HCl vial in the Techne DB-3 Dri Block heater with the thermometer in the block reading (75°C-76°C) for 10 minutes (not to exceed 15 minutes).
- If using a water bath, heat the doxorubicin HCl vial with the thermometer temperature reading 55°C-60°C for 10 minutes (not to exceed 15 minutes).
- While heating proceed to step 4.

Step 4. Adjust pH of liposomes

- Withdraw 1.9 ml of liposomes. Inject into the buffer vial to adjust the pH of liposomes. Pressure build-up may require venting.
- Shake well.

Step 5. Add pH-adjusted liposomes to doxorubicin

- Using a syringe, withdraw the entire vial contents of pH-adjusted liposomes from the buffer vial.
- Remove the reconstituted doxorubicin HCl vial from the water bath or dry heat block. SHAKE VIGOROUSLY. Carefully insert a pressure-venting device equipped with a hydrophobic filter. Then IMMEDIATELY (within 2 minutes) inject the pH-adjusted liposomes into the vial of heated reconstituted doxorubicin HCl. Remove venting device.
- SHAKE VIGOROUSLY.
- WAIT FOR A MINIMUM OF 10 MINUTES BEFORE USING, KEEPING THE MEDICINE AT ROOM TEMPERATURE.

The Techne DB-3 Dri Block Heater is fully validated for use in the constitution of Myocet liposomal. Three inserts, each with two 43.7mm openings per insert must be used. To ensure correct temperature control the use of a 35mm immersion thermometer is recommended.

The resulting reconstituted preparation of Myocet liposomal contains 50 mg of doxorubicin HCl/25 ml of concentrate for liposomal dispersion for infusion (2 mg/ml).

After reconstitution the finished product must be further diluted in 0.9% (w/v) sodium chloride solution for injection, or 5% (w/v) glucose solution for injection to a final volume of 40 ml to 120 ml per 50 mg reconstituted Myocet liposomal so that a final concentration of 0.4 mg/ml to 1.2 mg/ml doxorubicin is obtained.

Once constituted, the liposomal dispersion for infusion containing liposome encapsulated doxorubicin should be a red-orange opaque homogeneous dispersion. All parenteral medicinal products should be inspected visually for particulate matter and discoloration prior to administration. Do not use the preparation if foreign particulate matter is present.

It has been demonstrated that once reconstituted Myocet liposomal has a chemical and physical in-use stability at room temperature for up to 8 hours or in a refrigerator (2°C-8°C) for up to 5 days.

From a microbiological point of view, the product should be used immediately. If not used immediately, in-use storage times and conditions prior to use are the responsibility of the user and would normally not be longer than 24 hours at 2°C-8°C, unless reconstitution and dilution has taken place in controlled and validated aseptic conditions.

Myocet liposomal should be administered by intravenous infusion over a period of 1 hour.
Warning: Myocet liposomal must not be administered by the intramuscular or subcutaneous route or as a bolus injection.

4. DISPOSAL

Any unused product or waste material should be disposed of in accordance with local requirements.

Int. J. Cancer: **122,** 2148–2153 (2008)

Synergistic antitumor activity of the novel SN-38-incorporating polymeric micelles, NK012, combined with 5-fluorouracil in a mouse model of colorectal cancer, as compared with that of irinotecan plus 5-fluorouracil

Takako Eguchi Nakajima[1,2], Masahiro Yasunaga[2], Yasuhiko Kano[3], Fumiaki Koizumi[3], Ken Kato[1], Tetsuya Hamaguchi[1], Yasuhide Yamada[1], Kuniaki Shirao[1], Yasuhiro Shimada[1] and Yasuhiro Matsumura[2]*

[1]*Gastrointestinal Oncology Division, National Cancer Center Hospital, Tokyo, Japan*
[2]*Investigative Treatment Division, Research Center for Innovative Oncology, National Cancer Center Hospital East, Kashiwa, Chiba, Japan*
[3]*Hematology Oncology, Tochigi Cancer Center, Tochigi, Japan*
[4]*Shien Lab Medical Oncology Division, National Cancer Center Hospital, Tokyo, Japan*

The authors reported in a previous study that NK012, a 7-ethyl-10-hydroxy-camptothecin (SN-38)-releasing nano-system, exhibited high antitumor activity against human colorectal cancer xenografts. This study was conducted to investigate the advantages of NK012 over irinotecan hydrochloride (CPT-11) administered in combination with 5-fluorouracil (5FU). The cytotoxic effects of NK012 or SN-38 (an active metabolite of CPT-11) administered in combination with 5FU was evaluated *in vitro* in the human colorectal cancer cell line HT-29 by the combination index method. The effects of the same drug combinations was also evaluated *in vivo* using mice bearing HT-29 and HCT-116 cells. All the drugs were administered i.v. 3 times a week; NK012 (10 mg/kg) or CPT11 (50 mg/kg) was given 24 hr before 5FU (50 mg/kg). Cell cycle analysis in the HT-29 tumors administered NK012 or CPT-11 *in vivo* was performed by flow cytometry. NK012 exerted more synergistic activity with 5FU compared to SN-38. The therapeutic effect of NK012/5FU was significantly superior to that of CPT-11/5FU against HT-29 tumors ($p = 0.0004$), whereas no significant difference in the antitumor effect against HCT-116 tumors was observed between the 2-drug combinations ($p = 0.2230$). Cell-cycle analysis showed that both NK012 and CPT-11 tend to cause accumulation of cells in the S phase, although this effect was more pronounced and maintained for a more prolonged period with NK012 than with CPT-11. Optimal therapeutic synergy was observed between NK012 and 5FU, therefore, this regimen is considered to hold promise of clinical benefit, especially for patients with colorectal cancer.

Key words: NK012; SN-38; 5-fluorouracil; drug delivery system; colorectal cancer

The 5-year survival rates of colorectal cancer (CRC) have improved remarkably over the last 10 years, accounted for in large part by the extensively investigated agents after 5-fluorouracil (5FU), irinoetcan hydrochloride (CPT-11), a water-soluble, semi-synthetic derivative of camptothecin, is one such agent that has been shown to be highly effective, and currently represents a key-drug in first- and second-line treatment regimens for CRC. CPT-11 monotherapy, however, has not been shown to yield superior efficacy, including in terms of the median survival time, to bolus 5FU/leucovorin (LV) alone.[1] In 2 Phase III trials, the addition of CPT-11 to bolus or infusional 5FU/LV regimens clearly yielded greater efficacy than administration of 5FU/LV alone, with a doubling of the tumor response rate and prolongation of the median survival time by 2–3 months.[1,2]

CPT-11 is converted to 7-ethyl-10-hydroxy-camptothecin (SN-38), a biologically active and water-insoluble metabolite of CPT-11, by carboxylesterases in the liver and the tumor. SN-38 has been demonstrated to exhibit up to a 1,000-fold more potent cytotoxic activity than CPT-11 against various cancer cells *in vitro*.[3] The metabolic conversion rate is, however, very low, with only <10% of the original volume of CPT-11 being metabolized to SN-38[4,5]; conversion of CPT-11 to SN-38 also depends on genetic interindividual variability of the activity of carboxylesterases.[6] Direct use of SN-38 itself for clinical cancer treatment must be shown to be identical in terms of both efficacy and toxicity.

Some drugs incorporated in drug delivery systems (DDS), such as Abraxane and Doxil, are already in clinical use.[7,8] The clinical benefits of DDS are based on their EPR effect.[9] The EPR effect is based on the pathophysiological characteristics of solid tumor tissues: hypervascularity, incomplete vascular architecture, secretion of vascular permeability factors stimulating extravasation within cancer tissue, and absence of effective lymphatic drainage from the tumors that impedes the efficient clearance of macromolecules accumulated in solid tumor tissues. Several types of DDS can be used for incorporation of a drug. A liposome-based formulation of SN-38 (LE-SN38) has been developed, and a clinical trial to assess its efficacy is now under way.[10,11]

Recently, we demonstrated that NK012, novel SN-38-incorporating polymeric micelles, exerted superior antitumor activity and less toxicity than CPT-11.[12] NK012 is characterized by a smaller size of the particles than LE-SN38; the mean particle diameter of NK012 is 20 nm. NK012 can release SN-38 under neutral conditions even in the absence of a hydrolytic enzyme, because the bond between SN-38 and the block copolymer is a phenol ester bond, which is stable under acidic conditions and labile under mild alkaline conditions. The release rate of SN-38 from NK012 under physiological conditions is quite high; more than 70% of SN-38 is released within 48 hr. We speculated that the use of NK012, in place of CPT-11, in combination with 5FU may yield superior results in the treatment of CRC. In the present study, we evaluated the antitumor activity of NK012 administered in combination with 5FU as compared to that of CPT-11 administered in combination with 5FU against CRC in an experimental model.

Material and methods

Cells and animals

The human colorectal cancer cell lines used, namely, HT-29 and HCT-116, were purchased from the American Type Culture Collection (Rockville, MD). The HT-29 cells and HCT-116 cells were maintained in RPMI 1640 supplemented with 10% fetal bovine serum (Cell Culture Technologies, Gaggenau-Hoerden, Germany), penicillin, streptomycin, and amphotericin B (100 units/mL, 100 μg/mL, and 25 μg/mL, respectively; Sigma, St. Louis, MO) in a humidified atmosphere containing 5% CO_2 at 37°C.

BALB/c *nu/nu* mice were purchased from SLC Japan (Shizuoka, Japan). Six-week-old mice were subcutaneously (s.c.)

*Correspondence to: Investigative Treatment Division, Research Center for Innovative Oncology, National Cancer Center Hospital East, 6-5-1 Kashiwanoha, Kashiwa, Chiba 277-8577, Japan. Fax: +81-4-7134-6866.
E-mail: yhmatsum@east.ncc.go.jp
Received 2 September 2007; Accepted after revision 20 November 2007
DOI 10.1002/ijc.23381
Published online 14 January 2008 in Wiley InterScience (www.interscience.wiley.com).

inoculated with 1×10^6 cells of HT-29 or HCT-116 cell line in the flank region. The length (a) and width (b) of the tumor masses were measured twice a week, and the tumor volume (TV) was calculated as follows: $TV = (a \times b^2)/2$. All animal procedures were performed in compliance with the Guidelines for the Care and Use of Experimental Animals established by the Committee for Animal Experimentation of the National Cancer Center; these guidelines meet the ethical standards required by law and also comply with the guidelines for the use of experimental animals in Japan.

Drugs

The SN-38-incorporating polymeric micelles, NK012, and SN-38 were prepared by Nippon Kayaku (Tokyo, Japan).[12] CPT-11 was purchased from Yakult Honsha (Tokyo, Japan). 5FU was purchased from Kyowa Hakko (Tokyo, Japan).

Cell growth inhibition assay

HT-29 cells were seeded in 96-well plates at a density of 2,000 cells/well in a final volume of 90 μL. Twenty-four hours after seeding, a graded concentration of NK012 or SN-38 was added concurrently with 5FU to the culture medium of the HT-29 cells in a final volume of 100 μL for drug interaction studies. The culture was maintained in the CO_2 incubator for an additional 72 hr. Then, cell growth inhibition was measured by the tetrazolium salt-based proliferation assay (WST assay; Wako Chemicals, Osaka, Japan). WST-1 labeling solution (10 μL) was added to each well and the plates were incubated at 37°C for 3 hr. The absorbance of the formazan product formed was detected at 450 nm in a 96-well spectrophotometric plate reader. Cell viability was measured and compared to that of the control cells. Each experiment was carried out in triplicate and was repeated at least 3 times. Data were averaged and normalized against the nontreated controls to generate dose-response curves.

Drug interaction analysis

The nature of interaction between NK012 or SN-38 and 5FU against HT-29 cells was evaluated by median-effect plot analyses and the combination index (CI) method of Chou and Talalay.[15] Data analysis was performed using the Calcusyn software (Biosoft, NY, USA). NK012 or SN-38 was combined with 5FU at a fixed ratio that spanned the individual IC_{50} values of each drug. The IC_{50} values were determined on the basis of the dose-response curves using the WST assay. For any given drug combination, the CI is known to represent the degree of synergy, additivity or antagonism. It is expressed in terms of fraction-affected (Fa) values, which represents the percentage of cells killed or inhibited by the drug. Isobologram equations and Fa/CI plots were constructed by computer analysis of the data generated from the median effect analysis. Each experiment was performed in triplicate with 6 gradations and was repeated at least 3 times. The resultant dose-response curves were averaged, to create a single composite dose-response curve for each combination.

In vivo analysis of the effects of NK012 combined with 5FU as compared to those of CPT-11 combined with 5FU

When the mean tumor volumes reached ~93 mm^3, the mice were randomly divided into test groups consisting of 5 mice per group (Day 0). The drugs were administered i.v. *via* the tail vein of the mice. In the groups administered NK012 or 5FU as single agents, the drug was administered on Days 0, 7 and 14. In the combined treatment groups, NK012 or CPT-11 was administered 24 hr before 5FU on Days 0, 7 and 14, according to the previously reported combination schedule for CPT-11 and 5FU.[14] Complete response (CR) was defined as tumor not detectable by palpation at 90 days after the start of treatment, at which time-point the mice were sacrificed. Tumor volume and body weight were measured twice a week. As a general rule, animals in which the tumor volume exceeded 2,000 mm^3 were also sacrificed.

Experiment 1. Evaluation of the effects of NK012 combined with 5FU and determination of the maximum tolerated dose (MTD) of NK012/5FU. By comparing the data between NK012 administered as a single agent and NK012/5FU, we evaluated the effects of the combined regimen against the s.c HT-29 tumors. A preliminary experiment showed that combined administration of NK012 15 mg/kg + 5FU 50 mg/kg every 6 days caused drug-related lethality (data not shown). To determine the MTD, therefore, we set the dosing schedule of the combined regimen at 5 or 10 mg/kg of NK012 + 50 mg/kg of 5FU three times a week.

Experiment 2. Comparison of the antitumor effect of NK012/5FU and CPT-11/5FU. Based on a comparison of the data between NK012/5FU and CPT-11/5FU against the s.c. HT-29 and HCT-116 tumors, we investigated the feasibility of the clinical application of NK012/5FU for the treatment of CRC. CPT-11/5FU was administered three times a week at the respective MTDs of the 2 drugs as previously reported, that is, CPT11 at 50 mg/kg and 5FU at 50 mg/kg, respectively.[14] NK012/5FU was administered once three times a week at the respective MTDs of the 2 drugs determined from Experiment 1.

Cell cycle analysis

Samples from the HT-29 tumors that had grown to 80–100 mm^3 were removed from the mice at 6, 24, 48, 72 and 96 hr after the administration of NK012 alone at 10 mg/kg or CPT-11 alone at 50 mg/kg. The samples were excised, minced in PBS and fixed in 70% ethanol at −20°C for 48 hr. They were then digested with 0.04% pepsin (Sigma chemical Co., St Louis, MO) in 0.1 N HCL for 60 min at 37°C in a shaking bath to prepare single-nuclei suspensions. The nuclei were then centrifuged, washed twice with PBS and stained with 40 μg/mL of propidium iodide (Molecular Probes, OR) in the presence of 100 μg/mL RNase in 1 mL PBS for 30 min at 37°C. The stained nuclei were analyzed with B-D FACSCalibur (BD Biosciences, San Jose, CA), and the cell cycle distribution was analyzed using the Modfit program (Verity Software House Topsham, ME).

Statistical analyses

Data were expressed as mean ± SD. Data were analysed with Student's t test when the groups showed equal variances (F test), or Welch's test when they showed unequal variances (F test). $p < 0.05$ was regarded as statistically significant. All statistical tests were 2-sided.

Results

Antiproliferative effects of NK012 or SN-38 administered in combination with 5FU

Figure 1*a* shows the dose-response curves for NK012 alone, 5FU alone and a combination of the two. The IC_{50} levels of NK012 and 5FU against the HT-29 cells were 39 nM and 1 μM, respectively, and the IC_{50} level of SN-38 was 14 nM (data not shown). Based on these data, the molar ratio of NK012 or SN-38:5FU of 1:1,000 was used for the drug combination studies.

Figures 1*b* and 1*c* show the median-effect and the combination index plots. Combination indices (CIs) of <1.0 are indicative of synergistic interactions between 2 agents; additive interactions are indicated by CIs of 1.0, and antagonism by CIs of >1.0. Figure 1*c* shows the combination index for NK012 and 5FU, when 2 drugs are supposed to be mutually exclusive. Marked synergism was observed between Fa 0.2 and 0.6. Theoretically, the CI method is the most reliable around an Fa of 0.5, suggesting synergistic effects of the combination of NK012 and 5FU. This synergistic effect was more evident than that of SN-38/5FU (Fig. 1*d*).

In vivo *effect of combined NK012 and 5FU*

Experiment 1. Dose optimization and effect of combined NK012 and 5FU against HT-29 tumors. Comparison of the relative tumor volumes on Day 40 revealed significant differences between

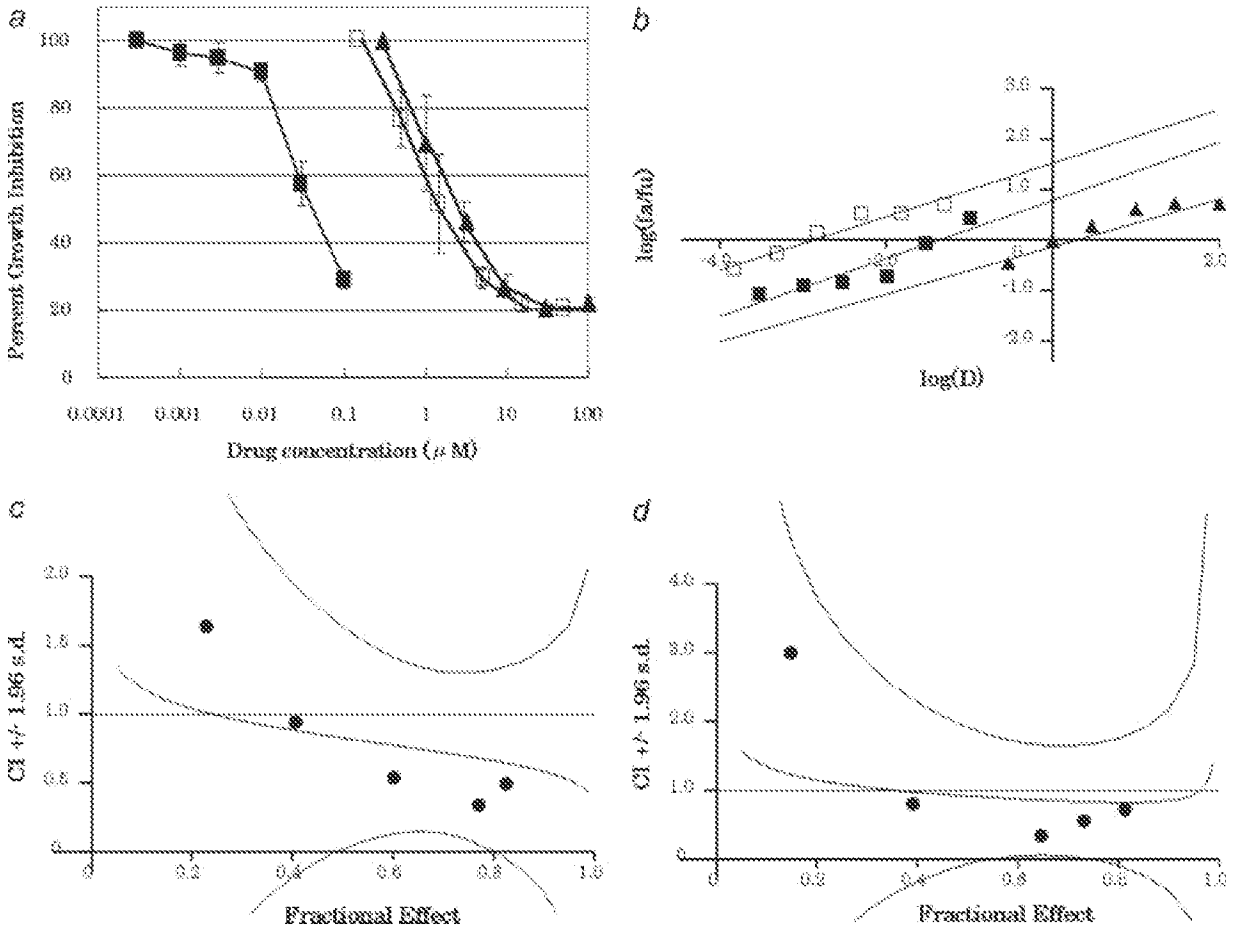

FIGURE 1 – Interaction of NK012 and 5FU *in vitro*. (*a*) Dose-response curves for NK012 alone (●), 5FU alone (▲) and their combination (□) against HT-29 cells. HT-29 cells were seeded at 2,000 cells/well. Twenty-four hours after seeding, a graded concentration of NK012 or 5FU was added to the culture medium of the HT-29 cells. Cell growth inhibition was measured by WST assay after 72 hr of treatment. Cell viability was measured and compared with that of the control cells. Each experiment was carried out independently and repeated at least 3 times. Points, mean of tripricates; bars, SD. (*b*) Median effect plot for the interaction of NK012 and 5FU. (*c*, *d*) Combination index for the interaction as a function of the level of effect (fraction effect = 0.5 is the IC_{50}). The straight line across the CI value of 1.0 indicates additive effect and CIs above and below indicate antagonism and synergism, respectively. The molar ratio of NK012/5FU (*c*) or SN-38/5FU (*d*) at 1:1,000 was tested by CI analysis. Black circles represent the CIs of the actual data points, solid lines represent the computer-derived CIs at effect levels ranging from 10 to 100% inhibition of cell growth, and the dotted lines represent the 95% confidence intervals.

those in the mice administered NK012 alone and those administered NK012/5FU at 5 mg/kg of NK012 ($p = 0.018$) (Fig. 2*a*). Although there was no statistically significant difference in the relative tumor volume measured on Day 54 between the mice administered NK012 alone and NK012/5FU at 10 mg/kg of NK012 ($p = 0.3050$), a trend of superior antitumor effect was demonstrated in the group treated with NK012/5FU at 10 mg/kg of NK012 (Fig. 2*a*). The CR rates were 20, 40 and 60% for 5 mg/kg NK012 + 50 mg/kg 5FU, 10 mg/kg NK012 alone and 10 mg/kg NK012 + 50 mg/kg 5FU, respectively. The schedule of 10 mg/kg NK012 + 50 mg/kg 5FU resulted in no remarkable toxicity in terms of body weight changes, and these doses were determined as representing the MTDs (Fig. 2*b*).

Experiment 2. Comparison of the antitumor effect of combined NK012/5FU and CPT-11/5FU against HT-29 and HCT-116 tumors. The therapeutic effect of NK012/5FU on Day 60 was significantly superior to that of CPT-11/5FU against the HT-29 tumors ($p = 0.0004$) (Fig. 3*a*). A more potent antitumor effect, namely, a 100% CR rate, was obtained in the NK012/5FU group as compared to the 0% CR rate in the CPT-11/5FU group. Although no statistically significant difference in the relative tumor volume on Day 61 was demonstrated between the NK012/5FU and CPT-11/5FU in the case of the HCT-116 tumors ($p = 0.2230$), a trend of superior antitumor effect against these tumors was observed in the NK012/5FU treatment group (Fig. 3*b*). The CR rates for the case of the HCT-116 tumors were 0% in both NK012/5FU and CPT-11/5FU groups.

Specificity of cell cycle perturbation

We studied the differences in the effects between NK012 10 mg/kg and CPT-11 50 mg/kg on the cell cycle (Fig. 4*a*). The data indicated that both NK012 and CPT-11 tended to cause accumulation of cells in the S phase, although the effect of NK012 was stronger and maintained for a more prolonged period than that of CPT-11; the maximal percentage of S-phase cells in the total cell population in the tumors was 34% at 24 hr after the administration of CPT-11, whereas it was 39% at 48 hr after the administration of NK012 (Figs. 4*b*, and 4*c*).

Discussion

Our primary endpoint was to clarify the advantages of NK012 over CPT-11 administered in combination with 5FU. We demonstrated that combined NK012 and 5FU chemotherapy exerts more

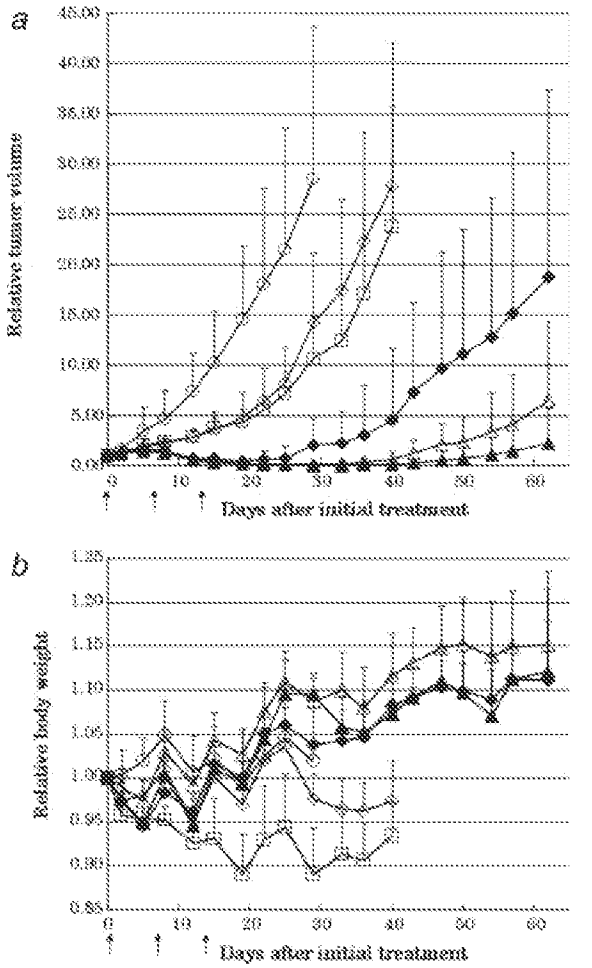

FIGURE 2 – Effect of NK012 alone or NK012 in combination with 5FU against HT-29 tumor-bearing mice. Points, mean; bars, SD. (*a*) Antitumor effect of each regimen on Days 0, 7 and 14. (○) control, (□) 5FU 50 mg/kg alone, (◇) NK012 5 mg/kg alone, (◆) NK012 5 mg/kg 24 hr before 5FU 50 mg/kg, (△) NK012 10 mg/kg alone, (▲) NK012 10 mg/kg 24 hr before 5FU 50 mg/kg. (*b*) Changes in the relative body weight. Data were derived from the same mice as those used in the present study.

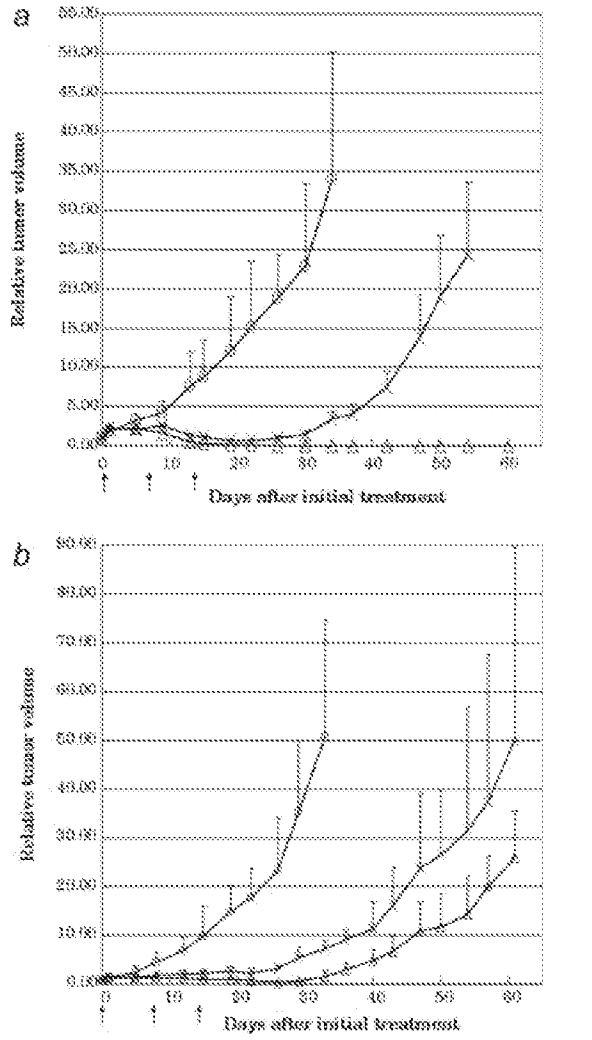

FIGURE 3 – Effect of NK012/5FU as compared with that of CPT11/5FU against HT-29 (*a*) or HCT-116 (*b*) tumor-bearing mice. Antitumor effect of each schedule on Days 0, 7 and 14. (○) control, (◇) CPT-11 50 mg/kg 24 hr before 5FU 50 mg/kg, (△) NK012 10 mg/kg 24 hr before 5FU 50 mg/kg. Points, mean; bars, SD.

synergistic activity *in vitro* and significantly greater antitumor activity against human CRC xenografts as compared to CPT-11/5FU. The combination of NK012 and 5FU is considered to hold promise of clinical benefit for patients with CRC.

CPT-11, a topoisomerase-I inhibitor, and 5FU, a thymidilate synthase inhibitor, have been demonstrated to be effective agents for the treatment of CRC. A combination of these 2 drugs has also been demonstrated to be clearly more effective than either CPT-11 or 5FU/LV administered alone *in vivo* and in clinical settings.[1,2,14] Administration of 5FU by infusion with CPT-11 was shown to be associated with reduced toxicity and an apparent improvement in survival as compared to that of administration of the drug by bolus injection with CPT-11.[1,2] This synergistic enhancement may result from the mechanism of action of the 2 drugs; CPT-11 has been reported to cause accumulation of cells in the S phase, and 5FU infusion is known to cause DNA damage specifically in cells of the S phase.[14] On the basis of this background, our results suggesting the more pronounced and more prolonged accumulation of the tumor cells in the S phase caused by NK012 as compared with that by CPT-11 may explain the more effective synergy of the former administered with 5FU infusion. This may be attributable to accumulation of NK012 due to the enhanced permeability and retention (EPR) effect.[9] It is also speculated that NK012 allows sustained release of free SN-38, which may move more freely in the tumor interstitium.[15] Otherwise NK012 itself could internalize into cells to localize in several cytoplasmic organelles as reported by Savic *et al.*[16] These characteristics of NK012 may be responsible for its more potent antitumor activity observed in this study, because CPT-11 has been reported to show time-dependent growth-inhibitory activity against the tumor cells.[17]

The major dose-limiting toxicities of CPT-11 are diarrhea and neutropenia. SN-38, the active metabolite of CPT-11, may cause CPT-11-related diarrhea as a result of mitotic -inhibitory activity.[18] Because it undergoes significant biliary excretion, SN-38 may have a potentially long residence time in the gastrointestinal tract that may be associated with prolonged diarrhea.[19,20] In our previous report, we evaluated the tissue distribution of SN-38 after administration of an equimolar amount of NK012 (20 mg/kg) and CPT-11 (30 mg/kg), and found no difference in the level of SN-38 accumulation in the small intestine.[12] A significant antitumor effect of NK012 with a lower incidence of diarrhea was also dem-

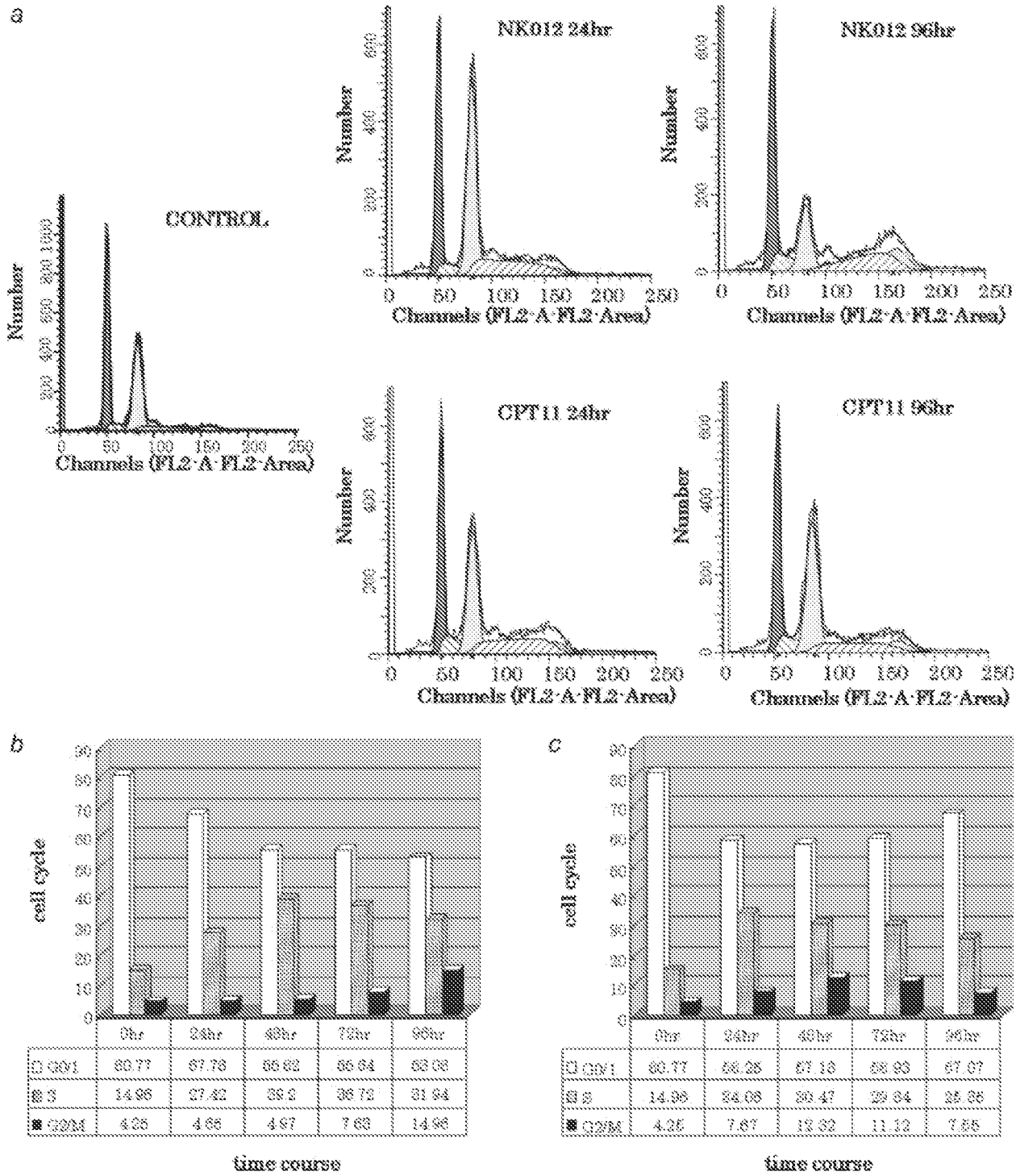

FIGURE 4 -- Cell cycle analysis of HT-29 tumor cells collected 24, 48, 72 and 96 hr after administration of NK012 at 10 mg/kg alone or CPT-11 at 50 mg/kg alone using the Modfit program (Verity Software House Topsham, ME). (*a*) Cell cycle analysis of HT-29 tumor cells 24 and 96 hr after administration of NK012 at 10 mg/kg or CPT-11 at 50 mg/kg, respectively. (*b*) Cell cycle distribution of tumor cells 0, 24, 48, 72 and 96 hr after treatment with NK012 at 10 mg/kg. (*c*) Cell cycle distribution of tumor cells 0, 24, 48, 72 and 96 hr after treatment with CPT-11 at 50 mg/kg.

onstrated as compared to that observed with CPT-11 in a rat mammary tumor model.[21] Combined administration of CPT-11 with 5FU/LV infusion appears to be associated with acceptable toxicity in patients with CRC. In addition, no significant difference in the frequency of Grade 3/4 diarrhea was noted between patients treated with FOLFIRI (CPT-11 regimen with bolus and infusional 5FU/LV) and those treated with FOLFOX6 (oxaliplatin regimen with bolus and infusional 5FU/LV).[22,23] Our *in vivo* data actually revealed no severe body weight loss in the NK012/5FU group. Consequently, we expect that the NK012/5FU regimen, especially

with infusional 5FU, may be an attractive arm for a Phase III trial in CRC, with CPT-11/5FU as the control arm. We have already initiated a Phase I trial of NK012 in patients with advanced solid tumors based on the data suggesting higher efficacy and lower toxicity of this preparation than CPT-11 *in vivo*.[12]

In conclusion, we demonstrated that combined NK012 and 5FU chemotherapy exerts significantly greater antitumor activity against human CRC xenografts as compared to CPT-11/5FU, indicating the necessity of clinical evaluation of this combined regimen.

References

1. Saltz LB, Douillard JY, Pirotta N, Alakl M, Gruia G, Awad L, Elfring GL, Locker PK, Miller LL. Irinotecan plus fluorouracil/leucovorin for metastatic colorectal cancer: a new survival standard. Oncologist 2001;6:81–91.
2. Douillard JY, Cunningham D, Roth AD, Navarro M, James RD, Karasek P, Jandik P, Iveson T, Carmichael J, Alaki M, Gruia G, Awad L, et al. Irinotecan combined with fluorouracil compared with fluorouracil alone as first-line treatment for metastatic colorectal cancer: a multicentre randomised trial. Lancet 2000;355:1041–7.
3. Takimoto CH, Arbuck SG. Topoisomerase I targeting agents: the camptothecins. In: Chabner BA, Lango DL, eds. Cancer chemotherapy and biotherapy: principal and practice, 3rd ed. Philadelphia, PA: Lippincott Williams and Wilkins, 2001. 579–646.
4. Slatter JG, Schaaf LJ, Sams JP, Feenstra KL, Johnson MG, Bombardt PA, Cathcart KS, Verburg MT, Pearson LK, Compton LD, Miller LL, Baker DS, et al. Pharmacokinetics, metabolism, and excretion of irinotecan (CPT-11) following I.V. infusion of [(14)C]CPT-11 in cancer patients. Drug Metab Dispos 2000;28:423–33.
5. Rothenberg ML, Kuhn JG, Burris HA, III, Nelson J, Eckardt JR, Tristan-Morales M, Hilsenbeck SG, Weiss GR, Smith LS, Rodriguez GI, Rock MK, Von Hoff DD. Phase I and pharmacokinetic trial of weekly CPT-11. J Clin Oncol 1993;11:2194–204.
6. Guichard S, Terret C, Hennebelle I, Lochon I, Chevreau P, Fretigny E, Selves J, Chatelut E, Bugat R, Canal P. CPT-11 converting carboxylesterase and topoisomerase activities in tumour and normal colon and liver tissues. Br J Cancer 1999;80:364–70.
7. Gradishar WJ, Tjulandin S, Davidson N, Shaw H, Desai N, Bhar P, Hawkins M, O'Shaughnessy J. Phase III trial of nanoparticle albumin-bound paclitaxel compared with polyethylated castor oil-based paclitaxel in women with breast cancer. J Clin Oncol 2005;23:7794–803.
8. Muggia FM. Liposomal encapsulated anthracyclines: new therapeutic horizons. Curr Oncol Rep 2001;3:156–62.
9. Matsumura Y, Maeda H. A new concept for macromolecular therapeutics in cancer chemotherapy: mechanism of tumoritropic accumulation of proteins and the antitumor agent smancs. Cancer Res 1986;46:6387–92.
10. Zhang JA, Xuan T, Parmar M, Ma L, Ugwu S, Ali S, Ahmad I. Development and characterization of a novel liposome-based formulation of SN-38. Int J Pharm 2004;270:93–107.
11. Kraut EH, Fishman MN, LoRusso PM, Gorden MS, Rubin EH, Haas A, Fetterly GJ, Cullinan P, Dul JL, Steinberg JL. Final result of a phase I study of liposome encapsulated SN-38 (LE-SN38): safety, pharmacogenomics, pharmacokinetics, and tumor response [abstract 2017]. Proc Am Soc Clin Oncol 2005;23:1398.
12. Koizumi F, Kitagawa M, Negishi T, Onda T, Matsumoto S, Hamaguchi T, Matsumura Y. Novel SN-38-incorporating polymeric micelles, NK012, eradicate vascular endothelial growth factor-secreting bulky tumors. Cancer Res 2006;66:10048–56.
13. Chou TC, Talalay P. Quantitative analysis of dose-effect relationships: the combined effects of multiple drugs or enzyme inhibitors. Adv Enzyme Regul 1984;22:27–55.
14. Azrak RG, Cao S, Slocum HK, Toth K, Durrani FA, Yin MB, Pendyala L, Zhang W, McLeod HL, Rustum YM. Therapeutic synergy between irinotecan and 5-fluorouracil against human tumor xenografts. Clin Cancer Res 2004;10:1121–9.
15. Jain RK. Barriers to drug delivery in solid tumors. Sci Am 1994; 271:58–65.
16. Savic R, Luo L, Eisenberg A, Maysinger D. Micellar nanocontainers distribute to defined cytoplasmic organelles. Science 2003;300:615–18.
17. Kawato Y, Aonuma M, Hirota Y, Kuga H, Sato K. Intracellular roles of SN-38, a metabolite of the camptothecin derivative CPT-11, in the antitumor effect of CPT-11. Cancer Res 1991;51:4187–91.
18. Slater R, Radstone D, Matthews L, McDaid J, Majeed A. Hepatic resection for colorectal liver metastasis after downstaging with irinotecan improves survival. Proc Am Soc Clin Oncol 2003;22(abstract 1287).
19. Araki E, Ishikawa M, Iigo M, Koide T, Itabashi M, Hoshi A. Relationship between development of diarrhea and the concentration of SN-38, an active metabolite of CPT-11, in the intestine and the blood plasma of athymic mice following intraperitoneal administration of CPT-11. Jpn J Cancer Res 1993;84:697–702.
20. Atsumi R, Suzuki W, Hakusui H. Identification of the metabolites of irinotecan, a new derivative of camptothecin, in rat bile and its biliary excretion. Xenobiotica 1991;21:1159–69.
21. Onda T, Nakamura I, Seno C, Matsumoto S, Kitagawa M, Okamoto K, Nishikawa K, Suzuki M. Superior antitumor activity of NK012, 7-ethyl-10-hydroxycamptothecin-incorporating micellar nanoparticle, to irinotecan. Proc Am Assoc Cancer Res 2006;47:720s(abstract 3062).
22. Tournigand C, Andre T, Achille E, Lledo G, Flesh M, Mery-Mignard D, Quinaux E, Couteau C, Buyse M, Ganem G, Landi B, Colin P, et al. FOLFIRI followed by FOLFOX6 or the reverse sequence in advanced colorectal cancer: a randomized GERCOR study. J Clin Oncol 2004;22:229–37.
23. Colucci G, Gebbia V, Paoletti G, Giuliani F, Caruso M, Gebbia N, Cartenì G, Agostara B, Pezzella G, Manzione L, Borsellino N, Misino A, et al. Phase III randomized trial of FOLFIRI versus FOLFOX4 in the treatment of advanced colorectal cancer: a multicenter study of the Gruppo Oncologico Dell'Italia Meridionale. J Clin Oncol 2005; 23:4866–75.

TUMOR BIOLOGY AND HUMAN GENETICS

Metronomic irinotecan and standard FOLFIRI regimen as first-line chemotherapy in metastatic colorectal cancer (MCRC). Final results of phase II study

M. Nardi , D. Azzarello , P. Del Medico , R. Giannicola , A. Falzea , C. GiuffrèR. Maisano , V. Panuccio , M. Raffaele , M. Zavettieri , A. Avallone

Azienda Ospedaliera, Reggio Calabria, Italy; IRCCS, Napoli, Italy

Show Less

Abstract

14520

Background: Angiogenesis is necessary to sustain the growth of both the primary tumour and the development of metastases in colorectal cancer. Before the clinical use of bevacizumab, metronomic chemotherapy was the only mean to block the growth of tumor microvessel. CPT-11 showed, in preclinical model, to have antiangiogenetic properties using low doses and weekly administration. We carried out this study in order to evaluate the activity and toxicity of mixed metronomic and standard FOLFIRI regimen in MCRC. **Methods:** From 10/03 to 9/05 we treated 46 pts (24M 22F), median age 66 years (range 41–79), ECOG PS 0–2 with this schedule: CPT- 11 10 mg/mq days 1, 7, 10 and CPT-11 150 mg/mq day 2, l-Folinic Acid 100 mg/mq days 2 and 3, 5-FU 400 mg/mq bolus days 2 and 3 and 5- FU 600 mg/mq 44 hours c.i. days 2 and 3 every two weeks for a maximum of 12 cycles. **Results:**All pts have been evaluable activity and toxicity. We obtained 9 CR (20%), 12 PR (26%) with an ORR of 46% (CI 95%: ±13%) and 17 SD. After a median follow-up of 24 months we registered a median TTP of 10 months and a median OS of 22 months. As regard toxicity, the chemotherapy has been well tolerated; no toxic deaths occurred and no therapy ended for toxicity. 6 pts had 25% dose reduction (standard schedule) for diarrhea G4 after the first cycle. The main toxicities recorded on a total of 440 cycles (cy) delivered were: diarrhea G4 1.7% and G3 2.3% of the cy. Neutropenia G3 5.8% and vomiting G3 0.5% of the cy. Anemia G2 was recorded in 14 pts. All pts suffered from partial alopecia and half of the pts from mild oral mucositis. **Conclusions:** This mixed schedule seems to be active and well tolerated, ORR, TTP and OS are similar to Hurwitz results (NEJM 2004; 350: 2335–42) but with less adverse events. The combination of this schedule with bevacizumab deserves further studies.

No significant financial relationships to disclose.

American Society of Clinical Oncology

NATIONAL CANCER INSTITUTE

Irinotecan Hydrochloride Liposome

(I-rih-noh-TEE-kan HY-droh-KLOR-ide LY-poh-some)

This page contains brief information about irinotecan hydrochloride liposome and a collection of links to more information about the use of this drug, research results, and ongoing clinical trials.

US Brand Name(s)	Onivyde
FDA Approved	Yes

FDA label information for this drug is available at DailyMed.

Use in Cancer

Irinotecan hydrochloride liposome is approved to be used with fluorouracil and leucovorin calcium to treat:

- **Pancreatic cancer** that has metastasized (spread to other parts of the body). It is used in patients whose disease has gotten worse after treatment with gemcitabine hydrochloride.

Irinotecan hydrochloride liposome is also being studied in the treatment of other types of cancer.

Irinotecan hydrochloride liposome is a form of irinotecan hydrochloride contained inside liposomes (very tiny particles of fat). This form may work better than other forms of irinotecan hydrochloride and have fewer side effects. Also, because its effects last longer in the body, it doesn't need to be given as often. For more information about irinotecan hydrochloride that may apply to irinotecan hydrochloride liposome, see the Drug Information Summary for Irinotecan Hydrochloride.

More About Irinotecan Hydrochloride Liposome

Definition from the NCI Drug Dictionary - Detailed scientific definition and other names for this drug.

MedlinePlus Information on Irinotecan Hydrochloride Liposome - A lay language summary of important information about this drug that may include the following:

- warnings about this drug,
- what this drug is used for and how it is used,
- what you should tell your doctor before using this drug,
- what you should know about this drug before using it,
- other drugs that may interact with this drug, and
- possible side effects.

Drugs are often studied to find out if they can help treat or prevent conditions other than the ones they are approved for. This patient information sheet applies only to approved uses of the drug. However, much of the

information may also apply to unapproved uses that are being studied.

Clinical Trials Accepting Patients

Find Clinical Trials for Irinotecan Hydrochloride Liposome - Check for trials from NCI's list of cancer clinical trials now accepting patients.

Important: The drug information on this page is meant to be educational. It is not a substitute for medical advice. The information may not cover all possible uses, actions, interactions, or side effects of this drug, or precautions to be taken while using it. Please see your health care professional for more information about your specific medical condition and the use of this drug.

Posted: October 27, 2015 | **Updated:** March 28, 2019

Vol 43 No 8 August 2005

dtb
Drug and Therapeutics Bulletin

The independent review of medical treatment

5HT$_3$-receptor antagonists as antiemetics in cancer

BNF 4.6 & 8.1

Effective antiemetic therapy is crucial for patients undergoing chemotherapy or radiotherapy for cancer. Severe nausea and vomiting associated with such cancer treatment can lead to anxiety, anorexia, dehydration, electrolyte disturbance and renal failure, and may interrupt cancer therapy, demoralise patients or even cause them to abandon treatment.[1,2] In 1992, we welcomed the introduction of ondansetron, the first selective serotonin type 3- (5HT$_3$-) receptor antagonist marketed in the UK, as an important advance in preventing chemotherapy-induced nausea and vomiting.[3] Several selective 5HT$_3$-receptor antagonists are now licensed. They are widely prescribed to patients receiving cancer treatment, but not always appropriately. Here we review their optimal use.

Treatment-induced nausea and vomiting

Chemotherapy-induced symptoms

The likelihood of nausea and vomiting occurring with chemotherapy will depend on individual patient factors (e.g. symptoms are more common in females, patients with pre-existing nausea and those with nausea and vomiting after previous chemotherapy), and on the chemotherapeutic agents used and their dose.[2,4]

Chemotherapeutic agents are often classed according to their emetogenic potential. Cisplatin is highly emetogenic: without antiemetic therapy, single doses above 50mg/m^2 almost always cause vomiting.[2,4,5] Among non-cisplatin drugs, cyclophosphamide, in doses above 1,000mg/m^2, and dacarbazine, are also highly emetogenic (i.e. likely to induce vomiting in over 90% of patients). With lower doses of cisplatin or cyclophosphamide, the risk of vomiting is still moderately high (60–90%); carboplatin, doxorubicin, ifosfamide, irinotecan and methotrexate are other drugs with a moderate or moderately high emetogenic risk (ranging from 30% to 90%, depending on the dose). Fluorouracil, etoposide and the taxanes have low-to-moderate emetogenicity (10–30%), while bleomycin, chlorambucil and the vinca alkaloids are classed as low risk (fewer than 10% of patients vomit after administration).[2,4,5] With combination therapy, the likelihood of vomiting tends be higher than with single-drug therapy, and is usually determined by the most emetogenic components.

Phases of nausea and vomiting

Specialists recognise three phases of nausea and vomiting associated with chemotherapy: 'acute' (occurring within 24 hours of administration of chemotherapy); 'delayed' (occurring more than 24 hours after administration and lasting for up to 5–7 days); and 'anticipatory' (occurring on the day or hours leading up to chemotherapy).[2,4,5] Anticipatory nausea and vomiting generally only develop when previous chemotherapy has been followed by severe nausea and vomiting, and is believed to represent a conditioned response.[1,2,5]

Prevention of acute nausea and vomiting after administration of chemotherapy is crucial, since poor emetic control in the first 24 hours markedly increases the likelihood both of delayed nausea and vomiting after the dose in question, and of any nausea and vomiting with subsequent chemotherapy.[2] Acute nausea and vomiting after highly emetogenic chemotherapy such as cisplatin are associated with a marked rise in the plasma concentration of serotonin and a corresponding increase in the urinary excretion of 5-hydroxyindoleacetic acid, the main metabolite of serotonin.[6,7] It is believed that the chemotherapy causes enterochromaffin cells in the upper gastrointestinal tract to release serotonin, which acts locally on 5HT$_3$-receptors, triggering afferent impulses to the vomiting centre in the medulla.[6] Selective 5HT$_3$-receptor antagonists appear to work by blocking this pathway.

Without effective prophylaxis, delayed nausea and vomiting reportedly occur in 20–93% of patients after high-dose cisplatin therapy.[8] Delayed vomiting is difficult to treat, and it increases the likelihood of both acute and delayed emesis in subsequent cycles.[2] Unlike with acute nausea and vomiting, there is no evidence that it is associated with release of serotonin and the underlying mechanism is not known.[7] However, recent evidence suggests that release of a neuropeptide, substance P (which acts by binding to a specific neuroreceptor, neurokinin 1), may be important in the genesis of chemotherapy-induced emesis, particularly in the delayed phase.[9]

Radiotherapy-induced nausea and vomiting

With radiotherapy, the degree of nausea and vomiting is related to the dose of radiation administered (per fraction and in total) and to the site and size of the irradiated field.[4,10] Symptoms most commonly follow radiotherapy that involves the whole body or the upper or whole abdomen; they are relatively uncommon after, for example, irradiation of the pelvis, breast or extremities.[4] Acute emesis after exposure to radiotherapy typically occurs after a latent period of 30 minutes to 4 hours and is followed by gradual recovery.[10] This pattern may be repeated after each treatment (which is usually daily), potentially leading to prolonged symptoms.[10]

Available evidence suggests that, as with acute emesis after chemotherapy, nausea and vomiting after radiotherapy may be triggered, at least in part, by serotonin (which is present in high concentrations in the upper abdomen) released from damaged tissues and acting on 5HT$_3$ receptors (locally and in the brain).[11]

The 5HT$_3$-receptor antagonists

Currently, five selective 5HT$_3$-receptor antagonists are licensed for use in the UK – ▼dolasetron, granisetron, ondansetron, ▼palonosetron and tropisetron. All work by the same mechanism and have high affinity and selectivity for the 5HT$_3$ receptor. All may be given by mouth or by injection (ondansetron may also be given as a suppository), except for palonosetron (the most recently licensed drug in this class) which is longer-acting (plasma elimination half-life around 40 hours) and is given as a single intravenous injection before chemotherapy.[12] Ondansetron and granisetron are licensed for use in the prevention and treatment of nausea and vomiting induced by either cancer chemotherapy or radiotherapy in both adults and children; tropisetron (in adults and children), dolasetron (in adults) and palonosetron (in adults) are licensed for use with chemotherapy but not radiotherapy. None of the drugs is indicated for symptomatic relief of nausea and vomiting that are associated with cancer but unrelated to cytotoxic therapy (i.e. that occur more than 7 days after the last treatment). There is very little evidence to support the use of 5HT$_3$-receptor antagonists outside their licensed indications and such use may be harmful.

Efficacy in chemotherapy

Acute nausea and vomiting

Prior to the introduction of selective 5HT$_3$-receptor antagonists in the early 1990s, the most effective regimen for prevention of acute nausea and vomiting after chemotherapy was a combination of the dopamine antagonist, metoclopramide, given in high dosage, with dexamethasone plus either lorazepam or diphenhydramine.[3,13] Subsequently, a meta-analysis of 30 randomised controlled trials (all published before 1996) showed that 5HT$_3$-receptor antagonists (usually given alone, but combined with dexamethasone in some studies) prevented acute chemotherapy-induced vomiting more effectively than did high-dose metoclopramide (with or without dexamethasone and other antiemetics).[14] In the trials involving patients treated with highly emetogenic chemotherapy such as cisplatin (15 studies, a total of 2,634 patients), fewer of those given a 5HT$_3$-receptor antagonist (granisetron, ondansetron or tropisetron) had one or more episodes of vomiting, compared with those given high-dose metoclopramide (40% vs. 51%, odds ratio [OR] 0.60, 95% CI 0.51–0.70). This corresponds to a number-needed-to-treat (NNT) of 9 to prevent 1 additional patient from vomiting at all in the first 24 hours. With moderately emetogenic chemotherapy (11 trials, a total of 1,848 patients), 32% of patients given 5HT$_3$-receptor antagonists vomited, compared with 49% given metoclopramide (in conventional dose) or other antiemetics (OR 0.47, 95% CI 0.39–0.58; NNT 6).[14]

Subsequent randomised trials have generally confirmed this advantage of 5HT$_3$-receptor antagonists, as a class, over dopamine antagonists and other antiemetics. Typically, currently available 5HT$_3$-receptor antagonists will completely protect around 50–80% of patients against acute vomiting in their first cycle of cisplatin-based therapy, and will prevent acute nausea in around 40–70% of patients.[4,9,15] In patients receiving highly emetogenic chemotherapy, a 5HT$_3$-receptor antagonist is generally better tolerated than high-dose metoclopramide.[4,5] In particular, it avoids the unpleasant extrapyramidal effects (such as acute dystonia) and sedation that are associated with the latter treatment.

5HT$_3$-receptor antagonists differ somewhat from one another in their binding affinity at 5HT$_3$ receptors and plasma elimination half-lives.[2] However, when given in currently recommended doses, they appear similarly effective in preventing acute chemotherapy-induced nausea and vomiting.[4,5,15–17] There is some evidence that patients in whom acute symptoms are not controlled by one 5HT$_3$-receptor antagonist may respond to a different 5HT$_3$-receptor antagonist in subsequent cycles.[18,19] Some patients rapidly metabolise certain drugs in this class, which in theory may lead to suboptimal plasma concentrations.[2,9] Since 5HT$_3$-receptor antagonists are not metabolised by precisely the same pathways, it is possible that changing to a different drug may result in better control for individual patients.

Many published studies of 5HT$_3$-receptor antagonists have investigated only the first cycle of chemotherapy. There is conflicting evidence on whether prophylactic efficacy against acute nausea and vomiting is completely maintained in subsequent cycles[16,18,20] or whether it tends to wane.[21]

5HT$_3$-receptor antagonists plus dexamethasone

The efficacy of a 5HT$_3$-receptor antagonist in preventing acute nausea and vomiting after chemotherapy is significantly increased by combination with dexamethasone.[4,5,14] In a meta-analysis of 11 randomised controlled trials (a total of 2,119 patients), comparing a 5HT$_3$-receptor antagonist with the same dose of 5HT$_3$-receptor antagonist plus dexamethasone, fewer patients given the combination vomited in the 24 hours after either highly or moderately emetogenic chemotherapy (24% vs. 41% with a 5HT$_3$-receptor antagonist alone, OR 0.42, 95% CI 0.34–0.51; NNT 6).[14]

In another meta-analysis, of 22 randomised comparisons (mostly double-blind trials in patients on highly emetogenic chemotherapy) involving a total of 3,791 patients, the combination of 5HT$_3$-receptor antagonist plus dexamethasone

increased the chance of having no acute vomiting when compared with 5HT$_3$-receptor antagonist plus either placebo or no treatment (OR 2.29 [95% CI not stated], p<0.0001; NNT 6).[22]

So which regimen for the acute phase?

These findings indicate that the combination of a 5HT$_3$-receptor antagonist plus dexamethasone will provide optimal protection against acute nausea and vomiting following chemotherapy with moderate-to-high emetogenic risk (e.g. above 30%).[4,5] For patients receiving chemotherapy with only a low-to-moderate risk of causing acute nausea and vomiting (e.g. 10–30%), dexamethasone alone (4–8mg intravenously before chemotherapy) will usually provide complete protection.[4,5] For patients receiving chemotherapy with a low emetogenic risk (less than 10%), an oral dopamine antagonist will usually provide satisfactory protection.[4] Domperidone may be a better choice than metoclopramide, as it is less likely to cause unwanted central effects.

Single oral or intravenous doses of 5HT$_3$-receptor antagonists, administered shortly before chemotherapy, appear to be as effective as multi-dose regimens over the first 24 hours after chemotherapy.[4,23,24] Also, clinical trials of 5HT$_3$-receptor antagonists have found little difference in efficacy across a wide range of doses; so for most adults, a single low dose (e.g. 100mg dolasetron, 1–3mg granisetron, 4–8mg ondansetron, 250μg palonosetron, 5mg tropisetron, each given intravenously) will often be adequate.[4] Higher doses may be indicated for highly emetogenic treatments in patients with individual risk factors for acute emesis.

In general, oral and intravenous administration of 5HT$_3$-receptor antagonists appear to provide similar acute antiemetic protection.[4,5] Although we know of no study that has directly compared the oral with the intravenous route for any individual 5HT$_3$-receptor antagonist, double-blind randomised trials have found oral granisetron as effective as intravenously administered ondansetron in patients receiving highly emetogenic[25] or moderately emetogenic chemotherapy.[26] Some guidelines suggest that oral treatment is likely to be more convenient for patients,[2,4] but we know of no evidence that patients undergoing potentially emetogenic chemotherapy prefer to take antiemetics by mouth. Also, many will have a temporary intravenous access line for administration of the cytotoxic drugs and so may prefer to receive antiemetics by this route.

Delayed nausea and vomiting

Following chemotherapy, 5HT$_3$-receptor antagonists are often continued by mouth for several days to help prevent delayed or prolonged emesis. Palonosetron is an exception; because of its long elimination half-life, it is given only once (intravenously) around 30 minutes before chemotherapy and the dose should not be repeated within 7 days.

A systematic review identified 10 double-blind randomised placebo-controlled trials of 5HT$_3$-receptor antagonists, given orally for 2–6 days beyond the first 24 hours after moderately or highly emetogenic chemotherapy.[15] Ondansetron was the most studied drug (used in seven trials). Meta-analysis of the 10 studies (a total of 3,468 patients) found a statistically significant, but small, advantage for 5HT$_3$-receptor antagonists over placebo for the complete prevention of delayed vomiting (overall risk ratio for at least one emetic episode 0.91, 95% CI 0.84–0.97, in favour of 5HT$_3$-receptor antagonists). The absolute difference in complete response rate was only 4–5%, indicating that 20–25 patients would need to be treated with a 5HT$_3$-receptor antagonist in order to prevent delayed vomiting in 1 patient.[15]

Compared with their efficacy in the acute phase, therefore, 5HT$_3$-receptor antagonists, as a class, are much less effective against delayed nausea and vomiting after chemotherapy.[4,5,15] This is in keeping with the finding that plasma serotonin concentrations are not raised during the delayed phase.[7] Preliminary evidence (based on secondary endpoints) from randomised controlled trials has suggested that the longer-acting 5HT$_3$-receptor antagonist, palonosetron, might give useful protection against delayed nausea and vomiting after moderately emetogenic chemotherapy.[12] However, this requires confirmation.

By contrast, a meta-analysis of 16 randomised trials (a total of 2,278 patients) found dexamethasone clearly more effective than placebo in preventing delayed vomiting (OR 2.04, 95% CI 1.63–2.56; NNT 6).[22] Also, in a randomised trial, dexamethasone alone gave significantly better protection against delayed nausea and vomiting than did granisetron.[27] In other randomised studies, ondansetron was no more effective than metoclopramide[28] and less effective than domperidone[29] in preventing delayed nausea or vomiting after highly emetogenic chemotherapy.

Combinations for delayed emesis?

Evidence suggests that, after highly emetogenic chemotherapy, dexamethasone plus another antiemetic may be more effective than dexamethasone alone in preventing delayed-phase vomiting. For example, in a randomised trial in 91 patients, fewer of those treated from day 2 to day 5 with a combination of metoclopramide plus dexamethasone developed delayed vomiting after cisplatin compared with those given dexamethasone alone (48% vs. 65%, p=0.006).[30] By contrast, in a randomised trial involving 708 patients receiving moderately emetogenic chemotherapy, protection against delayed vomiting was not significantly better with dexamethasone plus ondansetron compared with dexamethasone alone.[31]

There appear to be no major differences in efficacy between a 5HT$_3$-receptor antagonist plus dexamethasone combination and a dopamine antagonist plus dexamethasone combination for the prevention of delayed vomiting. In a randomised trial involving 322 patients undergoing cisplatin-based chemotherapy, the combinations of ondansetron (8mg twice daily) plus dexamethasone (4–8mg twice daily) and of metoclopramide (20mg every 6 hours) plus dexamethasone were similarly effective, each preventing delayed vomiting in around 60% of patients.[8] Only in the small subgroup of patients (22% of the total) who had vomiting during the acute phase were the rates of complete prevention of delayed vomiting slightly better with ondansetron plus dexamethasone (28.6% vs. 8.8% with metoclopramide plus dexamethasone, p<0.008).

Which regimen for delayed vomiting?

On the available evidence, dexamethasone (e.g. 4mg twice daily on days 1–3) is the best single agent for preventing delayed nausea and vomiting. Its use in combination with another antiemetic is appropriate after highly emetogenic chemotherapy. However, there seems to be no clear advantage for using a 5HT$_3$-receptor antagonist in preference to a dopamine antagonist (domperidone or metoclopramide), which is cheaper.[4,5,15] A consistent finding is that antiemetic control in the delayed phase is greatly dependent upon good control of emesis in the first 24 hours after chemotherapy.[2]

Anticipatory nausea and vomiting

Optimal prophylaxis against acute and delayed nausea and vomiting, from the start of chemotherapy, is the most effective way of preventing the development of anticipatory nausea and vomiting in subsequent cycles.[1,4] Benzodiazepines (e.g. lorazepam or alprazolam given on the day before or morning of chemotherapy), various behavioural and cognitive treatments, hypnosis and muscle relaxation therapy have been shown to ameliorate symptoms.[1,32] We know of no evidence that 5HT$_3$-receptor antagonists are useful for anticipatory symptoms.

Efficacy in radiotherapy

Evidence from randomised controlled trials on the efficacy of 5HT$_3$-receptor antagonists as antiemetics in patients undergoing radiotherapy is limited. A systematic review identified only five such trials of adequate quality (a total of 399 evaluable patients) and without confounding factors such as concomitant chemotherapy.[33] In one of the largest, involving 109 patients undergoing abdominal radiotherapy, ondansetron was more effective than placebo in achieving complete control of vomiting on the 'worst day' after radiotherapy (relative benefit 1.51, 95% CI 1.06–2.13; NNT around 4), but was not effective against nausea.[34] Another trial compared ondansetron with metoclopramide, both given orally before a single dose of radiotherapy to the upper abdomen, then three times daily.[35] On day 1, a higher proportion of patients on ondansetron were free from vomiting (97% vs. 46% on metoclopramide, $p<0.001$) and nausea (73% vs. 41%, $p=0.001$).[35] Over the first 3 post-treatment days as a whole, control of vomiting was significantly better with ondansetron.[35] In another trial, in 135 patients undergoing abdominal radiotherapy, ondansetron prevented vomiting (but not nausea) more effectively than did prochlorperazine.[36] Other, smaller randomised trials have suggested benefit from ondansetron (vs. placebo) or granisetron (vs. metoclopramide plus dexamethasone and lorazepam) in adults undergoing total body irradiation.[37,38]

Published guidelines recommend prophylaxis with a 5HT$_3$-receptor antagonist (usually with dexamethasone) before each fraction of radiotherapy, and for at least 24 hours afterwards, if the likelihood of nausea and vomiting after radiotherapy is considered high (e.g. when it involves 'high risk' areas of the body such as the upper abdomen).[4]

Approximate cost* of antiemetics in the licensed doses shown in adults receiving chemotherapy

Antiemetic	Regimen	Cost
For prevention of acute phase nausea and vomiting		
5HT$_3$-receptor antagonists	**Doses given before chemotherapy**	
▼dolasetron	100mg i.v. infusion	£13.00
	200mg orally	£14.00
granisetron	3mg by i.v. injection or infusion	£25.80
	1–2mg orally	£6.50–£13.10
ondansetron	8mg by i.v. injection	£12.00
	8mg orally	£7.20
▼palonosetron	250μg by i.v. injection	£55.90
tropisetron	5mg by i.v. injection or infusion	£12.20
Corticosteroids		
dexamethasone	8mg by i.v. injection	£2.00
	8mg orally	£0.40
For oral treatment during the delayed phase		
5HT$_3$-receptor antagonists	**Typical or commonly used regimens**	
▼dolasetron	200mg once daily for 2–3 days	£28.00–£42.00
granisetron	2mg daily for 2–3 days	£26.20–£39.30
ondansetron	8mg twice daily for 2–3 days	£28.80–£43.20
tropisetron	5mg once daily for 2–3 days	£21.50–£32.30
Corticosteroids		
dexamethasone	4mg twice daily for 2–3 days	£0.70–£1.00
Dopamine antagonists		
domperidone	10mg–20mg three to four times daily for 5 days	£0.70–£1.80
metoclopramide	10mg three times daily for 5 days	£0.70

* Based on information in the *Drug Tariff* and *Chemist & Druggist*

Efficacy in children

Antiemetic management, using traditional drugs such as dopamine antagonists or phenothiazines, is only modestly effective in children and adolescents undergoing cancer treatment, and commonly causes troublesome unwanted effects, especially extrapyramidal effects (e.g. acute dystonic reactions) and sedation.[5,39] Although randomised controlled studies are far fewer than in adults, the available evidence shows that, in children, 5HT$_3$-receptor antagonists are significantly more effective than these older drugs for the prevention of acute nausea and vomiting in the 24 hours after chemotherapy with agents with a high or moderately high emetogenic risk, and are much better tolerated.[16,40,41] As in adults, prophylactic efficacy is further enhanced if a 5HT$_3$-receptor antagonist is given with dexamethasone.[42]

Unwanted effects

The most commonly reported unwanted effects of 5HT$_3$-receptor antagonists are constipation and headache. Constipation caused by 5HT$_3$-receptor antagonists may be compounded by the patient's requirement for opiates or other constipating drugs, and can lead to serious problems for patients with cancer, for example, when underlying disease puts the patient at risk of intestinal obstruction. It is therefore crucial that 5HT$_3$-receptor antagonists are not given for longer than is indicated, nor used 'empirically' to reduce nausea that is unrelated to chemotherapy or radiotherapy. Other unwanted effects are generally mild and transient, including light-headedness, abdominal discomfort, fatigue and asymptomatic rises in liver transaminases. ECG changes, including prolongation of the QT_C interval, have been reported with 5HT$_3$-receptor antagonists, so caution is needed before prescribing these drugs to patients with pre-existing cardiac conduction defects or a history of cardiac rhythm disturbance.

Conclusion

Selective 5HT$_3$-receptor antagonists have significantly improved the control of acute nausea and vomiting associated with cancer chemotherapy and radiotherapy. Evidence suggests ▼dolasetron, granisetron, ondansetron and tropisetron have similar efficacy and safety, but their licensed indications differ. Experience with ▼palonosetron is more limited.

Prophylaxis with a 5HT$_3$-receptor antagonist, given orally or intravenously as a single low dose shortly before chemotherapy, together with dexamethasone, is recommended for any adult or child receiving cisplatin or other chemotherapy with a high or moderate-to-high (e.g. above 30%) likelihood of causing nausea and vomiting during the first 24 hours of treatment (the acute phase). For chemotherapy regimens with low-to-moderate emetic risk (10–30%), prophylaxis with dexamethasone alone is usually adequate to prevent acute nausea and vomiting. Use of a 5HT$_3$-receptor antagonist beyond the first 24 hours after chemotherapy, to prevent nausea and vomiting over the following 2–5 days (the delayed phase) offers marginal benefit at best. Dexamethasone, or dexamethasone plus either domperidone or metoclopramide, appears a more cost-effective option after the first day of chemotherapy with an emetogenic regimen.

Patients receiving radiotherapy likely to provoke vomiting (as in irradiation involving the upper abdomen) may benefit from prophylaxis with a 5HT$_3$-receptor antagonist, given as a single dose (usually with dexamethasone) before administration of each fraction.

5HT$_3$-receptor antagonists can cause constipation, which may be severe. For this and other reasons, the drugs should not be used outside their licensed indications, for instance, as empirical treatment for nausea, nor given for longer than is indicated.

[M=meta-analysis; R=randomised controlled trial]

1. Fallowfield LJ. Behavioural interventions and psychological aspects of care during chemotherapy. *Eur J Cancer* 1992; 28A (suppl 1): S39-41.
2. Schnell FM. Chemotherapy-induced nausea and vomiting: the importance of acute antiemetic control. *Oncologist* 2003; 8: 187-98.
3. Ondansetron to prevent chemotherapy-induced vomiting. *DTB* 1992; 30: 21-3.
4. Gralla RJ et al. Recommendations for the use of antiemetics: evidence-based, clinical practice guidelines. *J Clin Oncol* 1999; 17: 2971-94.
5. Antiemetic Subcommittee of the Multinational Association of Supportive Care in Cancer (MASCC). Prevention of chemotherapy- and radiotherapy-induced emesis: results of Perugia Consensus Conference. *Ann Oncol* 1998; 9: 811-9.
6. Cubeddu LX et al. Efficacy of ondansetron (GR 38032F) and the role of serotonin in cisplatin-induced nausea and vomiting. *N Engl J Med* 1990; 322: 810-6.
7. Wilder-Smith OH et al. Urinary serotonin metabolite excretion during cisplatin chemotherapy. *Cancer* 1993; 72: 2239-41.

R 8. The Italian Group for Antiemetic Research. Ondansetron versus metoclopramide, both combined with dexamethasone, in the prevention of cisplatin-induced delayed emesis. *J Clin Oncol* 1997; 15: 124-30.

9. de Wit R. Current position of 5HT$_3$ antagonists and the additional value of NK$_1$ antagonists; a new class of antiemetics. *Br J Cancer* 2003; 88: 1823-7.
10. Feyer PC et al. Aetiology and prevention of emesis induced by radiotherapy. *Support Care Cancer* 1998; 6: 253-60.
11. Scarantino CW et al. On the mechanism of radiation-induced emesis: the role of serotonin. *Int J Radiat Oncol Biol Phys* 1994; 30: 825-30.
12. Asif M et al. Palonosetron. *Drugs* 2004; 64: 1125-32.
13. Kris MG et al. Antiemetic control and prevention of side effects of anti-cancer therapy with lorazepam or diphenhydramine when used in combination with metoclopramide plus dexamethasone. *Cancer* 1987; 60: 2816-22.

M 14. Jantunen IT et al. An overview of randomised studies comparing 5-HT$_3$ receptor antagonists to conventional anti-emetics in the prophylaxis of acute chemotherapy-induced vomiting. *Eur J Cancer* 1997; 33: 66-74.

M 15. Cancer Care Ontario Practice Guidelines Initiative, 2003. *Use of 5-HT$_3$ receptor antagonists in patients receiving moderately or highly emetogenic chemotherapy. Practice Guideline Report #12-3* [online]. Available: http://www.cancercare.on.ca/pdf/full12_3.pdf [Accessed 19 July 2005].

16. Simpson K et al. Tropisetron. An update of its use in the prevention of chemotherapy-induced nausea and vomiting. *Drugs* 2000; 59: 1297-315.

M 17. del Giglio A et al. Granisetron is equivalent to ondansetron for prophylaxis of chemotherapy-induced nausea and vomiting. Results of a meta-analysis of randomized controlled trials. *Cancer* 2000; 89: 2301-8.

R 18. Mantovani G et al. Comparison of granisetron, ondansetron, and tropisetron in the prophylaxis of acute nausea and vomiting induced by cisplatin for the treatment of head and neck cancer: a randomized controlled trial. *Cancer* 1996; 77: 941-8.

R 19. de Wit R et al. Effective cross-over to granisetron after failure to ondansetron, a randomized double blind study in patients failing ondansetron plus dexamethasone during the first 24 hours following highly emetogenic chemotherapy. *Br J Cancer* 2001; 85: 1099-101.

R 20. Cunningham D et al. Optimum anti-emetic therapy for cisplatin induced emesis over repeat courses: ondansetron plus dexamethasone compared with metoclopramide, dexamethasone plus lorazepam. *Ann Oncol* 1996; 7: 277-82.

21. de Wit R et al. Analysis of cumulative probabilities shows that the efficacy of 5HT$_3$ antagonist prophylaxis is not maintained. *J Clin Oncol* 1996; 14: 644-51.

M 22. Ioannidis JP et al. Contribution of dexamethasone to control of chemotherapy-induced nausea and vomiting: a meta-analysis of randomized evidence. *J Clin Oncol* 2000; 18: 3409-22.
R 23. Seynaeve C et al. Comparison of the anti-emetic efficacy of different doses of ondansetron, given as either a continuous infusion or a single intravenous dose, in acute cisplatin-induced emesis. A multicentre, double-blind, randomised, parallel group study. *Br J Cancer* 1992; 66: 192-7.
R 24. Ettinger DS et al. A double-blind comparison of the efficacy of two dose regimens of oral granisetron in preventing acute emesis in patients receiving moderately emetogenic chemotherapy. *Cancer* 1996; 78: 144-51.
R 25. Gralla RJ et al. Single-dose oral granisetron has equivalent antiemetic efficacy to intravenous ondansetron for highly emetogenic cisplatin-based chemotherapy. *J Clin Oncol* 1998; 16: 1568-73.
R 26. Perez EA et al. Comparison of single-dose oral granisetron versus intravenous ondansetron in the prevention of nausea and vomiting induced by moderately emetogenic chemotherapy: a multicenter, double-blind, randomized parallel study. *J Clin Oncol* 1998; 16: 754-60.
R 27. The Italian Group for Antiemetic Research. Dexamethasone, granisetron, or both for the prevention of nausea and vomiting during chemotherapy for cancer. *N Engl J Med* 1995; 332: 1-5.
R 28. De Mulder PH et al. Ondansetron compared with high-dose metoclopramide in prophylaxis of acute and delayed cisplatin-induced nausea and vomiting. A multicenter, randomized, double-blind, crossover study. *Ann Intern Med* 1990; 113: 834-40.
R 29. Esseboom EU et al. Prophylaxis of delayed nausea and vomiting after cancer chemotherapy. *Neth J Med* 1995; 47: 12-7.
R 30. Kris MG et al. Controlling delayed vomiting: double-blind, randomized trial comparing placebo, dexamethasone alone, and metoclopramide plus dexamethasone in patients receiving cisplatin. *J Clin Oncol* 1989; 7: 108-14.
R 31. The Italian Group for Antiemetic Research. Dexamethasone alone or in combination with ondansetron for the prevention of delayed nausea and vomiting induced by chemotherapy. *N Engl J Med* 2000; 342: 1554-9.
R 32. Morrow GR, Morrell C. Behavioral treatment for the anticipatory nausea and vomiting induced by cancer chemotherapy. *N Engl J Med* 1982; 307: 1476-80.
M 33. Tramèr MR et al. Efficacy of 5-HT$_3$ receptor antagonists in radiotherapy-induced nausea and vomiting: a quantitative systematic review. *Eur J Cancer* 1998; 34: 1836-44.
R 34. Franzén L et al. A randomised placebo controlled study with ondansetron in patients undergoing fractionated radiotherapy. *Ann Oncol* 1996; 7: 587-92.
R 35. Priestman TJ et al. Results of a randomized, double-blind comparative study of ondansetron and metoclopramide in the prevention of nausea and vomiting following high-dose upper abdominal irradiation. *Clin Oncol* 1990; 2: 71-5.
R 36. Priestman TJ et al. A prospective randomized double-blind trial comparing ondansetron versus prochlorperazine for the prevention of nausea and vomiting in patients undergoing fractionated radiotherapy. *Clin Oncol* 1993; 5: 358-63.
R 37. Spitzer TR et al. Randomized double-blind, placebo-controlled evaluation of oral ondansetron in the prevention of nausea and vomiting associated with fractionated total-body irradiation. *J Clin Oncol* 1994; 12: 2432-8.
R 38. Prentice HG et al. Granisetron in the prevention of irradiation-induced emesis. *Bone Marrow Transplant* 1995; 15: 445-8.
39. Hewitt M et al. The efficacy and safety of ondansetron in the prophylaxis of cancer-chemotherapy induced nausea and vomiting in children. *Clin Oncol* 1993; 5: 11-4.
R 40. Dick GS et al. Randomised comparison of ondansetron and metoclopramide plus dexamethasone for chemotherapy induced emesis. *Arch Dis Child* 1995; 73: 243-5.
R 41. Hählen K et al. A randomized comparison of intravenously administered granisetron versus chlorpromazine plus dexamethasone in the prevention of ifosfamide-induced emesis in children. *J Pediatr* 1995; 126: 309-13.
R 42. Alvarez O et al. Randomized double-blind crossover ondansetron–dexamethasone versus ondansetron–placebo study for the treatment of chemotherapy-induced nausea and vomiting in pediatric patients with malignancies. *J Pediatr Hematol Oncol* 1995; 17: 145-50.

Ashley Publications
www.ashley-pub.com

Oncologic, Endocrine & Metabolic

Development of ligand-targeted liposomes for cancer therapy

Charles O Noble, Dmitri B Kirpotin, Mark E Hayes, Christoph Mamot, Keelung Hong, John W Park, Christopher C Benz, James D Marks & Daryl C Drummond†
†Hermes Biosciences, Inc., 61 Airport Boulevard, Suite D, South San Francisco, CA 94080, USA

The continued evolution of targeted liposomal therapeutics has resulted in new agents with remarkable antitumour efficacy and relatively mild toxicity profiles. A careful selection of the ligand is necessary to reduce immunogenicity, retain extended circulation lifetimes, target tumour-specific cell surface epitopes, and induce internalisation and subsequent release of the therapeutic substance from the liposome. Methods for assembling targeted liposomes, including a novel micellar insertion technology, for incorporation of targeting molecules that efficiently transforms a non-targeted liposomal therapeutic to a targeted one, greatly assist the translation of targeted liposome technology into the clinic. Targeting strategies with liposomes directed at solid tumours and vascular targets are discussed. The authors believe the development of ligand-targeted liposomes is now in the advanced stage and offers unique and important advantages among other targeted therapies. Anti-HER2 immunoliposomal doxorubicin is awaiting Phase I clinical trials, the results of which should provide new insights into the promise of ligand-targeted liposomal therapies.

Keywords: immunoliposomes, ligand-directed therapeutics, ligand-targeted liposomes, receptor-mediated endocytosis, receptor-targeted liposomes, targeted drug delivery

Expert Opin. Ther. Targets (2004) 8(4):335-353

1. Introduction

The majority of currently available chemotherapy options for the treatment of cancer involve small cytotoxic molecules. Most are relatively nonspecific, and upon administration result in substantial toxicity to other rapidly dividing cells in the body. Liposomes function as drug carriers, capable of altering the pharmacokinetic profile of a drug, delivering the encapsulated agent preferentially to solid tumours, and acting as a slow-release depot for the drug in the diseased tissue [1]. These attributes often result in a more favourable toxicity profile and an improved therapeutic window for use of the agent. Sterically stabilised liposomal doxorubicin, marketed in the USA under the trade name Doxil® (Alza Pharmaceuticals) has been extensively studied and is established as a successful liposomal drug. The poly(ethylene glycol)-grafted (PEGylated) surface of Doxil® liposomes provides for long circulation times and high concentrations of the drug accumulating in solid tumours. Clinical trials have shown clear cut antitumour activity with a largely improved toxicity profile, including reduced cardiotoxicity and haematological toxicities [1,2]. The clinical activity of Doxil® has been shown in a variety of malignancies, including breast cancer, when administered alone or in combination with other anticancer drugs [2-9]. Non-PEGylated liposomal formulations of daunorubicin (Daunoxome®, NeXstar Pharmaceuticals Inc. [10], doxorubicin (Evacet®, Elan Pharmaceuticals) [11], vincristine (Inex Pharmaceuticals) [12], and the camptothecin derivative lurtotecan (OSI Pharmaceuticals) [13]) have also shown activity in clinical trials. Although

present liposomal delivery methods have provided for significant advances in the treatment of cancer, the liposomal drugs developed to date do not afford precise targeting based on the molecular biology of cancer. Thus, improvements in the delivery strategy or encapsulated agent are necessary to engineer a genuinely disease-specific agent that can offer an expanded therapeutic window with which to work.

Therapeutic antibodies such as the anti-HER2 Herceptin® (Genentech), anti-CD20 Rituximab® (IDEC Pharmaceuticals), or anti-CD52 Alemtuzumab® (BTG), and antibody-directed therapeutics such as the anti-CD33 calicheamicin conjugate Mylotarg® (Wyeth/AHA) or anti-CD20 yittrium90 conjugate Ibritumomab® (IDEC Pharmaceuticals), are already playing a more prominent role in the treatment of human malignancies [14-16]. Their ability to alter normal receptor function or direct therapeutics specifically to target cells has resulted in remarkable antitumour efficacy and new hope for patients with previously difficult-to-treat cancers. Therapeutic antibodies can act by inhibiting binding of receptor ligands, regulating downstream receptor functions, inducing apoptosis, or modulating the activity of other therapeutic agents. Antibodies are also being used to direct therapeutics specifically to sites of disease, as is the case for ligand-targeted toxins, low molecular weight drug conjugates, and radioconjugates. Phage display libraries have resulted in rapid improvements in antibody discovery efforts and the development of a large number of antibody fragments, as well as smaller peptide ligands, currently being studied for various therapeutic applications.

The combination of the pharmacokinetic advantages and tumour-selective biodistribution of liposomes with the cell-specific binding and internalisation induced by antibodies or receptor ligands results in what may be considered one of the more attractive strategies for treating human malignancies. Ligand-directed liposomal therapeutics offer several unique characteristics that make them a desirable approach from both a therapeutic and a pharmaceutical development perspective. The 'payload', or amount of drug that can be delivered to a target per one ligand molecule (such as antibody or antibody fragment), is very high. A typical unilamellar immunoliposome with a size of ~ 100 nm encapsulates between 15,000 – 40,000 drug molecules per liposome, but requires only 15 – 40 antibody fragment ligands per liposome for optimum delivery. By contrast, a drug conjugated directly to an antibody usually has a maximum density of 8 – 12 drugs/antibody before antibody binding or physical stability are affected. Ligand-targeted liposomes (LT-Ls) have shown considerably greater efficacy in different tumour models than their corresponding non-targeted liposomal drugs, and in some instances have resulted in complete cures [17-19]. One of these agents, HER2-targeted liposomal doxorubicin, is awaiting Phase I clinical trials in HER2-overexpressing breast cancer patients. This review discusses important considerations in the choice of target for the ligand and design of the ligand-targeted liposomal construct, as well as examples of antibody, small-molecule, and peptide-targeted liposomal agents.

2. Mechanistic rationale for ligand-directed liposomal therapeutics

The rationale for using LT-Ls for the treatment of human cancers includes the combination of many favourable characteristics of both liposomes and the ligand employed for targeting. Liposomes in an aqueous medium have a vesicular structure characterised by one or more lipid bilayer membranes that enclose an aqueous interior space. Antineoplastic agents carried in the liposomal interior are protected from metabolic enzymes, binding to plasma proteins, and associated degradation (e.g., by hydrolysis). When properly formulated for targeted applications, the liposome formulation is stable in the circulation and releases the drug slowly enough to ensure that the bulk of drug release occurs primarily after reaching the target cells or tissues. The encapsulated drug then effectively takes on the pharmacokinetic profile of its liposomal carrier. PEGylation and the selection of highly saturated phospholipid- and cholesterol-containing lipid compositions for the liposome have been shown to result in extended circulation lifetimes [1,20], with a 79 h terminal half-life being reported in humans for PEGylated liposomal doxorubicin [21] and an area under the curve (AUC) for concentration versus time in plasma that is 200 – 1000 times greater than that for most unencapsulated drugs [1]. However, liposomal drugs can be thought of as prodrugs, where the rate of release from the carrier is an equally important determinant of activity. The reported AUC does not report on the concentration of 'active' therapeutic agent, but primarily of the encapsulated agent that must first be liberated from the carrier to act on its pharmacological target. The improved pharmacokinetics and stable encapsulation provide the opportunity for the drug to be effectively delivered to the target tissue, while reducing the delivery of the drug to healthy tissues or its premature metabolic degradation.

In addition, solid tumours are supported by a permeant and often discontinuous microvasculature that allows the passage of large biomolecules or nanoparticles [22]. The combination of this 'leaky' microvasculature and an impaired lymphatics supporting the tumour gives rise to a phenomenon referred to as the enhanced permeability and retention effect (EPR) [23], whereby large molecules or particles first enter and are subsequently retained in solid tumours. Liposomes have been shown to extravasate through the aberrant endothelium and localise in the tumour interstitium [24] or tumour-residing macrophages. This results in a tumour AUC for the liposomal drug that is considerably higher than the free drug, which localises in the tumour rapidly, but is also cleared from the tumour rapidly [25,26]. This passive targeting of tumours allows more of the drug to be delivered selectively to solid tumours, where the drug can be released slowly from its carrier. However, ultimately it is the rate of release from the carrier that determines the concentration of 'active' drug in the tumour.

The targeting ligand adds an additional dimension to the delivery technology, which, when optimised, can result in increased accumulation at the target in the case of readily accessible vascular targets or intracellular delivery in target cells. Blood-borne malignancies and angiogenic blood vessels represent targets readily accessible via the intravascular route, and therefore are less likely to benefit from the EPR phenomenon. However, because of their intravascular localisation, active targeting of these cells is also not limited by extravasation. Targeting ligands that specifically recognise tumour cells via unique or overexpressed epitopes can then direct liposomes to these targets and allow for greater drug delivery and efficacy than with non-targeted formulations or free small-molecule drugs. Ligands that can induce receptor-mediated endocytosis upon binding can deliver their contents intracellularly, where they can be released by degradative enzymes present in late endosomes or lysosomes [1,27]. Site-specific drug release after tumour-specific endocytosis and intracellular processing then results in increased bioavailability of the active drug at the site of the malignancy. Because the drug is delivered intracellularly in the case of optimised and stable ligand-targeted liposomal constructs, ligand targeting can also lead to reduced diffusion of the drug from the tumour, thus increasing its residency time in the tumour and its opportunity to act on cancerous cells. If the drug was not internalised and so released outside of the targeted cell population, then a smaller percentage of the active drug species would be expected to diffuse into the cell and reach the intracellular target for the drug. Finally, liposomes targeted to internalising receptors may be able to partially overcome drug resistance, for example, by circumventing multi-drug resistance transport proteins located at the plasma membrane [28,29]. These various characteristics of LT-Ls therapeutics illustrate the exciting potential of this strategy in treating malignancies.

There are many different barriers that must be overcome in the successful development of a ligand-targeted liposomal drug delivery approach. These include problems associated with specific and homogenous expression of receptors on tumour cells, the sequestration of liposomes by macrophages of the reticuloendothelial system (RES), immunogenicity of the targeting ligand, accessibility of the liposomes to the targeted receptor, the efficiency of endocytosis or the ability to induce endocytosis, the optimisation of drug-release rates from the carrier, and general formulation stability. Each of these obstacles will be addressed as the target selection and design considerations of our targeted carrier is considered.

3. Target selection

Target selection is critical to any immunotargeting approach, although the specific considerations may be quite different depending on what specifically is being targeted. For example, homogenous expression of the antigen is often considered an important criteria for many immunotargeting approaches [30]. Receptor expression in human cancer is both heterogeneous between patients and can show wide variations between tumours in the same patient, and this may complicate both the treatment and the assessment of suitable patients for these therapeutics. However, for liposomal therapeutics delivered to solid tumours where the released drug can act on neighbouring cells via a bystander effect, the question of heterogeneous expression becomes less critical. Taking into account the many complexities involved in the decision-making process and that oversimplification should be guarded against, some general considerations that can be taken into account when selecting a target antigen are now discussed.

The targeted antigen should be selectively expressed or overexpressed on the neoplastic target or on other target tissues, such as angiogenic blood vessels, that support the tumour. High levels of functional expression on accessible nontarget cells will result in nonspecific toxicities that will further complicate this therapeutic approach. The relative degree of overexpression and the tissue localisation of endogenous expression also play an important role in determining the practicality of a particular target. For example, the HER2/neu growth factor receptor is expressed on many breast cancer cell lines, but at significantly different receptor densities, ranging from ~ 10,000 receptors/cell for MCF-7 cells to more than a million receptors/cell for SKBR-3 or BT-474 breast cancer cells. Receptor-mediated endocytosis and cytotoxic activity of HER2-targeted immunoliposomes is observed in the latter cell lines, but not the former [31,32]. There appears to be a threshold effect for internalisation of the immunoliposome in this instance. Although HER/neu is expressed on some healthy tissues [33], including cardiac tissue [34], this threshold effect for activity should protect these healthy tissues, while providing for antitumour activity in receptor-overexpressing cancer cells. A similar dependency on receptor density was noted for liposomes targeted to CD19 [17], although relative to breast cancer cells, a significantly lower receptor density was required on B cells (~ 40,000 receptors/cell) for the targeted liposomes to have an increased therapeutic effect over non-targeted liposomes. The localisation of endogenous expression is also an important consideration. The folate receptor is expressed at low levels on several normal epithelial tissues [35,36]. For large macromolecular carriers, such as liposomes, access to these tissues is restricted by the generally poor permeability of a normal vasculature, while there is ready access to solid tumours overexpressing the folate receptor. Specific expression, antigen density, and endogenous distribution all combine to play a role in the suitability of a particular target for delivery via LT-Ls.

The ability to internalise the ligand-targeted therapeutic is also important in choosing a therapeutic target. Using HER2-targeted liposomal doxorubicin, the authors have observed significant antitumour activity when using an internalising ligand [18], whereas targeting to HER2/neu that did not result in efficient internalisation showed no improvement in antitumour activity when compared to non-targeted liposomes [37]. When liposomes targeted to the internalising CD19 were compared directly to those targeted to the

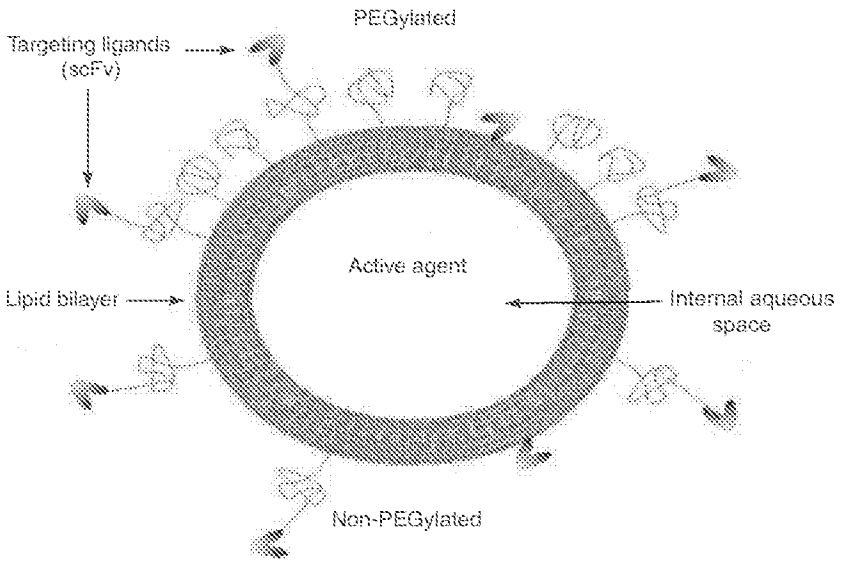

Figure 1. Schematic of a ligand-targeted liposomal therapeutic. The liposome is composed of a lipid bilayer capable of stably encapsulating a therapeutic drug while in the circulation and during prolonged storage. Hydrophilic polymers such as PEG can be attached to the surface of liposomes to increase circulation lifetimes and enhance accumulation in tumours. Finally, targeting molecules such as Fab' fragments can be attached, either directly to the membrane surface or via a spacer.
PEG: Polyethylene glycol.

noninternalising CD20 antigen, a considerable improvement in antitumour activity was seen in the former, but not the latter [38]. Increased anticancer activity has also been observed with other drugs encapsulated within the liposome interior, when they are targeted to internalising receptors [17,29,38,40]. On the other hand, drugs that are associated with the liposome membrane, rather than the liposome interior, only showed targeted activity *in vitro* or *in vivo* to readily accessible targets, even in the absence of internalisation, presumably due to increased drug transfer from the liposome membrane to the target cell subsequent to cell binding. Thus, at least for the drugs that are encapsulated within the liposome interior, liposome internalisation into target cells, as opposed to mere cell surface binding, seems to be important. Therefore, methods for rapidly screening and identifying internalising epitopes, as well as internalisable ligands, have been developed [41,42].

Other important considerations include the degree of shedding of the target antigen and the functionality of the receptor. Many cancers have been shown to shed their membrane antigens, particularly in situations of high tumour load [43,44]. A high degree of shedding will result in binding of the liposomes to soluble antigen and possibly accelerated clearance. The target antigen should also be vital to tumour progression in order that the receptors are not down-modulated during the course of treatment or tumour regression [45]. Careful selection and characterisation of the target antigen will provide a greater opportunity for *in vivo* activity and a reduced potential for unexpected toxicities due to targeting of healthy tissues upon reaching clinical trials.

4. Critical engineering considerations

There are many important design considerations and strategies for assembling LT-Ls therapeutics. Although these are reviewed here, more comprehensive and varying perspectives are given in separate reviews [27,46]. In general, the critical design characteristics include liposome formulation stability while in the general circulation, enablement of long circulating properties for the carrier, proper linkage of the targeting ligand to the liposomal membrane, selection of a stable, specific, and nonimmunogenic targeting ligand, and the choice and compatibility of the active agent for liposome encapsulation. Other important considerations include chemical conjugation strategies and the methods used for assembly of the targeted liposomal construct. Each of these design considerations has a critical role in determining the success of a LT-Ls drug delivery strategy. A schematic showing the basic construction of a LT-Ls drug is shown in Figure 1. In this design, the drug is encapsulated in an internal aqueous space enclosed by a lipid bilayer. The surface of the liposome may be covered with a polymer coat, as in the case of PEGylated, or 'Stealth®' liposomes, and the ligand is linked either close, or 'directly', to the membrane surface, or at a distance, via a polymer linker.

4.1 Development of the targeting ligand

Careful engineering of the targeting ligand for stability, specificity, lack of immunogenicity, internalisation, and ready access to the target receptor are critical to the successful construction of a LT-Ls therapeutic. The first obstacle to overcome is the

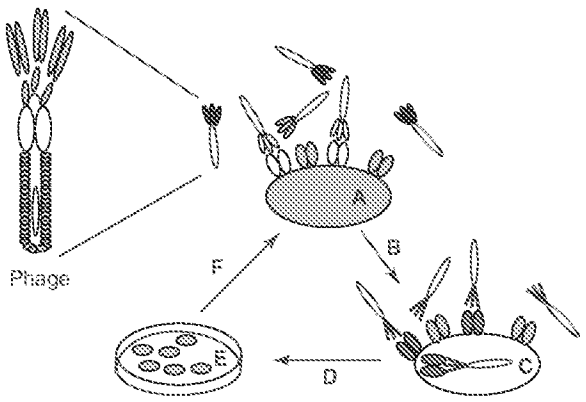

Figure 2. Illustration of phage display technique for selecting target-specific internalising peptide ligands, such as scFv antibodies, from a phage display library [41,42,124].
A. Deplete the number of non-specifically binding/internalising members of a phage display library by incubation with a control cell line that lacks a sufficient number of target epitopes. **B**. Incubate the depleted library with the target cells expressing the target epitope in sufficient number under the conditions (e.g., 37°C) that allow the epitope/phage complex to internalise. **C**. Remove all extracellular phages, including externally bound ones, by washing under epitope-antibody dissociative conditions (e.g., low pH buffer and/or trypsinisation). **D**. Lyse the cells and recover the internalised phage particles. **E**. Re-infect the recovered phage into bacterial host and propagate the phage. **F**. Repeat selection process as needed to obtain a number of highly specific internalising clones.

selection of an appropriate ligand. A wide array of targeting ligands have been utilised in the construction of LT-Ls. These include antibodies or antibody fragments [31,38,47,48], low molecular weight ligands [39,49], protein ligands such as transferrin [50], sugars [51], peptides [52,53], and RNA aptamers [54]. Low molecular weight ligands, such as folic acid [35] should offer the advantage of increased chemical stability, ease of manufacturing, and simple targeted formulation assembly when compared to larger biomolecules such as antibodies. Naturally occurring ligands such as folic acid and transferrin, while nonimmunogenic, may be relatively nonspecific and thus demonstrate considerable toxicities. However, as mentioned above, antigen density-dependent endocytosis and the accessibility of tissues overexpressing the target antigen to macromolecular carriers also play an important role in the feasibility of this approach and should be fully explored. Peptides are commonly incorporated at 300 – 1000 copies per liposome, compared to 20 – 40 copies for carefully optimised antibody fragments [52,55]. Although not fully explored, this elevated ligand density could lead to nonspecific interactions and result in increased clearance.

Libraries of low molecular weight receptor antagonists, RNA aptamers, peptides, and antibody fragments can be screened for specific binding or functional activity. Antibodies or antibody fragments are commonly employed targeting ligands. To reduce immunogenicity, these antibodies should be human or humanised. Administration of murine antibodies into humans generally results in a human antimouse antibody response (HAMA), with increased clearance of subsequent injections of antibodies or antibody-targeted therapeutics. Unfortunately, only a few of the antibodies reported to date in the construction of immunoliposomes have been human [18,29,47,48]. Antibody fragments, such as Fab', Fv, or single chain Fv antibodies, are also preferable to full IgG molecules in the construction of immunoliposomes [29,40,46,56]. The Fc domain of full IgG antibodies is recognised by the Fc receptor present on macrophages of the RES and results in increased clearance of the corresponding immunoliposomes [57,58]. Increased liposome clearance due to either an immune response to a foreign protein or to recognition by the Fc receptor on macrophages decreases the delivery of active agent to the target and thus the activity of the targeted liposomal agent. While technically more challenging, serious efforts to develop targeted liposomes desired for translation into the clinic should take into account these design constraints.

Efficient methods for selecting highly specific and internalising antibodies are essential for rapidly identifying successful targeting ligands. Phage and yeast display of scFv or Fab' nonimmune libraries [59,60] provides a powerful tool for selecting highly specific antibodies. Given the importance of internalisation to the success of targeted liposomal therapies, selection of these libraries based on internalisation, rather than simply binding, provides a narrower and more highly active resultant pool of antibody fragments [41,42]. A diagram depicting the selection process is shown in Figure 2. The authors have used the anti-HER2 scFv (F5), selected using this method, to develop HER2-immunoliposomal doxorubicin, which is currently being readied for Phase I clinical trials [47]. More recently, a prostate cancer-specific antibody was isolated using this approach [48].

4.2 Design of the liposomal carrier

Essential characteristics of the design of liposomes depend on the contemplated route of administration. For the systemic route, these characteristics include the choice of lipid composition, PEGylation, drug-loading methodologies, and size to maximise stability of the formulation in the circulation and efficient *in vivo* delivery to the site of disease. The importance of these various characteristics in the design of liposomal or LT-Ls therapeutics has been well-documented and the complexities involved in the development of long circulating and stable formulations of liposomal therapeutics are described in detail in several reviews [1,26,61]. In general, the preferred liposomes are small (70 – 120 nm in size), charge-neutral, and, in the absence of PEGylation, are composed of mixtures of high-phase transition phospholipids and cholesterol to allow for extended circulation lifetimes. Liposomes coated with polymers, such as PEG, have been shown to be long circulating and are less dependent with respect to clearance on size, membrane fluidity, and surface charge density [1,26].

Formulation stability is as important as extended circulation lifetimes for successful liposomal delivery, and is likely to be an even larger concern for LT-Ls than for non-targeted liposomes.

Some applications favour more rapid leakage of encapsulated agents when delivering via non-targeted liposomes. Liposomal mitoxantrone was shown to be more active when delivered in rapid release formulations in several different tumour models [62], and non-targeted liposomes may also be useful when used simply for drug solubilisation [63] as opposed to tumour-specific delivery. However, in the absence of a readily accessible vascular target, ligand-targeted liposomal therapeutics must stably encapsulate their active agent or there is no significant improvement provided for by increased tumour cell accumulation or internalisation because the drug has leaked from the carrier prior to interacting with the target. The presence of cholesterol and high-phase transition phospholipids help reduce transmembrane diffusion of liposome-encapsulated drugs, and thus improve formulation stability [1,64]. The substitution of sphingomyelin for phosphatidylcholine has also been shown to reduce drug leakage for some agents [65]. Negatively charged PEGylated lipid components have been shown to interfere with *in vivo* stability of liposomal vincristine [65,66], and thus their inclusion to prolong liposome circulation proved detrimental to the tumour-specific delivery of the active agent. Osmotic sensitivities must also be considered when formulating liposomes [67]. Finally, transmembrane gradient-based loading methods play a prominent role in helping stabilise liposomal drug formulations, especially in situations when the drug is gelated or precipitated inside the liposome, thus reducing the drug leakage rate while in circulation [68,69]. Careful attention to liposome formulation details will help ensure that the liposomal drug arrives at the tumour intact and in sufficient quantities to attain antitumour activity.

4.3 Assembly of targeted liposomal therapeutic

The conjugation methodologies for attaching the targeting ligand to the surface of the liposome are important in the stability and reactivity of the targeted formulation, as well as the scalability of the targeted liposomal agent. A lipophilic moiety merged within the lipid portion of the bilayer typically serves as an 'anchor' for ligand attachment. The linkage between the anchor and the ligand should be stable, nonimmunogenic, and should not affect the reactivity of the ligand or the stability of the liposomal drug. The anchor bears a functional group or moiety that forms a covalent or strong noncovalent bond with the ligand. A wide variety of covalent and noncovalent chemical linkages have been used to attach ligands to the surface of liposomes [70,71]. Several lipid-anchored targeting ligands are shown in Figure 3. For the conjugation of antibody fragments the authors prefer the use of maleimide chemistry using either the naturally occurring cysteine residue present in the hinge region for coupling of Fab' fragments or an engineered C-terminal cysteine in the case of scFv molecules (Figure 3a). Others have conjugated antibodies through the reaction of liposome-incorporated lipid-PEG hydrazides with periodate-oxidised sugar moieties [72] or sulfhydryls with pyridyldithiopropionoylamino-PEG--1,2-distearoyl-3-sn-pho-phatidylcholine (DSPE), with sulfhydryls preformed on an antibody molecule [73]. Unstable bonds, such as esters and disulfides, as well as lipid anchors of insufficient affinity to bilayers, may prove suboptimal if the targeting ligand is to remain intact on the liposome surface while in the circulation [71,74,75].

The nonspecific introduction of reactive groups for covalent coupling to lipid anchors can result in decreased cell binding, either due to reactivity with critical binding site residues or due to improper orientation of the ligand following conjugation. The use of molecularly engineered conjugation sites, such as the C-terminal cysteine in scFv [47], or naturally occurring reactive residues located distal to the antigen binding site, including the carbohydrate residues of IgG molecules [72] or reduced cysteines located in the hinge region of antibodies [31], allow for correct orientation of the targeting ligand and conjugation at a site distant from the antigen binding site where it can cause little interference with receptor binding. Coupling conditions, including temperature, pH, and ionic strength should be optimised to prevent denaturation of the protein while providing for sufficient reactivity of the ligand-coupling group. Modification of low molecular weight ligands faces similar challenges. Folate, for example, can be covalently modified at its γ-carboxylate (Figure 3c), but not its α-carboxylate without inhibiting binding to the folate receptor [76].

A polymer linker can also be important in retaining access of the ligand to the receptor. Liposomes targeted using folate were shown to require a PEG linker to distance the low molecular weight ligand from the liposome surface and allow receptor binding [77]. The length of the spacer was later determined to be important in liposomes that already contained PEG-derivatised lipids [78]. Using anti-HER2 Fab' fragments, the authors demonstrated superior binding and internalisation when the Fab' was conjugated to the distal end of PEG, as opposed to directly to the membrane surface [31]. Others have shown a similar improvement upon coupling through a polymer linker [79,80]. Two examples of lipid-anchored targeted ligands coupled through PEG spacers are shown in Figure 3.

Water-soluble, micellar conjugates of the ligand and an amphiphilic lipid anchor co-incubated with preformed liposomes spontaneously insert themselves into liposome bilayers without the loss of the liposome integrity [70]. This 'micellar insertion' technique has provided a rapid and relatively simple method for transforming non-targeted liposomal drugs into antibody-targeted drugs [81,82]. Amphiphilic conjugates of targeting ligands that typically include a hydrophilic polymer spacer between a lipid anchor and a ligand group can be prepared, purified, and characterised separately prior to inserting them into the outer membrane of the liposomal drug [47,83]. High insertion efficiencies (> 80%) are achievable when co-incubation conditions (temperature and duration) are optimised on a case-by-case basis, and remaining extraliposomal material can be subsequently removed using, for example, size

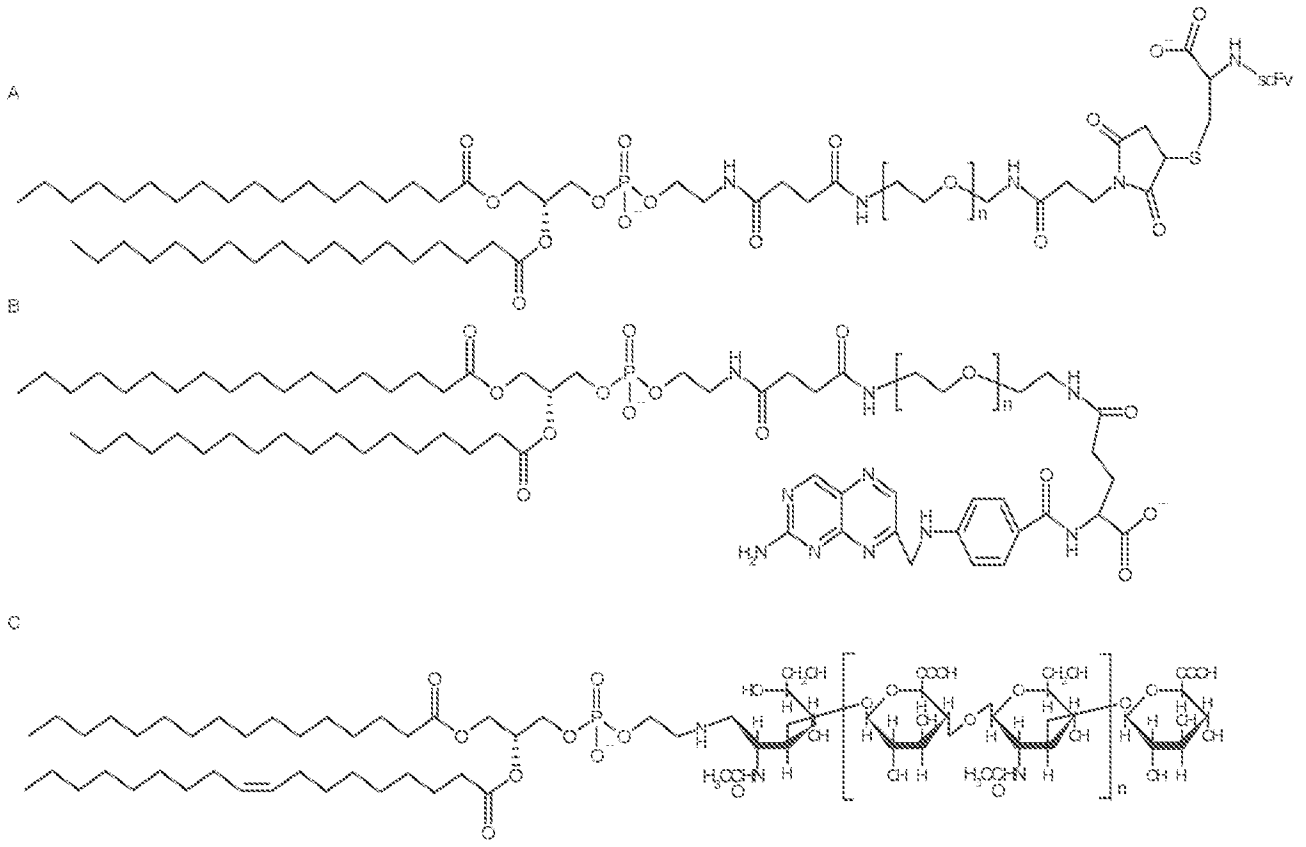

Figure 3. Illustration of various lipid-anchored ligand conjugates for incorporation into liposomes. A. scFv conjugated to maleimido-terminated PEG-DSPE. **B.** Folic acid-PEG conjugated to N-succinyl-DSPE. **C.** Hyaluronic acid conjugated directly to palmitoyl-2-oleoyl-3-phosphatidylethanolamine

DSPE: 1,2-Distearoyl-3-sn-phosphatidylcholine; PEG: Polyethylene glycol.

exclusion chromatography. When insertion is performed at elevated temperatures (55 – 60°C) to accommodate lipid bilayers with higher melting temperatures, denaturation of protein ligands is a concern. However, similar insertion efficiencies can be obtained in the same bilayers by overnight incubation at 37°C [47,81]. The use of micellar insertion avoids the need for exposure of a liposomal formulation to conjugation conditions that may result in destabilisation of the liposomal drug. Finally, the simplicity and reproducibility of this technique will undoubtedly reduce the manufacturing effort as well as batch-to-batch variability of manufactured ligand-targeted liposomes. The totality of the above mentioned intertwined considerations related to selection of a targeting ligand, liposome formulation, and conjugation process are important in developing a ligand-directed liposomal therapeutic with promise for reaching the clinic.

5. Targeting of solid tumours

Targeting of liposomes to both vascular accessible antigens and solid tumour antigens has been attempted with a wide range of targeting molecules, liposome constructs, and tumour types. A list of some of these targeting strategies is shown in **Table 1a** and **b**. The targeting of solid tumours provides a unique set of challenges and opportunities for anticancer therapy using LT-Ls. These are mostly related to the requirement of liposome extravasation for accumulation of drug at the tumour cells and have been addressed more thoroughly in Section 3. Below, the progress made in the development of several examples of LT-Ls directed at solid tumour antigens is described.

5.1 ErbB-targeted immunoliposomes

The epidermal growth factor (EGF) class of receptor tyrosine kinases represent a promising target for immunoliposome therapy. Both epidermal growth factor receptor (EGFR) and HER2 are overexpressed in a variety of different cancers [84] and occur only at low levels in some normal epithelial tissues [33]. The homogenous expression pattern of HER2, even being maintained on distant metastasis [30], lack of significant shedding, internalisation, and its critical role in pathogenesis, all make HER2 an attractive target. EGFR shares many of these traits and has been more widely targeted due in part to its more extensive overexpression in different cancers [85,86].

Table 1a. Drug delivery strategies explored using ligand-targeted liposomal therapeutics and probes in solid tumours.

Extracellular receptor target	Ligand	Active pharmaceutical ingredient	Model	Ref.
HER2	Humanised HER2 Fab' (Herceptin®)	Doxorubicin	Human breast carcinoma (SK-BR-3, BT-474)	[32]
	Human, Fab' and scFv C6.5	Doxorubicin	Human breast carcinoma (BT-474, MDA-MB-453, MCF-7/HER2)	[87]
	Human, scFv F5	Doxorubicin	Human breast carcinoma (BT-474, MDA-MB-453, MCF-7/HER2), human ovarian carcinoma (SKOV3)	[47]
	IgG (N-12A5)	Doxorubicin	HER2-positive human gastric carcinoma (N-87)	[37]
EGFR/EGFRvIII	Chimeric Fab' C225 (erbitux) and human scFv C10		Human epidermoid carcinoma (A-431), mouse fibroblast transfected with EGFRvIII (NR-6M), human breast carcinoma, (MDA-MB-468), human glioma (U87)	[83]
EGFR	Murine EGF	Acridine	Human glioma (U343MGaCl2:6)	[125]
EGFR, human insulin receptor	Murine IgG2a 528 (EGF), 83-14 (HIR)	Plasmid DNA	Human glioma (U87)	[126]
Folate	Folic acid	Doxorubicin	Human nasopharyngeal carcinoma (KB), human epithelial (HeLa)	[76]
		Plasmid DNA	Human nasopharyngeal carcinoma (KB)	[49]
		Doxorubicin	Human nasopharyngeal carcinoma (KB)	[76]
		Ara-C	Human nasopharyngeal carcinoma (KB)	[127]
		Oligonucleotides	Human nasopharyngeal carcinoma (KB)	[116]
Transferrin	IgG2a OX26	Daunomycin	Blood–brain barrier	[128]
Transferrin	Transferrin	Doxorubicin	Rat glioma (C6)	[129]
CD44	Hyaluronic acid	Doxorubicin	Murine melanoma (B16F10)	[51]
GD2	Murine IgG2a, 14.G2a, chimeric IgG ch14.18	Retinoid fenretinide (HPR)	Human melanoma cell line (MZ2-MEL), human melanoma (COLO 853)	[92]
GD2	Fab'	Doxorubicin	Human neuroblastoma (HTLA-230)	[91]
$\alpha_v\beta_3$-integrin	RGD (c(RGDf(e-S-acetylthioacetyl)K)	Doxorubicin	Murine colon carcinoma (C26)	[55]
β_1 integrin	Fab'	Doxorubicin	Non-small cell lung carcinomas	[40]
Anti-ED-B B-fibronectin scFv	ED-B domain of B-fibronectin	5-FdU-NOAC	Human colon epithelial Caco-2	[130]
Unknown (selected on human prostate cancer cells)	Human scFv	Fluorescent label	Prostate cancer (PC3)	[48]
Vasopressin, bradykinin	Antagonist G	Doxorubicin	Small cell lung cancer (NCI-H69)	[53]
Aminopeptidase N	NGR peptide	Doxorubicin	Human neuroblastoma (NB)	[104]

5'-fdU-NOAC: 2'-deoxy-5-fluorouridylyl-N(4)-octadecyl-1-beta-D-arabinofuranosylcytosine; EGF: Epidermal growth factor; EGFR: Epidermal growth factor receptor; HIR: Human insulin receptor.

Table 1b. Drug delivery strategies explored using ligand-targeted liposomal therapeutics and probes in vascular targets.

Extracellular receptor target	Ligand	Active pharmaceutical ingredient	Model	Ref.
VEGFR	Human scFv 4G7	Doxorubicin	Murine endothelial cells (BEND3), human breast carcinoma (SK-BR-3)	[102]
VEGFR (KDR)	Murine IgG 3G2	Calcein dye	CHO, HUVEC, HMEC-1	[100]
VEGFR	VEGF	Doxorubicin and plasmid DNA	Human transformed embryonic kidney cells (293/KDR)	[101]
Vasoactive intestinal peptide receptor	VIP	Tc99m-HMPAO	MNU-induced rat breast cancer	[131]
CD19	Murine IgG2a or Fab'	Doxorubicin and vincristine	Human B lymphoma (Namalwa)	[132]
CD19, CD20	Murine IgG	Doxorubicin	Human B lymphoma (Namalwa)	[38]
P-glycoprotein	Murine IgG MRK-16	Vincristine	Human myelogeneous leukaemia (K-562/ADM)	[133]

CHO: Chinese hamster ovary cells; HMEC: Human microvascular endothelial cells; HMPAO: Hexamethylpropylene amine oxime; HUVEC: Human umbilical vein endothelial cells; KDR: Kinase insert domain containing receptor; MNU: n-methyl nitrosourea; VEGF: Vascular epidermal growth factor; VEGFR: Vascular endothelial growth factor receptor; VIP: Vasoactive intestinal peptide.

The authors have conjugated hybridoma-generated recombinant humanised anti-HER2 Fab' 4D5 [86,87], phage display library-generated recombinant human scFv C6.5 and F5 [47,87], anti-EGFR Fab' proteolytically derived from the recombinant monoclonal antibody (mAb) C225, or phage display library-generated anti-EGFR human scFv (C10) [83], to the surface of liposomes using maleimide chemistry, most commonly utilising a PEG spacer. These liposomes were shown to undergo specific receptor-mediated endocytosis and demonstrated significant cytotoxic activity in receptor-overexpressing cells in culture [31,32,47,83]. An example of this is shown in Figure 4, where EGFR-mediated internalisation (4A) and cytotoxicity (4B) in MDA-MB468 breast cancer cells is demonstrated using anti-EGFR (C225 Fab') immunoliposomes encapsulating either a pH-sensitive fluorescent dye or the anticancer drug vinorelbine, respectively [83]. Control cells (MCF-7), expressing only low levels of the receptors, demonstrated no significant internalisation of the targeted liposomes and had cytotoxic activity similar to non-targeted liposomes. The pharmacokinetics of HER2-targeted liposomes was not affected by conjugation of anti-HER2 Fab' fragments to the surface, showing similar pharmacokinetics to non-targeted liposomes [87]. In addition, multiple injections of the targeted immunoliposomes showed no significant difference in clearance between the first and third weekly injections, suggesting low immunogenicity of this construct.

The antitumour efficacy of HER2-targeted immunoliposomal doxorubicin was studied in multiple xenograft models [87]. Activity was shown to correlate with the degree of receptor overexpression, with up to 55 – 60% complete cures being noted in a HER2-overexpressing BT474 model (Figure 5), and efficacy that was similar to non-targeted liposomal doxorubicin in control MCF7 tumours. Unexpectedly, considerable efficacy was observed in even relatively large tumours (~ 1000 mm^3). In addition, this activity did not appear to be dependent on the direct effects of the antibody on the tumour, as combinations of free Herceptin and liposomal doxorubicin or nondrug loaded HER2-immunoliposomes, showed inferior activity. This is not unexpected, considering the relatively low concentration of antibody fragments being delivered to the tumour. In addition, two of the single chains used for targeting to HER2 were examined for growth inhibition activity in a HER2-overexpressing breast cancer cell line and shown to not have any activity whether displayed monovalently or multivalently, helping to argue against activity for the antibody itself [88]. This suggests the antitumour activity is a result of the specific delivery of immunoliposomal doxorubicin intracellularly as initially proposed. Using a novel formulation of anti-EGFR (C225 Fab')-targeted immunoliposomal epirubicin, the authors were able to demonstrate EGFR-specific antitumour activity in a human glioblastoma (U87) xenograft model, overexpressing both EGFR and EGFRvIII [89]. Similar to the anti-HER2 immunoliposomes, the antitumour activity of the anti-EGFR-immunoliposomal epirubicin was greater than observed for a combination of Cetuximab (C225) and non-targeted liposomal epirubicin in the same U87 xenografts. Biodistribution studies comparing non-targeted and HER2-targeted liposomes have shown nearly identical tumour localisation in HER2-overexpressing cancers, suggesting that extravasation and the EPR effect are primarily responsible for tumour accumulation of liposomes in solid tumours [46]. This finding was substantiated in a separate model when targeting liposomes in a small cell lung cancer model resulted in similar tumour accumulation to non-targeted liposomes [90]. The intratumoural distribution of these liposomes, however, was considerably different. HER2-targeted liposomes delivered to a HER2-overexpressing tumour

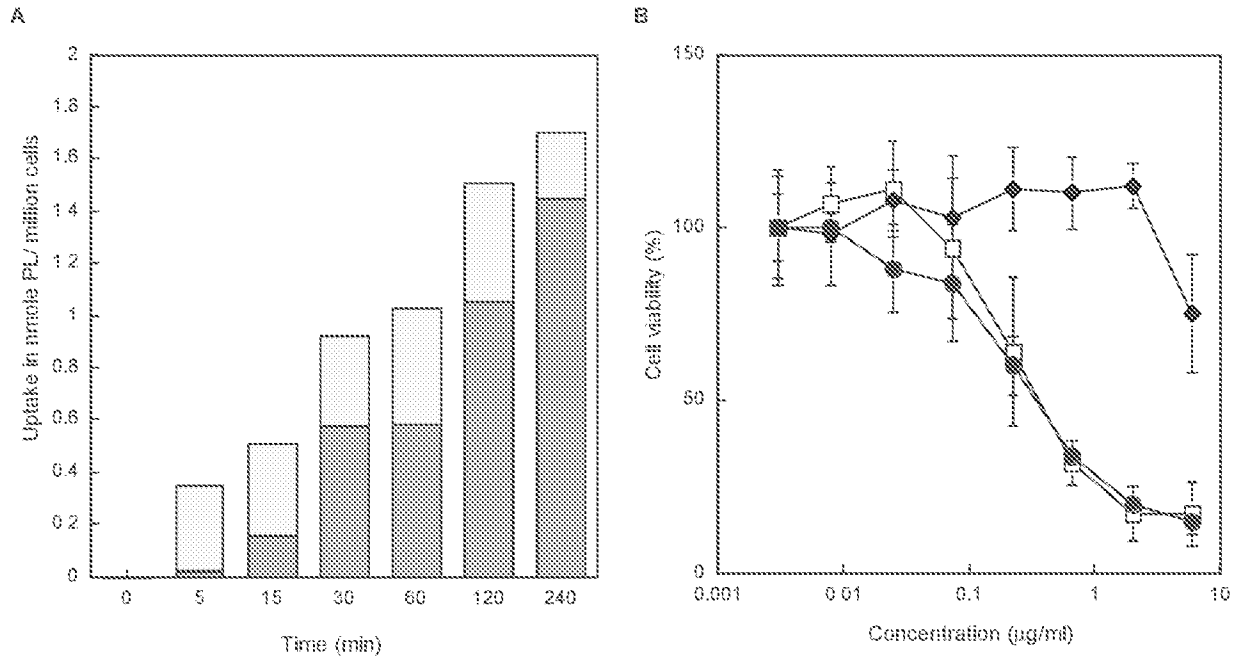

Figure 4. A. Kinetics of uptake of EGFR-targeted ILs in a cell line overexpressing EGFR. ILs loaded with the fluorophore HPTS and targeted with C225-Fab' by an insertion method described previously [46] were incubated with MDA-MB-468 cells at 37°C. At various time points, the fluorescence intensity was measured at excitation wavelengths of 460 and 413 nm (isosbestic point). On the basis of the pH sensitivity of HPTS, total uptake, internalised and surface bound fractions of liposomes were quantified [31]. Bar graph patterns indicate (not internalised; striped fill) versus endocytosed ILs at acidic pH (internalised; solid fill). Data indicate mean; bars, ± S.D.
B. *In vitro* cytotoxicity of EGFR-targeted ILs containing vinorelbine. MDA-MB-468 cells were treated for 2 h with EGFR-targeted ILs (circle), non-targeted liposomes (diamond), or free drug alone (square). The cells were incubated for another 3 days and the cytotoxicity evaluated by a colourimetric cell viability assay that uses MTT. This figure was adapted from [83] with permission from the American Association for Cancer Research.
EGFR: Epidermal growth factor receptor; HPTS: 1-hydroxypyrene-3,6,8-trisulfonic acid; MTT: 3-(4,5-Dimethylthiazol-2-yl)-2,5-diphenyltetrazolium bromide; S.D.: Standard deviation.

model were shown to reside intracellularly in tumour cells and had a more diffuse distribution within the tumour [46]. Non-targeted liposomes localised to the tumour interstitium and inside tumour-associated macrophages. The intratumoural distribution of HER2-targeted liposomes in control MCF-7 breast tumours (~ 10,000 receptors/cell) was similar to non-targeted liposomes. The totality of these results suggest that the marked highly specific antitumour activity observed with anti-HER2 immunoliposomal doxorubicin in HER2-overexpressing models is a result of the efficient *in vivo* delivery of the liposomal therapeutic intracellularly.

5.2 Targeting other solid tumour antigens

CD 44 [51], GD2 [91,92], the folate receptor [1,76,78], transferrin receptor [93], integrins [40], and an unidentified prostate cancer specific antigen [48] are a few of the receptors that have been studied as targets for LT-Ls. The targeting ligands in these studies have been sugars, small molecules (folate), peptides, and antibodies. CD44 expression is elevated in various carcinomas, melanoma, and lymphomas, but at low levels on healthy cells. Liposomal doxorubicin targeted to CD44 using hyaluronic acid oligosaccharides demonstrated CD44-specific binding and cytotoxic activity in B16F10 melanoma cells [51]. The relative difficulty of producing oligosaccharides of a defined structure and achieving site-specific conjugation to a liposome linker pose a challenge for the development of oligosaccharide-linked liposomes.

Another attractive target is disialoganglioside GD2, which is abundant in neuroblastomata and minimally expressed on healthy tissues. Anti-GD2 immunoliposomes containing fenretinide were shown to have cytotoxic activity in culture [92] and potent antitumour activity in a metastatic neuroblastoma model [91,94]. The activity of the targeted liposomal fenretinide was significantly greater than anti-GD2 immunoliposomes in the absence of fenretinide and anti-GD2 mAb alone. The targeting of metastasis is an appealing approach due to the greater accessibility of a targeted liposomal agent to the tumour cells. Liposomes targeted to solid tumours must often rely on a bystander effect to kill cells not located proximal to a discontinuous tumour vessel. Allen and co-workers have targeted metastases again using an IgG mAb directed against mammalian squamous carcinomas [19].

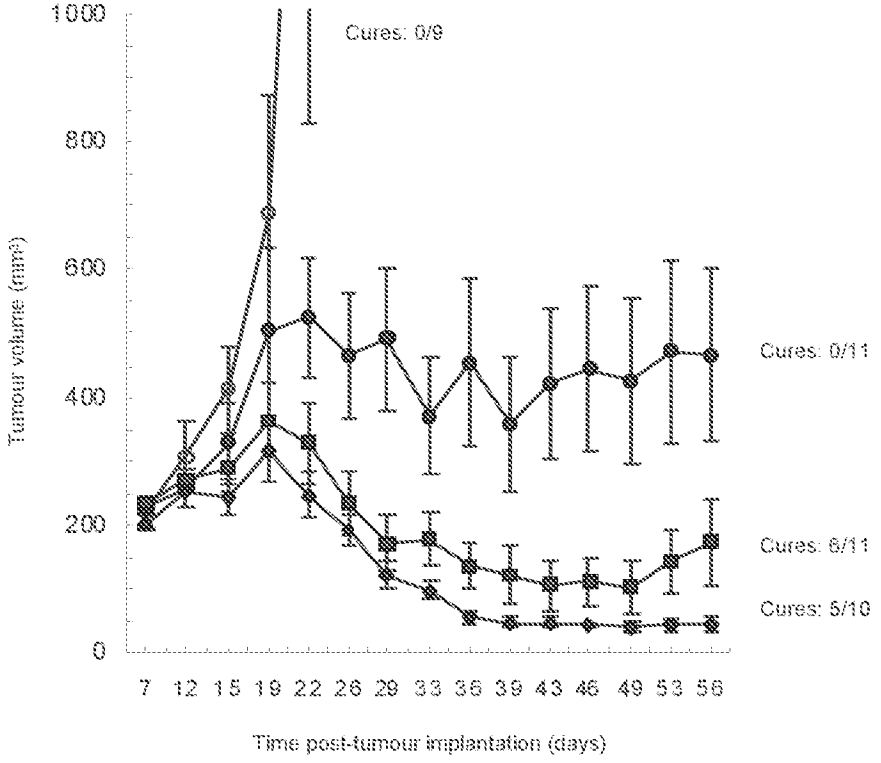

Figure 5. Efficacy of anti-HER2 immunoliposomes containing doxorubicin in a HER2-overexpressing breast cancer xenograft model (BT-474). The anti-HER2 immunoliposomes loaded with doxorubicin contain about 6 mol% PEG/PEG-MAb linkage and either rhuMAb HER2-Fab' (filled squares) or C6.5 scFv (filled diamonds). Control groups also included saline (hollow circles) and sterically stabilised liposomal doxorubicin (Lipodox; filled circles), prepared in an identical manner to the anti-HER2 immunoliposomes containing doxorubicin, but without mAb and given at the same dose and schedule. The liposomes were administered intravenously at a dose of 5 mg/kg every week for 3 weeks on the indicated days post-tumour implantation (arrows). Data represent mean tumour volumes; bars, SE. Adapted from [18] and used with permission from the American Association for Cancer Research.
mAb: Monoclonal antibody; PEG: Polyethylene glycol; SE: Standard error.

Targeted PEGylated liposomal doxorubicin was able to reduce the tumour burden substantially, and to a greater extent than either non-targeted liposomal doxorubicin or free doxorubicin. A study targeting the transferrin receptor with intraperitoneal liposomal cisplatin using human transferrin-conjugated liposomes demonstrated superior efficacy in a human gastric cancer model and elevated accumulation of cisplatin in the peritoneal cavity of nude mice where this cancer disseminated [93]. Immunoliposomal doxorubicin directed against β1-integrins suppressed tumour growth and prevented metastatic spread in a human lung tumour xenograft model [40]. These examples demonstrate the considerable promise of LT-Ls drugs in the treatment of cancer, and in particular in the treatment of metastatic cancers.

Unfortunately, antibody-directed liposome targeting has not always has been shown to lead to higher activity of the encapsulated drug [90,95-97]. In many of these studies it was too difficult to tell the precise reason for the lack of targeting-related improvement. Possible explanations include the lack of internalisation, inferior pharmacokinetics due to increased clearance of the targeted IgG-linked immunoliposome, poor drug encapsulation stability *in vivo*, receptor downregulation, reduced tumour penetration due to the binding site barrier associated with a particularly high affinity ligand, or insufficient antigen or antibody density. These studies underscore the need for careful engineering of the targeted liposomal construct as described in Section 4, and also careful selection of the target receptor.

6. Targeting of vascular antigens

Immunoliposomes targeted to vascular-accessible antigens are not as limited by pharmacokinetic considerations as are those targeted to malignant cells within the stroma of solid tumours. However, they are less likely to benefit from the bystander effect than their counterparts targeted to malignant cell antigens. As can be seen in Table 1a and b, vascular targets include both receptors on angiogenic or pathologic endothelial cells and

those on haematopoietic cells. Typical tumour endothelial targets are vascular endothelial growth factor receptor (VEGFR) and $\alpha_v\beta_3$-integrins. Haematopoietic cancers, including various lymphomas and leukaemias, have been targeted using CD19, CD20, and P-glycoprotein as antigens. The findings of a few of these studies are described in more detail below.

6.1 Angiogenic microvasculature as a target

The vasculature of growing tumours is an attractive target for ligand-directed therapy because of receptors involved with angiogenesis. Such markers can distinguish tumour vasculature from that of healthy tissue allowing for site-specific drug delivery. The nature of angiogenic vasculature lends itself to being a good target for ligand-directed treatment because of its direct exposure to intravenously injected therapeutics. The prospect of vascular targeting involves tumour growth inhibition by triggering apoptosis in the endothelial cells themselves rather than focusing directly on the tumour tissue. Diminishing the blood supply to the rapidly growing tumour cells by drug-induced damage to the vasculature is a promising method for cancer treatment.

A variety of cell surface targets are displayed on the neovasculature of growing tumours. One such target family of interest are integrins, which are involved in cell adhesion. Although their exact role in angiogenesis is not yet determined, it has been demonstrated that $\alpha_v\beta_3$ and $\alpha_v\beta_5$ integrins are overexpressed in tumour angiogenic endothelium [98]. Liposome conjugation of a cyclic 5-mer RGD-peptide (c(RGDf(ε-S-acetylthioacetyl)K, 300 copies/liposome) illustrates the use of these markers as effective endothelial targets [55,99]. Schiffelers *et al.* utilised this strategy for the delivery of doxorubicin to murine C26 colon carcinoma [55]. Biodistribution studies indicate an increase in liver and spleen uptake by the RGD-liposomes compared to that of a control RGD-liposome and non-targeted liposomes with no significant increase in tumour accumulation for the RGD-liposomes over either of the controls. However, efficacy results in the same mouse model indicated that tumour growth after a single intravenous treatment with RGD-LS-DOX (10 mg/kg) was approximately half of that observed for the two control liposomes and untreated tumours ($p < 0.05$).

Another frequently studied antigen of angiogenic tumour vessels is VEGFR. VEGFR-targeted liposomes have been shown to bind to target cells with a much higher affinity compared to non-targeted liposomes [100]. Backer *et al.* demonstrated the effective delivery of doxorubicin and plasmid DNA in cell culture with VEGFR-Ls [101]. The authors have targeted liposomes with an antiVEGFR scFv (4G7) for the delivery of a variety of drugs to endothelial cells overexpressing VEGFR, resulting in VEGFR-specific cytotoxic activity [102,103]. In addition to delivering encapsulated therapeutics, LT-Ls can be utilised to improve the pharmacokinetics of RNA aptamers for binding to the VEGF receptor and blocking its activity [54].

Targeting of liposomal doxorubicin to angiogenic endothelial cells using the NGR peptide to target aminopeptidase N, resulted in an ~ 10-fold increase in liposomal doxorubicin accumulation in orthotopic neuroblastoma xenograft tumours when compared to non-targeted liposomal doxorubicin [104]. The NGR-targeted liposomal doxorubicin resulted in apoptosis of the tumour endothelial cells, an inhibition of metastatic growth, and tumour regressions of the primary tumour. The results obtained while targeting various angiogenic endothelial cell receptors suggest that greater accessibility of the tumour endothelium holds great potential for delivering more liposomal drug to the tumour, considerable antitumour activity, and the flexibility for use with liposomal formulations of drugs where the drug may be released more rapidly than remote-loaded doxorubicin formulations, or cleared more quickly than with highly PEGylated, long-circulating, liposomal drug formulations.

6.2 Haematopoietic targets

One of the more extensively studied areas of LT-Ls research is in the treatment of haematological malignancies. Allen *et al.* thoroughly investigated targeting the CD19 antigen, specifically overexpressed on the surface of B cell malignancies [17,38,95]. Similar to antigens present on the angiogenic microvasculature, the receptors of haematological cancers are readily accessible to circulating liposomes. Targeting lymphoma with liposomes conjugated to antibodies against CD19 allows for selective damage to malignant B cells while leaving T cells unharmed [17]. This approach could help preserve the T cell immune response. An *in vitro* study demonstrating specificity for anti-CD19-LS targeting of $CD19^+$ B cells over CD T cells was demonstrated using flow cytometry [17]. CD19 possesses the desirable characteristic of internalisation upon binding with LT-Ls. Targeting the internalisable CD19 *in vivo* proved more efficacious than targeting the non-internalised CD20 [38]. *In vitro* studies indicate that Namalwa cells accumulate (bound and internalised) anti-CD20-LS to a greater extent that anti-CD19-LS. However, anti-CD19-LS are more efficacious in a mouse model injected with Namalwa cells (survival time of 45.6 ± 4.7 versus 34.3 ± 4.1 days), demonstrating the importance of internalisation for activity gain.

7. Targeted lipoplexes for delivery of therapeutic nucleic acids

Lipid-based vectors hold considerable advantages over their viral counterparts for gene delivery by having fewer immunogenic side effects, low acute toxicities, and a relative ease of preparation [105]. A significant paper by Felgner and co-workers showed that cationic liposomes could form a complex with negatively charged DNA through electrostatic interactions and could successfully introduce exogenous DNA intracellularly [106]. The efficiency of delivery was greater than previously seen with established non-viral delivery methods such as DEAE-dextran or calcium phosphate. Highest transfection efficiencies are typically seen with complexes of net positive charge [105,106], but the cationic component tends to react

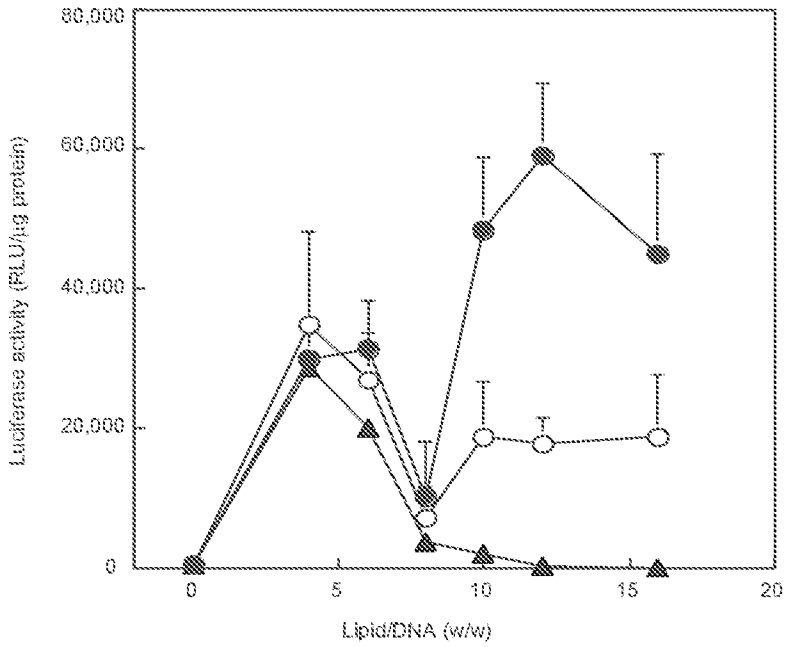

Figure 6. Enhanced expression of folate-targeted lipoplexes. Polylysine-DNA/lipid complexes containing the pRSVL plasmid carrying the luciferase reporter gene were prepare by mixing polylysine-DNA (0.75:1 w/w) complexes with anionic liposomes. KB cells were transfected in serum-free media for 4 h, after which time the media was removed and replaced with fresh serum (10%) containing media. Luciferase activity was measured 48 h post-transfection. Formulations: folate targeted complexes composed of DOPE/CHEMS/folate-PEG-DOPE (6:4:0.01 mol/mol/mol) (filled circle); folate-targeted complexes with 1 mM free folic acid (filled triangle); non-targeted complexes with the lipid composition DOPE/CHEMS (6:4 mol/mol) (empty circle). Error bar = 1 S.D. (n = 3). Adapted from [49] and used with permission from the American Society for Biochemistry and Molecular Biology.

CHEMS: Cholesteryl hemisuccinate; DOPE: Dioleoyl phosphatidylethanolamine; PEG: Polyethylene glycol; RLU: Relative light units; S.D.: Standard deviation.

indiscriminately and binds to most cell surfaces, rendering the particle non-specific and essentially limiting *in vivo* utility.

To this end, many novel methodologies have been devised that attempt to improve the properties of the cationic lipid/DNA complexes to provide suitable candidates for *in vivo* use [107-110]. To further increase the efficacy of lipid-based gene delivery, researchers have often adopted some of the approaches that have been used successfully to enhance liposomal drug delivery. One of these strategies has been to include PEG-lipid derivatives in the formulation in order to improve storage stability [111] and provide longer circulation times [112,113].

Another approach taken is the inclusion of target-specific ligands. Protein or small-molecule ligands that have been used for lipid-based gene targeting include transferrin [114], folic acid [49,115,116], and asialofetuin [117]. Lee and Huang presented a persuasive argument for the benefits of targeting DNA/lipid complexes to folate receptors on a carcinoma cell line *in vitro* (Figure 6) [49]. Using complexes composed of polylysine condensed DNA with dioleoyl phosphatidylethanolamine (DOPE) and the pH-sensitive lipid cholesteryl hemisuccinate (CHEMS), they were able to change the net surface charge by altering the relative lipid composition. At lower lipid/DNA ratios where the particles had a net cationic charge, gene expression levels indicated that there was no targeting effect. However, complexes with higher lipid composition (L/D > 8) were anionic and the differences in activity between targeted and non-targeted preparations were suggested to be a direct result of targeting. The fact that free folic acid partially inhibited transfection at high lipid/DNA ratios confirmed the mechanism of receptor-dependent delivery. Using complexes prepared from the cationic lipid, RPR209120, protamine, and DOPE, a 300 – 400-fold enhancement of gene expression was observed for complexes that were targeted to the folate receptor on M109 cells in the presence of 60% serum, and a 10-fold enhancement of the activity of targeted complexes was observed in mice bearing disseminated intraperitoneal tumours [115].

Recent antibody-targeted approaches to deliver nucleic acids in a lipid-based vector have, for example, utilised anti-CD19 [113], anti-GD2 [118,119], anti-E-selectin [120], anti-transferrin receptor [120,121], and anti-HER2 antibodies or fragments thereof [122,123]. The addition of an anti-HER2 Fab' conjugate to an equimolar DDAB/DOPE liposome/plasmid DNA complex conferred a 15-fold enhancement in transfection activity on HER2-overexpressing cells *in vitro* [122]. Indeed, a similar lipid formulation developed for the delivery of antisense oligonucleotide (asODN) revealed a more intricate targeting effect, demonstrating that HER2-mediated

endocytosis allowed for nuclear localisation of asODN. This was in contrast to the cytoplasmic distribution of oligo, associated with the cationic lipid-mediated internalisation of non-targeted cationic complexes [123]. An *in vitro* study using a 'coated' cationic liposomal (CCL) formulation coupled to an anti-CD19 mAb that recognises an internalising epitope on B cells was found to be effective at delivering the asODN to a multi-drug resistant B lymphoma cell line (Namalwa/MDR_{30}) [113]. The effectiveness of delivery was assessed by a fluorometric assay, which indirectly measured P-glycoprotein expression. This study showed the improved effectiveness of targeted over non-targeted constructs (~ 65% more effective than the targeted sense ODN or non-targeted formulations of either sODN or asODN). In a more recent study, *c-myb* asODN entrapped in a CCL targeted with a mAb against disialoganglioside (GD_2) inhibited the development of human melanoma lung metastases in mice when administered intravenously (10 mg/kg asODN). The inhibition was considerably greater than observed for non-targeted formulations, free asODN or a GD_2 targeted formulation containing a scrambled oligonucleotide [119]. The study also showed significant efficacy of the targeted preparations in the reduction in size of subcutaneous implanted human melanoma xenografts, providing one of the first examples of *in vivo* antitumour activity resulting from targeted delivery of a lipid-based nonviral vector of a therapeutic nucleic acid. Continuing developments in the areas of carrier design with characteristics particularly favourable for *in vivo* applications, and the discovery of suitable ligands for cancer cell recognition, should allow for practical gene therapy approaches for the treatment of cancer in the future.

8. Expert opinion and conclusion

The ability to specifically target anticancer chemotherapeutic drugs to cancer cells *in vivo* is an eagerly anticipated objective of many investigators and clinicians involved in the treatment of cancer. A successful approach holds the promise of reducing nonspecific toxicities to healthy tissues, allowing for both greater concentrations of the drug to be administered and to act at the site of disease. The clinically anticipated results include increased efficacy, a widening of the therapeutic window, greater patient tolerance for the treatment, and an increased quality of life. Under ideal conditions, liposomes at least partially fulfil this promise by securely carrying a cytotoxic drug while in the plasma and then preferentially delivering the drug to the tumour interstitium, due to a discontinuous microvasculature supporting the tumour. However, while liposomes have been shown to offer clear clinical benefits when compared to free drugs in some instances, this type of 'passive' tumour targeting is less than perfect due to difficulties in releasing the drug at appropriate release rates following accumulation in the tumour and partial accumulation in some healthy tissues. In addition, clinical studies offer the potential problem of nonspecific targeting of healthy tissues due to the presence of receptors on nontarget tissues. The resulting increase in toxicity could potentially offset the improvements in activity if this were to occur. The limitations of current animal models make this difficult to predict with absolute certainty, although staining of human tissues for the target receptors provides some guidance. Finally, the heterogeneous expression of receptors on tumour cells both between patients and within the same patient, as a function of time and tumour location, may limit treatment more than observed in more uniform and well-characterised animal models.

Receptor-targeted therapies, including both therapeutic antibodies acting directly on the tumour and ligand conjugates of therapeutic agents, are already making valuable contributions in the clinic for the treatment of cancer. Although the promise of targeted liposomes has not yet been fully recognised, the science is continuing to mature. Significant recent advances in liposome technology and immunoliposome construction, such as the development of novel drug loading methods and micellar insertion technology, have made manufacturing of these intricate liposomal constructs more pragmatic. Advances in construction and selection of appropriate targeting ligands continue to aid in the discovery and characterisation of new targets, and in the discovery of highly selective, stable, and active ligands. Selection based on function, most notably internalisation, has been a major advance. The authors believe the use of chimeric/human/humanised mAb fragments, such as the anti-EGFR Fab' (C225) and the anti-HER2 scFv (F5), should now be considered an absolute requirement in the construction of immunoliposomes. The technology has advanced to the stage where it is no longer out of reach for those seriously considering an immunotargeted therapeutic for translation into the clinic. In collaboration with the National Cancer Institute's Decision Network/Drug Development Group (DDG) program, we have scaled up human anti-HER2 scFv PEG-DSPE to levels required for early clinical trials. The final liposomal construct is currently being readied for Phase I clinical trials. The results of these initial trials and the lessons learned from their development should provide more prospective into both the potential this technology holds, and the direction to proceed forward.

Acknowledgements

This work was supported in part by the National Cancer Institute Specialized Programs of Research Excellence (SPORE) in Breast Cancer (P50-CA 58207-01; JWP, CCB) and Brain Tumours (P50 CA097257-01; JP), the NCI's U54CA90788 (JWP, DBK, JDM), and a contract from the NCI's Unconventional Innovations Programme (N01CO27031-16; KH). Additional support was from the Accelerated Brain Cancer Cure (ABC2) and Pharmacia Ellence Research Fund. DC Drummond is the recipient of a New Investigator Award from the Breast Cancer Research Programme of the University of California, grant number 7KB-0066A.

Bibliography

Papers of special note have been highlighted as either of interest (•) or of considerable interest (••) to readers.

1. DRUMMOND DC, MEYER OM, HONG K, KIRPOTIN DB, PAPAHADJOPOULOS D: Optimizing liposomes for delivery of chemotherapeutic agents to solid tumors. *Pharmacol. Rev.* (1999) 51:691-743.

•• **Detailed review describing criteria for optimising conventional and sterically stabilised liposomes.**

2. MUGGIA FM, HAINSWORTH JD, JEFFERS S *et al.*: Phase II study of liposomal doxorubicin in refractory ovarian cancer: antitumor activity and toxicity modification by liposomal encapsulation. *J. Clin. Oncol.* (1997) 15:987-993.

3. EANSON MR, CHEESEMAN S, WHITE S, MARGESON J: Caelyx (stealth liposomal doxorubicin) in the treatment of advanced breast cancer. *Crit. Rev. Oncol. Hematol.* (2001) 37:115-120.

4. CAMPOS SM, PENSON RT, MAYS AR *et al.*: The clinical utility of liposomal doxorubicin in recurrent ovarian cancer. *Gynecol. Oncol.* (2001) 81:206-212.

5. GORDON AN, FLEAGLE JT, GUTHRIE D *et al.*: Recurrent epithelial ovarian carcinoma: a randomized phase III study of pegylated liposomal doxorubicin versus topotecan. *J. Clin. Oncol.* (2001) 19:3312-3322.

6. SAFRA T, GROSHEN S, JEFFERS S *et al.*: Treatment of patients with ovarian carcinoma with pegylated liposomal doxorubicin: analysis of toxicities and predictors of outcome. *Cancer* (2001) 91:90-100.

7. NORTHFELT DW, DEZUBE BJ, THOMMES JA *et al.*: Efficacy of pegylated-liposomal doxorubicin in the treatment of AIDS-related Kaposi's sarcoma after failure of standard chemotherapy. *J. Clin. Oncol.* (1997) 15:653-659.

8. MARTINO R, PEREA G, CABALLERO MD *et al.*: Cyclophosphamide, pegylated liposomal doxorubicin (Caelyx), vincristine and prednisone (CCOP) in elderly patients with diffuse large B-cell lymphoma: results from a prospective Phase II study. *Haematologica* (2002) 87:822-827.

9. WOLLINA U, DRUMMER R, BROCKMEYER NH *et al.*: Multicenter study of pegylated liposomal doxorubicin in patients with cutaneous T-cell lymphoma. *Cancer* (2003) 98:993-1001

10. GILL PS, WERNZ J, SCADDEN DT *et al.*: Randomized Phase III trial of liposomal daunorubicin versus doxorubicin, bleomycin, and vincristine in AIDS-related Kaposi's sarcoma. *J. Clin. Oncol.* (1996) 14:2353-2364.

11. BATIST G, RAMAKRISHNAN G, RAO CS *et al.*: Reduced cardiotoxicity and preserved antitumor efficacy of liposome-encapsulated doxorubicin and cyclophosphamide compared with conventional doxorubicin and cyclophosphamide in a randomized, multicenter trial of metastatic breast cancer. *J. Clin. Oncol.* (2001) 19:1444-1454.

12. SARRIS AH, HAGEMEISTER F, ROMAGUERA J *et al.*: Liposomal vincristine in relapsed non-Hodgkin's lymphomas: early results of an ongoing Phase II trial. *Ann. Oncol.* (2000) 11:69-72.

13. KEHRER DF, BOS AM, VERWEIJ J *et al.*: Phase I and pharmacologic study of liposomal lurtotecan, NX 211: urinary excretion predicts hematologic toxicity. *J. Clin. Oncol.* (2002) 20:1222-1231.

14. ALLEN TM: Ligand-targeted therapeutics in anticancer therapy *Nat. Rev. Cancer* (2002) 2:750-763.

• **Review detailing various ligand-targeted therapeutics at various stages of development.**

15. NORMANNO N, BIANCO C, DE LUCA A, MAIELLO MR, SALOMON DS: Target-based agents against ErbB receptors and their ligands: a novel approach to cancer treatment. *Endocr. Relat. Cancer* (2003) 10:1-21.

16. ROSS JS, GRAY K, GRAY GS, WORLAND PJ, ROLFE M: Anticancer antibodies *Am. J. Clin Pathol.* (2003) 119:472-485.

17. LOPES DE MENEZES DE, PILARSKI LM, ALLEN TM: *In vitro* and *In vivo* targeting of immunoliposomal doxorubicin to human B-cell lymphoma. *Cancer Res.* (1998) 58:3320-3330.

18. PARK JW, HONG K, KIRPOTIN DB *et al.*: Anti-HER2 immunoliposomes: enhanced efficacy attributable to targeted delivery *Clin. Cancer Res.* (2002) 8:1172-1181.

•• **Demonstrates the target-specific antitumour efficacy of anti-HER2-immunoliposmomal doxorubicin in human breast tumours.**

19. AHMAD I, LONGENECKER M, SAMUEL J, ALLEN TM: Antibody-targeted delivery of doxorubicin entrapped in sterically stabilized liposomes can eradicate lung cancer in mice. *Cancer Res.* (1993) 53:1484-1488.

20. ALLEN TM, HANSEN CB, LOPES DE, MENEZES DE. Pharmacokinetics of long-circulating liposomes. *Adv. Drug Deliv. Rev.* (1995) 16:267-284.

•• **Excellent review describing the pharmacokinetics and mechanisms responsible for the clearance of long circulating liposomes.**

21. LYASS O, UZIELY B, BEN-YOSEF R *et al.*: Correlation of toxicity with pharmacokinetics of pegylated liposomal doxorubicin (Doxil®) in metastatic breast carcinoma *Cancer* (2000) 89:1037-1047.

22. HOBBS SK, MONSKY WL, YUAN F *et al.*: Regulation of transport pathways in tumor vessels: role of tumor type and microenvironment. *Proc. Natl. Acad. Sci. USA* (1998) 95:4607-4612.

23. MATSUMURA Y, MAEDA H: A new concept for macromolecular therapeutics in cancer chemotherapy: mechanism of tumoritropic accumulation of proteins and the antitumor agent SMANCS *Cancer Res.* (1986) 46:6387-6392.

24. HUANG SK, LEE KD, HONG K, FRIEND DS, PAPAHADJOPOULOS D: Microscopic localization of sterically stabilized liposomes in colon carcinoma-bearing mice. *Cancer Res.* (1992) 52:5135-5143.

25. GABIZON A, CHEMLA M, TZEMACH D, HOROWITZ AT, GOREN D: Liposome longevity and stability in circulation: effects on the *in vivo* delivery to tumors and therapeutic efficacy of encapsulated anthracyclines. *J. Drug Target.* (1996) 3:391-398.

26. MAYER LD, CULLIS PR, BALLY MB: In: *Medical Applications of Liposomes.* Papahadjopoulos La (Ed). Elsevier Science B.V., New York (1998).

27. SAPRA P, ALLEN TM: Ligand-targeted liposomal anticancer drugs. *Prog. Lipid Res.* (2003) 42:439-462.

• **Review detailing engineering considerations for immunoliposome construction.**

28. GABIZON AA: Pegylated liposomal doxorubicin: metamorphosis of an old drug into a new form of chemotherapy. *Cancer Invest.* (2001) 19:424-436.

29. MAMOT C, DRUMMOND DC, HONG K, KIRPOTIN DB, PARK JW: Liposome-based approaches to overcome anticancer drug resistance. *Drug Resist. Updat.* (2003) 6:271-279.

30. NIEHANS GA, SINGLETON TP, DYKOSKI D, KIANG DT: Stability of HER-2/neu expression over time and at multiple metastatic sites. *J. Natl. Cancer Inst.* (1993) 85:1230-1235.

31. KIRPOTIN D, PARK JW, HONG K *et al.*: Sterically stabilized anti-HER2 immunoliposomes: design and targeting to human breast cancer cells *in vitro*. *Biochemistry* (1997) 36:66-75.

32. PARK JW, HONG K, CARTER P *et al.*: Development of anti-p185^{HER2} immunoliposomes for cancer therapy. *Proc. Natl. Acad. Sci. USA* (1995) 92:1327-1331.

33. PRESS MF, CORDON-CARDO C, SLAMON DJ: Expression of the HER/2/neu proto-oncogene in normal human adult and fetal tissues. *Oncogene* (1990) 5:953-962.

34. ZHAO YY, SAWYER DR, BALIGA RR *et al.*: Neuregulins promote survival and growth of cardiac myocytes. Persistence of ErbB2 and ErbB4 expression in neonatal and adult ventricular myocytes. *J. Biol Chem.* (1998) 273:10261-10269.

35. DRUMMOND DC, HONG K, PARK JW, BENZ CC, KIRPOTIN DB: Liposome targeting to tumors using vitamin and growth factor receptors. *Vitam. Horm.* (2001) 60:285-332.

36. ROSS JF, CHAUDHURI PK, RATNAM M: Differential regulation of folate receptor isoforms in normal and malignant tissues *in vivo* and in established cell lines. *Cancer* (1994) 73:2432-2443.

37. GOREN D, HOROWITZ AT, ZALIPSKY S *et al.*: Targeting of stealth liposomes to erbB-2 (Her/2) receptor: *in vitro* and *in vivo* studies. *Br. J. Cancer* (1996) 74:1749-1756.

38. SAPRA P, ALLEN TM: Internalizing antibodies are necessary for improved therapeutic efficacy of antibody-targeted liposomal drugs. *Cancer Res.* (2002) 62:7190-7194.

39. GOREN D, HOROWITZ AT, TZEMACH D *et al.*: Nuclear delivery of doxorubicin via folate-targeted liposomes with bypass of multidrug-resistance efflux pump. *Clin. Cancer Res.* (2000) 6:1949-1957.

40. SUGANO M, EGILMEZ NK, YOKOTA SJ *et al.*: Antibody targeting of doxorubicin-loaded liposomes suppresses the growth and metastatic spread of established human lung tumor xenografts in severe combined immunodeficient mice. *Cancer Res.* (2000) 60:6942-6949.

41. BECERRIL B, POUL MA, MARKS JD: Toward selection of internalizing antibodies from phage libraries. *Biochem. Biophys. Res. Commun.* (1999) 255:386-393.

•• **Description of a novel method for selecting tumour-specific antibodies based on cell internalisation rather than binding.**

42. POUL MA, BECERRIL B, NIELSEN UB, MORISSON P, MARKS JD: Selection of tumor-specific internalizing human antibodies from phage libraries. *J. Mol. Biol.* (2000) 301:1149-1161.

•• **Description of a novel method for selecting tumour-specific antibodies based on cell internalisation rather than binding.**

43. LIEBERT M, WEDEMEYER GA, STEIN JA *et al.*: Identification by monoclonal antibodies of an antigen shed by human bladder cancer cells. *Cancer Res.* (1989) 49:6720-6726.

44. KATARI RS, FERNSTEN PD, SCHLOM J: Characterization of the shed form of the human tumor-associated glycoprotein (TAG-72) from serous effusions of patients with different types of carcinomas. *Cancer Res.* (1990) 50:4885-4890.

45. WALDMANN TA: Monoclonal antibodies in diagnosis and therapy. *Science* (1991) 252:1657-1662.

46. KIRPOTIN DB, PARK JW, HONG K *et al.*: Targeting of liposomes to solid tumors: the case of sterically stabilized anti-HER2 immunoliposomes. *J. Liposome Res.* (1997) 7:391-417.

47. NIELSEN UB, KIRPOTIN DB, PICKERING EM *et al.*: Therapeutic efficacy of anti-ErbB2 immunoliposomes targeted by a phage antibody selected for cellular endocytosis. *Biochim. Biophys. Acta.* (2002) 1591:109-118.

• **Description of a HER2-targeted immunoliposome targeted with a fully human anti-HER2 scFv antibody fragment.**

48. LIU B, CONRAD F, COOPERBERG MR, KIRPOTIN DB, MARKS JD: Mapping tumor epitope space by direct selection of single-chain Fv antibody libraries on prostate cancer cells *Cancer Res.* (2004) 64:704-710.

49. LEE RJ, HUANG L: Folate-targeted, anionic liposome-entrapped polylysine-condensed DNA for tumor cell-specific gene transfer. *J. Biol. Chem.* (1996) 271:8481-8487.

• **Demonstrates the physical properties of cationic lipid-DNA nonviral vectors required for target-specific activity using folic acid to target the folate receptor.**

50. XU L, PIROLLO KF, CHANG EH: Transferrin-liposome-mediated p53 sensitization of squamous cell carcinoma of the head and neck to radiation *in vitro*. *Hum. Gene Ther.* (1997) 8:467-475.

51. ELIAZ RE, SZOKA FC Jr: Liposome-encapsulated doxorubicin targeted to CD44: a strategy to kill CD44-overexpressing tumor cells. *Cancer Res.* (2001) 61:2592-2601.

• **Demonstrates the potential use of oligonucleotides as targeting ligands when targeting cancer cells.**

52. ZALIPSKY S, PUNTAMBEKAR B, BOULIKAS P, ENGBERS CM, WOODLE MC: Peptide attachment to extremities of liposomal surface grafted PEG chains: preparation of the long-circulating form of laminin pentapeptide, YIGSR. *Bioconjug. Chem.* (1995) 6:705-708.

53. MOREIRA JN, HANSEN CB, GASPAR R, ALLEN TM: A growth factor antagonist as a targeting agent for sterically stabilized liposomes in human small cell lung cancer. *Biochim. Biophys. Acta* (2001) 1514:303-317.

54. WILLIS MC, COLLINS B, ZHANG T *et al.*: Liposome-anchored vascular endothelial growth factor aptamers *Bioconjug. Chem.* (1998) 9:573-582.

55. SCHIFFELERS RM, KONING GA, TEN HAGEN TL *et al.*: Anti-tumor efficacy of tumor vasculature-targeted liposomal doxorubicin. *J. Control. Release* (2003) 91:115-122.

56. PASTORINO F, BRIGNOLE C, MARIMPIETRI D *et al.*: Doxorubicin-loaded Fab' fragments of anti-disialoganglioside immunoliposomes selectively inhibit the growth and dissemination of human neuroblastoma in nude mice. *Cancer Res.* (2003) 63:86-92.

57. ARAGNOL D, LESERMAN LD: Immune clearance of liposomes inhibited by an anti-Fc receptor antibody *in vivo*. *Proc. Natl. Acad. Sci. USA* (1986) 83:2699-2703.

58. HARDING JA, ENGBERS CM, NEWMAN MS, GOLDSTEIN NI, ZALIPSKY S: Immunogenicity and pharmacokinetic attributes of poly(ethylenegiycol)-grafted immunoliposomes. *Biochim. Biophys. Acta* (1997) 1327:181-192.

59. SHEETS MD, AMERSDORFER P, FINNERN R *et al.*: Efficient construction of a large nonimmune phage antibody library: the production of high-affinity human single-chain antibodies to protein antigens. *Proc. Natl. Acad. Sci. USA* (1998) 95:6157-6162.

60. BODER ET, MIDELFORT KS, WITTRUP KD: Directed evolution of antibody fragments with monovalent femtomolar antigen-binding affinity. *Proc. Natl. Acad. Sci. USA* (2000) 97:10701-10705.

61. ALLEN TM: Liposomal drug formulations. Rationale for development and what we can expect in the future. *Drugs* (1998) 56:747-756.

62. LIM HJ, MASIN D, MCINTOSH NL, MADDEN TD, BALLY MB: Role of drug release and liposome-mediated drug delivery in governing the therapeutic activity of liposomal mitoxantrone used to treat human A431 and LS180 solid tumors. *J. Pharmacol. Exp. Ther.* (2000) 292:337-345.

63. SHARMA A, STRAUBINGER RM: Novel taxol formulations: preparation and characterization of taxol-containing liposomes. *Pharm. Res.* (1994) 11:889-896.

64. GABIZON AA, BARENHOLZ Y, BIALER M: Prolongation of the circulation time of doxorubicin encapsulated in liposomes containing polyethylene glycol-derivatized phospholipid: pharmacokinetic studies in rodents and dogs. *Pharm. Res.* (1993) 10:703-708.

65. WEBB MS, HARASYM TO, MASIN D, BALLY MB, MAYER LD: Sphingomyelin-cholesterol liposomes significantly enhance the pharmacokinetic and therapeutic properties of vincristine in murine and human tumour models. *Br. J. Cancer* (1995) 72:896-904.

* **Describes the use of sphingomyelin and cholesterol liposome compositions for enhancing liposomal vincristine formulation stability.**

66. WEBB MS, SAXON D, WONG FM *et al.*: Comparison of different hydrophobic anchors conjugated to poly(ethylene glycol): effects on the pharmacokinetics of liposomal vincristine. *Biochim. Biophys. Acta* (1998) 1372:272-282.

67. MUI BL, CULLIS PR, PRITCHARD PH, MADDEN TD: Influence of plasma on the osmotic sensitivity of large unilamellar vesicles prepared by extrusion. *J. Biol. Chem.* (1994) 269:7364-7370.

68. LASIC DD, FREDERICK PM, STUART MC, BARENHOLZ Y, MCINTOSH TJ. Gelation of liposome interior: a novel method for drug encapsulation. *FEBS Lett.* (1992) 312:255-258.

69. CULLIS PR, HOPE MJ, BALLY MB *et al.*: Influence of pH gradients on the transbilayer transport of drugs, lipids, peptides and metal ions into large unilamellar vesicles. *Biochim. Biophys. Acta* (1997) 1331:187-211.

** **Review detailing various gradient-based loading strategies for encapsulating drugs inside liposomes.**

70. ZALIPSKY S: Functionalized poly(ethiene glycol) for preparation of biologically relevant conjugates. *Bioconjug. Chem.* (1995) 6:150-165.

71. HARASYM TO, BALLY MB, TARDI P: Clearance properties of liposomes involving conjugated proteins for targeting. *Adv. Drug Deliv. Rev.* (1998) 32:99-118.

72. HANSEN CB, KAO GY, MOASE EH, ZALIPSKY S, ALLEN TM: Attachment of antibodies to sterically stabilized liposomes: evaluation, comparison and optimization of coupling procedures. *Biochim. Biophys. Acta* (1995) 1239:133-144.

73. ALLEN TM, BRANDEIS E, HANSEN CB, KAO GY, ZALIPSKY S: A new strategy for attachment of antibodies to sterically stabilized liposomes resulting in efficient targeting to cancer cells. *Biochim. Biophys. Acta* (1995) 1237:99-108.

74. MARTIN FJ, HUBBELL WL, PAPAHADJOPOULOS D: Immunospecific targeting of liposomes to cells: a novel and efficient method for covalent attachment of Fab' fragments via disulfide bonds. *Biochemistry* (1981) 20:4229-4238.

75. PARR MJ, ANSELL SM, CHOI LS, CULLIS PR: Factors influencing the retention and chemical stability of poly(ethylene glycol)-lipid conjugates incorporated into large unilamellar vesicles. *Biochim. Biophys. Acta* (1994) 1195:21-30.

76. LEE RJ, LOW PS: Folate-mediated tumor cell targeting of liposome-entrapped doxorubicin *in vitro*. *Biochim. Biophys. Acta* (1995) 1233:134-144.

77. LEE RJ, LOW PS: Delivery of liposomes into cultured KB cells via folate receptor-mediated endocytosis. *J. Biol. Chem.* (1994) 269:3198-3204.

78. GABIZON A, HOROWITZ AT, GOREN D *et al.*: Targeting folate receptor with folate linked to extremeties of poly(ethlene glycol)-grafted liposomes: *in vitro* studies. *Bioconjug. Chem.* (1999) 10:289-298.

79. BLUME G, CEVC G, CROMMELIN MD *et al.*: Specific targeting with poly(ethylene glycol)-modified liposomes: coupling of homing devices to the ends of the polymeric chains combines effective target binding with long circulation times. *Biochim. Biophys. Acta* (1993) 1149:180-184.

80. MARUYAMA K, TAKIZAWA T, YUDA T *et al.*: Targetability of novel immunoliposomes modified with amphipathic poly(ethylene glycol)s conjugated at their distal terminals to monoclonal antibodies. *Biochim. Biophys. Acta* (1995) 1234:74-80.

81. ISHIDA T, IDEN DL, ALLEN TM: A combinatorial approach to producing sterically stabilized (Stealth) immunoliposomal drugs. *FEBS Lett.* (1999) 460:129-133.

** **First published description of the micellar insertion strategy for incorporating antibodies conjugated to PEG-lipid anchors into preformed liposomes.**

82. IDEN DL, ALLEN TM: *In vitro* and *in vivo* comparison of immunoliposomes made by conventional coupling techniques with those made by a new post-insertion approach. *Biochim. Biophys. Acta* (2001) 1513:207-216.

83 MAMOT C, DRUMMOND DC, CREISER U *et al.*: Epidermal growth factor receptor (EGFR)-targeted immunoliposomes mediate specific and efficient drug delivery to EGFR- and EGFRvIII-overexpressing tumor cells. *Cancer Res.* (2003) 63:3154-3161.

84. SALOMON DS, BRANDT R, CIARDIELLO F, NORMANNO N: Epidermal growth factor-related peptides and their receptors in human malignancies. *Crit. Rev. Oncol. Hematol.* (1995) 19:183-232.

85 MENDELSOHN J, BASELGA J: The EGF receptor family as targets for cancer therapy. *Oncogene* (2000) 19:6550-6565.

86. CIARDIELLO F, TORTORA G: A novel approach in the treatment of cancer: targeting the epidermal growth factor receptor. *Clin. Cancer Res.* (2001) 7:2958-2970.

87. PARK JW, HONG K, KIRPOTIN DB *et al.*: Anti-HER2 immunoliposomes: enhanced efficacy attributable to targeted delivery. *Clin. Cancer Res.* (2002) 8:1172-1181.

88. NEVE RM, NIELSEN UB, KIRPOTIN DB *et al.*: Biological effects of anti-ErbB2 single chain antibodies selected for internalizing function. *Biochem. Biophys. Res. Commun.* (2001) 280:274-279.

89. GUO Z, NOBLE CO, DRUMMOND DC *et al.*: HER2- and EGFR-targeted liposomal epirubicin. *Proc. Am. Assoc. Cancer Res.* (2003) 44:174.

90. MOREIRA JN, GASPAR R, ALLEN TM: Targeting Stealth liposomes in a murine model of human small cell lung cancer. *Biochim. Biophys. Acta* (2001) 1515:167-176.

91. ERIGNOLE C, MARIMPIETRI D, GAMBINI C *et al.*: Development of Fab' fragments of anti-GD(2) immunoliposomes entrapping doxorubicin for experimental therapy of human neuroblastoma. *Cancer Lett.* (2003) 197:199-204.

92. PAGNAN G, MONTALDO PG, PASTORINO F *et al.*: GD2-mediated melanoma cell targeting and cytotoxicity of liposome-entrapped fenretinide. *Int. J. Cancer* (1999) 81:268-274.

93. IINUMA H, MARUYAMA K, OKINAGA K *et al.*: Intracellular targeting therapy of cisplatin-encapsulated transferrin-polyethylene glycol liposome on peritoneal dissemination of gastric cancer. *Int. J. Cancer* (2002) 99:130-137.

94. RAFFAGHELLO L, PAGNAN G, PASTORINO F *et al.*: *In vitro* and *in vivo* antitumor activity of liposomal Fenretinide targeted to human neuroblastoma. *Int. J. Cancer* (2003) 104:559-567.

95. ALLEN TM, AHMAD I, LOPES DE MENEZES DE, MOASE EH: Immunoliposome-mediated targeting of anti-cancer drugs *in vivo*. *Biochem. Soc. Trans.* (1995) 23:1073-1079.

96. VINGERHOEDS MH, STEERENBERG PA, HENDRIKS JJ *et al.*: Immunoliposome-mediated targeting of doxorubicin to human ovarian carcinoma *in vitro* and *in vivo*. *Br. J. Cancer* (1996) 74:1023-1029.

97. MOASE EH, QU W, ISHIDA T *et al.*: Anti-MUC-1 immunoliposomal doxorubicin in the treatment of murine models of metastatic breast cancer. *Biochim. Biophys. Acta* (2001) 1510:43-55.

98. HYNES RO: A reevaluation of integrins as regulators of angiogenesis. *Nat. Med.* (2002) 8:918-921.

99. JANSSEN AP, SCHIFFELERS RM, TEN HAGEN TL *et al.*: Peptide-targeted PEG-liposomes in anti-angiogenic therapy. *Int. J. Pharm.* (2003) 254:55-58.

100. BENZINGER P, MARTINY-BARON C, REUSCH P *et al.*: Targeting of endothelial KDR receptors with 3C2 immunoliposomes *in vitro*. *Biochim. Biophys. Acta* (2000) 1466:71-78.

101. BACKER MV, ALOISE R, PEZEKOP K, STOLETOV K, BACKER JM: Molecular vehicles for targeted drug delivery. *Bioconjug. Chem.* (2002) 13:462-467.

102. GREISER U, DRUMMOND D, MAMOT C *et al.*: Targeting immunoliposomes to endothelial receptors. *Proc. Am. Assoc. Cancer Res.* (2002) 43:414

103. DRUMMOND DC, GUO Z, KIRPOTIN DB *et al.*: Immunoliposome delivery of novel anticancer compounds. *Proc. Am. Assoc. Cancer Res.* (2002) 43:418.

104. PASTORINO F, BRIGNOLE C, MARIMPIETRI D *et al.*: Vascular damage and anti-angiogenic effects of tumor vessel-targeted liposomal chemotherapy. *Cancer Res.* (2003) 63:7400-7409.

105. HUANG L, VIROONCHATAPAN E: Introduction. *Nonviral vectors for gene therapy* (1999) Ch.1:3-22.

106. FELGNER PL, GADEK TR, HOLM M *et al.*: Lipofectin: a highly efficient, lipid-mediated DNA-transfection procedure. *Proc. Natl. Acad. Sci. USA* (1987) 84:7413-7417.

107. STUART DD, ALLEN TM: A new liposomal formulation for antisense oligodeoxynucleotides with small size, high incorporation efficiency and good stability. *Biochim. Biophys. Acta* (2000) 1463:219-229.

108. HOFLAND HE, SHEPHARD L, SULLIVAN SM: Formation of stable cationic lipid/DNA complexes for gene transfer. *Proc. Natl. Acad. Sci. USA* (1996) 93:7305-7309.

109. MAURER N, WONG KF, STARK H *et al.*: Spontaneous entrapment of polynucleotides upon electrostatic interaction with ethanol-destabilized cationic liposomes. *Biophys. J.* (2001) 80:2310-2326.

110. ZHENG YP, REIMER DL, ZHANG G, LEE PH, BALLY MB: Self-assembling DNA-lipid particles for gene transfer. *Pharm. Res.* (1997) 14:190-196.

• **Description of a method for preparing small stable cationic lipid-DNA particles.**

111. HONG KL, ZHENG WW, BAKER A, PAPAHADJOPOULOS D: Stabilization of cationic liposome-plasmid DNA complexes by polyamines and poly(ethylene glycol)-phospholipid conjugates for efficient *in vivo* gene delivery. *FEBS Lett.* (1997) 400:233-237.

112. MONCK MA, MORI A, LEE D *et al.*: Stabilized plasmid-lipid particles: pharmacokinetics and plasmid delivery to distal tumors following intravenous injection. *J. Drug Target* (2000) 7:439-452.

113. STUART DD, KAO GY, ALLEN TM: A novel, long-circulating, and functional liposomal formulation of anti-sense oligodeoxynucleotides targeted against MDR1. *Cancer Gene Ther.* (2000) 7:468-475.

114. TROS DE ILARDUYA C, ARANGOA MA, MORENO-ALIAGA MJ, DUZGUNES N: Enhanced gene delivery *in vitro* and *in vivo* by improved transferrin-lipoplexes. *Biochim. Biophys. Acta.* (2002) 1561:209-221.

115. REDDY JA, ABBURI C, HOFLAND H *et al.*: Folate-targeted, cationic liposome-mediated gene transfer into disseminated peritoneal tumors. *Gene Ther.* (2002) 9:1542-1550.

116. LEAMON CP, COOPER SR, HARDEE GE: Folate-liposome-mediated antisense oligodeoxynucleotide targeting to cells. Evaluation *in vitro* and *in vivo*. *Bioconjug. Chem.* (2003) 14:738-747

117. KAO GY, CHANCE LJ, ALLEN TM: Use of targeted cationic liposomes in enhanced DNA delivery to cancer cells. *Cancer Gene Ther.* (1996) 4:250-256.

118. PASTORINO F, STUART D, PONZONI M, ALLEN TM: Targeted delivery of antisense oligonucleotides in cancer. *J. Control. Release* (2001) 74:69-75.

119. PASTORINO F, BRIGNOLE C, MARIMPIETRI D *et al.*: Targeted liposomal c-*myc* antisense oligonucleotides induce apoptosis and inhibit tumor growth and metastases in human melanoma models. *Clin. Cancer Res.* (2003) 9:4595-4605.

** **First description of *in vivo* activity for a cationic lipid-based therapeutic oligonucleotide.**

120. TAN PH, MANUNTA M, ARDJOMAND N *et al.*: Antibody targeted gene transfer to endothelium. *J. Gene Med.* (2003) 5:311-323.

121. SHI N, PARDRIDGE W: Noninvasive gene targeting to the brain. *Proc. Natl. Acad. Sci. USA* (2000) 97:7567-7572.

122. KIRPOTIN DB, PARK JW, HONG K *et al.*: In: *Medical Applications of Liposomes.* Lasic DD, Papahadjopoulos D (eds). Elsevier Science B.V., New York (1998).

123. MEYER O, KIRPOTIN D, HONG K *et al.*: Cationic liposomes coated with polyethylene glycol as carriers of oligonucleotides. *J. Biol. Chem.* (1998) 273:15621-15627.

124. BARRY MA, DOWER WJ, JOHNSTON SA: Toward cell-targeting gene therapy vectors: selection of cell-binding peptides from random peptide-presenting phage libraries. *Nat. Med.* (1996) 2:299-305.

125. BOHL KULLBERG E, BERGSTRAND N, CARLSSON J *et al.*: Development of EGF-conjugated liposomes for targeted delivery of boronated DNA-binding agents. *Bioconjug. Chem.* (2002) 13:737-743.

126. ZHANG Y, JEONG LEE H, BOADO RJ, PARDRIDGE WM: Receptor-mediated delivery of an antisense gene to human brain cancer cells. *J. Gene Med* (2002) 4:183-194.

127. RUI Y, WANG S, LOW PS, THOMSON DH. Diplasmenylcholine-folate liposomes: an efficient vehicle for intracellular drug delivery. *J. Am. Chem. Soc.* (1998) 120:11213-11218.

128. HUWYLER J, WU D, PARDRIDGE WM. Brain drug delivery of small molecules using immunoliposomes. *Proc. Natl. Acad Sci. USA* (1996) 93:14164-14169.

129. BAVARONE DA, YU X, BELLAMKONDA RV: Targeted drug delivery to C6 glioma by transferrin-coupled liposomes. *J. Biomed. Mater. Res.* (2000) 51:10-14.

130. MARTY C, ODERMATT B, SCHOTT H *et al.*: Cytotoxic targeting of F9 teratocarcinoma tumours with anti-ED-B fibronectin scFv antibody modified liposomes. *Br. J. Cancer* (2002) 87:106-112.

131. DAGAR S, KRISHNADAS A, RUBINSTEIN I, BLEND MJ, ONYUKSEL H: VIP grafted sterically stabilized liposomes for targeted imaging of breast cancer: *in vivo* studies. *J. Control. Release* (2003) 91:123-133.

132. SAPRA P, MOASE EH, MA J, ALLEN TM: Improved therapeutic responses in a xenograft model of human B lymphoma (Namalwa) for liposomal vincristine versus liposomal doxorubicin targeted via anti-CD19 IgG2a or Fab' fragments. *Clin. Cancer Res.* (2004) 10:1106-1111.

** **Comparison of antitumour activities of liposomes targeted to CD19 in a lymphoma model, containing either doxorubicin or vincristine.**

133. MATSUO H, WAKASUGI M, TAKANAGA H *et al.*: Possibility of the reversal of multidrug resistance and the aviodance of side effects by liposomes modified with MRK-16, a monoclonal antibody to P-glycoprotein. *J. Control. Release* (2001) 77:77-86.

Affiliation

Charles O Noble[1], Dmitri B Kirpotin[2], Mark E Hayes[2], Christoph Mamot[3], Keelung Hong[2], John W Park[4], Christopher C Benz[3], James D Marks[1] & Daryl C Drummond[1,4]

[†]Author for correspondence

[1]University of California at San Francisco, San Francisco, CA 94143, USA

[2]Hermes Biosciences, Inc., South San Francisco, CA 94080, USA

[3]Buck Institute for Age Research, Novato, CA 94945, USA

[4]Associate Director of Liposome Research, Hermes Biosciences, Inc., 61 Airport Boulevard., Suite D, South San Francisco, CA 94080, USA

Tel: +1 650 873 2583 (Ext. 109);

Fax: +1 650 873 2501;

E-mail: drummond@hermesbio.com

Original article

Annals of Oncology 15: 1025–1032, 2004
DOI: 10.1093/annonc/mdh264

5-Fluorouracil incorporation into RNA and DNA in relation to thymidylate synthase inhibition of human colorectal cancers

P. Noordhuis[1], U. Holwerda[2], C. L. Van der Wilt[1]†, C. J. Van Groeningen[1], K. Smid[1], S. Meijer[3], H. M. Pinedo[1] & G. J. Peters[1]*

Departments of [1]Medical Oncology, [2]Clinical Chemistry and [3]Surgical Oncology, VU University Medical Center, Amsterdam, The Netherlands

Received 5 September 2003; revised 23 February 2004; accepted 24 February 2004

Background: The mechanism of action of 5-fluorouracil (5-FU) has been associated with inhibition of thymidylate synthase (TS) and incorporation of 5-FU into RNA and DNA, but limited data are available in human tumor tissue for the latter. We therefore measured incorporation in human tumor biopsy specimens after administration of a test dose of 5-FU alone or with leucovorin.

Patients and methods: Patients received 5-FU (500 mg/m^2) with or without high-dose leucovorin, low-dose leucovorin or l-leucovorin, and biopsy specimens were taken after approximately 2, 24 or 48 h. Tissues were pulverized and extracted for nucleic acids. 5-FU incorporation was measured using gas chromatography/mass spectrometry after complete degradation to bases of isolated RNA and DNA.

Results: Maximal incorporation into RNA (1.0 pmol/μg RNA) and DNA (127 fmol/μg DNA) of 59 and 46 biopsy specimens, respectively, was found at 24 h after 5-FU administration. Incorporation into RNA but not DNA was significantly correlated with intratumoral 5-FU levels. However, DNA incorporation was significantly correlated with the RNA incorporation. Primary tumor tissue, liver metastasis and normal mucosa did not show significant differences, while leucovorin had no effect. Neither for RNA (30 patients) nor DNA (24 patients) incorporation was a significant correlation with response to 5-FU therapy found. However, in the same group of patients, response was significantly correlated to TS inhibition (mean TS in responding and non-responding groups 45 and 231 pmol/h/mg protein, respectively; $P = 0.001$).

Conclusions: 5-FU is incorporated at detectable levels into RNA and DNA of human tumor tissue, but no relation between the efficacy of 5-FU treatment and incorporation was found, in contrast to TS.

Key words: 5-fluorouracil, 5-FU incorporation into DNA, 5-FU incorporation into RNA, human colorectal cancer, leucovorin, thymidylate synthase inhibition

Introduction

Since 1957, 5-fluorouracil (5-FU) has played an important role in the treatment of colon cancer and is used for patients with breast cancer and cancer of the head and neck [1]. 5-FU is usually given in combination therapy. So far in colon cancer, response rates of 10–20% after bolus injection of 5-FU as single agent could be improved by leucovorin by up to 30%. A number of schedules are being used, although the choice is often a matter of local preference. For combinations with irinotecan or oxaliplatin, response rates up to 60% have been reported [2–6] for colon cancer.

Insight into the mechanism of action of 5-FU might improve the therapies in which 5-FU has been included. Various mechanisms including inhibition of thymidylate synthase (TS) by 5-fluoro-2′-deoxyuridine-5′-monophosphate (FdUMP), incorporation of 5-fluorouridine-5′-triphosphate (FUTP) into RNA and incorporation of 5-fluoro-2′-deoxyuridine-5′-triphosphate (FdUTP) into DNA have been reported. Although TS inhibition and its expression have been related to the antitumor effect of 5-FU [7–13], it has not yet been demonstrated clinically whether incorporation into RNA or DNA contribute to its antitumor effect.

Inhibition of TS, a key enzyme of pyrimidine *de novo* synthesis, has been studied extensively during recent last decades, *in vitro* as well as *in vivo* [1]. TS inhibition results in a depletion of dTTP and an increase in dUTP followed by decreased DNA synthesis and DNA repair. The inhibition of TS can be potentiated by leucovorin. Leucovorin acts as precursor for 5,10-methylene-tetrahydrofolate, which is necessary for the formation of the ternary complex with TS and FdUMP, essential for long-term maintenance of TS inhibition.

Correspondence to: Dr G. J. Peters, Department of Medical Oncology, VU University Medical Center, 1007 MB, Amsterdam, The Netherlands. Tel: +31-20-4442633; Fax: +31-20-4443844; E-mail: gj.peters@vumc.nl
† Present address: Comprehensive Cancer Center Amsterdam (IKA), Amsterdam, The Netherlands.

Incorporation of 5-FU into RNA has also been related to the cytotoxic action of 5-FU [14, 15] and has been postulated to be schedule dependent [16]. In a recent clinical study it was demonstrated that incorporation into RNA was higher after bolus administration of 5-FU, but not significantly different with continuous administration [17]. In an animal tumor model, the combination of 5-FU with thymidine, which bypasses the inhibition of TS, increased the antitumor activity of 5-FU, indicating that incorporation into RNA was the mechanism of action [18]. Evidence that this mechanism contributes to toxicity was obtained from studies with uridine protection. In normal epithelium of the intestine, p53-dependent apoptosis was only inhibited by uridine and not by thymidine after exposure to 5-FU [19]. Both UDPG, a precursor for uridine, and uridine decreased the incorporation of 5-FU into the RNA of tumors, but did not affect the inhibition of TS or the antitumor effect [20]. Uridine enabled an increase in the dose, resulting in increased TS inhibition and antitumor activity. Cytotoxicity by 5-FU incorporation into RNA is possibly mediated by its incorporation into snRNA, especially U2-RNA, which inhibits the splicing of pre-mRNA, resulting in impaired mRNA synthesis [21, 22]. Furthermore, it has been shown that pre-rRNA processing was inhibited after 5-FU administration and might be related to incorporation of 5-FU into U3-RNA [23, 24]. Incorporation of 5-FU into different RNA molecules may therefore lead to disturbance of mRNA processing and protein synthesis [25, 26].

5-FU can also be incorporated into DNA of murine bone marrow cells as well as human tumor cells and this may contribute to the cytotoxicity of 5-FU [27–31]. Misincorporation of 5-FU into DNA is associated with the formation of DNA strand breaks [32–34]. After incorporation into DNA, 5-FU can be excised by uracil–DNA-glycosylase followed by apurinic–apyrimidinic endonucleolytic cleavage, resulting in DNA strand breaks [35–37]. Also, when polymerase α is inhibited by a specific inhibitor like aphidicolin, strand break formation after 5-FU exposure remains, indicating a second mechanism of 5-FU-induced DNA strand break formation without incorporation of the drug [34], in which the imbalance of intracellular deoxyribonucleotide pools may play a role. This imbalance might be associated with the inhibition of TS, leading to a decrease in dTTP and an accumulation of dUTP with a subsequent decrease in DNA synthesis and repair. Misincorporation of dUTP and FdUTP into DNA can be prevented by the action of dUTPase [36].

Until now, incorporation of 5-FU into RNA and DNA has usually been determined in preclinical *in vitro* and *in vivo* model systems by using radiolabeled 5-FU. However, in order to determine the incorporation of 5-FU into RNA and DNA of patient samples, this is not a suitable method. We developed a non-radioactive method using gas chromatography coupled with mass spectrometry (GC–MS) to determine 5-FU incorporation into RNA [38, 39], which was adapted with minor changes to determine DNA incorporation as well. This is the first report describing the relevance of 5-FU incorporation into both RNA and DNA in a clinical setting and the possible relation with TS and response.

Patients and methods

Patient selection and drug administration

In this study, tissue samples of 68 patients (37 males) with a median age of 57 years (range 34–78 years) were included. All patients had advanced colorectal cancer. The protocol was approved by the Institutional Review Board and also aimed to evaluate the extent and retention of TS inhibition in relation to response to 5-FU [11]. All patients gave informed consent. The 5-FU schedules used are given routinely in our hospital. The study comprised two parts. (i) administration of an experimental dose of 5-FU at 500 mg/m^2 alone or in combination with leucovorin before a planned surgery (mostly implantation of a Port-a-Cath); and (ii) treatment of a selection of these patients with a hepatic artery infusion or an intravenous schedule. Twenty-two patients were treated with hepatic arterial infusions of 5-FU (1000 mg/m^2/day ×5 every 3 weeks). Of patients in whom only resection of the primary tumor took place, eight were subsequently treated with bolus injections of 5-FU (500 mg/m^2 weekly) and 10 were treated with a 2 h infusion of high-dose leucovorin (hd-LV) and a midway bolus injection of 5-FU (500 mg/m^2 leucovorin and 500 mg/m^2 5-FU weekly). Of the other patients, one was treated with a 2 h infusion of leucovorin and a midway bolus injection of 5-FU followed by oral uridine (500 mg/m^2 leucovorin, 600 mg/m^2 5-FU, 5 g/m^2 uridine every 6 h for 72 h, weekly). A total of 21 patients received no further treatment while the subsequent treatment of six patients was not fluoropyrimidine related. Of the eight patients who received 5-FU bolus injections, three were subsequently treated with hepatic arterial infusions of 5-FU. Also, one of the 10 patients receiving 5-FU with leucovorin was subsequently treated with hepatic arterial infusions of 5-FU.

Chemicals

5-FU, alkaline phosphatase type VII-S (APase, 1000 U/150 µl, EC 3.1.3.1) and thymidine phosphorylase (TPase, 600 U/ml, EC 2.4.2.4) were obtained from Sigma (St Louis, MO). 5-FU-$^{15}N_2$ was from Merck-Sharp and Dome (Montreal, Canada) and pentafluorobenzylbromide was from Pierce Chemicals (Rockford, IL). DNase I (2000 U/mg; EC 3.1.21.1), Nuclease P1 (300 U/mg, EC 3.1.30.1), RNase A (50 U/mg), RNase T1 (10^5 U/ml) and proteinase K were acquired from Roche Molecular Biochemicals (Almere, The Netherlands). Uridine phosphorylase [UPase (EC 2.4.2.3), 590 U/ml] was kindly provided by A. Komissarov. All other chemicals were of analytical grade. Solutions were made in water purified by a Millipore Reagent Q system (Millipore, Bedford, MA).

5-FU incorporation into RNA and DNA of human tumor tissue

From patients included in a study described elsewhere [11, 13, 38, 39], samples of primary colorectal cancer, liver metastasis and colon mucosa were analyzed for the incorporation of 5-FU into RNA and DNA. These patients received an experimental dose of 5-FU as an i.v. bolus injection at a dose of 500 mg/m^2 with or without a 2 h infusion of either hd-LV (500 mg/m^2), low-dose leucovorin (ld-LV; 25 mg/m^2) or l-leucovorin (l-LV; 250 mg/m^2) at approximately 2, 24 or 48 h before surgical resection of the tissues; biopsy specimens of the tissues were immediately frozen in liquid nitrogen and stored at −80°C.

The frozen tissue was pulverized as described previously [38]. Three volumes of ice-cold saline were added to the frozen pulverized tumor tissue and mixed thoroughly. After centrifugation for 10 min at 4000 r.p.m.

and 4°C, the resulting pellet, containing the RNA and DNA, was stored at −80°C until RNA and DNA extraction.

RNA isolation and degradation

RNA was isolated as described previously [39]. Precipitated nucleic acids from tissues were suspended in 5 ml lysis buffer, which consisted of 4 M guanidine-isothiocyanate, 25 mM sodium citrate, 0.5% *N*-lauroylsarcosine and 0.1 M β-mercaptoethanol. After suspension, 0.5 ml 2 M sodium acetate (pH 4) was added and mixed. Subsequently, 5 ml water-saturated phenol and 1 ml chloroform/isoamyl alcohol (49/1 v/v) were added. The resulting suspension was shaken thoroughly and centrifuged for 15 min at 4000 r.p.m. and 4°C. The RNA-containing upper layer was removed and precipitated with an equal volume of 2-propanol at −80°C for 2 h. After centrifugation at 4000 r.p.m. and 4°C for 10 min, the RNA pellet was resuspended in 1.8 ml lysis buffer and reprecipitated with 2 ml 2-propanol. The RNA was centrifuged again and reconstituted in 500 µl digestion buffer [40 mM Tris, 1 mM $MgCl_2$, 0.1 mM $ZnCl_2$ and 40 mM KH_2PO4 (pH 7.4)]. RNA concentration and purity were determined after measurement of the optical density at 260 and 280 nm. To 360 µl RNA suspension, 20 µl RNase A/RNase T1 (500/500 U/ml), 10 µl APase (1000 U/ml) and 10 µl UPase (590 U/ml) were added. The mixture was incubated at 37°C for 1 h to degrade the RNA to bases completely. After incubation the samples were stored at −20°C until extraction for GC–MS analysis [39].

DNA isolation and degradation

DNA isolation was essentially performed as described previously [40]. Precipitated nucleic acids from tissues were suspended in 7 ml lysis buffer [100 mM Tris, 5 mM EDTA, 0.2% SDS, 200 mM NaCl, 100 µg/ml proteinase K (pH 8.5)]. The suspension was incubated at 55°C overnight and subsequently for 1 h at 37°C with RNase A/T1 10/10 U/ml final concentration (RNase A/T1 was heated at 95°C for 15 min to inactivate DNase). In order to precipitate the DNA, an equal volume of 2-propanol was added and mixed until precipitation was complete. DNA was recovered from the solution and resuspended at 55°C in 2 ml buffer containing 10 mM Tris and 1 mM EDTA (pH 8.0). The suspension was purified further by extractions with an equal volume of phenol/chloroform/iso-amylalcohol (50/49/1 v/v/v) and chloroform/iso-amylalcohol (49/1 v/v). DNA was reprecipitated with an equal volume of 2-propanol and reconstituted in 0.5 ml digestion buffer [40 mM Tris, 1 mM $MgCl_2$, 0.1 mM $ZnCl_2$, 40 mM KH_2PO_4 (pH 7.4)] at 55°C. For measurement of concentration and purity, optical density was measured at 260 and 280 nm. For enzymatic degradation of the DNA, 20 µl DNase I (1 mg/ml), 20 µl Nuclease P1 (250 U/ml), 10 µl APase (1000 U/ml) and 10 µl TPase(600 U/ml) were added to 340 µl DNA suspension. In this composition the reaction mixture was optimal to degrade all DNA to bases after incubation overnight at 37°C. The digest was stored at −20°C until extraction for GC–MS analysis.

GC–MS extraction and measurement

Extraction for GC–MS was performed as described previously [39]. Briefly, 50 µl 5-FU-$^{15}N_2$ (1 µM for RNA and 0.1 µM for DNA samples), 1 ml milli-q water and 100 µl 2 M Tris (pH 6) were added to 300–350 µl enzyme digestion product. The solution was extracted twice with 4 ml di-ethyl-ether/2-propanol (80/20 v/v). The organic fraction was blown to dryness under N_2 at 60°C. The residue was reconstituted in 80 µl acetonitrile, and 10 µl triethylamine and 10 µl pentafluorobenzylbromide were added. The mixture was left at room temperature for at least 15 min. After the addition of 400 µl 0.1 M HCl the solution was extracted once with 1 ml hexane. The organic layer was blown to dryness under N_2 at 45°C and the residue was dissolved in 50 µl hexane/propanon (3/1 v/v). This sample was injected into the GC–MS system (Automass 2; ThermoQuest BV, Breda, The Netherlands). Chromatographic separation was carried out on a CPSil19 CB column (25 m × 0.25 internal diameter, film thickness 0.2 µm) (Chrompack, Middelburg, The Netherlands). The ions for 5-FU and 5-FU-$^{15}N_2$ (m/z-309 and m/z-311, respectively) were recorded with negative chemical ionization detection and methane as the moderating gas. More details of the 5-FU measurement with GC–MS have been described elsewhere [39].

Thymidylate synthase assays

Using the same samples in which we measured incorporation of 5-FU into RNA and DNA, we also evaluated the activity of TS. TS was assayed as described previously [11].

Statistics

In order to evaluate differences between the various groups of patients, we used SPSS for Windows version 11.5.

Results

Incorporation into RNA of human tissue

The assay to optimize the incorporation of 5-FU into RNA was described previously [39]. Figure 1 shows 5-FU incorporation into RNA of 59 human tumor tissues (17 primary tumors and 42 liver metastases) and nine colon mucosa samples obtained at approximately 2, 24 and 48 h after 5-FU administration, and the mean values of the different groups are summarized in Table 1. The incorporation of 5-FU into RNA of human tumor tissue showed a variation of 0.01–1.45 pmol/µg RNA. Variation in RNA incorporation within a tissue sample, determined in 11 samples, showed a mean variation of 37% (data not shown). Within 2 h of the administration of 5-FU it was incorporated into RNA, with mean values for primary colon tumors, liver metastasis and colon mucosa of 0.40, 0.74 and 0.21 pmol/µg RNA, respectively. At 24 h the incorporation

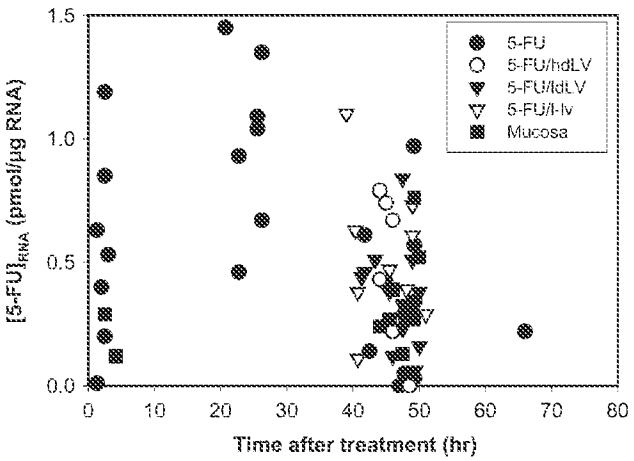

Figure 1. Incorporation of 5-fluorouracil (5-FU) into RNA of human tumor tissue at different time points after administration of 5-FU alone (closed circles) or 5-FU combined with high-dose leucovorin (hdLV; open circles), low-dose leucovorin (ldLV; closed triangles) or l-leucovorin (l-LV; open triangles), and mucosa (closed squares). Each point represents a single sample.

Table 1. Time dependence and the effect of leucovorin on the incorporation of 5-FU into RNA of human tumor tissue and mucosa

Treatment	Time, h	Tumor [mean ± SEM (*n*)], pmol/μg	Mucosa [mean ± SEM (*n*)], pmol/μg	Metastasis [mean ± SEM (*n*)], pmol/μg
5-FU	2	0.40 ± 0.19 (4)	0.29/0.12 (2)	0.74 ± 0.24 (3)
5-FU	24	0.96 ± 0.26 (3)	NA	1.02 ± 0.16 (4)
5-FU	48	0.20 ± 0.08 (3)	0.27 (1)	0.33 ± 0.10 (10)
5-FU/hd-LV	48	0.26/0.43 (2)	0.39/0.24 (2)	0.48 ± 0.16 (5)
5-FU/ld-LV	48	0.30 ± 0.04 (3)	0.47 ± 0.18 (3)	0.38 ± 0.07 (10)
5-FU/l-LV	48	0.47/0.38 (2)	0.27 (1)	0.53 ± 0.11 (8)

Tumors were excised at different time points after the administration of 5-FU alone or in combination with hd-LV, ld-LV or l-LV. In the case of one or two samples, individual values are given.
5-FU, 5-fluorouracil; hd-LV, high-dose leucovorin; ld-LV, low-dose leucovorin; l-LV, l-leucovorin; NA, not available.

Table 2. Statistical evaluation of the incorporation of 5-FU into RNA and DNA of human tumor tissue and mucosa

Parameter 1	Parameter 2	Test	RNA		DNA	
			Rho	*P* value	Rho	*P* value
5-FU 48 h	5-FU/hd-LV 48 h	Mann–Whitney *U*-test		0.344		0.250
5-FU 48 h	5-FU/ld-LV 48 h	Mann–Whitney *U*-test		0.244		0.782
5-FU 48 h	5-FU/l-LV 48 h	Mann–Whitney *U*-test		0.048		0.039
5-FU/hd-LV 48 h	5-FU/ld-LV 48 h	Mann–Whitney *U*-test		0.865		0.217
5-FU/hd-LV 48 h	5-FU/l-LV 48 h	Mann–Whitney *U*-test		0.648		0.064
5-FU/ld-LV 48 h	5-FU/l-LV 48 h	Mann–Whitney *U*-test		0.348		0.053
Colon tumor	Liver metastasis	Paired *t*-test		0.893		0.245
Colon tumor	Colon mucosa	Paired *t*-test		0.396		0.658
5-FU tissue	5-FU RNA/DNA	Spearman correlation	0.439	0.001	0.033	0.838
5-FU RNA/DNA	Response (i.v. LV/5-FU)	Spearman correlation	−0.070	0.848	0.000	1.000
5-FU RNA/DNA	Response (i.a. 5-FU)	Spearman correlation	0.171	0.511	0.347	0.205
5-FU RNA	5-FU DNA	Spearman correlation	0.309	0.024		
5-FU RNA	5-FU DNA	Pearson correlation	0.522	<0.001		

Evaluation was performed on data obtained after the administration of either 5-FU alone or in combination with hd-LV, ld-LV or l-LV. Correlation with response was evaluated at 48 h.
5-FU, 5-fluorouracil; hd-LV, high-dose leucovorin; ld-LV, low-dose leucovorin; l-LV, l-leucovorin.

increased to 0.96 and 1.02 pmol/μg RNA for primary colon tumors and liver metastasis, respectively. No colon mucosa samples were available at this time point. At 48 h after 5-FU administration the incorporation decreased to 0.20 pmol/μg RNA in primary colon tumor samples, 0.33 pmol/μg RNA in liver metastasis and 0.27 pmol/μg RNA in colon mucosa.

The addition of hd-LV, ld-LV or l-LV to 5-FU therapy was studied at 48 h after administration. Incorporation of 5-FU after the addition of hd-LV and ld-LV showed similar results as treatment with 5-FU alone and was not significantly different. Only l-LV seemed to increase the 5-FU incorporation as compared with 5-FU alone, but not with regimens including hd-LV and ld-LV (Table 2). Comparison of the incorporation of 5-FU into RNA of different tissues from the same patient showed that there was no significant difference between primary colon tumors and liver metastasis, and primary colon tumors and colon mucosa (Table 2). The incorporation of 5-FU into RNA is significantly correlated ($P = 0.001$) to the concentration of 5-FU in the tissue, as was also found previously in murine tumors [12] (Table 2).

The response to therapy with 5-FU was evaluable in 30 patients and was compared to the incorporation of 5-FU into RNA 48 h after administration (Figure 2). No significant relation was found, either when evaluating the whole group or the subgroups receiving different i.v. schedules of 5-FU (Table 2).

Incorporation into DNA of human tissue

The incorporation of 5-FU into DNA was measured using a novel sensitive assay, allowing the use of small tissue samples. Similar to the assay for 5-FU incorporation into RNA, it was first validated in a cell line and murine tissues. Similar results to those using classical methods (radioactive 5-FU) were observed (data not shown). Figure 3 shows

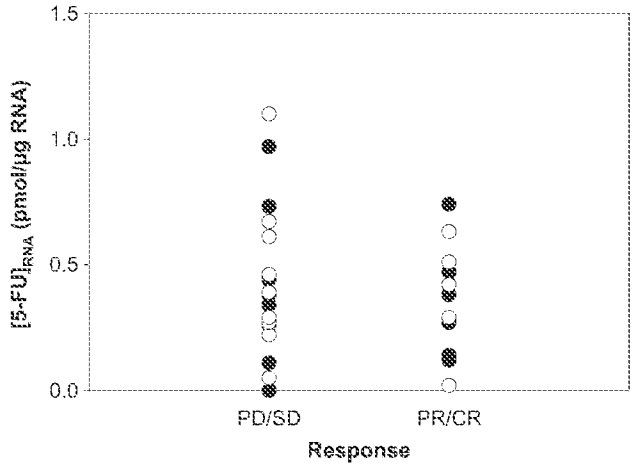

Figure 2. Incorporation of 5-fluorouracil (5-FU) into RNA 48 h after administration of 5-FU versus response to treatment with either i.v. leucovorin (LV)/5-FU (closed symbols) or i.a. 5-FU (open symbols). Each point represents a single sample. PD, progressive disease; SD, stable disease; PR, partial response; CR, complete remission.

the results of the incorporation of 5-FU into the DNA of 46 human tumor tissues (13 primary tumors and 33 liver metastases) and eight colon mucosa samples. The data are summarized as mean values in Table 3. These samples were obtained at approximately 2, 24 and 48 h after 5-FU administration. At the first time point, ~2 h after 5-FU administration, only three samples showing incorporation into DNA were available: 11.95 fmol/µg DNA for the primary colon tumor sample, 47.1 fmol/µg DNA for the liver metastasis and 4.5 fmol/µg DNA for the colon mucosa sample (Table 3). The DNA incorporation of 5-FU at 24 h showed the largest variation and ranged from 0.6 to 245 fmol of 5-FU/µg DNA, with mean values of 126.53 and 141.68 fmol/µg DNA for the primary colon tumors and liver metastases, respectively. The incorporation at 48 h after administration of 5-FU

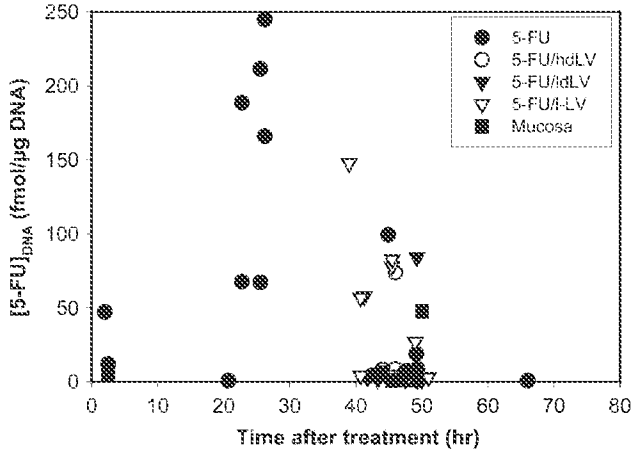

Figure 3. Incorporation of 5-fluorouracil (5-FU) into DNA of human tumor tissue at different time points after administration of 5-FU alone (closed circle) or 5-FU combined with high dose leucovorin (hd-LV; open circles), low-dose leucovorin (ld-LV; closed triangles) or l-leucovorin (l-LV; open triangles), and mucosa (closed squares). Each point represents a single sample.

decreased to 4.13 fmol/µg DNA for the primary colon tumors, 16.45 fmol/µg DNA for the liver metastases and 0.80 fmol/µg DNA in the only available colon mucosa sample. Also, for DNA incorporation LV seemed to increase incorporation compared with 5-FU alone (Table 2), but was not different compared to that of hd-LV and ld-LV. Primary colon tumors did not show a significantly different incorporation of 5-FU into DNA compared to liver metastasis from the same patients; also there was no difference between the primary tumor and normal mucosa (Table 2). In contrast to RNA incorporation there was no significant correlation between 5-FU concentration in the tissue and DNA incorporation of 5-FU. However, DNA incorporation was significantly correlated to RNA incorporation

Incorporation of 5-FU into DNA after 48 h could be evaluated in 24 patients receiving a 5-FU-containing regimen, and in whom response was evaluable (Figure 4), but similar to RNA there was no significant relation between 5-FU incorporation into DNA and response (Table 2), either for the whole group or for subgroups.

Thymidylate synthase levels

Previously we reported a relation between TS levels and response to 5-FU [11]. In order to determine the relative role of TS levels in the patient group for which we also measured incorporation into RNA and DNA, we evaluated TS levels in this particular subgroup (Figure 5). The mean residual TS activity in patients responding to 5-FU-based treatment was 45 pmol/h.mg protein, while that in the group not responding to 5-FU treatment the levels were significantly higher (245 pmol/h.mg protein; $P = 0.001$). Using other assays to evaluate TS expression, we observed similar differences.

Discussion

This is the first paper to describe the incorporation of 5-FU into both RNA and DNA in patient tumors without the use of radiolabeled drugs. In the same patients we also evaluated TS inhibition [11, 13], which was related to response to 5-FU treatment. It is unlikely that TS inhibition is related to 5-FU incorporation into RNA, but a prolonged TS inhibition might favor 5-FU incorporation into DNA. TS inhibition results in dTTP depletion, which favors the incorporation of FdUTP into DNA due to the lack of competition for DNA polymerase between FdUTP and dTTP. This condition would also favor incorporation of the increased dUTP into DNA. Apparently potential breakdown of FdUTP by dUTPase did not prevent its incorporation into DNA. The relatively long retention of FdUTP in DNA might be due to the favorable incorporation conditions, but also to rather inefficient DNA repair. The latter process is catalyzed by uracil-DNA-glycosylase [36, 37] and apparently functions at different rates in the various tumors, considering the large variation in the incorporation of 5-FU into DNA.

The kinetics of 5-FU incorporation into RNA of human tumor tissue differed to those in murine tumors [12, 20], while

Table 3. Time dependence and effect of leucovorin on incorporation of 5-FU into DNA of human tumor tissue and mucosa

Treatment	Time (h)	Tumor [mean ± SEM (*n*)], fmol/μg	Mucosa [mean ± SEM (*n*)], fmol/μg	Metastasis [mean ± SEM (*n*)], fmol/μg
5-FU	2	12.0(1)	4.5(1)	47.1(1)
5-FU	24	126.5 ± 59.1(3)	n.a.	141.7 ± 47.9(4)
5-FU	48	1.4/6.9(2)	0.8(1)	16.5 ± 10.5(9)
5-FU/hd-LV	48	8.6/8.1(2)	1.0/6.1(2)	26.6 ± 24.0(3)
5-FU/ld-LV	48	1.6 ± 0.15(3)	18.1 ± 14.8(3)	18.0 ± 10.3(9)
5-FU/l-LV	48	78.0/56.8(2)	0.60(1)	44.6 ± 24.1(6)

Tumors were excised at different time points after the administration of 5-FU alone or in combination with hd-LV, ld-LV or l-LV. In the case of one or two samples, individual values are given.
5-FU, 5-fluorouracil; hd-LV, high-dose leucovorin; ld-LV, low-dose leucovorin; l-LV, l-leucovorin; NA, not available.

5-FU tissue levels [38] were correlated with 5-FU incorporated into RNA. Incorporation in human tumors was greater after 24 h compared with 2 and 24 h, whereas in murine tumors the incorporation is maximal at 2 h. The large variation found for DNA incorporation, especially at 24 and 48 h post-administration, shows that incorporation is not only dependent on the intra-tumoral concentration of 5-FU, but that other mechanisms also play a role. Other mechanisms involved are dUTPase activity, inhibition of TS and excision of incorporated FdUTP by uracil-DNA-glycosylase [35, 36, 43, 44].

Repair may also be dependent on the availability of deoxynucleotides, which is dependent on the extent of TS inhibition. So far in the same patient samples, only TS inhibition, total TS activity and expression could be related to response to therapy [11, 13, 45], which was also shown in several studies by measurement of mRNA expression and protein expression [7–10]. A relationship between 5-FU RNA incorporation and response in tumor biopsy specimens was demonstrated in one limited study that evaluated 11 cases for incorporation of 5-FU into RNA [42]. It was postulated that 5-FU was effective at a 5-FU incorporation level higher than 200 ng 5-FU/mg RNA. The samples analyzed in our study showed a lower incorporation at a similar time point, which might explain why we could not demonstrate a significant relationship with response to treatment. Also, DNA incorporation in a limited number of patients failed to show a significant relationship with response to treatment. Possibly the imbalance of deoxynucleotides by depletion of dTTP after TS inhibition plays a more important role in the response to treatment of patients, leading to the apoptosis observed in these samples [46, 47].

Measurement of the incorporation of 5-FU into RNA and DNA of human tissue enabled evaluation of the role of 5-FU incorporation in the efficacy of patient treatment. We were able to measure in the tumor samples from the same patients not only 5-FU levels [39] and 5-FU incorporation into both RNA and DNA, but also TS levels and inhibition [11, 45], TS induction [46] and the downstream effects of TS inhibition

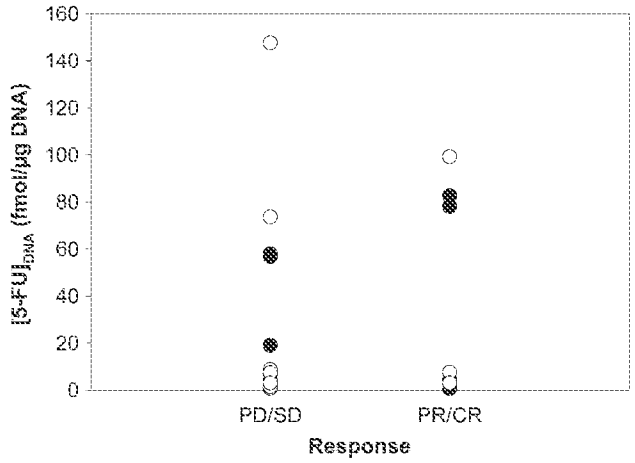

Figure 4. Incorporation of 5-fluorouracil (5-FU) into DNA 48 h after administration of 5-FU versus response to treatment with either i.v. leucovorin (LV)/5-FU (closed symbols) or i.a. 5-FU (open symbols). Each point represents a single sample. PD, progressive disease; SD, stable disease; PR, partial response; CR, complete remission.

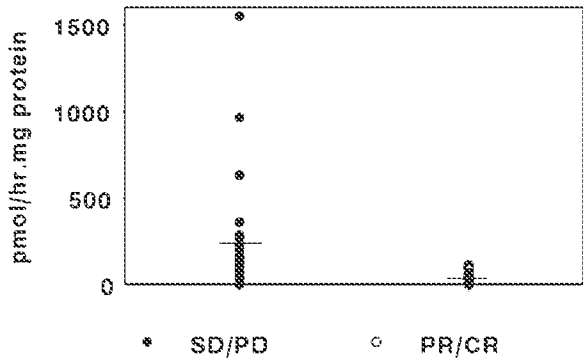

Figure 5. Relationship between thymidylate synthase (TS) levels and response to 5-fluorouracil (5-FU)-based treatment in the same group of patients referred to in Figures 2 and 4. TS levels are shown as the residual TS activity measured at 10 μM dUMP [11] in responding [partial response (PR)/complete remission (CR), 16 patients] and non-responding patients [progressive disease (PD)/stable disease (SD), 26 patients]. Lines indicate the means, (231 and 45 pmol/h.mg protein, respectively). TS levels were significantly different between both groups ($P = 0.001$; Mann–Whitney *U*-test). Other assays to evaluate TS levels showed a similar result.

[11, 45, 47]. These are all mechanisms by which fluoropyrimidines are postulated to act. This unique set of data obtained in the same group of patients clearly demonstrates that response to 5-FU treatment is related to TS levels and expression and not to 5-FU incorporation into RNA. These findings are supported by the observations that TS inhibition and response to treatment are increased by the addition of leucovorin [11]. Also in animal models [12, 14, 20], in which TS inhibition and incorporation into RNA were evaluated in the same tumor, response was related to TS inhibition. Evidence is also accumulating that incorporation of 5-FU into RNA is related to 5-FU toxicity [12, 19, 20], which does not exclude a relationship between TS inhibition and toxicity of 5-FU. It was postulated by Sobrero et al. [16] that 5-FU given as a bolus injection would act predominantly by its incorporation into RNA and that 5-FU given as a continuous infusion would act by inhibition of TS. However, in a recent study, the same group demonstrated that response to 5-FU given both as a bolus injection and as continuous infusion, was correlated with TS levels [48]. Only in the methotrexate-modulated arm was this relationship not found. These data are in line with the current findings and those in animal models, which also support TS as the main target. Toxicity caused by antifolate TS inhibitors such as Raltitrexed consists of myelotoxicity and gastrointestinal toxicity [49]. 5-FU can inhibit TS in normal gut mucosa and bone marrow [50]. In addition to novel antifolate TS inhibitors such as Raltitrexed, other new agents such as oxaliplatin and irinotecan can decrease TS expression in model systems [51, 52]. In patients, novel combinations or schedules should not aim to increase 5-FU incorporation into RNA, but should aim to increase 5-FU-induced TS inhibition in tumors.

References

1. Peters GJ, Köhne CH. Fluoropyrimidines as antifolate drugs. In Jackman JL (ed.): Antifolate Drugs in Cancer Therapy. Totowa, NJ: Humana Press 1999; 101–145.
2. Comella P, Casaretti R, De Vita F et al. Concurrent irinotecan 5-fluorouracil plus leuvo-folinic acid given every other week in the first line management of advanced colorectal carcinoma: a phase I study of the Southern Italy Cooperative Oncology Group. Ann Oncol 1999; 10: 915–921.
3. André T, Louvet C, Maindrault-Goebel F et al. CPT-11 (irinotecan) addition to bimonthly, high-dose leucovorin and bolus and continuous-infusion 5-fluorouracil (FOLFIRI) for pretreated metastatic colorectal cancer. Eur J Cancer 1999; 35: 1343–1347.
4. Douillard JY, Cunningham D, Roth AD et al. Irinotecan combined with fluorouracil compared with fluorouracil alone as first-line treatment for metastatic colorectal cancer: a multi-centre randomised trial. Lancet 2000; 355: 1041–1047.
5. Giachetti S, Perpoint B, Zidani R et al. Phase III multicenter randomized trial of oxaliplatin added to chronomodulated fluorouracil-leucovorin as first line treatment of metastatic colorectal cancer. J Clin Oncol 2000; 18: 136–147.
6. De Gramont A, Figer A, Seymour M. Leucovorin and fluorouracil with or without oxaliplatin as first-line treatment in advanced colorectal cancer. J Clin Oncol 2000; 18: 2938–2947.
7. Leichman CG, Lenz H-J, Leichman L et al. Quantitation of intratumoral thymidylate synthase expression predicts for disseminated colorectal cancer response and resistance to protracted infusion of 5-fluorouracil and weekly leucovorin. J Clin Oncol 1997; 15: 3223–3229.
8. Salonga D, Danenberg KD, Johnson M et al. Colorectal tumors responding to 5-fluorouracil have low gene expression levels of dihydropyrimidine dehydrogenase, thymidylate synthase, and thymidine phosphorylase. Clin Cancer Res 2000; 6: 1322–1327.
9. Davies MM, Johnston PG, Kaur S, Allen-Mersh TG. Colorectal liver metastasis thymidylate synthase staining correlates with response to hepatic arterial floxuridine. Clin Cancer Res 1999; 5: 325–328.
10. Lenz HJ, Leichman CG, Danenberg KD et al. Thymidylate synthase mRNA level in adenocarcinoma of the stomach: a predictor for primary tumor response and overall survival. J Clin Oncol 1996; 14: 176–182.
11. Peters GJ, Van der Wilt CL, Van Groeningen CJ et al. Thymidylate synthase inhibition after administration of fluorouracil with or without leucovorin in colon cancer patients: implications for treatment with fluorouracil. J Clin Oncol 1994; 12: 2035–2042.
12. Van Laar JAM, Van der Wilt CL, Smid K et al. Therapeutic efficacy of fluoropyrimidines depends on the duration of thymidylate synthase inhibition in the murine Colon 26-b carcinoma tumor model. Clin Cancer Res 1996; 2: 1327–1333.
13. Peters GJ, Van der Wilt CL, Van Groeningen CJ et al. Effect of different leucovorin formulations on 5-fluorouracil induced thymidylate synthase inhibition in colon tumors and normal tissues from patients in relation to response to 5-fluorouracil. In Pfleiderer W, Rokos H (eds): Chemistry and Biology of Pteridines and Folates (Proceedings of the 11th International Symposium. Berlin, Germany Blackwell Science 1997; 145–150.
14. Spears CP, Shani J, Shahinian AH et al. Assay and time course of 5-fluorouracil incorporation into RNA of L1210/0 ascites cells in vivo. Mol Pharmacol 1984; 27: 302–307.
15. Goshal K, Jacob ST. An alternative molecular mechanism of action of 5-fluorouracil, a potent anticancer drug. Biochem Pharmacol 1997; 53: 1569–1575.
16. Sobrero AF, Aschele C, Bertino JR. Fluorouracil in colorectal cancer—a tale of two drugs: implications for biochemical modulation. J Clin Oncol 1997; 15: 368–381.
17. Katsumata K, Tomioka H, Sumi T et al. Correlation between clinicopathologic factors and kinetics of metabolic enzymes for 5-fluorouracil given to patients with colon carcinoma by two different dosage regimens. Cancer Chemother Pharmacol 2003; 51: 155–160.
18. Spiegelman S, Nayak R, Sawyer R et al. Potentiation of the antitumor activity of 5FU by thymidine and its correlation with the formation of (5FU) RNA. Cancer 1980; 45: 1129–1134.
19. Pritchard DM, Watson AJM, Potten CS et al. Inhibition by uridine but not thymidine of p53-dependent intestinal apoptosis initiated by 5-fluorouracil: evidence for the involvement of RNA perturbation. Proc Natl Acad Sci USA 1997; 94: 1795–1799.
20. Codacci-Pisanelli G, Van der Wilt CL, Smid K et al. High-dose 5-fluorouracil with uridine-diphosphoglucose rescue increases thymidylate synthase inhibition but not 5-fluorouracil incorporation into RNA of murine tumors. Oncology 2002; 62: 363–370.
21. Lenz HJ, Manno DJ, Danenberg KD, Danenberg PV. Incorporation of 5-fluorouracil into U2 and U6 snRNA inhibits mRNA precursor splicing. J Biol Chem 1994; 269: 31962–31968.
22. Sierakowska H, Shukla RR, Dominski Z, Kole R. Inhibition of pre-mRNA splicing by 5-fluoro-, 5-chloro- and 5-bromouridine. J Biol Chem 1989; 264: 19185–19191.
23. Herrick D, Kufe DW. Lethality associated with incorporation of 5-fluorouracil into preribosomal RNA. Mol Pharmacol 1984; 26: 135–140.

24. Goshal K, Jacob ST. Specific inhibition of pre-ribosomal RNA processing in extracts of lymphosarcoma cells treated with 5-FU. Cancer Res 1994; 54: 632–636.
25. Will CL, Dolnick BJ. 5-Fluorouracil inhibits dihydrofolate reductase precursor mRNA processing and/or nuclear stability in methotrexate-resistant KB cells. J Biol Chem 1994; 264: 21413–21421.
26. Armstrong RD, Lewis M, Stern SG, Cadman EC. Acute effect of 5-fluorouracil on cytoplasmic and nuclear dihydrofolate reductase messenger RNA metabolism. J Biol Chem 1986; 261: 7366–7371.
27. Schuetz JD, Wallac HJ, Diasio RB. 5-Fluorouracil incorporation into DNA of CF-1 mouse bone marrow cells as a possible mechanism of toxicity. Cancer Res 1984; 44: 1358–1363.
28. Lönn U, Lönn S. Interaction between 5-fluorouracil and DNA of human colon adenocarcinoma. Cancer Res 1984; 44: 3414–3418.
29. Major PP, Egan E, Herrick D, Kufe DW. 5-Fluorouracil incorporation in DNA of human breast cancer cells. Cancer Res 1982; 42: 3005–3009.
30. Sawyer RC, Stolfi RL, Martin DS, Spiegelman S. Incorporation of 5-fluorouracil into murine bone marrow DNA in vivo. Cancer Res 1984; 44: 1847–1851.
31. Peters GJ, Laurensse E, Leyva A et al. Sensitivity of human, murine and rat cells to 5-fluorouracil and 5′-deoxy-5-fluorouridine in relation to drug-metabolizing enzymes. Cancer Res 1986; 46: 20–28.
32. Yin M-B, Rustum YM. Comparative DNA strand breakage induced by Fura and FdUrd in human ileocecal adenocarcinoma (HCT-8) cells: relevance to cell growth inhibition. Cancer Com 1991; 3: 45–51.
33. Lönn U, Lönn S. DNA lesions in human neoplastic cells and cytotoxicity of 5-fluoropyrimidines. Cancer Res 1986; 46: 3866–3870.
34. Lönn U, Lönn S. 5-Fluoropyrimidine induced DNA damage in human colon adenocarcinoma and its augmentation by nucleoside transport inhibitor dipyridamole. Cancer Res 1989; 49: 1085–1089.
35. Caradonna SJ, Cheng Y-C. Uracil DNA-Glycosylase. J Biol Chem 1980; 255: 2293–2300.
36. Caradonna SJ, Cheng Y-C. The role of deoxyuridine triphosphate nucleotidehydrolase, Uracil DNA Glycosylase, and DNA Polymerase-in the metabolism of FUdR in human tumor cells. Mol Pharmacol 1980; 18: 513–520.
37. Mauro DJ, De Riel JK, Tallarida RJ, Sirover MA. Mechanism of excision of 5-fluorouracil by Uracil DNA Glycosylase in normal human cells. Mol Pharmacol 1993; 43: 854–857.
38. Peters GJ, Lankelma J, Kok RM et al. Prolonged retention of high concentration of 5-fluorouracil in human and murine tumors as compared to plasma. Cancer Chemother Pharmacol 1993; 31: 269–276.
39. Peters GJ, Noordhuis P, Komissarov A et al. Quantification of 5-fluorouracil incorporation into RNA of human murine tumors as measured with a sensitive gas chromatography-mass spectrometry assay. Anal Biochem 1995; 231: 157–163.
40. Laird PW, Zijderveld A, Linders K et al. Simplified mammalian DNA isolation procedure. Nucleic Acids Res 1991; 19: 4293.
41. Van Riel JMGH, Van Groeningen CJ, Albers SHM et al. Hepatic arterial 5-fluorouracil in patients with liver metastases of colorectal cancer: single centre experience in 145 patients. Ann Oncol 2000; 11: 1563–1570.
42. Matsuoka H, Ueo H, Sugimachi K, Akiyoshi T. Preliminary evidence that incorporation of 5-fluorouracil into RNA correlates with antitumor response. Cancer Invest 1992; 10: 265–269.
43. Webly SD, Hardcastle A, Ladner RD et al. Deoxyuridine triphosphatase (dUTPase) expression and sensitivity to the thymidilate synthase (TS) inhibitor ZD9331. Br J Cancer 2000; 83: 792–799.
44. Aherne GW, Brown S. The role of uracil misincorporation in thymineless death. In Jackman AL (ed.): Antifolate Drugs in Cancer Therapy. Totowa, NJ: Humana Press 1999; 409–421.
45. Backus HHJ, Van Riel JMGH, Van Groeningen CJ et al. Rb, mcl-1 and p53 expression correlate with clinical outcome in patients with liver metasases from colorectal cancer. Ann Oncol 2001; 12: 231–239.
46. Peters GJ, Backus HHJ, Freemantle S et al. Induction of thymidylate synthase as a 5-fluorouracil resistance mechanism. Biochim Biophys Acta 2002; 1587: 194–205.
47. Backus HHJ, Van Riel JMGH, Van Groeningen CJ et al. Rb, mcl-1 and p53 expression correlate with clinical outcome in patients with liver metastases from colorectal cancer. Ann Oncol 2001; 12: 779–785.
48. Aschele C, Debernardis D, Bandellioni R et al. Thymidylate synthase protein expression in colorectal cancer metastases predicts for clinical outcome to leucovorin-modulated bolus or infusional 5-fluorouracil but not methotrexate-modulated bolus 5-fluorouracil. Ann Oncol 2002; 13: 1882–1892.
49. Jackman AL, Calvert AH. Folate-based thymidylate synthase inhibitors as anticancer drugs. Ann Oncol 1995; 6: 871–881.
50. Van der Wilt CL, Van Groeningen CJ, Pinedo HM et al. 5-Fluorouracil/leucovorin-induced inhibition of thymidylate synthase in normal tissues of mouse and man. J Cancer Res Clin Oncol 1997; 123: 595–601.
51. Guichard S, Hennebelle I, Bugat R, Canal P. Cellular interactions of 5-fluorouracil and the camptothecin analogue CPT-11 (irinotecan) in a human colorectal carcinoma cell line. Biochem Pharmacol 1998; 5: 667–676.
52. Fischel JL, Formento P, Ciccolini J et al. Impact of the oxaliplatin-5 fluorouracil-folinic acid combination on respective intracellular determinants of drug activity. Br J Cancer 2002; 7: 1162–1168.

Original Contribution

Kurume Medical Journal, 56, 1-7, 2009

Dosage Escalation Study of S-1 and Irinotecan in Metronomic Chemotherapy against Advanced Colorectal Cancer

YUTAKA OGATA*, **, TERUO SASATOMI*, **, YOSHITO AKAGI*, NOBUYA ISHIBASHI*, SHINJIROU MORI* AND KAZUO SHIROUZU*

**Department of Surgery, Kurume University School of Medicine, Kurume 830-0011 and **Surgery, Kurume University Medical Center, Kurume 839-0863, Japan*

Received 23 April 2009, accepted 7 June 2009

Edited by TAKASHI OKAMURA

Summary: The anti-angiogenic efficacy of chemotherapy would seem to be optimized by administering comparatively lower doses of drugs on a more frequent (daily, several times a week, or weekly) or continuous schedule, with no extended interruptions – sometimes referred to as 'metronomic' chemotherapy. This phase I study was performed to determine the recommended dosage (RD) of metronomic chemotherapy using oral fluoropyrimidine S-1 plus weekly irinotecan (CPT-11) in patients with previously untreated advanced or recurrent colorectal cancer. Patients received first-line chemotherapy consisting of 80 mg/m^2 of S-1 given on days 3 to 7, 10 to 14, and 17 to 21 with escalating dosages of CPT-11 (from 40 mg/m^2) administered intravenously on day 1, 8, and 15 of a 28-day cycle. Standard patient eligibility criteria were used. Based on the concept of metronomic chemotherapy, dose limiting toxicity (DLT) was defined any toxicity that resulted in skipping of CPT-11 administration, or more than 5 days suspension in S-1 administration, in addition to the conventional criteria. If the maximum tolerated dosage (MTD) was defined as the maximum dosage at which no suspension of CPT-11 or S-1 administration occurred, the RD was considered to be the dosage one rank lower than the MTD. On the other hand, in the present study the MTD was defined as the dosage at which at least one suspension of CPT-11 or S-1 administration occurred, the MTD was considered to be the RD. Two of the first 3 patients at level 4 received 60 mg/m^2 of CPT-11 and 80 mg/m^2 of S-1 experienced a suspension in CPT-11 administration, thus level 4 was defined as the MTD and RD. Sixty mg/m^2 of CPT-11 and 80 mg/m^2 of S-1 were the indicated RD for the following phase II study of metronomic chemotherapy.

Key words metronomic chemotherapy, S-1, irinotecan, advanced colorectal carcinoma

INTRODUCTION

Irinotecan (CPT-11) is a key drug in the management of metastatic colorectal cancer, as demonstrated by several randomized studies indicating a survival benefit. It has been shown that the response rate to CPT-11 was 11 to 25% in patients with advanced colorectal cancer refractory to 5-fluorouracil (5-FU) based chemotherapy [1,2]. These findings implied a lack in tumor cross-resistance to the two agents CPT-11 and 5-FU. Moreover, favorable results from combination chemotherapy using CPT-11 and 5-FU/leucovorin (LV) for advanced colorectal cancer have been reported [3,4], and a CPT-11 and infusion plus bolus

Correspondence to: Yutaka Ogata MD, PhD, Surgery, Kurume University Medical Center, 155-1 Kokubu-machi, Kurume, Fukuoka 839-0863, Japan. Tel: +81 942 22 6111 Fax: +81 942 22 6657 E-mail: yogata@med.kurume-u.ac.jp

Abbreviations: BSA, body surface area; CEA, carcinoembryonic antigen; CDHP, 5-chloro-2,4-dihydrooxypyridine; CPT-11, irinotecan; CR, complete response; CT, computed tomography; DLT, dosage limiting toxicity; ECG, electrocardiogram; ECOG, Eastern Cooperative Oncology Group; 5-FU, 5-fluorouracil; FBAL, F-beta-alanine, FOLFIRI, folinic acid+5-FU+irinotecan; FOLFOX, folinic acid+5-FU+oxaliplatin, LV, leucovorin, MTD, maximum tolerated dosage; NCI-CTC, National Cancer Institute Common Toxicity Criteria; Oxo, potassium oxonate; PD, disease progression; PR, partial response; PS, performance status; RECIST, Response Evaluation Criteria in Solid Tumors; RD, recommended dosage; SD, stable disease; UFT, uracil plus tegafur; VEGF, vascular endothelial growth factor.

5-FU/LV regimen FOLFIRI (folnic acid+5-FU+irinotecan) has been recommended as first-line therapy for advanced colorectal cancer, as well as FOLFOX (folnic acid+5-FU+oxaliplatin) regimens which added oxaliplatin to intravenous 5-FU/LV [5]. Since these regimens have consisted of the conventional maximum tolerated dosages (MTDs) of CPT-11 and 5-FU, adverse effects of grade 3 or worse are not uncommon. Moreover, administration of infusion 5-FU is becoming more complex because of the need for vascular access devices and a portable delivery system.

S-1 is an oral fluoropyrimidine preparation developed by Taiho Pharmaceutical Co., Ltd. (Tokyo, Japan) that combines tegafur with two 5-FU modulators 5-chloro-2,4-dihydrooxypyridine (CDHP) and potassium oxonate (Oxo) at a molar ratio of 1:0.4:1 [6]. Tegafur, a prodrug of 5-FU, is converted to 5-FU mainly in the liver and in the tumor cells. CDHP, a reversible inhibitor of dihydropyrimidine dehydrogenase, suppresses the degradation of 5-FU, thereby maintaining high concentrations of 5-FU in plasma and the tumor cells [6,7]. CDHP also decreases the cardiotoxic and neurotoxic effects by reducing the production of F-beta-alanine (FBAL), the main catabolite of 5-FU [8,9]. After peroral administration, Oxo is selectively distributed to the small and large bowels. High concentrations of Oxo in these organs inhibit the phosphorylation of 5-FU to fluoropyrimidine monophosphate, catabolized by orotate phosphoribosyltransferase within the gastrointestinal mucosal cells, thereby reducing the incidence of diarrhea [10].

In phase II trials of S-1 as a single agent, response rates ranging from 19 to 39% were obtained in patients with advanced colorectal cancer [11-13]. These studies demonstrated that S-1 had a high response rate and good compliance in patients with advanced colorectal cancer treated on an outpatient basis. Several regimens combining S-1 and CPT-11 were subsequently developed. Goto et al. [14] conducted a phase II study consisting of 150 mg/m^2 of CPT-11 given on day 1 with 40 mg/m^2 of S-1 twice daily on days 1 to 14 of a 21-day cycle to assess efficacy and safety. They concluded that the combined treatment with S-1 and CPT-11 was a promising regimen, offering benefits in terms of safety and survival as compared with conventional regimens such as FOLFIRI in patients with advanced colorectal cancer.

Conventional cytotoxic chemotherapeutics affect the endothelium of the growing tumor vasculature in addition to affecting the proliferating cancer cells and various types of normal cells [15]. The antiangiogenic efficacy of chemotherapy would seem to be optimized by administering comparatively low dosages of drugs on a more frequent (daily, several times a week, or weekly) or continuous schedule, with no extended interruptions -- sometimes referred to as 'metronomic' chemotherapy [16]. This would also have the advantage of being less acutely toxic, therefore making more prolonged treatments hypothetically possible. Thus, peroral fluoropyrimidine on a daily schedule would be a typical metronomic chemotherapy. In fact, the antitumor efficacy of capecitabine or UFT (uracil plus tegafur)/LV is not inferior to that of intravenous 5-FU/LV, and has lower toxicity in advanced colorectal cancer [17,18]. However, since grade 3 or 4 toxicities can be expected to necessitate temporary suspension of the chemotherapy, a high dosage of bi-weekly or tri-weekly CPT-11 as in Goto's regimen [14] might not realize the metronomic advantage of daily peroral fluoropyrimidine in combination therapy of CPT-11 and peroral fluoropyrimidine. We have previously reported the safety and efficacy of metronomic chemotherapy using low-dosage weekly CPT-11 and daily 5'-deoxy-5-fluorouridine, an intermediate metabolite of capecitabine, for advanced colorectal cancer, even in elderly patients [19]. Thus, combined metronomic administration of CPT-11 and peroral fluoropyrimidine is expected to be useful even in poor risk patients who are unable to receive standard CPT-11 and 5-FU (or S-1) chemotherapy. We have therefore postulated that a combination therapy of weekly CPT-11 and S-1 could realize the advantages of metronomic chemotherapy by having an antiangiogenic effect in addition to an antiproliferation effect. We conducted this phase I study to assess the recommended dosage (RD) of weekly CPT-11 combined with daily S-1 as a metronomic chemotherapy, in which treatment can be continued without temporary interruption.

PATIENTS AND METHODS

Eligibility

This was a non-randomized, open-label, phase I, dosage-escalating study, performed at Kurume University Hospital, between April 2004 and December 2005. The criteria for eligibility were histological findings of colorectal carcinoma indicating nonresectable metastatic or recurrent disease, no prior chemotherapy, no major surgery or radiation therapy within 2 weeks of beginning treatment, measurable tumors with at least one lesion having dimensions $\geqq$10 mm in longest diameter, a life expectancy of $\geqq$3 months and a

performance status (PS) according to the Eastern Cooperative Oncology Group (ECOG) criteria of 0-1, adequate bone marrow function (leucocytes ≧4000 per mm^3, platelets ≧100000 per mm^3), adequate liver function (bilirubin ≦1.5 mg/dl), adequate renal function (creatinine ≦1.1 mg/dl), no serious or uncontrolled concurrent medical illness, and no active other malignancy. Postoperative adjuvant chemotherapy excluding regimens including CPT-11 or S-1 was allowed. Patients were required to be ≧20 years and <75 years of age, and non-pregnant. All patients were informed of the investigative nature of this treatment, and gave their fully-informed written consent. This study was approved by the ethics committee of Kurume University (No. 2355).

Treatment protocol

CPT-11 was administered by infusion intravenously over 90 min for three consecutive weeks followed by one week of rest, in 4-week treatment cycles. S-1 was available as capsules containing 20 or 25 mg of tegafur. S-1 was given perorally twice daily on days 3 to 7, 10 to 14, and 17 to 21. Patients were assigned one of the following dosages, to be taken within an hour after breakfast and supper, on the basis of body surface area (BSA); level 1: 25 mg (BSA<1.25 m^2), 40 mg (BSA≧1.25 to <1.50 m^2), or 50 mg (BSA≧1.50), level 2 or after: 40 mg (BSA<1.25 m^2), 50 mg (BSA≧1.25 to <1.50 m^2), or 60 mg (BSA≧1.50). Cycles were repeated every 4 weeks (Fig. 1).

The CPT-11 administration was temporarily suspended for grade 2 or higher mucositis, any grade of diarrhea, grade 3 or higher other non-hematological toxicity, or for leucocytes <3000/mm^3, granulocytes <1500/mm^3, or platelets <100000/mm^3. The S-1 administration was also temporarily suspended for grade 2 or higher diarrhea, grade 2 or higher mucositis, grade 3 or higher other non-hematological toxicity, or for leucocytes <2000/mm^3, granulocytes <1000/mm^3, or platelets <75000/mm^3. The therapy was alternatively re-instituted using a dosage of minus 1 level after recovery from all toxicities, if leucocytes <2000/mm^3, granulocytes <1000/mm^3, platelets <50000/mm^3, or grade 3 or higher non-hematological toxicity (excluding nausea/vomiting and general fatigue) was noted during the cycle, or in any case where the treatment delay was longer than 14 days before the start of the next cycle of treatment. All treatment was performed on an outpatient basis.

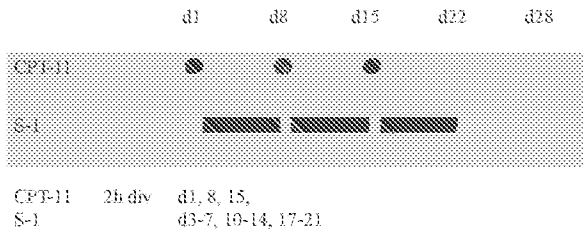

Fig. 1. Scheme of treatment protocol.

Dosage escalation

The dosage of S-1 was fixed at 80 mg/m^2 after level 2. The dosage of CPT-11 was started at 40 mg/m^2 and escalated after level 2, as shown in Table 1. Up to 6 patients at each dosage level completed one cycle of treatment before the next dosage level was tried. The dosage at which ≧2 of 3 or ≧2 of 6 patients experienced dosage limiting toxicity (DLT) during the first cycle of treatment was defined as the MTD. Adverse reactions were evaluated according to the National Cancer Institute Common Toxicity Criteria (NCI-CTC) version 3.0. Toxicity and laboratory variables were assessed weekly during the first and second treatment cycle. DLT was defined during the first treatment cycle as: grade 4 neutropenia, grade 4 thrombocytopenia, grade 3 neutropenia associated with fever ≧38°C, grade 3 or more non-hematological toxicity with the exception of alopecia, nausea and vomiting, and treatment delay of >7 days before the second cycle of treatment. Any skip in CPT-11 administration or more than 5 days suspension of S-1 administration with no relationship to the above DLTs was defined as an additional DLT.

Assessment of recommended dosage (RD)

If MTD is defined as the maximum dosage at which there was no skipping of CPT-11 or more than 5 days suspension in S-1 administration as an additional DLT, the RD is generally considered to be the dosage one rank lower than the MTD. However, for

TABLE 1.
Dose escalation scheme

	S-1	CPT-11
Level 1	60 mg/m^2	40 mg/m^2
Level 2	80 mg/m^2	40 mg/m^2
Level 3	80 mg/m^2	50 mg/m^2
Level 4	80 mg/m^2	60 mg/m^2

S-1 80 mg/m^2/day
BSA<1.25 80 mg/body/day
1.25≦BSA<1.5 100 mg/body/day
1.5≦BSA 120 mg/body/day
CPT-11: irinotecan, BSA: body surface area

the purposes of the present study if MTD is defined as the dosage at which at least one additional DLT of CPT-11 skipping or more than 5 days suspension in S-1 administration occurs, the RD is considered to be the same as the MTD at which a majority of patients will tolerate conventionally.

Follow-up evaluation

Within 2 weeks before initiating the chemotherapy, all patients were assessed by a physical examination, routine hematology and biochemistry analyses, ECG (electrocardiogram), chest X-ray and abdominal computed tomography (CT) scans to define the extent of disease. Complete blood cell counts with platelet and differential counts were recorded weekly during chemotherapy, and serum chemistries were repeated once or twice within every treatment cycle. Subjective symptoms, body weight, physical examination, performance status, and all adverse effects were recorded before each treatment course. Measurement of serum tumor marker carcinoembryonic antigen (CEA) level was performed at least once every 4 weeks.

Assessment of the objective response rate

Measurable lesions were reassessed every 8 weeks using CT scan, X-ray, and other techniques that allowed retrospective and independent evaluation. The response rate was assessed every 8 weeks using the RECIST (Response Evaluation Criteria in Solid Tumors) criteria. In cases of partial response or complete response, a further assessment at 4 weeks later was required for confirmation of the response; all tumor measurements were reviewed and confirmed by an independent panel of radiologists.

RESULTS

Patient characteristics

A total of 16 patients entered this study. The patient characteristics are shown in Table 2. The average age was 60 years, ranging from 36 to 74 years. Seven were male, and 9 were female. The PS according to the ECOG criteria was 0 in the majority of patients. Seven patients presented one affected organ, 8 patients presented two, and 1 patient presented three affected organs, with the most commonly affected organ being the distant lymph nodes. All eligible patients received at least 2 cycles of treatment.

MTD and RD

Adverse effects and DLT are shown in Table 3. Patient no. 2 experienced grade 3 diarrhea as a DLT after the third administration of CPT-11 on day15 at level 1.

TABLE 2.
Patient's characteristics

	Pt No.	Age	Sex	PS	Primary site	Affected organs	Treatment course
Level 1	1	53	M	0	Colon	Mediastinal LN, Spine	7
	2	63	M	1	Colon	Peritoneum	2
	3	36	F	0	Colon	Paraaortic LN	4
	4	55	M	1	Rectum	Intrapelvic, Peritoneum	4
	5	56	F	0	Colon	Mediastinal LN	4
	6	60	F	1	Colon	Liver, Lung, Neck LN	7
Level 2	7	74	M	0	Rectum	Lung	4
	8	57	F	0	Coon	Lung	5
	9	74	M	0	Rectum	Liver, Lung	4
Level 3	10	67	M	1	Colon	Mediastinal LN	2
	11	56	F	0	Colon	Iliac LN	8
	12	63	F	0	Colon	Peritoneum, Paraaortic LN	8
Level 4	13	53	F	1	Colon	Liver, Lung, Paraaortic LN	6
	14	57	F	0	Colon	Liver, Peritoneum	7
	15	58	M	0	Rectum	Lung, Paraaortic and iliac LN	2
	16	60	F	0	Rectum	Liver, Lung, Peritoneum, Primary	3

PS: performance status according to the Eastern Cooperative Oncology Group criteria.
M: male, F: female, LN: lymph nodes

TABLE 2.
Adverse effects during the first cycle, DLT and tumor response

	Pt No.	Adverse effects	DLT	Tumor Response
Level1	1	Fatigue (2)		SD
	2	Nausea (1), Fatigue (1)	Diarrhea (3)	SD
	3	Nausea (2), Fatigue (1)		SD
	4			PD
	5	Nausea (2), Fatigue (2)		PR
	6	Hand & Foot Syndrome (1)		PR
Level2	7	Fatigue (1)		PD
	8	Fatigue (2), Nausea (2)		PR
	9			PD
Level3	10	Fatigue (1), Stomatitis (1), Diarrhea (1)		SD
	11	Nausea (2)		CR
	12	Nausea (2), Fatigue (2), Neutropenia (1)		PR
Level4	13	Diarrhea (1), Fatigue (1)		PR
	14	Neutropenia (2)	CPT skip	PR
	15	Nausea (2), Rash, Diarrhea (2)	CPT skip	SD
	16	Nausea (2), Fatigue (1)	CPT skip	SD

( ): grade, DLT: dose limiting toxicity, CPT: irinotecan
CR: complete response, PR: partial response, SD: stable disease, PD: progression disease.

No DLT occurred in 3 additional patients enrolled at level 1. No DLT was observed at levels 2 or 3. Two of the first 3 patients at level 4 had to skip the third administration of CPT-11 due to grade 2 neutropenia (patient no. 14) and grade 1 diarrhea (patient no. 15), thus level 4 was defined as the MTD. According to the decision criteria for RD described in Patients and Methods, level 4 was therefore considered as the RD of this metronomic chemotherapy.

Tumor response

One patient at level 3 achieved a complete response (CR). Two patients at level 1, 1 at level 2, 1 at level 3, and 2 patients at level 4 achieved partial responses (PR). Three patients did not respond to chemotherapy and the disease progressed (PD); 6 patients showed a stable condition (stable disease: SD). The objective response rate was 43.8% with a 95% confidence interval (95% CI) ranging from 19.8 to 70.1% (Table 3).

Treatment continuation

The median number of treatment cycles in these patients was 4, with range of 2 to 8 cycles. The treatments were stopped for tumor progression in 9 patients, patient refusal in 2, conversion to surgery in 2, complete response in 1, and for adverse effects in 2 patients. The adverse effects leading to treatment discontinuation were diarrhea in the first (grade 3) and second (grade 2) cycle (patient no. 2) and intestinal bleeding in the second cycle (patient no. 15), respectively. Eight of 9 patients whose disease progressed, and 1 of 2 patients whose adverse effects disrupted the treatment, received second-line chemotherapies such as FOLFOX.

DISCUSSION

It has been shown that administration of peroral fluoropyrimidines on a daily schedule for an extended period of time may inhibit growth of the endothelium continuously without inducing drug resistance [20]. However, when bi-weekly or tri-weekly high-dosage CPT-11 is combined with peroral fluoropyrimidines, the combination therapy may often have to be temporarily suspended, which prevents the benefits of peroral fluoropyrimidines from being realized. The type of serious toxic effects, including neutropenia and diarrhea, often associated with a bi-weekly regimen FOLFIRI (irinotecan combined with bolus plus infusion 5-FU/LV), which is one of the standard therapies for metastatic colorectal cancer, were rarely observed

in the present study using low-dose metronomic weekly-CPT-11 and daily S-1. The lower toxicity of our metronomic regimen should be confirmed in a further phase II study, as compared with the regimen consisting of tri-weekly high dose CPT-11 and S-1 reported previously [14], or FOLFIRI.

The present study suggested that 60 mg/m^2 of CPT-11 and 80 mg/m^2 of S-1 were the RD for further metronomic chemotherapy study. Metronomic chemotherapy by definition should be continued without temporary suspension due to therapy-related toxic reactions. Therefore, it is reasonable to consider skipping of CPT-11 administration or several-days suspension in S-1 administration as a DLT using conventional dosage escalation criteria. If a skip in CPT-11 administration or a several-day suspension in S-1 administration were excluded as a DLT, a higher dosage than 60 mg/m^2 of CPT-11 might be considered the MTD. Such a higher dosage of CPT-11 may often result in a skip in the CPT-11 administration or interruption in S-1 administration, in this combination therapy of S-1 and CPT-11.

Metronomic chemotherapy has been summarized by Kerbel et al. [16] as showing that 1) conventional cytotoxic anticancer drugs have antiangiogenic effects which could contribute to their efficacy, 2) the antiangiogenic effects of chemotherapy seemed to be optimized by administering such drugs 'metronomically' – in other words in small dosages on a frequent schedule (daily, several times a week, or weekly) in an uninterrupted manner, over a relatively long period, 3) conventional chemotherapy, which is administered at more toxic MTD, requires 2- to 3-week breaks between successive cycles of therapy (which seems to counteract the potential for sustained therapeutically effective antiangiogenic effects), 4) in preclinical models, metronomic chemotherapy can be effective in treating tumors in which the cancer cells have developed resistance to the same chemotherapeutics in a MTD administration (which also has the advantage of being less acutely toxic, therefore making more extended treatments possible), 5) the efficacy of metronomic chemotherapy can be significantly increased when administered in combination with antiangiogenic drugs, such as antibodies against vascular endothelial growth factor (VEGF) or VEGF receptor 2, and 6) some metronomic chemotherapy regimens induce sustained suppression in circulating endothelial progenitor cells and increase the levels of the endogenous angiogenesis inhibitor thrombospondin-1, both of which can suppress neovascularization. However, no one yet knows an adequate dosage or definition of the dosage based on the concept of metronomic chemotherapy. This is a key reason why metronomic chemotherapy is not widely adopted in clinical trials. One possible means of determining the RD in metronomic chemotherapy might be to monitor the circulating endothelial cells and endothelial progenitor cells, which are known to be predictors for the effectiveness of antiangiogenic therapy [21,22].

It was interest that tumor responses were observed constantly at all therapy levels of our metronomic chemotherapy, even at the lowest-dosage of CPT-11. The findings suggested that this metronomic chemotherapy can be expected to have an antiangiogenic effect through continuous inhibition in endothelial cells, in addition to showing an antiproliferating effect against the tumor cells. With regard to antiangiogenic effects, in a preclinical study the 'doublet' combination metronomic chemotherapy using two oral drugs, UFT and cyclophosphamide, where the biologic optimal dosages were determined by effects on levels of circulating endothelial progenitor cells, showed a remarkable prolongation of survival with no evidence of overt toxicity despite long term continuous therapy compared to the monotherapy for advanced metastatic breast cancer [23]. Thus, when antitumor efficacy of metronomic chemotherapy is evaluated in phase II and III studies it is important to assess the duration of treatment, progression free survival, overall survival and the correlation with circulating endothelial cells and endothelial progenitor cells as surrogate markers for antiangiogenic therapy in addition to the tumor shrinkage (response rate).

Another advantage of our regimen is the schedule of drug administration. Previous *in vitro* studies have shown that CPT-11 down-regulated thymidylate synthase expression in tumor cells, leading to synergy between CPT-11 and 5-FU that was maximal when CPT-11 was given 24 h prior to 5-FU [24,25]. The administration of CPT-11 followed by S-1 with a 2-day interval in our regimen seems to be reasonable, in terms of the antiproliferation effects and of gastrointestinal toxicity.

In conclusion, 60 mg/m^2 of CPT-11 and 80 mg/m^2 of S-1 were found to be the RD for a further phase II study of metronomic chemotherapy consisting of weekly CPT-11 and daily S-1. Our new criteria, including a skipping or interruption of drug administration as a DLT in this dosage-escalating study may be useful for indicating the optimal dosages in metronomic chemotherapy.

ACKNOWLEDGMENTS: This work was supported by a Grant-in-Aid for Scientific Research (C) (No.20591597) from the Ministry of Education, Culture, Sports, Science and

Technology, of Japan.

REFERENCES

1. Shimada Y, Yoshino M, Wakui A, Nakao I, Futatsuki K et al. CPT-11 Gastrointestinal Cancer Study Group. Phase II study of CPT-11, a new camptothecin derivative, in metastatic colorectal cancer. J Clin Oncol 1993; 11:909-913.
2. Rothenberg ML, Cox JV, deVore RF, Hainsworth JD, Pazdur R et al. A multicenter, phase II trial of weekly irinotecan (CPT-11) in patients with previously treated colorectal carcinoma. Cancer 1999; 85:786-795.
3. Saltz LB, Cox JV, Blanke C, Rosen LS, Fehrenbacher L et al. Irinotecan Study Group. Irinotecan plus fluorouracil and leucovorin for metastatic colorectal cancer. N Engl J Med 2000; 343:905-914.
4. Douillard JY, Cunningham D, Roth AD, Navarro M, James RD et al. Irinotecan combined with fluorouracil compared with fluorouracil alone as first-line treatment for metastatic colorectal cancer: a multicentre randomised trial. Lancet 2000; 355:1041-1047.
5. de Gramont A, Figer A, Seymour M, Homerin M, Hmissi A et al. Leucovorin and fluorouracil with or without oxaliplatin as first-line treatment in advanced colorectal cancer. J Clin Oncol 2000; 18:2938-2947.
6. Shirasaka T, Nakano K, Takechi T, Satake H, Uchida J et al. Antitumor activity of 1 M tegafur-0.4 M 5-chloro-2,4-dihydroxypyridine-1 M potassium oxonate (S-1) against human colon carcinoma orthotopically implanted into nude rats. Cancer Res 1996; 56:2602-2606.
7. Takechi T, Nakano K, Uchida J, Mita A, Toko K et al. Antitumor activity and low intestinal toxicity of S-1, a new formulation of oral tegafur, in experimental tumor models in rats. Cancer Chemother Pharmacol 1997; 39:205-211.
8. Kato T, Shimamoto Y, Uchida J, Ohshimo H, Abe M et al. Possible regulation of 5-fluorouracil-induced neuro- and oral toxicities by two biochemical modulators consisting of S-1, a new oral formulation of 5-fluorouracil. Anticancer Res 2001; 21:1705-1712.
9. Robben NC, Pippas AW, and Moore JO. The syndrome of 5-fluorouracil cardiotoxicity. An elusive cardiopathy. Cancer 1993; 71:493-500.
10. Shirasaka T, Shimamoto Y, and Fukushima M. Inhibition by oxonic acid of gastrointestinal toxicity of 5-fluorouracil without loss of its antitumor activity in rats. Cancer Res 1993; 53:4004-4009.
11. Ohtsu A, Baba H, Sakata Y, Mitachi Y, Horikoshi N et al. Phase II study of S-1, a novel oral fluoropyrimidine derivative, in patients with metastatic colorectal carcinoma. S-1 Cooperative Colorectal Carcinoma Study Group. Br J Cancer 2000; 83:141-145.
12. Shirao K, Ohtsu A, Takada H, Mitachi Y, Hirakawa K et al. Phase II study of oral S-1 for treatment of metastatic colorectal carcinoma. Cancer 2004; 100:2355-2361.
13. Van den Brande J, Schöffski P, Schellens JH, Roth AD, Duffaud F et al. EORTC Early Clinical Studies Group early phase II trial of S-1 in patients with advanced or metastatic colorectal cancer. Br J Cancer 2003; 88:648-653.
14. Goto A, Yamada Y, Yasui H, Kato K, Hamaguchi T et al. Phase II study of combination therapy with S-1 and irinotecan in patients with advanced colorectal cancer. Ann Oncol 2006; 17:968-973.
15. Miller KD, Sweeney CJ, and Sledge GW Jr. Redefining the target: chemotherapeutics as antiangiogenics. J Clin Oncol 2001; 19:1195-1206.
16. Kerbel RS, and Kamen BA. The anti-angiogenic basis of metronomic chemotherapy. Nat Rev Cancer 2004; 4:423-436.
17. Hoff PM, Ansari R, Batist G, Cox J, Kocha W et al. Comparison of oral capecitabine versus intravenous fluorouracil plus leucovorin as first-line treatment in 605 patients with metastatic colorectal cancer: results of a randomized phase III study. J Clin Oncol 2001; 19:2282-2292.
18. Douillard JY, Hoff PM, Skillings JR, Eisenberg P, Davidson N et al. Multicenter phase III study of uracil/tegafur and oral leucovorin versus fluorouracil and leucovorin in patients with previously untreated metastatic colorectal cancer. J Clin Oncol 2002; 20:3605-3616.
19. Ogata Y, Sasatomi T, Mori S, Matono K, Ishibashi N et al. Significance of thymidine phosphorylase in metronomic chemotherapy using CPT-11 and doxifluridine for advanced colorectal carcinoma. Anticancer Res 2007; 27:2605-2611.
20. Yonekura K, Basaki Y, Chikahisa L, Okabe S, Hashimoto A et al. UFT and its metabolites inhibit the angiogenesis induced by murine renal cell carcinoma, as determined by a dorsal air sac assay in mice. Clin Cancer Res 1999; 5:2185-2191.
21. Duda DG, Cohen KS, di Tomaso E, Au P, Klein RJ et al. Differential CD146 expression on circulating *versus* tissue endothelial cells in rectal cancer patients: implications for circulating endothelial and progenitor cells as biomarkers for antiangiogenic therapy. J Clin Oncol 2006; 24:1449-1453.
22. Shaked Y, Emmenegger U, Man S, Cervi D, Bertolini F et al. Optimal biologic dose of metronomic chemotherapy regimens is associated with maximum antiangiogenic activity. Blood 2005; 106:3058-3061.
23. Munoz R, Man S, Shaked Y, Lee CR, Wong J et al. Highly efficacious nontoxic preclinical treatment for advanced metastatic breast cancer using combination oral UFT-cyclophosphamide metronomic chemotherapy. Cancer Res 2006; 66:3386-3391.
24. Guichard S, Hennebelle I, Bugat R, and Canal P. Cellular interactions of 5-fluorouracil and the camptothecin analogue CPT-11 (irinotecan) in a human colorectal carcinoma cell line. Biochem Pharmacol 1998; 55:667-676.
25. Torigoe S, Ogata Y, Matono K, and Shirouzu K. Molecular mechanisms of sequence-dependent antitumor effects of SN-38 and 5-fluorouracil combination therapy against colon cancer cells. Anticancer Res 2009; 29:2083-2090.

Experts Debate Bolus vs Continuous Infusion 5-FU

February 1, 2003
Oncology NEWS International, Oncology NEWS International Vol 12 No 2, Volume 12,Issue 2

PALM BEACH, Florida-What is the best method for administering fluorouracil (5-FU)? Should it be given as a continuous intravenous infusion, as often done in Europe? Or should 5-FU be administered as an intravenous bolus, as typically done by American physicians, at least partly to avoid the need for central venous access and pump devices.

PALM BEACH, Florida□What is the best method for administering fluorouracil (5-FU)? Should it be given as a continuous intravenous infusion, as often done in Europe? Or should 5-FU be administered as an intravenous bolus, as typically done by American physicians, at least partly to avoid the need for central venous access and pump devices.

In a debate over the best approach, Joseph R. Bertino, MD, argued in favor of bolus 5-FU in some situations on the ground that different effects can be expected depending on route of administration. He is associate director, Cancer Institute of New Jersey and professor of medicine and pharmacology, University of Medicine and Dentistry of New Jersey in New Brunswick. Robert B. Diasio, MD, argued that continuous infusion 5-FU is overall more effective and associated with less severe drug-related toxicity than bolus dosing. Dr. Diasio is chairman of pharmacology/toxicology, and associate director of the University of Alabama Comprehensive Cancer Center in Birmingham.

Two Different Drugs

"It is a little embarrassing that 40 years after the introduction of 5-FU we are still talking about how best to give this drug," Dr. Bertino admitted. "I want to suggest that some of the confusion is because 5-FU is actually two different drugs, depending on the dose schedule used. I'm not pushing for bolus vs infusional. I'm pushing for both."

Dr. Bertino said that 5-FU is activated by several pathways. Bolus 5-FU, which is active over 15 minutes to 24 hours, acts mainly by incorporation into RNA. Continuous infusion 5-FU, which is active for over 24 hours to 3 weeks, apparently acts mainly by inhibiting thymidylate synthase.

In vitro data using HCT-8 colorectal carcinoma cells showed that at the same dose, more 5-FU was incorporated into RNA following a bolus 4-hour exposure than following 7-day continuous exposure. "One mechanism of resistance to repeat bolus 5-FU is decreased incorporation into RNA, due to a decrease in UMP kinase activity," Dr. Bertino said. "A mechanism of resistance to 7-day continuous exposure to 5-FU is decreased thymidylate synthase inhibition."

Cytotoxicity caused by bolus 5-FU is not prevented by thymidine, but cytotoxicity produced by continuous infusion 5-FU is. Clinically, 5-FU-related toxicities also vary depending on dose schedule, Dr Bertino said. Bolus 5-FU causes leukopenia, mucositis, and diarrhea. Continuous infusion 5-FU causes more hand-foot syndrome and mucositis.

"Patients failing pulse 5-FU may still respond to continuous infusion 5-FU, capecitabine (Xeloda), or intra-arterial administration of the thymidylate synthase inhibitor fluorodeoxyuridine (FUDR)," Dr. Bertino said. Failure of bolus 5-FU has been correlated with decreased expression of UMP kinase in tumor samples. "This is one of the few mechanisms of resistance that has actually been identified in patients," Dr. Bertino said. Investigators had previously been puzzled by the fact that thymidylate synthase levels often do not predict tumor response to bolus 5-FU.

Revisiting Dose Schedules

Dr. Bertino said that a regimen of sequential pulses of methotrexate/5-FU and continuous infusion 5-FU/leucovorin produces response rates of about 40% but that oxaliplatin (Eloxatin) and/or irinotecan (CPT-11, Camptosar) may be more effective as partners for continuous infusion 5-FU/leucovorin. "This would amount to hitting the DNA directly at one level while preventing DNA synthesis at another level," he said.

Dr. Diasio agreed that 5-FU dose schedules need to be re-examined but contended that clinicians can produce the same efficacy with less toxicity by giving less 5-FU over a longer time as a continuous infusion. "This increases tumor exposure time to 5-FU. Capecitabine also increases exposure time, but by different pharmacokinetics," he said. "Oral capecitabine is more like a repeat minibolus effect with many small peaks and troughs."

Dr. Diasio pointed out that a continuous infusion schedule produces more complete responses (5% vs 0% with bolus 5-FU in one study) and a higher overall response rate (30% vs 7%, $P < .001$). He admitted that this has not generally translated into an improvement in survival in randomized trials, however. A meta-analysis of six trials of bolus vs infusional schedules reported a slight survival benefit for continuous infusion 5-FU, with 3-year survival of 39% vs 23% and 4-year survival of 16% vs 6%. Only three of these trials showed a survival benefit with continuous infusion 5-FU.

"Efficacy is maintained with an infusional schedule and there is less toxicity but little survival benefit," Dr. Diasio asserted.

Additional Issues

The waters are likely to be muddied a bit more by ongoing combination trials of 5-FU with oxaliplatin or irinotecan. These studies use infusional rather than bolus 5-FU, and Dr. Diasio pointed out that although there appear to be advantages to continuous infusion 5-FU, it would be helpful to have a bolus arm included in the study for comparison.

Finally, Dr. Diasio pointed to expense and reimbursement problems likely to occur in the United States due to the complexity of giving infusional 5-FU vs bolus 5-FU. "Oral fluoropyrimidines give increased exposure and may be able to maintain efficacy, as suggested by recent phase III studies with capecitabine," he said. Dr. Diasio also noted that because capecitabine is administered orally, it is associated with less toxicities than 5-FU, in particular, avoiding the problems associated with administration via IVs, catheters, and infusion pumps.

Related Content:
News

Editorial

Topotecan: What Dose, What Schedule, What Route?[1]

Seamus O'Reilly[2]
Waterford Regional Hospital, Waterford, Ireland

Topotecan is a semisynthetic water soluble analogue of camptothecin, which exerts its cytotoxic effects through inhibition of the enzyme topoisomerase I. This enzyme relaxes supercoiled DNA by covalently binding to it, leading to transient single-strand breaks that are resealed by topoisomerase I after strand passage. These breaks allow topological shifts in DNA strands and are essential steps in permitting DNA replication, repair, and transcription. Topotecan binds to the topoisomerase I-DNA complex and prevents the religation step. Consequently permanent strand breaks are created, and cell death ensues. Given such S-phase specificity, it is likely that topotecan's activity should be schedule dependent.

In Phase I trials of the i.v. formulation of topotecan, a variety of schedules were evaluated (1). On the basis of the schedule-dependent nature of topotecan's mechanism of action, its relatively short plasma half-life (2 h), and the antitumor activity observed in Phase I testing, a 30-min infusion schedule administered every 3 weeks was most extensively evaluated and was selected for pivotal, disease-specific studies. Antitumor activity in these Phase II and III studies resulted in the approval of this agent for patients with relapsed ovarian cancer in 1996 (2). Nonetheless, 2 years later, clinical investigators are still assessing the optimal dose and schedule for this agent.

Questions concerning the optimal schedule of topotecan were raised by investigators at New York University, who evaluated the use of ambulatory infusion schedules of topotecan administered for 21 days every 4 weeks (3, 4). Although it was cumbersome due to the requirements for central venous catheters, this schedule was felt to more optimally exploit the schedule-dependent nature of topotecan's effects. Correlative cellular pharmacodynamic studies demonstrated down-regulation of the topotecan target topoisomerase I over the 3 weeks of drug exposure, followed by recovery to normal in the week off treatment. Significant antitumor activity was demonstrated in patients with a variety of refractory solid tumor malignancies. Subsequent Phase II evaluations of this protracted schedule in patients with refractory ovarian cancer have produced response rates of 43% in one study (5) but only 10.5% in another (6). At this time, the optimal i.v. schedule of topotecan therapy is unknown. The most commonly used daily times 5 schedule is inconvenient for patients, and a less protracted daily times 3 schedule is being evaluated by some investigators. A recently completed randomized study compared the approved schedule with a 24-h infusion schedule administered once a week for 4 weeks every 6 weeks (7). In this well-conducted study of women with relapsed ovarian cancer, the response rate in the approved schedule arm was 22.6%, compared to 3.1% in the investigational arm. A similarly conducted trial comparing a 21-day infusion schedule of topotecan with the approved schedule would also be worthwhile, particularly because recently conducted xenograft studies have demonstrated that intermittent exposure schedules maybe the most efficacious (8).

Questions concerning the optimal dose of topotecan were raised following its approval for clinical use. In clinical practice, the hematological toxicity associated with the recommended Phase II dose of topotecan has been an area of concern, particularly in patients with renal impairment or those who have received extensive prior alkylating agent therapy, both of which are common clinical scenarios in patients with relapsed ovarian cancer (9, 10). Hematological toxicity has also been an issue with the development of combination regimens incorporating topotecan with alkylating agents or taxanes (e.g., Refs. 11 and 12). Dose reductions in therapy or hematopoietic growth factors have been used to circumvent these effects, the latter strategy adding considerably to the expense of therapy. In patients with renal impairment, dose reductions are required to compensate for reduced renal clearance. Anecdotal evidence suggests that antitumor activity is not compromised in these patients by this strategy (13). However, it is unknown whether efficacy is compromised by dose reductions in extensively pretreated patients. Population studies using limited sampling pharmacokinetics to assess the relationships between dose, drug exposure, and antitumor response (as have been performed with carboplatin; Ref. 14) would be helpful to clarify these issues. Indeed, dose intensification using granulocyte colony-stimulating factor to double the dose intensity of topotecan therapy in minimally pretreated patients with fluorouracil-refractory colorectal cancer did not impact on antitumor response rates (15).

Questions concerning the optimal dose and schedule of an oral formulation of topotecan are presented in the article by Gerrits *et al.* (16) elsewhere in this issue of *Clinical Cancer Research*. On the basis of observations that the i.v. formulation of topotecan was orally bioavailable and on the basis of efforts to mimic the continuous infusion schedule of topotecan that appeared most active, without the need for infusional pumps and central venous catheters, an oral formulation of topotecan was developed. In the article by Gerrits and colleagues (16), pharmacokinetic and pharmacodynamic relationships from Phase I studies of oral topotecan are presented and discussed. Four schedules were evaluated: once daily for 5 days every 21 days, once daily for 10 days every 21 days, twice daily for 10 days every 21 days, and twice daily for 21 days every 28 days. Several interesting observations were made. (a) With the more protracted schedules of oral administration, diarrhea rather than hematological toxicity was dose limiting. This toxicity appeared more severe than has been observed with the other camptothecin

Received 9/29/98; accepted 10/14/98.
The costs of publication of this article were defrayed in part by the payment of page charges. This article must therefore be hereby marked *advertisement* in accordance with 18 U.S.C. Section 1734 solely to indicate this fact.

[1] S. O. has received speaker's honoraria from SmithKline Beecham (the manufacturers of topotecan).

[2] To whom requests for reprints should be addressed, at Waterford Regional Hospital, Dunmore Road, Waterford, Ireland. Phone: 35351873321; Fax: 35351850406; E-mail: oreillys@setlb.ie.

analogue CPT-11, in that loperamide therapy was ineffective. The pathophysiology of these effects is unknown. These effects may relate to intestinal damage due to unabsorbed drug. (b) Hematological toxicity was the predominant toxicity associated with shorter administration schedules. However, with all schedules, this toxicity was less severe than that observed with the intravenous formulation. (c) Substantial intra- and interpatient variability in the pharmacokinetics of topotecan was observed. Mean intrapatient variations in the area under the plasma concentration *versus* time curve, ranging from 25.4 to 96.5% with the lowest intrapatient variability, was observed with the daily times 5 schedule. Interpatient variability in area under the concentration *versus* time curve varied from 40.1 to 73.4%. These results most likely reflect the relatively wide range in topotecan bioavailability reported previously by this group (17) and suggest that protocols for dose escalation should be incorporated into clinical trials of this formulation. On the basis of observations from this study, a daily times 5 schedule has been selected for further clinical development of oral topotecan.

Answers as to whether this 5-day oral schedule will replace the 5-day i.v. schedule will come from recently completed Phase II and III studies in women with relapsed ovarian cancer (18). In addition, these studies will address whether the favorable improvement in hematological toxicity profile of the oral formulation is at the expense of reduced antitumor activity. Results from such studies will also generate interest in developing combination regimens with oral topotecan, which may circumvent the hematological toxicities observed in combination regimens of the i.v. formulation.

These questions and answers pertaining to the optimal dose, schedule, and route of administration are not unique to topotecan. Similar issues of dose and schedule apply to other approved agents, such as paclitaxel (19) and CPT-11 (20), whereas issues of interpatient variability also pertain to all orally administered anticancer agents (21). Indeed, of the available anticancer agents, only carboplatin has been rigorously evaluated in clinical pharmacodynamic models relating drug exposure and antitumor activity. The story of the clinical development of topotecan is important because it emphasises the role of pharmacokinetic and pharmacodynamic studies in guiding drug development. A chapter of this story is elegantly demonstrated in the work of Gerrit *et al.* (16), in which pharmacokinetic and pharmacodynamic endpoints were used to determine the optimal schedule. This story emphasises the importance of Phase IV (postapproval) drug studies in which the majority of clinical drug development occurs and the need for both pharmacological evaluations and randomized comparisons as part of this process.

ACKNOWLEDGMENTS

The excellent secretarial assistance of Heretta Stanfield is gratefully acknowledged. I also acknowledge helpful discussions related to topotecan over the past several years with Drs. Eric Rowinsky, Ross Donehower, Louise Grochow, Sharyn Baker, and Deborah Armstrong.

REFERENCES

1. Takimoto, C. H., and Arbuck, S. Camptothecins. *In:* B. A. Chabner and D. L. Longo (eds.), Cancer Chemotherapy and Biotherapy: Principles and Practice, Ed. 2, pp. 463–484. Philadelphia: Lippincott-Raven Publishers, 1996.

2. ten Bokkel Huninink, W., Gore, M., Carmichael, J., Gordon, A., Malfetano, J., Hudson, I., Broom, C., Scarabelli, C., and Davidson, N. Topotecan *versus* paclitaxel for the treatment of recurrent epithelial ovarian cancer. J. Clin. Oncol., *15:* 2183–2193, 1997.

3. Hochster, H., Liebes, L., Speyer, J., Sorich, J., Taubes, B., Oratz, R., Wernz, J., Chachoua, A., Raphael, B., Vinci, R. Z., *et al.* Phase I trial of low-dose continuous topotecan infusion in patients with cancer: an active and well tolerated regimen. J. Clin. Oncol., *12:* 5553–5559, 1994.

4. Hochster, H., Speyer, J., Wadler, S., *et al.* Phase II study of topotecan 21 day infusion in platinum treated ovarian cancer: a highly active regimen. Proc. Am. Soc. Clin. Oncol., *15:* 285, 1996.

5. Hochster, H., Liebes, L., Speyer, J., Sorich, J., Taubes, B., Oratz, R., Wernz, J., Chachoua, A., Blum, R. H., and Zelenuich-Jacquotte, A. Effect of prolonged topotecan infusion on topoisomerase I levels: a Phase I and pharmacodynamic study. Clin. Cancer Res., *3:* 1245–1252, 1997.

6. Johnson, S., Pyle, L., King, K., *et al.* A Phase II study of topotecan given as a continuous 21 day infusion every 28 days in platinum pre-treated ovarian carcinoma. Eur. J. Cancer, *33* (Suppl. 8): S120, 1997.

7. Hoskins, P., Eisenhauer, E., Beare, S., Roy, M., Drouin, P., Stuart, G., Bryson, P., Grimshaw, R., Capstick, V., and Zee, B. Randomized Phase II study of two schedules of topotecan in previously treated patients with ovarian cancer: a National Cancer Institute of Canada Clinical Trials Group study. J. Clin. Oncol., *16:* 2233–2237, 1998.

8. Pawlik, C. A., Houghton, P. J., Stewart, C. F., Cheshire, P. J., Richmond, L. B., and Danks, M. K. Effective schedules of exposure of medulloblastoma and rhabdomyosarcoma xenografts to topotecan correlate with *in vitro* assays. Clin. Cancer Res., *4:* 1995–2002, 1998.

9. O'Reilly, S., Armstrong, D. K., and Grochow, L. B. Life threatening myelosuppression in patients with occult renal failure receiving topotecan. Gynecol. Oncol., 329–330, 1997.

10. Armstrong, D. K., and O'Reilly, S. Clinical guidelines for managing topotecan related hematologic toxicity. Oncologist, *3:* 4–10, 1998.

11. Miller, A. A., Lilenbaum, R. C., Lynch, T. J., Rosner, G. L., Ratain, M. J., Green, M. R., and Schilsky, R. L. Treatment related fatal sepsis from topotecan/cisplatin and topotecan/paclitaxel. J. Clin. Oncol., *14:* 1964–1965, 1996.

12. Lilenbaum, R. C., Ratain, M. J., Miller, A. A., Hargis, J. B., Hollis, D. R., Rosner, G. L., O'Brien, S. M., Brewster, L., Green, M. R., and Schilsky, R. L. Phase I study of paclitaxel and topotecan in patients with advanced tumors: a cancer and leukemia group B study. J. Clin. Oncol., *13:* 2230–2237, 1995.

13. O'Reilly, S., Rowinsky, E. K., Slichenmyer, W., Donehower, R. C., Forastiere, A. A., Ettinger, D. S., Chen, T. L., Sartorius, S., and Grochow, L. B. Phase I and pharmacologic study of topotecan in patients with impaired renal function. J. Clin. Oncol., *14:* 3062–3073, 1996.

14. Jodrell, D. I., Egorin, M. J., Canetta, R. M., Langenberg, P., Goldbloom, E. P., Burroughs, J. N., Goodlow, J. L., Tan, S., and Wiltshaw, E. Relationships between carboplatin exposure and tumor response and toxicity in patients with ovarian cancer. J. Clin. Oncol., *10:* 520–528, 1992.

15. Rowinsky, E. K., Baker, S. D., Burks, K., O'Reilly, S., Donehower, R. C., and Grochow, L. B. High-dose topotecan with granulocyte-colony stimulating factor in fluoropyrimidine-refractory colorectal cancer: a Phase II and pharmacodynamic study. Ann. Oncol., *9:* 173–180, 1998.

16. Gerrits, C. J. H., Schellens, J. H. M., Burris, H., Eckardt, J. R., Planting, A. S. T., van der Burg, M. E. L., Rodriguez, G. I., Loos, W. J., van Beurden, V., Hudson, I., von Hoff, D. D., and Verweij, J. A comparison of clinical pharmacodynamics of different administration schedules of topotecan (Hycamtin). Clin. Cancer Res., *5:* 69–75, 1999.

17. Schellens, J. H. M., Creemers, G. J., Beijnen, J. H., Rosing, H., de Boer-Dennert, M., McDonald, M., Davies, B., and Verweij, J. Bioavailability and pharmacokinetics of oral topotecan: a new topoisomerase I inhibitor. Br. J. Cancer, *73:* 1268–1271, 1996.

18. Gore, M., Rustin, G., Calvert, H., Bezwoda, W., Carmichael, J., Oza, A., Kaye, S., ten Bokkel Huinink, W., Malfetano, J., Falkson, G., Clarke Pearson, D., Ross, G. A., Dane, G. C., and Fields, S. Z. A multicenter randomized Phase III study of topotecan administered intravenously or orally for advanced epithelial ovarian carcinoma. Proc. Am. Soc. Clin. Oncol., *17:* 349a, 1998.

19. Arbuck, S. G., Canetta, R., and Onetto, N. Current dosage and schedule issues in the development of paclitaxel (Taxol). Semin. Oncol., *20* (Suppl. 3): 31–39, 1993.

20. O'Reilly, S., and Rowinsky, E. K. The clinical status of irinotecan (CPT-11), a novel water soluble camptothecin analogue: 1996. Crit. Rev. Oncol. Hematol., *24:* 47–70, 1996.

21. DeMario, M. D., and Ratain, M. J. Oral chemotherapy: rationale and future directions. J. Clin. Oncol., *16:* 2557–2567, 1998.

Clinical Cancer Research

Topotecan: What Dose, What Schedule, What Route?

Seamus O'Reilly

Clin Cancer Res 1999;5:3-5.

Preclinical Safety, Pharmacokinetics and Antitumor Efficacy Profile of Liposome-entrapped SN-38 Formulation

AJAI PAL, SUMSULLAH KHAN ,YUE-FEN WANG, NARAYAN KAMATH, ASIS K. SARKAR, ATEEQ AHMAD, SAIFUDDIN SHEIKH, SHAHID ALI, DANIELLE CARBONARO, ALLEN ZHANG and IMRAN AHMAD

NeoPharm, Inc., Research and Development, 1850 Lakeside Drive, Waukegan, IL 60085, U.S.A.

Abstract. *Background: SN-38, 7-ethyl-10-hydroxycamptothecin, is a biologically active metabolite of irinotecan. Its poor solubility restricted its development as an anticancer agent. We have developed an easy-to-use liposome-entrapped SN-38 (LE-SN38) and evaluated its toxicology, pharmacokinetics and antitumor efficacy profile. Materials and Methods: Toxicity and pharmacokinetics studies were conducted in CD2F1 mice and beagle dogs. Therapeutic efficacy studies were performed in murine leukemia (P388 and P388/ADR) and in a human pancreatic (Capan-1) tumor models. Results: Multiple dose administration (i.v. x 5) of LE-SN38 indicated a maximum tolerated dose (MTD) of 5.0 and 7.5 mg/kg/day for male and female mice, respectively. The MTD of LE-SN38 in dogs was 1.2 mg/kg. The elimination half-life ($t_{1/2}$) of SN-38 in mouse plasma was 6.38 h with volume of distribution (Vd_{ss}) 2.55 L/kg. In dogs, $t_{1/2}$ and Vd_{ss} were 1.38-6.42 h and 1.69-5.01 L/kg, respectively. P388 tumor-bearing mice dosed with LE-SN38 at 5.5 mg/kg (i.v. x 5) showed 100% survival. LE-SN38 at 4 or 8 mg/kg (i.v. x 5) inhibited 65% and 98% tumor growth, respectively, in a human pancreatic tumor model. Conclusion: LE-SN38 showed a favorable pharmacokinetics profile and can be administered safely at therapeutically effective doses.*

Camptothecin (CPT) and its analogues are broad-spectrum anticancer agents which target the nuclear enzyme topoisomerase I. This enzyme relieves torsional strain in DNA by inducing reversible single strand breaks, thereby permitting unwinding of DNA necessary for DNA replication, RNA transcription and DNA repair (1-3). Inhibition of topoisomerase I activity results in DNA damage, which leads to cell death. Among currently available camptothecin analogs, irinotecan (CPT-11) is recommended for the treatment of various types of cancer (4-6). CPT-11 is a prodrug that undergoes de-esterification *in* vivo by carboxylesterases (CE) to yield the biologically active metabolite, 7-ethyl-10-hydroxycamptothecin, SN-38 (7). This metabolic conversion of CPT-11 yields less than 10% SN-38, and further depends on the genetic inter-individual variability of CE activity (8). Low conversion to SN-38 limits the therapeutic potential of CPT-11. In addition, direct use of SN-38 has the advantage of being the active metabolite and, therefore, minimizes the inter-individual variability. It has been shown that SN-38 is up to 1000-fold more cytotoxic *in vitro* than CPT-11 (9). Despite the higher potency of SN-38, its poor solubility in aqueous media, as well as in physiologically compatible and acceptable solvents, hampered its development as an anticancer agent.

Among the available drug delivery systems, the use of liposome-entrapped drugs is an effective and viable approach to treat various diseases including cancer (10-12). Previous studies have shown that liposomal encapsulation of camptothecins conferred protection of the active lactone form (13). Liposome encapsulation of CPT-11 has been shown to reduce toxic side-effects with a better therapeutic profile compared to CPT-11 (14). Although the tissue distribution of CPT-11 was improved after liposome encapsulation, the SN-38 concentration in tissue was not increased (14).

To exploit the full therapeutic benefit of SN-38, we have successfully developed a novel easy-to-use liposome-entrapped SN-38 formulation, LE-SN38 (15). In the present study, we evaluated the safety, pharmacokinetics and toxicokinetics profile of SN-38 in CD2F1 mice and beagle dogs following intravenous (*i.v.*) administration of LE-SN38. The antitumor efficacy of LE-SN38 was evaluated in murine leukemia and human pancreatic tumor models. The results demonstrate that LE-SN38 is safe at a therapeutically effective dose, showed a favorable pharmacokinetic profile and was therapeutically effective in both murine and human tumor models.

Correspondence to: Imran Ahmad, NeoPharm Inc., 1850 Lakeside Drive, Waukegan, IL 60085. Fax: (847) 887-9281, e-mail: Imran@neopharm.com

Key Words: Camptothecin, CPT-11, SN-38, liposome, drug delivery.

Materials and Methods

Drug and chemicals. SN-38 was purchased from Qventas, Inc. (Newark, DE, USA). Irinotecan (irinotecan hydrochloride injection) was purchased from Pharmacia & Upjohn (Kalamazoo, MI, USA). Dioleoylphosphatidicholine, cardiolipin and cholesterol were purchased from Avanti Polar Lipids (Alabaster, AL, USA). All other chemicals were of reagent grade.

Preparation of liposomes. The liposome-entrapped formulation of SN-38 was prepared by the thin-film hydration method (15). The entrapment efficiency of SN-38 in liposomes was > 95% and the mean particle size of liposome was 150 ± 20 nm. Reconstituted LE-SN38 was stable at room temperature for up to 8 hours.

Cell culture. P388 and multidrug-resistant P388/ADR murine leukemia cells were obtained from the Biological Testing Branch, Developmental Therapeutics Program of the National Cancer Institute (Frederick, MD, USA). P388/ADR is a P-glycoprotein over-expressing multidrug-resistant tumor cell line derived from drug-sensitive P388 lymphocytic leukemia by long-term doxorubicin exposure. Leukemia cells were propagated in RPMI-1640 medium with 10% fetal bovine serum (FBS), 2 mM glutamine, 100 units/mL of penicillin and 100 μg/mL of streptomycin. Capan-1 was purchased from ATCC (Manassas, VA, USA) and grown in Iscoves' modified Dulbecco's medium supplemented with 20% FBS, 100 units/mL penicillin and 100 μg/mL streptomycin. All the cells were maintained at 37˚C in a humidified atmosphere of 5% CO_2. All culture media and related reagents were purchased from Invitrogen Co. (Carlsbad, CA, USA).

Animals. Male, female CD2F1 (6-7 weeks old) and female CB-17 SCID (3-4 weeks old) mice were obtained from Harlan Sprague Dawley Laboratories (Indianapolis, IN and Madison, WI , USA, respectively). The animals were housed in cages in temperature- and humidity-controlled rooms with a 12-h light/dark cycle. The CD2F1 mice were offered 2018S HT Rodent Diet (Harlan Teklad, Madison, WI, USA) and water *ad libitum*. The SCID mice were handled aseptically and housed in microisolators (Tecniplast, Italy). They were fed on autoclaved 2018S HT Rodent Diet (Harlan Teklad) and autoclaved water *ad libitum*.

Male and female purebred beagle dogs, weighing 8-10 kg (10-11 months of age), were purchased from Marshall Farms, Inc. (North Rose, NY, USA). Each dog was allowed access to Certified Canine Diet # 5007 (PMI Feeds, St. Louis, MO, USA) for approximately 2 h each day during the quarantine and study periods. Tap water was available *ad libitum*. The dogs were housed individually in stainless steel cages. The cage size and animal care were in accordance with the Guide for the Care and Use of Laboratory Animals (16), and the US Department of Agriculture through the Animal Welfare Act (Public Law 99-198).

Safety study in mice. For the single dose toxicity study, CD2F1 mice (5/group/sex) were administered *i.v.* with LE-SN38 at dose levels of 23, 46, or 65 mg/kg. Male animals also received LE-SN38 single additional doses of 28 or 37 mg/kg. The control group received placebo liposomes with a lipid dose equal to that of 65 mg/kg dose group. The mice were monitored for clinical signs, mortality and changes in body weight for up to 30 days.

Table I. *Effect of single and multiple treatments of LE-SN38 on survival of CD2F1 mice.*

Dose (mg/kg/day)	Number of doses	Cumulative dose (mg/kg)	Number surviving/Total	
			Female	Male
0[a]	1	0	5/5	5/5
23[b]	1	23	5/5	5/5
28[b]	1	28	ND	5/5
37[b]	1	37	ND	5/5
46[b]	1	46	5/5	0/5
65[b]	1	65	4/5	0/5
0[c]	5	0	10/10	10/10
5[d]	5	25	10/10	10/10
7.5[d]	5	37.5	10/10	9/10
10[d]	5	50	9/10	7/10

[a]Placebo liposomes were dosed at lipid amount 65 mg/kg dose.
[b]LE-SN38 was administered as a single dose on day 1.
[c]Placebo liposomes were dosed at lipid amount 10 mg/kg dose.
[d]LE-SN38 was administered for five consecutive days (once daily)
ND: not done

For the multiple dose toxicity study, LE-SN38 was administered *i.v.* to CD2F1 mice (20/group/sex) daily for 5 days at doses of 5.0, 7.5, or 10.0 mg/kg. The control group received placebo liposomes with a lipid dose equal to that of 10 mg/kg dose group. The animals were observed for clinical signs, mortality and changes in body weight for up to 30 days. Animals (five animals from each group) were sacrificed on days 6 and 20 for blood and organs collection for clinical analyses (hematology and clinical chemistry) and histopathology, respectively. Prior to blood collection, the animals were anesthetized by carbon dioxide and blood samples were collected by retro-orbital bleeding into tubes containing EDTA (hematology) or no anticoagulant (clinical chemistry). The heart, lung, kidney, spleen, liver and small intestine were removed and fixed in 10% neutral buffered formalin. The hematology parameters included: erythrocyte count (RBC), total white blood cells (WBC), platelets count, WBC differential, hemoglobin, hematocrit and erythrocyte indices (MCV, MCH, MCHC). The clinical chemistry analyses included: bilirubin, blood urea nitrogen (BUN), creatinine, alkaline amino phosphatase, alanine amino transferase (ALT) and aspartate amino transferase (AST).

Safety study in beagle dogs. The dogs were weighed prior to the start of study, and randomly assigned to one of the three LE-SN38 treatment groups (3 dogs/sex/treatment) or to the control group (placebo liposome). Each dog received a single slow bolus *i.v.* injection of the LE-SN38 at 0.4, 0.8 and 1.2mg/kg dose levels or placebo liposome with lipid dose equal to 1.2 mg/kg dose on days 1, 22, 43 and 64. All dogs in the study were observed twice daily during the study period for signs of mortality, moribundity and overt toxicity. Detailed clinical observations for each dog were recorded once weekly throughout the study. The examination included, but was not limited to, observations of the general condition, skin, fur, eyes, ears, nose, oral cavity, thorax, abdomen, external genitalia, limbs and feet. In addition, the dogs were observed immediately post-dose and at approximately 0.5 and 2 h after each dose administration (days 1, 22, 43, and 64) for pharmacotoxic signs resulting from acute effects of the LE-SN38 or placebo liposomes.

Body weight, food consumption, ophthalmology and electrocardiograms were also monitored. Blood samples were collected for clinical pathology (hematology, coagulation and clinical chemistry) prior to the start of study and on days 4, 25, 46, 67 and 84, and on days 10, 21, 31, 42, 52, 63 and 73 for hematology only. The hematology parameters included RBC, WBC, hemoglobin, hematocrit, MCV, MCH, MCHC, platelet count, reticulocyte count and reticulocyte percent, differential leukocyte counts and RBC morphology. Coagulation parameters included prothrombin time and activated partial thromboplastin time. Clinical chemistry parameters included BUN, creatinine, glucose, total protein, albumin, globulin, albumin/globulin ratio, sodium, potassium, chloride, calcium, phosphorus, ALT, AST, alkaline phosphatase, total bilirubin and cholesterol. On week 13, all animals were sacrificed and post mortem necropsy examination included a thorough inspection of all external surfaces, organs and orifices. The cranial, thoracic, abdominal and pelvic cavities were opened and tissues/organs within each cavity were examined. The tissues for histopathological examination including gross lesions, tumor masses and injection sites were collected. Organ weights of selected organs were also determined. Organ weights and terminal body weight were used for the calculation of organ to body and organ to brain weight ratios.

Pharmacokinetics, tissue distribution and toxicokinetics studies in mice. Plasma pharmacokinetic and tissue distribution analyses were performed in male CD2F1 mice. Mice received a single *i.v.* injection of LE-SN38 at a dose level of 10 mg/kg. Blood samples were collected by retro -orbital bleeding in microcontainer tubes containing heparin as anticoagulant at 5, 15, 30 min and 1, 2, 4, 8, 12 and 24 h post-dosing. Blood samples were centrifuged at 600xg for 10 min at 4˚C to separate the plasma. After blood collection, liver, kidneys, lungs, spleen and heart were rapidly collected and snap-frozen on dry ice. Both plasma and tissue samples were stored at -70˚C until analysis.

A multiple dose *i.v.* toxicokinetic study of LE-SN38 was conducted in CD2F1 mice at 5.0, 7.5 and 10 mg/kg/day x 5. Following administration of the last dose, blood samples were collected in heparinized tubes and plasma was separated as described above. Plasma samples were stored at -70˚C until analysis.

The concentrations of SN-38 in mouse plasma and in tissue samples were determined by an LC/MS/MS method. In brief, 100 µL plasma or tissue homogenate (5% w/v) was spiked with 200 µL of camptothecin (internal standard, IS) at 25 ng/mL in the extraction solvent (acetonitrile with 0.5% acetic acid) and vortexed. After centrifugation, the supernatant was evaporated and the residue was reconstituted with acetonitrile/ammonium acetate buffer, pH 3.5 (20/80, v/v), then injected onto a Zorbax SB-C18 HPLC column (2.0x50 mm, 5 µm). The HPLC column effluent was analyzed and quantified by MS/MS. The concentration of SN-38 was determined by using a standard curve generated from the peak area ratios of SN-38 standards *versus* IS. Plasma and tissue concentrations of SN-38 *vs.* time data were analyzed by a non-compartmental model using the WinNonlin program (Pharsight, Mountain View, CA, USA). Plasma and tissue area under the curve (AUC_{0-X}) values (X being the time of the last plasma concentration measured) were estimated using the linear trapezoidal method with uniform or $1/Y^2$ weighting. The terminal phase rate constant (K_{el}) was obtained by linear regression analysis of the terminal phase concentration-time data. $AUC_{X-\infty}$ was estimated by dividing the last plasma concentration value measured by the terminal plasma rate constant. Plasma clearance (CLp), terminal phase half-life ($t_{1/2}$) and volume of distribution at steady state (Vd_{ss}) were estimated based on standard methods.

Pharmacokinetics/toxicokinetics studies in dogs. The study design was the same as that described for the safety study in dogs. Serial blood samples (~ 2.5 mL) were collected from each dog by venipuncture from the jugular vein at 5 and 30 min, and 1, 2, 4, 8,12, 24 and 48 h after the first and fourth cycles (days 1 and 64 of dosing). Blood was transferred to heparinized vacutainer tubes and the plasma was collected by centrifugation and stored at -70˚C until analysis. The SN-38 concentration in dog plasma was determined by a HPLC fluorescence method (17). Plasma pharmacokinetics analysis was performed as described above.

Efficacy study in mouse leukemia models. P388 or P388/ADR cells ($1x10^5$) were injected *i.v. via* the tail vein into CD2F1 female mice. After 24 h of cell transplantation, the mice were randomly divided into different treatment groups (10 mice/group) and administered *i.v.* with placebo liposomes or LE-SN38. For the single dose study, the animals were treated with LE-SN38 at 15 or 30 mg/kg dose levels and were monitored for survival up to 30 days. In the multiple dose study, LE-SN38 was administered at 2.8 or 5.5 mg/kg dose levels for five consecutive days and the mice were monitored for survival up to 60 days. The median survival time (MST) for each group was calculated. Percent survival was also calculated and expressed as follows:

$$\text{Percent Survival} = \frac{\text{Number of Mice Surviving in Treatment Group}}{\text{Total Number of Mice in Group}} \times 100$$

Efficacy study in human xenograft tumor model. Logarithmically growing Capan-1 cells were injected (2.5×10^6 cells) subcutaneously to the flank region of SCID mice. The treatment was initiated when the tumor size reached 65-120 mm^3. Tumor-bearing mice were randomly divided into different treatment groups and treated with either placebo liposomes or LE-SN38 (15, 30 or 45 mg/kg) for the single dose study. In the multiple dose study, the animals received either placebo liposomes or LE-SN38 (4 or 8 mg/kg) once daily for 5 consecutive days. Tumor growth was monitored till day 28 post-treatment and the volume (mm^3) was measured every 3-5 days in two dimensions by calipers using the formula:

$$A \times (B/2)^2 \times \pi$$

where A and B are length and width of the tumor, respectively. To evaluate antitumor activity, the tumor volume was calculated as the percentage of pre-treatment tumor volume (day 1, the first day of dosing; 100%) by using the formula:

$$T_1 / T_0 \times 100$$

where T_1 represents mean tumor volume of the treated group on a particular day, and T_0 represents the mean tumor volume of the same treated group at the initiation of treatment.

Results

Safety profile of LE-SN38

Mice: Survival data for the single and multiple dose studies of LE-SN38 in mice are presented in Table I. The survival rate for animals at 23, 28 or 37 mg/kg dose level was 100%. The male mice treated as single dose with 46 or 65 mg/kg of LE-SN38

Table II. *Histopathological analysis: incidence/lesions on days 6 and 20 after initiation of treatment.*

Organ	Histopathological findings	Day 6 Dose (mg/kg/day)								Day 20 Dose (mg/kg/day)							
		0		5		7.5		10		0		5		7.5		10	
		M	F	M	F	M	F	M	F	M	F	M	F	M	F	M	F
	Degeneration and necrosis epithelium	0	0	4	3	5	5	5	5	0	0	0	0	0	0	0	1
	Hypertrophy/hyperplasis epithelium	0	0	3	3	4	5	5	5	0	0	0	0	0	0	0	0
Duodenum	Atrophy villi	0	0	0	0	0	0	3	4	0	0	0	0	0	0	0	0
	Atrophy crypts	0	0	0	0	0	0	2	0	0	0	0	0	0	0	0	0
	Degeneration and necrosis epithelium	0	0	4	3	5	5	5	5	0	0	0	0	0	0	0	1
Ileum	Hypertrophy/hyperplasis epithelium	0	0	2	3	5	5	5	5	0	0	0	0	0	0	0	0
	Atrophy villi	0	0	1	0	0	3	5	4	0	0	0	0	0	0	0	0
	Degeneration and necrosis epithelium	0	0	3	3	5	5	5	5	0	0	0	0	0	0	0	0
Jejunum	Hypertrophy/hyperplasis epithelium	0	0	1	3	4	5	5	5	0	0	0	0	0	0	0	0
	Atrophy villi	0	0	0	0	0	0	4	4	0	0	0	0	0	0	0	0
	Vacuolar degeneration hepatocellular	0	0	0	0	0	0	5	1	0	0	0	0	0	0	0	0
Liver	Necrosis hepatocellular	0	0	0	0	0	0	2	0	0	0	0	0	0	0	0	0
	Degeneration/necrosis cholangiocellular	0	0	0	0	1	0	5	0	0	0	0	0	0	0	1	0
	Hypertrophy/hyperplasis epithelium	0	0	0	0	1	0	5	0	0	0	0	0	0	0	0	0
Lung	Degeneration/necrosis artery wall	0	0	1	0	1	0	3	0	0	0	0	0	0	0	0	0
Spleen	Atrophy	0	0	3	2	5	5	5	4	0	0	0	0	0	0	0	0

CD2F1 mice (10 animals/group/sex) were administered LE-SN38 (*i.v.* once daily x 5 days) with doses of 5.0, 7.5 and 10.0 mg/kg. The control group received placebo liposomes with a lipid dose equal to that of 10 mg/kg group. Animals from each group were sacrificed on day 6 and day 20 and organs were collected for histopathological evaluation.
0 = mild; 1 = minimal; 2 = mild; 3 = moderate; 4 = marked; 5 = severe.

were either moribund sacrificed or died by day 9 of treatment initiation. All the female mice survived when dosed with 46 mg/kg, whereas the survival was 80% at the 65 mg/kg dose level.

No significant decreases in body weight were observed for animals treated with placebo liposomes or LE-SN38 at the 23 or 28 mg/kg dose levels. In male mice, the decrease in body weight was 16.9% at the 37 mg/kg dose level, however, the loss in body weight was recovered by day 19. Female mice administered at the 46 and 65 mg/kg LE-SN38 dose levels showed body weight losses of 9% and 19% on days 2 and 5, respectively, which was recovered by days 17 and 22, respectively.

Animals treated with placebo liposomes showed no clinical signs of toxicity, suggesting that the liposome itself was not toxic. The animals showed no clinical signs of toxicity at the 23, 28, or 37 mg/kg dose levels. Females at the 46 mg/kg dose level had no clinical signs of toxicity, whereas the males had rough coats, dehydration and hunched posture by day 3. These male mice were either moribund sacrificed or died due to toxicity by day 9. Both male and female animals at the 65 mg/kg dose level had clinical signs of toxicity including rough coats, hunched posture and dehydration.

Mice treated with placebo liposomes or LE-SN38 at 5.0 mg/kg for 5 days showed a 100% survival rate (Table I). At the 7.5 mg/kg x 5 dose level, the survival rate was 90% for male and 100% for female mice. The survival rate was 70% and 90% for males and females, respectively, at the 10 mg/kg x 5 dose level. A decrease in body weight of 4-6% on day 5 was observed at the 5.0 or 7.5 mg/kg dose levels, which was recovered by day 15. A 15% loss in body weight on day 9 was observed in animals administered with LE-SN38 at 10 mg/kg x 5. No clinical signs of toxicity were observed in any animals dosed with either the placebo liposomes or with LE-SN38 at the 5 and 7.5 mg/kg dose levels, however, animals at the 10 mg/kg dose level showed clinical signs of toxicity.

The clinical chemistry results suggest no LE-SN38-related toxicity either on day 6 or day 20 at the 5 and 7.5 mg/kg dose levels (data not shown). A slight increase in AST, ALT and alkaline phosphatase levels were observed in some animals at the 10 mg/kg x 5 dose level in comparison to the placebo liposome control. No changes in hematology parameters were noticed at any dose level of LE-SN38 compared to the placebo liposome control. The histopathological lesions observed in the small intestine, liver, lung and spleen of LE-SN38-treated animals on day 6 sacrifice were either greatly reduced or had disappeared by day 20 (Table II).

Beagle dogs: All of the dogs survived to scheduled necropsy. Dose-independent reversible swelling was noted at the site of injection in some dogs. No significant differences in body weight during the study period was observed in dogs from the LE-SN38-administered groups (data not shown). No

Table III. *Summary of the predominant hematology findings in beagle dogs following LE-SN38 administration.*

Day relative to start date	Dose (mg/kg) 0.4	0.8	1.2
4	↓ WBC (m, f) ↓ Lymphocytes (m, f) ↓ Reticulocytes (m, f)	↓ WBC (m, f) ↓ Lymphocytes (m, f) ↓ Neutrophils (m) ↓ Reticulocytes (m, f)	↓ WBC (m, f) ↓ Lymphocytes (m, f) ↓ Neutrophils (m) ↓ Reticulocytes (m, f)
10	↓ Neutrophils (f) ↓ Platelets (m, f)	↓ WBC (f) ↓ Neutrophils (m, f) ↓ Platelets (m, f)	↓ WBC (m, f) ↓ Neutrophils (m, f) ↓ Platelets (m, f)
21	None	None	None
25	↓ WBC (m, f) ↓ Lymphocytes (f) ↓ Neutrophils (m) ↓ Reticulocytes (m, f)	↓ Lymphocytes (m, f) ↓ Neutrophils (m) ↓ Reticulocytes (m, f)	↓ WBC (m, f) ↓ Lymphocytes (m, f) ↓ Neutrophils (m) ↓ Reticulocytes (m, f) ↓ RBC (m)
31	↓ Neutrophils (f) ↓ Platelets (m, f)	↓ Platelets (m, f)	↓ Neutrophils (f) ↓ Platelets (m, f)
42	None	None	None
46	↓ Lymphocytes (m, f) ↓ Reticulocytes (m, f)	↓ WBC (m, f) ↓ Lymphocytes (m, f) ↓ Reticulocytes (m, f)	↓ Lymphocytes (m, f) ↓ Reticulocytes (m, f) ↓ RBC (m)
52	↓ Platelets (m, f)	↓ Platelets (m, f) ↓ WBC (m) ↓ Neutrophils (m, f)	↓ Neutrophils (m) ↓ RBC (m) ↓ Platelets(m, f)
63	None	None	None
67	↓ Lymphocytes (m, f) ↓ Reticulocytes (m, f)	↓ Lymphocytes (m, f) ↓ Reticulocytes (m, f)	↓ Lymphocytes (m, f) ↓ Reticulocytes (m, f) ↓ RBC (m)
73	↓ Neutrophils (f) ↓ Platelets (m, f)	↓ WBC (m) ↓ Neutrophils (m) ↓ Platelets (m, f)	↓ WBC (f) ↓ Neutrophils (m, f) ↓ RBC (m) ↓ Platelets (m, f)
84	None	None	None

m= males, f= females

differences in group mean food consumption values, ophthalmologic and electrocardiographic irregularities were noted in LE-SN38-treated groups.

A summary of the hematology findings after LE-SN38 administration to animals is presented in Table III. Changes in group mean hematology parameters that were noted most consistently at approximately 72 h after LE-SN38 administration (days 4, 25, 46 and 67), included: decrease in reticulocytes percent, reticulocyte counts, lymphocyte count (except in males in the 0.4 mg/kg/dose group), monocyte and eosinophil values. Mild decreases in group means and in individual platelet, neutrophil and WBC counts that were observed for dogs in all LE-SN38 dose groups were also considered to be treatment-related. A trend towards a lower incidence of decreased neutrophil and WBC counts was observed for dogs in all LE-SN38 dose groups by the third and fourth cycles. Lower group mean RBC, HGB and HCT values observed for male dogs in the 1.2 mg/kg/dose group on days 5,

Table IV. *Pharmacokinetic parameters of SN-38 in plasma of CD2F1 male mice after single i.v. LE-SN38 (10 mg/kg) administration.*

$t_{1/2}$	C_{max}	Vd	Vd_{ss}	CL_p	AUC_{0-24h}	$AUC_{0-\infty}$
(h)	(μg/mL)	(L/kg)	(L/kg)	(L/h/kg)	(μg•h/mL)	(μg•h/mL)
6.38	14.7	23.4	4.55	2.55	3.87	3.92

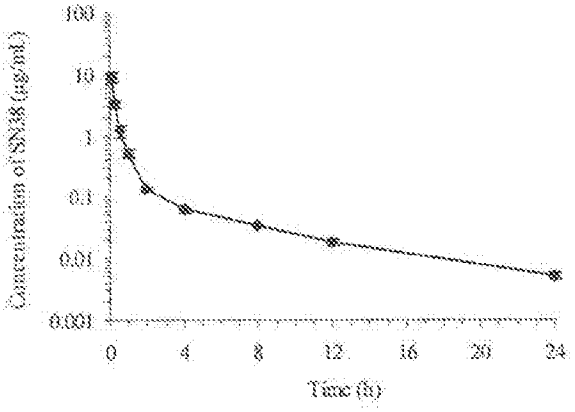

Figure 1. Plasma concentration-time profile of SN-38 in female CD2F1 mice. LE -SN38 was given to mice (n=3/time-point) at 10 mg/kg by i.v. injection via tail vein, and mean plasma concentrations of total SN-38 were measured by LC/MS/MS.

Table V. *Pharmacokinetic parameters of SN-38 in tissues of male CD2F1 mice after single i.v. LE-SN38 (10 mg/kg) administration.*

Tissue	C_{max} (μg/g)	AUC_{0-24h} (μg•h/g)	C_{max}/Dose[a]	AUC_{0-24h}/Dose[a]
Heart	17.1	11.9	1.72	1.19
Kidney	18.2	12.8	1.83	1.28
Liver	49.1	433	4.93	43.5
Lung	70.0	77.1	7.02	7.73
Spleen	65.2	385	6.54	38.6

[a] Mean dose given to the animals for tissue collection is 10 mg/kg

63 and 67 were considered treatment related, but of minimal toxicological relevance due to the small magnitude of the decreases observed in comparison to baseline values. Group mean reticulocyte, lymphocyte, monocyte and eosinophil values were comparable to or greater than values observed for dogs in the placebo liposome control group within 9 days after each dose (days 10, 31, 52 and 73). Mean platelet and neutrophil counts were comparable to or greater than the corresponding values for dogs in the placebo liposome control group by 20 days after each dose (days 21, 42, 63 and 84).

Increased (129% to 159% of placebo liposome control group values) group mean BUN values were observed for dogs in the 0.4 (female only), 0.8 (male only) and 1.2 mg/kg/dose groups on days 4, 25, 46 or 67. However, the changes were considered of minimal toxicological relevance due to the lack of a dose relationship and minimal magnitude of the changes. All other differences in group mean chemistry parameters that were observed were not considered to be toxicologically relevant as they were within their respective normal limits (data not shown).

There was no direct, treatment-related histopathological changes noted in the organs of dogs after LE-SN38 administration. Extramedullary hematopoiesis was noted in the livers of 1/3 male dogs (0.4 mg/kg/dose) and 3/3 male and 2/3 female dogs in each of the 0.8 and 1.2 mg/kg/dose groups. The severity of these lesions ranged from trace to mild. Extramedullary hematopoiesis (mild) was also detected in the spleens of 1/3 males dogs and 2/3 female dogs in the 1.2 mg/kg/dose group. This finding was consistent with decreases in reticulocyte, lymphocyte, monocyte, and eosinophil counts noted at approximately 72 h after each of the four doses (days 4, 25, 46 and 67).

LE-SN38 exhibits a favorable pharmacokinetic profile. The pharmacokinetics and tissue distribution of SN-38 were investigated in CD2F1 mice following a single *i.v.* dose administration at the 10 mg/kg dose level. Pharmacokinetic parameters are summarized in Table IV. The mean plasma concentrations of SN-38 *versus* time profile is shown in Figure 1. SN-38 was detected up to 24 h after dosing. The highest concentration detected was 8.83 μg/mL, which was observed at the first sampling time point (5 min). Following *i.v.* administration of LE-SN38, the total plasma clearance (CL_p) and the volume of distribution (Vd) were 2.55 L/h/kg and 23.4 L/kg, respectively, with an elimination half-life ($t_{1/2}$) of 6.38 h.

The exposure of SN-38 to the well-perfused tissues, *e.g.* liver, kidneys, heart, spleen and lungs, was higher as compared to plasma (Table V). The mean tissue-to-plasma concentration ratios of SN-38 at the observed T_{max} time (5 min for liver, kidneys, heart and lung; 30 min for spleen) were approximately 5.46, 1.59, 1.19, 7.38 and 4.79 for the liver, kidneys, heart, spleen and lungs, respectively. The level of total exposure (AUC_{0-24h}) in the tissues over 24h post-dose were detected in the following order: liver>spleen>lung>kidney>heart. The highest C_{max} 70.0 μg/g, was measured in the lung.

Table VI. *Toxicokinetic parameters of SN-38 in mice on day 5 following multiple i.v. dose administration of LE-SN38 (once daily x 5).*

Dose (mg/kg/day)	Sex	T_{max} (h)	C_{max} (μg/mL)	C_{max}/Dose	AUC_{0-24h} (μgh/mL)	AUC_{0-24h}/Dose
5	f	0.00	2.18	0.436	2.34	0.468
	m	0.00	2.50	0.500	2.55	0.510
7.5	f	0.00	2.50	0.333	3.38	0.451
	m	0.00	4.45	0.593	3.81	0.508
10	f	0.00	4.96	0.496	5.72	0.572
	m	0.00	4.85	0.485	4.54	0.454

m = males; f = females

The mean toxicokinetic parameters of SN-38 in mice on day 5 following LE-SN38 administration are presented in Table VI. The mean plasma AUC_{0-24} values at doses of 5, 7.5 and 10 mg/kg were 2.5, 5, 3.81 and 4.54 μg.h/mL for males and 2.34, 3.38 and 5.72 ug.h/mL for females respectively. The mean plasma C_{max} values at doses of 5, 7.5 and 10 mg/kg were 2.50, 4.45 and 4.85 μg /mL for males and 2.18, 2.50 and 4.96 μg /mL for females, respectively. There were no discernible differences in toxicokinetics parameters of SN-38 between male and female mice at all dose levels.

The mean plasma concentration-time profiles of SN-38 after the first (day 1) and the fourth doses (day 64) of LE-SN38 in beagle dogs are shown in Figure 2. Pharmacokinetic parameters are summarized in Table VII. Following *i.v.* administration of LE-SN38 on days 1 and 64, the peak plasma concentration of SN-38 in female and male dogs dosed at 1.2 mg/kg reached around 1200 ng/mL, and dropped to 2 ng/mL in 12 h. The observed C_{max} values were all achieved at the first sampling time-point (5 min). On day 1, the mean $t_{1/2}$, CLp, AUC_{0-12h} and $AUC_{0-\infty}$ values in female and male dogs were between 1.38 to 6.42 h, 1.56 to 2.90 L/h/kg, 144 to 543 ng•h/mL and 143 to 572 ng•h/mL, respectively. The Vd and Vd_{ss} values were between 5.15 to 19.0 L/kg and 2.99 to 5.01 L/kg, respectively. On day 64, the mean $t_{1/2}$, CLp, AUC_{0-12h} and $AUC_{0-\infty}$ values in female and male dogs were between 1.80 to 3.68 h, 1.34 to 2.40 L/h/kg, 209 to 541 ng•h/mL and 210 to 548 ng•h/mL, respectively. The Vd and Vd_{ss} values were between 5.11 to 12.7 L/kg and 1.69 to 3.21 L/kg, respectively.

LE-SN38 increased survival of P388 and P388/ADR tumor-bearing mice. The antitumor effect of a single dose administration of LE-SN38 against P388 leukemia is shown in Figure 3A. The MST for the control group (placebo liposome) was 12 days, while the MST was 25 days for LE-SN38 at the 15.0 mg/kg dose level. Treatment with LE-SN38 at 30 mg/kg increased the survival to 100% for the entire duration of the study (30 days).

The results for the antitumor effect of multiple dose studies are presented in Figure 3B. The MST of the control group (placebo liposome) was 13 days. In contrast, 60 and 100% survival was observed after LE-SN38 administration at the 2.8 and 5.5 mg/kg x 5 dose levels respectively, for the entire duration of the study (60 days).

In P388/ADR tumor-bearing mice, the MST for the control group was 11.5 days (Figure 4). The MST for mice treated with 4, 8 and 12 mg/kg x 5 of CPT-11 were 12.5, 14 and 14 days, respectively (data not shown). Treatment with LE-SN38 at the 4 and 8 mg/kg x 5 dose levels significantly increased the MST to 18.5 and 26.5 days, respectively.

LE-SN38 exhibits tumor growth inhibition of human pancreatic (Capan-1) xenograft tumor in SCID mice. In the single dose treatment schedule, animals treated with LE-SN38 at the 15, 30, or 45 mg/kg dose levels resulted in 53, 80 and 95% tumor growth inhibition, respectively, compared to the placebo liposome-treated group on day 28 post-treatment (Figure 5A). In the multiple dose treatment schedule (*i.v.* x 5), animals treated with LE-SN38 at the 4 or 8 mg/kg dose levels resulted in 65 and 98% tumor growth inhibition, respectively, compared to the control group (Figure 5B). No significant changes in body weights were observed in any LE-SN38-treated animals (data not shown).

Discussion

Advances in drug delivery technology have led to the development of several novel carriers, resulting in reduced toxicity and thereby improving the therapeutic efficacy of drugs. Liposomes are a well recognized drug delivery system that has been shown to increase therapeutic efficacy (10-14). Appropriately designed, liposomes preferentially accumulate at tumor sites as a result of their ability to extravasate through 'pores' or 'defects' in the capillary endothelium, which are usually not present in normal tissues or organs (18). The major toxicity associated with CPT-11 exposure is

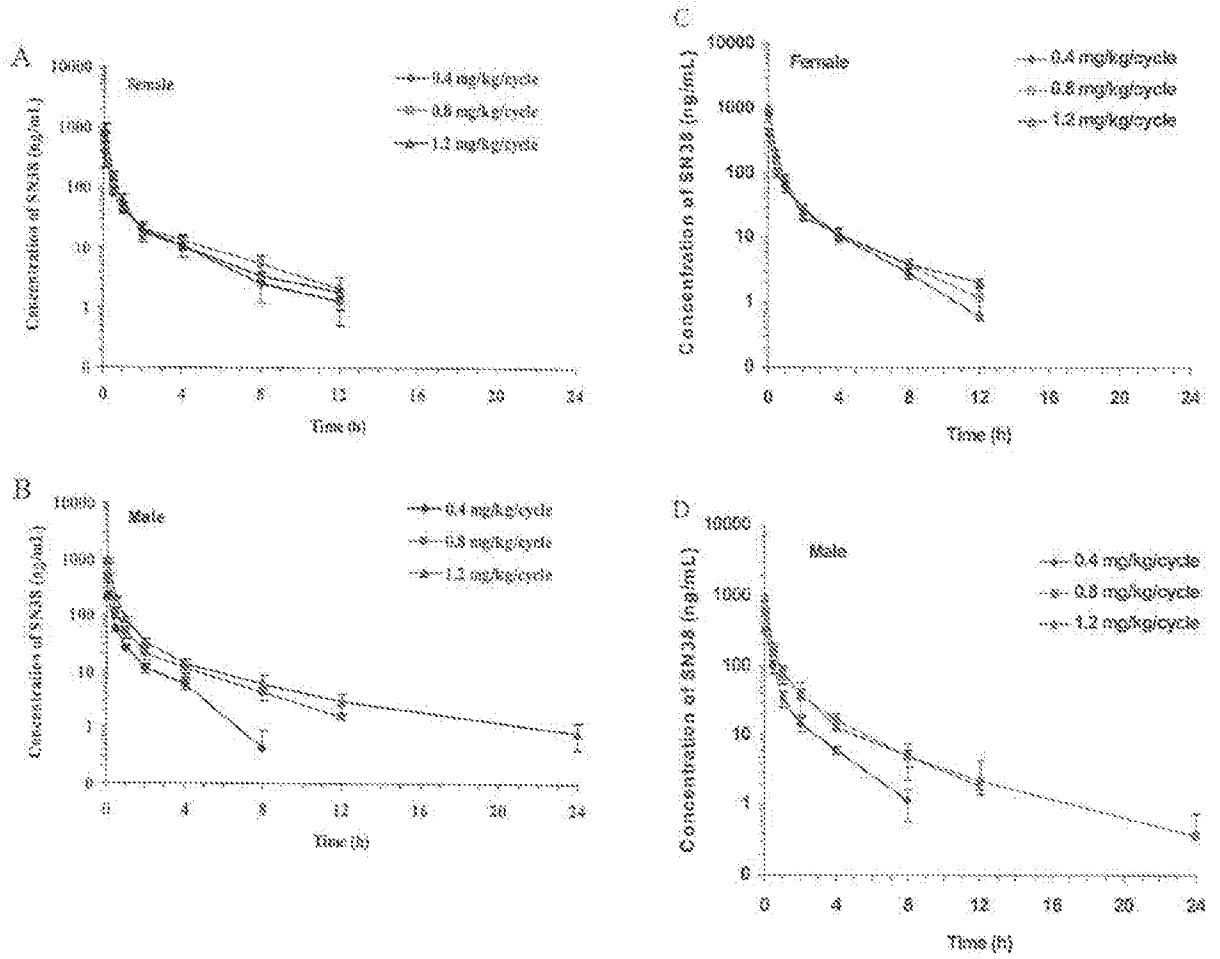

Figure 2. Plasma concentration-time profile of SN-38 in beagle dogs on days 1 and 64. LE-SN38 was given to beagle dogs (n=3/sex/group) as a 10-min i.v. infusion, and plasma concentrations of SN-38 were measured by HPLC on day 1, in female (A), male (B) and on day 64, female (C) and male (D).

severe acute diarrhea that leads to abdominal cramping, vomiting, flushing and diaphoresis (19-21). Several attempts have been made to incorporate camptothecin derivatives into liposomes to reduce the toxicity, while retaining the therapeutic efficacy (22,23). Sadzuka *et al.* (22) demonstrated that liposomal association of CPT-11 reduced the gastrointestinal toxicity of CPT-11. It also has been shown that lipid bilayer interactions stabilize the lactone moiety of camptothecin drugs, a pharmacophore that is essential for its antitumor activity (24). In order to overcome the potential problems associated with CPT-11, we have developed a well characterized easy-to-use liposome-entrapped SN-38 and evaluated its toxicity, pharmacokinetics, toxicokinetics, tissue distribution and therapeutic efficacy profile.

The toxicity results of LE-SN38 suggest that the MTDs were 37 and 46 mg/kg for single and 5 and 7.5 mg/kg/day (cumulative doses of 25 and 37.5 mg/kg) for multiple doses for male and female mice, respectively. Toxicity studies indicate that the therapeutically effective doses of LE-SN38 for murine and human tumor xenograft model are within the ranges of MTDs.

There were no unscheduled deaths during the study when LE-SN38 was administered to dogs as a single *i.v.* bolus at 0.4, 0.8 and 1.2 mg/kg dose levels on a 3-week schedule for four cycles. Dogs administered at the 1.2 mg/kg/dose level had occasional episodes of emesis. No clinical signs were noted in more than one dog in any LE-SN38-administered groups and then for only a single time during the study. Mean body weights did not decrease in any LE-SN38-treated groups when compared to controls (placebo liposome). Some individual animals, primarily in the 1.2 mg/kg/dose group, lost weight during one or more of the dosing cycles.

A LE-SN38-related decrease in hematopoiesis was observed in dogs approximately 72 h after administration

Table VII. *Pharmacokinetic parameters of SN-38 in beagle dogs on days 1 and 64 after LE-SN38 i.v. administration.*

Dose (mg/kg/cycle)	Sex	$t_{1/2}$ (h)	C_{max} (ng/mL)	Vd (L/kg)	Vd_{ss} (L/kg)	CL (L/h/kg)	AUC_{0-12h} (ngoh/mL)	$AUC_{0-\infty}$ (ngoh/mL)
Day 1								
0.4	f	2.16±0.78	536±277	5.15±2.29	2.99±1.37	1.56±0.13	256±26	260±21
	m	1.38±0.20	275±38	5.59±0.44	3.06±0.40	2.90±0.40	144±17	143±18
0.8	f	2.98±0.58	1000±263	8.69±1.19	3.19±0.40	2.16±0.51	396±74	407±78
	m	2.96±0.29	598±130	11.8±2.9	5.01±1.55	2.71±0.50	307±53	314±52
1.2	f	3.25±0.34	1290±241	13.1±3.3	3.12±0.55	2.70±0.45	468±93	476±93
	m	6.42±2.46	1210±107	19.0±6.8	4.28±0.82	2.13±0.19	543±36	572±48
Day 64								
0.4	f	2.62±0.62	522±146	5.13±1.29	2.12±0.39	1.34±0.04	295± 11	299±9
	m	1.80±0.17	398±58	5.11±0.66	2.16±0.27	2.00±0.31	209±34	210±34
0.8	f	2.68±0.29	1330±179	6.09±0.26	1.69±0.12	1.59±0.17	510±55	516±57
	m	2.34±1.00	699±154	7.34±1.33	3.21±0.47	2.08±0.53	426±107	444±123
1.2	f	3.68±0.19	1170±62	12.7±0.5	3.11±0.17	2.40±0.19	496±38	507±40
	m	2.90±0.05	1270±93	9.25±0.71	2.93±0.64	2.21±0.15	541±40	548 ±39

Values are expressed as mean±SEM
SEM: Standard error of the mean
m= males; f= females

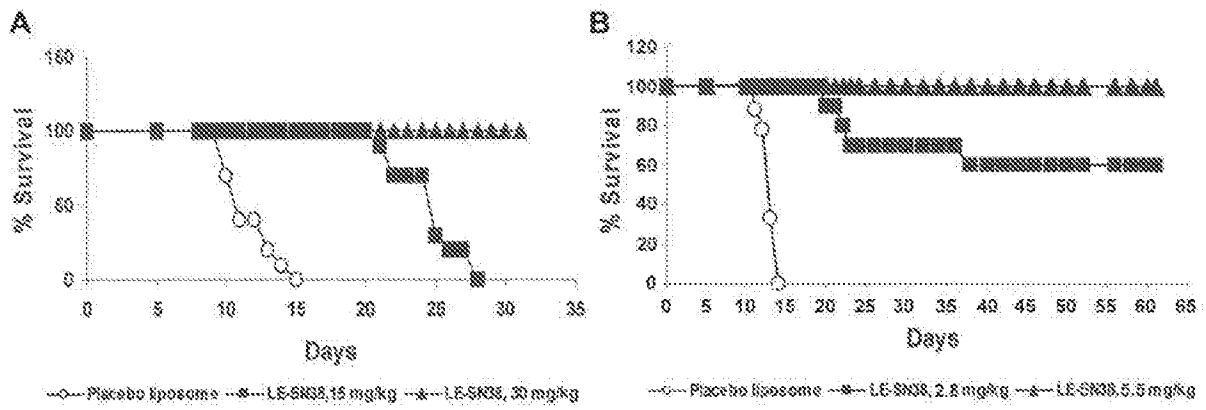

Figure 3. *A. Effect of single dose administration of LE-SN38 on survival of P388 leukemia tumor-bearing mice. Female CD2F1 mice were transplanted i.v. with $1x10^5$ P388 cells on day 0. Twenty-four hours after cell transplantation, treatment was initiated with the indicated doses of LE-SN38 i.v. once on day 1 (n=10). The animals were monitored for survival up to 30 days.*
B. Effects of multiple dose administration of LE-SN38 on the survival of P388 leukemia tumor-bearing CD2F1 mice. Female CD2F1 mice were transplanted i.v. with $1x10^5$ P388 cells on day 0. Twenty-four hours after cell transplantation, animals were injected i.v. with the indicated doses of LE-SN38 on day 1 through day 5 (n=10). The animals were monitored for survival up to 60 days.

of LE-SN38 at every cycle (days 4, 25, 46 and 73). However, the group mean values of hematology parameters were either comparable to or greater than the values observed in the placebo liposome group by day 9 after LE-SN38 administration (days 10, 31, 52 and 73). Fewer incidences of neutropenia and decreases in WBC counts were noticed in dogs dosed with LE-SN38 by the third and fourth cycles. The results suggest that the MTD in dogs was approximately 1.2 mg/kg/dose (24 mg/m^2/dose) and the No-Observed-Adverse-Effect-Level (NOAEL) was 0.8 mg/kg/dose.

SN-38 showed Vd_{ss} of 4.55 L/kg in mice, which is approximately 6.5 times of total body fluid at approximately 0.7 L/kg (25), indicating that SN-38 has a good tissue distribution and potential penetration to tumors. LE-SN38 showed a better pharmacokinetic profile in CD2F1 mice in comparison to an earlier study of mice given a comparable dose of CPT-11, a 10-fold higher plasma level than the equivalent dose of SN-38 and prolonged plasma $t_{1/2}$ of 6.38 h *vs* 1.7 h for SN-38 (8).

The mean exposure of SN-38 at the 1.2 mg/kg dose over 12h to female dogs were approximately 1.2 -and 1.8-fold

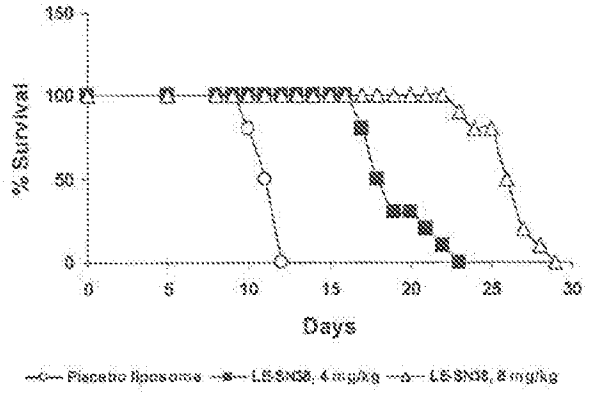

Figure 4. Effects of LE-SN38 on survival of P388/ADR leukemia tumor-bearing CD2F1 mice. Female CD2F1 mice were transplanted i.v. with $1x10^5$ P388/ADR cells on day 0. Twenty-four hours after cell transplantation, treatment was initiated with the indicated doses of LE-SN38 day 1 through day 5 (n=10). The study was monitored for survival up to 30 days.

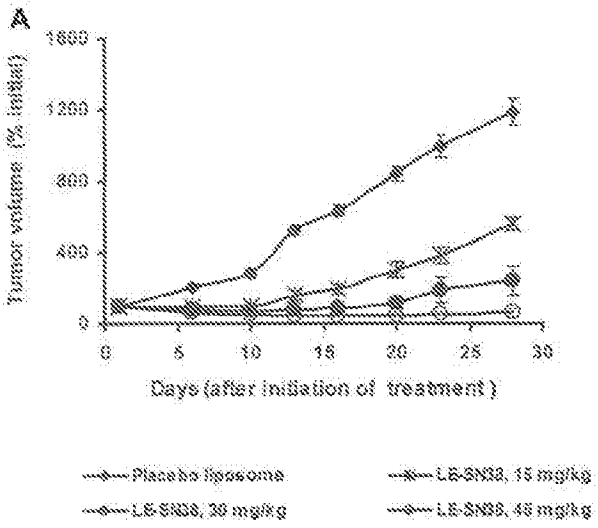

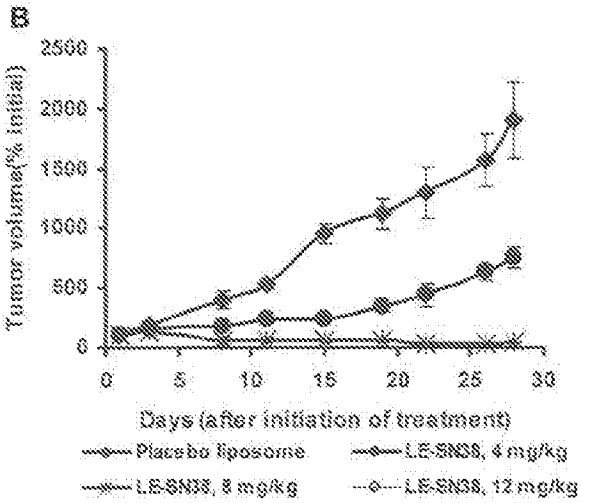

Figure 5. A. Single dose efficacy of LE-SN38 on growth of human pancreatic tumor model (Capan-1) in SCID mice. LE-SN38 was injected i.v. in mice when tumor volumes reached 65-120 mm^3 in size. Tumor growth was monitored for 28 days post-treatment and tumor volume was measured as described in Materials and Methods. The tumor size is expressed as mean ± SEM (n=5).

B. Multiple dose efficacy of LE-SN38 on growth of human pancreatic tumor model (Capan-1) in SCID mice. LE-SN38 was injected i.v. for five consecutive days once tumor volumes reached 65-120 mm^3 in size. Tumor growth was monitored for 28 days post-treatment and tumor volume was measured as described in Materials and Methods. The tumor size is expressed as mean ± SEM (n=4-6).

higher than at the 0.8 and 0.4 mg/kg dose levels, respectively, after the first cycle. In male dogs, the mean exposure of SN-38 over 12 h increased almost linearly with the dose levels after the first and fourth dose cycles. The exposure level of SN-38 at the 1.2 mg/kg dose was approximately 2.0- and 3.8-fold higher than that at the 0.8 and 0.4 mg/kg dose levels, respectively, after the first dose. The Vd_{ss} after the first and fourth doses was approximately 2 to 8 times greater than estimated dog body fluid (~0.6 L/kg) (25). Comparison of the pharmacokinetic parameters and exposure levels after the first and the fourth cycle doses showed no discernible differences, suggesting no accumulation in the tissues, and no major drug disposition or metabolism changes after dosing LE-SN38 once every three weeks in dogs.

LE-SN38 exhibited marked therapeutic efficacy against P388, P388/ADR murine leukemia cells transplanted in CD2F1 mice and against a human pancreatic tumor model. Single as well as multiple dose administration of LE-SN38 showed increased survival of P388 tumor-bearing mice compared to control (Figures 3 and 4). The multidrug-resistant cell line, P388/ADR is cross resistant to other anthracyclines, vinca alkaloids, epipodophylotoxins, CPT analogs and other structurally and functionally unrelated drugs (26). A marked increase in MST for LE-SN38-treated groups was observed compared to control (Figure 5) and CPT-11-treated groups (data not shown). The administration of single or multiple dose schedules of LE-SN38 in a human pancreatic tumor model showed significant tumor growth inhibition ($p<0.05$). This could be due to the optimal and prolonged bioavailability of SN-38, which is supported by our pharmacokinetics and tissue distribution data. This is also in agreement with an earlier study by Burke *et al.* (13), that liposome encapsulation of camptothecin protects the active lactone form for a prolonged period. It has been shown that liposome encapsulation of CPT-11 improved the tissue distribution profile and showed marginal increases in

therapeutic efficacy, however, conversion of CPT-11 to SN-38 was not increased (14). Therefore, the LE-SN38 formulation provides two major advantages: i) it does not require any metabolic conversion to exert its anticancer effect, and ii) liposomization may have provided the stability of the active lactone form and sustained exposure of SN-38.

In conclusion, these studies suggest that LE-SN38 is not toxic at a dose level with profound therapeutic benefits and favorable pharmacokinetics. The LE-SN38 formulation exhibited significant antitumor efficacy against murine and human tumor xenograft models. Thus, LE-SN38 may provide a potential therapeutic option for the treatment of human cancer. Phase I clinical trials of LE-SN38 are currently in progress.

Acknowledgements

The safety study in dogs was conducted at the Southern Research Institute (SRI, Birmingham, AL, USA). We thank Dr. Aqel W. Abu-Qare, Jennifer Ayoub, Wei Guo and Dr. Fadil Dahhani for their assistance in the mice pharmacokinetic studies and sample analyses.

References

1 Hsiang YH, Hertzberg R, Hecht S and Liu FJ: Camptothecin induces protein-linked DNA breaks *via* mammalian DNA topoisomerase I. J Biol Chem *260*: 14873-14878, 1985.

2 Hsiang YH and Liu F: Identification of mammalian DNA topoisomerase I as an intracellular target of the anticancer drug camptothecin. Cancer Res *48*: 1722-1726, 1988.

3 Stewart AF, Herrera RE and Nordheim A: Rapid induction of c-fos transcription reveals quantitative linkage of RNA polymerase II and DNA topoisomerase I enzyme activities. Cell *60*: 141-149, 1990.

4 Shimada Y, Yoshino M, Wakui A, Nakao I, Futatsuki K, Sakata Y, Kambe M, Taguchi T and Ogawa N: Phase II study of CPT-11, a new camptothecin derivative, in patients with metastatic colorectal cancer. J Clin Oncol *10*: 909-913, 1993.

5 Cardenal F, Domine M, Massuti B, Carrato A, Felip E, Garrido P, Juan O, Artal A, Barneto I, Lopez-Vivanco G, Balcells M and Rosell R: Three-week schedule of irinotecan and cisplatin in advanced non-small cell lung cancer: a multicentre phase II study. Lung Cancer *39*: 201-207, 2003.

6 Kollmannsberger C, Mross K, Jakob A, Kanz L and Bokemeyer C: Topotecan: A novel topoisomerase I inhibitor: pharmacology and clinical experience. Oncology 56: 1-12, 1999.

7 Humerickhouse R, Lohrbach K, Li L, Bosron WF and Dolan M E: Characterization of CPT-11 hydrolysis by human liver carboxylesterase isoforms hCE-1 and hCE-2. Cancer Res *60*: 1189-1192, 2000.

8 Kaneda N, Ngata H, Futura T and Yokokura T: Metabolism and pharmacokinetics of the camptothecin analogue CPT-11 in the mouse. Cancer Res *50*: 1715-1720, 1990.

9 Takimoto CH and Arbuck SG: Topoisomerase I targeting agents: the campothecins. *In*: Chabner BA, Lango DL (Eds). Cancer Chemotherapy and Biotherapy: Principal and Practice,3rd ed. Lippincot Williams & Wilkins, Philadelphia, 579-646, 2001.

10 Langer R: Drug delivery and targeting. Nature *392*: 5-10, 1998.

11 Gokhle PC, Pei J, Zhang C, Ahmad I, Rahman A and Kasid U: Improved safety, pharmacokinetics and therapeutic efficacy profiles of novel liposomal formulation of mitoxantrone. Anticancer Res *21*: 3313-3321, 2001.

12 Gabizon A and Papahadjopoulos D: Liposome formulations with prolonged circulation time in blood and enhanced uptake by tumors. Proc Natl Acd Sci USA *85*: 6949-6953, 1988.

13 Burke TG and Gao X: Stabilization of topotecan in low pH liposomes composed of distearoylphosphatidylcholine. J Pharma Sci *83*: 967-969, 1994.

14 Sadzuka Y, Hirotsu S and Hirota S: Effect of liposomalization on the antitumor activity, side-effects and tissue distribution of CPT-11. Cancer Lett *127*: 99-106, 1998.

15 Zhang JA, Xuan T, Parmar M, Ma L, Ugwu S, Ali S and Ahmad I: Development and characterization of a novel liposome-based formulation of SN-38. Int J Pharma *270*: 93-107, 2004.

16 Institute of Animal Laboratory Resources. Guide for Care and Use of Laboratory Animals. Commission on Life Sciences, National Research Council; National Academy Press; Washington D.C. 1996.

17 Guo W, Ahmad A, Khan S, Dahhani F, Wang YF and Ahmad I: Determination by liquid chromatography with fluorescence detection of total 7-ethyl-10-hydroxy-camptothecin (SN-38) in beagle dog plasma after intravenous administration of liposome-based SN-38 (LE-SN38). J Chromatography B *791*: 85-92, 2003.

18 Yuan F, Dellian M, Fukumura D, Leunig M, Berk DA, Torchilin VP and Jain RK: Vascular permeability in a human tumor xenograft: molecular size dependence and cutoff size. Cancer Res *55*: 3752-3756, 1995.

19 Kawato Y, Sekiguchi M, Akahane K, Tsutomi Y, Hirota Y, Kuga H, Suzuki W, Hakusui H and Sato K: Inhibitory activity of camptothecin derivatives against acetylcholinesterase in dogs and their binding activity to acetylcholine receptors in rats. J Pharm Pharmacol *45*: 444-448, 1993.

20 Morton CL, Wadkins RM, Danks MK and Potter PM: The anticancer prodrug CPT-11 is a potent inhibitor of acetylcholinesterase but is rapidly catalyzed to SN-38 by butyrylcholinesterase. Cancer Res *59*: 1458-1463, 1999.

21 Bleiberg H and Cvitkovic E: Characterisation and clinical management of CPT-11 (irinotecan)-induced adverse events: the European perspective. Eur J Cancer *3*: S18-23, 1996.

22 Sadzuka Y: Effective prodrug liposome and conversion to active metabolite. Curr Drug Metab *1*: 31-48, 2002.

23 Tardi P, Choice E, Masin D, Redelmeier T, Bally M and Madden TD: Liposomal encapsulation of topotecan enhances anticancer efficacy in murine and human xenograft models. Cancer Res *60*: 3389-3393, 2000.

24 Burke TG, Mishra AK, Wani MC and Wall ME: Lipid bilayer partitioning and stability of camptothecin drugs. Biochemistry, *32*: 5352-5364, 1993.

25 Davies B, and Morris T: Physiological parameters in laboratory animals and humans. Pharmaceutical Res *10*: 1093-1095, 1993.

26 Singer JW, De Vries P, Bhatt R, Tulinsky J, Klein P, Li C, Milas L, Lewis RA and Wallace S: Conjugation of camptothecins to poly-(L-glutamic acid). Ann NY Acad Sci 922: 136-150, 2000.

Received August 3, 2004
Accepted December 15, 2004

JOURNAL OF LIPOSOME RESEARCH, 8(4), 425–442 (1998)

REVIEW ARTICLE

TARGETING OF DRUGS TO SOLID TUMORS USING ANTI-HER2 IMMUNOLIPOSOMES†

Demetrios Papahadjopoulos[a,b], Dmitri B. Kirpotin[a,b], John W. Park[c], Keelung Hong[a,b], Yi Shao[a,b], Refaat Shalaby[a], Gail Colbern[a,+], and Christopher C. Benz[c]

[a]California Pacific Medical Center Research Institute, San Francisco, CA 94115.
[b]Liposome Research Laboratory, San Francisco, CA 94115.
[c]Department of Medicine, Division of Hematology-Oncology, University of California San Francisco, San Francisco, CA 94143.

ABSTRACT

Cancer therapy would clearly benefit from a carrier system capable of intracellular delivery of systemically administered drugs to cancer cells in solid tumors. Sterically stabilized immunoliposomes specific to the cells expressing HER2 protooncogene (anti-HER2 SIL), were designed by conjugating Fab' fragments of a recombinant humanized anti-HER2 MAb to the distal termini of poly(ethylene glycol) chains on the surface of unilamellar liposomes (size 90–100 nm) of phosphatidylcholine, cholesterol, and poly (ethylene glycol)–derivatized phosphatidylethanolamine. Anti-HER2 SIL avidly and specifically bound to cultured HER2-overexpressing cancer cells (8,000–23,000 vesicles per cell) and became endocytosed (k_e = 0.022–0.033 $min.^{-1}$) via the coated pit pathway. Anti-HER2 SIL showed prolonged circulation lifetime in rats (blood MRT approx. 24 hours) and significantly increased antitumor activity of encapsulated doxorubicin against HER2-overexpressing human breast

†This subject was addressed earlier as a part of a forum on "Liposome Targeting in Animal Models" in the *Journal of Liposome Research* 7(4):391–417 (1997).

+Present address: Sequus Pharmaceuticals, Menlo Park, CA 94025.

Editor's note: This article was contributed by D. Papahadjopoulos. Reprints can be ordered from D. Kirpotin. Tel.: (415) 561-1778; Fax: (415) 923-3594; E-Mail: dkirpo@cooper.cpmc.org

cancer xenografts in nude mice. Although the accumulation of anti-HER2 SIL in HER2-overexpressing tumor xenografts was not increased over that of non-targeted sterically stabilized liposomes (SL), microscopic examination revealed abundance of anti-HER2 SIL in the interstitial spaces, as well as within the cytoplasm of cancer cells, while identical liposomes lacking anti-HER2 Fab' were located predominantly within tumor-resident macrophages. Anti-HER2 SIL, a targeted vehicle capable of *in vivo* intracellular delivery of substances to HER2-overexpressing solid cancers, enhances the potential for tumor targeting and opens new avenues for better treatment of cancer.

INTRODUCTION

Targeted delivery of drugs to diseased tissues using liposomes as carrier vehicles has already been discussed (1). There is convincing experimental evidence for specific association of the cells exposing a characteristic ligand with liposomes bearing recognition molecules, such as antibodies or antigen-binding antibody fragments (2–5). Specific association with the target potentially leads to better therapeutic efficacy and less toxicity of liposome-encapsulated pharmaceuticals (2,3). This is especially important in cytotoxic chemotherapy of cancer, where therapeutic indices are narrow and systemic toxicity is high. Introduction of liposome designs which avoid early clearance by mononuclear phagocytic system (MPS), have longer circulation times and increased likelihood for a liposome drug to reach its intended destination in the body (6–10) attracted new attention to the targeting of liposomes. Grafting of hydrophilic, flexible chains of poly(ethylene glycol) on the liposome surface (sterically stabilized or Stealth® liposomes) has proved to be among the most successful methods for achieving long-circulating properties (8–10). Targeting of sterically stabilized liposomes containing phospholipids with poly(ethylene glycol)-modified head groups (PEG-DSPE) was at first effected by attachment of antibodies, via a hydrophobic anchor, in close proximity to the liposome surface (11). Such liposomes had long-circulating properties, but their interaction with the target was reduced presumably by the same mechanism which contributed to the MPS avoidance (12,13). More recently, target-specific molecules (antibodies, sugars, or peptides) were attached to the distal termini of liposome-grafted poly(ethylene glycol) chains, leading to a targeted sterically stabilized liposome with fully preserved target-binding capability (14–16).

This approach will be illustrated here by our studies with sterically stabilized liposomes targeted to cancer cells overexpressing the HER2 (c-erbB-2, *neu*) oncoprotein. Our evidence indicates that sterically stabilized anti-HER2 immunoliposomes (anti-HER2 SIL) are not only capable of target-specific binding and internalization by cancer cells in culture (17,18), but are also able to cross the vascular barrier and to be internalized by target cancer cells in solid tumor xenografts following intravenous injection (19). Anti-HER2 SIL carrying the anticancer drug doxorubicin are more efficient than their non-targeted counterparts in suppressing

the growth of HER2-overexpressing tumor xenografts (20,21). Inclusion of a cationic lipid in the composition of anti-HER2 SIL results in the vehicle for specific delivery of nucleic acids into HER2-overexpressing cancer cells (19,20,22).

TARGET MOLECULE: THE HER2 ONCOPROTEIN

The protooncogene HER2 (c-erbB-2, neu) encodes a 185 KDa (1255 amino acids) receptor tyrosine kinase ($p185^{HER2}$, erbB-2, or HER2) which belongs to the family of receptor tyrosine kinases including also the products of epidermal growth factor (EGFR), HER3 (erbB-3), and HER4 (erbB-4) genes (23,24). Studies have shown overexpression of HER2 in a variety of malignancies, including cancers of the breast (25,26), ovary (27), endometrium (28), lung (non-small cell) (29), stomach (30,31), pancreas (32), bladder (33), and prostate (34). Especially high incidence of HER2 overexpression (up to 50%) was found in breast ductal carcinoma in situ (DCIS), particularly in the lesions having high risk of recurrence (35,36). HER2 oncoprotein appears to be an important mediator of tumor growth directly contributing to tumor onset and progression, and conferring an especially aggressive malignant phenotype (23).

The obvious advantages of HER2 as a recognition marker for targeted delivery of anticancer agents are the following: HER2 is a readily accessible cell surface protein with substantial levels of overexpression ($10^5 - 10^6$ copies/cell) in various malignancies (37) . In normal adult tissues, HER2 occurs only in certain epithelial types, and at very low levels (38). HER2-overexpression is relatively homogenous within primary tumors, and is maintained at metastatic sites, suggesting continuous requirement for high levels of HER2 throughout the malignant process (39), while many other tumor-associated antigens show variable expression patterns within the tumor tissue and/or in the course of tumor progression. Last, but not least, is the fact that HER2 activation is accompanied by its internalization into the cell, which may occur upon interaction with an agonistic antibody (40–42). Therefore, ligands targeted to HER2 by means of such antibodies would have a better chance to enter the cell rather than stay attached to the cell surface.

Considerable effort has been devoted to achieve antitumor effect by blocking the function of this receptor protein. A variety of monoclonal antibodies (40–43) as well as phage-display library generated single-chain Fv's (44,45) reactive with the extracellular portion of HER2 have been reported, offering a vast palette of target-specific molecules suitable for liposome attachment. The variants with the highest antiproliferative effect have also demonstrated the highest rate of cell internalization (41). One such antibody, muMAb4D5, is highly reactive toward HER2 (43) and inhibitory for the growth of HER2 overexpressing tumor cells *in vitro* (37) and in animal models (46). This antibody was engineered into a fully humanized version, rhuMAbHER2, to reduce the potential for immunogenicity (47), and entered clinical trials showing antitumor responses (12% response rate) in patients with metastatic HER2-overexpressing breast cancer (48).

IMMUNOLIPOSOME DESIGN

Pharmaceutically acceptable liposomes, antibody-targeted for the treatment of solid tumors should satisfy a number of requirements aimed at maximum targeting effect of systemically administered immunoliposomes (Table 1). Antigen binding sites of the liposome-conjugated antibody must be accessible for unperturbed interaction with antigens on the surface of target cells. To ensure that immunoliposomes will reach their target cells, the rate of MPS clearance or other "nonproductive" elimination of blood-borne immunoliposomes must be minimized in comparison with the rate of extravasation in the tumor. Since the liposome-conjugated antibody is a foreign protein likely to elicit host immune response, their immunogenicity must be minimized. Immunoliposomes must allow efficient loading and retention of a selected anticancer drug. And finally, the drug and antibody incorporation must be stable enough to permit liposomal entry into the tumor tissue without the loss of either of these agents.

We have developed the present immunoliposome design to maximally satisfy these requirements. Lipid composition of anti-HER2 immunoliposomes was based on hydrogenated soy phosphatidylcholine (T_m = 54 ± C) so that at body temperature the liposome bilayer maintained the "solid" (gel) state. Cholesterol (40 mol.%) was included to increase bilayer stability in the presence of plasma (49). To reduce MPS clearance rate, the liposomes contained up to 5.7 mol.% of DSPE modified with methoxypoly(ethylene glycol) with molecular mass 1,900 (7). To assist extravasation, the liposomes were of uniform, small size (90–110 nm) achieved by extrusion of hydrated lipid suspension (multilamellar vesicles) through track-etched polycarbonate membranes (pore sizes 100 and 50 nm) after several cycles of freezing and thawing (50,52).

The use of Fab' fragments instead of intact anti-HER2 MAb carrying the Fc receptor, eliminates the immunogenic effects of the Fc portion, which is associated with increased MPS clearance through specific recognition by phagocytic cells, was achieved by. The use of Fab' fragments also allowed better way of conjugation to the liposome through unique thiol groups in the hinge region (51,52) providing predictable and correct orientation of the antigen-binding sites. The binding affinity of liposome-conjugated Fab' was not compromised in comparison with the binding of the whole antibody (see below) probably because the presence of multiple Fab' fragments on the liposome restored the multicenter interaction characteristic for the whole antibody which carries two antigen-binding sites (18). Anti-HER2 Fab' fragments were produced as a recombinant protein derived from a humanized anti-HER2 MAb (rhuMAbHER2) developed by Genentech, Inc. (South San Francisco, CA, USA) for the therapy of cancers overexpressing HER2 (47,48). This antibody was itself derived from a murine MAb muMAb4D5, which induces endocytosis of HER2 receptors upon binding to their extracellular domains (43). The use of Fab' antibody fragments with humanized sequence further reduces the risk of immune reaction in human patients; recombinant technology provided stable, reproducible and more economical

source of this protein, and the ability to induce internalization upon binding to the target antigen was favorable for intracellular delivery of liposome-associated pharmaceuticals.

Conjugation of anti-HER2 Fab' to sterically stabilized liposomes we have used two linkers both containing a hydrophobic anchor (DSPE or DPPE), and a thiol-reactive maleimide function. The use of aromatic maleimides, such as maleimidophenylbutyric acid derivatives (MPB-PE) (51,53) was avoided because of their reported ability to cause leakage of encapsulated drugs from liposomes (54) Linkers of the first type consisted of DPPE or DSPE with their amino groups acylated by hydroxysuccinimide esters of 4-(N-maleimido)methylcyclohexylcarboxylic acid (MMC-PE) or b-(N-maleimido)propionic acid (MP-PE) (17). These linkers positioned the conjugated Fab' fragment "in parallel" with the surface-attached PEG chains. The second type of linkers additionally included PEG chain (M_r = 2,000) between DSPE and the maleimido group (MMC or MP) (18,52). Linkers of this type positioned Fab' fragments "in series" with surface-attached PEG, i.e. outside of the PEG "cloud" surrounding the liposome. The second type of conjugation was essential for preservation of the target-binding and also for internalization of the anti-HER2 liposomes, as discussed below.

Attachment of Fab' were performed by incubation of SL containing 1.2 mol.% of appropriate linker with anti-HER2 Fab' (approx. 30 g/mol of liposomal phospholipid) for 2 hours to overnight at 4 ± C and pH 7.2 − 7.4. Under these conditions, the protein was covalently attached to liposomes, and co-eluted with liposomes in the void volume fraction during gel-exclusion chromatography on Sepharose 4B. More than 90% of Fab' bearing free thiol groups were coupled to the liposomes containing MP-PEG-DSPE as a conjugation linker, resulting in 50–60 Fab'/liposome. Coupling of Fab' fragments to MMC-PE-containing liposomes was quite efficient (40% yield) even at PEG densities associated with the "brush" regime, i.e. at PEG(M_r = 2,000) − DSPE > 5 mol.% of the liposome phospholipid, or, in our case, >3.3 mol.% or total lipid (55), which means that. Fab' molecules still were able to reach the liposome bilayer. Therefore, penetrability of the PEG layer for protein molecules may be higher than previously predicted (12,56).

The anticancer drug of choice for this study was Doxorubicin because it has been well characterized in a similar, non-targeted sterically stabilized liposome system, Doxil® (57–59). Drug loading (0.09–0.15 mg of doxorubicin/μmol of liposomal phospholipid) was performed prior to the conjugation of anti-HER2 Fab' by the ammonium sulfate gradient method (60) at the temperature above T_m of the bilayer.

SPECIFICITY OF BINDING AND ENDOCYTOSIS BY CANCER CELLS *IN VITRO*

The specificity of in vitro binding of anti-HER2 SIL was studied in cultures of human breast carcinoma cells with high (SK-BR-3, 10^6 HER2/cell) or low

(MCF-7, 10^4 HER2/cell) expression of HER2 (37) using confocal microscopy and spectrofluorometry of liposome-associated fluorescent markers. Liposomes of HSPC, cholesterol, 2.6 mol.% of methoxyPEG-DSPE, 1.2 mol.% of MMC-PEG-DSPE, and 0.2 mol.% of a fluorescent lipid marker N-lissamine-rhodamine B-dihexadecanoyl phosphatidylethanolamine (Rh-PE) were prepared and conjugated to anti-HER2 Fab' as described above. The liposomes were incubated with cells at 37°C in the presence of fluorescein-labeled (FITC) transferrin, which served as a marker for coated pit endocytosis. The liposomes were at first observed on the surface of SKBR-3 cells, and further entered the cells and became co-localized with FITC-transferrin, as it was evidenced by yellow color produced by overlapping green (FITC) and red (Rh-PE) fluorescences. Under the same experimental conditions, "target-negative" MCF-7 cells displayed only green punctate fluorescence of endocytosed FITC-transferrin, but not of the lipid label; similar results were obtained with SKBR-3 cells incubated with Rh-PE labeled SL lacking conjugated anti-HER2 Fab' (17). These results confirmed the ability of anti-HER2 SIL to specifically bind to target cells and undergo endocytosis. Endocytosis of anti-HER2 liposomes without PEG-DSPE by SKBR-3 cells was also shown by electron microscopy using liposomes labeled with colloidal gold (18).

Binding to cells and endocytosis were quantitatively assessed using liposomes with encapsulated pH-sensitive probe 1-hydroxypyrene-3,6,8-trisulfonic acid (HPTS, pyranine). Fluorescence excitation spectrum of HPTS undergoes rapid changes in response to the liposome entry into acidic environment of endosomes and lysosomes, but it also has a pH-independent isosbestic point for accurate quantitation of the probe (61) For faster equilibration of protons across the liposome bilayer, in these studies we substituted 1-palmitoyl-2-oleoylphosphatidyl-choline (POPC) for HPTS, since POPC bilayers are in more proton-permeable liquid crystalline state rather than gel state at ambient conditions. Upon incubation with HER2-overexpressing SKBR-3 cells, HPTS-loaded anti-HER2 SIL became rapidly associated with cells in a neutral compartment (cell surface), followed by acidification of the liposome environment indicating endocytosis. The amount of cell-associated anti-HER2 SSL reached a plateau after 3–4 hours of incubation, with more than 80% of liposomes endocytosed. At saturating concentrations, the uptake of anti-HER2 SIL by SKBR-3 cells, estimated from the fluorescence at HPTS isosbestic point, was in the range of 8,000–25,000 vesicles/cell, while the uptake of liposomes by "target-negative" MCF-7 cells was essentially undetectable (<100 vesicles/cell) (17).

The attachment of Fab' via hinge thiol group and maleimide-activated hydrophobic linker (51) was a high yield reaction without any loss of antigen-binding activity; however, the relative position of liposome-conjugated Fab' and PEG was crucial for maintaining high uptake of anti-HER2 SIL by target cells. During incubation of SKBR-3 cells at a constant concentration of liposomes (25 mM of liposome phospholipid) in the cell growth medium, the increasing PEG-DSPE content inhibited the uptake of anti-HER2 SIL prepared with MMC-DSPE linker, while no such inhibition occurred when anti-HER2 Fab' were attached via MP-PEG-

DSPE linker (17). Similar effect of the placement of a targeting antibody on the uptake of immuno-SIL by target cells/tissues was reported earlier (16,62) in studies utilizing whole antibodies rather than Fab' fragments. Since the cellular uptake of anti-HER2 liposomes includes steps of binding and subsequent endocytosis, we have studied the effect of PEG-DSPE and Fab' placement on each of these steps separately. Liposome-cell binding was characterized by dissociation constants (K_d) estimated from the amounts of cell-associated anti-HER2 liposomes after incubation of SKBR-3 cells at various liposome concentrations and low temperature (4 ± C) that completely inhibits endocytosis. For anti-HER2 liposomes without PEG coating, K_d normalized to the amount of liposome-conjugated Fab' was 12.0 ± 1.7 nM (mean ± SE), close to the reported values for the whole murine prototype anti-HER2 MAb 4D5 (6.0 nM) and its free Fab' fragment (19.0 nM) (41). As one may expect from the size of Fab' fragment, 6 nm in the longer aspect (63), and the thickness of PEG layer on the liposome surface, 5–7 nm for PEG with M_r = 2,000 in the "brush" regime (55,64), when Fab' fragments were conjugated through the "short" linker MMC-PE, the increase of PEG (Mr = 2,000) – DSPE amount to 1.2 mol.% reduced the affinity approximately threefold, and at 3.5–5.7 mol.% of PEG-DSPE the binding affinity was 20 to 75 times lower (K_d = 320–900 nM). On the contrary, conjugation of Fab' to the termini of PEG chains did not affect liposome binding to the target cells at increasing PEG-DSPE content (K_d 13–15 nM for 1.2–5.7 mol.% PEG-DSPE) (17). First-order rate constants of liposome endocytosis (k_e) were determined from the kinetic curves of cell surface-bound and endocytosed liposomes obtained by HPTS method (17), as the ratio of liposome internalization rate to the steady-state surface concentration of liposomes (65). Compared to K_d, k_e of anti-HER2 SSL prepared with the "short" linker MMC-PE was somewhat reduced at increased PEG-DSPE content (k_e decreased 2 times at 5.7 mol.% PEG-DSPE vs. 0%), and was not affected at all when MP-PEG-DSPE was used as a linker. Thus, PEG interfered with the ability of liposome-conjugated Fab' to bind to the cell surface antigen, and to the less extent, with its ability to induce endocytosis or the liposome; however, this interference was completely avoided by conjugation of anti-HER2 Fab' at the distal termini of liposome-grafted PEG chains.

Quantitation studies on the number of liposome-conjugated anti-HER2 Fab' and the cellular level of HER2 protein expression required to achieve specificity and effectiveness of liposome uptake were done using anti-HER2 liposomes without PEG coating (17,18). Binding of liposomes with the target cells increased in a linear manner as a function of Fab' density, and reached saturation (plateau) at ≈40 Fab'/vesicle; endocytosis of cell-bound liposomes occurred with 60% efficiency already at ≈10 Fab'/vesicle. That is, relatively few conjugated Fab' were needed for specific uptake. Similarly, the uptake of anti-HER2 liposomes by the cells with minimally elevated cellular levels of HER2 to allow classification as "HER2-positive" (MDA-MB-453, approx. 10^5 molecules/cell) was comparable to that by the cells with extremely high levels of HER2 expression (SK-BR-3, BT-474; approx. 10^6 molecules/cell). There was, however, pronounced difference

in the uptake of anti-HER2 liposomes between the cells with elevated levels of HER2 and those with only basal HER2 expression (MCF-7; approx. 10^4 molecules/cell) (17).

Immunoliposomes with rhuMAbHER2 Fab' conjugated via MMC-PE linker were loaded with doxorubicin using ammonium sulfate gradient method. In contrast to the liposomes conjugated via aromatic maleimide derivative, MPB-PE (16,54), the drug loading was practically quantitative even though the linker constituted 1.2 mol.% of total liposome lipid. Doxorubicin-loaded anti-HER2 liposomes showed efficient and specific *in vitro* cytotoxicity against HER2-overexpressing cancer cells. After 1 hour incubation, doxorubicin delivered by anti-HER2 liposomes to SKBR-3 cells was as cytotoxic as free doxorubicin (IC_{50} = 0.3 μg/ml), while cytotoxicity of doxorubicin in the liposomes with conjugated irrelevant Fab', or in anti-HER2 liposomes incubated with lung fibroblast cells (WI-38) expressing only minimal levels of HER2 was 20–30 times less than that of free drug (18). Goren and co-workers (66) reported doxorubicin-loaded anti-HER2 SIL bearing whole antibodies attached to PEG terminal groups via hydrazone formation with periodate-oxidized carbohydrate moieties. These liposomes bound quite well to HER2-overexpressing gastric cancer cells (N-87), but their cytotoxicity was equal to that of non-targeted doxorubicin-loaded liposomes, and much less than that of the free drug, presumably because of the inability of these liposomes to be internalized by the target cells (66). In contrast, doxorubicin-loaded immunoliposomes bearing conjugated anti-HER2 MAb SER4 were endocytosed by HER2 overexpressing cells SKBR-3 and MKN-7, and were 25 times more cytotoxic to these cells than the matching liposomes conjugated to an antibody against non-internalizable surface protein gp125 (67). Moreover, compared with anti-gp125 immunoliposomes, SER4-conjugated immuno-liposomes required 4.3–4.5 times less doxorubicin association with HER2 overexpressing cells for equal cytotoxicity (67). Evidently, endocytosis of doxorubicin-loaded anti-HER2 liposomes is important for increased cytotoxicity of the liposomal drug, presumably by creating an acidic environment and transmembrane pH gradients which favor escape of the drug from the liposome and its further distribution throughout the cell.

PHARMACOKINETIC AND THERAPEUTIC STUDIES

Studies on the pharmacokinetics of doxorubicin in anti-HER2 SSL were done in normal Lewis rats with indwelling jugular vein catheters. The animals received 5 μmol of liposomal phospholipid (0.8–1 mg of doxorubicin) intravenously at time 0; the blood was repeatedly sampled within 48 hours post injection and assayed for doxorubicin by spectrofluorometry after separation of blood cells and extraction with acidified alcohol. The drug showed biphasic elimination profile with $t_{1/2\alpha}$ = 6.1 min., $t_{1/2\beta}$ = 976 min., AUC = 93,100 min%, and blood MRT = 1460 min. (19,21). This pharmacokinetic behavior is characteristic of long-circulating liposomes and similar to that of non-targeted doxorubicin-loaded

SL, in contrast to free doxorubicin which had plasma half-life of about 5 min. (19). The use of Fab' instead of the whole antibody was of importance, since the analogous constructs bearing conjugated whole antibodies show lower circulation half-lives than corresponding non-conjugated SL (16,66). To analyze possible drug leakage or dissociation of Fab' from the liposomes in circulation, plasma pharmacokinetics of the anti-HER2 SIL-entrapped drug was compared to that of liposome-conjugated Fab' fragments. In this study, plasma concentration of anti-HER2 Fab' was determined by ELISA using extracellular domain of HER2 for capture, and HPR-linked goat anti-human IgG for detection. Drug and anti-HER2 Fab' showed identical pharmacokinetic profiles indicating the lack of drug or Fab' dissociation in from the liposomes in circulation (19,20).

We have studied the effect of tumor cell targeting on the therapeutic efficacy of sterically stabilized liposomes containing doxorubicin, using nude mice with subcutaneous xenografts of HER2-overexpressing human breast adenocarcinomas (BT-474 and MDA-MB-453) Treatment of animals with established (approximately 200 mm^3) xenografts of HER2-overexpressing human breast carcinomas (BT-474, MDA-MB-453) by three weekly injections of free or SL-encapsulated doxorubicin revealed superior activity of doxorubicin in anti-HER2 SIL (20,21). The average ratio of the volume of BT-474 tumors at the end of the experiment (48–60 days post tumor inoculation) to that at the beginning of the experiment (12–14 days post inoculation) was 19.13 ± 1.14 in the group treated with free doxorubicin at a total maximum tolerated dose (MTD) of 7.5 mg/kg, 2.59 ± 0.28 in the group receiving non-targeted doxorubicin-loaded SL (MTD, 15 mg/kg), and 0.63 ± 0.12 in the group injected with doxorubicin-loaded anti-HER2 SIL (15 mg/kg); in the case of MDA-MB-453 tumors (with lower expression of HER2), these values were 3.54 ± 0.53, 2.15 ± 0.29, and 1.17 ± 0.16, respectively. The difference between growth rates of tumors in the groups receiving doxorubicin in HER2-targeted vs. non-targeted SIL was statistically significant at $p = 0.001$ (BT-474) and $p = 0.004$ (MDA-MB-453) according to a modified Norton-Simon model of tumor growth (69). Administration of "empty" anti-HER2 SIL at equal dose/schedule did not produce antitumor effect in these models, ruling out the inhibitory effect of immunoliposome itself. Therefore the increased antitumor activity must be attributed to the targeting.

Increased accumulation in tumor tissue is often considered as the cause for the enhanced antitumor activity of immunotargeted drugs. To find out if this was the case for anti-HER2 SIL as well, we prepared non-targeted or HER2-targeted sterically stabilized liposomes with encapsulated chelating agent (DTPA) and remote-loaded them with a radiotracer ^{67}Ga *via* oxine complex (68). Nude mice bearing BT-474 or MCF-7 xenografts were injected via tail vein with ^{67}Ga-labeled anti-HER2 SIL or non-targeted SL (in the latter, the Fab'-conjugation step was omitted during the liposome preparation) in the dose of 1 mmol of liposome phospholipid per animal, which is equivalent to the dose of doxorubicin liposomes administered in the treatment efficacy studies. The animals were sacrificed 24 hours later, and the tissue concentrations of liposomes (% of injected dose/g tis-

sue) were determined by radioactivity measurements (70). Both HER2-targeted and non-targeted SSL were found in tumor tissue in high concentration, 4–8% of injected dose (i.d.)/g, which, assuming 10^9 cells per 1 g of tumor tissue and 80,000 phospholipid molecules per liposome, was consistent with an average of 300–600 vesicles per tumor cell. Biodistribution of ^{67}Ga-labeled anti-HER2 SIL in non-tumor tissues was characteristic of PEG-coated liposomes and was not significantly different from that of the similar non-targeted SL. Interestingly, no statistically significant difference was found between the accumulation of HER2-targeted SIL (8.34 ± 1.54% i.d./g) or non-targeted SL (7.32 ± 1.05% i.d./g) in HER2-overexpressing BT-474 tumors. In similarly established xenografts of MCF-7 tumors which express low levels of HER2, the difference of tumor uptake between targeted and non-targeted SSL was also insignificant, and both liposomes accumulated in MCF-7 tumors in similar amounts (7.2–8.6% i.d./g) regardless of the presence of anti-HER2 Fab' (70,71).

As indicated above, the biodistribution study ruled out the increased tumor uptake of targeted liposomes as an explanation of higher antitumor efficacy. Therefore, the mechanisms of this phenomenon had to be sought elsewhere. In fact, the lack of increase in the tumor concentration of tumor-cell targeted SSL over non-targeted ones is in accord with the view that the limiting step in the tumor accumulation of the blood-borne liposomes is extravasation (72) upon which this type of targeting evidently would have no effect. One cannot exclude that specific interaction with HER2-overexpressing tumor cells resulted in the extended residence time of anti-HER2 SIL in the tumor tissue, which calls for further pharmacokinetic studies of tumor cell-targeted vs. non-targeted SL in tumor tissue at longer post injection times. However, studies of liposome disposition within the tumor tissue revealed another mechanism that may explain higher antitumor efficacy of tumor cell targeted cytotoxic SIL.

The location and distribution of anti-HER2 SIL in the tumor tissue was visualized by using anti-HER2 SIL, as well as non-targeted SL labeled with entrapped colloidal gold (73). Liposomes of egg PC, cholesterol, PEG(M_r = 1,900) − DSPE, and maleimidopropionyl-amido-PEG-DSPE in molar ratio 3:2:0.24:0.06 were prepared in aqueous solution of $HAuCl_4$ by reverse phase evaporation, followed by sizing through 0.1 mm and 0.05 mm polycarbonate membranes. Colloidal gold particles were precipitated within liposomes by pH shift using citrate-carbonate buffer; unentrapped gold particles were removed by passing of the liposomes through Sephacryl S-400 in 144 mM NaCl, 20 mM HEPES-Na, pH 7.2. Nude mice bearing subcutaneous xenografts of the above tumors (200–600 mm^3 in size) were injected with gold-labeled liposomes or immunoliposomes via tail vein at the dose of 5 mmol phospholipid/animal, and sacrificed 48 hours later. Tumors were collected, fixed with 4% formaldehyde in phosphate-buffered saline, embedded in glycol metacrylate, and cut in 3 mm sections. Entrapment of gold had no effect on liposome stability or anti-HER2 Fab' conjugation. Tumor sections were enhanced with silver to visualize the location of gold particles, and microscopically examined at lower magnification (×400) using dark field illumination, and

at higher magnification (×1,250) using regular bright field illumination (69). In HER2-positive tumor (BT-474) anti-HER2 SIL were observed abundantly throughout the tumor tissue. In the absence of targeting, either through the lack of liposome-conjugated anti-HER2 Fab' fragments (non-targeted SL), or through insufficient expression of HER2 protein (MCF-7 tumors), the label was concentrated mostly within tumor-resident macrophages and in perivascular areas, in agreement with previous observations on non-targeted SL (74). At higher magnification, anti-HER2 SIL were frequently revealed within the cytoplasm and in the perinuclear spaces of HER2-positive cancer cells within the tumor tissue. In the absence of targeting, there was no clear deposition of silver granules within cancer cells: the label was detected in tumor stroma and especially within tumor-resident macrophages. Thus, anti-HER2 SIL not only crossed the vascular barrier into the solid tumor, but, in the case of HER2-overexpression, frequently became endocytosed by the cancer cells as they would be *in vitro*. Increased deposition in the intercellular spaces within the tumor tissue outside tumor-resident macrophages, as well as the intracellular delivery of the encapsulated drug *in vivo* may have contributed to superior antitumor efficacy of doxorubicin-loaded anti-HER2 SIL.

CONCLUDING REMARKS

The pharmaceutical science of liposomes has been greatly advanced over the last decade, by introduction of long-circulating liposomes (6–10), refinement of liposome preparation techniques (50,52) and "remote loading" methods for drug loading into liposomes (60,75). This is clearly evidenced by the recent approval of liposome-encapsulated drugs (Doxil, DaunoXome) for cancer treatment (76). It has also brought new enthusiasm to the area of liposome targeting. In this communication we presented a case study that illustrates, in our view, a "rational design" approach to antibody-targeted liposomes. Each element of this design addresses certain issues relating to the ultimate medical use of the targeted liposomal drug carrier. This design may be readily applied to other targeted drug delivery systems utilizing different drugs and/or different target-specific molecules, such as, for example, single chain anti-HER2 antibodies produced by phage display libraries (44,45). Doxorubicin-loaded HER2-targeted SIL constructed according to such design had superior antitumor activity compared to matched non-targeted liposomes in established solid tumor xenografts overexpressing HER2 oncoprotein. Interestingly, this phenomenon was not associated with the increased accumulation of targeted liposomes in HER2-overexpressing tumors, but apparently resulted from a different pattern of liposome disposition within the tumor tissue. This unexpected but important finding includes improved tumor tissue penetration and internalization of liposomes into HER2-overexpressing cancer cells. Such "rational design" of cancer cell-targeted sterically stabilized liposomes leads to a re-evaluation of the potential for tumor targeting and opens new avenues for better treatment of cancer.

ACKNOWLEDGEMENTS

This work was supported in part by the grants from National Cancer Institute (P50CA58207–01), California Breast Cancer Research Program (2CB-0004 and 2CB-0250), the US Army Medical Research and Materiel Command (DAMD 17-94-J-4195), and American Society of Clinical Oncology Young Investigator Award (J.W.P) sponsored by Don Shula Foundation.

REFERENCES

1. Papahadjopoulos, D. 1995. 30-Year progress for liposomes: from serendipity to molecular design. J Liposome Res 5:ix–xiv.
2. Lasic, D.D. and Papahadjopoulos, D. 1995. Liposomes revisited. Science 267:1275–1276.
3. Leserman, L. and Machy, P. Ligand targeting of liposomes *in* Liposomes: From Biophysics to Therapeutics. M.J. Ostro (Ed.), pp. 157–194, Marcel Dekker, New York. 1987.
4. Ranade, V.V. 1989. Drug delivery systems: Site-specific drug delivery using liposomes as carriers. J Clin Pharmacol 29:685–694.
5. Straubinger, R.M., Lopez, N.G., Debs, R.J, Hong, K. and Papahadjopoulos, D. 1988. Liposome-based therapy of human ovarian cancer: parameters determining potency of negatively charged and antibody-targeted liposomes. Cancer Res 48:5237–5245.
6. Allen, T.M. and Chonn, A. 1987. Large unilamellar liposomes with low uptake into the reticuloendothelial system. FEBS Lett 223:42–46.
7. Gabizon, A. and Papahadjopoulos, D. 1988. Liposome formulations with prolonged circulation time in blood and enhanced uptake by tumors. Proc Natl Acad Sci USA 85: 6949–6953.
8. Blume, G., and Cevc, G. 1990. Liposomes for the sustained drug release in vivo. Biochim Biophys Acta 1029:91–97.
9. Klibanov, A.L., Maruyama, K., Torchilin, V.P. and Huang, L. 1990. Amphipathic polyethyleneglycols effectively prolong the circulation time of liposomes. FEBS Lett 268:235–237.
10. Papahadjopoulos, D., Allen, T., Gabizon, A., Mayhew, E., Matthay, K., Huang, S.K., Lee, K.-D., Woodle, M.C., Lasic, D.D., Redemann, C. and Martin, F.J. 1991. Sterically stabilized liposomes: Improvements in pharmacokinetics and anti-tumor therapeutic efficacy. Proc Natl Acad Sci USA 88:11460–11464.
11. Torchilin, V.P., Klibanov, A.L., Huang, L., O'Donnell, S., Nossiff, N.D. and Khaw, B.A. 1992. Targeted accumulation of polyethylene glycol-coated immunoliposomes in infarcted rabbit myocardium. FASEB J 6:2716–2719.
12. Klibanov, A.L., Maruyama, K., Beckerleg, A.M., Torchilin, V.P. and Huang, L. 1991. Activity of amphipathic poly(ethylene glycol) 5000 to prolong the circulation lifetime of liposomes depends on the liposome size and is unfavorable for immunoliposome binding to target. Biochim Biophys Acta 1062:142–148.
13. Torchilin, V.P., Papisov, M.I., Bogdanov, A.A., Trubetskoy, V.S. and Omelyanenko, V.G. Molecular mechanism of liposome and immunoliposome steric protection with poly(ethylene glycol) *in* "Stealth Liposomes". D. Lasic, F. Martin (Eds.), pp. 51–62, CRC Press, Boca Raton, FL. 1995.

14. Allen, T.M., Brandeis, E., Hansen, C.B., Kao, G.Y. and Zalipsky, S. 1995. A new strategy for attachment of antibodies to sterically stabilized liposomes resulting in efficient targeting to cancer cells. Biochim Biophys Acta 1237:99–108.
15. Hansen, C.B., Kao, G.Y., Moase, E.H., Zalipsky, S. and Allen, T.M. 1995. Attachment of antibodies to sterically stabilized liposomes: evaluation, comparison and optimization of coupling procedures. Biochim Biophys Acta 1239:133–144.
16. Zalipsky, S., Hansen, C.B., Lopes de Menezes, D., E and Allen, T.M. 1996. Long-circulating, polyethylene glycol-grafted immunoliposomes. J Controlled Release 39: 153–161.
17. Kirpotin, D., Park, J.W., Hong, K., Zalipsky, S., Li, W.-L., Carter, P., Benz, C.C. and Papahadjopoulos, D. 1997. Sterically stabilized anti-HER2 immunoliposomes: desin and targeting to human breast cancer cells *in vitro*. Biochemistry 36:66–75.
18. Park, J.W., Hong, K., Carter, P., Asgari, H., Guo, L.Y., Wirth, C., Shalaby, R., Kotts, C., Keller, G.A., Wood, W.I., Papahadjopoulos, D and Benz, C.C. 1995. Development of anti-p185HER2 immunoliposomes for cancer therapy. Proc Natl Acad Sci USA 92:1327–1331.
19. Park, J.W., Hong, K., Kirpotin, D.B., Papahadjopoulos, D. and Benz C.C. 1997. Immunoliposomes for cancer treatment. Adv Pharmacol 40:399–436.
20. Park, J.W., Hong, K., Kirpotin, D.B., Meyer, O., Papahadjopoulos, D. and Benz C.C. 1997. Anti-HER2 immunoliposomes for targeted therapy of human tumors. Cancer Lett 118:153–160.
21. Park, J.W., Colbern, G., Hong, K., Kirpotin, D., Shao, Y., Baselga, J., Moore, D., Papahadjopoulos, D. and Benz, C.C. 1997. Targeted intracellular drug delivery via anti-HER2 immunoliposomes yields superior antitumor efficacy. Proc ASCO, 16: 430a.
22. Meyer, O., Kirpotin, D., Hong, K., Sternberg, B., Park, J.W., Woodle, M.C. and Papahadjopoulos, D. 1998. Poly(ethylene glycol)-coated cationic liposomes as carriers for cellular delivery of antisense oligonucleotides. J Biol Chem 283:15261–15267
23. Hynes, N.E. and Stern, D.F. 1994. The biology of erbB-2/neu/HER2 and its role in cancer. Biochim Biophys Acta 1198:165–184.
24. Carraway, K.L. and Cantley, L.C. 1994. A neu acquaintance for ErbB3 and ErbB4: a role for receptor heterodimerization in growth signaling. Cell 78:5–8.
25. Slamon, D.J., Clark, G.Mm, Wong, S.G., Levin, W.J., Ullrich, A. and McGuire, W.L. 1987. Human breast cancer: correlation of relapse and survival with amplification of HER2/neu oncogene. Science 235:177–182.
26. Slamon, D.J., Godolphin, W., Jones, L.A., Holt, J.A., Wong, S.G., Keith, D.E., Levin, W.J., Stuart, S.G., Udove, J., Ullrich, A. and Press, M. 1989. Studies of the HER2/neu proto-oncogene in human breast and ovarian cancer. Science 244:707–712.
27. Berchuck, A., Kamel, A., Whitaker, R., Kerns, B., Olt, G., Kinney, R., Soper, J.T., Dodge, R., Clarke-Pearson, D.L., Marks, P., McKenzie, S., Yin, S. and Bast, R.C. 1990. Overexpression of HER2/neu is associated with poor survival in advanced epithelial ovarian cancer. Cancer Res 50:4087–4091.
28. Berchuck, A., Rodriguez, G., Kinney, R.B., Soper, J.T., Dodge, R.K., Clarke-Pearson, D.L. and Bast, R.C. 1991. Overexpression of HER2/neu in endometrial cancer is associated with advanced stage disease. Am J Obstetrics Gynecol 164:15–21.

29. Kern, J.A., Schwartz, D.A., Nordberg, J.E., Weiner, D.B., Greene, M.I., Torney, L. and Robinson, R.A. 1990. p185neu expression in human lung adenocarcinomas predict shortened survival. Cancer Res 50:5184–5191.
30. Yokota, J., Yamamoto, T., Miyajima, N., Toyoshima, K., Nomura, N., Sakamoto, H., Yoshida, T., Terada, M. and Sugimura, T. 1988. Genetic alterations of the c-erbB-2 oncogene occur frequently in tubular adenocarcinoma of the stomach and are often accompanied by amplification of v-erbA homologue. Oncogene 2:283–287.
31. Park, J.B., Rhim, J.S., Park, S.C., Kimm, S.W. and Kraus, M.H. 1989. Amplification, overexpression and rearrangement of the erbB-2 proto-oncogene in primary human stomach carcinomas. Cancer Res 49:6605–6609.
32. Lei, A., Appert, H.E., Nakata, B., Domenico, D.R., Kim, K. and Howard, J.M. 1995. Overexpression of HER2/neu oncogene in pancreatic cancer correlates with shortened survival. In. J Pancreatology 17:15–21.
33. Zhau, H.E,, Zhang, X., von Eschenbach, A.C., Scorsone, K., Babaian, R.J., Ro, J.Y. and Hung, M.C. 1990. Amplification and expression of the c-erbB-2/neu proto-oncogene in human bladder cancer. Molec Carcinogenesis 3:254–257.
34. Gu, K., Mes-Masson, A.-M., Gauthier, J and Saad, F. 1996. Overexpression of her-2/*neu* in human prostate cancer and benign hyperplasia. Cancer Lett 99:185–189.
35. VandeVijver, M.J., Peterse , M.L., Mooi, W.J., Wisman, O., Lomans, J., Dalesio, O. and Nusse, R. 1988. Neu-protein expression in breast cancer. New Engl J Med 319:1239–1245.
36. Liu, E., Thor, A., He, M., Barcos, M., Ljung, B.M. and Benz, C.C. 1992. The HER2 (c-erbB-2) oncogene is frequently amplified in *in situ* carcinomas of the breast. Oncogene 7:1027–1032.
37. Lewis, G.D., Figari, I., Fendly, B.M., Wong, W.-L., Carter, P., Gorman, C. and Shepard, H.M. 1993. Differential responses of human tumor cell lines to anti-p185HER2 monoclonal antibodies. Cancer Immunol Immunother 37:255–263.
38. Press, M.F., Cordon-Cardo, C. and Slamon, D.J. 1990. Expression of the HER-2/neu proto-oncogene in normal human adult and fetal tissues. Oncogene 5:953–962.
39. Niehans, G.A., Singleton, T. P., Dykoski, D. and Kiang, D.T. 1993. Stability of HER-2/neu expression over time and at multiple metastatic sites. J Natl Cancer Inst 85:1230–1235.
40. Tagliabue, E., Centis, P., Campiglio, M., Mastroiannini, A., Martignone, S, Pellegrini, R., Casalani, P., Lanzi, C., Menard, S. and Colnaghi, M.I. 1991. Selecion of monoclonal antibodies which induce internalization and phosphorylation of p185HER2 and growth inhibition of cells with HER2/neu gene amplification. Int J Cancer 47:933–937.
41. Sarup, J.C., Johnson, R.M., King, K.L., Fendly, B.M., Lipari, M.T., Napier, M.A., Ullrich, A. and Shepard, H.M. 1991. Characterization of an anti-p185HER2 monoclonal antibody that stimulated receptor function and inhibits tumor cell growth. Growth Regulation 37:72–82.
42. Hurwitz, E., Stancovski, I., Sela, M. and, Yarden, Y. 1995. Suppression and promotion of tumor growth by monoclonal antibodies to ErbB-2 differentially correlate with cellular uptake. Proc Natl Acad Sci USA 92:3553–3557.
43. Fendly, B.M., Winget, M., Hudziak, R.M., Lipari, M.T., Napier, M.A. and Ullrich,

A. 1990. Characterization of murine monoclonal antibodies reactive to either the human epidermal growth factor receptor or HER2/neu gene product. Cancer Res 50:1550–1558.

44. Schier, R., Marks, J.D., Wolf, E.J., Apell, G., Wong, C., McCartney, J.E., Bookman, M.A., Huston, J.A., Houston, L.L., Weiner, L.M., Adams, G.P. 1995. *In vitro* and *in vivo* characterization of a human anti-c-erbB-2 single-chain Fv isolated from a filamentous phage antibody library. Immunotechnology 1:73–81.
45. Schier, R., McCal, A., Adams, G.P., Marshall, K.W., Merritt, H., Yim, M., Craford, R.S., Weiner, L.M., Marks, C., Marks, J.D. 1996. Isolation of picomolar affinity anti-c-erbB-2 single chain Fv by molecular evolution of the complementary determining regions in the center of the antibody binding site. J Mol Biol 263:551–567.
46. Park, J.W., Stagg, R., Lewis, G.D., Carter, P., Maneval, D., Slamon, D.J., Jaffe, H. and Shepard, H.M., Anti-p185HER2 monoclonal antibodies: biological properties and potential for immunotherapy *in* Genes, Oncogenes, and Hormones: Advances in Cellular and Molecular Biology of Breast Cancer. R.B. Dickson and M.E. Lippman (Eds.), pp. 193–211, Kluwer, Boston, MA. 1992.
47. Carter, P., Presta, L., Gorman, C.M., Ridgway, J.B.B., Henner, D., Wong, W.L.T., Rowland, A.M., Kotts, C., Carver, M.E. and Shepard, H.M. 1992. Humanization of an anti-p185HER2 antibody for human cancer therapy. Proc Natl Acad Sci USA 89:4285–4289.
48. Baselga, J., Tripathy, D., Mendelsohn, J., Baughman, S., Benz, C.C., Dantis, L., Sklarin, N.T., Seidman, A.D., Hudis, C.A., Moore, J., Rosen, P.P., Twaddell, T., Henderson, I.C. and Norton, L. 1996. Phase II study of weekly intravenous recombinant humanized anti-p185HER2 monoclonal antibody in patients with HER2/neu-overexpressing metastatic breast cancer. J Clin Oncol. 14:737–744.
49. Papahadjopoulos, D., Jacobson, K., Nir, S. and Isac, T. 1973. Phase transitions in phospholipid vesicles, fluorescence polarization and permeability measurements concerning the effect of temperature and cholesterol. Biochim Biophys Acta 311: 330–348.
50. Olson, F., Hunt, C.A., Szoka, F.C., Vail, W.J. and Papahadjopoulos, D. 1979. Preparation of liposomes of defined size distribution by extrusion through polycarbonate membranes. Biochim Biophys Acta 557:9–23.
51. Martin, F. and Papahadjopoulos, D. 1982. Irreversible coupling of immunoglobulin fragments to preformed vesicles. An improved method for liposome targeting. J Biol Chem 257:286–288.
52. Shahinian, S. and Silvius, J.R. 1995. A novel strategy affords high-yield coupling of antibody Fab' fragments to liposomes. Biochim Biophys Acta 1239:157–167.
53. Loughrey, H.C., Choi, L.S., Cullis, P.R. and Bally, M.B. 1990. Optimized procedures for the coupling of proteins to liposomes. J Immunol Methods 132:25–35.
54. Bredehorst, R., Ligler, F.S., Kusterbeck, A.W., Chang, E.L., Gaber, B.P. and Vogel, C.-W. 1986. Effect of covalent attachment of immunoglobulin fragments on liposomal integrity. Biochemistry 25:5693–5698.
55. Hristova, K. and Needham, D. Physical properties of polymer-grafted bilayers *in* Stealth Liposomes. D. Lasic, F. Martin (Eds.), pp. 35–49, CRC Press, Boca Raton, FL. 1995.
56. Mori, A., Klibanov, A.L., Torchilin, V.P. and Huang, L. 1991. Influence of the steric

barrier activity of amphipathic poly(ethylene glycol) and ganglioside GM1 on the circulation time of liposomes and on the target binding of immunoliposomes *in vivo*. FEBS Lett 284:263–266.

57. Huang, S.K., Mayhew, E., Gilani, S., Lasic, D.D., Martin, F.J. and Papahadjopoulos, D. 1992. Pharmacokinetics and therapeutics of sterically stabilized liposomes in mice bearing C-26 colon carcinoma. Cancer Res 52:6774–6781.
58. Working, P.W., Newman, M., Huang, S.K., Vaage, J., Mayhew, E. and Lasic, D.D. 1994. Pharmacokinetics, biodistribution and therapeutic efficacy of doxorubicin encapsulated in Stealth liposomes. J Liposome Res 4:667–675.
59. Bogner, J.R. and Goebel, F.-D. Efficacy of Dox-SL (Stealth® liposomal doxorubicin) in the treatment of advanced AIDS-related Kaposi's sarcoma *in* Stealth Liposomes. D. Lasic, F. Martin (Eds.), pp. 267–278, CRC Press, Boca Raton, FL. 1995.
60. Haran, G., Cohen, R., Bar, L.K. and Barenholz, Y. 1993. Transmembrane ammonium sulfate gradients in liposomes produce efficient and stable entrapment of amphipathic weak bases. Biochim Biophys Acta 1149:180–184.
61. Daleke, D.L., Hong, K. and Papahadjopoulos, D. 1990. Endocytosis of liposomes by macrophages: binding, acidification, and leakage of liposomes monitored by a new fluorescence assay. Biochim Biophys Acta 1024:352–366.
62. Maruyama, K., Takizawa, T., Yuda, T., Kennel, S.J., Huang, L. and Iwatsuru, M. 1995. Targetability of novel immunoliposomes modified with amphipathic poly(ethylene glycol)s conjugated at their distal terminals to monoclonal antibodies. Biochim Biophys Acta 1234:74–80.
63. Nezlin, R.C. 1977. Structure and biosynthesis of antibodies. Consultants Bureau, New York, NY, p. 174.
64. Kenworthy, A.K., Simon, S.A. and McIntosh, T.J. 1995. Structure and phase behavior of lipid suspensions containing phospholipids with covalently attached poly(ethylene glycol). Biophys J 68:1903–1920.
65. Lee, K.-D., Nir, S. and Papahadjopoulos, D. 1993. Quantitative analysis of liposome-cell interactions *in vitro*: rate constants of binding and endocytosis with suspension and adherent J774 cells and human monocytes. Biochemistry 32: 889–899.
66. Goren, D., Horowitz, A.T., Zalipsky, S., Woodle, M.C., Yarden, Y. and Gabizon, A. 1996. Targeting of stealth liposomes to erbB-2 (Her/2) receptor: *in vitro* and *in vivo* studies. Br J Cancer 74:1749–1756.
67. Suzuki, S., Uno, S., Fukuda, Y., Aoki, Y., Masuko, T. and Hashimoto, Y. 1995. Cytotoxicity of anti-c-erbB-2 immunoliposomes containing doxorubicin on human cancer cells. Br J Cancer 72:663–668.
68. Gabizon, A., Huberty, J., Straubinger, R., Price, D.C. and Papahadjopoulos, D. 1988. An improved method for *in vivo* tracing and imaging of liposomes using Gallium-67- deferoxamine complex. J Liposome Res 1:123–135.
69. Heitjan, D.F. 1991. Generalized Norton-Simon models of tumor growth. Statistics in Medicine 10:1075–1088.
70. Kirpotin DB, Park JW, Hong K, Shao Y, Shalaby R, Colbern G, Benz CC and Papahadjopoulos D. Targeting of liposomes to solid tumors: The case of the sterically stabilized anti-HER2 immunoliposomes. Forum on Liposomes targeting in animal models, J Lipo Res **7**(4):391–417, 1997
71. Kirpotin D.B., Park J.W., Hong K, Shao Y, Colbern G, Zheng W, Meyer O, Benz CC and Papahadjopoulos, D. Targeting of Sterically Stabilized Liposomes to Cancers Overexpressing HER2/neu Proto-oncogene *in* Medical Applications of Liposomes.

D Lasic and D Papahadjopoulos (Eds.). Elsevier Publishers, Amsterdam, The Netherlands. 1998.

72. Matzku, S., Krempel, H., Weckenmann, H.-P., Schirrmacher, V., Sinn, H. and Stricker, H. 1990. Tumour targeting with antibody-coupled liposomes: failure to achieve accumulation in xenografts and spontaneous liver metastases. Cancer Immunol Immunother 31:285–291.
73. Hong, K., Friend, D.S., Glabe C.G. and Papahadjopoulos, D. 1983. Liposomes containing colloidal gold are a useful probe of liposome-cell interactions. Biochim Biophys Acta 732:320–323.
74. Huang, S.K., Lee, K.-D., Hong, K., Friend, D.S. and Papahadjopoulos, D. 1992. Microscopic localization of sterically stabilized liposomes in colon-carcinoma bearing mice. Cancer Res 52:5135–5143.
75. Madden, T.D., Harrigan, P.R., Tai, L.C., Bally, M.B., Mayer, L.D., Redelmeier, T.E., Loughrey, H.C., Tilcock, C.P., Reinish, L.W. and Cullis, P.R. 1990. The accumulation of drugs within large unilamellar vesicles exhibiting a proton gradient: a survey. Chem Phys Lipids 53:37–46.
76. Janknegt, R. 1996. Liposomal formulations of cytotoxic drugs. Supportive Care Cancer, 4:298–304.

Proc. Natl. Acad. Sci. USA
Vol. 88, pp. 11460–11464, December 1991
Medical Sciences

Sterically stabilized liposomes: Improvements in pharmacokinetics and antitumor therapeutic efficacy

D. PAPAHADJOPOULOS*†, T. M. ALLEN‡, A. GABIZON§, E. MAYHEW¶, K. MATTHAY*‖, S. K. HUANG*, K.-D. LEE*, M. C. WOODLE**, D. D. LASIC**, C. REDEMANN**, AND F. J. MARTIN**

Cancer Research Institute, Departments of *Pharmacology and ‖Pediatrics, University of California, San Francisco, CA 94143; ‡Department of Pharmacology, University of Alberta, Edmonton, Alberta, Canada T6G 2H7; §Department of Oncology, Hadassah Medical Center, Jerusalem, Israel 91120; Department of Experimental Pathology, Roswell Park Cancer Institute, Buffalo, NY 14263; and **Liposome Technology, Inc., Menlo Park, CA 94025

Communicated by John A. Clements, July 30, 1991 (received for review May 6, 1991)

ABSTRACT **The results obtained in this study establish that liposome formulations incorporating a synthetic polyethylene glycol-derivatized phospholipid have a pronounced effect on liposome tissue distribution and can produce a large increase in the pharmacological efficacy of encapsulated antitumor drugs. This effect is substantially greater than that observed previously with conventional liposomes and is associated with a more than 5-fold prolongation of liposome circulation time in blood, a marked decrease in uptake by tissues such as liver and spleen, and a corresponding increased accumulation in implanted tumors. These and other properties described here have expanded considerably the prospects of liposomes as an effective carrier system for a variety of pharmacologically active macromolecules.**

Over the last 20 years, liposomes have served a dual role, as a valuable experimental tool for membrane research and in addition as an *in vivo* delivery system for enhancing the efficacy of various pharmacologically active molecules (1). Animal studies have shown that liposomes can decrease the toxicity of several antitumor and antifungal drugs, leading to several recent clinical trials with promising results (2–6). In addition, liposomes have been shown to be efficient carriers of antiparasitic drugs for treating intracellular infections of the reticuloendothelial system (RES), in activating macrophage cells to become tumoricidal in models of metastasis, and in enhancing the immune response to encapsulated antigens, thus facilitating the formulation of artificial vaccines (7, 8). All these effects stem from the capacity of macrophage cells in the liver and spleen (mononuclear phagocytic system or RES) to remove the majority of liposomes from the blood circulation within minutes (9). Such rapid clearance of conventional liposomes [i.e., liposomes composed of various phospholipids and cholesterol (Chol) and possibly other lipids, without specific components conferring the property of long circulation in blood] from the circulation, however, has limited their prospects as an *in vivo* delivery system for transporting drugs to sites of disease beyond the RES.

Recent reports from our laboratories have described liposome formulations (containing the monosialoganglioside G_{M1} or phosphatidylinositol) that exhibit a prolonged circulation time in blood and diminished uptake by the liver and spleen (10–12) and increased accumulation in implanted tumors (12–14). The term "stealth" has been proposed (15) for these long-circulating liposomes. We consider that such liposomes are sterically stabilized by the presence of the relevant headgroups on their surface (16). In this report we present several findings obtained with liposomes sterically stabilized by the PEG headgroups of a synthetic phospholipid (PEG-DSPE) included in the formulation (PEG-liposomes). Preliminary experiments with PEG-liposomes have been published recently (17–19). New microscopic evidence indicates that accumulation of liposomes in tumors involves extravasation, presumably due to increased permeability of the capillary endothelia (20, 21). Unlike conventional liposomes, which show dose-dependent blood clearance kinetics (9, 22, 23), the PEG-liposome formulations show prolonged circulation time in blood, with clearance kinetics that are completely independent of dosage over a wide range. Most importantly, they produce a marked enhancement of the antitumor activity of encapsulated doxorubicin and epirubicin in mice against both i.p. lymphoma and s.c. colon carcinoma, with a concomitant decrease in toxicity. This indicates an increase in the therapeutic index to a value that is much higher than that observed with conventional liposome formulations.

MATERIALS AND METHODS

Materials. Egg phosphatidylcholine (EPC), distearoyl phosphatidylcholine (DSPC), phosphatidylglycerol (PG) derived from EPC (EPG), and bovine brain sphingomyelin (SM) were purchased from Avanti Biochemicals (Birmingham, AL). The monosialoganglioside G_{M1} was obtained from Makor Chemical (Jerusalem). Chol was from either Sigma or Croda (Fullerton, CA). *N*-Tris[hydroxymethyl]-2-aminoethanesulfonic acid (Tes) was purchased from Sigma. Hydrogenated soy phosphatidylcholine [HSPC; NC-100-H, containing 98.2% phosphatidylcholine (PC) and 1.8% lyso-PC] was purchased from Natterman (Cologne, F.R.G.). Partially hydrogenated egg phosphatidylcholine (PHEPC) 99% pure, with an iodine value of 40, was obtained from Asahi Chemical Industries (Tokyo). Tyraminylinulin was synthesized and ^{125}I-labeled tyraminylinulin was prepared as before (24). Na^{25}I was obtained from the Edmonton Radiopharmaceutical Center; pyrogen-free saline for injection (0.9%, USP) was from Travenol Canada (Mississauga, ON). All test tubes, syringes, etc. were sterile and pyrogen-free. Desferal–gallium-67 (^{67}Ga-DF) was prepared as described (25). Dextran labeled with rhodamine B isothiocyanate (Rh-Dex; $M_r \approx$ 9000) was purchased from Sigma. Doxorubicin and epirubicin were obtained from Farmitalia, Carlo Erba (Milan). PEG (M_r = 1900)-derivatized distearoyl phosphatidylethanolamine (PEG-DSPE) was synthesized as described (26).

Abbreviations: RES, reticuloendothelial system; EPC, egg phosphatidylcholine; EPG, phosphatidylglycerol derived from EPC; SM, sphingomyelin; HSPC, hydrogenated soy phosphatidylcholine; PEG-DSPE, polyethylene glycol conjugated to distearoyl phosphatidylethanolamine; ^{67}Ga-DF, Desferal–gallium-67; Rh-Dex, dextran labeled with rhodamine B isothiocyanate; Chol, cholesterol; PC, phosphatidylcholine; PG, phosphatidylglycerol; DSPC, distearoyl phosphatidylcholine; PHEPC, partially hydrogenated EPC.

†To whom reprint requests should be addressed.

The publication costs of this article were defrayed in part by page charge payment. This article must therefore be hereby marked "*advertisement*" in accordance with 18 U.S.C. §1734 solely to indicate this fact.

Liposome Preparation. Liposomes were prepared by thin film hydration as described (10, 12). The resulting multilamellar vesicles at lipid concentrations of ≈10 μmol/ml were frozen (at −40°C) and thawed (at 60°C) several times and then passed repeatedly under pressure through 0.2- or 0.1- and 0.05-μm pore size polycarbonate membranes (27), and the extrusion was repeated until the average size distribution was ≈80–100 nm in diameter (mean Gaussian distribution by volume). Liposome morphology was occasionally examined by electron microscopy (28, 29).

For encapsulation of ^{67}Ga-DF, the liposomes were prepared with Desferal, and the ^{67}Ga was loaded just before use (25). Iodinated tyraminylinulin was encapsulated as before (10). Rh-Dex (M_r = 9000) was encapsulated passively by inclusion of the material at a concentration of 100 mg/ml in the preparation buffer. Free Rh-Dex was removed by gel permeation on a Sephadex G-150 column and an Amicon concentration unit with a M_r 30,000 cut-off filter. Liposomes containing doxorubicin or epirubicin were composed of PEG-DSPE/HSPC/Chol/α-tocopherol (0.15:1.85:1.00:0.018, mol/mol) and were prepared as described (30). The drug and total lipid concentrations of the final product were about 2 mg/ml and 20 μmol/ml, respectively (±10% for both), and the particle diameter was 85 ± 10 nm.

Animal Experimentation. Experiments with labeled inulin were performed in female ICR (outbred) mice (10), and tissue distribution experiments were performed with ^{67}Ga-DF in normal Swiss–Webster mice (12) and in tumor-bearing BALB/c mice inoculated s.c. with the C-26 colon carcinoma (31). Mice (three per group) were injected in the tail vein with ≈0.2 ml of 0.1–10 μmol of phospholipid. Blood correction factors (10, 12) were applied to tissues and the carcass. Male and female adult Sprague–Dawley rats (220–400 g) were surgically prepared under anesthesia for i.v. administration of a 0.3- to 0.4-ml sample via a femoral venous cannula and blood sampling via chronic femoral arterial cannula externalized at the back of the neck. The animals were awake and unrestrained during blood drawing except for the initial two time points, 1 and 15 min. The amount of lipid injected was 10–15 μmol of phospholipid per kg of animal weight.

Mouse colon carcinoma (C-26) cells were injected into BALB/c female mice (6–9 weeks old) as before (31). At day 0, mice were injected into the left flank s.c. with 4×10^5 cells in a volume of 0.1 ml. One day later drug was injected i.v. (tail vein, 0.2 ml or less, mouse weight between 16 and 21 g). Treatment was repeated at weekly intervals to a maximum of three injections. Tumor volume was measured as before (31).

The lymphoma cell line J6456 was inoculated i.p. into BALB/c female mice (32). When there was about 2 ml of ascitic fluid accumulated, containing between 10^8 and 10^9 tumor cells, the drug was injected i.v. either free in solution or in encapsulated form. The ascitic fluid was thereafter sampled at different intervals. Tumor cells were separated by centrifugation. Part of the supernatant was passed through a Dowex column to remove the non-liposome-associated drug (33). The drug concentration was determined as before (30). For therapeutic experiments, BALB/c female mice (20 in each treatment group) were inoculated i.p. on day 0 with 10^6 lymphoma cells (J6456). Treatment consisted of a single i.v. injection on day 5 containing either free or liposome-encapsulated doxorubicin.

RESULTS

Tissue Distribution and Pharmacokinetics. Recent studies with PEG-liposomes in mice demonstrate blood levels comparable to G_{M1} formulations (10, 12): 24–30% of total recovered dose at 24 h, regardless of whether the PC was rigid (DSPC) or fluid (EPC). In addition, similarly high liposome recoveries were obtained even when EPG was included in addition to PEG-DSPE. Average values for the percent recovered dose of PEG-DSPE/EPC/Chol liposomes (compared to the conventional formulation of EPG/EPC/Chol) at 24 h following i.v. injection in mice were as follows: blood, 29.3 ± 2.8 (1.2 ± 0.3); liver 17.9 ± 2.0 (61.3 ± 3.4); spleen, 2.7 ± 0.6 (4.3 ± 0.4); heart, 0.1 ± 0.7 (0.3 ± 0.1); skin, 15.6 ± 2.0 (4.7 ± 0.9); carcass, 20.5 ± 2.7 (15.3 ± 3.1). Our definition for carcass excludes all major organs such as liver, spleen, heart, kidneys, gut, and lungs.

We have also determined the blood clearance kinetics of several liposome formulations in rats by repeated sampling of blood, using ^{67}Ga-labeled liposomes as above. Fig. 1 compares the clearance curve of free ^{67}Ga-DF with that of the same label when encapsulated in liposomes of conventional composition (EPG/PHEPC/Chol or PHEPC/Chol) and when encapsulated in PEG-liposomes (PEG-DSPE/PHEPC/Chol). It is noteworthy that the clearance curve of the liposomes of the latter composition is linear on a semilogarithmic plot (Fig. 1), with a 5-fold increased $t_{1/2}$ value (to 15.3 h), as opposed to the presence of a fast and a slow component of clearance obtained with conventional liposomes, which show saturation of one or more of the components of uptake at doses of 40 mg/kg or lower (34). Pharmacokinetic studies with PEG-liposomes (Figs. 1 and 2) and additional work elsewhere (35) indicate that these compositions show single first-order clearance rates that are independent of dose over the entire dosage range examined (0.5–500 μmol/kg in mice and 3–70 μmol/kg in rats). Fig. 2 compares the blood levels and RES uptake obtained with PEG-DSPE/EPC/SM/Chol and EPC/Chol liposomes at 2 h after i.v. injection. These results indicate high, dose-independent blood levels for PEG-liposomes (35) as well as independence for the amount of label accumulating in the liver and spleen (Fig. 2*A*). Conventional liposomes (EPC/Chol) show decreasing percentages accumulating in liver and spleen with increasing dose, reaching a plateau at doses of >2 μmol of phospholipid per mouse. The results described above suggest that PEG-liposomes are not being recognized by high-affinity, saturable, binding sites, such as those expressed on resident macrophages in the liver and spleen, which recognize conventional liposomes (36). Indeed, the uptake of sterically stabilized liposomes *in vitro* by bone marrow-derived murine macrophages (37) and by CV1 cells, a primate cell line of epithelial origin (38), is significantly reduced compared to conventional liposomes.

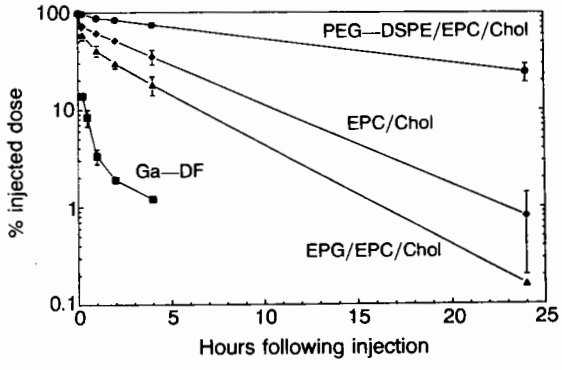

FIG. 1. Blood clearance kinetics of liposomes in rats. ^{67}Ga-DF was used as a marker for liposome contents. Results are expressed as the percentage of the injected dose present in blood at any particular time. Error bars represent the average (± SD) of three different experiments. ■, free ^{67}Ga-DF; ▲, ^{67}Ga-DF encapsulated in EPG/EPC/Chol (0.15:1.85:1, mol/mol) liposomes; ◆, ^{67}Ga-DF encapsulated in EPC/Chol (2:1, mol/mol) liposomes; ●, ^{67}Ga-DF encapsulated in PEG-DSPE/EPC/Chol (0.15:1.85:1, mol/mol) liposomes. In this figure, EPC stands for PHEPC.

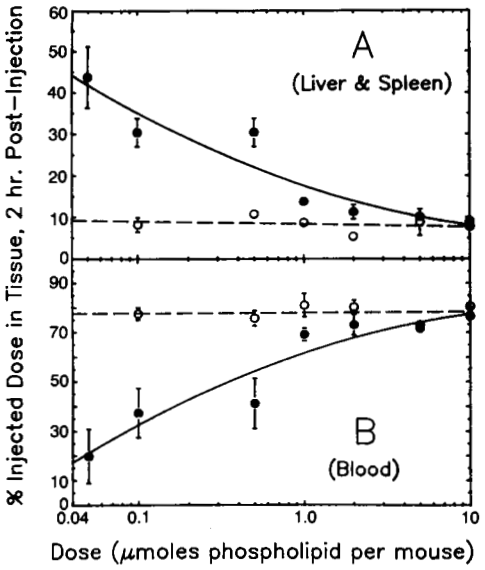

FIG. 2. Dose dependence of liposome distribution in mice. ^{125}I-labeled tyraminylinulin was used as a marker of liposome contents. The results are plotted as the percentage of the injected dose present 2 hours after injection in liver and spleen (corrected for blood) (*A*) or in blood (*B*). Each point represents an average (± SD) from three animals. One micromole per mouse represents a dose of 50 μmol/kg. ●, EPC/Chol (1:1, mol/mol) liposomes; ○, PEG-DSPE/EPC/SM/Chol (0.14:1:1:1, mol/mol) liposomes.

Uptake by Tumors and Extravasation of Liposome Label and Drug. *Accumulation in s.c.-implanted colon carcinoma.* We have compared liposomes composed of DSPC/Chol and PEG-DSPE/DSPC/Chol at the same dosage and particle size. The amount of ^{67}Ga present at different times in blood, liver, and tumor (C-26 cells injected s.c. 2–3 weeks earlier) was expressed as the percentage of the injected dose per gram of tissue. It was found that inclusion of PEG-DSPE increases the amount of label found in blood (by 4-fold) and tumor (by 2.3-fold) and decreases the amount found in liver (by 2-fold) at 48 h after i.v. injection. It should be noted here that DSPC/Chol and also SM/Chol have the longest circulation times compared to other conventional compositions (39–41). However, unlike sterically stabilized liposomes, they still show dose-dependent kinetics and saturation of liver uptake at high concentration (39). When a negatively charged phospholipid such as PG or phosphatidylserine was added to either of these two compositions, the uptake by the liver was much higher (12, 42) and that of the tumor much lower (12, 14).

We have also examined the tumor tissue microscopically to determine whether the accumulated liposomes have extravasated beyond the endothelial barrier of the tumor vasculature. Rh-Dex was used as a water-soluble liposome-encapsulated marker to study the distribution of liposomes within the tumor mass by fluorescence microscopy. Fig. 3 shows a phase-contrast picture of a frozen section of tumor tissue, along with a picture of the same section observed in dark-field fluorescence microscopy. When a solution of non-encapsulated Rh-Dex was injected i.v., there was no detectable fluorescence in the tumor after 24 h. The photograph shown in Fig. 3 is representative of a large number of photographs taken from various sections of the tumor mass. An uneven focal distribution of the fluorescence was observed within the tumor, with both dark areas and other highly fluorescent areas. Similar localization was observed by using a lipid fluorescent marker, rhodamine-labeled phosphatidylethanolamine, indicating that the fluorescence revealed by Rh-Dex in Fig. 3 probably represents intact liposomes. The fluorescence was localized well beyond the endothelial layer and was apparently extracellular, in the interstitial space surrounding living tumor cells. This conclusion has been confirmed more recently by silver enhancement of gold particles encapsulated into liposomes (43).

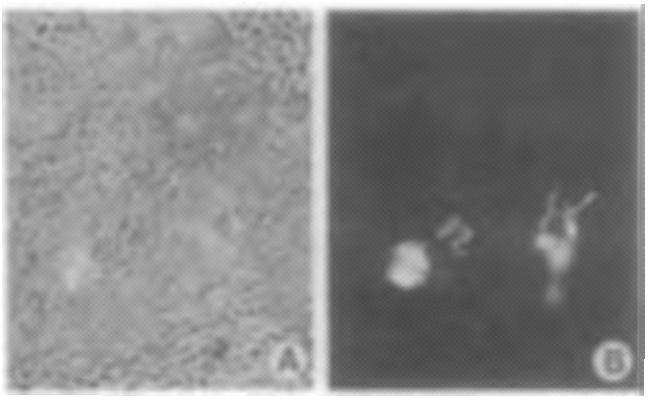

FIG. 3. Localization of liposomes in C-26 colon carcinoma. Liposomes with encapsulated Rh-Dex were injected into the tail vein of mice implanted with s.c. tumor. Colon carcinoma cells (C-26) were inoculated s.c. into BALB/c mice 2–3 weeks before the liposomes. Tumors at that time weighed ≈1 g. At 24 h after liposome injection, mice were perfused with heparinized buffer and subsequently with 4% paraformaldehyde. The tumors were collected and further fixed in 1% glutaraldehyde. Frozen sections of the tumors (≈5 μm thick) were examined in a fluorescence microscope with ×400 magnification. Most of the fluorescence signal was grossly associated with the vasculature inside the tumor mass, whereas a gradient of fluorescence away from them was usually observed. (*A*) Phase-contrast image of a representative section. (*B*) Corresponding fluorescence micrograph. Arrows and arrowheads point to an area with red blood cells in the blood vessel, which is dark in *B*. Rhodamine fluorescence is bright surrounding and away from that area, well beyond the endothelial layer of the vasculature.

Accumulation in i.p.-implanted lymphoma. The experimental model consisted of lymphoma grown i.p. with an i.v. injection of PEG-DSPE/HSPC/Chol liposomes encapsulating doxorubicin, an anthracycline used widely as an antitumor agent. Fig. 4 shows the concentration of drug in the liver,

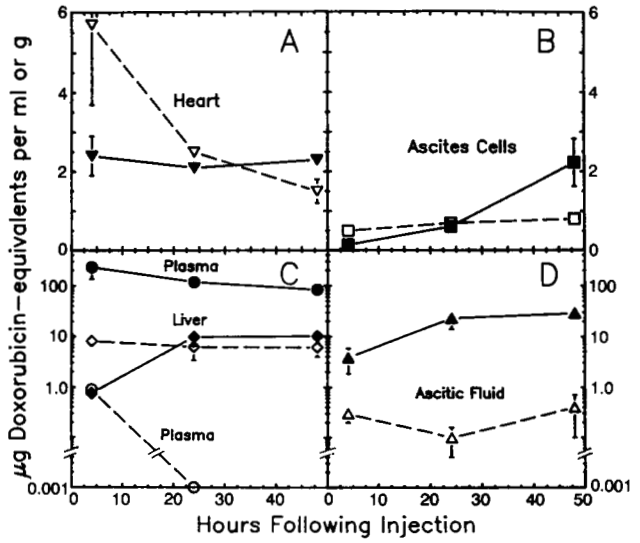

FIG. 4. Liposome-encapsulated doxorubicin in tumor-bearing mice. The presence of doxorubicin was measured directly by fluorimetric determination in various tissues of BALB/c mice inoculated (i.p.) with J6456 lymphoma, at different times following injection either as free drug (open symbols, dashed lines) or encapsulated in liposomes (closed symbols, solid lines) composed of PEG-DSPE/HSPC/Chol (0.2:2:1 mol/mol). ◇ and ◆, liver; ▽ and ▼, heart; ○ and ●, plasma; △ and ▲, ascitic fluid; □ and ■, ascitic cells.

heart, plasma, and ascitic fluid after i.v. injection of doxorubicin either free or encapsulated in PEG-liposomes. The ascitic fluid is an extravascular/extracellular fluid pool and is in direct contact with the tumor cells. The results indicate that encapsulation in PEG-liposomes diminished the early uptake of the drug by the heart and liver (lower values at 4 h) although the uptake in the liver was increased after 24 h, as observed earlier (12, 14). Most importantly, there was a much higher concentration of the drug in plasma and in the ascitic fluid with the encapsulated formulation compared to the free drug. Separation of free drug on a Dowex column (30) showed that the majority of the drug present in the ascitic fluid was in intact liposomes and only 15–25% was free drug between 24 and 48 h. The concentration of the drug in the ascitic cells (mostly tumor cells) was initially lower but increased with time (Fig. 4). These results, taken altogether, indicate that PEG-liposomes initially injected i.v. can extravasate into the peritoneal cavity where they provide a constantly high reservoir of encapsulated drug, available to be taken up by the tumor cells. Animals carrying no tumors did not accumulate any appreciable amount of liposomes into their peritoneal cavity, although liposomes are known to get transported from the peritoneal cavity to blood (11, 15).

Anti-Tumor Efficacy of Drug-Containing Liposomes. *Mouse colon carcinoma grown s.c.* For the therapeutic experiments, multiple injections of liposomes composed of PEG-DSPE/HSPC/Chol loaded with epirubicin were given i.v. starting 1 day after s.c. inoculation of 4×10^5 C-26 tumor cells. The dosage of drug per injection was 6 and 12 mg/kg, and the initial injection was repeated twice (total of three injections) at 7-day intervals. The antitumor effects were registered by measuring tumor size and the survival of mice up to 120 days after tumor implantation. The results presented in Fig. 5 show clearly that encapsulation causes a marked improvement in therapeutic efficacy, inhibiting the tumor growth (Fig. 5*A*) and producing a large percentage of long-term survivors (Fig. 5*B*). The controls with injections of free drug or drug and empty liposomes showed only a slight prolongation of mean survival over untreated animals. Similar effects were obtained when liposomes were injected with a delay of 3 or 10 days, and the effect was smaller but still significant, even with a delay of 14 days (E.M., D.D.L., S. Babar, and F. J. Martin, unpublished work).

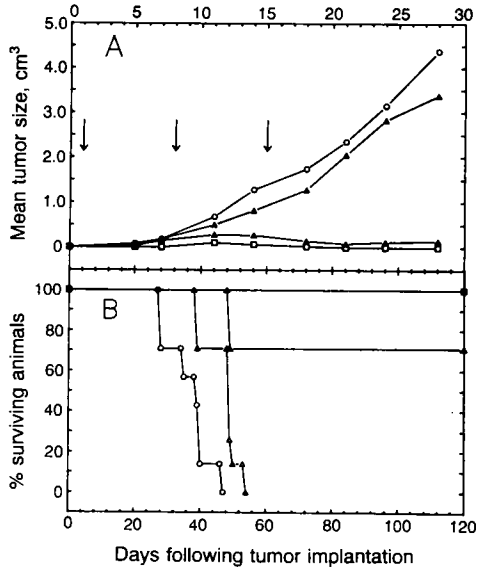

FIG. 5. Therapeutic experiment with colon carcinoma in mice. Colon carcinoma cells (C-26) were inoculated s.c. into BALB/c mice. Treatment started on day 1 and was repeated twice on days 8 and 15; it consisted of an i.v. injection of epirubicin either free or encapsulated in liposomes composed of PEG-DSPE/HSPC/Chol. There were four treatments as follows: ○, saline control; △, free epirubicin at 6 mg/kg (nonencapsulated); ▲, encapsulated epirubicin at 6 mg/kg; □, encapsulated epirubicin at 12 mg/kg. (*A*) Measurement of mean tumor size (volume in cm^3) between 0 and 30 days after tumor implantation. (*B*) Survival curves expressed as the percentage of surviving animals from 0 to 120 days postimplantation. The total number of animals was 6–10 per group.

The doses of free and encapsulated drug were chosen on the basis of toxicity experiments performed in animals without tumors, with a similar regime of three doses at weekly intervals. These studies indicated that a dose of epirubicin at 9 mg/kg encapsulated in liposomes and at 6 mg/kg as free drug resulted in no deaths up to 120 days following injection. In the same period three deaths out of five animals were observed with epirubicin at 12 mg/kg encapsulated in liposome and at 9 mg/kg as free drug. On the basis of these results, we can conclude that the acute toxicity of epirubicin, as exemplified by the maximum tolerated dose, is reduced slightly following liposome encapsulation. As already shown in Fig. 5, the therapeutic effect for a similar dose was increased markedly by liposome encapsulation. Thus, the therapeutic index of this drug (ratio of efficacy to toxicity) is considerably increased by encapsulation in PEG-liposomes. Earlier work had indicated that the C-26 colon carcinoma grown s.c. is not responsive to doxorubicin encapsulated into liposomes of conventional formulations (31).

Mouse lymphoma grown i.p. The antitumor efficacy of liposome-encapsulated doxorubicin was tested in this tumor model system after i.v. injection. The median survival time of the control (untreated) mice was 16 days. It was increased to 24 and 21 days with a single dose of free doxorubicin at 10 and 15 mg/kg, respectively. Encapsulation in PEG-DSPE/HSPC/Chol liposomes resulted in a substantial lengthening of the median survival to 30 and 44 days, respectively, for doses of 10 and 15 mg/kg. The last dose also resulted in two long-term survivors. Toxicity experiments with increasing doses (15, 20, and 25 mg/kg) of doxorubicin encapsulated in PEG-liposomes as above showed a substantial decrease in acute toxicity as compared to the free drug. From a comparison of the efficacy and the toxicity results, we conclude that encapsulation in PEG-liposomes produces a significant increase in the therapeutic index of doxorubicin against mouse lymphoma.

DISCUSSION

The clearance rate of liposomes from blood (41, 44, 45) as well as their accumulation in tumors (14) depends on particle size in addition to specific lipids (10, 12). Accumulation of small (≈50-nm diameter) neutral liposomes (DSPC/Chol) in tumors had been observed earlier (46). In our studies (12, 14) we have enhanced this accumulation by introducing liposome formulations with longer blood half-life and have increased their usefulness as a drug carrier by using liposomes of ≈100-nm diameter, which have a 16-fold higher internal volume as compared with smaller (50-nm) liposomes. We have recently proposed a mechanism for the prolonged blood clearance involving steric stabilization of the liposome surface (16).

The high recovery in blood reported here with PEG-liposomes and their accumulation in tumors (Fig. 3) may prove to be of considerable advantage to future clinical applications for the following reasons. (*i*) The PEG derivative is a synthetic phospholipid easily prepared at high purity in large quantities and considerably lower cost compared to the G_{M1} ganglioside, which is derived from bovine brain. (*ii*) Fluid and solid bilayer compositions give similar blood circulation times, adding considerably to the flexibility needed for various clinically relevant formulations. (*iii*) The additional presence of the negatively charged PG in the liposome

bilayer allows for better encapsulation of a variety of positively charged drugs and other macromolecules and reduces the likelihood of aggregation. (*iv*) Dose independence dictates that a constant percentage of the injected dose is taken up by various tissues, irrespective of the amount injected, allowing for a reliable prediction of drug levels during therapy (35). Finally, (*v*) reduced uptake by liver and spleen decreases the possibility for RES toxicity and enhances the chances for localization in other tissues for therapeutic and imaging applications.

Our therapeutic studies with PEG-DSPE/HSPC/Chol liposomes showed a significant increase in the therapeutic index of antitumor drugs in mice against both a lymphoma and a colon carcinoma. This is consistent with our earlier findings that phosphatidylinositol liposomes have a pronounced effect on the blood clearance kinetics of doxorubicin (30) and the accumulation of liposome markers in implanted tumors (12–14). The lower acute toxicity of anthracycline-loaded PEG-liposomes reported here is similar to that observed earlier with conventional liposomes (47–50). It is probably related to the delayed clearance of drug from the blood and the reduction of peak plasma levels of free drug, which adversely affect sensitive tissues such as the heart and others involved in the acute toxic effects. Whether the increased therapeutic efficacy is due to the improved (delayed) blood clearance as seen recently with arabinose cytosine encapsulated in G_{M1}-liposomes (51) or the increased local accumulation of drug within the tumor mass is not certain at present. It is possible that both factors contribute, although the latter is a more likely possibility.

The microscopic studies discussed above have indicated the presence of PEG-liposomes in the interstitial space around tumor cells. It is quite possible that their extravasation beyond the endothelial layer in tumors is the result of their long circulation time in blood and the increased permeability of the endothelial barrier in the newly vascularized tumors (12, 20, 21). Although diffusion and deep penetration within the tumor mass is not expected for particles of the size of liposomes (20, 21), it is possible that free drug can diffuse locally from the extravasated liposomes to the surrounding tumor cells. The presence of intact extracellular liposomes within the tumor area would provide a local depot for drug release. Enhanced localization of liposomes in other anatomically distinct regions might also be beneficial for other diseases involving areas of increased capillary permeability.

We thank Mary Newman, Lila Collins, and Jon Hidayat for technical assistance; Drs. R. Debs, N. Düzgünes, and K. Hong for helpful discussions; and Rita Spivey for skillful assistance with the manuscript. This study was supported by Grants CA35349 (D.P.) and CA39448 (K.M.) from the U.S. Public Health Service, MA9127 (T.A.) from the Canadian Medical Research Council, and RD264 (D.P.) from the American Cancer Society, and by Liposome Technology, Inc. (T.A., K.M., E.M., and A.G.).

1. Ostro, M. J., ed. (1987) *Liposomes from Biophysics to Therapeutics* (Dekker, New York), pp. 1–369.
2. Sculier, J. P., Caune, A., Meunier, F., Brassine, C., Laduzon, C., Hollaert, C., Collette, N., Heymans, C. & Klastersky, J. (1988) *Eur. J. Cancer Clin. Oncol.* **24**, 527–538.
3. Gabizon, A., Peretz, T., Sulkes, A., Amselem, S., Ben-Yosef, R., Ben-Baruch, N., Catane, R., Biran, S. & Barenholz, Y. (1989) *Eur. J. Cancer Clin. Oncol.* **25**, 1795–1803.
4. Treat, J., Greenspan, A., Forst, D., Sanchez, J. A., Ferrans, V. J., Potkul, L. A., Woolley, P. V. & Rahman, A. (1990) *J. Natl. Cancer Inst.* **82**, 1706–1710.
5. Lopez-Berestein, G., Fainstein, G. B., Hopfer, R., Mehta, K., Sullivan, M. P., Keating, M., Rosenblum, M. G., Mehta, R., Luna, M., Hersh, E. M., Reuben, J., Juliano, R. J. & Bodey, G. P. (1985) *J. Infect. Dis.* **151**, 704–710.
6. Presant, C. A., Proffitt, R. T., Turner, A. F., Williams, L. E., Winsor, D. W., Werner, J. L., Kennedy, P., Wiseman, C., Gala, K., McKenna, R., Smith, J. D., Bouzaglou, S. A., Calahan, R. A., Baldeschwieler, J. & Crossley, R. J. (1988) *Cancer* **62**, 905–911.
7. Lopez-Berestein, G. & Fidler, I. J., eds. (1989) *Liposomes in the Therapy of Infectious Diseases and Cancer* (Liss, NY).
8. Alving, C. R. & Richards, R. L. (1990) *Immunol. Lett.* **25**, 275–280.
9. Gregoriadis, G. ed. (1988) *Liposomes as Drug Carriers* (Wiley, New York), pp. 1–863.
10. Allen, T. M. & Chonn, A. (1987) *FEBS Lett.* **223**, 42–46.
11. Allen, T. M., Hansen, C. & Rutledge, J. (1989) *Biochim. Biophys. Acta* **981**, 27–35.
12. Gabizon, A. & Papahadjopoulos, D. (1988) *Proc. Natl. Acad. Sci. USA* **85**, 6949–6953.
13. Papahadjopoulos, D. & Gabizon, A. (1987) *Ann. N.Y. Acad. Sci.* **507**, 64–74.
14. Gabizon, A., Price, D. C., Huberty, J., Bresalier, R. S. & Papahadjopoulos, D. (1990) *Cancer Res.* **50**, 6371–6378.
15. Allen, T. M. (1989) in *Liposomes in the Therapy of Infectious Diseases and Cancer* eds., Lopez-Berestein, G. & Fidler, I. (Liss, New York), pp. 405–415.
16. Lasic, D. D., Martin, F. J., Gabizon, A., Huang, K. S. & Papahadjopoulos, D. (1991) *Biochim. Biophys. Acta* **1070**, 187–192.
17. Woodle, M. C., Neuman, M., Collins, L. R., Redemann, C. & Martin, F. J. (1990) *Proc. 17th Int. Symp. Control Release Bio-active Matr.* **17**, 77–78.
18. Klibanov, A. L., Maruyama, K., Torchilin, V. P. & Huang, L. (1990) *FEBS Lett.* **268**, 235–237.
19. Blume, G. & Cevc, C. (1990) *Biochim. Biophys. Acta* **1029**, 91–97.
20. Jain, R. K. (1987) *Cancer Metastasis Rev.* **6**, 559–593.
21. Jain, R. K. & Gerlowski, L. E. (1986) *CRC Crit. Rev. Oncol. Hematology* **5**, 115–170.
22. Mauk, M. R. & Gamble, R. E. (1979) *Proc. Natl. Acad. Sci. USA* **76**, 765–769.
23. Hwang, K. J. & Beaumier, P. L. (1988) in *Liposomes as Drug Carriers*, ed. Gregoriadis, G. (Wiley, New York), pp. 19–35.
24. Sommerman, E. F., Pritchard, P. H. & Cullis, P. R. (1984) *Biochem. Biophys. Res. Commun.* **122**, 319–325.
25. Gabizon, A., Huberty, J., Straubinger, R. M., Price, D. C. & Papahadjopoulos, D. (1988) *J. Liposome Res.* **1**, 123–135.
26. Allen, T. M., Hansen, C., Martin, F., Redemann, C. & Yau-Young, A. (1991) *Biochim. Biophys. Acta* **1066**, 29–36.
27. Olson, F., Hunt, C. A., Szoka, F. C., Vail, W. J. & Papahadjopoulos, D. (1979) *Biochim. Biophys. Acta* **557**, 9–23.
28. Düzgünes, N., Wilschut, J., Hong, K., Fraley, R., Perry, C., Friend, D. S., James, T. L. & Papahadjopoulos, D. (1983) *Biochim. Biophys. Acta* **732**, 289–299.
29. Hong, K., Friend, D. S., Glabe, G. & Papahadjopoulos, D. (1983) *Biochim. Biophys. Acta* **732**, 320–323.
30. Gabizon, A., Shiota, R. & Papahadjopoulos, D. (1989) *J. Natl. Cancer Inst.* **81**, 1484–1488.
31. Mayhew, E., Goldrosen, M., Vaage, J. & Rustum, Y. (1987) *J. Natl. Cancer Inst.* **78**, 707–713.
32. Gabizon, A. & Trainin, N. (1980) *Br. J. Cancer* **42**, 551–558.
33. Storm, G., Van Gloois, L., Brouwer, M. & Crommelin, D. J. (1985) *Biochim. Biophys. Acta* **818**, 343–351.
34. Abra, R. M. & Hunt, C. A. (1981) *Biochim. Biophys. Acta* **666**, 493–503.
35. Allen, T. M. & Hansen, C. (1991) *Biochim. Biophys. Acta* **1068**, 133–141.
36. Derksen, J. T. P., Morselt, H. W. M. & Scherphof, G. (1988) *Biochim. Biophys. Acta* **971**, 127–136.
37. Allen, T. M., Austin, G., Chonn, A., Lin, L. & Lee, K. C. (1991) *Biochim. Biophys. Acta* **1061**, 56–64.
38. Lee, K. D., Hong, K. & Papahadjopoulos, D. (1991) *Biochim. Biophys. Acta*, in press.
39. Hwang, K. J., Luk, K. S. & Beaumier, P. L. (1980) *Proc. Natl. Acad. Sci. USA* **77**, 4030–4034.
40. Senior, J. & Gregoriadis, G. (1982) *Life Sci.* **30**, 2123–2136.
41. Allen, T. M. & Everest, J. M. (1983) *J. Pharmacol. Exp. Ther.* **226**, 539–544.
42. Allen, T. M., Williamson, P. & Schlegel, R. A. (1988) *Proc. Natl. Acad. Sci. USA* **85**, 8067–8071.
43. Huang, S. K., Hong, K., Lee, K.-D., Papahadjopoulos, D. & Friend, D. S. (1991) *Biochim. Biophys. Acta* **1069**, 117–121.
44. Juliano, R. L. & Stamp, D. (1975) *Biochem. Biophys. Res. Commun.* **63**, 651–658.
45. Senior, J., Crawley, J. C. W. & Gregoriadis, G. (1985) *Biochim. Biophys. Acta* **839**, 1–8.
46. Proffitt, R. T., Williams, L. E., Presant, C. A., Tin, G. W., Bliana, J. A., Gamble, R. C. & Baldeschwieler, J. D. (1983) *Science* **220**, 502–505.
47. Forssen, E. A. & Tokes, Z. A. (1979) *Biochem. Biophys. Res. Commun.* **91**, 1295–1301.
48. Rahman, A., Kessler, A., More, B., Sikic, B., Rowden, P., Woolley, P. & Schein, P. S. (1980) *Cancer Res.* **40**, 1532–1537.
49. Olson, F., Mayhew, E., Maslow, D., Rustum, Y. & Szoka, F. (1982) *Eur. J. Cancer* **18**, 167–176.
50. Bally, M. B., Nayar, R., Masin, D., Hope, M. J., Cullis, P. R. & Mayer, L. D. (1990) *Biochim. Biophys. Acta* **1023**, 133–152.
51. Allen, T. M. & Mehra, T. (1989) *Proc. West. Pharmacol. Soc.* **32**, 111–114.

Nanoscale

PAPER

View Article Online
View Journal | View Issue

Cite this: Nanoscale, 2017, 9, 10327

Clinically approved PEGylated nanoparticles are covered by a protein corona that boosts the uptake by cancer cells†

M. Papi,‡[a] D. Caputo,‡[b] V. Palmieri,[a] R. Coppola,[b] S. Palchetti,[c,d] F. Bugli,[e] C. Martini,[e] L. Digiacomo,[c,f] D. Pozzi *[c,d] and G. Caracciolo *[c]

Today, liposomes are an advanced technology of drug carriers with a dozen drugs in clinical practice and many more in clinical trials. A bottleneck associated with the clinical translation of liposomes has long been 'opsonization', *i.e.* the adsorption of plasma proteins at the liposome surface resulting in their rapid clearance from circulation. For decades, the most popular way to avoid opsonization has been grafting polyethylene glycol (PEG) onto the liposome surface. Recent studies have clarified that grafting PEG onto the liposome surface reduces, but does not completely prevent protein binding. In this work, we employed dynamic light scattering, zeta-potential analysis, one-dimensional sodium dodecyl sulfate polyacrylamide gel electrophoresis (1D-SDS-PAGE), semi-quantitative densitometry and cell imaging to explore the bio-nano-interactions between human plasma (HP) and Onivyde, a PEGylated liposomal drug that has recently been approved by the Food and Drug Administration (FDA) for the treatment of metastatic pancreatic ductal adenocarcinoma (PDAC). To properly evaluate the role of PEGylation, an unPEGylated variant of Onivyde was used as a reference. Collectively, our findings suggest that: (i) although PEGylated, Onivyde is not "stealth" in HP; (ii) surface chemistry is more important than PEGylation in controlling the bio-nano-interactions between Onivyde and plasma components. Of note is that the PC was found to boost the cellular uptake of Onivyde in the pancreas ductal adenocarcinoma cell line (PANC-1) thus suggesting its prominent role in its indication for PDAC treatment. Relevant implications for drug delivery and drug design are discussed.

Received 28th April 2017,
Accepted 21st June 2017

DOI: 10.1039/c7nr03042h

rsc.li/nanoscale

Introduction

Nowadays, liposomes are the most successful drug delivery system with twelve drugs in routine clinical practice for a range of indications and many more in clinical development.[1,2] A common problem associated with the *in vivo* use of "first-generation" liposomes ("conventional" liposomes, Fig. 1, panel A) has long been their rapid clearance from circulation by uptake into the cells of the mononuclear phagocyte system (MPS).[3] The MPS does not recognize the liposomes themselves but, rather, recognizes opsonins (*e.g.* immunoglobulins, *etc.*) and complement proteins (*e.g.* C5b-9 complexes), which are bound to the surface of the liposomes.[4] Initial attempts to overcome the clearance of liposomes were: (i) the MPS blockade using large doses of empty liposomes;[5] (ii) reducing the vesicle size;[6] and (iii) lowering the surface charge.[7] As a matter of fact, all of these approaches did produce little improvements in the circulation half-life. Superior results were obtained using liposomes sterically stabilized with polyethylene glycol (PEG) that were termed "stealth" liposomes[8,9] (Fig. 1, panel B). Shortly thereafter, the first "stealth" liposomal

[a]Istituto di Fisica, Università Cattolica del Sacro Cuore, Largo F. Vito 1, 00168 Rome, Italy
[b]University Campus Bio-Medico di Roma, Via Alvaro del Portillo 200, 00128 Rome, Italy
[c]Department of Molecular Medicine, "Sapienza" University of Rome, Viale Regina Elena 291, 00161 Rome, Italy. E-mail: giulio.caracciolo@uniroma1.it, daniela.pozzi@uniroma1.it
[d]Istituti Fisioterapici Ospitalieri, Istituto Regina Elena, Via Elio Chianesi 53, 00144 Rome, Italy
[e]Istituto di Microbiologia, Università Cattolica del Sacro Cuore, Largo F. Vito 1, 00168 Rome, Italy
[f]Department of Bioscience and Biotechnology, University of Camerino, Via Gentile III da Varano, 62032 Camerino, MC, Italy

† Electronic supplementary information (ESI) available: Fig. S1. Representative one-dimensional SDS-PAGE gel of plasma proteins obtained from Onivyde and "unPEGylated Onivyde" following 1-hour incubation with plasma of four pancreatic ductal adenocarcinoma patients. Fig. S2. Temporal aggregation and sedimentation of liposomes and liposome–protein corona (PC) in phosphate-buffered saline (PBS) and cell culture medium (Dulbecco's modified Eagle's medium, DMEM) were explored by measuring the Optical Density (OD) at 600 nm. Table S1. Inclusion criteria in healthy and pancreatic cancer groups. Table S2. Clinical/pathological stage in the pancreatic cancer patients group. See DOI: 10.1039/c7nr03042h

‡ These authors contributed equally to this work.

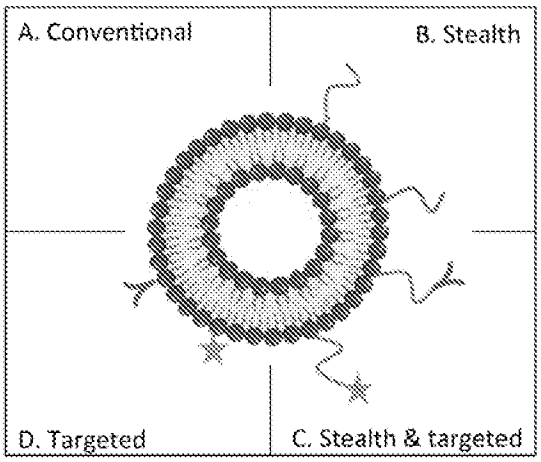

Fig. 1 (A) "First generation" vesicles, referred to as "conventional" liposomes have been the object of intense investigations. Manipulation of the lipid composition, size, and charge of the vesicle were the main strategies to increase their instability in plasma. (B) A significant step in the development of long-circulating liposomes came with inclusion of the synthetic polymer poly-(ethylene glycol) (PEG) in liposome composition (stealth liposomes). (C) Furthermore, by modifying the PEG-molecule terminus stealth liposomes can be actively targeted with monoclonal antibodies (Mabs) or ligands ("targeted stealth liposomes"). (D) The same strategy has been adopted to bind Mabs and/or ligand to conventional liposomes ("targeted liposomes").

formulation, named Doxil®,[10] was approved by the Food and Drug Administration (FDA) as a treatment for AIDS-related Kaposi's sarcoma in HIV patients. In general, PEGylation, although promising in concept,[11] has been frequently disappointing in practice.[12] For many diseases (*e.g.* breast cancer, acute lymphoblastic leukemia, *etc.*), "stealth" liposomes have resulted in no therapeutic improvement over their "conventional" (*i.e.* unPEGylated) counterpart. The scientific community soon realized that both "stealth" and "conventional" liposomes could also be an ideal nanodevice for the targeted delivery of nanomedicines (Fig. 1, panels C and D). However, despite the unprecedented efforts, no targeted liposomal therapeutics is available for clinical practice.[13] On the other hand, some "conventional" liposomes gained regulatory approval and reached the clinic. To date, four PEGylated liposomal drugs are used in the clinic and many more (*e.g.* MM302, MBP-426, *etc.*) are in clinical development.[14] Despite the huge amount of preclinical and clinical research work involving liposomes, it is still unclear why some lipid formulations require PEGylation to work properly *in vivo*, while others do not. According to our present understanding, this dichotomy is likely due to our limited knowledge of the new biological identity that liposomes acquire *in vivo*.[15] Indeed, when liposomes enter biological milieus (*e.g.* the blood, interstitial fluids, *etc.*), they are coated by a complex biomolecular layer that is commonly referred to as a "protein corona" (PC).[16–21] PC is the biological interface of liposomes that is 'seen' by the components of the physiological environment and influences the downstream biological behavior. PC becomes the biological identity of liposomes that is 'perceived' by cells, while the primary particle surface remains buried and inaccessible. As a consequence, liposome–PC is emerging as a key factor regulating the efficient delivery of liposomes at the target site, liposome–cell interactions and the cell response.[22–27] Recent studies[28–30] have clarified that grafting PEG onto the liposome surface reduces, but does not completely prevent PC formation *in vivo*. This unprecedented result has put forth the concept that PEGylated liposomes may not be actually "stealth" in nature (as believed so far). The most relevant implication is that proteins forming a PC of clinically approved PEGylated liposomes could drive particle accumulation at the target site as well as cellular association, internalization and intracellular destiny.[31] Thus, clarifying whether approved PEGylated liposomal drugs are covered by a PC *in vivo* is an unmet urgency with many implications in drug delivery and drug design. In this work, we explored the bio-nano-interactions between human plasma (HP) and Onivyde, a PEGylated liposomal formulation that has recently been approved by the FDA for the treatment of metastatic pancreatic ductal adenocarcinoma (PDAC). Its "conventional" counterpart was synthesized and used as a reference (hereafter referred to as "unPEGylated Onivyde"). Here we show that, following exposure to HP of PDAC patients, Onivyde, although PEGylated, is coated by a rich protein pattern that is similar to that of its unPEGylated counterpart. Our findings indicate that clinically approved PEGylated liposomal drugs might not be "stealth" in nature as generally assumed so far. Notably, PC increased the cellular uptake of Onivyde by pancreas ductal adenocarcinoma cell line (PANC-1) cells. Relevant implications for liposomal drug delivery and drug design are discussed.

Results and discussion

First, we thoroughly characterized the size and zeta-potential of liposomes and liposome–PC complexes. As Table 1 shows, the hydrodynamic radius of Onivyde was larger than that of "unPEGylated Onivyde". Such a size increase is a well-known effect due to the covalent attachment of PEG to the liposome surface.[32] The polydispersity index (PDI) of Onivyde liposomes (0.22 ± 0.02) was quite low,[33] but larger than that of "unPEGylated Onivyde" (0.10 ± 0.02). This observation means that: (i) both liposomal dispersions were quite monodisperse in size; (ii) the size distribution of Onivyde was broader than

Table 1 Hydrodynamic radius (R_H) and zeta-potential of bare liposomes (−HP) and liposome–PC complexes (+HP). Results given are mean ± standard deviation (s.d.) from three independent experiments

	R_H (nm)		Zeta-potential (mV)	
	Onivyde	unPEGylated Onivyde	Onivyde	unPEGylated Onivyde
−HP	59.3 ± 10.4	43.1 ± 3.2	−7.8 ± 2.5	−4.5 ± 0.7
+HP	84.2 ± 19.9	54.9 ± 10.7	−18.7 ± 7.0	−17.0 ± 7.2

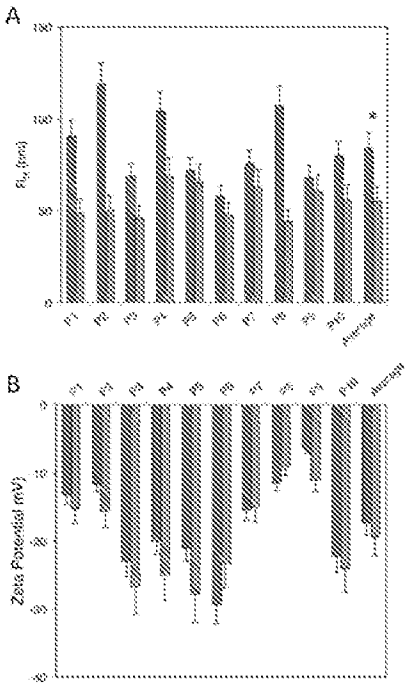

Fig. 2 (A) Hydrodynamic radius of Onivyde (blue hystograms) and "unPEGylated Onivyde" (red hystograms) liposomes following 1-hour incubation with human plasma (HP) of ten pancreatic cancer patients. Collected samples were not pooled and each liposome–HP sample was analyzed separately. Values are mean ± standard deviation (s.d.) from three independent experiments. (B) Zeta-potential of Onivyde (blue hystograms) and "unPEGylated Onivyde" (red hystograms) liposomes after 1-hour exposure to human plasma (HP) collected from pancreatic cancer patients. Values are mean ± s.d. from three independent experiments. The significance of size and zeta-potential measurements has been statistically evaluated by Student's *t*-test and (*$p < 0.05$).

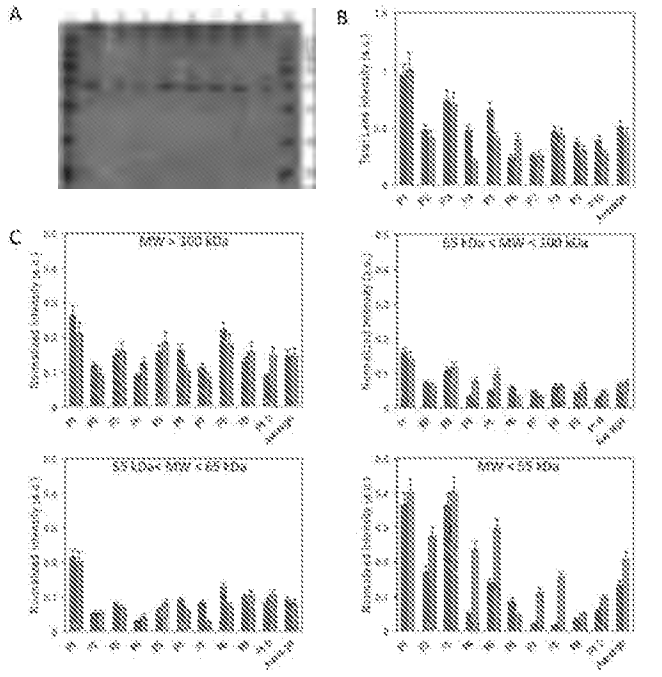

Fig. 3 (A) Representative one-dimensional SDS-PAGE gel of plasma proteins obtained from Onivyde following 1-hour incubation with the plasma of pancreatic ductal adenocarcinoma (PDAC) patients (lane 2: patient "P1"; lanes 3–4: patient "P2"; lanes 5–6: patient "P3"; lanes 7–8: patient "P4"; lane 9: patient "P1"). The molecular weights (kDa) of the proteins on the standard ladder are reported on lanes 1 and 10 (the amount of ladder in lane 1 is double that of lane 10). Red arrows indicate some of the most intense protein bands. (B) Histograms representing the total lane intensity of proteins recovered from Onivyde (blue hystograms) and "unPEGylated Onivyde" (red hystograms) from ten PDAC patients. Each value is the mean ± standard deviation (s.d.) from two independent experiments. (C) Lane intensity results of four molecular weight ranges (*i.e.*, >100 kDa, 65–100 kDa, 55–65 kDa and <55 kDa). No statistically significant differences between Onivyde (blue hystograms) and "unPEGylated Onivyde" (red hystograms) were found (evaluated by Student's *t*-test).

that of its unPEGylated counterpart. On the other hand, both formulations exhibited a weakly negative zeta-potential.

Following 1 h exposure to HP of PDAC patients, the size of Onivyde–PC complexes was larger than that of bare Onivyde (Fig. 2, panel A). According to the literature,[34] the observed increase in size is due to the formation of a protein layer at the liposome surface whose thickness (roughly between 10 and 80 nm) mainly depends on the particle surface chemistry.[34] Likewise, the zeta-potential of Onivyde–PC complexes was markedly lower than that of bare Onivyde (Fig. 2, panel B). Despite its complexity and variability between lipid vesicles,[35] the PC usually gives liposomes a zeta-potential in the range of −10 mV to −20 mV irrespective of the liposome surface chemistry. Such 'normalization' of the zeta-potential is due to the net negative charge carried by most plasma proteins at physiological pH.[17]

Similar effects were found for both the size and zeta-potential of "unPEGylated Onivyde" (Fig. 2, panels A and B). Globally, the results from Fig. 2 suggest that PEGylation could fail in preventing protein adsorption. To corroborate this hypothesis, the PCs of Onivyde and "unPEGylated Onivyde" were analyzed by 1D SDS PAGE. Fig. 3 panel A shows a representative 1D SDS PAGE image of the protein patterns of Onivyde after 1-hour incubation with HP from four PDAC patients. First, we observe that, after incubation with HP, Onivyde was coated by a rich PC. This result is noteworthy because it confirms the conclusions of size and zeta-potential results, *i.e.* grafting PEG onto the liposome surface did not prevent protein binding *in vitro* thus suggesting that Onivyde might not be actually "stealth" *in vivo*. To compare the PCs from liposomes incubated with different plasma samples, a semi-quantitative densitometry analysis of the protein bands was performed.[36,37] To provide insight into the change of the total protein content from various PDAC patients, the total lane intensities of proteins recovered from Onivyde and "unPEGylated Onivyde" (representative SDS-PAGE image reported in Fig. S1 in the ESI†) were calculated (Fig. 3, panel B). Since the total lane intensity is proportional to the protein amount, the densitometry analysis of 1D SDS-PAGE indicates that, for each PDAC patient, the PC of Onivyde is roughly as enriched as that of its unPEGylated counterpart. Fig. 3, panel

B also shows that, for each liposomal formulation, slight differences among individuals existed likely due to personalized plasma alterations. Similar results have been previously obtained by Mahmoudi and co-workers[38,39] who demonstrated that alterations in plasma protein concentrations and structures, as those induced by different diseases and/or disease stage, impact the formation of the PC. We envision that the innovative concept of the "personalized protein corona" (PPC) might have a tremendous impact on cancer for both therapeutic and diagnostic implications.[27,31] Fig. 3, panel C, shows the classification of lane intensities based on four molecular weight ranges (*i.e.*, >100 kDa, 65–100 kDa, 55–65 kDa and <55 kDa). Calculation was made as explained in ref. 40. As is evident, relevant differences in each molecular weight range were found. Next, principal component analysis (PCA) was performed using the four integral areas as input variables (Fig. 4). This method has proven to be very useful for distinguishing PCs of healthy subjects and cancer patients.[40] For both the liposome–PCs, PCA analysis reveals a first principal component (PC1) that mainly takes into account the changes in the protein patterns of the coronas, whereas the second and third principal components (PC2, PC3) are mainly related to the size and zeta-potential, respectively.

In Fig. 4, panel A, we report the whole dataset in the PC1–PC2 plane. Of note is that the PC1 values obtained for both Onivyde and "unPEGylated Onivyde" are indistinguishable and overlapping. In the PC1–PC2 plane, variability among the patients was the dominant factor for the observed variance. Differently, a separation between the two classes due to PC2 is appreciable. This result is clearly evident in the PC2–PC3 plane (Fig. 4, panel B), where Onivyde and "unPEGylated Onivyde" are appreciably separated from each other. In conclusion, PCA indicates that grafting PEG onto the liposome surface has a clear effect on the size and zeta-potential of liposome–PC complexes, while it has a minor, if any, effect on the protein pattern of the coronas.

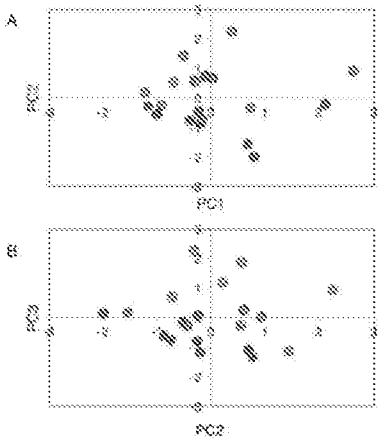

Fig. 4 Principal component analysis. (A) The PC1 value obtained for Onivyde (blue circles) and "unPEGylated Onivyde" (red circles) are indistinguishable and overlapping. The variability among the patients is the dominant factor for the observed variance. Differently, observing the PC2 value a separation between the two formulations is appreciable. (B) In the PC2–PC3 plane a remarkable separation between Onivyde (blue circles) and "unPEGylated Onivyde" (red circles) occurs with the largest part of variability being related to the particle shape and the zeta-potential.

Although many routes of administration have been used for liposomal and lipid-based products,[1] parenteral administration is the predominant one for clinically approved nanomedicines, in particular intravenous administration. Our results are likely to suggest that following parenteral administration clinically approved Onivyde could not actually be "stealth", but get covered by a complex PC. This is noteworthy since: (i) PEGylated liposomes have been always considered "stealth" so far;[4] and (ii) the existence of PC around PEGylated nanoparticles (NPs) has been only marginally addressed so far.[41] In addition, PC could produce relevant variations in circulation half-life, biodistribution, nanotoxicity, targeting ability and intracellular processes (*e.g.* lipid mixing with cellular membranes[42]). A PC enriched with opsonins and coagulation proteins could activate immune cells, and promote clearance of the NPs from the bloodstream. On the other hand, some other descriptors demonstrated a positive impact on NP–cell association.[26,43] For instance, human serum albumin (HSA) and apolipoproteins stimulate prolonged blood circulation and help towards crossing biological barriers. As a major protein found in the PC of many kinds of NPs, A1AT (alpha-1-antitrypsin) is an anti-inflammation protein serving as an immune system regulator of NPs that affects lymphocyte proliferation and cytotoxicity and mediates monocyte and neutrophil functions. Among other corona proteins, Vitronectin promotes efficient internalization in cancer cells over-expressing $\alpha_v\beta_3$ integrins (*i.e.* the Vitronectin receptor) which are overexpressed on many solid tumors and in the tumor neovasculature.[44] As we demonstrated the formation of a rich PC on both Onivyde and "unPEGylated Onivyde", the next step was investigating whether the PC could affect the cellular uptake of Onivyde in PANC-1 cells. This seemed to be a fundamental step towards providing new insights into the role of PC in the biological outcome of liposomal drugs. Here we underline that the relationship between the PC of an approved liposomal drug and its specificity for disease[14] has not been explored so far. If further demonstrated, this could represent a truly paradigm shift in the field of drug delivery.[26,45,46] Bare Onivyde (*i.e.* in the absence of PC) showed very low uptake (uptake ≈5%) by PANC-1 cells (Fig. 5, panels A and E). Anyway, pre-incubation with HP dramatically boosted cell uptake (cellular uptake ≈87%) (Fig. 5, panels C and E). Of note is that "unPEGylated Onivyde" exhibited similar behavior both in the absence (Fig. 5, panels B and E) and in the presence (Fig. 5, panels D and E) of PC. In detail, in the absence of PC, the cellular uptake of "unPEGylated Onivyde" was much larger (cellular uptake ≈33%) than that of Onivyde (cellular uptake ≈5%). This is a well known effect, known as the "PEG dilemma". While PEGylation increases the stealth properties of liposomes on one hand, on the other hand it could lead to a strong inhibition of cellular uptake and less efficient interaction and

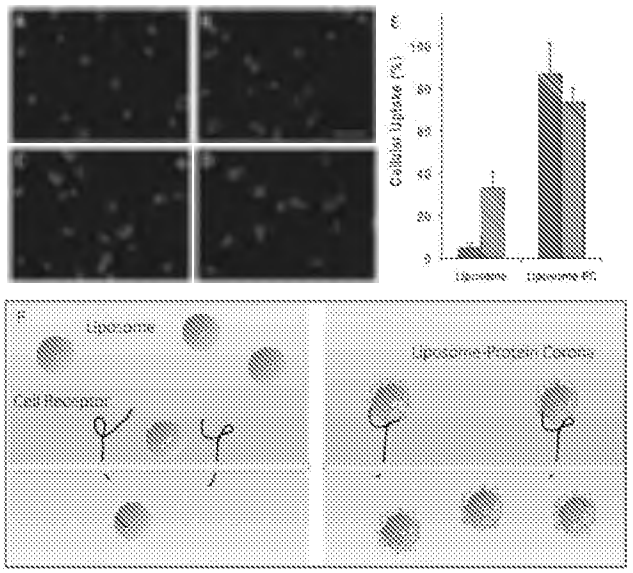

Fig. 5 Cellular uptake of bare Onivyde (A) and "unPEGylated Onivyde" (B) by PANC-1 cells. Following 1 h exposure to HP, Onivyde (C) and "unPEGylated Onivyde" (D) exhibit a marked increase in the mean fluoresce intensity per cell. (E) Cellular uptake (%) of Onivyde (blue hystograms) and "unPEGylated Onivyde" (red hystograms) by PANC-1 cells both in the absence (*i.e.* bare liposomes) and in the presence of a protein corona (*i.e.* liposome–PC). (F) Cartoon describing the cellular uptake of bare Onivyde liposomes and liposome–PC complexes. Naked liposomes are poorly internalized likely by a non-specific mechanism, while cellular uptake largely increases when a biomolecule corona adsorbs on the surface. Efficient internalization of liposome–PC complexes is likely due to some corona proteins that could have functional motifs presented appropriately to activate specific molecular recognition with receptors of PANC-1 cells. Imaging has been performed with a 4× objective. Cell contours have been traced from the bright field channel. Scale bar is 40 μm.

binding with protein targets, significantly lessening the ability of the delivery system. According to this interpretation, PC was found to increase the cellular uptake of "unPEGylated Onivyde" by PANC-1 cells (cellular uptake ≈73.3%), but by a factor (≈2.5) much lower than that observed in the case of Onivyde–PC complexes (≈18). In summary, cell imaging experiments showed that PC enhanced the cellular uptake of liposomes by PANC-1 cells. In principle, proteins bound to the liposome surface could change the colloidal stability of NPs that, in turn, could affect their cellular uptake by nonspecific mechanisms (*e.g.* size-dependent uptake mechanisms[47]). To explore the particle colloidal stability, both liposomes and liposome–PCs were incubated in cell-culture medium for 4-hours. During this time window, the occurrence of aggregation and/or sedimentation was investigated by monitoring the fluctuations in the sample optical density (OD) at 600 nm. As Fig. S2 in the ESI† clearly shows, both liposomes and liposome–PCs were stable, *i.e.* no evidence of particle aggregation or sedimentation was detected. In summary, the results of Fig. 5 indicate that PC strongly promotes association and cellular uptake by PANC-1 cells in a specific manner. To the best of our knowledge, this is the first report showing the active role of PC in boosting the cellular internalization of Onivyde within pancreatic cancer cells. This is most likely due to the molecular interactions between some "corona proteins" and cell receptors of PANC-1 cells. According to the literature,[48,49] some corona proteins could have functional motifs presented appropriately to activate specific molecular recognition with cell receptors of PANC-1 cells (Fig. 5, panel F). Considering the increase in the liposome ability to interact with PANC-1 cells as caused by the PC, we are prompted to conclude that the role of conjugation of PEG to therapeutics as an effective approach to increase the serum half-life should be reconsidered. Since liposomal drugs mainly differ in lipid composition, we suggest that surface chemistry might be definitely more important than PEGylation in controlling the bio-nano-interactions between lipid particles and plasma components. Whatever the mechanism of PC formation, the role of PC in lipid-mediated drug delivery must be properly evaluated. Latest research has focused on understanding the correlation between the PC composition of various nanomaterials and their physiological response[24,26,50–52] thus confirming that PC shall be a 'game-changer' for the clinical translation of nanoparticles.

Certainly, most investigations have shown that the PC of both organic and inorganic NPs could affect their biodistribution, cellular uptake and even intracellular trafficking. In a recent paper, Corbo *et al.*[53] demonstrated that even biomimetic NPs (referred to as "leukosomes") adsorb a PC and that this corona affects their biodistribution and interaction with cells. To date, liposomes are supposed to accumulate in regions of enhanced vascular permeability in humans. This effect is merely passive and was termed the enhanced permeability and retention (EPR) effect by the Maeda laboratory.[54,55] If accumulation of liposomes in the tumor region is likely due to the EPR effect, how to explain the indication of liposomal drugs for disease? In principle, the correlation between each liposomal formulation and its indication could be dependent on the biological identity of liposomes, *i.e.* on their PC that forms *in vivo*. The groundbreaking idea is that following *in vivo* administration, each liposomal formulation, being either "conventional" or PEGylated, will acquire a PC made of plasma components that are naturally targeted to the desired cells. At the site of action, the interaction between the exposed epitopes of "corona proteins" and the cell receptors[48] of target cells could lead to specific biological recognition leading to efficient drug internalization and optimized biological outcome. Thanks to the recent findings,[56,57] the *in situ* state of nanoparticles can now be looked at in detail by the combined use of antibody-labeled NPs, differential centrifugal sedimentation, and various imaging methods. This novel approach allows identifying the spatial location of corona proteins, their functional motifs and their binding sites. This methodological advancement will contribute to explore the interactions between multiple corona proteins and distinct cell receptors with a degree of accuracy never achieved before. For instance, it would of great help to demonstrate whether the "multivalent effect" (*i.e.* the multivalent binding between multiple ligands and multiple receptors, which frequently occurs

in many biological systems) could play a key role in controlling the bio-nano-interactions between NPs and cells[26] with a dramatic impact on clinical application.[31,46] Furthermore, we underline that the NP-PC is typically isolated from the physiological environment and characterized in different media such as water or phosphate saline buffer (PBS). In principle, this procedure could modify the BC. Thus, the possibility to characterize the BC *in situ*[57] could improve our understanding of the field.

Materials and methods

Human plasma collection

We collected blood samples from ten patients with consecutive histologically proven pancreatic adenocarcinoma that met the inclusion criteria reported in Table S1 in the ESI,† while Table S2 in the ESI† shows clinical characteristics of our series. Clinical and pathological stages are reported according to the seventh edition of the TNM staging system.[58] The Ethical Committee of University "Campus Bio-Medico di Roma" approved the study.

Liposomes preparation

1,2-Distearoyl-*sn-glycero*-3-phosphocholine (DSPC) and methoxy-terminated polyethylene glycol (MW 2000)-distearoylphosphatidyl ethanolamine (MPEG-2000-DSPE) were purchased from Avanti Polar Lipids (Alabaster, AL). Cholesterol (Chol) was purchased from Sigma-Aldrich (Milan, Italy). Texas Red® 1,2-dihexadecanoyl-*sn*-glycero-3-phosphoethanolamine, triethylammonium salt (TX-DHPE) was purchased from Invitrogen. Onyvide-like liposomes were synthesized at a molar ratio of DSPC : Chol : MPEG-2000-DSPE of 215 : 143 : 1 according to the standard protocols.[59] For cellular uptake experiments, liposomes were prepared using TX-DHPE at a molar ratio of DSPC : Chol : MPEG-2000-DSPE–TX-DHPE of 215 : 143 : 1 : 1. The same procedure was followed to synthesize "unPEGylated Onivyde" at a molar ratio of DSPC : Chol : MPEG-2000-DSPE of 215 : 143 : 0 and fluorescently labeled "unPEGylated Onivyde" at a molar ratio of DSPC : Chol : MPEG-2000-DSPE–TX-DHPE of 215 : 143 : 0 : 1.

Lipid films were hydrated with phosphate saline buffer PBS (10 mM, pH = 7.4) to a final lipid concentration of 1 mg mL^{-1}. The obtained liposome suspension was extruded 20 times through a 0.05 μm polycarbonate carbonate filter with the Avanti Mini-Extruder (Avanti Polar Lipids, Alabaster, AL).

Liposome–protein complexes

Liposome–protein complexes were prepared by incubating liposomes with HP (1 : 1 v/v) at 37 °C for 1 hour. Experimental conditions (*i.e.* plasma concentration, temperature and incubation time) were chosen according to previous investigations.[18,22,60,61] After incubation, liposome–protein complexes were isolated by centrifugation for 15 min at 14 000 rpm. Then pellets were washed three times with PBS to remove unbound proteins obtaining the "hard corona".

1D-SDS-PAGE experiments

Liposome–PC complexes were re-suspended in 20 μl of Laemmli loading buffer 1× (10 μl βME per 1 ml Laemmli loading buffer) and boiled for 5 min at 100 °C. Identical volumes (10 μl) of each sample were loaded on a gradient polyacrylamide gel (4–20% Criterion TGX precast gels, Bio-Rad) and run at 100 V for about 150 minutes. Gels were washed in double-distilled water (ddH_2O) and fixed overnight for 12 hours in a de-staining solution (MeOH 50% in ddH_2O) with gentle agitation at room temperature, with at least one solution change. In order to determine the differences in corona composition, we stained the proteins with highly sensitive silver-ammonia solution for 30 minutes. Then, gels were rinsed 3 times in ddH_2O, 40 seconds each rinse, then incubated with acidic developer solution from 3 to 5 minutes. Once all the protein bands started to clearly appear, the developer solution was removed and the stop solution (acetic acid 10%, methanol 45% in ddH2O) was added. Gel images were processed by means of customized software.

Dynamic light scattering and zeta-potential measurements

Size and zeta-potential measurements were carried out using a Zetasizer Nano ZS (Malvern, U.K.) at 25 °C. Liposomes and liposome/PC complexes were diluted 1 : 100 with 10 mM PBS. The results are given as mean ± standard deviation of five independent replicates.

Statistical analysis

Principal component analysis (PCA) is a method to project multidimensional data on a reduced set of orthogonal axes (principal component scores or eigenfunctions) with minimal loss of information.[62] The new eigenfunctions are linear combinations of the original data orthogonal by construction, each representing an independent aspect of the dataset. Original "*N*" variables are thus linearly transformed by the PCA in a set of variables (PC1, PC2..., PC*N*) ordered by the decreasing amount of the explained variance (information) of the dataset. To shed light on the main differences between Onivyde and "unPEGylated Onivyde" following exposure to HP of PDAC patients, we compared the values of the relative PC1 and PC2. PCs were obtained by 6 original variables: the integral areas of the average lane intensity profiles calculated for (i) MW < 55 kDa; (ii) 55 < MW < 65; (iii) 65 < MW < 100; (iv) MW > 100 kDa plus the hydrodynamic radius (R_H) and zeta-potential of liposome–PC complexes.

Cellular uptake

Pancreas ductal adenocarcinoma (PANC-1) cells (ATCC® CRL-1469™) were cultured in Dulbecco's modified Eagle's medium (DMEM) with Glutamax-I (Invitrogen, Carlsbad, CA, USA) supplemented with 1% penicillin–streptomycin (Invitrogen) and 10% fetal bovine serum (Invitrogen) at 37 °C and under a 5% CO_2 atmosphere, splitting the cells every 2–4 days to maintain the monolayer coverage. Onivyde and "unPEGylated Onivyde" were suspended in DMEM and used

for cell treatment. After 3 hours, cells were washed twice with PBS to eliminate unbound liposomes and fixed with 4% PFA for 10 min at room temperature for imaging as reported previously.[63] Imaging has been performed by using Cytation 3 (Biotek, USA) with a 4× objective, exciting with a led source at 580 nm and recording emission at 610 nm. After background subtraction, cellular uptake was quantified by ImageJ.[64] Brightfield images have been used to define the cell contour.

Conclusions

In this work, we explored the bio-nano-interactions between Onivyde, a PEGylated liposomal drug approved by the FDA, and HP. Although PEGylated, Onivyde was found to be not "stealth" in HP, but covered by a rich PC. Using an unPEGylated variant of Onivyde as a reference, we could demonstrate that surface chemistry is definitely more important than PEGylation in controlling the bio-nano-interactions between Onivyde and plasma components. Of note is that the PC was found to boost the cellular uptake in PANC-1 cells thus suggesting its prominent role in the indication of Onivyde for pancreatic cancer. The picture is still evolving, but this subject has an important general implication: if we understand which "corona proteins" dictate the cellular association of liposomes, we could manipulate the lipid composition and, in turn, liposomes' targeting ability. It is a simple idea, yet the high complexity of the PC makes its corroboration challenging. In this regard, characterizing the orientation of corona proteins[48,49,56] will be useful in developing liposomes with targeted protein adsorption and will provide the intriguing opportunity to manipulate the corona composition by liposome design.[35] Another relevant step towards clinical application of liposome formulations is to understand whether PC could affect the liposome interaction with intracellular barriers.[42,65,66] This aspect is being currently investigated in our laboratory.

Acknowledgements

The Italian Minister of Health ("Progetto Giovani Ricercatori 2011–2012", Grant No. GR-2011-02350094) is gratefully acknowledged.

Notes and references

1 T. M. Allen and P. R. Cullis, *Adv. Drug Delivery Rev.*, 2013, **65**, 36–48.
2 W. Gao, C.-M. J. Hu, R. H. Fang and L. Zhang, *J. Mater. Chem. B*, 2013, **1**, 6569–6585.
3 S. M. Moghimi, A. C. Hunter and J. C. Murray, *Pharmacol. Rev.*, 2001, **53**, 283–318.
4 M. L. Immordino, F. Dosio and L. Cattel, *Int. J. Nanomed.*, 2006, **1**, 297.
5 R. M. Abra, M. Bosworth and C. Hunt, *Res. Commun. Chem. Pathol. Pharmacol.*, 1988, **29**, 349–360.
6 K. J. Hwang, M. M. Padki, D. D. Chow, H. E. Essien, J. Lai and P. L. Beaumier, *Biochim. Biophys. Acta, Biomembr.*, 1987, **901**, 88–96.
7 A. Gabizon and D. Papahadjopoulos, *Proc. Natl. Acad. Sci. U. S. A.*, 1988, **85**, 6949–6953.
8 A. A. Gabizon, Y. Barenholz and M. Bialer, *Pharm. Res.*, 1993, **10**, 703–708.
9 A. Gabizon, R. Catane, B. Uziely, B. Kaufman, T. Safra, R. Cohen, F. Martin, A. Huang and Y. Barenholz, *Cancer Res.*, 1994, **54**, 987–992.
10 Y. C. Barenholz, *J. Controlled Release*, 2012, **160**, 117–134.
11 G. Pasut and F. M. Veronese, *J. Controlled Release*, 2012, **161**, 461–472.
12 J. J. Verhoef and T. J. Anchordoquy, *Drug Delivery Transl. Res.*, 2013, **3**, 499–503.
13 V. J. Venditto and F. C. Szoka Jr., *Adv. Drug Delivery Rev.*, 2013, **65**, 80–88.
14 G. Caracciolo, *Nanomedicine*, 2015, **11**, 543–557.
15 M. Mahmoudi, *Int. J. Biochem. Cell Biol.*, 2016, **75**, 141–142.
16 M. P. Monopoli, C. Åberg, A. Salvati and K. A. Dawson, *Nat. Nanotechnol.*, 2012, **7**, 779–786.
17 C. D. Walkey and W. C. W. Chan, *Chem. Soc. Rev.*, 2012, **41**, 2780–2799.
18 S. Tenzer, D. Docter, J. Kuharev, A. Musyanovych, V. Fetz, R. Hecht, F. Schlenk, D. Fischer, K. Kiouptsi and C. Reinhardt, *Nat. Nanotechnol.*, 2013, **8**, 772–781.
19 D. Docter, D. Westmeier, M. Markiewicz, S. Stolte, S. Knauer and R. Stauber, *Chem. Soc. Rev.*, 2015, **44**, 6094–6121.
20 M. Mahmoudi, N. Bertrand, H. Zope and O. C. Farokhzad, *Nano Today*, 2016, **11**, 817–832.
21 P. Del Pino, B. Pelaz, Q. Zhang, P. Maffre, G. U. Nienhaus and W. J. Parak, *Mater. Horiz.*, 2014, **1**, 301–313.
22 A. L. Barrán-Berdón, D. Pozzi, G. Caracciolo, A. L. Capriotti, G. Caruso, C. Cavaliere, A. Riccioli, S. Palchetti and A. Laganà, *Langmuir*, 2013, **29**, 6485–6494.
23 G. Caracciolo, S. Palchetti, V. Colapicchioni, L. Digiacomo, D. Pozzi, A. L. Capriotti, G. La Barbera and A. Laganà, *Langmuir*, 2015, **31**, 10764–10773.
24 A. Bigdeli, S. Palchetti, D. Pozzi, M. R. Hormozi-Nezhad, F. Baldelli Bombelli, G. Caracciolo and M. Mahmoudi, *ACS Nano*, 2016, **10**, 3723–3737.
25 S. Palchetti, V. Colapicchioni, L. Digiacomo, G. Caracciolo, D. Pozzi, A. L. Capriotti, G. La Barbera and A. Laganà, *Biochim. Biophys. Acta, Biomembr.*, 2016, **1858**, 189–196.
26 S. Palchetti, L. Digiacomo, D. Pozzi, G. Peruzzi, E. Micarelli, M. Mahmoudi and G. Caracciolo, *Nanoscale*, 2016, **8**, 12755–12763.
27 S. Palchetti, D. Pozzi, M. Mahmoudi and G. Caracciolo, *J. Mater. Chem. B*, 2016, **4**, 4376–4381.
28 D. Pozzi, V. Colapicchioni, G. Caracciolo, S. Piovesana, A. L. Capriotti, S. Palchetti, S. De Grossi, A. Riccioli, H. Amenitsch and A. Laganà, *Nanoscale*, 2014, **6**, 2782–2792.

29 M. Hadjidemetriou, Z. Al-Ahmady, M. Mazza, R. F. Collins, K. Dawson and K. Kostarelos, *ACS Nano*, 2015, **9**, 8142–8156.
30 M. Hadjidemetriou, Z. Al-Ahmady and K. Kostarelos, *Nanoscale*, 2016, **8**, 6948–6957.
31 C. Corbo, R. Molinaro, M. Tabatabaei, O. C. Farokhzad and M. Mahmoudi, *Biomater. Sci.*, 2017, **5**, 378–387.
32 A. R. Nicholas, M. J. Scott, N. I. Kennedy and M. N. Jones, *Biochim. Biophys. Acta, Biomembr.*, 2000, **1463**, 167–178.
33 M. Gaumet, A. Vargas, R. Gurny and F. Delie, *Eur. J. Pharm. Biopharm.*, 2008, **69**, 1–9.
34 G. Caracciolo, *Nanomedicine*, 2015, **11**, 543–557.
35 G. Caracciolo, D. Pozzi, A. L. Capriotti, C. Cavaliere, S. Piovesana, H. Amenitsch and A. Laganà, *RSC Adv.*, 2015, **5**, 5967–5975.
36 G. Caracciolo, D. Pozzi, A. L. Capriotti, C. Cavaliere, P. Foglia, H. Amenitsch and A. Laganà, *Langmuir*, 2011, **27**, 15048–15053.
37 M. P. Monopoli, D. Walczyk, A. Campbell, G. Elia, I. Lynch, F. Baldelli Bombelli and K. A. Dawson, *J. Am. Chem. Soc.*, 2011, **133**, 2525–2534.
38 M. J. Hajipour, S. Laurent, A. Aghaie, F. Rezaee and M. Mahmoudi, *Biomater. Sci.*, 2014, **2**, 1210–1221.
39 M. J. Hajipour, J. Raheb, O. Akhavan, S. Arjmand, O. Mashinchian, M. Rahman, M. Abdolahad, V. Serpooshan, S. Laurent and M. Mahmoudi, *Nanoscale*, 2015, **7**, 8978–8994.
40 D. Caputo, M. Papi, R. Coppola, S. Palchetti, L. Digiacomo, G. Caracciolo and D. Pozzi, *Nanoscale*, 2017, **9**, 349–354.
41 D. R. Hristov, L. Rocks, P. M. Kelly, S. S. Thomas, A. S. Pitek, P. Verderio, E. Mahon and K. A. Dawson, *Sci. Rep.*, 2015, **5**, 17040.
42 G. Caracciolo, D. Pozzi, R. Caminiti and H. Amenitsch, *Appl. Phys. Lett.*, 2005, **87**, 1–3.
43 R. Liu, W. Jiang, C. D. Walkey, W. C. Chan and Y. Cohen, *Nanoscale*, 2015, **7**, 9664–9675.
44 G. Caracciolo, F. Cardarelli, D. Pozzi, F. Salomone, G. Maccari, G. Bardi, A. L. Capriotti, C. Cavaliere, M. Papi and A. Laganà, *ACS Appl. Mater. Interfaces*, 2013, **5**, 13171–13179.
45 M. Mahmoudi, S. Sheibani, A. S. Milani, F. Rezaee, M. Gauberti, R. Dinarvand and H. Vali, *Nanomedicine*, 2015, **10**, 215–226.
46 G. Caracciolo, O. C. Farokhzad and M. Mahmoudi, *Trends Biotechnol.*, 2017, **35**, 257–264.
47 G. Caracciolo, L. Callipo, S. C. De Sanctis, C. Cavaliere, D. Pozzi and A. Laganà, *Biochim. Biophys. Acta, Biomembr.*, 2010, **1798**, 536–543.
48 P. M. Kelly, C. Åberg, E. Polo, A. O'Connell, J. Cookman, J. Fallon, Ž. Krpetić and K. A. Dawson, *Nat. Nanotechnol.*, 2015, **10**, 472–479.
49 L. M. Herda, D. R. Hristov, M. C. Lo Giudice, E. Polo and K. A. Dawson, *J. Am. Chem. Soc.*, 2017, **139**, 111–114.
50 G. Caracciolo, O. C. Farokhzad and M. Mahmoudi, *Trends Biotechnol.*, 2016, **35**, 257–264.
51 C. Corbo, R. Molinaro, A. Parodi, N. E. Toledano Furman, F. Salvatore and E. Tasciotti, *Nanomedicine*, 2016, **11**, 81–100.
52 C. Corbo, R. Molinaro, F. Taraballi, N. E. Toledano Furman, M. B. Sherman, A. Parodi, F. Salvatore and E. Tasciotti, *Int. J. Nanomed.*, 2016, **11**, 3049–3063.
53 C. Corbo, R. Molinaro, F. Taraballi, N. E. Toledano Furman, K. A. Hartman, M. B. Sherman, E. De Rosa, D. K. Kirui, F. Salvatore and E. Tasciotti, *ACS Nano*, 2017, **11**, 3262–3273.
54 J. Fang, H. Nakamura and H. Maeda, *Adv. Drug Delivery Rev.*, 2011, **63**, 136–151.
55 H. Maeda, *Adv. Drug Delivery Rev.*, 2015, **91**, 3–6.
56 M. C. L. Giudice, F. Meder, E. Polo, S. S. Thomas, K. Ainahdi, S. Lara and K. A. Dawson, *Nanoscale*, 2016, **8**, 16969–16975.
57 M. C. L. Giudice, L. M. Herda, E. Polo and K. A. Dawson, *Nat. Commun.*, 2016, **7**, 13475.
58 J. R. Egner, *J. Am. Med. Assoc.*, 2010, **304**, 1726–1727.
59 C. Marchini, M. Montani, A. Amici, H. Amenitsch, C. Marianecci, D. Pozzi and G. Caracciolo, *Langmuir*, 2009, **25**, 3013–3021.
60 G. Caracciolo, D. Pozzi, A. L. Capriotti, C. Cavaliere, P. Foglia, H. Amenitsch and A. Laganà, *Langmuir*, 2011, **27**, 15048–15053.
61 M. Mahmoudi, A. M. Abdelmonem, S. Behzadi, J. H. Clement, S. Dutz, M. R. Ejtehadi, R. Hartmann, K. Kantner, U. Linne and P. Maffre, *ACS Nano*, 2013, **7**, 6555–6562.
62 H. Abdi and L. J. Williams, *Wiley Interdiscip. Rev.: Comput. Stat.*, 2010, **2**, 433–459.
63 N. Di Simone, M. De Spirito, F. Di Nicuolo, C. Tersigni, R. Castellani, M. Silano, G. Mauiucci, M. Papi, R. Marana and G. Scambia, *Biol. Reprod.*, 2013, **89**, 88.
64 J. Schindelin, I. Arganda-Carreras, E. Frise, V. Kaynig, M. Longair, T. Pietzsch, S. Preibisch, C. Rueden, S. Saalfeld and B. Schmid, *Nat. Methods*, 2012, **9**, 676–682.
65 G. Caracciolo and H. Amenitsch, *Eur. Biophys. J.*, 2012, **41**, 815–829.
66 Z. u. Rehman, D. Hoekstra and I. S. Zuhorn, *ACS Nano*, 2013, **7**, 3767–3777.

ELSEVIER

Cancer Letters 118 (1997) 153–160

CANCER LETTERS

Anti-HER2 immunoliposomes for targeted therapy of human tumors

John W. Park[a,*], Keelung Hong[b], Dmitri B. Kirpotin[b], Olivier Meyer[b], Demetrios Papahadjopoulos[b], Christopher C. Benz[a]

[a]*Department of Medicine, Division of Hematology-Oncology, University of California, San Francisco, CA 94143, USA*
[b]*Department of Cellular and Molecular Pharmacology, University of California, San Francisco, CA 94143, USA*

Abstract

Anti-HER2 immunoliposomes (ILs) have been constructed by conjugation of Fab′ fragments of recombinant humanized monoclonal antibody rhuMAbHER2 to small sterically stabilized unilamellar liposomes, to create a targeted drug delivery vehicle for the treatment of HER2 (c-*erb*B-2, *neu*)-overexpressing cancers. Parameters affecting in vitro binding and internalization of ILs include liposome composition, Fab′ linkage site and Fab′ density. Anti-HER2 ILs have been constructed to optimize intracellular drug delivery. Doxorubicin (dox)-loaded ILs are highly stable and exhibit prolonged circulation in rats. In nude mice bearing HER2-overexpressing tumor xenografts, anti-HER2 ILs administered i.v. resulted in efficient tumor localization, with penetration of the ILs throughout the tumor mass and accumulation within tumor cells. In contrast, non-targeted liposomes resulted in extracellular tumor accumulation only. In multiple HER2-overexpressing human breast tumor xenograft models, treatment with dox-loaded anti-HER2 ILs produces significantly increased antitumor cytotoxicity as compared to free dox or dox-loaded non-targeted liposomes and significantly less systemic toxicity than free dox. To explore further the intracellular delivery advantages of ILs, anti-HER2 ILs bearing cationic lipids are being developed for nucleic acid delivery. These cationic immunoliposomes mediate efficient and specific transfection of target cells with reporter genes, as well as intracellular delivery of labeled oligonucleotides. Thus, anti-HER2 ILs represent an efficient and feasible strategy to achieve targeted intracellular delivery of therapeutic agents. © 1997 Elsevier Science Ireland Ltd.

Keywords: HER2; *neu*; c-*erb*B-2; Liposomes; Immunoliposomes; Gene therapy

1. Introduction

Anti-HER2 immunoliposomes represent a promising strategy to achieve targeted drug delivery for the treatment of HER2-overexpressing cancers. Advances in immunoliposome design have been facilitated by independent progress in the areas of antibody-based therapeutics and liposome research, which can now be exploited to yield tumor-targeted drug delivery [1].

The HER2 receptor is a logical focus for the development of targeted cancer therapies. The *HER2* (c-*erb*B-2, *neu*) protooncogene and its encoded $p185^{HER2}$ (ErbB-2) receptor tyrosine kinase play an important role in the pathogenesis of breast and other cancers (for review, see Ref. [2]). HER2 is highly and stably overexpressed in a significant pro-

* Corresponding author. 505 Parnassus Ave., Box 1270, San Francisco, CA 94143-1270, USA. Tel.: +1 415 4764149; fax: +1 415 4766998;
e-mail: benz@itsa.ucsf.edu or johnpark@quickmail.ucsf.edu

0304-3835/97/$17.00
PII S0304-3835(97)00326-1

portion of these cancers, but is expressed at much lower levels, if at all, in normal tissues. As a cell surface receptor it is readily accessible to antibody-based therapeutics and monoclonal antibodies directed against HER2 can inhibit tumor growth by affecting HER2 signal transduction. For example, muMAb4D5 and its humanized derivative, rhuMAbHER2, inhibit the growth of HER2-overexpressing breast cancer cells [3] and enhance the efficacy of certain chemotherapy drugs [4]. In phase II clinical trials, treatment with rhuMAbHER2 alone [5] or in combination with cisplatin chemotherapy [6] was associated with encouraging antitumor activity against advanced breast cancer. rhuMAbHER2 is currently being evaluated in phase III clinical trials for the treatment of advanced breast cancer in conjunction with first-line chemotherapy.

Improvements in liposomal delivery of chemotherapy include 'stealth' or 'sterically stabilized' liposomes, which are more resistant to reticulo-endothelial system (RES) clearance than so-called 'conventional' liposomes. These improvements produced substantially prolonged drug circulation with enhanced tumor accumulation [7–9]. The coupling of anti-HER2 antibody fragments to sterically stabilized liposomes represents a more recent design modification to further increase the therapeutic index of an encapsulated drug via selective delivery to HER2-overexpressing cancer cells. The receptor-mediated internalization property of this targeted delivery vehicle also affords an opportunity to achieve tumor-specific uptake of novel therapeutics such as genes and oligonucleotides.

2. Methods and results

2.1. Construction of anti-HER2 immunoliposomes (ILs)

Anti-HER2 immunoliposomes (ILs) incorporate multiple design elements to optimize intracellular delivery of encapsulated agent to tumor cells (Table 1). These include (1) rhuMAbHER2 Fab′ for reduced clearance and immunogenicity and to provide internalization and antipro-liferative activities, (2) PEG-Fab′ linkage (see below) to facilitate immunoliposome binding and internalization, (3) sterically stabilized immunoliposomes for prolongation of circulation and selective tumor extravasation and (4) encapsulated therapeutic agents (e.g. doxorubicin, nucleic acids) for enhanced therapeutic index via targeted intracellular delivery.

To test these designs we constructed multiple versions of anti-HER2 immunoliposomes containing covalently linked rhuMAbHER2 Fab′ (Genentech) and poly(ethylene glycol) (PEG)-phosphatidylethanolamine (PE) in varying proportions (0–12 mol% of total phospholipid). ILs were prepared by conjugation of conventional (phosphatidylcholine + cholesterol;

Table 1

Components of anti-HER2 immunoliposome design

Component	Rationale
Antibody: rhuMAbHER2-Fab′	Humanized to reduce immunogenicity. Fab′ to remove Fc region for reduced clearance. Efficient internalization for intracellular delivery. Expressed as recombinant protein in *E. coli* at high efficiency
Linkage: PEG-Fab′	Fab′ covalently attached to PEG. Specific, single sites on Fab′ and liposome. Avoids steric hindrance by PEG of binding and internalization. Highly efficient conjugation procedure
Liposome: sterically stabilized	Stable as intact constructs in vivo. Long circulation. Selective extravasation in tumors. Small diameter to improve tumor penetration
Agent:	
Doxorubicin	Efficient and high capacity encapsulation procedure. Small molecule drug to diffuse throughout tumor once released (bystander cytotoxicity). Cytotoxicity enhanced by antiproliferative activity of anti-HER2 antibody
Nucleic acid	Efficient and high capacity complexation with cationic lipids. Exploits intracellular delivery mechanism

PC/Chol) or sterically stabilized (PC/Chol/PEG-PE) small unilamellar liposomes with rhuMAbHER2-Fab′. Initially, Fab′ was conjugated to maleimido-phosphatidylethanolamine (M-PE), resulting in Fab′ directly linked to the liposome surface and hence alongside or in parallel with PEG (if present) [10]. Recently, we have also prepared ILs with Fab′ conjugated to maleimide-terminated PEG-PE (MMC-PEG-DSPE or MP-PEG-DSPE) [11], resulting in Fab′ linked to the distal end of PEG chains (Fig. 1, left). Both procedures were highly efficient, typically yielding 50–100 Fab′ fragments per liposome particle.

2.2. Binding and internalization of anti-HER2 immunoliposomes

Quantitative studies of immunoliposome binding, internalization and intracellular drug delivery were performed with ILs containing a pH-sensitive fluorescent probe (1-hydroxypyrene-3,6,8-trisulfonic acid (HPTS/pyranine)). These studies demonstrated a rapid uptake of ILs by SK-BR-3 cells into a neutral environment with subsequent accumulation in an acidic intracellular compartment, consistent with surface binding followed by receptor-mediated endocytosis [11]. The total uptake of ILs in SK-BR-3 cells reached 23 000 ILs/cell, while the total uptake of non-targeted control liposomes was essentially undetectable. In addition, the total uptake of ILs in non-HER2-overexpressing MCF-7 cells was 700-fold lower than in SK-BR-3 cells. With liposomes-Fab′-linked ILs, but not with PEG-Fab′-linked ILs, high PEG content was associated with reduced binding affinity and endocytosis. Binding and endocytosis also depended on the quantity of conjugated Fab′, reaching a plateau at ~40 Fab′/IL for binding and ~10 Fab′/IL for internalization.

The intracellular disposition of ILs containing colloidal gold particles was studied by electron microscopy [10]. SK-BR-3 cells treated with anti-HER2 ILs (0 mol% PEG) showed gold-loaded ILs at the cell surface and intracellularly in coated pits, coated vesicles, endosomes, multivesicular bodies and lysosomes, consistent with internalization occurring via the coated pit pathway. In addition, gold particles were noted free within the cytoplasm and not associated with a membrane-bound organelle, indicating that delivery outside the endolysomal pathway had also occurred.

2.3. Antiproliferative effects of anti-HER2 immunoliposomes

Although rhuMAbHER2 inhibits the growth of HER2-overexpressing breast cancer cells in monolayer culture, monovalent Fab and Fab′ fragments of rhuMAbHER2 are much less effective at inhibiting growth [12]. However, we have observed that empty

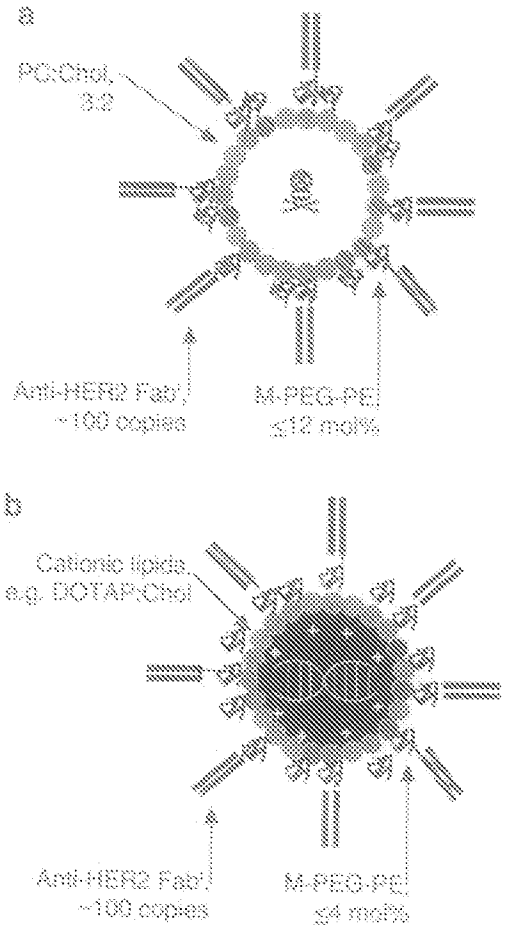

Fig. 1. Schematic representation of anti-HER2 immunoliposomes (ILs), showing rhuMAbHER2 Fab′ linked covalently to the termini of derivatized PEG molecules, which also provide steric stabilization. (a) Neutral immunoliposomes loaded with doxorubicin; (b) Nationic immunoliposomes complexed with nucleic acid. M-PEG-PE represents maleimide-terminated PEG-PE, either *N*-maleimidomethylcyclohexylcarboxamido-PEG-DSPE (MMC-PEG-DSPE) or *N*-maleimidopropionylcarboxamido-PEG-DSPE (MP-PEG-DSPE).

anti-HER2 ILs inhibit growth of SK-BR-3 cells in a dose-dependent manner, indicating that liposomal anchoring of rhuMAbHER2-Fab′ fragments restores antiproliferative activity that is comparable to intact rhuMAbHER2 [10]. This intrinsic antiproliferative activity of empty anti-HER2 ILs suggests that such ILs may provide an additional antitumor effect beyond tumor-specific delivery of an encapsulated drug.

2.4. Pharmacokinetics of anti-HER2 immunoliposomes

Pharmacokinetic (PK) studies of doxorubicin (dox)-loaded anti-HER2 immunoliposomes following single i.v. injection were performed in normal adult rats. Plasma dox levels following injection with either ILs or control (no Fab′) sterically stabilized liposomes were similar and indicated biexponential PK with terminal plasma half-lives of greater than 10 h and mean residence times of 16–24 h [13]. In comparison, dox levels following injection of free dox at the same dose (800 μg) were undetectable at 5 min. The integrity of dox-loaded anti-HER2 ILs in vivo was assayed by two-component PK studies, in which plasma PK of dox and of rhuMAbHER2-Fab′ were co-determined on identical plasma samples following single i.v. injection. The terminal plasma half-lives of rhuMAbHER2-Fab′ (as measured by ELISA) and that of dox (as measured fluorimetrically) were both approximately 10 h, indicating negligible dissociation or drug leakage.

2.5. Localization of anti-HER2 immunoliposomes to tumors in vivo

The biodistribution and tumor localization of dox-loaded anti-HER2 ILs were evaluated in HER2-overexpressing tumor xenograft models, in which nude mice carrying established subcutaneous (s.c.) BT-474 tumor xenografts received a single i.v. injection of ILs [13]. By 67 h post-injection, the concentration of dox in tumor tissue still exceeded 1%/g of tissue, which was significantly higher than dox levels in all other tissues except liver, the major site of liposome clearance. Tumor/blood and tumor/muscle ratios were both greater than 22-fold.

Tumor localization of ILs was studied histologically in two tumor xenograft models, BT-474 and MCF7/HER2 (MCF7 cells stably transfected with HER2), following administration of ILs containing colloidal gold [1]. Gold-loaded ILs were administered i.v. every 48 h for three doses and subsequently visualized by light microscopy within tumor tissue using a silver enhancement technique [14]. Silver grains indicating the presence of gold particles were observed throughout tumor tissue, both in perivascular areas and within cellular regions of the tumor. Importantly, silver grains were frequently observed within the cytoplasm of individual tumor cells, indicating intracellular delivery of gold particles. In contrast, treatment with control (no Fab′) sterically stabilized liposomes showed silver grains accumulating in predominantly extracellular and perivascular spaces, consistent with previous reports of the tumor interstitial localization of sterically stabilized liposomes [14]. These control liposomes were not observed within individual tumor cells.

To confirm the intracellular localization of anti-HER2 ILs in vivo, ILs were loaded with ^{67}Ga-DTPA chelate and administered by single i.v. injection in the MCF7/HER2 tumor xenograft model [13]. After 48 h, excised tumors were analyzed by electron microscopic autoradiography. Autoradiographic grains signifying ^{67}Ga emission resulting from immunoliposome delivery were frequently detected within tumor cells, at or near the cell surface, within the cytoplasm and within the nucleus. In contrast, tumors from mice treated with ^{67}Ga-loaded control liposomes showed no intracellular ^{67}Ga localization.

2.6. Doxorubicin-loaded anti-HER2 immunoliposomes

Targeted delivery of dox by anti-HER2 ILs may represent a particularly advantageous strategy for the treatment of HER2-overexpressing breast cancers, since these cancers appear to possess an especially steep dose-response relationship to dox-based therapy [15]. In addition, the significant clinical problem of dox toxicity to myocardium and hematopoietic cells may be largely mitigated by anti-HER2 immunoliposome delivery, as HER2 expression is negligible in these cell types [16]. Finally, the antiproliferative effect of the anti-HER2 immunoliposome vehicle (i.e. the rhuMAbHER2 effect) may work synergisti-

cally with dox, since it is has been shown that rhuMAbHER2 augments the efficacy of dox in animal models [17].

In vitro, dox-loaded anti-HER2 ILs showed efficient and specific cytotoxicity against HER2-overexpressing breast cancer cells [10]. Treatment of SK-BR-3 cells for 1 h with dox-loaded anti-HER2 ILs yielded dose-dependent cytotoxicity (IC50, 0.3 μg/ml) equivalent to that of free dox, indicating that ILs delivered dox as efficiently as the rapid diffusion of free dox into cells in vitro and were up to 30-fold more cytotoxic than dox-loaded ILs bearing irrelevant Fab′. The specificity of targeting was further confirmed by treatment of WI-38 cells, a non-malignant lung fibroblast cell line expressing minimal levels of HER2, wherein dox-loaded anti-HER2 ILs demonstrated cytotoxicity that was 20-fold less than free dox and equivalent to ILs with irrelevant Fab′.

In vivo, therapy studies using dox-loaded anti-HER2 ILs in multiple HER2-overexpressing tumor xenograft-nude mice models showed a significant increase in the therapeutic index of dox due to targeted delivery [13]. In these studies, experimental treatment was initiated 1–2 weeks after tumor implantation, at which time tumors were 200–1000 mm^3 in volume. ILs were administered at a total dox dose of 15 mg/kg, divided over three weekly i.v. injections. Therapeutic effects were compared to those of dox-loaded control (no Fab′) liposomes at the same dose and schedule. Additional control arms included treatment with free dox, which was given at its maximum tolerated dose (MTD) in these animals (7.5 mg/kg), free rhuMAbHER2 and saline. In each of the four models (two independent sublines of BT-474, MCF7/HER2 and MDA-MB-453), treatment with ILs resulted in marked tumor growth inhibition and/or regression (including some cured animals) and was significantly superior to all other treatment conditions. Furthermore, ILs did not produce any apparent acute toxicities or significant weight loss in the nude mice. The MTD determined for ILs represents a 2.5-fold increase over that of free dox.

2.7. Nucleic acid delivery via immunoliposomes

The above results suggest that anti-HER2 ILs may be particularly advantageous for tumor-specific treatment with agents that require intracellular delivery. For example, anti-HER2 ILs could represent a gene therapy vector system that provides targeted delivery of therapeutic genes or oligonucleotides to tumor cells. To overcome existing obstacles for successful implementation of this strategy, ILs must be reconstructed so as to efficiently package DNA, retain favorable drug delivery properties (such as stability, long circulation, minimal non-specific reactivity and reduced immunogenicity), selectively and efficiently deliver nucleic acids to tumor cells and provide intracellular delivery that results in adequate gene expression.

One approach to modifying anti-HER2 ILs for targeted gene therapy has been to include cationic lipids for efficient and high capacity packaging of DNA. Cationic liposomes, which readily form complexes with DNA molecules via electrostatic interactions and can mediate gene transfer to a variety of cell types, have previously attracted much attention as a gene therapy vector system. However, cationic liposomes developed to date have been limited by poor stability, high non-specific reactivity and lack of targeting. We recently reported cationic liposome-plasmid DNA complexes that are significantly more stable by manipulation of their lipid composition, inclusion of PEG-PE and condensation of plasmid DNA with polyamines [18]. These stable constructs show high gene transfer efficiency in vitro and in multiple tissue sites in vivo following i.v. administration. For targeting, rhuMAbHER2-Fab′ fragments have recently been conjugated covalently to PEG-containing cationic liposomes (Fig. 1b), thus generating anti-HER2 cationic immunoliposome-DNA complexes. In these cationic ILs, PEG-PE provides the attachment site for Fab′ and when present at an appropriate concentration, minimizes non-specific reactivity. By this design, anti-HER2 cationic ILs mediate efficient transfection of SK-BR-3 cells in vitro. The addition of Fab′ is associated with a 20-fold increase in reporter (firefly luciferase) gene expression as compared to cationic liposomes lacking Fab′, with minimal transfection observed in non-HER2-overexpressing MCF7 cells.

In a related strategy, anti-HER2 cationic ILs are also being developed for targeted delivery of oligonucleotides. As shown in Fig. 2, these ILs internalized in

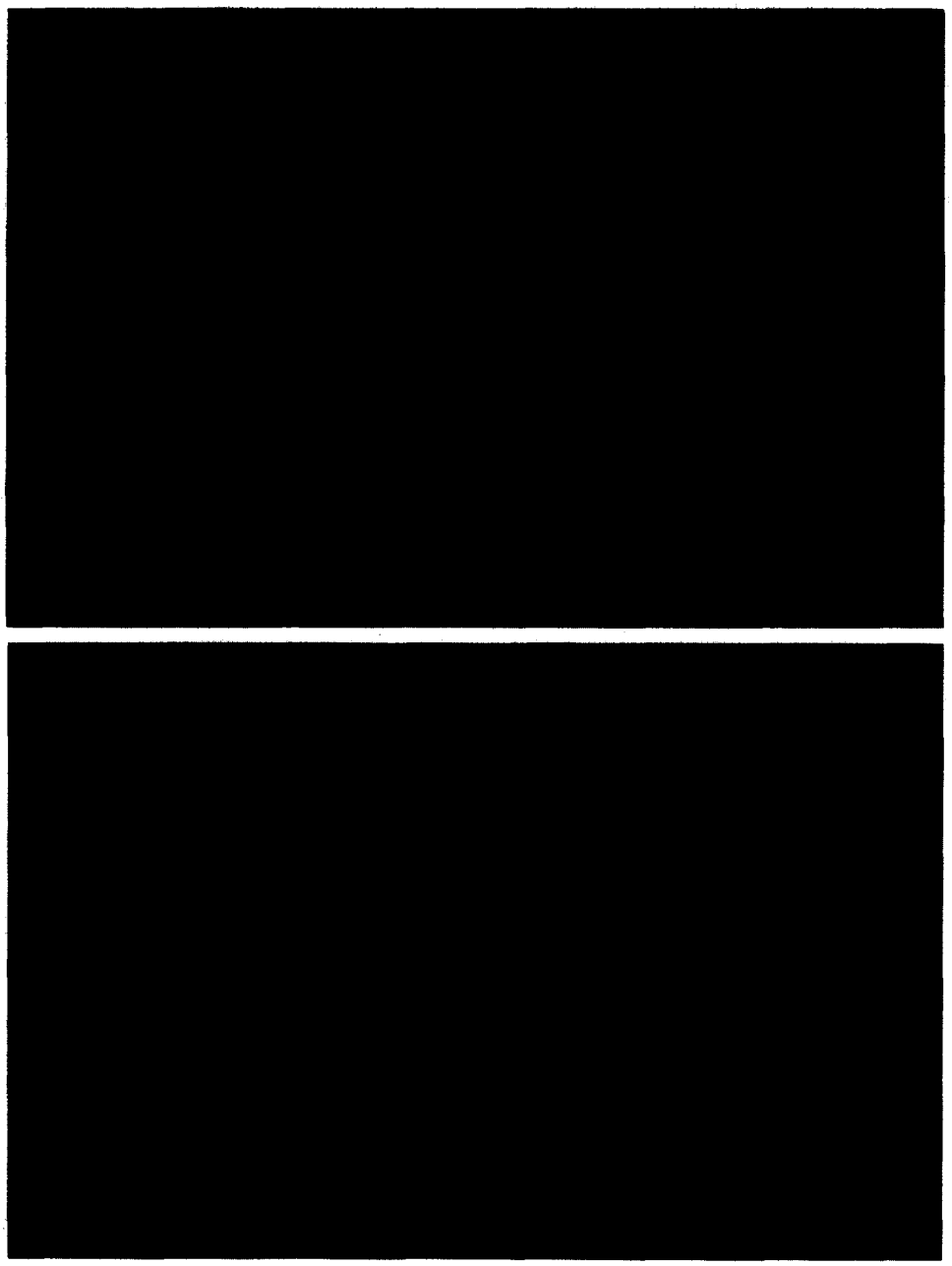

Fig. 2. Intracellular delivery of oligonucleotides via anti-HER2 cationic immunoliposomes (ILs) to SK-BR-3 cells. Anti-HER2 cationic ILs were prepared with dioleoyl-3-trimethylammonium propane (DOTAP) and dioleoylphosphatidylethanolamine (DOPE), with PEG-PE and rhodamine-PE included. Oligonucleotides were FITC-labeled phosphorothioate deoxynucleotide 18-mers with irrelevant specificity and were complexed with ILs. SK-BR-3 cells were incubated with ILs for 4 h at 37°C, then washed. After a further 20 h incubation, they were fixed and visualized by fluorescence microscopy. Above, immunoliposomes (red); below, oligonucleotides (green).

SK-BR-3 cells, resulting in rhodamine-labeled liposome accumulation within the cytosol, while the released FITC-labeled oligonucleotides accumulated within the nucleus.

3. Discussion

Because of their ability to provide tumor-targeted intracellular drug delivery, anti-HER2 ILs represent a potentially powerful strategy for the treatment of HER2-overexpressing cancers. Anti-HER2 ILs, like sterically stabilized liposomes, are stable and long circulating in vivo. Unlike liposomes, ILs bind to and internalize in target cells but are non-reactive with normal cells. In HER2-overexpressing tumor xenograft-nude mouse models, anti-HER2 ILs localize selectively in tumor tissue, where they deliver encapsulated agents intracellularly. In each animal model tested, dox-loaded anti-HER2 ILs greatly extend the therapeutic index of dox, both by increasing its antitumor efficacy and by reducing the systemic host toxicity; ILs exhibited significantly superior efficacy as compared with either dox-loaded sterically stabilized liposomes or free dox.

In addition to the targeted delivery of small molecule drugs like doxorubicin, the anti-HER2 immunoliposome strategy may enable new therapeutic applications, such as gene therapy. Compared with cationic liposomes, anti-HER2 cationic ILs provided significantly higher levels of reporter gene expression in target cells, but not in non-target cells. Anti-HER2 cationic ILs can also be developed to deliver oligonucleotides to target cells, resulting in the internalization of the complex and nuclear accumulation of oligonucleotides.

We conclude that the properties of anti-HER2 ILs described here make them a promising and novel strategy for tumor-targeted therapy. In particular, the development of immunoliposome constructs which are stable, long circulating and able to deliver encapsulated agents intracellularly in tumor cells appears to be important for the success of this strategy. These properties may confer sufficient pharmacokinetic and pharmacodynamic advantages to overcome the previous limitations of monoclonal antibody therapy and liposomal drug delivery.

Acknowledgements

The authors sincerely thank Paul Carter, Ph.D., Gilbert-Andre Keller, Ph.D. and William I. Wood, Ph.D. of Genentech, Inc. (South San Francisco, CA) and Yvonne S. Shao M.D. and Weiwen Zheng M.D. of UCSF (San Francisco, CA) for their contributions. The authors also thank Gail T. Colbern, DVM of the Geraldine Brush Cancer Research Institute/California Pacific Medical Center (San Francisco, CA) and Jose Baselga, MD and John Mendelsohn, MD of Memorial Sloan-Kettering Cancer Center (New York) for their contributions relating to the tumor xenograft-nude mouse studies. This work was partially supported by grants from the Breast Cancer SPORE Program of the National Cancer Institute and National Institutes of Health (P50-CA 58207-01), the US Army Medical Research and Materiel Command (DAMD17-94-J-4195), the California Breast Cancer Research Program (2CB-0250) and the American Society of Clinical Oncology Young Investigator Award (J.W.P.) sponsored by the Don Shula Foundation.

References

[1] J.W. Park, K. Hong, D.B. Kirpotin, D. Papahadjopoulos, C.C. Benz, Immunoliposomes for cancer treatment, in: J.T. August, J.T. Coyle, Gene Therapy, Advances in Pharmacology Vol. 40 Academic Press, San Diego, CA, 1997, pp. 399–435.

[2] N.E. Hynes, D.F. Stern, The biology of *erb*B-2/*neu*/HER-2 and its role in cancer, Biochim. Biophys. Acta 1198 (1994) 165–184.

[3] G.D. Lewis, I. Figari, B. Fendly, W.L. Wong, P. Carter, C. Gorman, H.M. Shepard, Differential responses of human tumor cell lines to anti-p185HER2 monoclonal antibodies, Cancer Immunol. Immunother. 37 (1993) 255–263.

[4] H.M. Shepard, G.D. Lewis, J.C. Sarup, B.M. Fendly, D. Maneval, J. Mordenti, I. Figari, C.E. Kotts, M.A. Palladino, A. Ullrich, D. Slamon, Monoclonal antibody therapy of human cancer: taking the HER2 protooncogene to the clinic, J. Clin. Immunol. 11 (1991) 117–127.

[5] J. Baselga, D. Tripathy, J. Mendelsohn, S. Baughman, C.C. Benz, L. Dantis, N.T. Sklarin, A.D. Seidman, C.A. Hudis, J. Moore, P.P. Rosen, T. Twaddell, I.C. Henderson, L. Norton, Phase II study of weekly intravenous recombinant humanized anti-p185^{HER2} monoclonal antibody in patients with HER/*neu*-overexpressing metastatic breast cancer, J. Clin. Oncol. 14 (1996) 737–744.

[6] M. Pegram, A. Lipton, R. Pietras, D. Hayes, B. Weber, J. Baselga, D. Tripathy, T. Twaddell, J. Glaspy, D. Slamon,

Phase II study of intravenous recombinant humanized anti-p185 HER-2 monoclonal antibody (rhuMAb HER-2) plus cisplatin in patients with HER-2/*neu* overexpressing metastatic breast cancer, Proc. Am. Soc. Clin. Oncol. 14 (1995) 106.

[7] D. Papahadjopoulos, T.M. Allen, A. Gabizon, E. Mayhew, K. Matthay, S.K. Huang, K.D. Lee, M.C. Woodle, D.D. Lasic, C. Redemann, F.J. Martin, Sterically stabilized liposomes: improvements in pharmacokinetics and antitumor therapeutic efficacy, Proc. Natl. Acad. Sci. USA 88 (1991) 11460–11464.

[8] S.K. Huang, E.M. Mayhew, S. Gilani, D.D. Lasic, F.J. Martin, D. Papahadjopoulos, Pharmacokinetics and therapeutics of sterically stabilized liposomes in mice bearing C-26 colon carcinoma, Cancer Res. 52 (1992) 6774–6781.

[9] D.D. Lasic, F.J. Martin, Stealth Liposomes, CRC Press, Boca Raton, FL, 1995.

[10] J.W. Park, K. Hong, P. Carter, H. Asgari, L.Y. Guo, G.A. Keller, C. Wirth, R. Shalaby, C. Kotts, W.I. Wood, D. Papahadjopoulos, C.C. Benz, Development of anti-p185HER2 immunoliposomes for cancer therapy, Proc. Natl. Acad. Sci. USA 92 (1995) 1327–1331.

[11] D. Kirpotin, J.W. Park, K. Hong, S. Zalipsky, W.L. Li, P. Carter, C.C. Benz, D. Papahadjopoulos, Sterically stabilized anti-HER2 immunoliposomes: design and targeting to human breast cancer cell *in vitro*, Biochemistry 36 (1997) 66–75.

[12] R.P. O'Connell, P. Carter, L. Presta, C. Eigenbrot, M. Covarrubias, B. Snedecor, R. Speckart, G. Blank, D. Vetterlein, C. Kotts, Characterization of humanized anti-p185HER2 antibody Fab fragments produced in *E. coli*, in: J.L. Cleland (Ed.), Protein Folding In Vivo and In Vitro, American Chemical Society, Washington, DC, 1993, pp. 218–239.

[13] J.W. Park, G. Colbern, J. Baselga, K. Hong, Y. Shao, D. Kirpotin, A. Nuijens, W. Wood, D. Papahadjopoulos, C. Benz, Antitumor efficacy of anti-p185HER2 immunoliposomes: enhanced therapeutic index due to targeted delivery, Proc. Am. Soc. Clin. Oncol. 15 (1996) 501.

[14] S.K. Huang, K.D. Lee, K. Hong, D.S. Friend, D. Papahadjopoulos, Microscopic localization of sterically stabilized liposomes in colon carcinoma-bearing mice, Cancer Res. 52 (1992) 5135–5143.

[15] H.B. Muss, A.D. Thor, D.A. Berry, T. Kute, E.T. Liu, F. Koerner, C.T. Cirrincione, D.R. Budman, W.C. Wood, M. Barcos, I.C. Henderson, c-*erb*B-2 expression and response to adjuvant chemotherapy in women with node-positive early breast cancer, N. Engl. J. Med. 330 (1994) 1260–1266.

[16] M.F. Press, C. Cordon-Cardo, D.J. Slamon, Expression of the HER-2/*neu* proto-oncogene in normal human adult and fetal tissues, Oncogene 5 (1990) 953–962.

[17] J. Baselga, L. Norton, R. Shalaby, J. Mendelsohn, Anti-HER2 humanized monoclonal antibody (MAb) alone and in combination with chemotherapy against breast carcinoma xenografts, Proc. Am. Soc. Clin. Oncol. 13 (1994) 63.

[18] K. Hong, W. Zheng, A. Baker, D. Papahadjopoulos, Stabilization of cationic liposome-plasmid DNA complexes by polyamines and poly(ethylene glycol)-phospholipid conjugates for efficient in vivo gene delivery, FEBS Lett. 400 (1997) 233–237.

Proc. Natl. Acad. Sci. USA
Vol. 92, pp. 1327–1331, February 1995
Medical Sciences

Development of anti-p185^{HER2} immunoliposomes for cancer therapy

J. W. PARK*†, K. HONG‡, P. CARTER§, H. ASGARI‡, L. Y. GUO‡, G. A. KELLER¶, C. WIRTH‖, R. SHALABY‖, C. KOTTS‖, W. I. WOOD†, D. PAPAHADJOPOULOS‡, and C. C. BENZ*‡

*Department of Medicine, Division of Hematology–Oncology and ‡Cancer Research Institute, University of California, San Francisco, San Francisco, CA 94143; and Departments of †Molecular Biology, §Cell Genetics, ‖Bioanalytical Technology, and ¶Pharmacology, Genentech, Inc., South San Francisco, CA 94080

Communicated by John A. Clements, University of California, San Francisco, CA, September 8, 1994 (received for review April 11, 1994)

ABSTRACT **The product of the *HER2* protooncogene, p185^{HER2}, represents an attractive target for cancer immunotherapies. We have prepared anti-p185^{HER2} immunoliposomes in which Fab′ fragments of a humanized anti-p185^{HER2} monoclonal antibody with antiproliferative properties (rhuMAb-HER2) were conjugated to either conventional or sterically stabilized liposomes. These immunoliposomes bind specifically to p185^{HER2}-overexpressing breast cancer cells (SK-BR-3 and BT-474). High-affinity binding of anti-p185^{HER2} immunoliposomes is comparable to that of free rhuMAbHER2-Fab′ or the intact antibody. Empty immunoliposomes inhibit the culture growth of p185^{HER2}-overexpressing breast cancer cells, and this antiproliferative effect is superior to that of free rhuMAbHER2-Fab′, indicating that liposomal anchoring of these anti-p185^{HER2} Fab′ fragments enhances their biological activity. Efficient internalization of anti-p185^{HER2} immunoliposomes, demonstrated by light and electron microscopy, occurs by receptor-mediated endocytosis via the coated pit pathway and also possibly by membrane fusion. Doxorubicin-loaded anti-p185^{HER2} immunoliposomes are markedly and specifically cytotoxic against p185^{HER2}-overexpressing tumor cells *in vitro*. Anti-p185^{HER2} immunoliposomes administered *in vivo* in Scid mice bearing human breast tumor (BT-474) xenografts can deliver doxorubicin to tumors. These results indicate that anti-p185^{HER2} immunoliposomes are a promising therapeutic vehicle for the treatment of p185^{HER2}-overexpressing human cancers.**

The *HER2* (c-*erbB2*, *neu*) protooncogene and p185^{HER2}, the growth factor receptor-tyrosine kinase it encodes, appear to play a central role in the pathogenesis of many human cancers. Overexpression of p185^{HER2} occurs in 20–30% of breast cancers, most commonly via gene amplification, and predicts a poor prognosis for these patients (1). Experimental evidence indicates that p185^{HER2} overexpression contributes to transformation and tumor progression and suggests that the prognostic significance of p185^{HER2} overexpression arises from the aggressive phenotype it confers (for review, see ref. 2).

The p185^{HER2} receptor represents an attractive target for antibody-based therapy. First, such therapies may be able to interfere with this important mediator of tumor growth and so inhibit tumor progression. Second, the stably overexpressed p185^{HER2} receptor provides an ideal target antigen. When present, p185^{HER2} overexpression generally occurs homogeneously within primary breast tumors as well as at synchronous or metachronous metastatic sites (3). In normal tissues, p185^{HER2} is expressed only at low levels in certain epithelial cell types (4). A murine anti-p185^{HER2} monoclonal antibody, muMAb4D5, inhibits the growth of p185^{HER2}-overexpressing breast cancer cells in culture and in animal models (2). A humanized version of this antibody, rhuMAbHER2, has been developed to retain these properties while reducing the potential for immunogenicity (5) and has entered clinical trials for the treatment of advanced breast cancer.

Here we describe the development of anti-p185^{HER2} immunoliposomes as a tumor-targeting vehicle, in which the anti-p185^{HER2} specificity and inhibitory activity of rhuMAbHER2 are combined with the pharmacokinetic and drug delivery advantages of liposomes. Recent advances in liposome development have yielded "sterically stabilized" or "stealth" liposomes, which are less susceptible to reticuloendothelial system uptake, resulting in prolonged circulation time and enhanced tumor extravasation (6, 7). Immunoliposomes represent another strategy to enhance liposomal drug delivery by linking liposomes to monoclonal antibodies directed against tumor-associated antigens to provide targeting (8, 9).

MATERIALS AND METHODS

Preparation of Liposomes and Immunoliposomes. Liposomes were prepared according to repeated freeze–thawing or the reverse-phase evaporation method (10), using phosphatidylcholine (PC) [either egg PC (EPC; Avanti Polar Lipids) or hydrogenated soy PC (HSPC, Natterman, Cologne, Germany)], cholesterol (Chol; Calbiochem), and polyethylene glycol (M_r, 1900)-derivatized phosphatidylethanolamine (PEG-PE) synthesized as described (11) and obtained from Liposome Technology (Menlo Park, CA). Liposome composition consisted of EPC/Chol (2:1) or HSPC/Chol (3:2) with PEG-PE (0–6 mol % of total phospholipid). For immunoliposomes, N-[4-(*p*-maleimidophenyl)butyryl]phosphatidylethanolamine (M-PE; Molecular Probes) was included at 2 mol % of total phospholipid (8). Liposomes were subsequently extruded repeatedly through polycarbonate membrane filters of defined pore size sequentially from 0.1 to 0.05 μm (12), yielding liposomes of 60–120 nm diameter as determined by dynamic light scattering. Liposome concentration was determined by phosphate assay. HSPC/Chol liposomes containing doxorubicin were prepared in 250 mM ammonium sulfate containing 1 mM desferrioxamine mesylate (desferal; CIBA–Geigy) at pH 5.5 (6, 13). The efficiency of drug loading reached >99% loading when 1 mg of drug per 10 μmol of phospholipid was used.

Cloned rhuMAbHER2 heavy- and light-chain genes were coexpressed in *Escherichia coli* and Fab′ was recovered as described (14). An irrelevant humanized Fab′ (rhuMAbH52-Fab′), which differs from rhuMAbHER2-Fab′ only by replacement of the antigen-binding loops and which shows no detectable binding to any known murine or human antigen (15), was used as a control. Fab′ was conjugated to the liposomes after drug loading via thioether linkage at pH >7.0 (8). Unreacted Fab′ was separated from immunoliposomes by gel filtration

The publication costs of this article were defrayed in part by page charge payment. This article must therefore be hereby marked "*advertisement*" in accordance with 18 U.S.C. §1734 solely to indicate this fact.

Abbreviations: Chol, cholesterol; PEG-PE, polyethylene glycol-derivatized phosphatidylethanolamine; liposome-C, conventional (no PEG-PE) liposome; liposome-SS, sterically stabilized (PEG-PE containing) liposome; PC, phosphatidylcholine; EPC, egg PC; HSPC, hydrogenated soy PC.

with Sephacryl S-400. The maleimide group on immunoliposomes was deactivated after conjugation by 2-fold excess of mercaptoethanol to M-PE. The amount of Fab' conjugated was determined by the Bio-Rad protein assay.

Immunoliposome Binding. For flow cytometric assay, cells in suspension were incubated in phosphate-buffered saline (PBS) with immunoliposomes for 45 min on ice, washed with PBS, stained with fluorescein isothiocyanate-labeled goat anti-human IgG, washed with PBS, and then subjected to flow cytometry. For competitive binding assays, cells in monolayer culture were treated with various concentrations of immunoliposomes in the presence of ^{125}I-labeled rhuMAbHER2 at 0.1 nM for 18 hr at 4°C. Counts bound were determined by γ counting.

Cell Proliferation and Cytotoxicity Studies. The antiproliferative activity of empty immunoliposomes was determined after continuous 4-day incubation with tumor cells in monolayer culture. Cell number and relative proliferation were determined by using crystal violet dye as described (16). The cytotoxicity of doxorubicin-loaded immunoliposomes was determined after a 1-hr incubation with tumor cells in monolayer culture. After 1 hr, the cells were extensively washed and then further incubated at 37°C for 3 days, after which cell number was estimated by crystal violet staining. Other assays of cell growth including alamar blue staining, 3-(4,5-dimethylthiazol-2-yl)-2,5-diphenyltetrazolium bromide staining, and direct cell counting yielded equivalent results.

Internalization Studies. For fluorescence microscopy, liposomes were prepared as described above with the addition of rhodamine phosphatidylethanolamine (Avanti Polar Lipids) at 1 mol % of total phospholipid. Cells grown on coverslips were incubated at 37°C with liposomes or immunoliposomes, fixed, mounted in glycerol, and observed with a Leitz Aristoplan fluorescence microscope or a Molecular Dynamics Multi-Probe 2001 confocal microscope. For electron microscopy, immunoliposomes were loaded with 5- to 15-nm gold particles as described (17). Cells were incubated at 37°C with gold-containing immunoliposomes and then fixed with tannic acid (17) and processed for electron microscopy.

***In Vivo* Tumor Localization and Biodistribution of Immunoliposomes and Immunoliposome Contents.** Female Scid mice (4–6 weeks old) implanted with estrogen pellets were injected with BT-474 cells in the subcutaneous tissue of the flank or mammary fat pad. When palpable tumors achieved a size of at least 300 mm^3 (typically 14 days postinoculation), immunoliposomes ($\approx$1 μmol of total lipid in 200 μl) were administered by single tail vein or intraperitoneal injection. After sacrifice, organs were immediately perfused with saline *in situ* and excised for analysis. For biodistribution and imaging analysis after injection of rhodamine-labeled immunoliposomes, freshly excised tissues were fixed and examined by confocal fluorescence microscopy. For quantitative localization of doxorubicin delivered by immunoliposomes, excised tissues were homogenized and subjected to acidified ethanol extraction; the extracted doxorubicin was then measured by spectrofluorimetric assay (6).

RESULTS

Preparation and Characterization of Anti-p185^{HER2} Immunoliposomes. Immunoliposomes were prepared by conjugation of conventional (PC/Chol; liposomes-C) or sterically stabilized (PC/Chol/PEG-PE; liposomes-SS) liposomes with Fab' fragments of rhuMAbHER2. Fab' was used because of the extremely efficient expression of rhuMAbHER2-Fab' in *E. coli* (14); and because the free thiol group in the Fab' hinge region provides a single site for covalent attachment to modified liposomes, which is distant from the antigen-binding site. Typically, conjugation yielded 50–100 Fab' molecules per liposome particle.

Binding of anti-p185^{HER2} immunoliposomes *in vitro* to breast cancer cells that overexpress p185^{HER2} was confirmed by flow cytometry, using a labeled secondary anti-human antibody to detect bound immunoliposomes (data not shown). Cells with p185^{HER2} overexpression [SK-BR-3 or BT-474 (16)] showed significant binding to anti-p185^{HER2} immunoliposomes, while cells without p185^{HER2} overexpression [MCF-7 (16)] showed undetectable binding. A competitive binding assay, in which breast cancer cells were simultaneously incubated with ^{125}I-labeled rhuMAbHER2 and increasing concentrations of anti-p185^{HER2} immunoliposomes, showed single component binding of immunoliposomes to both SK-BR-3 and BT-474 cells (data not shown). An approximation of binding affinity was obtained via Scatchard analysis by assuming that Fab' on immunoliposomes behaved as free ligand. Using this model, apparent binding constants for the immunoliposomes were comparable to those of free Fab' or intact rhuMAbHER2 (Table 1). Control liposomes lacking Fab' showed negligible binding.

Antiproliferative Effects of Anti-p185^{HER2} Immunoliposomes. While intact (bivalent) rhuMAbHER2 inhibits the growth of p185^{HER2}-overexpressing breast cancer cells in monolayer culture, monovalent Fab' fragments of this antibody are much less effective at inhibiting growth (18). This observation suggests that cross-linking of p185^{HER2} receptors by bivalent antibody is important for the antiproliferative effect. To determine whether liposomal anchoring of Fab' fragments might restore antiproliferative activity, the effect of anti-p185^{HER2} immunoliposomes on SK-BR-3 cells in monolayer culture was tested and compared to rhuMAbHER2 and rhuMAbHER2-Fab' (Fig. 1). Treatment with control liposomes lacking Fab' did not significantly affect cell growth. In contrast, anti-p185^{HER2} immunoliposomes inhibited growth in a dose-dependent manner. The growth inhibitory effect of the immunoliposomes reached a plateau of $\approx$30% growth inhibition (70% of control growth), approaching the 40% growth inhibition seen with free intact rhuMAbHER2. In contrast, free Fab' induced only modest growth inhibition. Thus, liposome-associated Fab' produced an antiproliferative effect markedly greater than the same amount of Fab' free in solution.

Internalization of Anti-p185^{HER2} Immunoliposomes. After binding to p185^{HER2}, rhuMAbHER2 is rapidly internalized via receptor-mediated endocytosis (19). To assess whether anti-p185^{HER2} immunoliposomes are internalized, fluorescence microscopy of SK-BR-3 cells treated with rhodamine-labeled immunoliposomes was performed. Cells treated with control liposomes lacking Fab' showed no rhodamine fluorescence (Fig. 2 *a* and *b*), consistent with their inability to bind to these cells. In contrast, cells treated with anti-p185^{HER2} immunoliposomes-C exhibited intense foci of fluorescence both at the cell surface and intracellularly within 30 min of treatment (Fig. 2*c*). Confocal fluorescence microscopy confirmed that rhodamine fluorescence was present both at the cell surface and intracellularly (Fig. 2*d*). Treatment with anti-p185^{HER2} immunoliposomes-SS containing 6 mol % PEG-PE, however, re-

Table 1. Binding of anti-p185^{HER2} immunoliposomes to BT-474 cells

Ligand	Apparent K_d, nM	EC_{50}, nM
Control liposomes-C	No displacement	>1000
Control liposomes-SS (6 mol % PEG-PE)	2500	>1000
Anti-p185^{HER2} immunoliposomes-C	9	15
Anti-p185^{HER2} immunoliposomes-SS (6 mol % PEG-PE)	58	78
rhuMAbHER2-Fab'	22	30
rhuMAbHER2	1	2

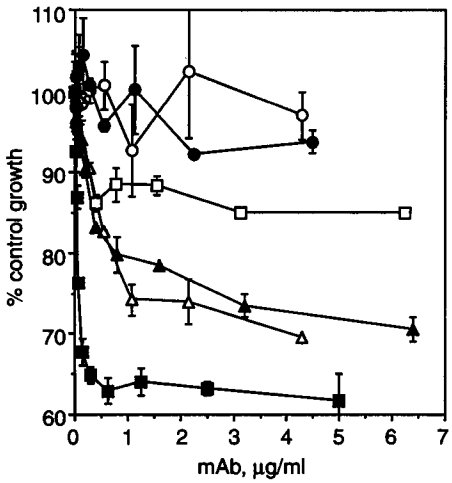

FIG. 1. Antiproliferative activity of anti-p185^{HER2} immunoliposomes against SK-BR-3 cells. Cells in monolayer culture were treated with immunoliposomes at monoclonal antibody (mAb) doses indicated on the abscissa, and relative cell proliferation was determined as described. Control liposomes lacking antibody were dosed according to liposome concentration and are plotted at equivalent liposome concentration with the appropriately matched immunoliposome. ○, Control (no antibody) liposomes-C; ●, control liposomes-SS (6 mol % PEG-PE); △, anti-p185^{HER2} immunoliposomes-C; ▲, anti-p185^{HER2} immunoliposomes-SS (6 mol % PEG-PE); □, free (nonliposomal) rhuMAbHER2-Fab'; ■, free rhuMAbHER2 bivalent antibody.

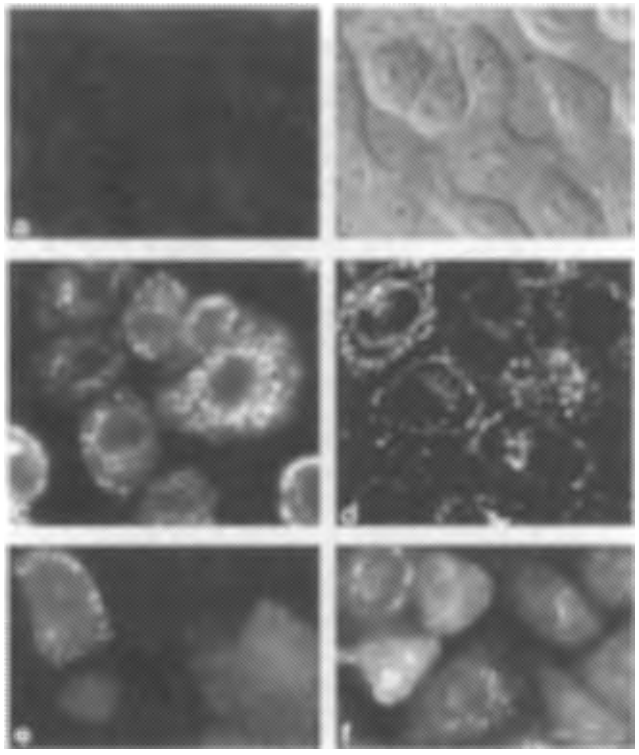

FIG. 2. Internalization of anti-p185^{HER2} immunoliposomes in SK-BR-3 cells. Conventional and confocal fluorescence microscopy of SK-BR-3 cells treated with rhodamine-labeled immunoliposomes or liposomes was performed as described. (*a*) SK-BR-3 cells treated with control (no antibody) liposomes-C for 30 min. (*b*) Same field as in *a*, using Nomarski optics. (*c*) Cells treated with anti-p185^{HER2} immunoliposomes-C for 30 min. (*d*) Same conditions as *c*, using confocal microscopy. (*e*) Cells treated with anti-p185^{HER2} immunoliposomes-SS (2 mol % PEG-PE) for 30 min. (*f*) Same conditions as *e* but after 2 hr of treatment. (Bar = 10 μm.)

sulted in minimal intracellular fluorescence after 30 min (data not shown), suggesting that the presence of PEG-PE appeared to retard immunoliposome internalization. Immunoliposomes-SS with 2 mol % PEG-PE yielded an intermediate degree of intracellular fluorescence after 30 min (Fig. 2*e*) and accumulated intracellularly after 2 hr (Fig. 2*f*). Thus, the rate of internalization of anti-p185^{HER2} immunoliposomes appeared to be inversely related to their PEG-PE content.

To study the intracellular disposition of immunoliposomes and their contents, electron microscopy was performed with anti-p185^{HER2} immunoliposomes-C containing gold particles (Fig. 3). SK-BR-3 cells treated with anti-p185^{HER2} immunoliposomes-C for 30 min showed numerous immunoliposomes at the cell surface (Fig. 3 *e* and *f*). Immunoliposomes were also observed in coated pits, coated vesicles, endosomes, multivesicular bodies, and lysosomes (Fig. 3 *a–d* and *g*), consistent with internalization via the coated pit pathway. However, immunoliposomes were also observed in apparent fusion with the cell membrane and not associated with coated pits (Fig. 3*f*). In addition, some gold particles appeared free within the cytoplasm and not associated with a liposome capsule or membrane-bound organelle (Fig. 3 *c*, *g*, and *h*), consistent with internalization via liposome–cell fusion or escape of gold particles from the coated pit pathway.

Cytotoxicity of Anti-p185^{HER2} Immunoliposomes Containing Doxorubicin. While empty anti-p185^{HER2} immunoliposomes displayed antiproliferative activity against p185^{HER2}-overexpressing breast cancer cells in culture, it was possible to augment the antineoplastic effect by loading the immunoliposomes with doxorubicin, thus producing a targeted, p185^{HER2}-specific drug delivery system. Because of the efficient internalization of anti-p185^{HER2} immunoliposomes, we reasoned that they might be just as effective at killing p185^{HER2}-overexpressing breast cancer cells in culture as free doxorubicin, a small (M_r, 544) amphipathic molecule that readily passes through the cell membrane. On the other hand, cells that do not overexpress p185^{HER2}, while susceptible to free doxorubicin, would escape cytotoxic injury. As shown in Fig. 4*a*, SK-BR-3 cells were treated for 1 hr with doxorubicin-loaded immunoliposomes. Under these conditions, the antiproliferative effect of rhuMAbHER2 is not apparent, as it requires continuous exposure of the cells to rhuMAbHER2 (20). Treatment with free doxorubicin for 1 hr yielded significant cytotoxicity, with an IC_{50} of 0.3 μg/ml. Doxorubicin-loaded anti-p185^{HER2} immunoliposomes showed comparable dose-dependent cytotoxicity, with an IC_{50} of 0.2 μg/ml for anti-p185^{HER2} immunoliposomes-C and 1.0 μg/ml for anti-p185^{HER2} immunoliposomes-SS. Thus, anti-p185^{HER2} immunoliposome delivery of doxorubicin to p185^{HER2}-overexpressing cells in culture was as efficient a process as the rapid diffusion of free doxorubicin into cells. Doxorubicin-loaded anti-p185^{HER2} immunoliposomes were 10- to 30-fold more cytotoxic than doxorubicin-loaded immunoliposomes bearing irrelevant Fab', which affected cell growth only at high concentrations (>3.3 μg/ml). WI-38 cells, a nonmalignant lung fibroblast cell line that expresses minimal levels of p185^{HER2} (16), were also treated with doxorubicin-loaded immunoliposomes (Fig. 4*b*). While free doxorubicin produced significant dose-dependent cytotoxicity against WI-38 cells, doxorubicin-loaded anti-p185^{HER2} immunoliposomes-C or -S produced much reduced (20-fold) cytotoxicity against these cells and were indistinguishable from doxorubicin-loaded irrelevant immunoliposomes. These results not only demonstrated the specificity of anti-p185^{HER2} immunoliposome treatment for p185^{HER2}-overexpressing targets but also confirmed that the cytotoxicity observed against SK-BR-3 cells was not simply due to leakage of doxorubicin out of immunoliposomes and into solution.

***In Vivo* Localization of Anti-p185^{HER2} Immunoliposomes to p185^{HER2}-Overexpressing Tumors.** The biodistribution of anti-

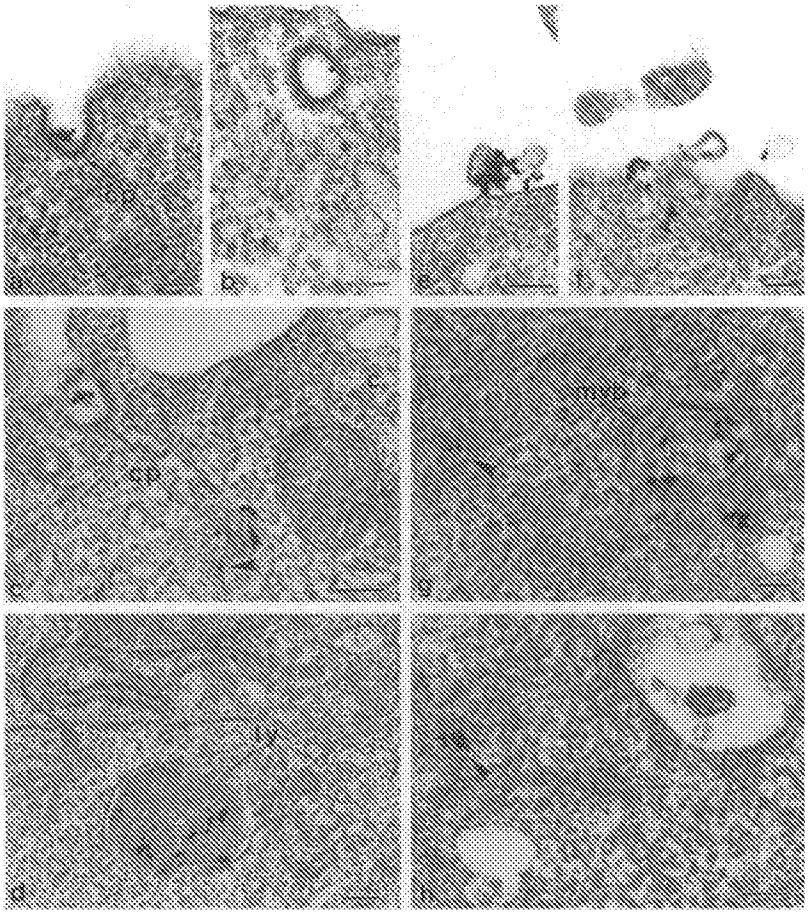

FIG. 3. Internalization of anti-p185^{HER2} immunoliposomes-C and intracellular delivery of encapsulated gold particles in SK-BR-3 cells. Electron microscopy of SK-BR-3 cells treated with EPC/Chol immunoliposomes-C containing encapsulated colloidal gold particles of 5–15 nm was performed as described. (*a*) Immunoliposomes in a coated pit (cp). (*b*) Immunoliposome within a coated vesicle. (*c*) Immunoliposomes in a coated pit (cp) and gold particles appearing free in the cytoplasm (arrowheads). (*d*) Gold within a lysosome (ly). (*e*) Surface-bound immunoliposomes. (*f*) Immunoliposomes apparently fusing with the cell membrane. (*g*) Gold particles appearing free in the cytoplasm (arrowhead) and in a multivesicular body (mvb). (*h*) Gold particles appearing free in the cytoplasm (arrowhead). (Bar = 0.1 μm.)

p185^{HER2} immunoliposomes and their ability to localize to and accumulate within tumors *in vivo* was evaluated in a tumor xenograft model. In this model, immunodeficient mice carrying established subcutaneous BT-474 tumor xenografts were treated with immunoliposomes by a single intravenous or intraperitoneal injection. Imaging studies with confocal fluorescence microscopy were performed to detect rhodamine-labeled immunoliposomes within various tissues of animals sacrificed after treatment. Within 6 hr of injection, rhodamine fluorescence was visualized within the xenografted tumor, while no significant fluorescence was observed within surrounding muscle (data not shown). For a quantitative evaluation of the biodistribution and localization of doxorubicin delivered by immunoliposomes, doxorubicin was assayed from tissue extracts of treated animals; 24 hr after intraperitoneal injection, doxorubicin delivered by anti-p185^{HER2} immunoliposomes-SS had accumulated within tumor xenografts, with lower levels of doxorubicin found in surrounding muscle and in blood (Table 2).

DISCUSSION

Recent reports have indicated the feasibility of using immunoliposomes for targeted drug delivery to augment the therapeutic index of an encapsulated anticancer agent (9). We have tried to increase the likelihood that such a strategy will succeed by (*i*) targeting p185^{HER2}, a growth factor receptor that is stably overexpressed by tumor cells and required for the maintenance of aggressive tumor growth; (*ii*) developing immunoliposomes that retain the antiproliferative activity of rhuMAbHER2 and thus have intrinsic antitumor properties; (*iii*) using humanized Fab′ to lessen potential immunogenicity; (*iv*) encapsulating a cytotoxic agent that provides an additive or synergistic antitumor effect when combined with antibody treatment; and (*v*) developing internalizing immunoliposomes for efficient intracellular delivery of encapsulated agents.

Anti-p185^{HER2} immunoliposomes not only bound to cell surface p185^{HER2} of tumor cells such as SK-BR-3 but could become rapidly internalized as well. Neutrally charged small unilamellar liposomes without associated ligands generally do not bind to tumor cells and are not efficiently internalized (21), as was observed with the control liposomes in this study. Antibody-bearing liposomes may be internalized at greatly varying rates, depending on the antibody and target receptor to which they bind (22). The differential internalization rates observed with conventional vs. sterically stabilized anti-p185^{HER2} immunoliposomes indicate that liposome composition can also affect internalization. It may be speculated that the slower internalization seen with sterically stabilized immunoliposomes may reflect the mechanism by which steric stabilization endows liposomes with relative resistance to phagocytic clearance. Furthermore, based on the unexpected result that anti-p185^{HER2} immunoliposomes can deliver some of their contents outside of the endolysosomal compartment, they may be useful for the intracellular delivery of agents susceptible to lysosomal degradation.

The delivery of doxorubicin via anti-p185^{HER2} immunoliposomes may substantially improve its therapeutic index. Increased tumor exposure to doxorubicin may be particularly advantageous in the case of p185^{HER2}-overexpressing tumors, since p185^{HER2}-overexpressing breast cancers may possess an especially steep dose–response relationship to doxorubicin-based therapy (23). In addition, the antiproliferative effect of anti-p185^{HER2} immunoliposomes themselves (derived from rhuMAbHER2) may act synergistically with doxorubicin, since rhuMAbHER2 augments the efficacy of doxorubicin (24), as well as cisplatin (25) and taxol (24). Finally, anti-p185^{HER2} immunoliposome delivery of doxorubicin provides a means of limiting the toxicity of doxorubicin in

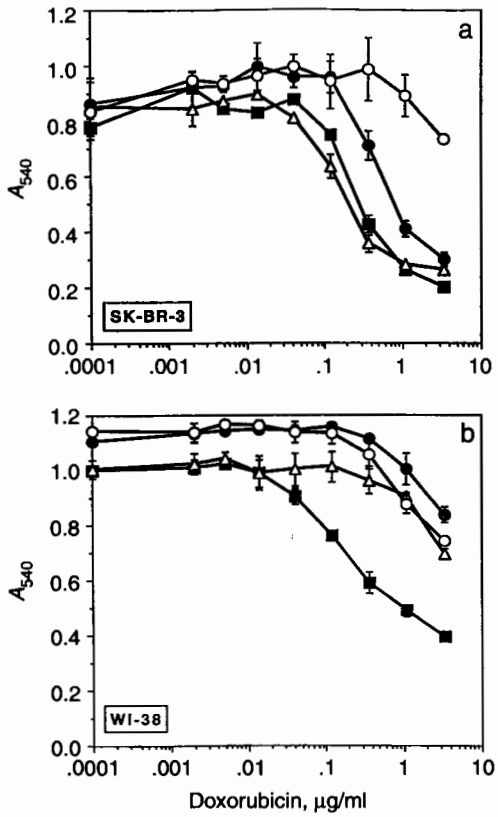

FIG. 4. Cytotoxicity of anti-p185^{HER2} immunoliposomes containing doxorubicin. HSPC/Chol immunoliposomes were loaded with doxorubicin as described. (*a*) SK-BR-3 cells. (*b*) WI-38 cells. Cells in culture were treated for 1 hr with anti-p185^{HER2} immunoliposomes-C (△), anti-p185^{HER2} immunoliposomes-SS (2 mol % PEG-PE) (●), control (irrelevant antibody) immunoliposomes-SS (2 mol % PEG-PE) (○), or free doxorubicin alone (■). Immunoliposomes contained 60–70 μg of antibody per μmol of phospholipid and 55–80 μg of doxorubicin per μmol of phospholipid; antibody/doxorubicin ratio was 0.8–1.2. Cells were counted 3 days after treatment as described.

normal tissues. p185^{HER2} receptor expression is negligible in myocardium and among hematopoietic cells (4), the critical sites of doxorubicin toxicity.

We conclude that the properties of anti-p185^{HER2} immunoliposomes described in this report make them a promising and feasible form of immunotherapy, in which cytotoxic agents such as doxorubicin can be targeted to p185^{HER2}-overexpressing tumors in combination with the antiproliferative effect induced by the immunoliposomes themselves. These properties may confer sufficient pharmacokinetic and pharmacodynamic advantage to overcome the previous limitations of monoclonal antibody therapy and liposomal drug delivery.

Table 2. Anti-p185^{HER2} immunoliposome delivery of doxorubicin *in vivo*: Biodistribution 24 hr after single i.p. injection

Tissue fluid	Doxorubicin level, % injected dose per g of tissue
Tumor	1.64
Muscle	0.61
Liver	13.46
Ventricular blood	0.88
Tumor/muscle ratio	2.69
Tumor/blood ratio	1.88

Anti-p185^{HER2} immunoliposomes-SS (2 mol % PEG-PE) loaded with doxorubicin were administered i.p. at a dose of 1 μmol of total lipid.

We are grateful to Gail T. Colbern, Helene S. Smith, and Alan J. Hiller for their establishment of the BT-474 tumor xenograft model and for assistance with our *in vivo* murine studies. J.W.P. is a recipient of the American Society of Clinical Oncology (ASCO) Young Investigator Award sponsored by The Don Shula Foundation. This work was supported by National Institutes of Health Grants CA36773, GM28117, and CA58207.

1. Slamon, D. J., Godolphin, W., Jones, L. A., Holt, J. A., Wong, S. G., Keith, D. E., Levin, W. J., Stuart, S. G., Udove, J., Ullrich, A. & Press, M. (1989) *Science* **244,** 707–712.
2. Park, J. W., Stagg, R., Lewis, G. D., Carter, P., Maneval, D., Slamon, D. J., Jaffe, H. & Shepard, H. M. (1992) in *Genes, Oncogenes, and Hormones: Advances in Cellular and Molecular Biology of Breast Cancer*, eds. Dickson, R. B. & Lippman, M. E. (Kluwer, Boston), pp. 193–211.
3. Niehans, G. A., Singleton, T. P., Dykoski, D. & Kiang, D. T. (1993) *J. Natl. Cancer Inst.* **85,** 1230–1235.
4. Press, M. F., Cordon-Cardo, C. & Slamon, D. J. (1990) *Oncogene* **5,** 953–962.
5. Carter, P., Presta, L., Gorman, C. M., Ridgway, J. B. B., Henner, D., Wong, W. L. T., Rowland, A. M., Kotts, C., Carver, M. E. & Shepard, H. M. (1992) *Proc. Natl. Acad. Sci. USA* **89,** 4285–4289.
6. Papahadjopoulos, D., Allen, T. M., Gabizon, A., Mayhew, E., Matthay, K., Huang, S. K., Lee, K. D., Woodle, M. C., Lasic, D. D., Redemann, C. & Martin, F. J. (1991) *Proc. Natl. Acad. Sci. USA* **88,** 11460–11464.
7. Huang, S. K., Mayhew, E. M., Gilani, S., Lasic, D. D., Martin, F. J. & Papahadjopoulos, D. (1992) *Cancer Res.* **52,** 6774–6781.
8. Martin, F. & Papahadjopoulos, D. (1982) *J. Biol. Chem.* **257,** 286–288.
9. Ahmad, I., Longenecker, M., Samuel, J. & Allen, T. M. (1993) *Cancer Res.* **55,** 1484–1488.
10. Szoka, F. & Papahadjopoulos, D. (1978) *Proc. Natl. Acad. Sci. USA* **75,** 4194–4198.
11. Allen, T. M., Hansen, C., Martin, F., Redemann, C. & Yau-Young, A. (1991) *Biochim. Biophys. Acta* **1066,** 29–36.
12. Szoka, F. C., Olson, F., Heath, T., Vail, W., Mayhew, E. & Papahadjopoulos, D. (1980) *Biochim. Biophys. Acta* **601,** 559–571.
13. Lasic, D. D., Frederik, P. M., Stuart, M. C. A., Barenholz, Y. & McIntosh, T. J. (1992) *FEBS Lett.* **312,** 255–258.
14. Carter, P., Kelley, R. F., Rodrigues, M. L., Snedecor, B. R., Covarrubias, M., Velligan, M. D., Wong, W. L., Rowland, A. M., Kotts, C. E., Carver, M. E., Yang, M., Bourell, J. H., Shepard, H. M. & Henner, D. (1992) *Biotechnology* **10,** 163–167.
15. Eigenbrot, C., Gonzalez, T., Mayeda, J., Carter, P., Werther, W., Hotaling, T., Fox, J. & Kessler, J. (1994) *Proteins: Struct. Funct. Genet.* **18,** 49–62.
16. Lewis, G. D., Figari, I., Fendly, B., Wong, W. L., Carter, P., Gorman, C. & Shepard, H. M. (1993) *Cancer Immunol. Immunother.* **37,** 255–263.
17. Straubinger, R. M., Hong, K., Friend, D. S. & Papahadjopoulos, D. (1983) *Cell* **32,** 1069–1079.
18. O'Connell, R. P., Carter, P., Presta, L., Eigenbrot, C., Covarrubias, M., Snedecor, B., Speckart, R., Blank, G., Vetterlein, D. & Kotts, C. (1993) in *Protein Folding In Vivo and In Vitro*, ed. Cleland, J. L. (Am. Chem. Soc., Washington, DC), pp. 218–239.
19. Sarup, J. C., Johnson, R. M., King, K. L., Fendly, B. M., Lipari, M. T., Napier, M. A., Ullrich, A. & Shepard, H. M. (1991) *Growth Regul.* **1,** 72–82.
20. Hudziak, R. M., Lewis, G. D., Winget, M., Fendly, B. M., Shepard, H. M. & Ullrich, A. (1989) *Mol. Cell. Biol.* **9,** 1165–1172.
21. Lee, K. D., Hong, K. & Papahadjopoulos, D. (1992) *Biochim. Biophys. Acta* **1103,** 185–197.
22. Matthay, K. K., Abai, A. A., Cobb, S., Hong, K., Papahadjopoulos, D. & Straubinger, R. M. (1989) *Cancer Res.* **49,** 4879–4886.
23. Muss, H. B., Thor, A. D, Berry, D. A., Kute, T., Liu, E. T., Koerner, F., Cirrincione, C. T., Budman, D. R., Wood, W. C., Barcos, M. & Henderson, I. C. (1994) *N. Engl. J. Med.* **330,** 1260–1266.
24. Baselga, J., Norton, L., Shalaby, R. & Mendelsohn, J. (1994) *Proc. Am. Soc. Clin. Oncol.* **13,** 63 (abstr.).
25. Pietras, R. J., Fendly, B. M., Chazin, V. R., Pegram, M. D., Howell, S. B. & Slamon, D. J. (1994) *Oncogene* **9,** 1829–1838.

John W. Park*
Keelung Hong†
Dmitri B. Kirpotin†
Demetrios Papahadjopoulos†
Christopher C. Benz*

*Department of Medicine
Division of Hematology-Oncology
University of California, San Francisco
San Francisco, California 94143

†Department of Cellular and Molecular Pharmacology
University of California, San Francisco
San Francisco, California 94143

Immunoliposomes for Cancer Treatment

I. Introduction

The notion of targeted drug delivery has long tantalized investigators in many fields, perhaps most of all in the treatment of cancer. Immunoliposomes represent a rational strategy to achieve targeted drug delivery for cancer treatment, and work suggests that optimization of immunoliposome design may finally lead to realization of this goal.

Despite more than a decade of preclinical work, immunoliposomes have yet to appear sufficiently promising to be evaluated in clinical trials. Early attempts to develop immunoliposomes as a targeted drug delivery system were plagued by multiple obstacles involving all of the components of immunoliposome construction: target antigen, antibody, antibody–liposome linkage, liposome composition and structure, and drug. In particular, progress in immunoliposome development ultimately had to await critical advances in the design of liposomes as a drug delivery system for cancer treatment.

Advances in Pharmacology, Volume 40

1054-3589/97 $25.00

These advances included liposomes with much improved pharmacologic properties, including long circulation and selective extravasation in tumors. Fortunately, advances in the liposome field were also paralleled by steady progress in monoclonal antibody-based therapy and in antibody engineering. As a result, immunoliposome development can now benefit from improved targeting technologies as well as important lessons learned from the extensive preclinical and clinical experience with antibody-based therapeutics.

This chapter reviews developments in the use of immunoliposomes for cancer treatment. The use of immunoliposomes for other therapeutic applications, such as the treatment of infectious or inflammatory disorders, is not discussed. Similarly, the use of immunoliposomes for diagnostic applications, such as imaging of solid tumors, also is not discussed. So-called ligandoliposomes, in which targeting ligands other than antibodies are linked to liposomes, also have been omitted from this chapter.

II. Lipsomes as a Drug Delivery System for Cancer Treatment

So-called "conventional" liposomes have been used in cancer treatment for more than two decades to deliver a number of anticancer agents, sometimes resulting in an improved therapeutic index owing to reduced toxicity to normal tissues. However, their clinical utility has been severely limited by the lack of specific tumor targeting, and by rapid clearance by phagocytic cells of the reticuloendothelial system (RES) (Gregoriadis, 1976). To circumvent this rapid clearance, we and other investigators have developed modified liposomes with altered lipid components, inclusion of substituents such as polyethylene glycol (PEG), small diameter, and reduction of surface charge (Gabizon and Papahadjopoulos, 1988). These so-called "stealth" or "sterically stabilized" liposomes possess much reduced reactivity with serum proteins and are less susceptible to RES uptake, resulting in significant prolongation of circulation time. In addition, sterically stabilized liposomes have been shown to accumulate preferentially within tumors in animal models and in humans (Papahadjopoulos *et al.*, 1991; Huang *et al.*, 1992b; Lasic and Martin, 1995). It appears that the mechanism for tumor localization of liposomes involves enhanced liposome extravasation from tumor-associated vasculature, which occurs because of endothelial fenestrations and other structural abnormalities associated with tumor angiogenesis. Because of their improved pharmacologic properties, sterically stabilized liposomes have generated renewed interest in liposomes as drug carriers (Lasic and Papahadjopoulos, 1995). Sterically stabilized liposomes containing doxorubicin have shown encouraging clinical activity (Lasic and Martin, 1995); and two versions of doxorubicin-loaded liposomes have been approved by the Food and Drug Administration (FDA) for the treatment of acquired

immunodeficiency syndrome (AIDS)-associated Kaposi's sarcoma. Clinical trials of sterically stabilized liposomes containing doxorubicin for the treatment of other solid tumors, including breast, lung, and liver cancer, are in progress.

III. Antibodies Useful for Targeting

A. General Considerations

Immunoliposomes (ILs) represent a further strategy to enhance liposomal drug delivery, by linking liposomes to monoclonal antibodies (MAbs) directed against tumor-associated antigens. Choice of target antigen and antibody is a critical aspect of immunoliposome design.

In the past, target antigens have often been chosen on the basis of availability of antibodies and model systems rather that rational therapeutic design. However, it is obvious that target antigen selection for monoclonal antibody-based therapies must involve careful consideration (Table I). Most tumor-associated antigens are quantitatively overexpressed on tumor cells as opposed to normal cells and tissues, but in cancer patients overexpression often does not occur homogeneously in all cells of a given tumor or in

TABLE I Components of Immunoliposome Design

Component	*Considerations for optimal design*
Target antigen	*Expression:* Homogeneously overexpressed
	Function: Vital to tumor progression, so that downmodulation does not occur or is associated with therapeutic benefit
	Shed antigen: Limited, to avoid binding to soluble antigen and accelerated clearance
Antibody	*Immunogenicity:* Humanized MAb, to remove murine sequences. MAb fragment (e.g., Fab, Fab', Fv), to remove Fc region
	Internalization: Efficiently endocytosed
	Biological activity: Intrinsic antitumor activity, to enhance antitumor effect
Linkage	*Stability:* Antibody covalently attached to hydrophobic anchor
	Attachment site: Specific sites on antibody and liposome. Avoids steric hindrance (e.g., due to PEG) of MAb binding and internalization
Liposome	*Stability:* Stable as intact construct *in vivo*
	Pharmacokinetics: Long circulating
	Tumor penetration: Selective extravasation in tumors (e.g., sterically stabilized). Small diameter to improve tumor penetration
Drug	*Encapsulation:* Efficient and high capacity
	Bystander toxicity: Small molecule drug to diffuse throughout tumor once released, or other mechanism to affect tumor cells not directly targeted
	Interaction with target antigen, MAb: Anticancer effect particularly suited to target cell population. Cytotoxicity enhanced by binding of MAb

cells from different metastatic sites. In addition, clinical studies involving monoclonal antibody therapies have shown that the expression of some target antigens can become significantly downmodulated during treatment or disease progression, including loss of the overexpression phenotype in some or all tumor cells (for review, see Waldmann, 1991). Finally, some antigens are shed or secreted by tumor cells in some patients, leading to potentially high circulating levels of soluble antigen that can bind antibody.

Monoclonal antibodies or antibody fragments to be used in immunoliposomes, even those directed against the same target antigen, vary in ways that are crucial to immunoliposome development. The immunogenicity of MAb-based therapeutic agents has constituted a major barrier to successful therapy, particularly owing to the use of murine MAbs and/or immunoconjugates containing immunogenic components. Similarly, immunoliposomes containing heterologous IgG have elicited high levels of anti-IgG antibodies in mice, resulting in marked reduction in circulation time with repeated administration (Phillips and Emili, 1991; Phillips *et al.*, 1994). In addition to the use of heterologous IgG, exposure of the Fc region and the use of an avidin–biotin linkage were also associated with increased immunogenicity in these studies.

Antibodies that are efficiently internalized after antigen binding, and that are capable of mediating immunoliposome internalization as well, offer a unique advantage for immunoliposomal drug delivery. Although immunoliposomes that do not efficiently internalize have been reported to produce enhanced cytotoxicity *in vitro* and *in vivo,* these immunoliposomes apparently act by slowly releasing encapsulated drug while bound at the cell membrane (Ahmad and Allen, 1992; Ahmad *et al.*, 1993). In contrast, internalizing immunoliposomes can directly deliver drug intracellularly as well as release drug extracellularly, leading in principle to more efficient delivery of drug and enhanced cytotoxicity. Furthermore, internalizing immunoliposomes allow strategies in which therapeutic agents otherwise unable to reach intracellular sites of action can be delivered intracellularly.

Another exploitable aspect of MAb-mediated targeting of immunoliposomes is the potential contribution of the biological activity of the antibody itself. Monoclonal antibodies that have anticancer properties, such as growth factor receptor antagonism or induction of apoptosis, may enhance the cytotoxic effect of encapsulated drug.

B. Antibodies Directed against the HER2/*neu* (c-*erb*B-2) Oncogene Product

1. The HER2 Oncogene Product as a Target for Cancer Treatment

The *HER2* (c-*erb*B-2, *neu*) proto-oncogene appears to play an important role in the development and progression of many breast and other

cancers. *HER2* encodes $p185^{HER2}$ (ErbB-2), a 1255-amino acid, 185-kDa receptor tyrosine kinase (RTK) that is a member of the class I RTK family, along with the proteins encoded by the epidermal growth factor receptor (*EGFR*), *HER3* (*erb*B-3), and *HER4* (*erb*B-4) genes (for review, see Carraway and Cantley, 1994). HER2 overexpression occurs in 20–30% of breast cancers, most commonly via gene amplification, and is associated with poor prognosis for these patients (Slamon *et al.*, 1987, 1989). HER2 overexpression also occurs in ≥40% of cases of ductal carcinoma *in situ* (DCIS) of the breast, and up to 80% of comedo-type DCIS lesions, which are associated with higher risk of recurrence (VandeVijver *et al.*, 1988; Liu *et al.*, 1992). In addition to breast cancer, HER2 overexpression also occurs frequently in other malignant diseases, including ovarian cancer (Slamon *et al.*, 1989; Berchuck *et al.*, 1990), endometrial cancer (Berchuck *et al.*, 1991), non-small-cell lung cancer (Kern *et al.*, 1990), gastric cancer (Yokota *et al.*, 1988; Park *et al.*, 1989; Yonemura *et al.*, 1991), bladder cancer (Zhau *et al.*, 1990), and prostate cancer (Zhau *et al.*, 1992). Much experimental evidence indicates that HER2 overexpression directly contributes to transformation and tumor progression, and suggests that its prognostic significance arises from the particularly aggressive phenotype it confers (for review, see Hynes and Stern, 1994).

The HER2 receptor is a logical focus for the development of targeted cancer therapies. First, such therapies may be able to antagonize or interfere with this important mediator of tumor growth. Second, HER2 provides an ideal target antigen. It is a readily accessible cell surface receptor, and, when overexpressed, provides a means for immunotherapies to target the tumor population. In contrast, in normal adult tissues, HER2 occurs only at low levels in certain epithelial cell types (Press *et al.*, 1990). In addition, HER2 overexpression occurs relatively homogeneously within primary breast tumors, and is maintained at synchronous or metachronous metastatic sites, suggesting a continuous requirement for HER2 overexpression throughout the malignant process (Niehans *et al.*, 1993). This is in contrast to most other tumor-associated antigens, which are often heterogeneously expressed and/or can undergo downmodulation of expression without significantly affecting tumor growth.

2. *Anti-HER2 Monoclonal Antibodies*

A number of monoclonal antibodies directed against HER2 have been developed for use in various forms of cancer immunotherapy (for review, see Park *et al.*, 1992). The use of "naked" anti-HER2 monoclonal antibodies for immunotherapy potentially offers two distinct mechanisms of action against HER2-overexpressing tumors: first, the antiproliferative (cytostatic) effect that some anti-HER2 monoclonal antibodies exert against HER2-overexpressing cells, which appears to be mediated by partial activation of HER2-dependent signal transduction and/or HER2 receptor downregula-

tion; and second, the activation or facilitation of endogenous host immune effector functions against antibody-bound tumor cells, e.g., via antibody-dependent cellular cytotoxicity. One such antibody, muMab4D5, reacts specifically with an epitope on the extracellular domain of $p185^{HER2}$ (Fendly *et al.*, 1990), and inhibits the growth of HER2-overexpressing breast cancer cells *in vitro* (Lewis *et al.*, 1993) and in animal models (Park *et al.*, 1992). Treatment with muMAb4D5 also renders HER2-overexpressing breast cancer cells more sensitive to the cytotoxic action of cisplatin (Shepard *et al.*, 1991; Pietras *et al.*, 1994) and doxorubicin (Baselga *et al.*, 1994). A fully humanized version of this antibody, rhuMAbHER2, has been developed to retain these properties while reducing the potential for immunogenicity (Carter *et al.*, 1992). In a phase II clinical trial, treatment with rhuMAbHER2 alone was well tolerated and associated with objective antitumor responses in 12% of patients with metastatic breast cancer (Baselga *et al.*, 1996). In another phase II study, treatment of metastatic breast cancer patients with rhuMAbHER2 and cisplatin resulted in an objective response rate of 25% (Pegram *et al.*, 1995). Use of rhuMAbHER2 has entered phase III clinical trials for the treatment of advanced breast cancer in conjunction with chemotherapy.

In addition to the use of "naked" anti-HER2 monoclonal antibodies by themselves or in combination with chemotherapy, therapeutic strategies in which anti-HER2 monoclonal antibodies or antibody fragments are used to target potent anticancer effectors of HER2-overexpressing cells have been developed. These strategies include anti-HER2 immunotoxins (Batra *et al.*, 1992; Wels *et al.*, 1992), bispecific antibodies directed against the HER2 receptor as well as against lymphocytes or other immune effector cells (Shalaby *et al.*, 1992; Weiner *et al.*, 1993; Valone *et al.*, 1995), constructs linking an anti-HER2 antibody domain with a prodrug-activating enzyme for antibody-dependent enzyme-prodrug therapy (ADEPT) (Rodrigues *et al.*, 1995), intracellular anti-HER2 single-chain antibody (scFv) expressed via adenoviral gene transfer (Deshane *et al.*, 1995), and constructs linking an anti-HER2 antibody domain with a DNA-binding domain for gene delivery (Fominaya and Wels, 1996).

IV. Immunoliposome Design and Construction

A. Conjugation Strategies

To form an immunoliposome, antibody or antibody fragments are linked to the liposome surface. The linkage must be stable enough to resist dissociation *in vivo*, should not impair the antigen-binding properties of the antibody, and should not disrupt the liposome and encapsulated drug (Table I). Importantly, the linkage procedure must be simple, efficient, and economical.

Considerable work has been performed to optimize antibody conjugation to liposomes (Heath, 1987; Leserman and Machy, 1987; Ranade, 1989; Torchilin, 1994). The solution offered by nature itself is to incorporate hydrophobic domains into antibodies to allow tight association with biomembranes. Early attempts to use the natural hydrophobicity of immunoglobulins to associate with liposomes helped to establish the concept of immunoliposome targeting, but were impractical owing to the weakness of the antibody association with the lipid bilayer (Gregoriadis and Neerunjun, 1975). Currently immunoliposomes are produced by linkage of antibody to a hydrophobic "anchor" stably rooted in the lipid bilayer of the liposome, sometimes with a spacer "arm" between the antibody and the anchor. Hence, antibody conjugation involves multiple elements, each of which can be addressed by a variety of strategies.

1. Antibody

Development of monoclonal antibodies, recombinant MAbs and their fragments, and single-chain antibody fragments (scFvs) generated by phage-display libraries has greatly expanded the scope of antigen-seeking molecules for immunoliposomes. Intact MAbs provide bivalent interaction with the target; however, major disadvantages include larger size and the presence of the Fc region, which is associated with higher immunogenicity and recognition by macrophage Fc receptors. Although IgG has been the most common type of antibody used for immunoliposomes, reduced IgM has two thiol groups conveniently located in the Fc region, and has also been used in immunoliposomes (Hashimoto *et al.,* 1986b). Monoclonal antibody fragments such as Fab′ offer a number of important advantages over intact MAb. Although Fab′ can be generated enzymatically from intact antibody. Fab′ can now be obtained far more efficiently using cloned antibody genes and high-level expression of Fab′ fragments in *Escherichia coli* (up to 2 g/liter)(Carter *et al.,* 1996). Fab′ fragments lack the Fc region, and their smaller size and greater flexibility relative to intact MAbs entail a reduction in the effective diameter of the immunoliposome. The thiol group in the Fab′ hinge region provides a single specific site for covalent coupling to a thiol-reactive anchor, and ensures that the antigen-binding site is oriented away from the liposome (Martin and Papahadjopoulos, 1982; Park *et al.,* 1995). Single-chain Fv fragments are becoming increasingly available through phage-display library screening, can also be expressed efficiently, and have also been linked to immunoliposomes (Laukkanen *et al.,* 1994). Attachment of several different antibodies (antibody "cocktail") to the same liposome can be used to create immunoliposomes with multiple specificities.

2. Hydrophobic Anchor

Early studies used long-chain fatty acids, such as palmitic acid, coupled to antibody (Harsch *et al.,* 1981; Huang *et al.,* 1982; Weissig *et al.,* 1986).

More recent and much more frequently used anchors include phospholipids [phosphatidylethanolamine (PE), phosphatidylinositol (PI)] with modified head groups to accommodate covalent binding, which are then linked either directly to the antibody or to an additional linker such as streptavidin (Leserman and Machy, 1987; Torchilin, 1994). Interest in fatty acid anchors has revived with the introduction of recombinant antibodies containing a lipophilic domain, thus avoiding the necessity for chemical coupling to a separate hydrophobic anchor (Keinanen and Laukkanen, 1994; Laukkanen *et al.*, 1994).

3. *Linkage*

As discussed, antibody can be covalently or noncovalently linked to the hydrophobic anchor. Noncovalent linkages have included biotinylated antibody bound to avidin-containing liposomes (Phillips and Tsoukas, 1990), or to streptavidin, which is in turn linked to biotinylated PE in the liposome bilayer (Loughrey *et al.*, 1987). The extremely high binding constant of the avidin (streptavidin)–biotin complex, as well as the commercial availability of many biotinylated antibodies, make this a feasible alternative to covalent binding; however, the introduction of additional bulky and potentially immunogenic proteins on the liposome surface is clearly undesirable. Another noncovalent linkage between liposome and antibody utilizes polyhistidine sequences, which are frequently added to recombinant proteins to facilitate their purification: a terminal polyhistidine sequence added to recombinant antibody was attached to the lipid bilayer via coordination complex with bivalent nickel ions immobilized on a membrane-anchored amphiphilic chelator (Dietrich *et al.*, 1996).

To achieve covalent linkage between antibody and hydrophobic anchor, a variety of biochemical strategies have been used. The coupling chemistry is similar to that of protein immobilization and modification. The functional group on the antibody molecule reacts with an active group on a liposome-associated hydrophobic anchor, or vice versa. Amino groups of lysine side chains on the antibody can be coupled to liposome-associated *N*-glutaryl-phosphatidylethanolamine activated with water-soluble carbodiimide, to palmitic acid via *N*-hydroxysuccinimide ester, or to periodate-oxidized PI through a Schiff base, further reduced by borohydride to stable amine (Torchilin, 1994). Thiol groups of reduced antibody or antibody fragment can be coupled to liposomes via thiol-reactive anchors such as pyridylthiopropionyl-phosphatidylethanolamine (PDP-PE), which forms a disulfide bond (Martin *et al.*, 1981; Wolff and Gregoriadis, 1984), maleimido-functionalized PE (Martin and Papahadjopoulos, 1982; Park *et al.*, 1995), or *N*-iodoacetyl derivatives of PE (Wolff and Gregoriadis, 1984; Hashimoto *et al.*, 1986a), which form a stable thioether bond. Thiol-reactive chemistry gives better prediction of the linking position and less possibility of lysine modification in the antigen-binding site. A convenient single thiol group is

present in the hinge region of Fab′ fragments, or may be introduced into the antibody molecule by treatment with heterobifunctional reagents, homocysteine thiolactone, or iminothiolane (Trout's reagent) (Thomas *et al.*, 1994). Alternatively, the antibody may be activated for linkage to a functional group exposed on the liposome surface. For example, oxidation of carbohydrate moieties in the antibody produces dialdehydes that can react with liposome-incorporated PE-hydrazide to form stable hydrazone linkages (Chua *et al.*, 1984). An important consideration with all of these approaches is the presence of excess active groups that remain after the coupling reaction; quenching of these groups may be required to avoid nonspecific reactivity of the remaining active groups with cell surface (Kirpotin *et al.*, 1997).

4. Linkage and Liposome Formation

Another vital consideration concerns when to perform antibody conjugation in relation to liposome formation: i.e., linkage of antibody to preformed liposomes containing activated anchor vs liposome formation in the presence of an anchor-modified antibody. To ensure stable "rooting" of the hydrophobic anchor in the lipid bilayer of the liposome, it should be present during bilayer formation. Since antibodies are often sensitive to conditions used in liposome preparation (e.g., organic solvents, shear forces, and elevated temperature), the most common strategy has been first to prepare liposomes containing a hydrophobic anchor with an active head group (see Section IV,A,2). Antibody is then allowed to react with the anchor head group, and uncoupled protein is separated from the resulting immunoliposomes by dialysis or size-exclusion chromatography (Chua *et al.*, 1984; Leserman and Machy, 1987; Torchilin, 1994). An exception to this rule is afforded by preparation of immunoliposomes using the detergent dialysis method, in which antibody is first coupled to a hydrophobic anchor molecule, and then solubilized in the presence of bilayer lipids under mild conditions using dialyzable detergents, such as octylglucoside; the hydrophobic anchor attached to the antibody becomes integrated into the liposome bilayer during detergent removal. This method can be useful when the accessibility of attachment sites on the hydrophobic anchor may be compromised by other components (e.g, surface-grafted polymers such as PEG) of the preformed liposome. Long-circulating immunoliposomes modified with polyethylene glycol chains and targeted to infarcted myocardium were prepared by this method, using anti-myosin antibody linked to the hydrophobic anchor *N*-glutaryl-phosphatidylethanolamine via lysine residues (Torchilin, 1994).

5. Site of Attachment on Sterically Stabilized (Polyethylene Glycol-Modified) Liposomes

An important case is represented by long-circulating sterically stabilized liposomes, which contain up to 6–7 mol% (of total lipid) of surface-grafted PEG. As discussed, the pharmacologic advantages of sterically stabilized

liposomes make them particularly suitable for use as immunoliposomes; however, surface-grafted PEG chains can inhibit the interaction between antibody and target antigen (Klibanov *et al.*, 1991). This inhibition depends on the chain length of PEG (Mori *et al.*, 1991), and is more pronounced when Fab′ fragments are used (Kirpotin *et al.*, 1997). To avoid this problem, several methods have been developed to allow linkage of antibodies to the distal ends of the liposome-grafted PEG chains themselves (Hansen *et al.*, 1995; Zalipsky *et al.*, 1996). These methods were facilitated by the development of functionalized polyethylene glycol-1,2-distearoyl-3-*sn*-glycerophosphoethanolamine (PEG-DSPE) derivatives containing hydrazido, 2-pyridyldithio-propionamide bromacetamido, or carboxy functions on the free terminus of PEG. These derivatives have been coupled to antibody via periodate-oxidized carbohydrate moiety, thiol groups, or active esters derived from amino groups (Hansen *et al.*, 1995; Zalipsky *et al.*, 1996). The resulting immunoliposomes retained the properties of sterically stabilized liposomes *in vivo* (Allen *et al.*, 1995). Two novel anchors, *N*-maleimidomethylcyclohexylcarboxamido-polyethylene glycol-1,2-distearoyl-3-*sn*-glycerophosphoethanolamine (MMC-PEG-DSPEC) and *N*-maleimidopropionylcarboxamido-polyethylene glycol-1,2-distearoyl-3-*sn*-glycerophosphoethanolamine (MP-PEG-DSPE), were developed for conjugation of humanized recombinant anti-HER2 Fab′ fragments, resulting in sterically stabilized immunoliposomes with nearly quantitative conjugation yield, extremely low nonspecific binding *in vitro*, and long circulation time *in vivo* (Kirpotin *et al.*, 1997; and below). The use of DSPE in these PEG-containing anchors was important, since PEG-PE with shorter acyl chains tended to leave the bilayer under *in vivo* conditions (Parr *et al.*, 1994).

B. Anti-HER2 Immunoliposomes

1. Construction of Anti-HER2 Immunoliposomes

We have described the development of sterically stabilized anti-HER2 immunoliposomes (ILs), in which the anti-HER2 specificity and inhibitory activity of the humanized monoclonal antibody rhuMAbHER2 are combined with the pharmacokinetic and drug delivery advantages of sterically stabilized ("stealth") liposomes (Park *et al.*, 1995). This strategy attempts to increase the likelihood of successful immunoliposome-mediated drug delivery to HER2-overexpressing cells by (1) use of humanized Fab′ to lessen the potential for immunogenicity, by removal of murine antibody sequences and of the antibody Fc region, (2) development of internalizing immunoliposomes for efficient intracellular delivery of encapsulated agents, (3) use of Fab′ derived from rhuMAbHER2, which has intrinsic antiproliferative and chemotherapy-sensitizing activities, and developing immunoliposomes that retain these properties, (4) use of PEG-containing sterically stabilized liposomes for prolongation of circulation and selective tumor extravasation,

and (5) encapsulation of a cytotoxic agent (doxorubicin) that provides an additive or synergistic antitumor effect when combined with antibody treatment, and that can readily diffuse through tumors when released to provide "bystander" cytotoxicity.

We have produced several versions of anti-HER2 immunoliposomes (ILs) containing covalently linked rhuMAbHER2-Fab′ fragments and PEG_{1900} (polyethylene glycol)-containing phosphatidylethanolamine (PEG-PE) included in varying amounts (0–12 mol% of total phospholipid). Immunoliposomes were prepared by conjugation of "conventional" (phosphatidylcholine plus cholesterol; PC/Chol) or "sterically stabilized" (PC/Chol/PEG-PE) small unilamellar liposomes with rhuMAbHER2-Fab′ (Carter *et al.*, 1996). Unlike previous so-called conventional liposomes, the PC used was hydrogenated soy phosphatidylcholine (HSPC), allowing for more rigid drug encapsulation as well as longer circulation *in vivo*. Although the inclusion of PEG-PE in these small HSPC liposomes and immunoliposomes was not required for long circulation, the addition of PEG-PE did provide further resistance to clearance and correspondingly improved pharmacokinetic properties (see Section IV,B,4). Recombinant Fab′ fragments were used because of their efficient expression in *E. coli*, single site attachment, smaller size, and lack of Fc sequences. In addition, rhuMAbHER2-Fab′ has much less antiproliferative activity than intact rhuMAbHER2, and thus it was of interest to see whether attachment of rhuMAbHER2-Fab′ to liposomes could reconstitute this activity (see Section IV,B,3). Initially, Fab′ was conjugated directly to maleimido-phosphatidylethanolamine (M-PE), resulting in Fab′ directly linked to the liposome surface (Ls-Fab′; Fig. 1), and hence alongside or in parallel with PEG (if present) (Park *et al.*, 1995). We have also prepared immunoliposomes in which Fab′ was conjugated to maleimide-terminated PEG-PE (MMC-PEG-DSPE or MP-PEG-DSPE) (Kirpotin *et al.*, 1997), resulting in Fab′ linked to the distal end of PEG chains (PEG-Fab′; Fig. 1). Both procedures were highly efficient, typically yielding 50–100 Fab′ fragments per liposome particle.

2. *Binding and Internalization of Anti-HER2 Immunoliposomes*

Specific binding of anti-HER2 immunoliposomes to HER2-overexpressing cancer cells in culture has been determined by flow cytometric assay, competitive binding assay, and spectrofluorometric assay. A flow cytometric assay showed binding of anti-HER2 immunoliposomes to cells with HER2 overexpression (BT-474 and SK-BR-3 breast cancer cells, 10^5–10^6 receptors/cell), but no detectable binding to cells lacking HER2 overexpression (MCF-7 breast cancer cells, 10^4 receptors/cell) (Park *et al.*, 1995). A competitive binding assay, in which breast cancer cells were simultaneously incubated with ^{125}I-labeled rhuMAbHER2 and increasing concentrations of anti-HER2 immunoliposomes, showed single-component binding of immunoliposomes to SK-BK-3 and BT-474 cells. An approximation of binding affinity was

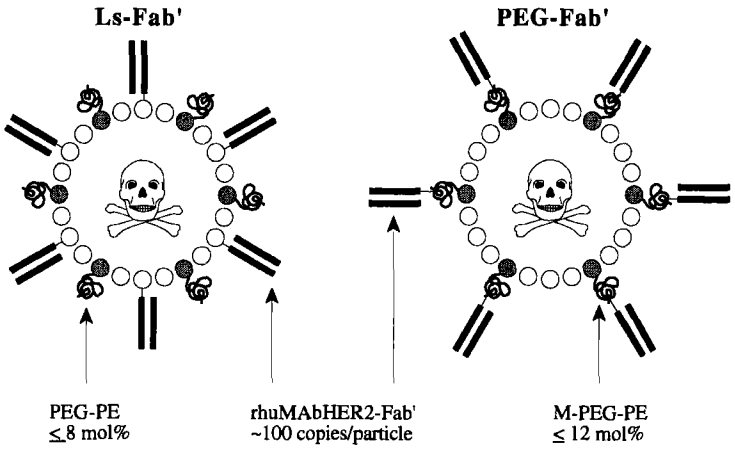

FIGURE 1 Schematic representation of anti-HER2 immunoliposomes (ILs), including immunoliposomes with Fab′ linked directly to the liposome surface (Ls-Fab′) or immunoliposomes with Fab′ linked to PEG (PEG-Fab′). M-PEG-PE, Maleimide-terminated PEG-PE [either *N*-maleimidomethylcyclohexylcarboxamido-PEG-DSPE (MMC-PEG-DSPE) or *N*-maleimidopropionylcarboxamido-PEG-DSPE (MP-PEG-DSPE)].

obtained via Scatchard analysis by assuming that Fab′ on immunoliposomes behaved as free ligand. With this model, immunoliposomes showed high-affinity binding comparable to that of free Fab′ or intact antibody. Binding affinity of immunoliposomes with the Ls-Fab′ linkage was reduced with increasing PEG content, indicating that high concentrations of PEG could interfere with Fab′ binding. Control liposomes lacking Fab′ showed negligible binding (Park *et al.*, 1995).

Monoclonal antibody rhuMAbHER2 is rapidly internalized by HER2-overexpressing tumor cells via receptor-mediated endocytosis (Sarup *et al.*, 1991). To assess whether anti-HER2 immunoliposomes internalize within target cells *in vitro*, a series of studies using conventional and confocal fluorescence microscopy of rhodamine-labeled immunoliposomes was performed. SK-BR-3 cells treated with rhodamine-labeled anti-HER2 immunoliposomes (Ls-Fab′ linkage, 0 mol% PEG) demonstrated intense foci of fluorescence both at the cell surface and intracellularly by 5 min (Park *et al.*, 1995), indicating rapid internalization. Treatment with anti-HER2 immunoliposomes containing high PEG concentrations (≥4 mol%) resulted in decreased intracellular fluorescence, indicating that the rate of internalization was inhibited by the PEG component of immunoliposomes containing the Ls-Fab′ linkage. Significantly, the inhibitory effect of PEG on internalization was not observed with immunoliposomes containing the PEG-Fab′ linkage rather than the Ls-Fab′ linkage: rapid internalization was observed regardless of PEG concentration (2–12 mol%). These results indicated that while PEG can inhibit binding and internalization of Ls-Fab′-linked immu-

noliposomes, shifting the Fab′ attachment site to the terminus of PEG (PEG-Fab′ linkage) prevents inhibition by PEG.

The specificity of immunoliposome uptake in SK-BR-3 cells was confirmed by preincubation of SK-BR-3 cells with rhuMAbHER2 at 10-fold excess over immunoliposomes, which totally blocked uptake of immunoliposomes but not of coadministered fluorescein isothiocyanate (FITC)-labeled transferrin (Kirpotin *et al.*, 1997). In addition, MCF-7 cells coincubated with immunoliposomes and transferrin showed efficient uptake of transferrin, but no detectable uptake of immunoliposomes.

For quantitative studies of immunoliposomes uptake, internalization, and intracellular drug delivery, immunoliposomes were loaded with pyranine (1-hydroxypyrene-3,6,8-trisulfonic acid; HPTS), a pH-sensitive fluorophore that can be readily encapsulated in liposomes (Daleke *et al.*, 1990). Intracellular disposition was determined by measurement of the pH-dependent fluorescence of HPTS, allowing quantitation of immunoliposome/HPTS in neutral compartments (surface bound) vs acidic compartments (endocytosis associated). Immunoliposomes were taken up rapidly into a neutral environment, with subsequent accumulation in acidic compartments, consistent with surface binding followed by receptor-mediated endocytosis (Kirpotin *et al.*, 1997). Total uptake of immunoliposomes in SK-BR-3 cells when present at saturating concentrations was 7.21 nmol of phospholipid per milligram of cell protein (SEM, 0.45), which corresponds to 23,000 immunoliposomes per cell. Selectivity of uptake was also extremely high: total uptake in non-HER2-overexpressing MCF-7 cells was <0.01 nmol of phospholipid per milligram of cell protein, a reduction of more than 700-fold. In addition, uptake of anti-HER2 immunoliposomes was 600-fold higher than uptake of nontargeted control liposomes in SK-BR-3 cells, but identical in MCF-7 cells. In immunoliposomes containing Fab′ linked at the liposome surface (Ls-Fab′ linkage), increasing concentrations of PEG-PE (2–10 mol%) reduced cell binding by up to 100-fold and endocytosis by 2-fold; however, when Fab′ fragments were instead conjugated to the termini of PEG-PE (PEG-Fab′ linkage), binding and endocytosis were unaffected by total PEG-PE content. Binding and endocytosis depended on quantity of conjugated Fab′, reaching a plateau at ~40 Fab′ per immunoliposome for binding and ~10 Fab′ per immunoliposome for internalization.

The intracellular disposition of immunoliposomes and their contents was also studied by electron microscopy, using immunoliposomes containing colliodal gold particles (Park *et al.*, 1995). SK-BR-3 cells treated with anti-HER2 immunoliposomes (0 mol% PEG) showed gold-laden immunoliposomes at the cell surface and intracellularly in coated pits, coated vesicles, endosomes, multivesicular bodies, and lysosomes. This intracellular distribution is consistent with internalization occurring via the coated pit pathway. However, observations were also made of immunoliposomes that appeared to fuse with the cell membrane, without coated pit formation. In addition,

gold particles were noted free within the cytoplasm, not associated with a membrane-bound organelle. Gold particles free within the cytoplasm might have resulted from fusion events between immunoliposomes and the cell membrane. Alternatively, they may have arisen following endocytosis, with escape of the encapsulated gold particles from the endosomal pathway. The ability of anti-HER2 immunoliposomes to internalize and efficiently deliver their contents intracellularly, including delivery outside of endolysosomal compartments, may be exploitable for the delivery of therapeutic genes. Anti-HER2 immunoliposomes may be particularly advantageous because of cytosolic delivery, thus reducing the potential for endosomal sequestration or lysosomal degradation that can accompany receptor-mediated endocytosis.

3. *Antiproliferative Effects of Anti-HER2 Immunoliposomes*

While the intact and bivalent antibody rhuMAbHER2 inhibits the growth of HER2-overexpressing breast cancer cells in monolayer culture, monovalent Fab and Fab′ fragments of rhuMAbHER2 are much less effective at inhibiting growth (O'Connell *et al.*, 1993). This observation suggested that cross-linking of HER2 receptors by bivalent antibody is important for the antiproliferative effect, and further suggested that liposomal anchoring of multiple rhuMAbHER2-Fab′ fragments might reconstitute antiproliferative activity comparable to that of intact rhuMAbHER2. The effect of empty anti-HER2 immunoliposomes on SK-BR-3 cells in monolayer culture was tested and compared to that of rhuMAbHER2 and rhuMAbHER2-Fab′ (Park *et al.*, 1995). Anti-HER2 immunoliposomes inhibited growth in a dose-dependent manner, indicating that empty anti-HER2 immunoliposomes retain the antiproliferative activity of rhuMAbHER2. Treatment with control liposomes lacking Fab′ did not significantly affect cell growth. Thus, anti-HER2 immunoliposomes possess intrinsic antiproliferative activity against HER2-overexpressing cells, and this unique property may act additively or synergistically with the cytotoxic activity of encapsulated drug.

4. *Pharmacokinetics of Anti-HER2 Immunoliposomes*

Pharmacokinetic (PK) studies of doxorubicin (dox)-loaded anti-HER2 immunoliposomes were performed in healthy, non-tumor-bearing adult rats. Dox-loaded immunoliposomes were prepared with 0–12 mol% PEG and with Fab′ linked to the liposome surface (Ls-Fab′) or to the distal end of PEG chains (PEG-Fab′). Doxorubicin levels obtained by sampling of venous blood following intravenous (i.v.) injection of immunoliposomes demonstrated greatly prolonged circulation of immunoliposomal dox. In comparison, blood and plasma dox levels following administration of free dox under these conditions were undetectable at 5 min, indicating a marked PK advantage for delivery by immunoliposomes. Pharmacokinetic analyses of the different versions of dox-loaded immunoliposomes revealed biexponen-

tial pharmacokinetics, with terminal plasma half-lives of approximately 10 hr (Table II) and mean residence times of 16–24 hr. These results are consistent with the PK of sterically stabilized liposomes, and are markedly superior to those of so-called "conventional" liposomes (Gabizon *et al.*, 1989). The addition of PEG to anti-HER2 immunoliposomes was associated with additional prolongation of mean residence time, but importantly was not required for long circulation. That is, immunoliposomes containing 0 mol% PEG still displayed a mean residence time of 16 hr. Anti-HER2 immunoliposomes and similarly constituted sterically stabilized liposomes lacking Fab′ showed similar plasma PK, indicating that the presence of Fab′ did not significantly increase clearance in normal, non-tumor-bearing rats.

To evaluate the integrity of dox-loaded anti-HER2 immunoliposomes in circulation, two-component PK studies were performed. For these studies, plasma PK of dox and of rhuMAbHER2-Fab′ were codetermined on identical plasma samples following a single i.v. injection of dox-loaded immunoliposomes . Levels of rhuMAbHER2-Fab′ were measured by enzyme-linked immunosorbent assay (ELISA), using HER2 extracellular domain (ECD)-coated wells for capture and horseradish peroxidate (HRP)-linked goat anti-human IgG for detection. Levels of rhuMAbHER2-Fab′ in plasma following immunoliposome administration indicated significantly prolonged circulation, in contrast to the relatively rapid clearance of free rhuMAbHER2-Fab′. As indicated in Table II, the terminal plasma half-life for rhuMAbHER2-Fab′ following immunoliposome administration was approximately 10 hr, as compared to 1–2 hr for free rhuMAbHER2-Fab′. Similarly, the terminal plasma half-life for dox in the same plasma samples following immunoliposome administration was also approximately 10 hr. These results indicate that dox-loaded immunoliposomes remain relatively stable in circulation, yielding equally long circulation times for both Fab′ and dox components, and suggesting negligible dissociation or drug leakage.

TABLE II Plasma Pharmacokinetics of Anti-HER2 Immunoliposomes in Rats[a]

Agent	*Terminal* $t_{1/2}$
Anti-HER2 immunoliposomes	
Doxorubicin component (Spectrophotometric assay)	10 hr
Anti-HER2 Fab′ component (ELISA)	10 hr
Free doxorubicin	<5 min
Free rhuMAbHER2-Fab′	1–2 hr

[a] Anti-HER2 immunoliposomes loaded with doxorubicin were administered i.v. via jugular vein catheter at a single dose of 5.0 μmol of total phospholipid (500 μg of doxorubicin), and plasma was collected serially via catheter for up to 48 hr postinjection. Pharmacokinetic analysis was performed using the ADAPT2 program.

5. Localization of Anti-HER2 Immunoliposomes to Tumors in Vivo

The biodistribution and tumor localization of dox-loaded anti-HER2 immunoliposomes were evaluated in an HER2-overexpressing tumor xenograft model. In this model, nude mice carrying established subcutaneous (s.c.) BT-474 tumor xenografts were treated with immunoliposomes by single intraperitoneal (i.p.) or i.v. injection, and tumor localization of dox determined by spectrofluorimetric assay of tissue extracts (Park et al., 1995). Twenty-four hours after i.p. injection, dox delivered by anti-HER2 immunoliposomes had accumulated within tumor xenografts, with significantly lower levels of doxorubicin found in surrounding muscle and in blood (Park *et al.,* 1995). However, we have subsequently observed that immunoliposomes administered i.p. in nude mice are erratically absorbed, resulting in highly variable systemic levels. When dox-loaded anti-HER2 immunoliposomes were administered by single i.v. (retroorbital) injection, dox attained consistently high levels in the blood, with a concentration of 6% of injected dose per gram of blood still present at 24 hr. This long circulation was consistent with formal pharmacokinetic studies performed in rats (see Section IV,B,4). High levels of dox were also observed in liver at 24 and 48 hr, consistent with its role in liposome clearance, with much reduced levels by 67 hr. Tumor localization was evident at 24 hr, with tumor-to-muscle and tumor-to-lung ratios of greater than 1. By 67 hr, the concentration of dox in tumor tissue was significantly higher than in all other tissues except liver. The tumor-to-blood ratio was greater than 22-fold.

Since anti-HER2 immunoliposomes produce efficient intracellular delivery of encapsulated agents to target cells *in vitro,* studies were performed to evaluate whether systemic treatment with anti-HER2 immunoliposomes results in intracellular delivery *in vivo,* using the NCF7/HER2 tumor xenograft-nude mouse model. The MCF7/HER2 cell line (MCF7 cells stably transfected with HER2) expresses high levels of HER2 *in vitro* and as xenografts in nude mice (10^6 receptors/cell). Anti-HER2 immunoliposomes loaded with gold particles were administered i.v. in nude mice containing s.c. MCF7/HER2 xenografts, and were visualized by light microscopy using the silver enhancement technique (Huang *et al.,* 1992a). These studies showed abundant accumulation of silver grains (indicating the presence of immunoliposomes) throughout tumor tissue, both in perivascular areas and within cellular regions of the tumor. Significantly, silver grains were frequently observed within the cytoplasm of individual tumor cells (Fig. 2). In contrast, treatment with control sterically stabilized liposomes, prepared identically to immunoliposomes but without Fab′, showed silver grains accumulating predominantly in the extracellular space of perivascular areas, consistent with previous reports of the tumor interstitial localization of sterically stabilized liposomes (Huang *et al.,* 1992a). Control liposomes,

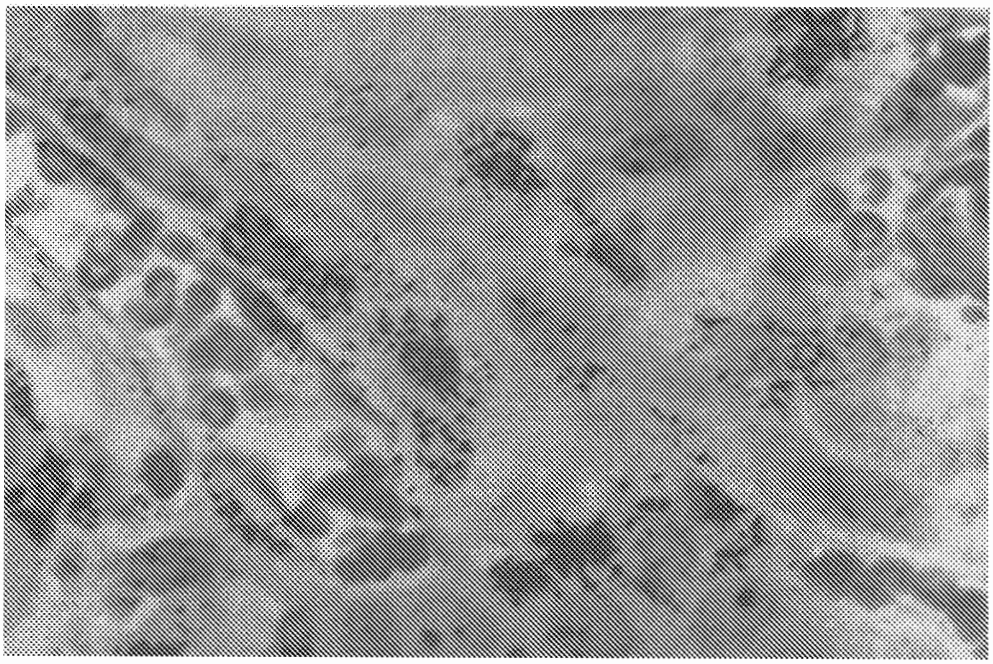

FIGURE 2 Localization of colloidal gold-loaded anti-HER2 immunoliposomes in tumor xenografts 24 hr following i.v. injection. Sterically stabilized immunoliposomes were prepared as described (Kirpotin *et al.*, 1997), labeled with entrapped colloidal gold as described (Huang *et al.*, 1992a), and injected i.v. in nude mice bearing established s.c. MCF7/HER2 tumor xenografts. Twenty-four hours after injection, mice were sacrificed and tumors excised. Tissues were fixed, embedded, and sections cut for silver enhancement (Huang *et al.*, 1992a). Silver grains, indicative of immunoliposome localization, can be seen throughout this representative section, including within the cytoplasm of individual tumor cells.

unlike immunoliposomes, did not produce any silver grains visible within individual tumor cells.

To confirm the intracellular localization of immunoliposomes *in vivo*, anti-HER2 immunoliposomes and control sterically stabilized liposomes (prepared exactly like immunoliposomes but without Fab') were radiolabeled with ^{67}Ga-diethylenetriamine pentaacetic acid (DTPA) chelates and administered by single i.v. injection in nude mice containing s.c. MCF7/HER2 xenografts. γ camera imaging of these mice 48 and 72 hr after treatment showed accumulation of immunoliposomes primarily in tumor xenografts and in the liver. Control sterically stabilized liposomes, which also preferentially localize to sites of tumor (see Section II), showed similar biodistribution but with less tumor localization. Similarly, γ counting of excised tumors after sacrifice at 72 hr confirmed high levels of ^{67}Ga accumulation in tumors following treatment with immunoliposomes (2.0% injected dose per gram of tissue) as well as with control liposomes (1.0% injected dose per gram of tissue). To evaluate intracellular delivery of ^{67}Ga to tumor xenografts *in vivo*, excised tumors were subjected to electron microscopic autoradiography. In tumors from mice treated with ^{67}Ga-loaded anti-HER2 immunoliposomes, autoradiographic grains signifying ^{67}Ga emission were frequently detected intracellularly within tumor cells (Fig. 3); autoradiographic grains were detected at or near the cell surface, within the cytoplasm, and within the nucleus. The intracellular distribution of ^{67}Ga in this *in vivo* study was consistent with the intracellular distribution observed by electron microscopy after colloidal gold delivery in SK-BR-3 cells *in vitro* (Park *et al.*, 1995); and in preceding discussion). In contrast, tumors from mice treated with ^{67}Ga-loaded control liposomes showed no intracellular ^{67}Ga localization.

C. Other Immunoliposomes

Immunoliposomes incorporating advances in liposome design have been developed for a variety of cancer treatment strategies. Sterically stabilized immunoliposomes directed against tumor-associated antigens have been used to target murine squamous cell lung cancer cells *in vitro* and *in vivo* (Ahmad and Allen, 1992; Ahmad *et al.*, 1993) (see subsequent discussion), and murine fibrosarcoma cells *in vitro* (Emanuel *et al.*, 1996). Immunoliposomes designed for intraperitoneal therapy have been used to target human ovarian cancer cells *in vitro* and in ascites fluid *in vivo* (Straubinger *et al.*, 1988; Nassander *et al.*, 1992, 1995).

In addition to targeting tumor-associated antigens, immunoliposomes have been developed to target endothelial cells. Huang and co-workers have developed sterically stabilized immunoliposomes directed against thrombomodulin, which is overexpressed by murine lung endothelium, for targeted

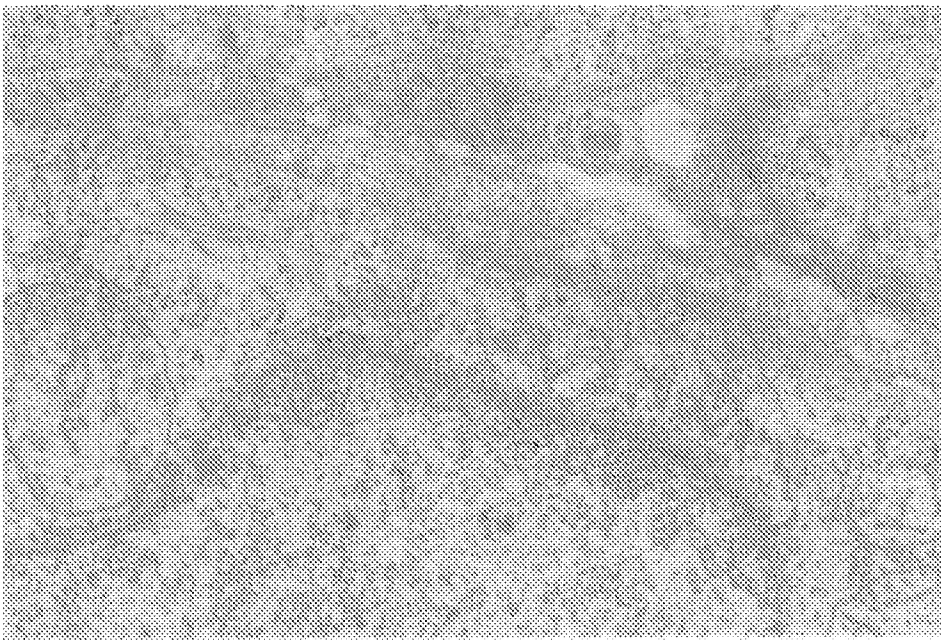

FIGURE 3 Intracellular localization in tumor xenograft cells *in vivo* of ^{67}Ga-loaded anti-HER2 immunoliposomes 72 hr following single i.v. injection. ^{67}Ga-loaded anti-HER2 immunoliposomes were injected i.v. in nude mice bearing established s.c. MCF7/HER2 tumor xenografts. Seventy-two hours after injection, mice were sacrificed and tumors excised. Tissues were fixed and ultrathin sections cut and processed for electron microscopic autoradiography. An autoradiographic grain can be seen in the juxtanuclear region of the cytoplasm. Original magnification: ×18,900.

delivery of a lipophilic prodrug of floxuridine (FUDR) to the lung (Mori *et al.*, 1993, 1995). These immunoliposomes were long circulating, and accumulated to high levels in mouse lung endothelium. Immunoliposome targeting of endothelial cells led to indirect delivery of prodrug to murine breast cancer cells within the lung in a mouse model of lung metastasis. In this strategy, immunoliposomes bound to thrombomodulin on endothelial cells subsequently release prodrug extracellularly, which then diffuses across the endothelium to nearby tumor cells. Strategies such as this, which target tumor-associated endothelium rather than the tumor cells themselves, although indirect, have the advantage of a highly accessible target cell population. Since tumor angiogenesis appears to be a critical determinant of tumor growth, immunoliposomes directed against tumor-associated endothelium could potentially be used to deliver cytotoxic agents to the endothelial cells.

V. Drug or Small-Molecule Delivery via Immunoliposomes

A. Doxorubicin

1. Doxorubicin-Loaded Immunoliposomes

Allen and co-workers have developed doxorubicin-loaded, sterically stabilized immunoliposomes that contain noncovalently linked murine MAb 174H.64, which is directed against an epitope associated with some squamous cell cancers (Ahmad and Allen, 1992; Ahmad *et al.*, 1993). These immunoliposomes specifically bound to murine squamous cell lung cancer cells expressing the epitope (although immunoliposome binding yielded only threefold higher uptake than control liposomes lacking antibody), and when loaded with doxorubicin were highly cytotoxic against these cells *in vitro* (Ahmad and Allen, 1992). *In vivo* therapy studies were performed in a murine model of nascent lung metastases: the same murine squamous cell lung cancer cells were administered i.v. in mice, where they begin to form lung metastases within 3 days, at which time dox-loaded immunoliposomes were administered i.v. Treatment with dox-loaded immunoliposomes produced a reduction in subsequent tumor burden, and prolongation of survival that was significantly superior to that associated with free doxorubicin or dox-loaded sterically stabilized liposomes without antibody.

2. Doxorubicin-Loaded Anti-HER2 Immunoliposomes

Anti-HER2 immunoliposome-mediated delivery of doxorubicin may represent a particularly advantageous strategy for the treatment of breast and other cancers with frequent HER2 overexpression. Increased tumor exposure to doxorubicin via immunoliposome delivery may be particularly beneficial in the case of HER2-overexpressing tumors, since HER2-overexpressing breast cancers appear to possess an especially steep dose–response relationship to doxorubicin-based therapy (Muss *et al.*, 1994). In addition, anti-HER2 immunoliposome delivery of doxorubicin provides a means of limiting the toxicity of doxorubicin in normal tissues. HER2 receptor expression is negligible in myocardium and among hematopoietic cells (Press *et al.*, 1990), the critical sites of doxorubicin toxicity in humans. Finally, the antiproliferative effect of anti-HER2 immunoliposomes themselves (derived from rhuMAbHER2) may act synergistically with doxorubicin, since rhuMAbHER2 augments the efficacy of doxorubicin (Baselga *et al.*, 1994), as well as cisplatin (Pietras *et al.*, 1994) and taxol (Baselga *et al.*, 1994).

We have evaluated the cytotoxicity of dox-loaded anti-HER2 immunoliposomes against HER2-overexpressing breast cancer cells and nonoverexpressing nonmalignant cells *in vitro* (Park *et al.*, 1995). Because of the efficient internalization of anti-HER2 immunoliposomes in HER2-overexpressing breast cancer cells, we reasoned that doxorubicin (dox) delivered by immunoliposomes might be just as effective at killing target cells *in vitro*

as free dox, a small (M_r 544), amphipathic molecule that readily passes through the cell membrane. Treatment of SK-BR-3 cells for 1 hr with dox-loaded anti-HER2 immunoliposomes yielded dose-dependent cytotoxicity equivalent to that of free dox, indicating that immunoliposomes delivered dox as efficiently as the rapid diffusion of free dox into cells *in vitro*. Doxorubicin-loaded anti-HER2 immunoliposomes were 10- to 30-fold more cytotoxic than dox-loaded immunoliposomes bearing irrelevant Fab'. The specificity of targeting was further confirmed by dox-loaded anti-HER2 immunoliposomes treatment of WI-38 cells, a nonmalignant lung fibroblast cell line that expresses minimal levels of HER2. While free dox produced significant dose-dependent cytotoxicity against WI-38 cells, dox-loaded anti-HER2 immunoliposomes demonstrated 20-fold less cytotoxicity, equivalent to dox-loaded irrelevant immunoliposomes.

Similar results were reported by Suzuki and co-workers, who developed their own doxorubicin-loaded anti-HER2 immunoliposome construct and have studied its cytotoxicity *in vitro* (Suzuki *et al.*, 1995). These small unilamellar immunoliposomes did not contain PEG, and were covalently coupled to intact murine MAb SER4. These dox-loaded anti-HER2 immunoliposomes showed slightly less cytotoxicity than free dox against SK-BR-3 cells *in vitro*, but much reduced cytotoxicity against non-HER2-overexpressing bladder cancer cells or peripheral blood mononuclear cells. When compared to dox-loaded immunoliposomes directed against gp125, a tumor-associated antigen abundantly present on SK-BR-3 cells, dox-loaded anti-HER2 immunoliposomes demonstrated significantly higher cytotoxicity than anti-gp125 immunoliposomes in SK-BR-3 cells despite lower total binding. Instead, cytotoxicity was correlated with internalization: anti-HER2 immunoliposomes were more efficiently internalized (90% at 1-hr incubation) than anti-gp125 immunoliposomes (60% at 1 hr). Interestingly, these investigators had previously shown that endocytosis of dox-loaded anti-gp125 immunoliposomes did not correlate with cytotoxicity (Suzuki *et al.*, 1994). Thus, these investigators concluded that dox-loaded anti-HER2 immunoliposomes can exploit efficient internalization to achieve effective intracellular drug delivery with enhanced cytotoxicity, while dox-loaded immunoliposomes directed against other antigens such as gp125 may not provide effective intracellular delivery, either because of less efficient endocytosis or different intracellular routing and processing.

We have performed a series of *in vivo* therapy studies using dox-loaded anti-HER2 sterically stabilized immunoliposomes in multiple tumor xenograft-nude mice models bearing established HER2-overexpressing tumors. Two independent versions of the BT-474 tumor xenograft–nude mouse model were used, one developed by our collaborators (J. Baselga and J. Mendelsohn) at Memorial Sloan-Kettering Cancer Center (New York, NY) and the other established by our collaborators (G. Colbern and H. Smith) at the Geraldine Brush Cancer Research Institute (San Francisco, CA). In

addition, therapy studies were performed using the MCF7/HER2 xenograft model described in Section IV,B,5 as well as an MDA-MB-453 xenograft model that expresses lower HER2 receptor levels ($\sim 10^5$ receptors per cell). In each study, experimental treatment was initiated 1–2 weeks after tumor implantation, at which time tumors were approximately 200–1000 mm^3 in volume. Immunoliposomes were administered at a total dox dose of 15 mg/kg, which was divided into weekly i.v. injection for a total of three doses. Therapeutic effects were compared to those of dox-loaded control liposomes, prepared exactly like immunoliposomes but without inclusion of Fab′ and given at the same dose and schedule. Additional control arms included treatment with free dox, which was given at its maximum tolerated dose (MTD) in these animals (7.5 mg/kg; see following discussion), and treatment with saline. Treatment with dox-loaded anti-HER2 immunoliposomes containing the 10% PEG/PEG-Fab′ linkage produced superior mean tumor growth suppression when compared with immunoliposomes containing the 2% PEG/Ls-Fab′ linkage (data not shown). With either immunoliposome construction, immunoliposomes produced significantly superior antitumor

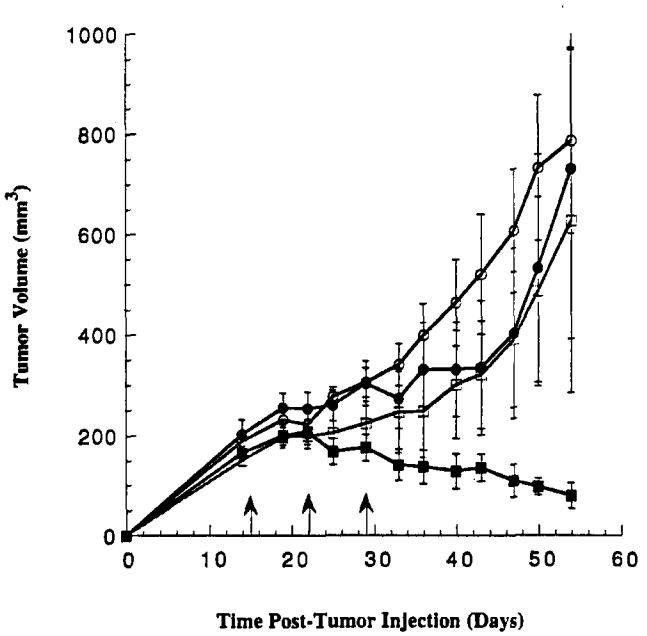

FIGURE 4 Antitumor efficacy of dox-loaded anti-HER2 immunoliposomes following i.v. injections in nude mice bearing established BT-474 tumor xenografts. Dox-loaded anti-HER2 immunoliposomes (■, anti-HER2 IL-dox) containing 2 mol% PEG were administered by i.v. (retroorbital) injection at a total doxorubicin dose of 15 mg/kg on days 15, 22, and 28 posttumor injection (arrows). Other groups included saline treated (○, control), free dox at its maximum tolerated dose (MTD) of 7.5 mg/kg (□), or dox-loaded liposomes (L-dox) containing 2 mol% PEG but no Fab′ at a total doxorubicin dose of 15 mg/kg (●). Data represent the mean (8 mice per group); bars, SEM.

efficacy than matched dox-loaded control liposomes, free dox, or saline (Fig. 4). Immunoliposome treatment yielded the greatest therapeutic efficacy in each of the animal models. In addition to regression of established tumors, treatment with immunoliposomes was occasionally associated with apparent cures (defined as complete regression of established tumor during the study without any regrowth up to time of sacrifice), which were not observed in any of the other treatment conditions (free dox, dox-loaded control sterically stabilized liposomes).

Treatment with anti-HER2 immunoliposomes resulted in no apparent acute toxicities or significant weight loss in the nude mice. In studies designed to determine MTD in nude mice, varying doses of free dox, dox-loaded liposomes, and dox-loaded anti-HER2 immunoliposomes were compared. The MTD was defined as the highest tested dose level that gave less than 20% weight loss and no treatment-related deaths. Free dox was associated with an MTD of 50 μg/dose over three doses (7.5 mg/kg). In contrast, dox-loaded anti-HER2 immunoliposomes and dox-loaded liposomes were both associated with a 2.5-fold increase in MTD, with an MTD of 100 μg dox/dose over four doses (20 mg/kg) or 125 μg of dox per dose over three doses (19 mg/kg). These results indicated that drug delivery via anti-HER2 immunoliposomes significantly increased the therapeutic index of dox, both by increasing antitumor efficacy and by reducing systemic toxicity. On the basis of these promising results, phase I clinical trials involving doxorubicin-loaded anti-HER2 immunoliposomes for the treatment of breast cancer are under consideration.

B. Other Cytotoxic Drugs

Although doxorubicin and other anthracyclines have been the most widely used drugs in liposomes and immunoliposomes, a number of other cytotoxic drugs have been encapsulated into immunoliposomes for targeted drug delivery. Immunoliposomes directed against placental alkaline phosphatase were used to deliver methotrexate to A431 cells *in vitro* (Jones and Hudson, 1993). As discussed above, sterically stabilized antithrombomodulin immunoliposomes have been used to deliver lipophilic prodrugs, including 3′,5′-O-dipalmitoyl-5-fluoro-2′-deoxyridine (dpFUDR), a prodrug of floxuridine (FUDR) (Mori *et al.*, 1993, 1995). In a mouse model of lung metastasis, dpFUDR-containing immunoliposomes were administered shortly after murine tumor cell injection, resulting in prlongation of median survival in the group of treated mice (Mori *et al.*, 1995). In another strategy, anti-carcinoembryonic antigen (CEA) immunoliposomes containing a ^{10}B-labeled compound were prepared and evaluated in an *in vitro* model of boron neutron capture therapy (Yanagie *et al.*, 1991).

VI. Macromolecule Delivery via Immunoliposomes

Immunoliposomes may prove useful as a tumor-targeted delivery system for a variety of anticancer agents, such as doxorubicin, by increasing tumor

exposure and reducing toxicity to normal cells and tissues. For certain applications, internalizing immunoliposomes may be particularly advantageous, such as for the delivery of agents that otherwise cannot readily gain intracellular access or that are susceptible to lysosomal degradation. Thus, potentially therapeutic macromolecules with intracellular sites of action (e.g., toxins) can in principle be encapsulated and delivered via internalizing immunoliposomes.

Several critical obstacles remain to be overcome for successful implementation of this strategy. First, macromolecular encapsulation must be efficient and reproducible. Methods of liposomal encapsulation, such as passive encapsulation, have in fact been developed for a number of therapeutic proteins. Use of these methods in conjunction with internalizing immunoliposome delivery may be feasible. Second, internalization must lead to release of the therapeutic agent in a biologically active state. Delivery to the endolysosomal compartment without escape into the cytoplasm or other intracellular site of action will obviously compromise any therapeutic effect, and for most proteins will result in degradation. For example, gelonin-loaded anti-HER2 immunoliposomes were able to efficiently deliver gelonin intracellularly in SK-BR-3 cells, but were not cytotoxic probably owing to gelonin remaining sequestered within the endocytic compartment (data not shown). However, certain proteins appear able to reach their sites of action following immunoliposome endocytosis; tumor necrosis factor (TNF) encapsulated in anti-CD4 immunoliposomes was cytotoxic *in vitro* against human T cell leukemia cells that had been TNF resistant (Morishige *et al.*, 1993).

VII. Nucleic Acid Delivery via Immunoliposomes

A. Delivery Systems for Cancer Gene Therapy

A number of strategies for the gene therapy of cancer have been proposed, and some of these have entered phase I clinical trials (for review, see Roth and Cristiano, 1997). Presently, *in vivo* gene therapy has been limited to locoregional routes of administration, typically by injection of vector directly into or around an identified tumor site. However, the clinical utility of such locoregional approaches, even if efficient gene transfer can be achieved, is extremely limited. Direct vector injection is unlikely to become an important modality for locoregional cancer treatment, in place of existing methods such as surgery or radiation therapy. Furthermore, in most cases of advanced cancer, direct injection of all actual or potential tumor sites in a patient is not usually feasible. Thus local gene therapy, while of scientific interest, is unlikely to become an important modality for cancer treatment or prevention. Ideally, *in vivo* gene therapy of cancer would involve systemic treatment to control or eradicate potentially all tumor cells, including cells at known and unknown metastatic sites.

To develop a feasible strategy for systemic *in vivo* gene therapy, what is needed is a vector or gene delivery system that is safe, nontoxic, stable in circulation, specifically targeted to tumor cells, and capable of mediating efficient gene transfer (Anderson, 1992; Vile and Russell, 1994). Current gene therapy vector technologies, which include modified viral vectors and cationic lipid complexes or liposomes, have not yet yielded vectors that satisfy all (or even most) of these requirements, and remain unsuitable for systemic gene therapy. Limitations of viral vectors include important safety concerns, the potential emergence of replication-competent virus, possible contaminating pathogens, induction of inflammation, and immunogenicity (Miller, 1992). Immunogenicity, in particular, is likely to be a critical obstacle to successful systemic gene therapy, as induction of a host immune response may severely compromise transduction efficiency as well as lead to additional toxicities. Since the efficiency of gene transfer is currently much less than 100% with any vector technology, it is likely that repeat administrations will be required to achieve gene transfer in a reasonable proportion of the tumor cell population.

Recombinant retroviral vectors have additional disadvantages, which include limited DNA insert size (<8 kb), potential for insertional mutagenesis, rapid complement-mediated inactivation following systemic administration, and difficulty in producing in high titers. This last problem has necessitated the local implantation of murine "producer cells" to release a greater amount of recombinant retroviral vector, rather than injection of the retroviral vector itself (Culver *et al.,* 1992). Retroviral vectors expressing ligand molecules on the viral envelope have been developed for tumor targeting (Han *et al.,* 1995). However, retroviral transduction is restricted to actively dividing cells (Miller *et al.,* 1990). This represents an important limitation in the treatment of most solid tumors, which typically have a low growth fraction and significant subpopulation of quiescent cells. Disadvantages of recombinant adenoviral vectors include its particularly high immunogenicity, as most patients are already seropositive for antibodies against the commonly used subgroup C adenovirus, and its lack of selectivity for tumor cells.

Lipid-based or liposomal gene delivery offers a number of potential advantages over viral vectors, particularly with regard to safety, immunogenicity, and ease of preparation. Debs and co-workers used cationic liposome–plasmid DNA complexes to achieve sustained reporter gene expression in multiple tissue sites following intravenous administration in mice (Zhu *et al.,* 1993). However, cationic lipid-based gene delivery technology must overcome problems of nonspecific reactivity and lack of tumor targeting. Molecular conjugate vectors have been developed to provide targeted delivery via attached ligand; these constructs contain a DNA-binding component, plasmid DNA, a ligand for receptor-mediated endocytosis, and additional components to provide subsequent escape from the endocytic path-

way. Although interesting, this approach is not yet suitable for systemic administration owing to problems with stability, immunogenicity, rapid clearance, and use of viral components (for review, see Michael and Curiel, 1994).

Immunoliposomes represent a potentially ideal gene delivery vehicle for the systemic gene therapy of cancer, provided they can be constructed so as to package plasmid DNA: retain favorable drug delivery properties, such as stability, long circulation, minimal nonspecific reactivity, and reduced immunogenicity; selectively deliver genes to tumor cells; and provide intracellular delivery that achieves reasonable gene expression.

B. Candidate Therapeutic Genes for Systemic Cancer Gene Therapy

An efficient and tumor-targeted immunoliposome vector suitable for systemic use would greatly improve the prospects for the gene therapy of cancer, and could be used to deliver many types of therapeutic genes, some examples, of which are discussed in the following sections.

1. Prodrug-Converting Enzyme Genes

Sometimes referred to as *suicide genes*, these genes have been used to subsequently activate cytotoxic drugs selectively in cells that have been transduced. For example, the herpes simplex virus thymidine kinase (HSVtk) gene, the most frequently used in gene therapy studies, converts the relatively nontoxic prodrug ganciclovir (GCV) to a phosphorylated metabolite that is highly cytocidal. This strategy has been used in the local treatment of gliomas, via direct implantation of retroviral-releasing producer cells into tumors, followed by subsequent i.v. GCV (Culver *et al.*, 1992). Since retroviral vectors only transduce dividing cells, tumor cells but not non-dividing normal cells will express HSVtk and so become susceptible to GCV. This treatment produced extensive tumor cell death in an animal model, even though only a small fraction of tumor cells actually expressed HSVtk. The mechanism for this phenomenon, sometimes referred to as the "bystander effect," has been attributed to toxic GCV metabolites moving from transduced cells via gap junctions to surrounding nontransduced cells (Ram *et al.*, 1993). Bystander toxicity may enable this strategy to produce significant tumor reduction even with suboptimal gene transfer efficiency. Stereotactic injection of retroviral vector-HSVtk producer cells into human gliomas is currently in phase I clinical trials (Oldfield *et al.*, 1993). A number of clinical studies of HSVtk gene therapy administered by other locoregional routes have now been approved by the Recombinant DNA Advisory Committee of the National Institutes of Health (NIH-RAC).

2. *Tumor Suppressor Genes*

Loss of function of the *p53* tumor suppressor gene by mutation and/or allelic loss occurs frequently in many types of human cancer, and appears to play a critical role in the pathogenesis of these diseases (for review, see Frebourg and Friend, 1993). Delivery of the wild-type *p53* gene to tumors lacking p53 function may be a useful therapeutic strategy, resulting in restoration of normal growth control and/or induction of apoptosis. For example, introduction of the wild-type *p53* gene in a colon cancer xenograft model has been shown to induce tumor regression due to apoptosis (Shaw *et al.*, 1992). In addition, introduction of the wild-type *p53* gene in an animal model of lung cancer produced moderately efficient gene transfer, which was associated with a disproportionately large antitumor effect consistent with a bystander effect (Fujiwara *et al.*, 1994). A recent report of a phase I clinical trial of *p53* gene therapy, which involved direct injection of endobronchial tumors of non-small-cell lung cancer with a retroviral vector containing the *p53* gene, described apoptosis and evidence of bystander effect following treatment (Roth *et al.*, 1996). Another locoregional *p53* gene strategy uses a modified adenoviral vector containing the wild-type *p53* gene, which is administered via hepatic artery infusion for the treatment of malignant liver tumors, including hepatocellular cancer and metastatic colorectal cancer (Bookstein *et al.*, 1996). In a rat model of orthotopic hepatocellular cancer, *p53* gene therapy via hepatic artery infusion markedly inhibited tumor progression. Formal toxicology studies demonstrated no significant p53-associated toxicities in animals treated either intravenously or by hepatic artery infusion; observed toxicities were tolerable and adenovirus related (data not shown). A clinical gene therapy protocol using this approach has been initiated at the University of California at San Francisco (UCSF).

3. *Immunoregulatory Genes*

A number of immunoregulatory genes have been proposed or are being included in gene therapy studies. Many of these strategies have the theoretical advantage that efficacy does not presuppose highly efficient gene transfer, as the resulting immune response may be effective against nontransduced tumor cells as well.

4. *Antisense Oligonucleotides*

The therapeutic use of antisense aptameric or triplex-forming oligonucleotides directed against oncogenes has been limited by their lack of stability *in vivo*, inefficient delivery to and uptake within tumor cells, and routing to lysosomes with resultant degradation (for review, see Calabretta, 1991). While their stability can be signifciantly improved by the use of derivatized nucleic acids, the problems of efficient cytoplasmic delivery remain. Immu-

noliposomes with the capacity for intracellular and cytoplasmic drug delivery represent a potentially advantageous delivery system for therapeutic oligonucleotides.

C. Strategies for the Development of Immunoliposomes for Gene Therapy

1. Immunoliposomes as a Targeted Gene Delivery System

It is possible to hypothesize that immunoliposome delivery of genes may produce specific and efficient expression of therapeutic genes within tumor cells, while avoiding many of the problems associated with current vector technology. A targeted gene delivery system of this kind may provide the means to achieve systemic gene therapy. Two type of immunoliposome–DNA construct designs can be envisioned: neutral immunoliposomes, with demonstrated long-circulating and tumor-localizing properties; and cationic immunoliposomes, in which neutral and cationic lipids are complexed with plasmid DNA, with further modification to block nonspecific reactivity and to allow inclusion of targeting antibody.

Neutral immunoliposomes, such as the sterically stabilized anti-HER2 immunoliposomes used to deliver doxorubicin (see Section V,A,2), can in principle be used to delivery DNA for systemic gene therapy. Indeed, anti-HER2 immunoliposomes possess highly desirable pharmacologic properties as gene carriers, including reproducibility of preparation, stability, long circulation, minimal reactivity with serum proteins, resistance to RES uptake, and ability to internalize and deliver contents cytoplasmically. However, efficient procedures for the loading of plasmid DNA into neutral liposomes or immunoliposomes have yet to be developed. Liposomes can be formed in the presence of concentrated solutions of supercoiled DNA to achieve encapsulation (Hoffman *et al.*, 1978; Fraley *et al.*, 1980; Wang and Huang, 1987). Although this method has been reported to be efficient, it is likely that highly efficient loading of plasmid DNA will require further technical developments beyond passive encapsulation. One approach may be to use polyamine polymers to condense DNA molecules for more efficient encapsulation (Arscott *et al.*, 1990; Plum *et al.*, 1990; Marquet and Houssier, 1991).

An alternative strategy to produce immunoliposome–DNA constructs is to package DNA within cationic liposomes or lipid complexes rather than neutral liposomes. These cationic liposomes can efficiently coat, via electrostatic interactions, DNA of virtually unlimited size. In addition, cationic liposomes appear to undergo fusion with the cell membrane, facilitating intracellular delivery of DNA (Felgner *et al.*, 1987), although the predominant entry pathway seems to involve endocytosis (Friend *et al.*, 1996). However, such cationic liposomes are limited by poor stability, high nonspecific reactivity, and lack of targeting. We were therefore interested in whether we could overcome the pharmacologic limitations of cationic

liposomes via structural modifications and addition of targeting antibody, while retaining their favorable properties. For example, we have developed formulations of cationic liposome–plasmid DNA complexes that are significantly more stable by manipulation of lipid composition, inclusion of PEG-PE, and condensation of plasmid DNA with polyamines (Hong *et al.*, 1997). These stable constructs showed high gene transfer efficiency *in vitro*, and in multiple tissues sites *in vivo* following systemic administration, with up to 1000-fold greater reporter gene expression than in previously published reports.

2. *In Vitro Gene Transfer Using Anti-HER2 Cationic Immunoliposomes*

To produce a targeted gene delivery vector, rhuMAbHER2-Fab′ fragments were conjugated covalently to PEG-PE on cationic liposomes (Fab′-PEG linkage), thus generating anti-HER2 cationic immunoliposome–DNA complexes (Park *et al.*, 1997). PEG-PE was included to reduce significantly the nonspecific reactivity of the cationic liposome component as well as to improve construct stability. Although cationic immunoliposome construction has yet to be optimized, anti-HER2 cationic immunoliposomes were prepared and tested for specific gene transfer *in vitro*. Cationic liposomes were prepared as described (Hong *et al.*, 1997), and loaded with an expression plasmid DNA containing the firefly luciferase (*lux*) gene as a reporter. Cationic liposomes yielded variable transfection in different cell types, including highly efficient transfection of SK-BR-3 cells. However, when cationic liposomes were prepared with the addition of PEG-PE to reduce nonspecific reactivity, the resulting PEG-containing cationic liposomes did yield significantly reduced Lux expression (17-fold) in SK-BR-3 cells. Next, rhuMAbHER2-Fab′ was conjugated to these PEG-containing cationic liposomes via M-PEG-PE (PEG-Fab′ linkage), thereby generating anti-HER2 cationic immunoliposomes for targeted gene delivery to HER2-overexpressing cells (Park *et al.*, 1997). Anti-HER2 cationic immunoliposomes mediated highly efficient transfection of SK-BR-3 cells: the addition of Fab′ was associated with an 18-fold increase in Lux expression as compared to PEG-containing cationic liposomes lacking Fab′. The specificity of immunoliposome-mediated transfection was confirmed by treatment of non-HER2-overexpressing MCF-7 cells with the same constructs. Unmodified cationic liposomes transfected MCF-7 cells with relatively low efficiency. Incorporation of PEG-PE inhibited transfection by four-fold. As expected, addition of rhuMAbHER2-Fab′ to PEG-containing cationic liposomes to form anti-HER2 cationic immunoliposomes failed to improve transfection in MCF-7 cells. These results suggest that the reactivity of cationic liposomes can be modulated by PEG-PE, and that the use of cationic immunoliposomes containing PEG-PE and specific Fab′ may then provide tumor-targeted gene transfer.

VIII. Conclusion

Successful development of immunoliposomes for targeted drug delivery will clearly require optimized immunoliposome design and construction. Critical parameters include (1) appropriate choice of target antigen, including expression pattern *in vivo*, cellular function, and presence of soluble antigen; (2) antibody, including reduced potential for immunogenicity, ability to promote internalization, and intrinsic biological activity; (3) antibody–liposome linkage, including stable attachment and specific attachment sites; (4) liposome composition and structure, including *in vivo* stability, long circulation, and ability to extravasate and penetrate at tumor sites; and (5) drug, including efficient encapsulation, ability to diffuse beyond the site of delivery, and usefulness in conjunction with target antigen and/or antibody.

Experience in manipulating these parameters to produce doxorubicin-loaded anti-HER2 immunoliposomes has resulted in an apparently optimized preparation that appears to have superior *in vitro* and *in vivo* therapeutic properties over free doxorubicin and nontargeted liposomes. Anti-HER2 immunoliposomes can deliver doxorubicin efficiently and specifically to HER2-overexpressing breast cancer cells while sparing nonoverexpressing normal cells, and, like sterically stabilized liposomes, are stable and long circulating *in vivo*. In HER2-overexpressing tumor xenograft–nude mouse models, anti-HER2 immunoliposomes localize in tumor tissue, deliver encapsulated agents intracellularly, and are associated with significantly increased antitumor cytotoxicity compared with free doxorubicin or doxorubicin-loaded sterically stabilized liposomes. In these animal models, delivery via doxorubicin-loaded anti-HER2 immunoliposomes greatly extends the therapeutic index of doxorubicin, both by increasing antitumor efficacy and by reducing systemic toxicity.

Although promising in animal models thus far, this new generation of immunoliposomes must still overcome questions regarding the therapeutic utility of immunoliposome-mediated drug delivery in cancer patients. Critical questions relating to immunoliposome biodistribution, tumor penetration, and immunogenicity are not fully evaluable in currently available animal models. On the basis of the preclinical experience with doxorubicin-loaded anti-HER2 immunoliposomes, targeted drug delivery by immunoliposomes may perhaps finally be ready for clinical evaluation in cancer patients.

In addition to targeted delivery of small molecule drugs, improvements in immunoliposome design and construction may lead to new therapeutic applications, such as gene therapy. Because of their advantageous properties of targeted intracellular delivery, along with new lipid composition enabling efficient DNA complex formation, immunoliposomes represent a potentially powerful strategy to achieve targeted gene delivery for the *in vivo* gene therapy of cancer.

Acknowledgments

The authors sincerely thank collaborating scientists Gail T. Colbern and Helene S. Smith (Geraldine Brush Cancer Research Institute, San Francisco, CA); Jose Baselga and John Mendelsohn (Memorial Sloan-Kettering Cancer Center, New York, NY); Gilbert-Andre Keller, William I. Wood, and Paul Carter (Genentech, Inc., South San Francisco, CA); and Weiwen Zhang and Yvonne S. Shao (UCSF, San Francisco, CA). This work was partially supported by grants from the SPORE Program of the National Cancer Institute and National Institutes of Health (P50-CA 58207-01); the U.S. Army Medical Research and Materiel Command (DAMD17-94-J-4195); and the American Society of Clinical Oncology Young Investigator Award (J.W.P) sponsored by the Don Shula Foundation.

References

Ahmad, I., and Allen, T. M. (1992). Antibody-mediated specific binding and cytotoxicity of liposome-entrapped doxorubicin to lung cancer cells *in vitro*. *Cancer Res.* **52**, 4817–4820.

Ahmad, I., Longenecker, M., Samuel, J., and Allen, T. M. (1993). Antibody-targeted delivery of doxorubicin entrapped in sterically stabilized liposomes can eradicate lung cancer in mice. *Cancer Res.* **55**, 1484–1488.

Allen, T. M., Brandeis, E., Hansen, C. B., Kao, G. Y., and Zalipsky, S. (1995). A new strategy for attachment of antibodies to sterically stabilized liposomes resulting in efficient targeting to cancer cells. *Biochim. Biophys. Acta* **1237**, 99–108.

Anderson, W. F. (1992). Human gene therapy. *Science* **256**, 808–813.

Arscott, P. G., Li, A.-Z., and Bloomfield, A. (1990). Condensation of DNA by trivalent cations. 1. Effects of DNA length and topology on the size and shape of condensed particles. *Biopolymers* **30**, 619–630.

Baselga, J., Norton, L., Shalaby, R., and Mendelsohn, J. (1994). Anti-HER2 humanized monoclonal antibody (MAb) alone and in combination with chemotherapy against breast carcinoma xenografts. *Proc. Am. Soc. Clin. Oncol.*, p. 63.

Baselga, J., Tripathy, D., Mendelsohn, J., Baughman, S., Benz, C. C., Dantis, L., Sklarin, N. T., Seidman, A. D., Hudis, C. A., Moore, J., Rosen, P. P., Twaddell, T., Henderson, I. C., and Norton, L. (1996). Phase II study of weekly intravenous recombinant humanized anti-p185^{HER2} monoclonal antibody in patients with HER/*neu*-overexpressing metastatic breast cancer. *J. Clin. Oncol.* **14**, 737–744.

Batra, J. K., Kasprzyk, P. G., Bird, R. E., Pastan, I., and King, C. R. (1992). Recombinant anti-*erb*B2 immunotoxins containing *Pseudomonas* exotoxin. *Proc. Natl. Acad. Sci. U.S.A.* **89**, 5867–5871.

Berchuck, A., Kamel, A., Whitaker, R., Kerns, B., Olt, G., Kinney, R., Soper, J. T., Dodge, R., Clarke-Pearson, D. L., Marks, P., McKenzie, S., Yin, S., and Bast, R. C. (1990). Overexpression of HER2/*neu* is associated with poor survival in advanced epithelial ovarian cancer. *Cancer Res.* **50**, 4087–4091.

Berchuck, A., Rodriguez, G., Kinney, R. B., Soper, J. T., Dodge, R. K., Clarke-Pearson, D. L., and Bast, R. C. (1991). Overexpression of HER-2/*neu* in endometrial cancer is associated with advanced stage disease. *Am J. Obstet. Gynecol.* **164**, 15–21.

Bookstein, R., Demers, W., Gregory, R., Maneval, D., Park, J. W., and Wills, K. (1996). p53 gene therapy *in vivo* of hepatocellular and liver-metastatic colorectal cancer. *Semin. Oncol.* **23**, 66–77.

Calabretta, B. (1991). Inhibition of protooncogene expression by antisense oligodeoxynucleotides: Biological and therapeutic implications. *Cancer Res.* **51**, 4505–4510.

Carraway, K. L., and Cantley, L. C. (1994). A neu acquaintance for ErbB3 and ErbB4: A role for receptor heterodimerization in growth signaling. *Cell* **78**, 5–8.

Carter, P., Presta, L., Gorman, C. M., Ridgway, J. B. B., Henner, D., Wong, W. L. T., Rowland, A. M., Kotts, C., Carver, M. E., and Shepard, H. M. (1992). Humanization of an anti-p185HER2 antibody for human cancer therapy. *Proc. Natl. Acad. Sci. U.S.A.* **89**, 4285–4289.

Carter, P., Rodrigues, M. L., Park, J. W., and Zapata, G. (1996). Preparation and uses of Fab' fragments from *E. coli*. *In* "Antibody Engineering: A Practical Approach" (H. H. R. McCafferty and D. J. Chiswell, eds.), pp. 291–308. IRL Press, Oxford, UK.

Chua, M. M., Fan, S. T., and Karush, F. (1984). Attachment of immunoglobulin to liposomal membrane via protein carbohydrate. *Biochim. Biophys. Acta* 800, 291–300.

Culver, K. W., Ram, Z., Wallbridge, S., Ishii, H., Oldfield, E. H., and Blaese, R. M. (1992). *In vivo* gene transfer with retroviral vector-producer cells for treatment of experimental brain tumors. *Science* **256**, 1550–1552.

Daleke, D. L., Hong, K., and Papahadjopoulos, D. (1990). Endocytosis of liposomes by macrophages: Binding, acidification and leakage of liposomes monitored by a new fluorescence assay. *Biochim. Biophys. Acta* **1024**, 352–366.

Deshane, J., Siegal, G. P., Alvarez, R. D., Wang, M. H., Feng, M., Cabrera, G., Liu, T., Kay, M., and Curiel, D. T. (1995). Targeted tumor killing via an intracellular antibody against erbB-2. *J. Clin. Invest.* **96**, 2980–2989.

Dietrich, C., Boscheinen, O., Scharf, K.-D., Schmitt, L., and Tampe, R. (1996). Functional immobilization of a DNA-binding protein at a membrane interface via histidine tag and synthetic chelator lipids. *Biochemistry* **35**, 1100–1105.

Emanuel, N., Kedar, E., Bolotin, E. M., Smorodinsky, N. I., and Barenholz, Y. (1996). Preparation and characterization of doxorubicin-loaded sterically stabilized immunoliposomes. *Pharm. Res.* **13**, 352–359.

Felgner, P. L., Gadek, T. R., Holm, M., Roman, R., Chan, H. W., Wenz, M., Northrop, J. P., Ringold, G. M., and Danielsen, M. (1987). Lipofection: A highly efficient, lipid mediated DNA-transfection procedure. *Proc. Natl. Acad. Sci. U.S.A.* **84**, 7413–7417.

Fendly, B. M., Winget, M., Hudziak, R. M., Lipari, M. T., Napier, M. A., and Ullrich, A. (1990). Characterization of murine monoclonal antibodies reactive to either the human epidermal growth factor receptor or HER2/*neu* gene product. *Cancer Res.* **50**, 1550–1558.

Fominaya, J., and Wels, W. (1996). Target cell-specific DNA transfer mediated by a chimeric multidomain protein: Novel non-viral gene delivery system. *J. Biol. Chem.* **371**, 1–9.

Fraley, R., Subramani, S., Berg, P., and Papahadjopoulos, D. (1980). Introduction of liposome-encapsulated SV40 DNA into cells. *J. Biol. Chem.* **255**, 10431–10435.

Frebourg, T., and Friend, S. H. (1993). The importance of p53 gene alterations in human cancer: Is there more than circumstantial evidence? *J. Natl. Cancer Inst.* **85**, 1554–1557.

Friend, D. S., Papahadjopoulos, D., and Debs, R. J. (1996). Endocytosis and intracellular processing accompanying transfection mediated by cationic liposomes. *Biochim. Biophys. Acta* **1278**, 41–50.

Fujiwara, T., Cai, D. W., Georges, R. N., Mukhopadhyay, T., Grimm, E. A., and Roth, J. A. (1994). Therapeutic effect of a retroviral wild-type p53 expression vector in an orthotopic lung cancer model. *J. Natl. Cancer Inst.* **86**, 1458–1462.

Gabizon, A., and Papahadjopoulos, D. (1988). Liposome formulations with prolonged circulation time in blood and enhanced uptake by tumors. *Proc. Natl. Acad. Sci. U.S.A.* **85**, 6949–6953.

Gabizon, A., Shiota, R., and Papahadjopoulos, D. (1989). Pharmacokinetics and tissue distribution of doxorubicin encapsulated in stable liposomes with long circulation times. *J. Natl. Cancer Inst.* **81**, 1484–1488.

Gregoriadis, G. (1976). The carrier potential of liposomes in biology and medicine. *N. Engl. J. Med.* **295**, 704–710.

Gregoriadis, G., and Neerunjun, E. D. (1975). Homing of liposomes to target cells. *Biochem. Biophys. Res. Commun.* **65**, 537–544.

Han, X., Kasahara, N., and Kan, Y. W. (1995). Ligand-directed retroviral targeting of human breast cancer cells. *Proc. Natl. Acad. Sci. U.S.A.* **92**, 9747–9751.

Hansen, C. B., Kao, G. Y., Moase, E. H., Zalipsky, S., and Allen, T. M. (1995). Attachment of antibodies to sterically stabilized liposomes: Evaluation, comparison and optimization of coupling procedures. *Biochim. Biophys. Acta* **1239**, 133–144.

Harsch, M., Walther, P., Weder, H. G., and Hengartner, H. (1981). Targeting of monoclonal antibody-coated liposomes to sheep red blood cells. *Biochem. Biophys. Res. Commun.* **103**, 1069–1076.

Hashimoto, K., Loader, J. E., and Kinsky, S. C. (1986a). Iodoacetylated and biotinylated liposomes: Effect of spacer length on sulfhydryl ligand binding and avidin precipitibility. *Biochim. Biophys. Acta* **856**, 556–565.

Hashimoto, Y., Sugawara, M., Kamiya, T., and Suzuki, S. (1986b). Coating of liposomes with subunits of monoclonal IgM antibody and targeting of the liposomes. *In* "Methods in Enzymology" (J. J. Langone and H. Van Vunakis, eds.), Vol. 121, pp. 817–828. Academic Press, New York.

Heath, T. D. (1987). Covalent attachment of proteins to lipopsomes. *In* "Methods in Enzymology" (K. J. Widder and R. Green, eds.), Vol. 149, pp. 111–119. Academic Press, Orlando, Florida.

Hoffman, R. M., Margolis, L. B., and Bergelson, L. D. (1978). Binding and entrapment of high molecular weight DNA by lecithin liposomes. *FEBS Lett.* **93**, 365–368.

Hong, K., Zheng, W., Baker, A., and Papahadjopoulos, D. (1997). Stabilization of cationic liposome–plasmid DNA complexes by polyamines and poly(ethylene glycol)-phospholipid conjugates for efficient *in vivo* gene delivery. *FEBS Lett.* **400**, 233–237.

Huang, A., Tsao, Y. S., Kennel, S., and Huang, L. (1982). Characterization of antibody covalently coupled to liposomes. *Biochim. Biophys. Acta* **716**, 140–150.

Huang, S. K., Lee, K. D., Hong, K., Friend, D. S., and Papahadjopoulos, D. (1992a). Microscopic localization of sterically stabilized liposomes in colon carcinoma-bearing mice. *Cancer Res.* **52**, 5135–5143.

Huang, S. K., Mayhew, E. M., Gilani, S., Lasic, D. D., Martin, F. J., and Papahadjopoulos, D. (1992b). Pharmacokinetics and therapeutics of sterically stabilized liposomes in mice bearing C-26 colon carcinoma. *Cancer Res.* **52**, 6774–6781.

Hynes, N. E., and Stern, D. F. (1994). The biology of *erb*B-2/*neu*/HER-2 and its role in cancer. *Biochim. Biophys. Acta* **1198**, 165–184.

Jones, M. N., and Hudson, M. J. H. (1993). The targeting of immunoliposomes to tumour cells (A431) and the effects of encapsulated methotrexate. *Biochim. Biophys. Acta* **1152**, 231–242.

Keinanen, K., and Laukkanen, M.-L. (1994). Biosynthetic lipid-tagging of antibodies. *FEBS Lett.* **346**, 123–126.

Kern, J. A., Schwartz, D. A., Nordberg, J. E., Weiner, D. B., Greene, M. I., Torney, L., and Robinson, R. A. (1990). p185*neu* expression in human lung adenocarcinomas predicts shortened survival. *Cancer Res.* **50**, 5184–5191.

Kirpotin, D., Park, J. W., Hong, K., Zalipsky, S., LI, W. L., Carter, P., Benz, C. C., and Papahadjopoulos, D. (1997). Sterically stabilized anti-HER2 immunoliposomes: Design and targeting to human breast cancer cell *in vitro*. *Biochemistry* **36**, 66–75.

Klibanov, A. L., Maruyama, K., Kecklerberg, A. M., Torchilin, V. P., and Huang, L. (1991). Activity of amphipathic poly(ethylene glycol) 5000 to prolong the circulation time of liposomes depends on the liposome size and is unfavorable for immunoliposome binding to target. *Biochim. Biophys. Acta* **1062**, 142–148.

Lasic, D. D., and Martin, F. J. (1995). "Stealth Liposomes." CRC Press, Boca Raton, Florida.

Lasic, D. D., and Papahadjopoulos, D. (1995). Liposomes revisited. *Science* **267**, 1275–1276.

Laukkanen, M.-L., Alfthan, K., and Keinanen, K. (1994). Functional immunoliposomes harboring a biosynthetically lipid-tagged single-chain antibody. *Biochemistry* **33**, 11664–11670.

Leserman, L., and Machy, P. (1987). Ligand targeting of liposomes. *In* "Liposomes: From Biophysics to Therapeutics" (M. J. Ostro, ed.), pp. 157–194. Dekker, New York.

Lewis, G. D., Figari, I., Fendly, B., Wong, W. L., Carter, P., Gorman, C., and Shepard, H. M. (1993). Differential responses of human tumor cell lines to anti-p185HER2 monoclonal antibodies. *Cancer Immunol. Immunother.* **37**, 255–263.

Liu, E., Thor, A., He, M., Barcos, M., Ljung, B.-M., and Benz, C. (1992). The *HER2* (c-*erbB*-2) oncogene is frequently amplified in *in situ* carcinomas of the breast. *Oncogene* **7**, 1027–1032.

Loughrey, H., Bally, M. B., and Cullis, P. R. (1987). A non-covalent method of attaching antibodies to liposomes. *Biochim. Biophys. Acta* **901**, 157–160.

Marquet, R., and Houssier, C. (1991). Thermodynamics of cation-induced DNA condensation. *J. Biomol. Struct. Dyn.* **9**, 159–167.

Martin, F. J., and Papahadjopoulos, D. (1982). Irreversible coupling of immunoglobulin fragments to preformed vesicles: An improved method for liposome targeting. *J. Biol. Chem.* **257**, 286–288.

Martin, F. J., Hubbell, L. W., and Papahadjopoulos, D. (1981). Immunospecific targeting of liposomes to cells: A novel and efficient method for covalent attachment of Fab′ fragments via disulfide bonds. *Biochemistry* **20**, 4429–4238.

Michael, S. I., and Curiel, D. T. (1994). Strategies to achieve targeted gene delivery via the receptor-mediated endocytosis pathway. *Gene Ther.* **1**, 223–232.

Miller, A. D. (1992). Human gene therapy comes of age. *Nature (London)* **357**, 455–460.

Miller, D. G., Adam, M. A., and Miller, A. D. (1990). Gene transfer by retrovirus vectors occurs only in cells that are actively replicating at the time of infection. *Mol. Cell. Biol.* **10**, 4239–4242.

Mori, A., Klibanov, A. L., Torchilin, V. P., and Huang, L. (1991). Influence of the steric barrier of amphipathic poly(ethylene glycol) and ganglioside GM1 on the circulation time of liposomes and on the target binding of immunoliposomes *in vivo*. *FEBS Lett.* **284**, 263–266.

Mori, A., Kennel, S. J., and Huang, L. (1993). Immunotargeting of liposomes containing lipophilic antitumor prodrugs. *Pharm. Res.* **10**, 507–514.

Mori, A., Kennel, S. J., Waalkes, M. van B., Scherphof, G. L., and Huang, L. (1995). Characterization of organ-specific immunoliposomes for delivery of 3′,5′-O-dipalmitoyl-5-fluoro-2′-deoxyridine in a mouse lung-metastasis model. *Cancer Chemother. Pharmacol.* **35**, 447–456.

Morishige, H., Ohkuma, T., and Kaji, A. (1993). *In vitro* cytostatic effect of TNF (tumor necrosis factor) entrapped in immunoliposomes on cells normally insensitive to TNF. *Biochim. Biophys. Acta* **1151**, 59–68.

Muss, H. B., Thor, A. D., Berry D. A., Kute, T., Liu, E. T., Koerner, F., Cirrincione, C. T., Budman, D. R., Wood, W. C., Barcos, M., and Henderson, I. C. (1994). c-*erb*B-2 expression and response to adjuvant chemotherapy in women with node-positive early breast cancer. *N. Engl. J. Med.* **330**, 1260–1266.

Nassander, U. K., Steerenberg, P. A., Poppe, H., Storm, G., Poels, L. G., Jong, W. H. D., and Crommelin, D. J. A. (1992). *In vivo* targeting of OV-TL 3 immunoliposomes to ascitic ovarian carcinoma cells (OVCAR-3) in athymic nude mice. *Cancer Res.* **52**, 646–653.

Nassander, U. K., Steerenberg, P. A., Jong, W. H. D., Overveld, W. O. W. M. V., Boekhorst, C. M. E. T., Poels, L. G., Jap, P. H. K., and Storm, G. (1995). Design of immunoliposomes directed against human ovarian carcinoma. *Biochim. Biophys. Acta* **1235**, 126–139.

Niehans, G. A., Singleton, T. P., Dykoski, D., and Kiang, D. T. (1993). Stability of HER-2/*neu* expression over time and at multiple metastatic sites. *J. Natl. Cancer Inst.* **85**, 1230–1235.

O'Connell, R. P., Carter, P., Presta, L., Eigenbrot, C., Covarrubias, M., Snedecor, B., Speckart, R., Blank, G., Vetterlein, D., and Kotts, C. (1993). Characterization of humanized anti-

p185HER2 antibody Fab fragments produced in *E. coli*. *In* "Protein Folding *in Vivo* and *in Vitro*" (J. L. Cleland, ed.), pp. 218–239. American Chemical Society, Washington, D.C.

Oldfield, E. H., Ram, Z., Culver, K. W., and Blaese, R. M. (1993). Clinical protocol: Gene therapy for the treatment of brain tumors using intra-tumoral transduction with the thymidine kinase gene and intravenous gancyclovir. *Hum. Gene Ther.* **4**, 39–69.

Papahadjopoulos, D., Allen, T. M., Gabizon, A., Mayhew, E., Matthay, K., Huang, S. K., Lee, K. D., Woodle, M. C., Lasic, D. D., Redemann, C., and Martin, F. J. (1991). Sterically stabilized liposomes: Improvements in pharmacokinetics and antitumor therapeutic efficacy. *Proc. Natl. Acad. Sci. U.S.A.* **88**, 11460–11464.

Park, J.-B., Rhim, J. S., Park, S.-C., Kimm, S.-W., and Kraus, M. H. (1989). Amplification, overexpression, and rearrangement of the *erb*B-2 proto-oncogene in primary human stomach carcinomas. *Cancer Res.* **49**, 6605–6609.

Park, J. W., Stagg, R., Lewis, G. D., Carter, P., Maneval, D., Slamon, D. J., Jaffe, H., and Shepard, H. M. (1992). Anti-p185HER2 monoclonal antibodies: Biological properties and potential for immunotherapy. *In* "Genes, Oncogenes, and Hormones: Advances in Cellular and Molecular Biology of Breast Cancer" (R. B. Dickson and M. E. Lippman, eds.), pp. 193–211. Kluwer Academic Publishers, Boston.

Park, J. W., Hong, K., Carter, P., Asgari, H., Guo, L. Y., Keller, G. A., Wirth, C., Shalaby, R., Kotts, C., Wood, W. I., Papahadjopoulos, D., and Benz, C. C. (1995). Development of anti-p185HER2 immunoliposomes for cancer therapy. *Proc. Natl. Acad. Sci. U.S.A.* **92**, 1327–1331.

Park, J. W., Hong, K., Zheng, W., Benz, C. C., and Papahadjopoulos, D. (1997). Development of liposome- and anti-HER2 immunoliposome-plasmid complexes for efficient and selective gene delivery. *Proc. Amer. Assoc. Cancer Res.* **38**, 342.

Parr, M. J., Ansell, S. M., Choi, L. S., and Cullis, P. R. (1994). Factors influencing the retention and chemical stability of poly(ethylene glycol)–lipid conjugates incorporated in large unilamellar vesicles. *Biochim. Biophys. Acta* **1195**, 21–30.

Pegram, M., Lipton, A., Pietras, R., Hayes, D., Weber, B., Baselga, J., Tripathy, D., Twaddell, T., Glaspy, J., and Slamon, D. (1995). Phase II study of intravenous recombinant humanized anti-p185 HER-2 monoclonal antibody (rhuMAb HER-2) plus cisplatin in patients with HER-2/*neu* overexpressing metastatic breast cancer. *Proc. Am. Soc. Clin. Oncol.* **14**, 106.

Phillips, N. C., and Emili, A. (1991). Immunogenicity of immunoliposomes. *Immunol. Lett.* **30**, 291–296.

Phillips, N. G., and Tsoukas, C. (1990). Immunoliposome targeting to CD4+ cells in human blood. *Cancer Detect. Prev.* **14**, 383–390.

Phillips, N. C., Gagne, L., Tsoukas, C., and Dahman, J. (1994). Immunoliposome targeting to murine CD4+ leucocytes is dependent on immune status. *J. Immunol.* **152**, 3168–3174.

Pietras, R. J., Fendly, B. M., Chazin, V. R., Pegram, M. D., Howell, S. B., and Slamon, D. J. (1994). Antibody to HER-2/*neu* receptor blocks DNA repair after cisplatin in human breast and ovarian cancer cells. *Oncogene* **9**, 1829–1838.

Plum, G. E., Arscott, P. G., and Bloomfield, V. A. (1990). Condensation of DNA by trivalent cations. 2. Effects of cation structure. *Biopolymers* **30**, 631–643.

Press, M. F., Cordon-Cardo, C., and Slamon, D. J. (1990). Expression of the HER-2/*neu* proto-oncogene in normal human adult and fetal tissues. *Oncogene* **5**, 953–962.

Ram, Z., Culver, K. W., Walbridge, S., Blaese, R. M., and Oldfield, E. H. (1993). *In situ* retroviral mediated gene transfer for the treatment of brain tumors in rats. *Cancer Res.* **53**, 83–88.

Ranade, V. (1989). Drug delivery systems. 1. Site-specific drug delivery using liposomes as carriers. *J. Clin. Pharmacol.* **29**, 685–694.

Rodrigues, M. L., Presta, L. G., Kotts, C. E., Wirth, C., Mordenti, J., Osaka, G., Wong, W. L., Nuijens, A., Blackburn, B., and Carter, P. (1995). Development of a humanized disulfide-

stabilized anti-p185HER2 Fv-β-lactamase fusion protein for activation of a cephalosporin doxorubicin prodrug. *Cancer Res.* **55**, 63–70.

Roth, J. A., and Cristiano, R. J. (1997). Gene therapy for cancer: What have we done and where are we going? *J. Natl. Cancer Inst.* **89**, 21–39.

Roth, J. A., Nguyen, D., Lawrence, D. D., Kemp, B. L., Carrasco, C. H., Ferson, D. Z., Hong, W. K., Komaki, R., Lee, J. J., Nesbitt, J. C., Pisters, K. M. W., Putnam, J. B., Schea, R., Shin, D. M., Walsh, G. L., Dolormente, M. M., Han, C.-I., Martin, F. D., Xu, K., Stephens, L. C., McDonnell, T. J., Mukhopadhyay, T., and Cai, D. (1996). Retrovirus-mediated wild-type *p53* gene transfer to tumors of patients with lung cancer. *Nat. Med.* **2**, 985–991.

Sarup, J.C., Johnson, R. M., King, K. L., Fendly, B. M., Lipari, M. T., Napier, M. A., Ullrich, A., and Shepard, H. M. (1991). Characterization of an anti-p185 HER2 monoclonal antibody that stimulates receptor function and inhibits tumor cell growth. *Growth Regul.* **1**, 72–82.

Shalaby, M. R., Shepard, H. M., Presta, L., Rodrigues, R. L., Beverley, P. L., Feldmann, M., and Carter, P. (1992). Development of humanized bispecific antibodies reactive with cytotoxic lymphocytes and tumor cells overexpressing the *HER2* protooncogene. *J. Exp. Med.* **175**, 217–225.

Shaw, P., Bovey, R., Tardy, S., Sahli, R., Sordat, B., and Costa, J. (1992). Induction of apoptosis by wild-type p53 in a human colon tumor-derived cell line. *Proc. Natl. Acad. Sci. U.S.A.* **89**, 4495–4499.

Shepard, H. M., Lewis, G. D., Sarup, J. C., Fendly, B. M., Maneval, D., Mordenti, J., Figari, I., Kotts, C. E., Palladino, M. A., Ullrich, A., and Slamon, D. (1991). Monoclonal antibody therapy of human cancer: Taking the HER2 protooncogene to the clinic. *J. Clin. Immunol.* **11**, 117–127.

Slamon, D. J., Clark, G. M., Wong, S. G., Levin, W. J., Ullrich, A., and McGuire, W. L. (1987). Human breast cancer: Correlation of relapse and survival with amplification of HER2/*neu* oncogene. *Science* **235**, 177–182.

Slamon, D. J., Godolphin, W., Jones, L. A., Holt, J. A., Wong, S. G., Keith, D. E., Levin, W. J., Stuart, S. G., Udove, J., Ullrich, A., and Press, M. (1989). Studies of the HER2/*neu* proto-oncogene in human breast and ovarian cancer. *Science* **244**, 707–712.

Straubinger, R. M., Lopez, N. G., Debs, R. J., Hong, K., and Papahadjopoulos, D. (1988). Liposome-based therapy of human ovarian cancer: Parameters determining potency of negatively charged and antibody-targeted liposomes. *Cancer Res.* **48**, 5237–5245.

Stribling, R., Brunette, E., Liggitt, D., Gaensler, K., and Debs, R. (1992). Aerosol gene delivery *in vivo*. *Proc. Natl. Acad. Sci. U.S.A.* **89**, 11277–11281.

Suzuki, S., Watanabe, S., Uno, S., Tanaka, M., Masuko, T., and Hashimoto, Y. (1994). Endocytosis does not necessarily augment the cytotoxicity of Adriamycin encapsulated in immunoliposomes. *Biochim. Biophys. Acta* **1224**, 445–453.

Suzuki, S., Uno, S., Fukuda, Y., Aoki, Y., Masuko, T., and Hashimoto, Y. (1995). Cytotoxicity of anti-c-*erb*B-2 immunoliposomes containing doxorubicin on human cancer cells. *Br. J. Cancer* **72**, 663–668.

Thomas, J. A., Chai, Y. C., and Jung, C. H. (1994). Protein S-thiolation and dethiolation. *In* "Methods in Enzymology" (L. Packer, ed.), Vol. 233, pp. 385–395. Academic Press, San Diego, California.

Torchilin, V. P. (1994). Immunoliposomes and PEGylated immunoliposomes: Possible use for targeted delivery of imaging agents. *Immunomethods* **4**, 244–258.

Valone, F. H., Kaufman, P. A., Guyre, P. M., Lewis, L. D., Memoli, V., Deo, Y., Graziano, R., Fisher, J. L., Meyer, L., Mrozek-Orlowski, M., Wardwell, K., Guyre, V., Morley, T. L., Arvizu, C., and Fanger, M. W. (1995). Phase Ia/Ib trial of bispecific antibody MDX-210 in patients with advanced breast or ovarian cancer that overexpress the proto-oncogene HER2/*neu*. *J. Clin. Oncol.* **13**, 2281–2292.

VandeVijver, M. J., Peterse, M. L., Mooi, W. J., Wisman, P., Lomans, J., Dalesio, O., and Nusse, R. (1988). *Neu*-protein expression in breast cancer. *N. Engl. J. Med.* **319**, 1239–1245.

Vile, R., and Russell, S. J. (1994). *Gene transfer technologies for the gene therapy of cancer. Gene Ther.* **1**, 88–98.

Waldmann, T. (1991). Monoclonal antibodies in diagnosis and therapy. *Science* **252**, 1657–1662.

Wang, C.-Y., and Huang, L. (1987). pH-sensitive immunoliposomes mediate target-cell-specific delivery and controlled expression of a foreign gene in mouse. *Proc. Natl. Acad. Sci. U.S.A.* **84**, 7851–7855.

Weiner, L. M., Holmes, M., Adams, G. P., LaCreta, F., Watts, P., and Garcia de Palazzo, I. (1993). A human tumor xenograft model of therapy with a bispecific monoclonal antibody targeting c-*erb*B-2 and CD16. *Cancer Res.* **53**, 94–100.

Weissig, V., Lasch, J., Klibanov, A. L., and Torchilin, V. P. (1986). A new hydrophobic anchor for the attachment of proteins to liposomal membranes. *FEBS Lett.* **202**, 86–90.

Wels, W., Harwerth, I.-M., Mueller, M., Groner, B., and Hynes, N. E. (1992). Selective inhibition of tumor cell growth by a recombinant single-chain antibody-toxin specific for the erbB-2 receptor. *Cancer Res.* **52**, 6310–6317.

Wolff, B., and Gregoriadis, G. (1984). The use of monoclonal anti-thy-1 IgG for the targeting of liposomes to AKR-A cells *in vitro* and *in vivo*. *Biochim. Biophys. Acta* **802**, 259–273.

Yanagie, H., Tomita, T., Kobayashi, H., Fujii, Y., Takahashi, T., Hasumi, K., and Nariuchi, H. (1991). Application of boronated anti-CEA immunoliposome to tumour cell growth inhibition in *in vitro* boron neutron capure therapy model. *Br. J. Cancer* **63**, 522–526.

Yokota, J., Yamamoto, T., Miyajima, N., Toyoshima, K., Nomura, N., Sakamoto, H., Yoshida, T., Terada, M., and Sugimura, T. (1988). Genetic alterations of the c-*erb*B-2 oncogene occur frequently in tubular adenocarcinoma of the stomach and are often accompanied by amplification of the v-*erb*A homologue. *Oncogene* **2**, 283–287.

Yonemura, Y., Ninomiya, I., Yamaguchi, A., Fushida, S., Kimura, H., Ohoyama, S., Miyazaki, I., Endou, Y., Tanaka, M., and Sasaki, T. (1991). Evaluation of immunoreactivity for *erb*B-2 protein as a marker of poor short term prognosis in gastric cancer. *Cancer Res.* **51**, 1034–1038.

Zalipsky, S., Hansen, C. B., Menezes, D. L. D., and Allen, T. M. (1996). Long-circulating, polyethylene glycol-grafted immunoliposomes. *J. Controlled Release* **39**, 153–161.

Zhau, H. E., Zhang, X., von Eschenbach, A. C., Scorsone, K., Babaian, R. J., Ro, J. Y., and Hung, M.-C. (1990). Amplification and expression of the c-*erb*B-2/*neu* proto-oncogene in human bladder cancer. *Mol. Carcinog.* **3**, 254–257.

Zhau, H. E., Wan, D. S., Zhou, J., Miller, G. J., and von Eschenbach, A. C. (1992). Expression of c-*erb*B-2/*neu* proto-oncogene in human prostatic cancer tissues and cell lines. *Mol. Carcinog.* **5**, 320–327.

Zhu, N., Liggitt, D., Liu, Y., and Debs, R. (1993). Systemic gene expression after intravenous DNA delivery into adult mice. *Science* **261**, 209–211.